

# Polymorphic transitions in single crystals: A new molec

Journal of Applied Physics

52, 7182-7190

DOI: 10.1063/1.328693

Citation Report

#	ARTICLE	IF	CITATIONS
202	Fluctuations and thermodynamic properties of anisotropic solids. Journal of Applied Physics, 1982, 53, 6441-6443.	2.5	38
203	Strain fluctuations and elastic constants. Journal of Chemical Physics, 1982, 76, 2662-2666.	3.0	724
204	Constant pressure molecular dynamics for molecular systems. Molecular Physics, 1983, 50, 1055-1076.	1.7	2,652
205	Molecular dynamics at constant pressure and temperature. Chemical Physics, 1983, 82, 285-301.	1.9	66
206	Special points for deformed face-centered cubic lattice under uniaxial loading. Solid State Communications, 1983, 48, 235-237.	1.9	0
207	Evidence for grain boundary phase transition in a 2d bicrystal. Scripta Metallurgica, 1983, 17, 915-918.	1.2	26
208	Observation of finite-temperature bain transformation (f.c.c. $\rightarrow$ b.c.c.) in Monte Carlo simulation of iron. Scripta Metallurgica, 1983, 17, 1199-1204.	1.2	79
209	New High-Pressure Phase of Solid He4 Is bcc. Physical Review Letters, 1983, 51, 670-673.	7.8	50
210	Molecular dynamics equations of motion for systems varying in shape and size. Journal of Chemical Physics, 1983, 79, 5128-5130.	3.0	38
211	Mineral and melt physics a summary of research in the United States, 1979-1982. Reviews of Geophysics, 1983, 21, 1487-1503.	23.0	46
212	Intermolecular force models and the crystal structure of carbon disulphide. Chemical Physics Letters, 1983, 103, 143-146.	2.6	8
213	Elastic-Constant Anomalies in Metallic Superlattices: A Molecular-Dynamics Study. Physical Review Letters, 1983, 50, 1377-1380.	7.8	83
214	Structural, elastic, and transport anomalies in molybdenum/nickel superlattices. Physical Review B, 1983, 27, 7186-7193.	3.2	230
215	A study of solid and liquid carbon tetrafluoride using the constant pressure molecular dynamics technique. Journal of Chemical Physics, 1983, 78, 6928-6939.	3.0	205
216	Polymorphic phase transitions in alkali cyanide crystals. Molecular Physics, 1983, 50, 243-246.	1.7	22
217	Elastic Moduli of H <sub>2</sub> O: Liquid, Ice VI and Ice VII. Materials Research Society Symposia Proceedings, 1983, 22, 143.	0.1	0
218	Molecular-dynamics studies of grain-boundary diffusion. I. Structural properties and mobility of point defects. Physical Review B, 1984, 29, 5354-5362.	3.2	46
219	Second-order elastic constants for the Lennard-Jones solid. Physical Review B, 1984, 29, 4368-4374.	3.2	87

#	ARTICLE	IF	CITATIONS
220	A unified formulation of the constant temperature molecular dynamics methods. Journal of Chemical Physics, 1984, 81, 511-519.	3.0	14,484
221	A molecular dynamics method for simulations in the canonical ensemble. Molecular Physics, 1984, 52, 255-268.	1.7	8,175
222	A simple intermolecular potential for liquid ammonia. Chemical Physics Letters, 1984, 104, 579-582.	2.6	81
223	Molecular dynamics study of structural instability of two-dimensional lattices. Journal of Applied Physics, 1984, 56, 1455-1461.	2.5	11
224	Statistical ensembles and molecular dynamics studies of anisotropic solids. Journal of Chemical Physics, 1984, 80, 4423-4428.	3.0	262
225	New Monte Carlo method to compute the free energy of arbitrary solids. Application to the fcc and hcp phases of hard spheres. Journal of Chemical Physics, 1984, 81, 3188-3193.	3.0	1,060
226	Mechanical responses of a stressed two-dimensional bicrystal. Scripta Metallurgica, 1984, 18, 159-164.	1.2	5
227	A molecular dynamics study of grain boundary phase equilibria: The case of the $\Sigma = 13$ boundary. Surface Science, 1984, 144, 77-83.	1.9	25
228	Phase transitions in diatomic molecular monolayers. Superlattices and Microstructures, 1985, 1, 517-527.	3.1	4
229	Molecular dynamics simulation of solid n-butane. Physica B: Physics of Condensed Matter & C: Atomic, Molecular and Plasma Physics, Optics, 1985, 131, 256-266.	0.9	34
230	New Molecular-Dynamics Method for Metallic Systems. Physical Review Letters, 1985, 54, 1679-1682.	7.8	24
231	Relative stability of dense crystalline packings. Physical Review B, 1985, 31, 7446-7448.	3.2	1
232	Simulation of the cubic to orthorhombic phase transition in potassium cyanide. Journal of Chemical Physics, 1985, 83, 3638-3644.	3.0	27
233	Inelastic Electron-Phonon Scattering and Time-Resolved Laser-Induced Phase Transformation in Aluminum. Physical Review Letters, 1985, 55, 1939-1939.	7.8	6
234	Statistical ensembles and molecular dynamics studies of anisotropic solids. II. Journal of Chemical Physics, 1985, 82, 4243-4247.	3.0	130
235	The migration of point defects on bcc surfaces using a metallic pair potential. Surface Science, 1985, 164, 526-542.	1.9	32
236	Molecular dynamics study of the liquid and plastic phases of neopentane. Journal of Chemical Physics, 1985, 82, 4236-4242.	3.0	24
237	Theory of melting based on lattice instability. Phase Transitions, 1985, 5, 1-47.	1.3	96

#	ARTICLE	IF	CITATIONS
238	Effect of grain boundary melting on sliding in bicrystals: A molecular dynamics study. Scripta Metallurgica, 1986, 20, 13-17.	1.2	9
239	Computational statistical mechanics methodology, applications and supercomputing. Advances in Physics, 1986, 35, 1-111.	14.4	284
240	Molecular dynamic calculation of elastic constants of silicon. Journal of Chemical Physics, 1986, 85, 4028-4031.	3.0	75
241	Calculation of free energies of Lennard-Jones crystals via molecular dynamics. Journal of Chemical Physics, 1986, 85, 2937-2942.	3.0	8
242	Molecular dynamics simulation of rigid molecules. Computer Physics Reports, 1986, 4, 346-392.	2.2	424
243	Hard spheres in the isobaric-isoenthalpic ensemble. Molecular Physics, 1986, 59, 625-635.	1.7	11
244	Phase diagrams of simple metals from molecular dynamics. Journal of Physics F: Metal Physics, 1986, 16, L35-L41.	1.6	11
245	Phase transitions in high-pressure He4: A study using molecular-dynamics and Monte Carlo methods. Physical Review B, 1986, 34, 178-188.	3.2	12
246	Constant-temperature-constant-pressure molecular-dynamics calculations for molecular solids: Application to solid nitrogen at high pressure. Physical Review B, 1986, 33, 339-342.	3.2	27
247	Constant-stress nonequilibrium molecular dynamics: Shearing of the soft-sphere crystal and fluid. Physical Review A, 1986, 34, 2093-2099.	2.5	21
248	Solid and liquid carbon monoxide studied with the use of constant-pressure molecular dynamics. Physical Review B, 1986, 33, 3441-3447.	3.2	11
249	Constant thermodynamic tension Monte Carlo studies of elastic properties of a two-dimensional system of hard cyclic hexamers. Molecular Physics, 1987, 61, 1247-1258.	1.7	366
250	Structural and thermodynamical behaviour of a solid surface under stress: a molecular dynamics study. Journal of Physics C: Solid State Physics, 1987, 20, 1231-1240.	1.5	1
251	Pulsed laser melting of silicon: A molecular dynamics study. Journal of Chemical Physics, 1987, 87, 2336-2339.	3.0	30
252	Phonon physics – a survey. , 1987, , 1-47.		12
253	Defect-Induced Crystal-to-Amorphous Transition in an Atomistic Simulation Model. Physical Review Letters, 1987, 59, 2760-2763.	7.8	47
254	Molecular dynamics studies of the condensed phases of n-butane and their transitions. Molecular Physics, 1987, 61, 669-692.	1.7	40
255	Fluctuation method for calculation of elastic constants of solids. Journal of Chemical Physics, 1987, 87, 1245-1247.	3.0	8

#	ARTICLE	IF	CITATIONS
256	Amorphous-silicon formation by rapid quenching: A molecular-dynamics study. Physical Review B, 1987, 36, 4234-4237.	3.2	153
257	Dynamical simulation of structural multiplicity in grain boundaries. Scripta Metallurgica, 1987, 21, 1153-1157.	1.2	22
258	Close-packed (polytypic) structures in molecular-dynamics simulations. Physical Review B, 1987, 35, 557-570.	3.2	9
259	The structure of internal interfaces: Report of a discussion meeting. Materials Science and Engineering, 1987, 89, 1-16.	0.1	28
260	Statistical mechanics of viscoelasticity. Journal of Statistical Physics, 1987, 46, 753-775.	1.2	9
261	A grain boundary phase transition studied by molecular dynamics. Acta Metallurgica, 1987, 35, 2719-2730.	2.1	39
262	Computer simulation of transformations in solids. Journal of Solid State Chemistry, 1987, 68, 193-213.	2.9	6
263	Molecular dynamics study of MgSiO <sub>3</sub> perovskite. Physics and Chemistry of Minerals, 1988, 16, 234.	0.8	63
264	Elastic constants and statistical ensembles in molecular dynamics. Computer Physics Reports, 1988, 8, 109-151.	2.2	186
265	Improved rigid ion model of molten zinc chloride. Physica B: Condensed Matter, 1988, 153, 85-92.	2.7	28
266	Molecular dynamics methods to study structural phase transformations in solids. Physica B: Physics of Condensed Matter & C: Atomic, Molecular and Plasma Physics, Optics, 1988, 150, 250-257.	0.9	9
267	Computer simulation studies of radiation induced amorphization. Journal of Non-Crystalline Solids, 1988, 99, 75-88.	3.1	44
268	Dynamical simulations of stress, strain, and finite deformations. Physical Review B, 1988, 38, 9522-9537.	3.2	44
269	Fundamental treatment of molecular-dynamics ensembles. Physical Review A, 1988, 37, 247-251.	2.5	58
270	Stress and elastic constants in anisotropic solids: Molecular dynamics techniques. Journal of Applied Physics, 1988, 64, 1152-1154.	2.5	204
271	New equations of motion for molecular dynamics systems that change shape. Journal of Chemical Physics, 1988, 89, 4987-4993.	3.0	66
272	Grain boundary segregation free energy: A molecular dynamics study. Scripta Metallurgica, 1988, 22, 1049-1054.	1.2	3
273	A molecular dynamics study of grain boundary behavior at elevated temperatures using an embedded atom potential. Scripta Metallurgica, 1988, 22, 1923-1928.	1.2	6

#	ARTICLE	IF	CITATIONS
274	Third-order elastic constants from molecular dynamics: Theory and an example calculation. Physical Review B, 1988, 38, 7940-7946.	3.2	61
275	Character of the $\sqrt{2}\sqrt{2}$ phase transition in solid oxygen. Physical Review B, 1988, 37, 5364-5370.	3.2	27
276	Molecular dynamics calculation of free energy. Journal of Chemical Physics, 1988, 88, 6525-6528.	3.0	34
277	Molecular-dynamics method for the simulation of bulk-solid interfaces at high temperatures. Physical Review B, 1988, 38, 11572-11581.	3.2	68
278	Electrical resistance of nickel in the range 300–725 K and 0–2 GPa. Physical Review B, 1988, 38, 12283-12289.	3.2	18
279	Atomistic model of orthorhombic YBa <sub>2</sub> Cu <sub>3</sub> O <sub>7</sub> . Physical Review B, 1988, 38, 6596-6603.	3.2	11
280	A New Model for the Simulation of Interfaces at High Temperature. Materials Research Society Symposia Proceedings, 1988, 122, 129.	0.1	0
281	Molecular Dynamics Simulation of a $\theta = 5^\circ$ Aluminum Bicrystal. Materials Research Society Symposia Proceedings, 1988, 122, 125.	0.1	0
282	Molecular Dynamics Studies of Twist Boundaries in Ionic Materials. Materials Research Society Symposia Proceedings, 1988, 122, 135.	0.1	1
283	Micromechanics and Microdynamics Via Atomistic Simulations. Materials Research Society Symposia Proceedings, 1988, 140, 101.	0.1	4
284	High-Temperature Behavior of Grain Boundaries from Embedded Atom Method Molecular Dynamics Simulation. Materials Research Society Symposia Proceedings, 1988, 141, 379.	0.1	0
285	A Computer Calorimetry Study of Segregation Free Energy: Cu in a Ni Grain Boundary. Materials Research Society Symposia Proceedings, 1988, 122, 275.	0.1	1
286	Molecular dynamics and defects in metals in relation to interatomic force laws. Philosophical Magazine A: Physics of Condensed Matter, Structure, Defects and Mechanical Properties, 1988, 58, 179-192.	0.6	9
287	The effective-medium theory beyond the nearest-neighbour interaction. Journal of Physics Condensed Matter, 1989, 1, 9765-9777.	1.8	27
288	Ferroelastic phase transition and phonons in a diatomic-molecular monolayer. Physical Review B, 1989, 39, 677-688.	3.2	2
289	Crystal-melt and melt-vapor interfaces of nickel. Physical Review B, 1989, 40, 924-932.	3.2	75
290	Glass formation in simple ionic systems via constant pressure molecular dynamics. Journal of Chemical Physics, 1989, 90, 7384-7394.	3.0	3
291	Elastic properties of grain boundaries in copper and their relationship to bulk elastic constants. Physical Review B, 1989, 40, 9479-9484.	3.2	62

#	ARTICLE	IF	CITATIONS
292	Atomistic simulation of defect-induced amorphization of binary lattices. Physical Review B, 1989, 39, 7476-7491.	3.2	36
293	Internal stress tensor in constant-pressure molecular dynamics of anisotropic molecular solids. Physical Review B, 1989, 39, 11928-11931.	3.2	1
294	Low temperature phase transformation in superionic conductors: A molecular dynamics study of silver sulfide. Journal of Chemical Physics, 1989, 90, 6580-6586.	3.0	22
295	Molecular-dynamics study of lattice-defect-nucleated melting in metals using an embedded-atom-method potential. Physical Review B, 1989, 40, 2841-2855.	3.2	223
296	Elastic moduli of a perfect hard disc crystal in two dimensions. Physics Letters, Section A: General, Atomic and Solid State Physics, 1989, 134, 314-318.	2.1	30
297	New pressure-induced structural transformations in silica obtained by computer simulation. Nature, 1989, 339, 209-211.	27.8	192
298	NEW FORMS OF MOLECULAR DYNAMICS AND SUPERIONIC CONDUCTORS. , 1989, , 553-567.		0
299	On the relevance of extrinsic defects to melting: A molecular dynamics study using an embedded atom potential. Scripta Metallurgica, 1989, 23, 333-338.	1.2	1
300	Mechanism of pressure-induced martensitic phase transformations: A molecular-dynamics study. Physical Review B, 1989, 39, 565-574.	3.2	23
301	Elastic constants of nickel: Variations with respect to temperature and pressure. Physical Review B, 1989, 39, 12484-12491.	3.2	34
302	Embedded Atom Potential for BCC Iron. , 1989, , 219-222.		26
303	Isothermalâ€isobaric molecular dynamics simulation of polymorphic phase transitions in alkali halides. Journal of Chemical Physics, 1989, 91, 3148-3159.	3.0	25
304	Molecular-dynamics study of lattice-defect-nucleated melting in silicon. Physical Review B, 1989, 40, 2831-2840.	3.2	157
305	Molecular dynamics study of the structural and thermodynamic properties of MgO crystal with quantum correction. Journal of Chemical Physics, 1989, 91, 489-494.	3.0	102
306	Structure and dynamic properties of twist boundaries in NaCl through a molecular dynamics study. Philosophical Magazine A: Physics of Condensed Matter, Structure, Defects and Mechanical Properties, 1989, 60, 525-544.	0.6	7
307	Molecular-Dynamics Study of Grain-Boundary Migration in Metals. Materials Research Society Symposia Proceedings, 1990, 193, 325.	0.1	0
308	Molecular Dynamics Study of the Elastic Response of Crystalline, Amorphous and Chemically Disordered NiZr <sub>2</sub> . Materials Research Society Symposia Proceedings, 1990, 205, 399.	0.1	1
309	Computer Simulation of Molecular Dynamics: Methodology, Applications, and Perspectives in Chemistry. Angewandte Chemie International Edition in English, 1990, 29, 992-1023.	4.4	1,352

#	ARTICLE	IF	CITATIONS
310	MolekÃ¼ldynamikâ€”Computersimulationen; Methodik, Anwendungen und Perspektiven in der Chemie. Angewandte Chemie, 1990, 102, 1020-1055.	2.0	114
311	Progress in the development of a molecular dynamics code for high-energy cascade studies. Journal of Nuclear Materials, 1990, 174, 151-157.	2.7	159
312	Dynamic properties of supercooled Lennard-Jones liquids: a molecular-dynamics study. Journal of Physics Condensed Matter, 1990, 2, 4991-5003.	1.8	9
313	Quantum isoenthalpic-isotension method for studying solid phase transformations. Physical Review B, 1990, 41, 6994-6997.	3.2	1
314	Molecular-dynamics study of amorphization by introduction of chemical disorder in crystallineNiZr <sub>2</sub> . Physical Review B, 1990, 41, 10486-10497.	3.2	142
315	Formalism for the calculation of local elastic constants at grain boundaries by means of atomistic simulation. Journal of Applied Physics, 1990, 67, 2370-2379.	2.5	113
316	Molecular-dynamics study of theÎ±toÎ²structural phase transition of quartz. Physical Review Letters, 1990, 64, 776-779.	7.8	108
317	Surface melting of Ni(110). Physical Review B, 1990, 41, 439-450.	3.2	137
318	Molecular dynamics simulations of some amorphous and crystalline photonic materials. Journal of Materials Research, 1990, 5, 1104-1109.	2.6	3
319	PARTICLE DEPOSITION AT A CHARGED SOLID/LIQUID INTERFACE. Chemical Engineering Communications, 1990, 91, 127-198.	2.6	29
320	Thermodynamic parallels between solid-state amorphization and melting. Journal of Materials Research, 1990, 5, 286-301.	2.6	199
321	Computer simulation studies of anisotropic systems. XIX. Mesophases formed by the Gay-Berne model mesogen. Liquid Crystals, 1990, 8, 451-464.	2.2	231
322	Deterministic Methods. , 1990, , 13-50.		0
323	Isobaric and Isothermal Molecular Dynamics Simulations of Diatomic Systems. Molecular Simulation, 1990, 4, 371-398.	2.0	3
324	Molecular dynamics studies of solid and liquid copper using the Finnis-Sinclair many-body potential. Journal of Physics Condensed Matter, 1990, 2, 1291-1300.	1.8	15
325	Molecular Dynamics Simulation of the Structural and Physical Properties of the Four Polymorphs of TiO <sub>2</sub> . Molecular Simulation, 1991, 6, 239-244.	2.0	413
326	Molecular dynamics with a variable number of molecules. Molecular Physics, 1991, 72, 169-175.	1.7	100
327	Invariant molecular-dynamics approach to structural phase transitions. Physical Review B, 1991, 44, 2358-2361.	3.2	321



#	ARTICLE	IF	CITATIONS
328	On the mechanism of grain-boundary migration in metals: A molecular dynamics study. Journal of Materials Research, 1991, 6, 2291-2304.	2.6	19
329	Development of an N-body interatomic potential for hcp and bcc zirconium. Physical Review B, 1991, 43, 11653-11665.	3.2	117
330	An Introduction to Molecular Dynamics, with Applications to the Glass Transition. , 1991, , 3-20.		1
331	Pressure-induced Structural Transformations in Framework Crystal Structures. Molecular Simulation, 1991, 6, 227-238.	2.0	6
332	Molecular Dynamics Simulations at Constant Temperature and Pressure. , 1991, , 21-41.		27
333	Microscopic Modeling of Amorphization by Solid State Reactions: Role of Chemical Disorder and Elastic Softening in the Intermetallic Alloy NiZr <sub>2</sub> . , 1991, , 349-363.		0
334	A survey of the phenomenon of polytypism in crystals. Solid State Ionics, 1991, 48, 3-70.	2.7	101
335	Vibrational properties of Ba <sub>1-x</sub> K <sub>x</sub> BiO <sub>3</sub> . Physica B: Condensed Matter, 1991, 168, 268-272.	2.7	2
336	Simulation of the pre-melting behaviour of MgSiO <sub>3</sub> perovskite at high pressures and temperatures. Nature, 1991, 351, 735-737.	27.8	114
337	Competing interactions and orientational ordering in (NaCN) <sub>1-x</sub> (KCN) <sub>x</sub> quadrupolar glasses. Physical Review Letters, 1991, 66, 624-627.	7.8	9
338	Dynamical models of hydrogenated amorphous silicon. Physical Review B, 1991, 43, 9810-9817.	3.2	37
339	Molecular-dynamics study of elasticity and failure of ideal solids. Physical Review B, 1991, 44, 378-381.	3.2	37
340	Analysis of point-defect diffusion and drift in cubic-type lattices: Constitutive modeling. Physical Review B, 1991, 44, 2567-2581.	3.2	1
341	Rate of microcrack nucleation. Physical Review A, 1991, 43, 5223-5227.	2.5	46
342	Molecular-dynamics study of the effects of strain on interstitial diffusion in a hard-sphere model of a binary crystalline solid. Physical Review B, 1991, 43, 8251-8263.	3.2	3
343	A Molecular Dynamics Simulation of Na <sub>2</sub> O·2SiO <sub>2</sub> -K <sub>2</sub> O·2SiO <sub>2</sub> Melts—Effect of Basic Cell Size. Molecular Simulation, 1991, 6, 245-255.	2.0	11
344	Effect of temperature and small-scale defects on the strength of solids. Journal of Chemical Physics, 1991, 95, 9128-9141.	3.0	30
345	Phase transformations and polytypism in silver iodide: A molecular-dynamics study. Physical Review B, 1991, 44, 9228-9239.	3.2	14

#	ARTICLE	IF	CITATIONS
346	Anomalies in the elastic properties of metallic multilayers. Physical Review Letters, 1991, 66, 1882-1885.	7.8	14
347	Surface premelting of Cu(110). Physical Review B, 1991, 44, 3226-3239.	3.2	106
348	MODELING OF MONOLAYERS. , 1991, , 305-338.		3
349	Molecular Dynamics and Diffusion in Silicate Melts. , 1991, , 1-50.		8
350	The fracture of perfect crystals under uniaxial tension at high temperatures. Journal of Physics Condensed Matter, 1992, 4, 2127-2138.	1.8	14
351	Computer Simulation of Surface Segregation. Molecular Simulation, 1992, 9, 83-98.	2.0	27
352	Finite temperature structure and properties of $\hat{\alpha} = 5$ (310) tilt grain boundaries in nacl a molecular dynamics study. Philosophical Magazine A: Physics of Condensed Matter, Structure, Defects and Mechanical Properties, 1992, 66, 11-26.	0.6	17
353	Percolation model for elastic softening in intermetallic compounds during solid-state amorphization. Physical Review B, 1992, 45, 2484-2487.	3.2	25
354	Nonlinear molecular dynamics and Monte Carlo algorithms. Physical Review B, 1992, 46, 12068-12071.	3.2	19
355	SolidC70: A molecular-dynamics study of the structure and orientational ordering. Physical Review B, 1992, 46, 4958-4962.	3.2	32
356	Temperature dependence of elastic constants of embedded-atom models of palladium. Physical Review B, 1992, 46, 8027-8035.	3.2	49
357	Thermodynamics, statistical thermodynamics, and computer simulation of crystals with vacancies and interstitials. Physical Review A, 1992, 46, 4539-4548.	2.5	50
358	Monte Carlo simulations in the isenthalpic-isotension-isobaric ensemble. Physical Review A, 1992, 46, 4645-4649.	2.5	33
359	A Percolation Model for Elastic Softening in Intermetallic Compounds During Solid-State Amorphization. Materials Research Society Symposia Proceedings, 1992, 278, 299.	0.1	0
360	Molecular Dynamics Modeling of Growth, Micro-Structure and Stresses in Sputter-Deposited Films with Impurity Atom Incorporation. Materials Research Society Symposia Proceedings, 1992, 280, 463.	0.1	2
361	Ergodicity and Convergence of Fluctuations in Parrinello-Rahman Molecular Dynamics. Materials Research Society Symposia Proceedings, 1992, 291, 285.	0.1	8
362	Nonlinear Molecular Dynamics and Monte Carlo Simulations of Crystals at Constant Temperature and Tensorial Pressure. Materials Research Society Symposia Proceedings, 1992, 291, 597.	0.1	0
363	Computer simulation methods and semi-empirical pair potentials for materials development and analysis.. Keikinzoku/Journal of Japan Institute of Light Metals, 1992, 42, 411-417.	0.4	0

#	ARTICLE	IF	CITATIONS
364	Molecular-dynamics investigation of orientational freezing in solid C <sub>60</sub> . Physical Review B, 1992, 45, 1889-1895.	3.2	111
365	Fluctuations and thermodynamic response functions in a Lennard-Jones solid. Physical Review B, 1992, 46, 5237-5241.	3.2	40
366	C60O: a molecular dynamics study of rotation in the solid phase solid phase. Journal of the Chemical Society, Faraday Transactions, 1992, 88, 1949.	1.7	11
367	Simulated quenching to the zero-temperature limit of the grand-canonical ensemble. Journal of Chemical Physics, 1992, 97, 2651-2658.	3.0	23
368	Theory of orientational glasses models, concepts, simulations. Advances in Physics, 1992, 41, 547-627.	14.4	238
369	Stress induced martensitic transition in a molecular dynamics model of $\epsilon$ -Fe. Journal of Applied Physics, 1992, 71, 4009-4014.	2.5	29
370	Molecular dynamics simulation of fluoride-perovskites. Journal of Physics Condensed Matter, 1992, 4, 2097-2108.	1.8	25
371	Ergodicity and dynamical properties of constant-temperature molecular dynamics. Physical Review A, 1992, 45, 7089-7097.	2.5	34
372	A molecular dynamics study of sodium beta $\gamma$ -alumina. Journal of Physics Condensed Matter, 1992, 4, 3215-3234.	1.8	25
373	Is There a Vacancy-Induced Premelting in a Molecular Crystal?. Europhysics Letters, 1992, 18, 245-250.	2.0	16
374	Computer simulation of the MgSiO <sub>3</sub> polymorphs. Physics and Chemistry of Minerals, 1992, 18, 365.	0.8	48
375	Molecular dynamics studies of defect production and clustering in energetic displacement cascades in copper. Journal of Nuclear Materials, 1992, 191-194, 108-115.	2.7	54
376	Molecular dynamics simulations of 45° [100] twist plus tilt grain boundaries in aluminum. Ultramicroscopy, 1992, 40, 240-246.	1.9	2
377	Mechanical stability of Pd-H systems: A molecular-dynamics study. Physical Review B, 1992, 46, 8099-8108.	3.2	31
378	Free-energy calculations and the melting point of Al. Physical Review B, 1992, 46, 21-25.	3.2	158
379	Computational materials science for microelectronics - the old and the new challenges. Physica D: Nonlinear Phenomena, 1993, 66, 154-165.	2.8	2
380	Computer simulation of hydrogen embrittlement in metals. Nature, 1993, 362, 435-437.	27.8	55
381	Hoover NPT dynamics for systems varying in shape and size. Molecular Physics, 1993, 78, 533-544.	1.7	1,003

#	ARTICLE	IF	CITATIONS
382	Simulation of site-site soft-core liquid crystal models. <i>Molecular Physics</i> , 1993, 80, 297-312.	1.7	37
383	Ferroelectric phases of dipolar hard spheres. <i>Physical Review E</i> , 1993, 48, 3728-3740.	2.1	160
384	A molecular dynamics study of atomic level stress distributions in defective intermetallics. <i>Journal of Alloys and Compounds</i> , 1993, 194, 417-427.	5.5	7
386	Activated dynamics, loss of ergodicity, and transport in supercooled liquids. <i>Physical Review E</i> , 1993, 47, 479-489.	2.1	134
387	Advanced Monte Carlo Techniques. , 1993, , 93-152.		14
388	Tight-binding potentials for transition metals and alloys. <i>Physical Review B</i> , 1993, 48, 22-33.	3.2	1,748
389	A molecular dynamics investigation of a stepped metal-ceramic interface. <i>Scripta Metallurgica Et Materialia</i> , 1993, 28, 943-947.	1.0	2
390	Analysis of Fe–Ni–Cr–N austenite using the Embedded-Atom Method. <i>Calphad: Computer Coupling of Phase Diagrams and Thermochemistry</i> , 1993, 17, 383-413.	1.6	49
391	Crystal instabilities at finite strain. <i>Physical Review Letters</i> , 1993, 71, 4182-4185.	7.8	742
392	Many-body potentials for Cu-Ti intermetallic alloys and a molecular dynamics study of vitrification and amorphization. <i>Modelling and Simulation in Materials Science and Engineering</i> , 1993, 1, 315-333.	2.0	17
393	Vibrational and elastic effects of point defects in silicon. <i>Physical Review B</i> , 1993, 48, 10899-10908.	3.2	27
394	Effect of gas impurity and ion bombardment on stresses in sputter-deposited thin films: A molecular-dynamics approach. <i>Journal of Applied Physics</i> , 1993, 74, 4472-4482.	2.5	43
395	Simulations of shear-induced melting and ordering. <i>Physical Review E</i> , 1993, 48, 3778-3792.	2.1	88
396	Quasiharmonic and molecular-dynamics study of the martensitic transformation in Ni-Al alloys. <i>Physical Review B</i> , 1993, 48, 99-111.	3.2	79
397	Anisotropy in the structure of pressure-induced disordered solids. <i>Physical Review Letters</i> , 1993, 70, 174-177.	7.8	59
398	Constant-temperature molecular dynamics with momentum conservation. <i>Physical Review E</i> , 1993, 47, 3145-3151.	2.1	45
399	Cu/Pd multilayers: An atomistic structural study. <i>Physical Review B</i> , 1993, 47, 13636-13642.	3.2	11
400	A force-balance Monte Carlo simulation of the surface tension of a hard-sphere fluid. <i>Molecular Physics</i> , 1993, 78, 943-959.	1.7	29

#	ARTICLE	IF	CITATIONS
401	A Computation of Elastic Constant of Metallic Multilayered Film Using EAM Potential. Materials Transactions, JIM, 1993, 34, 882-887.	0.9	4
402	Finite-Temperature Molecular Dynamics Study for Atomic Structures of Grain Boundary in Transition Metals Fe and Ni. Materials Research Society Symposia Proceedings, 1993, 318, 577.	0.1	0
403	Ideal chemical potential contribution in molecular dynamics simulations of the grand canonical ensemble. Molecular Physics, 1994, 82, 897-912.	1.7	46
404	Multiple time scale methods for constant pressure molecular dynamics simulations of molecular systems. Molecular Physics, 1994, 83, 255-272.	1.7	46
405	Structural variations in strained crystalline multilayers. Journal of Materials Research, 1994, 9, 2190-2197.	2.6	6
406	Finite size effects in the simulation of crystallization. Journal of Chemical Physics, 1994, 101, 6091-6095.	3.0	4
407	Atomistic simulations incorporating nonlinear elasticity: Slow-stress relaxation and symmetry breaking. Physical Review B, 1994, 49, 11619-11633.	3.2	12
408	Dislocation-mediated healing of ideal and adsorbed monolayers with vacancy damage. Physical Review B, 1994, 50, 8763-8772.	3.2	7
409	Computer simulations of disordering kinetics in irradiated intermetallic compounds. Physical Review B, 1994, 50, 13204-13213.	3.2	37
410	Lattice instability in $\text{SiC}$ and simulation of brittle fracture. Journal of Applied Physics, 1994, 76, 2719-2725.	2.5	58
411	Method of obtaining the stable unit-cell shape in the strained superlattice. Physical Review B, 1994, 50, 15138-15141.	3.2	0
412	Simulation of growth of Ni-Zr interfacial amorphous regions under nonequilibrium conditions. Physical Review B, 1994, 50, 2850-2857.	3.2	33
413	The temperature-size phase diagram of large $\text{SF}_6$ clusters by computer simulation. Chemical Physics Letters, 1994, 218, 122-127.	2.6	26
414	Multiresolution molecular dynamics algorithm for realistic materials modeling on parallel computers. Computer Physics Communications, 1994, 83, 197-214.	7.5	67
415	The integration of molecular dynamics simulations with imposed temperature and stress. Computer Physics Communications, 1994, 79, 219-248.	7.5	2
416	A fast grid search algorithm for molecular dynamics simulations with short-range interactions. Computer Physics Communications, 1994, 81, 19-55.	7.5	24
417	Molecular packing analysis: prediction of experimental crystal structures of benzene starting from unreasonable initial structures. Computational and Theoretical Chemistry, 1994, 313, 321-334.	1.5	19
418	The role of non-deformable units in pressure-induced reversible amorphization of clathrasils. Nature, 1994, 369, 724-727.	27.8	82

#	ARTICLE	IF	CITATIONS
419	Molecular dynamics of MgSiO <sub>3</sub> perovskite at high pressures: Equation of state, structure, and melting transition. <i>Geochimica Et Cosmochimica Acta</i> , 1994, 58, 4039-4047.	3.9	151
420	Theoretical Approach. , 0, , 1-23.		0
421	Ideal crystal stability and pressure-induced phase transition in silicon. <i>Physical Review B</i> , 1994, 50, 14952-14959.	3.2	114
422	Computer modelling as a technique in materials chemistry. <i>Journal of Materials Chemistry</i> , 1994, 4, 781.	6.7	84
423	Observation of a volume minimum in computer simulations of supercooled, amorphous silica. <i>Journal of Non-Crystalline Solids</i> , 1994, 167, 211-228.	3.1	14
424	The effect of molecular shape anisotropy on surface melting. <i>Surface Science</i> , 1994, 302, L331-L335.	1.9	1
425	VO <sub>2</sub> : Peierls or Mott-Hubbard? A view from band theory. <i>Physical Review Letters</i> , 1994, 72, 3389-3392.	7.8	588
426	Pressure Calculation in Molecular Dynamics Simulations of Molecular Crystals. <i>Molecular Simulation</i> , 1994, 13, 221-230.	2.0	6
427	Structure and Properties of Strained Crystalline Multilayers. <i>Materials Research Society Symposia Proceedings</i> , 1994, 351, 349.	0.1	0
428	Molecular Dynamics Study of BaB <sub>2</sub> O <sub>4</sub> in Crystalline and Molten States. <i>Molecular Simulation</i> , 1994, 12, 167-176.	2.0	0
429	A Heuristic Molecular-Dynamics Approach for the Prediction of a Molecular Crystal Structure. <i>Bulletin of the Chemical Society of Japan</i> , 1995, 68, 519-527.	3.2	27
430	Molecular dynamics simulation of the dipalmitoylphosphatidylcholine (DPPC) lipid bilayer in the fluid phase using the Nosé-Parrinello-Rahman NPT ensemble. <i>Chemical Physics Letters</i> , 1995, 232, 308-312.	2.6	38
431	Ab initio study of small gallium phosphate clusters. <i>Chemical Physics Letters</i> , 1995, 236, 609-615.	2.6	9
432	Martensitic transformation and phonon localization in Ni-Al alloys by atomistic simulations. <i>Meccanica</i> , 1995, 30, 439-448.	2.0	4
433	Calculated thermodynamic properties of silica polymorphs. <i>Physics and Chemistry of Minerals</i> , 1995, 22, 233.	0.8	10
434	Molecular packing analysis of benzene crystals. Part 2. Prediction of experimental crystal structure polymorphs at low and high pressure. <i>Computational and Theoretical Chemistry</i> , 1995, 333, 267-274.	1.5	21
435	Empirical atom-atom potential for a naphthalene crystal and transferability to other polyacene crystals. <i>Molecular Physics</i> , 1995, 85, 449-462.	1.7	7
436	Constant pressure molecular dynamics simulation: The Langevin piston method. <i>Journal of Chemical Physics</i> , 1995, 103, 4613-4621.	3.0	3,818

#	ARTICLE	IF	CITATIONS
437	Chapter 12. COMPUTER SIMULATIONS OF SILICATE MELTS. , 1995, , 563-616.		6
438	Solid-solid interface and solid solution of oxides with rock-salt structure: Lattice properties. Physical Review B, 1995, 51, 15732-15741.	3.2	4
439	Simulation of C60 through the plastic transition temperatures. Journal of Chemical Physics, 1995, 103, 1106-1108.	3.0	2
440	Atomic Size Effects in Pressure-Induced Amorphization of a Binary Covalent Lattice. Physical Review Letters, 1995, 75, 2738-2741.	7.8	44
441	Prediction and Observation of the bcc Structure in Pure Copper at a $\Sigma$ 3 Grain Boundary. Physical Review Letters, 1995, 75, 2160-2163.	7.8	56
442	Atomistic simulation of thermomechanical properties of $\beta$ -SiC. Physical Review B, 1995, 52, 15150-15159.	3.2	105
443	Molecular-dynamics simulations of nickel oxide surfaces. Physical Review B, 1995, 52, 5323-5329.	3.2	86
444	Embedded-atom model of glass-forming Si-metal alloys. Physical Review B, 1995, 51, 14962-14975.	3.2	23
445	Anomalous Phonon Behavior and Phase Fluctuations in bcc Zr. Physical Review Letters, 1995, 74, 1375-1378.	7.8	28
446	Molecular dynamics study of the plastic-crystalline phase transition of tetraphosphorus triselenide. Molecular Physics, 1995, 84, 727-742.	1.7	6
447	The pressure-induced phase transition of the $\alpha$ -cristobalite form of $\text{CaPO}_4$ . Journal of Physics Condensed Matter, 1995, 7, 8279-8286.	1.8	6
448	Selection of a simulation method. , 1995, , 203-233.		0
449	A molecular dynamics simulation of the effect of high pressure on fast-ion conduction in a $\text{MgSiO}_3$ -perovskite analogue; $\text{KCaF}_3$ . Physics of the Earth and Planetary Interiors, 1995, 89, 137-144.	1.9	10
450	Molecular dynamics of stishovite melting. Geochimica Et Cosmochimica Acta, 1995, 59, 1883-1889.	3.9	54
451	Melting in Two-Dimensional Lennard-Jones Systems: Observation of a Metastable Hexatic Phase. Physical Review Letters, 1995, 74, 4019-4022.	7.8	102
452	Study of copper precipitates in $\alpha$ -iron by computer simulation I. Interatomic potentials and properties of Fe and Cu. Philosophical Magazine A: Physics of Condensed Matter, Structure, Defects and Mechanical Properties, 1995, 72, 361-381.	0.6	65
453	Computer simulation of liquid/liquid interfaces. I. Theory and application to octane/water. Journal of Chemical Physics, 1995, 103, 10252-10266.	3.0	341
454	Monte Carlo algorithms for the atomistic simulation of condensed polymer phases. Journal of the Chemical Society, Faraday Transactions, 1995, 91, 2355.	1.7	48

#	ARTICLE	IF	CITATIONS
455	Molecular simulation: a view from the bond. Faraday Discussions, 1995, 100, C29.	3.2	10
456	Selection of a simulation method. , 1995, , 203-233.		0
457	Mechanical instabilities of homogeneous crystals. Physical Review B, 1995, 52, 12627-12635.	3.2	432
458	Molecular Dynamics Simulation of Structural Phase Transition of $\text{AlPO}_4$ Induced by Pressure. Molecular Simulation, 1996, 16, 375-386.	2.0	3
459	Constant-Pressure Molecular Dynamics Techniques Applied to Complex Molecular Systems and Solvated Proteins. The Journal of Physical Chemistry, 1996, 100, 4314-4322.	2.9	37
460	Molecular and lattice dynamics study of the $\text{MgO-SiO}_2$ system using a transferable interatomic potential. Geochimica Et Cosmochimica Acta, 1996, 60, 1645-1656.	3.9	43
461	Pressure-induced phase transition and structural changes under deviatoric stress of stishovite to $\text{CaCl}_2$ -like structure. Geochimica Et Cosmochimica Acta, 1996, 60, 3657-3663.	3.9	14
462	A computer simulation approach to the high pressure thermoelasticity of $\text{MgSiO}_3$ perovskite. Physics of the Earth and Planetary Interiors, 1996, 98, 55-63.	1.9	11
463	Million atom molecular dynamics simulations of materials on parallel computers. Current Opinion in Solid State and Materials Science, 1996, 1, 853-863.	11.5	8
464	Hydrogen-bonding behaviour in the hydrophobic hydration of simple hydrocarbons in water. Journal of the Chemical Society, Faraday Transactions, 1996, 92, 2547.	1.7	22
465	Molecular dynamics simulations of tethered membranes with periodic boundary conditions. Physical Review E, 1996, 53, 1422-1429.	2.1	17
466	The importance of the anisotropic energy term for the structure of the solid phases of nitrogen. Journal of Chemical Physics, 1996, 105, 3235-3244.	3.0	29
467	Molecular dynamics studies of titanylphthalocyanine crystals. Journal of the Chemical Society, Faraday Transactions, 1996, 92, 2463.	1.7	17
468	Molecular dynamics of $\text{NaCl}$ (B1 and B2) and $\text{MgO}$ (B1) melting; two-phase simulation. American Mineralogist, 1996, 81, 303-316.	1.9	143
469	Molecular Dynamics Study on Grain Boundary Diffusion in Aluminum under Hydrostatic Stress.. Nihon Kikai Gakkai Ronbunshu, A Hen/Transactions of the Japan Society of Mechanical Engineers, Part A, 1996, 62, 2791-2796.	0.2	0
470	A process model for sputter deposition of thin films using molecular dynamics. Thin Films, 1996, 22, 117-IN3.	0.1	2
471	DIFFUSION IN METALS AND ALLOYS. , 1996, , 535-668.		54
472	NpH-MD-Simulations of the Elastic Moduli of Cellulose II at Room Temperatue. Journal of Molecular Modeling, 1996, 2, 278-285.	1.8	14



#	ARTICLE	IF	CITATIONS
473	Silica under very large positive and negative pressures: Molecular dynamics simulations on parallel computers. International Journal of Thermophysics, 1996, 17, 169-178.	2.1	6
474	Molecular dynamics in curved hyperspace. Physics Letters, Section A: General, Atomic and Solid State Physics, 1996, 220, 258-262.	2.1	3
475	Molecular dynamics simulation of silica with a first-principles interatomic potential. Molecular Engineering, 1996, 6, 157.	0.2	9
476	Stability of Diamond at Megabar Pressures. Physica Status Solidi (B): Basic Research, 1996, 198, 447-453.	1.5	12
477	Pressure-induced phase transition of quartz-type GaPO <sub>4</sub> . Physical Review B, 1996, 53, 107-110.	3.2	13
478	Dielectric constant of polarizable water at elevated temperatures. Journal of Chemical Physics, 1996, 105, 10496-10499.	3.0	26
479	A molecular dynamics simulation study of the effects of defects on the transformation pressure of polymorphic phase transformations. Journal of Chemical Physics, 1996, 105, 3215-3218.	3.0	12
480	Quartzlike polymorph of ice. Physical Review B, 1996, 53, R8815-R8817.	3.2	41
481	Structural Transformations of Ice at High Pressures Via Molecular Dynamics Simulations. Molecular Simulation, 1996, 18, 115-132.	2.0	2
482	Evidence of diffusion-controlled vitrification in Ni/Zr bilayer at medium temperatures by molecular-dynamics simulation. Europhysics Letters, 1997, 39, 401-406.	2.0	4
483	Orthorhombic quartzlike polymorph of silica: A molecular-dynamics simulation study. Physical Review B, 1997, 55, 721-725.	3.2	17
484	A molecular dynamics study of the CO <sub>2</sub> /NaCl(001) system. Journal of Chemical Physics, 1997, 106, 5693-5705.	3.0	7
485	Comparison of Thermodynamic Properties of Simulated Liquid Silica and Water. Physical Review Letters, 1997, 79, 2281-2284.	7.8	158
486	Morphology of Pores and Interfaces and Mechanical Behavior of Nanocluster-Assembled Silicon Nitride Ceramic. Physical Review Letters, 1997, 78, 689-692.	7.8	67
487	Vacancy migration at the {410}/[001] symmetric tilt grain boundary of MgO: An atomistic simulation study. Physical Review B, 1997, 56, 11477-11484.	3.2	43
488	Molecular dynamics study of a lipid bilayer: Convergence, structure, and long-time dynamics. Journal of Chemical Physics, 1997, 106, 5731-5743.	3.0	61
489	Empirical bond-order potential description of thermodynamic properties of crystalline silicon. Journal of Applied Physics, 1997, 81, 96-106.	2.5	78
490	High-pressure infrared study of solid methane: Phase diagram up to 30 GPa. Physical Review B, 1997, 55, 14800-14809.	3.2	68

#	ARTICLE	IF	CITATIONS
491	Orientational ordering in the mixed crystal $\text{Ar1}\hat{\sim}\text{x}(\text{N2})\text{x}$ : A molecular dynamics study. Journal of Chemical Physics, 1997, 106, 8196-8203.	3.0	7
492	Structural Transformations of Ice at High Pressures via Molecular Dynamics Simulations II. Molecular Simulation, 1997, 18, 395-406.	2.0	2
493	A simulation study of induced failure and recrystallization of a perfect MgO crystal under non-hydrostatic compression; application to melting in the diamond-anvil cell. American Mineralogist, 1997, 82, 441-451.	1.9	22
494	Molecular Dynamics Simulation of Materio-Thermo-Mechanical Fields in the Melting/Solidification Process.. Nihon Kikai Gakkai Ronbunshu, A Hen/Transactions of the Japan Society of Mechanical Engineers, Part A, 1997, 63, 2135-2141.	0.2	1
495	Atomic Diffusion near Al Grain Boundary. (Molecular Dynamics Analysis Based on Effective-Medium) Tj ETQq0 0 0 rgBT /Overlock 10 Tf 5 203-210.	0.4	2
496	Predicted Effects of Site-Specific Aluminum Substitution on the Framework Geometry and Unit Cell Dimensions of Zeolite ZSM-5 Materialsâ€. Journal of Physical Chemistry B, 1997, 101, 9943-9950.	2.6	42
497	Structure and Dynamics of Zeolites Investigated by Molecular Dynamics. Chemical Reviews, 1997, 97, 2845-2878.	47.7	250
498	Structural Transformations of Ice at Normal and High Pressures via Molecular Dynamics Simulations. Journal of Physical Chemistry B, 1997, 101, 6293-6300.	2.6	9
499	Simulation of a Protein Crystal at Constant Pressure. Journal of Physical Chemistry B, 1997, 101, 2105-2108.	2.6	14
500	Origins of Solvation Forces in Confined Films. Journal of Physical Chemistry B, 1997, 101, 4013-4023.	2.6	125
501	Structure and solvation forces in confined films: Linear and branched alkanes. Journal of Chemical Physics, 1997, 106, 4309-4318.	3.0	202
502	Local structure analysis of the hard-disk fluid near melting. Physical Review E, 1997, 55, 6855-6859.	2.1	47
503	Temperature dependence of the elastic constants of Ni: reliability of EAM in predicting thermal properties. Modelling and Simulation in Materials Science and Engineering, 1997, 5, 337-346.	2.0	34
504	Study of copper precipitates in $\hat{1}\pm$ -iron by computer simulation. Philosophical Magazine A: Physics of Condensed Matter, Structure, Defects and Mechanical Properties, 1997, 75, 1097-1115.	0.6	37
505	Molecular Dynamics Methods. , 1997, , 83-115.		2
506	Atomic stress isobaric scaling for systems subjected to holonomic constraints. Journal of Chemical Physics, 1997, 106, 195-199.	3.0	31
507	Metric tensor as the dynamical variable for variable-cell-shape molecular dynamics. Physical Review B, 1997, 55, 8733-8742.	3.2	167
508	Core effects in dislocation intersection. Scripta Materialia, 1997, 36, 707-712.	5.2	14

#	ARTICLE	IF	CITATIONS
509	Strong relaxations at the Cr <sub>2</sub> O <sub>3</sub> (0001) surface as determined via low-energy electron diffraction and molecular dynamics simulations. Surface Science, 1997, 372, L291-L297.	1.9	140
510	A molecular dynamics study of MgO (111) slabs. Surface Science, 1997, 375, 374-384.	1.9	34
511	Lattice Dynamics of Martensitic Transformations Examined by Atomistic Simulations. European Physical Journal Special Topics, 1997, 07, C5-29-C5-34.	0.2	1
512	On the Thermodynamic Stability of Amorphous Intergranular Films in Covalent Materials. Journal of the American Ceramic Society, 1997, 80, 717-732.	3.8	72
513	Unifying two criteria of Born: Elastic instability and melting of homogeneous crystals. Physica A: Statistical Mechanics and Its Applications, 1997, 240, 396-403.	2.6	70
514	A molecular dynamics study of nickel vapor deposition: Temperature, incident angle, and adatom energy effects. Acta Materialia, 1997, 45, 1513-1524.	7.9	82
515	Molecular-Dynamics Method for the Simulation of Grain-Boundary Migration. Journal of Materials Science, 1997, 5, 245-262.	1.2	142
516	The analysis of dynamic simulations of polyethylene using the methods of "histograms and cumulants"™. Polymer, 1997, 38, 4769-4772.	3.8	2
517	Computer simulation of vacancy and interstitial clusters in bcc and fcc metals. Journal of Nuclear Materials, 1997, 251, 34-48.	2.7	66
518	Defect production and annealing kinetics in elemental metals and semiconductors. Journal of Nuclear Materials, 1997, 251, 13-33.	2.7	38
519	Local chain dynamics of a model polycarbonate near glass transition temperature: A molecular dynamics simulation. Macromolecular Theory and Simulations, 1997, 6, 83-102.	1.4	54
520	Use of test particle calculations for the derivation of van der Waals parameters used in force fields. Journal of Computational Chemistry, 1997, 18, 211-220.	3.3	17
521	Parallel short-range molecular dynamics using the "dhara" runtime system. Computer Physics Communications, 1997, 102, 28-43.	7.5	21
522	Dynamic-domain-decomposition parallel molecular dynamics. Computer Physics Communications, 1997, 102, 44-58.	7.5	15
523	The problem of the detaching shell in the shell model potential for oxides. Chemical Physics Letters, 1998, 289, 211-218.	2.6	5
524	Does salt increase the magnitude of the hydrophobic effect? A computer simulation study. Chemical Physics Letters, 1998, 296, 459-465.	2.6	33
525	Title is missing!. Journal of Computer-Aided Materials Design, 1998, 5, 243-264.	0.7	9
526	Molecular-Dynamics Simulation of Grain-Boundary Diffusion Creep. Journal of Materials Science, 1998, 6, 205-212.	1.2	88

#	ARTICLE	IF	CITATIONS
527	On the nucleation and growth of voids at high strain-rates. Journal of Computer-Aided Materials Design, 1998, 5, 193-206.	0.7	98
528	Segregation of niobium solute in nickel toward grain boundaries and free surfaces. Journal of Phase Equilibria and Diffusion, 1998, 19, 503-512.	0.3	3
529	Crystal Structure. , 0, , 295-344.		5
530	Melting of corundum using conventional and two-phase molecular dynamic simulation method. Physics and Chemistry of Minerals, 1998, 25, 138-141.	0.8	53
531	Atomistic modeling of finite-temperature properties of crystalline $\beta$ -SiC. Journal of Nuclear Materials, 1998, 255, 139-152.	2.7	244
532	Polyethylene (PEHD)/polypropylene (iPP) blends: mechanical properties, structure and morphology. Polymer, 1998, 39, 5283-5291.	3.8	25
533	Extended molecular dynamics scheme for crystals with fully relaxed size and shape. Solid State Communications, 1998, 105, 671-674.	1.9	2
534	The COMPASS force field: parameterization and validation for phosphazenes. Computational and Theoretical Polymer Science, 1998, 8, 229-246.	1.1	1,186
535	Selection of damage parameter "Art or science?". Mechanics of Materials, 1998, 28, 165-179.	3.2	39
536	Oxide ion diffusion along grain boundaries in zirconia: A molecular dynamics study. Solid State Ionics, 1998, 113-115, 311-318.	2.7	48
537	Molecular dynamics simulation of POPC at low hydration near the liquid crystal phase transition. Biochimie, 1998, 80, 415-419.	2.6	13
538	Computer Simulation of Crystallization from Solution. Journal of the American Chemical Society, 1998, 120, 9600-9604.	13.7	125
539	Computer simulations of martensitic transformations in NiAl alloys. Computational Materials Science, 1998, 10, 10-15.	3.0	21
540	Toward multiscale modelling: the role of atomistic simulations in the analysis of Si and SiC under hydrostatic compression. Journal of Alloys and Compounds, 1998, 279, 70-74.	5.5	7
541	Computer simulation of the effect of salt on the hydrophobic effect. Journal of the Chemical Society, Faraday Transactions, 1998, 94, 3549-3559.	1.7	32
542	Amorphous-crystal interface in silicon: A tight-binding simulation. Physical Review B, 1998, 58, 4579-4583.	3.2	69
543	Breathing shell model in molecular dynamics simulation: Application to MgO and CaO. Journal of Chemical Physics, 1998, 108, 3304-3309.	3.0	42
544	Molecular Dynamics Study on Electrostatic Properties of a Lipid Bilayer: Polarization, Electrostatic Potential, and the Effects on Structure and Dynamics of Water near the Interface. Journal of Physical Chemistry B, 1998, 102, 6647-6654.	2.6	54

#	ARTICLE	IF	CITATIONS
545	Variable-cell-shape-based structural optimization applied to calcium nitrides. <i>Physical Review B</i> , 1998, 57, 7615-7620.	3.2	32
546	Defect production, annealing kinetics and damage evolution in $\alpha$ -Fe: An atomic-scale computer simulation. <i>Philosophical Magazine A: Physics of Condensed Matter, Structure, Defects and Mechanical Properties</i> , 1998, 78, 995-1019.	0.6	275
547	Atomistic simulations of the vapor deposition of Ni/Cu/Ni multilayers: The effects of adatom incident energy. <i>Journal of Applied Physics</i> , 1998, 84, 2301-2315.	2.5	125
548	COMPASS: An ab Initio Force-Field Optimized for Condensed-Phase Applications Overview with Details on Alkane and Benzene Compounds. <i>Journal of Physical Chemistry B</i> , 1998, 102, 7338-7364.	2.6	4,882
549	Interatomic potential for silicon defects and disordered phases. <i>Physical Review B</i> , 1998, 58, 2539-2550.	3.2	406
550	Defect-unbinding transitions and inherent structures in two dimensions. <i>Physical Review E</i> , 1998, 58, 5748-5756.	2.1	18
551	Dynamics of viscoplastic deformation in amorphous solids. <i>Physical Review E</i> , 1998, 57, 7192-7205.	2.1	1,749
552	Comparison between the glass transition temperatures of the two PMMA tacticities: A molecular dynamics simulation point of view. <i>Macromolecular Symposia</i> , 1998, 133, 21-32.	0.7	62
553	Plastic behavior of nanophase metals studied by molecular dynamics. <i>Physical Review B</i> , 1998, 58, 11246-11251.	3.2	163
554	Melting and liquid structure of aluminum oxide using a molecular-dynamics simulation. <i>Physical Review E</i> , 1998, 57, 1673-1676.	2.1	54
555	Martensite-austenite transition and phonon dispersion curves of Fe <sub>1-x</sub> Ni <sub>x</sub> studied by molecular-dynamics simulations. <i>Physical Review B</i> , 1998, 57, 5140-5147.	3.2	142
556	Construction of an n-body potential and molecular-dynamics study of interfacial reaction in the Ni/Mo bilayer. <i>Europhysics Letters</i> , 1998, 43, 416-421.	2.0	7
557	Monte Carlo calculations of the hydrostatic compression of hexahydro-1,3,5-trinitro-1,3,5-triazine and 1,2-octahydro-1,3,5,7-tetranitro-1,3,5,7-tetrazocine. <i>Journal of Applied Physics</i> , 1998, 83, 4142-4145.	2.5	37
558	Structure formation during the crystallization induction period of a short chain-molecule system: A molecular dynamics study. <i>Journal of Chemical Physics</i> , 1998, 109, 5614-5621.	3.0	80
559	Computer-simulation study of high-temperature phase stability in iron. <i>Physical Review B</i> , 1998, 57, 755-763.	3.2	33
560	Quartz family of silica polymorphs: Comparative simulation study of quartz, moganite, and orthorhombic silica, and their phase transformations. <i>Physical Review B</i> , 1998, 57, 5639-5646.	3.2	28
561	Multiphonon effects in the one-phonon cross section of Al. <i>Physical Review B</i> , 1998, 58, 5429-5434.	3.2	4
562	Elastic constants of silicon using Monte Carlo simulations. <i>Physical Review B</i> , 1998, 58, 6019-6025.	3.2	29

#	ARTICLE	IF	CITATIONS
563	Effect of temperature and hydration on protein fluctuations: Molecular dynamics simulation of Cu, Zn superoxide dismutase at six different temperatures. Comparison with neutron scattering data. Journal of Chemical Physics, 1998, 108, 6033-6041.	3.0	22
564	Solid-state amorphization in Ni/Mo multilayers studied with molecular-dynamics simulation. Physical Review B, 1998, 58, 14020-14030.	3.2	31
565	Simulation of martensitic microstructural evolution in zirconium. Physical Review B, 1998, 58, 11252-11257.	3.2	54
566	Coordinates scaling and multiple time step algorithms for simulation of solvated proteins in the NPT ensemble. Journal of Chemical Physics, 1998, 109, 5194-5202.	3.0	97
567	Analysis of Serial and Parallel Algorithms for Use in Molecular Dynamics.. International Journal of Modern Physics C, 1998, 09, 179-194.	1.7	3
568	Molecular Modelling of the Mechanism of Action of Borate Retarders on Hydrating Cements at High Temperature. Molecular Simulation, 1998, 20, 331-356.	2.0	26
569	Diffusion-limited and asymmetric growth of amorphous layer in Ni/Zr bilayer upon annealing. Journal of Materials Research, 1998, 13, 1712-1716.	2.6	5
570	Molecular Dynamics Study on Grain Boundary Diffusion in Aluminum under Hydrostatic Stress.. JSME International Journal Series A-Solid Mechanics and Material Engineering, 1998, 41, 10-15.	0.4	5
571	Nonlocal Elastic Constants of Centrosymmetric Homogeneous Lattice Structure and Inhomogenous One.. JSME International Journal Series A-Solid Mechanics and Material Engineering, 1998, 41, 547-553.	0.4	1
572	Atomistic Aspects of Fracture Modelling in the Framework of Continuum Mechanics. Materials Research Society Symposia Proceedings, 1998, 538, 441.	0.1	1
573	Simulation of Void Growth at High Strain-Rate. Materials Research Society Symposia Proceedings, 1998, 539, 257.	0.1	8
574	Pressure Induced Structural Transformations in Nanocluster Assembled Gallium Arsenide. Materials Research Society Symposia Proceedings, 1998, 536, 545.	0.1	2
575	Computer simulation of pressure-induced structural transitions in MgO [001] tilt grain boundaries. American Mineralogist, 1999, 84, 138-143.	1.9	13
576	Experimental and Theoretical Studies on Composition Limits of Metallic Glass Formation in the Ni-Mo System. Chinese Physics Letters, 1999, 16, 667-669.	3.3	4
577	Thermal conductivity of model zeolites: molecular dynamics simulation study. Journal of Physics Condensed Matter, 1999, 11, 1261-1271.	1.8	26
578	Optimized Free-Energy Evaluation Using a Single Reversible-Scaling Simulation. Physical Review Letters, 1999, 83, 3973-3977.	7.8	100
579	Molecular dynamics simulation with reversible heat addition. Physical Review E, 1999, 59, R44-R47.	2.1	2
580	Morse Stretch Potential Charge Equilibrium Force Field for Ceramics: Application to the Quartz-Stishovite Phase Transition and to Silica Glass. Physical Review Letters, 1999, 82, 1708-1711.	7.8	173

#	ARTICLE	IF	CITATIONS
581	Variable-curvature-slab molecular dynamics as a method to determine surface stress. Physical Review B, 1999, 59, 7687-7696.	3.2	15
582	Correct microcanonical ensemble in molecular dynamics. Physical Review E, 1999, 59, 4781-4785.	2.1	32
583	Molecular-dynamics study of ductile and brittle fracture in model noncrystalline solids. Physical Review B, 1999, 60, 7062-7070.	3.2	172
584	Molecular Dynamics Machine: Special-Purpose Computer for Molecular Dynamics Simulations. Molecular Simulation, 1999, 21, 401-415.	2.0	73
585	Molecular-dynamics simulations of glass formation and crystallization in binary liquid metals: $\text{Cu-Ag}$ and $\text{Cu-Ni}$ . Physical Review B, 1999, 59, 3527-3533.	3.2	252
586	Do cylinders exhibit a cubatic phase?. Journal of Chemical Physics, 1999, 110, 11652-11659.	3.0	59
587	Glass-forming ability determined by the atomic interaction potential for the $\text{Ni-Mo}$ system. Physical Review B, 1999, 59, 13521-13524.	3.2	22
588	Molecular-dynamics study of melting on the shock Hugoniot of $\text{Al}$ . Physical Review B, 1999, 59, 329-333.	3.2	27
589	THE ORIENTATIONAL AND STRUCTURAL PROPERTIES OF $\text{N}_2$ and $\text{N}_2\text{-AR}$ SOLIDS AT HIGH PRESSURE. International Journal of Modern Physics C, 1999, 10, 445-453.	1.7	4
590	Excess energy of grain-boundary trijunctions: an atomistic simulation study. Acta Materialia, 1999, 47, 2821-2829.	7.9	66
591	Statistical models of brittle deformation Part I: introduction. International Journal of Plasticity, 1999, 15, 401-426.	8.8	13
592	Parallel molecular dynamics simulation: Implementation of PVM for a lipid membrane. Computer Physics Communications, 1999, 116, 295-310.	7.5	9
593	Co nanoprecipitates formed in $\text{Ag}$ upon ion implantation: their lattice dynamical properties. , 1999, 120/121, 291-296.		4
594	Molecular dynamics simulation of boundary lubricated interfaces. Journal of Computer-Aided Materials Design, 1999, 6, 69-80.	0.7	8
595	Molecular dynamics study of solid state interfacial reaction in the $\text{Ni-Mo}$ system. Journal of Computer-Aided Materials Design, 1999, 6, 103-116.	0.7	7
596	Title is missing!. Journal of Materials Science, 1999, 7, 15-31.	1.2	17
597	Diffusion and clustering on the titanium (0001) surface. Journal of Computer-Aided Materials Design, 1999, 6, 311-321.	0.7	14
598	Many-Body Effects in fcc Metals: A Lennard-Jones Embedded-Atom Potential. Physical Review Letters, 1999, 83, 2592-2595.	7.8	77



#	ARTICLE	IF	CITATIONS
599	Simulation of threshold displacements in NiAl. Nuclear Instruments & Methods in Physics Research B, 1999, 153, 99-104.	1.4	0
600	The primary damage state and its evolution over multiple length and time scales: Recent atomic-scale computer simulation studies. Radiation Effects and Defects in Solids, 1999, 148, 95-126.	1.2	14
601	Competing plastic deformation mechanisms in nanophase metals. Physical Review B, 1999, 60, 22-25.	3.2	319
602	Tight-binding Molecular Dynamics Simulation of Uniaxial Tensile Strength of Diamond. Molecular Simulation, 1999, 23, 143-150.	2.0	3
603	Structure and Mechanical Behavior of Bulk Nanocrystalline Materials. MRS Bulletin, 1999, 24, 44-53.	3.5	347
604	Lattice dynamics of Co nanoparticles in Ag. Scripta Materialia, 1999, 12, 299-302.	0.5	2
605	Solid-state amorphization of Ni/Zr bilayer through diffusion-limited-reaction observed by molecular-dynamics simulation. Computational Materials Science, 1999, 14, 163-168.	3.0	4
606	Molecular dynamics simulation for the crystal structure of synthetic sugar-based bolaamphiphiles. Computational Materials Science, 1999, 14, 267-276.	3.0	6
607	Microscopic analysis of the laser-induced femtosecond graphitization of diamond. Physical Review B, 1999, 60, R3701-R3704.	3.2	93
608	Hyperthermal vapor deposition of copper: athermal and biased diffusion effects. Surface Science, 1999, 431, 42-57.	1.9	64
609	Computer simulation of the Mg <sub>2</sub> SiO <sub>4</sub> phases with application to the 410 km seismic discontinuity. Physics of the Earth and Planetary Interiors, 1999, 116, 9-18.	1.9	23
610	The Riddle of Resorcinol Crystal Growth Revisited: Molecular Dynamics Simulations of Resorcinol Crystal-Water Interface. Journal of the American Chemical Society, 1999, 121, 8583-8591.	13.7	53
611	Structure and Electronic Properties of Ca-Doped CeO <sub>2</sub> and Implications on Catalytic Activity: An Experimental and Theoretical Study. Journal of Physical Chemistry B, 1999, 103, 7627-7636.	2.6	65
612	The change in phase behaviour and orientational order of solid N <sub>2</sub> at high pressure under the influence of Ar: a simulation study. Molecular Physics, 1999, 96, 1613-1622.	1.7	3
613	Molecular Dynamics Studies of the Phase Transitions of Homopolymers of p-Hydroxybenzoic Acid. Journal of Physical Chemistry B, 1999, 103, 7111-7121.	2.6	2
614	Phase diagram of MgO from density-functional theory and molecular-dynamics simulations. Physical Review B, 1999, 60, 15084-15093.	3.2	77
615	Free Energy Change of Amorphous Polymer Structure under Uniaxial Tension.. Nihon Kikai Gakkai Ronbunshu, A Hen/Transactions of the Japan Society of Mechanical Engineers, Part A, 1999, 65, 87-92.	0.2	2
616	Side Chain Dynamics in Poly(ethyl acrylate) Studied by Molecular Dynamics Simulation. Bulletin of the Chemical Society of Japan, 1999, 72, 1203-1211.	3.2	4



#	ARTICLE	IF	CITATIONS
617	Modeling of the Dislocation Formation at Pores and Inclusions under Thermo-Mechanical Shear Loads. Materials Research Society Symposia Proceedings, 1999, 578, 273.	0.1	3
618	Ion Exchange in High-Level Nuclear Waste Encapsulation: Atomistic Modeling of Equilibrium Coefficients and Isotherms. Materials Research Society Symposia Proceedings, 1999, 556, 1285.	0.1	1
619	Introduction to Molecular Dynamics.. Nippon Gomu Kyokaishi, 1999, 72, 632-638.	0.0	0
620	Molecular Dynamics Simulation in Investigation on Material Strength.. Nippon Gomu Kyokaishi, 1999, 72, 639-646.	0.0	0
621	Molecular Dynamics Simulation of Hydrogen-Induced Amorphization: Softening Effect by Incorporation of Hydrogen. Materials Transactions, JIM, 1999, 40, 1274-1280.	0.9	5
622	Deformation Mechanism of Diamond-Like Carbon. 1st Report. Change of Bonding Form Under Uniaxial Loading.. Nihon Kikai Gakkai Ronbunshu, A Hen/Transactions of the Japan Society of Mechanical Engineers, Part A, 2000, 66, 1794-1799.	0.2	2
623	Molecular modeling of the structure and dynamics of the interlayer and surface species of mixed-metal layered hydroxides: Chloride and water in hydrocalumite (Friedel's salt). American Mineralogist, 2000, 85, 1046-1052.	1.9	101
624	Molecular Dynamics Simulation of Nano-Sized Crystallization During Plastic Deformation in an Amorphous Metal. Materials Research Society Symposia Proceedings, 2000, 634, 191.	0.1	1
625	Atomic Scale Modelling of Supported and Assembled Nanoparticles. Materials Research Society Symposia Proceedings, 2000, 634, 821.	0.1	0
626	Calculation of Glass-Forming Ability in the Ni-Zr and Ni-Ti Systems from Interatomic Potentials. Materials Research Society Symposia Proceedings, 2000, 644, 421.	0.1	0
627	Moldy: a portable molecular dynamics simulation program for serial and parallel computers. Computer Physics Communications, 2000, 126, 310-329.	7.5	328
628	The role of point defects in melting of solid He. Physica B: Condensed Matter, 2000, 280, 142-145.	2.7	1
629	Irradiation induced amorphization in metallic multilayers and calculation of glass-forming ability from atomistic potential in the binary metal systems. Materials Science and Engineering Reports, 2000, 29, 1-48.	31.8	206
630	Towards first-principles modelling of the mechanical properties of oriented poly(ethylene) Tj ETQq1 1 0.784314 rgBT./Overlock 10 Tf 50	1.1	11
631	Computer simulation of structural changes in the ferroelectric phase transition of vinylidene fluoride-trifluoroethylene copolymers. Computational and Theoretical Polymer Science, 2000, 10, 323-333.	1.1	28
632	New advances in chemistry and materials science with CPMD and parallel computing. Parallel Computing, 2000, 26, 819-842.	2.1	146
633	Structures, solvation forces and shear of molecular films in a rough nano-confinement. Tribology Letters, 2000, 9, 3-13.	2.6	136
634	Atomistic studies of stress effects on self-interstitial diffusion in $\alpha$ -titanium*. Journal of Computer-Aided Materials Design, 2000, 7, 97-110.	0.7	10

#	ARTICLE	IF	CITATIONS
635	Atomistic model of plutonium. Physical Review B, 2000, 62, 15532-15537.	3.2	87
636	Role of point defects in martensitic transformations. Russian Physics Journal, 2000, 43, 493-497.	0.4	2
637	Phase transformation of poly(trimethylene terephthalate) in crystalline state: An atomistic modeling approach. Fibers and Polymers, 2000, 1, 18-24.	2.1	10
638	The Role Played By Two Parallel Free Surfaces In The Deformation Mechanism Of Nano-crystalline Metals: A Molecular Dynamics Simulation. Materials Research Society Symposia Proceedings, 2000, 634, 141.	0.1	1
639	Solid-state amorphization in Ni/Nb multilayers studied by molecular-dynamics simulation together with experiments. Journal of Physics Condensed Matter, 2000, 12, 6991-7004.	1.8	5
640	Structural Stability and Amorphization Transition in the Ni-Ti System Studied by Molecular Dynamics Simulation with an n-Body Potential. Journal of the Physical Society of Japan, 2000, 69, 2923-2937.	1.6	13
641	The MD simulation of the equation of state of MgO: Application as a pressure calibration standard at high temperature and high pressure. American Mineralogist, 2000, 85, 312-316.	1.9	124
642	Linear and nonlinear elasticity in atomistic simulations. Modelling and Simulation in Materials Science and Engineering, 2000, 8, 357-375.	2.0	3
643	Molecular Dynamics Simulation of Crystallization in an Amorphous Metal during Shear Deformation. Japanese Journal of Applied Physics, 2000, 39, L611-L613.	1.5	16
644	Monte Carlo simulations of the distribution of Ar and other noble-gas atoms in high-pressure solid N <sub>2</sub> . Physical Review B, 2000, 61, 9327-9335.	3.2	4
645	Simulations of the nucleation of AgBr from solution. Journal of Chemical Physics, 2000, 113, 6276-6284.	3.0	62
646	Glass-forming range of the Ni-Mo system derived from molecular dynamics simulation and generalized Lindemann criterion. Journal of Applied Physics, 2000, 87, 4147-4152.	2.5	20
647	Structure and relaxation in liquid and amorphous selenium. Physical Review B, 2000, 62, 3709-3716.	3.2	69
648	Thermal activation of shear modulus instabilities in pressure-induced bcc to hcp transitions. Physical Review B, 2000, 62, 13799-13802.	3.2	14
649	Molecular Dynamics Simulation of a Glissile Dislocation Interface Propagating a Martensitic Transformation. Physical Review Letters, 2000, 84, 5784-5787.	7.8	4
650	Interfacial reaction, amorphization transition, and associated elastic instability studied by molecular dynamics simulations in the Ni-Ta system. Physical Review B, 2000, 61, 9345-9355.	3.2	22
651	Mechanism for Negative Poisson Ratios over the $\beta_1$ - $\beta_2$ Transition of Cristobalite, SiO <sub>2</sub> : A Molecular-Dynamics Study. Physical Review Letters, 2000, 84, 5548-5551.	7.8	145
652	Conformational transition behavior around glass transition temperature. Journal of Chemical Physics, 2000, 112, 2016-2020.	3.0	23

#	ARTICLE	IF	CITATIONS
653	Deposition of Au clusters on Au(111) surfaces. <i>Atomic-scale modeling</i> . Physical Review B, 2000, 62, 2825-2834.	3.2	130
654	Bain transformation in $\text{Cu}_{1-x}\text{Pd}_x$ ( $x \sim 1/4$ to 0.5) alloys: An embedded-atom study. Physical Review B, 2000, 61, 24-27.	3.2	16
655	Mechanism for the $\alpha\text{-Al}_2\text{O}_3$ to the $\gamma\text{-Al}_2\text{O}_3$ transition and the stability of $\gamma\text{-Al}_2\text{O}_3$ under volume expansion. Physical Review B, 2000, 61, 3131-3134.	3.2	12
656	Growth and lattice dynamics of Co nanoparticles embedded in Ag: A combined molecular-dynamics simulation and Mössbauer study. Physical Review B, 2000, 62, 5117-5128.	3.2	64
657	Atomistic Studies of Plasticity in Nanophase Metals. Materials Research Society Symposia Proceedings, 2000, 634, 551.	0.1	5
658	Comparative study of quasiharmonic lattice dynamics, molecular dynamics and Debye model applied to $\text{MgSiO}_3$ perovskite. Physics of the Earth and Planetary Interiors, 2000, 122, 277-288.	1.9	108
659	Atomic structure and physical properties of $\text{Ni}_{40}\text{Nb}_{60}$ amorphous alloys determined by an n-body potential. Journal of Non-Crystalline Solids, 2000, 261, 137-145.	3.1	25
660	Molecular Dynamics Simulation of Water Mobility in Magnesium-Smectite Hydrates. Journal of the American Chemical Society, 2000, 122, 11459-11464.	13.7	100
661	Lattice stability of some Ni-Ti alloy phases versus their chemical composition and disordering. Journal of Physics Condensed Matter, 2000, 12, L53-L60.	1.8	92
662	Grain-boundary structures in polycrystalline metals at the nanoscale. Physical Review B, 2000, 62, 831-838.	3.2	333
663	Structural and thermodynamic properties of elemental and bimetallic nanoclusters: an atomic scale study. Journal of Physics Condensed Matter, 2000, 12, 6735-6754.	1.8	53
664	Large deformation and amorphization of Ni nanowires under uniaxial strain: A molecular dynamics study. Physical Review B, 2000, 62, 16950-16955.	3.2	190
665	Molecular Dynamics Study on Mechanical Properties and Fracture in Amorphous Metal. AIAA Journal, 2000, 38, 695-701.	2.6	25
666	Origin of asymmetric growth during solid-state amorphization studied with molecular-dynamics simulation. Journal of Applied Physics, 2000, 87, 7696-7701.	2.5	2
667	Monte Carlo calculations of the elastic moduli and pressure-volume-temperature equation of state for hexahydro-1,3,5-trinitro-1,3,5-triazine. Journal of Applied Physics, 2000, 88, 88-95.	2.5	59
668	Molecular-dynamics simulation of thermal stress at the (100) diamond/substrate interface: Effect of film continuity. Physical Review B, 2000, 62, 2920-2936.	3.2	23
669	Atomistic simulations of solid-phase epitaxial growth in silicon. Physical Review B, 2000, 61, 6696-6700.	3.2	64
670	Atomistic simulation of shear in a martensitic twinned microstructure. Physical Review B, 2000, 62, 5427-5434.	3.2	51

#	ARTICLE	IF	CITATIONS
671	High-pressure phases of group IV and III-V semiconductors. Reports on Progress in Physics, 2001, 64, 483-516.	20.1	230
672	Grain-boundary sliding in nanocrystalline fcc metals. Physical Review B, 2001, 64, .	3.2	498
673	Simulation of polyethylene oxide: Improved structure using better models for hydrogen and flexible walls. Journal of Chemical Physics, 2001, 115, 3957-3966.	3.0	17
674	Representation of mechanical loads in molecular dynamics simulations. Physical Review B, 2001, 65, .	3.2	42
675	Molecular Modeling of the Structure and Energetics of Hydrotalcite Hydration. Chemistry of Materials, 2001, 13, 145-150.	6.7	126
676	Dynamics of hydration in hen egg white lysozyme. Journal of Molecular Biology, 2001, 311, 409-419.	4.2	78
677	First Principles Theory of Mantle and Core Phases. Reviews in Mineralogy and Geochemistry, 2001, 42, 319-343.	4.8	6
678	A new constant-pressure ab initio/classical molecular dynamics method: simulation of pressure-induced amorphization in a Si35H36 cluster. Computational Materials Science, 2001, 20, 293-299.	3.0	31
679	Bent surface free energy differences from simulation. Surface Science, 2001, 482-485, 1331-1336.	1.9	2
680	Vibrational density of states of selenium through the glass transition. Journal of Chemical Physics, 2001, 114, 3236-3242.	3.0	7
681	Metric-tensor flexible-cell algorithm for isothermalâ€“isobaric molecular dynamics simulations. Journal of Chemical Physics, 2001, 115, 10282.	3.0	74
682	Molecular Dynamics Simulation of Liquid H2O, MeOH, EtOH, Si(OMe)4, and Si(OEt)4, as a Function of Temperature and Pressure. Journal of Physical Chemistry A, 2001, 105, 1909-1925.	2.5	35
683	First-principles studies of the stability of Zintl ions in alkali-tin alloys: II. Liquid alloys. Journal of Physics Condensed Matter, 2001, 13, 981-1021.	1.8	14
684	Simulation of Hydrated BPTI at High Pressure:â€“ Changes in Hydrogen Bonding and Its Relation with NMR Experiments. Journal of Physical Chemistry B, 2001, 105, 711-714.	2.6	33
685	Polarization reversal in a perovskite ferroelectric by molecular-dynamics simulation. Applied Physics Letters, 2001, 79, 4417-4419.	3.3	23
686	Intermixing of a system with positive heat of mixing at high strain rates. Physical Review B, 2001, 63, .	3.2	13
687	Atomic Assembly of Giant Magnetoresistive Multilayers. Materials Research Society Symposia Proceedings, 2001, 672, 1.	0.1	6
688	Self-interstitial Diffusion in Î±-Zirconium. Materials Research Society Symposia Proceedings, 2001, 677, 7311.	0.1	0

#	ARTICLE	IF	CITATIONS
689	Dislocation Nucleation and Propagation During Deposition of Cubic Metal Thin Films. Materials Research Society Symposia Proceedings, 2001, 677, 7321.	0.1	0
690	First principles multiscale modeling of physico-chemical aspects of tribology. Tribology Series, 2001, , 15-33.	0.1	1
691	Molecular dynamics interpretation of structural changes in quartz. Physics and Chemistry of Minerals, 2001, 28, 365-376.	0.8	33
692	GROMACS 3.0: a package for molecular simulation and trajectory analysis. Journal of Molecular Modeling, 2001, 7, 306-317.	1.8	6,085
693	Model of quasi-ductile deformations that bridges the scales. Theoretical and Applied Fracture Mechanics, 2001, 37, 167-182.	4.7	2
694	Computer simulation of structure and ferroelectric phase transition of vinylidene fluoride copolymers. Polymer, 2001, 42, 3409-3417.	3.8	18
695	Computer simulation of structure and ferroelectric phase transition of vinylidene fluoride copolymers. 5. Influence of orientational disorder of dipole moments and domain walls on phase transitional behavior. Polymer, 2001, 42, 9671-9678.	3.8	14
696	Molecular dynamics modeling of irradiation damage in pure and uranium-doped zircon. Journal of Nuclear Materials, 2001, 295, 167-178.	2.7	59
697	Atomic scale structure of sputtered metal multilayers. Acta Materialia, 2001, 49, 4005-4015.	7.9	664
698	Point defect interaction with dislocations in silicon. Materials Science & Engineering A: Structural Materials: Properties, Microstructure and Processing, 2001, 309-310, 129-132.	5.6	9
699	Strategies for multiscale modeling and simulation of organic materials: polymers and biopolymers. Computational and Theoretical Polymer Science, 2001, 11, 329-343.	1.1	36
700	Prediction of polyimide materials with high glass-transition temperatures. Journal of Polymer Science, Part B: Polymer Physics, 2001, 39, 2243-2251.	2.1	22
701	Computer simulation of structure and ferroelectric phase transition of vinylidene fluoride copolymers. IV. The factors governing the ferroelectric phase transition of VDF-TrFE copolymers. Journal of Polymer Science, Part B: Polymer Physics, 2001, 39, 689-702.	2.1	18
702	Atomic Computer Simulation: Large Scale Calculations of Defect Properties by Empirical Potentials. Physica Status Solidi (B): Basic Research, 2001, 227, 151-175.	1.5	1
703	Critical Solid Solubility of the Ni-Ti System Determined by Molecular Dynamics Simulation and Ion Mixing. Physica Status Solidi (B): Basic Research, 2001, 227, 503-514.	1.5	10
704	MD simulations of a doped ceria surface " very large surface ion motion. Chemical Physics Letters, 2001, 335, 517-523.	2.6	11
705	Molecular dynamics (MD) simulation of uniaxial tension of some single-crystal cubic metals at nanolevel. International Journal of Mechanical Sciences, 2001, 43, 2237-2260.	6.7	173
706	Solid-state crystal-to-amorphous transition in metal-metal multilayers and its thermodynamic and atomistic modelling. Advances in Physics, 2001, 50, 367-429.	14.4	118

#	ARTICLE	IF	CITATIONS
707	Application of Lattice Dynamics and Molecular Dynamics Techniques to Minerals and Their Surfaces. Reviews in Mineralogy and Geochemistry, 2001, 42, 63-82.	4.8	5
708	Molecular dynamics simulations to compute the bulk response of amorphous PMMA. Journal of Computer-Aided Materials Design, 2001, 8, 87-106.	0.7	31
709	Molecular dynamics simulations of HMX crystal polymorphs using a flexible molecule force field. Journal of Computer-Aided Materials Design, 2001, 8, 77-85.	0.7	102
710	Influence of Structural Defects on Martensitic Transformations in Systems with Low Elastic Moduli. Russian Physics Journal, 2001, 44, 151-161.	0.4	3
711	Condensed State Molecular Dynamics in Sorbitol and Maltitol: Mobility Gradients and Conformation Transitions. Molecular Simulation, 2001, 27, 243-265.	2.0	5
712	Glass-forming ability of the Ni-Zr and Ni-Ti systems determined by interatomic potentials. Journal of Materials Research, 2001, 16, 446-450.	2.6	11
713	Molecular Dynamics simulation of aqueous ZnCl <sub>2</sub> solutions. Molecular Physics, 2001, 99, 825-833.	1.7	37
714	Elastic constants of quantum solids by path integral simulations. Physical Review B, 2001, 63, .	3.2	19
715	Constant pressure molecular dynamics on a hypercylinder. Physical Review E, 2001, 64, 026112.	2.1	5
716	Ground-state structure of $\alpha$ -C <sub>3</sub> N <sub>4</sub> by first-principles calculations. Physical Review B, 2001, 64, .	3.2	3
717	Simulation of material properties below the Debye temperature: A path-integral molecular dynamics case study of quartz. Journal of Chemical Physics, 2001, 114, 6364-6370.	3.0	17
718	First principles molecular dynamics simulations of pressure-induced structural transformations in silicon clusters. Journal of Chemical Physics, 2001, 114, 5358-5365.	3.0	29
719	Atomistic simulations with slip boundary conditions. Physical Review B, 2001, 63, .	3.2	10
720	Nanoscale phase separation and local icosahedral order in amorphous alloys of immiscible elements. Physical Review B, 2001, 64, .	3.2	42
721	Fluctuations and thermodynamics properties of the constant shear strain ensemble. Journal of Chemical Physics, 2001, 114, 8769-8774.	3.0	15
722	Strain-induced structural phase transition of a Ni lattice through dissolving Ta solute atoms. Physical Review B, 2001, 63, .	3.2	6
723	Analysis of the elastic deformation of semicrystalline poly(trimethylene terephthalate) by the atomistic-continuum model. Journal of Chemical Physics, 2001, 114, 8159-8164.	3.0	10
724	Low-Frequency Vibrational Properties of Nanocrystalline Materials. Physical Review Letters, 2001, 87, 205501.	7.8	76

#	ARTICLE	IF	CITATIONS
725	Nodal Effects in Dislocation Mobility. Physical Review Letters, 2002, 89, 115501.	7.8	53
726	A molecular-dynamics simulation study of the influence of attractive dispersion interactions on the phase behavior of rigid bead-necklace molecules. Journal of Chemical Physics, 2002, 116, 9957-9963.	3.0	9
727	Influence of the quench rate and the pressure on the glass transition temperature in selenium. Journal of Chemical Physics, 2002, 117, 2814-2818.	3.0	19
729	Structural phase transformation in InSb: a molecular dynamics simulation. Physical Review B, 2002, 66, .	3.2	12
730	Molecular dynamics study of vibrational entropy in bcc and hcp zirconium. Physical Review B, 2002, 66, .	3.2	17
731	Atomic-scale modeling of cluster-assembled Ni <sub>3</sub> Al thin films. Physical Review B, 2002, 66, .	3.2	38
732	Atomistic modeling of solid-state amorphization in an immiscible Cu-Ta system. Physical Review B, 2002, 66, .	3.2	56
733	Flow state in molecular-dynamics-simulated deformed amorphous Ni <sub>0.5</sub> Zr <sub>0.5</sub> . Physical Review B, 2002, 66, .	3.2	21
734	Ferroelectric phase transitions and dynamical behavior in KNbO <sub>3</sub> /KTaO <sub>3</sub> superlattices by molecular-dynamics simulation. Journal of Applied Physics, 2002, 91, 3165-3171.	2.5	48
736	High-pressure behavior of bikitaite: An integrated theoretical and experimental approach. American Mineralogist, 2002, 87, 1415-1425.	1.9	56
737	Interfacial Reaction of W/Cu Examined by an n-body Potential through Molecular Dynamics Simulations. Japanese Journal of Applied Physics, 2002, 41, 4503-4508.	1.5	11
738	Instability of hcp structures in modified embedded atom method. Modelling and Simulation in Materials Science and Engineering, 2002, 10, 205-214.	2.0	10
739	Orientational phase transition between hexagonal solids in planar systems of hard cyclic pentamers and heptamers. Journal of Physics Condensed Matter, 2002, 14, 1261-1273.	1.8	15
741	Molecular Dynamics Simulations of HMX Crystal Polymorphs Using a Flexible Molecule Force Field. AIP Conference Proceedings, 2002, , .	0.4	5
742	Numerical Analysis of the Aggregate Structure of Ferrofluid under the Uniform Magnetic Fields. Study on the Mesoscopic System.. 880-02 Nihon Kikai Gakkai Ronbunshu Transactions of the Japan Society of Mechanical Engineers Series B B-hen, 2002, 68, 123-130.	0.2	0
743	Multiscale Modeling of Wave Propagation: FDTD/MD Hybrid Method. Materials Research Society Symposia Proceedings, 2002, 731, 471.	0.1	1
744	Molecular dynamics simulation of the pressure-induced phase transition in BaFCl. Radiation Effects and Defects in Solids, 2002, 157, 799-803.	1.2	2
745	Interlayer Structure and Dynamics of Cl <sup>-</sup> /LiAl <sub>2</sub> -Layered Double Hydroxide: <sup>35</sup> Cl NMR Observations and Molecular Dynamics Modeling. Chemistry of Materials, 2002, 14, 2078-2085.	6.7	54



#	ARTICLE	IF	CITATIONS
746	First-principles calculation of the piezoelectric tensor $d_{33}$ of $\text{AlN}$ nitrides. Applied Physics Letters, 2002, 80, 4145-4147.	3.3	125
747	Cooperative processes during plastic deformation in nanocrystalline fcc metals: A molecular dynamics simulation. Physical Review B, 2002, 66, .	3.2	153
748	Atomistic Aspects of Crack Propagation in Brittle Materials: Multimillion Atom Molecular Dynamics Simulations. Annual Review of Materials Research, 2002, 32, 377-400.	9.3	177
749	Synthesis of 3-spiroannulated hexahydro-6,8a-epoxyisoquinolines. Mendeleev Communications, 2002, 12, 32-33.	1.6	4
750	Atomistic model of gallium. Physical Review B, 2002, 66, .	3.2	56
751	Free-Energy Calculations in Materials Research. Annual Review of Materials Research, 2002, 32, 195-217.	9.3	104
752	Numerical evaluation of the exact phase diagram of an empirical Hamiltonian: Embedded atom model for the Au-Ni system. Physical Review B, 2002, 66, .	3.2	35
753	Cooling rate dependence of the glass transition temperature of polymer melts: Molecular dynamics study. Journal of Chemical Physics, 2002, 117, 7364-7372.	3.0	165
754	Development of transferable interaction models for water. III. Reparametrization of an all-atom polarizable rigid model (TTM2-R) from first principles. Journal of Chemical Physics, 2002, 116, 1500-1510.	3.0	173
755	Molecular dynamics simulation studies of atomic-level structures in rapidly quenched Ag-Cu nonequilibrium alloys. Physical Review B, 2002, 65, .	3.2	48
756	Molecular Simulation Approaches for Multiphase Polymer Systems. Advances in Polymer Science, 2002, , 1-51.	0.8	1
757	A molecular dynamics method for simulations in the canonical ensemble. Molecular Physics, 2002, 100, 191-198.	1.7	279
758	A new constant-pressure molecular dynamics method for finite systems. Journal of Physics Condensed Matter, 2002, 14, L487-L493.	1.8	28
759	Atomistic Simulation of the $\alpha$ -Relaxation in Crystalline Polyethylene. Macromolecules, 2002, 35, 4539-4549.	4.8	24
760	The role played by two parallel free surfaces in the deformation mechanism of nanocrystalline metals: A molecular dynamics simulation. Philosophical Magazine A: Physics of Condensed Matter, Structure, Defects and Mechanical Properties, 2002, 82, 1-15.	0.6	53
761	Molecular dynamics modeling of stishovite. Earth and Planetary Science Letters, 2002, 202, 147-157.	4.4	21
762	Amorphization of $\text{Ni-Al}$ alloys by fast quenching from the liquid state: a molecular dynamics study. Journal of Non-Crystalline Solids, 2002, 298, 60-66.	3.1	12
763	Atomic mechanism for dislocation emission from nanosized grain boundaries. Physical Review B, 2002, 66, .	3.2	385



#	ARTICLE	IF	CITATIONS
764	Correlation of lattice constant versus tungsten concentration of the Ni-based solid solution examined by molecular dynamics simulation. <i>Journal of Alloys and Compounds</i> , 2002, 337, 143-147.	5.5	30
765	Structural instability of uniaxially compressed $\alpha$ -quartz. <i>Computational Materials Science</i> , 2002, 23, 116-123.	3.0	6
766	Dislocation nucleation and propagation during thin film deposition under compression. <i>Computational Materials Science</i> , 2002, 23, 155-165.	3.0	17
767	Diffusion of clusters down aluminum islands. <i>Computational Materials Science</i> , 2002, 23, 85-94.	3.0	8
768	Order-Disorder Behavior in KNbO <sub>3</sub> and KNbO <sub>3</sub> /KTaO <sub>3</sub> Solid Solutions and Superlattices by Molecular-Dynamics Simulation. <i>AIP Conference Proceedings</i> , 2002, , .	0.4	1
769	Length scale effects in the simulation of deformation properties of nanocrystalline metals. <i>Scripta Materialia</i> , 2002, 47, 719-724.	5.2	95
770	Development of a strain induced planar film texture as revealed by molecular dynamics simulation. <i>Scripta Materialia</i> , 2002, 47, 677-682.	5.2	9
771	The competing crystalline and amorphous solid solutions in the Ag-Cu system. <i>Acta Materialia</i> , 2002, 50, 475-488.	7.9	100
772	On non-equilibrium grain boundaries and their effect on thermal and mechanical behaviour: a molecular dynamics computer simulation. <i>Acta Materialia</i> , 2002, 50, 3927-3939.	7.9	207
773	X-ray study and structure simulation of amorphous tungsten oxide. <i>Acta Crystallographica Section B: Structural Science</i> , 2002, 58, 576-586.	1.8	6
774	Ion association in concentrated NaCl brines from ambient to supercritical conditions: results from classical molecular dynamics simulations. <i>Geochemical Transactions</i> , 2002, 3, 1.	0.7	75
775	Theoretical description of the ultrafast ablation of diamond and graphite: dependence of thresholds on pulse duration. <i>Applied Surface Science</i> , 2002, 197-198, 107-113.	6.1	36
776	Laser ablation thresholds of silicon for different pulse durations: theory and experiment. <i>Applied Surface Science</i> , 2002, 197-198, 839-844.	6.1	124
777	Simulation of orientation of uniaxially stretched poly(vinyl phenol) by molecular dynamics. <i>Journal of Polymer Science, Part B: Polymer Physics</i> , 2002, 40, 1601-1625.	2.1	17
778	Molecular dynamics simulation of vanadium using an interatomic potential fitted to finite temperature properties. <i>Journal of Nuclear Materials</i> , 2002, 307-311, 1007-1010.	2.7	5
779	Energetic analysis of the two PMMA chain tacticities and PMA through molecular dynamics simulations. <i>Polymer</i> , 2002, 43, 4269-4275.	3.8	65
780	Glass transition temperature of low molecular weight poly(3-aminopropyl methyl siloxane). A molecular dynamics study. <i>Polymer</i> , 2002, 43, 6049-6055.	3.8	30
781	Mid-infrared optical properties of a polymer film: comparison between classical molecular simulations, spectrometry, and ellipsometry techniques. <i>Polymer</i> , 2002, 43, 6027-6035.	3.8	23

#	ARTICLE	IF	CITATIONS
782	Molecular modeling of the mobility of poly(allyl alcohol), PAA, and poly(vinyl alcohol), PVA. Polymer, 2002, 43, 5665-5677.	3.8	37
783	Dislocation processes in the deformation of nanocrystalline aluminium by molecular-dynamics simulation. Nature Materials, 2002, 1, 45-49.	27.5	865
784	A general-purpose coarse-grained molecular dynamics program. Computer Physics Communications, 2002, 145, 267-279.	7.5	126
785	Thermal evolution of cluster assembled $\text{Ni}_{3}\text{Al}$ materials modelled at the atomic scale. European Physical Journal D, 2003, 27, 231-237.	1.3	7
786	Methodological Issues in Lipid Bilayer Simulations. Journal of Physical Chemistry B, 2003, 107, 9424-9433.	2.6	337
787	A new empirical potential for simulating the formation of defects and their mobility in uranium dioxide. Philosophical Magazine, 2003, 83, 1533-1555.	1.6	158
788	Using the modified embedded-atom method to calculate the properties of Pu-Ga alloys. Jom, 2003, 55, 41-50.	1.9	38
789	Thermal stability of helium-vacancy clusters in iron. Nuclear Instruments & Methods in Physics Research B, 2003, 202, 76-81.	1.4	267
790	Anab initio force field for the cofactors of bacterial photosynthesis. Journal of Computational Chemistry, 2003, 24, 129-142.	3.3	79
791	SIA activity during irradiation of nanocrystalline Ni. Journal of Nuclear Materials, 2003, 323, 213-219.	2.7	32
792	Fast one-dimensional gas transport in molecular capillary embedded in polymer crystal. Chemical Physics Letters, 2003, 371, 217-222.	2.6	12
793	Reorientational dynamics of aromatic molecules clathrated in $\beta'$ form of crystalline syndiotactic polystyrene. Chemical Physics Letters, 2003, 371, 620-625.	2.6	25
794	Effect of tensile strain on adatom diffusion on Cu(111) surface. Surface Science, 2003, 545, 137-142.	1.9	8
795	Nanoscale molecular cavity in crystalline polymer membranes studied by molecular dynamics simulation. Polymer, 2003, 44, 3279-3289.	3.8	34
796	A molecular dynamics study on the role of localised lattice distortions in the formation of Ni-Zr metallic glasses. Materials Science & Engineering A: Structural Materials: Properties, Microstructure and Processing, 2003, 359, 52-61.	5.6	6
797	Dislocation-dislocation and dislocation-twin reactions in nanocrystalline Al by molecular dynamics simulation. Acta Materialia, 2003, 51, 4135-4147.	7.9	232
798	Stress induced crystallization of amorphous materials and mechanical properties of nanocrystalline materials: a molecular dynamics simulation study. Acta Materialia, 2003, 51, 6233-6240.	7.9	42
799	Metastable phase formation in an immiscible Cu-Ta system studied by ion-beam mixing, ab initio calculation, and molecular dynamics simulation. Acta Materialia, 2003, 51, 3885-3893.	7.9	17

#	ARTICLE	IF	CITATIONS
800	The Source of Helicity in Perfluorinated N-Alkanes. <i>Macromolecules</i> , 2003, 36, 5331-5341.	4.8	108
801	Multiscale modelling of nanomechanics and micromechanics: an overview. <i>Philosophical Magazine</i> , 2003, 83, 3475-3528.	1.6	145
802	Molecular Differences between Hydrocarbon and Fluorocarbon Surfactants at the CO <sub>2</sub> /Water Interface. <i>Journal of Physical Chemistry B</i> , 2003, 107, 10185-10192.	2.6	84
803	Elastic properties of two-dimensional hard disks in the close-packing limit. <i>Journal of Chemical Physics</i> , 2003, 119, 939-946.	3.0	23
804	Atomic positional disorder in fcc metal nanocrystalline grain boundaries. <i>Physical Review B</i> , 2003, 67, .	3.2	97
805	Atomistic simulation of dislocation emission in nanosized grain boundaries. <i>Philosophical Magazine</i> , 2003, 83, 3569-3575.	1.6	90
806	Improved simulation method for the calculation of the elastic constants of crystalline and amorphous systems using strain fluctuations. <i>Physical Review E</i> , 2003, 67, 011505.	2.1	30
807	Simulation and Modeling of the Rhodobacter sphaeroides Bacterial Reaction Center: A Structure and Interactions. <i>Journal of Physical Chemistry B</i> , 2003, 107, 1423-1431.	2.6	31
808	A Concurrent multiscale finite difference time domain/molecular dynamics method for bridging an elastic continuum to an atomic system. <i>Modelling and Simulation in Materials Science and Engineering</i> , 2003, 11, 487-501.	2.0	18
809	Molecular Dynamics Simulation of Conformational Change of Poly(Ala-Gly) from Silk I to Silk I <sup>TM</sup> in Relation to Fiber Formation Mechanism of Bombyx mori Silk Fibroin. <i>Macromolecules</i> , 2003, 36, 6766-6772.	4.8	51
810	Periodic image effects in dislocation modelling. <i>Philosophical Magazine</i> , 2003, 83, 539-567.	1.6	185
811	Dynamic properties of screw dislocations in Cu: A molecular dynamics study. <i>Physical Review B</i> , 2003, 67, .	3.2	46
812	Predicting Crystal Structures: The Parrinello-Rahman Method Revisited. <i>Physical Review Letters</i> , 2003, 90, 075503.	7.8	591
813	Maximum superheating and undercooling: Systematics, molecular dynamics simulations, and dynamic experiments. <i>Physical Review B</i> , 2003, 68, .	3.2	234
814	Membrane Protein Dynamics versus Environment: Simulations of OmpA in a Micelle and in a Bilayer. <i>Journal of Molecular Biology</i> , 2003, 329, 1035-1053.	4.2	130
815	The Implementation of Slab Geometry for Membrane-Channel Molecular Dynamics Simulations. <i>Biophysical Journal</i> , 2003, 85, 97-107.	0.5	76
816	Mixed Bilayer Containing Dipalmitoylphosphatidylcholine and Dipalmitoylphosphatidylserine: Lipid Complexation, Ion Binding, and Electrostatics. <i>Biophysical Journal</i> , 2003, 85, 3120-3131.	0.5	148
817	Structure of Sphingomyelin Bilayers: A Simulation Study. <i>Biophysical Journal</i> , 2003, 85, 3624-3635.	0.5	134

#	ARTICLE	IF	CITATIONS
818	Molecular Dynamics Simulation of a Dipalmitoylphosphatidylcholine Bilayer with NaCl. Biophysical Journal, 2003, 84, 3743-3750.	0.5	226
819	The calculations of P?T diagrams of Ni and Al using molecular dynamics simulation. Materials Letters, 2003, 57, 4336-4343.	2.6	13
820	Cell dynamics based on the metric tensor as extended variable for isothermalâ€isobaric molecular dynamics simulations. Computational Materials Science, 2003, 27, 212-218.	3.0	6
821	Trocadero: a multiple-algorithm multiple-model atomistic simulation program. Computational Materials Science, 2003, 28, 85-106.	3.0	75
822	Molecular dynamics study of isothermal and adiabatic elastic moduli prior to martensitic transformation. Journal of Alloys and Compounds, 2003, 355, 183-187.	5.5	4
823	Classical molecular dynamics simulation of UO2 to predict thermophysical properties. Journal of Alloys and Compounds, 2003, 360, 210-216.	5.5	148
824	Interface stability and solid-state amorphization in an immiscible Cuâ€Ta system. Applied Physics Letters, 2003, 83, 4515-4517.	3.3	29
825	A molecular dynamics simulation study of elastic properties of HMX. Journal of Chemical Physics, 2003, 119, 7417-7426.	3.0	195
826	Molecular dynamics simulation of dynamical properties of InSb. Physical Review B, 2003, 68, .	3.2	11
827	Phase diagram of an empirical potential: The case of Fe-Cu. Physical Review B, 2003, 68, .	3.2	56
828	Molecular Dynamics Simulations of Bulk Native Crystalline and Amorphous Structures of Cellulose. Journal of Physical Chemistry B, 2003, 107, 2394-2403.	2.6	319
829	Association Lifetimes of Hydrophobic Amino Acid Pairs Measured Directly from Molecular Dynamics Simulations. Journal of the American Chemical Society, 2003, 125, 13968-13969.	13.7	16
830	Molecular dynamics study of cristobalite silica using a charge transfer three-body potential: Phase transformation and structural disorder. Journal of Chemical Physics, 2003, 118, 1487-1498.	3.0	96
831	Calculation of the melting point of NaCl by molecular simulation. Journal of Chemical Physics, 2003, 118, 728-735.	3.0	119
832	Density functional and Monte Carlo studies of sulfur. II. Equilibrium polymerization of the liquid phase. Journal of Chemical Physics, 2003, 119, 8704-8715.	3.0	25
833	Orientation effects in shocked nickel single crystals via molecular dynamics. Journal of Applied Physics, 2003, 93, 3239-3247.	2.5	27
834	Molecular collective dynamics in solid para-hydrogen and ortho-deuterium: The Parrinelloâ€Rahman-type path integral centroid molecular dynamics approach. Journal of Chemical Physics, 2003, 119, 953-963.	3.0	45
835	Amorphous Alloy Formation in Immiscible Cu-Ta and Cu-W Systems by Atomistic Modeling and Ion-Beam Mixing. Materials Research Society Symposia Proceedings, 2003, 806, 220.	0.1	6

#	ARTICLE	IF	CITATIONS
836	Prediction of metastable phase formation in an immiscible Cu-Cr system from interatomic potential and ab initio calculation. Journal of Materials Research, 2003, 18, 2300-2303.	2.6	3
837	Liquid-liquid phase transition in compressed hydrogen from first-principles simulations. Proceedings of the National Academy of Sciences of the United States of America, 2003, 100, 3051-3053.	7.1	158
838	Experimental and Computational Studies of Ion-Solid Interactions in Silicon Carbide. Materials Research Society Symposia Proceedings, 2003, 792, 39.	0.1	3
839	Atomistic simulations of spherical indentations in nanocrystalline gold. Physical Review B, 2003, 67, .	3.2	84
840	Glass-forming ability determined by ann-body potential in a highly immiscible Cu-W system through molecular dynamics simulations. Physical Review B, 2003, 68, .	3.2	20
841	An algorithm to describe molecular scale rugged surfaces and its application to the study of a water/lipid bilayer interface. Journal of Chemical Physics, 2003, 119, 2199-2205.	3.0	90
842	Extended methods of molecular dynamic simulations under hydrostatic pressure and/or isostress. Journal of Chemical Physics, 2003, 118, 9926-9936.	3.0	13
843	Ab initioand finite-temperature molecular dynamics studies of lattice resistance in tantalum. Physical Review B, 2003, 68, .	3.2	44
844	Energy landscapes of model glasses. II. Results for constant pressure. Journal of Chemical Physics, 2003, 118, 4583-4593.	3.0	70
845	Phase stability and intrinsic stacking faults in aluminum under pressure. Physical Review B, 2003, 67, .	3.2	12
846	Anomalous Dislocation Multiplication in FCC Metals. Physical Review Letters, 2003, 91, 025503.	7.8	63
847	Molecular-dynamics study of the high-temperature elasticity of quartz above the $\hat{1}\pm\hat{1}^2$ phase transition. Physical Review B, 2003, 67, .	3.2	50
848	Coupling fields and underlying space curvature: An augmented Lagrangian approach. Physical Review E, 2003, 67, 047602.	2.1	0
849	Local elastic constants in thin films of an fcc crystal. Physical Review E, 2003, 67, 031601.	2.1	32
850	Elastic properties of dense solid phases of hard cyclic pentamers and heptamers in two dimensions. Physical Review E, 2003, 67, 036121.	2.1	91
851	Atomic-scale simulations of cascade overlap and damage evolution in silicon carbide. Journal of Materials Research, 2003, 18, 1877-1883.	2.6	23
852	Thermodynamic and mechanical properties of HMX from atomistic simulations. Theoretical and Computational Chemistry, 2003, , 279-326.	0.4	4
853	Molecular dynamics simulations for high-pressure induced B1-B2 transition in NaCl by MÃbius pair potentials. Modelling and Simulation in Materials Science and Engineering, 2003, 11, 331-338.	2.0	21

#	ARTICLE	IF	CITATIONS
854	Molecular Dynamics Simulation of Martensitic Transformations in NiAl Alloy Using the Modified Embedded Atom Method. Journal of the Physical Society of Japan, 2003, 72, 2539-2545.	1.6	6
855	Protein Explorer. , 2003, , .		56
856	Internal atomic stress near $\hat{A}5$ tilt grain boundary in aluminium under tension. Modelling and Simulation in Materials Science and Engineering, 2003, 11, 839-849.	2.0	5
857	Construction of an N-Body Cu $\hat{A}$ Ta Potential and Study of Interfacial Behavior between Immiscible Cu and Ta through Molecular Dynamics Simulation. Journal of the Physical Society of Japan, 2003, 72, 5-8.	1.6	5
858	Unconventional deformation mechanism in nanocrystalline metals?. International Journal of Materials Research, 2003, 94, 1106-1110.	0.8	24
859	Molecular Dynamics Simulation of Deformation-Induced Nanocrystallization in an Amorphous Metal.. Zairyo/Journal of the Society of Materials Science, Japan, 2003, 52, 235-240.	0.2	5
860	Nanostructured Polycrystals: Molecular-Dynamics Simulation of Plastic Deformation. , 2003, , 1-12.		3
861	First principles force field for metallic tantalum. Modelling and Simulation in Materials Science and Engineering, 2004, 12, S445-S459.	2.0	34
862	Structural Stability and the Correlation of Lattice Constant versus Tantalum Concentration of the Ag-Based Fcc Solid Solutions Studied by Molecular Dynamics Simulation. Japanese Journal of Applied Physics, 2004, 43, 2589-2593.	1.5	3
863	Calculating the Peierls energy and Peierls stress from atomistic simulations of screw dislocation dynamics: application to bcc tantalum. Modelling and Simulation in Materials Science and Engineering, 2004, 12, S371-S389.	2.0	31
864	Onset of Void Coalescence during Dynamic Fracture of Ductile Metals. Physical Review Letters, 2004, 93, 245503.	7.8	86
865	Potential energy constrained molecular dynamics simulations. Journal of Chemical Physics, 2004, 121, 4033-4042.	3.0	2
866	Cubatic liquid-crystalline behavior in a system of hard cuboids. Journal of Chemical Physics, 2004, 120, 9383-9389.	3.0	71
867	High-Frequency Vibrational Properties of Metallic Nanocrystalline Grain Boundaries. Physical Review Letters, 2004, 92, 035505.	7.8	26
868	Comment on "Collapse of Single-Wall Carbon Nanotubes is Diameter Dependent". Physical Review Letters, 2004, 93, 149601; author reply 149602.	7.8	15
869	Heat capacity effects associated with the hydrophobic hydration and interaction of simple solutes: A detailed structural and energetical analysis based on molecular dynamics simulations. Journal of Chemical Physics, 2004, 120, 10605-10617.	3.0	71
870	Stress-assisted grain boundary sliding and migration at finite temperature: A molecular dynamics study. Physical Review B, 2004, 70, .	3.2	34
871	Metastability of an immiscible Cu-Mo system calculated from first-principles and a derivedn-body potential. Physical Review B, 2004, 69, .	3.2	18

#	ARTICLE	IF	CITATIONS
872	Atomic pattern formation at the onset of stress-induced elastic instability: Fracture versus phase change. <i>Physical Review B</i> , 2004, 70, .	3.2	19
873	Atomistic modeling and thermodynamic interpretation of the bridging phenomenon observed in the Co-Au system. <i>Physical Review B</i> , 2004, 70, .	3.2	7
874	Microchemical inhomogeneity of multicomponent systems and its evaluation from interatomic potentials. <i>Physical Review B</i> , 2004, 69, .	3.2	7
875	Effect of encaged aromatic guests on the shape and connectivity of molecular cavity in crystalline polystyrene evaluated by molecular simulations. <i>Journal of Chemical Physics</i> , 2004, 121, 12085-12093.	3.0	17
876	Combinatorial entropy and phase diagram of partially ordered ice phases. <i>Journal of Chemical Physics</i> , 2004, 121, 10145-10158.	3.0	54
877	Structure and phase transitions of single-wall carbon nanotube bundles under hydrostatic pressure. <i>Physical Review B</i> , 2004, 70, .	3.2	46
878	Grown-in twin boundaries affecting deformation mechanisms in nc-metals. <i>Applied Physics Letters</i> , 2004, 85, 5863-5865.	3.3	74
879	Point-defect properties of and sputtering events in the {001} surfaces of Ni3Al I. Surface and point-defect properties. <i>Philosophical Magazine</i> , 2004, 84, 173-191.	1.6	6
880	Temperature dependence of the hydrophobic hydration and interaction of simple solutes: An examination of five popular water models. <i>Journal of Chemical Physics</i> , 2004, 120, 6674-6690.	3.0	259
881	Box length search algorithm for molecular simulation of systems containing periodic structures. <i>Journal of Chemical Physics</i> , 2004, 120, 2049-2055.	3.0	23
882	On the notion of average mechanical properties in MD simulation via homogenization. <i>Modelling and Simulation in Materials Science and Engineering</i> , 2004, 12, S333-S345.	2.0	16
883	Structural stability and magnetic properties of metastable Fe-Cu alloys studied by ab initio calculations and molecular dynamics simulations. <i>Physical Review B</i> , 2004, 69, .	3.2	17
884	Mechanical properties and elastic constants due to damage accumulation and amorphization in SiC. <i>Physical Review B</i> , 2004, 69, .	3.2	41
885	Combined Monte Carlo and molecular dynamics simulation of hydrated 18:0 sphingomyelin-cholesterol lipid bilayers. <i>Journal of Chemical Physics</i> , 2004, 120, 9841-9847.	3.0	73
886	Reconstruction of silicon surfaces: A stochastic optimization problem. <i>Physical Review B</i> , 2004, 70, .	3.2	32
887	Influence of interfacial texture on solid-state amorphization and associated asymmetric growth in immiscible Cu-Ta multilayers. <i>Physical Review B</i> , 2004, 70, .	3.2	9
888	Unusual alloying behavior at the equilibrium immiscible Cu-Nb interfaces. <i>Journal of Applied Physics</i> , 2004, 96, 3020-3022.	2.5	12
889	CONSTANT PRESSURE MD SIMULATION METHOD. <i>Molecular Crystals and Liquid Crystals</i> , 2004, 413, 109-116.	0.9	8



#	ARTICLE	IF	CITATIONS
890	Simulation of the plastic behavior of amorphous glassy bis-phenol-A-polycarbonate. Journal of Chemical Physics, 2004, 121, 4941-4950.	3.0	16
891	Atomic structures of nonequilibrium alloys in an immiscible Co–Ag system. Journal of Materials Research, 2004, 19, 1364-1368.	2.6	9
892	Non-classical nucleation in supercooled nickel. Modelling and Simulation in Materials Science and Engineering, 2004, 12, 1063-1068.	2.0	33
893	Exploration of Nanoscale Features of Thin Liquid Films on Solid Surfaces Using Molecular Dynamics Simulations. , 2004, , 27.		4
894	Structural transition and glass-forming ability of the Ni–Hf system studied by molecular dynamics simulation. Journal of Materials Research, 2004, 19, 3547-3555.	2.6	16
895	VORTICES IN BOSE–EINSTEIN CONDENSATES: SOME RECENT DEVELOPMENTS. Modern Physics Letters B, 2004, 18, 1481-1505.	1.9	85
896	Sorption Mechanism of Aromatic Molecules in the Interface between Liquid and Polymer Crystal. Molecular Simulation, 2004, 30, 901-906.	2.0	0
897	Perturbed Molecular Dynamics for Calculating Thermal Conductivity of Zirconia. Molecular Simulation, 2004, 30, 953-961.	2.0	27
898	Simple models of unusual elastic properties. AIP Conference Proceedings, 2004, , .	0.4	2
899	Deformation-mechanism map for nanocrystalline metals by molecular-dynamics simulation. Nature Materials, 2004, 3, 43-47.	27.5	740
900	A potential model for single crystals of the $\text{Li}_2\text{O-B}_2\text{O}_3$ system based on non-equivalence of boron atoms. European Physical Journal B, 2004, 41, 281-287.	1.5	6
901	Phonon spectra and heat capacity of $\text{Li}_2\text{B}_4\text{O}_7$ and $\text{Li}_3\text{BO}_5$ crystals. European Physical Journal B, 2004, 42, 461-466.	1.5	15
902	Grain-boundary free energy in an assembly of elastic disks. Physical Review E, 2004, 69, 026117.	2.1	6
903	Molecular Models of Hydroxide, Oxyhydroxide, and Clay Phases and the Development of a General Force Field. Journal of Physical Chemistry B, 2004, 108, 1255-1266.	2.6	2,281
904	Ab initio based force field and molecular dynamics simulations of crystalline TATB. Journal of Chemical Physics, 2004, 120, 7059-7066.	3.0	90
905	Molecular dynamics simulations of reduced $\text{CeO}_2$ : bulk and surfaces. Surface Science, 2004, 552, 273-280.	1.9	34
906	Atomistic simulation of the laser induced damage in single wall carbon nanotubes: Diameter and chirality dependence. Applied Physics A: Materials Science and Processing, 2004, 79, 899-901.	2.3	5
907	An atomistic study of solid/liquid interfaces in binary systems. Jom, 2004, 56, 45-48.	1.9	11



#	ARTICLE	IF	CITATIONS
908	A simple topological representation of protein structure: Implications for new, fast, and robust structural classification. <i>Proteins: Structure, Function and Bioinformatics</i> , 2004, 56, 487-501.	2.6	26
909	Can Nematic Transitions Be Predicted By Atomistic Simulations? A Computational Study of The Odd-Even Effect. <i>ChemPhysChem</i> , 2004, 5, 104-111.	2.1	114
910	Role of surface amorphous film in high-resolution high-angle annular dark field STEM imaging. <i>Ultramicroscopy</i> , 2004, 99, 125-135.	1.9	16
911	Second moment approximation of tight-binding potential for $^{57}\text{Fe}$ applicable up to 1700 K. <i>Science and Technology of Advanced Materials</i> , 2004, 5, 497-502.	6.1	3
912	Melting of thin $^{57}\text{Fe}/\text{C}$ films having (100), (110) and (111) surfaces in terms of molecular dynamics simulation. <i>Science and Technology of Advanced Materials</i> , 2004, 5, 677-682.	6.1	3
913	Size effects on the melting of nickel nanowires: a molecular dynamics study. <i>Physica E: Low-Dimensional Systems and Nanostructures</i> , 2004, 25, 47-54.	2.7	82
914	Molecular modelling of the uniaxial deformation of amorphous polyethylene terephthalate. <i>Polymer</i> , 2004, 45, 1401-1411.	3.8	14
915	Atomistic modeling: interfacial diffusion and adhesion of polycarbonate and silanes. <i>Polymer</i> , 2004, 45, 6399-6407.	3.8	53
916	Volume expansion and ultimate mechanical stability of crystalline phases in amorphisation and melting processes. <i>Materials Science &amp; Engineering A: Structural Materials: Properties, Microstructure and Processing</i> , 2004, 375-377, 675-678.	5.6	3
917	Molecular dynamics simulations of the elastic moduli of polymer-carbon nanotube composites. <i>Computer Methods in Applied Mechanics and Engineering</i> , 2004, 193, 1773-1788.	6.6	314
918	The influence of twins on the mechanical properties of nc-Al. <i>Acta Materialia</i> , 2004, 52, 2259-2268.	7.9	147
919	Thermal properties of thin and thick Ni <sub>3</sub> Al cluster assembled layers: an atomic scale simulation study. <i>Applied Surface Science</i> , 2004, 226, 161-166.	6.1	2
920	A molecular dynamics simulation of the melting points and glass transition temperatures of myo- and neo-inositol. <i>Journal of Chemical Physics</i> , 2004, 121, 9565-9573.	3.0	39
921	An Approach to Developing a Force Field for Molecular Simulation of Martensitic Phase Transitions between Phases with Subtle Differences in Energy and Structure. <i>Journal of the American Chemical Society</i> , 2004, 126, 396-405.	13.7	66
922	Molecular Simulations Suggest Protein Salt Bridges Are Uniquely Suited to Life at High Temperatures. <i>Journal of the American Chemical Society</i> , 2004, 126, 2208-2214.	13.7	83
923	Differences in deformation processes in nanocrystalline nickel with low- and high-angle boundaries from atomistic simulations. <i>Applied Physics Letters</i> , 2004, 84, 598-600.	3.3	39
924	Molecular Models for the Intercalation of Methane Hydrate Complexes in Montmorillonite Clay. <i>Journal of Physical Chemistry B</i> , 2004, 108, 15141-15149.	2.6	101
925	Proposed Definition of Microchemical Inhomogeneity and Application To Characterize Some Selected Miscible/Immiscible Binary Metal Systems. <i>Journal of Physical Chemistry B</i> , 2004, 108, 16071-16076.	2.6	20

#	ARTICLE	IF	CITATIONS
926	Molecular dynamic simulation methods for anisotropic liquids. Journal of Chemical Physics, 2004, 120, 5576-5584.	3.0	15
927	Dislocation Core Effects on Mobility. Dislocations in Solids, 2004, 12, 1-80.	1.6	120
928	Synthesis, Crystal Structure, and Molecular Modeling of a Layered Manganese(II) Phosphate: $\text{Mn}_3(\text{PO}_4)_4 \cdot 2(\text{H}_3\text{NCH}_2\text{CH}_2)_3\text{N} \cdot 6(\text{H}_2\text{O})$ . Chemistry of Materials, 2004, 16, 2068-2075.	6.7	13
929	Effect of stress triaxiality on void growth in dynamic fracture of metals: A molecular dynamics study. Physical Review B, 2004, 69, .	3.2	129
930	Molecular Dynamics Simulations of Electric Field Poled Nonlinear Optical Chromophores Incorporated in a Polymer Matrix. Journal of Physical Chemistry B, 2004, 108, 588-596.	2.6	54
931	Mechanisms of Nonexponential Relaxation in Supercooled Glucose Solutions: the Role of Water Facilitation. Journal of Physical Chemistry A, 2004, 108, 3699-3712.	2.5	30
932	Spectroscopic Characterization of Heterogeneous Structure of Samiacynthiaricini Silk Fibroin Induced by Stretching and Molecular Dynamics Simulation. Macromolecules, 2004, 37, 3497-3504.	4.8	26
933	Structures of Bombyxmori and Samiacynthiaricini Silk Fibroins Studied with Solid-State NMR. Biomacromolecules, 2004, 5, 680-688.	5.4	57
934	Molecular Modeling and Simulations of AOT $\sim$ Water Reverse Micelles in Isooctane: A Structural and Dynamic Properties. Journal of Physical Chemistry B, 2004, 108, 19458-19466.	2.6	209
935	On the Lennard-Jones EAM potential. Proceedings of the Royal Society A: Mathematical, Physical and Engineering Sciences, 2004, 460, 1649-1672.	2.1	14
936	Kinetic coefficient of Ni solid-liquid interfaces from molecular-dynamics simulations. Physical Review B, 2004, 69, .	3.2	126
937	Nonequilibrium melting and crystallization of a model Lennard-Jones system. Journal of Chemical Physics, 2004, 120, 11640-11649.	3.0	163
938	Size dependent ion hydration, its asymmetry, and convergence to macroscopic behavior. Journal of Chemical Physics, 2004, 120, 4457-4466.	3.0	140
939	Rapid estimation of elastic constants by molecular dynamics simulation under constant stress. Physical Review B, 2004, 69, .	3.2	900
940	Exterior Site Occupancy Infers Chloride-Induced Proton Gating in a Prokaryotic Homolog of the ClC Chloride Channel. Biophysical Journal, 2004, 87, 1686-1696.	0.5	54
941	The Range and Shielding of Dipole-Dipole Interactions in Phospholipid Bilayers. Biophysical Journal, 2004, 87, 2433-2445.	0.5	83
942	Simulation of the Early Stages of Nano-Domain Formation in Mixed Bilayers of Sphingomyelin, Cholesterol, and Dioleoylphosphatidylcholine. Biophysical Journal, 2004, 87, 3312-3322.	0.5	164
943	Molecular dynamics simulation of reconstructive phase transitions on an anhydrous zeolite. Physical Review B, 2004, 70, .	3.2	28

#	ARTICLE	IF	CITATIONS
944	Ultrafast dynamics in solids. Journal of Physics Condensed Matter, 2004, 16, R995-R1056.	1.8	55
945	Theoretical study of the local structure and Raman spectra of CaO-SiO <sub>2</sub> binary melts. Journal of Chemical Physics, 2004, 121, 7883.	3.0	49
946	First-principles study of hydrogen diffusion in $\alpha$ -Al <sub>2</sub> O <sub>3</sub> and liquid alumina. Physical Review B, 2004, 69, .	3.2	71
947	Computational study of imidazolium-based ionic solvents with alkyl substituents of different lengths. Molecular Physics, 2004, 102, 829-838.	1.7	164
948	Water at Hydrophobic Substrates: Curvature, Pressure, and Temperature Effects. Langmuir, 2004, 20, 4756-4763.	3.5	117
949	Coarse Grained Model for Semiquantitative Lipid Simulations. Journal of Physical Chemistry B, 2004, 108, 750-760.	2.6	2,027
950	Stress Distribution During Deformation of Polycrystalline Aluminum by Molecular-dynamics and Finite-element Modeling. , 2004, , .		0
951	Analytical evaluation of unstable deformation criterion of atomic structure and its application to nanostructure. Computational Materials Science, 2004, 29, 499-510.	3.0	46
952	Lattice distortion and thermal stability of nano-crystalline copper. Computational Materials Science, 2004, 30, 314-319.	3.0	11
953	Langevin dynamics in constant pressure extended systems. Journal of Chemical Physics, 2004, 120, 11432-11441.	3.0	116
954	Crystal-melt interfacial free energies and mobilities in fcc and bcc Fe. Physical Review B, 2004, 69, .	3.2	148
955	Structural phase transitions in the Cu-based Cu-V solid solutions studied by molecular dynamics simulation. Journal of Alloys and Compounds, 2004, 366, 205-212.	5.5	6
956	Jamming in hard sphere and disk packings. Journal of Applied Physics, 2004, 95, 989-999.	2.5	186
957	Structure and Dynamics of Sphingomyelin Bilayer: Insight Gained through Systematic Comparison to Phosphatidylcholine. Biophysical Journal, 2004, 87, 2976-2989.	0.5	141
958	Computer Simulation of Solid and Liquid Benzene with an Atomistic Interaction Potential Derived from ab Initio Calculations. Journal of the American Chemical Society, 2004, 126, 14278-14286.	13.7	74
959	Complexation of Phosphatidylcholine Lipids with Cholesterol. Biophysical Journal, 2004, 86, 1345-1356.	0.5	143
960	Structural Stability of the Metastable Solid Solution in the Equilibrium Immiscible Ag-W System Predicted by an ab Initio Derived Potential. Journal of the Physical Society of Japan, 2004, 73, 1222-1227.	1.6	5
961	Atomistic Modeling of Metastable Phase Selection of a Highly Immiscible Ag-W System. Journal of the Physical Society of Japan, 2004, 73, 2023-2027.	1.6	6

#	ARTICLE	IF	CITATIONS
962	Mechanical Properties Depending on Grain Sizes of Face-Centered-Cubic Nanocrystalline Metals Using Molecular Dynamics Simulation. JSME International Journal Series A-Solid Mechanics and Material Engineering, 2004, 47, 83-91.	0.4	14
963	Neighbor list collision-driven molecular dynamics simulation for nonspherical hard particles.II. Applications to ellipses and ellipsoids. Journal of Computational Physics, 2005, 202, 765-793.	3.8	17
964	Dual-Phase Metallic Glass and its Two-Dimensional Fractal Morphology. Journal of the Physical Society of Japan, 2005, 74, 2937-2940.	1.6	3
965	Structural Stability and Homogeneity of the Nonequilibrium Co-Al Ag Alloys. Journal of the Physical Society of Japan, 2005, 74, 375-381.	1.6	6
966	Molecular Dynamics Simulation on Anelasticity under Tensile and Shearing Stresses in Single Component Amorphous Metal. Materials Transactions, 2005, 46, 2875-2879.	1.2	2
967	High-Pressure Elasticity and Auxetic Property of $\alpha$ -Cristobalite. Materials Transactions, 2005, 46, 1161-1166.	1.2	18
968	Molecular dynamics simulations of basal and pyramidal system edge dislocations in sapphire. Journal of the European Ceramic Society, 2005, 25, 1431-1439.	5.7	26
969	Structural and thermodynamic properties of GaN at high pressures and high temperatures. Physica B: Condensed Matter, 2005, 368, 243-250.	2.7	19
970	Neighbor list collision-driven molecular dynamics simulation for nonspherical hard particles. I. Algorithmic details. Journal of Computational Physics, 2005, 202, 737-764.	3.8	279
971	Neighbor list collision-driven molecular dynamics simulation for nonspherical hard particles.. Journal of Computational Physics, 2005, 202, 765-793.	3.8	143
972	Elastic and plastic deformations of nickel nanowires under uniaxial compression. Physica E: Low-Dimensional Systems and Nanostructures, 2005, 30, 45-50.	2.7	20
973	A Parrinello-Rahman approach to vortex lattices. Physics Letters, Section A: General, Atomic and Solid State Physics, 2005, 341, 128-134.	2.1	15
974	Alloys created between immiscible elements. Progress in Materials Science, 2005, 50, 413-509.	32.8	324
975	On the definitions of effective stress and deformation gradient for use in MD: Hill's macro-homogeneity and the virial theorem. International Journal of Engineering Science, 2005, 43, 533-555.	5.0	33
976	Reorientational relaxation of aromatic molecules in the molecular cavity of crystalline syndiotactic polystyrene studied by molecular dynamics simulation. Journal of Molecular Structure, 2005, 739, 33-40.	3.6	19
977	Sorption of organic solvents on the surface of crystalline syndiotactic polystyrene studied by molecular dynamics simulation. Journal of Molecular Structure, 2005, 739, 27-32.	3.6	8
978	On the relationship between the mechanical and the thermal instabilities of crystalline lattices. Materials Science & Engineering A: Structural Materials: Properties, Microstructure and Processing, 2005, 403, 48-56.	5.6	7
979	Spontaneous disordering of nm-grain-sized polycrystals and clusters of silica stishovite. Solid State Communications, 2005, 136, 71-75.	1.9	8

#	ARTICLE	IF	CITATIONS
980	Crystallographic and lattice point correlations of a new hcp-to-fcc martensitic transformation observed in the Ni–Hf system. <i>Acta Materialia</i> , 2005, 53, 743-748.	7.9	5
981	Developing realistic grain boundary networks for use in molecular dynamics simulations. <i>Acta Materialia</i> , 2005, 53, 4847-4856.	7.9	58
982	A Lagrangian-based continuum homogenization approach applicable to molecular dynamics simulations. <i>International Journal of Solids and Structures</i> , 2005, 42, 6409-6432.	2.7	14
983	Intercalation of dimethyl sulfoxide in kaolinite: Molecular dynamics simulation study. <i>Chemical Physics Letters</i> , 2005, 411, 233-237.	2.6	36
984	Molecular dynamics simulation of the M intermediate of photoactive yellow protein in the crystalline state. <i>Chemical Physics Letters</i> , 2005, 414, 230-233.	2.6	8
985	The Microscopic Switching Mechanism of a [2]Catenane. <i>Journal of Physical Chemistry B</i> , 2005, 109, 17094-17099.	2.6	27
986	Radial distribution functions and densities for the SPC/E, TIP4P and TIP5P models for liquid water and ices Ih, Ic, II, III, IV, V, VI, VII, VIII, IX, XI and XII. <i>Physical Chemistry Chemical Physics</i> , 2005, 7, 1450.	2.8	111
987	Melting Behaviors of Nanocrystalline Ag. <i>Journal of Physical Chemistry B</i> , 2005, 109, 20339-20342.	2.6	68
988	Structure and dynamics of water at the interface with phospholipid bilayers. <i>Journal of Chemical Physics</i> , 2005, 123, 224702.	3.0	122
989	Molecular dynamics simulation of the structural and dynamical properties of crystalline BaO. <i>Physical Review B</i> , 2005, 71, .	3.2	13
990	Why Is the Partial Molar Volume of CO <sub>2</sub> So Small When Dissolved in a Room Temperature Ionic Liquid? Structure and Dynamics of CO <sub>2</sub> Dissolved in [Bmim] <sup>+</sup> [PF <sub>6</sub> ] <sup>-</sup> . <i>Journal of the American Chemical Society</i> , 2005, 127, 17842-17851.	13.7	335
991	Structural and energetic properties of unsupported Cu nanoparticles from room temperature to the melting point: Molecular dynamics simulations. <i>Physical Review B</i> , 2005, 72, .	3.2	95
992	Ensembles and Computer Simulation Calculation of Response Functions. , 2005, , 729-743.		4
993	Dynamics of Consolidation and Crack Growth in Nanocluster-Assembled Amorphous Silicon Nitride. <i>Journal of the American Ceramic Society</i> , 1998, 81, 433-436.	3.8	22
994	Atomistic Simulations of Materials Fracture and the Link between Atomic and Continuum Length Scales. <i>Journal of the American Ceramic Society</i> , 1998, 81, 501-516.	3.8	68
995	How pH Opens a H <sup>+</sup> Channel: The Gating Mechanism of Influenza A M2. <i>Structure</i> , 2005, 13, 1789-1798.	3.3	60
996	Vicinal twin boundaries providing dislocation sources in nanocrystalline Al. <i>Scripta Materialia</i> , 2005, 54, 477-477.	5.2	11
997	GROMACS: Fast, flexible, and free. <i>Journal of Computational Chemistry</i> , 2005, 26, 1701-1718.	3.3	13,676

#	ARTICLE	IF	CITATIONS
998	Polyamorphism in Silicon Nanocrystals under Pressure. ChemPhysChem, 2005, 6, 1765-1768.	2.1	12
999	Editorial: A Tribute to Michele Parrinello: From Physics via Chemistry to Biology. ChemPhysChem, 2005, 6, 1671-1676.	2.1	9
1000	A Tribute to Michele Parrinello: Publications in Peer-Reviewed Journals Including Review Articles (1971-2004). ChemPhysChem, 2005, 6, 1677-1684.	2.1	0
1001	Exploring Polymorphism: The Case of Benzene. Angewandte Chemie - International Edition, 2005, 44, 3769-3773.	13.8	138
1003	Twinning in Nanocrystalline fcc Metals. Advanced Engineering Materials, 2005, 7, 16-20.	3.5	81
1004	Peculiarities of electric field alignment of nonlinear optical chromophores incorporated into thin film polymer matrix. Theoretical Chemistry Accounts, 2005, 114, 153-158.	1.4	4
1005	Conformational analysis of xylan chains. Carbohydrate Research, 2005, 340, 2752-2760.	2.3	46
1006	Order-disorder behavior in KNbO <sub>3</sub> and KNbO <sub>3</sub> /KTaO <sub>3</sub> solid solutions and superlattices by molecular-dynamics simulation. Journal of Materials Science, 2005, 40, 3213-3217.	3.7	12
1007	Structural Micro-heterogeneities of Crystalline Î <sup>2</sup> -cellulose. Cellulose, 2005, 12, 339-349.	4.9	39
1008	The Molecular-Dynamics Method for Different Statistical Ensembles. Russian Physics Journal, 2005, 48, 122-130.	0.4	2
1009	Ab initio simulation in extreme conditions. Materials Today, 2005, 8, 26-32.	14.2	21
1010	Unwinding the helical linker of calcium-loaded calmodulin: A molecular dynamics study. Proteins: Structure, Function and Bioinformatics, 2005, 61, 829-839.	2.6	28
1011	Application of entropy calculations to the determination of transition temperature in zirconium. Physica Status Solidi (B): Basic Research, 2005, 242, 1598-1605.	1.5	4
1012	Molecular dynamics study of the high-temperature elasticity of SiO <sub>2</sub> polymorphs: Structural phase transition and elastic anomaly. Physica Status Solidi (B): Basic Research, 2005, 242, 607-620.	1.5	25
1013	Poisson's ratio of degenerate crystalline phases of three-dimensional hard dimers and hard cyclic trimers. Physica Status Solidi (B): Basic Research, 2005, 242, 626-631.	1.5	13
1014	Atomistic Computer Simulation of Diffusion. , 2005, , 113-171.		9
1015	Theoretical and Computational Studies of Energetic Salts. , 2005, , 431-471.		5
1016	Structural Phase Transformation in Niâ€“Hf and Niâ€“Ti Systems Studied by Molecular Dynamics Simulation. Journal of the Physical Society of Japan, 2005, 74, 2699-2702.	1.6	3

#	ARTICLE	IF	CITATIONS
1017	Electronic and Elastic Properties of Helical Nickel Nanowires. Chinese Physics Letters, 2005, 22, 1195-1198.	3.3	4
1018	Molecular dynamics. , 2005, , 425-441.		4
1019	Molecular Dynamics Exploration of Thin Liquid Films on Solid Surfaces. 1. Monatomic Fluid Films. Microscale Thermophysical Engineering, 2005, 9, 331-349.	1.2	18
1020	Defects and Ion-Solid Interactions in Silicon Carbide. Materials Science Forum, 2005, 475-479, 1345-1350.	0.3	0
1021	Molecular Dynamics Simulation of Compressive Mechanical Behavior of Nanocrystalline Fe. Materials Science Forum, 2005, 475-479, 3291-3294.	0.3	0
1022	Deducing solid-liquid interfacial energy from superheating or supercooling: application to H <sub>2</sub> O at high pressures. Modelling and Simulation in Materials Science and Engineering, 2005, 13, 321-328.	2.0	31
1023	Shear softening and structure in a simulated three-dimensional binary glass. Journal of Chemical Physics, 2005, 122, 154508.	3.0	50
1024	Molecular dynamics investigation on the role of sliding interfaces and friction in the formation of amorphous phases. Physical Review B, 2005, 71, .	3.2	43
1025	Metastable isomorphous phase diagram of the peritectic Ni-Ru system predicted by ab initio and molecular dynamics calculations. Physical Review B, 2005, 71, .	3.2	10
1026	Applicability of Born's stability criterion to face-centered-cubic crystals in [111] loading. Applied Physics Letters, 2005, 87, 251919.	3.3	14
1027	Effects of surface imperfections on deformation and failure of amorphous metals. Applied Physics Letters, 2005, 87, 031910.	3.3	37
1028	Boundary conditions for equilibrating incommensurate periodic patterns. Physical Review E, 2005, 72, 056707.	2.1	1
1029	Self-consistent mean-field model based on molecular dynamics: Application to lipid-cholesterol bilayers. Journal of Chemical Physics, 2005, 123, 034910.	3.0	39
1030	Numerical simulations of structural modifications at a Ni-Zr sliding interface. Physical Review B, 2005, 72, .	3.2	55
1031	Calculation of x-ray spectra for nanocrystalline materials. Physical Review B, 2005, 71, .	3.2	64
1032	Time reversible and symplectic integrators for molecular dynamics simulations of rigid molecules. Journal of Chemical Physics, 2005, 122, 224114.	3.0	149
1033	Grain-size dependence of the relationship between intergranular and intragranular deformation of nanocrystalline Al by molecular dynamics simulations. Physical Review B, 2005, 71, .	3.2	122
1034	Atomic-scale simulations of strain localization in a single-component three-dimensional model amorphous solid. Materials Research Society Symposia Proceedings, 2005, 903, 1.	0.1	1



#	ARTICLE	IF	CITATIONS
1035	Monte Carlo Simulations of Model Particles Forming Phases of Negative Poisson Ratio. , 2005, , 241-252.		5
1036	Strain-Modulated Adatom and Surface Vacancy Pair Interactions. Journal of Applied Mechanics, Transactions ASME, 2005, 72, 400-407.	2.2	1
1037	Vibrational density of states and Lindemann melting law. Journal of Chemical Physics, 2005, 122, 194709.	3.0	52
1038	Nature and extent of melting in superheated solids: Liquid-solid coexistence model. Physical Review B, 2005, 72, .	3.2	31
1039	Lattice vibrations in $\alpha$ -plutonium: Molecular dynamics calculation. Physical Review B, 2005, 72, .	3.2	30
1040	The role of particle softness in determining the value of Poisson's ratio for soft sphere solids. Molecular Simulation, 2005, 31, 937-944.	2.0	2
1041	Atomistic Methods for Structure-Property Correlations. , 2005, , 1931-1951.		0
1042	Molecular Dynamics Simulations of Salicylate Effects on the Micro- and Mesoscopic Properties of a Dipalmitoylphosphatidylcholine Bilayer. Biochemistry, 2005, 44, 13425-13438.	2.5	44
1043	Test of classical nucleation theory via molecular-dynamics simulation. Journal of Chemical Physics, 2005, 122, 224510.	3.0	61
1044	Three-dimensional molecular dynamics simulations of void coalescence during dynamic fracture of ductile metals. Physical Review B, 2005, 71, .	3.2	67
1045	Molecular dynamics (MD) simulation of uniaxial tension of $\alpha$ -Sn single crystals with nanocracks. , 0, , .		0
1046	Liquid Crystalline Formation of Semifluorinated n-Alkanes F <sub>n</sub> H <sub>m</sub> ; Molecular Dynamics Simulation Study Using Atomistic Model. Molecular Crystals and Liquid Crystals, 2005, 441, 307-317.	0.9	8
1047	Formation of Amorphous Alloys by Ion Beam Mixing and Its Multiscale Theoretical Modeling in the Equilibrium Immiscible Sc <sub>2</sub> W System. Journal of Physical Chemistry B, 2005, 109, 4391-4397.	2.6	13
1048	Effect of the Choice of the Pressure Coupling Method on the Spontaneous Aggregation of DPPC Molecules. Journal of Physical Chemistry B, 2005, 109, 14667-14674.	2.6	17
1049	Evolutionarily Conserved Functional Mechanics across Pepsin-like and Retroviral Aspartic Proteases. Journal of the American Chemical Society, 2005, 127, 3734-3742.	13.7	74
1050	Can simple models describe the phase diagram of water?. Journal of Physics Condensed Matter, 2005, 17, S3283-S3288.	1.8	72
1051	Computational Study of the Dynamics of Mannose Disaccharides Free in Solution and Bound to the Potent Anti-HIV Virucidal Protein Cyanovirin. Journal of Physical Chemistry B, 2005, 109, 3639-3647.	2.6	22
1052	Introducing Variable Cell Shape Methods in Field Theory Simulations of Polymers. Journal of Physical Chemistry B, 2005, 109, 6694-6700.	2.6	71



#	ARTICLE	IF	CITATIONS
1053	Molecular dynamics simulations of phase formation and stability in the Al(Ni) system under irradiation. Philosophical Magazine, 2005, 85, 737-743.	1.6	2
1054	Cooperative Dynamics and Self-Diffusion in Superheated Crystals. Journal of Physical Chemistry B, 2005, 109, 15291-15296.	2.6	12
1055	Atomic-level computer simulation of SiC: defect accumulation, mechanical properties and defect recovery. Philosophical Magazine, 2005, 85, 509-518.	1.6	8
1056	Solid-State Amorphization Observed in the Equilibrium-Immiscible Cu-Re System by Molecular Dynamics Simulations. Journal of Physical Chemistry B, 2005, 109, 16463-16468.	2.6	7
1057	Solubility of Methane in Water: The Significance of the Methane-Water Interaction Potential. Journal of Physical Chemistry B, 2005, 109, 23596-23604.	2.6	27
1058	The Effect of the Rigidity of Perfluoropolyether Surfactant on Its Behavior at the Water/Supercritical Carbon Dioxide Interface. Journal of Physical Chemistry B, 2005, 109, 21725-21731.	2.6	14
1059	Atomistic Modeling of Crystal-to-Amorphous Transition and Associated Kinetics in the Ni-Nb System by Molecular Dynamics Simulations. Journal of Physical Chemistry B, 2005, 109, 4717-4725.	2.6	12
1060	Molecular structure of the lecithin ripple phase. Proceedings of the National Academy of Sciences of the United States of America, 2005, 102, 5392-5396.	7.1	159
1061	The Role of the Peripheral Anionic Site and Cation Interactions in the Ligand Penetration of the Human AChE Gorge. Journal of the American Chemical Society, 2005, 127, 9147-9155.	13.7	94
1062	Interaction potential for ZnTe: A molecular dynamics study. Physical Review B, 2005, 72, .	3.2	10
1063	Molecular dynamics simulation of the titration of polyoxocations in aqueous solution. Geochimica Et Cosmochimica Acta, 2005, 69, 4397-4410.	3.9	39
1064	Glass transition phenomena observed in stereoregular PMMAs using molecular modeling. Composites Part A: Applied Science and Manufacturing, 2005, 36, 521-530.	7.6	25
1065	Molecular basis of the allosteric mechanism of cAMP in the regulatory PKA subunit. FEBS Letters, 2005, 579, 2679-2685.	2.8	9
1066	Nucleotide binding to the homodimeric MJ0796 protein: A computational study of a prokaryotic ABC transporter NBD dimer. FEBS Letters, 2005, 579, 4193-4199.	2.8	33
1067	Flexible Docking in Solution Using Metadynamics. Journal of the American Chemical Society, 2005, 127, 2600-2607.	13.7	266
1068	Structural phase transition and dynamical properties of PbTiO <sub>3</sub> simulated by molecular dynamics. Journal of Physics Condensed Matter, 2005, 17, 5771-5783.	1.8	20
1069	Differences between solid superheating and liquid supercooling. Journal of Chemical Physics, 2005, 123, 151102.	3.0	31
1070	Atomistic Computer Simulation of Diffusion. , 2005, , 113-171.		1

#	ARTICLE	IF	CITATIONS
1071	Molecular dynamics study of the binary Cu <sub>46</sub> Zr <sub>54</sub> metallic glass motivated by experiments: Glass formation and atomic-level structure. <i>Physical Review B</i> , 2005, 71, .	3.2	227
1072	A potential model for the study of ices and amorphous water: TIP4P/Ice. <i>Journal of Chemical Physics</i> , 2005, 122, 234511.	3.0	1,041
1073	Modified embedded-atom method interatomic potential for the Fe-Cu alloy system and cascade simulations on pure Fe and Fe-Cu alloys. <i>Physical Review B</i> , 2005, 71, .	3.2	55
1074	The melting temperature of the most common models of water. <i>Journal of Chemical Physics</i> , 2005, 122, 114507.	3.0	338
1075	Defect-Mediated Melting in Superheated Noble Gas Crystals. <i>Journal of Physical Chemistry B</i> , 2005, 109, 20295-20302.	2.6	4
1076	A general purpose model for the condensed phases of water: TIP4P/2005. <i>Journal of Chemical Physics</i> , 2005, 123, 234505.	3.0	2,907
1077	Mechanical properties of Au nanowires under uniaxial tension with high strain-rate by molecular dynamics. <i>Nanotechnology</i> , 2005, 16, 2972-2981.	2.6	46
1078	Low-temperature and high-pressure induced swelling of a hydrophobic polymer-chain in aqueous solution. <i>Physical Chemistry Chemical Physics</i> , 2005, 7, 2780.	2.8	39
1079	Electronic-Enthalpy Functional for Finite Systems Under Pressure. <i>Physical Review Letters</i> , 2005, 94, 145501.	7.8	41
1080	The DL_POLY molecular dynamics package. <i>Zeitschrift Fur Kristallographie - Crystalline Materials</i> , 2005, 220, .	0.8	31
1081	Preferential Solvation of Phenol in Binary Solvent Mixtures. A Molecular Dynamics Study. <i>Journal of Physical Chemistry A</i> , 2006, 110, 2253-2258.	2.5	7
1082	The Gay-Berne mesogen: a paradigm shift?. <i>Liquid Crystals</i> , 2006, 33, 1389-1405.	2.2	9
1083	Melting temperature: From nanocrystalline to amorphous phase. <i>Journal of Chemical Physics</i> , 2006, 125, 184504.	3.0	35
1084	Dynamics in atomistic simulations of phospholipid membranes: Nuclear magnetic resonance relaxation rates and lateral diffusion. <i>Journal of Chemical Physics</i> , 2006, 125, 204703.	3.0	109
1085	Phonon Transport in Molecular Dynamics Simulations: Formulation and Thermal Conductivity Prediction. <i>Advances in Heat Transfer</i> , 2006, , 169-255.	0.9	186
1086	A molecular dynamics study on intermediate structures during transition from amorphous to crystalline state. <i>Molecular Simulation</i> , 2006, 32, 443-449.	2.0	9
1087	DNA-decorated carbon nanotubes for chemical sensing. <i>Semiconductor Science and Technology</i> , 2006, 21, S17-S21.	2.0	45
1089	A classical mechanics approach to the determination of the stress-strain response of particle systems. <i>Modelling and Simulation in Materials Science and Engineering</i> , 2006, 14, 741-757.	2.0	23

#	ARTICLE	IF	CITATIONS
1090	Anthramycinâ€™DNA Binding Explored by Molecular Simulations. Journal of Physical Chemistry B, 2006, 110, 24687-24695.	2.6	23
1091	Duocarmycins Binding to DNA Investigated by Molecular Simulationâ€™. Journal of Physical Chemistry B, 2006, 110, 3647-3660.	2.6	26
1092	Calculation of solid-liquid interfacial free energy: A classical nucleation theory based approach. Journal of Chemical Physics, 2006, 124, 124707.	3.0	158
1093	The origin of (001) texture evolution in FePt thin films on amorphous substrates. Journal of Applied Physics, 2006, 99, 053906.	2.5	95
1094	Ionic conduction in the solid state. Journal of Chemical Sciences, 2006, 118, 135-154.	1.5	157
1095	Densification of silica glass at ambient pressure. Journal of Chemical Physics, 2006, 125, 154511.	3.0	9
1096	The melting point of ice Ih for common water models calculated from direct coexistence of the solid-liquid interface. Journal of Chemical Physics, 2006, 124, 144506.	3.0	386
1097	Phase Behavior of Elemental Aluminum Using Monte Carlo Simulations. Journal of Physical Chemistry B, 2006, 110, 26135-26142.	2.6	15
1098	Empirical Molecular Dynamics: Possibilities, Requirements, and Limitations. , 0, , 213-244.		3
1099	Parallelized-over-parts computation of absolute binding free energy with docking and molecular dynamics. Journal of Chemical Physics, 2006, 125, 084901.	3.0	92
1100	Temperature-Dependent Thermal and Elastic Properties of the Interlamellar Phase of Semicrystalline Polyethylene by Molecular Simulation. Macromolecules, 2006, 39, 439-447.	4.8	65
1101	The Influence of Amino Acid Protonation States on Molecular Dynamics Simulations of the Bacterial Porin OmpF. Biophysical Journal, 2006, 90, 112-123.	0.5	67
1102	Influence of Chain Length and Unsaturation on Sphingomyelin Bilayers. Biophysical Journal, 2006, 90, 851-863.	0.5	116
1103	Conformation and Environment of Channel-Forming Peptides: A Simulation Study. Biophysical Journal, 2006, 90, 1855-1864.	0.5	18
1104	Atomistic Simulation Studies of Cholesteryl Oleates: Model for the Core of Lipoprotein Particles. Biophysical Journal, 2006, 90, 2247-2257.	0.5	23
1105	Anionic Phospholipid Interactions with the Potassium Channel KcsA: Simulation Studies. Biophysical Journal, 2006, 90, 822-830.	0.5	77
1106	cAMP Modulation of the Cytoplasmic Domain in the HCN2 Channel Investigated by Molecular Simulations. Biophysical Journal, 2006, 90, 3428-3433.	0.5	17
1107	The Intrinsic Flexibility of the Kv Voltage Sensor and Its Implications for Channel Gating. Biophysical Journal, 2006, 90, 1598-1606.	0.5	37

#	ARTICLE	IF	CITATIONS
1108	Permeability of Psoralen Derivatives in Lipid Membranes. Biophysical Journal, 2006, 91, 2464-2474.	0.5	27
1109	Structure-Function Relationship in a Variant Hemoglobin: A Combined Computational-Experimental Approach. Biophysical Journal, 2006, 91, 3529-3541.	0.5	13
1110	Molecular Simulation of the Binding of Nerve Growth Factor Peptide Mimics to the Receptor Tyrosine Kinase A. Biophysical Journal, 2006, 91, 2063-2071.	0.5	19
1111	The Origin of Layer Structure Artifacts in Simulations of Liquid Water. Journal of Chemical Theory and Computation, 2006, 2, 1-11.	5.3	195
1112	Solid-state disordering and melting of silica stishovite: the role of defects. Journal of Physics Condensed Matter, 2006, 18, 659-668.	1.8	17
1113	Mechanistic Aspects of Homogeneous and Heterogeneous Melting Processes. Journal of Physical Chemistry B, 2006, 110, 12645-12652.	2.6	38
1114	Phase transitions of methane using molecular dynamics simulations. Journal of Chemical Physics, 2006, 124, 124517.	3.0	16
1115	Structural Disorder of the CD31 Transmembrane Domain Studied with 2D IR Spectroscopy and Molecular Dynamics Simulations. Journal of Physical Chemistry B, 2006, 110, 24740-24749.	2.6	64
1116	Cooperative Atomic Displacements and Melting at the Limit of Superheating. Journal of Physical Chemistry B, 2006, 110, 3281-3287.	2.6	10
1117	Effect of Surfactant Conformation on the Structures of Small Size Nonionic Reverse Micelles: A Molecular Dynamics Simulation Study. Langmuir, 2006, 22, 9112-9120.	3.5	40
1118	Molecular-dynamics simulation of a ceramide bilayer. Journal of Chemical Physics, 2006, 124, 014708.	3.0	51
1119	Formation and Structural Anomaly of the Metastable Phases in an Immiscible Ag-Mo System Studied by Ion Beam Mixing and Molecular Dynamics Simulation. Journal of Physical Chemistry B, 2006, 110, 595-606.	2.6	22
1120	Direct Observation of Salt Effects on Molecular Interactions through Explicit-Solvent Molecular Dynamics Simulations: A Differential Effects on Electrostatic and Hydrophobic Interactions and Comparisons to Poisson-Boltzmann Theory. Journal of the American Chemical Society, 2006, 128, 7796-7806.	13.7	45
1121	Absence of superheating for ice with a free surface: a new method of determining the melting point of different water models. Molecular Physics, 2006, 104, 3583-3592.	1.7	63
1122	A Molecular Dynamics Investigation of Hydrolytic Polymerization in a Metal-Hydroxide Gel. Journal of Physical Chemistry B, 2006, 110, 7107-7112.	2.6	12
1123	Confusing Cause and Effect: Energy-Entropy Compensation in the Preferential Solvation of a Nonpolar Solute in Dimethyl Sulfoxide/Water Mixtures. Journal of Physical Chemistry B, 2006, 110, 12104-12112.	2.6	26
1124	Molecular Dynamics Study of 2-Nitrophenyl Octyl Ether and Nitrobenzene. Journal of Physical Chemistry B, 2006, 110, 12530-12538.	2.6	24
1125	Molecular dynamics simulation of interface dynamics during the fcc-bcc transformation of a martensitic nature. Physical Review B, 2006, 73, .	3.2	52

#	ARTICLE	IF	CITATIONS
1126	Transmembrane Helix~Helix Interactions:~ Comparative Simulations of the Glycophorin A Dimer. Biochemistry, 2006, 45, 14298-14310.	2.5	65
1127	Atomic-scale simulations of strain localization in three-dimensional model amorphous solids. Physical Review B, 2006, 73, .	3.2	154
1128	Inverse Temperature Transition of a Biomimetic Elastin Model:~ Reactive Flux Analysis of Folding/Unfolding and Its Coupling to Solvent Dielectric Relaxation~. Journal of Physical Chemistry B, 2006, 110, 3576-3587.	2.6	28
1129	Epitaxial Transition from Gyroid to Cylinder in a Diblock Copolymer Melt. Macromolecules, 2006, 39, 2340-2349.	4.8	65
1130	Molecular Dynamics Modeling of the Structures and Binding Energies of ~-Nickel Hydroxides and Nickel~Aluminum Layered Double Hydroxides Containing Various Interlayer Guest Anions. Chemistry of Materials, 2006, 18, 4405-4414.	6.7	79
1131	Assessment of isobaric-isothermal (NPT) simulations for finite systems. Computational Materials Science, 2006, 37, 526-536.	3.0	17
1132	Molecular simulations of metal adsorption to bacterial surfaces. Geochimica Et Cosmochimica Acta, 2006, 70, 5075-5088.	3.9	32
1133	Atomic assembly during GaN film growth: Molecular dynamics simulations. Physical Review B, 2006, 73, .	3.2	56
1134	Exploring the Gating Mechanism in the ClC Chloride Channel via Metadynamics. Journal of Molecular Biology, 2006, 361, 390-398.	4.2	53
1135	Molecular dynamics simulation of intrinsic and extrinsic mechanical properties of amorphous metals. Intermetallics, 2006, 14, 1005-1010.	3.9	60
1136	Vacancy-induced densification of silica glass. Journal of Non-Crystalline Solids, 2006, 352, 3320-3325.	3.1	13
1137	Elastic properties of two-dimensional soft discs of various diameters at zero temperature. Journal of Non-Crystalline Solids, 2006, 352, 4292-4298.	3.1	8
1138	Poisson~ ratio of orientationally disordered hard dumbbell crystal in three dimensions. Journal of Non-Crystalline Solids, 2006, 352, 4269-4278.	3.1	10
1140	Mechanical Properties of Amorphous Metal with Dispersed Nanocrystalline Particles: Molecular Dynamics Study on Crystal Volume Fraction and Size Effects. JSME International Journal Series A-Solid Mechanics and Material Engineering, 2006, 49, 513-521.	0.4	3
1141	Evaluation of Mechanical Properties and Negative Poisson's Ratio Behavior in Crystalline SiO2 Materials: An Atomistic Approach. Nihon Kikai Gakkai Ronbunshu, A Hen/Transactions of the Japan Society of Mechanical Engineers, Part A, 2006, 72, 823-829.	0.2	1
1142	Atomistic Molecular Dynamics simulation of short~ chain branched polyethylene melts. Computer Aided Chemical Engineering, 2006, 22, 333-357.	0.5	0
1143	Solid-State Amorphization Observed in Ni~Sc System by Molecular Dynamics Simulation. Journal of the Physical Society of Japan, 2006, 75, 084603.	1.6	3
1144	The effect of water structure and surface charge correlations on the hydration force acting between model hydrophilic surfaces. Molecular Physics, 2006, 104, 3607-3617.	1.7	9

#	ARTICLE	IF	CITATIONS
1145	Molecular dynamics study of nitrobenzene and 2-nitrophenyloctyl ether saturated with water. <i>Molecular Physics</i> , 2006, 104, 3627-3634.	1.7	7
1146	Molecular Dynamics Simulations of Shape-Memory Behavior Based on Martensite Transformation and Shear Deformation. <i>JSME International Journal Series A-Solid Mechanics and Material Engineering</i> , 2006, 49, 300-306.	0.4	9
1147	A comparative study of helium atom diffusion via an interstitial mechanism in nickel and palladium. <i>Physica Status Solidi (B): Basic Research</i> , 2006, 243, 579-583.	1.5	22
1148	A study of the behavior of helium atoms at Ni grain boundaries. <i>Physica Status Solidi (B): Basic Research</i> , 2006, 243, 2702-2710.	1.5	20
1149	DNA-decorated carbon nanotubes for chemical sensing. <i>Physica Status Solidi (B): Basic Research</i> , 2006, 243, 3252-3256.	1.5	24
1150	Simulation and analysis of the migration mechanism of 15° tilt grain boundaries in an fcc metal. <i>Acta Materialia</i> , 2006, 54, 623-633.	7.9	46
1151	Direct, static measurement of single-crystal Young's moduli of the zeolite natrolite: Comparison with dynamic studies and simulations. <i>Acta Materialia</i> , 2006, 54, 2533-2545.	7.9	33
1152	Structure stability and magnetic properties of the Ni-Ru system studied by ab initio and molecular dynamics calculations together with ion beam mixing. <i>Acta Materialia</i> , 2006, 54, 3375-3381.	7.9	22
1153	Nonequilibrium solid phases studied by thermodynamic calculation, molecular dynamics simulation, ab initio calculation and ion-beam manipulation in an immiscible Au-Co system at equilibrium. <i>Acta Materialia</i> , 2006, 54, 5293-5304.	7.9	11
1154	Clustering of topological defects in superheated metals. <i>Materials Science &amp; Engineering A: Structural Materials: Properties, Microstructure and Processing</i> , 2006, 416, 33-39.	5.6	4
1155	Study on elastic constant softening in stress-induced martensitic transformation by molecular dynamics simulation. <i>Materials Science &amp; Engineering A: Structural Materials: Properties, Microstructure and Processing</i> , 2006, 438-440, 113-117.	5.6	10
1156	Temperature and pressure dependence of the some elastic and lattice dynamical properties of copper: a molecular dynamics study. <i>Physica B: Condensed Matter</i> , 2006, 381, 96-102.	2.7	10
1157	Anisotropic diffusion of Cu adatoms on strained Cu (1 1 1) surface. <i>Applied Surface Science</i> , 2006, 253, 1748-1752.	6.1	4
1158	High pressure melting of MgO. <i>Physics Letters, Section A: General, Atomic and Solid State Physics</i> , 2006, 353, 221-225.	2.1	16
1159	Thermal expansivity and bulk modulus of ZnO with NaCl-type cubic structure at high pressures and temperatures. <i>Physics Letters, Section A: General, Atomic and Solid State Physics</i> , 2006, 360, 362-366.	2.1	11
1160	Molecular-dynamics simulation-based cohesive zone representation of intergranular fracture processes in aluminum. <i>Journal of the Mechanics and Physics of Solids</i> , 2006, 54, 1899-1928.	4.8	196
1161	Molecular dynamics simulations of grain growth in nanocrystalline Ag. <i>Journal of Crystal Growth</i> , 2006, 286, 512-517.	1.5	16
1162	Study of martensitic transformation by use of Monte-Carlo method and molecular dynamics. <i>Materials Science &amp; Engineering A: Structural Materials: Properties, Microstructure and Processing</i> , 2006, 438-440, 95-98.	5.6	7

#	ARTICLE	IF	CITATIONS
1163	Heat capacity of ZnO with cubic structure at high temperatures. Solid State Communications, 2006, 140, 219-224.	1.9	35
1164	Vibrational spectroscopy of brucite: A molecular simulation investigation. American Mineralogist, 2006, 91, 1188-1196.	1.9	34
1165	The effect of pressure on the elastic constants of Cu, Ag and Au: a molecular dynamics study. Open Physics, 2006, 4, .	1.7	2
1166	Sum Rules for the Quasi-Static and Visco-Elastic Response of Disordered Solids at Zero Temperature. Journal of Statistical Physics, 2006, 123, 415-453.	1.2	151
1167	Atomic Scale Chemo-mechanics of Silica: Nano-rod Deformation and Water Reaction. Journal of Computer-Aided Materials Design, 2006, 13, 135-159.	0.7	16
1168	Model of the whole rat AT1 receptor and the ligand-binding site. Journal of Molecular Modeling, 2006, 12, 325-337.	1.8	29
1169	Equations of state of CaSiO <sub>3</sub> Perovskite: a molecular dynamics study. Physics and Chemistry of Minerals, 2006, 33, 126-137.	0.8	10
1170	Ab initio study of Ti <sub>3</sub> Si <sub>0.5</sub> Ge <sub>0.5</sub> C <sub>2</sub> under pressure. Journal of Physics and Chemistry of Solids, 2006, 67, 2149-2153.	4.0	5
1171	Piezoelectric coefficients by molecular dynamics simulations in the constant stress ensemble: A case study of quartz. Computer Physics Communications, 2006, 174, 17-23.	7.5	7
1172	Molecular dynamics simulation of thermal stability of nanocrystalline vanadium. Science in China Series D: Earth Sciences, 2006, 49, 400-407.	0.9	1
1173	Atomistic simulations of grain boundary migration in copper. Metallurgical and Materials Transactions A: Physical Metallurgy and Materials Science, 2006, 37, 1757-1771.	2.2	31
1174	Atomistic simulation of the effect of dislocations on temperature rise during high-strain-rate deformation. Metals and Materials International, 2006, 12, 331-338.	3.4	4
1175	Does metallic glass have a backbone? The role of percolating short range order in strength and failure. Scripta Materialia, 2006, 54, 381-386.	5.2	79
1176	The role of loop ZA and Pro371 in the function of yeast Gcn5p bromodomain revealed through molecular dynamics and experiment. Journal of Molecular Recognition, 2006, 19, 1-9.	2.1	20
1177	Glass Transition Temperature and Chain Flexibility of Ethylene-Norbornene Copolymers from Molecular Dynamics Simulations. Macromolecular Theory and Simulations, 2006, 15, 457-468.	1.4	10
1178	Early stages of disordering processes at the impact between rough surfaces: a molecular dynamics study. Journal of Physics Condensed Matter, 2006, 18, 8723-8736.	1.8	0
1179	Size Effects on Miscibility and Glass Transition Temperature of Binary Polymer Blend Films. Langmuir, 2006, 22, 1241-1246.	3.5	26
1180	Calculation of Elastic Constants of Ag/Pd Superlattice Thin Films by Molecular Dynamics with Many-Body Potentials. Chinese Physics Letters, 2006, 23, 2913-2916.	3.3	3



#	ARTICLE	IF	CITATIONS
1181	Coupling of structural and energetic fluctuations in Co nanometre-sized particles. Nanotechnology, 2006, 17, 2027-2031.	2.6	7
1182	Chapter 3 Ab initio Molecular Dynamics: Dynamics and Thermodynamic Properties. Contemporary Concepts of Condensed Matter Science, 2006, 2, 55-95.	0.5	1
1183	Investigation on quenching at a high-angle Cu grain boundary on an atomic scale. Chinese Physics B, 2006, 15, 610-617.	1.3	11
1184	Constant surface-tension molecular-dynamics simulation methods for anisotropic systems. Journal of Chemical Physics, 2006, 124, 064705.	3.0	14
1185	Fully flexible unit cell simulation with recursive thermostat chains. Journal of Chemical Physics, 2006, 125, 184105.	3.0	5
1186	Solid-liquid transitions of sodium chloride at high pressures. Journal of Chemical Physics, 2006, 125, 154510.	3.0	19
1187	Comparative study of microstructural evolution during melting and crystallization. Journal of Chemical Physics, 2006, 125, 014503.	3.0	31
1188	The behavior of reorientational correlation functions of water at the water-lipid bilayer interface. Journal of Chemical Physics, 2006, 125, 094713.	3.0	42
1189	The Jarzynski identity derived from general Hamiltonian or non-Hamiltonian dynamics reproducing NVT or NPT ensembles. Journal of Chemical Physics, 2006, 125, 144109.	3.0	41
1190	Computer simulation of two new solid phases of water: Ice XIII and ice XIV. Journal of Chemical Physics, 2006, 125, 116101.	3.0	15
1191	Modeling the Effect of Texture on the Deformation Mechanisms of Nanocrystalline Materials at the Atomistic Scale. , 2006, , 289-297.		2
1192	Collective motion of atoms in grain boundary migration of a bcc metal. Philosophical Magazine, 2006, 86, 5885-5895.	1.6	7
1193	Low-energy sputtering events at free surfaces near anti-phase and grain boundaries in Ni <sub>3</sub> Al. Philosophical Magazine, 2006, 86, 4243-4258.	1.6	2
1194	Numerical Simulation of Residual Stresses at the Grain and Sub-Grain Length Scale Using Atomistic Modeling. Materials Science Forum, 2006, 524-525, 517-522.	0.3	1
1195	Ab initio simulations in liquid caesium at high pressure and temperature. Physical Review B, 2006, 73, .	3.2	28
1196	Atomistic simulation of amorphization thermokinetics in lanthanum pyrozoirconate. Applied Physics Letters, 2006, 88, 051912.	3.3	42
1197	Exploration of NVE classical trajectories as a tool for molecular crystal structure prediction, with tests on ice polymorphs. Journal of Chemical Physics, 2006, 124, 204705.	3.0	26
1198	Stress distribution and mechanical properties of free and assembled Ni <sub>3</sub> Al nanoclusters. Physical Review B, 2006, 73, .	3.2	12



#	ARTICLE	IF	CITATIONS
1199	Precursors to stress-induced martensitic transformations and associated superelasticity: Molecular dynamics simulations and an analytical theory. <i>Physical Review B</i> , 2006, 74, .	3.2	30
1200	Adding salt to an aqueous solution of t-butanol: Is hydrophobic association enhanced or reduced?. <i>Journal of Chemical Physics</i> , 2006, 124, 154508.	3.0	17
1201	Nonplanar core and dynamical behavior of screw dislocations in copper at high velocities. <i>Physical Review B</i> , 2006, 74, .	3.2	26
1202	An Atomistic Study on Shape-Memory Effect by Shear Deformation and Phase Transformation. <i>Mechanics of Advanced Materials and Structures</i> , 2006, 13, 197-204.	2.6	12
1203	Hydration force between model hydrophilic surfaces: Computer simulations. <i>Journal of Chemical Physics</i> , 2006, 124, 101101.	3.0	50
1204	Analysis of elastic stability and structural response of face-centered cubic crystals subject to [110] loading. <i>Applied Physics Letters</i> , 2006, 89, 181907.	3.3	5
1205	Solubility of simple, nonpolar compounds in TIP4P-Ew. <i>Journal of Chemical Physics</i> , 2006, 124, 016102.	3.0	25
1206	Numerical simulations of atomic-scale disordering processes at impact between two rough crystalline surfaces. <i>Physical Review B</i> , 2006, 74, .	3.2	47
1207	Coarse-grained model for a molecular crystal. <i>Applied Physics Letters</i> , 2006, 89, 021919.	3.3	16
1209	TENSILE FAILURE OF SINGLE-CRYSTAL AND NANOCRYSTALLINE LENNARD-JONES SOLIDS UNDER UNIAXIAL STRAIN. <i>International Journal of Modern Physics C</i> , 2006, 17, 1551-1561.	1.7	10
1210	Only One Protomer Is Active in the Dimer of SARS 3C-like Proteinase*. <i>Journal of Biological Chemistry</i> , 2006, 281, 13894-13898.	3.4	104
1211	MD simulation of martensitic transformations in TiNi alloys with MEAM. <i>Molecular Simulation</i> , 2007, 33, 459-461.	2.0	32
1212	Atomistic Simulations of Interface Properties in Metals. , 2007, , .		2
1213	Conformational analysis of lipid molecules by self-organizing maps. <i>Journal of Chemical Physics</i> , 2007, 126, 054707.	3.0	17
1214	Molecular dynamics simulations of local field factors. <i>Journal of Chemical Physics</i> , 2007, 127, 014501.	3.0	4
1215	Deprotonation by Dehydration: The Origin of Ammonium Sensing in the AmtB Channel. <i>PLoS Computational Biology</i> , 2007, 3, e22.	3.2	40
1216	Cooperative atomic displacements at sheared twist (001) grain boundaries. <i>Journal of Physics Condensed Matter</i> , 2007, 19, 396005.	1.8	2
1217	Metastable phase formation in the immiscible Cu–Co system studied by thermodynamic, molecular dynamics and ab initio calculations together with ion beam mixing. <i>Journal of Physics Condensed Matter</i> , 2007, 19, 026219.	1.8	8

#	ARTICLE	IF	CITATIONS
1218	A methodology for coupling an atomic model with a continuum model using an extended Lagrange function. Journal of Physics Condensed Matter, 2007, 19, 246203.	1.8	3
1219	Demixing phenomena in NiAl nanometre-sized particles. Nanotechnology, 2007, 18, 065708.	2.6	21
1220	Heat Capacity and Gruneisen Parameter for GaN with Zinc-Blende Structure. Chinese Journal of Chemical Physics, 2007, 20, 233-236.	1.3	10
1221	The calculation of some thermoelastic properties and pressure-temperature ( $P$ - $T$ ) diagrams of Rh and Sr using molecular dynamics simulation. Journal of Physics Condensed Matter, 2007, 19, 326204.	1.8	3
1222	Dynamics of atomic species involved in shear-induced displacements at sliding symmetrical grain boundaries: a numerical study. Journal of Physics Condensed Matter, 2007, 19, 096008.	1.8	4
1223	Distinct atomic structures of the Ni-Nb metallic glasses formed by ion beam mixing. Journal of Applied Physics, 2007, 102, .	2.5	9
1224	Atomistic simulations of the hcp-to-fcc transition in nanometer-sized Co domains embedded in a Cu matrix under different pressure and stress conditions. Physical Review B, 2007, 76, .	3.2	1
1225	Monte Carlo Simulations of Semicrystalline Polyethylene: Interlamellar Domain and Crystal-Melt Interface. , 2007, , 261-284.		3
1226	Evolutionary approach for finding the atomic structure of steps on stable crystal surfaces. Physical Review B, 2007, 75, .	3.2	17
1227	Stability of simple cubic crystals. Applied Physics Letters, 2007, 90, 161910.	3.3	11
1228	Surface tension of the most popular models of water by using the test-area simulation method. Journal of Chemical Physics, 2007, 126, 154707.	3.0	635
1229	Simple monoclinic crystal phase in suspensions of hard ellipsoids. Physical Review E, 2007, 75, 020402.	2.1	54
1230	Structural stability and characteristics of the metastable Ag-W phases studied by ab initio and molecular dynamics calculations. Journal of Applied Physics, 2007, 101, 063512.	2.5	9
1231	Interatomic potential for the structure and energetics of tetrahedrally coordinated silica polymorphs. Physical Review B, 2007, 75, .	3.2	10
1232	Interaction of Voids and Nanoductility in Silica Glass. Physical Review Letters, 2007, 99, 155506.	7.8	60
1233	Formation and atomic configuration of binary metallic glasses studied by ion beam mixing and molecular dynamics simulation. Journal of Applied Physics, 2007, 101, 124905.	2.5	4
1234	Li Ion Diffusion Mechanisms in the Crystalline Electrolyte $\text{Li}_3\text{LiPO}_4$ . Journal of the Electrochemical Society, 2007, 154, A999.	2.9	66
1235	Molecular dynamics simulation of Ga penetration along symmetric tilt grain boundaries in an Al bicrystal. Physical Review B, 2007, 76, .	3.2	34

#	Mechanisms of $\text{Li}^+$ diffusion in crystalline $\text{Li}^3$ and $\text{Li}^2$	IF	CITATIONS
1236	First-principles study of the energy-gap composition dependence of Zn $\text{B}_{\text{S}}$ ternary alloys. Physical Review B, 2007, 75, .	3.2	93
1237	Dipole-Quadrupole Force Ratios Determine the Ability of Potential Models to Describe the Phase Diagram of Water. Physical Review Letters, 2007, 98, 237801.	7.8	69
1239	Computer simulation of model cohesive powders: Influence of assembling procedure and contact laws on low consolidation states. Physical Review E, 2007, 75, 011303.	2.1	111
1240	Mechanical properties of glass forming systems. Physical Review E, 2007, 76, 052401.	2.1	12
1241	Molecular dynamics calculations of the crystal-melt interfacial mobility for hexagonal close-packed Mg. Physical Review B, 2007, 75, .	3.2	55
1242	Atomistic simulations of crack nucleation and intergranular fracture in bulk nanocrystalline nickel. Physical Review B, 2007, 76, .	3.2	70
1243	Empirical potential for the interaction between molecular hydrogen and graphite. Physical Review B, 2007, 75, .	3.2	40
1244	Size Effects on Miscibility and Glass Transition Temperature of PS/TMPC Blend Films: a Simulation and Thermodynamic Approach. Key Engineering Materials, 2007, 334-335, 105-108.	0.4	1
1245	Elastic constants and thermodynamic properties of Mg-Pr, Mg-Dy, Mg-Y intermetallics with atomistic simulations. Journal Physics D: Applied Physics, 2007, 40, 7584-7592.	2.8	30
1246	Atomic Simulations on the Grain Subdivision of a Crystalline Metal. Materials Science Forum, 2007, 561-565, 1983-1986.	0.3	0
1247	Molecular dynamics studies of AChBP with nicotine and carbamylcholine: the role of water in the binding pocket. Protein Engineering, Design and Selection, 2007, 20, 353-359.	2.1	88
1248	Global vs. Local Instability of Disordered Systems: Local Lattice Instability Analysis on External Loading Conditions. Nihon Kikai Gakkai Ronbunshu, A Hen/Transactions of the Japan Society of Mechanical Engineers, Part A, 2007, 73, 66-72.	0.2	2
1249	Introduction to Zeolite Modeling. Reviews in Computational Chemistry, 2007, , 137-223.	1.5	8
1250	Combination method for the calculation of elastic constants. Physical Review B, 2007, 75, .	3.2	26
1252	Molecular dynamics simulations. , 0, , 197-262.		0
1253	The finite element method for partial differential equations. , 0, , 423-447.		1
1254	A Molecular Dynamics Study of the Epitaxial Growth of Metallic Nanoclusters Softly Deposited on Substrates with Very Different Lattice Parameter. Journal of Physics: Conference Series, 2007, 61, 915-919.	0.4	1

#	ARTICLE	IF	CITATIONS
1255	Dynamics and Function in a Bacterial ABC Transporter:Â Simulation Studies of the BtuCDF System and Its Componentsâ€. Biochemistry, 2007, 46, 2767-2778.	2.5	59
1256	A multidomain outer membrane protein from Pasteurella multocida: Modelling and simulation studies of PmOmpA. Biochimica Et Biophysica Acta - Biomembranes, 2007, 1768, 2831-2840.	2.6	19
1257	Classical molecular dynamics simulation of uranium monocarbide (UC). Computational Materials Science, 2007, 40, 562-568.	3.0	9
1258	Heterogeneity Even at the Speed Limit of Folding: Large-scale Molecular Dynamics Study of a Fast-folding Variant of the Villin Headpiece. Journal of Molecular Biology, 2007, 374, 806-816.	4.2	182
1259	An atomistic study of mechanical deformation of nanostructured Ni3Al synthesized by cluster compaction. Journal of Alloys and Compounds, 2007, 434-435, 559-564.	5.5	2
1260	Solid solution mechanism and thermodynamic properties of Tiâ€“Re alloy system: Experiment and theory. Intermetallics, 2007, 15, 1116-1121.	3.9	4
1261	Phases and Crystal Structures. Pergamon Materials Series, 2007, 12, 1-86.	0.2	5
1262	Atomistic mechanism of interfacial reaction and asymmetric growth kinetics in an immiscibleCuâ~Rusystem at equilibrium. Physical Review B, 2007, 75, .	3.2	22
1263	Picosecond fluctuating protein energy landscape mapped by pressure temperature molecular dynamics simulation. Proceedings of the National Academy of Sciences of the United States of America, 2007, 104, 17261-17265.	7.1	71
1264	Polyunsaturation in Lipid Membranes:â€™ Dynamic Properties and Lateral Pressure Profiles. Journal of Physical Chemistry B, 2007, 111, 3139-3150.	2.6	180
1265	A Statistical Approach for the Concurrent Coupling of Molecular Dynamics and Finite Element Methods. , 2007, , .		2
1266	Properties of ices at 0 K: A test of water models. Journal of Chemical Physics, 2007, 127, 154518.	3.0	32
1267	Size effects on the Kauzmann temperature and related thermodynamic parameters of Ag nanoparticles. Nanotechnology, 2007, 18, 255706.	2.6	20
1268	Water Permeation through a Subnanometer Boron Nitride Nanotube. Journal of the American Chemical Society, 2007, 129, 2748-2749.	13.7	205
1269	Molecular Dynamics Simulations of Hydrophobic Associations in Aqueous Salt Solutions Indicate a Connection between Water Hydrogen Bonding and the Hofmeister Effect. Journal of the American Chemical Society, 2007, 129, 14887-14898.	13.7	151
1270	Structure and UVâ~Vis Spectrum of C<sub>60</sub> Fullerene in Ethanol:â€™ A Sequential Molecular Dynamics/Quantum Mechanics Study. Journal of Physical Chemistry B, 2007, 111, 11935-11939.	2.6	40
1271	Off-Axis Elastic Properties and the Effect of Extraframework Species on Structural Flexibility of the NAT-Type Zeolites:Â Simulations of Structure and Elastic Properties. Chemistry of Materials, 2007, 19, 2423-2434.	6.7	59
1272	Applied Computational Materials Modeling. , 2007, , .		8

#	ARTICLE	IF	CITATIONS
1273	The mechanism of chemical disordering in Cu <sub>3</sub> Au nanometre-sized systems. <i>Nanotechnology</i> , 2007, 18, 235706.	2.6	19
1274	Bridging Molecular, Particulate, and Continuum Mechanics for Geomechanics Application. , 2007, , .		4
1275	Melting dynamics of superheated argon: Nucleation and growth. <i>Journal of Chemical Physics</i> , 2007, 126, 034505.	3.0	21
1276	Large-Scale Motions and Electrostatic Properties of Furin and HIV-1 Protease. <i>Journal of Physical Chemistry A</i> , 2007, 111, 12327-12332.	2.5	14
1277	Dynamical thermal conductivity of argon crystal. <i>Journal of Applied Physics</i> , 2007, 102, 043514.	2.5	47
1278	Coarse molecular-dynamics analysis of stress-induced structural transitions in crystals. <i>Applied Physics Letters</i> , 2007, 90, 171910.	3.3	8
1279	Size-dependent effects on equilibrium stress and strain in nickel nanowires. <i>Physical Review B</i> , 2007, 76, .	3.2	24
1280	New B <sub>2</sub> O <sub>3</sub> Crystals Predicted from Concurrent Molecular Dynamics Simulations and First-Principles Calculations. <i>Journal of Physical Chemistry C</i> , 2007, 111, 13712-13720.	3.1	21
1281	Internal states of model isotropic granular packings. III. Elastic properties. <i>Physical Review E</i> , 2007, 76, 061304.	2.1	126
1282	Equation of State, Thermal Expansion Coefficient, and Isothermal Compressibility for Ices Ih, II, III, V, and VI, as Obtained from Computer Simulation. <i>Journal of Physical Chemistry C</i> , 2007, 111, 15877-15888.	3.1	39
1283	Hydrophobic Solvation: Aqueous Methane Solutions. <i>Journal of Chemical Education</i> , 2007, 84, 864.	2.3	6
1284	Catabolite Activator Protein in Aqueous Solution: A Molecular Simulation Study. <i>Journal of Physical Chemistry B</i> , 2007, 111, 1496-1501.	2.6	14
1285	Molecular Dynamics Simulations of Bilayers Containing Mixtures of Sphingomyelin with Cholesterol and Phosphatidylcholine with Cholesterol. <i>Journal of Physical Chemistry B</i> , 2007, 111, 12888-12897.	2.6	57
1286	Intrinsic Structure and Dynamics of the Water/Nitrobenzene Interface. <i>Journal of Physical Chemistry C</i> , 2007, 111, 17612-17626.	3.1	113
1287	Coarse-Grained Protein Model Coupled with a Coarse-Grained Water Model: A Molecular Dynamics Study of Polyalanine-Based Peptides. <i>Journal of Chemical Theory and Computation</i> , 2007, 3, 2146-2161.	5.3	42
1288	Molecular Dynamics Simulation Studies of Self-Assembly of Racemic (R)/(S)-2-Bromohexadecanoic Acid on a Graphite Surface: Enantio-pure or Enantio-mixed Domains?. <i>Journal of Physical Chemistry C</i> , 2007, 111, 18243-18250.	3.1	10
1289	Molecular Thermodynamics of Methane Solvation in tert-Butanol~Water Mixtures. <i>Journal of Chemical Theory and Computation</i> , 2007, 3, 194-200.	5.3	19
1290	Insight into the Putative Specific Interactions between Cholesterol, Sphingomyelin, and Palmitoyl-Oleoyl Phosphatidylcholine. <i>Biophysical Journal</i> , 2007, 92, 1125-1137.	0.5	122

#	ARTICLE	IF	CITATIONS
1291	The cPLA2 C2 <sup>+</sup> Domain in Solution: Structure and Dynamics of Its Ca <sup>2+</sup> -activated and Cation-Free States. Biophysical Journal, 2007, 92, 966-976.	0.5	7
1292	Cholesterol Surrogates: A Comparison of Cholesterol and 16:0 Ceramide in POPC Bilayers. Biophysical Journal, 2007, 92, 920-927.	0.5	71
1293	Molecular Dynamics Simulations of SOPS and Sphingomyelin Bilayers Containing Cholesterol. Biophysical Journal, 2007, 92, 1284-1295.	0.5	47
1295	Internal states of model isotropic granular packings. I. Assembling process, geometry, and contact networks. Physical Review E, 2007, 76, 061302.	2.1	150
1296	Interaction of Hydrated Amino Acids with Metal Surfaces: A Multiscale Modeling Description. Journal of Physical Chemistry C, 2007, 111, 2631-2642.	3.1	50
1297	Role of defective icosahedra in undercooled copper. Physical Review B, 2007, 75, .	3.2	24
1298	Pressure and Salt Effects in Simulated Water: Two Sides of the Same Coin?. Angewandte Chemie - International Edition, 2007, 46, 8907-8911.	13.8	79
1300	Molecular Dynamic Simulations of Ionic Liquids: A Reliable Description of Structure, Thermodynamics and Dynamics. ChemPhysChem, 2007, 8, 2464-2470.	2.1	355
1301	Application of a shell model in molecular dynamics simulation to ZnO with zinc-blende cubic structure. Solid State Communications, 2007, 142, 15-19.	1.9	16
1302	First-principles investigation of pressure-induced changes in structural and electronic properties of Y 2C3 superconductor. Solid State Communications, 2007, 142, 536-540.	1.9	4
1303	Structural and thermodynamic properties of MgSiO3 perovskite under high pressure and high temperature. Solid State Communications, 2007, 144, 264-268.	1.9	8
1304	Molecular dynamics study of oxygen self-diffusion in reduced CeO2. Solid State Ionics, 2007, 178, 1421-1427.	2.7	72
1305	Theoretical and experimental studies of the structure and dynamics of the CaF2(111) surface. Surface Science, 2007, 601, 411-418.	1.9	12
1306	Epitaxial matching of small metallic nanoclusters in large-misfit systems. Vacuum, 2007, 81, 1515-1518.	3.5	4
1307	Simulations of nanoindentation in a thin amorphous metal film. Thin Solid Films, 2007, 515, 3179-3182.	1.8	20
1308	Mechanical response of He clusters in bcc iron. Nuclear Instruments & Methods in Physics Research B, 2007, 255, 57-62.	1.4	2
1309	Ice: A fruitful source of information about liquid water. Journal of Molecular Liquids, 2007, 136, 214-220.	4.9	15
1310	Comparative investigations of the P-V-T relationship of MgO with shell and breathing shell model molecular dynamics simulations. Physica B: Condensed Matter, 2007, 399, 9-16.	2.7	6

#	ARTICLE	IF	CITATIONS
1311	Structure of the spinning apparatus of a wild silkworm <i>Samia cynthia ricini</i> and molecular dynamics calculation on the structural change of the silk fibroin. <i>Polymer</i> , 2007, 48, 2064-2070.	3.8	28
1312	Molecular structure of side-chain liquid crystalline polysiloxane in the smectic C phase from X-ray diffraction and molecular modeling. <i>Polymer</i> , 2007, 48, 5161-5173.	3.8	1
1313	Molecular dynamics simulation of Pâ€“Vâ€“T relationship of ZnO with rock-salt structure using pair-wise interactions. <i>Journal of Physics and Chemistry of Solids</i> , 2007, 68, 249-255.	4.0	11
1314	Core charge distribution and self assembly of columnar phases: the case of triphenylenes and azatriphenylenes. <i>Chemistry Central Journal</i> , 2007, 1, 15.	2.6	20
1315	Positron annihilation at grain boundaries in metals. <i>Physica Status Solidi C: Current Topics in Solid State Physics</i> , 2007, 4, 3461-3464.	0.8	6
1316	Positron annihilation in structural vacancies in Alâ€“rich NiAl alloys. <i>Physica Status Solidi C: Current Topics in Solid State Physics</i> , 2007, 4, 3534-3537.	0.8	0
1317	Elastic properties of two-dimensional soft polydisperse trimers at zero temperature. <i>Physica Status Solidi (B): Basic Research</i> , 2007, 244, 943-954.	1.5	15
1318	Formation of amorphous phases in an immiscible Cuâ€“Nb system studied by molecular dynamics simulation and ion beam mixing. <i>Scripta Materialia</i> , 2007, 57, 157-160.	5.2	24
1319	The metallic glass-forming region of a ternary metal system predicted by interatomic potential through molecular dynamics simulation. <i>Scripta Materialia</i> , 2007, 57, 161-164.	5.2	4
1320	How Does a Voltage Sensor Interact with a Lipid Bilayer? Simulations of a Potassium Channel Domain. <i>Structure</i> , 2007, 15, 235-244.	3.3	96
1321	Conformational Change in an MFS Protein: MD Simulations of LacY. <i>Structure</i> , 2007, 15, 873-884.	3.3	70
1322	A molecular dynamics study on iridium. <i>Open Physics</i> , 2007, 5, .	1.7	3
1323	Nanoscale alloys and core-shell materials: Model predictions of the nanostructure and mechanical properties. <i>Physical Review B</i> , 2007, 75, .	3.2	14
1324	Concerted Molecular Displacements in a Thermally-Induced Solid-State Transformation in Crystals of DL-Norleucine. <i>Journal of the American Chemical Society</i> , 2007, 129, 2542-2547.	13.7	51
1325	On the calculation of velocity-dependent properties in molecular dynamics simulations using the leapfrog integration algorithm. <i>Journal of Chemical Physics</i> , 2007, 127, 184102.	3.0	95
1326	Void coalescence processes quantified through atomistic and multiscale simulation. <i>Journal of Computer-Aided Materials Design</i> , 2007, 14, 425-434.	0.7	29
1327	Molecular dynamics simulations of thermodynamics, elastic constants and solid solution strengths for Mg-Gd alloys. <i>European Physical Journal B</i> , 2007, 57, 305-312.	1.5	21
1328	Dynamics of nanoscale grain-boundary decohesion in aluminum by molecular-dynamics simulation. <i>Journal of Materials Science</i> , 2007, 42, 1466-1476.	3.7	21



#	ARTICLE	IF	CITATIONS
1329	Homogeneous and heterogeneous melting behavior of bulk and nanometer-sized Cu systems: a numerical study. Journal of Materials Science, 2007, 42, 6672-6683.	3.7	15
1330	Cold-active enzymes studied by comparative molecular dynamics simulation. Journal of Molecular Modeling, 2007, 13, 485-497.	1.8	42
1331	Numerical simulations of the melting behavior of bulk and nanometer-sized Cu systems. Physica B: Condensed Matter, 2007, 392, 288-297.	2.7	15
1332	Surface properties of rutile TiO <sub>2</sub> (110) from molecular dynamics and lattice dynamics at 300K: Variable-charge model results. Surface Science, 2007, 601, 5359-5367.	1.9	10
1333	Misfit dislocation network in Cu/Ni multilayers and its behaviors during scratching. Thin Solid Films, 2007, 515, 3698-3703.	1.8	35
1334	Plastic deformation by synchronized rotation of nanolayers under high stress in metals. Materials Science & Engineering A: Structural Materials: Properties, Microstructure and Processing, 2008, 489, 150-157.	5.6	0
1335	Isothermal isobaric molecular dynamics simulation of water. Computational and Theoretical Chemistry, 2008, 867, 39-46.	1.5	6
1336	Computation of interface interactions and mechanical properties of HMX-based PBX with Estane 5703 from atomic simulation. Journal of Materials Science, 2008, 43, 5685-5691.	3.7	21
1337	Multiscale modeling of intergranular fracture in aluminum: constitutive relation for interface debonding. Journal of Materials Science, 2008, 43, 7488-7494.	3.7	33
1338	Molecular dynamics simulations and membrane protein structure quality. European Biophysics Journal, 2008, 37, 403-409.	2.2	33
1339	Multiple shear banding in a computational amorphous alloy model. Applied Physics A: Materials Science and Processing, 2008, 91, 281-285.	2.3	26
1340	Molecular dynamics simulations of the hydration of poly(vinyl methyl ether): Hydrogen bonds and quasi-hydrogen bonds. Science in China Series B: Chemistry, 2008, 51, 736-742.	0.8	5
1341	Water penetration in the low and high pressure native states of ubiquitin. Proteins: Structure, Function and Bioinformatics, 2008, 70, 1175-1184.	2.6	62
1342	Effect of altered glycosylation on the structure of the $\alpha$ 1 domain of $\beta$ 21 integrin: A molecular dynamics study. Proteins: Structure, Function and Bioinformatics, 2008, 73, 989-1000.	2.6	40
1343	Epitaxy of softly deposited small Co nanoclusters on Cu(001) surfaces. Physica Status Solidi (A) Applications and Materials Science, 2008, 205, 1330-1336.	1.8	8
1344	Vibrational properties in nanocrystalline nickels: temperature effects and composite model for thermodynamics. Physica Status Solidi (B): Basic Research, 2008, 245, 1527-1533.	1.5	4
1345	Elastic properties of the fcc crystals of soft spheres with size dispersion at zero temperature. Physica Status Solidi (B): Basic Research, 2008, 245, 606-613.	1.5	13
1346	Pressure-induced phase transitions in silicon studied by neural network-based metadynamics simulations. Physica Status Solidi (B): Basic Research, 2008, 245, 2618-2629.	1.5	68



#	ARTICLE	IF	CITATIONS
1347	Elasticity of periodic and aperiodic structures of polydisperse dimers in two dimensions at zero temperature. <i>Physica Status Solidi (B): Basic Research</i> , 2008, 245, 2463-2468.	1.5	6
1348	Mechanism of Binding of Fluoroquinolones to the Quinolone Resistance-Determining Region of DNA Gyrase: Towards an Understanding of the Molecular Basis of Quinolone Resistance. <i>ChemBioChem</i> , 2008, 9, 2081-2086.	2.6	39
1349	NPT Ensemble MD Simulation Investigation on the Mechanical Properties of HMX/ $F_{2311}$ Polymer-Bonded Explosive. <i>Chinese Journal of Chemistry</i> , 2008, 26, 1969-1972.	4.9	9
1350	Ionic Liquids: Dissecting the Enthalpies of Vaporization. <i>ChemPhysChem</i> , 2008, 9, 549-555.	2.1	123
1351	On the Validity of Stokes-Einstein and Stokes-Einstein-Debye Relations in Ionic Liquids and Ionic-Liquid Mixtures. <i>ChemPhysChem</i> , 2008, 9, 1851-1858.	2.1	142
1352	The Solvent-Dependent Shift of the Amide I Band of a Fully Solvated Peptide as a Local Probe for the Solvent Composition in the Peptide/Solvent Interface. <i>ChemPhysChem</i> , 2008, 9, 2742-2750.	2.1	15
1353	Temperature and Concentration Effects on the Solvophobic Solvation of Methane in Aqueous Salt Solutions. <i>ChemPhysChem</i> , 2008, 9, 2722-2730.	2.1	14
1354	Salt Effects on the Structure of Water Probed by Attenuated Total Reflection Infrared Spectroscopy and Molecular Dynamics Simulations. <i>ChemPhysChem</i> , 2008, 9, 2731-2736.	2.1	25
1355	Modeling the hERG potassium channel in a phospholipid bilayer: Molecular dynamics and drug docking studies. <i>Journal of Computational Chemistry</i> , 2008, 29, 795-808.	3.3	47
1356	Variational boundary conditions for molecular dynamics simulations: Treatment of the loading condition. <i>Journal of Computational Physics</i> , 2008, 227, 10078-10093.	3.8	12
1357	Interatomic potentials of the binary transition metal systems and some applications in materials physics. <i>Physics Reports</i> , 2008, 455, 1-134.	25.6	112
1358	An atomistic investigation of the kinetics of detwinning. <i>Journal of the Mechanics and Physics of Solids</i> , 2008, 56, 1296-1319.	4.8	38
1359	Torsion and bending periodic boundary conditions for modeling the intrinsic strength of nanowires. <i>Journal of the Mechanics and Physics of Solids</i> , 2008, 56, 3242-3258.	4.8	36
1360	Atomistic calculations of lattice constants of mullite with its compositions. <i>Journal of the European Ceramic Society</i> , 2008, 28, 345-351.	5.7	11
1361	Positron annihilation in vacancies at grain boundaries in metals. <i>Applied Surface Science</i> , 2008, 255, 128-131.	6.1	9
1362	A space-time-ensemble parallel nudged elastic band algorithm for molecular kinetics simulation. <i>Computer Physics Communications</i> , 2008, 178, 280-289.	7.5	110
1363	Hydrogen effects on nanovoid nucleation in face-centered cubic single-crystals. <i>Acta Materialia</i> , 2008, 56, 95-104.	7.9	36
1364	Molecular dynamics investigation of deformation twinning in $\beta$ -TiAl sheared along the pseudo-twinning direction. <i>Acta Materialia</i> , 2008, 56, 1065-1074.	7.9	46

#	ARTICLE	IF	CITATIONS
1365	The stress-strain response of nanocrystalline metals: A statistical analysis of atomistic simulations. <i>Acta Materialia</i> , 2008, 56, 4846-4857.	7.9	63
1366	Local order influences initiation of plastic flow in metallic glass: Effects of alloy composition and sample cooling history. <i>Acta Materialia</i> , 2008, 56, 5263-5275.	7.9	378
1367	Continuum interpretation of virial stress in molecular simulations. <i>International Journal of Solids and Structures</i> , 2008, 45, 4340-4346.	2.7	373
1368	Atomistic simulation of Si-Ge clathrate alloys. <i>Chemical Physics</i> , 2008, 344, 299-308.	1.9	9
1369	A molecular dynamics study of interface interactions and mechanical properties of HMX-based PBXs with PEG and HTPB. <i>Computational and Theoretical Chemistry</i> , 2008, 851, 242-248.	1.5	53
1370	Liquid structure of N-butyl-N-methylpyrrolidinium bis-(trifluoromethanesulfonyl) amide ionic liquid studied by large angle X-ray scattering and molecular dynamics simulations. <i>Journal of Molecular Liquids</i> , 2008, 143, 2-7.	4.9	54
1371	Comparison of Protein Force Fields for Molecular Dynamics Simulations. <i>Methods in Molecular Biology</i> , 2008, 443, 63-88.	0.9	171
1372	Ca <sup>2+</sup> dissociation from the C-terminal EF-hand pair in calmodulin: A steered molecular dynamics study. <i>FEBS Letters</i> , 2008, 582, 1355-1361.	2.8	9
1373	A comparative study of two classical force fields on statics and dynamics of [EMIM][BF <sub>4</sub> ] investigated via molecular dynamics simulations. <i>Journal of Chemical Physics</i> , 2008, 129, 224501.	3.0	89
1374	Chapter 12 Molecular Modeling and Simulation Studies of Ion Channel Structures, Dynamics and Mechanisms. <i>Methods in Cell Biology</i> , 2008, 90, 233-265.	1.1	24
1375	Dislocation Cross-Slip in Nanocrystalline fcc Metals. <i>Physical Review Letters</i> , 2008, 100, 235501.	7.8	62
1376	A modified embedded-atom method interatomic potential for the Cu-Zr system. <i>Journal of Materials Research</i> , 2008, 23, 1095-1104.	2.6	45
1377	Pressure-induced structural transformation of CdSe nanocrystals studied with molecular dynamics. <i>Physical Review B</i> , 2008, 77, .	3.2	14
1378	Coarse-Grained Molecular Dynamics Simulations of the Energetics of Helix Insertion into a Lipid Bilayer. <i>Biochemistry</i> , 2008, 47, 11321-11331.	2.5	87
1379	Nonadiabaticity in the iron bcc to hcp phase transformation. <i>Journal of Chemical Physics</i> , 2008, 128, 104703.	3.0	25
1380	Numerical investigation of the stability of Ag-Cu nanorods and nanowires. <i>Physical Review B</i> , 2008, 78, .	3.2	13
1381	Size Effect on the Thermodynamic Properties of Silver Nanoparticles. <i>Journal of Physical Chemistry C</i> , 2008, 112, 2359-2369.	3.1	194
1382	Sliding of Alkylating Anticancer Drugs along the Minor Groove of DNA: New Insights on Sequence Selectivity. <i>Biophysical Journal</i> , 2008, 94, 550-561.	0.5	25

#	ARTICLE	IF	CITATIONS
1383	Molecular Dynamics Simulations of Asymmetric NaCl and KCl Solutions Separated by Phosphatidylcholine Bilayers: Potential Drops and Structural Changes Induced by Strong Na <sup>+</sup> -Lipid Interactions and Finite Size Effects. <i>Biophysical Journal</i> , 2008, 94, 3565-3576.	0.5	106
1384	A Method to Determine Dielectric Constants in Nonhomogeneous Systems: Application to Biological Membranes. <i>Biophysical Journal</i> , 2008, 94, 1185-1193.	0.5	89
1385	The Interaction of Phospholipase A2 with a Phospholipid Bilayer: Coarse-Grained Molecular Dynamics Simulations. <i>Biophysical Journal</i> , 2008, 95, 1649-1657.	0.5	41
1386	Protein-Protein Interaction Investigated by Steered Molecular Dynamics: The TCR-pMHC Complex. <i>Biophysical Journal</i> , 2008, 95, 3575-3590.	0.5	117
1387	Pressure Effects on the Ensemble Dynamics of Ubiquitin Inspected with Molecular Dynamics Simulations and Isotropic Reorientational Eigenmode Dynamics. <i>Biophysical Journal</i> , 2008, 95, 3943-3955.	0.5	10
1388	High-Pressure Studies of 1,3,5,7-Cyclooctatetraene: Experiment and Theory. <i>Journal of Physical Chemistry A</i> , 2008, 112, 11501-11507.	2.5	12
1389	Determination of phase diagrams via computer simulation: methodology and applications to water, electrolytes and proteins. <i>Journal of Physics Condensed Matter</i> , 2008, 20, 153101.	1.8	209
1390	Atomistic Simulations of Dislocations in FCC Metallic Nanocrystalline Materials. <i>Dislocations in Solids</i> , 2008, , 1-42.	1.6	24
1391	Influence of Temperature and Anisotropic Pressure on the Phase Transitions in $\text{In}_2\text{S}_3$ -Cristobalite. <i>Physical Review Letters</i> , 2008, 100, 165502.	7.8	38
1392	Molecular Dynamics Simulation of Self-Assembly of <i>n</i> -Decyltrimethylammonium Bromide Micelles. <i>Langmuir</i> , 2008, 24, 5714-5725.	3.5	94
1393	Molecular Dynamics Simulations. <i>Methods in Molecular Biology</i> , 2008, 443, 3-23.	0.9	51
1394	A Micromechanics-Based Notion of Stress for Use in the Determination of Continuum-Level Mechanical Properties via Molecular Dynamics. , 2008, , 203-234.		1
1395	Water Phase Transition Induced by a Stone-Wales Defect in a Boron Nitride Nanotube. <i>Journal of the American Chemical Society</i> , 2008, 130, 13649-13652.	13.7	26
1396	Conformational and Structural Relaxations of Poly(ethylene oxide) and Poly(propylene oxide) Melts: Molecular Dynamics Study of Spatial Heterogeneity, Cooperativity, and Correlated Forward-Backward Motion. <i>Macromolecules</i> , 2008, 41, 2949-2958.	4.8	32
1397	Cholesterol Packing around Lipids with Saturated and Unsaturated Chains: A Simulation Study. <i>Langmuir</i> , 2008, 24, 6858-6865.	3.5	97
1398	Formation of Ice-like Water Structure on the Surface of an Antifreeze Protein. <i>Journal of Physical Chemistry B</i> , 2008, 112, 6193-6202.	2.6	87
1399	Structure and Dynamics of Water Confined in a Boron Nitride Nanotube. <i>Journal of Physical Chemistry C</i> , 2008, 112, 1812-1818.	3.1	158
1400	Modeling and Molecular Dynamics Simulation of the Human Gonadotropin-Releasing Hormone Receptor in a Lipid Bilayer. <i>Journal of Physical Chemistry B</i> , 2008, 112, 10704-10713.	2.6	34

#	ARTICLE	IF	CITATIONS
1401	Metadynamics Simulations of the High-Pressure Phases of Silicon Employing a High-Dimensional Neural Network Potential. <i>Physical Review Letters</i> , 2008, 100, 185501.	7.8	207
1402	Role of the Active-Site Solvent in the Thermodynamics of Factor Xa Ligand Binding. <i>Journal of the American Chemical Society</i> , 2008, 130, 2817-2831.	13.7	594
1403	The effect of the water/methane interface on methane hydrate cages: The potential of mean force and cage lifetimes. <i>Journal of Chemical Physics</i> , 2008, 129, 034701.	3.0	43
1404	Molecular Modeling of Proteins. <i>Methods in Molecular Biology</i> , 2008, , .	0.9	45
1405	Computing the free energy of molecular solids by the Einstein molecule approach: Ices XIII and XIV, hard-dumbbells and a patchy model of proteins. <i>Journal of Chemical Physics</i> , 2008, 129, 104704.	3.0	58
1406	Surface structure and properties of NiZr model metallic glasses: A molecular dynamics simulation. <i>Journal of Non-Crystalline Solids</i> , 2008, 354, 2060-2065.	3.1	10
1407	Negative Poisson's ratio behavior in the planar model of asymmetric trimers at zero temperature. <i>Journal of Non-Crystalline Solids</i> , 2008, 354, 4242-4248.	3.1	32
1408	Effects of Ni, Ti and Hf on the glass forming ability of the Ni-Ti-Hf ternary alloys. <i>Journal of Alloys and Compounds</i> , 2008, 456, 358-363.	5.5	2
1409	Ring-diffusion mediated homogeneous melting in the superheating regime. <i>Physical Review B</i> , 2008, 77, .	3.2	57
1410	Probing the Structure of DNA~Carbon Nanotube Hybrids with Molecular Dynamics. <i>Nano Letters</i> , 2008, 8, 69-75.	9.1	371
1411	Melting temperature of Pb nanostructural materials from free energy calculation. <i>Journal of Chemical Physics</i> , 2008, 128, 074710.	3.0	23
1412	Solid-state amorphization of an immiscible Nb-Zr system simulated by molecular dynamics. <i>Computational Materials Science</i> , 2008, 42, 550-557.	3.0	9
1413	Development of n-body potentials for hcp-bcc and fcc-bcc binary transition metal systems. <i>Computational Materials Science</i> , 2008, 43, 1207-1215.	3.0	18
1414	Phase behavior and kinetics of a new bond-order potential for silicon. <i>Computational Materials Science</i> , 2008, 44, 274-279.	3.0	22
1415	Why Are Carbon Nanotubes Fast Transporters of Water?. <i>Nano Letters</i> , 2008, 8, 452-458.	9.1	727
1416	Molecular Dynamics Studies of Side Chain Effect on the $\beta$ -1,3-D-Glucan Triple Helix in Aqueous Solution. <i>Biomacromolecules</i> , 2008, 9, 783-788.	5.4	73
1417	Influence of Cu, Cr and C on the irradiation defect in Fe: A molecular dynamics simulation study. <i>Journal of Nuclear Materials</i> , 2008, 373, 28-38.	2.7	13
1418	Molecular Simulation of Water in Carbon Nanotubes. <i>Chemical Reviews</i> , 2008, 108, 5014-5034.	47.7	440

#	ARTICLE	IF	CITATIONS
1419	Comparing crystal–melt interfacial free energies through homogeneous nucleation rates. Journal of Physics Condensed Matter, 2008, 20, 375103.	1.8	2
1420	Systematic Comparison of Empirical Forcefields for Molecular Dynamic Simulation of Insulin. Journal of Physical Chemistry B, 2008, 112, 11137-11146.	2.6	53
1421	Monte Carlo Simulations of a Coarse Grain Model for Block Copolymers and Nanocomposites. Macromolecules, 2008, 41, 4989-5001.	4.8	198
1422	Unfolding and melting of DNA (RNA) hairpins: the concept of structure-specific 2D dynamic landscapes. Physical Chemistry Chemical Physics, 2008, 10, 4227.	2.8	29
1423	An optimized force field for crystalline phases of resorcinol. CrystEngComm, 2008, , .	2.6	3
1424	Computer simulation of model cohesive powders: Plastic consolidation, structural changes, and elasticity under isotropic loads. Physical Review E, 2008, 78, 031305.	2.1	62
1425	A novel model for the molecular dynamics simulation study on mechanical properties of HMX/F <sub>2311</sub> polymer-bonded explosive. Molecular Simulation, 2008, 34, 775-779.	2.0	12
1426	Modeling of Aqueous Poly(oxyethylene) Solutions: 1. Atomistic Simulations. Journal of Physical Chemistry B, 2008, 112, 2388-2398.	2.6	83
1427	Molecular Dynamics Study of the Interface between Water and 2-Nitrophenyl Octyl Ether. Journal of Physical Chemistry B, 2008, 112, 2415-2429.	2.6	44
1428	Molecular Dynamics Simulations of Monofunctionalized Polyhedral Oligomeric Silsesquioxane C <sub>6</sub> H <sub>13</sub> (H <sub>7</sub> Si <sub>8</sub> O <sub>12</sub> ). Journal of Physical Chemistry C, 2008, 112, 3473-3481.	3.1	19
1429	In Situ Polymerization of the 4-Vinylbenzenesulfonic Anion in Ni~Al~Layered Double Hydroxide and Its Molecular Dynamic Simulation. Journal of Physical Chemistry A, 2008, 112, 7671-7681.	2.5	31
1430	Insight into the Mechanism of Inactivation and pH Sensitivity in Potassium Channels from Molecular Dynamics Simulations. Biochemistry, 2008, 47, 7414-7422.	2.5	50
1431	Morphological Changes in Block Copolymer Melts Due to a Variation of Intramolecular Branching. Dissipative Particles Dynamics Study. Macromolecules, 2008, 41, 9904-9913.	4.8	5
1432	Molecular Dynamic Simulation of the Kv1.2 Voltage-Gated Potassium Channel in Open and Closed State Conformations. Journal of Physical Chemistry B, 2008, 112, 16966-16974.	2.6	10
1433	Multiscale Modeling and Simulation of Composite Materials and Structures. , 2008, , .		40
1434	Thermal and pressure-induced martensitic phase transformations in a Ni~Al alloy modelled by Sutton–Chen embedded atom method. Molecular Simulation, 2008, 34, 251-257.	2.0	4
1435	Energetics of Cholesterol Transfer between Lipid Bilayers. Journal of Physical Chemistry B, 2008, 112, 3807-3811.	2.6	62
1436	First-Principles Calculations for Thermodynamic Properties of Perovskite-Type Superconductor MgCNi <sub>3</sub> . Chinese Physics Letters, 2008, 25, 2603-2606.	3.3	6

#	ARTICLE	IF	CITATIONS
1437	Comparison of the Solid Solution Properties of Mg-RE (Gd, Dy, Y) Alloys with Atomistic Simulation. Research Letters in Physics, 2008, 2008, 1-4.	0.2	10
1438	HIV-1 Integrase-DNA Interactions Investigated by Molecular Modelling. Computational and Mathematical Methods in Medicine, 2008, 9, 231-243.	1.3	8
1439	Elastic and electronic properties of perovskite type superconductor MgCNi <sub>3</sub> under pressure. Journal of Physics Condensed Matter, 2008, 20, 325228.	1.8	11
1440	TWO-STATE STRUCTURE OF NANOMETER-SIZED Cu PARTICLES. International Journal of Nanoscience, 2008, 07, 137-150.	0.7	1
1441	Computing the stability diagram of the Trp-cage miniprotein. Proceedings of the National Academy of Sciences of the United States of America, 2008, 105, 17754-17759.	7.1	146
1442	A Role for Leu118 of Loop E in Agonist Binding to the $\alpha 7$ Nicotinic Acetylcholine Receptor. Molecular Pharmacology, 2008, 73, 1659-1667.	2.3	19
1443	Calculating the free energy of self-assembled structures by thermodynamic integration. Journal of Chemical Physics, 2008, 128, 024903.	3.0	87
1444	New concept of solute distribution around a diffusive crystal-solution interface of a binary Lennard-Jones mixture from the viewpoint of molecular dynamics. Journal of Chemical Physics, 2008, 128, 044716.	3.0	6
1445	Thr729 in human topoisomerase I modulates anti-cancer drug resistance by altering protein domain communications as suggested by molecular dynamics simulations. Nucleic Acids Research, 2008, 36, 5645-5651.	14.5	49
1446	A dislocation dynamics study of the strength of stacking fault tetrahedra. Part II: interactions with mixed and edge dislocations. Philosophical Magazine, 2008, 88, 841-863.	1.6	23
1447	Dissociation of minor groove binders from DNA: insights from metadynamics simulations. Nucleic Acids Research, 2008, 36, 5910-5921.	14.5	60
1448	BIOMOLECULAR SENSING USING CARBON NANOTUBES: A SIMULATION STUDY. International Journal of High Speed Electronics and Systems, 2008, 18, 879-887.	0.7	7
1449	An explicit algorithm for fully flexible unit cell simulation with recursive thermostat chains. Journal of Chemical Physics, 2008, 129, 164116.	3.0	1
1450	Abnormal alloying behaviour observed in an immiscible Zr-Nb system. Journal Physics D: Applied Physics, 2008, 41, 095310.	2.8	13
1451	Molecular dynamics simulations of homogeneous solids using multi-layered structures. Europhysics Letters, 2008, 83, 10003.	2.0	0
1452	Thermodynamic properties and elastic constants of Nd-Mg intermetallics: a molecular dynamics study. International Journal of Materials Research, 2008, 99, 42-49.	0.3	1
1453	Engineering molecular mechanics: an efficient static high temperature molecular simulation technique. Nanotechnology, 2008, 19, 285706.	2.6	11
1454	Molecular dynamics study of the hcp-bcc phase transformation in nanocrystalline zirconium. International Journal of Materials Research, 2008, 99, 626-631.	0.3	2



#	ARTICLE	IF	CITATIONS
1455	Thermal resistivity of Si-Ge alloys by molecular-dynamics simulation. Journal of Applied Physics, 2008, 103, .	2.5	50
1456	Structural phase transitions in high-pressure wurtzite to rocksalt phase in GaN and SiC. Applied Physics Letters, 2008, 92, .	3.3	18
1457	Metastable phase formation and magnetic properties of the Fe-Nb system studied by atomistic modeling and ion beam mixing. Journal of Applied Physics, 2008, 104, 014914.	2.5	7
1458	Atomic simulations of the dynamic properties of the $\partial \sigma / \partial \epsilon$ partial dislocation in Si crystal. Physical Review B, 2008, 77, .	3.2	10
1459	Test of the Gouy-Chapman Theory for a Charged Lipid Membrane against Explicit-Solvent Molecular Dynamics Simulations. Physical Review Letters, 2008, 101, 038103.	7.8	47
1460	Molecular dynamics simulations of the enzyme Catechol-O-Methyltransferase: methodological issues. SAR and QSAR in Environmental Research, 2008, 19, 179-189.	2.2	11
1461	Molecular transport across fluid interfaces: Coupling between solute dynamics and interface fluctuations. Physical Review E, 2008, 78, 041605.	2.1	12
1462	Solvophobic Solvation and Interaction of Small Apolar Particles in Imidazolium-Based Ionic Liquids. Physical Review Letters, 2008, 100, 115901.	7.8	19
1463	Solid-State Amorphization Observed in the Cu-Zr System by Molecular Dynamics Simulation. Journal of the Physical Society of Japan, 2008, 77, 104301.	1.6	5
1464	Raman Spectroscopic Study on Alkaline Metal Ion Solvation in 1-Butyl-3-methylimidazolium Bis(trifluoromethanesulfonyl)amide Ionic Liquid. Analytical Sciences, 2008, 24, 1297-1304.	1.6	38
1465	The thickness of a liquid layer on the free surface of ice as obtained from computer simulation. Journal of Chemical Physics, 2008, 129, 014702.	3.0	142
1466	Liquid Structure and the Ion-Ion Interactions of Ethylammonium Nitrate Ionic Liquid Studied by Large Angle X-Ray Scattering and Molecular Dynamics Simulations. Journal of Computer Chemistry Japan, 2008, 7, 125-134.	0.1	97
1467	Molecular Simulations of Nanoparticles in an Explicit Solvent. AIP Conference Proceedings, 2008, , .	0.4	3
1468	Amorphous phase formation, spinodal decomposition, and fractal growth of nanocrystals in an immiscible Hf-Nb system studied by ion beam mixing and atomistic modeling. Journal of Applied Physics, 2008, 103, 084910.	2.5	1
1469	Dinâmica molecular: teoria e aplicação em planejamento de fármacos. Ecletica Química, 2008, 33, 13-24.	0.5	24
1470	Relationship between Grain Boundary Structures and Mechanical Properties of Nanocrystalline Metals with Different Stacking Fault Energy Using Atomic Scale Computational Experiments. Zairyo/Journal of the Society of Materials Science, Japan, 2008, 57, 761-767.	0.2	0
1471	Glass Forming Ability in the Equilibrium Immiscible Ag-Ta System Studied by Molecular Dynamics Simulation and Ion Beam Mixing. Journal of the Physical Society of Japan, 2008, 77, 074601.	1.6	2
1472	Molecular Dynamics Simulations on the Deformation Behavior of Shape Memory Alloy using Multi-Grain Models. Zairyo/Journal of the Society of Materials Science, Japan, 2008, 57, 1217-1223.	0.2	2



#	ARTICLE	IF	CITATION
1473	Coarse-Grained Molecular Dynamics Study of the Interface of Polymer Blends. Nihon Reorogi Gakkaishi, 2009, 37, 75-79.	1.0	9
1474	Material Theories. Oberwolfach Reports, 2010, 6, 3033-3100.	0.0	0
1477	Free energy of a $\gamma$ interstitial defect in bcc Fe: Harmonic and anharmonic contributions. Physical Review B, 2009, 79, .	3.2	10
1478	Molecular dynamics of atomic rearrangements at perturbed surfaces. Physical Review B, 2009, 80, .	3.2	17
1479	Dynamics of the $\gamma$ in crystals under uniaxial stress. Physical Review B, 2009, 79, .	3.2	14
1480	Ground states and formal duality relations in the Gaussian core model. Physical Review E, 2009, 80, 061116.	2.1	23
1481	Isothermal-isobaric molecular dynamics using stochastic velocity rescaling. Journal of Chemical Physics, 2009, 130, 074101.	3.0	297
1482	Desipramine induces disorder in cholesterol-rich membranes: implications for viral trafficking. Physical Biology, 2009, 6, 046004.	1.8	10
1483	Long-range empirical potential model: extension to hexagonal close-packed metals. Journal of Physics Condensed Matter, 2009, 21, 385402.	1.8	23
1484	Structural-Dynamical Properties of the <i>Deinococcus Radiodurans</i> Topoisomerase IB in Absence of DNA: Correlation with the Human Enzyme. Journal of Biomolecular Structure and Dynamics, 2009, 27, 307-317.	3.5	30
1485	Kinase-activity-independent functions of atypical protein kinase C in Drosophila. Journal of Cell Science, 2009, 122, 3759-3771.	2.0	67
1486	Effect of pressure on the thermal expansion of MgO up to 200 GPa. Chinese Physics B, 2009, 18, 5001-5007.	1.4	5
1487	The role of grain boundary structure in stress-induced phase transformation in UO2. Modelling and Simulation in Materials Science and Engineering, 2009, 17, 064001.	2.0	6
1488	Phase Transition and Thermodynamics of Ruthenium Diboride via First-Principles Calculations. Chinese Physics Letters, 2009, 26, 097101.	3.3	5
1489	Evidence of the crucial role of the linker domain on the catalytic activity of human topoisomerase I by experimental and simulative characterization of the Lys681Ala mutant. Nucleic Acids Research, 2009, 37, 6849-6858.	14.5	29
1490	The reversibility of phase transitions in Ti/Co core/shell nanometre-sized particles. Nanotechnology, 2009, 20, 015702.	2.6	1
1491	Ab initiomolecular dynamics simulation of a pressure induced zinc blende to rocksalt phase transition in SiC. Journal of Physics Condensed Matter, 2009, 21, 245801.	1.8	10
1492	Structural aspects of the solvation shell of lysine and acetylated lysine: A Carâ€Parrinello and classical molecular dynamics investigation. Journal of Chemical Physics, 2009, 131, 225103.	3.0	5

#	ARTICLE	IF	CITATIONS
1493	A Review of Computational Methods in Materials Science: Examples from Shock-Wave and Polymer Physics. <i>International Journal of Molecular Sciences</i> , 2009, 10, 5135-5216.	4.1	86
1494	Progress and challenges in the automated construction of Markov state models for full protein systems. <i>Journal of Chemical Physics</i> , 2009, 131, 124101.	3.0	346
1495	Atomistic simulation of a dislocation shear loop interacting with grain boundaries in nanocrystalline aluminium. <i>Modelling and Simulation in Materials Science and Engineering</i> , 2009, 17, 055008.	2.0	27
1496	High-Rate Plastic Deformation of Nanocrystalline Tantalum to Large Strains: Molecular Dynamics Simulation. <i>Materials Science Forum</i> , 0, 633-634, 3-19.	0.3	19
1497	Glass-forming region of the Ni–Nb–Ta ternary metal system determined directly from n-body potential through molecular dynamics simulations. <i>Journal of Materials Research</i> , 2009, 24, 1815-1819.	2.6	11
1498	Stress-induced phase transformation in nanocrystalline UO <sub>2</sub> . <i>Scripta Materialia</i> , 2009, 60, 878-881.	5.2	23
1499	Atomistic simulation of surface segregation processes in unstrained and strained Ag–Cu nanowires. <i>Materials Chemistry and Physics</i> , 2009, 116, 112-118.	4.0	2
1500	Comparative investigations of the thermal expansivity of MgO at high temperature. <i>Materials Research Bulletin</i> , 2009, 44, 1729-1733.	5.2	6
1501	Modeling Polymer Dielectric/Pentacene Interfaces: On the Role of Electrostatic Energy Disorder on Charge Carrier Mobility. <i>Advanced Functional Materials</i> , 2009, 19, 3254-3261.	14.9	81
1502	Thermodynamic and structural analysis of interactions between peptide ligands and SEB. <i>Journal of Molecular Recognition</i> , 2010, 23, 369-378.	2.1	6
1503	A combined atomic force microscopy imaging and docking study to investigate the complex between p53 DNA binding domain and Azurin. <i>Journal of Molecular Recognition</i> , 2009, 22, 506-515.	2.1	13
1504	Mechanistic studies of displacer–protein binding in chemically selective displacement systems using NMR and MD simulations. <i>Biotechnology and Bioengineering</i> , 2009, 102, 1428-1437.	3.3	10
1505	An embedded statistical method for coupling molecular dynamics and finite element analyses. <i>International Journal for Numerical Methods in Engineering</i> , 2009, 78, 1292-1319.	2.8	53
1506	Molecular dynamics simulations of mouse ferrochelatase variants: what distorts and orientates the porphyrin?. <i>Journal of Biological Inorganic Chemistry</i> , 2009, 14, 1119-1128.	2.6	4
1507	Structure and dynamics of the influenza A M2 Channel: a comparison of three structures. <i>Journal of Molecular Modeling</i> , 2009, 15, 1317-1328.	1.8	11
1508	Multi-scale modeling of HIV-1 proteins. <i>Computational and Theoretical Chemistry</i> , 2009, 898, 97-105.	1.5	6
1509	Atomistic simulations of spontaneous formation and structural properties of linoleic acid micelles in water. <i>Chemical Physics Letters</i> , 2009, 481, 124-129.	2.6	8
1510	Estimation of Water Diffusion Coefficients in Freeze-Concentrated Matrices of Sugar Solutions Using Molecular Dynamics: Correlation Between Estimated Diffusion Coefficients and Measured Ice-Crystal Recrystallization Rates. <i>Food Biophysics</i> , 2009, 4, 340-346.	3.0	20

#	ARTICLE	IF	CITATIONS
1511	Molecular dynamics simulations of laser-induced damage of nanostructures and solids. Applied Physics A: Materials Science and Processing, 2009, 96, 33-42.	2.3	24
1512	G protein inactive and active forms investigated by simulation methods. Proteins: Structure, Function and Bioinformatics, 2009, 75, 919-930.	2.6	27
1513	Ion-ion interactions of LiPF <sub>6</sub> and LiBF <sub>4</sub> in propylene carbonate solutions. Journal of Molecular Liquids, 2009, 148, 99-108.	4.9	107
1514	Computer simulation of sputtering at the low index (100), (110) and (111) surfaces of Ni <sub>3</sub> Al in a STEM. Nuclear Instruments & Methods in Physics Research B, 2009, 267, 3076-3079.	1.4	2
1515	Prediction of partition coefficients and infinite dilution activity coefficients of 1-ethylpropylamine and 3-methyl-1-pentanol using force field methods. Fluid Phase Equilibria, 2009, 285, 19-23.	2.5	14
1516	Molecular hydrogen storage in Al-doped bulk graphite with wider layer distances. Solid State Communications, 2009, 149, 1363-1367.	1.9	15
1517	Molecular dynamics simulations of AP/HMX composite with a modified force field. Journal of Hazardous Materials, 2009, 167, 810-816.	12.4	65
1518	Conformational transition characterization of glass transition behavior of polymers. Polymer, 2009, 50, 3396-3402.	3.8	20
1519	Molecular modeling study on the effect of residues distant from the nucleotide-binding portion on RNA binding in Staphylococcus aureus Hfq. Journal of Molecular Graphics and Modelling, 2009, 28, 253-260.	2.4	4
1520	Mechanics of nanocrack: Fracture, dislocation emission, and amorphization. Journal of the Mechanics and Physics of Solids, 2009, 57, 840-850.	4.8	76
1521	Multiscale modelling of bi-crystal grain boundaries in bcc iron. Journal of Nuclear Materials, 2009, 385, 262-267.	2.7	39
1522	Molecular dynamics study of the mechanics for Ni single-wall nanowires. European Journal of Mechanics, A/Solids, 2009, 28, 877-881.	3.7	7
1523	Internal stress and mechanical deformation of Al and Al/Ni multilayered nanowires. Acta Materialia, 2009, 57, 453-465.	7.9	9
1524	Molecular dynamics simulation of water in cytochrome c oxidase reveals two water exit pathways and the mechanism of transport. Biochimica Et Biophysica Acta - Bioenergetics, 2009, 1787, 1140-1150.	1.0	43
1525	Atomistic simulations of elastic and plastic properties in amorphous silicon. Europhysics Letters, 2009, 86, 66005.	2.0	23
1526	Cationic transport mechanism in $\frac{1}{2}\text{-Ag}^{+} \times \text{Cu} \times \text{I}(\text{O} \&\text{lt; } x \&\text{lt; } 0.25)$ : Molecular-dynamics simulation. Crystallography Reports, 2009, 54, 292-298.	0.6	2
1527	Mitochondrial Membranes with Mono- and Divalent Salt: Changes Induced by Salt Ions on Structure and Dynamics. Journal of Physical Chemistry B, 2009, 113, 15513-15521.	2.6	41
1528	An Elemental Mercury Diffusion Coefficient for Natural Waters Determined by Molecular Dynamics Simulation. Environmental Science & Technology, 2009, 43, 3183-3186.	10.0	62

#	ARTICLE	IF	CITATIONS
1529	PIP <sub>2</sub> -Binding Site in Kir Channels: Definition by Multiscale Biomolecular Simulations. <i>Biochemistry</i> , 2009, 48, 10926-10933.	2.5	127
1530	Reordering Hydrogen Bonds Using Hamiltonian Replica Exchange Enhances Sampling of Conformational Changes in Biomolecular Systems. <i>Journal of Physical Chemistry B</i> , 2009, 113, 6484-6494.	2.6	12
1531	Universal Convergence of the Specific Volume Changes of Globular Proteins upon Unfolding. <i>Biochemistry</i> , 2009, 48, 10846-10851.	2.5	36
1532	Protein Conformational Transitions: The Closure Mechanism of a Kinase Explored by Atomistic Simulations. <i>Journal of the American Chemical Society</i> , 2009, 131, 244-250.	13.7	130
1533	Conformational Transition Behavior of Amorphous Polyethylene across the Glass Transition Temperature. <i>Journal of Physical Chemistry B</i> , 2009, 113, 9077-9083.	2.6	21
1534	Origin of the Hydration Force: Water-Mediated Interaction between Two Hydrophilic Plates. <i>Journal of Physical Chemistry B</i> , 2009, 113, 13222-13228.	2.6	47
1535	Solvent Effects on the Self-Assembly of 1-Bromoeicosane on Graphite. Part II. Theory. <i>Journal of Physical Chemistry C</i> , 2009, 113, 3641-3649.	3.1	9
1536	Proposed Long-Range Empirical Potential To Study the Metallic Glasses in the Ni-Nb-Ta System. <i>Journal of Physical Chemistry B</i> , 2009, 113, 7282-7290.	2.6	17
1537	Systematic Coarse-graining of a Multicomponent Lipid Bilayer. <i>Journal of Physical Chemistry B</i> , 2009, 113, 1501-1510.	2.6	99
1538	Perturbations of Membrane Structure by Cholesterol and Cholesterol Derivatives Are Determined by Sterol Orientation. <i>Journal of the American Chemical Society</i> , 2009, 131, 4854-4865.	13.7	77
1539	Cystic Fibrosis Transmembrane Conductance Regulator: Using Differential Reactivity toward Channel-Permeant and Channel-Impermeant Thiol-Reactive Probes To Test a Molecular Model for the Pore. <i>Biochemistry</i> , 2009, 48, 10078-10088.	2.5	69
1540	Molecular Dynamics Studies of the Interactions of Water and Amino Acid Analogues with Quartz Surfaces. <i>Langmuir</i> , 2009, 25, 1638-1644.	3.5	80
1541	Properties and Permeability of Hypericin and Brominated Hypericin in Lipid Membranes. <i>Journal of Chemical Theory and Computation</i> , 2009, 5, 3139-3149.	5.3	32
1542	Orientational Dynamics of Water in Phospholipid Bilayers with Different Hydration Levels. <i>Journal of Physical Chemistry B</i> , 2009, 113, 7676-7680.	2.6	57
1543	Raman Spectroscopic Study, DFT Calculations and MD Simulations on the Conformational Isomerism of <i>N</i> -Alkyl- <i>N</i> -methylpyrrolidinium Bis-(trifluoromethanesulfonyl) Amide Ionic Liquids. <i>Journal of Physical Chemistry B</i> , 2009, 113, 4338-4346.	2.6	56
1544	Experimental and simulation studies of a real-time polymerase chain reaction in the presence of a fullerene derivative. <i>Nanotechnology</i> , 2009, 20, 415101.	2.6	21
1545	Strain rates in molecular dynamics simulations of nanocrystalline metals. <i>Philosophical Magazine</i> , 2009, 89, 3465-3475.	1.6	64
1546	A molecular dynamics study on the impact of defects and functionalization on the Young modulus of boron nitride nanotubes. <i>Computational Materials Science</i> , 2009, 45, 1097-1103.	3.0	55

#	ARTICLE	IF	CITATIONS
1547	Semi-empirical atomistic study of point defect properties in BCC transition metals. Computational Materials Science, 2009, 47, 135-145.	3.0	61
1548	Molecular dynamics studies of the transmembrane domain of gp41 from HIV-1. Biochimica Et Biophysica Acta - Biomembranes, 2009, 1788, 1804-1812.	2.6	32
1549	Thermal conductivity of ZnTe investigated by molecular dynamics. Journal of Alloys and Compounds, 2009, 485, 488-492.	5.5	14
1550	Elucidating the Inhibition Mechanism of HIV-1 Non-Nucleoside Reverse Transcriptase Inhibitors through Multicopy Molecular Dynamics Simulations. Journal of Molecular Biology, 2009, 388, 644-658.	4.2	79
1551	Binding of Rabies Virus Polymerase Cofactor to Recombinant Circular Nucleoprotein-RNA Complexes. Journal of Molecular Biology, 2009, 394, 558-575.	4.2	46
1552	Calculation of the surface free energy of fcc copper nanoparticles. Modelling and Simulation in Materials Science and Engineering, 2009, 17, 015006.	2.0	30
1553	Interaction Between Amyloid-Î² (1-42) Peptide and Phospholipid Bilayers: A Molecular Dynamics Study. Biophysical Journal, 2009, 96, 785-797.	0.5	108
1554	Dynamic Structure Factors from Lipid Membrane Molecular Dynamics Simulations. Biophysical Journal, 2009, 96, 1828-1838.	0.5	23
1555	Energetics of Cholesterol Transfer between Lipid Bilayers. Biophysical Journal, 2009, 96, 163a.	0.5	5
1556	Evidence for a Partially Structured State of the Amylin Monomer. Biophysical Journal, 2009, 97, 2948-2957.	0.5	45
1557	Undulation Contributions to the Area Compressibility in Lipid Bilayer Simulations. Biophysical Journal, 2009, 97, 2754-2760.	0.5	82
1558	Temperature Dependence of the Solubility of Carbon Dioxide in Imidazolium-Based Ionic Liquids. Journal of Physical Chemistry B, 2009, 113, 12727-12735.	2.6	104
1559	Optimized Molecular Dynamics Force Fields Applied to the Helix-Coil Transition of Polypeptides. Journal of Physical Chemistry B, 2009, 113, 9004-9015.	2.6	767
1560	Simulated Tempering Distributed Replica Sampling, Virtual Replica Exchange, and Other Generalized-Ensemble Methods for Conformational Sampling. Journal of Chemical Theory and Computation, 2009, 5, 2640-2662.	5.3	50
1561	Anomalies in water as obtained from computer simulations of the TIP4P/2005 model: density maxima, and density, isothermal compressibility and heat capacity minima. Molecular Physics, 2009, 107, 365-374.	1.7	153
1562	Plastic crystal phases of simple water models. Journal of Chemical Physics, 2009, 130, 244504.	3.0	65
1563	Molecular dynamics simulation of shape memory behaviour using a multi-grain model. Modelling and Simulation in Materials Science and Engineering, 2009, 17, 035011.	2.0	20
1564	The phase diagram of water at high pressures as obtained by computer simulations of the TIP4P/2005 model: the appearance of a plastic crystal phase. Physical Chemistry Chemical Physics, 2009, 11, 543-555.	2.8	72

#	ARTICLE	IF	CITATIONS
1565	Docking Ligands on Protein Surfaces: The Case Study of Prion Protein. Journal of Chemical Theory and Computation, 2009, 5, 2565-2573.	5.3	34
1566	Triple points and coexistence properties of the dense phases of water calculated using computer simulation. Physical Chemistry Chemical Physics, 2009, 11, 556-562.	2.8	26
1567	Molecular Dynamics Simulations of Ammonium Surfactant Monolayers at the Heptane/Water Interface. Journal of Physical Chemistry B, 2009, 113, 12680-12686.	2.6	27
1568	Computational Study of a Nanobiosensor: A Single-Walled Carbon Nanotube Functionalized with the Cocksackie-Adenovirus Receptor. Journal of Physical Chemistry B, 2009, 113, 11589-11593.	2.6	38
1569	Paramagnetic Perturbation of the $^{19}\text{F}$ NMR Chemical Shift in Fluorinated Cysteine by $\text{O}_2$ : A Theoretical Study. Journal of Physical Chemistry B, 2009, 113, 10916-10922.	2.6	4
1570	Observation of $\alpha$ -Helical Lock-Formation in Molecular Dynamics Simulations of Wild-Type $\beta^1$ and $\beta^2$ Adrenergic Receptors. Biochemistry, 2009, 48, 4789-4797.	2.5	65
1571	Molecular dynamics study of prolyl oligopeptidase with inhibitor in binding cavity. SAR and QSAR in Environmental Research, 2009, 20, 595-609.	2.2	10
1572	Antihypertensive Drug Valsartan in Solution and at the $\text{AT}_{1\text{R}}$ Receptor: Conformational Analysis, Dynamic NMR Spectroscopy, <i>in Silico</i> Docking, and Molecular Dynamics Simulations. Journal of Chemical Information and Modeling, 2009, 49, 726-739.	5.4	39
1573	An Improved United Atom Force Field for Simulation of Mixed Lipid Bilayers. Journal of Physical Chemistry B, 2009, 113, 2748-2763.	2.6	267
1574	A Continuum-Atomistic Analysis of Transgranular Crack Propagation in Aluminum. , 2009, , .		2
1575	Molecular dynamics study of biomembrane/local anesthetics interactions. Molecular Physics, 2009, 107, 1437-1443.	1.7	19
1576	Copper $^{+1}$ ,10-Phenanthroline Complexes Binding to DNA: Structural Predictions from Molecular Simulations. Journal of Physical Chemistry B, 2009, 113, 10881-10890.	2.6	78
1577	Al doped graphene: A promising material for hydrogen storage at room temperature. Journal of Applied Physics, 2009, 105, .	2.5	212
1578	Temperature-Dependent Mechanisms for the Dynamics of Protein-Hydration Waters: A Molecular Dynamics Simulation Study. Journal of Physical Chemistry B, 2009, 113, 9386-9392.	2.6	35
1579	Effect of Cross-Linking on the Diffusion of Water, Ions, and Small Molecules in Hydrogels. Journal of Physical Chemistry B, 2009, 113, 3512-3520.	2.6	171
1580	What ice can teach us about water interactions: a critical comparison of the performance of different water models. Faraday Discussions, 2009, 141, 251-276.	3.2	375
1581	Interaction of Monotopic Membrane Enzymes with a Lipid Bilayer: A Coarse-Grained MD Simulation Study. Biochemistry, 2009, 48, 2135-2145.	2.5	44
1582	Molecular Dynamics Simulation of the Early Stages of the Synthesis of Periodic Mesoporous Silica. Journal of Physical Chemistry B, 2009, 113, 708-718.	2.6	41



#	ARTICLE	IF	CITATIONS
1583	The phase diagram of water at negative pressures: Virtual ices. <i>Journal of Chemical Physics</i> , 2009, 131, 034510.	3.0	69
1584	Void growth in bcc metals simulated with molecular dynamics using the Finnis-Sinclair potential. <i>Philosophical Magazine</i> , 2009, 89, 3133-3161.	1.6	64
1585	Encapsulation of Myoglobin in a Cetyl Trimethylammonium Bromide Micelle in Vacuo: A Simulation Study. <i>Biochemistry</i> , 2009, 48, 1006-1015.	2.5	36
1586	Vibrational properties of grain boundaries in nanocrystalline Ni using second moment potentials. <i>Philosophical Magazine</i> , 2009, 89, 3511-3529.	1.6	3
1587	Self-assembling dipeptides: conformational sampling in solvent-free coarse-grained simulation. <i>Physical Chemistry Chemical Physics</i> , 2009, 11, 2077.	2.8	79
1588	Self-assembling dipeptides: including solvent degrees of freedom in a coarse-grained model. <i>Physical Chemistry Chemical Physics</i> , 2009, 11, 2068.	2.8	55
1589	Investigation on thermal properties of crosslinked epoxy resin by MD simulation. , 2009, , .		1
1590	Role of Cardiolipins in the Inner Mitochondrial Membrane: Insight Gained through Atom-Scale Simulations. <i>Journal of Physical Chemistry B</i> , 2009, 113, 3413-3422.	2.6	62
1591	Detection of Functional Modes in Protein Dynamics. <i>PLoS Computational Biology</i> , 2009, 5, e1000480.	3.2	126
1592	Water permeation through stratum corneum lipid bilayers from atomistic simulations. <i>Soft Matter</i> , 2009, 5, 4549.	2.7	61
1593	Umbrella Sampling Simulations of Biotin Carboxylase: Is a Structure with an Open ATP Grasp Domain Stable in Solution?. <i>Journal of Physical Chemistry B</i> , 2009, 113, 10097-10103.	2.6	6
1594	Scaling of Multimillion-Atom Biological Molecular Dynamics Simulation on a Petascale Supercomputer. <i>Journal of Chemical Theory and Computation</i> , 2009, 5, 2798-2808.	5.3	94
1595	Molecular Simulation of Cross-Linked Epoxy and Epoxy~POSS Nanocomposite. <i>Macromolecules</i> , 2009, 42, 4319-4327.	4.8	171
1596	Molecular Dynamics Simulations of Methane Hydrate Decomposition. <i>Journal of Physical Chemistry A</i> , 2009, 113, 1913-1921.	2.5	141
1597	How Does Solute-Polarization Affect the Hydrophobic Hydration of Methane?. <i>Zeitschrift Fur Physikalische Chemie</i> , 2009, 223, 1091-1104.	2.8	8
1598	Correlation of Static and Dynamic Heterogeneities in Supercooled Water by Means of Molecular Dynamics Simulations. <i>Zeitschrift Fur Physikalische Chemie</i> , 2009, 223, 1001-1010.	2.8	5
1599	A Molecular Dynamics Study of an hcp-to-fcc Martensitic Transformation and Its Crystallographic Correlation in a Ti Lattice, upon Dissolution of Cu Atoms. <i>Journal of the Physical Society of Japan</i> , 2010, 79, 104601.	1.6	1
1600	Simulated tempering distributed replica sampling: A practical guide to enhanced conformational sampling. <i>Journal of Physics: Conference Series</i> , 2010, 256, 012011.	0.4	2



#	ARTICLE	IF	CITATIONS
1601	An insight into the opening path to semi-open conformation of HIV-1 protease by molecular dynamics simulation. <i>Aids</i> , 2010, 24, 1121-1125.	2.2	3
1602	Reliability of methods of computer simulation of structure of amorphous alloys. <i>Journal of Applied Physics</i> , 2010, 107, .	2.5	17
1603	Ordered equilibrium structures of soft particles in thin layers. <i>Journal of Chemical Physics</i> , 2010, 133, 224504.	3.0	11
1604	Phase transition in nanocrystalline iron: Atomistic-level simulations. <i>International Journal of Materials Research</i> , 2010, 101, 1361-1368.	0.3	7
1605	Fluctuating Charge Molecular Dynamics Study on the Nanoscale Structures of Polymer Electrolytes. <i>Kobunshi Ronbunshu</i> , 2010, 67, 28-38.	0.2	0
1606	Molecular Dynamics Simulation for the Impact of N-Decanol Surfactants on the Liquid-Vapor Interface of Lithium Bromide Aqueous Solution. , 2010, , .		0
1607	Molecular dynamics simulations of cytochrome c unfolding in AOT reverse micelles: The first steps. <i>European Physical Journal E</i> , 2010, 32, 399-409.	1.6	32
1608	Destabilizing Alzheimer's A $\beta$ <sub>42</sub> Protofibrils with Morin: Mechanistic Insights from Molecular Dynamics Simulations. <i>Biochemistry</i> , 2010, 49, 3935-3946.	2.5	162
1609	Top Leads for Swine Influenza A/H1N1 Virus Revealed by Steered Molecular Dynamics Approach. <i>Journal of Chemical Information and Modeling</i> , 2010, 50, 2236-2247.	5.4	84
1610	Working Mechanism for a Redox Switchable Molecular Machine Based on Cyclodextrin: A Free Energy Profile Approach. <i>Journal of Physical Chemistry B</i> , 2010, 114, 6561-6566.	2.6	46
1611	Practical Considerations for Building GROMOS-Compatible Small-Molecule Topologies. <i>Journal of Chemical Information and Modeling</i> , 2010, 50, 2221-2235.	5.4	180
1612	pH-driven helix rotations in the influenza M2 H <sup>+</sup> channel: a potential gating mechanism. <i>European Biophysics Journal</i> , 2010, 39, 1043-1049.	2.2	5
1613	Hindering of rotational motion of guest molecules in the Type I clathrate hydrate. <i>Chemical Physics Letters</i> , 2010, 494, 206-212.	2.6	12
1614	Atomistic simulations of surface segregation of defects in solid oxide electrolytes. <i>Acta Materialia</i> , 2010, 58, 2197-2206.	7.9	78
1615	Simulation studies of the insolubility of cellulose. <i>Carbohydrate Research</i> , 2010, 345, 2060-2066.	2.3	166
1616	Computational approach to ensure the stability of the favorable ATP binding site in <i>E. coli</i> Hfq. <i>Journal of Molecular Graphics and Modelling</i> , 2010, 29, 573-580.	2.4	4
1617	Molecular dynamics simulation of anionic clays containing glutamic acid. <i>Journal of Molecular Structure</i> , 2010, 977, 165-169.	3.6	6
1618	Thrombin allosteric modulation revisited: a molecular dynamics study. <i>Journal of Molecular Modeling</i> , 2010, 16, 725-735.	1.8	16

#	ARTICLE	IF	CITATIONS
1619	Distinct interactions between the human adrenergic $\beta_2$ receptor and G $\beta\gamma$ in an in silico study. <i>Journal of Molecular Modeling</i> , 2010, 16, 1307-1318.	1.8	6
1620	Isoform-specific determinants in the HP1 binding to histone 3: insights from molecular simulations. <i>Amino Acids</i> , 2010, 38, 1571-1581.	2.7	9
1621	Temperature-dependent structural and transport properties of liquid transition metals. <i>Metals and Materials International</i> , 2010, 16, 921-929.	3.4	1
1622	Tyrosine aminotransferase: biochemical and structural properties and molecular dynamics simulations. <i>Protein and Cell</i> , 2010, 1, 1023-1032.	11.0	36
1623	Molecular simulations of clay minerals: a study considering the change of cell size and shape. <i>Acta Geotechnica</i> , 2010, 5, 151-167.	5.7	1
1624	Glass transition and structural properties of glycidylxypropyl-heptaphenyl polyhedral oligomeric silsesquioxane-epoxy nanocomposites. <i>Journal of Thermal Analysis and Calorimetry</i> , 2010, 102, 461-467.	3.6	22
1625	A computational study on cannabinoid receptors and potent bioactive cannabinoid ligands: homology modeling, docking, de novo drug design and molecular dynamics analysis. <i>Molecular Diversity</i> , 2010, 14, 257-276.	3.9	31
1626	On (Andersen's) Parrinello's Rahman Molecular Dynamics, the Related Metadynamics, and the Use of the Cauchy-Born Rule. <i>Journal of Elasticity</i> , 2010, 100, 145-153.	1.9	30
1627	Pressure effects on icosahedral short range order in undercooled copper. <i>Solid State Sciences</i> , 2010, 12, 179-182.	3.2	1
1628	Free energy profiles of amino acid side chain analogs near water's vapor interface obtained via MD simulations. <i>Journal of Computational Chemistry</i> , 2010, 31, 204-216.	3.3	11
1629	Atomistic insight into chondroitin-6-sulfate glycosaminoglycan chain through quantum mechanics calculations and molecular dynamics simulation. <i>Journal of Computational Chemistry</i> , 2010, 31, 1670-1680.	3.3	11
1630	Solvent mediated stabilisation of dissolution at the resorcinol-water interface. <i>Crystal Research and Technology</i> , 2010, 45, 149-157.	1.3	1
1631	Sugar treatment of human lipoprotein particles and their separation by capillary electrophoresis. <i>Journal of Separation Science</i> , 2010, 33, 2528-2535.	2.5	5
1632	Cooperative behavior of poly(vinyl alcohol) and water as revealed by molecular dynamics simulations. <i>Polymer</i> , 2010, 51, 4452-4460.	3.8	64
1633	Why pyridine containing pyrido[2,3-d]pyrimidin-7-ones selectively inhibit CDK4 than CDK2: Insights from molecular dynamics simulation. <i>Journal of Molecular Graphics and Modelling</i> , 2010, 28, 695-706.	2.4	16
1634	Plasticity of metal wires in torsion: Molecular dynamics and dislocation dynamics simulations. <i>Journal of the Mechanics and Physics of Solids</i> , 2010, 58, 1011-1025.	4.8	65
1635	Molecular dynamics simulation of polyethylene under cyclic loading: Effect of loading condition and chain length. <i>International Journal of Mechanical Sciences</i> , 2010, 52, 136-145.	6.7	20
1636	Polydispersity effect on solid-fluid transition in hard sphere systems. <i>Physics Procedia</i> , 2010, 3, 1475-1479.	1.2	1

#	ARTICLE	IF	CITATIONS
1637	Atomic simulations of dislocation emission from Cu/Cu and Co/Cu grain boundaries. Materials Science & Engineering A: Structural Materials: Properties, Microstructure and Processing, 2010, 528, 260-267.	5.6	12
1638	Molecular force field investigation for Sulfur Hexafluoride: A computer simulation study. Fluid Phase Equilibria, 2010, 291, 81-89.	2.5	35
1639	Molecular dynamics simulations of imidazolium-based ionic liquid/water mixtures: Alkyl side chain length and anion effects. Fluid Phase Equilibria, 2010, 294, 148-156.	2.5	182
1640	Structure of cationic surfactant micelles from molecular simulations of self-assembly. Computational and Theoretical Chemistry, 2010, 946, 88-93.	1.5	13
1641	Structure of the interface between water and self-assembled monolayers of neutral, anionic and cationic alkane thiols. Computational and Theoretical Chemistry, 2010, 946, 83-87.	1.5	10
1642	The melting curve of perovskite under lower mantle pressures. Solid State Communications, 2010, 150, 590-593.	1.9	9
1643	Atomistic simulations of void migration under thermal gradient in UO <sub>2</sub> . Acta Materialia, 2010, 58, 330-339.	7.9	24
1644	Plastic deformation of nanocrystalline aluminum at high temperatures and strain rate. Acta Materialia, 2010, 58, 2176-2185.	7.9	30
1645	Massive oxidation of phospholipid membranes leads to pore creation and bilayer disintegration. Chemical Physics Letters, 2010, 486, 99-103.	2.6	90
1646	Filling carbon nanotubes with liquid acetonitrile. Chemical Physics Letters, 2010, 496, 50-55.	2.6	26
1647	Should carbon nanotubes be degasified before filling?. Chemical Physics Letters, 2010, 500, 35-40.	2.6	23
1648	Structural facets of disease-linked human prion protein mutants: A molecular dynamic study. Proteins: Structure, Function and Bioinformatics, 2010, 78, 3270-3280.	2.6	46
1649	The Nature of DNA-Base-Carbon-Nanotube Interactions. Small, 2010, 6, 31-34.	10.0	108
1650	Tunable Water Channels with Carbon Nanoscrolls. Small, 2010, 6, 739-744.	10.0	110
1651	Mapping the Druggable Allosteric Space of G-Protein Coupled Receptors: a Fragment-Based Molecular Dynamics Approach. Chemical Biology and Drug Design, 2010, 76, 201-217.	3.2	106
1652	An aqueous H <sup>+</sup> permeation pathway in the voltage-gated proton channel Hv1. Nature Structural and Molecular Biology, 2010, 17, 869-875.	8.2	160
1654	15. Computer Simulations on Phase Transitions in Ice. , 2010, , 315-336.		0
1655	Constant-Pressure Molecular-Dynamics Study of Carbon Nanotubes and Electronic Structure of New Phases. Japanese Journal of Applied Physics, 2010, 49, 02BB05.	1.5	4

#	ARTICLE	IF	CITATIONS
1656	Molecular Structural Transformation of 2:1 Clay Minerals by a Constant-Pressure Molecular Dynamics Simulation Method. <i>Journal of Nanomaterials</i> , 2010, 2010, 1-13.	2.7	0
1657	Structural and Dynamical Effects Induced by the Anticancer Drug Topotecan on the Human Topoisomerase I-DNA Complex. <i>PLoS ONE</i> , 2010, 5, e10934.	2.5	32
1658	Thermal transport property of Ge <sub>34</sub> and d-Ge investigated by molecular dynamics and the Slack's equation. <i>Chinese Physics B</i> , 2010, 19, 076501.	1.4	11
1659	Systematic determination of order parameters for chain dynamics using diffusion maps. <i>Proceedings of the National Academy of Sciences of the United States of America</i> , 2010, 107, 13597-13602.	7.1	142
1660	Local structure of the Zr-Al metallic glasses studied by proposed $\langle i \rangle_n$ -body potential through molecular dynamics simulation. <i>Journal of Materials Research</i> , 2010, 25, 1679-1688.	2.6	9
1661	Interatomic potential to predict the binary metallic glass formation. <i>Journal of Materials Research</i> , 2010, 25, 976-981.	2.6	4
1662	Electrostatic hot spot on DNA-binding domains mediates phosphate desolvation and the pre-organization of specificity determinant side chains. <i>Nucleic Acids Research</i> , 2010, 38, 2134-2144.	14.5	9
1663	Bias-dependent amino-acid-induced conductance changes in short semi-metallic carbon nanotubes. <i>Nanotechnology</i> , 2010, 21, 015202.	2.6	19
1664	Formation of the Ni-Zr-Al Ternary Metallic Glasses Investigated by Interatomic Potential through Molecular Dynamic Simulation. <i>Journal of the Physical Society of Japan</i> , 2010, 79, 064607.	1.6	7
1665	Phase behavior of symmetric disk-coil molecules. <i>Journal of Chemical Physics</i> , 2010, 132, 174901.	3.0	3
1666	Separation of gases from gas-water mixtures using carbon nanotubes. <i>Applied Physics Letters</i> , 2010, 96, .	3.3	33
1667	Electrolytes in a nanometer slab-confinement: Ion-specific structure and solvation forces. <i>Journal of Chemical Physics</i> , 2010, 133, 164511.	3.0	37
1668	Transverse resonant properties of strained gold nanowires. <i>Journal of Applied Physics</i> , 2010, 108, .	2.5	37
1669	Computational investigation of lipid hydration water of 1-palmitoyl-2-oleoyl-sn-glycero-3-phosphocholine at three hydration levels. <i>Molecular Physics</i> , 2010, 108, 2027-2036.	1.7	17
1670	Energy dissipation and defect generation in nanocrystalline silicon carbide. <i>Physical Review B</i> , 2010, 81, .	3.2	42
1671	Gypsum under pressure: A first-principles study. <i>Physical Review B</i> , 2010, 81, .	3.2	12
1672	Molecular dynamics of collisions between rough surfaces. <i>Physical Review B</i> , 2010, 82, .	3.2	34
1673	Evidence for short-time limit of martensite deaging in shape-memory alloys: Experiment and atomistic simulation. <i>Applied Physics Letters</i> , 2010, 97, 171902.	3.3	4

#	ARTICLE	IF	CITATIONS
1674	Computer simulations of aqua metal ions for accurate reproduction of hydration free energies and structures. Journal of Chemical Physics, 2010, 132, 104505.	3.0	15
1675	Complex martensitic nanostructure in Zr nanowires: A molecular dynamics study. Physical Review B, 2010, 81, .	3.2	9
1676	Stability of simple cubic calcium at high pressure: A first-principles study. Physical Review B, 2010, 82, .	3.2	23
1677	Role of Lipids in Spheroidal High Density Lipoproteins. PLoS Computational Biology, 2010, 6, e1000964.	3.2	81
1678	Spontaneous Quaternary and Tertiary T-R Transitions of Human Hemoglobin in Molecular Dynamics Simulation. PLoS Computational Biology, 2010, 6, e1000774.	3.2	57
1679	Puckering free energy of pyranoses: A NMR and metadynamics-umbrella sampling investigation. Journal of Chemical Physics, 2010, 133, 095104.	3.0	47
1680	Theoretical study on the structure and energetics of intergranular glassy film in $\text{Si}_3\text{N}_4\text{-SiO}_2$ ceramics. International Journal of Materials Research, 2010, 101, 57-65.	0.3	9
1681	Proposed truncated Cu-Hf tight-binding potential to study the crystal-to-amorphous phase transition. Journal of Applied Physics, 2010, 108, .	2.5	8
1682	Stretched exponential dynamics in lipid bilayer simulations. Journal of Chemical Physics, 2010, 133, 115101.	3.0	26
1683	Free energy surfaces for the interaction of D-glucose with planar aromatic groups in aqueous solution. Journal of Chemical Physics, 2010, 133, 155103.	3.0	24
1685	Structure and dynamics of the protic ionic liquid monomethylammonium nitrate ( $[\text{CH}_3\text{NH}_3][\text{NO}_3]$ ) from <i>ab initio</i> molecular dynamics simulations. Journal of Chemical Physics, 2010, 132, 124506.	3.0	111
1686	pH response of conformation of poly(propylene imine) dendrimer in water: a molecular simulation study. Molecular Simulation, 2010, 36, 1164-1172.	2.0	19
1687	Thermo-mechanical stability and strength of peptide nanostructures from molecular dynamics: self-assembled cyclic peptide nanotubes. Nanotechnology, 2010, 21, 115703.	2.6	10
1688	Molecular Dynamics Applications in Packaging. , 2010, , 665-694.		0
1689	Toward an Understanding of the Aqueous Solubility of Amino Acids in the Presence of Salts: A Molecular Dynamics Simulation Study. Journal of Physical Chemistry B, 2010, 114, 16450-16459.	2.6	34
1690	Prediction of high-pressure polymorphism in $\text{NiS}_2$ at megabar pressures. Journal of Physics Condensed Matter, 2010, 22, 235401.	1.8	5
1691	A Coarse-Grained Model Based on Morse Potential for Water and <i>n</i> -Alkanes. Journal of Chemical Theory and Computation, 2010, 6, 851-863.	5.3	75
1692	Modeling the Relationship between the p53 C-Terminal Domain and Its Binding Partners Using Molecular Dynamics. Journal of Physical Chemistry B, 2010, 114, 13201-13213.	2.6	18

#	ARTICLE	IF	CITATIONS
1693	Heat-Driven Release of a Drug Molecule from Carbon Nanotubes: A Molecular Dynamics Study. Journal of Physical Chemistry B, 2010, 114, 13481-13486.	2.6	70
1694	Diffusivities and Viscosities of Poly(ethylene oxide) Oligomers. Journal of Chemical & Engineering Data, 2010, 55, 4273-4280.	1.9	15
1695	Protein Thermostability Calculations Using Alchemical Free Energy Simulations. Biophysical Journal, 2010, 98, 2309-2316.	0.5	176
1696	Simulation of Nanoparticle Permeation through a Lipid Membrane. Biophysical Journal, 2010, 99, 144-152.	0.5	55
1697	Chemomechanical Regulation of SNARE Proteins Studied with Molecular Dynamics Simulations. Biophysical Journal, 2010, 99, 1221-1230.	0.5	17
1698	Crystallization and Melting Simulations of Oligomeric $\hat{1}$ Isotactic Polypropylene. Macromolecules, 2010, 43, 5455-5469.	4.8	35
1699	Local Chain Dynamics and Dynamic Heterogeneity in Cross-Linked Epoxy in the Vicinity of Glass Transition. Macromolecules, 2010, 43, 6505-6510.	4.8	35
1700	Effects of the Lipid Bilayer Phase State on the Water Membrane Interface. Journal of Physical Chemistry B, 2010, 114, 11784-11792.	2.6	58
1701	Crystalline to Amorphous Transition and Relative Stability of Amorphous Phase versus Solid Solution in the Cuâ€Ti System Studied by Molecular Dynamics Simulations. Journal of the Physical Society of Japan, 2010, 79, 064603.	1.6	2
1702	Microscopic mechanism of martensitic stabilization in shape-memory alloys: Atomic-level processes. Physical Review B, 2010, 81, .	3.2	24
1703	A Complete Thermodynamic Characterization of Electrostatic and Hydrophobic Associations in the Temperature Range 0 to 100 Å°C from Explicit-Solvent Molecular Dynamics Simulations. Journal of Chemical Theory and Computation, 2010, 6, 1293-1306.	5.3	25
1704	Glass Forming Region of Cuâ~Tiâ~Hf Ternary Metal System Derived from the $\langle i \rangle n \langle /i \rangle$ -Body Potential through Molecular Dynamics Simulation. Journal of Physical Chemistry B, 2010, 114, 9540-9545.	2.6	10
1705	Effects of DPH on DPPCâ~Cholesterol Membranes with Varying Concentrations of Cholesterol: From Local Perturbations to Limitations in Fluorescence Anisotropy Experiments. Journal of Physical Chemistry B, 2010, 114, 2704-2711.	2.6	39
1706	Phase Transitions and Mechanical Properties of Octahydro-1,3,5,7-tetranitro-1,3,5,7-tetrazocine in Different Crystal Phases by Molecular Dynamics Simulation. Journal of Chemical & Engineering Data, 2010, 55, 3121-3129.	1.9	30
1707	Thermodynamic and Hydrogen-Bonding Analyses of the Interaction between Model Lipid Bilayers. Journal of Physical Chemistry B, 2010, 114, 3013-3019.	2.6	20
1708	In Silico Prediction of the 3D Structure of Trimeric Asialoglycoprotein Receptor Bound to Triantennary Oligosaccharide. Journal of the American Chemical Society, 2010, 132, 9087-9095.	13.7	16
1709	Solvation of the Amphiphilic Diol Molecule in Aliphatic Alcoholâ~Water and Fluorinated Alcoholâ~Water Solutions. Journal of Physical Chemistry B, 2010, 114, 4252-4260.	2.6	23
1710	Analysis of dissociation process for gas hydrates by molecular dynamics simulation. Molecular Simulation, 2010, 36, 246-253.	2.0	40

#	ARTICLE	IF	CITATIONS
1711	Behavior of 2,6-Bis(decyloxy)naphthalene Inside Lipid Bilayer. Journal of Physical Chemistry B, 2010, 114, 15483-15494.	2.6	11
1712	Dielectric Constant of Ice Ih and Ice V: A Computer Simulation Study. Journal of Physical Chemistry B, 2010, 114, 6089-6098.	2.6	31
1713	Smooth Size Effects in Pd and PdH Nanoparticles. Journal of Physical Chemistry C, 2010, 114, 18085-18090.	3.1	8
1714	Another Coarse Grain Model for Aqueous Solvation: WAT FOUR?. Journal of Chemical Theory and Computation, 2010, 6, 3793-3807.	5.3	111
1715	Unfolding of Hydrophobic Polymers in Guanidinium Chloride Solutions. Journal of Physical Chemistry B, 2010, 114, 2246-2254.	2.6	66
1716	Dynamic Correlation between Pressure-Induced Protein Structural Transition and Water Penetration. Journal of Physical Chemistry B, 2010, 114, 2281-2286.	2.6	63
1717	Comparing the Efficiency of Biased and Unbiased Molecular Dynamics in Reconstructing the Free Energy Landscape of Met-Enkephalin. Journal of Chemical Theory and Computation, 2010, 6, 3640-3646.	5.3	51
1718	Orientation-Dependent Plasticity in Metal Nanowires under Torsion: Twist Boundary Formation and Eshelby Twist. Nano Letters, 2010, 10, 139-142.	9.1	56
1719	Numerical Investigation of the Cubic-to-Tetragonal Phase Transition in Ag Nanorods. Journal of Physical Chemistry C, 2010, 114, 3364-3370.	3.1	18
1720	Fluctuations in Number of Water Molecules Confined between Nanoparticles. Journal of Physical Chemistry B, 2010, 114, 13410-13414.	2.6	30
1721	Characterization of Perfluorooctylbromide-Based Nanoemulsion Particles Using Atomistic Molecular Dynamics Simulations. Journal of Physical Chemistry B, 2010, 114, 10086-10096.	2.6	15
1722	Molecular Design of Functionalized <i>m</i> -Poly(phenylene ethynylene) Foldamers: from Simulation to Synthesis. Macromolecules, 2010, 43, 5932-5942.	4.8	10
1723	Solution Study of Engineered Quartz Binding Peptides Using Replica Exchange Molecular Dynamics. Biomacromolecules, 2010, 11, 3266-3274.	5.4	28
1724	Nanoscale Tensile, Shear, and Failure Properties of Layered Silicates as a Function of Cation Density and Stress. Journal of Physical Chemistry C, 2010, 114, 1763-1772.	3.1	64
1725	Automated force field optimisation of small molecules using a gradient-based workflow package. Molecular Simulation, 2010, 36, 1182-1196.	2.0	21
1726	Experimental Verification of Force Fields for Molecular Dynamics Simulations Using Gly-Pro-Gly-Gly. Journal of Physical Chemistry B, 2010, 114, 12358-12375.	2.6	42
1727	Potentials of Mean Force and Permeabilities for Carbon Dioxide, Ammonia, and Water Flux across a Rhesus Protein Channel and Lipid Membranes. Journal of the American Chemical Society, 2010, 132, 13251-13263.	13.7	88
1728	Implementation of the CHARMM Force Field in GROMACS: Analysis of Protein Stability Effects from Correction Maps, Virtual Interaction Sites, and Water Models. Journal of Chemical Theory and Computation, 2010, 6, 459-466.	5.3	866



#	ARTICLE	IF	CITATIONS
1729	Exploring the Changes in the Structure of $\alpha$ -Helical Peptides Adsorbed onto a Single Walled Carbon Nanotube Using Classical Molecular Dynamics Simulation. Journal of Physical Chemistry B, 2010, 114, 14048-14058.	2.6	55
1730	Dynamics of Water Clusters Confined in Proteins: A Molecular Dynamics Simulation Study of Interfacial Waters in a Dimeric Hemoglobin. Journal of Physical Chemistry B, 2010, 114, 16989-16996.	2.6	62
1731	Dynamics and Structural Changes Induced by ATP Binding in SAV1866, a Bacterial ABC Exporter. Journal of Physical Chemistry B, 2010, 114, 15948-15957.	2.6	43
1732	Phase behavior of colloidal superballs: Shape interpolation from spheres to cubes. Physical Review E, 2010, 81, 061105.	2.1	107
1733	Structure of 1-Butylpyridinium Tetrafluoroborate Ionic Liquid: Quantum Chemistry and Molecular Dynamic Simulation Studies. Journal of Physical Chemistry A, 2010, 114, 3990-3996.	2.5	43
1734	Temperature-evolution of structure and diffusion properties of liquid transition metals. Journal of Non-Crystalline Solids, 2010, 356, 1061-1069.	3.1	8
1735	Elastic properties of degenerate f.c.c. crystal of polydisperse soft dimers at zero temperature. Journal of Non-Crystalline Solids, 2010, 356, 2026-2032.	3.1	35
1736	ADP/ATP mitochondrial carrier MD simulations to shed light on the structural "dynamical events that, after an additional mutation, restore the function in a pathological single mutant. Journal of Structural Biology, 2010, 172, 225-232.	2.8	10
1737	A Conserved Protonation-Induced Switch can Trigger "Ionic-Lock" Formation in Adrenergic Receptors. Journal of Molecular Biology, 2010, 397, 1339-1349.	4.2	36
1738	X-ray Crystallographic and MD Simulation Studies on the Mechanism of Interfacial Activation of a Family I.3 Lipase with Two Lids. Journal of Molecular Biology, 2010, 400, 82-95.	4.2	28
1739	Ab initio molecular dynamics simulation of structural transformation in zinc blende GaN under high pressure. Journal of Alloys and Compounds, 2010, 490, 537-540.	5.5	6
1740	Interactions at the bilayer interface and receptor site induced by the novel synthetic pyrrolidinone analog MMK3. Biochimica Et Biophysica Acta - Biomembranes, 2010, 1798, 422-432.	2.6	22
1741	Membrane simulations mimicking acidic pH reveal increased thickness and negative curvature in a bilayer consisting of lysophosphatidylcholines and free fatty acids. Biochimica Et Biophysica Acta - Biomembranes, 2010, 1798, 938-946.	2.6	57
1742	Thermal conductivity of A-site doped pyrochlore oxides studied by molecular-dynamics simulation. Computational Materials Science, 2010, 48, 336-342.	3.0	22
1743	Continuum mechanics ability to predict the material response at atomic scale. Computational Materials Science, 2010, 48, 372-380.	3.0	4
1744	Computer Simulations on Phase Transitions in Ice. Reviews in Mineralogy and Geochemistry, 2010, 71, 315-335.	4.8	9
1745	Assessing the Stability of Alzheimer's Amyloid Protofibrils Using Molecular Dynamics. Journal of Physical Chemistry B, 2010, 114, 1652-1660.	2.6	398
1746	Dynamical study of a polydisperse hard-sphere system. Physical Review E, 2010, 82, 021201.	2.1	10

#	ARTICLE	IF	CITATIONS
1747	Molecular Modeling of the Additional Inhibitor Site Located in Secretory Phospholipase A <sub>2</sub> . Journal of Biomolecular Structure and Dynamics, 2010, 27, 489-499.	3.5	21
1748	Transferability of Nonbonded Interaction Potentials for Coarse-Grained Simulations: Benzene in Water. Journal of Chemical Theory and Computation, 2010, 6, 2434-2444.	5.3	66
1749	Nano-Bio- Electronic, Photonic and MEMS Packaging. , 2010, , .		38
1750	On the Self-Assembly of a Highly Selective Benzothiazole-Based TIM Inhibitor in Aqueous Solution. Langmuir, 2010, 26, 16681-16689.	3.5	10
1751	Sequence-Dependent Configurational Entropy Change of DNA upon Intercalation. Journal of Physical Chemistry B, 2010, 114, 13446-13454.	2.6	27
1752	Simulation of structural phase transitions in NiTi. Physical Review B, 2010, 82, .	3.2	59
1753	Molecular dynamics simulations of pentacene thin films: The effect of surface on polymorph selection. Journal of Materials Chemistry, 2010, 20, 10397.	6.7	46
1754	Determining the three-phase coexistence line in methane hydrates using computer simulations. Journal of Chemical Physics, 2010, 133, 064507.	3.0	201
1755	Dependence of the Conformational Isomerism in 1- <i>n</i> -Butyl-3-methylimidazolium Ionic Liquids on the Nature of the Halide Anion. Journal of Physical Chemistry B, 2010, 114, 11715-11724.	2.6	66
1756	Melting point and phase diagram of methanol as obtained from computer simulations of the OPLS model. Journal of Chemical Physics, 2010, 132, 094505.	3.0	20
1757	Oxidation Changes Physical Properties of Phospholipid Bilayers: Fluorescence Spectroscopy and Molecular Simulations. Langmuir, 2010, 26, 6140-6144.	3.5	108
1758	Chain-Length Dependence of the Segmental Relaxation in Polymer Melts: Molecular Dynamics Simulation Studies on Poly(propylene oxide). Macromolecules, 2010, 43, 8985-8992.	4.8	26
1759	Lateral confinement effects on the structural properties of surfactant aggregates: SDS on graphene. Physical Chemistry Chemical Physics, 2010, 12, 13137.	2.8	50
1760	Atomistic Evidence of How Force Dynamically Regulates Thiol/Disulfide Exchange. Journal of the American Chemical Society, 2010, 132, 16790-16795.	13.7	63
1761	Cholesterol Orientation and Tilt Modulus in DMPC Bilayers. Journal of Physical Chemistry B, 2010, 114, 7524-7534.	2.6	81
1762	Lateral pressure profiles in lipid monolayers. Faraday Discussions, 2010, 144, 393-409.	3.2	51
1763	Sequence-Dependent Interaction of $\beta^2$ -Peptides with Membranes. Journal of Physical Chemistry B, 2010, 114, 13585-13592.	2.6	31
1764	Experimental Test of the Thermodynamic Model of Protein Cooperativity Using Temperature-Induced Unfolding of a Ubiquitin-UIM Fusion Protein. Biochemistry, 2010, 49, 8455-8467.	2.5	7

#	ARTICLE	IF	CITATIONS
1765	Can gas hydrate structures be described using classical simulations?. Journal of Chemical Physics, 2010, 132, 114503.	3.0	44
1766	The crystal structure and superconducting properties of monatomic bromine. Journal of Physics Condensed Matter, 2010, 22, 015702.	1.8	10
1767	Influence of endohedral water on diameter sorting of single-walled carbon nanotubes by density gradient centrifugation. Physical Chemistry Chemical Physics, 2010, 12, 902-908.	2.8	19
1768	Dynamics and energetics of solute permeation through the Plasmodium falciparum aquaglyceroporin. Physical Chemistry Chemical Physics, 2010, 12, 10246.	2.8	34
1769	Predicting water uptake in poly(perfluorosulfonic acids) using force field simulation methods. Physical Chemistry Chemical Physics, 2010, 12, 14543.	2.8	11
1770	Volumetric properties of human islet amyloid polypeptide in liquid water. Physical Chemistry Chemical Physics, 2010, 12, 4233.	2.8	15
1771	Thermodynamic calculation and interatomic potential to predict the favored composition region for the Cu-Zr-Al metallic glass formation. Physical Chemistry Chemical Physics, 2011, 13, 4103.	2.8	29
1772	Structural properties of polystyrene oligomers in different environments: a molecular dynamics study. Physical Chemistry Chemical Physics, 2011, 13, 18107.	2.8	3
1773	Pickett angles and Cremer-Pople coordinates as collective variables for the enhanced sampling of six-membered ring conformations. Molecular Physics, 2011, 109, 141-148.	1.7	24
1774	Binding Affinity of a Small Molecule to an Amorphous Polymer in a Solvent. Part 1: Free Energy of Binding to a Binding Site. Langmuir, 2011, 27, 12381-12395.	3.5	6
1775	Charybdotoxin Unbinding from the <i>Kv1.3</i> Potassium Channel: A Combined Computational and Experimental Study. Journal of Physical Chemistry B, 2011, 115, 11490-11500.	2.6	28
1776	Molecular dynamics study of the interactions between phenolic compounds and alginate/alginate acid chains. New Journal of Chemistry, 2011, 35, 1607.	2.8	16
1777	N,N-Dimethylformamide-induced phase separation of hexafluoroisopropanol-water mixtures. Physical Chemistry Chemical Physics, 2011, 13, 11222.	2.8	16
1778	Free energy analysis of vesicle-to-bicelle transformation. Soft Matter, 2011, 7, 9012.	2.7	40
1779	An all atom computer simulation study of the liquid crystalline phase behaviour of alkenic fluoroterphenyls. Soft Matter, 2011, 7, 10266.	2.7	11
1780	Arrhenius analysis of anisotropic surface self-diffusion on the prismatic facet of ice. Physical Chemistry Chemical Physics, 2011, 13, 19960.	2.8	29
1781	Study of structural and dynamic properties of liquid phenyltrimethoxysilane. Physical Chemistry Chemical Physics, 2011, 13, 11864.	2.8	7
1782	Spatially inhomogeneous bimodal inherent structure of simulated liquid water. Physical Chemistry Chemical Physics, 2011, 13, 19918.	2.8	136

#	ARTICLE	IF	CITATIONS
1783	Conditional reversible work method for molecular coarse graining applications. Physical Chemistry Chemical Physics, 2011, 13, 10468.	2.8	77
1784	Predicting hydration Gibbs energies of alkyl-aromatics using molecular simulation: a comparison of current force fields and the development of a new parameter set for accurate solvation data. Physical Chemistry Chemical Physics, 2011, 13, 17384.	2.8	22
1785	Polarizability versus mobility: atomistic force field for ionic liquids. Physical Chemistry Chemical Physics, 2011, 13, 16055.	2.8	149
1786	Limiting diffusion coefficients of ionic liquids in water and methanol: a combined experimental and molecular dynamics study. Physical Chemistry Chemical Physics, 2011, 13, 3268.	2.8	34
1787	Entropy and the driving force for the filling of carbon nanotubes with water. Proceedings of the National Academy of Sciences of the United States of America, 2011, 108, 11794-11798.	7.1	287
1788	2DIR Spectroscopy of Human Amylin Fibrils Reflects Stable $\beta^2$ -Sheet Structure. Journal of the American Chemical Society, 2011, 133, 16062-16071.	13.7	114
1789	Atomistic Molecular Dynamics Simulations of the Interactions of Oleic and 2-Hydroxyoleic Acids with Phosphatidylcholine Bilayers. Journal of Physical Chemistry B, 2011, 115, 11727-11738.	2.6	21
1790	Molecular Dynamics Study of Water Interacting with Siloxane Surface Modified by Poly(ethylene) Tj ETQq1 1 0.784314 rgBT /Overlock 3.1 8	3.1	8
1791	Direct Observations of Conformational Distributions of Intrinsically Disordered p53 Peptides Using UV Raman and Explicit Solvent Simulations. Journal of Physical Chemistry A, 2011, 115, 9520-9527.	2.5	18
1792	Self-Organization of 1-Methylnaphthalene on the Surface of Artificial Snow Grains: A Combined Experimentalâ€“Computational Approach. Journal of Physical Chemistry A, 2011, 115, 11412-11422.	2.5	43
1793	Coenzyme A Binding to the Aminoglycoside Acetyltransferase (3)-IIIb Increases Conformational Sampling of Antibiotic Binding Site. Biochemistry, 2011, 50, 10559-10565.	2.5	11
1794	Hofmeister Ion Interactions with Model Amide Compounds. Journal of Physical Chemistry B, 2011, 115, 13781-13787.	2.6	95
1795	Dislocation mediated plasticity in nanocrystalline Al: the strongest size. Modelling and Simulation in Materials Science and Engineering, 2011, 19, 074005.	2.0	20
1796	Non-adiabatic dynamics of interfacial systems: a case study of a nanoparticle penetration into a lipid bilayer. Molecular Simulation, 2011, 37, 525-536.	2.0	5
1797	Effect of Curvature on the $\beta$ -Helix Breaking Tendency of Carbon Based Nanomaterials. Journal of Physical Chemistry C, 2011, 115, 8886-8892.	3.1	57
1798	Molecular Dynamics Simulations Predict a Favorable and Unique Mode of Interaction between Lithium ( $\text{Li}^{+}$ ) Ions and Hydrophobic Molecules in Aqueous Solution. Journal of Chemical Theory and Computation, 2011, 7, 818-824.	5.3	8
1799	Stability of Elastically Deformed Massive and Nanometer-Sized Pd Hydrides. Journal of Physical Chemistry C, 2011, 115, 12803-12807.	3.1	2
1800	A Molecular Dynamics Approach for the Association of ApolipoproteinB-100 and Chondroitin-6-sulfate. Journal of Physical Chemistry B, 2011, 115, 4818-4825.	2.6	5

#	ARTICLE	IF	CITATIONS
1801	Effect of Galactosylceramide on the Dynamics of Cholesterol-Rich Lipid Membranes. Journal of Physical Chemistry B, 2011, 115, 14424-14434.	2.6	17
1802	Importance of Each Residue within Secretin for Receptor Binding and Biological Activity. Biochemistry, 2011, 50, 2983-2993.	2.5	24
1803	Composition Dependence of Glass Forming Propensity in Al <sup>~</sup> Ni Alloys. Journal of Physical Chemistry C, 2011, 115, 2320-2331.	3.1	18
1804	Coarse-Grained Molecular Dynamics Simulations of the Sphere to Rod Transition in Surfactant Micelles. Langmuir, 2011, 27, 6628-6638.	3.5	130
1805	Properties of the Membrane Binding Component of Catechol- <i>O</i> -methyltransferase Revealed by Atomistic Molecular Dynamics Simulations. Journal of Physical Chemistry B, 2011, 115, 13541-13550.	2.6	15
1806	Prediction of Favored and Optimized Compositions for Cu <sup>~</sup> Zr <sup>~</sup> Ni Metallic Glasses by Interatomic Potential. Journal of Physical Chemistry B, 2011, 115, 4703-4708.	2.6	9
1807	Solvation Structure and Dynamics of <i>cis</i> - and <i>trans</i> -1,2 Dichloroethene Isomers in Supercritical Carbon Dioxide. A Molecular Dynamics Simulation Study.. Journal of Physical Chemistry B, 2011, 115, 12098-12107.	2.6	13
1808	Proline 68 Enhances Photoisomerization Yield in Photoactive Yellow Protein. Journal of Physical Chemistry B, 2011, 115, 6668-6677.	2.6	17
1809	The Influence of Cholesterol on the Properties and Permeability of Hypericin Derivatives in Lipid Membranes. Journal of Chemical Theory and Computation, 2011, 7, 560-574.	5.3	45
1810	Characterization of Interactions between PilA from Pseudomonas aeruginosa Strain K and a Model Membrane. Journal of Physical Chemistry B, 2011, 115, 8004-8008.	2.6	21
1811	Liquid Structure of and Li <sup>+</sup> Ion Solvation in Bis(trifluoromethanesulfonyl)amide Based Ionic Liquids Composed of 1-Ethyl-3-methylimidazolium and <i>N</i> -Methyl- <i>N</i> -propylpyrrolidinium Cations. Journal of Physical Chemistry B, 2011, 115, 12179-12191.	2.6	102
1812	Reversible Hydrogen Bond Network Dynamics: Molecular Dynamics Simulations of Calix[4]arene-Catenanes. Journal of Physical Chemistry B, 2011, 115, 6445-6454.	2.6	18
1813	Mechanistic Analysis of Gas Enrichment in Gas- <sup>~</sup> Water Mixtures near Extended Surfaces. Journal of Physical Chemistry C, 2011, 115, 17495-17502.	3.1	8
1814	Simulations of High-Pressure Phases in RDX. Journal of Physical Chemistry B, 2011, 115, 4378-4386.	2.6	108
1815	On the Role of London Dispersion Forces in Biomolecular Structure Determination. Journal of Physical Chemistry B, 2011, 115, 8038-8046.	2.6	41
1816	Molecular Dynamics Simulations of Pregelification Mixtures for the Production of Imprinted Xerogels. Langmuir, 2011, 27, 5062-5070.	3.5	14
1817	Parsing Partial Molar Volumes of Small Molecules: A Molecular Dynamics Study. Journal of Physical Chemistry B, 2011, 115, 4856-4862.	2.6	40
1818	Controlling them-Poly(phenylene ethynylene) Helical Cavity Environment: Hydrogen Bond Stabilized Helical Structures. Macromolecules, 2011, 44, 60-67.	4.8	8

#	ARTICLE	IF	CITATIONS
1819	Characterizing the Dynamics and Ligand-Specific Interactions in the Human Leukocyte Elastase through Molecular Dynamics Simulations. <i>Journal of Chemical Information and Modeling</i> , 2011, 51, 1690-1702.	5.4	8
1820	An Analysis of the Influence of Protein Intrinsic Dynamical Properties on its Thermal Unfolding Behavior. <i>Journal of Biomolecular Structure and Dynamics</i> , 2011, 29, 105-121.	3.5	10
1821	Simulated Glass Transition of Poly(ethylene oxide) Bulk and Film: A Comparative Study. <i>Journal of Physical Chemistry B</i> , 2011, 115, 11044-11052.	2.6	53
1822	Molecular Transport through Surfactant-Covered Oil-Water Interfaces: Role of Physical Properties of Solutes and Surfactants in Creating Energy Barriers for Transport. <i>Langmuir</i> , 2011, 27, 2420-2436.	3.5	16
1823	Dielectric Constant of Ices and Water: A Lesson about Water Interactions. <i>Journal of Physical Chemistry A</i> , 2011, 115, 5745-5758.	2.5	108
1824	Lactam Constraints Provide Insights into the Receptor-Bound Conformation of Secretin and Stabilize a Receptor Antagonist. <i>Biochemistry</i> , 2011, 50, 8181-8192.	2.5	21
1825	Molecular Dynamics Simulation Study of Interaction between Model Rough Hydrophobic Surfaces. <i>Journal of Physical Chemistry A</i> , 2011, 115, 6059-6067.	2.5	13
1826	Phase Behavior of Disk-Coil Macromolecules. <i>Macromolecules</i> , 2011, 44, 7016-7025.	4.8	9
1827	Interaction of Melittin Peptides with Perfluorocarbon Nanoemulsion Particles. <i>Journal of Physical Chemistry B</i> , 2011, 115, 15271-15279.	2.6	24
1828	Systematic Coarse Graining of 4-Cyano-4'-pentylbiphenyl. <i>Industrial &amp; Engineering Chemistry Research</i> , 2011, 50, 546-556.	3.7	35
1829	Entropy Balance in the Intercalation Process of an Anti-Cancer Drug Daunomycin. <i>Journal of Physical Chemistry Letters</i> , 2011, 2, 3021-3026.	4.6	39
1830	Urea-Induced Drying of Hydrophobic Nanotubes: Comparison of Different Urea Models. <i>Journal of Physical Chemistry B</i> , 2011, 115, 2988-2994.	2.6	52
1831	Thermodynamic stability of nanometre-sized Cu <sub>3</sub> Au systems. <i>Nanotechnology</i> , 2011, 22, 155704.	2.6	5
1832	Using molecular simulation to predict solute solvation and partition coefficients in solvents of different polarity. <i>Physical Chemistry Chemical Physics</i> , 2011, 13, 9155.	2.8	30
1833	Simulation Analysis of the Temperature Dependence of Lignin Structure and Dynamics. <i>Journal of the American Chemical Society</i> , 2011, 133, 20277-20287.	13.7	126
1834	Enhanced small-angle scattering connected to the Widom line in simulations of supercooled water. <i>Journal of Chemical Physics</i> , 2011, 134, 214506.	3.0	67
1835	Theoretical and Computational Analysis of Static and Dynamic Anomalies in Water-DMSO Binary Mixture at Low DMSO Concentrations. <i>Journal of Physical Chemistry B</i> , 2011, 115, 685-692.	2.6	99
1836	Interpretation of Fluctuation Spectra in Lipid Bilayer Simulations. <i>Biophysical Journal</i> , 2011, 100, 2104-2111.	0.5	117



#	ARTICLE	IF	CITATIONS
1837	Glu-286 Rotation and Water Wire Reorientation Are Unlikely the Gating Elements for Proton Pumping in Cytochrome c Oxidase. <i>Biophysical Journal</i> , 2011, 101, 61-69.	0.5	34
1838	Toward a Predictive Understanding of Slow Methyl Group Dynamics in Proteins. <i>Biophysical Journal</i> , 2011, 101, 910-915.	0.5	37
1839	Oxidized Phosphatidylcholines Facilitate Phospholipid Flip-Flop in Liposomes. <i>Biophysical Journal</i> , 2011, 101, 1376-1384.	0.5	87
1840	Thermodynamics of liquids: standard molar entropies and heat capacities of common solvents from 2PT molecular dynamics. <i>Physical Chemistry Chemical Physics</i> , 2011, 13, 169-181.	2.8	144
1841	Using Molecular Dynamics to Study Liquid Phase Behavior: Simulations of the Ternary Sodium Laurate/Sodium Oleate/Water System. <i>Langmuir</i> , 2011, 27, 11381-11393.	3.5	35
1842	Molecular Insight into Conformational Transition of Amyloid $\beta$ -Peptide 42 Inhibited by ( $\alpha^*$ )-Epigallocatechin-3-gallate Probed by Molecular Simulations. <i>Journal of Physical Chemistry B</i> , 2011, 115, 11879-11887.	2.6	122
1843	<i>In Vitro</i> Polymerization of Microtubules with a Fullerene Derivative. <i>ACS Nano</i> , 2011, 5, 6306-6314.	14.6	55
1844	Electroporation of the E. coli and S. Aureus Membranes: Molecular Dynamics Simulations of Complex Bacterial Membranes. <i>Journal of Physical Chemistry B</i> , 2011, 115, 13381-13388.	2.6	219
1845	Molecular Simulations of Dodecyl- $\beta$ -maltoside Micelles in Water: Influence of the Headgroup Conformation and Force Field Parameters. <i>Journal of Physical Chemistry B</i> , 2011, 115, 487-499.	2.6	69
1846	Optical Properties of Ag/Polyvinylidene Fluoride Nanocomposites: A Theoretical Study. <i>Journal of Physical Chemistry C</i> , 2011, 115, 8316-8324.	3.1	17
1847	Molecular Dynamics Study of Carbon Dioxide Hydrate Dissociation. <i>Journal of Physical Chemistry A</i> , 2011, 115, 6102-6111.	2.5	107
1848	Molecular Dynamics Study of Hydrated Poly(ethylene oxide) Chains Grafted on Siloxane Surface. <i>Macromolecules</i> , 2011, 44, 3639-3648.	4.8	20
1849	Multiple stepwise pattern for potential of mean force in unfolding the thrombin binding aptamer in complex with Sr <sup>2+</sup> . <i>Journal of Chemical Physics</i> , 2011, 135, 225104.	3.0	18
1850	Helium-vacancy cluster in a single bcc iron crystal lattice. <i>Journal of Physics Condensed Matter</i> , 2011, 23, 245403.	1.8	23
1851	How Is Charge Transport Different in Ionic Liquids and Electrolyte Solutions?. <i>Journal of Physical Chemistry B</i> , 2011, 115, 13212-13221.	2.6	190
1852	Molecular Dynamics Simulations of the Structural and Thermodynamic Properties of Imidazolium-Based Ionic Liquid Mixtures. <i>Journal of Physical Chemistry B</i> , 2011, 115, 11170-11182.	2.6	58
1853	A flexible model for water based on TIP4P/2005. <i>Journal of Chemical Physics</i> , 2011, 135, 224516.	3.0	153
1854	Investigation of the Structure Requirement for 5-HT <sub>6</sub> Binding Affinity of Arylsulfonyl Derivatives: A Computational Study. <i>International Journal of Molecular Sciences</i> , 2011, 12, 5011-5030.	4.1	15



#	ARTICLE	IF	CITATIONS
1855	Direct Measurement of the Kinetics and Thermodynamics of Association of Hydrophobic Molecules from Molecular Dynamics Simulations. <i>Journal of Physical Chemistry Letters</i> , 2011, 2, 19-24.	4.6	28
1856	Adsorption of collagen onto single walled carbon nanotubes: a molecular dynamics investigation. <i>Physical Chemistry Chemical Physics</i> , 2011, 13, 13046.	2.8	21
1857	A Coarse-Grained Model for Molecular Dynamics Simulations of Native Cellulose. <i>Journal of Chemical Theory and Computation</i> , 2011, 7, 753-760.	5.3	79
1858	A molecular dynamics simulation study to investigate the elastic properties of PVDF and POSS nanocomposites. <i>Modelling and Simulation in Materials Science and Engineering</i> , 2011, 19, 025005.	2.0	24
1859	Benzofurans from <i>Styrax agrestis</i> As Acetylcholinesterase Inhibitors: Structure–Activity Relationships and Molecular Modeling Studies. <i>Journal of Natural Products</i> , 2011, 74, 2081-2088.	3.0	30
1860	NANOINDENTATION SIMULATION ON MECHANICAL BEHAVIOR OF NANOCRYSTALLINE $\text{Ni}$ . <i>International Journal of Modern Physics B</i> , 2011, 25, 1689-1700.	2.0	5
1861	An Atomistic Simulation for 4-Cyano-4'-pentylbiphenyl and Its Homologue with a Reoptimized Force Field. <i>Journal of Physical Chemistry B</i> , 2011, 115, 2214-2227.	2.6	38
1862	Properties and behaviour of tetracyclic allopsoralen derivatives inside a DPPC lipid bilayer model. <i>Physical Chemistry Chemical Physics</i> , 2011, 13, 10174.	2.8	5
1863	Impact of sterol tilt on membrane bending rigidity in cholesterol and 7DHC-containing DMPC membranes. <i>Soft Matter</i> , 2011, 7, 10299.	2.7	18
1864	Wide-angle X-ray diffraction and molecular dynamics study of medium-range order in ambient and hot water. <i>Physical Chemistry Chemical Physics</i> , 2011, 13, 19997.	2.8	63
1865	Temperature effect on ideal shear strength of Al and Cu. <i>Physical Review B</i> , 2011, 84, .	3.2	45
1866	DNA Base Pair Hybridization and Water-Mediated Metastable Structures Studied by Molecular Dynamics Simulations. <i>Biochemistry</i> , 2011, 50, 9628-9632.	2.5	21
1867	Surface Hydroxyl Identity and Reactivity in Akaganite. <i>Journal of Physical Chemistry C</i> , 2011, 115, 17036-17045.	3.1	30
1868	From Coarse Grained to Atomistic: A Serial Multiscale Approach to Membrane Protein Simulations. <i>Journal of Chemical Theory and Computation</i> , 2011, 7, 1157-1166.	5.3	240
1869	Molecular dynamics simulation of pressure-driven water flow in silicon-carbide nanotubes. <i>Journal of Chemical Physics</i> , 2011, 135, 204509.	3.0	52
1870	Kinetic aspects of the thermostatted growth of ice from supercooled water in simulations. <i>Journal of Chemical Physics</i> , 2011, 135, 034701.	3.0	39
1871	Molecular Dynamics Simulation Study of Chlorophyll a in Different Organic Solvents. <i>Journal of Chemical Theory and Computation</i> , 2011, 7, 1131-1140.	5.3	34
1872	A new force field model of 1-butyl-3-methylimidazolium tetrafluoroborate ionic liquid and acetonitrile mixtures. <i>Physical Chemistry Chemical Physics</i> , 2011, 13, 19345.	2.8	57

#	ARTICLE	IF	CITATIONS
1873	Dynamical Properties of Alcohol + 1-Hexyl-3-methylimidazolium Ionic Liquid Mixtures: A Computer Simulation Study. <i>Journal of Physical Chemistry B</i> , 2011, 115, 15313-15322.	2.6	33
1874	Study of Tamiflu Sensitivity to Variants of A/H5N1 Virus Using Different Force Fields. <i>Journal of Chemical Information and Modeling</i> , 2011, 51, 2266-2276.	5.4	36
1875	Steered Molecular Dynamics Simulations Reveal Important Mechanisms in Reversible Monoamine Oxidase B Inhibition. <i>Biochemistry</i> , 2011, 50, 6441-6454.	2.5	23
1876	A new force field model for the simulation of transport properties of imidazolium-based ionic liquids. <i>Physical Chemistry Chemical Physics</i> , 2011, 13, 7910.	2.8	168
1877	Using the Wimleyâ€“White Hydrophobicity Scale as a Direct Quantitative Test of Force Fields: The MARTINI Coarse-Grained Model. <i>Journal of Chemical Theory and Computation</i> , 2011, 7, 2316-2324.	5.3	47
1878	An analysis on nanovoid growth in body-centered cubic single crystalline vanadium. <i>Computational Materials Science</i> , 2011, 50, 2411-2421.	3.0	34
1879	Molecular dynamics simulation of a novel kind of polymer composite incorporated with polyhedral oligomeric silsesquioxane (POSS). <i>Computational Materials Science</i> , 2011, 50, 3282-3289.	3.0	28
1880	Hydrogen hardening effect in heavily deformed single crystal $\alpha$ -Fe. <i>Computational Materials Science</i> , 2011, 50, 3397-3402.	3.0	21
1881	Structure and hydrogen bonding in aqueous sodium chloride solutions using theoretical water model AB4: Effects of concentration. <i>Computational and Theoretical Chemistry</i> , 2011, 977, 97-102.	2.5	15
1882	Exploring the conformational dynamics and membrane interactions of PorB from <i>C. glutamicum</i> : A multi-scale molecular dynamics simulation study. <i>Biochimica Et Biophysica Acta - Biomembranes</i> , 2011, 1808, 1746-1752.	2.6	6
1883	Influence of the arrangement and secondary structure of melittin peptides on the formation and stability of toroidal pores. <i>Biochimica Et Biophysica Acta - Biomembranes</i> , 2011, 1808, 2258-2266.	2.6	36
1884	Ions and the Protein Surface Revisited: Extensive Molecular Dynamics Simulations and Analysis of Protein Structures in Alkali-Chloride Solutions. <i>Journal of Physical Chemistry B</i> , 2011, 115, 9213-9223.	2.6	32
1885	Thermal Stability and Unfolding Pathways of Sso7d and its Mutant F31A: Insight from Molecular Dynamics Simulation. <i>Journal of Biomolecular Structure and Dynamics</i> , 2011, 28, 717-727.	3.5	21
1886	Molecular Dynamics Simulations Reveal Insights into Key Structural Elements of Adenosine Receptors. <i>Biochemistry</i> , 2011, 50, 4194-4208.	2.5	64
1887	Ultrashort-pulse laser ablation of nanocrystalline aluminum. <i>Physical Review B</i> , 2011, 84, .	3.2	29
1888	Common Structural Traits across Pathogenic Mutants of the Human Prion Protein and Their Implications for Familial Prion Diseases. <i>Journal of Molecular Biology</i> , 2011, 411, 700-712.	4.2	66
1889	Dynamical behaviour of the human $\beta$ 21-adrenoceptor under agonist binding. <i>Molecular Simulation</i> , 2011, 37, 907-913.	2.0	10
1890	Catalytic Mechanism and Roles of Arg197 and Thr183 in the <i>Staphylococcus aureus</i> Sortase A Enzyme. <i>Journal of Physical Chemistry B</i> , 2011, 115, 13003-13011.	2.6	28

#	ARTICLE	IF	CITATIONS
1891	Size and Sequence and the Volume Change of Protein Folding. Journal of the American Chemical Society, 2011, 133, 6020-6027.	13.7	101
1892	Bilayer Structure and Lipid Dynamics in a Model Stratum Corneum with Oleic Acid. Journal of Physical Chemistry B, 2011, 115, 3164-3171.	2.6	64
1893	Thermo-activated Dislocation Emission at the Cu/Nb Interface Revealed by Molecular Dynamics Simulations. Journal of Materials Science and Technology, 2011, 27, 714-718.	10.7	2
1894	Keep It Flexible: Driving Macromolecular Rotary Motions in Atomistic Simulations with GROMACS. Journal of Chemical Theory and Computation, 2011, 7, 1381-1393.	5.3	42
1895	Combined 3D-QSAR, Molecular Docking, and Molecular Dynamics Study on Piperazinyl-Glutamate-Pyridines/Pyrimidines as Potent P2Y12 Antagonists for Inhibition of Platelet Aggregation. Journal of Chemical Information and Modeling, 2011, 51, 2560-2572.	5.4	38
1896	Absorption and Fluorescence of PRODAN in Phospholipid Bilayers: A Combined Quantum Mechanics and Classical Molecular Dynamics Study. Journal of Physical Chemistry A, 2011, 115, 11428-11437.	2.5	43
1897	Atom-centered symmetry functions for constructing high-dimensional neural network potentials. Journal of Chemical Physics, 2011, 134, 074106.	3.0	1,014
1898	The effect of lipid oxidation on the water permeability of phospholipids bilayers. Physical Chemistry Chemical Physics, 2011, 13, 17555.	2.8	83
1899	Study of PEGylated Lipid Layers as a Model for PEGylated Liposome Surfaces: Molecular Dynamics Simulation and Langmuir Monolayer Studies. Langmuir, 2011, 27, 7788-7798.	3.5	95
1900	A Comparative Study for Molecular Dynamics Simulations of Liquid Benzene. Journal of Chemical Theory and Computation, 2011, 7, 2240-2252.	5.3	74
1901	The Role of Conformational Ensembles in Ligand Recognition in G-Protein Coupled Receptors. Journal of the American Chemical Society, 2011, 133, 13197-13204.	13.7	72
1902	Physical Properties at the Base for the Development of an All-Atom Force Field for Ethylene Glycol. Journal of Physical Chemistry B, 2011, 115, 3013-3019.	2.6	37
1903	The cages, dynamics, and structuring of incipient methane clathrate hydrates. Physical Chemistry Chemical Physics, 2011, 13, 19951.	2.8	127
1904	How Do Aminoadamantanes Block the Influenza M2 Channel, and How Does Resistance Develop?. Journal of the American Chemical Society, 2011, 133, 9903-9911.	13.7	73
1905	Use of Umbrella Sampling to Calculate the Entrance/Exit Pathway for Z-Pro-Prolinal Inhibitor in Prolyl Oligopeptidase. Journal of Chemical Theory and Computation, 2011, 7, 1583-1594.	5.3	28
1906	MD Simulation of Single-wall Carbon Nanotubes Employed as Container in Self-healing Materials. Polymers and Polymer Composites, 2011, 19, 333-338.	1.9	4
1908	Interaction of $\beta$ -Sheet Folds with a Gold Surface. PLoS ONE, 2011, 6, e20925.	2.5	61
1909	Computational Study of Interstitial Hydrogen Atoms in Nano-Diamond Grains Embedded in an Amorphous Carbon Shell. Communications in Computational Physics, 2011, 9, 843-858.	1.7	2

#	ARTICLE	IF	CITATIONS
1910	Formation of dislocation loops during He clustering in bcc Fe. Journal of Physics Condensed Matter, 2011, 23, 442201.	1.8	26
1911	Effects of Carbon Nanotubes on Structure and Elasticity of Lipid Bilayers. Current Nanoscience, 2011, 7, 674-689.	1.2	3
1912	A Molecular Dynamic Simulation of Crosslinking of Bisphenol and Triazine by United Atom Model: A Polycyanurate Model. Chemistry Letters, 2011, 40, 309-311.	1.3	9
1914	Structural Study for Helical Biomacromolecular Complexes of $\beta$ -1,3-D-glucans and Polynucleotide by Molecular Dynamics Simulation. Kobunshi Ronbunshu, 2011, 68, 711-718.	0.2	2
1915	Accuracy of existing atomic potentials for the CdTe semiconductor compound. Journal of Chemical Physics, 2011, 134, 244703.	3.0	37
1916	Enhancement of nanovoid formation in annealed amorphous Al <sub>2</sub> O <sub>3</sub> including W. Journal of Applied Physics, 2011, 110, 064324.	2.5	13
1917	Symmetry-adapted non-equilibrium molecular dynamics of chiral carbon nanotubes under tensile loading. Journal of Applied Physics, 2011, 109, .	2.5	13
1918	Phase behavior of symmetric disk-coil macromolecules with stacking interactions. Journal of Chemical Physics, 2011, 135, 024902.	3.0	5
1919	Interatomic potential to calculate the driving force, optimized composition, and atomic structure of the Cu-Hf-Al metallic glasses. Applied Physics Letters, 2011, 99, .	3.3	6
1920	Opposite photo-induced deformations in azobenzene-containing polymers with different molecular architecture: Molecular dynamics study. Journal of Chemical Physics, 2011, 135, 044901.	3.0	58
1921	Molecular Mimicry and Ligand Recognition in Binding and Catalysis by the Histone Demethylase LSD1-CoREST Complex. Structure, 2011, 19, 212-220.	3.3	85
1922	Biophysical and Computational Studies of Membrane Penetration by the GRP1 Pleckstrin Homology Domain. Structure, 2011, 19, 1338-1346.	3.3	56
1923	Anisotropic behavior of energetic materials at elevated pressure and temperature. Journal of Loss Prevention in the Process Industries, 2011, 24, 805-805.	3.3	2
1924	Development of in silico models for pyrazoles and pyrimidine derivatives as cyclin-dependent kinase 2 inhibitors. Journal of Molecular Graphics and Modelling, 2011, 30, 67-81.	2.4	15
1925	Simulated strength and structure of carbon-carbon reinforced composite. Materials Chemistry and Physics, 2011, 129, 1240-1246.	4.0	12
1926	Structural, electronic properties and chemical bonding in protonated lithium metallates Li <sub>2</sub> x H x MO <sub>3</sub> (M = Ti, Zr, Sn). Journal of Structural Chemistry, 2011, 52, 1043-1050.	1.0	13
1927	The MOLDY short-range molecular dynamics package. Computer Physics Communications, 2011, 182, 2587-2604.	7.5	36
1928	The adsorption of DNA bases on neutral and charged (8, 8) carbon-nanotubes. Chemical Physics Letters, 2011, 514, 311-316.	2.6	32

#	ARTICLE	IF	CITATIONS
1929	The adsorption of xyloglucan on cellulose: effects of explicit water and side chain variation. Carbohydrate Research, 2011, 346, 2595-2602.	2.3	53
1930	Free Energy Calculations of Gramicidin Dimer Dissociation. Journal of Physical Chemistry B, 2011, 115, 13765-13770.	2.6	8
1931	Water Boiling Inside Carbon Nanotubes: Toward Efficient Drug Release. ACS Nano, 2011, 5, 5647-5655.	14.6	108
1932	Cholesterol Effect on Water Permeability through DPPC and PSM Lipid Bilayers: A Molecular Dynamics Study. Journal of Physical Chemistry B, 2011, 115, 15241-15250.	2.6	106
1933	Effects of grain boundary and boundary inclination on hydrogen diffusion in $\delta$ -iron. Journal of Materials Research, 2011, 26, 2735-2743.	2.6	32
1934	Molecular-dynamic simulation of DPPC bilayer in different phase state: Hydration and electric field distribution in the presence of Be <sup>2+</sup> cations. Biochemistry (Moscow) Supplement Series A: Membrane and Cell Biology, 2011, 5, 370-378.	0.6	3
1935	Atomistic simulations of pressure-induced structural transformations in solids. European Physical Journal B, 2011, 79, 241-252.	1.5	22
1936	Molecular dynamics characterization of icosahedral short range order in undercooled copper. European Physical Journal: Special Topics, 2011, 196, 35-43.	2.6	4
1937	Promiscuity of Carbonic Anhydrase II. Unexpected Ester Hydrolysis of Carbohydrate-Based Sulfamate Inhibitors. Journal of the American Chemical Society, 2011, 133, 18452-18462.	13.7	38
1938	Design of Covalent Organic Frameworks for Methane Storage. Journal of Physical Chemistry A, 2011, 115, 13852-13857.	2.5	92
1939	Methane Hydrate Nucleation Rates from Molecular Dynamics Simulations: Effects of Aqueous Methane Concentration, Interfacial Curvature, and System Size. Journal of Physical Chemistry C, 2011, 115, 21241-21248.	3.1	187
1940	Ligand Conformational and Solvation/Desolvation Free Energy in Protein-Ligand Complex Formation. Journal of Physical Chemistry B, 2011, 115, 4718-4724.	2.6	24
1941	Ab initio molecular dynamics simulation of pressure-induced phase transformation in BeO. Journal of Materials Science, 2011, 46, 6408-6415.	3.7	4
1942	Hydration Structure of Cocaine and its Metabolites: A Molecular Dynamics Study. Journal of Solution Chemistry, 2011, 40, 656-679.	1.2	1
1943	A molecular dynamics study of the thermal response of crystalline cellulose $\beta$ . Cellulose, 2011, 18, 207-221.	4.9	39
1944	Trajectory NG: portable, compressed, general molecular dynamics trajectories. Journal of Molecular Modeling, 2011, 17, 2669-2685.	1.8	14
1945	A systematic study of fundamentals in $\alpha$ -helical coiled coil mimicry by alternating sequences of $\beta$ - and $\gamma$ -amino acids. Amino Acids, 2011, 41, 733-742.	2.7	12
1946	Orientations of special water dipoles that accelerate water molecules exiting from carbon nanotube. Applied Mathematics and Mechanics (English Edition), 2011, 32, 1101-1108.	3.6	2

#	ARTICLE	IF	CITATIONS
1947	Comparison of thermal effects of stilbenoid analogs in lipid bilayers using differential scanning calorimetry and molecular dynamics: correlation of thermal effects and topographical position with antioxidant activity. <i>European Biophysics Journal</i> , 2011, 40, 865-875.	2.2	20
1948	Study of the Alzheimer's A $\beta$ 240 peptide in SDS micelles using molecular dynamics simulations. <i>Biophysical Chemistry</i> , 2011, 153, 179-186.	2.8	9
1949	Structural properties of hydroxyl-substituted alkyl benzenesulfonates at the water/vapor and water/decane interfaces. <i>Science China Chemistry</i> , 2011, 54, 1078-1085.	8.2	10
1950	Revealing the functionality of hypothetical protein KPN00728 from <i>Klebsiella pneumoniae</i> MGH78578: molecular dynamics simulation approaches. <i>BMC Bioinformatics</i> , 2011, 12, S11.	2.6	7
1951	How T cell receptors interact with peptide-MHCs: A multiple steered molecular dynamics study. <i>Proteins: Structure, Function and Bioinformatics</i> , 2011, 79, 3007-3024.	2.6	43
1952	Competitive absorption of epoxy monomers on carbon nanotube: A molecular simulation study. <i>Journal of Polymer Science, Part B: Polymer Physics</i> , 2011, 49, 1123-1130.	2.1	15
1953	Lipid composition influences the release of Alzheimer's amyloid $\beta$ peptide from membranes. <i>Protein Science</i> , 2011, 20, 1530-1545.	7.6	81
1954	Insights into the structural stability of Bax from molecular dynamics simulations at high temperatures. <i>Protein Science</i> , 2011, 20, 2035-2046.	7.6	9
1955	Partial interdigitation of lipid bilayers. <i>International Journal of Quantum Chemistry</i> , 2011, 111, 1172-1183.	2.0	20
1956	Effect of solute flexibility and polarization on the solvatochromic shift of a brominated merocyanine dye in water: A sequential MD/QM study. <i>International Journal of Quantum Chemistry</i> , 2011, 111, 1607-1615.	2.0	6
1957	Modelling the interaction between the p53 DNA-binding domain and the p28 peptide fragment of Azurin. <i>Journal of Molecular Recognition</i> , 2011, 24, 1043-1055.	2.1	25
1958	Mapping the Catechol Binding Site in Dopamine D <sub>1</sub> Receptors: Synthesis and Evaluation of Two Parallel Series of Bicyclic Dopamine Analogues. <i>ChemMedChem</i> , 2011, 6, 1024-1040.	3.2	17
1959	Combination of the CHARMM27 force field with united-atom lipid force fields. <i>Journal of Computational Chemistry</i> , 2011, 32, 1400-1410.	3.3	75
1960	Molecular basis of calcium binding by polyguluronate chains. Revising the egg-box model. <i>Journal of Computational Chemistry</i> , 2011, 32, 2988-2995.	3.3	86
1961	Design and Synthesis of Sphingomyelin-Cholesterol Conjugates and Their Formation of Ordered Membranes. <i>Chemistry - A European Journal</i> , 2011, 17, 8568-8575.	3.3	8
1962	Comparing the structural properties of human and rat islet amyloid polypeptide by MD computer simulations. <i>Biophysical Chemistry</i> , 2011, 156, 43-50.	2.8	49
1963	Structural basis for the role of LYS220 as proton donor for nucleotidyl transfer in HIV-1 reverse transcriptase. <i>Biophysical Chemistry</i> , 2011, 157, 1-6.	2.8	4
1964	Least square method for the calculation of elastic constants. <i>Computer Physics Communications</i> , 2011, 182, 1447-1451.	7.5	8



#	ARTICLE	IF	CITATIONS
1965	Stiffening of organosilicate glasses by organic cross-linking. <i>Acta Materialia</i> , 2011, 59, 44-52.	7.9	63
1966	A molecular dynamics study of structural and dynamical correlations of CaTiO <sub>3</sub> . <i>Acta Materialia</i> , 2011, 59, 1409-1423.	7.9	22
1967	Nanovoid formation by change in amorphous structure through the annealing of amorphous Al <sub>2</sub> O <sub>3</sub> thin films. <i>Acta Materialia</i> , 2011, 59, 4631-4640.	7.9	22
1968	New potent human acetylcholinesterase inhibitors in the tetracyclic triterpene series with inhibitory potency on amyloid $\beta^2$ aggregation. <i>European Journal of Medicinal Chemistry</i> , 2011, 46, 2193-2205.	5.5	36
1969	Melting of Pb clusters encapsulated in large fullerenes. <i>Chemical Physics</i> , 2011, 383, 12-18.	1.9	0
1970	Effects of pressure and temperature on the isothermal bulk modulus of CaO. <i>Physica B: Condensed Matter</i> , 2011, 406, 293-296.	2.7	10
1971	Investigating the temperature dependence of elastic constants by thermal fluctuation formula. <i>Physica B: Condensed Matter</i> , 2011, 406, 3018-3022.	2.7	1
1972	Grain-boundary activated pyramidal dislocations in nano-textured Mg by molecular dynamics simulation. <i>Materials Science &amp; Engineering A: Structural Materials: Properties, Microstructure and Processing</i> , 2011, 528, 5411-5420.	5.6	42
1973	Atomistic theory for predicting the binary metallic glass formation. <i>Materials Science and Engineering Reports</i> , 2011, 72, 1-28.	31.8	80
1974	Pressure-induced structural phase transition of small-diameter carbon nanotubes. <i>Physica E: Low-Dimensional Systems and Nanostructures</i> , 2011, 43, 673-676.	2.7	14
1975	The equivalence between volume averaging and method of planes definitions of the pressure tensor at a plane. <i>Journal of Chemical Physics</i> , 2011, 135, 024512.	3.0	37
1976	Finnisâ€Sinclair potentials for fcc Auâ€Pd and Agâ€Pt alloys. <i>International Journal of Materials Research</i> , 2011, 102, 381-388.	0.3	17
1977	Reactive force field simulation of proton diffusion in BaZrO <sub>3</sub> using an empirical valence bond approach. <i>Journal of Physics Condensed Matter</i> , 2011, 23, 334213.	1.8	31
1978	The melting curve of MgSiO <sub>3</sub> perovskite from molecular dynamics simulation. <i>Physica Scripta</i> , 2011, 83, 045602.	2.5	5
1979	On the existence of a third-order phase transition beyond the Andrews critical point: A molecular dynamics study. <i>Journal of Chemical Physics</i> , 2011, 135, 224506.	3.0	6
1980	Thermodynamics and kinetics of silicon under conditions of strong electronic excitation. <i>Journal of Applied Physics</i> , 2011, 109, 073503.	2.5	27
1981	Elastic constants of hcp $\langle \text{mml:math xmlns:mml="http://www.w3.org/1998/Math/MathML" display="inline">\langle \text{mml:msup}>\langle \text{mml:mrow}>\langle \text{mml:mn}>4</\text{mml:mn}></\text{mml:msup}></\text{mml:math}>\text{He}$ Path-integral Monte Carlo results versus experiment. <i>Physical Review B</i> , 2011, 84, .	3.2	10
1982	Design of high $\langle \text{i}>\text{T}</\text{i}></\text{sub}>\langle \text{i}>\text{g}</\text{i}></\text{sub}>$ Zr-based metallic glasses using atomistic simulation and experiment. <i>Philosophical Magazine</i> , 2011, 91, 3393-3405.	1.6	3



#	ARTICLE	IF	CITATIONS
1983	Self-consistent mean-field model for palmitoylphosphatidylcholine–palmitoyl sphingomyelin–cholesterol lipid bilayers. <i>Physical Review E</i> , 2011, 83, 031925.	2.1	6
1984	Transition of creep mechanism in nanocrystalline metals. <i>Physical Review B</i> , 2011, 84, .	3.2	51
1985	Bayesian Inference of Atomic Diffusivity in a Binary Ni/Al System Based on Molecular Dynamics. <i>Multiscale Modeling and Simulation</i> , 2011, 9, 486-512.	1.6	29
1986	Ignition of an exothermal reaction by collision between Al and Ni crystals. <i>Journal of Applied Physics</i> , 2011, 110, 103505.	2.5	11
1987	Subtleties in the calculation of the pressure and pressure tensor of anisotropic particles from volume-perturbation methods and the apparent asymmetry of the compressive and expansive contributions. <i>Molecular Physics</i> , 2011, 109, 169-189.	1.7	27
1988	Glass-forming ability and atomic-level structure of the ternary Ag–Ni–Zr metallic glasses studied by molecular dynamics simulations. <i>Journal of Applied Physics</i> , 2011, 109, 053505.	2.5	7
1989	Atomistic study of nanotwins in NiTi shape memory alloys. <i>Journal of Applied Physics</i> , 2011, 110, .	2.5	90
1990	Multiscale simulations suggest a mechanism for integrin inside-out activation. <i>Proceedings of the National Academy of Sciences of the United States of America</i> , 2011, 108, 11890-11895.	7.1	62
1991	Towards computational specificity screening of DNA-binding proteins. <i>Nucleic Acids Research</i> , 2011, 39, 8281-8290.	14.5	20
1992	Integrating diffusion maps with umbrella sampling: Application to alanine dipeptide. <i>Journal of Chemical Physics</i> , 2011, 134, 135103.	3.0	64
1993	Optimization of linear and branched alkane interactions with water to simulate hydrophobic hydration. <i>Journal of Chemical Physics</i> , 2011, 135, 054510.	3.0	36
1994	Molecular Determinants for Activation of Human Ether-Å-go-go-related Gene 1 Potassium Channels by 3-Nitro-N-(4-phenoxyphenyl) Benzamide. <i>Molecular Pharmacology</i> , 2011, 80, 630-637.	2.3	33
1995	Metallic glass-forming composition range of the Cu–Zr–Ti ternary system determined by molecular dynamics simulations with many-body potentials. <i>Journal of Materials Research</i> , 2011, 26, 547-560.	2.6	7
1996	Mechanical Behavior and Size Sensitivity of Nanocrystalline Nickel Wires Using Molecular Dynamics Simulation. <i>Journal of Aerospace Engineering</i> , 2011, 24, 147-153.	1.4	14
1997	Experimentally Justified Model-Like Description of Consolidation of Precipitated Silica. <i>Polymers</i> , 2011, 3, 2156-2171.	4.5	2
1998	Torsional elasticity and energetics of F <sub>1</sub> -ATPase. <i>Proceedings of the National Academy of Sciences of the United States of America</i> , 2011, 108, 7408-7413.	7.1	46
1999	Polymorphisms in fibronectin binding protein A of <i>Staphylococcus aureus</i> are associated with infection of cardiovascular devices. <i>Proceedings of the National Academy of Sciences of the United States of America</i> , 2011, 108, 18372-18377.	7.1	69
2000	A Novel Current Pathway Parallel to the Central Pore in a Mutant Voltage-gated Potassium Channel. <i>Journal of Biological Chemistry</i> , 2011, 286, 20031-20042.	3.4	8

#	ARTICLE	IF	CITATIONS
2001	Favored composition region for metallic glass formation and atomic configurations in the ternary Niâ€“Zrâ€“Ti system derived from n-body potential through molecular dynamics simulations. Journal of Materials Research, 2011, 26, 2050-2064.	2.6	6
2002	Interaction of Actin with Carcinoembryonic Antigen-related Cell Adhesion Molecule 1 (CEACAM1) Receptor in Liposomes Is Ca <sup>2+</sup> - and Phospholipid-dependent. Journal of Biological Chemistry, 2011, 286, 27528-27536.	3.4	9
2003	Mutant alcohol dehydrogenase leads to improved ethanol tolerance in <i>Clostridium thermocellum</i> . Proceedings of the National Academy of Sciences of the United States of America, 2011, 108, 13752-13757.	7.1	159
2005	Disordered Binding of Small Molecules to A <sup>12</sup> (12â€“28). Journal of Biological Chemistry, 2011, 286, 41578-41588.	3.4	46
2006	The multiscale coarse-graining method. VII. Free energy decomposition of coarse-grained effective potentials. Journal of Chemical Physics, 2011, 134, 224107.	3.0	65
2007	Condensed phase molecular dynamics using interpolated potential energy surfaces with application to the resolution process of coumarin 153. Journal of Chemical Physics, 2011, 135, 014107.	3.0	26
2008	Predicting Novel Binding Modes of Agonists to $\beta_2$ Adrenergic Receptors Using All-Atom Molecular Dynamics Simulations. PLoS Computational Biology, 2011, 7, e1001053.	3.2	38
2009	Putting the squeeze on cavities in liquids: Quantifying pressure effects on solvation using simulations and scaled-particle theory. Journal of Chemical Physics, 2011, 134, 014507.	3.0	15
2010	Response of water to electric fields at temperatures below the glass transition: A molecular dynamics analysis. Journal of Chemical Physics, 2011, 135, 134507.	3.0	14
2011	Response of fcc metals and $L_{12}$ and $D_{022}$ -type trialuminides to uniaxial loading along [100] and [001]: <i>ab initio</i> DFT calculations. Philosophical Magazine, 2011, 91, 491-516.	1.6	11
2012	Anchoring Intrinsically Disordered Proteins to Multiple Targets: Lessons from N-Terminus of the p53 Protein. International Journal of Molecular Sciences, 2011, 12, 1410-1430.	4.1	21
2013	Cubic-to-Tetragonal Phase Transitions in Agâ€“Cu Nanorods. Journal of Nanomaterials, 2012, 2012, 1-8.	2.7	1
2014	Finding a Needle in a Haystack: The Role of Electrostatics in Target Lipid Recognition by PH Domains. PLoS Computational Biology, 2012, 8, e1002617.	3.2	35
2015	Molecular Dynamics Simulation of Palmitate Ester Self-Assembly with Diclofenac. International Journal of Molecular Sciences, 2012, 13, 9572-9583.	4.1	20
2016	Binding of Two Intrinsically Disordered Peptides to a Multi-Specific Protein: A Combined Monte Carlo and Molecular Dynamics Study. PLoS Computational Biology, 2012, 8, e1002682.	3.2	37
2017	Phase Behavior of a Lipid Bilayer System Studied by a Replica-Exchange Molecular Dynamics Simulation. Journal of the Physical Society of Japan, 2012, 81, 024002.	1.6	16
2018	Computational studies on a new cationic peroxidase isoenzyme from artichoke leaves. Bioengineered, 2012, 3, 60-66.	3.2	0
2019	Natural polarizability and flexibility via explicit valency: The case of water. Journal of Chemical Physics, 2012, 136, 084109.	3.0	26

#	ARTICLE	IF	CITATIONS
2020	Atomistic simulations of liquid crystal mixtures of alkoxy substituted phenylpyrimidines 2PhP and PhP14. Journal of Chemical Physics, 2012, 136, 124506.	3.0	11
2021	Nanosize icosahedral quasicrystal in Mg <sub>90</sub> Ca <sub>10</sub> glass: An ab initio molecular dynamics study. Journal of Chemical Physics, 2012, 137, 034503.	3.0	4
2022	The influence of internal rotational barriers and temperature on static and dynamic properties of bulk atactic polystyrene. Journal of Chemical Physics, 2012, 137, 244903.	3.0	13
2023	Investigation of the interfacial tension of complex coacervates using field-theoretic simulations. Journal of Chemical Physics, 2012, 136, 024903.	3.0	96
2024	Water-induced ethanol dewetting transition. Journal of Chemical Physics, 2012, 137, 024703.	3.0	17
2025	Collective degrees of freedom involved in absorption and desorption of surfactant molecules in spherical non-ionic micelles. Journal of Chemical Physics, 2012, 137, 164902.	3.0	7
2026	Free-energy analysis of water affinity in polymer studied by atomistic molecular simulation combined with the theory of solutions in the energy representation. Journal of Chemical Physics, 2012, 137, 234903.	3.0	32
2027	Molecular modeling study of agglomeration of [6,6]-phenyl-C61-butyric acid methyl ester in solvents. Journal of Chemical Physics, 2012, 137, 244308.	3.0	24
2028	Computational methodology for analysis of the Soret effect in crystals: Application to hydrogen in palladium. Journal of Applied Physics, 2012, 112, .	2.5	15
2029	Core/shell structural transformation and brittle-to-ductile transition in nanowires. Applied Physics Letters, 2012, 100, .	3.3	12
2030	Quadrupolar spectra of nuclear spins in strained In <sub>x</sub> Ga <sub>1-x</sub> As quantum dots. Physical Review B, 2012, 85, .	3.2	55
2031	Length-scale dependence of elastic strain from scattering measurements in metallic glasses. Physical Review B, 2012, 85, .	3.2	31
2032	Explicit all-atom modeling of realistically sized ligand-capped nanocrystals. Journal of Chemical Physics, 2012, 136, 114702.	3.0	41
2033	Molecular dynamics simulations of He bubble nucleation at grain boundaries. Journal of Physics Condensed Matter, 2012, 24, 305005.	1.8	15
2034	Molecular dynamics simulation of replacement of methane hydrate with carbon dioxide. Molecular Simulation, 2012, 38, 481-490.	2.0	23
2035	High-fidelity simulations of CdTe vapor deposition from a bond-order potential-based molecular dynamics method. Physical Review B, 2012, 85, .	3.2	19
2036	Molecular modelling of the mass density of single proteins. Journal of Biomolecular Structure and Dynamics, 2012, 30, 318-327.	3.5	2
2037	Effects of temperature and pressure on the thermal expansion of sodium chloride. Physica Scripta, 2012, 85, 045707.	2.5	2

#	ARTICLE	IF	CITATIONS
2038	Direct observation of proteolytic cleavage at the S2 site upon forced unfolding of the Notch negative regulatory region. Proceedings of the National Academy of Sciences of the United States of America, 2012, 109, E2757-65.	7.1	60
2039	Identification of a Small Molecule That Modulates Platelet Glycoprotein Ib-von Willebrand Factor Interaction. Journal of Biological Chemistry, 2012, 287, 9461-9472.	3.4	13
2040	New insights into the role of the glutamic acid of the E $\epsilon$ box motif in group B Streptococcus pilus 2a assembly. FASEB Journal, 2012, 26, 2008-2018.	0.5	11
2041	Interaction of Edge Dislocation With Stacking Fault Tetrahedron in Cu. Journal of Engineering Materials and Technology, Transactions of the ASME, 2012, 134, .	1.4	1
2042	Analytical bond-order potential for the Cd-Zn-Te ternary system. Physical Review B, 2012, 86, .	3.2	30
2043	Nonlinear elastic model for faceting of vesicles with soft grain boundaries. Physical Review E, 2012, 85, 050501.	2.1	15
2044	SHAPE DEPENDENCE OF THE PREMELTING OF NANOWIRE: A MOLECULAR DYNAMICS STUDY. International Journal of Modern Physics B, 2012, 26, 1250022.	2.0	1
2045	Chemically transferable coarse-grained potentials from conditional reversible work calculations. Journal of Chemical Physics, 2012, 137, 154113.	3.0	58
2046	Atomistic simulations of dislocation pinning points in pure face-centered-cubic nanopillars. Modelling and Simulation in Materials Science and Engineering, 2012, 20, 075001.	2.0	18
2047	The Energy State and Phase Transition of Cu Clusters in bcc-Fe Studied by a Molecular Dynamics Simulation. Chinese Physics Letters, 2012, 29, 096102.	3.3	5
2048	Molecular Dynamics Simulation of the Mechanical Properties of NR/TPI. Advanced Materials Research, 2012, 560-561, 1114-1118.	0.3	4
2049	Proteome-wide Analysis of Lysine Acetylation Suggests its Broad Regulatory Scope in Saccharomyces cerevisiae. Molecular and Cellular Proteomics, 2012, 11, 1510-1522.	3.8	255
2050	Correlated motion of protein subdomains and large-scale conformational flexibility of RecA protein filament. Journal of Physics: Conference Series, 2012, 340, 012094.	0.4	5
2051	Combined Modeling and Biophysical Characterisation of CO <sub>2</sub> Interaction with Class II Hydrophobins: New Insight into the Mechanism Underpinning Primary Gushing. Journal of the American Society of Brewing Chemists, 2012, 70, 249-256.	1.1	23
2052	Prediction of glass-forming ability and characterization of atomic structure of the Co-Ni-Zr metallic glasses by a proposed long range empirical potential. Journal of Applied Physics, 2012, 111, 033521.	2.5	4
2053	On Accurate Approach for Molecular Dynamics Study of Ideal Strength at Elevated Temperature. Journal of Solid Mechanics and Materials Engineering, 2012, 6, 29-38.	0.5	4
2054	Grain Size Dependence of Creep in Nanocrystalline Copper by Molecular Dynamics. Materials Transactions, 2012, 53, 156-160.	1.2	35
2055	Microstructure Evolution in Polycrystalline Metal under Severe Plastic Deformation by Strain-Controlled Molecular Dynamics. Journal of Solid Mechanics and Materials Engineering, 2012, 6, 48-60.	0.5	1

#	ARTICLE	IF	CITATIONS
2056	Interfacial Tension and Surface Pressure of High Density Lipoprotein, Low Density Lipoprotein, and Related Lipid Droplets. <i>Biophysical Journal</i> , 2012, 103, 1236-1244.	0.5	42
2057	Nanoscale Elastic Properties of Montmorillonite upon Water Adsorption. <i>Langmuir</i> , 2012, 28, 16855-16863.	3.5	104
2058	Long-range n-body potential and applied to atomistic modeling the formation of ternary metallic glasses. <i>Intermetallics</i> , 2012, 31, 292-320.	3.9	18
2059	Uncertainty Quantification in MD Simulations. Part I: Forward Propagation. <i>Multiscale Modeling and Simulation</i> , 2012, 10, 1428-1459.	1.6	55
2060	Binding and reorientation of melittin in a POPC bilayer: Computer simulations. <i>Biochimica Et Biophysica Acta - Biomembranes</i> , 2012, 1818, 2975-2981.	2.6	56
2061	Molecular Dynamics Investigations of PRODAN in a DLPC Bilayer. <i>Journal of Physical Chemistry B</i> , 2012, 116, 2713-2721.	2.6	26
2062	Photodynamic Efficiency of Cationic <i>meso</i> -Porphyrins at Lipid Bilayers: Insights from Molecular Dynamics Simulations. <i>Journal of Physical Chemistry B</i> , 2012, 116, 14618-14627.	2.6	35
2063	Local Fluctuations and Conformational Transitions in Proteins. <i>Journal of Chemical Theory and Computation</i> , 2012, 8, 4775-4785.	5.3	37
2064	GROMOS 53A6 <sub>GLYC</sub> , an Improved GROMOS Force Field for Hexopyranose-Based Carbohydrates. <i>Journal of Chemical Theory and Computation</i> , 2012, 8, 4681-4690.	5.3	132
2065	Molecular Dynamics Simulations of a Characteristic DPC Micelle in Water. <i>Journal of Chemical Theory and Computation</i> , 2012, 8, 4610-4623.	5.3	62
2066	Uncovering Molecular Details of Urea Crystal Growth in the Presence of Additives. <i>Journal of the American Chemical Society</i> , 2012, 134, 17221-17233.	13.7	182
2067	Study of Interaction Between PEG Carrier and Three Relevant Drug Molecules: Piroxicam, Paclitaxel, and Hematoporphyrin. <i>Journal of Physical Chemistry B</i> , 2012, 116, 7334-7341.	2.6	51
2068	Grand canonical-like molecular dynamics simulations: Application to anisotropic mass diffusion in a nanoporous medium. <i>Journal of Chemical Physics</i> , 2012, 136, 184702.	3.0	22
2069	Phase Transitions in Coarse-Grained Lipid Bilayers Containing Cholesterol by Molecular Dynamics Simulations. <i>Biophysical Journal</i> , 2012, 103, 2125-2133.	0.5	55
2070	Protein Pharmacophore Selection Using Hydration-Site Analysis. <i>Journal of Chemical Information and Modeling</i> , 2012, 52, 1046-1060.	5.4	43
2071	Peptide-Lipid Interactions of the Stress-Response Peptide TisB That Induces Bacterial Persistence. <i>Biophysical Journal</i> , 2012, 103, 1460-1469.	0.5	50
2072	Probing Structure–Nanoaggregation Relations of Polyaromatic Surfactants: A Molecular Dynamics Simulation and Dynamic Light Scattering Study. <i>Journal of Physical Chemistry B</i> , 2012, 116, 5907-5918.	2.6	97
2073	Derivation and Systematic Validation of a Refined All-Atom Force Field for Phosphatidylcholine Lipids. <i>Journal of Physical Chemistry B</i> , 2012, 116, 3164-3179.	2.6	486

#	ARTICLE	IF	CITATIONS
2074	Hydrophobic Segregation, Phase Transitions and the Anomalous Thermodynamics of Water/Methanol Mixtures. <i>Journal of Physical Chemistry B</i> , 2012, 116, 13905-13912.	2.6	46
2075	Invariance of Parrinello-Rahman molecular dynamics and its relation to continuum mechanics. <i>Proceedings in Applied Mathematics and Mechanics</i> , 2012, 12, 419-420.	0.2	0
2076	Side-chain hydrophobicity and the stability of $\alpha$ -helical aggregates. <i>Protein Science</i> , 2012, 21, 1837-1848.	7.6	50
2077	Predicting the effects of amino acid replacements in peptide hormones on their binding affinities for class B GPCRs and application to the design of secretin receptor antagonists. <i>Journal of Computer-Aided Molecular Design</i> , 2012, 26, 835-845.	2.9	5
2078	First-principles molecular dynamics simulations to study the crystal-to-amorphous transition in the Mg-Zn system. <i>Intermetallics</i> , 2012, 29, 75-79.	3.9	13
2079	Peptide Chain Dynamics in Light and Heavy Water: Zooming in on Internal Friction. <i>Journal of the American Chemical Society</i> , 2012, 134, 6273-6279.	13.7	86
2080	GABA Binding to an Insect GABA Receptor: A Molecular Dynamics and Mutagenesis Study. <i>Biophysical Journal</i> , 2012, 103, 2071-2081.	0.5	43
2081	Phase behavior of rounded hard-squares. <i>Soft Matter</i> , 2012, 8, 4675.	2.7	104
2082	Molecular wire of urea in carbon nanotube: a molecular dynamics study. <i>Nanoscale</i> , 2012, 4, 652-658.	5.6	20
2083	Multi-Scale Simulation of the Simian Immunodeficiency Virus Fusion Peptide. <i>Journal of Physical Chemistry B</i> , 2012, 116, 13713-13721.	2.6	11
2084	Screening for the Location of RNA using the Chloride Ion Distribution in Simulations of Virus Capsids. <i>Journal of Chemical Theory and Computation</i> , 2012, 8, 2474-2483.	5.3	24
2085	Proton Transport in a Membrane Protein Channel: Two-Dimensional Infrared Spectrum Modeling. <i>Journal of Physical Chemistry B</i> , 2012, 116, 6336-6345.	2.6	8
2086	Numerical Validation of IFT in the Analysis of Protein-Surfactant Complexes with SAXS and SANS. <i>Langmuir</i> , 2012, 28, 12593-12600.	3.5	22
2087	Investigation of the Local Structure of Mixtures of an Ionic Liquid with Polar Molecular Species through Molecular Dynamics: Cluster Formation and Angular Distributions. <i>Journal of Physical Chemistry B</i> , 2012, 116, 5941-5950.	2.6	25
2088	Anesthetic molecules embedded in a lipid membrane: a computer simulation study. <i>Physical Chemistry Chemical Physics</i> , 2012, 14, 12956.	2.8	27
2089	Atomistic simulations of rare events using gentlest ascent dynamics. <i>Journal of Chemical Physics</i> , 2012, 136, 124104.	3.0	31
2090	Molecular structure of human GM-CSF in complex with a disease-associated anti-human GM-CSF autoantibody and its potential biological implications. <i>Biochemical Journal</i> , 2012, 447, 205-215.	3.7	15
2091	Structural and Functional Characterization of the Kindlin-1 Pleckstrin Homology Domain. <i>Journal of Biological Chemistry</i> , 2012, 287, 43246-43261.	3.4	27



#	ARTICLE	IF	CITATIONS
2092	Fast relaxation and elasticity-related properties of trehalose-glycerol mixtures. <i>Soft Matter</i> , 2012, 8, 4936.	2.7	18
2093	Exploring the mineralization of hydrophobins at a liquid interface. <i>Soft Matter</i> , 2012, 8, 11343.	2.7	12
2094	Thermally Induced Protein Unfolding Probed by Isotope-Edited IR Spectroscopy. <i>Journal of Physical Chemistry B</i> , 2012, 116, 9627-9634.	2.6	17
2095	Molecular Dynamics Study of a MARTINI Coarse-Grained Polystyrene Brush in Good Solvent: Structure and Dynamics. <i>Macromolecules</i> , 2012, 45, 563-571.	4.8	30
2096	Water activity coefficients in aqueous amino acid solutions by molecular dynamics simulation: 1. Force field development. <i>Molecular Simulation</i> , 2012, 38, 132-138.	2.0	3
2097	Molecular Simulation of the Thermophysical Properties of N-Functionalized Alkylimidazoles. <i>Journal of Physical Chemistry B</i> , 2012, 116, 6529-6535.	2.6	26
2098	Water Structure and Hydrogen Bonding at Goethite/Water Interfaces: Implications for Proton Affinities. <i>Journal of Physical Chemistry C</i> , 2012, 116, 4714-4724.	3.1	59
2099	Thermodynamic transferability of coarse-grained potentials for polymer-additive systems. <i>Physical Chemistry Chemical Physics</i> , 2012, 14, 11896.	2.8	26
2100	Force and Stress along Simulated Dissociation Pathways of Cucurbituril-Guest Systems. <i>Journal of Chemical Theory and Computation</i> , 2012, 8, 966-976.	5.3	14
2101	RNA Unwinding from Reweighted Pulling Simulations. <i>Journal of the American Chemical Society</i> , 2012, 134, 5173-5179.	13.7	40
2102	Structure and Dynamics of Ethanol Adsorbed on a Mica Surface. <i>Communications in Theoretical Physics</i> , 2012, 57, 308-314.	2.5	7
2103	Three-dimensional structure of human Î²-defensin 28 via homology modelling and molecular dynamics. <i>Molecular Simulation</i> , 2012, 38, 90-101.	2.0	4
2104	Structural Heterogeneity and Unique Distorted Hydrogen Bonding in Primary Ammonium Nitrate Ionic Liquids Studied by High-Energy X-ray Diffraction Experiments and MD Simulations. <i>Journal of Physical Chemistry B</i> , 2012, 116, 2801-2813.	2.6	116
2105	Nonintercalating Nanosubstrates Create Asymmetry between Bilayer Leaflets. <i>Langmuir</i> , 2012, 28, 2842-2848.	3.5	12
2106	Free Energy Barriers for Escape of Water Molecules from Protein Hydration Layer. <i>Journal of Physical Chemistry B</i> , 2012, 116, 2958-2968.	2.6	40
2107	Modification of Lipid Bilayer Structure by Diacylglycerol: A Comparative Study of Diacylglycerol and Cholesterol. <i>Journal of Chemical Theory and Computation</i> , 2012, 8, 749-758.	5.3	41
2108	Definition and Computation of Intermolecular Contact in Liquids Using Additively Weighted Voronoi Tessellation. <i>Journal of Physical Chemistry A</i> , 2012, 116, 4657-4666.	2.5	12
2109	Temperature- and Pressure-Dependent Densities, Self-Diffusion Coefficients, and Phase Behavior of Monoacid Saturated Triacylglycerides: Toward Molecular-Level Insights into Processing. <i>Journal of Agricultural and Food Chemistry</i> , 2012, 60, 5243-5249.	5.2	21



#	ARTICLE	IF	CITATIONS
2110	Interpolated Mechanicsâ€“Molecular Mechanics Study of Internal Rotation Dynamics of the Chromophore Unit in Blue Fluorescent Protein and Its Variants. <i>Journal of Physical Chemistry B</i> , 2012, 116, 11137-11147.	2.6	16
2111	Parallel Î²-Sheet Vibrational Couplings Revealed by 2D IR Spectroscopy of an Isotopically Labeled Macrocycle: Quantitative Benchmark for the Interpretation of Amyloid and Protein Infrared Spectra. <i>Journal of the American Chemical Society</i> , 2012, 134, 19118-19128.	13.7	91
2112	Role of the Subunit Interactions in the Conformational Transitions in Adult Human Hemoglobin: An Explicit Solvent Molecular Dynamics Study. <i>Journal of Physical Chemistry B</i> , 2012, 116, 11004-11009.	2.6	21
2113	Investigations into the Bending Constant and Edge Energy of Bilayers of Salt-Free Catanionic Vesicles. <i>Langmuir</i> , 2012, 28, 5927-5933.	3.5	13
2114	Computer Simulation of the Nonlinear Optical Properties of Langmuirâ€“Blodgett Films of a Squaraine Derivative. <i>Journal of Physical Chemistry C</i> , 2012, 116, 15449-15457.	3.1	5
2115	Early Events in Helix Unfolding under External Forces: A Milestoning Analysis. <i>Journal of Physical Chemistry B</i> , 2012, 116, 8662-8691.	2.6	22
2116	Replica-exchange molecular dynamics simulation of a lipid bilayer system with a coarse-grained model. <i>Molecular Simulation</i> , 2012, 38, 437-441.	2.0	13
2117	Conformational Study of Glycal-Type Neuraminidase Inhibitors. <i>Journal of Carbohydrate Chemistry</i> , 2012, 31, 114-129.	1.1	1
2118	The <i>Streptomyces</i> -Produced Antibiotic Fosfomycin Is a Promiscuous Substrate for Archaeal Isopentenyl Phosphate Kinase. <i>Biochemistry</i> , 2012, 51, 917-925.	2.5	8
2119	Interaction of Hematoporphyrin with Lipid Membranes. <i>Journal of Physical Chemistry B</i> , 2012, 116, 4889-4897.	2.6	36
2120	Molecular Dynamics Study of Poly(Ethylene Oxide) Chains Densely Grafted on Siloxane Surface in Dry Conditions. <i>Journal of Physical Chemistry C</i> , 2012, 116, 3576-3584.	3.1	8
2121	Modeling the Closed and Open State Conformations of the GABA <sub>A</sub> Ion Channel - Plausible Structural Insights for Channel Gating. <i>Journal of Chemical Information and Modeling</i> , 2012, 52, 2958-2969.	5.4	14
2122	On the Cis to Trans Isomerization of Prolylâ€“Peptide Bonds under Tension. <i>Journal of Physical Chemistry B</i> , 2012, 116, 9346-9351.	2.6	14
2123	Structure Formation of Toluene around C60: Implementation of the Adaptive Resolution Scheme (AdResS) into GROMACS. <i>Journal of Chemical Theory and Computation</i> , 2012, 8, 398-403.	5.3	52
2124	Environment Polarity in Proteins Mapped Noninvasively by FTIR Spectroscopy. <i>Journal of Physical Chemistry Letters</i> , 2012, 3, 939-944.	4.6	22
2125	Characterization of a Disordered Protein during Micellation: Interactions of Î±-Synuclein with Sodium Dodecyl Sulfate. <i>Journal of Physical Chemistry B</i> , 2012, 116, 4417-4424.	2.6	15
2126	Poly(Ethylene Glycol) in Drug Delivery, Why Does it Work, and Can We do Better? All Atom Molecular Dynamics Simulation Provides Some Answers. <i>Physics Procedia</i> , 2012, 34, 24-33.	1.2	63
2127	Molecular dynamics study of water diffusivity at low concentrations in non-swollen and swollen polyurethanes. <i>Polymer</i> , 2012, 53, 3253-3260.	3.8	9

#	ARTICLE	IF	CITATIONS
2128	Interaction of C70 fullerene with the Kv1.2 potassium channel. <i>Physical Chemistry Chemical Physics</i> , 2012, 14, 12526.	2.8	17
2129	Molecular Dynamics Simulations of the Bacterial ABC Transporter SAV1866 in the Closed Form. <i>Journal of Physical Chemistry B</i> , 2012, 116, 2934-2942.	2.6	38
2130	Molecular Dynamics Simulations of Ice Growth from Supercooled Water When Both Electric and Magnetic Fields Are Applied. <i>Journal of Physical Chemistry C</i> , 2012, 116, 19773-19780.	3.1	17
2131	Assessing Polyglutamine Conformation in the Nucleating Event by Molecular Dynamics Simulations. <i>Journal of Physical Chemistry B</i> , 2012, 116, 10259-10265.	2.6	31
2132	REACH Coarse-Grained Simulation of a Cellulose Fiber. <i>Biomacromolecules</i> , 2012, 13, 2634-2644.	5.4	33
2133	Molecular dynamics simulations of the Ca <sup>2+</sup> -pump: a structural analysis. <i>Physical Chemistry Chemical Physics</i> , 2012, 14, 3543.	2.8	14
2134	An Extension and Further Validation of an All-Atomistic Force Field for Biological Membranes. <i>Journal of Chemical Theory and Computation</i> , 2012, 8, 2938-2948.	5.3	408
2135	Peptide friction in water nanofilm on mica surface. <i>Chinese Physics B</i> , 2012, 21, 026801.	1.4	3
2136	Comparison of Secondary Structure Formation Using 10 Different Force Fields in Microsecond Molecular Dynamics Simulations. <i>Journal of Chemical Theory and Computation</i> , 2012, 8, 2725-2740.	5.3	171
2137	Insights on P-Glycoprotein's Efflux Mechanism Obtained by Molecular Dynamics Simulations. <i>Journal of Chemical Theory and Computation</i> , 2012, 8, 1853-1864.	5.3	102
2138	Morin Inhibits the Early Stages of Amyloid $\beta$ -Peptide Aggregation by Altering Tertiary and Quaternary Interactions to Produce $\alpha$ -Off-Pathway Structures. <i>Biochemistry</i> , 2012, 51, 5990-6009.	2.5	64
2139	Fluorescence Probing of Thiol-Functionalized Gold Nanoparticles: Is Alkylthiol Coating of a Nanoparticle as Hydrophobic as Expected?. <i>Journal of Physical Chemistry C</i> , 2012, 116, 21059-21068.	3.1	33
2140	Modelling elasticity and memory effects in liquid crystalline elastomers by molecular dynamics simulations. <i>Soft Matter</i> , 2012, 8, 11123.	2.7	30
2141	DNA Base Dimers Are Stabilized by Hydrogen-Bonding Interactions Including Non-Watson-Crick Pairing Near Graphite Surfaces. <i>Journal of Physical Chemistry B</i> , 2012, 116, 12088-12094.	2.6	26
2142	Vibrational Spectra of Water Solutions of Azoles from QM/MM Calculations: Effects of Solvation. <i>Journal of Physical Chemistry A</i> , 2012, 116, 10160-10171.	2.5	14
2143	Molecular Dynamics Simulations of Phosphatidylcholine Membranes: A Comparative Force Field Study. <i>Journal of Chemical Theory and Computation</i> , 2012, 8, 4593-4609.	5.3	176
2144	Strong preferences of dopamine and L-dopa towards lipid head group: importance of lipid composition and implication for neurotransmitter metabolism. <i>Journal of Neurochemistry</i> , 2012, 122, 681-690.	3.9	51
2145	Temperature-dependent structure of ionic liquids: X-ray scattering and simulations. <i>Faraday Discussions</i> , 2012, 154, 133-143.	3.2	171

#	ARTICLE	IF	CITATIONS
2146	Mechanism of <i>Taq</i> DNA Polymerase Inhibition by Fullerene Derivatives: Insight from Computer Simulations. <i>Journal of Physical Chemistry B</i> , 2012, 116, 10676-10683.	2.6	22
2147	Molecular dynamics simulation study of the vanillate transport channel of Opdk. <i>Archives of Biochemistry and Biophysics</i> , 2012, 524, 132-139.	3.0	8
2148	In silico prediction of inhibitory effects of pyrazol-5-one and indazole derivatives on GSK3 $\beta$ kinase enzyme. <i>Journal of Molecular Structure</i> , 2012, 1024, 94-103.	3.6	2
2149	Structural effect of the L16Q, K50E, and R53P mutations on homeodomain of pituitary homeobox protein 2. <i>International Journal of Biological Macromolecules</i> , 2012, 51, 305-313.	7.5	9
2150	A detailed kinetic Monte Carlo study of growth from solution using MD-derived rate constants. <i>Journal of Crystal Growth</i> , 2012, 354, 34-43.	1.5	7
2151	Characterization of a potent antimicrobial lipopeptide via coarse-grained molecular dynamics. <i>Biochimica Et Biophysica Acta - Biomembranes</i> , 2012, 1818, 212-218.	2.6	41
2152	Saturation with cholesterol increases vertical order and smoothes the surface of the phosphatidylcholine bilayer: A molecular simulation study. <i>Biochimica Et Biophysica Acta - Biomembranes</i> , 2012, 1818, 520-529.	2.6	49
2153	Structure, dynamics, and hydration of POPC/POPS bilayers suspended in NaCl, KCl, and CsCl solutions. <i>Biochimica Et Biophysica Acta - Biomembranes</i> , 2012, 1818, 609-616.	2.6	98
2154	Molecular dynamics, crystallography and mutagenesis studies on the substrate gating mechanism of prolyl oligopeptidase. <i>Biochimie</i> , 2012, 94, 1398-1411.	2.6	47
2155	Atomistic simulations on multilayer graphene reinforced epoxy composites. <i>Composites Part A: Applied Science and Manufacturing</i> , 2012, 43, 1293-1300.	7.6	116
2156	Massively parallel chemical potential calculation on graphics processing units. <i>Computer Physics Communications</i> , 2012, 183, 2054-2062.	7.5	25
2157	Conformational properties of acidic oligo- and disaccharides and their ability to bind calcium: a molecular modeling study. <i>Carbohydrate Research</i> , 2012, 357, 111-117.	2.3	14
2158	Predicting CO <sub>2</sub> -water interfacial tension under pressure and temperature conditions of geologic CO <sub>2</sub> storage. <i>Geochimica Et Cosmochimica Acta</i> , 2012, 81, 28-38.	3.9	135
2159	A novel dimerization interface of cyclic nucleotide binding domain, which is disrupted in presence of cAMP: implications for CNG channels gating. <i>Journal of Molecular Modeling</i> , 2012, 18, 4053-4060.	1.8	1
2160	Are Protein Force Fields Getting Better? A Systematic Benchmark on 524 Diverse NMR Measurements. <i>Journal of Chemical Theory and Computation</i> , 2012, 8, 1409-1414.	5.3	347
2161	Interaction of wild type, G68R and L125M isoforms of the arylamine-N-acetyltransferase from <i>Mycobacterium tuberculosis</i> with isoniazid: a computational study on a new possible mechanism of resistance. <i>Journal of Molecular Modeling</i> , 2012, 18, 4013-4024.	1.8	22
2162	Experimental and Computational Studies Reveal an Alternative Supramolecular Structure for Fmoc-Dipeptide Self-Assembly. <i>Biomacromolecules</i> , 2012, 13, 3562-3571.	5.4	79
2163	Competitive Binding of Cations to Duplex DNA Revealed through Molecular Dynamics Simulations. <i>Journal of Physical Chemistry B</i> , 2012, 116, 12946-12954.	2.6	105

#	ARTICLE	IF	CITATIONS
2164	Efficient Free Energy Calculation of Biomolecules from Diffusion-Biased Molecular Dynamics. Journal of Chemical Theory and Computation, 2012, 8, 4657-4662.	5.3	10
2165	The <i>lac</i> Repressor Displays Facilitated Diffusion in Living Cells. Science, 2012, 336, 1595-1598.	12.6	361
2166	Molecular dynamic simulation studies on the effect of one residue chain staggering on the structure and stability of heterotrimeric collagen-like peptides with interruption. Biopolymers, 2012, 97, 847-863.	2.4	10
2167	Study on Molecular Cavity of Oligoamide Macrocycles by Using Scanning Tunneling Microscopy. ChemPhysChem, 2012, 13, 3598-3604.	2.1	7
2168	The Boson peak of model glass systems and its relation to atomic structure. European Physical Journal B, 2012, 85, 1.	1.5	52
2169	Atomistic response of a model silica glass under shear and pressure. European Physical Journal B, 2012, 85, 1.	1.5	74
2170	Amyloid Inspired Self-Assembled Peptide Nanofibers. Biomacromolecules, 2012, 13, 3377-3387.	5.4	46
2171	Proton Delivery and Removal in $[\text{Ni}(\text{P}^{\text{R}}_2\text{N}^{\text{R}}_2)^2]^+_{2+}$ Hydrogen Production and Oxidation Catalysts. Journal of the American Chemical Society, 2012, 134, 19409-19424.	13.7	122
2172	Interactions between CD44 protein and hyaluronan: insights from the computational study. Molecular BioSystems, 2012, 8, 543-547.	2.9	23
2173	On the absolute thermodynamics of water from computer simulations: A comparison of first-principles molecular dynamics, reactive and empirical force fields. Journal of Chemical Physics, 2012, 137, 244507.	3.0	59
2174	MD Simulation of Crosslinked Epoxy Resin at Different Temperatures. Advanced Materials Research, 2012, 602-604, 747-750.	0.3	1
2175	Atomistic Simulations of Micellization of Sodium Hexyl, Heptyl, Octyl, and Nonyl Sulfates. Journal of Physical Chemistry B, 2012, 116, 2430-2437.	2.6	76
2176	All-Atom Stability and Oligomerization Simulations of Polyglutamine Nanotubes with and without the 17-Amino-Acid N-Terminal Fragment of the Huntingtin Protein. Journal of Physical Chemistry B, 2012, 116, 12168-12179.	2.6	15
2177	A GROMOS Parameter Set for Vicinal Diether Functions: Properties of Polyethyleneoxide and Polyethyleneglycol. Journal of Chemical Theory and Computation, 2012, 8, 3943-3963.	5.3	61
2178	New Soft-Core Potential Function for Molecular Dynamics Based Alchemical Free Energy Calculations. Journal of Chemical Theory and Computation, 2012, 8, 2373-2382.	5.3	92
2179	Molecular Dynamics. , 2012, , 249-265.		24
2180	Molecular dynamics method to locally resolve Poisson's ratio: Mechanical description of the solid-soft-matter interphase. Physical Review E, 2012, 86, 036704.	2.1	13
2181	INTERACTION BETWEEN THE 30° PARTIAL DISLOCATION AND HEX-VACANCY IN SILICON. Modern Physics Letters B, 2012, 26, 1250154.	1.9	3

#	ARTICLE	IF	CITATIONS
2182	Insight into the Structural Deformations of Beta-Cyclodextrin Caused by Alcohol Cosolvents and Guest Molecules. <i>Journal of Physical Chemistry B</i> , 2012, 116, 3880-3889.	2.6	37
2183	Force Field Development for Actinyl Ions via Quantum Mechanical Calculations: An Approach to Account for Many Body Solvation Effects. <i>Journal of Physical Chemistry B</i> , 2012, 116, 10885-10897.	2.6	38
2184	Molecular dynamics simulation study of the water-mediated interaction between zwitterionic and charged surfaces. <i>Journal of Chemical Physics</i> , 2012, 136, 024501.	3.0	10
2185	Exploring the Multidimensional Free Energy Surface of Phosphoester Hydrolysis with Constrained QM/MM Dynamics. <i>Journal of Chemical Theory and Computation</i> , 2012, 8, 3596-3604.	5.3	23
2186	Molecular Dynamics Simulation Studies of the Interactions between Ionic Liquids and Amino Acids in Aqueous Solution. <i>Journal of Physical Chemistry B</i> , 2012, 116, 1831-1842.	2.6	64
2187	Differential Solubility of Ethylene and Acetylene in Room-Temperature Ionic Liquids: A Theoretical Study. <i>Journal of Physical Chemistry B</i> , 2012, 116, 3944-3953.	2.6	42
2188	Structural Properties of Nonionic Tween80 Micelle in Water Elucidated by Molecular Dynamics Simulation. <i>APCBEE Procedia</i> , 2012, 3, 287-297.	0.5	40
2189	Mechanical Force Can Fine-Tune Redox Potentials of Disulfide Bonds. <i>Biophysical Journal</i> , 2012, 102, 622-629.	0.5	51
2190	A Novel Dendrimeric Peptide with Antimicrobial Properties: Structure-Function Analysis of SB056. <i>Biophysical Journal</i> , 2012, 102, 1039-1048.	0.5	41
2191	Predicting the Effect of Ions on the Conformation of the H-NS Dimerization Domain. <i>Biophysical Journal</i> , 2012, 103, 89-98.	0.5	14
2192	The Role of Magnesium for Geometry and Charge in GTP Hydrolysis, Revealed by Quantum Mechanics/Molecular Mechanics Simulations. <i>Biophysical Journal</i> , 2012, 103, 293-302.	0.5	46
2193	Elucidating the Locking Mechanism of Peptides onto Growing Amyloid Fibrils through Transition Path Sampling. <i>Biophysical Journal</i> , 2012, 103, 1296-1304.	0.5	37
2194	Retention of Conformational Entropy upon Calmodulin Binding to Target Peptides Is Driven by Transient Salt Bridges. <i>Biophysical Journal</i> , 2012, 103, 1576-1584.	0.5	17
2195	Polymer-polymer adhesion via connector chains: An MD study of the competition between bulk dissipation and connector pull-out. <i>Computational Materials Science</i> , 2012, 64, 187-191.	3.0	7
2196	Ab initio modeling of metallic Pd <sub>80</sub> Si <sub>20</sub> glass. <i>Computational Materials Science</i> , 2012, 65, 44-47.	3.0	29
2197	Colonic amyloidosis, computational analysis of the major amyloidogenic species, Serum Amyloid A. <i>Computational Biology and Chemistry</i> , 2012, 39, 29-34.	2.3	18
2198	Study on structure, sensitivity and mechanical properties of HMX and HMX-based PBXs with molecular dynamics simulation. <i>Computational and Theoretical Chemistry</i> , 2012, 999, 21-27.	2.5	57
2199	Understanding the binding of daunorubicin and doxorubicin to NADPH-dependent cytosolic reductases by computational methods. <i>European Journal of Medicinal Chemistry</i> , 2012, 56, 145-154.	5.5	12

#	ARTICLE	IF	CITATIONS
2200	Exploring the structure determinants of pyrazinone derivatives as PDE5 3HC8 inhibitors: An in silico analysis. <i>Journal of Molecular Graphics and Modelling</i> , 2012, 38, 112-122.	2.4	4
2201	Breakdown of the Schmid law in homogeneous and heterogeneous nucleation events of slip and twinning in magnesium. <i>Journal of the Mechanics and Physics of Solids</i> , 2012, 60, 2084-2099.	4.8	111
2202	Lipase B from <i>Candida antarctica</i> binds to hydrophobic substrateâ€“water interfaces via hydrophobic anchors surrounding the active site entrance. <i>Journal of Molecular Catalysis B: Enzymatic</i> , 2012, 84, 48-54.	1.8	39
2203	Analytical bond-order potential for the cadmium telluride binary system. <i>Physical Review B</i> , 2012, 85, .	3.2	64
2204	Prediction of the Hydration Properties of Diamondoids from Free Energy and Potential of Mean Force Calculations. <i>Journal of Physical Chemistry B</i> , 2012, 116, 13467-13471.	2.6	8
2205	Aspirin Loading and Release from MCM-41 Functionalized with Aminopropyl Groups via Co-condensation or Postsynthesis Modification Methods. <i>Journal of Physical Chemistry C</i> , 2012, 116, 18358-18366.	3.1	97
2206	A Coarse-Grained MARTINI Model of Polyethylene Glycol and of Polyoxyethylene Alkyl Ether Surfactants. <i>Journal of Physical Chemistry B</i> , 2012, 116, 14353-14362.	2.6	90
2207	Atomistic molecular dynamics study of cross-linked phenolic resins. <i>Soft Matter</i> , 2012, 8, 5283.	2.7	59
2208	Force Field Benchmark of Organic Liquids: Density, Enthalpy of Vaporization, Heat Capacities, Surface Tension, Isothermal Compressibility, Volumetric Expansion Coefficient, and Dielectric Constant. <i>Journal of Chemical Theory and Computation</i> , 2012, 8, 61-74.	5.3	609
2209	Confinement induced conformational changes in n-alkanes sequestered within a narrow carbon nanotube. <i>Physical Chemistry Chemical Physics</i> , 2012, 14, 2702.	2.8	22
2210	Charybdotoxin and Margatoxin Acting on the Human Voltage-Gated Potassium Channel $\gamma$ 1.3 and Its H399N Mutant: An Experimental and Computational Comparison. <i>Journal of Physical Chemistry B</i> , 2012, 116, 5132-5140.	2.6	15
2211	Elastic Properties of Co/Cu Nanocomposite Nanowires. <i>Advanced Structured Materials</i> , 2012, , 337-350.	0.5	1
2212	Roles of Grain Boundaries in the Strength of Metals by Using Atomic Simulations. , 2012, , 55-75.		1
2213	Mixing Properties of Sphingomyelin Ceramide Bilayers: A Simulation Study. <i>Journal of Physical Chemistry B</i> , 2012, 116, 4500-4509.	2.6	29
2214	Molecular Mechanism of Direct Proflavineâ€“DNA Intercalation: Evidence for Drug-Induced Minimum Base-Stacking Penalty Pathway. <i>Journal of Physical Chemistry B</i> , 2012, 116, 12208-12212.	2.6	37
2215	Molecular dynamics simulation of diffusion of hydrogen in binary hydrogenâ€“tetrahydrofuran hydrate. <i>Molecular Simulation</i> , 2012, 38, 333-340.	2.0	10
2216	Calculation of the melting point of alkali halides by means of computer simulations. <i>Journal of Chemical Physics</i> , 2012, 137, 104507.	3.0	41
2217	Molecular dynamics study on the relationships of modeling, structural and energy properties with sensitivity for RDX-based PBXs. <i>Science China Chemistry</i> , 2012, 55, 2587-2594.	8.2	32



#	ARTICLE	IF	CITATIONS
2218	A Molecular Trajectory of $\hat{\Gamma}$ -Actinin Activation. Biophysical Journal, 2012, 103, 2050-2059.	0.5	29
2219	Dimethyl sulfoxide induced structural transformations and non-monotonic concentration dependence of conformational fluctuation around active site of lysozyme. Journal of Chemical Physics, 2012, 136, 115103.	3.0	67
2220	Monte Carlo simulations of charge transport in organic systems with true off-diagonal disorder. Journal of Chemical Physics, 2012, 137, 114901.	3.0	16
2221	Prediction of glass forming ability and glass forming range for electrodeposited binary Co-W alloys. Journal of Applied Physics, 2012, 111, .	2.5	8
2222	Coarse-Grained Modeling of Polystyrene in Various Environments by Iterative Boltzmann Inversion. Macromolecules, 2012, 45, 9205-9219.	4.8	72
2223	Ligand migration in myoglobin: A combined study of computer simulation and x-ray crystallography. Journal of Chemical Physics, 2012, 136, 165101.	3.0	7
2224	Solubility of NaCl in water by molecular simulation revisited. Journal of Chemical Physics, 2012, 136, 244508.	3.0	133
2225	Optimization of the Additive CHARMM All-Atom Protein Force Field Targeting Improved Sampling of the Backbone $\hat{\Gamma}$ , $\hat{\Gamma}$ and Side-Chain $\hat{\Gamma}_{1</sub>}$ and $\hat{\Gamma}_{2</sub>}$ Dihedral Angles. Journal of Chemical Theory and Computation, 2012, 8, 3257-3273.	5.3	3,696
2226	Molecular Dynamics Study of Catanionic Bilayers Composed of Ion Pair Amphiphile with Double-Tailed Cationic Surfactant. Langmuir, 2012, 28, 8156-8164.	3.5	23
2227	Activity Coefficients of Complex Molecules by Molecular Simulation and Gibbs-Duhem Integration. Soft Materials, 2012, 10, 26-41.	1.7	24
2228	Effects of Location of Twin Boundaries and Grain Size on Plastic Deformation of Nanocrystalline Copper. Metallurgical and Materials Transactions A: Physical Metallurgy and Materials Science, 2012, 43, 3547-3555.	2.2	10
2229	The effects of electronic polarization on water adsorption in metal-organic frameworks: H <sub>2</sub> O in MIL-53(Cr). Journal of Chemical Physics, 2012, 137, 054704.	3.0	45
2230	Molecular modeling of Ca <sup>2+</sup> -oligo( $\hat{\Gamma}$ -l-guluronate) complexes: toward the understanding of the junction zone structure in calcium alginate gels. Structural Chemistry, 2012, 23, 1409-1415.	2.0	24
2231	Ionic Vapor: What Does It Consist Of?. Journal of Physical Chemistry Letters, 2012, 3, 1657-1662.	4.6	32
2232	Are Pentacene Monolayer and Thin-Film Polymorphs Really Substrate-Induced? A Molecular Dynamics Simulation Study. Journal of Physical Chemistry C, 2012, 116, 791-795.	3.1	21
2233	Computer Simulation of Water Sorption on Flexible Protein Crystals. Journal of Physical Chemistry Letters, 2012, 3, 2713-2718.	4.6	16
2234	Variable Hydrogen Bond Strength in Akaganite. Journal of Physical Chemistry C, 2012, 116, 2303-2312.	3.1	32
2235	Adsorption of Organic Electron Acceptors on Graphene-like Molecules: Quantum Chemical and Molecular Mechanical Study. Journal of Physical Chemistry C, 2012, 116, 25328-25336.	3.1	23



#	ARTICLE	IF	CITATIONS
2236	Large Influence of Cholesterol on Solute Partitioning into Lipid Membranes. <i>Journal of the American Chemical Society</i> , 2012, 134, 5351-5361.	13.7	145
2237	Atomistic simulation for the size-dependent melting behaviour of vanadium nanowires. <i>Journal Physics D: Applied Physics</i> , 2012, 45, 485304.	2.8	7
2239	Molecular dynamics simulation of orientational glass formation in anisotropic particle systems in three dimensions. <i>Europhysics Letters</i> , 2012, 100, 16006.	2.0	4
2241	Difference between Magainin-2 and Melittin Assemblies in Phosphatidylcholine Bilayers: Results from Coarse-Grained Simulations. <i>Journal of Physical Chemistry B</i> , 2012, 116, 3021-3030.	2.6	81
2242	How Chemistry, Nanoscale Roughness, and the Direction of Heat Flow Affect Thermal Conductance of Solid–Water Interfaces. <i>Industrial &amp; Engineering Chemistry Research</i> , 2012, 51, 1767-1773.	3.7	78
2243	Coarse-Grained Molecular Dynamics Simulations of the Phase Behavior of the 4-Cyano-4'-pentylbiphenyl Liquid Crystal System. <i>Journal of Physical Chemistry B</i> , 2012, 116, 2075-2089.	2.6	31
2244	Molecular Dynamics Simulation of the Unfolding of Individual Bacteriorhodopsin Helices in Sodium Dodecyl Sulfate Micelles. <i>Biochemistry</i> , 2012, 51, 1061-1069.	2.5	21
2245	The Origin of the LCST on the Liquid–Liquid Equilibrium of Thiophene with Ionic Liquids. <i>Journal of Physical Chemistry B</i> , 2012, 116, 5985-5992.	2.6	16
2246	Valence Force Field for Layered Double Hydroxide Materials Based on the Parameterization of Octahedrally Coordinated Metal Cations. <i>Journal of Physical Chemistry C</i> , 2012, 116, 3421-3431.	3.1	38
2247	Virus Capsid Dissolution Studied by Microsecond Molecular Dynamics Simulations. <i>PLoS Computational Biology</i> , 2012, 8, e1002502.	3.2	70
2248	Dynamic Prestress in a Globular Protein. <i>PLoS Computational Biology</i> , 2012, 8, e1002509.	3.2	28
2249	Cupricyclins, Novel Redox-Active Metallopeptides Based on Conotoxins Scaffold. <i>PLoS ONE</i> , 2012, 7, e30739.	2.5	6
2250	Dimer Formation Enhances Structural Differences between Amyloid $\beta$ -Protein (1–40) and (1–42): An Explicit-Solvent Molecular Dynamics Study. <i>PLoS ONE</i> , 2012, 7, e34345.	2.5	101
2251	The Impact of Small Molecule Binding on the Energy Landscape of the Intrinsically Disordered Protein C-Myc. <i>PLoS ONE</i> , 2012, 7, e41070.	2.5	61
2252	Quantifying the Effect of Polymer Blending through Molecular Modelling of Cyanurate Polymers. <i>PLoS ONE</i> , 2012, 7, e44487.	2.5	8
2253	Conformations of Islet Amyloid Polypeptide Monomers in a Membrane Environment: Implications for Fibril Formation. <i>PLoS ONE</i> , 2012, 7, e47150.	2.5	30
2254	SP-C, a Putative New Surfactant Protein Tissue Localization and 3D Structure. <i>PLoS ONE</i> , 2012, 7, e47789.	2.5	27
2255	Engineering Tocopherol Selectivity in $\beta$ -TTP: A Combined In Vitro/In Silico Study. <i>PLoS ONE</i> , 2012, 7, e49195.	2.5	10

#	ARTICLE	IF	CITATIONS
2256	Binding of an Indenoisoquinoline to the Topoisomerase-DNA Complex Induces Reduction of Linker Mobility and Strengthening of Protein-DNA Interaction. PLoS ONE, 2012, 7, e51354.	2.5	14
2257	T-Cell Receptors Binding Orientation over Peptide/MHC Class I Is Driven by Long-Range Interactions. PLoS ONE, 2012, 7, e51943.	2.5	8
2258	Influence of Energy and Temperature in Cluster Coalescence Induced by Deposition. Advances in Condensed Matter Physics, 2012, 2012, 1-7.	1.1	0
2259	The Method of Microscopic Strain Analysis Based on Evolution of Atomic Configuration for the Simulation of Nanostructured Materials. Zairyo/Journal of the Society of Materials Science, Japan, 2012, 61, 162-168.	0.2	2
2260	Monitoring the Contractile Properties of Optically Patterned Liquid Crystal Based Elastomers. , 2012, , .		0
2261	Dynamic properties of reconstruction defect on 90° partial dislocation in Si. Physica Status Solidi (B): Basic Research, 2012, 249, 531-534.	1.5	1
2262	Carâ€Parrinello molecular dynamics. Wiley Interdisciplinary Reviews: Computational Molecular Science, 2012, 2, 604-612.	14.6	128
2263	Computational investigation of the HIVâ€1 Rev multimerization using molecular dynamics simulations and binding free energy calculations. Proteins: Structure, Function and Bioinformatics, 2012, 80, 1633-1646.	2.6	9
2264	Exploring the essential collective dynamics of interacting proteins: Application to prion protein dimers. Proteins: Structure, Function and Bioinformatics, 2012, 80, 1847-1865.	2.6	14
2265	Benzothiadiazoles as DNA intercalators: Docking and simulation. International Journal of Quantum Chemistry, 2012, 112, 3296-3302.	2.0	12
2266	Molecular Dynamics Studies of the STAT3 Homodimer:DNA Complex: Relationships between STAT3 Mutations and Proteinâ€DNA Recognition. Journal of Chemical Information and Modeling, 2012, 52, 1179-1192.	5.4	21
2267	Ionic liquids studied across different scales: A computational perspective. Faraday Discussions, 2012, 154, 111-132.	3.2	99
2268	Designing biomimetic pores based on carbon nanotubes. Proceedings of the National Academy of Sciences of the United States of America, 2012, 109, 6939-6944.	7.1	78
2269	Multidimensional View of Amyloid Fibril Nucleation in Atomistic Detail. Journal of the American Chemical Society, 2012, 134, 3886-3894.	13.7	78
2270	Modeling crystal growth from solution with molecular dynamics simulations: Approaches to transition rate constants. Journal of Chemical Physics, 2012, 136, 034704.	3.0	19
2271	Kirkwoodâ€Buff Coarse-Grained Force Fields for Aqueous Solutions. Journal of Chemical Theory and Computation, 2012, 8, 1802-1807.	5.3	62
2272	Confinement by Carbon Nanotubes Drastically Alters the Boiling and Critical Behavior of Water Droplets. ACS Nano, 2012, 6, 2766-2773.	14.6	59
2273	Tracking a complete voltage-sensor cycle with metal-ion bridges. Proceedings of the National Academy of Sciences of the United States of America, 2012, 109, 8552-8557.	7.1	132

#	ARTICLE	IF	CITATIONS
2274	Docking, molecular dynamics and quantitative structure-activity relationship studies for HEPTs and DABOs as HIV-1 reverse transcriptase inhibitors. <i>Journal of Molecular Modeling</i> , 2012, 18, 2185-2198.	1.8	32
2275	On Atomistic and Coarse-Grained Models for C <sub>60</sub> Fullerene. <i>Journal of Chemical Theory and Computation</i> , 2012, 8, 1370-1378.	5.3	127
2276	Evaluating nonpolarizable nucleic acid force fields: A systematic comparison of the nucleobases hydration free energies and chloroform-water partition coefficients. <i>Journal of Computational Chemistry</i> , 2012, 33, 2225-2232.	3.3	25
2277	From Quantum Mechanics to Quantum Chemistry. , 2012, , 167-222.		0
2278	Force-Field Development and Molecular Dynamics of [NiFe] Hydrogenase. <i>Journal of Chemical Theory and Computation</i> , 2012, 8, 2103-2114.	5.3	26
2279	Binary Interactions and Salt-Induced Coalescence of Spherical Micelles of Cationic Surfactants from Molecular Dynamics Simulations. <i>Langmuir</i> , 2012, 28, 1127-1135.	3.5	43
2280	Proton transport in functionalised additives for PEM fuel cells: contributions from atomistic simulations. <i>Chemical Society Reviews</i> , 2012, 41, 5143.	38.1	27
2281	The Method of Molecular Dynamics Simulations. <i>Springer Series in Materials Science</i> , 2012, , 35-57.	0.6	0
2282	Comparison of selected polarizable and nonpolarizable water models in molecular dynamics simulations of ice Ih. <i>Physical Chemistry Chemical Physics</i> , 2012, 14, 11371.	2.8	25
2283	The Role of Pendant Amines in the Breaking and Forming of Molecular Hydrogen Catalyzed by Nickel Complexes. <i>Chemistry - A European Journal</i> , 2012, 18, 6493-6506.	3.3	102
2284	The Effect of Neutral Ion Aggregate Formation on the Electrical Conductivity of an Ionic Liquid and its Mixtures with Chloroform. <i>ChemPhysChem</i> , 2012, 13, 1748-1752.	2.1	29
2285	Comparative Study of Flavins Binding with Human Serum Albumin: A Fluorometric, Thermodynamic, and Molecular Dynamics Approach. <i>ChemPhysChem</i> , 2012, 13, 2142-2153.	2.1	31
2286	Crystal habit prediction – Including the liquid as well as the solid side. <i>Crystal Research and Technology</i> , 2012, 47, 597-602.	1.3	11
2287	Development of a united-atom force field for 1-ethyl-3-methylimidazolium tetracyanoborate ionic liquid. <i>Molecular Physics</i> , 2012, 110, 1115-1126.	1.7	28
2288	Hybrid QM/MM Molecular Dynamics Study of Benzocaine in a Membrane Environment: How Does a Quantum Mechanical Treatment of Both Anesthetic and Lipids Affect Their Interaction. <i>Journal of Chemical Theory and Computation</i> , 2012, 8, 2197-2203.	5.3	20
2289	Functional Domain Motions in Proteins on the ~100 ns Timescale: Comparison of Neutron Spin-Echo Spectroscopy of Phosphoglycerate Kinase with Molecular-Dynamics Simulation. <i>Biophysical Journal</i> , 2012, 102, 1108-1117.	0.5	42
2290	A Novel Approach to the Investigation of Passive Molecular Permeation through Lipid Bilayers from Atomistic Simulations. <i>Journal of Physical Chemistry B</i> , 2012, 116, 8714-8721.	2.6	63
2291	Different effects of zwitterion and ethylene glycol on proteins. <i>Journal of Chemical Physics</i> , 2012, 136, 225101.	3.0	39

#	ARTICLE	IF	CITATIONS
2292	Structural phase transitions in Si under hydrostatic and uniaxial compression. <i>Physical Review B</i> , 2012, 85, .	3.2	12
2293	Formation, migration, and clustering of delocalized vacancies and interstitials at a solid-state semicoherent interface. <i>Physical Review B</i> , 2012, 85, .	3.2	38
2294	Positioning of Antioxidant Quercetin and Its Metabolites in Lipid Bilayer Membranes: Implication for Their Lipid-Peroxidation Inhibition. <i>Journal of Physical Chemistry B</i> , 2012, 116, 1309-1318.	2.6	119
2295	Molecular Dynamics Simulation of PEGylated Bilayer Interacting with Salt Ions: A Model of the Liposome Surface in the Bloodstream. <i>Journal of Physical Chemistry B</i> , 2012, 116, 4212-4219.	2.6	64
2296	Heterogeneity of properties in Ar nanoparticles. <i>Journal of Nanoparticle Research</i> , 2012, 14, 1.	1.9	3
2297	Deciphering the binding mode of Zolpidem to GABAA $\alpha 1$ receptor – insights from molecular dynamics simulation. <i>Journal of Molecular Modeling</i> , 2012, 18, 1345-1354.	1.8	10
2298	Ligand-based 3-D pharmacophore generation and molecular docking of mTOR kinase inhibitors. <i>Journal of Molecular Modeling</i> , 2012, 18, 1611-1624.	1.8	19
2299	Structural requirements of pyrimidine, thienopyridine and ureido thiophene carboxamide-based inhibitors of the checkpoint kinase 1: QSAR, docking, molecular dynamics analysis. <i>Journal of Molecular Modeling</i> , 2012, 18, 3227-3242.	1.8	6
2300	Free energy calculation of single molecular interaction using Jarzynski's identity method: the case of HIV-1 protease inhibitor system. <i>Acta Mechanica Sinica/Lixue Xuebao</i> , 2012, 28, 891-903.	3.4	22
2301	A hybrid molecular continuum method using point wise coupling. <i>Advances in Engineering Software</i> , 2012, 46, 85-92.	3.8	60
2302	A Novel Pseudo-En Approach in Classical MD Simulation: A Case Study on ( $U_{0.8}Pu_{0.2}O_{2.7}$ ) Mixed Oxide. <i>Journal of the American Ceramic Society</i> , 2012, 95, 1435-1439.	3.8	27
2303	A theoretical evaluation of the effects of carbon nanotube entanglement and bundling on the structural and mechanical properties of buckypaper. <i>Carbon</i> , 2012, 50, 1793-1806.	10.3	97
2304	Prediction of the mutual solubility of water and dipropylene glycol dimethyl ether using molecular dynamics simulation. <i>Fluid Phase Equilibria</i> , 2012, 314, 1-6.	2.5	8
2305	Properties of oxidized phospholipid monolayers: An atomistic molecular dynamics study. <i>Chemical Physics Letters</i> , 2012, 519-520, 93-99.	2.6	28
2306	A possible alloying mechanism in idealized collisions between Cu and Sn crystals. <i>Chemical Physics Letters</i> , 2012, 521, 125-129.	2.6	18
2307	Aberrant structures of Parkinson's disease-associated ubiquitin C-terminal hydrolase L1 predicted by molecular dynamics. <i>Chemical Physics Letters</i> , 2012, 535, 163-168.	2.6	3
2308	Prediction of drug-packaging interactions via molecular dynamics (MD) simulations. <i>International Journal of Pharmaceutics</i> , 2012, 431, 26-32.	5.2	14
2309	Analysis of cause of failure of new targeting peptide in PEGylated liposome: Molecular modeling as rational design tool for nanomedicine. <i>European Journal of Pharmaceutical Sciences</i> , 2012, 46, 121-130.	4.0	58

#	ARTICLE	IF	CITATIONS
2310	Size dependence of cavity volume: A molecular dynamics study. Biophysical Chemistry, 2012, 161, 46-49.	2.8	27
2311	Structure and stability of a thermostable carboxylesterase from the thermoacidophilic archaeon <i>Sulfolobus tokodaii</i> . FEBS Journal, 2012, 279, 3071-3084.	4.7	41
2312	Atomistic modeling of solid-state amorphization and atomic structure of the Cu-Hf system. Materials Letters, 2012, 76, 77-80.	2.6	0
2313	A long-range U-Nb potential for the calculation of some chemical and physical properties of the U-Nb system. Journal of Nuclear Materials, 2012, 427, 239-244.	2.7	12
2314	Distribution of local elastic constants in nanofilms of metals. Journal of Physics and Chemistry of Solids, 2012, 73, 881-885.	4.0	3
2315	Effects of crystal orientation on the tensile and shear deformation of nickel-silicon interfaces: A molecular dynamics simulation. Materials Science & Engineering A: Structural Materials: Properties, Microstructure and Processing, 2012, 543, 217-223.	5.6	8
2316	Molecular dynamic study of the melting temperature in MgF <sub>2</sub> with the fluorite structure. Physica B: Condensed Matter, 2012, 407, 551-554.	2.7	5
2317	Atomistic simulation on the shape dependence of the melting behavior of V nanowire. European Physical Journal D, 2012, 66, 1.	1.3	5
2318	Probing the oligomeric state and interaction surfaces of Fukutin-I in dilauroylphosphatidylcholine bilayers. European Biophysics Journal, 2012, 41, 199-207.	2.2	13
2319	Study of intermolecular contacts in the proline-rich homeodomain (PRH)-DNA complex using molecular dynamics simulations. European Biophysics Journal, 2012, 41, 329-340.	2.2	8
2320	Concentration enrichment of urea at cellulose surfaces: results from molecular dynamics simulations and NMR spectroscopy. Cellulose, 2012, 19, 1-12.	4.9	38
2321	Nuclear magnetic resonance signal chemical shifts and molecular simulations: a multidisciplinary approach to modeling copper protein structures. Journal of Biological Inorganic Chemistry, 2012, 17, 71-79.	2.6	3
2322	The mechanism of hydrogen uptake in [NiFe] hydrogenase: first-principles molecular dynamics investigation of a model compound. Journal of Biological Inorganic Chemistry, 2012, 17, 149-164.	2.6	3
2323	Structural determinants of benzodiazepinedione/peptide-based p53-HDM2 inhibitors using 3D-QSAR, docking and molecular dynamics. Journal of Molecular Modeling, 2012, 18, 295-306.	1.8	19
2324	Studies of H4R antagonists using 3D-QSAR, molecular docking and molecular dynamics. Journal of Molecular Modeling, 2012, 18, 991-1001.	1.8	17
2325	Solvation dynamics of tryptophan in water-dimethyl sulfoxide binary mixture: In search of molecular origin of composition dependent multiple anomalies. Journal of Chemical Physics, 2013, 139, 034308.	3.0	47
2326	Elastic Anomalies of Crystalline 4He at T=0. Journal of Low Temperature Physics, 2013, 173, 143-151.	1.4	2
2327	Molecular dynamics simulations with many-body potentials on multiple GPUs-The implementation, package and performance. Computer Physics Communications, 2013, 184, 2091-2101.	7.5	51

#	ARTICLE	IF	CITATIONS
2328	Small-molecule G-quadruplex interactions: Systematic exploration of conformational space using multiple molecular dynamics. Biopolymers, 2013, 99, n/a-n/a.	2.4	29
2329	Transient Polymorphism in NaCl. Journal of Chemical Theory and Computation, 2013, 9, 2526-2530.	5.3	44
2330	Free energy calculations for molecular solids using <scp>GROMACS</scp>. Journal of Chemical Physics, 2013, 139, 034104.	3.0	46
2331	Phase Behavior and Molecular Dynamics Simulation Studies of New Aqueous Two-Phase Separation Systems Induced by HEPES Buffer. Journal of Physical Chemistry B, 2013, 117, 563-582.	2.6	28
2332	Molecular dynamics simulations of isoleucine-release pathway in GAF domain of N-CodY from Bacillus Subtilis. Journal of Molecular Graphics and Modelling, 2013, 44, 232-240.	2.4	2
2333	A morphometric approach for the accurate solvation thermodynamics of proteins and ligands. Journal of Computational Chemistry, 2013, 34, 1969-1974.	3.3	9
2334	Aggregation of Alzheimer's Amyloid $\beta$ -Peptide in Biological Membranes: A Molecular Dynamics Study. Biochemistry, 2013, 52, 4971-4980.	2.5	51
2335	Understanding the effect of side groups in ionic liquids on carbon-capture properties: a combined experimental and theoretical effort. Physical Chemistry Chemical Physics, 2013, 15, 3264.	2.8	28
2336	Novel Ultrathin Membranes Composed of Organic Ions. Journal of Physical Chemistry Letters, 2013, 4, 1216-1220.	4.6	13
2337	Kinetic sonication effects in aqueous acetonitrile solutions. Reaction rate levelling by ultrasound. Ultrasonics Sonochemistry, 2013, 20, 1414-1418.	8.2	6
2338	Effects of elevated temperature on the structure and properties of calcium-silicate-hydrate gels: the role of confined water. Soft Matter, 2013, 9, 6418.	2.7	54
2339	Interactions and Stabilities of the UV RESISTANCE LOCUS8 (UVR8) Protein Dimer and Its Key Mutants. Journal of Chemical Information and Modeling, 2013, 53, 1736-1746.	5.4	8
2340	Evaluation of the Role of Water in the $H_2$ Bond Formation by Ni(II)-Based Electrocatalysts. Journal of Chemical Theory and Computation, 2013, 9, 3505-3514.	5.3	7
2341	Modeling, docking and dynamics simulations of a non-specific lipid transfer protein from Peganum harmala L.. Computational Biology and Chemistry, 2013, 47, 56-65.	2.3	11
2342	Mechanistic Explanation of Different Unfolding Behaviors Observed for Transmembrane and Soluble $\beta$ -Barrel Proteins. Structure, 2013, 21, 1317-1324.	3.3	14
2343	A new mechanism of loop formation and transformation in bcc iron without dislocation reaction. Journal of Nuclear Materials, 2013, 441, 216-221.	2.7	41
2344	Aqueous citrate: a first-principles and force-field molecular dynamics study. RSC Advances, 2013, 3, 16399.	3.6	22
2345	On the Nature of DNA Hyperchromic Effect. Journal of Physical Chemistry B, 2013, 117, 8697-8704.	2.6	44



#	ARTICLE	IF	CITATIONS
2346	The sintering and densification behaviour of many copper nanoparticles: A molecular dynamics study. Computational Materials Science, 2013, 74, 1-11.	3.0	63
2347	Towards an Understanding of Channelrhodopsin Function: Simulations Lead to Novel Insights of the Channel Mechanism. Journal of Molecular Biology, 2013, 425, 1795-1814.	4.2	62
2348	Liquid Mixtures Involving Hydrogenated and Fluorinated Chains: ( <i>p</i> , <i>t</i> , <i>x</i> ) Surface of (Ethanol + 2,2,2-Trifluoroethanol), Experimental and Simulation. Journal of Physical Chemistry B, 2013, 117, 9709-9717.	2.6	31
2349	Structural features of falcipain-3 inhibitors: an in silico study. Molecular BioSystems, 2013, 9, 2296.	2.9	16
2350	Structural and functional insights on folate receptor $\hat{F}_1$ (FR $\hat{F}_1$ ) by homology modeling, ligand docking and molecular dynamics. Journal of Molecular Graphics and Modelling, 2013, 44, 197-207.	2.4	22
2351	Spectroscopic, docking and molecular dynamics simulation studies on the interaction of two Schiff base complexes with human serum albumin. Journal of Luminescence, 2013, 141, 166-172.	3.1	31
2352	The Influence of Water on the Solubility of Carbon Dioxide in Imidazolium Based Ionic Liquids. Zeitschrift Fur Physikalische Chemie, 2013, 227, 167-176.	2.8	16
2353	Computer modeling of the dynamic properties of the cAMP-dependent protein kinase catalytic subunit. Computational Biology and Chemistry, 2013, 47, 66-70.	2.3	2
2354	Simulation of Fracture Nucleation in Cross-Linked Polymer Networks. Jom, 2013, 65, 147-167.	1.9	30
2355	Identification of MDP (muramyl dipeptide)-binding key domains in NOD2 (nucleotide-binding and) Tj ETQq1 1 0.784314 rgBT /Overlook 1007-1023.	2.3	20
2356	Comments on a Continuum-Related Parrinello-Rahman Molecular Dynamics Formulation. Journal of Elasticity, 2013, 113, 93-112.	1.9	8
2357	A two-domain elevator mechanism for sodium/proton antiport. Nature, 2013, 501, 573-577.	27.8	221
2358	Structure of 1-Alkyl-1-methylpyrrolidinium Bis(trifluoromethylsulfonyl)amide Ionic Liquids with Linear, Branched, and Cyclic Alkyl Groups. Journal of Physical Chemistry B, 2013, 117, 15328-15337.	2.6	121
2359	Molecular Dynamics Perspective on the Protein Thermal Stability: A Case Study Using SAICAR Synthetase. Journal of Chemical Information and Modeling, 2013, 53, 2448-2461.	5.4	29
2360	Thermophysical Properties of the Ionic Liquids [EMIM][B(CN) <sub>4</sub> ] and [HMIM][B(CN) <sub>4</sub> ]. Journal of Physical Chemistry B, 2013, 117, 8512-8523.	2.6	39
2361	Comparison of Force Fields on the Basis of Various Model Approachesâ€”How To Design the Best Model for the [C <sub>n</sub> MIM][NTf <sub>2</sub> ] Family of Ionic Liquids. ChemPhysChem, 2013, 14, 3368-3374.	2.1	34
2362	Combined QM/MM Investigation on the Light-Driven Electron-Induced Repair of the (6â€”4) Thymine Dimer Catalyzed by DNA Photolyase. Journal of Physical Chemistry B, 2013, 117, 10071-10079.	2.6	24
2363	MD simulations of loading rate dependence of detwinning deformation in nanocrystalline Ni. Science China: Physics, Mechanics and Astronomy, 2013, 56, 491-497.	5.1	6



#	ARTICLE	IF	CITATIONS
2364	A coarse-grained model for polyethylene glycol in bulk water and at a water/air interface. <i>Physical Chemistry Chemical Physics</i> , 2013, 15, 17093.	2.8	49
2365	Rearrangement of Nanoporous Cavity Structures in Crystalline Syndiotactic Polystyrene Associated with Stress-Induced Phase Transition. <i>ACS Macro Letters</i> , 2013, 2, 834-838.	4.8	11
2366	Flexibility of the Bacterial Chaperone Trigger Factor in Microsecond-Timescale Molecular Dynamics Simulations. <i>Biophysical Journal</i> , 2013, 105, 732-744.	0.5	17
2367	Molecular dynamics simulation of oleic acid/oleate bilayers: An atomistic model for a ufasome membrane. <i>Chemistry and Physics of Lipids</i> , 2013, 175-176, 79-83.	3.2	23
2368	Computing Gibbs free energy differences by interface pinning. <i>Physical Review B</i> , 2013, 88, .	3.2	64
2369	Molecular Dynamics Simulations of Highly Crowded Amino Acid Solutions: Comparisons of Eight Different Force Field Combinations with Experiment and with Each Other. <i>Journal of Chemical Theory and Computation</i> , 2013, 9, 4585-4602.	5.3	36
2370	New Computational Approach to Determine Liquid-Solid Phase Equilibria of Water Confined to Slit Nanopores. <i>Journal of Chemical Theory and Computation</i> , 2013, 9, 3299-3310.	5.3	25
2371	Self-assembly of DNA duplex in graphene bilayer. <i>Molecular Physics</i> , 2013, 111, 1053-1060.	1.7	3
2372	Self-assembly of cationic surfactants on the carbon nanotube surface: insights from molecular dynamics simulations. <i>Journal of Molecular Modeling</i> , 2013, 19, 4319-4335.	1.8	15
2373	Time-resolved force distribution analysis. <i>BMC Biophysics</i> , 2013, 6, 5.	4.4	60
2374	Are structural properties of dendrimers sensitive to the symmetry of branching? Computer simulation of lysine dendrimers. <i>Journal of Chemical Physics</i> , 2013, 139, 064903.	3.0	43
2375	Double Resolution Model for Studying TMAO/Water Effective Interactions. <i>Journal of Physical Chemistry B</i> , 2013, 117, 13268-13277.	2.6	93
2376	Interbilayer repulsion forces between tension-free lipid bilayers from simulation. <i>Soft Matter</i> , 2013, 9, 10705.	2.7	22
2377	Water permeation through single-layer graphyne membrane. <i>Journal of Chemical Physics</i> , 2013, 139, 064705.	3.0	58
2378	Isopeptide Bonds Mechanically Stabilize Spy0128 in Bacterial Pili. <i>Biophysical Journal</i> , 2013, 104, 2051-2057.	0.5	19
2379	Interactions of the Auxilin-1 PTEN-like Domain with Model Membranes Result in Nanoclustering of Phosphatidyl Inositol Phosphates. <i>Biophysical Journal</i> , 2013, 105, 137-145.	0.5	24
2380	Structural Basis for Ternary Complex Formation between Tau, Hsp90, and FKBP51. <i>Biophysical Journal</i> , 2013, 104, 387a-388a.	0.5	0
2381	Propofol modulates the lipid phase transition and localizes near the headgroup of membranes. <i>Chemistry and Physics of Lipids</i> , 2013, 175-176, 84-91.	3.2	18

#	ARTICLE	IF	CITATIONS
2382	Investigation into the Feasibility of Thioditaloside as a Novel Scaffold for Galectinâ€³â€³-Specific Inhibitors. <i>ChemBioChem</i> , 2013, 14, 1331-1342.	2.6	36
2383	Direct calculation of the solid-liquid Gibbs free energy difference in a single equilibrium simulation. <i>Journal of Chemical Physics</i> , 2013, 139, 104102.	3.0	66
2384	Conformational Analysis of the Frog Skin Peptide, Plasticin-L1, and Its Effects on Production of Proinflammatory Cytokines by Macrophages. <i>Biochemistry</i> , 2013, 52, 7231-7241.	2.5	27
2385	Short-Range Order in Polyethylene Melts: Identification and Characterization. <i>Macromolecules</i> , 2013, 46, 7977-7988.	4.8	3
2386	Interactions between Fengycin and Model Bilayers Quantified by Coarse-Grained Molecular Dynamics. <i>Biophysical Journal</i> , 2013, 105, 1612-1623.	0.5	34
2387	Refining classical force fields for ionic liquids: theory and application to [MMIM][Cl]. <i>Physical Chemistry Chemical Physics</i> , 2013, 15, 2037-2049.	2.8	23
2388	Molecular Mechanisms of Water-Mediated Proton Transport in MIL-53 Metalâ€³â€³Organic Frameworks. <i>Journal of Physical Chemistry C</i> , 2013, 117, 19508-19516.	3.1	42
2389	Effect of Proline Mutations on the Monomer Conformations of Amylin. <i>Biophysical Journal</i> , 2013, 105, 1227-1235.	0.5	51
2390	One-dimensional potential of mean force underestimates activation barrier for transport across flexible lipid membranes. <i>Journal of Chemical Physics</i> , 2013, 139, 134906.	3.0	29
2391	Glyceride Lipid Formulations: Molecular Dynamics Modeling of Phase Behavior During Dispersion and Molecular Interactions Between Drugs and Excipients. <i>Pharmaceutical Research</i> , 2013, 30, 3238-3253.	3.5	33
2392	Exploitation of the Catalytic Site and 150 Cavity for Design of Influenza A Neuraminidase Inhibitors. <i>Journal of Organic Chemistry</i> , 2013, 78, 10867-10877.	3.2	29
2393	On fluid-solid direct coexistence simulations: The pseudo-hard sphere model. <i>Journal of Chemical Physics</i> , 2013, 139, 144502.	3.0	92
2394	Atomistic simulation for the size effect on the mechanical properties of Ni/Ni3Al nanowire. <i>Journal of Applied Physics</i> , 2013, 114, 094303.	2.5	12
2395	Molecular Dynamics Simulation of SDS and CTAB Micellization and Prediction of Partition Equilibria with COSMOmic. <i>Langmuir</i> , 2013, 29, 11582-11592.	3.5	52
2396	Ion Permeation in the NanC Porin from <i>Escherichia coli</i> : Free Energy Calculations along Pathways Identified by Coarse-Grain Simulations. <i>Journal of Physical Chemistry B</i> , 2013, 117, 13534-13542.	2.6	6
2397	Accurate and efficient integration for molecular dynamics simulations at constant temperature and pressure. <i>Journal of Chemical Physics</i> , 2013, 139, 164106.	3.0	159
2398	Calcium- $\beta$ -Guluronate Complexes: $\text{Ca}^{2+}$ Binding Modes from DFT-MD Simulations. <i>Journal of Physical Chemistry B</i> , 2013, 117, 12105-12112.	2.6	29
2399	B4â€³B1 phase transition of GaN under isotropic and uniaxial compression. <i>Physical Review B</i> , 2013, 88, .	3.2	27

#	ARTICLE	IF	CITATIONS
2400	Theoretical predictions for hexagonal BN based nanomaterials as electrocatalysts for the oxygen reduction reaction. <i>Physical Chemistry Chemical Physics</i> , 2013, 15, 2809.	2.8	95
2401	A New Ionic Pair Potential for Evaluation the Thermal Properties of Uranium Dioxide by Molecular Dynamics. , 2013, , .		0
2402	Transient Protein States in Designing Inhibitors of the MDM2-p53 Interaction. <i>Structure</i> , 2013, 21, 2143-2151.	3.3	57
2403	Molecular Basis for the Long Duration of Action and Kinetic Selectivity of Tiotropium for the Muscarinic M3 Receptor. <i>Journal of Medicinal Chemistry</i> , 2013, 56, 8746-8756.	6.4	85
2404	Transferable Mixing of Atomistic and Coarse-Grained Water Models. <i>Journal of Physical Chemistry B</i> , 2013, 117, 14438-14448.	2.6	43
2405	Hydration Patterns of Graphene-Based Nanomaterials (GBNMs) Play a Major Role in the Stability of a Helical Protein: A Molecular Dynamics Simulation Study. <i>Langmuir</i> , 2013, 29, 14230-14238.	3.5	43
2406	The identification of novel, high affinity AQP9 inhibitors in an intracellular binding site. <i>Molecular Membrane Biology</i> , 2013, 30, 246-260.	2.0	33
2407	Structural characterization of NETNES glycopeptide from <i>Trypanosoma cruzi</i> . <i>Carbohydrate Research</i> , 2013, 373, 28-34.	2.3	3
2408	Solvation Structures and Dynamics of the Magnesium Chloride ( $Mg^{2+}Cl^{-}$ ) Ion Pair in Water-Ethanol Mixtures. <i>Journal of Physical Chemistry A</i> , 2013, 117, 8703-8709.	2.5	27
2409	Lennard-Jones Lattice Summation in Bilayer Simulations Has Critical Effects on Surface Tension and Lipid Properties. <i>Journal of Chemical Theory and Computation</i> , 2013, 9, 3527-3537.	5.3	138
2410	Mutations and Seeding of Amylin Fibril-Like Oligomers. <i>Journal of Physical Chemistry B</i> , 2013, 117, 16076-16085.	2.6	30
2411	Insights on Hydrogen-Bond Lifetimes in Liquid and Supercooled Water. <i>Journal of Physical Chemistry B</i> , 2013, 117, 16188-16195.	2.6	50
2412	Interdiffusion of Ni-Al multilayers: A continuum and molecular dynamics study. <i>Journal of Applied Physics</i> , 2013, 114, .	2.5	44
2413	Another Piece of the Membrane Puzzle: Extending Slipids Further. <i>Journal of Chemical Theory and Computation</i> , 2013, 9, 774-784.	5.3	237
2414	An Atomistic Model for Assembly of Transmembrane Domain of T cell Receptor Complex. <i>Journal of the American Chemical Society</i> , 2013, 135, 2188-2197.	13.7	19
2415	Conformational Biases of Linear Motifs. <i>Journal of Physical Chemistry B</i> , 2013, 117, 15943-15957.	2.6	18
2416	Local Partition Coefficients Govern Solute Permeability of Cholesterol-Containing Membranes. <i>Biophysical Journal</i> , 2013, 105, 2760-2770.	0.5	67
2417	The Role of Cross-Chain Ionic Interactions for the Stability of Collagen Model Peptides. <i>Biophysical Journal</i> , 2013, 105, 1681-1688.	0.5	29

#	ARTICLE	IF	CITATIONS
2418	Method for calculating small-angle neutron scattering spectra using all-atom molecular dynamics trajectories. <i>Journal of Surface Investigation</i> , 2013, 7, 1124-1127.	0.5	6
2419	Recent Advances in Broadband Dielectric Spectroscopy. NATO Science for Peace and Security Series B: Physics and Biophysics, 2013, , .	0.3	10
2420	An analysis of fluctuations in supercooled TIP4P/2005 water. <i>Journal of Chemical Physics</i> , 2013, 138, 184502.	3.0	51
2421	Solvation structure and dynamics of potassium chloride ion pair in dimethyl sulfoxideâ€“water mixtures. <i>Journal of Molecular Liquids</i> , 2013, 188, 5-12.	4.9	23
2422	Calculating the binding free energies of charged species based on explicit-solvent simulations employing lattice-sum methods: An accurate correction scheme for electrostatic finite-size effects. <i>Journal of Chemical Physics</i> , 2013, 139, 184103.	3.0	187
2423	Molecular mechanism of the camptothecin resistance of Glu710Gly topoisomerase IB mutant analyzed in vitro and in silico. <i>Molecular Cancer</i> , 2013, 12, 100.	19.2	29
2424	Detection of persistent organic pollutants binding modes with androgen receptor ligand binding domain by docking and molecular dynamics. <i>BMC Structural Biology</i> , 2013, 13, 16.	2.3	7
2425	Water molecular flow control with a (5,5) nanocoil switch. <i>Journal of Nanoparticle Research</i> , 2013, 15, 1889.	1.9	2
2426	The role of solvent exclusion in the interaction between D124 and the metal site in SOD1: implications for ALS. <i>Journal of Biological Inorganic Chemistry</i> , 2013, 18, 931-938.	2.6	7
2427	Ab initio studies of the short-range atomic structure of liquid ironâ€“carbon alloys. <i>Journal of Molecular Liquids</i> , 2013, 179, 12-17.	4.9	14
2428	A Molecular Dynamics Simulation of Fracture in Nanocrystalline Copper. <i>Journal of Nano Research</i> , 0, 23, 50-56.	0.8	2
2429	Embedding AÎ²42 in Heterogeneous Membranes Depends on Cholesterol Asymmetries. <i>Biophysical Journal</i> , 2013, 105, 899-910.	0.5	18
2430	Solventâ€“driven symmetry of selfâ€“assembled nanocrystal superlatticesâ€“A computational study. <i>Journal of Computational Chemistry</i> , 2013, 34, 523-532.	3.3	41
2431	In Silico Cross Seeding of AÎ²2 and Amylin Fibril-like Oligomers. <i>ACS Chemical Neuroscience</i> , 2013, 4, 1488-1500.	3.5	62
2432	Atomistic Simulations of Wimleyâ€“White Pentapeptides: Sampling of Structure and Dynamics in Solution. <i>Journal of Chemical Theory and Computation</i> , 2013, 9, 1657-1666.	5.3	8
2433	Reaction Pathways for Oxygen Evolution Promoted by Cobalt Catalyst. <i>Journal of the American Chemical Society</i> , 2013, 135, 15353-15363.	13.7	228
2434	Molecular Dynamics Simulations of Water Sorption in a Perfluorosulfonic Acid Membrane. <i>Journal of Physical Chemistry B</i> , 2013, 117, 12649-12660.	2.6	40
2435	Molecular dynamics simulation of dipalmitoylphosphatidylcholine modified with a MTSL nitroxide spin label in a lipid membrane. <i>Biochimica Et Biophysica Acta - Biomembranes</i> , 2013, 1828, 2770-2777.	2.6	8

#	ARTICLE	IF	CITATIONS
2436	Quantification of Solvent Contribution to the Stability of Noncovalent Complexes. <i>Journal of Chemical Theory and Computation</i> , 2013, 9, 4542-4551.	5.3	37
2437	Modeling Self-Assembly of Silica/Surfactant Mesostructures in the Templated Synthesis of Nanoporous Solids. <i>Langmuir</i> , 2013, 29, 2387-2396.	3.5	44
2438	Molecular Dynamics Simulations of Graphene Oxide Frameworks. <i>Journal of Chemical Theory and Computation</i> , 2013, 9, 4890-4900.	5.3	35
2439	Homogeneous Ice Nucleation at Moderate Supercooling from Molecular Simulation. <i>Journal of the American Chemical Society</i> , 2013, 135, 15008-15017.	13.7	256
2440	Benzene adsorption at the aqueous (011)-quartz interface: is surface flexibility important?. <i>Molecular Simulation</i> , 2013, 39, 1093-1102.	2.0	11
2441	Atomistic understanding of diffusion kinetics in nanocrystals from molecular dynamics simulations. <i>Physical Review B</i> , 2013, 88, .	3.2	17
2442	Studies on sensitivity to tension and gating pathway of MscL by molecular dynamic simulation. <i>Acta Mechanica Sinica/Lixue Xuebao</i> , 2013, 29, 256-266.	3.4	3
2443	Selective inhibition of the unfolded protein response: targeting catalytic sites for Schiff base modification. <i>Molecular BioSystems</i> , 2013, 9, 2408.	2.9	26
2444	Three-dimensional failure envelopes and the brittle-ductile transition. <i>Journal of Geophysical Research: Solid Earth</i> , 2013, 118, 1378-1392.	3.4	34
2445	Tension moderation and fluctuation spectrum in simulated lipid membranes under an applied electric potential. <i>Journal of Chemical Physics</i> , 2013, 139, 164902.	3.0	7
2446	Simulation optimization of spherical non-polar guest recognition by deep-cavity cavitands. <i>Journal of Chemical Physics</i> , 2013, 139, 234502.	3.0	13
2447	Electrostatic frequency shifts in amide I vibrational spectra: Direct parameterization against experiment. <i>Journal of Chemical Physics</i> , 2013, 138, 134116.	3.0	87
2448	Insight into the structural requirements of benzimidazole derivatives as interleukin-2 inducible tyrosine kinase inhibitors by computational explorations. <i>International Journal of Quantum Chemistry</i> , 2013, 113, 2385-2396.	2.0	4
2449	Permeation of polystyrene nanoparticles across model lipid bilayer membranes. <i>Soft Matter</i> , 2013, 9, 10265.	2.7	25
2450	Polyelectrolyte multilayers as a platform for pH-responsive lipid bilayers. <i>Soft Matter</i> , 2013, 9, 8938.	2.7	17
2451	Membrane penetration and curvature induced by single-walled carbon nanotubes: the effect of diameter, length, and concentration. <i>Physical Chemistry Chemical Physics</i> , 2013, 15, 16334.	2.8	11
2452	Structure determinants of indolin-2-on-3-spirothiazolidinones as MptpB inhibitors: An in silico study. <i>Soft Matter</i> , 2013, 9, 11054.	2.7	5
2453	Interaction of Piscidin-1 with zwitterionic versus anionic membranes: a comparative molecular dynamics study. <i>Journal of Biomolecular Structure and Dynamics</i> , 2013, 31, 1393-1403.	3.5	13

#	ARTICLE	IF	CITATIONS
2454	Interactions of monovalent salts with cationic lipid bilayers. Faraday Discussions, 2013, 160, 341-358.	3.2	17
2455	Molecular dynamics simulations of the water adsorption around malonic acid aerosol models. Physical Chemistry Chemical Physics, 2013, 15, 10942.	2.8	17
2456	Insight into the Molecular Properties of Chitlac, a Chitosan Derivative for Tissue Engineering. Journal of Physical Chemistry B, 2013, 117, 13578-13587.	2.6	25
2457	Aggregation of Oligoarginines at Phospholipid Membranes: Molecular Dynamics Simulations, Time-Dependent Fluorescence Shift, and Biomimetic Colorimetric Assays. Journal of Physical Chemistry B, 2013, 117, 11530-11540.	2.6	34
2458	Computational and Experimental Study of the Effect of PEG in the Preparation of Damascenone-Imprinted Xerogels. Langmuir, 2013, 29, 2024-2032.	3.5	9
2459	Wagging the Tail: Essential Role of Substrate Flexibility in FAAH Catalysis. Journal of Chemical Theory and Computation, 2013, 9, 1202-1213.	5.3	24
2460	Utilization of efficient gradient and Hessian computations in the force field optimization process of molecular simulations. Computational Science & Discovery, 2013, 6, 015005.	1.5	3
2461	Atomistic force field for alumina fit to density functional theory. Journal of Chemical Physics, 2013, 139, 204704.	3.0	13
2462	Kinetic sonication effects in light of molecular dynamics simulation of the reaction medium. Ultrasonics Sonochemistry, 2013, 20, 703-707.	8.2	4
2463	Ionic specific effects on the structure, mechanics and interfacial softness of a polyelectrolyte brush. Faraday Discussions, 2013, 160, 297-309.	3.2	20
2464	The Power Stroke Driven by ATP Binding in CFTR As Studied by Molecular Dynamics Simulations. Journal of Physical Chemistry B, 2013, 117, 83-93.	2.6	32
2465	Are polar liquids less simple?. Journal of Chemical Physics, 2013, 138, 12A502.	3.0	15
2466	Simple Quantitative Tests to Validate Sampling from Thermodynamic Ensembles. Journal of Chemical Theory and Computation, 2013, 9, 909-926.	5.3	61
2467	A Candidate Ion-Retaining State in the Inward-Facing Conformation of Sodium/Galactose Symporter: Clues from Atomistic Simulations. Journal of Chemical Theory and Computation, 2013, 9, 1240-1246.	5.3	26
2468	Dynamics and structural changes induced by ATP and/or substrate binding in the inward-facing conformation state of P-glycoprotein. Chemical Physics Letters, 2013, 557, 145-149.	2.6	13
2469	Anions, the Reporters of Structure in Ionic Liquids. Journal of Physical Chemistry Letters, 2013, 4, 105-110.	4.6	116
2470	Biomolecular Simulations. Methods in Molecular Biology, 2013, , .	0.9	33
2471	Computational modeling of human coreceptor CCR5 antagonist as a HIV-1 entry inhibitor: using an integrated homology modeling, docking, and membrane molecular dynamics simulation analysis approach. Journal of Biomolecular Structure and Dynamics, 2013, 31, 1251-1276.	3.5	13

#	ARTICLE	IF	CITATIONS
2472	Anomalous and normal diffusion of proteins and lipids in crowded lipid membranes. Faraday Discussions, 2013, 161, 397-417.	3.2	170
2473	Discovery of Novel Human Aquaporin-1 Blockers. ACS Chemical Biology, 2013, 8, 249-256.	3.4	58
2474	Characterization of the structures and dynamics of phosphoric acid doped benzimidazole mixtures: a molecular dynamics study. Journal of Molecular Modeling, 2013, 19, 109-118.	1.8	7
2475	Molecular dynamics study on the correlation between structure and sensitivity for defective RDX crystals and their PBXs. Journal of Molecular Modeling, 2013, 19, 803-809.	1.8	32
2476	ESPreSo++: A modern multiscale simulation package for soft matter systems. Computer Physics Communications, 2013, 184, 1129-1149.	7.5	99
2477	Implicit inclusion of atomic polarization in modeling of partitioning between water and lipid bilayers. Physical Chemistry Chemical Physics, 2013, 15, 4677.	2.8	43
2478	Atomistic simulation study of brittle failure in nanocrystalline graphene under uniaxial tension. Applied Physics Letters, 2013, 102, .	3.3	65
2479	Role of tyrosine hot-spot residues at the interface of colicin E9 and immunity protein 9: A comparative free energy simulation study. Proteins: Structure, Function and Bioinformatics, 2013, 81, 461-468.	2.6	10
2480	Molecular insights into the AT1 antagonism based on biophysical and in silico studies of telmisartan. Medicinal Chemistry Research, 2013, 22, 4842-4857.	2.4	8
2481	Atomic rearrangements in metallic glass: Their nucleation and self-organization. Acta Materialia, 2013, 61, 6050-6060.	7.9	8
2483	Fluid simulations with atomistic resolution: a hybrid multiscale method with field-wise coupling. Journal of Computational Physics, 2013, 255, 149-165.	3.8	27
2484	Grain size effect on microstructural properties of 3D nanocrystalline magnesium under tensile deformation. Computational Materials Science, 2013, 79, 247-251.	3.0	23
2485	3D numerical simulation study of quasistatic grinding process on a model granular material. Mechanics of Materials, 2013, 66, 88-109.	3.2	21
2486	Effects of surface curvature and surface characteristics of carbon-based nanomaterials on the adsorption and activity of acetylcholinesterase. Carbon, 2013, 62, 222-232.	10.3	39
2487	On the weak dependence of water diffusivity on the degree of hydrophobicity of acetylated hydroxypropyl xylan. Carbohydrate Polymers, 2013, 98, 644-649.	10.2	5
2488	Atomic structure of amorphous Mg <sub>40</sub> Cu <sub>35</sub> Ti <sub>25</sub> alloy: An ab initio molecular dynamics study. Solid State Communications, 2013, 154, 30-33.	1.9	3
2489	Guidance to design grain boundary mobility experiments with molecular dynamics and phase-field modeling. Acta Materialia, 2013, 61, 1373-1382.	7.9	15
2490	NaCl crystallization in apolar nanometer-sized confinement studied by atomistic simulations. Physical Review E, 2013, 88, 062312.	2.1	4



#	ARTICLE	IF	CITATIONS
2491	The Structural Basis for Endotoxin-induced Allosteric Regulation of the Toll-like Receptor 4 (TLR4) Innate Immune Receptor. <i>Journal of Biological Chemistry</i> , 2013, 288, 36215-36225.	3.4	51
2492	Effect of Carbon Spacer Length on Zwitterionic Carboxybetaines. <i>Journal of Physical Chemistry B</i> , 2013, 117, 1357-1366.	2.6	101
2493	Pivot Algorithm and Push-off Method for Efficient System Generation of All-atom Polymer Melts: Application to Hydroxyl-terminated Polybutadiene. <i>Macromolecular Theory and Simulations</i> , 2013, 22, 344-353.	1.4	8
2494	Modelling the effect of osmolytes on peptide mechanical unfolding. <i>Chemical Physics Letters</i> , 2013, 578, 138-143.	2.6	5
2495	Resisting resistant <i>Mycobacterium tuberculosis</i> naturally: Mechanistic insights into the inhibition of the parasite's sole signal peptidase Leader peptidase B. <i>Biochemical and Biophysical Research Communications</i> , 2013, 433, 552-557.	2.1	6
2496	Designing thermoplastic oligomers with programmed degradation mechanisms using a combined empirical and simulation approach. <i>Polymer Degradation and Stability</i> , 2013, 98, 829-838.	5.8	4
2497	The human topoisomerase 1B Arg634Ala mutation results in camptothecin resistance and loss of inter-domain motion correlation. <i>Biochimica Et Biophysica Acta - Proteins and Proteomics</i> , 2013, 1834, 2712-2721.	2.3	14
2498	Role of the fluidity of a liquid phase in determining the surface properties of the opposite phase at the liquid-liquid interface. <i>Journal of Molecular Liquids</i> , 2013, 186, 7.	4.9	1
2499	Unfolding stabilities of two paralogous proteins from <i>Naja naja naja</i> (Indian cobra) as probed by molecular dynamics simulations. <i>Toxicon</i> , 2013, 72, 11-22.	1.6	7
2500	Signal intensities in $1\text{H}$ - $^{13}\text{C}$ CP and INEPT MAS NMR of liquid crystals. <i>Journal of Magnetic Resonance</i> , 2013, 230, 165-175.	2.1	78
2501	Analysis of structural changes during plastic deformations of amorphous polyethylene. <i>Polymer</i> , 2013, 54, 819-840.	3.8	14
2502	Insights into eukaryotic Rubisco assembly - Crystal structures of RbcX chaperones from <i>Arabidopsis thaliana</i> . <i>Biochimica Et Biophysica Acta - General Subjects</i> , 2013, 1830, 2899-2906.	2.4	20
2503	Nanoscale insight into the exfoliation mechanism of graphene with organic dyes: effect of charge, dipole and molecular structure. <i>Nanoscale</i> , 2013, 5, 4205.	5.6	116
2504	Taste of Sugar at the Membrane: Thermodynamics and Kinetics of the Interaction of a Disaccharide with Lipid Bilayers. <i>Biophysical Journal</i> , 2013, 104, 622-632.	0.5	22
2505	Simulations: The dark side. <i>European Physical Journal Plus</i> , 2013, 128, 1.	2.6	113
2506	MD Simulations of the Formation of Stable Clusters in Mixtures of Alkaline Salts and Imidazolium-Based Ionic Liquids. <i>Journal of Physical Chemistry B</i> , 2013, 117, 3207-3220.	2.6	92
2507	Carbon nanotube bundling: influence on layer-by-layer assembly and antimicrobial activity. <i>Soft Matter</i> , 2013, 9, 2136.	2.7	32
2508	String-like cooperative motion in homogeneous melting. <i>Journal of Chemical Physics</i> , 2013, 138, 12A538.	3.0	69

#	ARTICLE	IF	CITATIONS
2509	Conical Lipids in Flat Bilayers Induce Packing Defects Similar to that Induced by Positive Curvature. <i>Biophysical Journal</i> , 2013, 104, 585-593.	0.5	149
2510	Amphipathic Lipid Packing Sensor Motifs: Probing Bilayer Defects with Hydrophobic Residues. <i>Biophysical Journal</i> , 2013, 104, 575-584.	0.5	171
2511	Inhibition mechanism exploration of quinoline derivatives as PDE10A inhibitors by in silico analysis. <i>Molecular BioSystems</i> , 2013, 9, 386.	2.9	6
2512	Structural features of the apelin receptor N-terminal tail and first transmembrane segment implicated in ligand binding and receptor trafficking. <i>Biochimica Et Biophysica Acta - Biomembranes</i> , 2013, 1828, 1471-1483.	2.6	34
2513	Theoretical study on the structures and properties of mixtures of urea and choline chloride. <i>Journal of Molecular Modeling</i> , 2013, 19, 2433-2441.	1.8	172
2514	Defining the Membrane-Associated State of the PTEN Tumor Suppressor Protein. <i>Biophysical Journal</i> , 2013, 104, 613-621.	0.5	42
2515	Prediction of Micelle/Water and Liposome/Water Partition Coefficients Based on Molecular Dynamics Simulations, COSMO-RS, and COSMOmic. <i>Langmuir</i> , 2013, 29, 3527-3537.	3.5	75
2516	Chemical Unfolding of Chicken Villin Headpiece in Aqueous Dimethyl Sulfoxide Solution: Cosolvent Concentration Dependence, Pathway, and Microscopic Mechanism. <i>Journal of Physical Chemistry B</i> , 2013, 117, 4488-4502.	2.6	24
2517	GROMACS 4.5: a high-throughput and highly parallel open source molecular simulation toolkit. <i>Bioinformatics</i> , 2013, 29, 845-854.	4.1	6,072
2519	Molecular Dynamics Simulations of the Adenosine A2a Receptor: Structural Stability, Sampling, and Convergence. <i>Journal of Chemical Information and Modeling</i> , 2013, 53, 1168-1178.	5.4	42
2520	Convergence of Sampling Kirkwoodâ€œBuff Integrals of Aqueous Solutions with Molecular Dynamics Simulations. <i>Journal of Chemical Theory and Computation</i> , 2013, 9, 1347-1355.	5.3	147
2521	Cytochrome C on a gold surface: investigating structural relaxations and their role in proteinâ€œsurface electron transfer by molecular dynamics simulations. <i>Physical Chemistry Chemical Physics</i> , 2013, 15, 5945.	2.8	20
2522	Theoretical studies on the transport mechanism of 5-fluorouracil through cyclic peptide based nanotubes. <i>Physical Chemistry Chemical Physics</i> , 2013, 15, 1260-1270.	2.8	32
2523	Effect of Organochloride Guest Molecules on the Stability of Homo/Hetero Self-Assembled $\beta$ -Cyclic Peptide Structures: A Computational Study Toward the Control of Nanotube Length. <i>Journal of Physical Chemistry C</i> , 2013, 117, 10143-10162.	3.1	12
2524	Interaction of Human Synovial Phospholipase A2 with Mixed Lipid Bilayers: A Coarse-Grain and All-Atom Molecular Dynamics Simulation Study. <i>Biochemistry</i> , 2013, 52, 1477-1489.	2.5	17
2525	Structure and dynamics of supercooled water in neutral confinements. <i>Journal of Chemical Physics</i> , 2013, 138, 134503.	3.0	40
2526	Force Field for Tricalcium Silicate and Insight into Nanoscale Properties: Cleavage, Initial Hydration, and Adsorption of Organic Molecules. <i>Journal of Physical Chemistry C</i> , 2013, 117, 10417-10432.	3.1	141
2527	Computational Study of Synthetic Agonist Ligands of Ionotropic Glutamate Receptors. <i>PLoS ONE</i> , 2013, 8, e58774.	2.5	11

#	ARTICLE	IF	CITATIONS
2528	Conformational changes of $\beta$ -carotene and zeaxanthin immersed in a model membrane through atomistic molecular dynamics simulations. <i>Physical Chemistry Chemical Physics</i> , 2013, 15, 6527.	2.8	21
2529	Assessing the Accuracy and Performance of Implicit Solvent Models for Drug Molecules: Conformational Ensemble Approaches. <i>Journal of Physical Chemistry B</i> , 2013, 117, 5950-5962.	2.6	60
2530	Crystal structure of a eukaryotic phosphate transporter. <i>Nature</i> , 2013, 496, 533-536.	27.8	202
2531	A partition function-based weighting scheme in force field parameter development using <i>ab initio</i> calculation results in global configurational space. <i>Journal of Computational Chemistry</i> , 2013, 34, 1271-1282.	3.3	1
2532	Ethanol promotes dewetting transition at low concentrations. <i>Soft Matter</i> , 2013, 9, 4655.	2.7	20
2533	Dimers of human $\beta$ -defensins and their interactions with the POPG membrane. <i>Molecular Simulation</i> , 2013, 39, 849-859.	2.0	4
2534	How Cholesterol Tilt Modulates the Mechanical Properties of Saturated and Unsaturated Lipid Membranes. <i>Journal of Physical Chemistry B</i> , 2013, 117, 2411-2421.	2.6	62
2535	On the plasticity event in metallic glass. <i>Philosophical Magazine Letters</i> , 2013, 93, 158-165.	1.2	11
2536	3D-QSAR, docking and molecular dynamics for factor Xa inhibitors as anticoagulant agents. <i>Molecular Simulation</i> , 2013, 39, 453-471.	2.0	11
2537	DMSO Transport across Water/Hexane Interface by Molecular Dynamics Simulation. <i>Industrial &amp; Engineering Chemistry Research</i> , 2013, 52, 6550-6558.	3.7	15
2538	Toward quantitative estimates of binding affinities for protein-ligand systems involving large inhibitor compounds: A steered molecular dynamics simulation route. <i>Journal of Computational Chemistry</i> , 2013, 34, 1561-1576.	3.3	41
2539	Molecular dynamics simulation of cetyltrimethylammonium bromide and sodium octyl sulfate mixtures: aggregate shape and local surfactant distribution. <i>Physical Chemistry Chemical Physics</i> , 2013, 15, 5563.	2.8	35
2540	Comparing Simulations of Lipid Bilayers to Scattering Data: The GROMOS 43A1-S3 Force Field. <i>Journal of Physical Chemistry B</i> , 2013, 117, 5065-5072.	2.6	47
2541	Sequence Effects on Peptide Assembly Characteristics Observed by Using Scanning Tunneling Microscopy. <i>Journal of the American Chemical Society</i> , 2013, 135, 2181-2187.	13.7	50
2542	Inhibition of CK2 Activity by TCDD via binding to ATP-competitive binding site of catalytic subunit: Insight from computational studies. <i>Chemical Research in Chinese Universities</i> , 2013, 29, 299-306.	2.6	1
2543	Analytical model and multiscale simulations of $\beta$ peptide aggregation in lipid membranes: towards a unifying description of conformational transitions, oligomerization and membrane damage. <i>Physical Chemistry Chemical Physics</i> , 2013, 15, 8940.	2.8	45
2544	Theoretical prediction of the protein-protein interaction between <i>Arabidopsis thaliana</i> COP1 and UVR8. <i>Theoretical Chemistry Accounts</i> , 2013, 132, 1.	1.4	8
2545	Insights on the Solubility of CO <sub>2</sub> in 1-Ethyl-3-methylimidazolium Bis(trifluoromethylsulfonyl)imide from the Microscopic Point of View. <i>Environmental Science &amp; Technology</i> , 2013, 47, 7421-7429.	10.0	65

#	ARTICLE	IF	CITATIONS
2546	Materialsâ€Scale Implications of Solvent and Temperature on [6,6]â€Phenylâ€C61â€Butyric Acid Methyl Ester (PCBM): A Theoretical Perspective. <i>Advanced Functional Materials</i> , 2013, 23, 5800-5813.	14.9	43
2547	Lengthâ€dependent stability of Î±â€helical peptide upon adsorption to singleâ€walled carbon nanotube. <i>Biopolymers</i> , 2013, 99, 357-369.	2.4	13
2548	Study of base pair mutations in proline-rich homeodomain (PRH)â€DNA complexes using molecular dynamics. <i>European Biophysics Journal</i> , 2013, 42, 427-440.	2.2	0
2549	Molecular Mechanism of Misfolding and Aggregation of AÎ²(13â€23). <i>Journal of Physical Chemistry B</i> , 2013, 117, 6175-6186.	2.6	46
2550	Molecular Dynamics Simulations of Carbon Dioxide Intercalation in Hydrated Na-Montmorillonite. <i>Journal of Physical Chemistry C</i> , 2013, 117, 11028-11039.	3.1	107
2551	Classical Molecular Dynamics in a Nutshell. <i>Methods in Molecular Biology</i> , 2013, 924, 127-152.	0.9	11
2552	Estimation of Ligand Efficacies of Metabotropic Glutamate Receptors from Conformational Forces Obtained from Molecular Dynamics Simulations. <i>Journal of Chemical Information and Modeling</i> , 2013, 53, 1337-1349.	5.4	3
2553	Fuzzy Complex Formation between the Intrinsically Disordered Prothymosin Î± and the Kelch Domain of Keap1 Involved in the Oxidative Stress Response. <i>Journal of Molecular Biology</i> , 2013, 425, 1011-1027.	4.2	38
2554	Water Vapor Diffusion into a Nanostructured Iron Oxyhydroxide. <i>Inorganic Chemistry</i> , 2013, 52, 7107-7113.	4.0	11
2555	Simulation Study of Structural Changes in Zeolite RHO. <i>Journal of Physical Chemistry C</i> , 2013, 117, 11592-11599.	3.1	23
2556	Design and evaluation of new chemotherapeutics of aloe-emodin (AE) against the deadly cancer disease: an in silico study. <i>Journal of Chemical Biology</i> , 2013, 6, 141-153.	2.2	5
2557	Heat Transfer Calculations for Decomposition of Structure I Methane Hydrates by Molecular Dynamics Simulation. <i>Journal of Physical Chemistry C</i> , 2013, 117, 12172-12182.	3.1	36
2558	Thermodynamic properties of poly(vinyl alcohol) with different tacticities estimated from molecular dynamics simulation. <i>Polymer</i> , 2013, 54, 4212-4219.	3.8	26
2559	Side pockets provide the basis for a new mechanism of Kv channelâ€specific inhibition. <i>Nature Chemical Biology</i> , 2013, 9, 507-513.	8.0	50
2560	Molecular Dynamics Simulation Study on the Absorption of Ethylene and Acetylene in Ionic Liquids. <i>Industrial &amp; Engineering Chemistry Research</i> , 2013, 52, 9308-9316.	3.7	37
2561	Performance of Different Force Fields in Force Probe Simulations. <i>Journal of Physical Chemistry B</i> , 2013, 117, 1862-1871.	2.6	17
2562	Anisotropic Dielectric Relaxation of the Water Confined in Nanotubes for Terahertz Spectroscopy Studied by Molecular Dynamics Simulations. <i>Journal of Physical Chemistry B</i> , 2013, 117, 7967-7971.	2.6	24
2563	Simulating the Shapeâ€Memory Behavior of Amorphous Switching Domains of Poly(L-lactide) by Molecular Dynamics. <i>Macromolecular Chemistry and Physics</i> , 2013, 214, 1273-1283.	2.2	26

#	ARTICLE	IF	CITATIONS
2564	Dissimilar stability of proteins in graphene bilayer: a molecular dynamics study. <i>Molecular Physics</i> , 2013, 111, 545-552.	1.7	7
2565	Systematic Parametrization of Polarizable Force Fields from Quantum Chemistry Data. <i>Journal of Chemical Theory and Computation</i> , 2013, 9, 452-460.	5.3	164
2566	Optimal Superpositioning of Flexible Molecule Ensembles. <i>Biophysical Journal</i> , 2013, 104, 196-207.	0.5	25
2567	The dynamics of camphor in the cytochrome P450 CYP101D2. <i>Protein Science</i> , 2013, 22, 1218-1229.	7.6	13
2568	Salting-in with a Salting-out Agent: Explaining the Cation Specific Effects on the Aqueous Solubility of Amino Acids. <i>Journal of Physical Chemistry B</i> , 2013, 117, 6116-6128.	2.6	85
2569	Atomistic simulations of grain boundary segregation in nanocrystalline yttria-stabilized zirconia and gadolinia-doped ceria solid oxide electrolytes. <i>Acta Materialia</i> , 2013, 61, 3872-3887.	7.9	68
2570	Molecular modeling, dynamics, and an insight into the structural inhibition of cofactor independent phosphoglycerate mutase isoform 1 from <i>Wuchereria bancrofti</i> using cheminformatics and mutational studies. <i>Journal of Biomolecular Structure and Dynamics</i> , 2013, 31, 765-778.	3.5	12
2571	Interatomic potential to predict favored composition for Hf-Cu-Ni metallic glasses formation. <i>Journal of Alloys and Compounds</i> , 2013, 552, 55-59.	5.5	6
2572	Molecular Dynamics Simulations of Membrane-Sugar Interactions. <i>Journal of Physical Chemistry B</i> , 2013, 117, 6667-6673.	2.6	43
2573	Effect of melatonin and cholesterol on the structure of DOPC and DPPC membranes. <i>Biochimica Et Biophysica Acta - Biomembranes</i> , 2013, 1828, 2247-2254.	2.6	92
2574	Top-leads from natural products for treatment of Alzheimer's disease: docking and molecular dynamics study. <i>Molecular Simulation</i> , 2013, 39, 279-291.	2.0	50
2575	Lipid Bilayer Membrane Affinity Rationalizes Inhibition of Lipid Peroxidation by a Natural Lignan Antioxidant. <i>Journal of Physical Chemistry B</i> , 2013, 117, 5043-5049.	2.6	22
2576	Dynamic Heterogeneity in Random and Gradient Copolymers: A Computational Investigation. <i>Macromolecules</i> , 2013, 46, 5066-5079.	4.8	32
2577	Free Energy of Solvated Salt Bridges: A Simulation and Experimental Study. <i>Journal of Physical Chemistry B</i> , 2013, 117, 7254-7259.	2.6	40
2578	Atomistic simulation for the $\beta$ -phase volume fraction dependence of the interfacial behavior of Ni-base superalloy. <i>Applied Surface Science</i> , 2013, 264, 563-569.	6.1	10
2579	Conformational dynamics and membrane interactions of the <i>E. coli</i> outer membrane protein FecA: A molecular dynamics simulation study. <i>Biochimica Et Biophysica Acta - Biomembranes</i> , 2013, 1828, 284-293.	2.6	66
2580	Stability and membrane interactions of an autotransport protein: MD simulations of the Hia translocator domain in a complex membrane environment. <i>Biochimica Et Biophysica Acta - Biomembranes</i> , 2013, 1828, 715-723.	2.6	26
2581	Lipid peroxidation and water penetration in lipid bilayers: A W-band EPR study. <i>Biochimica Et Biophysica Acta - Biomembranes</i> , 2013, 1828, 510-517.	2.6	21

#	ARTICLE	IF	CITATIONS
2582	Molecular dynamics of paclitaxel encapsulated by salicylic acid-grafted chitosan oligosaccharide aggregates. <i>Biomaterials</i> , 2013, 34, 1843-1851.	11.4	58
2583	Quantifying Changes in Intrinsic Molecular Motion Using Support Vector Machines. <i>Journal of Chemical Theory and Computation</i> , 2013, 9, 868-875.	5.3	9
2584	Unusual Li <sup>+</sup> Ion Solvation Structure in Bis(fluorosulfonyl)amide Based Ionic Liquid. <i>Journal of Physical Chemistry C</i> , 2013, 117, 19314-19324.	3.1	133
2585	Graphitic Carbonâ€“Water Nonbonded Interaction Parameters. <i>Journal of Physical Chemistry B</i> , 2013, 117, 8802-8813.	2.6	138
2586	Structure and Dynamics of [PF <sub>6</sub> ][P <sub>1,2,2,4</sub> ] from Molecular Dynamics Simulations. <i>Journal of Physical Chemistry B</i> , 2013, 117, 15176-15183.	2.6	13
2587	Theoretical Elucidation of the Origin for Assembly of the DAP12 Dimer with Only One NKG2C in the Lipid Membrane. <i>Journal of Physical Chemistry B</i> , 2013, 117, 4789-4797.	2.6	6
2588	Pressure Reentrant Assembly: Direct Simulation of Volumes of Micellization. <i>Langmuir</i> , 2013, 29, 14743-14747.	3.5	9
2589	8.1.6.6 Fibrous zeolites. , 2013, , 1-128.		0
2590	Insight into the Molecular Mechanisms of Protein Stabilizing Osmolytes from Global Force-Field Variations. <i>Journal of Physical Chemistry B</i> , 2013, 117, 8310-8321.	2.6	102
2591	Conformational Fluctuations of UreG, an Intrinsically Disordered Enzyme. <i>Biochemistry</i> , 2013, 52, 2949-2954.	2.5	33
2592	Alcohol-induced drying of carbon nanotubes and its implications for alcohol/water separation: A molecular dynamics study. <i>Journal of Chemical Physics</i> , 2013, 138, 204711.	3.0	39
2593	Representability and Transferability of Kirkwoodâ€“Buff Iterative Boltzmann Inversion Models for Multicomponent Aqueous Systems. <i>Journal of Chemical Theory and Computation</i> , 2013, 9, 5247-5256.	5.3	34
2594	RNA/Peptide Binding Driven by Electrostaticsâ€“Insight from Bidirectional Pulling Simulations. <i>Journal of Chemical Theory and Computation</i> , 2013, 9, 1720-1730.	5.3	48
2595	Comparative Computer Simulation Study of Cholesterol in Hydrated Unary and Binary Lipid Bilayers and in an Anhydrous Crystal. <i>Journal of Physical Chemistry B</i> , 2013, 117, 8758-8769.	2.6	23
2596	Insight into Î±-Synuclein Plasticity and Misfolding from Differential Micelle Binding. <i>Journal of Physical Chemistry B</i> , 2013, 117, 11448-11459.	2.6	12
2597	Toward Understanding the Outer Membrane Uptake of Small Molecules by <i>Pseudomonas aeruginosa</i> . <i>Journal of Biological Chemistry</i> , 2013, 288, 12042-12053.	3.4	51
2598	Enhancement of Lithium Ion Mobility in Ionic Liquid Electrolytes in Presence of Additives. <i>Journal of Physical Chemistry C</i> , 2013, 117, 25343-25351.	3.1	61
2599	Transcription-factor binding and sliding on DNA studied using micro- and macroscopic models. <i>Proceedings of the National Academy of Sciences of the United States of America</i> , 2013, 110, 19796-19801.	7.1	79



#	ARTICLE	IF	CITATIONS
2600	Appraisal of sildenafil binding on the structure and promiscuous esterase activity of native and histidine-modified forms of carbonic anhydrase II. <i>Biophysical Chemistry</i> , 2013, 175-176, 1-16.	2.8	7
2601	The "order-to-disorder"™ conformational transition in CD44 protein: An umbrella sampling analysis. <i>Journal of Molecular Graphics and Modelling</i> , 2013, 45, 122-127.	2.4	10
2602	Interactions between Voltage Sensor and Pore Domains in a hERG K <sup>+</sup> Channel Model from Molecular Simulations and the Effects of a Voltage Sensor Mutation. <i>Journal of Chemical Information and Modeling</i> , 2013, 53, 1358-1370.	5.4	19
2603	Inclusion of Multiple Fragment Types in the Site Identification by Ligand Competitive Saturation (SILCS) Approach. <i>Journal of Chemical Information and Modeling</i> , 2013, 53, 3384-3398.	5.4	101
2604	Solvent Sensitivity of Protein Unfolding: Dynamical Study of Chicken Villin Headpiece Subdomain in Water–Ethanol Binary Mixture. <i>Journal of Physical Chemistry B</i> , 2013, 117, 15625-15638.	2.6	48
2605	Softening due to disordered grain boundaries in nanocrystalline Co. <i>Journal of Physics Condensed Matter</i> , 2013, 25, 345702.	1.8	2
2606	Conformational Dynamics and Proton Relay Positioning in Nickel Catalysts for Hydrogen Production and Oxidation. <i>Organometallics</i> , 2013, 32, 7034-7042.	2.3	36
2607	Refined OPLS All-Atom Force Field Parameters for <i>n</i> -Pentadecane, Methyl Acetate, and Dimethyl Phosphate. <i>Journal of Physical Chemistry B</i> , 2013, 117, 16388-16396.	2.6	56
2608	Modelling family 2 cystatins and their interaction with papain. <i>Journal of Biomolecular Structure and Dynamics</i> , 2013, 31, 649-664.	3.5	17
2609	Adaptive molecular decomposition: Large-scale quantum chemistry for liquids. <i>Journal of Chemical Physics</i> , 2013, 138, 104108.	3.0	0
2610	Homogeneous bubble nucleation in water at negative pressure: A Voronoi polyhedra analysis. <i>Journal of Chemical Physics</i> , 2013, 138, 084508.	3.0	35
2611	Atomic-scale mechanism for pressure-induced amorphization of $\beta^2$ -eucryptite. <i>Journal of Applied Physics</i> , 2013, 114, 083520.	2.5	13
2612	Layerwise decomposition of water dynamics in reverse micelles: A simulation study of two-dimensional infrared spectrum. <i>Journal of Chemical Physics</i> , 2013, 139, 144906.	3.0	23
2613	Understanding the Molecular Determinants Driving the Immunological Specificity of the Protective Pilus 2a Backbone Protein of Group B Streptococcus. <i>PLoS Computational Biology</i> , 2013, 9, e1003115.	3.2	82
2614	The HAMP Signal Relay Domain Adopts Multiple Conformational States through Collective Piston and Tilt Motions. <i>PLoS Computational Biology</i> , 2013, 9, e1002913.	3.2	15
2615	The Recent Developments of Molecular Dynamics Simulation. <i>Applied Mechanics and Materials</i> , 0, 444-445, 1370-1373.	0.2	1
2616	Formation and Structure of Pd–Zr Metallic Glasses Studied by Molecular Dynamics Simulations. <i>Journal of the Physical Society of Japan</i> , 2013, 82, 064802.	1.6	2
2617	The Molecular Mechanism of Substrate Engagement and Immunosuppressant Inhibition of Calcineurin. <i>PLoS Biology</i> , 2013, 11, e1001492.	5.6	123



#	ARTICLE	IF	CITATIONS
2618	Engineering a More Thermostable Blue Light Photo Receptor Bacillus subtilis YtvA LOV Domain by a Computer Aided Rational Design Method. PLoS Computational Biology, 2013, 9, e1003129.	3.2	29
2619	Two Misfolding Routes for the Prion Protein around pH 4.5. PLoS Computational Biology, 2013, 9, e1003057.	3.2	18
2620	Conformational Changes in Talin on Binding to Anionic Phospholipid Membranes Facilitate Signaling by Integrin Transmembrane Helices. PLoS Computational Biology, 2013, 9, e1003316.	3.2	30
2621	Structural basis for alternating access of a eukaryotic calcium/proton exchanger. Nature, 2013, 499, 107-110.	27.8	87
2622	Are rare, long waiting times between rearrangement events responsible for the slowdown of the dynamics at the glass transition?. Journal of Chemical Physics, 2013, 138, 12A527.	3.0	21
2623	Role of the protein in the DNA sequence specificity of the cleavage site stabilized by the camptothecin topoisomerase IB inhibitor: a metadynamics study. Nucleic Acids Research, 2013, 41, 9977-9986.	14.5	26
2624	Study of lattice thermal conductivity of alpha-zirconium by molecular dynamics simulation. Chinese Physics B, 2013, 22, 076601.	1.4	9
2625	Structural Basis for Activation of ZAP-70 by Phosphorylation of the SH2-Kinase Linker. Molecular and Cellular Biology, 2013, 33, 2188-2201.	2.3	90
2626	Planar sheets meet negative-curvature liquid interfaces. Europhysics Letters, 2013, 101, 44007.	2.0	8
2627	Î±-Helical Structures Drive Early Stages of Self-Assembly of Amyloidogenic Amyloid Polypeptide Aggregate Formation in Membranes. Scientific Reports, 2013, 3, 2781.	3.3	91
2628	Free Energy Generalization of the Peierls Potential in Iron. Physical Review Letters, 2013, 111, 095502.	7.8	31
2629	On a Deformation-Driven Continuum-Related Parrinello-Rahman Molecular Dynamics. Proceedings in Applied Mathematics and Mechanics, 2013, 13, 175-176.	0.2	0
2630	Catch bond-like kinetics of helix cracking: Network analysis by molecular dynamics and Milestoning. Journal of Chemical Physics, 2013, 139, 121902.	3.0	25
2631	Variation and decomposition of the partial molar volume of small gas molecules in different organic solvents derived from molecular dynamics simulations. Journal of Chemical Physics, 2013, 139, 244506.	3.0	7
2632	Sequence dependent free energy profiles of localized B- to A-form transition of DNA in water. Journal of Chemical Physics, 2013, 139, 155102.	3.0	15
2633	A comparative study on shock compression of nanocrystalline Al and Cu: Shock profiles and microscopic views of plasticity. Journal of Applied Physics, 2013, 114, .	2.5	11
2634	Fitting coarse-grained distribution functions through an iterative force-matching method. Journal of Chemical Physics, 2013, 139, 121906.	3.0	77
2635	The stability of cylindrin Î²-barrel amyloid oligomer modelsâ€”A molecular dynamics study. Proteins: Structure, Function and Bioinformatics, 2013, 81, 1542-1555.	2.6	43

#	ARTICLE	IF	CITATIONS
2636	Calculation of driving force and local order to predict the favored and optimized compositions for Mg-Cu-Ni metallic glass formation. Journal of Applied Physics, 2013, 114, 153503.	2.5	3
2637	Combination of COSMOmic and molecular dynamics simulations for the calculation of membraneâ€“water partition coefficients. Journal of Computational Chemistry, 2013, 34, 1332-1340.	3.3	50
2638	Assessing the Stabilization of Pâ€“Glycoproteinâ€™s Nucleotideâ€“Binding Domains by the Linker, Using Molecular Dynamics. Molecular Informatics, 2013, 32, 529-540.	2.5	17
2639	Long-time mean-square displacements in proteins. Physical Review E, 2013, 88, 052706.	2.1	17
2640	Role of temperature in the formation and growth of gold monoatomic chains: A molecular dynamics study. Physical Review B, 2013, 88, .	3.2	7
2641	TES buffer-induced phase separation of aqueous solutions of several water-miscible organic solvents at 298.15 K: Phase diagrams and molecular dynamic simulations. Journal of Chemical Physics, 2013, 138, 244501.	3.0	24
2642	The 2.5 Å... Structure of the Enterococcus Conjugation Protein TraM resembles VirB8 Type IV Secretion Proteins. Journal of Biological Chemistry, 2013, 288, 2018-2028.	3.4	50
2643	Stability of fluctuating and transient aggregates of amphiphilic solutes in aqueous binary mixtures: Studies of dimethylsulfoxide, ethanol, and tert-butyl alcohol. Journal of Chemical Physics, 2013, 139, 164301.	3.0	27
2644	The effects on the lattice dynamical properties of the temperature and pressure in random NiPd alloy. Canadian Journal of Physics, 2013, 91, 833-838.	1.1	6
2645	Ordering simulation of high thermal conductivity epoxy resins. Polymer Journal, 2013, 45, 444-448.	2.7	20
2646	Determining the phase diagram of water from direct coexistence simulations: The phase diagram of the TIP4P/2005 model revisited. Journal of Chemical Physics, 2013, 139, 154505.	3.0	61
2647	Dominant-negative effects in prion diseases: insights from molecular dynamics simulations on mouse prion protein chimeras. Journal of Biomolecular Structure and Dynamics, 2013, 31, 829-840.	3.5	9
2648	Prediction of Glass-Forming Ability and Atomic-Level Structure of the Alâ€“Zrâ€“Pd Metallic Glasses by Molecular Dynamics Simulations. Journal of the Physical Society of Japan, 2013, 82, 124006.	1.6	1
2649	ICA-105574 Interacts with a Common Binding Site to Elicit Opposite Effects on Inactivation Gating of EAG and ERG Potassium Channels. Molecular Pharmacology, 2013, 83, 805-813.	2.3	21
2650	Orientation-strain glass formation in anisotropic particle systems with impurities. , 2013, , .		0
2652	High-Performance Modeling of CO2 Sequestration by Coupling Reservoir Simulation and Molecular Dynamics. , 2013, , .		2
2653	High end GPCR design: crafted ligand design and druggability analysis using protein structure, lipophilic hotspots and explicit water networks. In Silico Pharmacology, 2013, 1, .	3.3	72
2654	Atomistic Design of High Strength Crystalline-Amorphous Nanocomposites. Materials Transactions, 2013, 54, 1592-1596.	1.2	9

#	ARTICLE	IF	CITATIONS
2655	Binding of disordered proteins to a protein hub. Scientific Reports, 2013, 3, 2305.	3.3	28
2656	5 Modeling mechanical properties of nanocomposites. , 2013, , 145-182.		0
2657	Activation Free Energy of Nucleation of a Dislocation Pair in Magnesium. Materials Transactions, 2013, 54, 680-685.	1.2	8
2658	Characterization of three cinnamyl alcohol dehydrogenases from Carthamus tinctorius. Plant Biotechnology, 2013, 30, 315-326.	1.0	3
2659	Ion Concentration-Dependent Ion Conduction Mechanism of a Voltage-Sensitive Potassium Channel. PLoS ONE, 2013, 8, e56342.	2.5	13
2660	Ammonium Transport Proteins with Changes in One of the Conserved Pore Histidines Have Different Performance in Ammonia and Methylamine Conduction. PLoS ONE, 2013, 8, e62745.	2.5	20
2661	How Fast Does a Signal Propagate through Proteins?. PLoS ONE, 2013, 8, e64746.	2.5	12
2662	Two Distinct States of the HAMP Domain from Sensory Rhodopsin Transducer Observed in Unbiased Molecular Dynamics Simulations. PLoS ONE, 2013, 8, e66917.	2.5	19
2663	Molecular Dynamics Simulations of Water/Mucus Partition Coefficients for Feeding Stimulants in Fish and the Implications for Olfaction. PLoS ONE, 2013, 8, e72271.	2.5	6
2664	Biochemical and Structural Characterization of SplD Protease from Staphylococcus aureus. PLoS ONE, 2013, 8, e76812.	2.5	29
2665	Stability of Transmembrane Amyloid Î²-Peptide and Membrane Integrity Tested by Molecular Modeling of Site-Specific AÎ²42 Mutations. PLoS ONE, 2013, 8, e78399.	2.5	27
2666	Acetylation of Lysine 382 and Phosphorylation of Serine 392 in p53 Modulate the Interaction between p53 and MDC1 In Vitro. PLoS ONE, 2013, 8, e78472.	2.5	16
2667	Ponatinib Is a Pan-BCR-ABL Kinase Inhibitor: MD Simulations and SIE Study. PLoS ONE, 2013, 8, e78556.	2.5	19
2668	Familial Hypertrophic Cardiomyopathy Related Cardiac Troponin C L29Q Mutation Alters Length-Dependent Activation and Functional Effects of Phosphomimetic Troponin I*. PLoS ONE, 2013, 8, e79363.	2.5	26
2669	Energetic and Molecular Water Permeation Mechanisms of the Human Red Blood Cell Urea Transporter B. PLoS ONE, 2013, 8, e82338.	2.5	27
2670	Exploration of Virtual Candidates for Human HMG-CoA Reductase Inhibitors Using Pharmacophore Modeling and Molecular Dynamics Simulations. PLoS ONE, 2013, 8, e83496.	2.5	17
2671	Theoretical Investigation of the D83V Mutation within the Myocyte-Specific Enhancer Factor-2 Beta and Its Role in Cancer. Journal of Theoretical Chemistry, 2013, 2013, 1-10.	1.5	3
2672	New Hexagonal-rhombic Trilayer Ice Structure Confined between Hydrophobic Plates. Chinese Journal of Chemical Physics, 2014, 27, 15-19.	1.3	14

#	ARTICLE	IF	CITATIONS
2673	Molecular mechanics and dynamics: numerical tools to sample the configuration space. <i>Frontiers in Bioscience - Landmark</i> , 2014, 19, 578.	3.0	13
2674	Atomic resolution view into the structure–function relationships of the human myelin peripheral membrane protein P2. <i>Acta Crystallographica Section D: Biological Crystallography</i> , 2014, 70, 165-176.	2.5	41
2675	The C-Terminal Random Coil Region Tunes the Ca <sup>2+</sup> -Binding Affinity of S100A4 through Conformational Activation. <i>PLoS ONE</i> , 2014, 9, e97654.	2.5	11
2676	GSK3 $\beta$ -Dependent Phosphorylation Alters DNA Binding, Transactivity and Half-Life of the Transcription Factor USF2. <i>PLoS ONE</i> , 2014, 9, e107914.	2.5	6
2677	Two Polymorphisms Facilitate Differences in Plasticity between Two Chicken Major Histocompatibility Complex Class I Proteins. <i>PLoS ONE</i> , 2014, 9, e89657.	2.5	20
2678	Functional Mechanism of C-Terminal Tail in the Enzymatic Role of Porcine Testicular Carbonyl Reductase: A Combined Experiment and Molecular Dynamics Simulation Study of the C-Terminal Tail in the Enzymatic Role of PTCR. <i>PLoS ONE</i> , 2014, 9, e90712.	2.5	2
2679	Organization of Lipids in the Tear Film: A Molecular-Level View. <i>PLoS ONE</i> , 2014, 9, e92461.	2.5	41
2680	Inter-Species Cross-Seeding: Stability and Assembly of Rat - Human Amylin Aggregates. <i>PLoS ONE</i> , 2014, 9, e97051.	2.5	28
2681	Structural Basis for the Recognition in an Idiotypic-Anti-Idiotypic Antibody Complex Related to Celiac Disease. <i>PLoS ONE</i> , 2014, 9, e102839.	2.5	9
2682	Thermostability of In Vitro Evolved <i>Bacillus subtilis</i> Lipase A: A Network and Dynamics Perspective. <i>PLoS ONE</i> , 2014, 9, e102856.	2.5	24
2683	Enzymatic Oxidation of Cholesterol: Properties and Functional Effects of Cholestenone in Cell Membranes. <i>PLoS ONE</i> , 2014, 9, e103743.	2.5	50
2684	Insights from Molecular Dynamics Simulations: Structural Basis for the V567D Mutation-Induced Instability of Zebrafish Alpha-Dystroglycan and Comparison with the Murine Model. <i>PLoS ONE</i> , 2014, 9, e103866.	2.5	34
2685	On Calculation of the Electrostatic Potential of a Phosphatidylinositol Phosphate-Containing Phosphatidylcholine Lipid Membrane Accounting for Membrane Dynamics. <i>PLoS ONE</i> , 2014, 9, e104778.	2.5	3
2686	Co-Exposure with Fullerene May Strengthen Health Effects of Organic Industrial Chemicals. <i>PLoS ONE</i> , 2014, 9, e114490.	2.5	9
2687	Effects of Water Models on Binding Affinity: Evidence from All-Atom Simulation of Binding of Tamiflu to A/H5N1 Neuraminidase. <i>Scientific World Journal</i> , The, 2014, 2014, 1-14.	2.1	42
2688	Molecular dynamics and first-principles study of grain boundary sliding in metals. <i>Transactions of the Materials Research Society of Japan</i> , 2014, 39, 31-34.	0.2	1
2689	Anisotropy of Thermal-expansion for $\beta$ -Octahydro-1,3,5,7-tetranitro- 1,3,5,7-tetrazocine: Quantum Chemistry Calculation and Molecular Dynamics Simulation. <i>Chinese Journal of Chemical Physics</i> , 2014, 27, 57-62.	1.3	1
2690	Insight into Capture of Greenhouse Gas (CO <sub>2</sub> ) based on Guanidinium Ionic Liquids. <i>Chinese Journal of Chemical Physics</i> , 2014, 27, 144-148.	1.3	3

#	ARTICLE	IF	CITATIONS
2691	Role of solvation in pressure-induced helix stabilization. <i>Journal of Chemical Physics</i> , 2014, 141, 22D522.	3.0	16
2692	Lattice-switching Monte Carlo method for crystals of flexible molecules. <i>Physical Review E</i> , 2014, 90, 063313.	2.1	6
2693	Molecular Dynamics Analysis on Compressive Strength of PAN-Based Carbon Fibers. <i>International Journal of Nanoscience</i> , 2014, 13, 1440004.	0.7	2
2694	Tensile deformation and failure of amyloid and amyloid-like protein fibrils. <i>Nanotechnology</i> , 2014, 25, 105703.	2.6	37
2695	Sensitivity of polarization fluctuations to the nature of protein-water interactions: Study of biological water in four different protein-water systems. <i>Journal of Chemical Physics</i> , 2014, 141, 22D531.	3.0	23
2696	An extended molecular statics algorithm simulating the electromechanical continuum response of ferroelectric materials. <i>Computational Mechanics</i> , 2014, 54, 1515-1527.	4.0	8
2697	Molecular dynamics simulations of the Nip7 proteins from the marine deep- and shallow-water <i>Pyrococcus</i> species. <i>BMC Structural Biology</i> , 2014, 14, 23.	2.3	6
2698	Lipid Converter, A Framework for Lipid Manipulations in Molecular Dynamics Simulations. <i>Journal of Membrane Biology</i> , 2014, 247, 1137-1140.	2.1	7
2699	Phospholamban C-terminal Residues Are Critical Determinants of the Structure and Function of the Calcium ATPase Regulatory Complex. <i>Journal of Biological Chemistry</i> , 2014, 289, 25855-25866.	3.4	14
2700	Anomalous lateral diffusion in lipid bilayers observed by molecular dynamics simulations with atomistic and coarse-grained force fields. <i>Molecular Simulation</i> , 2014, 40, 245-250.	2.0	17
2701	Allosteric Response and Substrate Sensitivity in Peptide Binding of the Signal Recognition Particle. <i>Journal of Biological Chemistry</i> , 2014, 289, 30868-30879.	3.4	2
2702	Understanding the structural and dynamic consequences of DNA epigenetic modifications: Computational insights into cytosine methylation and hydroxymethylation. <i>Epigenetics</i> , 2014, 9, 1604-1612.	2.7	47
2703	Towards the Realization of Ab Initio Dynamics at the Speed of Molecular Mechanics: Simulations with Interpolated Diabatic Hamiltonian. <i>ChemPhysChem</i> , 2014, 15, 3183-3193.	2.1	12
2704	Structural Characterization of the Drug Translocation Path of MRP1/ABCC1. <i>Israel Journal of Chemistry</i> , 2014, 54, 1382-1393.	2.3	9
2705	A Critical Residue Selectively Recruits Nucleotides for T7 RNA Polymerase Transcription Fidelity Control. <i>Biophysical Journal</i> , 2014, 107, 2130-2140.	0.5	22
2706	Dynamic characterization and substrate binding of cis-2,3-dihydrobiphenyl-2,3-diol dehydrogenase—an enzyme used in bioremediation. <i>Journal of Molecular Modeling</i> , 2014, 20, 2531.	1.8	6
2707	The Free Energy Profile of Tubulin Straight-Bent Conformational Changes, with Implications for Microtubule Assembly and Drug Discovery. <i>PLoS Computational Biology</i> , 2014, 10, e1003464.	3.2	35
2708	Dewetting transition assisted clearance of (NFGAILS) amyloid fibrils from cell membranes by graphene. <i>Journal of Chemical Physics</i> , 2014, 141, 22D520.	3.0	16

#	ARTICLE	IF	CITATIONS
2709	A Hybrid Molecular Dynamics/Atomic-Scale Finite Element Method for Quasi-Static Atomistic Simulations at Finite Temperature. Journal of Applied Mechanics, Transactions ASME, 2014, 81, .	2.2	5
2710	Molecular Simulation-Based Structural Prediction of Protein Complexes in Mass Spectrometry: The Human Insulin Dimer. PLoS Computational Biology, 2014, 10, e1003838.	3.2	13
2711	Phase stability and in situ growth stresses in Ti/Nb thin films. Acta Materialia, 2014, 80, 490-497.	7.9	16
2712	Structure of the Membrane Anchor of Pestivirus Glycoprotein Erns, a Long Tilted Amphipathic Helix. PLoS Pathogens, 2014, 10, e1003973.	4.7	30
2713	Revisiting the conundrum of trehalose stabilization. Physical Chemistry Chemical Physics, 2014, 16, 26746-26761.	2.8	33
2714	How Anacetrapib Inhibits the Activity of the Cholesteryl Ester Transfer Protein? Perspective through Atomistic Simulations. PLoS Computational Biology, 2014, 10, e1003987.	3.2	17
2715	Structural Insights into E. coli Porphobilinogen Deaminase during Synthesis and Exit of 1-Hydroxymethylbilane. PLoS Computational Biology, 2014, 10, e1003484.	3.2	12
2716	Hydrophobic Compounds Reshape Membrane Domains. PLoS Computational Biology, 2014, 10, e1003873.	3.2	58
2717	Theoretical Methods of Domain Structures in Ultrathin Ferroelectric Films: A Review. Materials, 2014, 7, 6502-6568.	2.9	17
2718	Hydration of chloride anions in the NanC Porin from Escherichia coli: A comparative study by QM/MM and MD simulations. Journal of Chemical Physics, 2014, 141, 22D521.	3.0	3
2719	A flexible volumetric comparison of protein cavities can reveal patterns in ligand binding specificity. , 2014, , .		5
2720	Variational Bayesian clustering on protein cavity conformations for detecting influential amino acids. , 2014, , .		7
2721	Evaluation of metastable region boundaries for liquid and solid states in MD simulations. Journal of Physics: Conference Series, 2014, 500, 172004.	0.4	3
2722	A combined MD/QM and experimental exploration of conformational richness in branched oligothiophenes. Physical Chemistry Chemical Physics, 2014, 16, 24841-24852.	2.8	13
2723	Simulation of polyethylene glycol and calcium-mediated membrane fusion. Journal of Chemical Physics, 2014, 140, 124905.	3.0	44
2724	Precursory signatures of protein folding/unfolding: From time series correlation analysis to atomistic mechanisms. Journal of Chemical Physics, 2014, 140, 204905.	3.0	3
2725	Hydrophobic hydration driven self-assembly of curcumin in water: Similarities to nucleation and growth under large metastability, and an analysis of water dynamics at heterogeneous surfaces. Journal of Chemical Physics, 2014, 141, 18C501.	3.0	40
2726	Boundary-controlled barostats for slab geometries in molecular dynamics simulations. Physical Review E, 2014, 90, 043302.	2.1	21



#	ARTICLE	IF	CITATIONS
2727	A fully atomistic computer simulation study of cold denaturation of a $\beta^2$ -hairpin. Nature Communications, 2014, 5, 5773.	12.8	44
2728	Multidimensional free energy surface of unfolding of HP-36: Microscopic origin of ruggedness. Journal of Chemical Physics, 2014, 141, 135101.	3.0	13
2729	Local structural excitations in model glasses. Physical Review B, 2014, 89, .	3.2	34
2730	Dicarba Analogues of $\beta^1$ -Conotoxin RgIA. Structure, Stability, and Activity at Potential Pain Targets. Journal of Medicinal Chemistry, 2014, 57, 9933-9944.	6.4	56
2731	Monte Carlo simulations for the free energies of C60 and C70 fullerene crystals by acceptance ratio method and expanded ensemble method. Journal of Chemical Physics, 2014, 140, 084110.	3.0	2
2732	Diffusion maps, clustering and fuzzy Markov modeling in peptide folding transitions. Journal of Chemical Physics, 2014, 141, 114102.	3.0	23
2733	Structural Basis for Autoinhibition of CTP:Phosphocholine Cytidyltransferase (CCT), the Regulatory Enzyme in Phosphatidylcholine Synthesis, by Its Membrane-binding Amphipathic Helix. Journal of Biological Chemistry, 2014, 289, 1742-1755.	3.4	35
2734	The interaction of local anesthetics with lipid membranes. Journal of Molecular Graphics and Modelling, 2014, 53, 200-205.	2.4	17
2735	Is there a third order phase transition for supercritical fluids?. Journal of Chemical Physics, 2014, 140, 014502.	3.0	1
2736	Atomistic Description of the Solubilisation of Testosterone Propionate in a Sodium Dodecyl Sulfate Micelle. Journal of Physical Chemistry B, 2014, 118, 13192-13201.	2.6	15
2737	R102Q Mutation Shifts the Salt-Bridge Network and Reduces the Structural Flexibility of Human Neuronal Calcium Sensor-1 Protein. Journal of Physical Chemistry B, 2014, 118, 13112-13122.	2.6	12
2738	Calcium Binding to Calmodulin by Molecular Dynamics with Effective Polarization. Journal of Physical Chemistry Letters, 2014, 5, 3964-3969.	4.6	60
2739	A sub-nanometre view of how membrane curvature and composition modulate lipid packing and protein recruitment. Nature Communications, 2014, 5, 4916.	12.8	230
2740	Molecular Insight into the Effect of Lipid Bilayer Environments on Thrombospondin-1 and Calreticulin Interactions. Biochemistry, 2014, 53, 6309-6322.	2.5	24
2741	Communication: Minimum in the thermal conductivity of supercooled water: A computer simulation study. Journal of Chemical Physics, 2014, 140, 161104.	3.0	16
2742	First Principles Modeling of Electrolyte Materials in All-Solid-State Batteries. Physics Procedia, 2014, 57, 29-37.	1.2	7
2743	Insights into the Role of Asp79 <sup>&gt;2.50&lt;/sup&gt; in <math>\beta^2</math><sub>2</sub> Adrenergic Receptor Activation from Molecular Dynamics Simulations. Biochemistry, 2014, 53, 7283-7296.</sup>	2.5	67
2744	Water Dynamics at Protein-Protein Interfaces: Molecular Dynamics Study of Virus-Host Receptor Complexes. Journal of Physical Chemistry B, 2014, 118, 141212105050009.	2.6	17



#	ARTICLE	IF	CITATIONS
2745	Influence of electric fields on the structure and structure transition of water confined in a carbon nanotube. <i>Journal of Chemical Physics</i> , 2014, 140, 154508.	3.0	26
2746	Dynamical and structural properties of monohydroxy alcohols exhibiting a Debye process. <i>Journal of Chemical Physics</i> , 2014, 140, 144507.	3.0	17
2747	Motional timescale predictions by molecular dynamics simulations: Case study using proline and hydroxyproline sidechain dynamics. <i>Proteins: Structure, Function and Bioinformatics</i> , 2014, 82, 195-215.	2.6	202
2748	Analysis of Solvation and Gelation Behavior of Methylcellulose Using Atomistic Molecular Dynamics Simulations. <i>Journal of Physical Chemistry B</i> , 2014, 118, 13992-14008.	2.6	34
2749	Ab initio calculation of the electronic absorption spectrum of liquid water. <i>Journal of Chemical Physics</i> , 2014, 140, 164511.	3.0	8
2750	Controlling water flow inside carbon nanotube with lipid membranes. <i>Journal of Chemical Physics</i> , 2014, 141, 094901.	3.0	13
2751	Mechanical properties and plasticity of a model glass loaded under stress control. <i>Physical Review E</i> , 2014, 90, 052402.	2.1	7
2752	Homogeneous ice nucleation evaluated for several water models. <i>Journal of Chemical Physics</i> , 2014, 141, 18C529.	3.0	128
2753	Molecular dynamics simulation study on the interaction of collagen-like peptides with gelatinase (MMP-2). <i>Biopolymers</i> , 2014, 101, 779-794.	2.4	12
2754	Communication: Kinetic and pairing contributions in the dielectric spectra of electrolyte solutions. <i>Journal of Chemical Physics</i> , 2014, 140, 211101.	3.0	25
2755	Glucose oxidase from <i>Penicillium amagasakiense</i> : Characterization of the transition state of its denaturation from molecular dynamics simulations. <i>Proteins: Structure, Function and Bioinformatics</i> , 2014, 82, 2353-2363.	2.6	13
2756	Short-Range Solvation Effects on Chiroptical Properties: A Time-Dependent Density Functional Theory and ab Initio Molecular Dynamics Computational Case Study on Austdiol. <i>Journal of Physical Chemistry A</i> , 2014, 118, 11751-11757.	2.5	7
2757	The behaviour of tributyl phosphate in an organic diluent. <i>Molecular Physics</i> , 2014, 112, 2203-2214.	1.7	13
2758	Mesoscale properties of clay aggregates from potential of mean force representation of interactions between nanoplatelets. <i>Journal of Chemical Physics</i> , 2014, 140, .	3.0	73
2759	Electrophoretic mobilities of neutral analytes and electroosmotic flow markers in aqueous solutions of Hofmeister salts. <i>Electrophoresis</i> , 2014, 35, 617-624.	2.4	9
2760	Detecting vapour bubbles in simulations of metastable water. <i>Journal of Chemical Physics</i> , 2014, 141, 18C511.	3.0	19
2761	Understanding electrofreezing in water simulations. <i>Journal of Chemical Physics</i> , 2014, 141, 074501.	3.0	27
2762	Stability of Iowa mutant and wild type A $\beta$ -peptide aggregates. <i>Journal of Chemical Physics</i> , 2014, 141, 175101.	3.0	22

#	ARTICLE	IF	CITATIONS
2763	Multiscale Simulations Give Insight into the Hydrogen In and Out Pathways of [NiFe]-Hydrogenases from <i>Aquifex aeolicus</i> and <i>Desulfovibrio fructosovorans</i> . Journal of Physical Chemistry B, 2014, 118, 13800-13811.	2.6	26
2764	Does fluoride disrupt hydrogen bond network in cationic lipid bilayer? Time-dependent fluorescence shift of Laurdan and molecular dynamics simulations. Journal of Chemical Physics, 2014, 141, 22D516.	3.0	6
2765	Peptide dynamics by molecular dynamics simulation and diffusion theory method with improved basis sets. Journal of Chemical Physics, 2014, 140, 104910.	3.0	3
2766	Communication: Thermodynamics of stacking disorder in ice nuclei. Journal of Chemical Physics, 2014, 141, 121101.	3.0	32
2767	Constant pressure hybrid Monte Carlo simulations in GROMACS. Journal of Molecular Modeling, 2014, 20, 2487.	1.8	15
2768	UO <sub>2</sub> <sup>2+</sup> Uptake by Proteins: Understanding the Binding Features of the Super Uranyl Binding Protein and Design of a Protein with Higher Affinity. Journal of the American Chemical Society, 2014, 136, 17484-17494.	13.7	74
2769	Interplay of spin-orbit and entropic effects in cerium. Physical Review B, 2014, 90, .	3.2	20
2770	Vibrations of Bioionic Liquids by Ab Initio Molecular Dynamics and Vibrational Spectroscopy. Journal of Physical Chemistry A, 2014, 118, 12229-12240.	2.5	27
2771	Communication: Anomalous temperature dependence of the intermediate range order in phosphonium ionic liquids. Journal of Chemical Physics, 2014, 140, 111102.	3.0	49
2772	de Gennes Narrowing Describes the Relative Motion of Protein Domains. Physical Review Letters, 2014, 112, 158102.	7.8	30
2773	How distributed charge reduces the melting points of model ionic salts. Journal of Chemical Physics, 2014, 140, 104504.	3.0	8
2774	Peptide-induced membrane curvature in edge-stabilized open bilayers: A theoretical and molecular dynamics study. Journal of Chemical Physics, 2014, 141, 024901.	3.0	15
2775	Equilibrium Conformational Ensemble of the Intrinsically Disordered Peptide n16N: Linking Subdomain Structures and Function in Nacre. Biomacromolecules, 2014, 15, 4467-4479.	5.4	24
2776	Reparameterized United Atom Model for Molecular Dynamics Simulations of Gel and Fluid Phosphatidylcholine Bilayers. Journal of Chemical Theory and Computation, 2014, 10, 5706-5715.	5.3	32
2777	Role of Desolvation in Thermodynamics and Kinetics of Ligand Binding to a Kinase. Journal of Chemical Theory and Computation, 2014, 10, 5696-5705.	5.3	61
2778	Molecular dynamics approach to locally resolve elastic constants in nanocomposites and thin films: Mechanical description of solid-soft matter interphases via Young's modulus, Poisson's ratio and shear modulus. European Physical Journal E, 2014, 37, 103.	1.6	8
2779	Tilt orientationally disordered hexagonal columnar phase of phthalocyanine discotic liquid crystals. Physical Review E, 2014, 89, 062505.	2.1	23
2780	Thermodynamics of surface defects at the aspirin/water interface. Journal of Chemical Physics, 2014, 141, 124702.	3.0	3

#	ARTICLE	IF	CITATIONS
2781	Quantification of the stiffness and strength of cadherin ectodomain binding with different ions. Theoretical and Applied Mechanics Letters, 2014, 4, 034001.	2.8	10
2782	Molecular dynamics simulations show how the FMRP Ile304Asn mutation destabilizes the KH2 domain structure and affects its function. Journal of Biomolecular Structure and Dynamics, 2014, 32, 337-350.	3.5	21
2783	Widom line and dynamical crossovers as routes to understand supercritical water. Nature Communications, 2014, 5, 5806.	12.8	116
2784	Restriction of HIV-1 by Rhesus TRIM5 $\alpha$ Is Governed by Alpha Helices in the Linker2 Region. Journal of Virology, 2014, 88, 8911-8923.	3.4	9
2785	Molecular Dynamics Study of Aqueous NaCl Solutions: Flash Crystallization Caused by Solution Phase Change. Journal of Solution Chemistry, 2014, 43, 1799-1809.	1.2	4
2786	Dependence of critical stress on temperature and shear strain rate in grain boundary of W. Materials Research Innovations, 2014, 18, S4-1078-S4-1081.	2.3	0
2787	Structure of the type VI secretion phospholipase effector Tle1 provides insight into its hydrolysis and membrane targeting. Acta Crystallographica Section D: Biological Crystallography, 2014, 70, 2175-2185.	2.5	26
2788	The Crystal Structure of Giardia duodenalis 14-3-3 in the Apo Form: When Protein Post-Translational Modifications Make the Difference. PLoS ONE, 2014, 9, e92902.	2.5	12
2789	Effective interaction between small unilamellar vesicles as probed by coarse-grained molecular dynamics simulations. Pure and Applied Chemistry, 2014, 86, 215-222.	1.9	11
2790	Molecular dynamics simulations of the formation of 1D spin-valves from stretched Au-Co and Pt-Co nanowires. Journal of Physics Condensed Matter, 2014, 26, 474206.	1.8	8
2791	Computational analysis of amino acids and their sidechain analogs in crowded solutions of RNA nucleobases with implications for the mRNA-protein complementarity hypothesis. Nucleic Acids Research, 2014, 42, 12984-12994.	14.5	19
2792	The investigation of the secondary structure propensities and free-energy landscapes of peptide ligands by replica exchange molecular dynamics simulations. Molecular Simulation, 2014, 40, 1015-1025.	2.0	2
2793	Comparing atomistic molecular mechanics force fields for a difficult target: a case study on the Alzheimer's amyloid $\beta$ -peptide. Journal of Biomolecular Structure and Dynamics, 2014, 32, 1817-1832.	3.5	74
2794	Bindings of hMRP1 transmembrane peptides with dodecylphosphocholine and dodecyl- $\beta$ -D-maltoside micelles: A molecular dynamics simulation study. Biochimica Et Biophysica Acta - Biomembranes, 2014, 1838, 493-509.	2.6	5
2795	Molecular origins of bending rigidity in lipids with isolated and conjugated double bonds: The effect of cholesterol. Chemistry and Physics of Lipids, 2014, 178, 18-26.	3.2	27
2796	i-PI: A Python interface for ab initio path integral molecular dynamics simulations. Computer Physics Communications, 2014, 185, 1019-1026.	7.5	189
2797	Effect of chirality, length and diameter of carbon nanotubes on the adsorption of 20 amino acids: a molecular dynamics simulation study. Molecular Simulation, 2014, 40, 392-398.	2.0	33
2798	Nickel(ii), copper(ii) and zinc(ii) metallo-intercalators: structural details of the DNA-binding by a combined experimental and computational investigation. Dalton Transactions, 2014, 43, 6108.	3.3	79

#	ARTICLE	IF	CITATIONS
2799	Interactions between clay portions with various contacts and subjected to specific environmental conditions. <i>Applied Surface Science</i> , 2014, 292, 311-318.	6.1	7
2800	Membrane attachment and structure models of lipid storage droplet protein 1. <i>Biochimica Et Biophysica Acta - Biomembranes</i> , 2014, 1838, 874-881.	2.6	16
2801	Grain boundary migration of substitutional and interstitial atoms in $\delta$ -iron. <i>Acta Materialia</i> , 2014, 69, 105-113.	7.9	39
2802	Conformational Analysis of Processivity Clamps in Solution Demonstrates that Tertiary Structure Does Not Correlate with Protein Dynamics. <i>Structure</i> , 2014, 22, 572-581.	3.3	30
2803	Kinetic and Mechanistic Study of COF-1 Phase Change from a Staggered to Eclipsed Model upon Partial Removal of Mesitylene. <i>Journal of Physical Chemistry C</i> , 2014, 118, 399-407.	3.1	32
2804	Accurate Determination of the Orientational Distribution of a Fluorescent Molecule in a Phospholipid Membrane. <i>Journal of Physical Chemistry B</i> , 2014, 118, 855-863.	2.6	30
2805	Effect of PEGylation on Drug Entry into Lipid Bilayer. <i>Journal of Physical Chemistry B</i> , 2014, 118, 144-151.	2.6	26
2806	Comprehensive portrait of cholesterol containing oxidized membrane. <i>Biochimica Et Biophysica Acta - Biomembranes</i> , 2014, 1838, 1769-1776.	2.6	17
2807	Local fivefold symmetry in liquid and undercooled Ni probed by x-ray absorption spectroscopy and computer simulations. <i>Physical Review B</i> , 2014, 89, .	3.2	37
2808	Molecular dynamics study of HIV-1 RT-DNA-nevirapine complexes explains NNRTI inhibition and resistance by connection mutations. <i>Proteins: Structure, Function and Bioinformatics</i> , 2014, 82, 815-829.	2.6	15
2809	Encapsulation of sodium radio-iodide in fullerene C60. <i>Journal of Molecular Modeling</i> , 2014, 20, 2130.	1.8	4
2810	How well does cholesteryl hemisuccinate mimic cholesterol in saturated phospholipid bilayers?. <i>Journal of Molecular Modeling</i> , 2014, 20, 2121.	1.8	44
2811	Mechanistic insights into mode of actions of novel oligopeptidase B inhibitors for combating leishmaniasis. <i>Journal of Molecular Modeling</i> , 2014, 20, 2099.	1.8	17
2812	Homology modeling and virtual screening for antagonists of protease from yellow head virus. <i>Journal of Molecular Modeling</i> , 2014, 20, 2116.	1.8	4
2813	The gamma-butyrolactone receptors BulR1 and BulR2 of <i>Streptomyces tsukubaensis</i> : tacrolimus (FK506) and butyrolactone synthetases production control. <i>Applied Microbiology and Biotechnology</i> , 2014, 98, 4919-4936.	3.6	40
2814	Steered molecular dynamics identifies critical residues of the Nodamura virus B2 suppressor of RNAi. <i>Journal of Molecular Modeling</i> , 2014, 20, 2092.	1.8	11
2815	The archetype-genome exemplar in molecular dynamics and continuum mechanics. <i>Computational Mechanics</i> , 2014, 53, 687-737.	4.0	16
2816	Insights into the conformational perturbations of novel agonists with $\beta_3$ -adrenergic receptor using molecular dynamics simulations. <i>Biochimie</i> , 2014, 101, 168-182.	2.6	4

#	ARTICLE	IF	CITATIONS
2817	Theoretical Considerations and Computational Tools. <i>Advances in Experimental Medicine and Biology</i> , 2014, 794, 69-93.	1.6	0
2818	How to link pyrene to its host lipid to minimize the extent of membrane perturbations and to optimize pyrene dimer formation. <i>Chemistry and Physics of Lipids</i> , 2014, 177, 19-25.	3.2	7
2819	Combined Monte Carlo and molecular dynamics simulation of methane adsorption on dry and moist coal. <i>Fuel</i> , 2014, 122, 186-197.	6.4	195
2820	Plasticity and conformational equilibria of influenza fusion peptides in model lipid bilayers. <i>Biochimica Et Biophysica Acta - Biomembranes</i> , 2014, 1838, 1169-1179.	2.6	10
2821	Fast, metadynamicsâ€‘based method for prediction of the stereochemistryâ€‘dependent relative free energies of ligandâ€‘receptor interactions. <i>Journal of Computational Chemistry</i> , 2014, 35, 876-882.	3.3	10
2822	Photochemical Reaction Mechanism of UV-B-Induced Monomerization of UVR8 Dimers as the First Signaling Event in UV-B-Regulated Gene Expression in Plants. <i>Journal of Physical Chemistry B</i> , 2014, 118, 951-965.	2.6	27
2823	The molecular structure of a phosphatidylserine bilayer determined by scattering and molecular dynamics simulations. <i>Soft Matter</i> , 2014, 10, 3716.	2.7	84
2824	A new method for characterizing the interphase regions of carbon nanotube composites. <i>International Journal of Solids and Structures</i> , 2014, 51, 1781-1791.	2.7	73
2825	Combined molecular docking, molecular dynamics simulation and quantitative structureâ€‘activity relationship study of pyrimido[1,2-c][1,3]benzothiazin-6-imine derivatives as potent anti-HIV drugs. <i>Journal of Molecular Structure</i> , 2014, 1067, 1-13.	3.6	7
2826	Generic force fields for ionic liquids. <i>Journal of Molecular Liquids</i> , 2014, 192, 32-37.	4.9	32
2827	Simulations of monomeric amyloid Î²-peptide (1â€‘40) with varying solution conditions and oxidation state of Met35: Implications for aggregation. <i>Archives of Biochemistry and Biophysics</i> , 2014, 545, 44-52.	3.0	33
2828	Perspective: Crystal structure prediction at high pressures. <i>Journal of Chemical Physics</i> , 2014, 140, 040901.	3.0	135
2829	Stable Polyglutamine Dimers Can Contain Î²-Hairpins with Interdigitated Side Chainsâ€‘But Not Î±-Helices, Î²-Nanotubes, Î²-Pseudohelices, or Steric Zippers. <i>Biophysical Journal</i> , 2014, 106, 1721-1728.	0.5	9
2830	Adhesive characteristics of low dimensional carbon nanomaterial on actin. <i>Applied Physics Letters</i> , 2014, 104, .	3.3	14
2831	Path-integral simulation of solids. <i>Journal of Physics Condensed Matter</i> , 2014, 26, 233201.	1.8	47
2832	Fully atomistic molecularâ€‘mechanical model of liquid alkane oils: Computational validation. <i>Journal of Computational Chemistry</i> , 2014, 35, 776-788.	3.3	6
2833	The alloying element dependence of the local lattice deformation and the elastic properties of Ni3Al: A molecular dynamics simulation. <i>Journal of Applied Physics</i> , 2014, 115, .	2.5	19
2834	Studies of (â€‘)-Pironetin Binding to Î±-Tubulin: Conformation, Docking, and Molecular Dynamics. <i>Journal of Organic Chemistry</i> , 2014, 79, 3752-3764.	3.2	20

#	ARTICLE	IF	CITATIONS
2835	Vapor Pressures and Heats of Sublimation of Crystalline Î²-Cellobiose from Classical Molecular Dynamics Simulations with Quantum Mechanical Corrections. <i>Journal of Physical Chemistry B</i> , 2014, 118, 5365-5373.	2.6	13
2836	Computationally Efficient Prediction of Ionic Liquid Properties. <i>Journal of Physical Chemistry Letters</i> , 2014, 5, 1973-1977.	4.6	16
2837	Drug promiscuity of P-glycoprotein and its mechanism of interaction with paclitaxel and doxorubicin. <i>Soft Matter</i> , 2014, 10, 438-445.	2.7	36
2838	Imidazolium Ionic Liquid Helps to Disperse Fullerenes in Water. <i>Journal of Physical Chemistry Letters</i> , 2014, 5, 1795-1800.	4.6	38
2839	Molecular Dynamics Investigation on the Aggregation of Violanthrone78-Based Model Asphaltenes in Toluene. <i>Energy &amp; Fuels</i> , 2014, 28, 3604-3613.	5.1	79
2840	Ion Transport through a Water-Organic Solvent Liquid-Liquid Interface: A Simulation Study. <i>Journal of Physical Chemistry B</i> , 2014, 118, 5957-5970.	2.6	14
2841	Exploring the free energy landscape of a model Î²-hairpin peptide and its isoform. <i>Proteins: Structure, Function and Bioinformatics</i> , 2014, 82, 2394-2402.	2.6	2
2842	Study of Orientation and Penetration of LAH4 into Lipid Bilayer Membranes: pH and Composition Dependence. <i>Chemical Biology and Drug Design</i> , 2014, 84, 242-252.	3.2	10
2843	In silico identification of novel kinase inhibitors targeting wild-type and T315I mutant ABL1 from FDA-approved drugs. <i>Molecular BioSystems</i> , 2014, 10, 1524.	2.9	22
2844	Size-Selective, Noncovalent Dispersion of Carbon Nanotubes by PEGylated Lipids: A Coarse-Grained Molecular Dynamics Study. <i>Journal of Chemical &amp; Engineering Data</i> , 2014, 59, 3080-3089.	1.9	23
2845	Flexible Gates Generate Occluded Intermediates in the Transport Cycle of LacY. <i>Journal of Molecular Biology</i> , 2014, 426, 735-751.	4.2	70
2846	Quantifying Artifacts in Ewald Simulations of Inhomogeneous Systems with a Net Charge. <i>Journal of Chemical Theory and Computation</i> , 2014, 10, 381-390.	5.3	176
2847	G Protein-Coupled Receptors - Modeling and Simulation. <i>Advances in Experimental Medicine and Biology</i> , 2014, , .	1.6	7
2848	Atomistic Simulations of Poly(ethylene oxide) in Water and an Ionic Liquid at Room Temperature. <i>Macromolecules</i> , 2014, 47, 438-446.	4.8	50
2849	Going Backward: A Flexible Geometric Approach to Reverse Transformation from Coarse Grained to Atomistic Models. <i>Journal of Chemical Theory and Computation</i> , 2014, 10, 676-690.	5.3	566
2850	A stochastic thermostat algorithm for coarse-grained thermomechanical modeling of large-scale soft matters: Theory and application to microfilaments. <i>Journal of Computational Physics</i> , 2014, 263, 177-184.	3.8	1
2851	Dynamic structure of unentangled polymer chains in the vicinity of non-attractive nanoparticles. <i>Soft Matter</i> , 2014, 10, 1723.	2.7	73
2852	Synthesis and characterisation of new MO(OH) <sub>2</sub> (M = Zr, Hf) oxyhydroxides and related Li <sub>2</sub> MO <sub>3</sub> salts. <i>Dalton Transactions</i> , 2014, 43, 2755-2763.	3.3	12



#	ARTICLE	IF	CITATIONS
2853	Exploring binding properties of naringenin with bovine $\beta$ -lactoglobulin: A fluorescence, molecular docking and molecular dynamics simulation study. <i>Biophysical Chemistry</i> , 2014, 187-188, 33-42.	2.8	45
2854	Coarse-grained versus atomistic simulations: realistic interaction free energies for real proteins. <i>Bioinformatics</i> , 2014, 30, 326-334.	4.1	40
2855	Primary and Secondary Dimer Interfaces of the Fibroblast Growth Factor Receptor 3 Transmembrane Domain: Characterization via Multiscale Molecular Dynamics Simulations. <i>Biochemistry</i> , 2014, 53, 323-332.	2.5	24
2856	Solvation of Lithium Salts in Protic Ionic Liquids: A Molecular Dynamics Study. <i>Journal of Physical Chemistry B</i> , 2014, 118, 761-770.	2.6	87
2857	X-ray structure, thermodynamics, elastic properties and MD simulations of cardiolipin/dimyristoylphosphatidylcholine mixed membranes. <i>Chemistry and Physics of Lipids</i> , 2014, 178, 1-10.	3.2	42
2858	Genetic and structural characterization of PvSERA4: potential implication as therapeutic target for <i>Plasmodium vivax</i> malaria. <i>Journal of Biomolecular Structure and Dynamics</i> , 2014, 32, 580-590.	3.5	7
2859	Molecular dynamics studies on the structures of polymer electrolyte membranes and diffusion mechanism of protons and small molecules. <i>Polymer</i> , 2014, 55, 6309-6319.	3.8	22
2860	Hydration Control of the Mechanical and Dynamical Properties of Cellulose. <i>Biomacromolecules</i> , 2014, 15, 4152-4159.	5.4	44
2861	The structure of interfacial water on gold electrodes studied by x-ray absorption spectroscopy. <i>Science</i> , 2014, 346, 831-834.	12.6	391
2862	Peptide Backbone Effect on Hydration Free Energies of Amino Acid Side Chains. <i>Journal of Physical Chemistry B</i> , 2014, 118, 13162-13168.	2.6	11
2863	Diabatic Population Matrix Formalism for Performing Molecular Mechanics Style Simulations with Multiple Electronic States. <i>Journal of Chemical Theory and Computation</i> , 2014, 10, 5238-5253.	5.3	9
2864	Molecular Dynamics Simulations of Plastic Damage in Metals. , 2014, , 1-30.		1
2865	Structural basis of thymosin- $\beta$ 4/profilin exchange leading to actin filament polymerization. <i>Proceedings of the National Academy of Sciences of the United States of America</i> , 2014, 111, E4596-605.	7.1	68
2866	Different aggregation dynamics of benzene-water mixtures. <i>Physical Chemistry Chemical Physics</i> , 2014, 16, 21957-21963.	2.8	7
2867	Quantum Mechanics/Molecular Mechanics Modeling of Photoelectron Spectra: The Carbon 1s Core-Electron Binding Energies of Ethanol-Water Solutions. <i>Journal of Physical Chemistry B</i> , 2014, 118, 13217-13225.	2.6	14
2868	Testing the inter-operability of the CHARMM and SPC/Fw force fields for conformational sampling. <i>Molecular Simulation</i> , 2014, 40, 912-921.	2.0	6
2869	Anomalies in bulk supercooled water at negative pressure. <i>Proceedings of the National Academy of Sciences of the United States of America</i> , 2014, 111, 7936-7941.	7.1	103
2870	Intrinsic $\alpha$ -helical and $\beta$ -sheet conformational preferences: A computational case study of alanine. <i>Protein Science</i> , 2014, 23, 970-980.	7.6	18



#	ARTICLE	IF	CITATIONS
2871	Simulation of high-density water: Its glass transition for various water models. <i>Journal of Chemical Physics</i> , 2014, 140, 134504.	3.0	5
2872	Molecular simulation of Tyr105 phosphorylated pyruvate kinase M2 to understand its structure and dynamics. <i>Journal of Molecular Modeling</i> , 2014, 20, 2447.	1.8	8
2873	Endohedral confinement of a DNA dodecamer onto pristine carbon nanotubes and the stability of the canonical B form. <i>Journal of Chemical Physics</i> , 2014, 140, 225103.	3.0	17
2874	Interatomic potential to predict the glass-forming ability of Ni–Nb–Mo ternary alloys. <i>Journal of Materials Science</i> , 2014, 49, 7263-7272.	3.7	4
2875	Effect of Including Torsional Parameters for Histidine–Metal Interactions in Classical Force Fields for Metalloproteins. <i>Journal of Physical Chemistry B</i> , 2014, 118, 13106-13111.	2.6	13
2876	Toward a Materials Genome Approach for Ionic Liquids: Synthesis Guided by Ab Initio Property Maps. <i>Journal of Physical Chemistry B</i> , 2014, 118, 13609-13620.	2.6	19
2877	Induced Ice Melting by the Snow Flea Antifreeze Protein from Molecular Dynamics Simulations. <i>Journal of Physical Chemistry B</i> , 2014, 118, 13527-13534.	2.6	17
2878	Molecular Dynamics Simulation on Nucleation of Ammonium Perchlorate from an Aqueous Solution. <i>Crystal Growth and Design</i> , 2014, 14, 5897-5903.	3.0	18
2879	Infinitely Dilute Partial Molar Properties of Proteins from Computer Simulation. <i>Journal of Physical Chemistry B</i> , 2014, 118, 12844-12854.	2.6	11
2880	Suppression of sub-surface freezing in free-standing thin films of a coarse-grained model of water. <i>Physical Chemistry Chemical Physics</i> , 2014, 16, 25916-25927.	2.8	65
2881	Accelerating the Conformational Sampling of Intrinsically Disordered Proteins. <i>Journal of Chemical Theory and Computation</i> , 2014, 10, 5081-5094.	5.3	38
2882	Bicontinuity and Multiple Length Scale Ordering in Triphasic Hydrogen-Bonding Ionic Liquids. <i>Journal of Physical Chemistry B</i> , 2014, 118, 12706-12716.	2.6	69
2883	Protein modeling and molecular dynamics simulation of the two novel surfactant proteins SP-G and SP-H. <i>Journal of Molecular Modeling</i> , 2014, 20, 2513.	1.8	16
2884	The scaled-charge additive force field for amino acid based ionic liquids. <i>Chemical Physics Letters</i> , 2014, 616-617, 205-211.	2.6	41
2885	Molecular Dynamics Simulations of Complex Mixtures Aimed at the Preparation of Naproxen-Imprinted Xerogels. <i>Journal of Chemical Information and Modeling</i> , 2014, 54, 3330-3343.	5.4	6
2886	Viscosity of Nafion Oligomers as a Function of Hydration and Counterion Type: A Molecular Dynamics Study. <i>Journal of Physical Chemistry B</i> , 2014, 118, 13981-13991.	2.6	11
2887	Atomistic amorphous/crystalline interface modelling for superlattices and core/shell nanowires. <i>Journal of Physics Condensed Matter</i> , 2014, 26, 055011.	1.8	30
2888	Disorder in Cholesterol-Binding Functionality of CRAC Peptides: A Molecular Dynamics Study. <i>Journal of Physical Chemistry B</i> , 2014, 118, 13169-13174.	2.6	31

#	ARTICLE	IF	CITATIONS
2889	Designing and understanding permanent microporosity in liquids. <i>Physical Chemistry Chemical Physics</i> , 2014, 16, 9422-9431.	2.8	80
2890	Spontaneous dimer states of the A <sup>21</sup> decapeptide. <i>Physical Chemistry Chemical Physics</i> , 2014, 16, 13069-13073.	2.8	7
2891	Surface Energetics of the Hydroxyapatite Nanocrystal-Water Interface: A Molecular Dynamics Study. <i>Langmuir</i> , 2014, 30, 13283-13292.	3.5	56
2892	Molecular Origin of the Self-Assembled Morphological Difference Caused by Varying the Order of Charged Residues in Short Peptides. <i>Journal of Physical Chemistry B</i> , 2014, 118, 12501-12510.	2.6	24
2893	Molecular interactions of ethylcellulose with sucrose particles. <i>RSC Advances</i> , 2014, 4, 55048-55061.	3.6	35
2894	Characterizing protein crystal contacts and their role in crystallization: rubredoxin as a case study. <i>Soft Matter</i> , 2014, 10, 290-302.	2.7	48
2895	Nucleation free-energy barriers with Hybrid Monte-Carlo/Umbrella Sampling. <i>Physical Chemistry Chemical Physics</i> , 2014, 16, 24913-24919.	2.8	13
2896	Selective G-quadruplex stabilizers: Schiff-base metal complexes with anticancer activity. <i>RSC Advances</i> , 2014, 4, 33245-33256.	3.6	78
2897	Insights into ordered microstructures and ordering mechanisms of ABC star terpolymers by integrating dynamic self-consistent field theory and variable cell shape methods. <i>Soft Matter</i> , 2014, 10, 5916-5927.	2.7	10
2898	Atomistic Molecular-Dynamics Simulations Enable Prediction of the Arginine Permeation Pathway through OccD1/OprD from <i>Pseudomonas Aeruginosa</i> . <i>Biophysical Journal</i> , 2014, 107, 1853-1861.	0.5	23
2899	Molecular Dynamics Study of Surfactant-Like Peptide Based Nanostructures. <i>Journal of Physical Chemistry B</i> , 2014, 118, 12215-12222.	2.6	49
2900	Thermodynamics of Antimicrobial Lipopeptide Binding to Membranes: Origins of Affinity and Selectivity. <i>Biophysical Journal</i> , 2014, 107, 1862-1872.	0.5	31
2901	Improved Coarse-Grained Modeling of Cholesterol-Containing Lipid Bilayers. <i>Journal of Chemical Theory and Computation</i> , 2014, 10, 2137-2150.	5.3	48
2902	A Highly Viscous Imidazolium Ionic Liquid inside Carbon Nanotubes. <i>Journal of Physical Chemistry B</i> , 2014, 118, 6234-6240.	2.6	50
2903	Modeling and simulation of the water gradient within a Nafion membrane. <i>Physical Chemistry Chemical Physics</i> , 2014, 16, 3173.	2.8	19
2904	Diversity of transition pathways in the course of crystallization into ice VII. <i>Physical Chemistry Chemical Physics</i> , 2014, 16, 16419-16425.	2.8	25
2905	Finite element models and molecular dynamic simulations for studying the response of mast cell under mechanical activation. <i>Science Bulletin</i> , 2014, 59, 3562-3572.	1.7	0
2906	Structural states of the flexible catalytic loop of <i>M. tuberculosis</i> tyrosyl-tRNA synthetase in different enzyme-substrate complexes. <i>European Biophysics Journal</i> , 2014, 43, 613-622.	2.2	8

#	ARTICLE	IF	CITATIONS
2907	Amphiphilic interactions of ionic liquids with lipid biomembranes: a molecular simulation study. <i>Soft Matter</i> , 2014, 10, 8641-8651.	2.7	116
2908	Molecular Mechanism of Viral Resistance to a Potent Non-nucleoside Inhibitor Unveiled by Molecular Simulations. <i>Biochemistry</i> , 2014, 53, 6941-6953.	2.5	33
2909	Graphyne as the membrane for water desalination. <i>Nanoscale</i> , 2014, 6, 1865-1870.	5.6	230
2910	Molecular Dynamics Simulations Identify Time Scale of Conformational Changes Responsible for Conformational Selection in Molecular Recognition of HIV-1 Transactivation Responsive RNA. <i>Journal of the American Chemical Society</i> , 2014, 136, 15631-15637.	13.7	35
2911	A mechanical nanogate based on a carbon nanotube for reversible control of ion conduction. <i>Nanoscale</i> , 2014, 6, 3686-3694.	5.6	22
2912	The dynamics of the conformational changes in the hexopyranose ring: a transition path sampling approach. <i>RSC Advances</i> , 2014, 4, 25028-25039.	3.6	17
2913	Exploring the Local Elastic Properties of Bilayer Membranes Using Molecular Dynamics Simulations. <i>Journal of Physical Chemistry B</i> , 2014, 118, 12883-12891.	2.6	9
2914	Free energy landscapes of the encapsulation mechanism of DNA nucleobases onto carbon nanotubes. <i>RSC Advances</i> , 2014, 4, 1310-1321.	3.6	15
2915	Multiscale simulation of surfactantâ€œaquaporin complex formation and water permeability. <i>RSC Advances</i> , 2014, 4, 37592-37599.	3.6	6
2916	Binding Difference of Fipronil with GABA <sub>A</sub> Rs in Fruitfly and Zebrafish: Insights from Homology Modeling, Docking, and Molecular Dynamics Simulation Studies. <i>Journal of Agricultural and Food Chemistry</i> , 2014, 62, 10646-10653.	5.2	35
2917	Study on the agonists for the human Toll-like receptor-8 by molecular modeling. <i>Molecular BioSystems</i> , 2014, 10, 2202.	2.9	4
2918	Design of coordination polymers with 4-â€²-substituted functionalized terpyridyls in the backbone and pendent cyclopentadienyliron moieties. <i>Polymer Chemistry</i> , 2014, 5, 3453-3465.	3.9	23
2919	Assessing the hydration free energy of a homologous series of polyols with classical and quantum mechanical solvation models. <i>Physical Chemistry Chemical Physics</i> , 2014, 16, 17863-17868.	2.8	2
2920	Reaction mechanism and free energy profile for acylation of <i>Candida Antarctica</i> lipase B with methylcaprylate and acetylcholine: Density functional theory calculations. <i>Journal of Molecular Graphics and Modelling</i> , 2014, 54, 131-140.	2.4	10
2921	Molecular Mechanism of Na <sup>+</sup> ,K <sup>+</sup> -ATPase Malfunction in Mutations Characteristic of Adrenal Hypertension. <i>Biochemistry</i> , 2014, 53, 746-754.	2.5	23
2922	COFFDROP: A Coarse-Grained Nonbonded Force Field for Proteins Derived from All-Atom Explicit-Solvent Molecular Dynamics Simulations of Amino Acids. <i>Journal of Chemical Theory and Computation</i> , 2014, 10, 5178-5194.	5.3	16
2923	Atomistic Force Field for Pyridinium-Based Ionic Liquids: Reliable Transport Properties. <i>Journal of Physical Chemistry B</i> , 2014, 118, 10716-10724.	2.6	50
2924	Local Structures of Methanolâ€œWater Binary Solutions Studied by Soft X-ray Absorption Spectroscopy. <i>Journal of Physical Chemistry B</i> , 2014, 118, 4388-4396.	2.6	81

#	ARTICLE	IF	CITATIONS
2925	Molecular Dynamics Study of the Diffusivity of a Hydrophobic Drug Cucurbitacin B in Pseudo-poly(ethylene oxide-b-caprolactone) Micelle Environments. <i>Langmuir</i> , 2014, 30, 7798-7803.	3.5	11
2926	Single Water Entropy: Hydrophobic Crossover and Application to Drug Binding. <i>Journal of Physical Chemistry B</i> , 2014, 118, 10553-10564.	2.6	22
2927	Carbon Dioxide Hydrate Phase Equilibrium and Cage Occupancy Calculations Using <i>Ab Initio</i> Intermolecular Potentials. <i>Journal of Physical Chemistry B</i> , 2014, 118, 577-589.	2.6	39
2928	Dynamic heterogeneity controls diffusion and viscosity near biological interfaces. <i>Nature Communications</i> , 2014, 5, 3034.	12.8	58
2929	Single Lipid Extraction: The Anchoring Strength of Cholesterol in Liquid-Ordered and Liquid-Disordered Phases. <i>Biophysical Journal</i> , 2014, 107, 1167-1175.	0.5	26
2930	Energetics of Hydrophilic Protein-Protein Association and the Role of Water. <i>Journal of Chemical Theory and Computation</i> , 2014, 10, 3512-3524.	5.3	27
2931	Self-Assembly of Calcium Carbonate Nanoparticles in Water and Hydrophobic Solvents. <i>Journal of Physical Chemistry C</i> , 2014, 118, 21092-21103.	3.1	7
2932	Interface-Limited Growth of Heterogeneously Nucleated Ice in Supercooled Water. <i>Journal of Physical Chemistry B</i> , 2014, 118, 752-760.	2.6	29
2933	Small molecule-mediated control of hydroxyapatite growth: Free energy calculations benchmarked to density functional theory. <i>Journal of Computational Chemistry</i> , 2014, 35, 70-81.	3.3	42
2934	Lipid Organization of the Plasma Membrane. <i>Journal of the American Chemical Society</i> , 2014, 136, 14554-14559.	13.7	734
2935	Hopping-Mediated Anion Transport through a Mannitol-Based Rosette Ion Channel. <i>Journal of the American Chemical Society</i> , 2014, 136, 14128-14135.	13.7	89
2936	Benchmarking of Force Fields for Molecule-Membrane Interactions. <i>Journal of Chemical Theory and Computation</i> , 2014, 10, 4143-4151.	5.3	73
2937	Solubilization in Mixed Micelles Studied by Molecular Dynamics Simulations and COSMOmic. <i>Journal of Physical Chemistry B</i> , 2014, 118, 3593-3604.	2.6	32
2938	Interfacial Thermodynamics of Water and Six Other Liquid Solvents. <i>Journal of Physical Chemistry B</i> , 2014, 118, 5943-5956.	2.6	32
2939	Development of a highly potent anti-angiogenic <i>VEGF</i> <sub>8</sub> heterodimer by directed blocking of its <i>VEGFR</i> binding site. <i>FEBS Journal</i> , 2014, 281, 4479-4494.	4.7	18
2940	Dynamic Structure of NGF and proNGF Complexed with p75NTR: Pro-Peptide Effect. <i>Journal of Chemical Information and Modeling</i> , 2014, 54, 2051-2067.	5.4	4
2941	Accelerating All-Atom MD Simulations of Lipids Using a Modified Virtual-Sites Technique. <i>Journal of Chemical Theory and Computation</i> , 2014, 10, 5690-5695.	5.3	34
2942	Relationship between Nonlinear Pressure-Induced Chemical Shift Changes and Thermodynamic Parameters. <i>Journal of Physical Chemistry B</i> , 2014, 118, 5681-5690.	2.6	20

#	ARTICLE	IF	CITATIONS
2943	Sensitivity of Water Dynamics to Biologically Significant Surfaces of Monomeric Insulin: Role of Topology and Electrostatic Interactions. <i>Journal of Physical Chemistry B</i> , 2014, 118, 3805-3813.	2.6	30
2944	CO <sub>2</sub> Diffusion in Champagne Wines: A Molecular Dynamics Study. <i>Journal of Physical Chemistry B</i> , 2014, 118, 1839-1847.	2.6	20
2945	Modulation of Dipalmitoylphosphatidylcholine Monolayers by Dimethyl Sulfoxide. <i>Langmuir</i> , 2014, 30, 8803-8811.	3.5	29
2946	Electroporation of Asymmetric Phospholipid Membranes. <i>Journal of Physical Chemistry B</i> , 2014, 118, 9909-9918.	2.6	45
2947	Solvent Polarity Considerations Are Unable to Describe Fullerene Solvation Behavior. <i>Journal of Physical Chemistry B</i> , 2014, 118, 3378-3384.	2.6	25
2948	Can xenon in water inhibit ice growth? Molecular dynamics of phase transitions in waterâ€“Xe system. <i>Journal of Chemical Physics</i> , 2014, 141, 034503.	3.0	13
2949	Polystyrene Nanoparticles Perturb Lipid Membranes. <i>Journal of Physical Chemistry Letters</i> , 2014, 5, 241-246.	4.6	266
2950	Computational Approaches Elucidate the Allosteric Mechanism of Human Aromatase Inhibition: A Novel Possible Route to Small-Molecule Regulation of CYP450s Activities?. <i>Journal of Chemical Information and Modeling</i> , 2014, 54, 2856-2868.	5.4	41
2951	Improving <i>Trichoderma reesei</i> Cel7B Thermostability by Targeting the Weak Spots. <i>Journal of Chemical Information and Modeling</i> , 2014, 54, 2826-2833.	5.4	19
2952	Structure-Based Drug Design of Diphenyl Î±-Aminoalkylphosphonates as Prostate-Specific Antigen Antagonists. <i>Journal of Chemical Information and Modeling</i> , 2014, 54, 2967-2979.	5.4	5
2953	Atomistic Description of Fullerene-Based Membranes. <i>Journal of Physical Chemistry B</i> , 2014, 118, 12471-12477.	2.6	6
2954	Solvation free energies in [bmim]-based ionic liquids: Anion effect toward solvation of amino acid side chain analogues. <i>Chemical Physics Letters</i> , 2014, 615, 69-74.	2.6	11
2955	Dissipative Particle Dynamics with an Effective Pair Potential from Integral Equation Theory of Molecular Liquids. <i>Journal of Physical Chemistry B</i> , 2014, 118, 12034-12049.	2.6	9
2956	Molecular dynamics simulations of strain-controlled fatigue behaviour of amorphous polyethylene. <i>Journal of Polymer Research</i> , 2014, 21, 1.	2.4	10
2957	Dissolution study of active pharmaceutical ingredients using molecular dynamics simulations with classical force fields. <i>Journal of Crystal Growth</i> , 2014, 405, 122-130.	1.5	22
2958	Data Filtering for Effective Analysis of Crystalâ€“Solution Interface Molecular Dynamics Simulations. <i>Journal of Chemical Theory and Computation</i> , 2014, 10, 1686-1697.	5.3	8
2959	Importance of Force Decomposition for Local Stress Calculations in Biomembrane Molecular Simulations. <i>Journal of Chemical Theory and Computation</i> , 2014, 10, 691-702.	5.3	124
2960	Extended Narrowâ€“Bandgap Diketopyrrolopyrrole-Based Oligomers for Solutionâ€“Processed Inverted Organic Solar Cells. <i>Advanced Energy Materials</i> , 2014, 4, 1400879.	19.5	47

#	ARTICLE	IF	CITATIONS
2961	One-Dimensional Self-Assembly of Polyaromatic Compounds Revealed by Molecular Dynamics Simulations. <i>Journal of Physical Chemistry B</i> , 2014, 118, 12772-12780.	2.6	45
2962	Molecular Recognition of Platinated DNA from Chromosomal HMGB1. <i>Journal of Chemical Theory and Computation</i> , 2014, 10, 3578-3584.	5.3	12
2963	Molecular Basis of the Mechanical Hierarchy in Myomesin Dimers for Sarcomere Integrity. <i>Biophysical Journal</i> , 2014, 107, 965-973.	0.5	17
2964	Adsorption, Mobility, and Self-Association of Naphthalene and 1-Methylnaphthalene at the Water–Vapor Interface. <i>Journal of Physical Chemistry A</i> , 2014, 118, 1052-1066.	2.5	21
2965	Automated Optimization of Water–Water Interaction Parameters for a Coarse-Grained Model. <i>Journal of Physical Chemistry B</i> , 2014, 118, 1603-1611.	2.6	17
2966	Comparative Study of Protein Unfolding in Aqueous Urea and Dimethyl Sulfoxide Solutions: Surface Polarity, Solvent Specificity, and Sequence of Secondary Structure Melting. <i>Journal of Physical Chemistry B</i> , 2014, 118, 5691-5697.	2.6	42
2967	Atomistic mechanisms of huntingtin N-terminal fragment insertion on a phospholipid bilayer revealed by molecular dynamics simulations. <i>Proteins: Structure, Function and Bioinformatics</i> , 2014, 82, 1409-1427.	2.6	16
2968	Structural Insights into Trapping and Dissociation of Small Molecules in $K^{+}$ Channels. <i>Journal of Chemical Information and Modeling</i> , 2014, 54, 3218-3228.	5.4	6
2969	Impact of Ionic Liquids in Aqueous Solution on Bacterial Plasma Membranes Studied with Molecular Dynamics Simulations. <i>Journal of Physical Chemistry B</i> , 2014, 118, 10444-10459.	2.6	67
2970	Favored Composition Design and Atomic Structure Characterization for Ternary Al–Cu–Y Metallic Glasses via Proposed Interatomic Potential. <i>Journal of Physical Chemistry B</i> , 2014, 118, 4442-4449.	2.6	16
2971	Layer-by-Layer Formation of Oligoelectrolyte Multilayers: A Combined Experimental and Computational Study. <i>Soft Materials</i> , 2014, 12, S14-S21.	1.7	13
2972	Deviatoric Stress-Driven Fusion of Nanoparticle Superlattices. <i>Nano Letters</i> , 2014, 14, 4951-4958.	9.1	37
2973	Assembly and stability of Salmonella enterica ser. Typhi TolC protein in POPE and DMPE. <i>Journal of Biological Physics</i> , 2014, 40, 387-400.	1.5	4
2974	The NorM MATE Transporter from <i>N. gonorrhoeae</i> : Insights into Drug and Ion Binding from Atomistic Molecular Dynamics Simulations. <i>Biophysical Journal</i> , 2014, 107, 460-468.	0.5	20
2975	Direct Osmolyte–Macromolecule Interactions Confer Entropic Stability to Folded States. <i>Journal of Physical Chemistry B</i> , 2014, 118, 7327-7334.	2.6	87
2976	Interactions of Phosphatase and Tensin Homologue (PTEN) Proteins with Phosphatidylinositol Phosphates: Insights from Molecular Dynamics Simulations of PTEN and Voltage Sensitive Phosphatase. <i>Biochemistry</i> , 2014, 53, 1724-1732.	2.5	42
2977	Electrostatic Potential within the Free Volume Space of Imidazole-Based Solvents: Insights into Gas Absorption Selectivity. <i>Journal of Physical Chemistry B</i> , 2014, 118, 255-264.	2.6	26
2978	Molecular Description of Surfactant-like Peptide Based Membranes. <i>Journal of Physical Chemistry C</i> , 2014, 118, 9598-9603.	3.1	29



#	ARTICLE	IF	CITATIONS
2979	Methyl-methoxypyrrolinone and flavinium nucleus binding signatures on falcipain-2 active site. <i>Journal of Molecular Modeling</i> , 2014, 20, 2386.	1.8	15
2980	Insight into HIV-1 reverse transcriptaseâ€‘aptamer interaction from molecular dynamics simulations. <i>Journal of Molecular Modeling</i> , 2014, 20, 2380.	1.8	12
2981	Parallel Optimization of a Reactive Force Field for Polycondensation of Alkoxysilanes. <i>Journal of Physical Chemistry B</i> , 2014, 118, 10966-10978.	2.6	37
2982	Molecular Dynamics Simulation of Inverse-Phosphocholine Lipids. <i>Journal of Physical Chemistry C</i> , 2014, 118, 19444-19449.	3.1	14
2983	Urea Induced Unfolding Dynamics of Flavin Adenine Dinucleotide (FAD): Spectroscopic and Molecular Dynamics Simulation Studies from Femto-Second to Nanosecond Regime. <i>Journal of Physical Chemistry B</i> , 2014, 118, 1881-1890.	2.6	14
2984	Initial Partition and Aggregation of Uncharged Polyaromatic Molecules at the Oilâ€‘Water Interface: A Molecular Dynamics Simulation Study. <i>Journal of Physical Chemistry B</i> , 2014, 118, 1040-1051.	2.6	76
2985	Novel Human Butyrylcholinesterase Variants: Toward Organophosphonate Detoxication. <i>Biochemistry</i> , 2014, 53, 4476-4487.	2.5	9
2986	Dehydroergosterol as an Analogue for Cholesterol: Why It Mimics Cholesterol So Wellâ€‘or Does It?. <i>Journal of Physical Chemistry B</i> , 2014, 118, 7345-7357.	2.6	31
2987	Equation of state, elastic constants, and melting curve of solid neon using an effective two-body potential including quantum corrections. <i>Fluid Phase Equilibria</i> , 2014, 379, 167-174.	2.5	6
2988	Octapeptide-based affinity chromatography of human immunoglobulin G: Comparisons of three different ligands. <i>Journal of Chromatography A</i> , 2014, 1359, 100-111.	3.7	26
2989	Molecular Monte Carlo Simulation Method of Systems Connected to Three Reservoirs. <i>Journal of the Physical Society of Japan</i> , 2014, 83, 054003.	1.6	0
2990	Binding mode analysis of a major <i>Pseudomonas aeruginosa</i> translocator protein <i>PopB</i> with its chaperone <i>PcrH</i> from <i>Pseudomonas aeruginosa</i> . <i>Proteins: Structure, Function and Bioinformatics</i> , 2014, 82, 3273-3285.	2.6	4
2991	Accurate Description of Calcium Solvation in Concentrated Aqueous Solutions. <i>Journal of Physical Chemistry B</i> , 2014, 118, 7902-7909.	2.6	125
2992	Transferability of Coarse-Grained Force Field for <i>nCB</i> Liquid Crystal Systems. <i>Journal of Physical Chemistry B</i> , 2014, 118, 4647-4660.	2.6	23
2993	Molecular Dynamics Simulations of Self-Emulsifying Drug-Delivery Systems (SEDDS): Influence of Excipients on Droplet Nanostructure and Drug Localization. <i>Langmuir</i> , 2014, 30, 8471-8480.	3.5	40
2994	Ligandâ€‘Receptor Affinities Computed by an Adapted Linear Interaction Model for Continuum Electrostatics and by Protein Conformational Averaging. <i>Journal of Chemical Information and Modeling</i> , 2014, 54, 2309-2319.	5.4	17
2995	Identification of Allosteric Disulfides from Prestress Analysis. <i>Biophysical Journal</i> , 2014, 107, 672-681.	0.5	36
2996	Probing carbon nanotubeâ€‘amino acid interactions in aqueous solution with molecular dynamics simulations. <i>Carbon</i> , 2014, 78, 500-509.	10.3	78



#	ARTICLE	IF	CITATIONS
2997	A Method to Predict Blood-Brain Barrier Permeability of Drug-Like Compounds Using Molecular Dynamics Simulations. Biophysical Journal, 2014, 107, 630-641.	0.5	202
2998	Nanoscale Carbon Greatly Enhances Mobility of a Highly Viscous Ionic Liquid. ACS Nano, 2014, 8, 8190-8197.	14.6	65
2999	Ionic liquid confined in silica nanopores: molecular dynamics in the isobaric-isothermal ensemble. Molecular Physics, 2014, 112, 1350-1361.	1.7	71
3000	Isomerization of $\hat{5}$ -Androstene-3,17-dione into $\hat{4}$ -Androstene-3,17-dione Catalyzed by Human Glutathione Transferase A3-3: A Computational Study Identifies a Dual Role for Glutathione. Journal of Physical Chemistry A, 2014, 118, 5790-5800.	2.5	14
3001	Molecular View of Polymer/Water Interfaces in Latex Paint. Macromolecules, 2014, 47, 6441-6452.	4.8	18
3002	Computational study on ice growth inhibition of Antarctic bacterium antifreeze protein using coarse grained simulation. Journal of Chemical Physics, 2014, 140, 225101.	3.0	9
3003	Molecular Dynamics Simulations of the Ionic Liquid 1- <i>n</i> -Butyl-3-Methylimidazolium Chloride and Its Binary Mixtures with Ethanol. Journal of Chemical Theory and Computation, 2014, 10, 4465-4479.	5.3	50
3004	Acceleration of Lateral Equilibration in Mixed Lipid Bilayers Using Replica Exchange with Solute Tempering. Journal of Chemical Theory and Computation, 2014, 10, 4264-4272.	5.3	38
3005	Analytical Bond-Order Potential for the Cd-Te-Se Ternary System. Journal of Physical Chemistry C, 2014, 118, 20661-20679.	3.1	13
3006	Dynamics of the $\hat{1}$ and $\hat{2}$ Polymorphs of <i>N</i> -Norleucine at Different Temperatures: Sliding to a Partial Phase Transition. Crystal Growth and Design, 2014, 14, 3343-3351.	3.0	10
3007	Aneesur Rahman. Resonance, 2014, 19, 671-683.	0.3	0
3008	Effective interactions in molecular dynamics simulations of lysozyme solutions. European Physical Journal B, 2014, 87, 1.	1.5	3
3009	From Side Chains Rattling on Picoseconds to Ensemble Simulations of Protein Folding. Israel Journal of Chemistry, 2014, 54, 1274-1285.	2.3	0
3010	Substrate Channel in Nitrogenase Revealed by a Molecular Dynamics Approach. Biochemistry, 2014, 53, 2278-2285.	2.5	28
3011	Molecular dynamics study of the conformation and dynamics of precisely branched polyethylene. Polymer, 2014, 55, 5734-5738.	3.8	9
3012	Determining Structural and Mechanical Properties from Molecular Dynamics Simulations of Lipid Vesicles. Journal of Chemical Theory and Computation, 2014, 10, 4160-4168.	5.3	25
3013	Prediction of the structure of a silk-like protein in oligomeric states using explicit and implicit solvent models. Soft Matter, 2014, 10, 5362.	2.7	11
3014	Molecular Dynamics Simulation of Aqueous Urea Solution: Is Urea a Structure Breaker?. Journal of Physical Chemistry B, 2014, 118, 11757-11768.	2.6	103

#	ARTICLE	IF	CITATIONS
3015	Extension and validation of the GROMOS 53A6 <sub>glyc</sub> parameter set for glycoproteins. Journal of Computational Chemistry, 2014, 35, 2087-2095.	3.3	42
3016	Complex Roles of Hybrid Lipids in the Composition, Order, and Size of Lipid Membrane Domains. Langmuir, 2014, 30, 1361-1369.	3.5	30
3017	Structure of the Neisserial Outer Membrane Protein Opa <sub>60</sub> : Loop Flexibility Essential to Receptor Recognition and Bacterial Engulfment. Journal of the American Chemical Society, 2014, 136, 9938-9946.	13.7	52
3018	Analysis of the Structural and Functional Roles of Coupling Helices in the ATP-Binding Cassette Transporter MsbA through Enzyme Assays and Molecular Dynamics Simulations. Biochemistry, 2014, 53, 4261-4272.	2.5	20
3019	New Insights into the Thermal Stability of the Smectic C Phase. Journal of Physical Chemistry B, 2014, 118, 4037-4043.	2.6	8
3020	Effect of arginine-rich cell penetrating peptides on membrane pore formation and life-times: a molecular simulation study. Physical Chemistry Chemical Physics, 2014, 16, 20785-20795.	2.8	53
3021	Influence of metal ions (Zn <sup>2+</sup> , Cu <sup>2+</sup> , Ca <sup>2+</sup> , Mg <sup>2+</sup> and Tj ETQq0 0 0 rgBT /Overlock Advances, 2014, 4, 49040-49052.	3.6	12
3022	Interdomain communication in the endonuclease/motor subunit of type I restriction-modification enzyme EcoR124I. Journal of Molecular Modeling, 2014, 20, 2334.	1.8	6
3023	Molecular dynamics simulation of dissociation behavior of various crystalline celluloses treated with hot-compressed water. Cellulose, 2014, 21, 3203-3215.	4.9	13
3024	Structural Determinants in Prion Protein Folding and Stability. Journal of Molecular Biology, 2014, 426, 3796-3810.	4.2	28
3025	Dimerization of the EphA1 Receptor Tyrosine Kinase Transmembrane Domain: Insights into the Mechanism of Receptor Activation. Biochemistry, 2014, 53, 6641-6652.	2.5	43
3026	Modest Influence of FRET Chromophores on the Properties of Unfolded Proteins. Biophysical Journal, 2014, 107, 1654-1660.	0.5	29
3027	V-type nerve agents phosphorylate ubiquitin at biologically relevant lysine residues and induce intramolecular cyclization by an isopeptide bond. Analytical and Bioanalytical Chemistry, 2014, 406, 5171-5185.	3.7	33
3028	Evaluation of active designs of cephalosporin C acylase by molecular dynamics simulation and molecular docking. Journal of Molecular Modeling, 2014, 20, 2314.	1.8	11
3029	Chemotherapy efficiency increase via shock wave interaction with biological membranes: a molecular dynamics study. Microfluidics and Nanofluidics, 2014, 16, 613-622.	2.2	12
3030	ZIBgridfree: efficient conformational analysis by partition-of-unity coupling. Journal of Mathematical Chemistry, 2014, 52, 781-804.	1.5	5
3031	Does the Like Dissolves Like Rule Hold for Fullerene and Ionic Liquids?. Journal of Solution Chemistry, 2014, 43, 1019-1031.	1.2	40
3032	Orientalational glass in mixtures of elliptic and circular particles: Structural heterogeneities, rotational dynamics, and rheology. Physical Review E, 2014, 89, 022308.	2.1	9

#	ARTICLE	IF	CITATIONS
3033	Mechanism of the pH-Controlled Self-Assembly of Nanofibers from Peptide Amphiphiles. <i>Journal of Physical Chemistry C</i> , 2014, 118, 16272-16278.	3.1	52
3034	Discerning intersecting fusion–activation pathways in the Nipah virus using machine learning. <i>Proteins: Structure, Function and Bioinformatics</i> , 2014, 82, 3241-3254.	2.6	7
3035	Ermol: Fast and versatile computation software for solvation free energy with approximate theory of solutions. <i>Journal of Computational Chemistry</i> , 2014, 35, 1592-1608.	3.3	58
3036	WATsite: Hydration site prediction program with PyMOL interface. <i>Journal of Computational Chemistry</i> , 2014, 35, 1255-1260.	3.3	60
3037	Transmembrane Permeation Mechanism of Charged Methyl Guanidine. <i>Journal of Chemical Theory and Computation</i> , 2014, 10, 1717-1726.	5.3	29
3038	Modeling Cell Membrane Perturbation by Molecules Designed for Transmembrane Electron Transfer. <i>Langmuir</i> , 2014, 30, 2429-2440.	3.5	55
3039	Molecular dynamics simulation study of glass transition in hydrated Nafion. <i>Journal of Polymer Science, Part B: Polymer Physics</i> , 2014, 52, 907-915.	2.1	26
3040	Melatonin directly interacts with cholesterol and alleviates cholesterol effects in dipalmitoylphosphatidylcholine monolayers. <i>Soft Matter</i> , 2014, 10, 206-213.	2.7	47
3041	Protein–Ligand Docking Using Hamiltonian Replica Exchange Simulations with Soft Core Potentials. <i>Journal of Chemical Information and Modeling</i> , 2014, 54, 1669-1675.	5.4	32
3042	Exploring the Conformational Dynamics of Alanine Dipeptide in Solution Subjected to an External Electric Field: A Nonequilibrium Molecular Dynamics Simulation. <i>Journal of Chemical Theory and Computation</i> , 2014, 10, 1376-1386.	5.3	17
3043	Investigation of crack tip dislocation emission in aluminum using multiscale molecular dynamics simulation and continuum modeling. <i>Journal of the Mechanics and Physics of Solids</i> , 2014, 65, 35-53.	4.8	57
3044	Direct Evaluation of Polypeptide Partial Molar Volumes in Water Using Molecular Dynamics Simulations. <i>Journal of Chemical &amp; Engineering Data</i> , 2014, 59, 3130-3135.	1.9	8
3045	On the Hofmeister Effect: Fluctuations at the Protein–Water Interface and the Surface Tension. <i>Journal of Physical Chemistry B</i> , 2014, 118, 8496-8504.	2.6	22
3046	Possible Dynamically Gated Conductance along Heme Wires in Bacterial Multiheme Cytochromes. <i>Journal of Physical Chemistry B</i> , 2014, 118, 8505-8512.	2.6	1
3047	A Fixed-Charge Model for Alcohol Polarization in the Condensed Phase, and Its Role in Small Molecule Hydration. <i>Journal of Physical Chemistry B</i> , 2014, 118, 6438-6446.	2.6	54
3048	Copper-transporting P-type ATPases use a unique ion-release pathway. <i>Nature Structural and Molecular Biology</i> , 2014, 21, 43-48.	8.2	98
3049	Cholesterol-Induced Condensing and Disordering Effects on a Rigid Catanionic Bilayer: A Molecular Dynamics Study. <i>Langmuir</i> , 2014, 30, 55-62.	3.5	27
3050	1,3,5-Tris(4-bromophenyl)benzene prenucleation clusters from metadynamics. <i>Acta Crystallographica Section C, Structural Chemistry</i> , 2014, 70, 132-136.	0.5	21

#	ARTICLE	IF	CITATIONS
3051	Thermal activation analysis of enthalpic and entropic contributions to the activation free energy of basal and prismatic slips in Mg. <i>Physical Review B</i> , 2014, 89, .	3.2	11
3052	Mutagenesis and molecular dynamics simulations revealed the chitooligosaccharide entry and exit points for chitinase D from <i>Serratia proteamaculans</i> . <i>Biochimica Et Biophysica Acta - General Subjects</i> , 2014, 1840, 2685-2694.	2.4	14
3053	MDcons: Intermolecular contact maps as a tool to analyze the interface of protein complexes from molecular dynamics trajectories. <i>BMC Bioinformatics</i> , 2014, 15, S1.	2.6	29
3054	Historical contingency and its biophysical basis in glucocorticoid receptor evolution. <i>Nature</i> , 2014, 512, 203-207.	27.8	132
3055	Molecular dynamics study of mixed alkanethiols covering a gold surface at three different arrangements. <i>Chemical Physics Letters</i> , 2014, 600, 79-86.	2.6	13
3056	Molecular dynamics study on the interaction between doxorubicin and hydrophobically modified chitosan oligosaccharide. <i>RSC Advances</i> , 2014, 4, 23730-23739.	3.6	29
3057	Deformation-induced structural transition in body-centred cubic molybdenum. <i>Nature Communications</i> , 2014, 5, 3433.	12.8	95
3058	Molecular Dynamics Simulation of PEGylated Membranes with Cholesterol: Building Toward the DOXIL Formulation. <i>Journal of Physical Chemistry C</i> , 2014, 118, 15541-15549.	3.1	25
3059	Ferroelectric hexagonal and rhombic monolayer ice phases. <i>Chemical Science</i> , 2014, 5, 1757-1764.	7.4	94
3060	Computer Simulation Study of the Structure of LiCl Aqueous Solutions: Test of Non-Standard Mixing Rules in the Ion Interaction. <i>Journal of Physical Chemistry B</i> , 2014, 118, 7680-7691.	2.6	36
3061	Modeling the Interaction of Interferon $\hat{1}\pm$ -1b to Bovine Serum Albumin as a Drug Delivery System. <i>Journal of Physical Chemistry B</i> , 2014, 118, 8566-8574.	2.6	8
3062	Analysis of Factors Influencing Hydration Site Prediction Based on Molecular Dynamics Simulations. <i>Journal of Chemical Information and Modeling</i> , 2014, 54, 2987-2995.	5.4	15
3063	Polyelectrolyte Decomplexation via Addition of Salt: Charge Correlation Driven Zipper. <i>Journal of Physical Chemistry B</i> , 2014, 118, 3226-3234.	2.6	35
3064	Surface Adsorption and Bulk Aggregation of Cyclodextrins by Computational Molecular Dynamics Simulations as a Function of Temperature: $\hat{1}\pm$ -CD vs $\hat{1}^2$ -CD. <i>Journal of Physical Chemistry B</i> , 2014, 118, 6999-7011.	2.6	38
3065	Comparative study on structure, energetic and mechanical properties of a $\hat{1}\mu$ -CL-20/HMX cocrystal and its composite with molecular dynamics simulation. <i>Journal of Materials Chemistry A</i> , 2014, 2, 13898.	10.3	94
3066	A Cooperative Mechanism of Clotrimazoles in P450 Revealed by the Dissociation Picture of Clotrimazole from P450. <i>Journal of Chemical Information and Modeling</i> , 2014, 54, 1218-1225.	5.4	6
3067	Refined OPLS All-Atom Force Field for Saturated Phosphatidylcholine Bilayers at Full Hydration. <i>Journal of Physical Chemistry B</i> , 2014, 118, 4571-4581.	2.6	139
3068	Molecular Dynamics Simulations of Turbostratic Dry and Hydrated Montmorillonite with Intercalated Carbon Dioxide. <i>Journal of Physical Chemistry A</i> , 2014, 118, 7454-7468.	2.5	28

#	ARTICLE	IF	CITATIONS
3069	Quantum molecular dynamics simulations of liquid benzene using orbital optimization. Theoretical Chemistry Accounts, 2014, 133, 1.	1.4	2
3070	Fluctuating micro-heterogeneity in water-tert-butyl alcohol mixtures and lambda-type divergence of the mean cluster size with phase transition-like multiple anomalies. Journal of Chemical Physics, 2014, 140, 194502.	3.0	49
3071	Ab initio Kinetic Monte Carlo simulations of dissolution at the NaCl-water interface. Physical Chemistry Chemical Physics, 2014, 16, 22545-22554.	2.8	30
3072	Spectroscopic Properties of Benzene at the Air-Ice Interface: A Combined Experimental-Computational Approach. Journal of Physical Chemistry A, 2014, 118, 7535-7547.	2.5	27
3073	Intrinsic Autocorrelation Time of Picoseconds for Thermal Noise in Water. Journal of Physical Chemistry A, 2014, 118, 8936-8941.	2.5	9
3074	Looking at Human Cytosolic Sialidase NEU2 Structural Features with an Interdisciplinary Approach. Biochemistry, 2014, 53, 5343-5355.	2.5	3
3075	Effect of fullerene surface chemistry on nanoparticle binding-induced protein misfolding. Nanoscale, 2014, 6, 8340-8349.	5.6	41
3076	Interactions of a Water-Soluble Fullerene Derivative with Amyloid- $\beta$ Protofibrils: Dynamics, Binding Mechanism, and the Resulting Salt-Bridge Disruption. Journal of Physical Chemistry B, 2014, 118, 6733-6741.	2.6	50
3077	Diffusion Coefficients of Fluorinated Surfactants in Water: Experimental Results and Prediction by Computer Simulation. Journal of Chemical & Engineering Data, 2014, 59, 3151-3159.	1.9	31
3078	Multiple Scale Dynamics in Proteins Probed at Multiple Time Scales through Fluctuations of NMR Chemical Shifts. Journal of Physical Chemistry B, 2014, 118, 3823-3831.	2.6	7
3079	Molecular dynamics study of the volumetric and hydrophobic properties of the amphiphilic molecule C8E6. Journal of Molecular Liquids, 2014, 189, 74-80.	4.9	44
3080	Evidence for the Interactions Occurring Between Ionic Liquids and Tetraethylene Glycol in Binary Mixtures and Aqueous Biphasic Systems. Journal of Physical Chemistry B, 2014, 118, 4615-4629.	2.6	18
3081	Can pyrene probes be used to measure lateral pressure profiles of lipid membranes? Perspective through atomistic simulations. Biochimica Et Biophysica Acta - Biomembranes, 2014, 1838, 1406-1411.	2.6	16
3082	Molecular dynamics simulations of lipid membranes with lateral force: Rupture and dynamic properties. Biochimica Et Biophysica Acta - Biomembranes, 2014, 1838, 994-1002.	2.6	30
3083	Galectin-3 Interactions with Glycosphingolipids. Journal of Molecular Biology, 2014, 426, 1439-1451.	4.2	65
3084	Role of atomic variability and mechanical constraints on the martensitic phase transformation of a model disordered shape memory alloy via molecular dynamics. Acta Materialia, 2014, 69, 30-36.	7.9	19
3085	Interactions of beta-blockers with model lipid membranes: Molecular view of the interaction of acebutolol, oxprenolol, and propranolol with phosphatidylcholine vesicles by time-dependent fluorescence shift and molecular dynamics simulations. European Journal of Pharmaceutics and Biopharmaceutics, 2014, 87, 559-569.	4.3	28
3086	Molecular simulation of adsorption of hydrophobin HFBI to the air-water, DPPC-water and decane-water interfaces. Food Hydrocolloids, 2014, 42, 66-74.	10.7	16

#	ARTICLE	IF	CITATIONS
3087	Studying structure–property relationships in oligomeric engineering thermoplastics by controlled preparation of low molecular weight polymers. <i>Reactive and Functional Polymers</i> , 2014, 81, 22-32.	4.1	2
3088	Elastic Properties of Swelling Clay Particles at Finite Temperature upon Hydration. <i>Journal of Physical Chemistry C</i> , 2014, 118, 8933-8943.	3.1	83
3089	Electric-Field-Induced Phase Transition of Confined Water Nanofilms between Two Graphene Sheets. <i>Journal of Physical Chemistry A</i> , 2014, 118, 8922-8928.	2.5	16
3090	Ebolavirus Entry Requires a Compact Hydrophobic Fist at the Tip of the Fusion Loop. <i>Journal of Virology</i> , 2014, 88, 6636-6649.	3.4	44
3091	Free Energy of PAMAM Dendrimer Adsorption onto Model Biological Membranes. <i>Journal of Physical Chemistry B</i> , 2014, 118, 6792-6802.	2.6	19
3092	Molecular Dynamics Simulation of Oxygen Ion Diffusion in Ytria Stabilized Zirconia Single Crystals and Bicrystals. <i>Fuel Cells</i> , 2014, 14, 574-580.	2.4	24
3093	Dispersion of Carbon Nanotubes Using Mixed Surfactants: Experimental and Molecular Dynamics Simulation Studies. <i>Journal of Physical Chemistry B</i> , 2014, 118, 3094-3103.	2.6	79
3094	Rotation Triggers Nucleotide-Independent Conformational Transition of the Empty $\hat{F}_1$ Subunit of $F_1F_0$ -ATPase. <i>Journal of the American Chemical Society</i> , 2014, 136, 6960-6968.	13.7	25
3095	Atomistic Simulations of Properties and Phenomena at High Temperatures. , 2014, , 287-393.		2
3096	Choice of the center of water molecules in calculations of partial molar volume of single ions immersed in water: A molecular simulation study. <i>Journal of Molecular Liquids</i> , 2014, 200, 67-71.	4.9	1
3097	Porphyrin–phospholipid liposomes permeabilized by near-infrared light. <i>Nature Communications</i> , 2014, 5, 3546.	12.8	282
3098	Efficient Characterization of Protein Cavities within Molecular Simulation Trajectories: $\langle i \rangle_{trj\_cavity} \langle /i \rangle$ . <i>Journal of Chemical Theory and Computation</i> , 2014, 10, 2151-2164.	5.3	129
3099	Variable-cell method for stress-controlled jamming of athermal, frictionless grains. <i>Physical Review E</i> , 2014, 89, 042203.	2.1	30
3100	Computational Study of the Stability of the Miniprotein Trp-Cage, the GB1 $\hat{F}_2$ -Hairpin, and the AK16 Peptide, under Negative Pressure. <i>Journal of Physical Chemistry B</i> , 2014, 118, 7761-7769.	2.6	37
3101	Structure and Supersaturation of Highly Concentrated Solutions of Buckyball in 1-Butyl-3-Methylimidazolium Tetrafluoroborate. <i>Journal of Physical Chemistry B</i> , 2014, 118, 7376-7382.	2.6	12
3102	Molecular Dynamics Simulations of the Adenosine A2a Receptor in POPC and POPE Lipid Bilayers: Effects of Membrane on Protein Behavior. <i>Journal of Chemical Information and Modeling</i> , 2014, 54, 573-581.	5.4	33
3103	Efficient Method To Characterize the Context-Dependent Hydrophobicity of Proteins. <i>Journal of Physical Chemistry B</i> , 2014, 118, 1564-1573.	2.6	75
3104	Insights into the role of cyclic ladderane lipids in bacteria from computer simulations. <i>Chemistry and Physics of Lipids</i> , 2014, 181, 76-82.	3.2	9



#	ARTICLE	IF	CITATIONS
3105	Rate-Dependent Behavior of the Amorphous Phase of Spider Dragline Silk. Biophysical Journal, 2014, 106, 2511-2518.	0.5	26
3106	Insights into proteinâ€™TNS (2-p-toluidinylnaphthalene-6-sulfonate) interaction using molecular dynamics simulation. Journal of Molecular Structure, 2014, 1068, 261-269.	3.6	4
3107	3D Hydrophobic Moment Vectors as a Tool to Characterize the Surface Polarity of Amphiphilic Peptides. Biophysical Journal, 2014, 106, 2385-2394.	0.5	61
3108	Reprint of â€œRole of the fluidity of a liquid phase in determining the surface properties of the opposite phaseâ€• Journal of Molecular Liquids, 2014, 189, 122-128.	4.9	2
3109	The structure of the CD31 transmembrane dimer in lipid bilayers. Biochimica Et Biophysica Acta - Biomembranes, 2014, 1838, 739-746.	2.6	5
3110	Insight into the binding mode and the structural features of the pyrimidine derivatives as human A2A adenosine receptor antagonists. BioSystems, 2014, 115, 13-22.	2.0	12
3111	Plastic strain localization in metals: origins and consequences. Progress in Materials Science, 2014, 59, 1-160.	32.8	340
3112	Profiling the Interaction Mechanism of Quinoline/Quinazoline Derivatives as MCHR1 Antagonists: An in Silico Method. International Journal of Molecular Sciences, 2014, 15, 15475-15502.	4.1	9
3113	Spatial-decomposition analysis of electrical conductivity in ionic liquid. Journal of Chemical Physics, 2014, 141, 244507.	3.0	14
3114	ABSINTH Implicit Solvation Model and Force Field Paradigm for Use in Simulations of Intrinsically Disordered Proteins. , 2014, , 208-231.		0
3115	Lipid-associated aggregate formation of superoxide dismutase-1 is initiated by membrane-targeting loops. Proteins: Structure, Function and Bioinformatics, 2014, 82, 3194-3209.	2.6	10
3116	Dyes in Liquid Crystals: Experimental and Computational Studies of a Guestâ€™Host System Based on a Combined DFT and MD Approach. Chemistry - A European Journal, 2015, 21, 10123-10130.	3.3	36
3117	Stability analysis of the martensitic phase transformation in<mml:math xmlns:mml="http://www.w3.org/1998/Math/MathML"><mml:mrow><mml:msub><mml:mi>Co</mml:mi><mml:mns>2</mml:mns></mml:msub></mml:mrow></mml:math> alloy. Physical Review B, 2015, 92, .	3.2	34
3118	Development and application of a Ni-Ti interatomic potential with high predictive accuracy of the martensitic phase transition. Physical Review B, 2015, 92, .	3.2	187
3119	Universal enthalpy-entropy compensation rule for the deformation of metallic glasses. Physical Review B, 2015, 92, .	3.2	19
3120	Negative thermal expansion of<mml:math xmlns:mml="http://www.w3.org/1998/Math/MathML"><mml:msub><mml:mi>ScF</mml:mi><mml:mns>3</mml:mns></mml:msub></mml:math> Insights from density-functional molecular dynamics in the isothermal-isobaric ensemble. Physical Review B. 2015, 92, .	3.2	34
3121	Molecular dynamics study of rhodamine 6G diffusion at<mml:math xmlns:mml="http://www.w3.org/1998/Math/MathML"><mml:mi>n</mml:mi></mml:math>-decaneâ€™water interfaces. Physical Review E, 2015, 91, 053308.	2.1	13
3122	Protein-fluctuation-induced water-pore formation in ion channel voltage-sensor translocation across a lipid bilayer membrane. Physical Review E, 2015, 92, 052719.	2.1	3



#	ARTICLE	IF	CITATIONS
3123	Stretched Exponential Relaxation of Glasses at Low Temperature. <i>Physical Review Letters</i> , 2015, 115, 165901.	7.8	53
3124	Generalized ensemble method applied to study systems with strong first order transitions. <i>Journal of Physics: Conference Series</i> , 2015, 640, 012003.	0.4	2
3125	Hidden scale invariance of metals. <i>Physical Review B</i> , 2015, 92, .	3.2	36
3126	Motional displacements in proteins: The origin of wave-vector-dependent values. <i>Physical Review E</i> , 2015, 91, 052705.	2.1	12
3127	Atomistic structure of a PAN-based carbon fibre constructed by molecular dynamics simulations and lifetime measurement of positron annihilation. <i>International Journal of Sustainable Aviation</i> , 2015, 1, 269.	0.2	2
3128	Origin of the structure-directing effect resulting in identical topological open-framework materials. <i>Scientific Reports</i> , 2015, 5, 14940.	3.3	14
3129	Modelling heat conduction in polycrystalline hexagonal boron-nitride films. <i>Scientific Reports</i> , 2015, 5, 13228.	3.3	104
3130	Melting point trends and solid phase behaviors of model salts with ion size asymmetry and distributed cation charge. <i>Journal of Chemical Physics</i> , 2015, 143, 024508.	3.0	20
3131	The Widom line and dynamical crossover in supercritical water: Popular water models versus experiments. <i>Journal of Chemical Physics</i> , 2015, 143, 114502.	3.0	35
3132	Transition fields in organic materials: From percolation to inverted Marcus regime. A consistent Monte Carlo simulation in disordered PPV. <i>Journal of Chemical Physics</i> , 2015, 142, 094503.	3.0	14
3133	The C-terminal region of the non-structural protein 2B from Hepatitis A Virus demonstrates lipid-specific viroporin-like activity. <i>Scientific Reports</i> , 2015, 5, 15884.	3.3	19
3134	Pairwise-additive force fields for selected aqueous monovalent ions from adaptive force matching. <i>Journal of Chemical Physics</i> , 2015, 143, 194505.	3.0	38
3135	A computer simulation approach to quantify the $\langle i \rangle_{true}$ area and $\langle i \rangle_{true}$ area compressibility modulus of biological membranes. <i>Journal of Chemical Physics</i> , 2015, 143, 034706.	3.0	31
3136	Mass dependence of the activation enthalpy and entropy of unentangled linear alkane chains. <i>Journal of Chemical Physics</i> , 2015, 143, 144905.	3.0	47
3137	Strong influence of periodic boundary conditions on lateral diffusion in lipid bilayer membranes. <i>Journal of Chemical Physics</i> , 2015, 143, 243113.	3.0	70
3138	Composition dependent multiple structural transformations of myoglobin in aqueous ethanol solution: A combined experimental and theoretical study. <i>Journal of Chemical Physics</i> , 2015, 143, 015103.	3.0	16
3139	Self-sorting heterodimeric coiled coil peptides with defined and tuneable self-assembly properties. <i>Scientific Reports</i> , 2015, 5, 14063.	3.3	54
3140	Energetics of Endotoxin Recognition in the Toll-Like Receptor 4 Innate Immune Response. <i>Scientific Reports</i> , 2015, 5, 17997.	3.3	25

#	ARTICLE	IF	CITATIONS
3141	In silico mechanistic analysis of IRF3 inactivation and high-risk HPV E6 species-dependent drug response. Scientific Reports, 2015, 5, 13446.	3.3	33
3142	Molecular dynamics simulations of cholesterol-rich membranes using a coarse-grained force field for cyclic alkanes. Journal of Chemical Physics, 2015, 143, 243144.	3.0	55
3143	Nested sampling of isobaric phase space for the direct evaluation of the isothermal-isobaric partition function of atomic systems. Journal of Chemical Physics, 2015, 143, 154108.	3.0	8
3144	Remarkably stable amorphous metal oxide grown on Zr-Cu-Be metallic glass. Scientific Reports, 2015, 5, 18196.	3.3	16
3145	Ionic liquid induced dehydration and domain closure in lysozyme: FCS and MD simulation. Journal of Chemical Physics, 2015, 143, 125103.	3.0	38
3146	Mode coupling theory analysis of electrolyte solutions: Time dependent diffusion, intermediate scattering function, and ion solvation dynamics. Journal of Chemical Physics, 2015, 142, 124502.	3.0	9
3147	Improving the description of interactions between $\text{Ca}^{2+}$ and protein carboxylate groups, including $^{13}\text{C}$ -carboxylglutamic acid: revised CHARMM22* parameters. RSC Advances, 2015, 5, 67820-67828.	3.6	14
3148	Reducing the cost of evaluating the committor by a fitting procedure. Journal of Chemical Physics, 2015, 143, 174103.	3.0	14
3149	A molecular dynamics simulations study on the relations between dynamical heterogeneity, structural relaxation, and self-diffusion in viscous liquids. Journal of Chemical Physics, 2015, 143, 164502.	3.0	38
3150	Phosphatidylcholine reverse micelles on the wrong track in molecular dynamics simulations of phospholipids in an organic solvent. Journal of Chemical Physics, 2015, 142, 094902.	3.0	25
3151	Molecular dynamics simulations of the structure and single-particle dynamics of mixtures of divalent salts and ionic liquids. Journal of Chemical Physics, 2015, 143, 124507.	3.0	17
3152	Competition between ices Ih and Ic in homogeneous water freezing. Journal of Chemical Physics, 2015, 143, 134504.	3.0	65
3153	Ionic liquids—Conventional solvent mixtures, structurally different but dynamically similar. Journal of Chemical Physics, 2015, 143, 134505.	3.0	33
3154	Machine learning of single molecule free energy surfaces and the impact of chemistry and environment upon structure and dynamics. Journal of Chemical Physics, 2015, 142, 105101.	3.0	34
3155	Parameters for Martini sterols and hopanoids based on a virtual-site description. Journal of Chemical Physics, 2015, 143, 243152.	3.0	125
3156	Hydrogen bond network in the hydration layer of the water confined in nanotubes increasing the dielectric constant parallel along the nanotube axis. Journal of Chemical Physics, 2015, 143, 114708.	3.0	14
3157	Shearing of the CENP-A dimerization interface mediates plasticity in the octameric centromeric nucleosome. Scientific Reports, 2015, 5, 17038.	3.3	35
3158	Insights into the species-specific TLR4 signaling mechanism in response to Rhodobacter sphaeroides lipid A detection. Scientific Reports, 2015, 5, 7657.	3.3	44

#	ARTICLE	IF	CITATIONS
3159	Intrinsic Localized Modes in Proteins. Scientific Reports, 2015, 5, 18128.	3.3	11
3160	Diffusivity and short-time dynamics in two models of silica. Journal of Chemical Physics, 2015, 142, 104506.	3.0	18
3161	A classical force field for tetrahedral oxyanions developed using hydration properties: The examples of pertechnetate (TcO <sub>4</sub> <sup>2-</sup> ) and sulfate (SO <sub>4</sub> <sup>2-</sup> ). Journal of Chemical Physics, 2015, 143, 174502.	3.0	24
3162	DNA sequencing with MspA: Molecular Dynamics simulations reveal free-energy differences between sequencing and non-sequencing mutants. Scientific Reports, 2015, 5, 12783.	3.3	6
3163	Force-Sensitive Autoinhibition of the von Willebrand Factor Is Mediated by Interdomain Interactions. Biophysical Journal, 2015, 108, 2312-2321.	0.5	64
3164	A computer model of a polyunsaturated monogalactolipid bilayer. Biochimie, 2015, 118, 129-140.	2.6	15
3165	Pore-Filling Nature of CH <sub>4</sub> Adsorption Behavior in Kerogen Nanopores: A Molecular View Based on Full-Atom Kerogen Models. , 2015, , .		9
3166	Ion assisted structural collapse of a single stranded DNA: A molecular dynamics approach. Chemical Physics, 2015, 459, 137-147.	1.9	22
3167	Molecular simulations study of novel 1,4-dihydropyridines derivatives with a high selectivity for $\text{Ca}^{2+}$ calcium channel. Protein Science, 2015, 24, 1737-1747.	7.6	9
3168	The anisotropic character of Snoek relaxation in Fe <sub>1-x</sub> C system: A kinetic Monte Carlo and molecular dynamics simulation. Physica Status Solidi (B): Basic Research, 2015, 252, 1382-1387.	1.5	3
3169	Self-Assembled Peptide-Polyfluorene Nanocomposites for Biodegradable Organic Electronics. Advanced Materials Interfaces, 2015, 2, 1500265.	3.7	35
3170	Three-dimensional structure model and predicted ATP interaction rewiring of a deviant RNA ligase 2. BMC Structural Biology, 2015, 15, 20.	2.3	4
3171	Non-Ideal Behaviour and Solution Interactions in Binary DMSO Solutions. ChemPhysChem, 2015, 16, 3814-3823.	2.1	6
3172	Effect of Cholesterol on Ethanol-Induced Disruption of a $\text{POPC}$ Bilayer: A Molecular Dynamics Simulation Study. Bulletin of the Korean Chemical Society, 2015, 36, 2569-2572.	1.9	2
3173	Transient Interactions of a Cytosolic Protein with Macromolecular and Vesicular Cosolutes: Unspecific and Specific Effects. ChemBioChem, 2015, 16, 2633-2645.	2.6	10
3174	Increased Microbial Butanol Tolerance by Exogenous Membrane Insertion Molecules. ChemSusChem, 2015, 8, 3718-3726.	6.8	19
3175	Analysis of water channels by molecular dynamics simulation of heterotetrameric sarcosine oxidase. Biophysics and Physicobiology, 2015, 12, 131-138.	1.0	4
3176	Intermolecular-Interaction and Mechanical Properties of MNs-Plasticizer Modified 2,4,6-Trinitrotoluene/1,3,5-Trinitrohexahydro-1,3,5-Triazine Molten-Energetic-Composite(MEC). Key Engineering Materials, 2015, 645-646, 252-258.	0.4	1

#	ARTICLE	IF	CITATIONS
3177	Structural, elastic, and electronic properties of sodium atoms encapsulated type-I silicon clathrate compound under high pressure. Chinese Physics B, 2015, 24, 107101.	1.4	2
3178	Integrating Pharmacophore into Membrane Molecular Dynamics Simulations to Improve Homology Modeling of $G$ Protein-coupled Receptors with Ligand Selectivity: $A_{2A}$ Adenosine Receptor as an Example. Chemical Biology and Drug Design, 2015, 86, 1438-1450.	3.2	7
3179	The Dependence of Amyloid $\beta$ Dynamics on Protein Force Fields and Water Models. ChemPhysChem, 2015, 16, 3278-3289.	2.1	103
3180	A Study of the Solvation Structure of $L$ -Leucine in Alcohol-Water Binary Solvents through Molecular Dynamics Simulations and FTIR and NMR Spectroscopy. ChemPhysChem, 2015, 16, 3190-3199.	2.1	9
3181	Enhanced stability of the model mini-protein in amino acid ionic liquids and their aqueous solutions. Journal of Computational Chemistry, 2015, 36, 2044-2051.	3.3	35
3182	Effect of single point mutations in a form of systemic amyloidosis. Protein Science, 2015, 24, 1451-1462.	7.6	8
3183	Effect of intrinsic and extrinsic factors on the simulated D-band length of type I collagen. Proteins: Structure, Function and Bioinformatics, 2015, 83, 1800-1812.	2.6	20
3184	$\Delta$ 1-25-Derived Sphingolipid-Domain Tracer Peptide SBD Interacts with Membrane Ganglioside Clusters via a Coil-Helix-Coil Motif. International Journal of Molecular Sciences, 2015, 16, 26318-26332.	4.1	3
3185	Aqueous Molecular Dynamics Simulations of the M. tuberculosis Enoyl-ACP Reductase-NADH System and Its Complex with a Substrate Mimic or Diphenyl Ethers Inhibitors. International Journal of Molecular Sciences, 2015, 16, 23695-23722.	4.1	15
3186	Palate Lung Nasal Clone (PLUNC), a Novel Protein of the Tear Film: Three-Dimensional Structure, Immune Activation, and Involvement in Dry Eye Disease (DED). , 2015, 56, 7312.		13
3187	Penetration of HIV-1 Tat47-57 into PC/PE Bilayers Assessed by MD Simulation and X-ray Scattering. Membranes, 2015, 5, 473-494.	3.0	11
3188	3D Modeling of Dengue Virus NS4B and Chikungunya Virus nsP4: Identification of a Common Drug Target and Designing a Single Antiviral Inhibitor. Current Computer-Aided Drug Design, 2015, 10, 361-373.	1.2	5
3189	Assembly of Influenza Hemagglutinin Fusion Peptides in a Phospholipid Bilayer by Coarse-grained Computer Simulations. Frontiers in Molecular Biosciences, 2015, 2, 66.	3.5	8
3190	Identification of the antiepileptic racetam binding site in the synaptic vesicle protein 2A by molecular dynamics and docking simulations. Frontiers in Cellular Neuroscience, 2015, 9, 125.	3.7	29
3191	Structure, Dynamics, and Interaction of Mycobacterium tuberculosis (Mtb) DprE1 and DprE2 Examined by Molecular Modeling, Simulation, and Electrostatic Studies. PLoS ONE, 2015, 10, e0119771.	2.5	38
3192	Binding of the Antagonist Caffeine to the Human Adenosine Receptor hA2AR in Nearly Physiological Conditions. PLoS ONE, 2015, 10, e0126833.	2.5	12
3193	Structural Determinants for the Binding of Morphinan Agonists to the $\mu$ -Opioid Receptor. PLoS ONE, 2015, 10, e0135998.	2.5	20
3194	A Jump-from-Cavity Pyrophosphate Ion Release Assisted by a Key Lysine Residue in T7 RNA Polymerase Transcription Elongation. PLoS Computational Biology, 2015, 11, e1004624.	3.2	31

#	ARTICLE	IF	CITATIONS
3195	Dynamics of the Glycophorin A Dimer in Membranes of Native-Like Composition Uncovered by Coarse-Grained Molecular Dynamics Simulations. PLoS ONE, 2015, 10, e0133999.	2.5	19
3196	Insight into the Mechanism of Intramolecular Inhibition of the Catalytic Activity of Sirtuin 2 (SIRT2). PLoS ONE, 2015, 10, e0139095.	2.5	11
3197	Differential Regulation of 6- and 7-Transmembrane Helix Variants of $\mu$ -Opioid Receptor in Response to Morphine Stimulation. PLoS ONE, 2015, 10, e0142826.	2.5	14
3198	Deciphering the Dynamics of Non-Covalent Interactions Affecting Thermal Stability of a Protein: Molecular Dynamics Study on Point Mutant of Thermus thermophilus Isopropylmalate Dehydrogenase. PLoS ONE, 2015, 10, e0144294.	2.5	21
3199	Macromolecular crowding studies of amino acids using NMR diffusion measurements and molecular dynamics simulations. Frontiers in Physics, 2015, 3, .	2.1	12
3201	Atomistic Simulations of Clathrate Hydrates. , 2015, , 351-359.		2
3202	Properties of water hydrating the galactolipid and phospholipid bilayers: a molecular dynamics simulation study. Acta Biochimica Polonica, 2015, 62, 475-481.	0.5	10
3203	Chemistry specificity of DNAâ€“polycation complex salt response: a simulation study of DNA, polylysine and polyethyleneimine. Physical Chemistry Chemical Physics, 2015, 17, 5279-5289.	2.8	37
3204	A molecular dynamics study of model SI clathrate hydrates: the effect of guest size and guestâ€“water interaction on decomposition kinetics. Physical Chemistry Chemical Physics, 2015, 17, 9509-9518.	2.8	28
3205	Reparametrized E3B (Explicit Three-Body) Water Model Using the TIP4P/2005 Model as a Reference. Journal of Chemical Theory and Computation, 2015, 11, 2268-2277.	5.3	43
3206	Mechanism of Bismuth Telluride Exfoliation in an Ionic Liquid Solvent. Langmuir, 2015, 31, 3644-3652.	3.5	45
3207	Reduced Cytotoxicity of Graphene Nanosheets Mediated by Blood-Protein Coating. ACS Nano, 2015, 9, 5713-5724.	14.6	271
3208	Distribution of Residence Time of Water around DNA Base Pairs: Governing Factors and the Origin of Heterogeneity. Journal of Physical Chemistry B, 2015, 119, 11371-11381.	2.6	36
3209	A lazy learning-based QSAR classification study for screening potential histone deacetylase 8 (HDAC8) inhibitors. SAR and QSAR in Environmental Research, 2015, 26, 397-420.	2.2	17
3210	Transformation pathways in high-pressure solid nitrogen: From molecular N2 to polymeric cg-N. Journal of Chemical Physics, 2015, 142, 094505.	3.0	27
3211	Interaction of rhyolite melts with monazite, xenotime, and zircon surfaces. Contributions To Mineralogy and Petrology, 2015, 169, 1.	3.1	3
3212	PEGylated Liposomes as Carriers of Hydrophobic Porphyrins. Journal of Physical Chemistry B, 2015, 119, 6646-6657.	2.6	47
3213	Salting-Out of Methane in the Aqueous Solutions of Urea and Glycineâ€“Betaine. Journal of Physical Chemistry B, 2015, 119, 10941-10953.	2.6	13

#	ARTICLE	IF	CITATIONS
3214	Temperature and Pressure Dependence of Methane Correlations and Osmotic Second Virial Coefficients in Water. <i>Journal of Physical Chemistry B</i> , 2015, 119, 6280-6294.	2.6	31
3215	Conformational Dynamics of Two Natively Unfolded Fragment Peptides: Comparison of the AMBER and CHARMM Force Fields. <i>Journal of Physical Chemistry B</i> , 2015, 119, 7902-7910.	2.6	16
3216	Insights into the unfolding pathway and identification of thermally sensitive regions of phytase from <i>Aspergillus niger</i> by molecular dynamics simulations. <i>Journal of Molecular Modeling</i> , 2015, 21, 163.	1.8	7
3217	Novel chemical scaffolds of the tumor marker AKR1B10 inhibitors discovered by 3D QSAR pharmacophore modeling. <i>Acta Pharmacologica Sinica</i> , 2015, 36, 998-1012.	6.1	25
3218	Tristearin bilayers: structure of the aqueous interface and stability in the presence of surfactants. <i>RSC Advances</i> , 2015, 5, 49933-49943.	3.6	3
3219	Kirkwood's Buff Approach Rescues Overcollapse of a Disordered Protein in Canonical Protein Force Fields. <i>Journal of Physical Chemistry B</i> , 2015, 119, 7975-7984.	2.6	70
3220	Methyl-branched lipids promote the membrane adsorption of $\beta$ -synuclein by enhancing shallow lipid-packing defects. <i>Physical Chemistry Chemical Physics</i> , 2015, 17, 15589-15597.	2.8	42
3221	Characterization of interactions and pharmacophore development for DFG-out inhibitors to RET tyrosine kinase. <i>Journal of Molecular Modeling</i> , 2015, 21, 167.	1.8	11
3222	Quantitative Interpretation of FRET Experiments via Molecular Simulation: Force Field and Validation. <i>Biophysical Journal</i> , 2015, 108, 2721-2731.	0.5	59
3223	Molecular basis of laccase bound to lignin: insight from comparative studies on the interaction of <i>Trametes versicolor</i> laccase with various lignin model compounds. <i>RSC Advances</i> , 2015, 5, 52307-52313.	3.6	52
3224	On the lack of polymorphism in $\text{A}\beta$ peptide aggregates derived from patient brains. <i>Protein Science</i> , 2015, 24, 923-935.	7.6	17
3225	Molecular Dynamics. <i>Interdisciplinary Applied Mathematics</i> , 2015, , .	0.3	115
3226	Extended Variable Methods. <i>Interdisciplinary Applied Mathematics</i> , 2015, , 329-401.	0.3	1
3227	Role of grain size on the martensitic transformation and ultra-fast superelasticity in shape memory alloys. <i>Acta Materialia</i> , 2015, 95, 37-43.	7.9	28
3228	Steered molecular dynamics approach for promising drugs for influenza A virus targeting M2 channel proteins. <i>European Biophysics Journal</i> , 2015, 44, 447-455.	2.2	16
3229	A molecular dynamics study of water transport inside an epoxy polymer matrix. <i>Computational Materials Science</i> , 2015, 106, 29-37.	3.0	53
3230	Cholesterol under oxidative stress—How lipid membranes sense oxidation as cholesterol is being replaced by oxysterols. <i>Free Radical Biology and Medicine</i> , 2015, 84, 30-41.	2.9	57
3231	Solvation structure of sodium chloride ( $\text{Na}^+\text{Cl}^-$ ) ion pair in dimethyl sulfoxide-acetonitrile mixtures. <i>Journal of Molecular Liquids</i> , 2015, 207, 279-285.	4.9	13



#	ARTICLE	IF	CITATIONS
3232	Controlled Rejuvenation of Amorphous Metals with Thermal Processing. Scientific Reports, 2015, 5, 10545.	3.3	110
3233	Response of Calcium Carbonate Nanoparticles in Hydrophobic Solvent to Pressure, Temperature, and Water. Journal of Physical Chemistry C, 2015, 119, 16879-16888.	3.1	7
3234	MARTINI Coarse-Grained Models of Polyethylene and Polypropylene. Journal of Physical Chemistry B, 2015, 119, 8209-8216.	2.6	82
3235	Properties of Organic Liquids when Simulated with Long-Range Lennard-Jones Interactions. Journal of Chemical Theory and Computation, 2015, 11, 2938-2944.	5.3	116
3236	Quaternary structures of GroEL and na <sup>+</sup> -ve-Hsp60 chaperonins in solution: a combined SAXS-MD study. RSC Advances, 2015, 5, 49871-49879.	3.6	12
3237	The N Terminus of Sarcolipin Plays an Important Role in Uncoupling Sarco-endoplasmic Reticulum Ca <sup>2+</sup> -ATPase (SERCA) ATP Hydrolysis from Ca <sup>2+</sup> Transport. Journal of Biological Chemistry, 2015, 290, 14057-14067.	3.4	56
3238	Computational Study of Uniaxial Deformations in Silica Aerogel Using a Coarse-Grained Model. Journal of Physical Chemistry B, 2015, 119, 8640-8650.	2.6	27
3239	Determining the dielectric losses in polymers by using Molecular Dynamics simulations. , 2015, , .		10
3240	Predicting protein-ligand binding specificity based on ensemble clustering. , 2015, , .		1
3241	Coarse-Grained Ions for Nucleic Acid Modeling. Journal of Chemical Theory and Computation, 2015, 11, 5436-5446.	5.3	26
3242	Variable-Cell Double-Ended Surface Walking Method for Fast Transition State Location of Solid Phase Transitions. Journal of Chemical Theory and Computation, 2015, 11, 4885-4894.	5.3	58
3243	Empirical Optimization of Interactions between Proteins and Chemical Denaturants in Molecular Simulations. Journal of Chemical Theory and Computation, 2015, 11, 5543-5553.	5.3	23
3244	Role of the central cations in the mechanical unfolding of DNA and RNA G-quadruplexes. Nucleic Acids Research, 2015, 43, 7638-7647.	14.5	38
3245	Structural Degradation and Swelling of Lipid Bilayer under the Action of Benzene. Journal of Physical Chemistry B, 2015, 119, 15006-15013.	2.6	13
3246	Mechanism of Polymer Collapse in Miscible Good Solvents. Journal of Physical Chemistry B, 2015, 119, 15780-15788.	2.6	95
3247	Inhibition of cyclin-dependent kinase CDK1 by oxindolimine ligands and corresponding copper and zinc complexes. Journal of Biological Inorganic Chemistry, 2015, 20, 1205-1217.	2.6	18
3248	Molecular Dynamics Simulation of Na <sup>+</sup> •••Cl <sup>-</sup> Ion-Pair in Water•••Methanol Mixtures under Supercritical and Ambient Conditions. Journal of Physical Chemistry B, 2015, 119, 15471-15484.	2.6	13
3249	Pathways through Equilibrated States with Coexisting Phases for Gas Hydrate Formation. Journal of Physical Chemistry B, 2015, 119, 15857-15865.	2.6	18



#	ARTICLE	IF	CITATIONS
3250	Revisiting the Anomalous Bending Elasticity of Sharply Bent DNA. <i>Biophysical Journal</i> , 2015, 109, 2338-2351.	0.5	27
3251	Molecular dynamics study of the effect of active site protonation on <i>Helicobacter pylori</i> 5â€²-methylthioadenosine/S-adenosylhomocysteine nucleosidase. <i>European Biophysics Journal</i> , 2015, 44, 685-696.	2.2	6
3252	The role of lipids in mechanosensation. <i>Nature Structural and Molecular Biology</i> , 2015, 22, 991-998.	8.2	160
3253	MOLECULAR DYNAMICS SIMULATION OF THE SIZE EFFECT ON THE ELASTIC PROPERTIES OF THE B2-NiAl NANOFILM. <i>Surface Review and Letters</i> , 2015, 22, 1550042.	1.1	0
3254	The effect of anaesthetics on the properties of a lipid membrane in the biologically relevant phase: a computer simulation study. <i>Physical Chemistry Chemical Physics</i> , 2015, 17, 14750-14760.	2.8	31
3255	Molecular Dynamics Simulation of Iron â€” A Review. <i>Spin</i> , 2015, 05, 1540007.	1.3	5
3256	Using Pseudocontact Shifts and Residual Dipolar Couplings as Exact NMR Restraints for the Determination of Protein Structural Ensembles. <i>Biochemistry</i> , 2015, 54, 7470-7476.	2.5	19
3257	Water Freezing and Ice Melting. <i>Journal of Chemical Theory and Computation</i> , 2015, 11, 5613-5623.	5.3	19
3258	A calcium-accumulating region, CAR, in the channel Orai1 enhances Ca <sup>2+</sup> permeation and SOCE-induced gene transcription. <i>Science Signaling</i> , 2015, 8, ra131.	3.6	51
3259	Dislocation-nucleation-controlled deformation of Ni <sub>3</sub> Al nanocubes in molecular dynamics simulations. <i>Modelling and Simulation in Materials Science and Engineering</i> , 2015, 23, 085004.	2.0	19
3260	Selective targeting of the BRG/PB1 bromodomains impairs embryonic and trophoblast stem cell maintenance. <i>Science Advances</i> , 2015, 1, e1500723.	10.3	112
3261	A Rigid Hinge Region Is Necessary for High-Affinity Binding of Dimannose to Cyanovirin and Associated Constructs. <i>Biochemistry</i> , 2015, 54, 6951-6960.	2.5	15
3262	Epitope mapping of monoclonal antibody HPT-101: a study combining dynamic force spectroscopy, ELISA and molecular dynamics simulations. <i>Physical Biology</i> , 2015, 12, 066018.	1.8	3
3263	How Well Does BODIPY-Cholesteryl Ester Mimic Unlabeled Cholesteryl Esters in High Density Lipoprotein Particles?. <i>Journal of Physical Chemistry B</i> , 2015, 119, 15848-15856.	2.6	4
3264	Structure, Dynamics, and Allosteric Potential of Ionotropic Glutamate Receptor N-Terminal Domains. <i>Biophysical Journal</i> , 2015, 109, 1136-1148.	0.5	27
3265	Contribution of Electrostatics in the Fibril Stability of a Model Ionic-Complementary Peptide. <i>Biomacromolecules</i> , 2015, 16, 3792-3801.	5.4	15
3266	Controlling in Vitro Insulin Amyloidosis with Stable Peptide Conjugates: A Combined Experimental and Computational Study. <i>Journal of Physical Chemistry B</i> , 2015, 119, 15395-15406.	2.6	30
3267	Force-Field Induced Bias in the Structure of Å <sup>2</sup> <sub>21</sub> “ <sub>30</sub> : A Comparison of OPLS, AMBER, CHARMM, and GROMOS Force Fields. <i>Journal of Chemical Information and Modeling</i> , 2015, 55, 2587-2595.	5.4	82

#	ARTICLE	IF	CITATIONS
3268	Aggregation of photosensitizers: the role of dispersion and solvation on dimer formation energetics. Theoretical Chemistry Accounts, 2015, 134, 1.	1.4	16
3269	Role of Water in the Puzzling Mechanism of the Final Aromatization Step Promoted by the Human Aromatase Enzyme. Insights from QM/MM MD Simulations. Journal of Chemical Information and Modeling, 2015, 55, 2218-2226.	5.4	25
3270	Molecular-dynamics simulations of urea nucleation from aqueous solution. Proceedings of the National Academy of Sciences of the United States of America, 2015, 112, E6-14.	7.1	142
3271	Thermodynamic properties and microstructures of the mixture of N-butylpyridinium tetrafluoroborate with acetonitrile studied by molecular dynamics simulation. Journal of Molecular Liquids, 2015, 203, 153-158.	4.9	9
3272	Interaction of collagen like peptides with gold nanosurfaces: a molecular dynamics investigation. Physical Chemistry Chemical Physics, 2015, 17, 5172-5186.	2.8	26
3273	Molecular Dynamics Study on the Equilibrium and Kinetic Properties of Tetrahydrofuran Clathrate Hydrates. Journal of Physical Chemistry C, 2015, 119, 1400-1409.	3.1	34
3274	Rational design of hyper-glycosylated interferon beta analogs: A computational strategy for glycoengineering. Journal of Molecular Graphics and Modelling, 2015, 56, 31-42.	2.4	16
3275	A molecular view of the role of chirality in charge-driven polypeptide complexation. Soft Matter, 2015, 11, 1525-1538.	2.7	55
3276	Analysis of crystal growth of methane hydrate using molecular dynamics simulation. Molecular Simulation, 2015, 41, 918-922.	2.0	6
3277	Evolution of the active site of human glutathione transferase A2-2 for enhanced activity with dietary isothiocyanates. Biochimica Et Biophysica Acta - General Subjects, 2015, 1850, 742-749.	2.4	8
3278	K <sup>+</sup> Congeners That Do Not Compromise Na <sup>+</sup> Activation of the Na <sup>+</sup> ,K <sup>+</sup> -ATPase. Journal of Biological Chemistry, 2015, 290, 3720-3731.	3.4	9
3279	Effect of the hydroaffinity and topology of pore walls on the structure and dynamics of confined water. Journal of Chemical Physics, 2015, 142, 034703.	3.0	28
3280	Computational and Experimental Study of the Behavior of Cyano-Based Ionic Liquids in Aqueous Solution. Journal of Physical Chemistry B, 2015, 119, 1567-1578.	2.6	25
3281	Structural basis for amyloidogenic peptide recognition by sorLA. Nature Structural and Molecular Biology, 2015, 22, 199-206.	8.2	55
3282	Molecular dynamics study-based mechanism of nefiracetam-induced NMDA receptor potentiation. Computational Biology and Chemistry, 2015, 55, 14-22.	2.3	15
3283	Monte Carlo simulation of free energy for the solid-liquid equilibrium of methane. Korean Journal of Chemical Engineering, 2015, 32, 939-949.	2.7	2
3284	Hydrogen bonding in a mixture of protic ionic liquids: a molecular dynamics simulation study. Physical Chemistry Chemical Physics, 2015, 17, 8431-8440.	2.8	74
3285	Targeting the intersubunit cavity of Plasmodium falciparum glutathione reductase by a novel natural inhibitor: Computational and experimental evidence. International Journal of Biochemistry and Cell Biology, 2015, 61, 72-80.	2.8	15

#	ARTICLE	IF	CITATIONS
3286	Theoretical Study of Structural Changes in DNA under High External Hydrostatic Pressure. <i>Journal of Physical Chemistry B</i> , 2015, 119, 3348-3355.	2.6	3
3287	Quantitative Assessments of the Distinct Contributions of Polypeptide Backbone Amides versus Side Chain Groups to Chain Expansion via Chemical Denaturation. <i>Journal of the American Chemical Society</i> , 2015, 137, 2984-2995.	13.7	104
3288	Solvation of an Excess Electron in Pyrrolidinium Dicyanamide Based Ionic Liquids. <i>Journal of Physical Chemistry B</i> , 2015, 119, 532-542.	2.6	19
3289	Short Hydrogen Bonds and Negative Charge in Photoactive Yellow Protein Promote Fast Isomerization but not High Quantum Yield. <i>Journal of Physical Chemistry B</i> , 2015, 119, 2372-2383.	2.6	10
3290	Influence of Antifreeze Proteins on the Ice/Water Interface. <i>Journal of Physical Chemistry B</i> , 2015, 119, 3407-3413.	2.6	20
3291	Structure of Alkylimidazolium-Based Ionic Liquids at the Interface with Vacuum and Water—A Molecular Dynamics Study. <i>Journal of Physical Chemistry B</i> , 2015, 119, 3795-3807.	2.6	40
3292	Single Chain Structure of a Poly( <i>N</i> -isopropylacrylamide) Surfactant in Water. <i>Journal of Physical Chemistry B</i> , 2015, 119, 3837-3845.	2.6	53
3293	Ionic Clusters vs Shear Viscosity in Aqueous Amino Acid Ionic Liquids. <i>Journal of Physical Chemistry B</i> , 2015, 119, 3824-3828.	2.6	23
3294	Native Conformational Dynamics of the Spliceosomal U1A Protein. <i>Journal of Physical Chemistry B</i> , 2015, 119, 3651-3661.	2.6	10
3295	Structure of Mixed Self-Assembled Monolayers on Gold Nanoparticles at Three Different Arrangements. <i>Journal of Physical Chemistry C</i> , 2015, 119, 3199-3209.	3.1	28
3296	Solvent Driving Force Ensures Fast Formation of a Persistent and Well-Separated Radical Pair in Plant Cryptochrome. <i>Journal of the American Chemical Society</i> , 2015, 137, 1147-1156.	13.7	70
3297	Controlling Carbon-Nanotube—Phospholipid Solubility by Curvature-Dependent Self-Assembly. <i>Journal of Physical Chemistry B</i> , 2015, 119, 4020-4032.	2.6	18
3298	Concurrent Cooperativity and Substrate Inhibition in the Epoxidation of Carbamazepine by Cytochrome P450 3A4 Active Site Mutants Inspired by Molecular Dynamics Simulations. <i>Biochemistry</i> , 2015, 54, 711-721.	2.5	42
3299	Electrolyte Diffusion in Gyroidal Nanoporous Carbon. <i>Journal of Physical Chemistry C</i> , 2015, 119, 2896-2903.	3.1	8
3300	Molecular Dynamics Simulations of 441 Two-Residue Peptides in Aqueous Solution: Conformational Preferences and Neighboring Residue Effects with the Amber ff99SB-ildn-NMR Force Field. <i>Journal of Chemical Theory and Computation</i> , 2015, 11, 1315-1329.	5.3	13
3301	Multiscale Modeling of Four-Component Lipid Mixtures: Domain Composition, Size, Alignment, and Properties of the Phase Interface. <i>Journal of Physical Chemistry B</i> , 2015, 119, 4240-4250.	2.6	85
3302	A Structural Mechanism for Calcium Transporter Headpiece Closure. <i>Journal of Physical Chemistry B</i> , 2015, 119, 1407-1415.	2.6	24
3303	Hydration of Kr(aq) in Dilute and Concentrated Solutions. <i>Journal of Physical Chemistry B</i> , 2015, 119, 9098-9102.	2.6	20

#	ARTICLE	IF	CITATIONS
3304	Potentials of Mean Force and Escape Times of Surfactants from Micelles and Hydrophobic Surfaces Using Molecular Dynamics Simulations. <i>Langmuir</i> , 2015, 31, 1336-1343.	3.5	54
3305	Carboxylâ€“Peptide Plane Stacking Is Important for Stabilization of Buried E305 of <i>Trichoderma reesei</i> Cel5A. <i>Journal of Chemical Information and Modeling</i> , 2015, 55, 104-113.	5.4	3
3306	Molecular Dynamics Characterizations of the Supercritical CO <sub>2</sub> -Mediated Hexaneâ€“Brine Interface. <i>Industrial &amp; Engineering Chemistry Research</i> , 2015, 54, 2489-2496.	3.7	45
3307	A comparative study of structural and conformational properties of casein kinase-1 isoforms: Insights from molecular dynamics and principal component analysis. <i>Journal of Theoretical Biology</i> , 2015, 371, 59-68.	1.7	4
3308	Creepâ€“Fatigue Relationship in Polymer: Molecular Dynamics Simulations Approach. <i>Macromolecular Theory and Simulations</i> , 2015, 24, 65-73.	1.4	15
3309	Allosteric Regulation of Focal Adhesion Kinase by PIP2 and ATP. <i>Biophysical Journal</i> , 2015, 108, 698-705.	0.5	32
3310	Integrating docking and molecular dynamics approaches for a series of proline-based 2,5-diketopiperazines as novel $\beta$ -tubulin inhibitors. <i>Journal of Biomolecular Structure and Dynamics</i> , 2015, 33, 2285-2295.	3.5	11
3311	A Computational Study of the Effect of Matrix Structural Order on Water Sorption by Trp-Cage Miniproteins. <i>Journal of Physical Chemistry B</i> , 2015, 119, 1847-1856.	2.6	9
3312	<i>In silico</i> characterization of binding mode of CCR8 inhibitor: homology modeling, docking and membrane based MD simulation study. <i>Journal of Biomolecular Structure and Dynamics</i> , 2015, 33, 2491-2510.	3.5	16
3313	Chirality-selected phase behaviour in ionic polypeptide complexes. <i>Nature Communications</i> , 2015, 6, 6052.	12.8	208
3314	Formation of bilayer clathrate hydrates. <i>Journal of Materials Chemistry A</i> , 2015, 3, 5547-5555.	10.3	17
3315	Role of Arginine in Mediating Proteinâ€“Carbon Nanotube Interactions. <i>Langmuir</i> , 2015, 31, 1683-1692.	3.5	30
3316	Mechanisms of Anion Conduction by Coupled Glutamate Transporters. <i>Cell</i> , 2015, 160, 542-553.	28.9	114
3317	Path Integral Metadynamics. <i>Journal of Chemical Theory and Computation</i> , 2015, 11, 1383-1388.	5.3	21
3318	Conformational Sampling of Oligosaccharides Using Hamiltonian Replica Exchange with Two-Dimensional Dihedral Biasing Potentials and the Weighted Histogram Analysis Method (WHAM). <i>Journal of Chemical Theory and Computation</i> , 2015, 11, 788-799.	5.3	38
3319	Synthetic Peptides Reproducing Tissue Transglutaminaseâ€“Gliadin Complex Neo-epitopes as Probes for Antibody Detection in Celiac Disease Patientsâ€™ Sera. <i>Journal of Medicinal Chemistry</i> , 2015, 58, 1390-1399.	6.4	6
3320	Conformational changes and allosteric communications in human serum albumin due to ligand binding. <i>Journal of Biomolecular Structure and Dynamics</i> , 2015, 33, 2192-2204.	3.5	12
3321	Glass transition investigations on highly crosslinked epoxy resins by molecular dynamics simulations. <i>Molecular Simulation</i> , 2015, 41, 1515-1527.	2.0	31

#	ARTICLE	IF	CITATIONS
3322	Simulating the antimicrobial mechanism of human $\beta$ 2-defensin-3 with coarse-grained molecular dynamics. <i>Journal of Biomolecular Structure and Dynamics</i> , 2015, 33, 2522-2529.	3.5	18
3323	Molecular effects of encapsulation of glucose oxidase dimer by graphene. <i>RSC Advances</i> , 2015, 5, 13570-13578.	3.6	19
3324	The energy landscape of adenylate kinase during catalysis. <i>Nature Structural and Molecular Biology</i> , 2015, 22, 124-131.	8.2	150
3325	Correlation of Drug and Carbon Nanotube Size in Encapsulation and Free Energy Calculation: A Molecular Insight. <i>Bulletin of the Korean Chemical Society</i> , 2015, 36, 168-179.	1.9	6
3326	Kinetic dielectric decrement revisited: phenomenology of finite ion concentrations. <i>Physical Chemistry Chemical Physics</i> , 2015, 17, 130-133.	2.8	40
3327	The effects of globotriaosylceramide tail saturation level on bilayer phases. <i>Soft Matter</i> , 2015, 11, 1352-1361.	2.7	22
3328	Estimation of the Binding Free Energy of AC1NX476 to HIV-1 Protease Wild Type and Mutations Using Free Energy Perturbation Method. <i>Chemical Biology and Drug Design</i> , 2015, 86, 546-558.	3.2	24
3329	Design of sweet protein based sweeteners: Hints from structure–function relationships. <i>Food Chemistry</i> , 2015, 173, 1179-1186.	8.2	40
3330	General order parameter based correlation analysis of protein backbone motions between experimental NMR relaxation measurements and molecular dynamics simulations. <i>Biochemical and Biophysical Research Communications</i> , 2015, 457, 467-472.	2.1	3
3331	Alanine Scan of $\pm$ -Conotoxin RegIIA Reveals a Selective $\beta$ 3 $\beta$ 4 Nicotinic Acetylcholine Receptor Antagonist. <i>Journal of Biological Chemistry</i> , 2015, 290, 1039-1048.	3.4	38
3332	Evaluation of conformational changes in diabetes-associated mutation in insulin a chain: A molecular dynamics study. <i>Proteins: Structure, Function and Bioinformatics</i> , 2015, 83, 662-669.	2.6	9
3333	Ion Transport in Na <sub>2</sub> M <sub>2</sub> TeO <sub>6</sub> : Insights from Molecular Dynamics Simulation. <i>Journal of Physical Chemistry C</i> , 2015, 119, 1651-1658.	3.1	34
3334	Nucleation rate analysis of methane hydrate from molecular dynamics simulations. <i>Faraday Discussions</i> , 2015, 179, 463-474.	3.2	57
3335	Size dependence of yield strength simulated by a dislocation-density function dynamics approach. <i>Modelling and Simulation in Materials Science and Engineering</i> , 2015, 23, 035001.	2.0	6
3336	Effect of replacing [NTf <sub>2</sub> ] by [PF <sub>6</sub> ] anion on the [BMIm][NTf <sub>2</sub> ] ionic liquid confined by gold. <i>Molecular Simulation</i> , 2015, 41, 455-462.	2.0	17
3337	Role of surfactant structure in aqueous dispersions of carbon nanotubes. <i>Fluid Phase Equilibria</i> , 2015, 394, 19-28.	2.5	29
3338	Dependence of Internal Friction on Folding Mechanism. <i>Journal of the American Chemical Society</i> , 2015, 137, 3283-3290.	13.7	41
3339	Mechanistic insight into the functional transition of the enzyme guanylate kinase induced by a single mutation. <i>Scientific Reports</i> , 2015, 5, 8405.	3.3	4

#	ARTICLE	IF	CITATIONS
3340	Multi-scale simulations for predicting material properties of a cross-linked polymer. Computational Materials Science, 2015, 102, 68-77.	3.0	26
3341	Study of the sensitisation process of a duplex stainless steel (UNS 1.4462) by means of confocal microscopy and localised electrochemical techniques. Corrosion Science, 2015, 94, 327-341.	6.6	29
3342	Hierarchical multi-scale simulations of adhesion at polymer-metal interfaces: dry and wet conditions. Physical Chemistry Chemical Physics, 2015, 17, 8935-8944.	2.8	12
3343	Mutation V111I in HIV-2 Reverse Transcriptase Increases the Fitness of the Nucleoside Analogue-Resistant K65R and Q151M Viruses. Journal of Virology, 2015, 89, 833-843.	3.4	15
3344	Evaluating Force Fields for the Computational Prediction of Ionized Arginine and Lysine Side-Chains Partitioning into Lipid Bilayers and Octanol. Journal of Chemical Theory and Computation, 2015, 11, 1775-1791.	5.3	34
3345	Binding of bivalent metal cations by $\alpha$ -glucuronate: insights from the DFT-MD simulations. New Journal of Chemistry, 2015, 39, 3987-3994.	2.8	19
3346	Phosphorylation of PPAR $\beta$ Affects the Collective Motions of the PPAR $\beta$ -RXR $\alpha$ -DNA Complex. PLoS ONE, 2015, 10, e0123984.	2.5	15
3347	Diffusion mechanism of CO <sub>2</sub> in a crystalline polymer membrane studied using model gases. Molecular Simulation, 2015, 41, 974-979.	2.0	5
3348	Do adsorbed drugs onto P-glycoprotein influence its efflux capability?. Physical Chemistry Chemical Physics, 2015, 17, 22023-22034.	2.8	14
3349	The water-catalyzed mechanism of the ring-opening reaction of glucose. Physical Chemistry Chemical Physics, 2015, 17, 21622-21629.	2.8	19
3350	Hexagonal nanosheets in amorphous BN: A first principles study. Journal of Non-Crystalline Solids, 2015, 427, 41-45.	3.1	13
3351	Effect of Phosphatidic Acid on Biomembrane: Experimental and Molecular Dynamics Simulations Study. Journal of Physical Chemistry B, 2015, 119, 10042-10051.	2.6	20
3352	Stability and softening of a lipid monolayer in the presence of a pain-killer drug. Colloids and Surfaces B: Biointerfaces, 2015, 132, 34-44.	5.0	12
3353	Novel high-pressure phase of ZrO <sub>2</sub> : An ab initio prediction. Journal of Solid State Chemistry, 2015, 230, 233-236.	2.9	10
3354	Hydrogen/Deuterium Exchange and Molecular Dynamics Analysis of Amyloid Fibrils Formed by a D69K Charge-Pair Mutant of Human Apolipoprotein C-II. Biochemistry, 2015, 54, 4805-4814.	2.5	15
3356	Nascent $\beta$ -Hairpin Formation of a Natively Unfolded Peptide Reveals the Role of Hydrophobic Contacts. Biophysical Journal, 2015, 109, 630-638.	0.5	6
3357	Mapping the Dynamics Landscape of Conformational Transitions in Enzyme: The Adenylate Kinase Case. Biophysical Journal, 2015, 109, 647-660.	0.5	61
3358	Effects of variation in chain length on ternary polymer electrolyte " Ionic liquid mixture " A molecular dynamics simulation study. Journal of Power Sources, 2015, 293, 983-992.	7.8	9



#	ARTICLE	IF	CITATIONS
3359	Direct calculation of ice homogeneous nucleation rate for a molecular model of water. Proceedings of the National Academy of Sciences of the United States of America, 2015, 112, 10582-10588.	7.1	199
3360	Peridynamic theory of solids from the perspective of classical statistical mechanics. Physica A: Statistical Mechanics and Its Applications, 2015, 437, 162-183.	2.6	6
3361	Molecular dynamics simulations of Na <sup>+</sup> -Cl <sup>-</sup> ion-pair in supercritical methanol. Journal of Supercritical Fluids, 2015, 103, 61-69.	3.2	10
3362	In silico research to assist the investigation of carboxamide derivatives as potent TRPV1 antagonists. Molecular BioSystems, 2015, 11, 2885-2899.	2.9	9
3363	Theoretical Approaches for Understanding the Interplay Between Stress and Chemical Reactivity. Topics in Current Chemistry, 2015, 369, 37-96.	4.0	23
3364	Development and application of in situ/operando soft X-ray transmission cells to aqueous solutions and catalytic and electrochemical reactions. Journal of Electron Spectroscopy and Related Phenomena, 2015, 200, 293-310.	1.7	32
3365	Molecular Dynamics Study of the Gold/Ionic Liquids Interface. Journal of Physical Chemistry B, 2015, 119, 9883-9892.	2.6	35
3366	Dynamical equations for the period vectors in a periodic system under constant external stress. Canadian Journal of Physics, 2015, 93, 974-978.	1.1	1
3367	A multiscale molecular dynamics method for isothermal dynamic problems using the seamless heterogeneous multiscale method. Computer Methods in Applied Mechanics and Engineering, 2015, 295, 510-524.	6.6	10
3368	Investigating the Structural Variability and Binding Modes of the Glioma Targeting NFL-TBS.40-63 Peptide on Tubulin. Biochemistry, 2015, 54, 3660-3669.	2.5	8
3369	Mutual and Self-Diffusivities in Binary Mixtures of [EMIM][B(CN) <sub>4</sub> ] with Dissolved Gases by Using Dynamic Light Scattering and Molecular Dynamics Simulations. Journal of Physical Chemistry B, 2015, 119, 8583-8592.	2.6	31
3370	Temperature Dependence of Hydroxymethyl Group Rotamer Populations in Celooligomers. Journal of Physical Chemistry B, 2015, 119, 9559-9570.	2.6	11
3371	Structural Properties of the Water/Membrane Interface of a Bilayer Built of the <i>E. coli</i> Lipid A. Journal of Physical Chemistry B, 2015, 119, 5846-5856.	2.6	14
3372	Molecular dynamics of dibenz[a,h]anthracene and its metabolite interacting with lung surfactant phospholipid bilayers. Physical Chemistry Chemical Physics, 2015, 17, 20912-20922.	2.8	15
3373	Effect of Chromophore Potential Model on the Description of Exciton-Phonon Interactions. Journal of Physical Chemistry Letters, 2015, 6, 2875-2880.	4.6	27
3374	In silico Investigation of the PglB Active Site Reveals Transient Catalytic States and Octahedral Metal Ion Coordination. Glycobiology, 2015, 25, 1183-1195.	2.5	13
3375	Effect of graphene oxide on the conformational transitions of amyloid beta peptide: A molecular dynamics simulation study. Journal of Molecular Graphics and Modelling, 2015, 61, 175-185.	2.4	72
3376	Interaction preferences between nucleobase mimetics and amino acids in aqueous solutions. Physical Chemistry Chemical Physics, 2015, 17, 21414-21422.	2.8	15



#	ARTICLE	IF	CITATIONS
3377	Atomistic simulations of the structure of highly crosslinked sulfonated poly(styrene-co-divinylbenzene) ion exchange resins. <i>Soft Matter</i> , 2015, 11, 2251-2267.	2.7	10
3378	Effects of Concentration on Like-Charge Pairing of Guanidinium Ions and on the Structure of Water: An All-Atom Molecular Dynamics Simulation Study. <i>Journal of Physical Chemistry B</i> , 2015, 119, 11262-11274.	2.6	27
3379	Molecular Dynamics Simulations of the Bacterial UraA H <sup>+</sup> -Uracil Symporter in Lipid Bilayers Reveal a Closed State and a Selective Interaction with Cardiolipin. <i>PLoS Computational Biology</i> , 2015, 11, e1004123.	3.2	40
3380	Interaction of the Antimicrobial Peptide Polymyxin B1 with Both Membranes of <i>E. coli</i> : A Molecular Dynamics Study. <i>PLoS Computational Biology</i> , 2015, 11, e1004180.	3.2	134
3381	Oligomer Formation of Toxic and Functional Amyloid Peptides Studied with Atomistic Simulations. <i>Journal of Physical Chemistry B</i> , 2015, 119, 9696-9705.	2.6	29
3382	In silico ligand binding studies of cyanogenic $\beta$ -glucosidase, dhurrinase-2 from <i>Sorghum bicolor</i> . <i>Journal of Molecular Modeling</i> , 2015, 21, 184.	1.8	5
3383	Higher-Affinity Agonists of 5-HT <sub>1A</sub> R Discovered through Tuning the Binding-Site Flexibility. <i>Journal of Chemical Information and Modeling</i> , 2015, 55, 1616-1627.	5.4	11
3384	Reversible and Irreversible Adsorption Energetics of Poly(ethylene glycol) and Sorbitan Poly(ethoxylate) at a Water/Alkane Interface. <i>Langmuir</i> , 2015, 31, 7503-7511.	3.5	30
3385	Asphaltene Subfractions Responsible for Stabilizing Water-in-Crude Oil Emulsions. Part 2: Molecular Representations and Molecular Dynamics Simulations. <i>Energy &amp; Fuels</i> , 2015, 29, 4783-4794.	5.1	122
3386	Site-directed mutagenesis substituting cysteine for serine in 2-Cys peroxiredoxin (2-Cys Prx A) of <i>Arabidopsis thaliana</i> effectively improves its peroxidase and chaperone functions. <i>Annals of Botany</i> , 2015, 116, 713-725.	2.9	26
3387	Insights into Stability and Folding of GNRA and UNCG Tetraloops Revealed by Microsecond Molecular Dynamics and Well-Tempered Metadynamics. <i>Journal of Chemical Theory and Computation</i> , 2015, 11, 3866-3877.	5.3	60
3388	Molecular dynamics simulation of CO <sub>2</sub> hydrates: Prediction of three phase coexistence line. <i>Journal of Chemical Physics</i> , 2015, 142, 124505.	3.0	96
3389	Structural asymmetry in a conserved signaling system that regulates division, replication, and virulence of an intracellular pathogen. <i>Proceedings of the National Academy of Sciences of the United States of America</i> , 2015, 112, E3709-18.	7.1	52
3390	Characterization of the Dielectric Constant in the <i>Trichoderma reesei</i> Cel7B Active Site. <i>Journal of Chemical Information and Modeling</i> , 2015, 55, 1369-1376.	5.4	5
3391	Structural Order of Water Molecules around Hydrophobic Solutes: Length-Scale Dependence and Solute-Solvent Coupling. <i>Journal of Physical Chemistry B</i> , 2015, 119, 11346-11357.	2.6	33
3392	Dissolving process of a cellulose bunch in ionic liquids: a molecular dynamics study. <i>Physical Chemistry Chemical Physics</i> , 2015, 17, 17894-17905.	2.8	92
3393	Exploring the Balance between Folding and Functional Dynamics in Proteins and RNA. <i>International Journal of Molecular Sciences</i> , 2015, 16, 6868-6889.	4.1	20
3394	Nanoplasmonics, Nano-Optics, Nanocomposites, and Surface Studies. <i>Springer Proceedings in Physics</i> , 2015, , .	0.2	6

#	ARTICLE	IF	CITATIONS
3395	Atomistic Molecular Insight into the Time Dependence of Polymer Glass Transition. Journal of Physical Chemistry B, 2015, 119, 9959-9969.	2.6	19
3396	Structural Changes in Ceramide Bilayers Rationalize Increased Permeation through Stratum Corneum Models with Shorter Acyl Tails. Journal of Physical Chemistry B, 2015, 119, 9811-9819.	2.6	46
3397	Waterâ€“methanol separation with carbon nanotubes and electric fields. Nanoscale, 2015, 7, 12659-12665.	5.6	33
3398	Properties of Nafion Under Uniaxial Loading at Different Temperatures: A Molecular Dynamics Study. Polymer-Plastics Technology and Engineering, 2015, 54, 806-813.	1.9	11
3400	Conformational Properties of Sodium Polystyrenesulfonate in Water: Insights from a Coarse-Grained Model with Explicit Solvent. Journal of Physical Chemistry B, 2015, 119, 11010-11018.	2.6	24
3401	A Combined Experimental and Molecular Dynamics Study of Iodide-Based Ionic Liquid and Water Mixtures. Journal of Physical Chemistry B, 2015, 119, 8764-8772.	2.6	31
3402	Effects of drug-resistant mutations on the dynamic properties of HIV-1 protease and inhibition by Amprenavir and Darunavir. Scientific Reports, 2015, 5, 10517.	3.3	39
3403	Freezing point depression in model Lennard-Jones solutions. Molecular Physics, 2015, 113, 2725-2734.	1.7	5
3404	A fast recoiling silk-like elastomer facilitates nanosecond nematocyst discharge. BMC Biology, 2015, 13, 3.	3.8	34
3405	Electrochemical Model for Ionic Liquid Electrolytes in Lithium Batteries. Electrochimica Acta, 2015, 176, 301-310.	5.2	21
3406	Force Field Benchmark of Organic Liquids. 2. Gibbs Energy of Solvation. Journal of Chemical Information and Modeling, 2015, 55, 1192-1201.	5.4	77
3407	The juxtamembrane regions of human receptor tyrosine kinases exhibit conserved interaction sites with anionic lipids. Scientific Reports, 2015, 5, 9198.	3.3	89
3408	Interaction of P-glycoprotein with anti-tumor drugs: the site, gate and pathway. Soft Matter, 2015, 11, 6633-6641.	2.7	18
3409	Appraisal of the realistic accuracy of molecular dynamics of high-pressure hydrogen. Cogent Physics, 2015, 2, 1049477.	0.7	11
3410	In silico investigation of action mechanism of four novel angiotensin-I converting enzyme inhibitory peptides modified with Trp. Journal of Functional Foods, 2015, 17, 632-639.	3.4	14
3411	Quantifying the co-solvent effects on trypsin from the digestive system of carp Catla catla by biophysical techniques and molecular dynamics simulations. RSC Advances, 2015, 5, 43023-43035.	3.6	3
3412	Molecular mechanisms for the adhesion of chitin and chitosan to montmorillonite clay. RSC Advances, 2015, 5, 54580-54588.	3.6	22
3413	Broad spectrum assessment of the epitope fluctuationâ€“immunogenicity hypothesis. Vaccine, 2015, 33, 5945-5949.	3.8	3

#	ARTICLE	IF	CITATIONS
3414	Improving the LIE Method for Binding Free Energy Calculations of Proteinâ€“Ligand Complexes. Journal of Chemical Information and Modeling, 2015, 55, 1867-1877.	5.4	31
3415	Understanding the cation specific effects on the aqueous solubility of amino acids: from mono to polyvalent cations. RSC Advances, 2015, 5, 15024-15034.	3.6	9
3416	Design, synthesis and characterization of a new blue phosphorescent Ir complex. Journal of Materials Chemistry C, 2015, 3, 8675-8683.	5.5	14
3417	Monoterpenes as nitrofurantoin resistance modulating agents: minimal structural requirements, molecular dynamics simulations, and the effect of piperitone on the emergence of nitrofurantoin resistance in Enterobacteriaceae. Journal of Molecular Modeling, 2015, 21, 198.	1.8	3
3418	Thermodynamics of Na <sup>+</sup> Cl <sup>-</sup> ion pair association in acetonitrileâ€“dimethyl sulfoxide mixtures. Chemical Physics Letters, 2015, 620, 134-138.	2.6	13
3419	Insight into the nucleation of urea crystals from the melt. Chemical Engineering Science, 2015, 121, 51-59.	3.8	70
3420	Thermodynamic and Transport Properties of H <sub>2</sub> O + NaCl from Polarizable Force Fields. Journal of Chemical Theory and Computation, 2015, 11, 3802-3810.	5.3	63
3421	Temperature dependent structural, elastic, and polar properties of ferroelectric polyvinylidene fluoride (PVDF) and trifluoroethylene (TrFE) copolymers. Journal of Materials Chemistry C, 2015, 3, 8389-8396.	5.5	51
3422	Retardation of Water Reorientation at the Oil/Water Interface. Journal of Physical Chemistry C, 2015, 119, 16639-16648.	3.1	16
3423	Phosphatidylserine transport by ORP/Osh proteins is driven by phosphatidylinositol 4-phosphate. Science, 2015, 349, 432-436.	12.6	301
3424	Insight into the impact of environments on structure of chimera C3 of human Î²-defensins 2 and 3 from molecular dynamics simulations. Journal of Biomolecular Structure and Dynamics, 2015, 33, 1989-2002.	3.5	3
3425	A multiscale molecular dynamics allowing macroscale mechanical loads. Europhysics Letters, 2015, 110, 60005.	2.0	5
3426	On the Mg <sup>2+</sup> binding site of the Î¼ subunit from bacterial F-type ATP synthases. Biochimica Et Biophysica Acta - Bioenergetics, 2015, 1847, 1101-1112.	1.0	9
3427	Molecular dynamic simulation of asphaltene co-aggregation with humic acid during oil spill. Chemosphere, 2015, 138, 412-421.	8.2	44
3428	Temperature dependent dynamics of DegP-trimer: A molecular dynamics study. Computational and Structural Biotechnology Journal, 2015, 13, 329-338.	4.1	3
3429	Modeling Diffusion of Linear Hydrocarbons in Silica Zeolite LTA Using Transition Path Sampling. Journal of Physical Chemistry C, 2015, 119, 15643-15653.	3.1	22
3430	Molecular Dynamics Simulations for the Description of Experimental Molecular Conformation, Melt Dynamics, and Phase Transitions in Polyethylene. Macromolecules, 2015, 48, 5016-5027.	4.8	76
3431	Cloud computing approaches for prediction of ligand binding poses and pathways. Scientific Reports, 2015, 5, 7918.	3.3	54

#	ARTICLE	IF	CITATIONS
3432	Martini Coarse-Grained Force Field: Extension to DNA. <i>Journal of Chemical Theory and Computation</i> , 2015, 11, 3932-3945.	5.3	239
3433	Effect of surfactant SDS on DMSO transport across water/hexane interface by molecular dynamics simulation. <i>Chemical Engineering Science</i> , 2015, 134, 813-822.	3.8	22
3434	Vapor-Liquid Equilibria of Imidazolium Ionic Liquids with Cyano Containing Anions with Water and Ethanol. <i>Journal of Physical Chemistry B</i> , 2015, 119, 10287-10303.	2.6	52
3435	Unfolding stabilities of two structurally similar proteins as probed by temperature-induced and force-induced molecular dynamics simulations. <i>Journal of Biomolecular Structure and Dynamics</i> , 2015, 33, 2037-2047.	3.5	5
3436	Interatomic potential for the ternary Ni-Al-Co system and application to atomistic modeling of the B2-L1 <sub>0</sub> martensitic transformation. <i>Modelling and Simulation in Materials Science and Engineering</i> , 2015, 23, 065006.	2.0	75
3437	Lipocarbazole, an efficient lipid peroxidation inhibitor anchored in the membrane. <i>Bioorganic and Medicinal Chemistry</i> , 2015, 23, 4866-4870.	3.0	13
3438	SAXS-Guided Metadynamics. <i>Journal of Chemical Theory and Computation</i> , 2015, 11, 3491-3498.	5.3	37
3439	Direct Coexistence Methods to Determine the Solubility of Salts in Water from Numerical Simulations. Test Case NaCl. <i>Journal of Physical Chemistry B</i> , 2015, 119, 8389-8396.	2.6	43
3440	Comparative Study of the Mechanical Unfolding Pathways of Î±- and Î²-Peptides. <i>Journal of Physical Chemistry B</i> , 2015, 119, 8313-8320.	2.6	3
3441	Free energy landscape of activation in a signalling protein at atomic resolution. <i>Nature Communications</i> , 2015, 6, 7284.	12.8	75
3442	Surface Curvature Relation to Protein Adsorption for Carbon-based Nanomaterials. <i>Scientific Reports</i> , 2015, 5, 10886.	3.3	97
3443	A theoretical study on the molecular determinants of the affibody protein Z <sub>A23</sub> bound to an amyloid Î² peptide. <i>Physical Chemistry Chemical Physics</i> , 2015, 17, 16886-16893.	2.8	4
3444	Model-free estimation of the effective correlation time for C-H bond reorientation in amphiphilic bilayers: 1H-13C solid-state NMR and MD simulations. <i>Journal of Chemical Physics</i> , 2015, 142, 044905.	3.0	27
3445	Insights into the Interactions of Fasciola hepatica Cathepsin L3 with a Substrate and Potential Novel Inhibitors through In Silico Approaches. <i>PLoS Neglected Tropical Diseases</i> , 2015, 9, e0003759.	3.0	17
3446	Catalytic pathway, substrate binding and stability in SAICAR synthetase: A structure and molecular dynamics study. <i>Journal of Structural Biology</i> , 2015, 191, 22-31.	2.8	6
3447	Exposure of thiol groups in the heat-induced denaturation of Î²-lactoglobulin. <i>Molecular Simulation</i> , 2015, 41, 1006-1014.	2.0	17
3448	Interplay of Dynamical Properties between Ionic Liquids and Ionic Surfactants: Mechanism and Aggregation. <i>Journal of Physical Chemistry B</i> , 2015, 119, 9925-9932.	2.6	8
3449	How To Minimize Artifacts in Atomistic Simulations of Membrane Proteins, Whose Crystal Structure Is Heavily Engineered: Î² <sub>2</sub> -Adrenergic Receptor in the Spotlight. <i>Journal of Chemical Theory and Computation</i> , 2015, 11, 3432-3445.	5.3	16

#	ARTICLE	IF	CITATIONS
3450	Membrane Recognition and Dynamics of the RNA Degradosome. PLoS Genetics, 2015, 11, e1004961.	3.5	93
3451	Structures of water molecules in carbon nanotubes under electric fields. Journal of Chemical Physics, 2015, 142, 124701.	3.0	45
3452	Molecular-Scale Understanding of Cohesion and Fracture in P3HT:Fullerene Blends. ACS Applied Materials & Interfaces, 2015, 7, 9957-9964.	8.0	60
3453	Bias-Exchange Metadynamics Simulations: An Efficient Strategy for the Analysis of Conduction and Selectivity in Ion Channels. Journal of Chemical Theory and Computation, 2015, 11, 1896-1906.	5.3	43
3454	Building Markov State Models for Periodically Driven Non-Equilibrium Systems. Journal of Chemical Theory and Computation, 2015, 11, 1819-1831.	5.3	20
3455	Effect of Hydrostatic Pressure on Gas Solubilization in Micelles. Langmuir, 2015, 31, 3318-3325.	3.5	6
3456	Spontaneous Adsorption of Coiled-Coil Model Peptides K and E to a Mixed Lipid Bilayer. Journal of Physical Chemistry B, 2015, 119, 4396-4408.	2.6	29
3457	Identification of Alcohol Conformers by Raman Spectra in the C-H Stretching Region. Journal of Physical Chemistry A, 2015, 119, 3209-3217.	2.5	45
3458	Oxidation of Cholesterol Does Not Alter Significantly Its Uptake into High-Density Lipoprotein Particles. Journal of Physical Chemistry B, 2015, 119, 4594-4600.	2.6	6
3459	The General AMBER Force Field (GAFF) Can Accurately Predict Thermodynamic and Transport Properties of Many Ionic Liquids. Journal of Physical Chemistry B, 2015, 119, 5882-5895.	2.6	319
3460	Urea enhances the photodynamic efficiency of methylene blue. Journal of Photochemistry and Photobiology B: Biology, 2015, 150, 31-37.	3.8	45
3461	New Insights into the Molecular Mechanism of E-Cadherin-Mediated Cell Adhesion by Free Energy Calculations. Journal of Chemical Theory and Computation, 2015, 11, 1354-1359.	5.3	7
3462	Molecular dynamic simulation of Ca <sup>2+</sup> -ATPase interacting with lipid bilayer membrane. IET Nanobiotechnology, 2015, 9, 85-94.	3.8	7
3463	Systematic characterization of protein folding pathways using diffusion maps: Application to Trp-cage miniprotein. Journal of Chemical Physics, 2015, 142, 085101.	3.0	53
3464	Molecular dynamics study of montmorillonite crystalline swelling: Roles of interlayer cation species and water content. Chemical Physics, 2015, 455, 23-31.	1.9	63
3465	Liquid boron and amorphous boron: An ab initio molecular dynamics study. Journal of Non-Crystalline Solids, 2015, 417-418, 10-14.	3.1	10
3466	Prediction of diffusion coefficients of chlorophenols in water by computer simulation. Fluid Phase Equilibria, 2015, 396, 9-19.	2.5	20
3467	Elasticity of Crystalline Molecular Explosives. Propellants, Explosives, Pyrotechnics, 2015, 40, 333-350.	1.6	51

#	ARTICLE	IF	CITATIONS
3468	Solubilization of Single-Walled Carbon Nanotubes Using a Peptide Aptamer in Water below the Critical Micelle Concentration. <i>Langmuir</i> , 2015, 31, 3482-3488.	3.5	17
3469	Brittle versus ductile fracture behaviour in nanotwinned FCC crystals. <i>Materials Letters</i> , 2015, 152, 65-67.	2.6	13
3470	Effects of multivalency and hydrophobicity of polyamines on enzyme hyperactivation of $\beta$ -chymotrypsin. <i>Journal of Molecular Catalysis B: Enzymatic</i> , 2015, 115, 135-139.	1.8	18
3471	Solution Properties of Hemicellulose Polysaccharides with Four Common Carbohydrate Force Fields. <i>Journal of Chemical Theory and Computation</i> , 2015, 11, 1765-1774.	5.3	41
3472	The structural impact of DNA mismatches. <i>Nucleic Acids Research</i> , 2015, 43, 4309-4321.	14.5	113
3473	Agonist binding by the $\beta_2$ -adrenergic receptor: an effect of receptor conformation on ligand association-dissociation characteristics. <i>European Biophysics Journal</i> , 2015, 44, 149-163.	2.2	15
3474	Nano-Encapsulation of Glucose Oxidase Dimer by Graphene. <i>Materials Research Society Symposia Proceedings</i> , 2015, 1725, 1.	0.1	1
3475	Retention-time prediction for polycyclic aromatic compounds in reversed-phase capillary electro-chromatography. <i>Journal of Molecular Modeling</i> , 2015, 21, 124.	1.8	2
3476	Computational Lipidomics with <i>insane</i> : A Versatile Tool for Generating Custom Membranes for Molecular Simulations. <i>Journal of Chemical Theory and Computation</i> , 2015, 11, 2144-2155.	5.3	847
3477	Structural importance of the C-terminal region in pig aldo-keto reductase family 1 member C1 and their effects on enzymatic activity. <i>BMC Structural Biology</i> , 2015, 15, 1.	2.3	16
3478	Molecular dynamics of the asymmetric dimers of EGFR: Simulations on the active and inactive conformations of the kinase domain. <i>Journal of Molecular Graphics and Modelling</i> , 2015, 58, 16-29.	2.4	11
3479	Effect of free volume redistribution on the diffusivity of water and benzene in poly(vinyl alcohol). <i>Chemical Engineering Science</i> , 2015, 121, 258-267.	3.8	17
3480	Mutation of Gly717Phe in human topoisomerase 1B has an effect on enzymatic function, reactivity to the camptothecin anticancer drug and on the linker domain orientation. <i>Biochimica Et Biophysica Acta - Proteins and Proteomics</i> , 2015, 1854, 860-868.	2.3	11
3481	Synthetic 1,2,3-triazole-linked glycoconjugates bind with high affinity to human galectin-3. <i>Bioorganic and Medicinal Chemistry</i> , 2015, 23, 3414-3425.	3.0	26
3482	Intra-helical salt-bridge and helix destabilizing residues within the same helical turn: Role of functionally important loop E half-helix in channel regulation of major intrinsic proteins. <i>Biochimica Et Biophysica Acta - Biomembranes</i> , 2015, 1848, 1436-1449.	2.6	13
3483	Lysine-Based Site-Directed Mutagenesis Increased Rigid $\beta$ -Sheet Structure and Thermostability of Mesophilic 1,4- $\beta$ -Glucanase. <i>Journal of Agricultural and Food Chemistry</i> , 2015, 63, 5249-5256.	5.2	28
3484	Interpretation of Solution X-Ray Scattering by Explicit-Solvent Molecular Dynamics. <i>Biophysical Journal</i> , 2015, 108, 2573-2584.	0.5	99
3485	Sec14-nodulin proteins and the patterning of phosphoinositide landmarks for developmental control of membrane morphogenesis. <i>Molecular Biology of the Cell</i> , 2015, 26, 1764-1781.	2.1	44



#	ARTICLE	IF	CITATIONS
3486	Smoothing of contact lines in spreading droplets by trisiloxane surfactants and its relevance for superspreading. <i>Soft Matter</i> , 2015, 11, 4527-4539.	2.7	13
3487	Role of hydration in phosphatidylcholine reverse micelle structure and gelation in cyclohexane: a molecular dynamics study. <i>Physical Chemistry Chemical Physics</i> , 2015, 17, 14951-14960.	2.8	17
3488	Acyl-2-aminobenzimidazoles: A novel class of neuroprotective agents targeting mGluR5. <i>Bioorganic and Medicinal Chemistry</i> , 2015, 23, 2211-2220.	3.0	21
3489	Identification of Mutational Hot Spots for Substrate Diffusion: Application to Myoglobin. <i>Journal of Chemical Theory and Computation</i> , 2015, 11, 1919-1927.	5.3	12
3490	On the urea induced hydrophobic collapse of a water soluble polymer. <i>Physical Chemistry Chemical Physics</i> , 2015, 17, 8491-8498.	2.8	56
3491	Structure of dimers of glycyrrhizic acid in water and their complexes with cholesterol: Molecular dynamics simulation. <i>Journal of Structural Chemistry</i> , 2015, 56, 67-76.	1.0	21
3492	<i>N</i> -Glycosylation as determinant of epidermal growth factor receptor conformation in membranes. <i>Proceedings of the National Academy of Sciences of the United States of America</i> , 2015, 112, 4334-4339.	7.1	135
3493	Exploring volume, compressibility and hydration changes of folded proteins upon compression. <i>Physical Chemistry Chemical Physics</i> , 2015, 17, 8499-8508.	2.8	23
3494	Stacking Free Energies of All DNA and RNA Nucleoside Pairs and Dinucleoside-Monophosphates Computed Using Recently Revised AMBER Parameters and Compared with Experiment. <i>Journal of Chemical Theory and Computation</i> , 2015, 11, 2315-2328.	5.3	86
3495	Phase Diagram and Electronic Structure of Praseodymium and Plutonium. <i>Physical Review X</i> , 2015, 5, .	8.9	67
3496	Structural conservation of the short $\alpha$ -helix in modified higher and lower polarity water solutions. <i>RSC Advances</i> , 2015, 5, 9627-9634.	3.6	3
3497	Nanosopic Characterization of DNA within Hydrophobic Pores: Thermodynamics and Kinetics. <i>Biochemical Engineering Journal</i> , 2015, 104, 41-47.	3.6	9
3498	Molecular dynamics of Kv1.3 ion channel and structural basis of its inhibition by scorpion toxin-OSK1 derivatives. <i>Biophysical Chemistry</i> , 2015, 203-204, 1-11.	2.8	11
3499	A molecular dynamics study of CaCO <sub>3</sub> nanoparticles in a hydrophobic solvent with a stearate co-surfactant. <i>Physical Chemistry Chemical Physics</i> , 2015, 17, 13575-13581.	2.8	3
3500	Composition dependent structural organization in trihexyl(tetradecyl)phosphonium chloride ionic liquid-methanol mixtures. <i>Journal of Chemical Physics</i> , 2015, 142, 134503.	3.0	32
3501	Parametrization of Backbone Flexibility in a Coarse-Grained Force Field for Proteins (COFFDROP) Derived from All-Atom Explicit-Solvent Molecular Dynamics Simulations of All Possible Two-Residue Peptides. <i>Journal of Chemical Theory and Computation</i> , 2015, 11, 2341-2354.	5.3	16
3502	Structural transformation between long and short-chain form of liquid sulfur from <i>ab initio</i> molecular dynamics. <i>Journal of Chemical Physics</i> , 2015, 142, 154502.	3.0	18
3503	Linear Basis Function Approach to Efficient Alchemical Free Energy Calculations. 2. Inserting and Deleting Particles with Coulombic Interactions. <i>Journal of Chemical Theory and Computation</i> , 2015, 11, 2536-2549.	5.3	41



#	ARTICLE	IF	CITATIONS
3504	Resveratrol interferes with the aggregation of membrane-bound human-IAPP: A molecular dynamics study. <i>European Journal of Medicinal Chemistry</i> , 2015, 92, 876-881.	5.5	47
3505	Cholesterol level affects surface charge of lipid membranes in saline solution. <i>Scientific Reports</i> , 2014, 4, 5005.	3.3	157
3506	New mimetic peptides inhibitors of $\beta$ aggregation. Molecular guidance for rational drug design. <i>European Journal of Medicinal Chemistry</i> , 2015, 95, 136-152.	5.5	19
3507	Conformational changes in MetNI: steered molecular dynamic studies of the methionine ABC transporter with and without substrates. <i>Molecular Simulation</i> , 2015, 41, 613-621.	2.0	1
3508	<i>In Silico</i> and <i>In Vitro</i> Study of Binding Affinity of Tripeptides to Amyloid $\beta$ Fibrils: Implications for Alzheimer's Disease. <i>Journal of Physical Chemistry B</i> , 2015, 119, 5145-5155.	2.6	30
3509	Intermolecular interaction and mechanical properties of energetic plasticizer MN reinforced 2,4,6-trinitrotoluene/1,3,5-trinitrohexahydro-1,3,5-triazine molten-energetic-composite (MEC). <i>RSC Advances</i> , 2015, 5, 33755-33761.	3.6	7
3510	In silico identification of novel kinase inhibitors by targeting B-Rafv660e from natural products database. <i>Journal of Molecular Modeling</i> , 2015, 21, 102.	1.8	6
3511	A phosphatidylinositol-4-phosphate powered exchange mechanism to create a lipid gradient between membranes. <i>Nature Communications</i> , 2015, 6, 6671.	12.8	166
3512	Systematic Refinement of Canongia Lopes's Force Field for Pyrrolidinium-Based Ionic Liquids. <i>Journal of Physical Chemistry B</i> , 2015, 119, 6242-6249.	2.6	55
3513	Molecular Dynamics Simulations of KirBac1.1 Mutants Reveal Global Gating Changes of Kir Channels. <i>Journal of Chemical Information and Modeling</i> , 2015, 55, 814-822.	5.4	21
3514	Urea homogeneous nucleation mechanism is solvent dependent. <i>Faraday Discussions</i> , 2015, 179, 291-307.	3.2	50
3515	Structural basis for regulation of stability and activity in glyceraldehyde-3-phosphate dehydrogenases. Differential scanning calorimetry and molecular dynamics. <i>Journal of Structural Biology</i> , 2015, 190, 224-235.	2.8	9
3516	PAMAM Dendrimers and Graphene: Materials for Removing Aromatic Contaminants from Water. <i>Environmental Science &amp; Technology</i> , 2015, 49, 4490-4497.	10.0	40
3517	The Bacterial Hydrophobin BslA is a Switchable Ellipsoidal Janus Nanocolloid. <i>Langmuir</i> , 2015, 31, 11558-11563.	3.5	28
3518	Effects of lysine residues on structural characteristics and stability of tau proteins. <i>Biochemical and Biophysical Research Communications</i> , 2015, 466, 486-492.	2.1	12
3519	Structure of Bolaamphiphile Sophorolipid Micelles Characterized with SAXS, SANS, and MD Simulations. <i>Journal of Physical Chemistry B</i> , 2015, 119, 13113-13133.	2.6	55
3520	Stability of Osaka Mutant and Wild-Type Fibril Models. <i>Journal of Physical Chemistry B</i> , 2015, 119, 13063-13070.	2.6	20
3521	On the Nature of an Extended Stokes Shift in the mPlum Fluorescent Protein. <i>Journal of Physical Chemistry B</i> , 2015, 119, 13052-13062.	2.6	35

#	ARTICLE	IF	CITATIONS
3522	Mixtures of amino-acid based ionic liquids and water. <i>Journal of Molecular Modeling</i> , 2015, 21, 236.	1.8	17
3523	Association of small aromatic molecules with PAMAM dendrimers. <i>Physical Chemistry Chemical Physics</i> , 2015, 17, 29548-29557.	2.8	9
3524	Molecular dynamics simulations for designing biomimetic pores based on internally functionalized self-assembling $\alpha$ , $\beta$ -peptide nanotubes. <i>Physical Chemistry Chemical Physics</i> , 2015, 17, 28586-28601.	2.8	9
3525	Thermo-responsive behavior of borinic acid polymers: experimental and molecular dynamics studies. <i>Soft Matter</i> , 2015, 11, 7159-7164.	2.7	20
3526	Origin of structural analogies and differences between the atomic structures of GeSe <sub>4</sub> and GeS <sub>4</sub> glasses: A first principles study. <i>Journal of Chemical Physics</i> , 2015, 143, 034504.	3.0	35
3527	First-principles calculations for thermodynamic properties of type-I silicon clathrate intercalated by sodium atoms. <i>Modern Physics Letters B</i> , 2015, 29, 1550166.	1.9	2
3528	Structure and Hydrogen Bonding of Water in Polyacrylate Gels: Effects of Polymer Hydrophilicity and Water Concentration. <i>Journal of Physical Chemistry B</i> , 2015, 119, 15381-15393.	2.6	36
3529	The molecular mechanism behind reactive aldehyde action on transmembrane translocations of proton and potassium ions. <i>Free Radical Biology and Medicine</i> , 2015, 89, 1067-1076.	2.9	39
3530	Simulation assisted characterization of kaolinite $\alpha$ -methanol intercalation complexes synthesized using cost-efficient homogenization method. <i>Applied Surface Science</i> , 2015, 357, 626-634.	6.1	28
3531	Computation assisted design of favored composition for ternary Mg $\alpha$ -Cu $\alpha$ -Y metallic glass formation. <i>Physical Chemistry Chemical Physics</i> , 2015, 17, 14879-14889.	2.8	3
3532	Hydration shell of the TS-Kappa protein: Higher density than bulk water. <i>Physica A: Statistical Mechanics and Its Applications</i> , 2015, 439, 48-58.	2.6	19
3533	Exploring binding properties of sertraline with human serum albumin: Combination of spectroscopic and molecular modeling studies. <i>Chemico-Biological Interactions</i> , 2015, 242, 235-246.	4.0	40
3534	A Comparison of Barostats for the Mechanical Characterization of Metal $\alpha$ -Organic Frameworks. <i>Journal of Chemical Theory and Computation</i> , 2015, 11, 5583-5597.	5.3	83
3535	Understanding the Thermodynamics of Hydrogen Bonding in Alcohol-Containing Mixtures: Self Association. <i>Journal of Physical Chemistry B</i> , 2015, 119, 14086-14101.	2.6	31
3536	Derivation of coarse-grained simulation models of chlorophyll molecules in lipid bilayers for applications in light harvesting systems. <i>Physical Chemistry Chemical Physics</i> , 2015, 17, 22054-22063.	2.8	11
3537	Atomistic Molecular Simulations Suggest a Kinetic Model for Membrane Translocation by Arginine-Rich Peptides. <i>Journal of Physical Chemistry B</i> , 2015, 119, 14413-14420.	2.6	31
3538	Direct-Space Corrections Enable Fast and Accurate Lorentz $\alpha$ -Berthelot Combination Rule Lennard-Jones Lattice Summation. <i>Journal of Chemical Theory and Computation</i> , 2015, 11, 5737-5746.	5.3	112
3539	Extension of the LOPLS-AA Force Field for Alcohols, Esters, and Monoolein Bilayers and its Validation by Neutron Scattering Experiments. <i>Journal of Physical Chemistry B</i> , 2015, 119, 15287-15299.	2.6	42

#	ARTICLE	IF	CITATIONS
3540	A computational study of the self-assembly of the RFFFR peptide. <i>Physical Chemistry Chemical Physics</i> , 2015, 17, 30023-30036.	2.8	13
3541	Molecular simulation studies of hydrocarbon and carbon dioxide adsorption on coal. <i>Petroleum Science</i> , 2015, 12, 692-704.	4.9	25
3542	Phase Transition of Glycolipid Membranes Studied by Coarse-Grained Simulations. <i>Langmuir</i> , 2015, 31, 9379-9387.	3.5	15
3543	Structure Characterization and Properties of Metal–Surfactant Complexes Dispersed in Organic Solvents. <i>Langmuir</i> , 2015, 31, 9006-9016.	3.5	10
3544	The effect of time step, thermostat, and strain rate on ReaxFF simulations of mechanical failure in diamond, graphene, and carbon nanotube. <i>Journal of Computational Chemistry</i> , 2015, 36, 1587-1596.	3.3	81
3545	Computing the crystal growth rate by the interface pinning method. <i>Journal of Chemical Physics</i> , 2015, 142, 044104.	3.0	15
3546	A concurrent multiscale micromorphic molecular dynamics. <i>Journal of Applied Physics</i> , 2015, 117, .	2.5	21
3547	Bubble nucleation in simple and molecular liquids via the largest spherical cavity method. <i>Journal of Chemical Physics</i> , 2015, 142, 154903.	3.0	15
3548	Molecular dynamics simulations of solutions at constant chemical potential. <i>Journal of Chemical Physics</i> , 2015, 142, 144113.	3.0	63
3549	Role of string-like collective atomic motion on diffusion and structural relaxation in glass forming Cu-Zr alloys. <i>Journal of Chemical Physics</i> , 2015, 142, 164506.	3.0	97
3550	The crystal-fluid interfacial free energy and nucleation rate of NaCl from different simulation methods. <i>Journal of Chemical Physics</i> , 2015, 142, 194709.	3.0	59
3551	Impact of secondary structure and hydration water on the dielectric spectrum of poly-alanine and possible relation to the debate on slaved versus slaving water. <i>Journal of Chemical Physics</i> , 2015, 142, 215104.	3.0	6
3552	Complete catalytic cycle of cofactor-independent phosphoglycerate mutase involves a spring-loaded mechanism. <i>FEBS Journal</i> , 2015, 282, 1097-1110.	4.7	8
3553	Uncovering Nanoclusters in Amorphous AlN: An <i>Ab Initio</i> Study. <i>Journal of the American Ceramic Society</i> , 2015, 98, 1095-1098.	3.8	5
3554	Water density fluctuations relevant to hydrophobic hydration are unaltered by attractions. <i>Journal of Chemical Physics</i> , 2015, 142, 024502.	3.0	22
3555	Molecular Origin of DNA Kinking by Transcription Factors. <i>Journal of Physical Chemistry B</i> , 2015, 119, 11590-11596.	2.6	10
3556	Mechanical unfolding pathway of a model $\alpha$ -peptide foldamer. <i>Journal of Chemical Physics</i> , 2015, 142, 204901.	3.0	7
3557	The structure and IR signatures of the arginine-glutamate salt bridge. Insights from the classical MD simulations. <i>Journal of Chemical Physics</i> , 2015, 142, 215106.	3.0	18

#	ARTICLE	IF	CITATIONS
3558	Reference interaction site model with hydrophobicity induced density inhomogeneity: An analytical theory to compute solvation properties of large hydrophobic solutes in the mixture of polyatomic solvent molecules. <i>Journal of Chemical Physics</i> , 2015, 143, 054110.	3.0	9
3559	How Hydrophilic Proteins Form Nonspecific Complexes. <i>Journal of Physical Chemistry B</i> , 2015, 119, 10524-10530.	2.6	9
3560	Probing the mechanism of CO <sub>2</sub> capture in diamine-appended metal-organic frameworks using measured and simulated X-ray spectroscopy. <i>Physical Chemistry Chemical Physics</i> , 2015, 17, 21448-21457.	2.8	43
3561	Solvation thermodynamics of amino acid side chains on a short peptide backbone. <i>Journal of Chemical Physics</i> , 2015, 142, 144502.	3.0	16
3562	Understanding Nanopore Window Distortions in the Reversible Molecular Valve Zeolite RHO. <i>Chemistry of Materials</i> , 2015, 27, 5657-5667.	6.7	42
3563	Phase Segregation at the Liquid-Air Interface Prior to Liquid-Liquid Equilibrium. <i>Journal of Physical Chemistry B</i> , 2015, 119, 10304-10315.	2.6	8
3564	Destruction of amyloid fibrils by graphene through penetration and extraction of peptides. <i>Nanoscale</i> , 2015, 7, 18725-18737.	5.6	101
3565	Exploring LacDNA Dynamics by Multiscale Simulations Using the SIRAH Force Field. <i>Journal of Chemical Theory and Computation</i> , 2015, 11, 5012-5023.	5.3	28
3566	Predicting RNA Duplex Dimerization Free-Energy Changes upon Mutations Using Molecular Dynamics Simulations. <i>Journal of Physical Chemistry Letters</i> , 2015, 6, 4348-4351.	4.6	19
3567	Influence of the size and charge of gold nanoclusters on complexation with siRNA: a molecular dynamics simulation study. <i>Physical Chemistry Chemical Physics</i> , 2015, 17, 30307-30317.	2.8	12
3568	Chelerythrine-lysozyme interaction: spectroscopic studies, thermodynamics and molecular modeling exploration. <i>Physical Chemistry Chemical Physics</i> , 2015, 17, 16630-16645.	2.8	67
3569	How the spontaneous insertion of amphiphilic imidazolium-based cations changes biological membranes: a molecular simulation study. <i>Physical Chemistry Chemical Physics</i> , 2015, 17, 29171-29183.	2.8	48
3570	Molecular Basis for Differential Sensitivity of $\alpha$ -Conotoxin RegIIA at Rat and Human Neuronal Nicotinic Acetylcholine Receptors. <i>Molecular Pharmacology</i> , 2015, 88, 993-1001.	2.3	19
3571	The impact of interchain hydrogen bonding on $\hat{\tau}^2$ hairpin stability is readily predicted by molecular dynamics simulation. <i>Biopolymers</i> , 2015, 104, 703-706.	2.4	2
3572	Solution NMR and molecular dynamics reveal a persistent alpha helix within the dynamic region of PsbQ from photosystem II of higher plants. <i>Proteins: Structure, Function and Bioinformatics</i> , 2015, 83, 1677-1686.	2.6	4
3573	Direct Correlation of Cell Toxicity to Conformational Ensembles of Genetic A $\beta$ Variants. <i>ACS Chemical Neuroscience</i> , 2015, 6, 1990-1996.	3.5	16
3574	The molecular mechanism of Zinc acquisition by the neisserial outer-membrane transporter ZnuD. <i>Nature Communications</i> , 2015, 6, 7996.	12.8	58
3575	Arginine analogues incorporating carboxylate bioisosteric functions are micromolar inhibitors of human recombinant DDAH-1. <i>Organic and Biomolecular Chemistry</i> , 2015, 13, 11315-11330.	2.8	18

#	ARTICLE	IF	CITATIONS
3576	Effects of the C-Terminal Tail on the Conformational Dynamics of Human Neuronal Calcium Sensor-1 Protein. <i>Journal of Physical Chemistry B</i> , 2015, 119, 14236-14244.	2.6	5
3577	New High- and Low-Temperature Phase Changes of ZIF-7: Elucidation and Prediction of the Thermodynamics of Transitions. <i>Journal of the American Chemical Society</i> , 2015, 137, 13603-13611.	13.7	66
3578	Structural Ensembles of Intrinsically Disordered Proteins Depend Strongly on Force Field: A Comparison to Experiment. <i>Journal of Chemical Theory and Computation</i> , 2015, 11, 5513-5524.	5.3	368
3579	Glass Transition and Molecular Mobility in Styrene-Butadiene Rubber Modified Asphalt. <i>Journal of Physical Chemistry B</i> , 2015, 119, 14261-14269.	2.6	102
3580	Molecular Dynamics Investigation of Ion Sorption and Permeation in Desalination Membranes. <i>Journal of Physical Chemistry B</i> , 2015, 119, 14168-14179.	2.6	37
3581	Synaptobrevin Transmembrane Domain Dimerization Studied by Multiscale Molecular Dynamics Simulations. <i>Biophysical Journal</i> , 2015, 109, 760-771.	0.5	22
3582	Functional insights from molecular modeling, docking, and dynamics study of a cypoviral RNA dependent RNA polymerase. <i>Journal of Molecular Graphics and Modelling</i> , 2015, 61, 160-174.	2.4	5
3583	Multistep Molecular Dynamics Simulations Identify the Highly Cooperative Activity of Melittin in Recognizing and Stabilizing Membrane Pores. <i>Langmuir</i> , 2015, 31, 9388-9401.	3.5	45
3584	Coarse grained simulation reveals antifreeze properties of hyperactive antifreeze protein from Antarctic bacterium <i>Colwellia</i> sp.. <i>Chemical Physics Letters</i> , 2015, 638, 137-143.	2.6	5
3585	Ab Initio-Based Kinetic Modeling for the Design of Molecular Catalysts: The Case of H <sub>2</sub> Production Electrocatalysts. <i>ACS Catalysis</i> , 2015, 5, 5436-5452.	11.2	38
3586	From molecular systems to continuum solids: A multiscale structure and dynamics. <i>Journal of Chemical Physics</i> , 2015, 143, 064101.	3.0	16
3587	G Protein-Coupled Receptors in Drug Discovery. <i>Methods in Molecular Biology</i> , 2015, 1335, v.	0.9	7
3588	Thermodynamics of Micelle Formation and Membrane Fusion Modulate Antimicrobial Lipopeptide Activity. <i>Biophysical Journal</i> , 2015, 109, 750-759.	0.5	37
3589	External electric field reverses helical handedness of a supramolecular columnar stack. <i>Chemical Communications</i> , 2015, 51, 16049-16052.	4.1	22
3590	Mechanistic insights into protonation state as a critical factor in hFPPS enzyme inhibition. <i>Journal of Computer-Aided Molecular Design</i> , 2015, 29, 667-680.	2.9	2
3591	Effect of hydrogen on degradation mechanism of zirconium: A molecular dynamics study. <i>Journal of Nuclear Materials</i> , 2015, 466, 172-178.	2.7	18
3592	Atomistic modeling study of surface effect on oxide ion diffusion in yttria-stabilized zirconia. <i>Solid State Ionics</i> , 2015, 279, 46-52.	2.7	4
3593	Kinetic characteristics of conformational changes in the hexopyranose rings. <i>Carbohydrate Research</i> , 2015, 416, 41-50.	2.3	10

#	ARTICLE	IF	CITATIONS
3594	Thermodynamic and Structural Evidence for Reduced Hydrogen Bonding among Water Molecules near Small Hydrophobic Solutes. <i>Journal of Physical Chemistry B</i> , 2015, 119, 12108-12116.	2.6	35
3595	Swelling Properties of Montmorillonite and Beidellite Clay Minerals from Molecular Simulation: Comparison of Temperature, Interlayer Cation, and Charge Location Effects. <i>Journal of Physical Chemistry C</i> , 2015, 119, 20880-20891.	3.1	184
3596	An Analysis of Biomolecular Force Fields for Simulations of Polyglutamine in Solution. <i>Biophysical Journal</i> , 2015, 109, 1009-1018.	0.5	40
3597	Molecular View of Ligands Specificity for CAG Repeats in Anti-Huntington Therapy. <i>Journal of Chemical Theory and Computation</i> , 2015, 11, 4911-4922.	5.3	15
3598	Molecular Dynamics Study on the Growth Mechanism of Methane plus Tetrahydrofuran Mixed Hydrates. <i>Journal of Physical Chemistry C</i> , 2015, 119, 19883-19890.	3.1	31
3599	Evolution of network topology of bifunctional epoxy thermosets during cure and its relationship to thermo-mechanical properties: A molecular dynamics study. <i>Polymer</i> , 2015, 75, 151-160.	3.8	35
3600	Conformational Polymorphism in Autophagy-Related Protein GATE-16. <i>Biochemistry</i> , 2015, 54, 5469-5479.	2.5	17
3601	The binding of small carbazole derivative (P7C3) to protofibrils of the Alzheimer's disease and $\beta$ -secretase: Molecular dynamics simulation studies. <i>Chemical Physics</i> , 2015, 459, 31-39.	1.9	11
3602	PIP2 and Talin Join Forces to Activate Integrin. <i>Journal of Physical Chemistry B</i> , 2015, 119, 12381-12389.	2.6	27
3603	Atomic-scale investigation of creep behavior in nanocrystalline Mg and Mg-Y alloys. <i>Acta Materialia</i> , 2015, 99, 382-391.	7.9	66
3604	Variational cross-validation of slow dynamical modes in molecular kinetics. <i>Journal of Chemical Physics</i> , 2015, 142, 124105.	3.0	173
3605	Folding and binding energy of a calmodulin-binding cell antiproliferative peptide. <i>Journal of Molecular Graphics and Modelling</i> , 2015, 61, 281-289.	2.4	0
3606	The effect of amino substituents on the interactions of quinazalone derivatives with c-KIT G-quadruplex: insight from molecular dynamics simulation study for rational design of ligands. <i>RSC Advances</i> , 2015, 5, 76642-76650.	3.6	7
3607	Spatio-temporal correlations in aqueous systems: computational studies of static and dynamic heterogeneity by 2D-IR spectroscopy. <i>Faraday Discussions</i> , 2015, 177, 313-328.	3.2	7
3608	Structure and Function of the Escherichia coli Tol-Pal Stator Protein TolR. <i>Journal of Biological Chemistry</i> , 2015, 290, 26675-26687.	3.4	35
3609	Simulating Gram-Negative Bacterial Outer Membrane: A Coarse Grain Model. <i>Journal of Physical Chemistry B</i> , 2015, 119, 14668-14682.	2.6	69
3610	Structural studies on choline-carboxylate bio-ionic liquids by x-ray scattering and molecular dynamics. <i>Journal of Chemical Physics</i> , 2015, 143, 114506.	3.0	28
3611	Exploring the structure and conformational landscape of human leptin. A molecular dynamics approach. <i>Journal of Theoretical Biology</i> , 2015, 385, 90-101.	1.7	3



#	ARTICLE	IF	CITATIONS
3612	Multiscale Molecular Dynamics Simulations of Model Hydrophobically Modified Ethylene Oxide Urethane Micelles. <i>Journal of Physical Chemistry B</i> , 2015, 119, 12540-12551.	2.6	14
3613	Molecular Models of Nanodiscs. <i>Journal of Chemical Theory and Computation</i> , 2015, 11, 4923-4932.	5.3	33
3614	Mechanism of anisotropic surface self-diffusivity at the prismatic ice–vapor interface. <i>Physical Chemistry Chemical Physics</i> , 2015, 17, 22947-22958.	2.8	8
3615	Conformational Changes of the Antibacterial Peptide ATP Binding Cassette Transporter McjD Revealed by Molecular Dynamics Simulations. <i>Biochemistry</i> , 2015, 54, 5989-5998.	2.5	21
3616	Calculating the Fugacity of Pure, Low Volatile Liquids via Molecular Simulation with Application to Acetanilide, Acetaminophen, and Phenacetin. <i>Industrial &amp; Engineering Chemistry Research</i> , 2015, 54, 9027-9037.	3.7	24
3617	Decoding the Role of Water Dynamics in Ligand–Protein Unbinding: CRF <sub>1</sub> as a Test Case. <i>Journal of Chemical Information and Modeling</i> , 2015, 55, 1857-1866.	5.4	57
3618	Hydrophobicity: effect of density and order on water's rotational slowing down. <i>Soft Matter</i> , 2015, 11, 7977-7985.	2.7	13
3619	Polypeptide A9K at nanoscale carbon: a simulation study. <i>Physical Chemistry Chemical Physics</i> , 2015, 17, 26386-26393.	2.8	4
3620	The Dynamic Process of Drug–GPCR Binding at Either Orthosteric or Allosteric Sites Evaluated by Metadynamics. <i>Methods in Molecular Biology</i> , 2015, 1335, 277-294.	0.9	26
3621	Molecular dynamics simulations of self-assembled peptide amphiphile based cylindrical nanofibers. <i>RSC Advances</i> , 2015, 5, 66582-66590.	3.6	23
3622	Graphene exfoliation in ionic liquids: unified methodology. <i>RSC Advances</i> , 2015, 5, 81229-81234.	3.6	26
3623	How endoglucanase enzymes act on cellulose nanofibrils: role of amorphous regions revealed by atomistic simulations. <i>Cellulose</i> , 2015, 22, 2911-2925.	4.9	20
3624	Potential Application and Molecular Mechanisms of Soy Protein on the Enhancement of Graphite Nanoplatelet Dispersion. <i>Journal of Physical Chemistry C</i> , 2015, 119, 26760-26767.	3.1	13
3625	The tricyanomethanide anion favors low viscosity of the pure ionic liquid and its aqueous mixtures. <i>Physical Chemistry Chemical Physics</i> , 2015, 17, 31839-31849.	2.8	24
3626	Membrane accessibility of glutathione. <i>Biochimica Et Biophysica Acta - Biomembranes</i> , 2015, 1848, 2430-2436.	2.6	12
3627	Biochemical stability and molecular dynamic characterization of <i>Aspergillus fumigatus</i> cystathionine $\beta$ -lyase in response to various reaction effectors. <i>Enzyme and Microbial Technology</i> , 2015, 81, 31-46.	3.2	33
3628	Mutational analysis of the Notch2 negative regulatory region identifies key structural elements for mechanical stability. <i>FEBS Open Bio</i> , 2015, 5, 625-633.	2.3	3
3629	Influence of missing guest and host atoms on the mechanical and electronic properties of type-I clathrate compound Ba8Si46. <i>Journal of Alloys and Compounds</i> , 2015, 653, 77-87.	5.5	5



#	ARTICLE	IF	CITATIONS
3630	Evaluation of the GROMOS 56A<sub>CARBO</sub> Force Field for the Calculation of Structural, Volumetric, and Dynamic Properties of Aqueous Glucose Systems. Journal of Physical Chemistry B, 2015, 119, 15310-15319.	2.6	14
3631	Thin Water Films at Multifaceted Hematite Particle Surfaces. Langmuir, 2015, 31, 13127-13137.	3.5	24
3632	The influence of the hexopyranose ring geometry on the conformation of glycosidic linkages investigated using molecular dynamics simulations. Carbohydrate Research, 2015, 415, 17-27.	2.3	27
3633	Reactive Molecular Dynamics Simulations of Siliceous Solids Polycondensed from Tetra- and Trihydroxysilane. Journal of Non-Crystalline Solids, 2015, 429, 183-189.	3.1	10
3634	Intrinsic Structure of the Interface of Partially Miscible Fluids: An Application to Ionic Liquids. Journal of Physical Chemistry C, 2015, 119, 28448-28461.	3.1	15
3635	Anti-solvent crystallization of a ternary Lennard-Jones mixture performed by molecular dynamics. Journal of Molecular Liquids, 2015, 209, 1-5.	4.9	7
3636	Cosolvent Effects on Solute-Solvent Hydrogen-Bond Dynamics: Ultrafast 2D IR Investigations. Journal of Physical Chemistry B, 2015, 119, 15334-15343.	2.6	31
3637	Effects of thermodynamic inhibitors on the dissociation of methane hydrate: a molecular dynamics study. Physical Chemistry Chemical Physics, 2015, 17, 32347-32357.	2.8	67
3638	1-Butanol absorption in poly(styrene-divinylbenzene) ion exchange resins for catalysis. Soft Matter, 2015, 11, 9144-9149.	2.7	6
3639	A New Method for Navigating Optimal Direction for Pulling Ligand from Binding Pocket: Application to Ranking Binding Affinity by Steered Molecular Dynamics. Journal of Chemical Information and Modeling, 2015, 55, 2731-2738.	5.4	47
3640	Large-Scale Analysis of 48 DNA and 48 RNA Tetranucleotides Studied by 1 $\mu$ s Explicit-Solvent Molecular Dynamics Simulations. Journal of Chemical Theory and Computation, 2015, 11, 5906-5917.	5.3	20
3641	Binding assessment of two arachidonic-based synthetic derivatives of adrenalin with $\beta$ -lactoglobulin: Molecular modeling and chemometrics approach. Biophysical Chemistry, 2015, 207, 97-106.	2.8	3
3642	Femtosecond coherent anti-Stokes Raman scattering spectroscopy of hydrogen bonded structure in water and aqueous solutions. Spectrochimica Acta - Part A: Molecular and Biomolecular Spectroscopy, 2015, 151, 262-273.	3.9	18
3643	Influence of the Compatible Solute Ectoine on the Local Water Structure: Implications for the Binding of the Protein G5P to DNA. Journal of Physical Chemistry B, 2015, 119, 15212-15220.	2.6	51
3644	Liquids with permanent porosity. Nature, 2015, 527, 216-220.	27.8	402
3645	SIRAH: A Structurally Unbiased Coarse-Grained Force Field for Proteins with Aqueous Solvation and Long-Range Electrostatics. Journal of Chemical Theory and Computation, 2015, 11, 723-739.	5.3	139
3646	Basic structural units in carbon fibers: Atomistic models and tensile behavior. Carbon, 2015, 85, 72-78.	10.3	36
3647	What can we learn from molecular dynamics simulations for GPCR drug design?. Computational and Structural Biotechnology Journal, 2015, 13, 111-121.	4.1	60

#	ARTICLE	IF	CITATIONS
3648	The atomistic mechanism of hcp-to-bcc martensitic transformation in the Ti–Nb system revealed by molecular dynamics simulations. <i>Physical Chemistry Chemical Physics</i> , 2015, 17, 4184-4192.	2.8	8
3649	Exploring a Non-ATP Pocket for Potential Allosteric Modulation of PI3K $\beta$ . <i>Journal of Physical Chemistry B</i> , 2015, 119, 1002-1016.	2.6	30
3650	pmx: Automated protein structure and topology generation for alchemical perturbations. <i>Journal of Computational Chemistry</i> , 2015, 36, 348-354.	3.3	199
3651	Understanding the Thermostability and Activity of <i>Bacillus subtilis</i> Lipase Mutants: Insights from Molecular Dynamics Simulations. <i>Journal of Physical Chemistry B</i> , 2015, 119, 392-409.	2.6	58
3652	Conformational Dynamics of Shaker-Type Kv1.1 Ion Channel in Open, Closed, and Two Mutated States. <i>Journal of Membrane Biology</i> , 2015, 248, 241-255.	2.1	6
3653	Enhancement of Internal Motions of Lysozyme through Interaction with Gold Nanoclusters and its Optical Imaging. <i>Journal of Physical Chemistry C</i> , 2015, 119, 653-664.	3.1	15
3654	Primary radiation damage near grain boundary in bcc tungsten by molecular dynamics simulations. <i>Journal of Nuclear Materials</i> , 2015, 458, 138-145.	2.7	46
3655	Interactions of the EGFR juxtamembrane domain with PIP2-containing lipid bilayers: Insights from multiscale molecular dynamics simulations. <i>Biochimica Et Biophysica Acta - General Subjects</i> , 2015, 1850, 1017-1025.	2.4	66
3656	Enhancement of Thermostability and Kinetic Efficiency of <i>Aspergillus niger</i> PhyA Phytase by Site-Directed Mutagenesis. <i>Applied Biochemistry and Biotechnology</i> , 2015, 175, 2528-2541.	2.9	19
3657	Characterization of thermal oxide films formed on a duplex stainless steel by means of confocal-Raman microscopy and electrochemical techniques. <i>Thin Solid Films</i> , 2015, 576, 1-10.	1.8	28
3658	Toward structure prediction of cyclic peptides. <i>Physical Chemistry Chemical Physics</i> , 2015, 17, 4210-4219.	2.8	50
3659	The role of inversion domain boundaries in fabricating crack-free GaN films on sapphire substrates by hydride vapor phase epitaxy. <i>Materials Science and Engineering B: Solid-State Materials for Advanced Technology</i> , 2015, 193, 105-111.	3.5	7
3660	The role of hopping on transport above T <sub>c</sub> in glycerol. <i>Journal of Non-Crystalline Solids</i> , 2015, 407, 118-125.	3.1	6
3661	Accurate Multiple Time Step in Biased Molecular Simulations. <i>Journal of Chemical Theory and Computation</i> , 2015, 11, 139-146.	5.3	31
3662	Thermal- and urea-induced unfolding processes of glutathione S-transferase by molecular dynamics simulation. <i>Biopolymers</i> , 2015, 103, 247-259.	2.4	2
3663	Dry Martini, a Coarse-Grained Force Field for Lipid Membrane Simulations with Implicit Solvent. <i>Journal of Chemical Theory and Computation</i> , 2015, 11, 260-275.	5.3	236
3664	Thermodynamics of the self-assembly of non-ionic chromonic molecules using atomistic simulations. The case of TP6EO2M in aqueous solution. <i>Soft Matter</i> , 2015, 11, 680-691.	2.7	27
3665	Molecular mechanics and equation of state modeling of compressible polyolefin solutions: Impact of pressure and cut-off radius of intermolecular potentials. <i>Chemical Engineering Science</i> , 2015, 121, 100-109.	3.8	1

#	ARTICLE	IF	CITATIONS
3666	Molecular dynamics simulations of negatively charged DPPC/DPPI lipid bilayers at two levels of resolution. Computational and Theoretical Chemistry, 2015, 1058, 61-66.	2.5	15
3667	Engineering molecular dynamics simulation in chemical engineering. Chemical Engineering Science, 2015, 121, 200-216.	3.8	18
3668	Automatic GROMACS Topology Generation and Comparisons of Force Fields for Solvation Free Energy Calculations. Journal of Physical Chemistry B, 2015, 119, 810-823.	2.6	88
3669	Self-Assembly of Phenylalanine-Based Molecules. Journal of Physical Chemistry A, 2015, 119, 1609-1615.	2.5	67
3670	Experimental determination and computational interpretation of biophysical properties of lipid bilayers enriched by cholesterol hemisuccinate. Biochimica Et Biophysica Acta - Biomembranes, 2015, 1848, 422-432.	2.6	45
3671	Electronic and structural properties of bulk arsenopyrite and its cleavage surfaces – a DFT study. RSC Advances, 2015, 5, 2013-2023.	3.6	34
3672	A simulation study on the significant nanomechanical heterogeneous properties of collagen. Biomechanics and Modeling in Mechanobiology, 2015, 14, 445-457.	2.8	13
3673	Molecular mechanisms for intrafibrillar collagen mineralization in skeletal tissues. Biomaterials, 2015, 39, 59-66.	11.4	89
3674	Coupling the finite element method and molecular dynamics in the framework of the heterogeneous multiscale method for quasi-static isothermal problems. Journal of the Mechanics and Physics of Solids, 2015, 74, 1-18.	4.8	23
3675	Structural signature of the G719S-T790M double mutation in the EGFR kinase domain and its response to inhibitors. Scientific Reports, 2014, 4, 5868.	3.3	37
3676	Interactions of Lipids and Detergents with a Viral Ion Channel Protein: Molecular Dynamics Simulation Studies. Journal of Physical Chemistry B, 2015, 119, 764-772.	2.6	21
3677	Stability analysis for binary sll hydrogen-promoter hydrates by molecular dynamics simulation. Molecular Simulation, 2015, 41, 735-740.	2.0	4
3678	An <i>in silico</i> structural insights into <i>Plasmodium</i> LytB protein and its inhibition. Journal of Biomolecular Structure and Dynamics, 2015, 33, 1198-1210.	3.5	7
3679	Investigation for antimicrobial resistance-modulating activity of diethyl malate and 1-methyl malate against beta-lactamase class A from <i>Bacillus licheniformis</i> by molecular dynamics, <i>in vitro</i> and <i>in vivo</i> studies. Journal of Biomolecular Structure and Dynamics, 2015, 33, 1016-1026.	3.5	12
3680	The effect of structural parameters and positive charge distance on the interaction free energy of antimicrobial peptides with membrane surface. Journal of Biomolecular Structure and Dynamics, 2015, 33, 502-512.	3.5	1
3681	Dielectric and Terahertz Spectroscopy of Polarizable and Nonpolarizable Water Models: A Comparative Study. Journal of Physical Chemistry A, 2015, 119, 1539-1547.	2.5	47
3682	In silico 3D structure modeling and inhibitor binding studies of human male germ cell-associated kinase. Journal of Biomolecular Structure and Dynamics, 2015, 33, 1710-1719.	3.5	5
3683	Molecular scale study on solutions of asphaltene deposition problems in oil production. Journal of the Japanese Association for Petroleum Technology, 2016, 81, 469-478.	0.0	2

#	ARTICLE	IF	CITATIONS
3684	Ab-Initio Modeling of Adhesive Behaviors at Material Interfaces. , 2016, , .		0
3685	Calculation of thermophysical properties of magnesium antimonide ( $\alpha$ -Mg <sub>3</sub> Sb <sub>2</sub> ). Turkish Journal of Physics, 2016, 40, 264-269.	1.1	1
3686	Effect of Post-Translational Amidation on Islet Amyloid Polypeptide Conformational Ensemble: Implications for Its Aggregation Early Steps. International Journal of Molecular Sciences, 2016, 17, 1896.	4.1	7
3687	Dynamics of the Large Progenitor Toxin Complex of Clostridium botulinum. Journal of Computer Science and Systems Biology, 2016, 09, .	0.0	0
3688	Assembling the Tat protein translocase. ELife, 2016, 5, .	6.0	62
3689	Structural Dynamics of Human Argonaute2 and Its Interaction with siRNAs Designed to Target Mutant tdp43. Advances in Bioinformatics, 2016, 2016, 1-13.	5.7	19
3690	Molecular Dynamics Simulation Study of the Selectivity of a Silica Polymer for Ibuprofen. International Journal of Molecular Sciences, 2016, 17, 1083.	4.1	7
3691	Development of novel HER2 inhibitors against gastric cancer derived from flavonoid source of <em>Syzygium alternifolium</em> through molecular dynamics and pharmacophore-based screening. Drug Design, Development and Therapy, 2016, Volume 10, 3611-3632.	4.3	16
3692	Combined computational and experimental studies of molecular interactions of albuterol sulfate with bovine serum albumin for pulmonary drug nanoparticles. Drug Design, Development and Therapy, 2016, Volume 10, 2973-2987.	4.3	9
3693	The D173G mutation in ADAMTS-13 causes a severe form of congenital thrombotic thrombocytopenic purpura. Thrombosis and Haemostasis, 2016, 115, 51-62.	3.4	14
3694	Structure and Ionic Conductivity of Li <sub>2</sub> S-P <sub>2</sub> S <sub>5</sub> Glass Electrolytes Simulated with First-Principles Molecular Dynamics. Frontiers in Energy Research, 2016, 4, .	2.3	33
3695	High Transmembrane Voltage Raised by Close Contact Initiates Fusion Pore. Frontiers in Molecular Neuroscience, 2016, 9, 136.	2.9	10
3696	Computational Analysis of Structure-Based Interactions for Novel H1-Antihistamines. International Journal of Molecular Sciences, 2016, 17, 129.	4.1	21
3697	A Theoretical Study of the Hydration of Methane, from the Aqueous Solution to the sl Hydrate-Liquid Water-Gas Coexistence. International Journal of Molecular Sciences, 2016, 17, 378.	4.1	11
3698	Lattice Dynamics Study of Phonon Instability and Thermal Properties of Type-I Clathrate K <sub>8</sub> Si <sub>46</sub> under High Pressure. Materials, 2016, 9, 616.	2.9	2
3699	As Simple As Possible, but Not Simpler: Exploring the Fidelity of Coarse-Grained Protein Models for Simulated Force Spectroscopy. PLoS Computational Biology, 2016, 12, e1005211.	3.2	32
3700	Membrane Mediated Antimicrobial and Antitumor Activity of Cathelicidin 6: Structural Insights from Molecular Dynamics Simulation on Multi-Microsecond Scale. PLoS ONE, 2016, 11, e0158702.	2.5	14
3701	Coenzyme Q Biosynthesis: Evidence for a Substrate Access Channel in the FAD-Dependent Monooxygenase Coq6. PLoS Computational Biology, 2016, 12, e1004690.	3.2	10

#	ARTICLE	IF	CITATIONS
3702	Multiscale Simulations Suggest a Mechanism for the Association of the Dok7 PH Domain with PIP-Containing Membranes. <i>PLoS Computational Biology</i> , 2016, 12, e1005028.	3.2	24
3703	Induced Fit in Protein Multimerization: The HFBI Case. <i>PLoS Computational Biology</i> , 2016, 12, e1005202.	3.2	4
3704	Cholesterol Corrects Altered Conformation of MHC-II Protein in <i>Leishmania donovani</i> Infected Macrophages: Implication in Therapy. <i>PLoS Neglected Tropical Diseases</i> , 2016, 10, e0004710.	3.0	25
3705	Exploration of Novel Inhibitors for Bruton's Tyrosine Kinase by 3D QSAR Modeling and Molecular Dynamics Simulation. <i>PLoS ONE</i> , 2016, 11, e0147190.	2.5	24
3706	Viral Evolved Inhibition Mechanism of the RNA Dependent Protein Kinase PKR's Kinase Domain, a Structural Perspective. <i>PLoS ONE</i> , 2016, 11, e0153680.	2.5	4
3707	Rational Design of Disulfide Bonds Increases Thermostability of a Mesophilic 1,3-1,4- $\beta$ -Glucanase from <i>Bacillus terquilensis</i> . <i>PLoS ONE</i> , 2016, 11, e0154036.	2.5	31
3708	Bending-Twisting Motions and Main Interactions in Nucleoplasmin Nuclear Import. <i>PLoS ONE</i> , 2016, 11, e0157162.	2.5	3
3709	Crystal Structures of the Global Regulator DasR from <i>Streptomyces coelicolor</i> : Implications for the Allosteric Regulation of GntR/HutC Repressors. <i>PLoS ONE</i> , 2016, 11, e0157691.	2.5	21
3710	Microscopic Dynamics and Topology of Polymer Rings Immersed in a Host Matrix of Longer Linear Polymers: Results from a Detailed Molecular Dynamics Simulation Study and Comparison with Experimental Data. <i>Polymers</i> , 2016, 8, 283.	4.5	29
3711	The Role of Cholesterol in Driving IAPP-Membrane Interactions. <i>Biophysical Journal</i> , 2016, 111, 140-151.	0.5	74
3712	The Molecular Switching Mechanism at the Conserved D(E)RY Motif in Class-A GPCRs. <i>Biophysical Journal</i> , 2016, 111, 79-89.	0.5	19
3713	Replica Exchange Molecular Dynamics Study of Dimerization in Prion Protein: Multiple Modes of Interaction and Stabilization. <i>Journal of Physical Chemistry B</i> , 2016, 120, 7332-7345.	2.6	12
3714	Iminoguanidines as Allosteric Inhibitors of the Iron-Regulated Heme Oxygenase (Hemo) of <i>Pseudomonas aeruginosa</i> . <i>Journal of Medicinal Chemistry</i> , 2016, 59, 6929-6942.	6.4	33
3715	Partial auxeticity induced by nanoslits in the Yukawa crystal. <i>Physica Status Solidi - Rapid Research Letters</i> , 2016, 10, 566-569.	2.4	36
3716	A Dewetting-Induced Assembly Strategy for Precisely Patterning Organic Single Crystals in OFETs. <i>ACS Applied Materials &amp; Interfaces</i> , 2016, 8, 18978-18984.	8.0	18
3717	Exploration of the presence of bulk-like water in AOT reverse micelles and water-in-oil nanodroplets: the role of charged interfaces, confinement size and properties of water. <i>Physical Chemistry Chemical Physics</i> , 2016, 18, 21767-21779.	2.8	26
3718	DIRECT: An automated method to identify and quantify conformational variations' application to $\beta_2$ -adrenergic GPCR. <i>Journal of Computational Chemistry</i> , 2016, 37, 416-425.	3.3	13
3719	A role for loop C in the $\beta_1$ strand in GABA <sub>A</sub> receptor activation. <i>Journal of Physiology</i> , 2016, 594, 5555-5571.	2.9	7

#	ARTICLE	IF	CITATIONS
3720	Engineered human angiogenin mutations in the placental ribonuclease inhibitor complex for anticancer therapy: Insights from enhanced sampling simulations. <i>Protein Science</i> , 2016, 25, 1451-1460.	7.6	11
3721	Vortex formation in coalescence of droplets with a reservoir using molecular dynamics simulations. <i>Journal of Colloid and Interface Science</i> , 2016, 479, 189-198.	9.4	8
3722	Reactive Molecular Dynamics Simulations of the Silanization of Silica Substrates by Methoxysilanes and Hydroxysilanes. <i>Langmuir</i> , 2016, 32, 7045-7055.	3.5	8
3723	Predicting the Structure-Activity Relationship of Hydroxyapatite-Binding Peptides by Enhanced-Sampling Molecular Simulation. <i>Langmuir</i> , 2016, 32, 7009-7022.	3.5	39
3724	Accurately modeling nanosecond protein dynamics requires at least microseconds of simulation. <i>Journal of Computational Chemistry</i> , 2016, 37, 558-566.	3.3	51
3725	Polyamorphism in Aluminum Nitride: A First Principles Molecular Dynamics Study. <i>Journal of the American Ceramic Society</i> , 2016, 99, 1594-1600.	3.8	8
3726	Free energy simulations with the AMOEBA polarizable force field and metadynamics on GPU platform. <i>Journal of Computational Chemistry</i> , 2016, 37, 614-622.	3.3	12
3727	Small Peptides Derived from Penetratin as Antibacterial Agents. <i>Archiv Der Pharmazie</i> , 2016, 349, 242-251.	4.1	8
3728	Identification of 1 <i>H</i> -indene-(1,3,5,6)-tetrol derivatives as potent pancreatic lipase inhibitors using molecular docking and molecular dynamics approach. <i>Biotechnology and Applied Biochemistry</i> , 2016, 63, 765-778.	3.1	8
3729	Controlling the Integration of Polyvinylpyrrolidone onto Substrate by Quartz Crystal Microbalance with Dissipation To Achieve Excellent Protein Resistance and Detoxification. <i>ACS Applied Materials &amp; Interfaces</i> , 2016, 8, 18684-18692.	8.0	12
3730	Permeability Coefficients of Lipophilic Compounds Estimated by Computer Simulations. <i>Journal of Chemical Theory and Computation</i> , 2016, 12, 4093-4099.	5.3	22
3731	Molecular Dynamics Simulation Study of Parallel Telomeric DNA Quadruplexes at Different Ionic Strengths: Evaluation of Water and Ion Models. <i>Journal of Physical Chemistry B</i> , 2016, 120, 7380-7391.	2.6	28
3732	Structural studies and SH3 domain binding properties of a human antiviral salivary proline-rich peptide. <i>Biopolymers</i> , 2016, 106, 714-725.	2.4	6
3733	Tailoring Poisson's ratio by introducing auxetic layers. <i>Physica Status Solidi (B): Basic Research</i> , 2016, 253, 1318-1323.	1.5	48
3734	Thermal Imprint Introduced Crystallization of A Solution Processed Subphthalocyanine Thin Film. <i>Advanced Materials Interfaces</i> , 2016, 3, 1600179.	3.7	5
3735	Simulation of coupled folding and binding of an intrinsically disordered protein in explicit solvent with metadynamics. <i>Journal of Molecular Graphics and Modelling</i> , 2016, 68, 114-127.	2.4	21
3736	Thermostability Mechanism for the Hyperthermophilicity of Extremophile Cellulase <i>TmCel12A</i> : Implied from Molecular Dynamics Simulation. <i>Journal of Physical Chemistry B</i> , 2016, 120, 7346-7352.	2.6	4
3737	Molecular Simulation Study of the Early Stages of Formation of Bioinspired Mesoporous Silica Materials. <i>Langmuir</i> , 2016, 32, 7228-7240.	3.5	9



#	ARTICLE	IF	CITATIONS
3738	A variational approach to nucleation simulation. <i>Faraday Discussions</i> , 2016, 195, 557-568.	3.2	15
3739	Solvation structure of sodium chloride ( $\text{Na}^+\text{Cl}^-$ ) ion pair in acetonitrile (AN)-dimethyl formamide (DMF) mixtures. <i>Molecular Simulation</i> , 2016, 42, 1193-1201.	2.0	6
3740	Improved model of hydrated calcium ion for molecular dynamics simulations using classical biomolecular force fields. <i>Biopolymers</i> , 2016, 105, 752-763.	2.4	40
3741	Avalanche mediated devitrification in a glass of pseudo hard-spheres. <i>Journal of Statistical Mechanics: Theory and Experiment</i> , 2016, 2016, 094005.	2.3	12
3742	Atomistic Molecular Dynamics Simulations of Carbon Dioxide Diffusivity in <i>n</i> -Hexane, <i>n</i> -Decane, <i>n</i> -Hexadecane, Cyclohexane, and Squalane. <i>Journal of Physical Chemistry B</i> , 2016, 120, 12890-12900.	2.6	53
3743	Stearylated cycloarginine nanosystems for intracellular delivery – simulations, formulation and proof of concept. <i>RSC Advances</i> , 2016, 6, 113538-113550.	3.6	17
3744	On the ability of molecular dynamics simulation and continuum electrostatics to treat interfacial water molecules in protein-protein complexes. <i>Scientific Reports</i> , 2016, 6, 38259.	3.3	11
3745	Unravelling the Structural Changes in $\alpha$ -Helical Peptides on Interaction with Convex, Concave, and Planar Surfaces of Boron-Nitride-Based Nanomaterials. <i>Journal of Physical Chemistry C</i> , 2016, 120, 28246-28260.	3.1	14
3746	Creating new layered structures at high pressures: SiS <sub>2</sub> . <i>Scientific Reports</i> , 2016, 6, 37694.	3.3	21
3747	Photocontrollable Self-Assembly of Azobenzene-Decorated Nanoparticles in Bulk: Computer Simulation Study. <i>Macromolecules</i> , 2016, 49, 9272-9282.	4.8	23
3748	Key diffusion mechanisms involved in regulating bidirectional water permeation across <i>E. coli</i> outer membrane lectin. <i>Scientific Reports</i> , 2016, 6, 28157.	3.3	7
3749	Theoretical approaches for studying anisotropic negative thermal expansion: A case of cordierite. <i>Journal of the Ceramic Society of Japan</i> , 2016, 124, 744-749.	1.1	4
3750	Light-induced structural changes in a monomeric bacteriophytochrome. <i>Structural Dynamics</i> , 2016, 3, 054701.	2.3	34
3751	Tackling amyloidogenesis in Alzheimer's disease with A2V variants of Amyloid- $\beta$ . <i>Scientific Reports</i> , 2016, 6, 20949.	3.3	26
3752	Spotting the difference in molecular dynamics simulations of biomolecules. <i>Journal of Chemical Physics</i> , 2016, 145, 074116.	3.0	14
3753	A comprehensive scenario of the thermodynamic anomalies of water using the TIP4P/2005 model. <i>Journal of Chemical Physics</i> , 2016, 145, 054505.	3.0	48
3754	Structural and activity characterization of human PHPT1 after oxidative modification. <i>Scientific Reports</i> , 2016, 6, 23658.	3.3	13
3755	Structural relaxation of acridine orange dimer in bulk water and inside a single live lung cell. <i>Journal of Chemical Physics</i> , 2016, 144, 065101.	3.0	18



#	ARTICLE	IF	CITATIONS
3756	On the calculation of solubilities via direct coexistence simulations: Investigation of NaCl aqueous solutions and Lennard-Jones binary mixtures. <i>Journal of Chemical Physics</i> , 2016, 145, 154111.	3.0	80
3757	A map of binding cavity conformations reveals differences in binding specificity. , 2016, , .		0
3758	Liquid-liquid phase separation of N-isopropylpropionamide aqueous solutions above the lower critical solution temperature. <i>Scientific Reports</i> , 2016, 6, 24657.	3.3	19
3759	Molecular Dynamics Study of the Structure and Permeability of Polymer Electrolyte Membranes for Fuel Cells. <i>Kobunshi Ronbunshu</i> , 2016, 73, 520-531.	0.2	0
3760	Detecting O <sub>2</sub> binding sites in protein cavities. <i>Scientific Reports</i> , 2016, 6, 20534.	3.3	18
3761	A molecular dynamics simulations study on ethylene glycol-water mixtures in mesoporous silica. <i>Journal of Chemical Physics</i> , 2016, 145, 104703.	3.0	21
3762	Molecular dynamics simulation elucidates the preferential binding affinity of sodium and tetramethylammonium ions for tetrameric Nafion unit under aqueous conditions. <i>RSC Advances</i> , 2016, 6, 97961-97968.	3.6	6
3763	The allosteric switching mechanism in bacteriophage MS2. <i>Journal of Chemical Physics</i> , 2016, 145, 035101.	3.0	12
3764	On the interpretation of reflectivity data from lipid bilayers in terms of molecular-dynamics models. <i>Acta Crystallographica Section D: Structural Biology</i> , 2016, 72, 1227-1240.	2.3	10
3765	Solvent organization around the perfluoro group of coumarin 153 governs its photophysical properties: An experimental and simulation study of coumarin dyes in ethanol as well as fluorinated ethanol solvents. <i>Journal of Chemical Physics</i> , 2016, 144, 184504.	3.0	15
3766	Temperature and pressure dependence of the interfacial free energy against a hard surface in contact with water and decane. <i>Journal of Chemical Physics</i> , 2016, 145, 124710.	3.0	6
3767	Two distinct crystallization processes in supercooled liquid. <i>Journal of Chemical Physics</i> , 2016, 144, 194505.	3.0	7
3768	The effects of replacing the water model while decoupling water-water and water-solute interactions on computed properties of simple salts. <i>Journal of Chemical Physics</i> , 2016, 145, 044501.	3.0	5
3769	Structure and dynamics of ionic liquids: Trimethylsilylpropyl-substituted cations and bis(sulfonyl)amide anions. <i>Journal of Chemical Physics</i> , 2016, 145, 244506.	3.0	27
3770	Elastic properties of gold supracrystals: Effects of nanocrystal size, ligand length, and nanocrystallinity. <i>Journal of Chemical Physics</i> , 2016, 144, 144507.	3.0	16
3771	Temperature of maximum density and excess thermodynamics of aqueous mixtures of methanol. <i>Journal of Chemical Physics</i> , 2016, 144, 184505.	3.0	18
3772	Size effects of 109 Å domain walls in rhombohedral barium titanate single crystals—A molecular statics analysis. <i>Journal of Applied Physics</i> , 2016, 119, .	2.5	6
3773	Effect of Polydispersity of Clay Platelets on the Aggregation and Mechanical Properties of Clay at the Mesoscale. <i>Clays and Clay Minerals</i> , 2016, 64, 425-437.	1.3	14

#	ARTICLE	IF	CITATIONS
3774	Super-Maxwellian helium evaporation from pure and salty water. Journal of Chemical Physics, 2016, 144, 044707.	3.0	15
3775	Low-frequency dynamics of aqueous alkali chloride solutions as probed by terahertz spectroscopy. Journal of Chemical Physics, 2016, 144, 234501.	3.0	12
3776	Striped gold nanoparticles: New insights from molecular dynamics simulations. Journal of Chemical Physics, 2016, 144, 244710.	3.0	12
3777	Structural Dynamics of the Heterodimeric ABC Transporter TM287/288 Induced by ATP and Substrate Binding. Biochemistry, 2016, 55, 6730-6738.	2.5	10
3778	Hysteresis and the Cholesterol Dependent Phase Transition in Binary Lipid Mixtures with the Martini Model. Journal of Physical Chemistry B, 2016, 120, 13086-13093.	2.6	14
3779	The thermodynamics and kinetics of a nucleotide base pair. Journal of Chemical Physics, 2016, 144, 115101.	3.0	30
3780	Structure of ionic liquids with cationic silicon-substitutions. Journal of Chemical Physics, 2016, 145, .	3.0	21
3781	A one-way shooting algorithm for transition path sampling of asymmetric barriers. Journal of Chemical Physics, 2016, 145, 164112.	3.0	28
3782	Effect of alcohol on the structure of cytochrome C: FCS and molecular dynamics simulations. Journal of Chemical Physics, 2016, 145, 235102.	3.0	25
3783	Mechanisms and rate of dislocation nucleation in aluminum-copper alloys near Guinier-Preston zones. Journal of Applied Physics, 2016, 120, 235106.	2.5	13
3784	A multiscale transport model for Lennard-Jones binary mixtures based on interfacial friction. Journal of Chemical Physics, 2016, 145, 074115.	3.0	5
3785	Pressure-dependent morphology of trihexyl(tetradecyl)phosphonium ionic liquids: A molecular dynamics study. Journal of Chemical Physics, 2016, 145, 134506.	3.0	33
3786	Delayed yield in colloidal gels: Creep, flow, and re-entrant solid regimes. Journal of Rheology, 2016, 60, 783-807.	2.6	79
3787	Structure of cyano-anion ionic liquids: X-ray scattering and simulations. Journal of Chemical Physics, 2016, 145, 024503.	3.0	54
3788	Molecular dynamics simulation of a binary mixture near the lower critical point. Journal of Chemical Physics, 2016, 145, 014501.	3.0	10
3789	Structure of ring-shaped A $\beta$ 242 oligomers determined by conformational selection. Scientific Reports, 2016, 6, 21429.	3.3	32
3790	Properties of high-density, well-ordered, and high-energy metallic glass phase designed by pressurized quenching. Applied Physics Letters, 2016, 109, .	3.3	14
3791	First Principles Calculations of Stress-Induced Structural Changes of Supercooled Borosilicate Glass. Key Engineering Materials, 0, 725, 399-404.	0.4	0

#	ARTICLE	IF	CITATIONS
3792	Unveiling the Pathogenic Molecular Mechanisms of the Most Common Variant (p.K329E) in Medium-Chain Acyl-CoA Dehydrogenase Deficiency by <i>in Vitro</i> and <i>in Silico</i> Approaches. <i>Biochemistry</i> , 2016, 55, 7086-7098.	2.5	5
3793	Distinct Roles of Histone H3 and H2A Tails in Nucleosome Stability. <i>Scientific Reports</i> , 2016, 6, 31437.	3.3	79
3794	CL-20/DNB co-crystal based PBX with PEG: molecular dynamics simulation. <i>Modelling and Simulation in Materials Science and Engineering</i> , 2016, 24, 085008.	2.0	9
3795	Towards a structural biology of the hydrophobic effect in protein folding. <i>Scientific Reports</i> , 2016, 6, 28285.	3.3	91
3796	Communication: Nanoscale structure of tetradecyltriethylphosphonium based ionic liquids. <i>Journal of Chemical Physics</i> , 2016, 144, 121102.	3.0	44
3797	Molecular dynamics at constant Cauchy stress. <i>Journal of Chemical Physics</i> , 2016, 144, 184107.	3.0	21
3798	Ion Pathways in the Na <sup>+</sup> /K <sup>+</sup> -ATPase. <i>Journal of Chemical Information and Modeling</i> , 2016, 56, 2434-2444.	5.4	21
3799	Collapse/Swelling Transitions of a Thermoresponsive, Single Poly( <i>N</i> -isopropylacrylamide) Chain in Water. <i>Journal of Physical Chemistry B</i> , 2016, 120, 13184-13192.	2.6	49
3800	Structure of small associates of glycyrrhizic acid with cholesterol in aqueous solution: Molecular dynamics simulation. <i>Journal of Structural Chemistry</i> , 2016, 57, 940-946.	1.0	1
3801	Two-state thermodynamics and the possibility of a liquid-liquid phase transition in supercooled TIP4P/2005 water. <i>Journal of Chemical Physics</i> , 2016, 144, 144504.	3.0	145
3802	Coarse-grained models using local-density potentials optimized with the relative entropy: Application to implicit solvation. <i>Journal of Chemical Physics</i> , 2016, 145, 034109.	3.0	83
3803	On the time required to freeze water. <i>Journal of Chemical Physics</i> , 2016, 145, 211922.	3.0	64
3804	Molecular dynamics and simulations study on the vibrational and electronic solvatochromism of benzophenone. <i>Journal of Chemical Physics</i> , 2016, 144, 064302.	3.0	21
3805	Membrane Anchoring and Ion-Entry Dynamics in P-type ATPase Copper Transport. <i>Biophysical Journal</i> , 2016, 111, 2417-2429.	0.5	16
3806	Characterization of the Annonaceous acetogenin, annonacinone, a natural product inhibitor of plasminogen activator inhibitor-1. <i>Scientific Reports</i> , 2016, 6, 36462.	3.3	8
3807	Nanobubbles, cavitation, shock waves and traumatic brain injury. <i>Physical Chemistry Chemical Physics</i> , 2016, 18, 32638-32652.	2.8	37
3808	Genetic Algorithm Managed Peptide Mutant Screening: Optimizing Peptide Ligands for Targeted Receptor Binding. <i>Journal of Chemical Information and Modeling</i> , 2016, 56, 2378-2387.	5.4	10
3809	Probing the Soft and Nanoductile Mechanical Nature of Single and Polycrystalline Organic-Inorganic Hybrid Perovskites for Flexible Functional Devices. <i>ACS Nano</i> , 2016, 10, 11044-11057.	14.6	89

#	ARTICLE	IF	CITATIONS
3810	Influence of the anions on the N-cationic benzethonium salts in the solid state and solution: Chloride, bromide, hydroxide and citrate hydrates. AIP Advances, 2016, 6, .	1.3	4
3811	A critical appraisal of the zero-multipole method: Structural, thermodynamic, dielectric, and dynamical properties of a water system. Journal of Chemical Physics, 2016, 144, 114503.	3.0	23
3812	Full-length model of the human galectin-4 and insights into dynamics of inter-domain communication. Scientific Reports, 2016, 6, 33633.	3.3	15
3813	Design principles for high- pressure force fields: Aqueous TMAO solutions from ambient to kilobar pressures. Journal of Chemical Physics, 2016, 144, 144104.	3.0	79
3814	Molecular modeling and simulation of atactic polystyrene/amorphous silica nanocomposites. Journal of Physics: Conference Series, 2016, 738, 012021.	0.4	2
3815	Conformational Flexibility of a Short Loop near the Active Site of the SARS-3CLpro is Essential to Maintain Catalytic Activity. Scientific Reports, 2016, 6, 20918.	3.3	20
3816	System-size corrections for self-diffusion coefficients calculated from molecular dynamics simulations: The case of CO <sub>2</sub> , <i>n</i> -alkanes, and poly(ethylene glycol) dimethyl ethers. Journal of Chemical Physics, 2016, 145, 074109.	3.0	101
3817	The temperature dependence of intermediate range oxygen-oxygen correlations in liquid water. Journal of Chemical Physics, 2016, 145, 084503.	3.0	33
3818	Molecular dynamics analysis of the effect of electronic polarization on the structure and single-particle dynamics of mixtures of ionic liquids and lithium salts. Journal of Chemical Physics, 2016, 145, 204507.	3.0	28
3819	Predictions of thermal expansion coefficients of rare-earth zirconate pyrochlores: A quasi-harmonic approximation based on stable phonon modes. Journal of Applied Physics, 2016, 119, .	2.5	7
3820	A canonical replica exchange molecular dynamics implementation with normal pressure in each replica. Journal of Chemical Physics, 2016, 145, 044903.	3.0	6
3821	A first principle particle mesh method for solution SAXS of large bio-molecular systems. Journal of Chemical Physics, 2016, 145, 045101.	3.0	7
3822	Exploration of multiple Sortase A protein conformations in virtual screening. Scientific Reports, 2016, 6, 20413.	3.3	14
3823	Multi-scale computational evaluation of hole mobility in amorphous polyethylene. , 2016, , .		14
3824	On the structure of crystalline and molten cryolite: Insights from the <i>ab initio</i> molecular dynamics in NpT ensemble. Journal of Chemical Physics, 2016, 144, 064502.	3.0	18
3825	Silicon-wall interfacial free energy via thermodynamics integration. Journal of Chemical Physics, 2016, 145, 184702.	3.0	6
3826	New Insights into Molecular Organization of Human Neuraminidase-1: Transmembrane Topology and Dimerization Ability. Scientific Reports, 2016, 6, 38363.	3.3	44
3827	A link between structure, diffusion and rotations of hydrogen bonding tracers in ionic liquids. Journal of Chemical Physics, 2016, 144, 204504.	3.0	36

#	ARTICLE	IF	CITATIONS
3828	Seeding approach to crystal nucleation. Journal of Chemical Physics, 2016, 144, 034501.	3.0	155
3829	Prediction of pressure-promoted thermal rejuvenation in metallic glasses. Npj Computational Materials, 2016, 2, .	8.7	67
3830	Adenylylation of Tyr77 stabilizes Rab1b GTPase in an active state: A molecular dynamics simulation analysis. Scientific Reports, 2016, 6, 19896.	3.3	13
3831	A new intermolecular potential for simulations of methanol: The OPLS/2016 model. Journal of Chemical Physics, 2016, 145, 034508.	3.0	30
3832	Adaptive resolution simulation of oligonucleotides. Journal of Chemical Physics, 2016, 145, 234101.	3.0	14
3833	Influence of Tacticity on Hydrophobicity of Poly(N-isopropylacrylamide): A Single Chain Molecular Dynamics Simulation Study. Journal of Physical Chemistry B, 2016, 120, 3765-3776.	2.6	45
3834	A Critical Comparison of Biomembrane Force Fields: Structure and Dynamics of Model DMPC, POPC, and POPE Bilayers. Journal of Physical Chemistry B, 2016, 120, 3888-3903.	2.6	138
3835	Modeling of Thermal Effect on the Electronic Properties of Photovoltaic Perovskite $\text{CH}_3\text{NH}_3\text{PbI}_3$ : The Case of Tetragonal Phase. Journal of Physical Chemistry C, 2016, 120, 7976-7986.	3.1	25
3836	Computational Approach to Explore the B/A Junction Free Energy in DNA. ChemPhysChem, 2016, 17, 147-154.	2.1	2
3837	Enhanced auxeticity in Yukawa systems due to introduction of nanochannels in $[001]$ -direction. Smart Materials and Structures, 2016, 25, 054007.	3.5	44
3838	Simulation of Temperature-Dependent Charge Transport in Organic Semiconductors with Various Degrees of Disorder. Journal of Chemical Theory and Computation, 2016, 12, 3087-3096.	5.3	27
3839	Finite-size effects on the molecular dynamics simulation of fast-ion conductors: A case study of lithium garnet oxide $\text{Li}_7\text{La}_3\text{Zr}_2\text{O}_{12}$ . Solid State Ionics, 2016, 289, 143-149.	2.7	36
3840	Lower critical solution temperature (LCST) phase behaviour of an ionic liquid and its control by supramolecular host-guest interactions. Chemical Communications, 2016, 52, 7970-7973.	4.1	43
3841	Relative Orientation of POTRA Domains from Cyanobacterial Omp85 Studied by Pulsed EPR Spectroscopy. Biophysical Journal, 2016, 110, 2195-2206.	0.5	21
3842	Molecular dynamics simulation and free energy landscape methods in probing L215H, L217R and L225M $\beta$ -tubulin mutations causing paclitaxel resistance in cancer cells. Biochemical and Biophysical Research Communications, 2016, 476, 273-279.	2.1	45
3843	Effect of the amino acid l-histidine on methane hydrate growth kinetics. Journal of Natural Gas Science and Engineering, 2016, 35, 1453-1462.	4.4	114
3844	Role of hydrogen bonding in cellulose deformation: the leverage effect analyzed by molecular modeling. Cellulose, 2016, 23, 2315-2323.	4.9	29
3845	Exploring the Formation and the Structure of Synaptobrevin Oligomers in a Model Membrane. Biophysical Journal, 2016, 110, 2004-2015.	0.5	13

#	ARTICLE	IF	CITATIONS
3846	Empirical Corrections to the Amber RNA Force Field with Target Metadynamics. <i>Journal of Chemical Theory and Computation</i> , 2016, 12, 2790-2798.	5.3	54
3847	ReaxFF <sup>+</sup> A New Reactive Force Field Method for the Accurate Description of Ionic Systems and Its Application to the Hydrolyzation of Aluminosilicates. <i>Journal of Physical Chemistry C</i> , 2016, 120, 10849-10856.	3.1	8
3848	Molecular dynamics study of CO <sub>2</sub> sorption and transport properties in coal. <i>Fuel</i> , 2016, 177, 53-62.	6.4	41
3849	Penetration of HIV-1 Tat47-57 into PC/PE Bilayers Assessed by MD Simulation and X-Ray Scattering. <i>Biophysical Journal</i> , 2016, 110, 204a.	0.5	0
3850	Ganglioside and Protein-Ganglioside Interactions in Martini and Atomistic Molecular Dynamics Simulations. <i>Biophysical Journal</i> , 2016, 110, 254a.	0.5	0
3851	Design of cholesterol arabinogalactan anchored liposomes for asialoglycoprotein receptor mediated targeting to hepatocellular carcinoma: In silico modeling, in vitro and in vivo evaluation. <i>International Journal of Pharmaceutics</i> , 2016, 509, 149-158.	5.2	28
3852	Time-, stress-, and temperature-dependent deformation in nanostructured copper: Creep tests and simulations. <i>Journal of the Mechanics and Physics of Solids</i> , 2016, 94, 191-206.	4.8	54
3853	Effect of type of poly(ethylene glycol) (PEG) based amphiphilic copolymer on antifouling properties of copolymer/poly(vinylidene fluoride) (PVDF) blend membranes. <i>Journal of Membrane Science</i> , 2016, 514, 429-439.	8.2	106
3854	Cononsolvency behavior of hydrophobes in water + methanol mixtures. <i>Physical Chemistry Chemical Physics</i> , 2016, 18, 16188-16195.	2.8	18
3855	Predicting Dissolution Kinetics for Active Pharmaceutical Ingredients on the Basis of Their Molecular Structures. <i>Crystal Growth and Design</i> , 2016, 16, 4154-4164.	3.0	15
3856	The radical mechanism of biological methane synthesis by methyl-coenzyme M reductase. <i>Science</i> , 2016, 352, 953-958.	12.6	129
3857	Amorphous boron nitride at high pressure. <i>Philosophical Magazine</i> , 2016, 96, 1950-1964.	1.6	5
3858	Time, stress, and temperature-dependent deformation in nanostructured copper: Stress relaxation tests and simulations. <i>Acta Materialia</i> , 2016, 108, 252-263.	7.9	66
3859	Atomistic Simulation of Solubilization of Polycyclic Aromatic Hydrocarbons in a Sodium Dodecyl Sulfate Micelle. <i>Langmuir</i> , 2016, 32, 3645-3654.	3.5	16
3860	Sparse Sampling of Water Density Fluctuations in Interfacial Environments. <i>Journal of Chemical Theory and Computation</i> , 2016, 12, 706-713.	5.3	36
3861	Computational Analysis of Sugar Alcohols as Phase-Change Material: Insight into the Molecular Mechanism of Thermal Energy Storage. <i>Journal of Physical Chemistry C</i> , 2016, 120, 7903-7915.	3.1	38
3862	Molecular dynamics of water and monovalent-ions transportation mechanisms of pentameric sarcolipin. <i>Proteins: Structure, Function and Bioinformatics</i> , 2016, 84, 73-81.	2.6	6
3863	Hydrated nonpolar solute volumes: Interplay between size, Attractiveness, and molecular structure. <i>Biophysical Chemistry</i> , 2016, 213, 1-5.	2.8	6



#	ARTICLE	IF	CITATIONS
3864	Mechanism of pKID/KIX Association Studied by Molecular Dynamics Free Energy Simulations. <i>Journal of Physical Chemistry B</i> , 2016, 120, 8186-8192.	2.6	7
3865	Dynamics of the Water Molecules at the Intrinsic Liquid Surface As Seen from Molecular Dynamics Simulation and Identification of Truly Interfacial Molecules Analysis. <i>Journal of Physical Chemistry C</i> , 2016, 120, 8578-8588.	3.1	21
3866	Membrane invagination induced by Shiga toxin B-subunit: from molecular structure to tube formation. <i>Soft Matter</i> , 2016, 12, 5164-5171.	2.7	82
3867	Sphingolipids contribute to acetic acid resistance in <i>Zygosaccharomyces bailii</i> . <i>Biotechnology and Bioengineering</i> , 2016, 113, 744-753.	3.3	54
3868	Spontaneous Unzipping of Xylonucleic Acid Assisted by a Single-Walled Carbon Nanotube: A Computational Study. <i>Journal of Physical Chemistry B</i> , 2016, 120, 3642-3652.	2.6	17
3869	Structure and thermodynamics of nondipolar molecular liquids and solutions from integral equation theory. <i>Molecular Physics</i> , 2016, 114, 2461-2476.	1.7	5
3870	Determining the Lipid Tilt Modulus by Simulating Membrane Buckles. <i>Journal of Physical Chemistry B</i> , 2016, 120, 6061-6073.	2.6	28
3871	Multiscale Model for the Templated Synthesis of Mesoporous Silica: The Essential Role of Silica Oligomers. <i>Chemistry of Materials</i> , 2016, 28, 2715-2727.	6.7	32
3872	Ice-Water Interfacial Free Energy for the TIP4P, TIP4P/2005, TIP4P/Ice, and mW Models As Obtained from the Mold Integration Technique. <i>Journal of Physical Chemistry C</i> , 2016, 120, 8068-8075.	3.1	79
3873	Characterization of Mn(II) ion binding to the amyloid- $\beta$ peptide in Alzheimer's disease. <i>Journal of Trace Elements in Medicine and Biology</i> , 2016, 38, 183-193.	3.0	60
3874	Computational Study of Excess Electron Mobility in High-Pressure Liquid Benzene. <i>Journal of Physical Chemistry C</i> , 2016, 120, 8490-8501.	3.1	27
3875	Interaction of the N-Acetyl(13 <sup>23</sup> )NH <sub>2</sub> segment of the beta amyloid peptide with beta-sheet-blocking peptides: site and edge specificity. <i>Canadian Journal of Chemistry</i> , 2016, 94, 583-592.	1.1	5
3876	A niosomal bilayer of sorbitan monostearate in complex with flavones: a molecular dynamics simulation study. <i>Journal of Liposome Research</i> , 2016, 26, 336-344.	3.3	8
3877	Predicting Octanol/Water Partition Coefficients of Alcohol Ethoxylate Surfactants Using a Combination of Molecular Dynamics and the Conductor-like Screening Model for Realistic Solvents. <i>Industrial &amp; Engineering Chemistry Research</i> , 2016, 55, 4782-4789.	3.7	25
3878	Indocyanine Green-Loaded Liposomes for Light-Triggered Drug Release. <i>Molecular Pharmaceutics</i> , 2016, 13, 2095-2107.	4.6	102
3879	Molecular dynamics simulation of nanometer scale mechanical properties of hexagonal MgLi alloy. <i>Journal of Magnesium and Alloys</i> , 2016, 4, 36-43.	11.9	23
3880	Carnosine and Homocarnosine Degradation Mechanisms by the Human Carnosinase Enzyme CN1: Insights from Multiscale Simulations. <i>Biochemistry</i> , 2016, 55, 2772-2784.	2.5	20
3881	Timing Correlations in Proteins Predict Functional Modules and Dynamic Allostery. <i>Journal of the American Chemical Society</i> , 2016, 138, 5036-5043.	13.7	14



#	ARTICLE	IF	CITATIONS
3882	Identification and Structural Characterization of an Intermediate in the Folding of the Measles Virus X Domain. <i>Journal of Biological Chemistry</i> , 2016, 291, 10886-10892.	3.4	18
3883	Dynamics of Hydration Water around Native and Misfolded Î±-Lactalbumin. <i>Journal of Physical Chemistry B</i> , 2016, 120, 4756-4766.	2.6	39
3884	Insights on the mechanical behavior of keratin fibrils. <i>International Journal of Biological Macromolecules</i> , 2016, 89, 477-483.	7.5	13
3885	Free Energy Landscape of Lipid Interactions with Regulatory Binding Sites on the Transmembrane Domain of the EGF Receptor. <i>Journal of Physical Chemistry B</i> , 2016, 120, 8154-8163.	2.6	60
3886	Developing a Predictive Form of MOSCED for Nonelectrolyte Solids Using Molecular Simulation: Application to Acetanilide, Acetaminophen, and Phenacetin. <i>Industrial &amp; Engineering Chemistry Research</i> , 2016, 55, 5415-5430.	3.7	24
3887	Multi-Conformation Monte Carlo: A Method for Introducing Flexibility in Efficient Simulations of Many-Protein Systems. <i>Journal of Physical Chemistry B</i> , 2016, 120, 8115-8126.	2.6	12
3888	Ensemble Structure of the Highly Flexible Complex Formed between Vesicular Stomatitis Virus Unassembled Nucleoprotein and its Phosphoprotein Chaperone. <i>Journal of Molecular Biology</i> , 2016, 428, 2671-2694.	4.2	16
3889	Polyunsaturated Lipids Regulate Membrane Domain Stability by Tuning Membrane Order. <i>Biophysical Journal</i> , 2016, 110, 1800-1810.	0.5	155
3890	Hydrophobicity and Hydrophilicity Balance Determines Shape Selectivity of Suzuki Coupling Reactions Inside Pd@meso-SiO <sub>2</sub> Nanoreactor. <i>Journal of Physical Chemistry C</i> , 2016, 120, 10244-10251.	3.1	3
3891	New insight into probe-location dependent polarity and hydration at lipid/water interfaces: comparison between gel- and fluid-phases of lipid bilayers. <i>Physical Chemistry Chemical Physics</i> , 2016, 18, 24185-24197.	2.8	14
3892	The function of the two-pore channel TPC1 depends on dimerization of its carboxy-terminal helix. <i>Cellular and Molecular Life Sciences</i> , 2016, 73, 2565-2581.	5.4	28
3893	Lytic Polysaccharide Monooxygenases <i>Sc</i>LPMO10B and <i>Sc</i>LPMO10C Are Stable in Ionic Liquids As Determined by Molecular Simulations. <i>Journal of Physical Chemistry B</i> , 2016, 120, 3863-3872.	2.6	15
3894	Hybrid Atomistic and Coarse-Grained Molecular Dynamics Simulations of Polyethylene Glycol (PEG) in Explicit Water. <i>Journal of Physical Chemistry B</i> , 2016, 120, 4160-4173.	2.6	29
3895	Correlating Nitrile IR Frequencies to Local Electrostatics Quantifies Noncovalent Interactions of Peptides and Proteins. <i>Journal of Physical Chemistry B</i> , 2016, 120, 4034-4046.	2.6	75
3896	Interactions of Polyethylenimines with Zwitterionic and Anionic Lipid Membranes. <i>Langmuir</i> , 2016, 32, 5004-5018.	3.5	37
3897	Behavior of Bilayer Leaflets in Asymmetric Model Membranes: Atomistic Simulation Studies. <i>Journal of Physical Chemistry B</i> , 2016, 120, 8438-8448.	2.6	19
3898	Quantifying the Relationship between Curvature and Electric Potential in Lipid Bilayers. <i>Journal of Physical Chemistry B</i> , 2016, 120, 4812-4817.	2.6	24
3899	Adsorption-Induced Surface Stresses of the Water/Quartz Interface: Ab Initio Molecular Dynamics Study. <i>Langmuir</i> , 2016, 32, 5259-5266.	3.5	18

#	ARTICLE	IF	CITATIONS
3900	Effect of lipid head group interactions on membrane properties and membrane-induced cationic $\beta$ -hairpin folding. <i>Physical Chemistry Chemical Physics</i> , 2016, 18, 17836-17850.	2.8	19
3901	An atomistic-to-continuum molecular dynamics: Theory, algorithm, and applications. <i>Computer Methods in Applied Mechanics and Engineering</i> , 2016, 306, 452-478.	6.6	35
3902	Energy barriers and mechanisms in solid–solid polymorphic transitions exhibiting cooperative motion. <i>CrystEngComm</i> , 2016, 18, 4420-4430.	2.6	18
3903	Investigation of the Effect of Sulfur Heteroatom on Asphaltene Aggregation. <i>Energy &amp; Fuels</i> , 2016, 30, 4758-4766.	5.1	53
3905	Entry of water into the distal heme pocket of soluble guanylate cyclase $\beta$ 1 H-NOX domain alters the ligated CO structure: a resonance Raman and in silico simulation study. <i>RSC Advances</i> , 2016, 6, 43707-43714.	3.6	2
3906	MD simulation study of direct permeation of a nanoparticle across the cell membrane under an external electric field. <i>Nanoscale</i> , 2016, 8, 11897-11906.	5.6	46
3907	Formation of Clathrate Hydrates of Water-Soluble Guest Molecules. <i>Journal of Physical Chemistry C</i> , 2016, 120, 21512-21521.	3.1	40
3908	The aliphatic chain of cholesterol modulates bilayer interleaflet coupling and domain registration. <i>FEBS Letters</i> , 2016, 590, 3368-3374.	2.8	20
3909	Morphologies Observed in Ultraflexible Microemulsions with and without the Presence of a Strong Acid. <i>ACS Central Science</i> , 2016, 2, 467-475.	11.3	37
3910	Introduction to Atomistic Simulation Methods. <i>Springer Series in Materials Science</i> , 2016, , 1-52.	0.6	2
3911	Conformational Thermodynamics of DNA Strands in Hydrophilic Nanopores. <i>Journal of Physical Chemistry C</i> , 2016, 120, 20357-20367.	3.1	5
3912	Isoexergonic Conformations of Surface-Bound Citrate Regulated Bioinspired Apatite Nanocrystal Growth. <i>ACS Applied Materials &amp; Interfaces</i> , 2016, 8, 28116-28123.	8.0	20
3913	Characterization of kaolinite-cetyltrimethylammonium chloride intercalation complex synthesized through eco-friend kaolinite-urea pre-intercalation complex. <i>Colloids and Surfaces A: Physicochemical and Engineering Aspects</i> , 2016, 508, 265-273.	4.7	21
3914	The effect of urea and taurine osmolytes on hydrophobic association and solvation of methane and neopentane molecules. <i>Journal of Molecular Liquids</i> , 2016, 223, 660-671.	4.9	6
3915	Sparse Neural Network Models of Antimicrobial Peptide–Activity Relationships. <i>Molecular Informatics</i> , 2016, 35, 606-614.	2.5	15
3916	Pharmacophore-based virtual screening, biological evaluation and binding mode analysis of a novel protease-activated receptor 2 antagonist. <i>Journal of Computer-Aided Molecular Design</i> , 2016, 30, 625-637.	2.9	3
3917	Antibacterial efficacy of fractions and compounds from <i>Indigofera barberi</i> : Identification of DNA gyrase B inhibitors through pharmacophore based virtual screening. <i>Process Biochemistry</i> , 2016, 51, 2208-2221.	3.7	10
3918	Binding of Pollutants to Biomolecules: A Simulation Study. <i>Chemical Research in Toxicology</i> , 2016, 29, 1679-1688.	3.3	7

#	ARTICLE	IF	CITATIONS
3919	Experimental and molecular dynamics studies of anthraquinone dyes in a nematic liquid-crystal host: a rationale for observed alignment trends. <i>Physical Chemistry Chemical Physics</i> , 2016, 18, 20651-20663.	2.8	12
3920	Near-atomic cryo-EM structure of PRC1 bound to the microtubule. <i>Proceedings of the National Academy of Sciences of the United States of America</i> , 2016, 113, 9430-9439.	7.1	70
3921	Fast and slow dynamics and the local structure of liquid and supercooled water next to a hydrophobic amino acid. <i>Physical Chemistry Chemical Physics</i> , 2016, 18, 27639-27647.	2.8	12
3922	Structural mechanism for the recognition and ubiquitination of a single nucleosome residue by Rad6/Bre1. <i>Proceedings of the National Academy of Sciences of the United States of America</i> , 2016, 113, 10553-10558.	7.1	44
3923	Parameterization and optimization of the menthol force field for molecular dynamics simulations. <i>Journal of Molecular Modeling</i> , 2016, 22, 234.	1.8	7
3924	Ultrafast anisotropic protein quake propagation after CO photodissociation in myoglobin. <i>Proceedings of the National Academy of Sciences of the United States of America</i> , 2016, 113, 10565-10570.	7.1	47
3925	Unzipping of Double-Stranded Ribonucleic Acids by Graphene and Single-Walled Carbon Nanotube: Helix Geometry versus Surface Curvature. <i>Journal of Physical Chemistry C</i> , 2016, 120, 22681-22693.	3.1	19
3926	Structures of Ionic Liquids Having Both Anionic and Cationic Octyl Tails: Lamellar Vacuum Interface vs Sponge-Like Bulk Order. <i>Journal of Physical Chemistry Letters</i> , 2016, 7, 3785-3790.	4.6	46
3927	Structural Plasticity of Cholesteryl Ester Transfer Protein Assists the Lipid Transfer Activity. <i>Journal of Biological Chemistry</i> , 2016, 291, 19462-19473.	3.4	20
3928	Molecular Dynamics Simulations of Amyloid I <sup>2</sup> -Peptide (1-42): Tetramer Formation and Membrane Interactions. <i>Biophysical Journal</i> , 2016, 111, 937-949.	0.5	84
3929	Molecular dynamics simulations of Ca <sup>2+</sup> +Cl <sup>-</sup> ion pair in polar mixtures of acetone and water: Solvation and dynamical studies. <i>Chemical Physics Letters</i> , 2016, 662, 306-316.	2.6	9
3930	Towards a Multiscale Simulation Approach of Nanofluids for Volumetric Solar Receivers: Assessing Inter-particle Potential Energy. <i>Energy Procedia</i> , 2016, 91, 3-10.	1.8	7
3931	Structural and dynamical aspects of uranyl ions in supercritical water: A molecular dynamics simulation study. <i>Journal of Molecular Liquids</i> , 2016, 224, 599-606.	4.9	7
3932	L30A Mutation of Phospholemman Mimics Effects of Cardiac Glycosides in Isolated Cardiomyocytes. <i>Biochemistry</i> , 2016, 55, 6196-6204.	2.5	5
3933	Molecular Dynamics Simulations Predict the Pathways via Which Pristine Fullerenes Penetrate Bacterial Membranes. <i>Journal of Physical Chemistry B</i> , 2016, 120, 11170-11179.	2.6	68
3934	Effect of Lipid Charge on Membrane Immersion of Cytochrome P450 3A4. <i>Journal of Physical Chemistry B</i> , 2016, 120, 11205-11213.	2.6	24
3935	Interactions of Pleckstrin Homology Domains with Membranes: Adding Back the Bilayer via High-Throughput Molecular Dynamics. <i>Structure</i> , 2016, 24, 1421-1431.	3.3	68
3936	Effect of polyelectrolyte size on multilayer conformation and dynamics at different temperatures and salt concentrations. <i>Journal of Molecular Graphics and Modelling</i> , 2016, 70, 246-252.	2.4	17

#	ARTICLE	IF	CITATIONS
3937	Superionic-Superionic Phase Transitions in Body-Centered Cubic $H_2O_2$ Ice. Physical Review Letters, 2016, 117, 135503.	7.8	53
3938	A Dynamic Picture of the Early Events in Nociceptin Binding to the NOP Receptor by Metadynamics. Biophysical Journal, 2016, 111, 1203-1213.	0.5	10
3939	Efficient Blue Electroluminescence Using Quantum-Confined Two-Dimensional Perovskites. ACS Nano, 2016, 10, 9720-9729.	14.6	299
3940	Synaptic Vesicle Protein 2A as a Novel Pharmacological Target with Broad Potential for New Antiepileptic Drugs. Methods in Pharmacology and Toxicology, 2016, , 53-81.	0.2	1
3941	The Solvent-Exposed C-Terminus of the Cytolysin A Pore-Forming Toxin Directs Pore Formation and Channel Function in Membranes. Biochemistry, 2016, 55, 5952-5961.	2.5	17
3942	Effects of point mutations on the thermostability of B. subtilis lipase: investigating nonadditivity. Journal of Computer-Aided Molecular Design, 2016, 30, 899-916.	2.9	11
3943	Molecular Simulation of $n$ -Octacosane-Water Mixture in Titania Nanopores at Elevated Temperature and Pressure. Journal of Physical Chemistry C, 2016, 120, 24743-24753.	3.1	14
3944	Structural and conformational insights into SOX2/OCT4-bound enhancer DNA: a computational perspective. RSC Advances, 2016, 6, 90138-90153.	3.6	4
3945	Solvent effects on optical excitations of poly para phenylene ethynylene studied by QM/MM simulations based on many-body Green's functions theory. European Physical Journal: Special Topics, 2016, 225, 1743-1756.	2.6	6
3946	Toward elucidating the heat activation mechanism of the TRPV1 channel gating by molecular dynamics simulation. Proteins: Structure, Function and Bioinformatics, 2016, 84, 1938-1949.	2.6	21
3947	Effects of interface mutations on the dimerization of alanine glyoxylate aminotransferase and implications in the mistargeting of the pathogenic variants F152I and I244T. Biochimie, 2016, 131, 137-148.	2.6	17
3948	Mutation-Induced Population Shift in the MexR Conformational Ensemble Disengages DNA Binding: A Novel Mechanism for MarR Family Derepression. Structure, 2016, 24, 1311-1321.	3.3	16
3949	Role of donor-acceptor macrocycles in sequence specific peptide recognition and their optoelectronic properties: a detailed computational insight. Physical Chemistry Chemical Physics, 2016, 18, 20682-20690.	2.8	4
3950	Cycling of a Lithium-Ion Battery with a Silicon Anode Drives Large Mechanical Actuation. Advanced Materials, 2016, 28, 10236-10243.	21.0	40
3951	POPC Bilayers Supported on Nanoporous Substrates: Specific Effects of Silica-Type Surface Hydroxylation and Charge Density. Langmuir, 2016, 32, 6766-6774.	3.5	11
3952	Fast and accurate determination of the relative binding affinities of small compounds to HIV-1 protease using non-equilibrium work. Journal of Computational Chemistry, 2016, 37, 2734-2742.	3.3	70
3953	Systematic and Automated Development of Quantum Mechanically Derived Force Fields: The Challenging Case of Halogenated Hydrocarbons. Journal of Chemical Theory and Computation, 2016, 12, 5525-5540.	5.3	35
3954	Structural basis of steroid binding and oxidation by the cytochrome P450 CYP109E1 from <i>Bacillus megaterium</i> . FEBS Journal, 2016, 283, 4128-4148.	4.7	49

#	ARTICLE	IF	CITATIONS
3955	How Does a Hydrophobic Macromolecule Respond to a Mixed Osmolyte Environment?. Journal of Physical Chemistry B, 2016, 120, 10969-10978.	2.6	16
3956	Ionic liquid induced G-quadruplex formation and stabilization: spectroscopic and simulation studies. Physical Chemistry Chemical Physics, 2016, 18, 29740-29746.	2.8	10
3957	Conserved Mechanism of Conformational Stability and Dynamics in G-Protein-Coupled Receptors. Journal of Chemical Theory and Computation, 2016, 12, 5575-5584.	5.3	23
3958	A stochastic approximation approach to improve the convergence behavior of hierarchical atomistic-to-continuum multiscale models. Journal of the Mechanics and Physics of Solids, 2016, 95, 480-500.	4.8	5
3959	Adsorption of Synthetic Cationic Polymers on Model Phospholipid Membranes: Insight from Atomic-Scale Molecular Dynamics Simulations. Langmuir, 2016, 32, 10402-10414.	3.5	41
3960	Development of simulation methods for dielectrics. , 2016, , .		2
3961	Electric Field Keeps Chromophore Planar and Produces High Yield Fluorescence in Green Fluorescent Protein. Journal of the American Chemical Society, 2016, 138, 13619-13629.	13.7	72
3962	Raman Spectroscopic Speciation Analyses and Liquid Structures by High-Energy X-ray Total Scattering and Molecular Dynamics Simulations for <i>N</i>-methylimidazolium-Based Protic Ionic Liquids. Bulletin of the Chemical Society of Japan, 2016, 89, 965-972.	3.2	5
3963	Effect of polyvinylpyrrolidone at methane hydrate-liquid water interface. Application in flow assurance and natural gas hydrate exploitation. Fuel, 2016, 186, 613-622.	6.4	35
3964	Development and assessment of atomistic models for predicting static friction coefficients. Physical Review B, 2016, 94, .	3.2	4
3965	Molecular Dynamics Simulations of Hydration Effects on Solvation, Diffusivity, and Permeability in Chitosan/Chitin Films. Journal of Physical Chemistry B, 2016, 120, 8997-9010.	2.6	32
3966	Promiscuous Histone Mis-Assembly Is Actively Prevented by Chaperones. Journal of the American Chemical Society, 2016, 138, 13207-13218.	13.7	28
3968	Comparison of Different TMAO Force Fields and Their Impact on the Folding Equilibrium of a Hydrophobic Polymer. Journal of Physical Chemistry B, 2016, 120, 8757-8767.	2.6	36
3969	Multiscale simulations of PSâ€SiO2nanocomposites: from melt to glassy state. Soft Matter, 2016, 12, 7585-7605.	2.7	23
3970	Dislocation Structure and Mobility in hcpHe4. Physical Review Letters, 2016, 117, 045301.	7.8	17
3971	Origin of the Surfactantâ€Dependent Redox Chemistry of Singleâ€Wall Carbon Nanotubes. ChemNanoMat, 2016, 2, 911-920.	2.8	16
3972	Dispersion Corrections to the Surface Tension at Planar Surfaces. Journal of Chemical Theory and Computation, 2016, 12, 4025-4032.	5.3	19
3973	Structural and Functional Basis for Lipid Synergy on the Activity of the Antibacterial Peptide ABC Transporter McjD. Journal of Biological Chemistry, 2016, 291, 21656-21668.	3.4	33

#	ARTICLE	IF	CITATIONS
3974	Destabilization of the metal site as a hub for the pathogenic mechanism of five ALS-linked mutants of copper, zinc superoxide dismutase. <i>Metallomics</i> , 2016, 8, 1141-1150.	2.4	5
3975	Polyarginine Interacts More Strongly and Cooperatively than Polylysine with Phospholipid Bilayers. <i>Journal of Physical Chemistry B</i> , 2016, 120, 9287-9296.	2.6	76
3976	Multiscale Materials Modeling for Nanomechanics. <i>Springer Series in Materials Science</i> , 2016, , .	0.6	20
3977	De novo design of VEGFR-2 tyrosine kinase inhibitors based on a linked-fragment approach. <i>Journal of Molecular Modeling</i> , 2016, 22, 222.	1.8	11
3978	Predicting the Chemical Potential and Osmotic Pressure of Polysaccharide Solutions by Molecular Simulations. <i>Journal of Chemical Theory and Computation</i> , 2016, 12, 4375-4384.	5.3	39
3979	COGNAC: Coarse-Grained Molecular Dynamics Simulator. , 2016, , 29-65.		0
3980	Strongly correlated breeding of high-speed dislocations. <i>Acta Materialia</i> , 2016, 119, 229-241.	7.9	21
3981	Molecular dynamics studies of a Î²-sheet blocking peptide with the full-length amyloid beta peptide of Alzheimer's disease. <i>Canadian Journal of Chemistry</i> , 2016, 94, 833-841.	1.1	6
3982	Molecular dynamics simulation of diffusion and structure of n -alkane/ n -alkanol mixtures at infinite dilution. <i>Journal of Molecular Liquids</i> , 2016, 223, 489-496.	4.9	3
3983	Estimation of Liposome Penetration Barriers of Drug Molecules with All-Atom and Coarse-Grained Models. <i>Journal of Chemical Theory and Computation</i> , 2016, 12, 4651-4661.	5.3	11
3984	Probing the Action of Chemical Denaturant on an Intrinsically Disordered Protein by Simulation and Experiment. <i>Journal of the American Chemical Society</i> , 2016, 138, 11702-11713.	13.7	121
3985	Atomically precise understanding of nanofluids: nanodiamonds and carbon nanotubes in ionic liquids. <i>Physical Chemistry Chemical Physics</i> , 2016, 18, 26865-26872.	2.8	10
3986	Insights into the molecular basis for substrate binding and specificity of the wild-type L-arginine/agmatine antiporter AdiC. <i>Proceedings of the National Academy of Sciences of the United States of America</i> , 2016, 113, 10358-10363.	7.1	82
3987	Restrictive Cardiomyopathy Troponin I R145W Mutation Does Not Perturb Myofilament Length-dependent Activation in Human Cardiac Sarcomeres. <i>Journal of Biological Chemistry</i> , 2016, 291, 21817-21828.	3.4	35
3988	Prediction of cyclohexane-water distribution coefficients for the SAMPL5 data set using molecular dynamics simulations with the OPLS-AA force field. <i>Journal of Computer-Aided Molecular Design</i> , 2016, 30, 1045-1058.	2.9	19
3989	Destabilization of Hydrophobic Core of Chicken Villin Headpiece in Guanidinium Chloride Induced Denaturation: Hint of Î€-Cation Interaction. <i>Journal of Physical Chemistry B</i> , 2016, 120, 9599-9607.	2.6	15
3990	Evaluation of Methods for the Calculation of the $pK_a$ of Cysteine Residues in Proteins. <i>Journal of Chemical Theory and Computation</i> , 2016, 12, 4662-4673.	5.3	88
3991	Lowered pH Leads to Fusion Peptide Release and a Highly Dynamic Intermediate of Influenza Hemagglutinin. <i>Journal of Physical Chemistry B</i> , 2016, 120, 9654-9660.	2.6	13



#	ARTICLE	IF	CITATIONS
3992	Molecular dynamics simulations of mixtures of protic and aprotic ionic liquids. <i>Physical Chemistry Chemical Physics</i> , 2016, 18, 23932-23943.	2.8	25
3993	Conformational dynamics of cancer-associated MyD88-TIR domain mutant L252P (L265P) allosterically tilts the landscape toward homo-dimerization. <i>Protein Engineering, Design and Selection</i> , 2016, 29, 347-354.	2.1	18
3994	Microsecond Molecular Dynamics Simulation of Methane Hydrate Formation in Humic-Acid-Amended Sodium Montmorillonite. <i>Energy &amp; Fuels</i> , 2016, 30, 7206-7213.	5.1	35
3995	Coarse-Grained Molecular Dynamics Simulations of Membrane-Trehalose Interactions. <i>Journal of Physical Chemistry B</i> , 2016, 120, 9621-9631.	2.6	7
3996	Diffusion of Aromatics in Silicalite-1: Experimental and Theoretical Evidence of Entropic Barriers. <i>Journal of Physical Chemistry C</i> , 2016, 120, 21410-21426.	3.1	20
3997	Harmonic effects in atomistic phase interactions between phonons and dislocations moving at relativistic velocities. <i>Computational Materials Science</i> , 2016, 124, 259-266.	3.0	1
3998	Structural basis of control of inward rectifier Kir2 channel gating by bulk anionic phospholipids. <i>Journal of General Physiology</i> , 2016, 148, 227-237.	1.9	66
3999	Efficient molecular packing of glycerol monostearate in Langmuir monolayers at the air-water interface. <i>Colloids and Surfaces A: Physicochemical and Engineering Aspects</i> , 2016, 508, 85-92.	4.7	14
4000	Molecular Properties of Astaxanthin in Water/Ethanol Solutions from Computer Simulations. <i>Journal of Physical Chemistry B</i> , 2016, 120, 9322-9328.	2.6	7
4001	Molecular-dynamic simulation of aliphatic alcohols distribution between the micelle of 3-methyl-1-dodecylimidazolium bromide and their aqueous surrounding. <i>Colloids and Surfaces A: Physicochemical and Engineering Aspects</i> , 2016, 508, 93-100.	4.7	4
4002	Nanoscale Spatial Heterogeneity in Deep Eutectic Solvents. <i>Journal of Physical Chemistry B</i> , 2016, 120, 6712-6720.	2.6	123
4003	Interfacial Diffusion and Bonding in Multilayer Polymer Films: A Molecular Dynamics Simulation. <i>Journal of Physical Chemistry B</i> , 2016, 120, 10018-10029.	2.6	16
4004	Drug-Specific Design of Telodendrimer Architecture for Effective Doxorubicin Encapsulation. <i>Journal of Physical Chemistry B</i> , 2016, 120, 9766-9777.	2.6	13
4005	Local lateral environment of the molecules at the surface of DMSO-water mixtures. <i>Journal of Physics Condensed Matter</i> , 2016, 28, 404002.	1.8	5
4006	Structural and viscosity properties of CaO-SiO <sub>2</sub> -Al <sub>2</sub> O <sub>3</sub> -FeO slags based on molecular dynamic simulation. <i>Journal of Non-Crystalline Solids</i> , 2016, 450, 23-31.	3.1	67
4007	The Free Energy of Small Solute Permeation through the <i>Escherichia coli</i> Outer Membrane Has a Distinctly Asymmetric Profile. <i>Journal of Physical Chemistry Letters</i> , 2016, 7, 3446-3451.	4.6	57
4008	Mediation mechanism of tyrosine 185 on the retinal isomerization equilibrium and the proton release channel in the seven-transmembrane receptor bacteriorhodopsin. <i>Biochimica Et Biophysica Acta - Bioenergetics</i> , 2016, 1857, 1786-1795.	1.0	6
4009	Molecular dynamics simulation of cyclodextrin aggregation and extraction of Anthracene from non-aqueous liquid phase. <i>Journal of Hazardous Materials</i> , 2016, 320, 169-175.	12.4	15



#	ARTICLE	IF	CITATIONS
4010	An analysis of key characteristics of the Frank-Read source process in FCC metals. Journal of the Mechanics and Physics of Solids, 2016, 96, 460-476.	4.8	55
4011	Structures, Properties, and Dynamics of Intermediates in eEF2-Diphthamide Biosynthesis. Journal of Chemical Information and Modeling, 2016, 56, 1776-1786.	5.4	3
4012	QSAR modeling to design selective histone deacetylase 8 (HDAC8) inhibitors. Archives of Pharmacal Research, 2016, 39, 1356-1369.	6.3	12
4013	Estimation of Relative Proteinâ€“RNA Binding Strengths from Fluctuations in the Bound State. Journal of Chemical Theory and Computation, 2016, 12, 4593-4599.	5.3	4
4014	Conformational Thermodynamics of DNA Strands in Hydrophilic Nanopores. Journal of Physical Chemistry B, 2016, , .	2.6	0
4015	Minicollagen cysteine-rich domains encode distinct modes of polymerization to form stable nematocyst capsules. Scientific Reports, 2016, 6, 25709.	3.3	18
4016	Binding Free Energy and the structural changes determination in hGH protein with different concentrations of copper ions (A molecular dynamics simulation study). Journal of Theoretical and Computational Chemistry, 2016, 15, 1650045.	1.8	4
4017	Probabilistic Analysis and Design of HCP Nanowires: An Efficient Surrogate Based Molecular Dynamics Simulation Approach. Journal of Materials Science and Technology, 2016, 32, 1345-1351.	10.7	43
4018	Partitioning into Colloidal Structures of Fasted State Intestinal Fluid Studied by Molecular Dynamics Simulations. Langmuir, 2016, 32, 12732-12740.	3.5	19
4019	Microscopic Origin of Strain Hardening in Methane Hydrate. Scientific Reports, 2016, 6, 23548.	3.3	15
4020	Functional Annotation of Ion Channel Structures by Molecular Simulation. Structure, 2016, 24, 2207-2216.	3.3	69
4021	OmpA: A Flexible Clamp for Bacterial Cell Wall Attachment. Structure, 2016, 24, 2227-2235.	3.3	76
4022	Temperature Dependence of Static and Dynamic Heterogeneities in a Waterâ€“Ethanol Binary Mixture and a Study of Enhanced, Short-Lived Fluctuations at Low Concentrations. Journal of Physical Chemistry B, 2016, 120, 12568-12583.	2.6	19
4023	Competitive Adsorption of Naphthenic Acids and Polyaromatic Molecules at a Tolueneâ€“Water Interface. Journal of Physical Chemistry B, 2016, 120, 12901-12910.	2.6	13
4024	Probing the Thermodynamic Stability and Phonon Transport in Two-Dimensional Hexagonal Aluminum Nitride Monolayer. Journal of Physical Chemistry C, 2016, 120, 27675-27681.	3.1	22
4025	Antimicrobial Peptide Potency is Facilitated by Greater Conformational Flexibility when Binding to Gram-negative Bacterial Inner Membranes. Scientific Reports, 2016, 6, 37639.	3.3	64
4026	Structural insight into inhibition of human Class II PI3K isoforms: homology modeling, binding site characterization, docking and molecular dynamics studies. RSC Advances, 2016, 6, 112455-112467.	3.6	3
4027	Water modulates the ultraslow dynamics of hydrated ionic liquids near CG rich DNA: consequences for DNA stability. Physical Chemistry Chemical Physics, 2016, 18, 32107-32115.	2.8	9

#	ARTICLE	IF	CITATIONS
4028	Binding Characteristics of Sphingosine-1-Phosphate to ApoM hints to Assisted Release Mechanism via the ApoM Calyx-Opening. <i>Scientific Reports</i> , 2016, 6, 30655.	3.3	21
4029	Linker dependent chirality of solvent induced self-assembled structures of porphyrin- $\alpha$ -helical peptide conjugates. <i>Organic and Biomolecular Chemistry</i> , 2016, 14, 9568-9577.	2.8	16
4030	Molecular Dynamics Simulation of Bismuth Telluride Exfoliation Mechanisms in Different Ionic Liquid Solvents. <i>Langmuir</i> , 2016, 32, 9982-9992.	3.5	13
4031	An atomic-scale insight into the effects of hydrogen microalloying on the glass-forming ability and ductility of Zr-based bulk metallic glasses. <i>Computational Materials Science</i> , 2016, 125, 197-205.	3.0	11
4032	Interaction between arginine conformers and Hofmeister halide anions. <i>Computational and Theoretical Chemistry</i> , 2016, 1095, 93-103.	2.5	0
4033	Improved Force Field Model for the Deep Eutectic Solvent Ethaline: Reliable Physicochemical Properties. <i>Journal of Physical Chemistry B</i> , 2016, 120, 10124-10137.	2.6	63
4034	Putative membrane lytic sites of P-type and S-type cardiotoxins from snake venoms as probed by all-atom molecular dynamics simulations. <i>Journal of Molecular Modeling</i> , 2016, 22, 238.	1.8	9
4035	Energetics of Ion Permeation in an Open-Activated TRPV1 Channel. <i>Biophysical Journal</i> , 2016, 111, 1214-1222.	0.5	21
4036	Structure and aggregation of $\beta$ -cyclodextrin-pyrene-analyte supramolecular sensor: Absorption/emission spectra and simulations. <i>Journal of Luminescence</i> , 2016, 180, 328-340.	3.1	12
4037	Succession of Alkane Conformational Motifs Bound within Hydrophobic Supramolecular Capsular Assemblies. <i>Journal of Physical Chemistry B</i> , 2016, 120, 10394-10402.	2.6	19
4038	On the Structural and Dynamical Properties of DOPC Reverse Micelles. <i>Langmuir</i> , 2016, 32, 10610-10620.	3.5	35
4039	Molecular Origins of Dynamic Coupling between Water and Hydrated Polyacrylate Gels. <i>Macromolecules</i> , 2016, 49, 7551-7562.	4.8	21
4040	Large-scale molecular dynamics simulation of crosslinked phenolic resins using pseudo-reaction model. <i>Polymer</i> , 2016, 103, 261-276.	3.8	34
4041	Elucidating the mechanisms of nanodiamond-promoted structural disruption of crystallised lipid. <i>Soft Matter</i> , 2016, 12, 8338-8347.	2.7	1
4042	A Fast Convergent Simulated Annealing Algorithm for Protein-Folding: Simulated Annealing Outlier FLOODing (SA-OFLOOD) Method. <i>Bulletin of the Chemical Society of Japan</i> , 2016, 89, 1361-1367.	3.2	19
4043	A systematic study on the intradiffusion and structure of N,N-dimethylformamide-water mixtures: by experiment and molecular dynamics simulation. <i>RSC Advances</i> , 2016, 6, 85603-85611.	3.6	15
4044	Adapting the semi-explicit assembly solvation model for estimating water-cyclohexane partitioning with the SAMPL5 molecules. <i>Journal of Computer-Aided Molecular Design</i> , 2016, 30, 1067-1077.	2.9	3
4045	Transmembrane dynamics of the Thr-5 phosphorylated sarcolipin pentameric channel. <i>Archives of Biochemistry and Biophysics</i> , 2016, 604, 143-151.	3.0	18

#	ARTICLE	IF	CITATIONS
4046	Theoretical study of the interactions between the first transmembrane segment of NS2 protein and a POPC lipid bilayer. Biophysical Chemistry, 2016, 217, 1-7.	2.8	8
4047	Spectroscopic and dynamic properties of arachidonoyl serotonin-Î²-lactoglobulin complex: A molecular modeling and chemometric study. Journal of Photochemistry and Photobiology B: Biology, 2016, 162, 519-528.	3.8	2
4048	Structural origin of proton mobility in a protic ionic liquid/imidazole mixture: insights from computational and experimental results. Physical Chemistry Chemical Physics, 2016, 18, 23195-23206.	2.8	28
4049	Computational investigation of cold denaturation in the Trp-cage miniprotein. Proceedings of the National Academy of Sciences of the United States of America, 2016, 113, 8991-8996.	7.1	48
4050	Multiscale simulations on conformational dynamics and membrane interactions of the non-structural 2 (NS2) transmembrane domain. Biochemical and Biophysical Research Communications, 2016, 478, 193-198.	2.1	4
4051	Mesoscale Simulation of Asphaltene Aggregation. Journal of Physical Chemistry B, 2016, 120, 8016-8035.	2.6	68
4052	Water adsorption behaviour of CAU-10-H: a thorough investigation of its structureâ€“property relationships. Journal of Materials Chemistry A, 2016, 4, 11859-11869.	10.3	166
4053	A molecular dynamics study of the effect of glycosidic linkage type in the hemicellulose backbone on the molecular chain flexibility. Plant Journal, 2016, 88, 56-70.	5.7	58
4054	Structural basis of Smoothed regulation by its extracellular domains. Nature, 2016, 535, 517-522.	27.8	300
4055	Pressure-induced structural changes in the network-forming isostatic glass<mml:math xmlns:mml="http://www.w3.org/1998/Math/MathML"><mml:msub><mml:mi>GeSe</mml:mi><mml:mn>4</mml:mn></mml:msub></mml:math> An investigation by neutron diffraction and first-principles molecular dynamics. Physical Review B, 2016, 93, .	3.2	24
4056	Hydrogen Incorporation in Crystalline Jadeite: Insight from First Principles Calculations. Acta Geologica Sinica, 2016, 90, 939-945.	1.4	1
4057	Multi-scale molecular dynamics study of cholera pentamer binding to a GM1-phospholipid membrane. Journal of Molecular Graphics and Modelling, 2016, 68, 236-251.	2.4	15
4058	Calculating Partition Coefficients of Small Molecules in Octanol/Water and Cyclohexane/Water. Journal of Chemical Theory and Computation, 2016, 12, 4015-4024.	5.3	137
4059	Impact of Ions on Individual Water Entropy. Journal of Physical Chemistry B, 2016, 120, 7471-7479.	2.6	19
4060	Interaction Dynamics in Inhibiting the Aggregation of AÎ² Peptides by SWCNTs: A Combined Experimental and Coarse-Grained Molecular Dynamic Simulation Study. ACS Chemical Neuroscience, 2016, 7, 1232-1240.	3.5	24
4061	The solvation structure of alprazolam. Physical Chemistry Chemical Physics, 2016, 18, 22416-22425.	2.8	7
4062	Improved QM/MM Linear-Interaction Energy Model for Substrate Recognition in Zinc-Containing Metalloenzymes. Journal of Physical Chemistry B, 2016, 120, 7824-7835.	2.6	1
4064	Crystal Structure of a Group I Energy Coupling Factor Vitamin Transporter S Component in Complex with Its Cognate Substrate. Cell Chemical Biology, 2016, 23, 827-836.	5.2	9

#	ARTICLE	IF	CITATIONS
4065	Hydrophobic Association in Mixed Urea/TMAO Solutions. <i>Journal of Physical Chemistry Letters</i> , 2016, 7, 3052-3059.	4.6	44
4066	12-Crown-4 Ether Disrupts the Patient Brain-Derived Amyloid- $\beta$ -Fibril Trimer: Insight from All-Atom Molecular Dynamics Simulations. <i>ACS Chemical Neuroscience</i> , 2016, 7, 1433-1441.	3.5	37
4067	Product Release Pathways in Human and <i>Plasmodium falciparum</i> Phosphoribosyltransferase. <i>Journal of Chemical Information and Modeling</i> , 2016, 56, 1528-1538.	5.4	4
4068	Nanomechanics of Type I Collagen. <i>Biophysical Journal</i> , 2016, 111, 50-56.	0.5	67
4069	Structure-based virtual screening efforts against HIV-1 reverse transcriptase to introduce the new potent non-nucleoside reverse transcriptase inhibitor. <i>Journal of Molecular Structure</i> , 2016, 1125, 592-600.	3.6	10
4070	Peculiar Aqueous Solubility Trend in Cucurbiturils Unraveled by Atomistic Simulations. <i>Journal of Physical Chemistry B</i> , 2016, 120, 7511-7516.	2.6	11
4071	Aggregation Kinetics and Stability Mechanisms of Pristine and Oxidized Nanocarbons in Polar Solvents. <i>Journal of Physical Chemistry C</i> , 2016, 120, 16804-16814.	3.1	14
4072	Structural and dynamic evolution of the amphipathic N-terminus diversifies enzyme thermostability in the glycoside hydrolase family 12. <i>Physical Chemistry Chemical Physics</i> , 2016, 18, 21340-21350.	2.8	26
4073	Structure and dynamics of <i>H. pylori</i> 98-10 C5-cytosine specific DNA methyltransferase in complex with S-adenosyl-methionine and DNA. <i>Molecular BioSystems</i> , 2016, 12, 3111-3123.	2.9	4
4074	Nonlinear reconstruction of single-molecule free-energy surfaces from univariate time series. <i>Physical Review E</i> , 2016, 93, 032412.	2.1	26
4075	Comparison of systematic coarse-graining strategies for soluble conjugated polymers. <i>European Physical Journal: Special Topics</i> , 2016, 225, 1441-1461.	2.6	17
4076	Molecular Dynamics Approach for Predicting Helical Twisting Powers of Metal Complex Dopants in Nematic Solvents. <i>Journal of Physical Chemistry B</i> , 2016, 120, 6858-6864.	2.6	16
4077	In silico study of amphiphilic nanotubes based on cyclic peptides in polar and non-polar solvent. <i>Journal of Molecular Modeling</i> , 2016, 22, 264.	1.8	5
4078	Protein remains stable at unusually high temperatures when solvated in aqueous mixtures of amino acid based ionic liquids. <i>Journal of Molecular Modeling</i> , 2016, 22, 258.	1.8	14
4079	Exploring the Structural Properties of Positively Charged Peptide Dendrimers. <i>Journal of Physical Chemistry B</i> , 2016, 120, 11323-11330.	2.6	16
4080	Protein-dependent Membrane Interaction of A Partially Disordered Protein Complex with Oleic Acid: Implications for Cancer Lipidomics. <i>Scientific Reports</i> , 2016, 6, 35015.	3.3	9
4081	Lattice mold technique for the calculation of crystal nucleation rates. <i>Faraday Discussions</i> , 2016, 195, 569-582.	3.2	4
4082	Structural elements of an NRPS cyclization domain and its intermodule docking domain. <i>Proceedings of the National Academy of Sciences of the United States of America</i> , 2016, 113, 12432-12437.	7.1	65

#	ARTICLE	IF	CITATIONS
4083	Surface Rebound of Relativistic Dislocations Directly and Efficiently Initiates Deformation Twinning. Physical Review Letters, 2016, 117, 165501.	7.8	6
4084	Construction of Digital Oil for Investigation of Crude Oil Properties at Different Thermodynamic Conditions. , 2016, , .		3
4085	Separation of water-ethanol solutions with carbon nanotubes and electric fields. Physical Chemistry Chemical Physics, 2016, 18, 33310-33319.	2.8	33
4086	2H-NMR and MD Simulations Reveal Membrane-Bound Conformation of Magainin 2 and Its Synergy with PGLa. Biophysical Journal, 2016, 111, 2149-2161.	0.5	31
4087	Role of Hydration Layer in Dynamical Transition in Proteins: Insights from Translational Self-Diffusivity. Journal of Physical Chemistry B, 2016, 120, 12031-12039.	2.6	14
4088	Anion Dependent Dynamics and Water Solubility Explained by Hydrogen Bonding Interactions in Mixtures of Water and Aprotic Heterocyclic Anion Ionic Liquids. Journal of Physical Chemistry B, 2016, 120, 12679-12686.	2.6	18
4089	How Is the Surface Tension of Various Liquids Distributed along the Interface Normal?. Journal of Physical Chemistry C, 2016, 120, 27468-27477.	3.1	37
4090	On the determination of defect dipoles from atomistic simulations using periodic boundary conditions. Philosophical Magazine Letters, 2016, 96, 447-453.	1.2	6
4091	Direct evidence for sequence-dependent attraction between double-stranded DNA controlled by methylation. Nature Communications, 2016, 7, 11045.	12.8	64
4092	Structural insights and functional implications of inter-individual variability in $\beta_2$ -adrenergic receptor. Scientific Reports, 2016, 6, 24379.	3.3	15
4093	Probing Hydration Patterns in Class-A GPCRs via Biased MD: The $\alpha_2A$ Receptor. Journal of Chemical Theory and Computation, 2016, 12, 6049-6061.	5.3	18
4094	Imidazolium-Based Lipid Analogues and Their Interaction with Phosphatidylcholine Membranes. Langmuir, 2016, 32, 12579-12592.	3.5	50
4095	Effects of temperature, pH and counterions on the stability of peptide amphiphile nanofiber structures. RSC Advances, 2016, 6, 104201-104214.	3.6	36
4096	Molecular Mechanism and Energy Basis of Conformational Diversity of Antibody SPE7 Revealed by Molecular Dynamics Simulation and Principal Component Analysis. Scientific Reports, 2016, 6, 36900.	3.3	23
4097	Determination of functional collective motions in a protein at atomic resolution using coherent neutron scattering. Science Advances, 2016, 2, e1600886.	10.3	30
4098	Full-Length OmpA: Structure, Function, and Membrane Interactions Predicted by Molecular Dynamics Simulations. Biophysical Journal, 2016, 111, 1692-1702.	0.5	67
4099	How Oliceridine (TRV-130) Binds and Stabilizes a $\mu$ -Opioid Receptor Conformational State That Selectively Triggers G Protein Signaling Pathways. Biochemistry, 2016, 55, 6456-6466.	2.5	87
4100	Molecular Mechanism behind Solvent Concentration-Dependent Optimal Activity of <i>Thermomyces lanuginosus</i> Lipase in a Biocompatible Ionic Liquid: Interfacial Activation through Arginine Switch. Journal of Physical Chemistry B, 2016, 120, 11720-11732.	2.6	16

#	ARTICLE	IF	CITATIONS
4101	Resolving the Origins of Crystalline Anharmonicity Using Terahertz Time-Domain Spectroscopy and <i>ab Initio</i> Simulations. <i>Journal of Physical Chemistry B</i> , 2016, 120, 11733-11739.	2.6	42
4102	Characterization of Mg <sup>2+</sup> Distributions around RNA in Solution. <i>ACS Omega</i> , 2016, 1, 680-688.	3.5	40
4103	Modelling proteins' hidden conformations to predict antibiotic resistance. <i>Nature Communications</i> , 2016, 7, 12965.	12.8	113
4104	Constructing an Interpolated Potential Energy Surface of a Large Molecule: A Case Study with Bacteriochlorophyll <i>a</i> Model in the Fenna-Matthews-Olson Complex. <i>Journal of Chemical Theory and Computation</i> , 2016, 12, 5235-5246.	5.3	23
4105	Scaling Atomic Partial Charges of Carbonate Solvents for Lithium Ion Solvation and Diffusion. <i>Journal of Chemical Theory and Computation</i> , 2016, 12, 5709-5718.	5.3	64
4106	What Can We Learn about Cholesterol's Transmembrane Distribution Based on Cholesterol-Induced Changes in Membrane Dipole Potential?. <i>Journal of Physical Chemistry Letters</i> , 2016, 7, 4585-4590.	4.6	19
4107	Investigation into Biological Environments through (Non)linear Optics: A Multiscale Study of Laurdan Derivatives. <i>Journal of Chemical Theory and Computation</i> , 2016, 12, 6169-6181.	5.3	25
4108	Lipid-Loving ANTs: Molecular Simulations of Cardiolipin Interactions and the Organization of the Adenine Nucleotide Translocase in Model Mitochondrial Membranes. <i>Biochemistry</i> , 2016, 55, 6238-6249.	2.5	63
4109	Molecular Dynamics and Free Energy Simulations of Phenylacetate and CO <sub>2</sub> Release from AMDase and Its G74C/C188S Mutant: A Possible Rationale for the Reduced Activity of the Latter. <i>Journal of Physical Chemistry B</i> , 2016, 120, 11644-11653.	2.6	2
4110	Effect of Mutation on an Aggregation-Prone Segment of p53: From Monomer to Dimer to Multimer. <i>Journal of Physical Chemistry B</i> , 2016, 120, 11665-11673.	2.6	12
4111	Molecular Dynamics Study of the Morphology of Hydrated Perfluorosulfonic Acid Polymer Membranes. <i>Journal of Physical Chemistry C</i> , 2016, 120, 25832-25842.	3.1	62
4112	Crystal structure of an invertebrate cytolysin pore reveals unique properties and mechanism of assembly. <i>Nature Communications</i> , 2016, 7, 11598.	12.8	71
4113	Aggregation tendencies in the p53 family are modulated by backbone hydrogen bonds. <i>Scientific Reports</i> , 2016, 6, 32535.	3.3	47
4114	Mechanistic Understanding of the Effect of Temperature and Salinity on the Water/Toluene Interfacial Tension. <i>Energy &amp; Fuels</i> , 2016, 30, 10228-10235.	5.1	32
4115	Determination of structural requirements of Mer kinase inhibitors and binding interaction analysis using in silico approaches. <i>Medicinal Chemistry Research</i> , 2016, 25, 3021-3029.	2.4	2
4116	Supercritical CO <sub>2</sub> Confined in Palygorskite and Sepiolite Minerals: A Classical Molecular Dynamics Investigation. <i>Journal of Physical Chemistry C</i> , 2016, 120, 26945-26954.	3.1	17
4117	Preferential solvation and ion association properties in aqueous dimethyl sulfoxide solutions. <i>Physical Chemistry Chemical Physics</i> , 2016, 18, 31312-31322.	2.8	30
4118	Nonclassical Crystal Growth as Explanation for the Riddle of Polarity in Centrosymmetric Glycine Crystals. <i>Journal of the American Chemical Society</i> , 2016, 138, 14756-14763.	13.7	14



#	ARTICLE	IF	CITATIONS
4119	A method of solidâ€“solid phase equilibrium calculation by molecular dynamics. Journal of Physics Condensed Matter, 2016, 28, 495201.	1.8	1
4120	Molecular dynamics simulations of atomistic hydration structures of poly(vinyl methyl ether). Chinese Journal of Polymer Science (English Edition), 2016, 34, 1396-1410.	3.8	2
4121	Optimized atomistic force fields for aqueous solutions of Magnesium and Calcium Chloride: Analysis, achievements and limitations. European Physical Journal: Special Topics, 2016, 225, 1391-1409.	2.6	10
4122	Comparison of iterative inverse coarse-graining methods. European Physical Journal: Special Topics, 2016, 225, 1323-1345.	2.6	27
4123	Rheological Study and Molecular Dynamics Simulation of Biopolymer Blend Thermogels of Tunable Strength. Biomacromolecules, 2016, 17, 3474-3484.	5.4	18
4124	Molecular Dynamics Study of Mg <sup>2+</sup> /Li <sup>+</sup> Separation via Biomimetic Graphene-Based Nanopores: The Role of Dehydration in Second Shell. Langmuir, 2016, 32, 13778-13786.	3.5	58
4125	Temperature-sensitive gating of TRPV1 channel as probed by atomistic simulations of its trans- and juxtamembrane domains. Scientific Reports, 2016, 6, 33112.	3.3	49
4126	Atomistic migration mechanisms of atomically flat, stepped, and kinked grain boundaries. Physical Review B, 2016, 94, .	3.2	33
4127	On the anomalous temperature dependence of cellulose aqueous solubility. Cellulose, 2016, 23, 2375-2387.	4.9	12
4128	Stimulation of Nipah Fusion: Small Intradomain Changes Trigger Extensive Interdomain Rearrangements. Biophysical Journal, 2016, 111, 1621-1630.	0.5	9
4129	Directly Modifying the Nonbonded Potential Based on the Standard Iterative Boltzmann Inversion Method for Coarse-Grained Force Fields. Journal of Physical Chemistry B, 2016, 120, 11834-11844.	2.6	13
4130	Functional annotation of rare gene aberration drivers of pancreatic cancer. Nature Communications, 2016, 7, 10500.	12.8	58
4131	Adaptive molecular resolution approach in Hamiltonian form: An asymptotic analysis. Physical Review E, 2016, 94, 043321.	2.1	7
4132	Domain Stability in Biomimetic Membranes Driven by Lipid Polyunsaturation. Journal of Physical Chemistry B, 2016, 120, 11930-11941.	2.6	52
4133	Liquid Structure of CO <sub>2</sub> â€“Reactive Aprotic Heterocyclic Anion Ionic Liquids from X-ray Scattering and Molecular Dynamics. Journal of Physical Chemistry B, 2016, 120, 11951-11960.	2.6	12
4134	Structural basis for Mep2 ammonium transceptor activation by phosphorylation. Nature Communications, 2016, 7, 11337.	12.8	52
4135	Modelling temperature-dependent properties of polymorphic organic molecular crystals. Physical Chemistry Chemical Physics, 2016, 18, 31132-31143.	2.8	81
4136	The singular behavior of a Î²-type semi-synthetic two branched polypeptide: three-dimensional structure and mode of action. Physical Chemistry Chemical Physics, 2016, 18, 30998-31011.	2.8	14



#	ARTICLE	IF	CITATIONS
4137	Nanosegregated amorphous AlBN <sub>2</sub> alloy. Philosophical Magazine, 2016, 96, 3200-3210.	1.6	4
4138	The Dry Preservation of Giant Vesicles Using a Group 3 LEA Protein Model Peptide and Its Molecular Mechanism. Bulletin of the Chemical Society of Japan, 2016, 89, 1493-1499.	3.2	10
4139	Structural basis for the membrane association of ankyrinG via palmitoylation. Scientific Reports, 2016, 6, 23981.	3.3	18
4140	Anomalous Dynamics of a Lipid Recognition Protein on a Membrane Surface. Scientific Reports, 2016, 5, 18245.	3.3	38
4141	Computational investigation of dynamical transitions in Trp-cage miniprotein powders. Scientific Reports, 2016, 6, 25612.	3.3	15
4142	Energetics of side-chain snorkeling in transmembrane helices probed by nonproteinogenic amino acids. Proceedings of the National Academy of Sciences of the United States of America, 2016, 113, 10559-10564.	7.1	26
4143	Sampling the isothermal-isobaric ensemble by Langevin dynamics. Journal of Chemical Physics, 2016, 144, 124113.	3.0	14
4144	Molecular dynamics simulation of structural change at metal/semiconductor interface induced by nanoindenter. Chinese Physics B, 2016, 25, 114601.	1.4	1
4145	Mechanism of L-leucine in promoting methane hydrate formation by molecular dynamic simulation. , 2016, , .		2
4146	Structure of zirconium tetrahydroborate Zr(BH <sub>4</sub> ) <sub>4</sub> : A molecular dynamics study. Journal of Structural Chemistry, 2016, 57, 1068-1073.	1.0	3
4147	Cellulose chain binding free energy drives the processive move of cellulases on the cellulose surface. Biotechnology and Bioengineering, 2016, 113, 1873-1880.	3.3	7
4148	Efficient enzymatic cyclization of an inhibitory cystine knot-containing peptide. Biotechnology and Bioengineering, 2016, 113, 2202-2212.	3.3	22
4149	Enantioselective Benzylic Hydroxylation Catalysed by P450 Monooxygenases: Characterisation of a P450cam Mutant Library and Molecular Modelling. ChemBioChem, 2016, 17, 426-432.	2.6	29
4150	Molecular interactions of UvrB protein and DNA from Helicobacter pylori: Insight into a molecular modeling approach. Computers in Biology and Medicine, 2016, 75, 181-189.	7.0	13
4151	A Discontinuous Potential Model for Protein-Protein Interactions. Molecular Modeling and Simulation, 2016, 2016, 1-20.	0.2	0
4152	DFT calculation of NMR $\hat{\gamma}$ ( <sup>113</sup> Cd) in cadmium complexes. Polyhedron, 2016, 117, 48-56.	2.2	9
4153	Radical Formation Initiates Solvent-Dependent Unfolding and $\beta^2$ -sheet Formation in a Model Helical Peptide. Journal of Physical Chemistry B, 2016, 120, 4878-4889.	2.6	3
4154	Osmotic Pressure Simulations of Amino Acids and Peptides Highlight Potential Routes to Protein Force Field Parameterization. Journal of Physical Chemistry B, 2016, 120, 8217-8229.	2.6	28

#	ARTICLE	IF	CITATIONS
4155	Salting-out of methane in the aqueous solutions of urea and sarcosine. <i>Journal of Chemical Sciences</i> , 2016, 128, 599-612.	1.5	5
4156	Dual Function of Phosphoubiquitin in E3 Activation of Parkin. <i>Journal of Biological Chemistry</i> , 2016, 291, 16879-16891.	3.4	12
4157	Predicting light absorption properties of anthocyanidins in solution: a multi-level computational approach. <i>Theoretical Chemistry Accounts</i> , 2016, 135, 1.	1.4	16
4158	Influence of Glu/Arg, Asp/Arg, and Glu/Lys Salt Bridges on $\alpha$ -Helical Stability and Folding Kinetics. <i>Biophysical Journal</i> , 2016, 110, 2328-2341.	0.5	72
4159	Confined water in imidazolium based ionic liquids: a supramolecular guest@host complex case. <i>Physical Chemistry Chemical Physics</i> , 2016, 18, 18297-18304.	2.8	36
4160	A first-principles study of stable few-layer penta-silicene. <i>Physical Chemistry Chemical Physics</i> , 2016, 18, 18486-18492.	2.8	51
4161	Elucidating the influence of polymorph-dependent interfacial solvent structuring at chitin surfaces. <i>Carbohydrate Polymers</i> , 2016, 151, 916-925.	10.2	8
4162	Molecular Dynamics Study of Nanoaggregation in Asphaltene Mixtures: Effects of the N, O, and S Heteroatoms. <i>Energy &amp; Fuels</i> , 2016, 30, 5656-5664.	5.1	73
4163	Effect of monoglycerides and fatty acids on a ceramide bilayer. <i>Physical Chemistry Chemical Physics</i> , 2016, 18, 17446-17460.	2.8	26
4164	The first crystal structure of human RNase 6 reveals a novel substrate-binding and cleavage site arrangement. <i>Biochemical Journal</i> , 2016, 473, 1523-1536.	3.7	44
4165	Distribution and dynamics of quinones in the lipid bilayer mimicking the inner membrane of mitochondria. <i>Biochimica Et Biophysica Acta - Biomembranes</i> , 2016, 1858, 2116-2122.	2.6	47
4166	Solution Conditions Affect the Ability of the K30D Mutation To Prevent Amyloid Fibril Formation by Apolipoprotein C-II: Insights from Experiments and Theoretical Simulations. <i>Biochemistry</i> , 2016, 55, 3815-3824.	2.5	5
4167	Ligand binding to anti-cancer target CD44 investigated by molecular simulations. <i>Journal of Molecular Modeling</i> , 2016, 22, 165.	1.8	12
4168	Controlling the Dissociation of Ligands from the Adenosine A <sub>2A</sub> Receptor through Modulation of Salt Bridge Strength. <i>Journal of Medicinal Chemistry</i> , 2016, 59, 6470-6479.	6.4	151
4169	Why are some cyano-based ionic liquids better glucose solvents than water?. <i>Physical Chemistry Chemical Physics</i> , 2016, 18, 18958-18970.	2.8	13
4170	Lid closure dynamics of porcine pancreatic lipase in aqueous solution. <i>Biochimica Et Biophysica Acta - General Subjects</i> , 2016, 1860, 2313-2325.	2.4	12
4171	Parametrization of halogen bonds in the CHARMM general force field: Improved treatment of ligand-protein interactions. <i>Bioorganic and Medicinal Chemistry</i> , 2016, 24, 4812-4825.	3.0	168
4172	The structure of liquid water beyond the first hydration shell. <i>Physical Chemistry Chemical Physics</i> , 2016, 18, 19420-19425.	2.8	16

#	ARTICLE	IF	CITATIONS
4173	Role of Preferential Ions of Ammonium Ionic Liquid in Destabilization of Collagen. <i>Journal of Physical Chemistry B</i> , 2016, 120, 6515-6524.	2.6	24
4174	Atomic-Scale Molecular Dynamics Simulations of DNA–Polycation Complexes: Two Distinct Binding Patterns. <i>Journal of Physical Chemistry B</i> , 2016, 120, 6546-6554.	2.6	31
4175	Conformation Transitions of Recombinant Spidroins via Integration of Time-Resolved FTIR Spectroscopy and Molecular Dynamic Simulation. <i>ACS Biomaterials Science and Engineering</i> , 2016, 2, 1298-1308.	5.2	21
4176	Unraveling the aggregation effect on amorphous phase AIE luminogens: a computational study. <i>Nanoscale</i> , 2016, 8, 15173-15180.	5.6	112
4177	Ab Initio Molecular Dynamics Simulations of an Excess Proton in a Triethylene Glycol–Water Solution: Solvation Structure, Mechanism, and Kinetics. <i>Journal of Physical Chemistry B</i> , 2016, 120, 5223-5242.	2.6	5
4178	Liquid structure of dibutyl sulfoxide. <i>Physical Chemistry Chemical Physics</i> , 2016, 18, 15980-15987.	2.8	10
4179	Crystal structure and dynamics of Spt16N-domain of FACT complex from <i>Cicer arietinum</i> . <i>International Journal of Biological Macromolecules</i> , 2016, 88, 36-43.	7.5	8
4180	Molecular Dynamics Simulations of Intrinsically Disordered Proteins: On the Accuracy of the TIP4P-D Water Model and the Representativeness of Protein Disorder Models. <i>Journal of Chemical Theory and Computation</i> , 2016, 12, 3407-3415.	5.3	82
4181	Behavior of P85 and P188 Poloxamer Molecules: Computer Simulations Using United-Atom Force-Field. <i>Journal of Physical Chemistry B</i> , 2016, 120, 8631-8641.	2.6	14
4182	UO <sub>2</sub> bicrystal phonon grain-boundary resistance by molecular dynamics and predictive models. <i>International Journal of Heat and Mass Transfer</i> , 2016, 100, 243-249.	4.8	7
4183	Interfacial water thickness at inorganic nanoconstructs and biomolecules: Size matters. <i>Physics Letters, Section A: General, Atomic and Solid State Physics</i> , 2016, 380, 1735-1740.	2.1	21
4184	Adsorption of Plasma Proteins onto PEGylated Lipid Bilayers: The Effect of PEG Size and Grafting Density. <i>Biomacromolecules</i> , 2016, 17, 1757-1765.	5.4	75
4185	Coarse-Grained Interface Surfactant Density Maps for Calculation of the Fractional Conversion of Tetrameric Carboxylic Acids to Calcium Naphthenate Precipitates. <i>Industrial &amp; Engineering Chemistry Research</i> , 2016, 55, 5090-5099.	3.7	2
4186	Design, Synthesis, and Characterization of Cyclic Peptidomimetics of the Inducible Nitric Oxide Synthase Binding Epitope That Disrupt the Protein–Protein Interaction Involving SPRY Domain-Containing Suppressor of Cytokine Signaling Box Protein (SPSB) 2 and Inducible Nitric Oxide Synthase. <i>Journal of Medicinal Chemistry</i> , 2016, 59, 5799-5809.	6.4	19
4187	Divalent Ion Parameterization Strongly Affects Conformation and Interactions of an Anionic Biomimetic Polymer. <i>Journal of Physical Chemistry B</i> , 2016, 120, 2198-2208.	2.6	18
4188	Comparative Molecular Dynamics Study on Tri- <i>n</i> -butyl Phosphate in Organic and Aqueous Environments and Its Relevance to Nuclear Extraction Processes. <i>Journal of Physical Chemistry B</i> , 2016, 120, 5183-5193.	2.6	28
4189	Jumping Diffusion of Water Intercalated in Layered Double Hydroxides. <i>Journal of Physical Chemistry C</i> , 2016, 120, 12924-12931.	3.1	18
4190	High-Performance Modeling of Carbon Dioxide Sequestration by Coupling Reservoir Simulation and Molecular Dynamics. <i>SPE Journal</i> , 2016, 21, 0853-0863.	3.1	6

#	ARTICLE	IF	CITATIONS
4191	Traction boundary conditions for molecular static simulations. <i>Computer Methods in Applied Mechanics and Engineering</i> , 2016, 308, 310-329.	6.6	3
4192	Reduction of Water/Oil Interfacial Tension by Model Asphaltenes: The Governing Role of Surface Concentration. <i>Journal of Physical Chemistry B</i> , 2016, 120, 5646-5654.	2.6	105
4193	Mechanical properties of silica glass predicted by a pair-wise potential in molecular dynamics simulations. <i>Journal of Non-Crystalline Solids</i> , 2016, 445-446, 102-109.	3.1	23
4194	Stability of a Split Streptomycin Binding Aptamer. <i>Journal of Physical Chemistry B</i> , 2016, 120, 6479-6489.	2.6	11
4195	Probing the Adsorption of Polycyclic Aromatic Compounds onto Water Droplets Using Molecular Dynamics Simulations. <i>Journal of Physical Chemistry C</i> , 2016, 120, 14170-14179.	3.1	19
4196	Melting Point and Solid-Liquid Coexistence Properties of $\hat{1}$ Isotactic Polypropylene as Functions of Its Molar Mass: A Molecular Dynamics Study. <i>Macromolecules</i> , 2016, 49, 4663-4673.	4.8	17
4197	Multiscale coupling of molecular dynamics and peridynamics. <i>Journal of the Mechanics and Physics of Solids</i> , 2016, 95, 169-187.	4.8	59
4198	Effects of Asphaltenes on the Formation and Decomposition of Methane Hydrate: A Molecular Dynamics Study. <i>Energy &amp; Fuels</i> , 2016, 30, 5643-5650.	5.1	41
4199	Localization model description of diffusion and structural relaxation in glass-forming Cu-Zr alloys. <i>Journal of Statistical Mechanics: Theory and Experiment</i> , 2016, 2016, 054048.	2.3	62
4200	Structure of a low-population binding intermediate in protein-RNA recognition. <i>Proceedings of the National Academy of Sciences of the United States of America</i> , 2016, 113, 7171-7176.	7.1	54
4201	Single-molecule force spectroscopy study of the effect of cigarette carcinogens on thrombomodulin-thrombin interaction. <i>Science Bulletin</i> , 2016, 61, 1187-1194.	9.0	7
4202	Oligomerization of the Tetraspanin CD81 via the Flexibility of Its $\hat{1}$ -Loop. <i>Biophysical Journal</i> , 2016, 110, 2463-2474.	0.5	26
4203	A highly efficient hybrid method for calculating the hydration free energy of a protein. <i>Journal of Computational Chemistry</i> , 2016, 37, 712-723.	3.3	6
4204	Reaction kinetics and solubility in water-organic binary solutions are governed by similar solvation equilibria. <i>Journal of Physical Organic Chemistry</i> , 2016, 29, 118-126.	1.9	5
4205	Identification of the active site of human mitochondrial malonyl-coenzyme a decarboxylase: A combined computational study. <i>Proteins: Structure, Function and Bioinformatics</i> , 2016, 84, 792-802.	2.6	2
4206	Influence of nanochannels on Poisson's ratio of degenerate crystal of hard dimers. <i>Physica Status Solidi (B): Basic Research</i> , 2016, 253, 1324-1330.	1.5	17
4207	Effects of a More Accurate Polarizable Hamiltonian on Polymorph Free Energies Computed Efficiently by Reweighting Point-Charge Potentials. <i>Journal of Chemical Theory and Computation</i> , 2016, 12, 3491-3505.	5.3	24
4208	Structural Elements in the $\hat{1}$ s and $\hat{1}$ q C Termini That Mediate Selective G Protein-coupled Receptor (GPCR) Signaling. <i>Journal of Biological Chemistry</i> , 2016, 291, 17929-17940.	3.4	38

#	ARTICLE	IF	CITATIONS
4209	Synthesis, base pairing and structure studies of geranylated RNA. <i>Nucleic Acids Research</i> , 2016, 44, 6036-6045.	14.5	26
4210	A coarse-grained model for polylactide: glass transition temperature and conformational properties. <i>Journal of Polymer Research</i> , 2016, 23, 1.	2.4	15
4211	In silico designing of hyper-glycosylated analogs for the human coagulation factor IX. <i>Journal of Molecular Graphics and Modelling</i> , 2016, 68, 39-47.	2.4	38
4212	Free energy of solvation of carbon nanotubes in pyridinium-based ionic liquids. <i>Physical Chemistry Chemical Physics</i> , 2016, 18, 20357-20362.	2.8	7
4213	Molecular simulations of the effects of phospholipid and cholesterol peroxidation on lipid membrane properties. <i>Biochimica Et Biophysica Acta - Biomembranes</i> , 2016, 1858, 2191-2198.	2.6	38
4214	Computational Study Exploring the Interaction Mechanism of Benzimidazole Derivatives as Potent Cattle Bovine Viral Diarrhea Virus Inhibitors. <i>Journal of Agricultural and Food Chemistry</i> , 2016, 64, 5941-5950.	5.2	20
4215	Assessing Spectral Simulation Protocols for the Amide I Band of Proteins. <i>Journal of Chemical Theory and Computation</i> , 2016, 12, 3982-3992.	5.3	32
4216	Understanding the dynamics of monomeric, dimeric, and tetrameric $\alpha$ -synuclein structures in water. <i>FEBS Open Bio</i> , 2016, 6, 666-686.	2.3	14
4217	Linker-Region Modified Derivatives of the Deoxyhypusine Synthase Inhibitor CN1493 Suppress HIV-1 Replication. <i>Archiv Der Pharmazie</i> , 2016, 349, 91-103.	4.1	6
4218	Insights into Medium-chain Acyl-CoA Dehydrogenase Structure by Molecular Dynamics Simulations. <i>Chemical Biology and Drug Design</i> , 2016, 88, 281-292.	3.2	9
4219	Effect of Polarization on the Mobility of C <sub>60</sub> : A Kinetic Monte Carlo Study. <i>Journal of Chemical Theory and Computation</i> , 2016, 12, 812-824.	5.3	23
4220	Local structure of As <sub>2</sub> O <sub>3</sub> glass from first principles simulations. <i>Journal of Non-Crystalline Solids</i> , 2016, 436, 18-21.	3.1	3
4221	Characterization of the Free State Ensemble of the CoNR Box Motif by Molecular Dynamics Simulations. <i>Journal of Physical Chemistry B</i> , 2016, 120, 1060-1068.	2.6	12
4222	Pressure-induced changes in structural and dynamic properties of liquid Fe close to the melting line. An <i>ab initio</i> study. <i>Journal of Physics Condensed Matter</i> , 2016, 28, 075101.	1.8	18
4223	Probing molecular basis of single-walled carbon nanotube degradation and nondegradation by enzymes based on manganese peroxidase and lignin peroxidase. <i>RSC Advances</i> , 2016, 6, 3592-3599.	3.6	27
4224	Direct Interaction between the Voltage Sensors Produces Cooperative Sustained Deactivation in Voltage-gated H <sup>+</sup> Channel Dimers. <i>Journal of Biological Chemistry</i> , 2016, 291, 5935-5947.	3.4	11
4225	Molecular principles behind pyrazinamide resistance due to mutations in panD gene in <i>Mycobacterium tuberculosis</i> . <i>Gene</i> , 2016, 581, 31-42.	2.2	34
4226	Atomistic Molecular Dynamics Simulations of Charged Latex Particle Surfaces in Aqueous Solution. <i>Langmuir</i> , 2016, 32, 428-441.	3.5	23

#	ARTICLE	IF	CITATIONS
4227	Carbon dioxide induced bubble formation in a $\text{CH}_4\text{-CO}_2\text{-H}_2\text{O}$ ternary system: a molecular dynamics simulation study. <i>Physical Chemistry Chemical Physics</i> , 2016, 18, 3746-3754.	2.8	19
4228	Shock Wave-Induced Damage of a Protein by Void Collapse. <i>Biophysical Journal</i> , 2016, 110, 147-156.	0.5	22
4229	Molecular Dynamics Simulation of Tensile Deformation and Fracture of $\text{TiAl}$ with and without Surface Defects. <i>Journal of Materials Science and Technology</i> , 2016, 32, 1033-1042.	10.7	40
4230	Effects of normal stresses on the homogeneous nucleation of a basal dislocation in magnesium. <i>Computational Materials Science</i> , 2016, 113, 143-147.	3.0	3
4231	Properties of Poloxamer Molecules and Poloxamer Micelles Dissolved in Water and Next to Lipid Bilayers: Results from Computer Simulations. <i>Journal of Physical Chemistry B</i> , 2016, 120, 5823-5830.	2.6	45
4232	Enhanced, targeted sampling of high-dimensional free-energy landscapes using variationally enhanced sampling, with an application to chignolin. <i>Proceedings of the National Academy of Sciences of the United States of America</i> , 2016, 113, 1150-1155.	7.1	47
4233	Predictive Sampling of Rare Conformational Events in Aqueous Solution: Designing a Generalized Orthogonal Space Tempering Method. <i>Journal of Chemical Theory and Computation</i> , 2016, 12, 41-52.	5.3	11
4234	Driving forces for the pressure-induced aggregation of poly(N-isopropylacrylamide) in water. <i>Physical Chemistry Chemical Physics</i> , 2016, 18, 4697-4703.	2.8	27
4235	On the ATP binding site of the $\text{F}_1$ subunit from bacterial F-type ATP synthases. <i>Biochimica Et Biophysica Acta - Bioenergetics</i> , 2016, 1857, 332-340.	1.0	14
4236	Principal Component Analysis of Lipid Molecule Conformational Changes in Molecular Dynamics Simulations. <i>Journal of Chemical Theory and Computation</i> , 2016, 12, 1019-1028.	5.3	26
4237	Acetone as a polar cosolvent for pyridinium-based ionic liquids. <i>RSC Advances</i> , 2016, 6, 8906-8912.	3.6	20
4238	Molecular dynamics simulations of the formation of ethane clathrate hydrates. <i>Fluid Phase Equilibria</i> , 2016, 413, 229-234.	2.5	21
4239	CHARMM-GUI Input Generator for NAMD, GROMACS, AMBER, OpenMM, and CHARMM/OpenMM Simulations Using the CHARMM36 Additive Force Field. <i>Journal of Chemical Theory and Computation</i> , 2016, 12, 405-413.	5.3	2,567
4240	Atomistic modeling of BN nanofillers for mechanical and thermal properties: a review. <i>Nanoscale</i> , 2016, 8, 22-49.	5.6	82
4241	Soft particles at a fluid interface. <i>Soft Matter</i> , 2016, 12, 1062-1073.	2.7	46
4242	Simulations of flow induced structural transition of the $\text{I}^2$ -switch region of glycoprotein $\text{Ib}\alpha$ . <i>Biophysical Chemistry</i> , 2016, 209, 9-20.	2.8	16
4243	Mechanism for Asymmetric Nanoscale Electrowetting of an Ionic Liquid on Graphene. <i>Langmuir</i> , 2016, 32, 140-150.	3.5	23
4244	Dynamic conformational ensembles regulate casein kinase-1 isoforms: Insights from molecular dynamics and molecular docking studies. <i>Computational Biology and Chemistry</i> , 2016, 61, 39-46.	2.3	1



#	ARTICLE	IF	CITATIONS
4245	Different nanostructures caused by competition of intra- and inter- $\beta^2$ -sheet interactions in hierarchical self-assembly of short peptides. <i>Journal of Colloid and Interface Science</i> , 2016, 464, 219-228.	9.4	42
4246	Improved Parameterization of Amine-Carboxylate and Amine-Phosphate Interactions for Molecular Dynamics Simulations Using the CHARMM and AMBER Force Fields. <i>Journal of Chemical Theory and Computation</i> , 2016, 12, 430-443.	5.3	132
4247	Phosphonium based ionic liquids-stabilizing or destabilizing agents for collagen?. <i>RSC Advances</i> , 2016, 6, 4022-4033.	3.6	23
4248	Binding of Disordered Peptides to Kelch: Insights from Enhanced Sampling Simulations. <i>Journal of Chemical Theory and Computation</i> , 2016, 12, 395-404.	5.3	23
4249	Inclusion complexes of propiconazole nitrate with substituted $\beta^2$ -cyclodextrins: the synthesis and in silico and in vitro assessment of their antifungal properties. <i>New Journal of Chemistry</i> , 2016, 40, 1765-1776.	2.8	12
4250	Molecular dynamics simulations of $K^+Cl^-$ ion pair in polar mixtures of acetone and water: Preferential solvation and structural studies. <i>Journal of Molecular Liquids</i> , 2016, 213, 276-288.	4.9	2
4251	Epiregulin Recognition Mechanisms by Anti-epiregulin Antibody 9E5. <i>Journal of Biological Chemistry</i> , 2016, 291, 2319-2330.	3.4	11
4252	Interdigitation of long-chain sphingomyelin induces coupling of membrane leaflets in a cholesterol dependent manner. <i>Biochimica Et Biophysica Acta - Biomembranes</i> , 2016, 1858, 281-288.	2.6	76
4253	Force field development and simulations of senior dialkyl sulfoxides. <i>Physical Chemistry Chemical Physics</i> , 2016, 18, 10507-10515.	2.8	19
4254	Understanding the Thermodynamics of Hydrogen Bonding in Alcohol-Containing Mixtures: Cross-Association. <i>Journal of Physical Chemistry B</i> , 2016, 120, 3388-3402.	2.6	46
4255	How the Structure of Pyrrolidinium Ionic Liquids Is Susceptible to High Pressure. <i>Journal of Physical Chemistry B</i> , 2016, 120, 3206-3214.	2.6	41
4256	Structure and dynamics of proflavine association around DNA. <i>Physical Chemistry Chemical Physics</i> , 2016, 18, 10383-10391.	2.8	7
4257	Dielectric Relaxation of Ethylene Carbonate and Propylene Carbonate from Molecular Dynamics Simulations. <i>Journal of Physical Chemistry B</i> , 2016, 120, 1849-1853.	2.6	42
4258	Permeability of 5-aminolevulinic acid oxime derivatives in lipid membranes. <i>Theoretical Chemistry Accounts</i> , 2016, 135, 1.	1.4	0
4259	$Li^{+}$ Local Structure in Hydrofluoroether Diluted Li-Glyme Solvate Ionic Liquid. <i>Journal of Physical Chemistry B</i> , 2016, 120, 3378-3387.	2.6	81
4260	Defects in the calcium-binding region drastically affect the cadherin-like domains of RET tyrosine kinase. <i>Physical Chemistry Chemical Physics</i> , 2016, 18, 8673-8681.	2.8	2
4261	Temperature-Dependent Conformational Properties of Human Neuronal Calcium Sensor-1 Protein Revealed by All-Atom Simulations. <i>Journal of Physical Chemistry B</i> , 2016, 120, 3551-3559.	2.6	4
4262	Docking and molecular dynamics simulation study of EGFR1 with EGF-like peptides to understand molecular interactions. <i>Molecular BioSystems</i> , 2016, 12, 1987-1995.	2.9	11



#	ARTICLE	IF	CITATIONS
4263	n-type conductivity in Si-doped amorphous AlN: anab initioinvestigation. Philosophical Magazine, 2016, 96, 1110-1121.	1.6	0
4264	Direct Phase Equilibrium Simulations of NIPAM Oligomers in Water. Journal of Physical Chemistry B, 2016, 120, 3434-3440.	2.6	42
4265	Transmembrane Potential Modeling: Comparison between Methods of Constant Electric Field and Ion Imbalance. Journal of Chemical Theory and Computation, 2016, 12, 2418-2425.	5.3	34
4266	Two-dimensional interlocked pentagonal bilayer ice: how do water molecules form a hydrogen bonding network?. Physical Chemistry Chemical Physics, 2016, 18, 14216-14221.	2.8	26
4267	On the physiological/pathological link between AÎ² peptide, cholesterol, calcium ions and membrane deformation: A molecular dynamics study. Biochimica Et Biophysica Acta - Biomembranes, 2016, 1858, 1380-1389.	2.6	14
4268	Diffusivity of Cucurbitacin B in water swollen polyethylene oxide-b-polycaprolactone matrices with different PCL/PEO weight ratios. Computational Materials Science, 2016, 118, 97-102.	3.0	3
4269	Acyclic forms of aldohexoses and ketohexoses in aqueous and DMSO solutions: conformational features studied using molecular dynamics simulations. Physical Chemistry Chemical Physics, 2016, 18, 9626-9635.	2.8	15
4270	Morphological dependence of silver electrodeposits investigated by changing the ionic liquid solvent and the deposition parameters. Physical Chemistry Chemical Physics, 2016, 18, 7242-7250.	2.8	10
4271	Ring inversion properties of 1â†'2, 1â†'3 and 1â†'6-linked hexopyranoses and their correlation with the conformation of glycosidic linkages. Carbohydrate Research, 2016, 423, 43-48.	2.3	13
4272	Pharmacophore based virtual screening for identification of marine bioactive compounds as inhibitors against macrophage infectivity potentiator (Mip) protein of Chlamydia trachomatis. RSC Advances, 2016, 6, 18946-18957.	3.6	7
4273	The recognition mechanism of crizotinib on MTH1: influence of chirality on the bioactivity. Molecular Physics, 2016, 114, 2364-2372.	1.7	3
4274	Self-aggregation and coaggregation of the p53 core fragment with its aggregation gatekeeper variant. Physical Chemistry Chemical Physics, 2016, 18, 8098-8107.	2.8	23
4275	Structural features determining thermal adaptation of esterases. Protein Engineering, Design and Selection, 2016, 29, 65-76.	2.1	46
4276	TRPV1 channel as a target for cancer therapy using CNT-based drug delivery systems. European Biophysics Journal, 2016, 45, 423-433.	2.2	19
4277	Accurate calculation of the absolute free energy of binding for drug molecules. Chemical Science, 2016, 7, 207-218.	7.4	248
4278	Sequence diversity and ligand-induced structural rearrangements of viper hyaluronidase. Molecular BioSystems, 2016, 12, 1128-1138.	2.9	13
4279	Effect of dimerization on the mechanism of action of aurein 1.2. Biochimica Et Biophysica Acta - Biomembranes, 2016, 1858, 1129-1138.	2.6	16
4280	Novel actin filaments fromBacillus thuringiensisform nanotubules for plasmid DNA segregation. Proceedings of the National Academy of Sciences of the United States of America, 2016, 113, E1200-E1205.	7.1	16

#	ARTICLE	IF	CITATIONS
4281	Structural perturbation of a dipalmitoylphosphatidylcholine (DPPC) bilayer by warfarin and its bolaamphiphilic analogue: A molecular dynamics study. <i>Journal of Colloid and Interface Science</i> , 2016, 468, 227-237.	9.4	13
4282	A molecular understanding of the phase-behavior of thiophene in the ionic liquid [C4mim] <sup>+</sup> [BF4] <sup>-</sup> for extraction from petroleum streams. <i>Fuel</i> , 2016, 175, 225-231.	6.4	19
4283	Structural basis of outer membrane protein insertion by the BAM complex. <i>Nature</i> , 2016, 531, 64-69.	27.8	234
4284	Molecular Dynamics Simulation of Methane Hydrate Growth in the Presence of the Natural Product Pectin. <i>Journal of Physical Chemistry C</i> , 2016, 120, 5392-5397.	3.1	51
4285	Rapid Computation of Thermodynamic Properties over Multidimensional Nonbonded Parameter Spaces Using Adaptive Multistate Reweighting. <i>Journal of Chemical Theory and Computation</i> , 2016, 12, 1806-1823.	5.3	13
4286	Uncertainty quantification in molecular dynamics studies of the glass transition temperature. <i>Polymer</i> , 2016, 87, 246-259.	3.8	75
4287	Atomistic Simulation of Oligoelectrolyte Multilayers Growth. , 2016, , 215-228.		1
4288	The dynamic mechanism of presenilin-1 function: Sensitive gate dynamics and loop unplugging control protein access. <i>Neurobiology of Disease</i> , 2016, 89, 147-156.	4.4	52
4289	Towards Next Generation Lithium-Sulfur Batteries: Non-Conventional Carbon Compartments/Sulfur Electrodes and Multi-Scale Analysis. <i>Journal of the Electrochemical Society</i> , 2016, 163, A730-A741.	2.9	43
4290	P3HT:DiPBI bulk heterojunction solar cells: morphology and electronic structure probed by multiscale simulation and UV/vis spectroscopy. <i>Physical Chemistry Chemical Physics</i> , 2016, 18, 6217-6227.	2.8	15
4291	The Structural Basis for Lipid and Endotoxin Binding in RP105-MD-1, and Consequences for Regulation of Host Lipopolysaccharide Sensitivity. <i>Structure</i> , 2016, 24, 200-211.	3.3	11
4292	Role of Electroosmosis in the Permeation of Neutral Molecules: CymA and Cyclodextrin as an Example. <i>Biophysical Journal</i> , 2016, 110, 600-611.	0.5	55
4293	Synthesis, biological evaluation and molecular modeling of pseudo-peptides based statine as inhibitors for human tissue kallikrein 5. <i>European Journal of Medicinal Chemistry</i> , 2016, 112, 39-47.	5.5	10
4294	Gaussian-Charge Polarizable and Nonpolarizable Models for CO <sub>2</sub> . <i>Journal of Physical Chemistry B</i> , 2016, 120, 984-994.	2.6	34
4295	Probing the Salt Concentration Dependent Nucleobase Distribution in a Single-Stranded DNA@Single-Walled Carbon Nanotube Hybrid with Molecular Dynamics. <i>Journal of Physical Chemistry B</i> , 2016, 120, 455-466.	2.6	25
4296	The good, the bad and the user in soft matter simulations. <i>Biochimica Et Biophysica Acta - Biomembranes</i> , 2016, 1858, 2529-2538.	2.6	93
4297	COMPASS II: extended coverage for polymer and drug-like molecule databases. <i>Journal of Molecular Modeling</i> , 2016, 22, 47.	1.8	566
4298	Mechanism of Slow Crystal Growth of Tetrahydrofuran Clathrate Hydrate. <i>Journal of Physical Chemistry C</i> , 2016, 120, 3305-3313.	3.1	44

#	ARTICLE	IF	CITATIONS
4299	Crystal structures reveal the molecular basis of ion translocation in sodium/proton antiporters. <i>Nature Structural and Molecular Biology</i> , 2016, 23, 248-255.	8.2	83
4300	Allostery in BAX protein activation. <i>Journal of Biomolecular Structure and Dynamics</i> , 2016, 34, 2469-2480.	3.5	11
4301	Pressure-induced phase transformations in amorphous arsenic. <i>Journal of Non-Crystalline Solids</i> , 2016, 437, 6-9.	3.1	0
4302	Structures of the EphA2 Receptor at the Membrane: Role of Lipid Interactions. <i>Structure</i> , 2016, 24, 337-347.	3.3	31
4303	Understanding the Solubility of Acetaminophen in 1- <i>n</i> -Alkyl-3-methylimidazolium-Based Ionic Liquids Using Molecular Simulation. <i>Journal of Physical Chemistry B</i> , 2016, 120, 3360-3369.	2.6	17
4304	Effects of temperature, salt concentration, and the protonation state on the dynamics and hydrogen-bond interactions of polyelectrolyte multilayers on lipid membranes. <i>Physical Chemistry Chemical Physics</i> , 2016, 18, 6691-6700.	2.8	15
4305	Enhanced sampling simulation analysis of the structure of lignin in the THF-water miscibility gap. <i>Physical Chemistry Chemical Physics</i> , 2016, 18, 6394-6398.	2.8	24
4306	Interaction of wine anthocyanin derivatives with lipid bilayer membranes. <i>Computational and Theoretical Chemistry</i> , 2016, 1077, 80-86.	2.5	34
4307	A Flexible Domain-Domain Hinge Promotes an Induced-fit Dominant Mechanism for the Loading of Guide-DNA into Argonaute Protein in <i>Thermus thermophilus</i> . <i>Journal of Physical Chemistry B</i> , 2016, 120, 2709-2720.	2.6	25
4308	Molecular dynamics simulation of coarse-grained poly(L-lysine) dendrimers. <i>Journal of Molecular Modeling</i> , 2016, 22, 59.	1.8	27
4309	Interaction mechanism exploration of HEA derivatives as BACE1 inhibitors by in silico analysis. <i>Molecular BioSystems</i> , 2016, 12, 1151-1165.	2.9	11
4310	Molecular Insights into the Adsorption Mechanism of Human $\beta$ 2-Defensin-3 on Bacterial Membranes. <i>Langmuir</i> , 2016, 32, 1782-1790.	3.5	55
4311	Dynamics and mechanisms of interactions between ring-shaped heterohexameric TIP49a/b protein complexes and double-stranded DNA. <i>Cell and Tissue Biology</i> , 2016, 10, 47-54.	0.4	0
4312	Self-stability of C60 nanocapsules with radio-iodide content and its interaction with calcium atoms. <i>Journal of Molecular Modeling</i> , 2016, 22, 28.	1.8	3
4313	The biophysical properties of ethanolamine plasmalogens revealed by atomistic molecular dynamics simulations. <i>Biochimica Et Biophysica Acta - Biomembranes</i> , 2016, 1858, 97-103.	2.6	69
4314	Choline salicylate ionic liquid by X-ray scattering, vibrational spectroscopy and molecular dynamics. <i>Journal of Molecular Liquids</i> , 2016, 218, 39-49.	4.9	19
4315	Lipid Bilayer Membrane Perturbation by Embedded Nanopores: A Simulation Study. <i>ACS Nano</i> , 2016, 10, 3693-3701.	14.6	44
4316	Molecular simulations of cytochrome c adsorption on positively charged surfaces: the influence of anion type and concentration. <i>Physical Chemistry Chemical Physics</i> , 2016, 18, 9979-9989.	2.8	29

#	ARTICLE	IF	CITATIONS
4317	Selective Removal of Technetium from Water Using Graphene Oxide Membranes. Environmental Science & Technology, 2016, 50, 3875-3881.	10.0	53
4318	Role of Naphthenic Acids in Controlling Self-Aggregation of a Polyaromatic Compound in Toluene. Journal of Physical Chemistry B, 2016, 120, 3516-3526.	2.6	14
4319	Understanding the mechanism of CO <sub>2</sub> capture by 1,3 di-substituted imidazolium acetate based ionic liquids. Physical Chemistry Chemical Physics, 2016, 18, 1911-1917.	2.8	37
4320	Computational investigation of structure, dynamics and nucleation kinetics of a family of modified Stillingers-Weber model fluids in bulk and free-standing thin films. Physical Chemistry Chemical Physics, 2016, 18, 4102-4111.	2.8	28
4321	Alteration of lipid membrane structure and dynamics by diacylglycerols with unsaturated chains. Biochimica Et Biophysica Acta - Biomembranes, 2016, 1858, 253-263.	2.6	21
4322	The inhibition of glycerol permeation through aquaglyceroporin-3 induced by mercury(II): A molecular dynamics study. Journal of Inorganic Biochemistry, 2016, 160, 78-84.	3.5	27
4323	Computational microscopy™ of cellular membranes. Journal of Cell Science, 2016, 129, 257-68.	2.0	119
4324	Emission shaping in fluorescent proteins: role of electrostatics and $\pi$ -stacking. Physical Chemistry Chemical Physics, 2016, 18, 3944-3955.	2.8	24
4325	Exploring the Effects of Subfreezing Temperature and Salt Concentration on Ice Growth Inhibition of Antarctic Gram-Negative Bacterium Marinomonas Primoryensis Using Coarse-Grained Simulation. Applied Biochemistry and Biotechnology, 2016, 178, 1534-1545.	2.9	1
4326	Modeling of carbon nanotubes and carbon nanotube-polymer composites. Progress in Aerospace Sciences, 2016, 80, 33-58.	12.1	77
4327	Exploration of Interfacial Hydration Networks of Target-Ligand Complexes. Journal of Chemical Information and Modeling, 2016, 56, 148-158.	5.4	30
4328	Surface Reconstructions in Organic Crystals: Simulations of the Effect of Temperature and Defectivity on Bulk and (001) Surfaces of 2,2',2''-Ternaphthalene. Crystal Growth and Design, 2016, 16, 3.0 412-422.		7
4329	Hydrogen bond in imidazolium based protic and aprotic ionic liquids. Journal of Molecular Liquids, 2016, 217, 35-42.	4.9	45
4330	Formation of randomly dispersed pores in Ga-doped ZnO between Al <sub>2</sub> O <sub>3</sub> and glass via promoted atomic diffusion: Experimental and computational study. Materials and Design, 2016, 93, 304-310.	7.0	4
4331	Kinetic and Structural Insights into the Mechanism of Binding of Sulfonamides to Human Carbonic Anhydrase by Computational and Experimental Studies. Journal of Medicinal Chemistry, 2016, 59, 4245-4256.	6.4	60
4332	Molecular assembly of lethal factor enzyme and pre-pore heptameric protective antigen in early stage of translocation. Journal of Molecular Modeling, 2016, 22, 7.	1.8	4
4333	Mutants and molecular dockings reveal that the primary L-thyroxine binding site in human serum albumin is not the one which can cause familial dysalbuminemic hyperthyroxinemia. Biochimica Et Biophysica Acta - General Subjects, 2016, 1860, 648-660.	2.4	11
4334	Conformational ensemble of human $\beta$ -synuclein physiological form predicted by molecular simulations. Physical Chemistry Chemical Physics, 2016, 18, 5702-5706.	2.8	32

#	ARTICLE	IF	CITATIONS
4335	Multi-scale simulation of degradation of polymer coatings: Thermo-mechanical simulations. Polymer Degradation and Stability, 2016, 123, 1-12.	5.8	6
4336	Molecular Dynamics Simulations of Sulfobetaine-Type Zwitterionic Surfactant at the Decane/Water Interface. Journal of Dispersion Science and Technology, 2016, 37, 1480-1485.	2.4	15
4337	Consistent Embedding Frameworks for Predictive Multi-theory Multiscale Simulations. Springer Series in Materials Science, 2016, , 249-297.	0.6	0
4338	A Validation Study of the General Amber Force Field Applied to Energetic Molecular Crystals. Journal of Energetic Materials, 2016, 34, 62-75.	2.0	5
4339	Insights into structural and dynamical features of water at halloysite interfaces probed by DFT and classical molecular dynamics simulations. Physical Chemistry Chemical Physics, 2016, 18, 2164-2174.	2.8	37
4340	Computer Simulation of Side-Chain Liquid Crystal Polymer Melts and Elastomers. , 2016, , 93-129.		2
4341	Fluorinated surfactants in solution: Diffusion coefficients of fluorinated alcohols in water. Fluid Phase Equilibria, 2016, 407, 322-333.	2.5	9
4342	Coarse-grained bond and angle distributions from atomistic simulations: On the systematic parameterisation of lipid models. Journal of Molecular Graphics and Modelling, 2016, 63, 57-64.	2.4	3
4343	Structural and biochemical characterization of two heme binding sites on Î± 1 -microglobulin using site directed mutagenesis and molecular simulation. Biochimica Et Biophysica Acta - Proteins and Proteomics, 2016, 1864, 29-41.	2.3	20
4344	Nonequilibrium free-energy calculation of solids using LAMMPS. Computational Materials Science, 2016, 112, 333-341.	3.0	111
4345	Comparative study of structural models of Leishmania donovani and human GDP-mannose pyrophosphorylases. European Journal of Medicinal Chemistry, 2016, 107, 109-118.	5.5	12
4346	Molecular Dynamics Study of N-Dodecyl-N,N-Dimethyl-3-Ammonio-1-Propanesulfonate Mono-Layer Adsorbed at the Air/Water Interface. Journal of Dispersion Science and Technology, 2016, 37, 1067-1075.	2.4	9
4347	Accurate Estimation of the Entropy of Rotationâ€“Translation Probability Distributions. Journal of Chemical Theory and Computation, 2016, 12, 1-8.	5.3	21
4348	Capturing state-dependent dynamic events of GABA <sub>A</sub> -receptors: a microscopic look into the structural and functional insights. Journal of Biomolecular Structure and Dynamics, 2016, 34, 1818-1837.	3.5	8
4349	Molecular dynamics simulations of the free and inhibitor-bound cruzain systems in aqueous solvent: insights on the inhibition mechanism in acidic pH. Journal of Biomolecular Structure and Dynamics, 2016, 34, 1969-1978.	3.5	12
4350	Thermodynamics of site-specific small molecular ion interactions with DNA duplex: a molecular dynamics study. Molecular Simulation, 2016, 42, 715-724.	2.0	6
4351	Protein conformational perturbations in hereditary amyloidosis: Differential impact of single point mutations in ApoA1 amyloidogenic variants. Biochimica Et Biophysica Acta - General Subjects, 2016, 1860, 434-444.	2.4	23
4352	Stability of the kaolinite-guest molecule intercalation system: A molecular simulation study. Fluid Phase Equilibria, 2016, 409, 434-438.	2.5	5

#	ARTICLE	IF	CITATIONS
4353	Martini straight: Boosting performance using a shorter cutoff and GPUs. Computer Physics Communications, 2016, 199, 1-7.	7.5	352
4354	Analysis of non-peptidic compounds as potential malarial inhibitors against <i>Plasmodial</i> cysteine proteases via integrated virtual screening workflow. Journal of Biomolecular Structure and Dynamics, 2016, 34, 2084-2101.	3.5	25
4355	Hydrogen bonds in Zif268 proteins – a theoretical perspective. Journal of Biomolecular Structure and Dynamics, 2016, 34, 1607-1624.	3.5	5
4356	OpenGrowth: An Automated and Rational Algorithm for Finding New Protein Ligands. Journal of Medicinal Chemistry, 2016, 59, 4171-4188.	6.4	53
4357	Peroxidised phospholipid bilayers: insight from coarse-grained molecular dynamics simulations. Soft Matter, 2016, 12, 263-271.	2.7	32
4358	Size-dependent plastic deformation and failure mechanisms of nanotwinned Ni3Al: Insights from an atomistic cracking model. Materials Science & Engineering A: Structural Materials: Properties, Microstructure and Processing, 2016, 649, 449-460.	5.6	19
4359	Measurement artifacts identified in the UV-vis spectroscopic study of adduct formation within the context of molecular imprinting of naproxen. Spectrochimica Acta - Part A: Molecular and Biomolecular Spectroscopy, 2016, 153, 661-668.	3.9	13
4360	Molecular dynamics simulation for self-diffusion coefficients of ginger bioactive compounds in subcritical water with and without ethanol. Fluid Phase Equilibria, 2016, 407, 197.e1-197.e10.	2.5	6
4361	Effect of lipid peroxidation on membrane permeability of cancer and normal cells subjected to oxidative stress. Chemical Science, 2016, 7, 489-498.	7.4	307
4362	Exploring the biological consequences of conformational changes in aspartame models containing constrained analogues of phenylalanine. Journal of Enzyme Inhibition and Medicinal Chemistry, 2016, 31, 953-963.	5.2	14
4363	Accounting for Electronic Polarization Effects in Aqueous Sodium Chloride via Molecular Dynamics Aided by Neutron Scattering. Journal of Physical Chemistry B, 2016, 120, 1454-1460.	2.6	102
4364	Heterogeneous behavior of metalloproteins toward metal ion binding and selectivity: insights from molecular dynamics studies. Journal of Biomolecular Structure and Dynamics, 2016, 34, 1470-1485.	3.5	7
4365	A review of constitutive models and modeling techniques for shape memory alloys. International Journal of Plasticity, 2016, 76, 244-284.	8.8	267
4366	An <i>in silico</i> approach towards the identification of novel inhibitors of the TLR-4 signaling pathway. Journal of Biomolecular Structure and Dynamics, 2016, 34, 1345-1362.	3.5	3
4367	Hydrogen bonding in ethanol-water and trifluoroethanol-water mixtures studied by NMR and molecular dynamics simulation. Journal of Molecular Liquids, 2016, 217, 3-11.	4.9	47
4368	Molecular dynamics simulations of the diffusion coefficients of light n-alkanes in water over a wide range of temperature and pressure. Fluid Phase Equilibria, 2016, 407, 236-242.	2.5	39
4369	Molecular dynamics simulations for the prediction of the dielectric spectra of alcohols, glycols and monoethanolamine. Molecular Simulation, 2016, 42, 370-390.	2.0	28
4370	Cis and trans unsaturated phosphatidylcholine bilayers: A molecular dynamics simulation study. Chemistry and Physics of Lipids, 2016, 195, 12-20.	3.2	69



#	ARTICLE	IF	CITATIONS
4371	Multiscale modeling of sensory properties of Co–Ni–Al shape memory particles embedded in an Al metal matrix. <i>Journal of Materials Science</i> , 2016, 51, 1204-1216.	3.7	25
4372	Study of curcumin behavior in two different lipid bilayer models of liposomal curcumin using molecular dynamics simulation. <i>Journal of Biomolecular Structure and Dynamics</i> , 2016, 34, 327-340.	3.5	19
4373	Change in specific interactions between lactose repressor protein and DNA induced by ligand binding: molecular dynamics and molecular orbital calculations. <i>Molecular Simulation</i> , 2016, 42, 242-256.	2.0	6
4374	Computational studies of pandemic 1918 and 2009 H1N1 hemagglutinins bound to avian and human receptor analogs. <i>Journal of Biomolecular Structure and Dynamics</i> , 2016, 34, 272-289.	3.5	9
4375	Molecular dynamics simulations on the interaction of the transmembrane NavAb channel with cholesterol and lipids in the membrane. <i>Journal of Biomolecular Structure and Dynamics</i> , 2016, 34, 318-326.	3.5	5
4376	A coarse grained molecular dynamics study on the structure and stability of small-sized liposomes. <i>Molecular Simulation</i> , 2016, 42, 122-130.	2.0	9
4377	Derivation of original RESP atomic partial charges for MD simulations of the LDAO surfactant with AMBER: applications to a model of micelle and a fragment of the lipid kinase PI4KA. <i>Journal of Biomolecular Structure and Dynamics</i> , 2017, 35, 159-181.	3.5	4
4378	Mapping intermolecular interactions and active site conformations: from human MMP-1 crystal structure to molecular dynamics free energy calculations. <i>Journal of Biomolecular Structure and Dynamics</i> , 2017, 35, 564-573.	3.5	15
4379	Investigations of Takeout proteins <sup>TM</sup> ligand binding and release mechanism using molecular dynamics simulation. <i>Journal of Biomolecular Structure and Dynamics</i> , 2017, 35, 1464-1473.	3.5	3
4380	Influence of V54M mutation in giant muscle protein titin: a computational screening and molecular dynamics approach. <i>Journal of Biomolecular Structure and Dynamics</i> , 2017, 35, 917-928.	3.5	44
4381	Insights into the structural dynamics of Liver kinase B1 (LKB1) by the binding of STe20 Related Adapter <sup>1</sup> ± (STRAD <sup>1</sup> ±) and Mouse protein 25 <sup>1</sup> ± (MO25 <sup>1</sup> ±) co-activators. <i>Journal of Biomolecular Structure and Dynamics</i> , 2017, 35, 1138-1152.	3.5	2
4382	Critical effects on binding of epidermal growth factor produced by amino acid substitutions. <i>Journal of Biomolecular Structure and Dynamics</i> , 2017, 35, 1085-1101.	3.5	6
4383	Role of sequence evolution and conformational dynamics in the substrate specificity and oligomerization mode of thymidylate kinases. <i>Journal of Biomolecular Structure and Dynamics</i> , 2017, 35, 2136-2154.	3.5	1
4384	Molecular dynamics simulations of ternary lipid bilayers containing plant sterol and glucosylceramide. <i>Chemistry and Physics of Lipids</i> , 2017, 203, 24-32.	3.2	13
4385	Effects of Lithium and Other Monovalent Ions on Palmitoyl Oleoyl Phosphatidylcholine Bilayer. <i>Langmuir</i> , 2017, 33, 1105-1115.	3.5	14
4386	Local Mode Analysis: Decoding IR Spectra by Visualizing Molecular Details. <i>Journal of Physical Chemistry B</i> , 2017, 121, 3483-3492.	2.6	6
4387	Conformational Transitions of the Amyloid <sup>2</sup> Peptide Upon Copper(II) Binding and pH Changes. <i>Israel Journal of Chemistry</i> , 2017, 57, 771-784.	2.3	20
4388	Interfacial Structure Analysis for the Morphology Prediction of Adipic Acid Crystals from Aqueous Solution. <i>Crystal Growth and Design</i> , 2017, 17, 1088-1095.	3.0	6



#	ARTICLE	IF	CITATIONS
4389	Carbon Nanotubes Mediate Fusion of Lipid Vesicles. <i>ACS Nano</i> , 2017, 11, 1273-1280.	14.6	36
4390	Investigation of changes in structure and thermodynamic of spruce budworm antifreeze protein under subfreezing temperature. <i>Scientific Reports</i> , 2017, 7, 40032.	3.3	5
4391	TMAO and urea in the hydration shell of the protein SNase. <i>Physical Chemistry Chemical Physics</i> , 2017, 19, 6345-6357.	2.8	46
4392	The presence of non-native helical structure in the unfolding of a beta-sheet protein MPT63. <i>Protein Science</i> , 2017, 26, 536-549.	7.6	11
4393	Molecular-Scale Biophysical Modulation of an Endothelial Membrane by Oxidized Phospholipids. <i>Biophysical Journal</i> , 2017, 112, 325-338.	0.5	41
4394	Structure-based virtual screening to identify the beta-lactamase CTX-M-9 inhibitors: An in silico effort to overcome antibiotic resistance in <i>E. coli</i> . <i>Computational Biology and Chemistry</i> , 2017, 67, 174-181.	2.3	7
4395	Microscopic Structure and Solubility Predictions of Multifunctional Solids in Supercritical Carbon Dioxide: A Molecular Simulation Study. <i>Journal of Physical Chemistry B</i> , 2017, 121, 1660-1674.	2.6	17
4396	Sampling conformational space of intrinsically disordered proteins in explicit solvent: Comparison between well-tempered ensemble approach and solute tempering method. <i>Journal of Molecular Graphics and Modelling</i> , 2017, 72, 136-147.	2.4	8
4397	Molecular dynamics simulations on the heterocyclic cyclodecapeptide and its linear analogous in water and octanol solvents. <i>Journal of Molecular Liquids</i> , 2017, 229, 583-590.	4.9	2
4398	Performance of various models in structural characterization of n-butanol: Molecular dynamics and X-ray scattering studies. <i>Journal of Molecular Liquids</i> , 2017, 229, 346-357.	4.9	21
4399	Protein-ion Interactions: Simulations of Bovine Serum Albumin in Physiological Solutions of NaCl, KCl and LiCl. <i>Israel Journal of Chemistry</i> , 2017, 57, 403-412.	2.3	16
4400	N6-Adenosine DNA Methyltransferase from <i>H. pylori</i> 98-10 Strain in Complex with DNA and AdoMet: Structural Insights from in Silico Studies. <i>Journal of Physical Chemistry B</i> , 2017, 121, 365-378.	2.6	0
4401	Hampering Effect of Cholesterol on the Permeation of Reactive Oxygen Species through Phospholipids Bilayer: Possible Explanation for Plasma Cancer Selectivity. <i>Scientific Reports</i> , 2017, 7, 39526.	3.3	76
4402	Distributions of therapeutically promising neurosteroids in cellular membranes. <i>Chemistry and Physics of Lipids</i> , 2017, 203, 78-86.	3.2	3
4403	Long-time atomistic dynamics through a new self-adaptive accelerated molecular dynamics method. <i>Journal of Physics Condensed Matter</i> , 2017, 29, 145201.	1.8	10
4404	Heterogeneous nanomechanical properties of type I collagen in longitudinal direction. <i>Biomechanics and Modeling in Mechanobiology</i> , 2017, 16, 1023-1033.	2.8	20
4405	Dynamic disorder can explain non-exponential kinetics of fast protein mechanical unfolding. <i>Journal of Structural Biology</i> , 2017, 197, 43-49.	2.8	10
4406	Molecular Dynamics Simulations Illuminate the Role of Counterion Condensation in the Electrophoretic Transport of Homogalacturonans. <i>Biomacromolecules</i> , 2017, 18, 505-516.	5.4	13

#	ARTICLE	IF	CITATIONS
4407	Increased Binding of Calcium Ions at Positively Curved Phospholipid Membranes. <i>Journal of Physical Chemistry Letters</i> , 2017, 8, 518-523.	4.6	27
4408	Three-dimensional Morphology and X-ray Scattering Structure of Aqueous tert-Butanol Mixtures: A Molecular Dynamics Study. <i>Journal of Chemical Sciences</i> , 2017, 129, 103-116.	1.5	8
4409	Solid-liquid and liquid-solid transitions in metal nanoparticles. <i>Physical Chemistry Chemical Physics</i> , 2017, 19, 5994-6005.	2.8	13
4410	Towards open boundary molecular dynamics simulation of ionic liquids. <i>Physical Chemistry Chemical Physics</i> , 2017, 19, 4701-4709.	2.8	17
4411	Effect of piroxicam on lipid membranes: Drug encapsulation and gastric toxicity aspects. <i>European Journal of Pharmaceutical Sciences</i> , 2017, 100, 116-125.	4.0	16
4412	Simulation Studies on the Role of Lauryl Betaine in Modulating the Stability of AOS Surfactant-Stabilized Foams Used in Enhanced Oil Recovery. <i>Energy &amp; Fuels</i> , 2017, 31, 1512-1518.	5.1	24
4413	Crystal structure and molecular dynamics studies of L-amino acid oxidase from <i>Bothrops atrox</i> . <i>Toxicon</i> , 2017, 128, 50-59.	1.6	16
4414	A Spectroscopic and Molecular Simulation Approach toward the Binding Affinity between Lysozyme and Phenazinium Dyes: An Effect on Protein Conformation. <i>Journal of Physical Chemistry B</i> , 2017, 121, 1475-1484.	2.6	64
4415	Glutamine Amide Flip Elicits Long Distance Allosteric Responses in the LOV Protein Vivid. <i>Journal of the American Chemical Society</i> , 2017, 139, 2972-2980.	13.7	31
4416	Computational smart polymer design based on elastin protein mutability. <i>Biomaterials</i> , 2017, 127, 49-60.	11.4	49
4417	Voltage Gating of a Biomimetic Nanopore: Electrowetting of a Hydrophobic Barrier. <i>ACS Nano</i> , 2017, 11, 1840-1847.	14.6	59
4418	Trimesic acid on Cu in ethanol: Potential-dependent transition from 2-D adsorbate to 3-D metal-organic framework. <i>Journal of Electroanalytical Chemistry</i> , 2017, 793, 226-234.	3.8	6
4419	Features of solvation of phenolic acids in supercritical carbon dioxide modified by methanol and acetone. <i>Journal of Supercritical Fluids</i> , 2017, 124, 50-56.	3.2	11
4420	Lid domain plasticity and lipid flexibility modulate enzyme specificity in human monoacylglycerol lipase. <i>Biochimica Et Biophysica Acta - Molecular and Cell Biology of Lipids</i> , 2017, 1862, 441-451.	2.4	15
4421	Mutation G1629E Increases von Willebrand Factor Cleavage via a Cooperative Destabilization Mechanism. <i>Biophysical Journal</i> , 2017, 112, 57-65.	0.5	11
4422	One-Way Allosteric Communication between the Two Disulfide Bonds in Tissue Factor. <i>Biophysical Journal</i> , 2017, 112, 78-86.	0.5	7
4423	Understanding the molecular mechanism for the differential inhibitory activities of compounds against MTH1. <i>Scientific Reports</i> , 2017, 7, 40557.	3.3	9
4424	On the existence of a scattering pre-peak in the mono-ols and diols. <i>Chemical Physics Letters</i> , 2017, 671, 37-43.	2.6	11

#	ARTICLE	IF	CITATIONS
4425	Role of base arrangements and intermolecular hydrogen bonding in charge-transfer states of thymine-adenine dinucleotide in aqueous solution. <i>Journal of Photochemistry and Photobiology A: Chemistry</i> , 2017, 337, 1-5.	3.9	6
4426	Elucidating the Bacterial Membrane Disruption Mechanism of Human $\alpha$ -Defensin 5: A Theoretical Study. <i>Journal of Physical Chemistry B</i> , 2017, 121, 741-748.	2.6	17
4427	Electrostatic Stabilization Plays a Central Role in Autoinhibitory Regulation of the Na <sup>+</sup> ,K <sup>+</sup> -ATPase. <i>Biophysical Journal</i> , 2017, 112, 288-299.	0.5	22
4428	A blended NPT/NVT scheme for simulating metallic glasses. <i>Computational Materials Science</i> , 2017, 130, 130-137.	3.0	5
4429	Alpha-tocopherol inhibits pore formation in oxidized bilayers. <i>Physical Chemistry Chemical Physics</i> , 2017, 19, 5699-5704.	2.8	29
4430	Structural studies of a vasorelaxant lectin from <i>Dioclea reflexa</i> Hook seeds: Crystal structure, molecular docking and dynamics. <i>International Journal of Biological Macromolecules</i> , 2017, 98, 12-23.	7.5	27
4431	Coarse-Grained Molecular Simulation of the Hierarchical Self-Assembly of $\beta$ -Conjugated Optoelectronic Peptides. <i>Journal of Physical Chemistry B</i> , 2017, 121, 1684-1706.	2.6	43
4432	Structural insights into human microsomal epoxide hydrolase by combined homology modeling, molecular dynamics simulations, and molecular docking calculations. <i>Proteins: Structure, Function and Bioinformatics</i> , 2017, 85, 720-730.	2.6	11
4433	Structural Insights How PIP2 Imposes Preferred Binding Orientations of FAK at Lipid Membranes. <i>Journal of Physical Chemistry B</i> , 2017, 121, 3523-3535.	2.6	28
4434	Synergistic effect of electric field and lipid oxidation on the permeability of cell membranes. <i>Biochimica Et Biophysica Acta - General Subjects</i> , 2017, 1861, 839-847.	2.4	116
4435	Combined Molecular Dynamics, Atoms in Molecules, and IR Studies of the Bulk Monofluoroethanol and Bulk Ethanol To Understand the Role of Organic Fluorine in the Hydrogen Bond Network. <i>Journal of Physical Chemistry A</i> , 2017, 121, 1250-1260.	2.5	20
4436	Potential of Mean Force Calculations of Solute Permeation Across UT-B and AQP1: A Comparison between Molecular Dynamics and 3D-RISM. <i>Journal of Physical Chemistry B</i> , 2017, 121, 1506-1519.	2.6	6
4437	Epigallocatechin-3-gallate preferentially induces aggregation of amyloidogenic immunoglobulin light chains. <i>Scientific Reports</i> , 2017, 7, 41515.	3.3	23
4438	Thermal rejuvenation in metallic glasses. <i>Science and Technology of Advanced Materials</i> , 2017, 18, 152-162.	6.1	82
4439	Capturing Entropic Contributions to Temperature-Mediated Polymorphic Transformations Through Molecular Modeling. <i>Crystal Growth and Design</i> , 2017, 17, 1775-1787.	3.0	43
4440	Electrical Energy Storage by a Magnesium-Copper-Sulfide Rechargeable Battery. <i>Journal of the Electrochemical Society</i> , 2017, 164, A770-A774.	2.9	8
4441	Deconstruction of the human connexin 26 hemichannel due to an applied electric field; A molecular dynamics simulation study. <i>Journal of Molecular Graphics and Modelling</i> , 2017, 73, 108-114.	2.4	7
4442	Long-chain GM1 gangliosides alter transmembrane domain registration through interdigitation. <i>Biochimica Et Biophysica Acta - Biomembranes</i> , 2017, 1859, 870-878.	2.6	20

#	ARTICLE	IF	CITATIONS
4443	Computing the Rotational Diffusion of Biomolecules via Molecular Dynamics Simulation and Quaternion Orientations. <i>Journal of Physical Chemistry B</i> , 2017, 121, 1812-1823.	2.6	19
4444	Formation mechanism of glyoxal-DNA adduct, a DNA cross-link precursor. <i>International Journal of Biological Macromolecules</i> , 2017, 98, 664-675.	7.5	8
4445	Self-host blue-emitting iridium dendrimer for solution-processed non-doped phosphorescent organic light-emitting diodes with flat efficiency roll-off and less phase segregation. <i>Organic Electronics</i> , 2017, 45, 49-56.	2.6	12
4446	Combining the MARTINI and Structure-Based Coarse-Grained Approaches for the Molecular Dynamics Studies of Conformational Transitions in Proteins. <i>Journal of Chemical Theory and Computation</i> , 2017, 13, 1366-1374.	5.3	136
4447	Amorphous zirconia: <i>ab initio</i> molecular dynamics simulations. <i>Philosophical Magazine</i> , 2017, 97, 1334-1345.	1.6	7
4448	Intra- and Intersubunit Ion-Pair Interactions Determine the Ability of Apolipoprotein C-II Mutants To Form Hybrid Amyloid Fibrils. <i>Biochemistry</i> , 2017, 56, 1757-1767.	2.5	5
4449	Molecular modeling, docking and dynamics simulations of the Dioclea lasiophylla Mart. Ex Benth seed lectin: An edematogenic and hypernociceptive protein. <i>Biochimie</i> , 2017, 135, 126-136.	2.6	11
4450	Bulk Heterojunction Morphologies with Atomistic Resolution from Coarse-Grain Solvent Evaporation Simulations. <i>Journal of the American Chemical Society</i> , 2017, 139, 3697-3705.	13.7	133
4451	Proton Dynamics in Protein Mass Spectrometry. <i>Journal of Physical Chemistry Letters</i> , 2017, 8, 1105-1112.	4.6	34
4452	Glycosylation and Lipids Working in Concert Direct CD2 Ectodomain Orientation and Presentation. <i>Journal of Physical Chemistry Letters</i> , 2017, 8, 1060-1066.	4.6	22
4453	Aggregation and insertion of melittin and its analogue MelP5 into lipid bilayers at different concentrations: effects on pore size, bilayer thickness and dynamics. <i>Physical Chemistry Chemical Physics</i> , 2017, 19, 7195-7203.	2.8	17
4454	Extension of CAVS coarse-grained model to phospholipid membranes: The importance of electrostatics. <i>Journal of Computational Chemistry</i> , 2017, 38, 971-980.	3.3	8
4455	Microscopic Structure, Conformation, and Dynamics of Ring and Linear Poly(ethylene oxide) Melts from Detailed Atomistic Molecular Dynamics Simulations: Dependence on Chain Length and Direct Comparison with Experimental Data. <i>Macromolecules</i> , 2017, 50, 2565-2584.	4.8	50
4456	Size and shape effects on the thermodynamic properties of nanoscale volumes of water. <i>Physical Chemistry Chemical Physics</i> , 2017, 19, 9016-9027.	2.8	27
4457	Crystallographic Snapshots of Class A $\beta$ -Lactamase Catalysis Reveal Structural Changes That Facilitate $\beta$ -Lactam Hydrolysis. <i>Journal of Biological Chemistry</i> , 2017, 292, 4022-4033.	3.4	24
4458	Computational prediction of the preferred glycation sites of model helical peptides derived from human serum albumin (HSA) and lysozyme helix 4 (LH4). <i>Theoretical Chemistry Accounts</i> , 2017, 136, 1.	1.4	10
4459	Computationally connecting organic photovoltaic performance to atomistic arrangements and bulk morphology. <i>Molecular Simulation</i> , 2017, 43, 756-773.	2.0	22
4460	Lateral Pressure Profile and Free Volume Properties in Phospholipid Membranes Containing Anesthetics. <i>Journal of Physical Chemistry B</i> , 2017, 121, 2814-2824.	2.6	17

#	ARTICLE	IF	CITATIONS
4461	Mechanics of water pore formation in lipid membrane under electric field. <i>Acta Mechanica Sinica/Lixue Xuebao</i> , 2017, 33, 234-242.	3.4	8
4462	Effects of Membrane PEGylation on Entry and Location of Antifungal Drug Itraconazole and Their Pharmacological Implications. <i>Molecular Pharmaceutics</i> , 2017, 14, 1057-1070.	4.6	19
4463	Structural properties of amyloid $\beta$ (1-40) dimer explored by replica exchange molecular dynamics simulations. <i>Proteins: Structure, Function and Bioinformatics</i> , 2017, 85, 1024-1045.	2.6	18
4464	Lattice Instabilities and Phase Transformations in Fe from Atomistic Simulations. <i>Journal of Phase Equilibria and Diffusion</i> , 2017, 38, 185-194.	1.4	1
4465	Polyphenols in combination with $\beta$ -cyclodextrin can inhibit and disaggregate $\beta$ -synuclein amyloids under cell mimicking conditions: A promising therapeutic alternative. <i>Biochimica Et Biophysica Acta - Proteins and Proteomics</i> , 2017, 1865, 589-603.	2.3	49
4466	Nucleotide Selectivity at a Preinsertion Checkpoint of T7 RNA Polymerase Transcription Elongation. <i>Journal of Physical Chemistry B</i> , 2017, 121, 3777-3786.	2.6	11
4467	Microscopic Origin of Hysteresis in Water Sorption on Protein Matrices. <i>Journal of Physical Chemistry Letters</i> , 2017, 8, 1185-1190.	4.6	3
4468	Photoswitching of Azobenzene-Based Reverse Micelles above and at Subzero Temperatures As Studied by NMR and Molecular Dynamics Simulations. <i>Langmuir</i> , 2017, 33, 2306-2317.	3.5	10
4469	Why Only Ionic Liquids with Unsaturated Heterocyclic Cations Can Dissolve Cellulose: A Simulation Study. <i>ACS Sustainable Chemistry and Engineering</i> , 2017, 5, 3417-3428.	6.7	80
4470	Maltose-binding protein effectively stabilizes the partially closed conformation of the ATP-binding cassette transporter MalFGK <sub>2</sub> . <i>Physical Chemistry Chemical Physics</i> , 2017, 19, 9366-9373.	2.8	8
4471	Molecular basis of interactions between SH3 domain-containing proteins and the proline-rich region of the ubiquitin ligase Itch. <i>Journal of Biological Chemistry</i> , 2017, 292, 6325-6338.	3.4	13
4472	Molecular dynamics study of nanoscale organization and hydrogen bonding in binary mixtures of butylammonium nitrate ionic liquid and primary alcohols. <i>Journal of Chemical Physics</i> , 2017, 146, 064503.	3.0	9
4473	Different locations of adenine in AOT and CTAB reverse micelles. <i>Journal of Molecular Liquids</i> , 2017, 232, 236-242.	4.9	9
4474	Through the Lipopolysaccharide Glass: A Potent Antimicrobial Peptide Induces Phase Changes in Membranes. <i>Biochemistry</i> , 2017, 56, 1672-1679.	2.5	39
4475	Can an ammonium-based room temperature ionic liquid counteract the urea-induced denaturation of a small peptide?. <i>Physical Chemistry Chemical Physics</i> , 2017, 19, 7772-7787.	2.8	23
4476	Spontaneous NaCl-doped ice at seawater conditions: focus on the mechanisms of ion inclusion. <i>Physical Chemistry Chemical Physics</i> , 2017, 19, 9566-9574.	2.8	53
4477	Unraveling Mg <sup>2+</sup> -RNA binding with atomistic molecular dynamics. <i>Rna</i> , 2017, 23, 628-638.	3.5	61
4478	Stiff phase nucleation in a phase-transforming bar due to the collision of non-stationary waves. <i>Archive of Applied Mechanics</i> , 2017, 87, 1019-1036.	2.2	2

#	ARTICLE	IF	CITATIONS
4479	Engineering of CYP106A2 for steroid 9 $\alpha$ - and 6 $\beta$ -hydroxylation. <i>Steroids</i> , 2017, 120, 41-48.	1.8	20
4480	Albociclib can overcome mutations in cyclin dependent kinase 6 that break hydrogen bonds between the drug and the protein. <i>Protein Science</i> , 2017, 26, 870-879.	7.6	20
4481	Structural Basis of cis- and trans-Combretastatin Binding to Tubulin. <i>CheM</i> , 2017, 2, 102-113.	11.7	164
4482	Calcium Assists Dopamine Release by Preventing Aggregation on the Inner Leaflet of Presynaptic Vesicles. <i>ACS Chemical Neuroscience</i> , 2017, 8, 1242-1250.	3.5	21
4483	A refined polarizable water model for the coarse-grained MARTINI force field with long-range electrostatic interactions. <i>Journal of Chemical Physics</i> , 2017, 146, 054501.	3.0	69
4484	The Startle Disease Mutation E103K Impairs Activation of Human Homomeric $\alpha 1$ Glycine Receptors by Disrupting an Intersubunit Salt Bridge across the Agonist Binding Site. <i>Journal of Biological Chemistry</i> , 2017, 292, 5031-5042.	3.4	8
4485	Coarse-Grained Simulation of Rodlike Higher-Order Quadruplex Structures at Different Salt Concentrations. <i>ACS Omega</i> , 2017, 2, 386-396.	3.5	8
4486	Structure-mechanical property relationships in crosslinked phenolic resin investigated by molecular dynamics simulation. <i>Polymer</i> , 2017, 116, 506-514.	3.8	38
4487	Interactions of Polyaromatic Compounds. Part 1: Nanoaggregation Probed by Electrospray Ionization Mass Spectrometry and Molecular Dynamics Simulation. <i>Energy &amp; Fuels</i> , 2017, 31, 3465-3474.	5.1	13
4488	Efficient Conformational Search Based on Structural Dissimilarity Sampling: Applications for Reproducing Structural Transitions of Proteins. <i>Journal of Chemical Theory and Computation</i> , 2017, 13, 1411-1423.	5.3	26
4489	Engineering a pH responsive pore forming protein. <i>Scientific Reports</i> , 2017, 7, 42231.	3.3	27
4490	A nontoxic pain killer designed by modeling of pathological receptor conformations. <i>Science</i> , 2017, 355, 966-969.	12.6	175
4491	$\alpha$ -Synuclein's Uniquely Long Amphipathic Helix Enhances its Membrane Binding and Remodeling Capacity. <i>Journal of Membrane Biology</i> , 2017, 250, 183-193.	2.1	27
4492	Ca <sup>2+</sup> -Induced Rigidity Change of the Myosin VIIa IQ Motif-Single $\alpha$ Helix Lever Arm Extension. <i>Structure</i> , 2017, 25, 579-591.e4.	3.3	25
4493	Adsorption of the natural protein surfactant Rsn-2 onto liquid interfaces. <i>Physical Chemistry Chemical Physics</i> , 2017, 19, 8584-8594.	2.8	14
4494	Janus Gold Nanoparticles from Nanodroplets of Alkyl Thiols: A Molecular Dynamics Study. <i>Langmuir</i> , 2017, 33, 3056-3067.	3.5	10
4495	Prednisolone adsorption on lung surfactant models: insights on the formation of nanoaggregates, monolayer collapse and prednisolone spreading. <i>RSC Advances</i> , 2017, 7, 5272-5281.	3.6	30
4496	Elucidation of Binding Mechanism of Photodynamic Therapeutic Agent Toluidine Blue O with Chicken Egg White Lysozyme by Spectroscopic and Molecular Dynamics Studies. <i>Photochemistry and Photobiology</i> , 2017, 93, 1043-1056.	2.5	12



#	ARTICLE	IF	CITATIONS
4497	Single Residue Acts as Gate in Occk Channels. Journal of Physical Chemistry B, 2017, 121, 2614-2621.	2.6	15
4498	Mechanics of deformations in terms of scalar variables. Continuum Mechanics and Thermodynamics, 2017, 29, 715-729.	2.2	3
4499	Unveiling Amyloid- $\beta$ 42 Interaction with Zinc in Water and Mixed Hexafluoroisopropanol Solution in Alzheimer's Disease. International Journal of Peptide Research and Therapeutics, 2017, 23, 393-407.	1.9	2
4500	Structure and Characterisation of a Key Epitope in the Conserved C-Terminal Domain of the Malaria Vaccine Candidate MSP2. Journal of Molecular Biology, 2017, 429, 836-846.	4.2	6
4501	Binding and Packing in Two-Component Colloidal Quantum Dot Ligand Shells: Linear versus Branched Carboxylates. Journal of the American Chemical Society, 2017, 139, 3456-3464.	13.7	58
4502	Partitioning of caffeine in lipid bilayers reduces membrane fluidity and increases membrane thickness. Physical Chemistry Chemical Physics, 2017, 19, 7101-7111.	2.8	33
4503	Insights into the ion-coupling mechanism in the MATE transporter NorM-VC. Physical Biology, 2017, 14, 045009.	1.8	16
4504	Thermodynamics of hydration of fullerols [C60(OH) <sub>n</sub> ] and hydrogen bond dynamics in their hydration shells. Journal of Chemical Physics, 2017, 146, 074501.	3.0	12
4505	Protein Tunnels: The Case of Urease Accessory Proteins. Journal of Chemical Theory and Computation, 2017, 13, 2322-2331.	5.3	25
4506	Solution behaviour of poly(N-isopropylacrylamide) stereoisomers in water: a molecular dynamics simulation study. Physical Chemistry Chemical Physics, 2017, 19, 11892-11903.	2.8	17
4507	Differential binding and activity of the pore-forming toxin sticholysin II in model membranes containing diverse ceramide-derived lipids. Biochimie, 2017, 138, 20-31.	2.6	14
4508	Estimating yield-strain via deformation-recovery simulations. Polymer, 2017, 116, 295-303.	3.8	3
4509	Aptamer based electrostatic-stimuli responsive surfaces for on-demand binding/unbinding of a specific ligand. Journal of Materials Chemistry B, 2017, 5, 3675-3685.	5.8	13
4510	On the parallelism between the mechanisms behind chromatography and drug delivery: the role of interactions with a stationary phase. Physical Chemistry Chemical Physics, 2017, 19, 11518-11528.	2.8	8
4511	Interdigitation between Triglycerides and Lipids Modulates Surface Properties of Lipid Droplets. Biophysical Journal, 2017, 112, 1417-1430.	0.5	102
4512	The pH-dependent assembly of Chaplin E from Streptomyces coelicolor. Journal of Structural Biology, 2017, 198, 82-91.	2.8	8
4513	Amino acid polymorphisms in the fibronectin-binding repeats of fibronectin-binding protein A affect bond strength and fibronectin conformation. Journal of Biological Chemistry, 2017, 292, 8797-8810.	3.4	16
4514	Mechanism-based selection of stabilization strategy for amorphous formulations: Insights into crystallization pathways. Journal of Controlled Release, 2017, 256, 193-202.	9.9	63



#	ARTICLE	IF	CITATIONS
4515	Effect of an ionic liquid/air Interface on the structure and dynamics of amphiphilic peptides. Journal of Molecular Liquids, 2017, 236, 404-413.	4.9	8
4516	Molecular dynamics simulations of early steps in RNA $\alpha$ -mediated conversion of prions. Protein Science, 2017, 26, 1524-1534.	7.6	11
4517	Full-length, Oligomeric Structure of Wzz Determined by Cryoelectron Microscopy Reveals Insights into Membrane-Bound States. Structure, 2017, 25, 806-815.e3.	3.3	31
4518	Hydrogen-Doped Polymeric Carbon Monoxide at High Pressure. Journal of Physical Chemistry C, 2017, 121, 10078-10086.	3.1	11
4519	Solvation Structure of 1,3-Butanediol in Aqueous Binary Solvents with Acetonitrile, 1,4-Dioxane, and Dimethyl Sulfoxide Studied by IR, NMR, and Molecular Dynamics Simulation. Journal of Physical Chemistry B, 2017, 121, 4864-4872.	2.6	7
4520	Performance of extended Lagrangian schemes for molecular dynamics simulations with classical polarizable force fields and density functional theory. Journal of Chemical Physics, 2017, 146, 124115.	3.0	26
4521	Homogeneous nucleation of water in argon. Nucleation rate computation from molecular simulations of TIP4P and TIP4P/2005 water model. Journal of Chemical Physics, 2017, 146, 084309.	3.0	10
4522	Assembly of trivalent particles under confinement: from an exotic solid phase to a liquid phase at low temperature. Soft Matter, 2017, 13, 3221-3229.	2.7	5
4523	Importance of side-chain anchoring atoms on electron donor/fullerene interfaces for high-performance organic solar cells. Journal of Materials Chemistry A, 2017, 5, 9316-9321.	10.3	34
4524	Small static electric field strength promotes aggregation-prone structures in amyloid- $\beta$ (29-42). Journal of Chemical Physics, 2017, 146, 145101.	3.0	17
4525	Identification of a conserved 8 aa insert in the PIP5K protein in the <i>Saccharomycetaceae</i> family of fungi and the molecular dynamics simulations and structural analysis to investigate its potential functional role. Proteins: Structure, Function and Bioinformatics, 2017, 85, 1454-1467.	2.6	22
4526	A multiscale model for amorphous materials. Computational Materials Science, 2017, 135, 64-77.	3.0	15
4527	Is the Solution Activity Derivative Sufficient to Parametrize Ion-Ion Interactions? Ions for TIP5P Water. Journal of Chemical Theory and Computation, 2017, 13, 2112-2122.	5.3	17
4528	Novel 1, 4-dihydropyridines for L-type calcium channel as antagonists for cadmium toxicity. Scientific Reports, 2017, 7, 45211.	3.3	28
4529	On the role of residue phosphorylation in 14-3-3 partners: AANAT as a case study. Scientific Reports, 2017, 7, 46114.	3.3	9
4530	Influence of phase stability on the in situ growth stresses in Cu/Nb multilayered films. Acta Materialia, 2017, 132, 149-161.	7.9	15
4531	Defect-induced change of temperature-dependent elastic constants in BCC iron. Journal of Nuclear Materials, 2017, 490, 125-129.	2.7	3
4532	Mesoscale Simulation and Machine Learning of Asphaltene Aggregation Phase Behavior and Molecular Assembly Landscapes. Journal of Physical Chemistry B, 2017, 121, 4923-4944.	2.6	32

#	ARTICLE	IF	CITATIONS
4533	Nature's Selection of Geranyl Group as a tRNA Modification: The Effects of Chain Length on Base-Pairing Specificity. <i>ACS Chemical Biology</i> , 2017, 12, 1504-1513.	3.4	7
4534	Terminal $\pi$ - $\pi$ stacking determines three-dimensional molecular packing and isotropic charge transport in an A $\pi$ -A electron acceptor for non-fullerene organic solar cells. <i>Journal of Materials Chemistry C</i> , 2017, 5, 4852-4857.	5.5	192
4535	How a short pore forming peptide spans the lipid membrane. <i>Biointerphases</i> , 2017, 12, 02D405.	1.6	6
4536	Analysis of Biphenyl-Type Inhibitors Targeting the Eg5 $\pm 4/\pm 6$ Allosteric Pocket. <i>ACS Omega</i> , 2017, 2, 1836-1849.	3.5	2
4537	Mapping the ionic fingerprints of molecular monolayers. <i>Physical Chemistry Chemical Physics</i> , 2017, 19, 15098-15109.	2.8	22
4538	Second Harmonic Generation Guided Raman Spectroscopy for Sensitive Detection of Polymorph Transitions. <i>Analytical Chemistry</i> , 2017, 89, 5958-5965.	6.5	12
4539	On the prediction of transport properties of ionic liquid using 1-n-butylmethylpyridinium tetrafluoroborate as an example. <i>Molecular Simulation</i> , 2017, 43, 1502-1512.	2.0	17
4540	Pressure modulates the self-cleavage step of the hairpin ribozyme. <i>Nature Communications</i> , 2017, 8, 14661.	12.8	22
4541	Revisiting Partition in Hydrated Bilayer Systems. <i>Journal of Chemical Theory and Computation</i> , 2017, 13, 2290-2299.	5.3	13
4542	Structural investigation of room-temperature ionic liquids and high-temperature ionic melts using triplet correlation functions. <i>Journal of Chemical Physics</i> , 2017, 146, .	3.0	11
4543	Computation of elastic constants of solids using molecular simulation: comparison of constant volume and constant pressure ensemble methods. <i>Molecular Simulation</i> , 2017, 43, 1413-1422.	2.0	36
4544	A New Strategy for Deleting Animal drugs from Traditional Chinese Medicines based on Modified Yimusake Formula. <i>Scientific Reports</i> , 2017, 7, 1504.	3.3	45
4545	Nucleation of urea from aqueous solution: Structure, critical size, and rate. <i>Journal of Chemical Physics</i> , 2017, 146, 134501.	3.0	18
4546	Molecular characterization and application of lipase from <i>Bacillus</i> sp. PU1 and investigation of structural changes based on pH and temperature using MD simulation. <i>International Journal of Biological Macromolecules</i> , 2017, 103, 47-56.	7.5	16
4547	Combined effects of headgroup charge and tail unsaturation of lipids on lateral organization and diffusion of lipids in model biomembranes. <i>Chinese Physics B</i> , 2017, 26, 048701.	1.4	3
4548	Structural insights into the mechanism of the drastic changes in enzymatic activity of the cytochrome P450 vitamin D <sub>3</sub> hydroxylase (CYP107BR1) caused by a mutation distant from the active site. <i>Acta Crystallographica Section F, Structural Biology Communications</i> , 2017, 73, 266-275.	0.8	12
4549	Antioxidant and Membrane Binding Properties of Serotonin Protect Lipids from Oxidation. <i>Biophysical Journal</i> , 2017, 112, 1863-1873.	0.5	66
4550	Thermodynamic formalism for transport coefficients with an application to the shear modulus and shear viscosity. <i>Journal of Chemical Physics</i> , 2017, 146, 124130.	3.0	4

#	ARTICLE	IF	CITATIONS
4551	Mechanistic Principles Behind Molecular Mechanism of Rifampicin Resistance in Mutant RNA Polymerase Beta Subunit of <i>Mycobacterium tuberculosis</i> . Journal of Cellular Biochemistry, 2017, 118, 4594-4606.	2.6	38
4552	Analysis of O <sub>2</sub> -binding Sites in Proteins Using Gas-Pressure NMR Spectroscopy: Outer Surface Protein A. Biophysical Journal, 2017, 112, 1820-1828.	0.5	8
4553	Broadband terahertz dielectric spectroscopy of alcohols. Chemical Physics Letters, 2017, 678, 65-71.	2.6	17
4554	A comparison of ligand behaviors and interactions during supramolecular assembly using molecular dynamics simulation: Synthesis, solid state and solution studies of two Ni(II) compounds. Polyhedron, 2017, 133, 24-32.	2.2	1
4555	V67L Mutation Fills an Internal Cavity To Stabilize RecA <i>Mtu</i> Intein. Biochemistry, 2017, 56, 2715-2722.	2.5	9
4556	Simulated Force Quench Dynamics Shows GB1 Protein Is Not a Two State Folder. Journal of Physical Chemistry B, 2017, 121, 5162-5173.	2.6	14
4557	Adsorption of plasma proteins onto PEGylated single-walled carbon nanotubes: The effects of protein shape, PEG size and grafting density. Journal of Molecular Graphics and Modelling, 2017, 75, 1-8.	2.4	11
4558	Testing High Concentrations of Membrane Active Antibiotic Chlorhexidine Via Computational Titration and Calorimetry. Journal of Physical Chemistry B, 2017, 121, 4657-4668.	2.6	8
4559	Defeating Bacterial Resistance and Preventing Mammalian Cells Toxicity Through Rational Design of Antibiotic-Functionalized Nanoparticles. Scientific Reports, 2017, 7, 1326.	3.3	33
4560	Elasticity and Stability of Clathrate Hydrate: Role of Guest Molecule Motions. Scientific Reports, 2017, 7, 1290.	3.3	41
4561	Two successive amorphous-to-amorphous phase transformations in TiO <sub>2</sub> . Journal of the American Ceramic Society, 2017, 100, 3903-3911.	3.8	6
4562	BayesWHAM: A Bayesian approach for free energy estimation, reweighting, and uncertainty quantification in the weighted histogram analysis method. Journal of Computational Chemistry, 2017, 38, 1583-1605.	3.3	46
4563	Effect of Model Polycyclic Aromatic Compounds on the Coalescence of Water-in-Oil Emulsion Droplets. Journal of Physical Chemistry C, 2017, 121, 10382-10391.	3.1	27
4564	Effects of the asphaltene structure and the tetralin/heptane solvent ratio on the size and shape of asphaltene aggregates. Physical Chemistry Chemical Physics, 2017, 19, 13931-13940.	2.8	16
4565	Multilayer Nanofilms via Inkjet Printing for Stabilizing Growth Factor and Designing Desired Cell Developments. Advanced Healthcare Materials, 2017, 6, 1700216.	7.6	8
4566	Enhancing thermal stability of a highly concentrated insulin formulation with Pluronic F-127 for long-term use in microfabricated implantable devices. Drug Delivery and Translational Research, 2017, 7, 529-543.	5.8	21
4567	Characterizing the structure–function relationship reveals the mode of action of a novel antimicrobial peptide, P1, from jumper ant <i>Myrmecia pilosula</i> . Molecular BioSystems, 2017, 13, 1193-1201.	2.9	12
4568	Force probe simulations of a reversibly rebinding system: Impact of pulling device stiffness. Journal of Chemical Physics, 2017, 146, 124901.	3.0	6

#	ARTICLE	IF	CITATIONS
4569	Thermophysical properties of liquid UO <sub>2</sub> , ZrO <sub>2</sub> and corium by molecular dynamics and predictive models. Journal of Nuclear Materials, 2017, 491, 126-137.	2.7	31
4570	Diffusion-Controlled Recrystallization of Water Sorbed into Poly(meth)acrylates Revealed by Variable-Temperature Mid-Infrared Spectroscopy and Molecular Dynamics Simulation. Journal of Physical Chemistry B, 2017, 121, 5133-5141.	2.6	20
4571	Molecular dynamics simulations of the structure and the morphology of graphene/polymer nanocomposites. Physical Chemistry Chemical Physics, 2017, 19, 12959-12969.	2.8	40
4572	Molecular Simulations of Mixed Lipid Bilayers with Sphingomyelin, Glycerophospholipids, and Cholesterol. Journal of Physical Chemistry B, 2017, 121, 5197-5208.	2.6	54
4573	Efficient affinity maturation of antibody variable domains requires co-selection of compensatory mutations to maintain thermodynamic stability. Scientific Reports, 2017, 7, 45259.	3.3	77
4574	Direct experimental observation of mesoscopic fluorine domains in fluorinated room temperature ionic liquids. Physical Chemistry Chemical Physics, 2017, 19, 13101-13110.	2.8	32
4575	Coupling of helix E-F motion with the O-nitrito and 2-nitrovinyl coordination in myoglobin. Biophysical Chemistry, 2017, 221, 10-16.	2.8	4
4576	Effect of small amount of water on the dynamics properties and microstructures of ionic liquids. AIChE Journal, 2017, 63, 2248-2256.	3.6	48
4577	Hydrogen-bond dynamics at the bio-water interface in hydrated proteins: a molecular-dynamics study. Physical Chemistry Chemical Physics, 2017, 19, 318-329.	2.8	28
4578	Thermodynamic origins of the solvent-dependent stability of lithium polysulfides from first principles. Physical Chemistry Chemical Physics, 2017, 19, 1441-1448.	2.8	41
4579	Hydration and self-aggregation of a neutral cosolute from dielectric relaxation spectroscopy and MD simulations: the case of 1,3-dimethylurea. Physical Chemistry Chemical Physics, 2017, 19, 219-230.	2.8	21
4580	Targeting Type 2 Diabetes with <i>l</i> -Glucosyl Dihydrochalcones as Selective Sodium Glucose Co-Transporter 2 (SGLT2) Inhibitors: Synthesis and Biological Evaluation. Journal of Medicinal Chemistry, 2017, 60, 568-579.	6.4	50
4581	Structural Basis of Egg Coat-Sperm Recognition at Fertilization. Cell, 2017, 169, 1315-1326.e17.	28.9	78
4582	Coherent Experimental and Simulation Approach To Explore the Underlying Mechanism of Denaturation of Stem Bromelain in Osmolytes. Journal of Physical Chemistry B, 2017, 121, 6456-6470.	2.6	12
4583	Identification of potent cholecystokinin-B receptor antagonists: synthesis, molecular modeling and anti-cancer activity against pancreatic cancer cells. MedChemComm, 2017, 8, 1561-1574.	3.4	6
4584	Size and strain rate effects in tensile strength of penta-twinned Ag nanowires. Acta Mechanica Sinica/Lixue Xuebao, 2017, 33, 792-800.	3.4	17
4585	Water structure around hydrophobic amino acid side chain analogs using different water models. Journal of Chemical Physics, 2017, 146, 225104.	3.0	18
4586	Software tools for high-throughput CALPHAD from first-principles data. Calphad: Computer Coupling of Phase Diagrams and Thermochemistry, 2017, 58, 70-81.	1.6	57

#	ARTICLE	IF	CITATIONS
4587	Structure-Activity Relationship in TLR4 Mutations: Atomistic Molecular Dynamics Simulations and Residue Interaction Network Analysis. <i>Scientific Reports</i> , 2017, 7, 43807.	3.3	54
4588	Connecting diffusion and entropy of bulk water at the single particle level. <i>Journal of Chemical Sciences</i> , 2017, 129, 825-832.	1.5	3
4589	The unfolding mechanism of monomeric mutant SOD1 by simulated force spectroscopy. <i>Biochimica Et Biophysica Acta - Proteins and Proteomics</i> , 2017, 1865, 1631-1642.	2.3	14
4590	Buckling Under Pressure: Curvature-Based Lipid Segregation and Stability Modulation in Cardiolipin-Containing Bilayers. <i>Langmuir</i> , 2017, 33, 6937-6946.	3.5	68
4591	Structure of the full-length glucagon class B G-protein-coupled receptor. <i>Nature</i> , 2017, 546, 259-264.	27.8	179
4592	Isobaric vapor-liquid equilibrium of 2-propanone+2-butanol system at 101.325 kPa: Experimental and molecular dynamics simulation. <i>Korean Journal of Chemical Engineering</i> , 2017, 34, 2011-2018.	2.7	4
4593	Control of the hierarchical assembly of Ñ-conjugated optoelectronic peptides by pH and flow. <i>Organic and Biomolecular Chemistry</i> , 2017, 15, 5484-5502.	2.8	19
4594	Hidden electrostatic basis of dynamic allostery in a PDZ domain. <i>Proceedings of the National Academy of Sciences of the United States of America</i> , 2017, 114, E5825-E5834.	7.1	78
4595	New insights into human farnesyl pyrophosphate synthase inhibition by second-generation bisphosphonate drugs. <i>Journal of Computer-Aided Molecular Design</i> , 2017, 31, 675-688.	2.9	3
4596	Comparison of the Structural Response to Pressure of Ionic Liquids with Ether and Alkyl Functionalities. <i>Journal of Physical Chemistry B</i> , 2017, 121, 6890-6897.	2.6	19
4597	A Spring-Loaded Mechanism Governs the Clamp-like Dynamics of the Skp Chaperone. <i>Structure</i> , 2017, 25, 1079-1088.e3.	3.3	34
4598	Pressure-Induced Disorder in SnO <sub>2</sub> Nanoparticles. <i>Journal of Physical Chemistry C</i> , 2017, 121, 15463-15471.	3.1	23
4599	Suppression of homogeneous crystal nucleation of the NiAl intermetallic by a composition gradient: A molecular dynamics study. <i>Journal of Chemical Physics</i> , 2017, 146, .	3.0	10
4600	Are Pro8/Pro18 really critical for functional dynamic behavior of human endostatin N-terminal peptide? A comparative molecular dynamics study. <i>Journal of the Iranian Chemical Society</i> , 2017, 14, 2023-2039.	2.2	6
4601	Monitoring the different micelle species and the slow kinetics of tetraethylammonium perfluorooctane-sulfonate by 19F NMR spectroscopy. <i>Advances in Colloid and Interface Science</i> , 2017, 246, 153-164.	14.7	12
4602	Optimizing purification process of MIM-I-BAR domain by introducing atomic force microscope and dynamics simulations. <i>Colloids and Surfaces B: Biointerfaces</i> , 2017, 157, 391-397.	5.0	1
4603	Polar N-terminal Residues Conserved in Type 2 Secretion Pseudopilins Determine Subunit Targeting and Membrane Extraction Steps during Fibre Assembly. <i>Journal of Molecular Biology</i> , 2017, 429, 1746-1765.	4.2	18
4604	Structural Characterization of Histatin 5â€Spermidine Conjugates: A Combined Experimental and Theoretical Study. <i>Journal of Chemical Information and Modeling</i> , 2017, 57, 1330-1341.	5.4	8

#	ARTICLE	IF	CITATIONS
4605	Production of Medium Chain Fatty Acids by <i>Yarrowia lipolytica</i> : Combining Molecular Design and TALEN to Engineer the Fatty Acid Synthase. ACS Synthetic Biology, 2017, 6, 1870-1879.	3.8	71
4606	Effect of applied force and atomic organization of copper on its adhesion to a graphene substrate. RSC Advances, 2017, 7, 25118-25131.	3.6	15
4607	Computational methodology for solubility prediction: Application to the sparingly soluble solutes. Journal of Chemical Physics, 2017, 146, 214110.	3.0	71
4608	Characterization of 1,2-Distearoyl-sn-glycero-3-phosphoethanolamineâ€“[Methoxy(polyethylene) Tj ETQq1 1 0.784314rgBT /Overlock 10 T and Molecular Dynamics. Bioconjugate Chemistry, 2017, 28, 1777-1790.	3.6	6
4609	First-principle simulations of electronic structure in semicrystalline polyethylene. Journal of Chemical Physics, 2017, 146, 204901.	3.0	43
4610	The effects of single-walled carbon nanotubes (SWCNTs) on the structure and function of human serum albumin (HSA): Molecular docking and molecular dynamics simulation studies. Structural Chemistry, 2017, 28, 1815-1822.	2.0	9
4611	Mapping the Free Energy of Lithium Solvation in the Protic Ionic Liquid Ethylammonium Nitrate: A Metadynamics Study. ChemSusChem, 2017, 10, 3083-3090.	6.8	10
4612	A combined molecular dynamics simulation, atoms in molecule analysis and IR study on the biologically important bulk fluorinated ethanols to understand the role of weak interactions in their cluster formation and hydrogen bond network. Journal of Molecular Liquids, 2017, 240, 708-716.	4.9	16
4613	Modulation of the Conformational Dynamics of Apo-Adenylate Kinase through a â€“Cation Interaction. Journal of Physical Chemistry B, 2017, 121, 5699-5708.	2.6	13
4614	Curcumin Protects Membranes through a Carpet or Insertion Model Depending on Hydration. Langmuir, 2017, 33, 8516-8524.	3.5	24
4615	Lifshitz phase: the microscopic structure of aqueous and ethanol mixtures of 1,n-diols. Physical Chemistry Chemical Physics, 2017, 19, 14992-15004.	2.8	3
4616	Effect of sampling on BACE-1 ligands binding free energy predictions via MM-PBSA calculations. Journal of Computational Chemistry, 2017, 38, 1941-1951.	3.3	14
4617	Gold-Induced Unfolding of Lysozyme: Toward the Formation of Luminescent Clusters. Journal of Physical Chemistry C, 2017, 121, 13335-13344.	3.1	14
4618	Imidazolium Ionic Liquid Mediates Black Phosphorus Exfoliation while Preventing Phosphorene Decomposition. ACS Nano, 2017, 11, 6459-6466.	14.6	43
4619	2D lattice model of a lipid bilayer: Microscopic derivation and thermodynamic exploration. Journal of Chemical Physics, 2017, 146, 064305.	3.0	6
4620	Structural dissimilarity sampling with dynamically self-guiding selection. Journal of Computational Chemistry, 2017, 38, 1921-1929.	3.3	11
4621	Temperature Effect on Interfacial Structure and Dynamics Properties in Polymer/Single-Chain Nanoparticle Composite. Macromolecular Chemistry and Physics, 2017, 218, 1700029.	2.2	11
4622	Inhibition of A $\beta$ Amyloid Growth and Toxicity by Silybins: The Crucial Role of Stereochemistry. ACS Chemical Neuroscience, 2017, 8, 1767-1778.	3.5	72



#	ARTICLE	IF	CITATIONS
4623	Structural and functional effects of nucleotide variation on the human TB drug metabolizing enzyme arylamine N -acetyltransferase 1. <i>Journal of Molecular Graphics and Modelling</i> , 2017, 75, 330-339.	2.4	13
4624	Computational Studies of the Active and Inactive Regulatory Domains of Response Regulator PhoP Using Molecular Dynamics Simulations. <i>Molecular Informatics</i> , 2017, 36, 1700031.	2.5	4
4625	Metadynamic metainference: Convergence towards force field independent structural ensembles of a disordered peptide. <i>Journal of Chemical Physics</i> , 2017, 146, 165102.	3.0	47
4626	1,3,5-tris(4-bromophenyl)-benzene Nucleation: From Dimers to Needle-like Clusters. <i>Crystal Growth and Design</i> , 2017, 17, 4137-4143.	3.0	9
4627	<i>Staphylococcus aureus</i> $\hat{\Gamma}$ -toxin in aqueous solution: Behavior in monomeric and multimeric states. <i>Biophysical Chemistry</i> , 2017, 227, 21-28.	2.8	4
4628	$\hat{\Gamma}$ -Conotoxin [S9A]TxID Potently Discriminates between $\hat{\Gamma}\pm 3\hat{\Gamma}^{24}$ and $\hat{\Gamma}\pm 6/\hat{\Gamma}\pm 3\hat{\Gamma}^{24}$ Nicotinic Acetylcholine Receptors. <i>Journal of Medicinal Chemistry</i> , 2017, 60, 5826-5833.	6.4	30
4629	Determining dominant driving forces affecting controlled protein release from polymeric nanoparticles. <i>Biointerphases</i> , 2017, 12, 02D412.	1.6	5
4630	A structural perspective on the interactions of TRAF6 and $\langle \text{scp} \rangle \text{B} \langle / \text{scp} \rangle$ asigin during the onset of melanoma: A molecular dynamics simulation study. <i>Journal of Molecular Recognition</i> , 2017, 30, e2643.	2.1	6
4631	The study of peculiarities of parabens solvation in methanol- and acetone-modified supercritical carbon dioxide by computer simulation. <i>Journal of Supercritical Fluids</i> , 2017, 126, 47-54.	3.2	14
4632	Amorphous phase stability and the interplay between electronic structure and topology. <i>Acta Materialia</i> , 2017, 131, 131-140.	7.9	12
4633	Anesthetics mechanism on a DMPC lipid membrane model: Insights from molecular dynamics simulations. <i>Biophysical Chemistry</i> , 2017, 226, 1-13.	2.8	16
4634	Intercolumnar Interactions Control the Local Orientations within Columnar Stacks of Sumanene and Sumanene Derivatives. <i>Journal of Physical Chemistry C</i> , 2017, 121, 8541-8547.	3.1	9
4635	Rational Design of New Antimicrobial Peptides Targeting Gram Negative Bacteria. <i>Biophysical Journal</i> , 2017, 112, 386a.	0.5	1
4636	Anomalous Protein-Protein Interactions in Multivalent Salt Solution. <i>Journal of Physical Chemistry B</i> , 2017, 121, 3000-3006.	2.6	23
4637	Modeling and Experiment Reveal Structure and Nanomechanics across the Inverse Temperature Transition in <i>B. mori</i> Silk-Elastin-like Protein Polymers. <i>ACS Biomaterials Science and Engineering</i> , 2017, 3, 2889-2899.	5.2	20
4638	Structure and dynamics of Type III periplasmic proteins VcFhuD and VcHutB reveal molecular basis of their distinctive ligand binding properties. <i>Scientific Reports</i> , 2017, 7, 42812.	3.3	8
4639	<i>Yersinia</i> effector protein (YopO)-mediated phosphorylation of host gelsolin causes calcium-independent activation leading to disruption of actin dynamics. <i>Journal of Biological Chemistry</i> , 2017, 292, 8092-8100.	3.4	13
4640	Mobility of dissociated mixed dislocations under an Escaig stress. <i>Modelling and Simulation in Materials Science and Engineering</i> , 2017, 25, 045001.	2.0	5



#	ARTICLE	IF	CITATIONS
4641	Dislocation Core Structure at Finite Temperature Inferred by Molecular Dynamics Simulations for 1,3,5-Triamino-2,4,6-trinitrobenzene Single Crystal. <i>Journal of Physical Chemistry C</i> , 2017, 121, 7442-7449.	3.1	21
4642	The atomic simulation environmentâ€”a Python library for working with atoms. <i>Journal of Physics Condensed Matter</i> , 2017, 29, 273002.	1.8	1,933
4643	Study of the cold charge transfer state separation at the TQ1/PC<sub>71</sub>BM interface. <i>Journal of Computational Chemistry</i> , 2017, 38, 1039-1048.	3.3	2
4644	Molecular docking, molecular dynamics simulation, biological evaluation and 2D QSAR analysis of flavonoids from <i>Syzygium alternifolium</i> as potent anti- <i>Helicobacter pylori</i> agents. <i>RSC Advances</i> , 2017, 7, 18277-18292.	3.6	60
4645	Breakdown of nonlinear elasticity in stress-controlled thermal amorphous solids. <i>Physical Review E</i> , 2017, 95, 031001.	2.1	7
4646	Subtle Effects of Aliphatic Alcohol Structure on Water Extraction and Solute Aggregation in Biphasic Water/n-Dodecane. <i>Langmuir</i> , 2017, 33, 3776-3786.	3.5	15
4647	Internal Water Dynamics Control the Transglycosylation/Hydrolysis Balance in the Agarase (AgaD) of <i>Zobellia galactanivorans</i> . <i>ACS Catalysis</i> , 2017, 7, 3357-3367.	11.2	23
4648	Structural heterogeneity of the Î¼-opioid receptorâ€™s conformational ensemble in the apo state. <i>Scientific Reports</i> , 2017, 7, 45761.	3.3	23
4649	Phosphatidylserine flipâ€”flop induced by oxidation of the plasma membrane: a better insight by atomic scale modeling. <i>Plasma Processes and Polymers</i> , 2017, 14, 1700013.	3.0	18
4650	Molecular Dynamics Study of Morphology of Doped PEDOT: From Solution to Dry Phase. <i>Journal of Physical Chemistry B</i> , 2017, 121, 4299-4307.	2.6	68
4651	Stability, Structure, and Electronic Properties of the Pyrite/Arsenopyrite Solidâ€”Solid Interfaceâ€”A DFT Study. <i>Journal of Physical Chemistry C</i> , 2017, 121, 8042-8051.	3.1	34
4652	Replica exchange molecular dynamics study of the amyloid beta (11â€”40) trimer penetrating a membrane. <i>RSC Advances</i> , 2017, 7, 7346-7357.	3.6	38
4653	Critical Comparison of Biomembrane Force Fields: Proteinâ€”Lipid Interactions at the Membrane Interface. <i>Journal of Chemical Theory and Computation</i> , 2017, 13, 2310-2321.	5.3	62
4654	Switchable Redox Chemistry of the Hexameric Tyrosine-Coordinated Heme Protein. <i>Journal of Physical Chemistry B</i> , 2017, 121, 3955-3964.	2.6	8
4655	Interface-Mediated Self-Assembly in Inkjet Printing of Single-Crystal Organic Semiconductor Films. <i>Journal of Physical Chemistry C</i> , 2017, 121, 8796-8803.	3.1	25
4656	Formation of novel transition metal hydride complexes with ninefold hydrogen coordination. <i>Scientific Reports</i> , 2017, 7, 44253.	3.3	32
4657	The molecular behavior of a single Î²-amyloid inside a dipalmitoylphosphatidylcholine bilayer at three different temperatures: An atomistic simulation study: AÎ² interaction with DPPC: Atomistic simulation. <i>Proteins: Structure, Function and Bioinformatics</i> , 2017, 85, 1298-1310.	2.6	7
4658	Structural insights into type I and type II of nsp4 porcine reproductive and respiratory syndrome virus (nsp4 PRRSV) by molecular dynamics simulations. <i>Journal of Molecular Graphics and Modelling</i> , 2017, 74, 125-134.	2.4	2

#	ARTICLE	IF	CITATIONS
4659	Molecular Mechanism of Nucleotide-Dependent Allosteric Regulation in AMP-Activated Protein Kinase. <i>Journal of Physical Chemistry B</i> , 2017, 121, 2919-2930.	2.6	0
4660	Deformation physics of shape memory alloys “ Fundamentals at atomistic frontier. <i>Progress in Materials Science</i> , 2017, 88, 49-88.	32.8	124
4661	Molecular dynamics simulation studies of the $\mu$ -CL-20/HMX co-crystal-based PBXs with HTPB. <i>Structural Chemistry</i> , 2017, 28, 1645-1651.	2.0	16
4662	Opposing Intermolecular Tuning of Ca <sup>2+</sup> Affinity for Calmodulin by Neurogranin and CaMKII Peptides. <i>Biophysical Journal</i> , 2017, 112, 1105-1119.	0.5	11
4663	Transport Behavior of the Enantiomers of Lactic Acid through the Cyclic Peptide Nanotube: Enantiomer Discrimination. <i>Journal of Physical Chemistry C</i> , 2017, 121, 8165-8176.	3.1	8
4664	Allosteric cross-talk in chromatin can mediate drug-drug synergy. <i>Nature Communications</i> , 2017, 8, 14860.	12.8	61
4665	Diffusion of the small, very polar, drug piracetam through a lipid bilayer: an MD simulation study. <i>Theoretical Chemistry Accounts</i> , 2017, 136, 1.	1.4	20
4666	Molecular dynamics study of water diffusion in an amphiphilic block copolymer with large difference in the blocks’ glass transition temperatures. <i>Frontiers of Chemical Science and Engineering</i> , 2017, 11, 440-447.	4.4	4
4667	Functional and Structural Characterization of a Thermostable Phospholipase A <sub>2</sub> from a Sparidae Fish ( <i>Diplodus annularis</i> ). <i>Journal of Agricultural and Food Chemistry</i> , 2017, 65, 2468-2480.	5.2	3
4668	Brigatinib combined with anti-EGFR antibody overcomes osimertinib resistance in EGFR-mutated non-small-cell lung cancer. <i>Nature Communications</i> , 2017, 8, 14768.	12.8	306
4669	Molecular dynamics simulation of effect of glycerol monostearate on amorphous polyethylene in the presence of water. <i>Journal of Molecular Modeling</i> , 2017, 23, 115.	1.8	13
4670	Potential entry inhibitors of the envelope protein (E2) of Chikungunya virus: in silico structural modeling, docking and molecular dynamic studies. <i>VirusDisease</i> , 2017, 28, 39-49.	2.0	18
4671	Modelling the Polymer Electrolyte/Li-Metal Interface by Molecular Dynamics simulations. <i>Electrochimica Acta</i> , 2017, 234, 43-51.	5.2	50
4672	High-density amorphous phase of CdO. <i>Journal of Non-Crystalline Solids</i> , 2017, 463, 64-67.	3.1	0
4673	Combined virtual screening, MMPBSA, molecular docking and dynamics studies against deadly anthrax: An in silico effort to inhibit <i>Bacillus anthracis</i> nucleoside hydrolase. <i>Journal of Theoretical Biology</i> , 2017, 420, 180-189.	1.7	23
4674	Direct Comparison of Amino Acid and Salt Interactions with Double-Stranded and Single-Stranded DNA from Explicit-Solvent Molecular Dynamics Simulations. <i>Journal of Chemical Theory and Computation</i> , 2017, 13, 1794-1811.	5.3	22
4675	Molecular modeling and structural characterization of a high glycine-tyrosine hair keratin associated protein. <i>Physical Chemistry Chemical Physics</i> , 2017, 19, 8575-8583.	2.8	16
4676	Ligand-induced allostery in the interaction of the <i>Pseudomonas aeruginosa</i> heme binding protein with heme oxygenase. <i>Proceedings of the National Academy of Sciences of the United States of America</i> , 2017, 114, 3421-3426.	7.1	18

#	ARTICLE	IF	CITATIONS
4677	Computational investigation of surface freezing in a molecular model of water. Proceedings of the National Academy of Sciences of the United States of America, 2017, 114, 3316-3321.	7.1	58
4678	Collective excitations in liquid dimethyl sulfoxide (DMSO): FIR spectrum, low frequency vibrational density of states, and ultrafast dipolar solvation dynamics. Journal of Chemical Physics, 2017, 146, 024505.	3.0	9
4679	Identification of the Crucial Residues in the Early Insertion of Pardaxin into Different Phospholipid Bilayers. Journal of Chemical Information and Modeling, 2017, 57, 929-941.	5.4	13
4680	Reparametrization of Protein Force Field Nonbonded Interactions Guided by Osmotic Coefficient Measurements from Molecular Dynamics Simulations. Journal of Chemical Theory and Computation, 2017, 13, 1812-1826.	5.3	37
4681	Local environment structure and dynamics of CO <sub>2</sub> in the 1-ethyl-3-methylimidazolium bis(trifluoromethanesulfonyl)imide and related ionic liquids. Journal of Chemical Physics, 2017, 146, 104502.	3.0	8
4682	Efficient systematic scheme to construct second-principles lattice dynamical models. Physical Review B, 2017, 95, .	3.2	23
4683	Determination of the absolute binding free energies of HIV-1 protease inhibitors using non-equilibrium molecular dynamics simulations. Chemical Physics Letters, 2017, 676, 12-17.	2.6	27
4684	Accurate, Large-Scale Density Functional Melting of Hg: Relativistic Effects Decrease Melting Temperature by 160 K. Journal of Physical Chemistry Letters, 2017, 8, 1407-1412.	4.6	21
4685	A computational study suggests that replacing PEG with PMOZ may increase exposure of hydrophobic targeting moiety. European Journal of Pharmaceutical Sciences, 2017, 103, 128-135.	4.0	17
4686	Signature of an aggregation-prone conformation of tau. Scientific Reports, 2017, 7, 44739.	3.3	69
4687	Cry1A(b)16 toxin from <i>Bacillus thuringiensis</i> : Theoretical refinement of three-dimensional structure and prediction of peptides as molecular markers for detection of genetically modified organisms. Proteins: Structure, Function and Bioinformatics, 2017, 85, 1248-1257.	2.6	3
4688	Mobility and Core-Protein Binding Patterns of Disordered C-Terminal Tails in $\beta$ -Tubulin Isotypes. Biochemistry, 2017, 56, 1746-1756.	2.5	15
4689	Self-Assembly Nanostructures of Triglyceride-Water Interfaces Determine Functional Conformations of <i>Candida antarctica</i> Lipase B. Langmuir, 2017, 33, 3151-3159.	3.5	10
4690	Stability and dynamics of membrane-spanning DNA nanopores. Nature Communications, 2017, 8, 14784.	12.8	61
4691	Stereoselective binding of agonists to the $\beta_2$ -adrenergic receptor: insights into molecular details and thermodynamics from molecular dynamics simulations. Molecular BioSystems, 2017, 13, 910-920.	2.9	8
4692	Efficient solvation free energy simulations: impact of soft-core potential and a new adaptive $\lambda$ -spacing method. Molecular Physics, 2017, 115, 1322-1334.	1.7	16
4693	A BEST example of channel structure annotation by molecular simulation. Channels, 2017, 11, 347-353.	2.8	26
4694	Structural insights into adiponectin receptors suggest ceramidase activity. Nature, 2017, 544, 120-123.	27.8	168

#	ARTICLE	IF	CITATIONS
4695	Drug Target miRNA. <i>Methods in Molecular Biology</i> , 2017, , .	0.9	2
4696	Ionic Liquids with Symmetric Diether Tails: Bulk and Vacuum-Liquid Interfacial Structures. <i>Journal of Physical Chemistry B</i> , 2017, 121, 174-179.	2.6	15
4697	A simple guiding principle for the temperature dependence of the solubility of light gases in imidazolium-based ionic liquids derived from molecular simulations. <i>Physical Chemistry Chemical Physics</i> , 2017, 19, 1770-1780.	2.8	29
4698	Topological insulating states in 2D transition metal dichalcogenides induced by defects and strain. <i>Nanoscale</i> , 2017, 9, 562-569.	5.6	28
4699	Molecular Modeling of Human CCR2 Receptor within POPC Lipid Bilayer. <i>Structural Chemistry</i> , 2017, 28, 849-857.	2.0	5
4700	Interfacial activation of M37 lipase: A multi-scale simulation study. <i>Biochimica Et Biophysica Acta - Biomembranes</i> , 2017, 1859, 340-349.	2.6	21
4701	Predicting the Kinetics of RNA Oligonucleotides Using Markov State Models. <i>Journal of Chemical Theory and Computation</i> , 2017, 13, 926-934.	5.3	26
4702	From Cooperative Self-Assembly to Water-Soluble Supramolecular Polymers Using Coarse-Grained Simulations. <i>ACS Nano</i> , 2017, 11, 1000-1011.	14.6	82
4703	Solid-State Polymerization of CO <sub>2</sub> from Catalytic Photoexcitation: An Ab Initio Molecular Dynamics Study. <i>Journal of Physical Chemistry C</i> , 2017, 121, 115-122.	3.1	2
4704	Computer Simulation Studies on the pH-Responsive Self-Assembly of Amphiphilic Carboxy-Terminated Polyester Dendrimers in Aqueous Solution. <i>Langmuir</i> , 2017, 33, 388-399.	3.5	22
4705	Complexation of short ds RNA/DNA oligonucleotides with Gemini micelles: a time resolved SAXS and computational study. <i>Physical Chemistry Chemical Physics</i> , 2017, 19, 3046-3055.	2.8	6
4706	The Proprotein Convertase Subtilisin/Kexin Type 9-resistant R410S Low Density Lipoprotein Receptor Mutation. <i>Journal of Biological Chemistry</i> , 2017, 292, 1573-1590.	3.4	30
4707	Disrupting a key hydrophobic pair in the oligomerization interface of the actinoporins impairs their pore-forming activity. <i>Protein Science</i> , 2017, 26, 550-565.	7.6	25
4708	Molecular Dynamics Simulation and Analysis of the Antimicrobial Peptide-Lipid Bilayer Interactions. <i>Methods in Molecular Biology</i> , 2017, 1548, 103-118.	0.9	8
4709	Molecular interactions accounting for protein denaturation by urea. <i>Journal of Molecular Liquids</i> , 2017, 228, 168-175.	4.9	27
4710	Femtosecond Raman-Induced Kerr Effect Study of Temperature-Dependent Intermolecular Dynamics in Imidazolium-Based Ionic Liquids: Effects of Anion Species and Cation Alkyl Groups. <i>Journal of Physical Chemistry B</i> , 2017, 121, 250-264.	2.6	32
4711	Predictions of Ligand Selectivity from Absolute Binding Free Energy Calculations. <i>Journal of the American Chemical Society</i> , 2017, 139, 946-957.	13.7	132
4712	Novel flavonolignan hybrid antioxidants: From enzymatic preparation to molecular rationalization. <i>European Journal of Medicinal Chemistry</i> , 2017, 127, 263-274.	5.5	25

#	ARTICLE	IF	CITATIONS
4713	On Atomistic Models for Molecular Oxygen. Journal of Physical Chemistry B, 2017, 121, 518-528.	2.6	19
4714	Partially Assembled Nucleosome Structures at Atomic Detail. Biophysical Journal, 2017, 112, 460-472.	0.5	50
4715	Increase in the $\beta$ -Sheet Character of an Amyloidogenic Peptide upon Adsorption onto Gold and Silver Surfaces. ChemPhysChem, 2017, 18, 526-536.	2.1	11
4716	Human Neuronal Calcium Sensor-1 Protein Avoids Histidine Residues To Decrease pH Sensitivity. Journal of Physical Chemistry B, 2017, 121, 508-517.	2.6	2
4717	Swelling and dimensional stability of xyloglucan/montmorillonite nanocomposites in moist conditions from molecular dynamics simulations. Computational Materials Science, 2017, 128, 191-197.	3.0	4
4718	Beneficial roles of H-donors as diluent and H-shuttle for asphaltenes in catalytic upgrading of vacuum residue. Chemical Engineering Journal, 2017, 314, 1-10.	12.7	41
4719	Mechanism of Unfolding of Human Prion Protein. Journal of Physical Chemistry B, 2017, 121, 550-564.	2.6	33
4720	Accurate Three States Model for Amino Acids with Two Chemically Coupled Titrating Sites in Explicit Solvent Atomistic Constant pH Simulations and pK <sub>a</sub> Calculations. Journal of Chemical Theory and Computation, 2017, 13, 147-160.	5.3	27
4721	Role of the hydrophobic and hydrophilic sites in the dynamic crossover of the protein-hydration water. Physica A: Statistical Mechanics and Its Applications, 2017, 468, 733-739.	2.6	20
4722	On the micro-heterogeneous structure of neat and aqueous propylamine mixtures: A computer simulation study. Journal of Molecular Liquids, 2017, 227, 210-217.	4.9	7
4723	A computational approach for studying antibody-antigen interactions without prior structural information: the anti-testosterone binding antibody as a case study. Proteins: Structure, Function and Bioinformatics, 2017, 85, 322-331.	2.6	4
4724	Influence of sequence and lipid type on membrane perturbation by human and rat amyloid $\beta$ -peptide (1-42). Archives of Biochemistry and Biophysics, 2017, 614, 1-13.	3.0	18
4725	Molecular dynamics study of micelles properties according to their size. Journal of Molecular Graphics and Modelling, 2017, 72, 6-15.	2.4	25
4726	Elucidating Mechanisms of Molecular Recognition Between Human Argonaute and miRNA Using Computational Approaches. Methods in Molecular Biology, 2017, 1517, 251-275.	0.9	1
4727	Computational study of the interplay between intermolecular interactions and CO <sub>2</sub> orientations in type I hydrates. Physical Chemistry Chemical Physics, 2017, 19, 3384-3393.	2.8	17
4728	Experimental and theoretical evidence for bilayer-by-bilayer surface melting of crystalline ice. Proceedings of the National Academy of Sciences of the United States of America, 2017, 114, 227-232.	7.1	131
4729	Structural insight into the antiprion compound inhibition mechanism of native prion folding over misfolding. Chemical Biology and Drug Design, 2017, 89, 907-917.	3.2	2
4730	Interatomic potential that describes martensitic phase transformations in pure lithium. Computational Materials Science, 2017, 129, 202-210.	3.0	10

#	ARTICLE	IF	CITATIONS
4731	Interplay between Protein Thermal Flexibility and Kinetic Stability. <i>Structure</i> , 2017, 25, 167-179.	3.3	29
4732	Repurposing designed mutants: a valuable strategy for computer-aided laccase engineering – the case of POXA1b. <i>Catalysis Science and Technology</i> , 2017, 7, 515-523.	4.1	17
4733	Simulation of Asphaltene Aggregation through Molecular Dynamics: Insights and Limitations. <i>Energy &amp; Fuels</i> , 2017, 31, 1108-1125.	5.1	170
4734	Molecular Insights into Glass Transition in Condensed Core Asphaltenes. <i>Energy &amp; Fuels</i> , 2017, 31, 1182-1192.	5.1	18
4735	Solubility origin at the nanoscale: enthalpic and entropic contributions in polar and nonpolar environments. <i>Physical Chemistry Chemical Physics</i> , 2017, 19, 3903-3910.	2.8	6
4736	Lipid and Peptide Diffusion in Bilayers: The Saffman–Delbrück Model and Periodic Boundary Conditions. <i>Journal of Physical Chemistry B</i> , 2017, 121, 3443-3457.	2.6	91
4737	Hydration Effects Turn a Highly Stretched Polymer from an Entropic into an Energetic Spring. <i>ACS Nano</i> , 2017, 11, 702-712.	14.6	68
4738	Role of Salt and Water in the Plasticization of PDAC/PSS Polyelectrolyte Assemblies. <i>Journal of Physical Chemistry B</i> , 2017, 121, 322-333.	2.6	72
4739	Exfoliation of Graphene in Ionic Liquids: Pyridinium versus Pyrrolidinium. <i>Journal of Physical Chemistry C</i> , 2017, 121, 911-917.	3.1	30
4740	Disrupting domain-domain interactions is indispensable for EngA-ribosome interactions. <i>Biochimica Et Biophysica Acta - Proteins and Proteomics</i> , 2017, 1865, 289-303.	2.3	7
4741	Procedure for Transferable Coarse-Grained Models of Aqueous Polysaccharides. <i>Journal of Chemical Theory and Computation</i> , 2017, 13, 223-236.	5.3	22
4742	Crystal structures of an archaeal thymidylate kinase from <i>Sulfolobus tokodaii</i> provide insights into the role of a conserved active site Arginine residue. <i>Journal of Structural Biology</i> , 2017, 197, 236-249.	2.8	15
4743	Natural Gas Evolution in a Gas Hydrate Melt: Effect of Thermodynamic Hydrate Inhibitors. <i>Journal of Physical Chemistry B</i> , 2017, 121, 153-163.	2.6	26
4744	Structure and lipid-binding properties of the kindlin-3 pleckstrin homology domain. <i>Biochemical Journal</i> , 2017, 474, 539-556.	3.7	40
4745	Thermal Ripples in Model Molybdenum Disulfide Monolayers. <i>Zeitschrift Fur Anorganische Und Allgemeine Chemie</i> , 2017, 643, 152-154.	1.2	2
4746	Sliding of coherent twin boundaries. <i>Nature Communications</i> , 2017, 8, 1108.	12.8	44
4747	Regular Motifs in Xylan Modulate Molecular Flexibility and Interactions with Cellulose Surfaces. <i>Plant Physiology</i> , 2017, 175, 1579-1592.	4.8	79
4748	Structural Disruption of an Adenosine-Binding DNA Aptamer on Graphene: Implications for Aptasensor Design. <i>ACS Sensors</i> , 2017, 2, 1602-1611.	7.8	18



#	ARTICLE	IF	CITATIONS
4749	Mutation L1196M-induced conformational changes and the drug resistant mechanism of anaplastic lymphoma kinase studied by free energy perturbation and umbrella sampling. <i>Physical Chemistry Chemical Physics</i> , 2017, 19, 30239-30248.	2.8	45
4750	Cholera toxin B subunit induces local curvature on lipid bilayers. <i>FEBS Open Bio</i> , 2017, 7, 1638-1645.	2.3	38
4751	Entropy based fingerprint for local crystalline order. <i>Journal of Chemical Physics</i> , 2017, 147, 114112.	3.0	92
4752	Combined x-ray crystallography and computational modeling approach to investigate the Hsp90 C-terminal peptide binding to FKBP51. <i>Scientific Reports</i> , 2017, 7, 14288.	3.3	30
4753	Effects of mutations on active site conformation and dynamics of RNA-dependent RNA polymerase from Cocksackievirus B3. <i>Journal of Molecular Graphics and Modelling</i> , 2017, 77, 330-337.	2.4	1
4754	Effects of High Pressure on Phospholipid Bilayers. <i>Journal of Physical Chemistry B</i> , 2017, 121, 9597-9606.	2.6	27
4755	Ion-induced alterations of the local hydration environment elucidate Hofmeister effect in a simple classical model of Trp-cage miniprotein. <i>Journal of Molecular Modeling</i> , 2017, 23, 298.	1.8	2
4756	Structure of the triose-phosphate/phosphate translocator reveals the basis of substrate specificity. <i>Nature Plants</i> , 2017, 3, 825-832.	9.3	51
4757	Braunâ€™s Lipoprotein Facilitates OmpA Interaction with the Escherichia coli Cell Wall. <i>Biophysical Journal</i> , 2017, 113, 1496-1504.	0.5	55
4758	Assessing the Structure and Stability of Transmembrane Oligomeric Intermediates of an Î±-Helical Toxin. <i>Langmuir</i> , 2017, 33, 11496-11510.	3.5	25
4759	Comparative Molecular Dynamics Analysis of RNase-S Complex Formation. <i>Biophysical Journal</i> , 2017, 113, 1466-1474.	0.5	8
4760	Micellization and Partition Equilibria in Mixed Nonionic/Ionic Micellar Systems: Predictions with Molecular Models. <i>Langmuir</i> , 2017, 33, 12306-12316.	3.5	14
4761	Molecular Dynamics Simulations of the [2Feâ€™2S] Cluster-Binding Domain of NEET Proteins Reveal Key Molecular Determinants That Induce Their Cluster Transfer/Release. <i>Journal of Physical Chemistry B</i> , 2017, 121, 10648-10656.	2.6	18
4762	Insights on the Mechanism of Action of INH-C<sub>10</sub> as an Antitubercular Prodrug. <i>Molecular Pharmaceutics</i> , 2017, 14, 4597-4605.	4.6	15
4763	Spatially Heterogeneous Surface Water Diffusivity around Structured Protein Surfaces at Equilibrium. <i>Journal of the American Chemical Society</i> , 2017, 139, 17890-17901.	13.7	60
4764	Structural Basis for Polyproline-Mediated Ribosome Stalling and Rescue by the Translation Elongation Factor EF-P. <i>Molecular Cell</i> , 2017, 68, 515-527.e6.	9.7	118
4765	Comparative Assessment of Computational Methods for Free Energy Calculations of Ionic Hydration. <i>Journal of Chemical Information and Modeling</i> , 2017, 57, 2763-2775.	5.4	20
4766	Validation of Trimethylamine-oxide (TMAO) Force Fields Based on Thermophysical Properties of Aqueous TMAO Solutions. <i>Journal of Physical Chemistry B</i> , 2017, 121, 10674-10688.	2.6	26



#	ARTICLE	IF	CITATIONS
4767	Structural determinants and functional consequences of protein affinity for membrane rafts. <i>Nature Communications</i> , 2017, 8, 1219.	12.8	231
4768	A glycerophospholipid-specific pocket in the RVFV class II fusion protein drives target membrane insertion. <i>Science</i> , 2017, 358, 663-667.	12.6	66
4769	Force probe simulations using a hybrid scheme with virtual sites. <i>Journal of Chemical Physics</i> , 2017, 147, 134909.	3.0	2
4770	A conserved degron containing an amphipathic helix regulates the cholesterol-mediated turnover of human squalene monooxygenase, a rate-limiting enzyme in cholesterol synthesis. <i>Journal of Biological Chemistry</i> , 2017, 292, 19959-19973.	3.4	51
4771	Modeling Thermodynamic Properties of Propane or Tetrahydrofuran Mixed with Carbon Dioxide or Methane in Structure-II Clathrate Hydrates. <i>Journal of Physical Chemistry C</i> , 2017, 121, 23911-23925.	3.1	15
4772	Temperature-Dependent Structure and Dynamics of Water Intercalated in Layered Double Hydroxides with Different Hydration States. <i>Journal of Physical Chemistry C</i> , 2017, 121, 23752-23762.	3.1	10
4773	Molecular Modeling of the Interaction of Protein L with Antibodies. <i>ACS Omega</i> , 2017, 2, 6464-6472.	3.5	8
4774	Pore formation in lipid membrane I: Continuous reversible trajectory from intact bilayer through hydrophobic defect to transversal pore. <i>Scientific Reports</i> , 2017, 7, 12152.	3.3	102
4775	A review on simulation of methane production from gas hydrate reservoirs: Molecular dynamics prospective. <i>Journal of Petroleum Science and Engineering</i> , 2017, 159, 754-772.	4.2	72
4776	Molecular determinant of the effects of hydrostatic pressure on protein folding stability. <i>Nature Communications</i> , 2017, 8, 14561.	12.8	75
4777	Probing the communication of deoxythymidine triphosphate in HIV-1 reverse transcriptase by communication maps and interaction energy studies. <i>Physical Chemistry Chemical Physics</i> , 2017, 19, 29608-29616.	2.8	3
4778	Mechanistic principles underlying regulation of the actin cytoskeleton by phosphoinositides. <i>Proceedings of the National Academy of Sciences of the United States of America</i> , 2017, 114, E8977-E8986.	7.1	106
4779	Studies of DNA- and HSA-binding properties of new nano-scale green synthesized Ni (II) complex as anticancer agent using spectroscopic methods, viscosity measurement, molecular docking, MD simulation and QM/MM. <i>Journal of Molecular Liquids</i> , 2017, 248, 24-35.	4.9	24
4780	2D IR spectroscopy of high-pressure phases of ice. <i>Journal of Chemical Physics</i> , 2017, 147, 144501.	3.0	14
4781	A Quantum Mechanically Derived Force Field To Predict CO <sub>2</sub> Adsorption on Calcite {10.4} in an Aqueous Environment. <i>Journal of Physical Chemistry C</i> , 2017, 121, 24025-24035.	3.1	18
4782	Self-association of a highly charged arginine-rich cell-penetrating peptide. <i>Proceedings of the National Academy of Sciences of the United States of America</i> , 2017, 114, 11428-11433.	7.1	63
4783	<i>in silico</i> screening of drug-membrane thermodynamics reveals linear relations between bulk partitioning and the potential of mean force. <i>Journal of Chemical Physics</i> , 2017, 147, 125101.	3.0	37
4784	Solvation of Carbon Nanoparticles in Water/Alcohol Mixtures: Using Molecular Simulation To Probe Energetics, Structure, and Dynamics. <i>Journal of Physical Chemistry C</i> , 2017, 121, 22926-22938.	3.1	14

#	ARTICLE	IF	CITATIONS
4785	Binding of protofibrillar A $\beta$ 2 trimers to lipid bilayer surface enhances A $\beta$ 2 structural stability and causes membrane thinning. <i>Physical Chemistry Chemical Physics</i> , 2017, 19, 27556-27569.	2.8	32
4786	Molecular Basis of Altered hERG1 Channel Gating Induced by Ginsenoside Rg3. <i>Molecular Pharmacology</i> , 2017, 92, 437-450.	2.3	6
4787	Theoretical insight into the cocrystal explosive of 2,4,6,8,10,12-hexanitrohexaazaisowurtzitane (CL-20)/1-Methyl-4,5-dinitro-1H-imidazole (MDNI). <i>Journal of Theoretical and Computational Chemistry</i> , 2017, 16, 1750061.	1.8	5
4788	Effect of temperature, water content and free fatty acid on reverse micelle formation of phospholipids in vegetable oil. <i>Colloids and Surfaces B: Biointerfaces</i> , 2017, 160, 355-363.	5.0	50
4789	Commonalities in frequency-dependent viscoelastic damping in glasses in the MHz to THz regime. <i>Journal of Applied Physics</i> , 2017, 122, .	2.5	12
4790	pH-Induced interfacial properties of Chaplin E from <i>Streptomyces coelicolor</i> . <i>Colloids and Surfaces B: Biointerfaces</i> , 2017, 160, 589-597.	5.0	1
4791	Evaluation and Optimization of Interface Force Fields for Water on Gold Surfaces. <i>Journal of Chemical Theory and Computation</i> , 2017, 13, 5610-5623.	5.3	34
4792	Structural basis for maintenance of bacterial outer membrane lipid asymmetry. <i>Nature Microbiology</i> , 2017, 2, 1616-1623.	13.3	118
4793	Molecular Simulations of Melittin-Induced Membrane Pores. <i>Journal of Physical Chemistry B</i> , 2017, 121, 10209-10214.	2.6	27
4794	Structural insights into the competitive inhibition of the ATP-gated P2X receptor channel. <i>Nature Communications</i> , 2017, 8, 876.	12.8	75
4795	Dependence of the structure and dynamics of liquid silicon on the choice of density functional approximation. <i>Physical Review B</i> , 2017, 96, .	3.2	26
4796	Switch Loop Flexibility Affects Substrate Transport of the AcrB Efflux Pump. <i>Journal of Molecular Biology</i> , 2017, 429, 3863-3874.	4.2	33
4797	Evolution of the micro-structure of aqueous alcohol mixtures with cooling: A computer simulation study. <i>Journal of Molecular Liquids</i> , 2017, 248, 602-609.	4.9	4
4798	Phase and vacancy behaviour of hard $\alpha$ -cubes. <i>Journal of Chemical Physics</i> , 2017, 147, 124501.	3.0	6
4799	Quasiharmonic analysis of protein energy landscapes from pressure-temperature molecular dynamics simulations. <i>Journal of Chemical Physics</i> , 2017, 147, 125103.	3.0	7
4800	Mobility field and mobility temperature dependence in PC61BM: A kinetic Monte-Carlo study. <i>Chemical Physics Letters</i> , 2017, 689, 74-81.	2.6	7
4801	The origin of uniaxial negative thermal expansion in layered perovskites. <i>Npj Computational Materials</i> , 2017, 3, .	8.7	38
4802	Interplay between alkyl chain asymmetry and cholesterol addition in the rigid ion pair amphiphile bilayer systems. <i>Journal of Chemical Physics</i> , 2017, 146, 035102.	3.0	6

#	ARTICLE	IF	CITATIONS
4803	Substrate-triggered position switching of TatA and TatB during Tat transport in <i>Escherichia coli</i> . <i>Open Biology</i> , 2017, 7, 170091.	3.6	24
4804	Molecular-Level Insight into the Interaction of Phospholipid Bilayers with Cellulose. <i>Langmuir</i> , 2017, 33, 12793-12803.	3.5	11
4805	Dynamic Histogram Analysis To Determine Free Energies and Rates from Biased Simulations. <i>Journal of Chemical Theory and Computation</i> , 2017, 13, 6328-6342.	5.3	54
4806	Highly Porous Silicon Embedded in a Ceramic Matrix: A Stable High-Capacity Electrode for Li-Ion Batteries. <i>ACS Nano</i> , 2017, 11, 11409-11416.	14.6	73
4807	Conversion of OprO into an OprP-like Channel by Exchanging Key Residues in the Channel Constriction. <i>Biophysical Journal</i> , 2017, 113, 829-834.	0.5	10
4808	Membrane Dynamics of $\beta$ -Secretase Provides a Molecular Basis for $\beta$ -Amyloid Binding and Processing. <i>ACS Chemical Neuroscience</i> , 2017, 8, 2424-2436.	3.5	54
4809	Embedded-atom method potential for modeling hydrogen and hydrogen-defect interaction in tungsten. <i>Journal of Physics Condensed Matter</i> , 2017, 29, 435401.	1.8	26
4810	Improvement of molecular dynamics simulation method applied to nematics doped with racemic metal complexes. <i>Molecular Crystals and Liquid Crystals</i> , 2017, 647, 235-243.	0.9	3
4811	Understanding the pH-dependent adsorption of ionizable compounds on graphene oxide using molecular dynamics simulations. <i>Environmental Science: Nano</i> , 2017, 4, 1935-1943.	4.3	26
4812	Interaction between 1-phenylethanone, 2-phenyl-2-propanol, and isopropenylbenzene with water molecules: A computational study. <i>Computational and Theoretical Chemistry</i> , 2017, 1117, 188-195.	2.5	6
4813	Protocol for fast screening of multi-target drug candidates: Application to Alzheimer's disease. <i>Journal of Molecular Graphics and Modelling</i> , 2017, 77, 121-129.	2.4	31
4814	Self-assembly of donor-acceptor semiconducting polymers in solution thin films: a molecular dynamics simulation study. <i>Journal of Materials Chemistry C</i> , 2017, 5, 9602-9610.	5.5	5
4815	Hydrophobic fluorine mediated switching of the hydrogen bonding site as well as orientation of water molecules in the aqueous mixture of monofluoroethanol: IR, molecular dynamics and quantum chemical studies. <i>Physical Chemistry Chemical Physics</i> , 2017, 19, 24667-24677.	2.8	10
4816	Directional mechanical stability of Bacteriophage $\phi$ 29 motor's 3WJ-pRNA: Extraordinary robustness along portal axis. <i>Science Advances</i> , 2017, 3, e1601684.	10.3	17
4817	Structural Insights into the Mode of Action of the Peptide Antibiotic Copsin. <i>Biochemistry</i> , 2017, 56, 4992-5001.	2.5	8
4818	Characterization of Ciprofloxacin Permeation Pathways across the Porin OmpC Using Metadynamics and a String Method. <i>Journal of Chemical Theory and Computation</i> , 2017, 13, 4553-4566.	5.3	41
4819	Stability of Proteins in Carbohydrates and Other Additives during Freezing: The Human Growth Hormone as a Case Study. <i>Journal of Physical Chemistry B</i> , 2017, 121, 8652-8660.	2.6	28
4820	Ability of the Poisson-Boltzmann equation to capture molecular dynamics predicted ion distribution around polyelectrolytes. <i>Physical Chemistry Chemical Physics</i> , 2017, 19, 24583-24593.	2.8	38

#	ARTICLE	IF	CITATIONS
4821	Evaluation of mapping schemes for systematic coarse graining of higher alkanes. <i>Physical Chemistry Chemical Physics</i> , 2017, 19, 23034-23042.	2.8	22
4822	Influence of co-non-solvency on hydrophobic molecules driven by excluded volume effect. <i>Physical Chemistry Chemical Physics</i> , 2017, 19, 23915-23918.	2.8	7
4823	Molecular simulation of caloric properties of fluids modelled by force fields with intramolecular contributions: Application to heat capacities. <i>Journal of Chemical Physics</i> , 2017, 147, 034508.	3.0	5
4824	Interplay Between Membrane Composition and Structural Stability of Membrane-Bound hIAPP. <i>Journal of Physical Chemistry B</i> , 2017, 121, 8661-8668.	2.6	25
4825	Interaction of lysozyme with a tear film lipid layer model: A molecular dynamics simulation study. <i>Biochimica Et Biophysica Acta - Biomembranes</i> , 2017, 1859, 2289-2296.	2.6	21
4826	How kanamycin A interacts with bacterial and mammalian mimetic membranes. <i>Biochimica Et Biophysica Acta - Biomembranes</i> , 2017, 1859, 2242-2252.	2.6	33
4827	Pseudo-peptide amyloid- $\beta^2$ blocking inhibitors: molecular dynamics and single molecule force spectroscopy study. <i>Biochimica Et Biophysica Acta - Proteins and Proteomics</i> , 2017, 1865, 1707-1718.	2.3	15
4828	Active site gate of M32 carboxypeptidases illuminated by crystal structure and molecular dynamics simulations. <i>Biochimica Et Biophysica Acta - Proteins and Proteomics</i> , 2017, 1865, 1406-1415.	2.3	8
4829	Single-Walled Carbon Nanotube Engendered Pseudo-1D Morphologies of Silver Nanowire. <i>Journal of Physical Chemistry C</i> , 2017, 121, 20468-20480.	3.1	10
4830	Lattice instability during phase transformations under multiaxial stress: Modified transformation work criterion. <i>Physical Review B</i> , 2017, 96, .	3.2	38
4831	Simulating Bilayers of Nonionic Surfactants with the GROMOS-Compatible 2016H66 Force Field. <i>Langmuir</i> , 2017, 33, 10225-10238.	3.5	12
4832	Involvement of G-triplex and G-hairpin in the multi-pathway folding of human telomeric G-quadruplex. <i>Nucleic Acids Research</i> , 2017, 45, 11401-11412.	14.5	67
4833	Dynamic Specification of Initial Structures in Parallel Cascade Selection Molecular Dynamics (PaCS-MD) Efficiently Promotes Biologically Relevant Rare Events. <i>Bulletin of the Chemical Society of Japan</i> , 2017, 90, 1236-1243.	3.2	8
4834	Dynamics at a Peptide-TiO <sub>2</sub> Anatase (101) Interface. <i>Journal of Physical Chemistry B</i> , 2017, 121, 8869-8877.	2.6	8
4835	Contact angles from Young's equation in molecular dynamics simulations. <i>Journal of Chemical Physics</i> , 2017, 147, 084708.	3.0	48
4836	Thermodynamic properties of the 1-butyl-3-methylimidazolium mesilate ionic liquid [C4mim][OMs] in condensed phase, using molecular simulations. <i>Journal of Molecular Liquids</i> , 2017, 244, 422-432.	4.9	9
4837	Molecular Dynamics Study on the Mechanical Deformation of Hydrated Perfluorosulfonic Acid Polymer Membranes. <i>Journal of Physical Chemistry C</i> , 2017, 121, 21374-21382.	3.1	11
4838	Distinct Electrostatic Interactions Govern the Chiro-Optical Properties and Architectural Arrangement of Peptide-Oligothiophene Hybrid Materials. <i>Macromolecules</i> , 2017, 50, 7102-7110.	4.8	14

#	ARTICLE	IF	CITATIONS
4839	Resolving the Atomistic Modes of Anle138b Inhibitory Action on Peptide Oligomer Formation. ACS Chemical Neuroscience, 2017, 8, 2791-2808.	3.5	26
4840	Membrane Tubulation in Lipid Vesicles Triggered by the Local Application of Calcium Ions. Langmuir, 2017, 33, 11010-11017.	3.5	51
4841	The mechano-sensing role of the unique SH3 insertion in plakin domains revealed by Molecular Dynamics simulations. Scientific Reports, 2017, 7, 11669.	3.3	28
4842	Common behaviors associated with the glass transitions of water-like models. Journal of Chemical Physics, 2017, 147, 034505.	3.0	20
4843	Molecular dynamics simulations of structural transitions of crystalline polystyrene in response to external stresses and temperatures. Polymer, 2017, 128, 177-187.	3.8	4
4844	Atomic theory of viscoelastic response and memory effects in metallic glasses. Physical Review B, 2017, 96, .	3.2	27
4845	Photoinduced Bimolecular Electron Transfer in Ionic Liquids. Journal of the American Chemical Society, 2017, 139, 14568-14585.	13.7	30
4846	Polymorphic phase transitions: Macroscopic theory and molecular simulation. Advanced Drug Delivery Reviews, 2017, 117, 47-70.	13.7	49
4847	Graphene engendered 2-D structural morphology of aluminium atoms: Molecular dynamics simulation study. Materials Chemistry and Physics, 2017, 202, 329-339.	4.0	17
4848	On deformation behavior of Fe-Mn based structural alloys. Materials Science and Engineering Reports, 2017, 122, 1-28.	31.8	102
4849	Structural and Kinetic Characterization of the Intrinsically Disordered Protein SeV N<sub>TAIL</sub> through Enhanced Sampling Simulations. Journal of Physical Chemistry B, 2017, 121, 9572-9582.	2.6	23
4850	Dynamics of water bound to crystalline cellulose. Scientific Reports, 2017, 7, 11840.	3.3	82
4851	A potential model for sodium chloride solutions based on the TIP4P/2005 water model. Journal of Chemical Physics, 2017, 147, 104501.	3.0	82
4852	Molecular dynamics simulations of ether- and ester-linked phospholipids. Biochimica Et Biophysica Acta - Biomembranes, 2017, 1859, 2297-2307.	2.6	11
4853	Unveiling subsurface hydrogen-bond structure of hexagonal water ice. Physical Review B, 2017, 96, .	3.2	40
4854	Computational study on acetophenone in amorphous polyethylene. Journal of Molecular Modeling, 2017, 23, 274.	1.8	9
4855	Molecular dynamics simulation study of hydration of uranyl nitrate in supercritical water: Dissecting the effect of uranyl ion concentration from solvent density. Chemical Physics, 2017, 495, 48-58.	1.9	2
4856	Thermodynamic Anomalies in Stretched Water. Langmuir, 2017, 33, 11771-11778.	3.5	27

#	ARTICLE	IF	CITATIONS
4857	In vitro blood cell viability profiling of polymers used in molecular assembly. Scientific Reports, 2017, 7, 9481.	3.3	76
4858	Simulation of Reversible Protein-Protein Binding and Calculation of Binding Free Energies Using Perturbed Distance Restraints. Journal of Chemical Theory and Computation, 2017, 13, 5697-5708.	5.3	36
4859	Effects of Coarse Graining and Saturation of Hydrocarbon Chains on Structure and Dynamics of Simulated Lipid Molecules. Scientific Reports, 2017, 7, 11476.	3.3	14
4860	Fv-clasp: An Artificially Designed Small Antibody Fragment with Improved Production Compatibility, Stability, and Crystallizability. Structure, 2017, 25, 1611-1622.e4.	3.3	31
4861	Crystal structure of a novel prolidase from <i>Deinococcus radiodurans</i> identifies new subfamily of bacterial prolidases. Proteins: Structure, Function and Bioinformatics, 2017, 85, 2239-2251.	2.6	3
4862	Effects of disulfide bridges and backbone connectivity on water sorption by protein matrices. Scientific Reports, 2017, 7, 7957.	3.3	4
4863	Structural insights into HIV-1 protease flap opening processes and key intermediates. RSC Advances, 2017, 7, 45121-45128.	3.6	16
4864	Multiple interactions between an Arf/GEF complex and charged lipids determine activation kinetics on the membrane. Proceedings of the National Academy of Sciences of the United States of America, 2017, 114, 11416-11421.	7.1	38
4865	Influence of side chain linker length on ion transport properties of polymeric ionic liquids. Journal of Polymer Science, Part B: Polymer Physics, 2017, 55, 1718-1723.	2.1	30
4866	Energetics and mechanism of anion permeation across formate-nitrite transporters. Scientific Reports, 2017, 7, 12027.	3.3	32
4867	Accessibility explains preferred thiol-disulfide isomerization in a protein domain. Scientific Reports, 2017, 7, 9858.	3.3	31
4868	The Molecular Dynamics Study of Vacancy Formation During Solidification of Pure Metals. Scientific Reports, 2017, 7, 10241.	3.3	19
4869	Dynamic and Kinetic Elements of $\mu$ -Opioid Receptor Functional Selectivity. Scientific Reports, 2017, 7, 11255.	3.3	44
4870	Publisher's note. Journal of Molecular Graphics and Modelling, 2017, 77, 250.	2.4	19
4871	Estimation of adsorbed-phase density of methane in realistic overmature kerogen models using molecular simulations for accurate gas in place calculations. Journal of Natural Gas Science and Engineering, 2017, 46, 865-872.	4.4	36
4872	An allosteric ligand-binding site in the extracellular cap of K2P channels. Nature Communications, 2017, 8, 378.	12.8	30
4873	Structural basis for antibacterial peptide self-immunity by the bacterial ABC transporter McjD. EMBO Journal, 2017, 36, 3062-3079.	7.8	64
4874	Thermodynamics of association of water soluble fullerene derivatives [ $C_{60}(OH)_n$ , $n = 0, 2, 4, 8$ and $12$ ] in aqueous media. Journal of Chemical Sciences, 2017, 129, 1327-1340.	1.5	8



#	ARTICLE	IF	CITATIONS
4875	Liquid Adsorption of Organic Compounds on Hematite $\alpha$ -Fe <sub>2</sub> O <sub>3</sub> Using ReaxFF. <i>Langmuir</i> , 2017, 33, 11257-11263.	3.5	18
4876	Morphology of a self-doped conducting oligomer for green energy applications. <i>Nanoscale</i> , 2017, 9, 13717-13724.	5.6	19
4878	Simulation Studies on the Lipid Interaction and Conformation of Novel Drug-Delivery Pseudopeptidic Polymers. <i>Journal of Physical Chemistry B</i> , 2017, 121, 9113-9125.	2.6	0
4879	MD Simulations of Viruslike Particles with Supra CG Solvation Affordable to Desktop Computers. <i>Journal of Chemical Theory and Computation</i> , 2017, 13, 5106-5116.	5.3	29
4880	Orcein-Related Small Molecule O4 Destabilizes hIAPP Protofibrils by Interacting Mostly with the Amyloidogenic Core Region. <i>Journal of Physical Chemistry B</i> , 2017, 121, 9203-9212.	2.6	30
4881	Agonist-induced dimer dissociation as a macromolecular step in G protein-coupled receptor signaling. <i>Nature Communications</i> , 2017, 8, 226.	12.8	57
4882	Structural Properties of Human IAPP Dimer in Membrane Environment Studied by All-Atom Molecular Dynamics Simulations. <i>Scientific Reports</i> , 2017, 7, 7915.	3.3	17
4883	Path lumping: An efficient algorithm to identify metastable path channels for conformational dynamics of multi-body systems. <i>Journal of Chemical Physics</i> , 2017, 147, 044112.	3.0	11
4884	Hydration properties of the polyanilines by atomistic molecular dynamics. <i>Journal of Molecular Liquids</i> , 2017, 244, 285-290.	4.9	6
4885	On the Calculation of Acyl Chain Order Parameters from Lipid Simulations. <i>Journal of Chemical Theory and Computation</i> , 2017, 13, 5683-5696.	5.3	92
4886	Pea PSII-LHCII supercomplexes form pairs by making connections across the stromal gap. <i>Scientific Reports</i> , 2017, 7, 10067.	3.3	30
4887	The influence of solid scaffolds on flat and curved lipid membranes. <i>AIP Advances</i> , 2017, 7, 075007.	1.3	5
4888	Effective charges of ionic liquid determined self-consistently through combination of molecular dynamics simulation and density-functional theory. <i>Journal of Computational Chemistry</i> , 2017, 38, 2559-2569.	3.3	20
4889	Fully Atomistic $\text{Al}^{240}$ and $\text{Al}^{242}$ Oligomers in Water: Observation of Porelike Conformations. <i>Journal of Chemical Theory and Computation</i> , 2017, 13, 4567-4583.	5.3	24
4890	Dynamics of B-DNA in Electrically Charged Solid Nanopores. <i>Journal of Physical Chemistry C</i> , 2017, 121, 16568-16575.	3.1	2
4891	The mechanism for the complexation and dissociation between siRNA and PMAL: a molecular dynamics simulation study based on a coarse-grained model. <i>Molecular Simulation</i> , 2017, 43, 1385-1393.	2.0	6
4892	Characterization of crystal polymorphs of the organic semiconductor non-peripheral octa-hexyl phthalocyanine. <i>Japanese Journal of Applied Physics</i> , 2017, 56, 081601.	1.5	8
4893	Toward Understanding the Environmental Control of Hydrogel Film Properties: How Salt Modulates the Flexibility of Chitosan Chains. <i>Macromolecules</i> , 2017, 50, 5946-5952.	4.8	35



#	ARTICLE	IF	CITATIONS
4894	Assessing the interaction between surfactant-like peptides and lipid membranes. RSC Advances, 2017, 7, 35973-35981.	3.6	22
4895	Computational Calorimetry of PNIPAM Cononsolvency in Water/Methanol Mixtures. Journal of Physical Chemistry B, 2017, 121, 7741-7748.	2.6	63
4896	Nucleotide Dependent Switching in Rho GTPase: Conformational Heterogeneity and Competing Molecular Interactions. Scientific Reports, 2017, 7, 45829.	3.3	18
4897	Sequence Specificity in the Entropy-Driven Binding of a Small Molecule and a Disordered Peptide. Journal of Molecular Biology, 2017, 429, 2772-2779.	4.2	62
4898	Organic and Third Phase in HNO <sub>3</sub> /TBP/n-Dodecane System: No Reverse Micelles. Solvent Extraction and Ion Exchange, 2017, 35, 251-265.	2.0	24
4899	Investigation of naphthofuran moiety as potential dual inhibitor against BACE-1 and GSK-3 $\beta$ : molecular dynamics simulations, binding energy, and network analysis to identify first-in-class dual inhibitors against Alzheimer's disease. Journal of Molecular Modeling, 2017, 23, 239.	1.8	20
4900	Dynamical Transition of Collective Motions in Dry Proteins. Physical Review Letters, 2017, 119, 048101.	7.8	27
4901	The properties of residual water molecules in ionic liquids: a comparison between direct and inverse Kirkwood-Buff approaches. Physical Chemistry Chemical Physics, 2017, 19, 18924-18937.	2.8	35
4902	Dynamics and energetics of the mammalian phosphatidylinositol transfer protein phospholipid exchange cycle. Journal of Biological Chemistry, 2017, 292, 14438-14455.	3.4	25
4903	A polar SxxS motif drives assembly of the transmembrane domains of Toll-like receptor 4. Biochimica Et Biophysica Acta - Biomembranes, 2017, 1859, 2086-2095.	2.6	12
4904	All-Atom MD Simulation of DNA Condensation Using <i>Ab Initio</i> Derived Force Field Parameters of Cobalt(III)-Hexammine. Journal of Physical Chemistry B, 2017, 121, 7761-7770.	2.6	16
4905	pH Dependence of $\beta$ -Aminobutyric Acid Iontronic Transport. Journal of Physical Chemistry B, 2017, 121, 7284-7289.	2.6	21
4906	Biomolecular conformational changes and ligand binding: from kinetics to thermodynamics. Chemical Science, 2017, 8, 6466-6473.	7.4	51
4907	Enthalpy Landscape Dictates the Irradiation-Induced Disordering of Quartz. Physical Review X, 2017, 7, .	8.9	27
4908	Rationally designed peptide nanosponges for cell-based cancer therapy. Nanomedicine: Nanotechnology, Biology, and Medicine, 2017, 13, 2555-2564.	3.3	14
4909	Theoretical and computational validation of the Kuhn barrier friction mechanism in unfolded proteins. Scientific Reports, 2017, 7, 269.	3.3	31
4910	Effect of lipid shape on toroidal pore formation and peptide orientation in lipid bilayers. Physical Chemistry Chemical Physics, 2017, 19, 21340-21349.	2.8	14
4911	Connecting Structural and Transport Properties of Ionic Liquids with Cationic Oligoether Chains. Journal of the Electrochemical Society, 2017, 164, H5247-H5262.	2.9	33

#	ARTICLE	IF	CITATIONS
4912	Atomistic insight into the role of amine groups in thermoresponsive poly(2-dialkylaminoethyl) Tj ETQq0 0 0 rgBT /Ovgrlock 10 Tf 50 742	3.8	13
4913	Structural Dependence of the Sulfur Reduction Mechanism in Carbon-Based Cathodes for Lithiumâ€“Sulfur Batteries. Journal of Physical Chemistry C, 2017, 121, 18369-18377.	3.1	17
4914	Influence of doxorubicin on model cell membrane properties: insights from in vitro and in silico studies. Scientific Reports, 2017, 7, 6343.	3.3	70
4915	Interaction of hydrophobic polymers with model lipid bilayers. Scientific Reports, 2017, 7, 6357.	3.3	56
4916	Molecular mechanisms of Charcot-Marie-Tooth neuropathy linked to mutations in human myelin protein P2. Scientific Reports, 2017, 7, 6510.	3.3	33
4917	Direct Observation of Percolation in the Yielding Transition of Colloidal Glasses. Physical Review Letters, 2017, 118, 148001.	7.8	49
4918	Mean Activity Coefficients of NaCl in the Mixture of 2-Hydroxyethylammonium Butyrate + H<sub>2</sub>O at 298.15 K. Journal of Chemical & Engineering Data, 2017, 62, 2384-2391.	1.9	2
4919	Shuffling Active Site Substate Populations Affects Catalytic Activity: The Case of Glucose Oxidase. ACS Catalysis, 2017, 7, 6188-6197.	11.2	46
4920	Glutamate Water Gates in the Ion Binding Pocket of Na+ Bound Na+, K+-ATPase. Scientific Reports, 2017, 7, 39829.	3.3	8
4921	Crystal structure of Pisum arvense seed lectin (PAL) and characterization of its interaction with carbohydrates by molecularÂdocking and dynamics. Archives of Biochemistry and Biophysics, 2017, 630, 27-37.	3.0	9
4922	Intermolecular interactions and its effect within Cr 3+ -containing atmospheric particulate matter using molecular dynamics simulations. Atmospheric Environment, 2017, 166, 334-339.	4.1	4
4923	Molecular dynamics simulation of the aggregation behavior of N-Dodecyl-N,N-Dimethyl-3-Ammonio-1-Propanesulfonate/sodium dodecyl benzene sulfonate surfactant mixed system at oil/water interface. Colloids and Surfaces A: Physicochemical and Engineering Aspects, 2017, 531, 73-80.	4.7	26
4924	A comparison of classical interatomic potentials applied to highly concentrated aqueous lithium chloride solutions. Journal of Molecular Liquids, 2017, 242, 845-858.	4.9	25
4925	A Multiâ€“Level Theoretical Study to Disclose the Binding Mechanisms of Gold(III)â€“Bipyridyl Compounds as Selective Aquaglyceroporin Inhibitors. Chemistry - A European Journal, 2017, 23, 13802-13813.	3.3	31
4926	Structure-function studies of BPP-BrachyNH2 and synthetic analogues thereof with Angiotensin I-Converting Enzyme. European Journal of Medicinal Chemistry, 2017, 139, 401-411.	5.5	5
4927	A tale of two tails: The importance of unstructured termini in the aggregation pathway of Î²2â€“microglobulin. Proteins: Structure, Function and Bioinformatics, 2017, 85, 2045-2057.	2.6	17
4928	Identification of Key Interactions in the Initial Self-Assembly of Amylin in a Membrane Environment. Biochemistry, 2017, 56, 4884-4894.	2.5	27
4929	Overcoming the Limitations of the MARTINI Force Field in Simulations of Polysaccharides. Journal of Chemical Theory and Computation, 2017, 13, 5039-5053.	5.3	83

#	ARTICLE	IF	CITATIONS
4930	<i>Ab initio</i> molecular dynamics study of the structural and electronic transition in $\text{VO}_2$ . Physical Review B, 2017, 96, .		
4931	Sampling Long- versus Short-Range Interactions Defines the Ability of Force Fields To Reproduce the Dynamics of Intrinsically Disordered Proteins. Journal of Chemical Theory and Computation, 2017, 13, 3964-3974.	5.3	22
4932	Conjugated Polymer Nanoparticles in Aqueous Media by Assembly with Phospholipids via Dense Alkyl Chain Packing. Macromolecules, 2017, 50, 6935-6944.	4.8	17
4933	Investigations of binding mode insight in Salmonella typhi type-III secretion system tip protein (SipD): A molecular docking and MD simulation study. Informatics in Medicine Unlocked, 2017, 9, 166-172.	3.4	14
4934	$\text{Mg}^{2+}$ -Channel-Inspired Nanopores for $\text{Mg}^{2+}/\text{Li}^{+}$ Separation: The Effect of Coordination on the Ionic Hydration Microstructures. Langmuir, 2017, 33, 9201-9210.	3.5	38
4935	Analysing the microenvironment of 2-p-toluidinylnaphthalene-6-sulfonate (TNS) in solvents and in different conformational states of proteins in relation to its fluorescence properties: a computational study. Physical Chemistry Chemical Physics, 2017, 19, 24656-24666.	2.8	2
4936	A spectroscopic and molecular dynamics simulation approach towards the stabilizing effect of ammonium-based ionic liquids on bovine serum albumin. New Journal of Chemistry, 2017, 41, 10712-10722.	2.8	42
4937	Assessment of empirical potential for MOX nuclear fuels and thermomechanical properties. Journal of Nuclear Materials, 2017, 495, 67-77.	2.7	29
4938	Ferromagnetism in amorphous MgO. Philosophical Magazine, 2017, 97, 2129-2141.	1.6	1
4939	The molecular mechanism behind resistance of the kinase FLT3 to the inhibitor quizartinib. Proteins: Structure, Function and Bioinformatics, 2017, 85, 2143-2152.	2.6	24
4940	Molecular Dynamics Simulations Reveal Key Roles of the Interleukin-6 Alpha Receptor in the Assembly of the Human Interleukin-6 Receptor Complex. Journal of Physical Chemistry B, 2017, 121, 8113-8122.	2.6	7
4941	Molecular Structuring and Phase Transition of Lipid-Based Formulations upon Water Dispersion: A Coarse-Grained Molecular Dynamics Simulation Approach. Molecular Pharmaceutics, 2017, 14, 4145-4153.	4.6	17
4942	The opening/closure of the P-loop and hinge of BCR-ABL1 decodes the low/high bioactivities of dasatinib and axitinib. Physical Chemistry Chemical Physics, 2017, 19, 22444-22453.	2.8	9
4943	Structure, Dynamics, and Electron Transfer of Azurin Bound to a Gold Electrode. Langmuir, 2017, 33, 9190-9200.	3.5	5
4944	Modeling DMPC lipid membranes with SIRAH force-field. Journal of Molecular Modeling, 2017, 23, 259.	1.8	24
4945	Long Distance Modulation of Disorder-to-Order Transitions in Protein Allostery. Biochemistry, 2017, 56, 4478-4488.	2.5	12
4946	Molecular insights into the role of a distal F240A mutation that alters CYP1A1 activity towards persistent organic pollutants. Biochimica Et Biophysica Acta - General Subjects, 2017, 1861, 2852-2860.	2.4	12
4947	Physical mechanism for biopolymers to aggregate and maintain in non-equilibrium states. Scientific Reports, 2017, 7, 3105.	3.3	3

#	ARTICLE	IF	CITATIONS
4948	Ring-like N-fold Models of A $\beta$ 242 fibrils. <i>Scientific Reports</i> , 2017, 7, 6588.	3.3	26
4949	Arginine mutations in antibody complementarity-determining regions display context-dependent affinity/specificity trade-offs. <i>Journal of Biological Chemistry</i> , 2017, 292, 16638-16652.	3.4	51
4950	Statistical Analysis on the Performance of Molecular Mechanics Poisson-Boltzmann Surface Area versus Absolute Binding Free Energy Calculations: Bromodomains as a Case Study. <i>Journal of Chemical Information and Modeling</i> , 2017, 57, 2203-2221.	5.4	108
4951	Mapping Putative B-Cell Zika Virus NS1 Epitopes Provides Molecular Basis for Anti-NS1 Antibody Discrimination between Zika and Dengue Viruses. <i>ACS Omega</i> , 2017, 2, 3913-3920.	3.5	41
4952	Molecular Structure Inhibiting Synergism in Charged Surfactant Mixtures: An Atomistic Molecular Dynamics Simulation Study. <i>Langmuir</i> , 2017, 33, 14093-14104.	3.5	13
4953	Network of Conformational Transitions Revealed by Molecular Dynamics Simulations of the Carbonic Anhydrase II Apo-Enzyme. <i>ACS Omega</i> , 2017, 2, 8414-8420.	3.5	8
4954	Different carotenoid conformations have distinct functions in light-harvesting regulation in plants. <i>Nature Communications</i> , 2017, 8, 1994.	12.8	83
4955	Molecular dynamics simulations for CL-20/TNT co-crystal based polymer-bonded explosives. <i>Journal of Theoretical and Computational Chemistry</i> , 2017, 16, 1750072.	1.8	9
4956	Initiation of prolyl cis-trans isomerisation in the CDR-H3 loop of an antibody in response to antigen binding. <i>Scientific Reports</i> , 2017, 7, 16964.	3.3	13
4957	Superhard and superconducting B6C. <i>Materials Today Physics</i> , 2017, 3, 76-84.	6.0	13
4958	Bulk and interfacial structures of reline deep eutectic solvent: A molecular dynamics study. <i>Journal of Chemical Physics</i> , 2017, 147, 194507.	3.0	90
4959	Structure-Based Insights into the Dynamics and Function of Two-Domain SlpA from <i>Escherichia coli</i> . <i>Biochemistry</i> , 2017, 56, 6533-6543.	2.5	2
4960	Identification of Two New Cholesterol Interaction Sites on the A2A Adenosine Receptor. <i>Biophysical Journal</i> , 2017, 113, 2415-2424.	0.5	61
4961	Denaturation of dsDNA Induced by Specific Major Groove Binding of Cadmium Ion to Thymine. <i>ACS Omega</i> , 2017, 2, 8490-8494.	3.5	6
4962	Modulation of the <i>Neisseria gonorrhoeae</i> drug efflux conduit MtrE. <i>Scientific Reports</i> , 2017, 7, 17091.	3.3	6
4963	Simulation of Ti-Al intermetallic compound synthesis using cold spraying. <i>AIP Conference Proceedings</i> , 2017, , .	0.4	0
4964	Anisotropic formation mechanism and nanomechanics for the self-assembly process of cross-linked peptides. <i>Chinese Physics B</i> , 2017, 26, 128701.	1.4	1
4965	Control of zeolite framework flexibility and pore topology for separation of ethane and ethylene. <i>Science</i> , 2017, 358, 1068-1071.	12.6	304

#	ARTICLE	IF	CITATIONS
4966	Structural similarities in the CPC clip motif explain peptide-binding promiscuity between glycosaminoglycans and lipopolysaccharides. <i>Journal of the Royal Society Interface</i> , 2017, 14, 20170423.	3.4	4
4967	Protein crowding and lipid complexity influence the nanoscale dynamic organization of ion channels in cell membranes. <i>Scientific Reports</i> , 2017, 7, 16647.	3.3	68
4968	Poly[ <i>n</i> ]catenanes: Synthesis of molecular interlocked chains. <i>Science</i> , 2017, 358, 1434-1439.	12.6	196
4969	Structure-function relationships in ABCG2: insights from molecular dynamics simulations and molecular docking studies. <i>Scientific Reports</i> , 2017, 7, 15534.	3.3	48
4970	Elucidating the stability of bolaamphiphilic polypeptide nanosheets using atomistic molecular dynamics. <i>Physical Chemistry Chemical Physics</i> , 2017, 19, 31921-31928.	2.8	26
4971	Ammonium based stabilizers effectively counteract urea-induced denaturation in a small protein: insights from molecular dynamics simulations. <i>RSC Advances</i> , 2017, 7, 52888-52906.	3.6	24
4972	Comparative computational assessment of the pathogenicity of mutations in the Aspartoacylase enzyme. <i>Metabolic Brain Disease</i> , 2017, 32, 2105-2118.	2.9	34
4973	New Force Field Model for Propylene Glycol: Insight to Local Structure and Dynamics. <i>Journal of Physical Chemistry B</i> , 2017, 121, 10906-10921.	2.6	24
4974	Parameterization of Palmitoylated Cysteine, Farnesylated Cysteine, Geranylgeranylated Cysteine, and Myristoylated Glycine for the Martini Force Field. <i>Journal of Physical Chemistry B</i> , 2017, 121, 11132-11143.	2.6	33
4975	Hydration peculiarities of graphene oxides with multiple oxidation degrees. <i>Physical Chemistry Chemical Physics</i> , 2017, 19, 32333-32340.	2.8	21
4976	Conditional Reversible Work Coarse-Grained Models of Molecular Liquids with Coulomb Electrostatics – A Proof of Concept Study on Weakly Polar Organic Molecules. <i>Journal of Chemical Theory and Computation</i> , 2017, 13, 6158-6166.	5.3	11
4977	Multiple pathways in pressure-induced phase transition of coesite. <i>Proceedings of the National Academy of Sciences of the United States of America</i> , 2017, 114, 12894-12899.	7.1	7
4978	Mechanism of Competitive Inhibition and Destabilization of <i>Acidothermus cellulolyticus</i> Endoglucanase 1 by Ionic Liquids. <i>Journal of Physical Chemistry B</i> , 2017, 121, 10793-10803.	2.6	20
4979	Structural and dynamical characterization of the pH-dependence of the pectin methylesterase-pectin methylesterase inhibitor complex. <i>Journal of Biological Chemistry</i> , 2017, 292, 21538-21547.	3.4	19
4980	Antiviral potential of natural compounds against influenza virus hemagglutinin. <i>Computational Biology and Chemistry</i> , 2017, 71, 207-218.	2.3	33
4981	Alchemical Free Energy Calculations for Nucleotide Mutations in Protein-DNA Complexes. <i>Journal of Chemical Theory and Computation</i> , 2017, 13, 6275-6289.	5.3	42
4982	Changing the shape of hair with keratin peptides. <i>RSC Advances</i> , 2017, 7, 51581-51592.	3.6	38
4983	Interaction between Water and Alkali Metal Ions and Its Temperature Dependence Revealed by Oxygen K-Edge X-ray Absorption Spectroscopy. <i>Journal of Physical Chemistry B</i> , 2017, 121, 10957-10964.	2.6	41

#	ARTICLE	IF	CITATIONS
4984	A coarse-grained polarizable force field for the ionic liquid 1-butyl-3-methylimidazolium hexafluorophosphate. <i>Journal of Physics Condensed Matter</i> , 2017, 29, 504004.	1.8	16
4985	Dynamic changes in binding interaction networks of sex steroids establish their non-classical effects. <i>Scientific Reports</i> , 2017, 7, 14847.	3.3	3
4986	Transferable coarse-grained model for perfluorosulfonic acid polymer membranes. <i>Journal of Chemical Physics</i> , 2017, 147, 094904.	3.0	25
4987	Guest Controlled Nonmonotonic Deep Cavity Cavitand Assembly State Switching. <i>Journal of Physical Chemistry B</i> , 2017, 121, 10717-10725.	2.6	12
4988	Computational Lipidomics of the Neuronal Plasma Membrane. <i>Biophysical Journal</i> , 2017, 113, 2271-2280.	0.5	197
4989	Squid Suckerin Biomimetic Peptides Form Amyloid-like Crystals with Robust Mechanical Properties. <i>Biomacromolecules</i> , 2017, 18, 4240-4248.	5.4	21
4990	Self-Avoiding Conformational Sampling Based on Histories of Past Conformational Searches. <i>Journal of Chemical Information and Modeling</i> , 2017, 57, 3070-3078.	5.4	7
4991	Temperature-Dependent Implicit-Solvent Model of Polyethylene Glycol in Aqueous Solution. <i>Journal of Chemical Theory and Computation</i> , 2017, 13, 6317-6327.	5.3	22
4992	How the Incorporation of Pluronic Block Copolymers Modulates the Response of Lipid Membranes to Mechanical Stress. <i>Langmuir</i> , 2017, 33, 13284-13294.	3.5	14
4993	Tunable fluorescence behaviors of a supramolecular system based on a fluorene derivative and cucurbit[8]uril and its application for ATP sensing. <i>Physical Chemistry Chemical Physics</i> , 2017, 19, 31306-31315.	2.8	21
4994	Inhibition of $\beta$ -Amyloid Channels with a Drug Candidate wxg-50 Revealed by Molecular Dynamics Simulations. <i>Journal of Chemical Information and Modeling</i> , 2017, 57, 2811-2821.	5.4	31
4995	Structural and Dynamical Properties of Alkaline Earth Metal Halides in Supercritical Water: Effect of Ion Size and Concentration. <i>Journal of Physical Chemistry B</i> , 2017, 121, 10543-10555.	2.6	10
4996	Influence of molecular weight on ion-transport properties of polymeric ionic liquids. <i>Physical Chemistry Chemical Physics</i> , 2017, 19, 29134-29145.	2.8	49
4997	Dielectric properties of pyridine derivative-water clusters: Molecular dynamics simulation. <i>Journal of Molecular Liquids</i> , 2017, 241, 984-991.	4.9	6
4998	Magnesium sulfate against oxidative damage of membrane lipids: A theoretical model. <i>International Journal of Quantum Chemistry</i> , 2017, 117, e25423.	2.0	8
4999	Understanding the Roles of Solution Chemistries and Functionalization on the Aggregation of Graphene-Based Nanomaterials Using Molecular Dynamic Simulations. <i>Journal of Physical Chemistry C</i> , 2017, 121, 13888-13897.	3.1	24
5000	Stability and growth mechanism of self-assembling putative antifreeze cyclic peptides. <i>Physical Chemistry Chemical Physics</i> , 2017, 19, 19032-19042.	2.8	13
5001	Role of Dynamic Heterogeneities in Ionic Liquids: Insights from All-Atom and Coarse-Grained Molecular Dynamics Simulation Studies. <i>ChemPhysChem</i> , 2017, 18, 2233-2242.	2.1	16



#	ARTICLE	IF	CITATIONS
5002	Elucidating sequence and solvent specific design targets to protect and stabilize enzymes for biocatalysis in ionic liquids. <i>Physical Chemistry Chemical Physics</i> , 2017, 19, 17426-17433.	2.8	21
5003	Changes in the hydration structure of imidazole upon protonation: Neutron scattering and molecular simulations. <i>Journal of Chemical Physics</i> , 2017, 146, .	3.0	14
5004	Multiscale design and optimization of polymer-based photonic crystals for solar shielding. <i>Solar Energy Materials and Solar Cells</i> , 2017, 171, 166-179.	6.2	4
5005	Three-dimensional buckled honeycomb boron lattice with vacancies as an intermediate phase on the transition pathway from $\Gamma$ -B to $\Gamma$ -B. <i>NPG Asia Materials</i> , 2017, 9, e400-e400.	7.9	4
5006	Developing structure and thermodynamic properties-consistent coarse-grained model for random copolymer systems. <i>Polymer</i> , 2017, 123, 107-120.	3.8	12
5007	Molecular origin of urea driven hydrophobic polymer collapse and unfolding depending on side chain chemistry. <i>Physical Chemistry Chemical Physics</i> , 2017, 19, 18156-18161.	2.8	37
5008	Interconversion of inactive to active conformation of MARK2: Insights from molecular modeling and molecular dynamics simulation. <i>Archives of Biochemistry and Biophysics</i> , 2017, 630, 66-80.	3.0	9
5009	Why human anti-Gal $\alpha$ 1 $\rightarrow$ 4Gal $\beta$ 1 $\rightarrow$ 4Glc natural antibodies do not recognize the trisaccharide on erythrocyte membrane? Molecular dynamics and immunochemical investigation. <i>Molecular Immunology</i> , 2017, 90, 87-97.	2.2	8
5010	Phase and interface determination in computer simulations of liquid mixtures with high partial miscibility. <i>Physical Chemistry Chemical Physics</i> , 2017, 19, 18968-18974.	2.8	11
5011	Ground state structure of high-energy-density polymeric carbon monoxide. <i>Physical Review B</i> , 2017, 95, .	3.2	22
5012	Probe-location dependent resonance energy transfer at lipid/water interfaces: comparison between the gel- and fluid-phase of lipid bilayer. <i>Physical Chemistry Chemical Physics</i> , 2017, 19, 25870-25885.	2.8	9
5013	Utilizing Computational Techniques to Accelerate Discovery in Peanut Allergenicity. , 2017, , .		0
5014	The tyrosine Y2502.39 in Frizzled 4 defines a conserved motif important for structural integrity of the receptor and recruitment of Dishevelled. <i>Cellular Signalling</i> , 2017, 38, 85-96.	3.6	16
5015	Molecular dynamic studies of $\pi$ - $\pi$ stacked imidazolium/imidazolate ion pairs in chloroform solution. <i>Journal of Molecular Liquids</i> , 2017, 245, 103-108.	4.9	5
5016	Flexible Force Field Parameterization through Fitting on the Ab Initio-Derived Elastic Tensor. <i>Journal of Chemical Theory and Computation</i> , 2017, 13, 3722-3730.	5.3	13
5017	Structural insights into the mechanism of the membrane integral N-acyltransferase step in bacterial lipoprotein synthesis. <i>Nature Communications</i> , 2017, 8, 15952.	12.8	52
5018	Insight into increased stability of methane hydrates at high pressure from phase equilibrium data and molecular structure. <i>Fluid Phase Equilibria</i> , 2017, 450, 24-29.	2.5	30
5019	Effect of Polycation Structure on Interaction with Lipid Membranes. <i>Journal of Physical Chemistry B</i> , 2017, 121, 7318-7326.	2.6	27



#	ARTICLE	IF	CITATIONS
5020	Liquid-liquid phase transition in an ionic model of silica. <i>Journal of Chemical Physics</i> , 2017, 146, 234503.	3.0	29
5021	Molecular Recognition in Asymmetric Counteranion Catalysis: Understanding Chiral Phosphate-Mediated Desymmetrization. <i>Journal of the American Chemical Society</i> , 2017, 139, 8886-8896.	13.7	47
5022	Methodology for Estimation of Nanoscale Hardness via Atomistic Simulations. <i>Journal of Nanomechanics &amp; Micromechanics</i> , 2017, 7, .	1.4	16
5023	Enhancing Entropy and Enthalpy Fluctuations to Drive Crystallization in Atomistic Simulations. <i>Physical Review Letters</i> , 2017, 119, 015701.	7.8	74
5024	Impact of molecular flexibility on the site energy shift of chlorophylls in Photosystem II. <i>Biophysical Chemistry</i> , 2017, 229, 93-98.	2.8	8
5025	Follicle-stimulating hormone encapsulation in the cholesterol-modified chitosan nanoparticles via molecular dynamics simulations and binding free energy calculations. <i>European Journal of Pharmaceutical Sciences</i> , 2017, 107, 126-137.	4.0	25
5026	Distinct Protein Hydration Water Species Defined by Spatially Resolved Spectra of Intermolecular Vibrations. <i>Journal of Physical Chemistry B</i> , 2017, 121, 7431-7442.	2.6	30
5027	Structure of Hydrated Gibbsite and Brucite Edge Surfaces: DFT Results and Further Development of the ClayFF Classical Force Field with Metal-H Angle Bending Terms. <i>Journal of Physical Chemistry C</i> , 2017, 121, 14757-14771.	3.1	91
5028	Self-Assembled DNA/Peptide-Based Nanoparticle Exhibiting Synergistic Enzymatic Activity. <i>ACS Nano</i> , 2017, 11, 7251-7258.	14.6	67
5029	Continuum balances from extended Hamiltonian dynamics. <i>Journal of Chemical Physics</i> , 2017, 146, 224102.	3.0	2
5030	A novel method for constructing continuous intrinsic surfaces of nanoparticles. <i>Journal of Molecular Modeling</i> , 2017, 23, 219.	1.8	10
5031	StreAM- $\text{gTg}$ : algorithms for analyzing coarse grained RNA dynamics based on Markov models of connectivity-graphs. <i>Algorithms for Molecular Biology</i> , 2017, 12, 15.	1.2	5
5032	Integrative modelling of TIR domain-containing adaptor molecule inducing interferon- $\beta$ (TRIF) provides insights into its autoinhibited state. <i>Biology Direct</i> , 2017, 12, 9.	4.6	10
5033	Internal modifications in the CENP-A nucleosome modulate centromeric dynamics. <i>Epigenetics and Chromatin</i> , 2017, 10, 17.	3.9	31
5034	Efficient estimation of binding free energies between peptides and an MHC class II molecule using coarse-grained molecular dynamics simulations with a weighted histogram analysis method. <i>Journal of Computational Chemistry</i> , 2017, 38, 2007-2019.	3.3	16
5035	Prediction of self-assemblies of sodium dodecyl sulfate and fragrance additives using coarse-grained force fields. <i>Journal of Molecular Modeling</i> , 2017, 23, 211.	1.8	3
5036	Membrane localization and dynamics of geranylgeranylated Rab5 hypervariable region. <i>Biochimica Et Biophysica Acta - Biomembranes</i> , 2017, 1859, 1335-1349.	2.6	18
5037	Regulation of the Equilibrium between Closed and Open Conformations of Annexin A2 by N-Terminal Phosphorylation and S100A4-Binding. <i>Structure</i> , 2017, 25, 1195-1207.e5.	3.3	42

#	ARTICLE	IF	CITATIONS
5038	Molecular Dynamics Studies of Overbased Detergents on a Water Surface. <i>Langmuir</i> , 2017, 33, 7263-7270.	3.5	5
5039	Guest-host systems containing anthraquinone dyes with multiple visible transitions giving positive and negative dichroic order parameters: an assessment of principal molecular axes and computational methods. <i>Liquid Crystals</i> , 0, , 1-17.	2.2	2
5040	Transport properties of mixtures composed of acetone, water, and supercritical carbon dioxide by molecular dynamics simulation. <i>Journal of Supercritical Fluids</i> , 2017, 130, 321-326.	3.2	17
5041	Temperature dependence of protein-water interactions in a gated yeast aquaporin. <i>Scientific Reports</i> , 2017, 7, 4016.	3.3	9
5042	Delineating residues for haemolytic activities of snake venom cardiotoxin 1 from <i>Naja naja</i> as probed by molecular dynamics simulations and in vitro validations. <i>International Journal of Biological Macromolecules</i> , 2017, 95, 1022-1036.	7.5	8
5043	Molecular Dynamics Analysis of 4E-BP2 Protein Fold Stabilization Induced by Phosphorylation. <i>Journal of Physical Chemistry B</i> , 2017, 121, 3387-3393.	2.6	11
5044	Aliphatic isocyanurates and polyisocyanurate networks. <i>Polymers for Advanced Technologies</i> , 2017, 28, 1299-1304.	3.2	21
5045	Unveiling the impact of regioisomerism defects in the glass transition temperature of PVDF by the mean of the activation energy. <i>Journal of Polymer Science Part A</i> , 2017, 55, 419-426.	2.3	16
5046	The effect of dichlorvos on the structural alteration of serum albumins: a combined spectroscopic and molecular dynamic simulation approach. <i>Monatshefte für Chemie</i> , 2017, 148, 1141-1151.	1.8	18
5047	Engineering disulfide bonds in <i>Selenomonas ruminantium</i> $\beta$ -xylosidase by experimental and computational methods. <i>International Journal of Biological Macromolecules</i> , 2017, 95, 248-255.	7.5	14
5048	Molecular basis and potential activity of HIV-1 reverse transcriptase toward trimethylamine-based compounds. <i>Biotechnology and Applied Biochemistry</i> , 2017, 64, 810-826.	3.1	1
5049	Deciphering the Multisite Interactions of a Protein and Its Ligand at Atomic Resolution by Using Sensitive Paramagnetic Effects. <i>Chemistry - A European Journal</i> , 2017, 23, 926-934.	3.3	1
5050	Molecular Dynamics Simulations. <i>Topics in Applied Physics</i> , 2017, , 355-414.	0.8	6
5051	Exploration of the binding properties of the human serum albumin sites with neurology drugs by docking and molecular dynamics simulation. <i>Journal of the Iranian Chemical Society</i> , 2017, 14, 19-35.	2.2	5
5052	Essential dynamics of the cold denaturation: pressure and temperature effects in yeast frataxin. <i>Proteins: Structure, Function and Bioinformatics</i> , 2017, 85, 125-136.	2.6	11
5053	Shear stress- and line length-dependent screw dislocation cross-slip in FCC Ni. <i>Acta Materialia</i> , 2017, 122, 412-419.	7.9	48
5054	Which fullerenols are water soluble? Systematic atomistic investigation. <i>New Journal of Chemistry</i> , 2017, 41, 184-189.	2.8	16
5055	Detailed Molecular Dynamics Simulation of the Structure and Self-Diffusion of Linear and Cyclic $\alpha$ -Alkanes in Melt and Blends. <i>Macromolecular Theory and Simulations</i> , 2017, 26, 1600049.	1.4	10

#	ARTICLE	IF	CITATIONS
5056	Uncoupling of an ammonia channel as a mechanism of allosteric inhibition in anthranilate synthase of <i>Serratia marcescens</i> : dynamic and graph theoretical analysis. <i>Molecular BioSystems</i> , 2017, 13, 142-155.	2.9	13
5057	Compromise in competition between free energy and binding effect of intrinsically disordered protein p53 C-terminal domain. <i>Molecular Simulation</i> , 2017, 43, 110-120.	2.0	2
5058	Exploring the structure and stability of cholesterol dimer formation in multicomponent lipid bilayers. <i>Journal of Computational Chemistry</i> , 2017, 38, 1479-1488.	3.3	25
5059	Molecular dynamics study on the grain size, temperature, and stress dependence of creep behavior in nanocrystalline nickel. <i>Journal of Materials Science</i> , 2017, 52, 2180-2191.	3.7	50
5060	Atomic scale processes of phase transformations in nanocrystalline NiTi shape-memory alloys. <i>Acta Materialia</i> , 2017, 123, 90-101.	7.9	161
5061	Estimation of relative free energies of binding using pre-computed ensembles based on the single-step free energy perturbation and the site-identification by Ligand competitive saturation approaches. <i>Journal of Computational Chemistry</i> , 2017, 38, 1238-1251.	3.3	26
5062	Solvation structures of sodium halides in dimethyl sulfoxide (DMSO)-methanol (MeOH) mixtures. <i>Molecular Simulation</i> , 2017, 43, 154-168.	2.0	7
5063	Mechanical equilibrium, a prerequisite to unveil auxetic properties in molecular compounds. <i>Molecular Simulation</i> , 2017, 43, 169-175.	2.0	7
5064	Convergence and Sampling in Determining Free Energy Landscapes for Membrane Protein Association. <i>Journal of Physical Chemistry B</i> , 2017, 121, 3364-3375.	2.6	93
5065	The effect of porosity on the vibrational and low temperature equilibrium thermodynamic properties of amorphous silicon via computer simulation. <i>Journal of Non-Crystalline Solids</i> , 2017, 455, 42-51.	3.1	1
5066	Molecular modeling, dynamics studies and density functional theory approaches to identify potential inhibitors of SIRT4 protein from <i>Homo sapiens</i> : a novel target for the treatment of type 2 diabetes. <i>Journal of Biomolecular Structure and Dynamics</i> , 2017, 35, 3316-3329.	3.5	39
5067	In vivo and in silico studies to identify mechanisms associated with Nurr1 modulation following early life exposure to permethrin in rats. <i>Neuroscience</i> , 2017, 340, 411-423.	2.3	30
5068	Dynamic conformational changes in the rhesus TRIM5 $\alpha$ dimer dictate the potency of HIV-1 restriction. <i>Virology</i> , 2017, 500, 161-168.	2.4	10
5069	Calcium-induced conformational changes of Thrombospondin-1 signature domain: implications for vascular disease. <i>Journal of Receptor and Signal Transduction Research</i> , 2017, 37, 239-251.	2.5	1
5070	Insight into the mechanism of chemical modification of antibacterial agents by antibiotic resistance enzyme <i>O</i> <sup>6</sup> -phosphotransferase- $\alpha$ -NIA. <i>Chemical Biology and Drug Design</i> , 2017, 89, 84-97.	3.2	1
5071	Study of conformational changes in serum albumin by binding of chlorfenvinphos using multispectroscopic techniques and molecular dynamic simulation. <i>Monatshefte für Chemie</i> , 2017, 148, 781-791.	1.8	18
5072	The Study of the Concentration Increasing Effect in the Combination of Zinc Ion with Human Growth Hormone by Molecular Dynamics Simulation. <i>Iranian Journal of Science and Technology, Transaction A: Science</i> , 2017, 41, 329-335.	1.5	1
5073	Novel virtual lead identification in the discovery of hematopoietic cell kinase (HCK) inhibitors: application of 3D QSAR and molecular dynamics simulation. <i>Journal of Receptor and Signal Transduction Research</i> , 2017, 37, 224-238.	2.5	9

#	ARTICLE	IF	CITATIONS
5074	Integrated Modeling and Experimental Approaches to Control Silica Modification of Design Silk-Based Biomaterials. <i>ACS Biomaterials Science and Engineering</i> , 2017, 3, 2877-2888.	5.2	14
5075	Eliminating a Protein Folding Intermediate by Tuning a Local Hydrophobic Contact. <i>Journal of Physical Chemistry B</i> , 2017, 121, 3276-3284.	2.6	5
5076	A molecular dynamics strategy for CSÎ±Î² peptides disulfide-assisted model refinement. <i>Journal of Biomolecular Structure and Dynamics</i> , 2017, 35, 2736-2744.	3.5	1
5077	Computational Methodologies for Developing Structureâ€“Morphologyâ€“Performance Relationships in Organic Solar Cells: A Protocol Review. <i>Chemistry of Materials</i> , 2017, 29, 346-354.	6.7	61
5078	Ganglioside-Lipid and Ganglioside-Protein Interactions Revealed by Coarse-Grained and Atomistic Molecular Dynamics Simulations. <i>Journal of Physical Chemistry B</i> , 2017, 121, 3262-3275.	2.6	81
5079	Rational design of thermostability in bacterial 1,3-1,4-Î²-glucanases through spatial compartmentalization of mutational hotspots. <i>Applied Microbiology and Biotechnology</i> , 2017, 101, 1085-1097.	3.6	27
5080	Study of procaine and tetracaine in the lipid bilayer using molecular dynamics simulation. <i>European Biophysics Journal</i> , 2017, 46, 265-282.	2.2	10
5081	Molecular dynamics simulation on structural evolution during crystallization of rapidly super-cooled Cu50Ni50 alloy. <i>Journal of Alloys and Compounds</i> , 2017, 690, 633-639.	5.5	21
5082	Comparison of force fields for Alzheimer's A: A case study for intrinsically disordered proteins. <i>Protein Science</i> , 2017, 26, 174-185.	7.6	118
5083	Double phosphorylationâ€“induced structural changes in the signalâ€“receiving domain of Î²BÎ± in complex with NFâ€“B. <i>Proteins: Structure, Function and Bioinformatics</i> , 2017, 85, 17-29.	2.6	9
5084	A green process for recovery of 1-propanol/2-propanol from their aqueous solutions: Experimental and MD simulation studies. <i>Journal of Chemical Thermodynamics</i> , 2017, 105, 76-85.	2.0	8
5085	Highly clean and efficient enzymatic dehairing in green solvents. <i>Journal of Cleaner Production</i> , 2017, 140, 1578-1586.	9.3	9
5086	Structure of the SLC4 transporter Bor1p in an inwardâ€“facing conformation. <i>Protein Science</i> , 2017, 26, 130-145.	7.6	34
5087	A coarse-grained model for PCL: conformation, self-assembly of MePEG-b-PCL amphiphilic diblock copolymers. <i>Molecular Simulation</i> , 2017, 43, 92-101.	2.0	13
5088	Antiâ€“HIVâ€“1 Activity Prediction of Novel Gp41 Inhibitors Using Structureâ€“Based Virtual Screening and Molecular Dynamics Simulation. <i>Molecular Informatics</i> , 2017, 36, 1600060.	2.5	18
5089	PCLa-H tandem-repeat peptides active against multidrug resistant clinical bacterial isolates. <i>Biochimica Et Biophysica Acta - Biomembranes</i> , 2017, 1859, 228-237.	2.6	23
5090	Resolving solvophobic interactions inferred from experimental solvation free energies and evaluated from molecular simulations. <i>Chemical Physics Letters</i> , 2017, 667, 62-67.	2.6	1
5091	Molecular dynamics simulations and Kelvin probe force microscopy to study of cholesterol-induced electrostatic nanodomains in complex lipid mixtures. <i>Soft Matter</i> , 2017, 13, 355-362.	2.7	8

#	ARTICLE	IF	CITATIONS
5092	The IM30/Vipp1 C-terminus associates with the lipid bilayer and modulates membrane fusion. <i>Biochimica Et Biophysica Acta - Bioenergetics</i> , 2017, 1858, 126-136.	1.0	26
5093	Assessing gastric toxicity of xanthone derivatives of anti-inflammatory activity using simulation and experimental approaches. <i>Biophysical Chemistry</i> , 2017, 220, 20-33.	2.8	5
5094	Computational modeling and molecular dynamics simulations of mammalian cytoplasmic tyrosyl-tRNA synthetase and its complexes with substrates. <i>Journal of Biomolecular Structure and Dynamics</i> , 2017, 35, 2772-2788.	3.5	5
5095	Catalytic efficiency and thermostability improvement of Suc2 invertase through rational site-directed mutagenesis. <i>Enzyme and Microbial Technology</i> , 2017, 96, 14-22.	3.2	13
5096	Structural plasticity mediates distinct $\text{GAP}$ -dependent $\text{GTP}$ hydrolysis mechanisms in Rab33 and Rab5. <i>FEBS Journal</i> , 2017, 284, 4358-4375.	4.7	4
5097	Oxidation Mechanism of Arsenopyrite in the Presence of Water. <i>Journal of Physical Chemistry C</i> , 2017, 121, 26887-26894.	3.1	14
5098	High precision determination of the melting points of water TIP4P/2005 and water TIP4P/Ice models by the direct coexistence technique. <i>Journal of Chemical Physics</i> , 2017, 147, 244506.	3.0	60
5099	Atomistic Insights into Structural Differences between E3 and E4 Isoforms of Apolipoprotein E. <i>Biophysical Journal</i> , 2017, 113, 2682-2694.	0.5	17
5100	Structural Characterization and computational approach to doped hafnium oxide nano crystals for thermo and photoluminescence applications. <i>MRS Advances</i> , 2017, 2, 2793-2798.	0.9	0
5101	Impact of protein-ligand solvation and desolvation on transition state thermodynamic properties of adenosine A2A ligand binding kinetics. <i>In Silico Pharmacology</i> , 2017, 5, 16.	3.3	20
5102	Modulation of the Vault Protein-Protein Interaction for Tuning of Molecular Release. <i>Scientific Reports</i> , 2017, 7, 14816.	3.3	8
5103	Designing Fcabs: well-expressed and stable high affinity antigen-binding Fc fragments. <i>Protein Engineering, Design and Selection</i> , 2017, 30, 657-671.	2.1	12
5104	The role of $\text{Zn}^{2+}$ , dimerization and N-glycosylation in the interaction of Auxin-Binding Protein 1 (ABP1) with different auxins. <i>Glycobiology</i> , 2017, 27, 1109-1119.	2.5	4
5105	Nucleation mechanism of clathrate hydrates of water-soluble guest molecules. <i>Journal of Chemical Physics</i> , 2017, 147, 204503.	3.0	32
5106	Comparison of coarse-grained (MARTINI) and atomistic molecular dynamics simulations of $\alpha$ and $\beta$ toxin nanopores in lipid membranes. <i>Journal of Chemical Sciences</i> , 2017, 129, 1017-1030.	1.5	18
5107	Macroscopic chiral symmetry breaking in monolayers of achiral nonconvex platelets. <i>Soft Matter</i> , 2017, 13, 8618-8624.	2.7	5
5108	Origin of the blueshift of water molecules at interfaces of hydrophilic cyclic compounds. <i>Science Advances</i> , 2017, 3, e1701400.	10.3	22
5109	Aggregation-induced emission in lamellar solids of colloidal perovskite quantum wells. <i>Science Advances</i> , 2017, 3, eaaq0208.	10.3	65

#	ARTICLE	IF	CITATIONS
5110	Predicting Critical Micelle Concentrations with Molecular Dynamics Simulations and COSMOmic. <i>Chemie-Ingenieur-Technik</i> , 2017, 89, 1288-1296.	0.8	11
5111	Computer simulations of alkali-acetate solutions: Accuracy of the forcefields in difference concentrations. <i>Journal of Chemical Physics</i> , 2017, 147, 194102.	3.0	9
5112	Evaluation of Sox2 binding affinities for distinct <scp>DNA</scp> patterns using steered molecular dynamics simulation. <i>FEBS Open Bio</i> , 2017, 7, 1750-1767.	2.3	18
5113	Molecular Dynamics Simulation Study of ClF in Water: Halogen Bonding Interaction in Liquid. <i>Chinese Journal of Chemical Physics</i> , 2017, 30, 25-28.	1.3	3
5114	Molecular Simulation Study on the Interaction of Nanoparticles with Clay Minerals: C <sub>60</sub> on Surfaces of Pyrophyllite and Kaolinite. <i>Clays and Clay Minerals</i> , 2017, 65, 398-409.	1.3	4
5115	P-gp and BCRP inhibition induced by some new 1,4-Dihydropyridine and Dihydropyrimidines. <i>International Journal of Bioinformatics Research and Applications</i> , 2017, 13, 62.	0.2	1
5116	Decoding Corticotropin-Releasing Factor Receptor Type 1 Crystal Structures. <i>Current Molecular Pharmacology</i> , 2017, 10, 334-344.	1.5	25
5117	Water Molecules in a Carbon Nanotube under an Applied Electric Field at Various Temperatures and Pressures. <i>Water (Switzerland)</i> , 2017, 9, 473.	2.7	29
5118	Auxeticity of Yukawa Systems with Nanolayers in the (111) Crystallographic Plane. <i>Materials</i> , 2017, 10, 1338.	2.9	18
5119	Protein Stability and Unfolding Following Glycine Radical Formation. <i>Molecules</i> , 2017, 22, 655.	3.8	7
5120	Supporting the Identification of Novel Fragment-Based Positive Allosteric Modulators Using a Supervised Molecular Dynamics Approach: A Retrospective Analysis Considering the Human A2A Adenosine Receptor as a Key Example. <i>Molecules</i> , 2017, 22, 818.	3.8	19
5121	Mechanism Exploration of Arylpiperazine Derivatives Targeting the 5-HT <sub>2A</sub> Receptor by In Silico Methods. <i>Molecules</i> , 2017, 22, 1064.	3.8	13
5122	Coupling Form and Function: How the Oligomerisation Symmetry of the SAS-6 Protein Contributes to the Architecture of Centriole Organelles. <i>Symmetry</i> , 2017, 9, 74.	2.2	0
5123	T7 RNA polymerase translocation is facilitated by a helix opening on the fingers domain that may also prevent backtracking. <i>Nucleic Acids Research</i> , 2017, 45, 7909-7921.	14.5	25
5124	Tacticity-Dependent Interchain Interactions of Poly(N-Isopropylacrylamide) in Water: Toward the Molecular Dynamics Simulation of a Thermoresponsive Microgel. <i>Gels</i> , 2017, 3, 13.	4.5	8
5125	The Effects of Alkyl Chain Combinations on the Structural and Mechanical Properties of Biomimetic Ion Pair Amphiphile Bilayers. <i>Bioengineering</i> , 2017, 4, 84.	3.5	9
5126	An Atomistic Carbide-Derived Carbon Model Generated Using ReaxFF-Based Quenched Molecular Dynamics. <i>Journal of Carbon Research</i> , 2017, 3, 32.	2.7	13
5127	Bladder-cancer-associated mutations in RXRA activate peroxisome proliferator-activated receptors to drive urothelial proliferation. <i>ELife</i> , 2017, 6, .	6.0	55



#	ARTICLE	IF	CITATIONS
5128	A new molecular mechanism underlying the EGCG-mediated autophagic modulation of AFP in HepG2 cells. <i>Cell Death and Disease</i> , 2017, 8, e3160-e3160.	6.3	48
5129	Stabilization and structural analysis of a membrane-associated hIAPP aggregation intermediate. <i>ELife</i> , 2017, 6, .	6.0	61
5130	His-FLAG Tag as a Fusion Partner of Glycosylated Human Interferon-Gamma and Its Mutant: Gain or Loss?. <i>BioMed Research International</i> , 2017, 2017, 1-12.	1.9	4
5131	Computational Exploration for Lead Compounds That Can Reverse the Nuclear Morphology in Progeria. <i>BioMed Research International</i> , 2017, 2017, 1-15.	1.9	10
5132	Sulfonanilide Derivatives in Identifying Novel Aromatase Inhibitors by Applying Docking, Virtual Screening, and MD Simulations Studies. <i>BioMed Research International</i> , 2017, 2017, 1-17.	1.9	20
5133	Modeling the Mechanisms of Clay Damage by Molecular Dynamic Simulation. <i>Geofluids</i> , 2017, 2017, 1-8.	0.7	5
5134	Biophysical and Computational Studies of the vCCI:vMIP-II Complex. <i>International Journal of Molecular Sciences</i> , 2017, 18, 1778.	4.1	4
5135	Investigation of Binding Modes and Functional Surface of Scorpion Toxins ANEP to Sodium Channels 1.7. <i>Toxins</i> , 2017, 9, 387.	3.4	10
5136	Waterdock 2.0: Water placement prediction for Holo-structures with a pymol plugin. <i>PLoS ONE</i> , 2017, 12, e0172743.	2.5	35
5137	Differential roles of 3-Hydroxyflavone and 7-Hydroxyflavone against nicotine-induced oxidative stress in rat renal proximal tubule cells. <i>PLoS ONE</i> , 2017, 12, e0179777.	2.5	21
5138	Modeling of annexin A2â€™Membrane interactions by molecular dynamics simulations. <i>PLoS ONE</i> , 2017, 12, e0185440.	2.5	26
5139	Insight into the interactions, residue snorkeling, and membrane disordering potency of a single antimicrobial peptide into different lipid bilayers. <i>PLoS ONE</i> , 2017, 12, e0187216.	2.5	27
5140	Assemblies of amyloid-Î²30â€™36 hexamer and its G33V/L34T mutants by replica-exchange molecular dynamics simulation. <i>PLoS ONE</i> , 2017, 12, e0188794.	2.5	13
5141	Water permeation through the internal water pathway in activated GPCR rhodopsin. <i>PLoS ONE</i> , 2017, 12, e0176876.	2.5	14
5142	Sequence dependency of canonical base pair opening in the DNA double helix. <i>PLoS Computational Biology</i> , 2017, 13, e1005463.	3.2	31
5143	Atomistic fingerprint of hyaluronanâ€™CD44 binding. <i>PLoS Computational Biology</i> , 2017, 13, e1005663.	3.2	33
5144	Concerted regulation of npc2 binding to endosomal/lysosomal membranes by bis(monoacylglycero)phosphate and sphingomyelin. <i>PLoS Computational Biology</i> , 2017, 13, e1005831.	3.2	27
5145	A new class of hybrid secretion system is employed in <i>Pseudomonas</i> amyloid biogenesis. <i>Nature Communications</i> , 2017, 8, 263.	12.8	56



#	ARTICLE	IF	CITATIONS
5146	PknB remains an essential and a conserved target for drug development in susceptible and MDR strains of M. Tuberculosis. <i>Annals of Clinical Microbiology and Antimicrobials</i> , 2017, 16, 56.	3.8	13
5147	Transferability of Polymer Chain Properties between Coarse-Grained and Atomistic Models of Natural Rubber Molecule Validated by Molecular Dynamics Simulations. <i>Journal of Physics: Conference Series</i> , 2017, 901, 012096.	0.4	2
5148	Trigonella seed extract ameliorates inflammation via regulation of the inflammasome adaptor protein ASC. <i>Frontiers in Bioscience - Elite</i> , 2017, 9, 246-257.	1.8	7
5149	Uncertainty Quantification and Reduction of Molecular Dynamics Models. , 0, , .		4
5150	Debye-Waller coefficient of heavily deformed nanocrystalline iron. <i>Journal of Applied Crystallography</i> , 2017, 50, 508-518.	4.5	21
5151	Comparative molecular dynamics study of dimeric and monomeric forms of HIV-1 protease in ligand bound and unbound state. <i>General Physiology and Biophysics</i> , 2017, 36, 141-154.	0.9	2
5152	Structural insights into dynamics of RecU-HJ complex formation elucidates key role of NTR and stalk region toward formation of reactive state. <i>Nucleic Acids Research</i> , 2017, 45, 975-986.	14.5	5
5153	Structural Ordering of Molybdenum Disulfide Studied via Reactive Molecular Dynamics Simulations. <i>ACS Applied Materials &amp; Interfaces</i> , 2018, 10, 8937-8946.	8.0	34
5154	Addressing the temperature transferability of structure based coarse graining models. <i>Physical Chemistry Chemical Physics</i> , 2018, 20, 6617-6628.	2.8	32
5155	Intermolecular Interactions of Pyridine in Liquid Phase and Aqueous Solution Studied by Soft X-ray Absorption Spectroscopy. <i>Zeitschrift Fur Physikalische Chemie</i> , 2018, 232, 705-722.	2.8	21
5156	Comment to: "Martini straight: Boosting performance using a shorter cutoff and GPUs" by D.H. de Jong, S. Baoukina, H.I. IngÅlfsson, and S.J.A.Marrink. <i>Computer Physics Communications</i> , 2018, 228, 146-151.	7.5	3
5157	Statistical Model To Decipher Protein Folding/Unfolding at a Local Scale. <i>Journal of Physical Chemistry B</i> , 2018, 122, 3540-3549.	2.6	6
5158	Transferable Coarse-Grained Models of Liquid-Liquid Equilibrium Using Local Density Potentials Optimized with the Relative Entropy. <i>Journal of Physical Chemistry B</i> , 2018, 122, 5678-5693.	2.6	57
5159	Structural principles that enable oligomeric small heat-shock protein paralogs to evolve distinct functions. <i>Science</i> , 2018, 359, 930-935.	12.6	51
5160	Molecular Photophysics under Shock Compression: Ab Initio Nonadiabatic Molecular Dynamics of Rhodamine Dye. <i>Journal of Physical Chemistry C</i> , 2018, 122, 13600-13607.	3.1	4
5161	Probing spatial locality in ionic liquids with the grand canonical adaptive resolution molecular dynamics technique. <i>Journal of Chemical Physics</i> , 2018, 148, 193804.	3.0	19
5162	Insight into microtubule destabilization mechanism of 3,4,5-trimethoxyphenyl indanone derivatives using molecular dynamics simulation and conformational modes analysis. <i>Journal of Computer-Aided Molecular Design</i> , 2018, 32, 559-572.	2.9	13
5163	Interpretation of cytochrome P450 monooxygenase kinetics by modeling of thermodynamic activity. <i>Journal of Inorganic Biochemistry</i> , 2018, 183, 172-178.	3.5	6

#	ARTICLE	IF	CITATIONS
5164	Computational Signaling Protein Dynamics and Geometric Mass Relations in Biomolecular Diffusion. <i>Journal of Physical Chemistry B</i> , 2018, 122, 5599-5609.	2.6	1
5165	Temperature-Dependent Lipid Extraction from Membranes by Boron Nitride Nanosheets. <i>ACS Nano</i> , 2018, 12, 2764-2772.	14.6	44
5166	Blood Proteins and Their Interactions with Nanoparticles Investigated Using Molecular Dynamics Simulations. , 2018, , 5-19.		0
5167	Molecular Mechanism, Dynamics, and Energetics of Protein-Mediated Dinucleotide Flipping in a Mismatched DNA: A Computational Study of the RAD4-DNA Complex. <i>Journal of Chemical Information and Modeling</i> , 2018, 58, 647-660.	5.4	3
5168	Revisiting imidazolium based ionic liquids: Effect of the conformation bias of the [NTf2] anion studied by molecular dynamics simulations. <i>Journal of Chemical Physics</i> , 2018, 148, 193828.	3.0	42
5169	Impact of Edge Groups on the Hydration and Aggregation Properties of Graphene Oxide. <i>Journal of Physical Chemistry B</i> , 2018, 122, 2578-2586.	2.6	15
5170	Water entrapment and structure ordering as protection mechanisms for protein structural preservation. <i>Journal of Chemical Physics</i> , 2018, 148, 055102.	3.0	16
5171	Simulations of CYP51A from <i>Aspergillus fumigatus</i> in a model bilayer provide insights into triazole drug resistance. <i>Medical Mycology</i> , 2018, 56, 361-373.	0.7	10
5172	Efficient Osmotic Pressure Calculations Using Coarse-Grained Molecular Simulations. <i>Journal of Chemical Theory and Computation</i> , 2018, 14, 1171-1176.	5.3	4
5173	Solvent-enabled control of reactivity for liquid-phase reactions of biomass-derived compounds. <i>Nature Catalysis</i> , 2018, 1, 199-207.	34.4	211
5174	A simulation study of homogeneous ice nucleation in supercooled salty water. <i>Journal of Chemical Physics</i> , 2018, 148, 222811.	3.0	33
5175	Formation of a nanobubble and its effect on the structural ordering of water in a CH <sub>4</sub> -N <sub>2</sub> -CO <sub>2</sub> -H <sub>2</sub> O mixture. <i>Physical Chemistry Chemical Physics</i> , 2018, 20, 9157-9166.	2.8	13
5176	The structurally similar TRFH domain of TRF1 and TRF2 dimers shows distinct behaviour towards TIN2. <i>Archives of Biochemistry and Biophysics</i> , 2018, 642, 52-62.	3.0	5
5177	Self-assembled monolayer formation of distorted cylindrical AOT micelles on gold surfaces. <i>Colloids and Surfaces A: Physicochemical and Engineering Aspects</i> , 2018, 546, 20-27.	4.7	12
5178	Clarifying the role of cryo- and lyo-protectants in the biopreservation of proteins. <i>Physical Chemistry Chemical Physics</i> , 2018, 20, 8267-8277.	2.8	21
5179	On the distinct binding modes of expansin and carbohydrate-binding module proteins on crystalline and nanofibrous cellulose: implications for cellulose degradation by designer cellulosomes. <i>Physical Chemistry Chemical Physics</i> , 2018, 20, 8278-8293.	2.8	12
5180	Simulation-Guided Design of Cytochrome P450 for Chemo- and Regioselective Macrocyclic Oxidation. <i>Journal of Chemical Information and Modeling</i> , 2018, 58, 848-858.	5.4	14
5181	An auto-inhibitory helix in CTP:phosphocholine cytidyltransferase hijacks the catalytic residue and constrains a pliable, domain-bridging helix pair. <i>Journal of Biological Chemistry</i> , 2018, 293, 7070-7084.	3.4	12

#	ARTICLE	IF	CITATIONS
5182	Prediction of the Crystal Morphology of $\hat{1}^2$ -HMX using a Generalized Interfacial Structure Analysis Model. <i>Crystal Growth and Design</i> , 2018, 18, 2349-2357.	3.0	15
5183	Water Confined in Nanocapillaries: Two-Dimensional Bilayer Squarelike Ice and Associated Solid $\hat{1}^2$ -Liquid $\hat{1}^2$ -Solid Transition. <i>Journal of Physical Chemistry C</i> , 2018, 122, 6704-6712.	3.1	27
5184	Pressure- and Temperature-Induced Monoclinic-to-Orthorhombic Phase Transition in Silicalite-1. <i>Journal of Physical Chemistry C</i> , 2018, 122, 6217-6229.	3.1	5
5185	A molecular dynamics study of lithium-containing aprotic heterocyclic ionic liquid electrolytes. <i>Journal of Chemical Physics</i> , 2018, 148, 193834.	3.0	37
5186	Aspirin locally disrupts the liquid-ordered phase. <i>Royal Society Open Science</i> , 2018, 5, 171710.	2.4	7
5187	Computer simulations of the catalytic mechanism of wild-type and mutant $\hat{1}^2$ -phosphoglucosyltransferase. <i>Organic and Biomolecular Chemistry</i> , 2018, 16, 2060-2073.	2.8	11
5188	Mesoscopic structural organization in fluorinated room temperature ionic liquids. <i>Comptes Rendus Chimie</i> , 2018, 21, 757-770.	0.5	12
5189	Molecular dynamics study of structure and vibrational spectra at zwitterionic lipid/aqueous KCl, NaCl, and CaCl <sub>2</sub> solution interfaces. <i>Journal of Chemical Physics</i> , 2018, 148, 222801.	3.0	15
5190	Highly Disordered Amyloid- $\hat{1}^2$ Monomer Probed by Single-Molecule FRET and MD Simulation. <i>Biophysical Journal</i> , 2018, 114, 870-884.	0.5	88
5191	$\langle i \rangle$ Ab initio $\langle /i \rangle$ molecular dynamics study of 1-D superionic conduction and phase transition in $\hat{1}^2$ -eucryptite. <i>Journal of Materials Chemistry A</i> , 2018, 6, 5052-5064.	10.3	22
5192	Competition between Supramolecular Interaction and Protein $\hat{1}^2$ -Protein Interaction in Protein Crystallization: Effects of Crystallization Method and Small Molecular Bridge. <i>Industrial &amp; Engineering Chemistry Research</i> , 2018, 57, 6726-6733.	3.7	10
5193	Phase Diagram of Kob-Andersen-Type Binary Lennard-Jones Mixtures. <i>Physical Review Letters</i> , 2018, 120, 165501.	7.8	45
5194	The $\hat{1}^2$ -pre-assembled state $\hat{1}^2$ of magainin 2 lysine-linked dimer determines its enhanced antimicrobial activity. <i>Colloids and Surfaces B: Biointerfaces</i> , 2018, 167, 432-440.	5.0	15
5195	ReaxFF Molecular Dynamics Simulation for the Graphitization of Amorphous Carbon: A Parametric Study. <i>Journal of Chemical Theory and Computation</i> , 2018, 14, 2322-2331.	5.3	44
5196	Water and hydrophobic gates in ion channels and nanopores. <i>Faraday Discussions</i> , 2018, 209, 231-247.	3.2	48
5197	Sparse sampling of water density fluctuations near liquid-vapor coexistence. <i>Molecular Simulation</i> , 2018, 44, 1124-1135.	2.0	9
5198	Comparison of single-ion molecular dynamics in common solvents. <i>Journal of Chemical Physics</i> , 2018, 148, 222821.	3.0	5
5199	Machine learning approaches to evaluate correlation patterns in allosteric signaling: A case study of the PDZ2 domain. <i>Journal of Chemical Physics</i> , 2018, 148, 241726.	3.0	14

#	ARTICLE	IF	CITATIONS
5200	On the electrophoretic mobilities of partially charged oligosaccharides as a function of charge patterning and degree of polymerization. <i>Electrophoresis</i> , 2018, 39, 1497-1503.	2.4	2
5201	Refined description of liquid and supercooled silicon from <i>ab initio</i> simulations. <i>Physical Review B</i> , 2018, 97, .	3.2	9
5202	A simple two dimensional model of methanol. <i>Journal of Molecular Liquids</i> , 2018, 262, 46-57.	4.9	8
5203	$\beta$ -N-Methylamino-L-alanine (BMAA) Not Involved in Alzheimer's Disease. <i>Journal of Physical Chemistry B</i> , 2018, 122, 4472-4480.	2.6	12
5204	Computational Design of High- $\beta$ Block Oligomers for Accessing 1 nm Domains. <i>ACS Nano</i> , 2018, 12, 4351-4361.	14.6	25
5205	Rotational and translational dynamics and their relation to hydrogen bond lifetimes in an ionic liquid by means of NMR relaxation time experiments and molecular dynamics simulation. <i>Journal of Chemical Physics</i> , 2018, 148, 193843.	3.0	22
5206	StreaMD: Advanced analysis of molecular dynamics using R. <i>Journal of Computational Chemistry</i> , 2018, 39, 1666-1674.	3.3	3
5207	Semi-flexible polymer engendered aggregation/dispersion of fullerene (C60) nano-particles: An atomistic investigation. <i>Chemical Physics Letters</i> , 2018, 701, 22-29.	2.6	7
5208	Simulations Study of Single-Component and Mixed <i>n</i> -Alkyl-PEG Micelles. <i>Journal of Physical Chemistry B</i> , 2018, 122, 4851-4860.	2.6	15
5209	Electric field mediated separation of water-ethanol mixtures in carbon-nanotubes integrated in nanoporous graphene membranes. <i>Faraday Discussions</i> , 2018, 209, 259-271.	3.2	5
5210	$\beta$ 1 subunit stabilises sodium channel Nav1.7 against mechanical stress. <i>Journal of Physiology</i> , 2018, 596, 2433-2445.	2.9	16
5211	Truncation- and motif-based pan-cancer analysis reveals tumor-suppressing kinases. <i>Science Signaling</i> , 2018, 11, .	3.6	10
5212	Evidence that TLR4 Is Not a Receptor for Saturated Fatty Acids but Mediates Lipid-Induced Inflammation by Reprogramming Macrophage Metabolism. <i>Cell Metabolism</i> , 2018, 27, 1096-1110.e5.	16.2	309
5213	Absolute Alchemical Free Energy Calculations for Ligand Binding: A Beginner's Guide. <i>Methods in Molecular Biology</i> , 2018, 1762, 199-232.	0.9	38
5214	Rare Dissipative Transitions Punctuate the Initiation of Chemical Denaturation in Proteins. <i>Biophysical Journal</i> , 2018, 114, 812-821.	0.5	0
5215	Influence of Cosolutes on Chemical Equilibrium: a Kirkwood-Buff Theory for Ion Pair Association-Dissociation Processes in Ternary Electrolyte Solutions. <i>Journal of Physical Chemistry C</i> , 2018, 122, 10293-10302.	3.1	22
5216	Protein-protein interactions within photosystem II under photoprotection: the synergy between CP29 minor antenna, subunit S (PsbS) and zeaxanthin at all-atom resolution. <i>Physical Chemistry Chemical Physics</i> , 2018, 20, 11843-11855.	2.8	28
5217	Interaction of lecithin:cholesterol acyltransferase with lipid surfaces and apolipoprotein A-I-derived peptides. <i>Journal of Lipid Research</i> , 2018, 59, 670-683.	4.2	16

#	ARTICLE	IF	CITATIONS
5218	Molecular Dynamics Simulations of Cross-Linked Phenolic Resins Using a United-Atom Model. <i>Macromolecular Theory and Simulations</i> , 2018, 27, 1700103.	1.4	18
5219	Programed dynamical ordering in self-organization processes of a nanocube: a molecular dynamics study. <i>Physical Chemistry Chemical Physics</i> , 2018, 20, 9115-9122.	2.8	7
5220	On flexible force fields for metal-organic frameworks: Recent developments and future prospects. <i>Wiley Interdisciplinary Reviews: Computational Molecular Science</i> , 2018, 8, e1363.	14.6	49
5221	Molecular Dynamics Simulations of Nanopolycrystals. , 2018, , 1-30.		0
5222	Cell penetrating peptide modulation of membrane biomechanics by Molecular dynamics. <i>Journal of Biomechanics</i> , 2018, 73, 137-144.	2.1	40
5223	On the molecular origin of the cooperative coil-to-globule transition of poly( <i>N</i> -isopropylacrylamide) in water. <i>Physical Chemistry Chemical Physics</i> , 2018, 20, 9997-10010.	2.8	97
5224	Salt effects in surfactant-free microemulsions. <i>Journal of Chemical Physics</i> , 2018, 148, 222818.	3.0	8
5225	pH-Induced Rotation of Lidless Lipase LipA from <i>Bacillus subtilis</i> at Lipase-Detergent Interface. <i>Journal of Physical Chemistry B</i> , 2018, 122, 4802-4812.	2.6	8
5226	Evaluating Ylehd, a recombinant epoxide hydrolase from <i>Yarrowia lipolytica</i> as a potential biocatalyst for the resolution of benzyl glycidyl ether. <i>RSC Advances</i> , 2018, 8, 12918-12926.	3.6	9
5227	Molecular dynamics simulations of freezing-point depression of TIP4P/2005 water in solution with NaCl. <i>Journal of Molecular Liquids</i> , 2018, 261, 513-519.	4.9	43
5228	Processive Degradation of Crystalline Cellulose by a Multimodular Endoglucanase via a Wirewalking Mode. <i>Biomacromolecules</i> , 2018, 19, 1686-1696.	5.4	40
5229	Arginine side chain stacking with peptide plane stabilizes the protein helix conformation in a cooperative way. <i>Proteins: Structure, Function and Bioinformatics</i> , 2018, 86, 684-692.	2.6	1
5230	Role of the Bound Phospholipids in the Structural Stability of Cholesteryl Ester Transfer Protein. <i>Journal of Physical Chemistry B</i> , 2018, 122, 4239-4248.	2.6	16
5231	The effect of alkyl chain length on the structure and thermodynamics of protic-aprotic ionic liquid mixtures: a molecular dynamics study. <i>Physical Chemistry Chemical Physics</i> , 2018, 20, 9938-9949.	2.8	20
5232	Forward flux sampling calculation of homogeneous nucleation rates from aqueous NaCl solutions. <i>Journal of Chemical Physics</i> , 2018, 148, 044505.	3.0	47
5233	Lipopeptide daptomycin: Interactions with bacterial and phospholipid membranes, stability of membrane aggregates and micellation in solution. <i>Biochimica Et Biophysica Acta - Biomembranes</i> , 2018, 1860, 1949-1954.	2.6	9
5234	Mutations Alter RNA-Mediated Conversion of Human Prions. <i>ACS Omega</i> , 2018, 3, 3936-3944.	3.5	6
5235	Elucidating the key role of fluorine in improving the charge mobility of electron acceptors for non-fullerene organic solar cells by multiscale simulations. <i>Journal of Materials Chemistry C</i> , 2018, 6, 4912-4918.	5.5	35

#	ARTICLE	IF	CITATIONS
5236	Single molecule FRET investigation of pressure-driven unfolding of cold shock protein A. <i>Journal of Chemical Physics</i> , 2018, 148, 123336.	3.0	4
5237	How do glycerol and dimethyl sulphoxide affect local tetrahedral structure of water around a nonpolar solute at low temperature? Importance of preferential interaction. <i>Journal of Chemical Physics</i> , 2018, 148, 134501.	3.0	31
5238	Effect of low levels of lipid oxidation on the curvature, dynamics, and permeability of lipid bilayers and their interactions with cationic nanoparticles. <i>Journal Physics D: Applied Physics</i> , 2018, 51, 164002.	2.8	13
5239	Physiologically-relevant levels of sphingomyelin, but not GM1, induces a $\beta$ -sheet-rich structure in the amyloid- $\beta$ (1-42) monomer. <i>Biochimica Et Biophysica Acta - Biomembranes</i> , 2018, 1860, 1709-1720.	2.6	22
5240	Preferential Binding of Urea to Single-Stranded DNA Structures: A Molecular Dynamics Study. <i>Biophysical Journal</i> , 2018, 114, 1551-1562.	0.5	30
5241	Use of a Compact Tripodal Tris(bipyridine) Ligand to Stabilize a Single-Metal-Centered Chirality: Stereoselective Coordination of Iron(II) and Ruthenium(II) on a Semirigid Hexapeptide Macrocyclic. <i>Inorganic Chemistry</i> , 2018, 57, 5475-5485.	4.0	7
5242	Ionic Liquid Designed for PEDOT:PSS Conductivity Enhancement. <i>Journal of the American Chemical Society</i> , 2018, 140, 5375-5384.	13.7	112
5243	Surfactants as stabilizers for biopharmaceuticals: An insight into the molecular mechanisms for inhibition of protein aggregation. <i>European Journal of Pharmaceutics and Biopharmaceutics</i> , 2018, 128, 98-106.	4.3	20
5244	Strategy for Stabilization of CutA1 Proteins Due to Ion-Ion Interactions at Temperatures of over 100 $^{\circ}\text{C}$ . <i>Biochemistry</i> , 2018, 57, 2649-2656.	2.5	7
5245	DNP-Enhanced MAS NMR: A Tool to Snapshot Conformational Ensembles of $\beta$ -Synuclein in Different States. <i>Biophysical Journal</i> , 2018, 114, 1614-1623.	0.5	38
5246	Comparative experimental/theoretical studies on the EGFR dimerization under the effect of EGF/EGF analogues binding: Highlighting the importance of EGF/EGFR interactions at site III interface. <i>International Journal of Biological Macromolecules</i> , 2018, 115, 401-417.	7.5	11
5247	Force Field Benchmark of Amino Acids: I. Hydration and Diffusion in Different Water Models. <i>Journal of Chemical Information and Modeling</i> , 2018, 58, 1037-1052.	5.4	70
5248	A Computational Study of the Ionic Liquid-Induced Destabilization of the Miniprotein Trp-Cage. <i>Journal of Physical Chemistry B</i> , 2018, 122, 5707-5715.	2.6	8
5249	Decoupling of bilayer leaflets under gas supersaturation: nitrogen nanobubbles in a membrane and their implication in decompression sickness. <i>Journal Physics D: Applied Physics</i> , 2018, 51, 184001.	2.8	0
5250	Adaptive enhanced sampling by force-biasing using neural networks. <i>Journal of Chemical Physics</i> , 2018, 148, 134108.	3.0	39
5251	Structure and dynamics of the peptide strand KRFL from the thrombospondin TSP-1 in water. <i>Journal of Molecular Modeling</i> , 2018, 24, 54.	1.8	1
5252	Molecular polydispersity improves prediction of asphaltene aggregation. <i>Journal of Molecular Liquids</i> , 2018, 256, 382-394.	4.9	56
5253	Ion association in binary mixtures of water-CO <sub>2</sub> in supercritical conditions through classical molecular dynamics simulations. <i>Journal of Molecular Liquids</i> , 2018, 257, 82-92.	4.9	6



#	ARTICLE	IF	CITATIONS
5254	From a Highly Disordered to a Metastable State: Uncovering Insights of $\beta$ -Synuclein. ACS Chemical Neuroscience, 2018, 9, 1051-1065.	3.5	22
5255	Role of Counterions in Constant-pH Molecular Dynamics Simulations of PAMAM Dendrimers. ACS Omega, 2018, 3, 2001-2009.	3.5	20
5256	Ge-based bipolar small molecular host for highly efficient blue OLEDs: multiscale simulation of charge transport. Journal of Materials Chemistry C, 2018, 6, 6146-6152.	5.5	23
5257	Structural basis for the interaction of the beta-secretase with copper. Biochimica Et Biophysica Acta - Biomembranes, 2018, 1860, 1105-1113.	2.6	7
5258	The Molecular Basis of the Sodium Dodecyl Sulfate Effect on Human Ubiquitin Structure: A Molecular Dynamics Simulation Study. Scientific Reports, 2018, 8, 2150.	3.3	37
5259	Influence of electric field on the amyloid- $\beta$ (29-42) peptides embedded in a membrane bilayer. Journal of Chemical Physics, 2018, 148, 045105.	3.0	21
5260	Impact of graphene-based nanomaterials (GBNMs) on the structural and functional conformations of hepcidin peptide. Journal of Computer-Aided Molecular Design, 2018, 32, 487-496.	2.9	4
5261	Characterization of Interactions between Curcumin and Different Types of Lipid Bilayers by Molecular Dynamics Simulation. Journal of Physical Chemistry B, 2018, 122, 2341-2354.	2.6	45
5262	Insight into the Microenvironments of the Metal-Ionic Liquid Interface during Electrochemical $\text{CO}_2$ Reduction. ACS Catalysis, 2018, 8, 2420-2427.	11.2	77
5263	Effects of 1-hexanol on C12E10 micelles: a molecular simulations and light scattering study. Physical Chemistry Chemical Physics, 2018, 20, 6287-6298.	2.8	17
5264	Structural analysis of zwitterionic liquids vs. homologous ionic liquids. Journal of Chemical Physics, 2018, 148, 193807.	3.0	24
5265	Computing the absolute Gibbs free energy in atomistic simulations: Applications to defects in solids. Physical Review B, 2018, 97, .	3.2	53
5266	Extracting functional groups of ALLINI to design derivatives of FDA-approved drugs: Inhibition of HIV-1 integrase. Biotechnology and Applied Biochemistry, 2018, 65, 594-607.	3.1	0
5267	Coarse-grained modelling of self-assembling poly(ethylene glycol)/poly(lactic acid) diblock copolymers. Journal of Polymer Research, 2018, 25, 1.	2.4	6
5268	Insights into the homo-oligomerization properties of N-terminal coiled-coil domain of Ebola virus VP35 protein. Virus Research, 2018, 247, 61-70.	2.2	14
5269	Application of the Quality by Design Approach to the Freezing Step of Freeze-Drying: Building the Design Space. Journal of Pharmaceutical Sciences, 2018, 107, 1586-1596.	3.3	33
5270	A secondary RET mutation in the activation loop conferring resistance to vandetanib. Nature Communications, 2018, 9, 625.	12.8	75
5271	Pressure control in interfacial systems: Atomistic simulations of vapor nucleation. Journal of Chemical Physics, 2018, 148, 064706.	3.0	19



#	ARTICLE	IF	CITATIONS
5272	Nanoscale organization in the fluorinated room temperature ionic liquid: Tetraethyl ammonium (trifluoromethanesulfonyl)(nonafluorobutylsulfonyl)imide. Journal of Chemical Physics, 2018, 148, 193816.	3.0	19
5273	Atomic scale simulation of H <sub>2</sub> O <sub>2</sub> permeation through aquaporin: toward the understanding of plasma cancer treatment. Journal Physics D: Applied Physics, 2018, 51, 125401.	2.8	42
5274	Controlling anticancer drug mediated G-quadruplex formation and stabilization by a molecular container. Physical Chemistry Chemical Physics, 2018, 20, 7808-7818.	2.8	7
5275	The nearest neighbor and next nearest neighbor effects on the thermodynamic and kinetic properties of RNA base pair. Journal of Chemical Physics, 2018, 148, 045101.	3.0	13
5276	Communication between N terminus and loop2 tunes Orai activation. Journal of Biological Chemistry, 2018, 293, 1271-1285.	3.4	44
5277	Fully Flexible Docking via Reaction-Coordinate-Independent Molecular Dynamics Simulations. Journal of Chemical Information and Modeling, 2018, 58, 490-500.	5.4	9
5278	Fully Anisotropic Rotational Diffusion Tensor from Molecular Dynamics Simulations. Journal of Physical Chemistry B, 2018, 122, 5630-5639.	2.6	18
5279	Investigating the effect of key mutations on the conformational dynamics of toll-like receptor dimers through molecular dynamics simulations and protein structure networks. Proteins: Structure, Function and Bioinformatics, 2018, 86, 475-490.	2.6	9
5280	A Molecular Dynamics Study of the Effect of Asphaltenes on Toluene/Water Interfacial Tension: Surfactant or Solute?. Energy & Fuels, 2018, 32, 3225-3231.	5.1	39
5281	Core Binding Site of a Thioflavin-T-Derived Imaging Probe on Amyloid $\beta$ Fibrils Predicted by Computational Methods. ACS Chemical Neuroscience, 2018, 9, 957-966.	3.5	14
5282	The influence of like-charge attraction on the structure and dynamics of ionic liquids: NMR chemical shifts, quadrupole coupling constants, rotational correlation times and failure of Stokes-Einstein-Debye. Physical Chemistry Chemical Physics, 2018, 20, 5617-5625.	2.8	26
5283	Water structure and dynamics in the hydration layer of a type III anti-freeze protein. Physical Chemistry Chemical Physics, 2018, 20, 6996-7006.	2.8	23
5284	Probing subtle conformational changes induced by phosphorylation and point mutations in the $\text{TIR}$ domains of $\text{TLR}_2$ and $\text{TLR}_3$ . Proteins: Structure, Function and Bioinformatics, 2018, 86, 524-535.	2.6	16
5285	Structural basis of the molecular ruler mechanism of a bacterial glycosyltransferase. Nature Communications, 2018, 9, 445.	12.8	31
5286	Computational investigation on DNA sequencing using functionalized graphene nanopores. Physical Chemistry Chemical Physics, 2018, 20, 9063-9069.	2.8	23
5287	Structure and dynamics of stereo-regular poly(methyl-methacrylate) melts through atomistic molecular dynamics simulations. Soft Matter, 2018, 14, 1449-1464.	2.7	21
5288	The role of d - allo -isoleucine in the deposition of the anti- Leishmania peptide bombinin H4 as revealed by 31 P solid-state NMR, VCD spectroscopy, and MD simulation. Biochimica Et Biophysica Acta - Proteins and Proteomics, 2018, 1866, 789-798.	2.3	24
5289	Hard boron rich boron nitride nanoglasses. Journal of the American Ceramic Society, 2018, 101, 1929-1939.	3.8	6

#	ARTICLE	IF	CITATIONS
5290	âœln silicoâœstudy of the binding of two novel antagonists to the nociceptin receptor. Journal of Computer-Aided Molecular Design, 2018, 32, 385-400.	2.9	9
5291	Convergence of KirkwoodâœBuff Integrals of Ideal and Nonideal Aqueous Solutions Using Molecular Dynamics Simulations. Journal of Physical Chemistry B, 2018, 122, 5515-5526.	2.6	64
5292	What Gives an Insulin Hexamer Its Unique Shape and Stability? Role of Ten Confined Water Molecules. Journal of Physical Chemistry B, 2018, 122, 1631-1637.	2.6	39
5293	Structural basis for chitin acquisition by marine Vibrio species. Nature Communications, 2018, 9, 220.	12.8	37
5294	Lipids Shape the Electron Acceptor-Binding Site of the Peripheral Membrane Protein Dihydroorotate Dehydrogenase. Cell Chemical Biology, 2018, 25, 309-317.e4.	5.2	25
5295	Umbrella Sampling and X-ray Crystallographic Analysis Unveil an ArgâœAsp Gate Facilitating Inhibitor Binding Inside Phosphopantetheine Adenylyltransferase Allosteric Cleft. Journal of Physical Chemistry B, 2018, 122, 1551-1559.	2.6	2
5296	Essence of Small Molecule-Mediated Control of Hydroxyapatite Growth: Free Energy Calculations of Amino Acid Side Chain Analogues. Journal of Physical Chemistry C, 2018, 122, 4372-4380.	3.1	17
5297	Salting-in of neopentane in the aqueous solutions of urea and glycine-betaine. Molecular Simulation, 2018, 44, 677-687.	2.0	4
5298	Balancing Force Field ProteinâœLipid Interactions To Capture Transmembrane HelixâœHelix Association. Journal of Chemical Theory and Computation, 2018, 14, 1706-1715.	5.3	40
5299	Effect of Dimethyl Sulfoxide on the Binding of 1-Adamantane Carboxylic Acid to Î²- and Î³-Cyclodextrins. ACS Omega, 2018, 3, 1014-1021.	3.5	12
5300	Molecular mechanism for inhibition of twinfilin by phosphoinositides. Journal of Biological Chemistry, 2018, 293, 4818-4829.	3.4	15
5301	Binding of Divalent Cations to Insulin: Capillary Electrophoresis and Molecular Simulations. Journal of Physical Chemistry B, 2018, 122, 5640-5648.	2.6	45
5303	Assessment of Simple Models for Molecular Simulation of Ethylene Carbonate and Propylene Carbonate as Solvents for Electrolyte Solutions. Topics in Current Chemistry, 2018, 376, 7.	5.8	15
5304	Atomistic-level study of the interactions between hIAPP protofibrils and membranes: Influence of pH and lipid composition. Biochimica Et Biophysica Acta - Biomembranes, 2018, 1860, 1818-1825.	2.6	33
5305	Dissecting the Forces that Dominate Dimerization of the Nucleotide Binding Domains of ABCB1. Biophysical Journal, 2018, 114, 331-342.	0.5	19
5306	Destabilizing the AXH Tetramer by Mutations: Mechanisms and Potential Antiaggregation Strategies. Biophysical Journal, 2018, 114, 323-330.	0.5	14
5307	Molecular details of spontaneous insertion and interaction of HCV nonâœstructure 3 protease protein domain with PIP2âœcontaining membrane. Proteins: Structure, Function and Bioinformatics, 2018, 86, 423-433.	2.6	1
5308	Superrepression through Altered CorepressorâœActivated Protein:Protein Interactions. Biochemistry, 2018, 57, 1119-1129.	2.5	6

#	ARTICLE	IF	CITATIONS
5309	Out-of-Register A $\beta$ <sub>42</sub> Assemblies as Models for Neurotoxic Oligomers and Fibrils. Journal of Chemical Theory and Computation, 2018, 14, 1099-1110.	5.3	22
5310	The fold preference and thermodynamic stability of $\beta$ -synuclein fibrils is encoded in the non-amyloid- $\beta$ component region. Physical Chemistry Chemical Physics, 2018, 20, 4502-4512.	2.8	19
5311	First-Principles Parametrization of Polarizable Coarse-Grained Force Fields for Ionic Liquids. Journal of Chemical Theory and Computation, 2018, 14, 1471-1486.	5.3	26
5312	Mechanistic and structural insight into promiscuity based metabolism of cardiac drug digoxin by gut microbial enzyme. Journal of Cellular Biochemistry, 2018, 119, 5287-5296.	2.6	20
5313	Exploring the effect of 5-Fluorouracil on conformation, stability and activity of lysozyme by combined approach of spectroscopic and theoretical studies. Journal of Photochemistry and Photobiology B: Biology, 2018, 179, 23-31.	3.8	34
5314	Nucleation of Molecular Crystals Driven by Relative Information Entropy. Journal of Chemical Theory and Computation, 2018, 14, 959-972.	5.3	27
5315	Molecular dynamics simulations of asymmetric heterodimers of HER1/HER2 complexes. Journal of Molecular Modeling, 2018, 24, 30.	1.8	1
5316	Multi-periodic boundary conditions and the Contact Dynamics method. Comptes Rendus - Mecanique, 2018, 346, 263-277.	2.1	8
5317	Multiscale molecular dynamics simulations of lipid interactions with P-glycoprotein in a complex membrane. Journal of Molecular Graphics and Modelling, 2018, 80, 147-156.	2.4	34
5318	Adsorption of Kinetic Hydrate Inhibitors on Growing Surfaces: A Molecular Dynamics Study. Journal of Physical Chemistry B, 2018, 122, 3396-3406.	2.6	65
5319	Structure analysis of collagen fibril at atomic-level resolution and its implications for intra-fibrillar transport in bone biomineralization. Physical Chemistry Chemical Physics, 2018, 20, 1513-1523.	2.8	33
5320	MgCu metallic glass. Philosophical Magazine, 2018, 98, 633-645.	1.6	1
5321	Locating Large, Flexible Ligands on Proteins. Journal of Chemical Information and Modeling, 2018, 58, 315-327.	5.4	6
5322	Coarse-Grained Molecular Dynamics Force-Field for Polyacrylamide in Infinite Dilution Derived from Iterative Boltzmann Inversion and MARTINI Force-Field. Journal of Physical Chemistry B, 2018, 122, 1516-1524.	2.6	16
5323	Fast Calculation of Protein-Protein Binding Free Energies Using Umbrella Sampling with a Coarse-Grained Model. Journal of Chemical Theory and Computation, 2018, 14, 991-997.	5.3	38
5324	Validation and Comparison of Force Fields for Native Cyclodextrins in Aqueous Solution. Journal of Physical Chemistry B, 2018, 122, 1608-1626.	2.6	39
5325	Molecular dynamics simulations of lattice site preference and phase separation in B2-NiAl with Pt addition. Journal of Alloys and Compounds, 2018, 740, 863-869.	5.5	3
5326	Computational characterisation of dried and hydrated graphene oxide membranes. Nanoscale, 2018, 10, 1946-1956.	5.6	28

#	ARTICLE	IF	CITATIONS
5327	The effect of pressure on open-framework silicates: elastic behaviour and crystalâ€“fluid interaction. <i>Physics and Chemistry of Minerals</i> , 2018, 45, 115-138.	0.8	44
5328	New Aspects of the Gold Nanorod Formation Mechanism via Seed-Mediated Methods Revealed by Molecular Dynamics Simulations. <i>Langmuir</i> , 2018, 34, 366-375.	3.5	40
5329	GADDLE Maps: General Algorithm for Discrete Object Deformations Based on Local Exchange Maps. <i>Journal of Chemical Theory and Computation</i> , 2018, 14, 466-478.	5.3	5
5330	Mechanism of Urea Crystal Dissolution in Water from Molecular Dynamics Simulation. <i>Journal of Physical Chemistry B</i> , 2018, 122, 1213-1222.	2.6	12
5331	A Novel Microemulsion Phase Transition: Toward the Elucidation of Third-Phase Formation in Spent Nuclear Fuel Reprocessing. <i>Journal of Physical Chemistry B</i> , 2018, 122, 1439-1452.	2.6	37
5332	Spontaneous protein desorption from self-assembled monolayer (SAM)-coated gold nanoparticles. <i>Physical Chemistry Chemical Physics</i> , 2018, 20, 68-74.	2.8	7
5333	Solvation of alcohols in ionic liquids â€“ understanding the effect of the anion and cation. <i>Physical Chemistry Chemical Physics</i> , 2018, 20, 2536-2548.	2.8	17
5334	Transport Properties and Ion Aggregation in Mixtures of Room Temperature Ionic Liquids with Aprotic Dipolar Solvents. <i>Springer Proceedings in Physics</i> , 2018, , 67-109.	0.2	6
5335	Crystal structure of UDP- N -acetylglucosamine-enolpyruvate reductase (MurB) from <i>Mycobacterium tuberculosis</i> . <i>Biochimica Et Biophysica Acta - Proteins and Proteomics</i> , 2018, 1866, 397-406.	2.3	27
5336	All-Atom Molecular Dynamics Study of Waterâ€“Dodecane Interface in the Presence of Octanol. <i>Journal of Physical Chemistry C</i> , 2018, 122, 687-693.	3.1	12
5337	Accurate non-asymptotic thermodynamic properties of near-critical N2 and O2 computed from molecular dynamics simulations. <i>Journal of Supercritical Fluids</i> , 2018, 135, 225-233.	3.2	6
5338	A Computational Assay of Estrogen Receptor Î± Antagonists Reveals the Key Common Structural Traits of Drugs Effectively Fighting Refractory Breast Cancers. <i>Scientific Reports</i> , 2018, 8, 649.	3.3	57
5339	Solubility of CO2 in triglycerides using Monte Carlo simulations. <i>Fluid Phase Equilibria</i> , 2018, 476, 39-47.	2.5	10
5340	Mechanism and Determinants of Amphipathic Helix-Containing Protein Targeting to Lipid Droplets. <i>Developmental Cell</i> , 2018, 44, 73-86.e4.	7.0	175
5341	Surfactant Interactions and Organization at the Gasâ€“Water Interface (CTAB with Added Salt). <i>Langmuir</i> , 2018, 34, 1855-1864.	3.5	26
5342	Effect of Ceramide Tail Length on the Structure of Model Stratum Corneum Lipid Bilayers. <i>Biophysical Journal</i> , 2018, 114, 113-125.	0.5	36
5343	Decrypting the Heat Activation Mechanism of TRPV1 Channel by Molecular Dynamics Simulation. <i>Biophysical Journal</i> , 2018, 114, 40-52.	0.5	30
5344	Graphene Engendered aluminium crystal growth and mechanical properties of its composite: An atomistic investigation. <i>Materials Chemistry and Physics</i> , 2018, 208, 41-48.	4.0	30

#	ARTICLE	IF	CITATIONS
5345	Identification of Factors Promoting HBV Capsid Self-Assembly by Assembly-Promoting Antivirals. <i>Journal of Chemical Information and Modeling</i> , 2018, 58, 328-337.	5.4	12
5346	A Study of the Morphology, Dynamics, and Folding Pathways of Ring Polymers with Supramolecular Topological Constraints Using Molecular Simulation and Nonlinear Manifold Learning. <i>Macromolecules</i> , 2018, 51, 598-616.	4.8	15
5347	Widom line, dynamical crossover, and percolation transition of supercritical oxygen via molecular dynamics simulations. <i>Journal of Chemical Physics</i> , 2018, 148, 014502.	3.0	21
5348	Superior HIV-1 TAR Binders with Conformationally Constrained R52 Arginine Mimics in the Tat(48-57) Peptide. <i>ChemMedChem</i> , 2018, 13, 220-226.	3.2	0
5349	Studies on DNA binding properties of new Schiff base ligands using spectroscopic, electrochemical and computational methods: Influence of substitutions on DNA-binding. <i>Journal of Molecular Liquids</i> , 2018, 253, 61-71.	4.9	78
5350	CO <sub>2</sub> Diffusion in Various Carbonated Beverages: A Molecular Dynamics Study. <i>Journal of Physical Chemistry B</i> , 2018, 122, 1655-1661.	2.6	15
5351	Force Field Benchmark of the TraPPE-UA for Polar Liquids: Density, Heat of Vaporization, Dielectric Constant, Surface Tension, Volumetric Expansion Coefficient, and Isothermal Compressibility. <i>Journal of Physical Chemistry B</i> , 2018, 122, 1669-1678.	2.6	21
5352	pH-Dependent cooperativity and existence of a dry molten globule in the folding of a miniprotein BBL. <i>Physical Chemistry Chemical Physics</i> , 2018, 20, 3523-3530.	2.8	10
5353	Modulating interactions between ligand-coated nanoparticles and phase-separated lipid bilayers by varying the ligand density and the surface charge. <i>Nanoscale</i> , 2018, 10, 2481-2491.	5.6	46
5354	Biological activity and interaction mechanism of the diketopiperazine derivatives as tubulin polymerization inhibitors. <i>RSC Advances</i> , 2018, 8, 1055-1064.	3.6	16
5355	Size of graphene sheets determines the structural and mechanical properties of 3D graphene foams. <i>Nanotechnology</i> , 2018, 29, 104001.	2.6	29
5356	Identification of potential inhibitors against nuclear Dam1 complex subunit Ask1 of <i>Candida albicans</i> using virtual screening and MD simulations. <i>Computational Biology and Chemistry</i> , 2018, 72, 33-44.	2.3	9
5357	Method Evaluations for Adsorption Free Energy Calculations at the Solid/Water Interface through Metadynamics, Umbrella Sampling, and Jarzynski's Equality. <i>ChemPhysChem</i> , 2018, 19, 690-702.	2.1	18
5358	Ab Initio Prediction of NMR Spin Relaxation Parameters from Molecular Dynamics Simulations. <i>Journal of Chemical Theory and Computation</i> , 2018, 14, 1009-1019.	5.3	23
5359	Effect of Chain Flexibility and Interlayer Interactions on the Local Dynamics of Layered Polymer Systems. <i>Macromolecules</i> , 2018, 51, 576-588.	4.8	9
5360	Structure of the glucagon receptor in complex with a glucagon analogue. <i>Nature</i> , 2018, 553, 106-110.	27.8	109
5361	Origins of biological function in DNA and RNA hairpin loop motifs from replica exchange molecular dynamics simulation. <i>Physical Chemistry Chemical Physics</i> , 2018, 20, 2990-3001.	2.8	11
5362	Molecular-Scale Description of SPAN80 Desorption from a Squalane-Water Interface. <i>Journal of Physical Chemistry B</i> , 2018, 122, 3378-3383.	2.6	5

#	ARTICLE	IF	CITATIONS
5363	Molecular Dynamics Investigation of the Influence of the Hydrogen Bond Networks in Ethanol/Water Mixtures on Dielectric Spectra. <i>Journal of Physical Chemistry B</i> , 2018, 122, 1505-1515.	2.6	41
5364	Selective binding of pyrene in subdomain IB of human serum albumin: Combining energy transfer spectroscopy and molecular modelling to understand protein binding flexibility. <i>Spectrochimica Acta - Part A: Molecular and Biomolecular Spectroscopy</i> , 2018, 194, 36-44.	3.9	17
5365	Molecular Simulation Results on Charged Carbon Nanotube Forest-Based Supercapacitors. <i>ChemSusChem</i> , 2018, 11, 1927-1932.	6.8	7
5366	Intrinsic Conformational Preferences and Interactions in Î±-Synuclein Fibrils: Insights from Molecular Dynamics Simulations. <i>Journal of Chemical Theory and Computation</i> , 2018, 14, 3298-3310.	5.3	24
5367	Lipid tempering simulation of model biological membranes on parallel platforms. <i>Biochimica Et Biophysica Acta - Biomembranes</i> , 2018, 1860, 1480-1488.	2.6	4
5368	Structural insights from lipid-bilayer nanodiscs link Î±-Synuclein membrane-binding modes to amyloid fibril formation. <i>Communications Biology</i> , 2018, 1, 44.	4.4	79
5369	Distinctive phosphoinositide- and Ca <sup>2+</sup> -binding properties of normal and cognitive performance-linked variant forms of KIBRA C2 domain. <i>Journal of Biological Chemistry</i> , 2018, 293, 9335-9344.	3.4	8
5370	Docosahexaenoic acid regulates the formation of lipid rafts: A unified view from experiment and simulation. <i>Biochimica Et Biophysica Acta - Biomembranes</i> , 2018, 1860, 1985-1993.	2.6	65
5371	Effect of Surface Charge and Hydrophobicity on Phospholipid-Nanoparticle Corona Formation: A Molecular Dynamics Simulation Study. <i>Colloids and Interface Science Communications</i> , 2018, 25, 7-11.	4.1	18
5372	The Interplay of Methyl-Group Distribution and Hydration Pattern of Isomeric Amphiphilic Osmolytes. <i>Journal of Physical Chemistry B</i> , 2018, 122, 5972-5983.	2.6	12
5373	Anomalous diffusion of water molecules at grain boundaries in ice I <sub>h</sub> . <i>Physical Chemistry Chemical Physics</i> , 2018, 20, 13944-13951.	2.8	15
5374	Interactions of HP1 Bound to H3K9me3 Dinucleosome by Molecular Simulations and Biochemical Assays. <i>Biophysical Journal</i> , 2018, 114, 2336-2351.	0.5	28
5375	How cardiolipin peroxidation alters the properties of the inner mitochondrial membrane?. <i>Chemistry and Physics of Lipids</i> , 2018, 214, 15-23.	3.2	35
5376	Cosolubilization of phenanthrene and pyrene in surfactant micelles: Experimental and atomistic simulations studies. <i>Journal of Molecular Liquids</i> , 2018, 263, 1-9.	4.9	9
5377	Refining Collective Coordinates and Improving Free Energy Representation in Variational Enhanced Sampling. <i>Journal of Chemical Theory and Computation</i> , 2018, 14, 2889-2894.	5.3	25
5378	Influence of Na <sup>+</sup> and Mg <sup>2+</sup> ions on RNA structures studied with molecular dynamics simulations. <i>Nucleic Acids Research</i> , 2018, 46, 4872-4882.	14.5	76
5379	Size- and temperature-dependent Young's modulus and size-dependent thermal expansion coefficient of nanowires. <i>Science China Technological Sciences</i> , 2018, 61, 687-698.	4.0	20
5380	In silico assessment of the conduction mechanism of the Ryanodine Receptor 1 reveals previously unknown exit pathways. <i>Scientific Reports</i> , 2018, 8, 6886.	3.3	13



#	ARTICLE	IF	CITATIONS
5381	Bowl-in-bowl complex formation with mixed sized calixarenes: adaptivity towards guest binding. Chemical Communications, 2018, 54, 7131-7134.	4.1	7
5382	Optical Properties of Vibronically Coupled Cy3 Dimers on DNA Scaffolds. Journal of Physical Chemistry B, 2018, 122, 5020-5029.	2.6	58
5383	Unusual Temperature Dependence of Nanoscale Structural Organization in Deep Eutectic Solvents. Journal of Physical Chemistry B, 2018, 122, 5242-5250.	2.6	36
5384	Erythromycin leads to differential protein expression through differences in electrostatic and dispersion interactions with nascent proteins. Scientific Reports, 2018, 8, 6460.	3.3	3
5385	Identification of a novel small-molecule Keap1-Nrf2 PPI inhibitor with cytoprotective effects on LPS-induced cardiomyopathy. Journal of Enzyme Inhibition and Medicinal Chemistry, 2018, 33, 833-841.	5.2	50
5386	Protein Partitioning into Ordered Membrane Domains: Insights from Simulations. Biophysical Journal, 2018, 114, 1936-1944.	0.5	63
5387	Targeting natural compounds against HER2 kinase domain as potential anticancer drugs applying pharmacophore based molecular modelling approaches. Computational Biology and Chemistry, 2018, 74, 327-338.	2.3	34
5388	In silico data analyses of the hotspot mutations of CHM gene in choroideremia disease. Data in Brief, 2018, 18, 1217-1223.	1.0	4
5389	The Preservation of Lyophilized Human Growth Hormone Activity: how Do Buffers and Sugars Interact?. Pharmaceutical Research, 2018, 35, 131.	3.5	8
5390	Lipid Configurations from Molecular Dynamics Simulations. Biophysical Journal, 2018, 114, 1895-1907.	0.5	14
5391	Analysis of the influence of simulation parameters on biomolecule-linked water networks. Journal of Molecular Graphics and Modelling, 2018, 82, 117-128.	2.4	2
5392	Thermal conductivity of ice polymorphs: a computational study. Physical Chemistry Chemical Physics, 2018, 20, 11028-11036.	2.8	8
5393	A molecular dynamics investigation of the surface tension of water nanodroplets and a new technique for local pressure determination through density correlation. Journal of Chemical Physics, 2018, 148, 144503.	3.0	10
5394	Molecular dynamics simulation study on the structural instability of the most common cystic fibrosis-associated mutant I <sup>505</sup> F508-CFTR. Biophysics and Physicobiology, 2018, 15, 33-44.	1.0	10
5395	Penetration of antimicrobial peptides in a lung surfactant model. Colloids and Surfaces B: Biointerfaces, 2018, 167, 345-353.	5.0	26
5396	Conformational Ensemble and Biological Role of the TCTP Intrinsically Disordered Region: Influence of Calcium and Phosphorylation. Journal of Molecular Biology, 2018, 430, 1621-1639.	4.2	7
5397	The aldehyde dehydrogenase AldA contributes to the hypochlorite defense and is redox-controlled by protein S-bacillithiolation in Staphylococcus aureus. Redox Biology, 2018, 15, 557-568.	9.0	38
5398	Effects of Hydrophilic Residues and Hydrophobic Length on Flip-Flop Promotion by Transmembrane Peptides. Journal of Physical Chemistry B, 2018, 122, 4318-4324.	2.6	16



#	ARTICLE	IF	CITATIONS
5399	Antimicrobial action of the cationic peptide, chrysopsin-3: a coarse-grained molecular dynamics study. <i>Soft Matter</i> , 2018, 14, 2796-2807.	2.7	19
5400	Molecular dynamics characterization of the SAMHD1 Aicardi-Goutières Arg145Gln mutant: structural determinants for the impaired tetramerization. <i>Journal of Computer-Aided Molecular Design</i> , 2018, 32, 623-632.	2.9	1
5401	Paradoxical Effect of Trehalose on the Aggregation of $\beta$ -Synuclein: Expedites Onset of Aggregation yet Reduces Fibril Load. <i>ACS Chemical Neuroscience</i> , 2018, 9, 1477-1491.	3.5	27
5402	Empirical temperature-dependent intermolecular potentials determined by data mining from crystal data. <i>Chemical Physics Letters</i> , 2018, 699, 115-124.	2.6	7
5403	Reinforced dynamics for enhanced sampling in large atomic and molecular systems. <i>Journal of Chemical Physics</i> , 2018, 148, 124113.	3.0	48
5404	Structural Transitions in Ceramide Cubic Phases during Formation of the Human Skin Barrier. <i>Biophysical Journal</i> , 2018, 114, 1116-1127.	0.5	13
5405	On the Calculation of SAXS Profiles of Folded and Intrinsically Disordered Proteins from Computer Simulations. <i>Journal of Molecular Biology</i> , 2018, 430, 2521-2539.	4.2	64
5406	Crystal structure of undecaprenyl-pyrophosphate phosphatase and its role in peptidoglycan biosynthesis. <i>Nature Communications</i> , 2018, 9, 1078.	12.8	47
5407	Supramolecular complexes of DNA with cationic polymers: The effect of polymer concentration. <i>Polymer</i> , 2018, 142, 277-284.	3.8	16
5408	Study of the Gemini Surfactants' Self-Assembly on Graphene Nanosheets: Insights from Molecular Dynamic Simulation. <i>Journal of Physical Chemistry A</i> , 2018, 122, 3873-3885.	2.5	10
5409	Interaction of N-terminal peptide analogues of the Na <sup>+</sup> ,K <sup>+</sup> -ATPase with membranes. <i>Biochimica Et Biophysica Acta - Biomembranes</i> , 2018, 1860, 1282-1291.	2.6	26
5410	Conformational Sampling of the Intrinsically Disordered C-Terminal Tail of DERA Is Important for Enzyme Catalysis. <i>ACS Catalysis</i> , 2018, 8, 3971-3984.	11.2	15
5411	Carbapenems and Lipid Bilayers: Localization, Partitioning, and Energetics. <i>ACS Infectious Diseases</i> , 2018, 4, 926-935.	3.8	14
5412	A single NaK channel conformation is not enough for non-selective ion conduction. <i>Nature Communications</i> , 2018, 9, 717.	12.8	52
5413	Identification of inhibitor against <i>H. pylori</i> HtrA protease using structure-based virtual screening and molecular dynamics simulations approaches. <i>Microbial Pathogenesis</i> , 2018, 118, 365-377.	2.9	4
5414	Extension of the GROMOS 56a6 CARBO/CARBO <sub>R</sub> Force Field for Charged, Protonated, and Esterified Uronates. <i>Journal of Physical Chemistry B</i> , 2018, 122, 3696-3710.	2.6	17
5415	Structural Polymorphism in a Self-Assembled Tri-Aromatic Peptide System. <i>ACS Nano</i> , 2018, 12, 3253-3262.	14.6	72
5416	Prediction of striped cylindrical micelles (SCMs) formed by dodecyl- $\beta$ -D-maltoside (DDM) surfactants. <i>Soft Matter</i> , 2018, 14, 2694-2700.	2.7	8

#	ARTICLE	IF	CITATIONS
5417	Sequence-dependent response of DNA to torsional stress: a potential biological regulation mechanism. <i>Nucleic Acids Research</i> , 2018, 46, 1684-1694.	14.5	40
5418	Protein adsorption onto polysaccharides: Comparison of chitosan and chitin polymers. <i>Carbohydrate Polymers</i> , 2018, 191, 191-197.	10.2	36
5419	Role of proton balance in formation of self-assembled chitosan nanoparticles. <i>Colloids and Surfaces B: Biointerfaces</i> , 2018, 166, 127-134.	5.0	18
5420	Mechanism by which DHA inhibits the aggregation of KLVFFA peptides: A molecular dynamics study. <i>Journal of Chemical Physics</i> , 2018, 148, 115102.	3.0	7
5421	Antithrombin conformational modulation by D-myo-inositol 3,4,5,6-tetrakisphosphate (TMI), a novel scaffold for the development of antithrombotic agents. <i>Journal of Biomolecular Structure and Dynamics</i> , 2018, 36, 4045-4056.	3.5	5
5422	Structures of monomeric and oligomeric forms of the <i>Toxoplasma gondii</i> perforin-like protein 1. <i>Science Advances</i> , 2018, 4, eaq0762.	10.3	32
5423	Molecular Insight into the Growth of Hydrogen and Methane Binary Hydrates. <i>Journal of Physical Chemistry C</i> , 2018, 122, 7771-7778.	3.1	30
5424	Lipid composition dictates serum stability of reconstituted high-density lipoproteins: implications for in vivo applications. <i>Nanoscale</i> , 2018, 10, 7420-7430.	5.6	12
5425	Characterization of a <i>Drosophila</i> glutathione transferase involved in isothiocyanate detoxification. <i>Insect Biochemistry and Molecular Biology</i> , 2018, 95, 33-43.	2.7	49
5426	Determination of Dynamical Heterogeneity from Dynamic Neutron Scattering of Proteins. <i>Biophysical Journal</i> , 2018, 114, 2397-2407.	0.5	5
5427	Molecular Dynamics Modeling of Methylene Blue~DOPC Lipid Bilayer Interactions. <i>Langmuir</i> , 2018, 34, 4314-4323.	3.5	19
5428	Dynamic coarse-graining fills the gap between atomistic simulations and experimental investigations of mechanical unfolding. <i>Journal of Chemical Physics</i> , 2018, 148, 044109.	3.0	7
5429	Molecular Dynamics Simulation of Water Confinement in Disordered Aluminosilicate Subnanopores. <i>Scientific Reports</i> , 2018, 8, 3761.	3.3	17
5430	Designing phenylalanine-based hybrid biological materials: controlling morphology <i>via</i> molecular composition. <i>Organic and Biomolecular Chemistry</i> , 2018, 16, 2499-2507.	2.8	13
5431	Cholesterol Protects the Oxidized Lipid Bilayer from Water Injury: An All-Atom Molecular Dynamics Study. <i>Journal of Membrane Biology</i> , 2018, 251, 521-534.	2.1	12
5432	Solvent scaling scheme for studying solvent restructuring thermodynamics in solvation processes. <i>Journal of Molecular Liquids</i> , 2018, 270, 114-127.	4.9	2
5433	Design of Polyphosphate Inhibitors: A Molecular Dynamics Investigation on Polyethylene Glycol-Linked Cationic Binding Groups. <i>Biomacromolecules</i> , 2018, 19, 1358-1367.	5.4	12
5434	Antibacterial Activity Affected by the Conformational Flexibility in Glycine~Lysine Based $\alpha$ -Helical Antimicrobial Peptides. <i>Journal of Medicinal Chemistry</i> , 2018, 61, 2924-2936.	6.4	48

#	ARTICLE	IF	CITATIONS
5435	Nanopatterns of Phospholipid Assemblies on Carbon Nanotubes: A Molecular Dynamics Simulation Study. <i>Journal of Physical Chemistry C</i> , 2018, 122, 7455-7463.	3.1	4
5436	Does an electronic continuum correction improve effective short-range ion-ion interactions in aqueous solution?. <i>Journal of Chemical Physics</i> , 2018, 148, 222816.	3.0	33
5437	Fast estimation of protein conformational preference at air/water interface via molecular dynamics simulations. <i>Journal of the Taiwan Institute of Chemical Engineers</i> , 2018, 92, 42-49.	5.3	3
5438	Phase boundaries, nucleation rates and speed of crystal growth of the water-to-ice transition under an electric field: a simulation study. <i>Journal of Physics Condensed Matter</i> , 2018, 30, 174002.	1.8	12
5439	Characterization of the structural ensembles of p53 TAD2 by molecular dynamics simulations with different force fields. <i>Physical Chemistry Chemical Physics</i> , 2018, 20, 8676-8684.	2.8	24
5440	Elucidating the amphiphilic character of graphene oxide. <i>Physical Chemistry Chemical Physics</i> , 2018, 20, 9507-9515.	2.8	40
5441	Predicting rates of <i>in vivo</i> degradation of recombinant spider silk proteins. <i>Journal of Tissue Engineering and Regenerative Medicine</i> , 2018, 12, e97-e105.	2.7	21
5442	Effects of different force fields on the structural character of $\alpha$ -synuclein $\beta$ -hairpin peptide (35-56) in aqueous environment. <i>Journal of Biomolecular Structure and Dynamics</i> , 2018, 36, 302-317.	3.5	13
5443	Exploring the binding mechanism and kinetics of Piperine with snake venom secretory Phospholipase A <sub>2</sub> . <i>Journal of Biomolecular Structure and Dynamics</i> , 2018, 36, 209-220.	3.5	3
5444	Atomic insight into designed carbamate-based derivatives as acetylcholine esterase (AChE) inhibitors: a computational study by multiple molecular docking and molecular dynamics simulation. <i>Journal of Biomolecular Structure and Dynamics</i> , 2018, 36, 126-138.	3.5	17
5445	Molecular dynamics analysis of the structural and dynamic properties of the functionally enhanced hepta-variant of mouse 5-aminolevulinate synthase. <i>Journal of Biomolecular Structure and Dynamics</i> , 2018, 36, 152-165.	3.5	4
5446	Structure and interactions of RecA: plasticity revealed by molecular dynamics simulations. <i>Journal of Biomolecular Structure and Dynamics</i> , 2018, 36, 98-111.	3.5	30
5447	<i>In silico</i> modelling and molecular dynamics simulation studies of thiazolidine based PTP1B inhibitors. <i>Journal of Biomolecular Structure and Dynamics</i> , 2018, 36, 1195-1211.	3.5	25
5448	A theoretical study on the stability of CNT encased cyclic peptide beyond hydrogen bond cut-off. <i>Journal of Biomolecular Structure and Dynamics</i> , 2018, 36, 1108-1117.	3.5	6
5449	Exploring the sequence-structure-function relationship for the intrinsically disordered $\beta$ -crystallin Hahellin. <i>Journal of Biomolecular Structure and Dynamics</i> , 2018, 36, 1171-1181.	3.5	4
5450	Experimental and computational studies on the binding of diazinon to human serum albumin. <i>Journal of Biomolecular Structure and Dynamics</i> , 2018, 36, 1490-1510.	3.5	42
5451	Structural Insight into Binding Mode of 9-Hydroxy Aristolochic Acid, Diclofenac and Indomethacin to PLA2. <i>Interdisciplinary Sciences, Computational Life Sciences</i> , 2018, 10, 400-410.	3.6	3
5452	Analysis of Species-Selectivity of Human, Mouse and Rat Cytochrome P450 1A and 2B Subfamily Enzymes using Molecular Modeling, Docking and Dynamics Simulations. <i>Cell Biochemistry and Biophysics</i> , 2018, 76, 91-110.	1.8	1

#	ARTICLE	IF	CITATIONS
5453	Molecular dynamics simulation of the membrane binding and disruption mechanisms by antimicrobial scorpion venom-derived peptides. <i>Journal of Biomolecular Structure and Dynamics</i> , 2018, 36, 2070-2084.	3.5	22
5454	Simulation Based Investigation of Deleterious nsSNPs in ATXN2 Gene and Its Structural Consequence Toward Spinocerebellar Ataxia. <i>Journal of Cellular Biochemistry</i> , 2018, 119, 499-510.	2.6	16
5455	A computational study to identify the key residues of peroxisome proliferator-activated receptor gamma in the interactions with its antagonists. <i>Journal of Biomolecular Structure and Dynamics</i> , 2018, 36, 1822-1833.	3.5	5
5456	Wing 1 of protein HOP2 is as important as helix 3 in DNA binding by MD simulation. <i>Journal of Biomolecular Structure and Dynamics</i> , 2018, 36, 1853-1866.	3.5	3
5457	Addressing the Environment Electrostatic Effect on Ballistic Electron Transport in Large Systems: A QM/MM-NEGF Approach. <i>Journal of Physical Chemistry B</i> , 2018, 122, 485-492.	2.6	21
5458	Evidence of anomalous behavior of intermolecular interactions at low concentration of methanol in ethanol-methanol binary system. <i>Spectrochimica Acta - Part A: Molecular and Biomolecular Spectroscopy</i> , 2018, 188, 301-310.	3.9	13
5459	Molecular dynamics studies on the domain swapped <i>Salmonella typhimurium</i> survival protein SurE: insights on the possible reasons for catalytic cooperativity. <i>Journal of Biomolecular Structure and Dynamics</i> , 2018, 36, 2303-2311.	3.5	0
5460	Steered Molecular Dynamics for Investigating the Interactions Between Insulin Receptor Tyrosine Kinase (IRK) and Variants of Protein Tyrosine Phosphatase 1B (PTP1B). <i>Applied Biochemistry and Biotechnology</i> , 2018, 184, 401-413.	2.9	8
5461	Permanent densification of amorphous zinc oxide under pressure: A first principles study. <i>Journal of Non-Crystalline Solids</i> , 2018, 481, 27-32.	3.1	4
5462	Charge transport and structure in semimetallic polymers. <i>Journal of Polymer Science, Part B: Polymer Physics</i> , 2018, 56, 97-104.	2.1	53
5463	Structures and anti-inflammatory properties of 4-halogenated -mofebutazones. <i>Journal of Molecular Structure</i> , 2018, 1154, 204-218.	3.6	0
5464	Unveiling the Role of Macrodipolar Interactions in the Properties of Self-Assembled Supramolecular Materials. <i>Chemistry - A European Journal</i> , 2018, 24, 2609-2617.	3.3	7
5465	Is the cholesterol bilayer domain a barrier to oxygen transport into the eye lens?. <i>Biochimica Et Biophysica Acta - Biomembranes</i> , 2018, 1860, 434-441.	2.6	28
5466	Conformational transitions of uracil transporter UraA from <i>Escherichia coli</i> : a molecular simulation study. <i>Journal of Biomolecular Structure and Dynamics</i> , 2018, 36, 3398-3410.	3.5	1
5467	Kinetic Origin of Substrate Specificity in Post-Transfer Editing by Leucyl-tRNA Synthetase. <i>Journal of Molecular Biology</i> , 2018, 430, 1-16.	4.2	19
5468	Structural studies and nociceptive activity of a native lectin from <i>Platypodium elegans</i> seeds (nPELa). <i>International Journal of Biological Macromolecules</i> , 2018, 107, 236-246.	7.5	10
5469	Ethane clathrates using different water-ethane models: Molecular dynamics. <i>Physica A: Statistical Mechanics and Its Applications</i> , 2018, 491, 89-100.	2.6	1
5470	Metabolism-dependent cytotoxicity of citrinin and ochratoxin A alone and in combination as assessed adopting integrated discrete multiple organ co-culture (IdMOC). <i>Toxicology in Vitro</i> , 2018, 46, 166-177.	2.4	16

#	ARTICLE	IF	CITATIONS
5471	A major serendipitous contribution to continuum mechanics. <i>Mechanics Research Communications</i> , 2018, 93, 41-46.	1.8	7
5472	Pore formation and the key factors in antibacterial activity of aurein 1.2 and LLAA inside lipid bilayers, a molecular dynamics study. <i>Biochimica Et Biophysica Acta - Biomembranes</i> , 2018, 1860, 347-356.	2.6	2
5473	Role of <i>pncA</i> gene mutations W68R and W68G in pyrazinamide resistance. <i>Journal of Cellular Biochemistry</i> , 2018, 119, 2567-2578.	2.6	29
5474	Interatomic potential suitable for the modeling of penta-graphene: Molecular statics/molecular dynamics studies. <i>Carbon</i> , 2018, 126, 165-175.	10.3	37
5475	Connections between the Anomalous Volumetric Properties of Alcohols in Aqueous Solution and the Volume of Hydrophobic Association. <i>Journal of Physical Chemistry B</i> , 2018, 122, 3242-3250.	2.6	7
5476	The role of the oximes HI-6 and HS-6 inside human acetylcholinesterase inhibited with nerve agents: a computational study. <i>Journal of Biomolecular Structure and Dynamics</i> , 2018, 36, 3444-3452.	3.5	11
5477	Membrane-induced organization and dynamics of the N-terminal domain of chemokine receptor CXCR1: insights from atomistic simulations. <i>Chemistry and Physics of Lipids</i> , 2018, 210, 142-148.	3.2	9
5478	Multivalent interacting glycodendrimer to prevent amyloid-peptide fibril formation induced by Cu(II): A multidisciplinary approach. <i>Nano Research</i> , 2018, 11, 1204-1226.	10.4	27
5479	Understanding the molecular mechanism of improved proliferation and osteogenic potential of human mesenchymal stem cells grown on a polyelectrolyte complex derived from non-mulberry silk fibroin and chitosan. <i>Biomedical Materials (Bristol)</i> , 2018, 13, 015011.	3.3	25
5480	Computational design of Phe-Tyr dipeptide and preparation, characterization, cytotoxicity studies of Phe-Tyr dipeptide loaded PLGA nanoparticles for the treatment of hypertension. <i>Journal of Biomolecular Structure and Dynamics</i> , 2018, 36, 2893-2907.	3.5	15
5481	Structural elucidation of transmembrane domain zero (TMD0) of EcdL: A multidrug resistance-associated protein (MRP) family of ATP-binding cassette transporter protein revealed by atomistic simulation. <i>Journal of Biomolecular Structure and Dynamics</i> , 2018, 36, 2938-2950.	3.5	20
5482	Efficient potential of mean force calculation from multiscale simulations: Solute insertion in a lipid membrane. <i>Biochemical and Biophysical Research Communications</i> , 2018, 498, 282-287.	2.1	20
5483	Molecular dynamics for near melting temperatures simulations of metals using modified embedded-atom method. <i>Journal of Physics and Chemistry of Solids</i> , 2018, 112, 61-72.	4.0	78
5484	Protein surface roughness accounts for binding free energy of Plasmepsin II ligand complexes. <i>Journal of Molecular Recognition</i> , 2018, 31, e2661.	2.1	0
5485	A molecular dynamics study of components of the ginger ( <i>Zingiber officinale</i> ) extract inside human acetylcholinesterase: implications for Alzheimer disease. <i>Journal of Biomolecular Structure and Dynamics</i> , 2018, 36, 3843-3855.	3.5	19
5486	A revised worm-like chain model for elasticity of polypeptide chains. <i>Journal of Polymer Science, Part B: Polymer Physics</i> , 2018, 56, 297-307.	2.1	5
5487	Unfolding dynamics of small peptides biased by constant mechanical forces. <i>Molecular Systems Design and Engineering</i> , 2018, 3, 204-213.	3.4	4
5488	The role of caveolin-1 in lipid droplets and their biogenesis. <i>Chemistry and Physics of Lipids</i> , 2018, 211, 93-99.	3.2	18

#	ARTICLE	IF	CITATIONS
5489	Probing the inhibitory potency of epigallocatechin gallate against human $\beta$ -crystallin aggregation: Spectroscopic, microscopic and simulation studies. <i>Spectrochimica Acta - Part A: Molecular and Biomolecular Spectroscopy</i> , 2018, 192, 318-327.	3.9	10
5490	A Single Mutation is Sufficient to Modify the Metal Selectivity and Specificity of a Eukaryotic Manganese Superoxide Dismutase to Encompass Iron. <i>Chemistry - A European Journal</i> , 2018, 24, 5303-5308.	3.3	10
5491	Ordering of lipid membranes altered by boron nitride nanosheets. <i>Physical Chemistry Chemical Physics</i> , 2018, 20, 3903-3910.	2.8	22
5492	Protein-Ligand Dissociation Simulated by Parallel Cascade Selection Molecular Dynamics. <i>Journal of Chemical Theory and Computation</i> , 2018, 14, 404-417.	5.3	34
5493	Ligand-induced action of the W2866.48 rotamer toggle switch in the $\beta$ 2-adrenergic receptor. <i>Physical Chemistry Chemical Physics</i> , 2018, 20, 581-594.	2.8	6
5494	Understanding homogeneous nucleation in solidification of aluminum by molecular dynamics simulations. <i>Modelling and Simulation in Materials Science and Engineering</i> , 2018, 26, 025007.	2.0	79
5495	Differential targeting of membrane lipid domains by caffeic acid and its ester derivatives. <i>Free Radical Biology and Medicine</i> , 2018, 115, 232-245.	2.9	42
5496	Metastable State during Melting and Solid-Solid Phase Transition of [C <sub>3</sub> Mim][NO <sub>3</sub> ] ( $\rho = 4 \times 10^{-12}$ ) Ionic Liquids by Molecular Dynamics Simulation. <i>Journal of Physical Chemistry B</i> , 2018, 122, 229-239.	2.6	26
5497	Functional role of an unusual tyrosine residue in the electron transfer chain of a prokaryotic (6-4) photolyase. <i>Chemical Science</i> , 2018, 9, 1259-1272.	7.4	17
5498	Multiscale simulations of ligand adsorption and exchange on gold nanoparticles. <i>Physical Chemistry Chemical Physics</i> , 2018, 20, 1381-1394.	2.8	25
5499	Biochemical and Biophysical Characterisation of Higher Oligomeric Structure of Rat Nucleosome Assembly Protein 1. <i>Protein Journal</i> , 2018, 37, 58-69.	1.6	3
5500	Exploring the Nanotoxicology of MoS <sub>2</sub> : A Study on the Interaction of MoS <sub>2</sub> Nanoflakes and K <sup>+</sup> Channels. <i>ACS Nano</i> , 2018, 12, 705-717.	14.6	44
5501	Effects of force fields on the conformational and dynamic properties of amyloid $\beta$ (1-40) dimer explored by replica exchange molecular dynamics simulations. <i>Proteins: Structure, Function and Bioinformatics</i> , 2018, 86, 279-300.	2.6	23
5502	Molecular Dynamics Simulation of Methane Hydrate Formation and Dissociation in the Clay Pores with Fatty Acids. <i>Journal of Physical Chemistry C</i> , 2018, 122, 1318-1325.	3.1	49
5503	Integration of molecular dynamics simulation and hotspot residues grafting for de novo scFv design against <i>Salmonella</i> Typhi TolC protein. <i>Journal of Molecular Recognition</i> , 2018, 31, e2695.	2.1	4
5504	Conformational dynamics of human protein kinase CK2 $\alpha$ and its effect on function and inhibition. <i>Proteins: Structure, Function and Bioinformatics</i> , 2018, 86, 344-353.	2.6	8
5505	Structural dissection of an interaction between transcription initiation and termination factors implicated in promoter-terminator cross-talk. <i>Journal of Biological Chemistry</i> , 2018, 293, 1651-1665.	3.4	15
5506	Double-layer carbon nanocapsules with radioiodine content and its interaction with calcium, phosphorus, and strontium. <i>Journal of Molecular Modeling</i> , 2018, 24, 2.	1.8	1



#	ARTICLE	IF	CITATIONS
5507	Effects of Silica Surfaces on the Structure and Dynamics of Room-Temperature Ionic Liquids: A Molecular Dynamics Simulation Study. <i>Journal of Physical Chemistry C</i> , 2018, 122, 624-634.	3.1	29
5508	Binding of 12-Crown-4 with Alzheimer's A $\beta$ 40 and A $\beta$ 42 Monomers and Its Effect on Their Conformation: Insight from Molecular Dynamics Simulations. <i>Molecular Pharmaceutics</i> , 2018, 15, 289-299.	4.6	26
5509	The inhibitory performance of flavonoid cyanidin-3-sambubioside against H274Y mutation in H1N1 influenza virus. <i>Journal of Biomolecular Structure and Dynamics</i> , 2018, 36, 4255-4269.	3.5	24
5510	Trimethylamine <i>N</i> -oxide Counteracts Urea Denaturation by Inhibiting Protein-Urea Preferential Interaction. <i>Journal of the American Chemical Society</i> , 2018, 140, 483-492.	13.7	94
5511	Stress-dependence of kinetic transitions at atomistic defects. <i>Modelling and Simulation in Materials Science and Engineering</i> , 2018, 26, 015007.	2.0	0
5512	ForceGen: atomic covalent bond value derivation for Gromacs. <i>Journal of Molecular Modeling</i> , 2018, 24, 5.	1.8	13
5513	Effect of number of hydroxyl groups of fullereneol C <sub>60</sub> (OH) <sub>n</sub> on its interaction with cell membrane. <i>Journal of the Taiwan Institute of Chemical Engineers</i> , 2018, 90, 18-24.	5.3	9
5514	Molecular dynamics simulation of aspirin dissolution. <i>Journal of Molecular Liquids</i> , 2018, 270, 243-250.	4.9	5
5515	Cooperative effects of inorganic and organic structure-directing agents in ZSM-5 crystallization. <i>Molecular Systems Design and Engineering</i> , 2018, 3, 159-170.	3.4	51
5516	Dislocation interactions at reduced strain rates in atomistic simulations of nanocrystalline Al. <i>Acta Materialia</i> , 2018, 144, 68-79.	7.9	21
5517	Molecular dynamics study of the interaction between nanoscale interstitial dislocation loops and grain boundaries in BCC iron. <i>Journal of Nuclear Materials</i> , 2018, 498, 378-386.	2.7	18
5518	Molecular dynamics simulation and experimental validation by X-ray data of hydroxyapatite crystalline structures. <i>Fluid Phase Equilibria</i> , 2018, 470, 60-67.	2.5	5
5519	Molecular simulations of electrolyte structure and dynamics in lithium-sulfur battery solvents. <i>Journal of Power Sources</i> , 2018, 373, 70-78.	7.8	79
5520	Permeation pathways through lateral domains in model membranes of skin lipids. <i>Physical Chemistry Chemical Physics</i> , 2018, 20, 2162-2174.	2.8	32
5521	Adsorption of water, sulfates and chloride on arsenopyrite surface. <i>Applied Surface Science</i> , 2018, 434, 389-399.	6.1	20
5522	Hydration and Ion Pairing in Aqueous Mg <sup>2+</sup> and Zn <sup>2+</sup> Solutions: Force-Field Description Aided by Neutron Scattering Experiments and Ab Initio Molecular Dynamics Simulations. <i>Journal of Physical Chemistry B</i> , 2018, 122, 3296-3306.	2.6	75
5523	d-Peptides as inhibitors of PR3-membrane interactions. <i>Biochimica Et Biophysica Acta - Biomembranes</i> , 2018, 1860, 458-466.	2.6	4
5524	Inference of Calmodulin's Ca <sup>2+</sup> -Dependent Free Energy Landscapes via Gaussian Mixture Model Validation. <i>Journal of Chemical Theory and Computation</i> , 2018, 14, 63-71.	5.3	23



#	ARTICLE	IF	CITATIONS
5525	Simulation of Ductile Fracture in Amorphous and Polycrystalline Materials by Multiscale Cohesive Zone Model. <i>Mathematics for Industry</i> , 2018, , 39-50.	0.4	0
5526	Modern drug design: the implication of using artificial neuronal networks and multiple molecular dynamic simulations. <i>Journal of Computer-Aided Molecular Design</i> , 2018, 32, 299-311.	2.9	6
5527	Exploring the Roles of Proline in Three-Dimensional Domain Swapping from Structure Analysis and Molecular Dynamics Simulations. <i>Protein Journal</i> , 2018, 37, 13-20.	1.6	8
5528	Pyranose ring puckering in aldopentoses, ketohexoses and deoxyaldohexoses. A molecular dynamics study. <i>Carbohydrate Research</i> , 2018, 455, 62-70.	2.3	11
5529	Excited state energy fluctuations in the Fennaâ€“Matthewsâ€“Olson complex from molecular dynamics simulations with interpolated chromophore potentials. <i>Physical Chemistry Chemical Physics</i> , 2018, 20, 3310-3319.	2.8	31
5530	Improvement in the Thermostability of a Î²â€“Amino Acid Converting Î³â€“Transaminase by Using FoldX. <i>ChemBioChem</i> , 2018, 19, 379-387.	2.6	28
5531	Density functional study of the thermodynamic properties and phase diagram of the magnesium hydride. <i>Calphad: Computer Coupling of Phase Diagrams and Thermochemistry</i> , 2018, 60, 7-15.	1.6	4
5532	Molecular dynamics simulation of the thermosensitivity of the human connexin 26 hemichannel. <i>Chemical Physics</i> , 2018, 500, 7-14.	1.9	7
5533	Simulation study of intercalation complexes of kaolinite with simple amides as primary intercalation reagents. <i>Computational Materials Science</i> , 2018, 143, 118-125.	3.0	19
5534	Membrane phase transition during heating and cooling: molecular insight into reversible melting. <i>European Biophysics Journal</i> , 2018, 47, 151-164.	2.2	29
5535	An assessment of optimal time scale of conformational resampling for parallel cascade selection molecular dynamics. <i>Molecular Simulation</i> , 2018, 44, 206-212.	2.0	6
5536	Neutron and X-ray crystal structures of <i>Lactobacillus brevis</i> alcohol dehydrogenase reveal new insights into hydrogen-bonding pathways. <i>Acta Crystallographica Section F, Structural Biology Communications</i> , 2018, 74, 754-764.	0.8	6
5537	Molecular docking and dynamics studies of 4-anilino quinazolines for epidermal growth factor receptor tyrosine kinase to find potent inhibitor. <i>Journal of Receptor and Signal Transduction Research</i> , 2018, 38, 475-483.	2.5	4
5538	Molecular dynamics study of binary POPC bilayers: molecular condensing effects on membrane structure and dynamics. <i>Journal of Physics: Conference Series</i> , 2018, 1136, 012022.	0.4	10
5539	Dynamics and deformability of Î±-, 310- and Î²-helices. <i>Archives of Biological Sciences</i> , 2018, 70, 21-31.	0.5	10
5540	Construction of Novel Aspartokinase Mutant A380I and Its Characterization by Molecular Dynamics Simulation. <i>Molecules</i> , 2018, 23, 3379.	3.8	6
5541	Molecular Dynamics Simulations. , 2018, , .		0
5542	High Partial Auxeticity Induced by Nanochannels in [111]-Direction in a Simple Model with Yukawa Interactions. <i>Materials</i> , 2018, 11, 2550.	2.9	9

#	ARTICLE	IF	CITATIONS
5543	Water phase transitions from the perspective of hydrogen-bond network analysis. <i>Physical Chemistry Chemical Physics</i> , 2018, 20, 28308-28318.	2.8	8
5544	Understanding the temperature effect on transport dynamics and structures in polyamide reverse osmosis system <i>via</i> molecular dynamics simulations. <i>Physical Chemistry Chemical Physics</i> , 2018, 20, 29996-30005.	2.8	20
5545	Molecular basis for the increased affinity of an RNA recognition motif with re-engineered specificity: A molecular dynamics and enhanced sampling simulations study. <i>PLoS Computational Biology</i> , 2018, 14, e1006642.	3.2	14
5546	Nanoparticles based on lipidyl- $\beta$ -cyclodextrins: synthesis, characterization, and experimental and computational biophysical studies for encapsulation of atazanavir. <i>New Journal of Chemistry</i> , 2018, 42, 20171-20179.	2.8	5
5547	Comparative studies on structure, sensitivity and mechanical properties of CL-20/DNDAP cocrystal and composite by molecular dynamics simulation. <i>RSC Advances</i> , 2018, 8, 34690-34698.	3.6	15
5548	Ion transport through a nanoporous C <sub>2</sub> N membrane: the effect of electric field and layer number. <i>RSC Advances</i> , 2018, 8, 36705-36711.	3.6	8
5549	Effects of lipid composition on membrane permeation. <i>Soft Matter</i> , 2018, 14, 8496-8508.	2.7	26
5550	Quantifying the influence of the ion cloud on SAXS profiles of charged proteins. <i>Physical Chemistry Chemical Physics</i> , 2018, 20, 26351-26361.	2.8	9
5551	Influence of compatible solute ectoine on distinct DNA structures: thermodynamic insights into molecular binding mechanisms and destabilization effects. <i>Physical Chemistry Chemical Physics</i> , 2018, 20, 25861-25874.	2.8	24
5552	Molecular simulations reveal that a short helical loop regulates thermal stability of type I cohesin-dockerin complexes. <i>Physical Chemistry Chemical Physics</i> , 2018, 20, 28445-28451.	2.8	3
5553	Aggregation response of triglyceride hydrolysis products in cyclohexane and triolein. <i>Physical Chemistry Chemical Physics</i> , 2018, 20, 27192-27204.	2.8	8
5554	Exploring thermal transitions in anthradithiophene-based organic semiconductors to reveal structure-packing relationships. <i>Journal of Materials Chemistry C</i> , 2018, 6, 10924-10934.	5.5	4
5555	Assessment of anti-arthritis potential of traditionally fermented ayurvedic polyherbal product chandanasava by molecular modelling, docking and dynamics approaches. <i>International Journal of Computational Biology and Drug Design</i> , 2018, 11, 346.	0.3	2
5556	Partitioning of nanoscale particles on a heterogeneous multicomponent lipid bilayer. <i>Physical Chemistry Chemical Physics</i> , 2018, 20, 28241-28248.	2.8	14
5557	Molecular Dynamics Simulations of the Thermal and Transport Properties of Molten NaNO <sub>2</sub> -NaNO <sub>3</sub> Systems. <i>Electrochemistry</i> , 2018, 86, 104-108.	1.4	3
5558	Identification and Characterization of NTB451 as a Potential Inhibitor of Necroptosis. <i>Molecules</i> , 2018, 23, 2884.	3.8	11
5559	Effects of Salt Ions on the Methane Hydrate Formation and Dissociation in the Clay Pore Water and Bulk Water. <i>Energy &amp; Fuels</i> , 2018, 32, 12486-12494.	5.1	32
5560	Self-Assembly of a Structurally Defined Chiro-Optical Peptide-Oligothiophene Hybrid Material. <i>ACS Omega</i> , 2018, 3, 15066-15075.	3.5	2

#	ARTICLE	IF	CITATIONS
5561	The Antibody Light-Chain Linker Regulates Domain Orientation and Amyloidogenicity. <i>Journal of Molecular Biology</i> , 2018, 430, 4925-4940.	4.2	27
5562	Influence of Hydration on the Structure of Reline Deep Eutectic Solvent: A Molecular Dynamics Study. <i>ACS Omega</i> , 2018, 3, 15246-15255.	3.5	122
5563	Molecular Dynamics Simulations of Water-Mediated Cholesterol Capture within an Open-Ended Single-Walled Carbon Nanotube. <i>ChemPhysChem</i> , 2018, 20, 142-147.	2.1	2
5564	Investigation of grain formation mechanism in CuAl shape memory alloy by molecular dynamic simulation. <i>AIP Conference Proceedings</i> , 2018, , .	0.4	2
5565	Probing inhibition mechanisms of adenosine deaminase by using molecular dynamics simulations. <i>PLoS ONE</i> , 2018, 13, e0207234.	2.5	7
5566	Nanoscale domains in ionic liquids: A statistical mechanics definition for molecular dynamics studies. <i>Journal of Chemical Physics</i> , 2018, 149, 184502.	3.0	10
5567	A biophysical study on the mechanism of interactions of DOX or PTX with $\alpha$ -lactalbumin as a delivery carrier. <i>Scientific Reports</i> , 2018, 8, 17345.	3.3	17
5568	Superior Compatibility of C <sub>2</sub> N with Human Red Blood Cell Membranes and the Underlying Mechanism. <i>Small</i> , 2018, 14, e1803509.	10.0	33
5569	Understanding Adsorption of Violanthrone-79 as a Model Asphaltene Compound on Quartz Surface Using Molecular Dynamics Simulations. <i>Journal of Physical Chemistry C</i> , 2018, 122, 28787-28796.	3.1	30
5570	Mapping the Substrate Recognition Pathway in Cytochrome P450. <i>Journal of the American Chemical Society</i> , 2018, 140, 17743-17752.	13.7	42
5571	Electronic Excitations in Complex Molecular Environments: Many-Body Green's Functions Theory in VOTCA-XTP. <i>Journal of Chemical Theory and Computation</i> , 2018, 14, 6253-6268.	5.3	28
5572	Exploring the Ligand Efficacy of Cannabinoid Receptor 1 (CB1) using Molecular Dynamics Simulations. <i>Scientific Reports</i> , 2018, 8, 13787.	3.3	25
5573	Targeting the Pentose Phosphate Pathway: Characterization of a New 6PGL Inhibitor. <i>Biophysical Journal</i> , 2018, 115, 2114-2126.	0.5	6
5574	The Formation of Hydrophobic Core Regulates the Protein Folding of Villin Elucidated with Parallel Cascade Selection Molecular Dynamics. <i>Chemistry Letters</i> , 2018, 47, 1300-1303.	1.3	0
5575	Nanocrystalline Oligo(ethylene sulfide)- <i>b</i> -poly(ethylene glycol) Micelles: Structure and Stability. <i>Macromolecules</i> , 2018, 51, 9538-9546.	4.8	7
5576	Molecular Mechanism of Depolarization-Dependent Inactivation in W366F Mutant of Kv1.2. <i>Journal of Physical Chemistry B</i> , 2018, 122, 10825-10833.	2.6	4
5577	Targeted Molecular Dynamics Calculations of Free Energy Profiles Using a Nonequilibrium Friction Correction. <i>Journal of Chemical Theory and Computation</i> , 2018, 14, 6175-6182.	5.3	41
5578	Exploring pH-Responsive, Switchable Crosslinking Mechanisms for Programming Reconfigurable Hydrogels Based on Aminopolysaccharides. <i>Chemistry of Materials</i> , 2018, 30, 8597-8605.	6.7	19

#	ARTICLE	IF	CITATIONS
5579	The potential of natural product vs neurodegenerative disorders: In silico study of artoflavanocoumarin as BACE-1 inhibitor. Computational Biology and Chemistry, 2018, 77, 307-317.	2.3	10
5580	BUMPy: A Model-Independent Tool for Constructing Lipid Bilayers of Varying Curvature and Composition. Journal of Chemical Theory and Computation, 2018, 14, 6642-6652.	5.3	29
5581	Protein assemblies ejected directly from native membranes yield complexes for mass spectrometry. Science, 2018, 362, 829-834.	12.6	155
5582	Probing the mechanism of SIRT1 activation by a 1,4-dihydropyridine. Journal of Molecular Modeling, 2018, 24, 340.	1.8	14
5583	Molecular Dynamics Simulation of Structural Signals of Shear-Band Formation in Zr46Cu46Al8 Metallic Glasses. Materials, 2018, 11, 2564.	2.9	3
5584	Computational Studies on the Inhibitor Selectivity of Human JAMM Deubiquitinylases Rpn11 and CSN5. Frontiers in Chemistry, 2018, 6, 480.	3.6	17
5585	Creating a Coating from a Titanium-Aluminum Intermetallic Compound By the Cold Spray Technology. Journal of Applied Mechanics and Technical Physics, 2018, 59, 1126-1135.	0.5	6
5586	Silicon Liquid Structure and Crystal Nucleation from <i>Ab Initio</i> Deep Metadynamics. Physical Review Letters, 2018, 121, 265701.	7.8	109
5587	Refinement of the OPLSAA Force-Field for Liquid Alcohols. ACS Omega, 2018, 3, 18089-18099.	3.5	27
5588	Loop-punching suppression induced by growth of helium bubble pair in tungsten. Journal of Applied Physics, 2018, 124, 235105.	2.5	8
5589	Simulation of Capture and Release Processes of Hydrogen by $\beta$ -Hydroquinone Clathrate. ACS Omega, 2018, 3, 18771-18782.	3.5	16
5590	Coarse-grained model of titrating peptides interacting with lipid bilayers. Journal of Chemical Physics, 2018, 149, 244108.	3.0	4
5591	Bottom-up approach to represent dynamic properties in coarse-grained molecular simulations. Journal of Chemical Physics, 2018, 149, 244114.	3.0	25
5592	Improved general-purpose five-point model for water: TIP5P/2018. Journal of Chemical Physics, 2018, 149, 224507.	3.0	23
5593	Natural Compound Modulates the Cervical Cancer Microenvironment-A Pharmacophore Guided Molecular Modelling Approaches. Journal of Clinical Medicine, 2018, 7, 551.	2.4	11
5594	Discovery of Potential Plant-Derived Peptide Deformylase (PDF) Inhibitors for Multidrug-Resistant Bacteria Using Computational Studies. Journal of Clinical Medicine, 2018, 7, 563.	2.4	21
5595	Understanding the Exceptional Properties of Nitroacetamides in Water: A Computational Model Including the Solvent. Molecules, 2018, 23, 3308.	3.8	3
5596	Comparative analysis of interactions between aryl hydrocarbon receptor ligand binding domain with its ligands: a computational study. BMC Structural Biology, 2018, 18, 15.	2.3	17

#	ARTICLE	IF	CITATIONS
5597	Molecular modelling and simulation studies of the Mycobacterium tuberculosis multidrug efflux pump protein Rv1258c. PLoS ONE, 2018, 13, e0207605.	2.5	23
5598	Self-assembly of aromatic amino acids: a molecular dynamics study. Physical Chemistry Chemical Physics, 2018, 20, 30525-30536.	2.8	29
5599	First principles study of hole transport properties in amorphous polyethylene: Effect of bromine doping. Journal of Applied Physics, 2018, 124, .	2.5	6
5600	Equilibrium and Transport Properties of Methane at the Methane/Water Interface with the Presence of SDS. Journal of Physical Chemistry C, 2018, 122, 29259-29267.	3.1	15
5601	Inhibitor binding mode and allosteric regulation of Na <sup>+</sup> -glucose symporters. Nature Communications, 2018, 9, 5245.	12.8	35
5602	Spatially Resolving the Condensing Effect of Cholesterol in Lipid Bilayers. Biophysical Journal, 2018, 115, 2179-2188.	0.5	38
5603	<i>Stercobilin-HCl</i> and <i>Urobilin-HCl</i> . Analysis of Their Chiroptical and Conformational Properties by VCD, ECD, and CPL Experiments and MD and DFT Calculations. Journal of Physical Chemistry B, 2018, 122, 12351-12362.	2.6	17
5604	Characterizing Molecular Adsorption on Biodegradable MnO <sub>2</sub> Nanoscaffolds. Journal of Physical Chemistry C, 2018, 122, 29017-29027.	3.1	11
5607	Molecular Origin of Spatiotemporal Heterogeneity in Biomembranes With Coexisting Liquid Phases: Insights From Topological Rearrangements and Lipid Packing Defects. Advances in Biomembranes and Lipid Self-Assembly, 2018, , 87-114.	0.6	5
5608	High and low density patches in simulated liquid water. Journal of Chemical Physics, 2018, 149, 204507.	3.0	33
5609	Disassembly and trimer formation of E2 protein cage: the effects of C-terminus, salt, and protonation state. Journal Physics D: Applied Physics, 2018, 51, 365402.	2.8	0
5610	Distribution of mechanical stress in the Escherichia coli cell envelope. Biochimica Et Biophysica Acta - Biomembranes, 2018, 1860, 2566-2575.	2.6	66
5611	Insight into novel clinical mutants of RpsA-S324F, E325K, and G341R of Mycobacterium tuberculosis associated with pyrazinamide resistance. Computational and Structural Biotechnology Journal, 2018, 16, 379-387.	4.1	28
5612	Simultaneous and Independent Dual Site-Specific Self-Labeling of Recombinant Antibodies. Bioconjugate Chemistry, 2018, 29, 3586-3594.	3.6	9
5613	Best of Two Worlds? How MD Simulations of Amphiphilic Helical Peptides in Membranes Can Complement Data from Oriented Solid-State NMR. Journal of Chemical Theory and Computation, 2018, 14, 6002-6014.	5.3	12
5614	Molecular Insights into the Unusual Structure of an Antifreeze Protein with a Hydrated Core. Journal of Physical Chemistry B, 2018, 122, 9827-9839.	2.6	15
5615	Unexplored Nucleotide Binding Modes for the ABC Exporter MsbA. Journal of the American Chemical Society, 2018, 140, 14112-14125.	13.7	32
5616	Binding modes of CYP106A2 redox partners determine differences in progesterone hydroxylation product patterns. Communications Biology, 2018, 1, 99.	4.4	29

#	ARTICLE	IF	CITATIONS
5617	Exploring Rigid and Flexible Core Trivalent Sialosides for Influenza Virus Inhibition. Chemistry - A European Journal, 2018, 24, 19373-19385.	3.3	14
5618	pH dependent membrane binding of the Solanum tuberosum plant specific insert: An in silico study. Biochimica Et Biophysica Acta - Biomembranes, 2018, 1860, 2608-2618.	2.6	4
5619	Interactions between the Molecular Components of the Cowpea Chlorotic Mottle Virus Investigated by Molecular Dynamics Simulations. Journal of Physical Chemistry B, 2018, 122, 9490-9498.	2.6	8
5620	Structure and Dynamics of the Quasi-Liquid Layer at the Surface of Ice from Molecular Simulations. Journal of Physical Chemistry C, 2018, 122, 24780-24787.	3.1	38
5621	Mechanistic basis for the evolution of chalcone synthase catalytic cysteine reactivity in land plants. Journal of Biological Chemistry, 2018, 293, 18601-18612.	3.4	38
5622	Structure and dynamics of Helicobacter pylori nickel-chaperone HypA: an integrated approach using NMR spectroscopy, functional assays and computational tools. Journal of Biological Inorganic Chemistry, 2018, 23, 1309-1330.	2.6	20
5623	Self-Assembled Micellar Structures of Lipopeptides with Variable Number of Attached Lipid Chains Revealed by Atomistic Molecular Dynamics Simulations. Journal of Physical Chemistry B, 2018, 122, 9605-9615.	2.6	8
5624	Solidâ€State Rechargeable Zn//NiCo and Znâ€Air Batteries with Ultralong Lifetime and High Capacity: The Role of a Sodium Polyacrylate Hydrogel Electrolyte. Advanced Energy Materials, 2018, 8, 1802288.	19.5	253
5625	Prion protein conversion triggered by acidic condition: a molecular dynamics study through different force fields. Journal of Computational Chemistry, 2018, 39, 2000-2011.	3.3	6
5626	d-Amino Acid Pseudopeptides as Potential Amyloid-Beta Aggregation Inhibitors. Molecules, 2018, 23, 2387.	3.8	9
5627	Dissipative particle dynamics modeling of hydrogel swelling by osmotic ensemble method. Journal of Chemical Physics, 2018, 149, 094904.	3.0	22
5628	Insight into the Self-Assembling Properties of Peptergents: A Molecular Dynamics Simulation Study. International Journal of Molecular Sciences, 2018, 19, 2772.	4.1	3
5629	Structures, intermolecular interactions, and chemical hardness of binary waterâ€organic solvents: a molecular dynamics study. Journal of Molecular Modeling, 2018, 24, 292.	1.8	3
5630	Anomalous behavior of membrane fluidity caused by copper-copper bond coupled phospholipids. Scientific Reports, 2018, 8, 14093.	3.3	13
5631	Improvement of versatile peroxidase activity and stability by a cholinium-based ionic liquid. Journal of Molecular Liquids, 2018, 272, 597-608.	4.9	28
5632	Stretch and Breakage of Wormlike Micelles under Uniaxial Strain: A Simulation Study and Comparison with Experimental Results. Langmuir, 2018, 34, 12600-12608.	3.5	10
5633	The evolution of multiple active site configurations in a designed enzyme. Nature Communications, 2018, 9, 3900.	12.8	75
5634	<i>Tannerella forsythia</i> Tfo belongs to <i>Porphyromonas gingivalis</i> HmuY-like family of proteins but differs in heme-binding properties. Bioscience Reports, 2018, 38, .	2.4	24



#	ARTICLE	IF	CITATIONS
5635	Unraveling the mechanism of l-gulonate-3-dehydrogenase inhibition by ascorbic acid: Insights from molecular modeling. <i>Computational Biology and Chemistry</i> , 2018, 77, 146-153.	2.3	2
5636	Disulfide bonds elimination of endoglucanase II from <i>Trichoderma reesei</i> by site-directed mutagenesis to improve enzyme activity and thermal stability: An experimental and theoretical approach. <i>International Journal of Biological Macromolecules</i> , 2018, 120, 1572-1580.	7.5	23
5637	Origin of Internal Friction in Disordered Proteins Depends on Solvent Quality. <i>Journal of Physical Chemistry B</i> , 2018, 122, 11478-11487.	2.6	19
5638	Study of Thermal Stability of Hydrotalcite and Carbon Dioxide Adsorption Behavior on Hydrotalcite-Derived Mixed Oxides Using Atomistic Simulations. <i>ACS Omega</i> , 2018, 3, 12041-12051.	3.5	11
5639	Dielectric relaxation in acetamide + urea deep eutectics and neat molten urea: Origin of time scales via temperature dependent measurements and computer simulations. <i>Journal of Chemical Physics</i> , 2018, 149, 124501.	3.0	34
5640	Insights into the Folding of Disulfide-Rich Î¼-Conotoxins. <i>ACS Omega</i> , 2018, 3, 12330-12340.	3.5	19
5641	Designed peptide with a flexible central motif from ranatuerins adapts its conformation to bacterial membranes. <i>Biochimica Et Biophysica Acta - Biomembranes</i> , 2018, 1860, 2655-2668.	2.6	8
5642	Water Splits To Degrade Two-Dimensional Group-IV Monochalcogenides in Nanoseconds. <i>ACS Central Science</i> , 2018, 4, 1436-1446.	11.3	53
5643	Outward open conformation of a Major Facilitator Superfamily multidrug/H <sup>+</sup> antiporter provides insights into switching mechanism. <i>Nature Communications</i> , 2018, 9, 4005.	12.8	46
5644	Open and closed states of Mrlip1 DAG lipase revealed by molecular dynamics simulation. <i>Molecular Simulation</i> , 2018, 44, 1520-1528.	2.0	5
5645	Antimicrobial and Antibiofilm Activity of a Recombinant Fragment of Î²-Thymosin of Sea Urchin <i>Paracentrotus lividus</i> . <i>Marine Drugs</i> , 2018, 16, 366.	4.6	14
5646	Interactions of cantharidin-like inhibitors with human protein phosphatase-5 in a Mg <sup>2+</sup> system: molecular dynamics and quantum calculations. <i>Journal of Molecular Modeling</i> , 2018, 24, 303.	1.8	0
5647	Enzymeâ€“Polyelectrolyte Complexes Boost the Catalytic Performance of Enzymes. <i>ACS Catalysis</i> , 2018, 8, 10876-10887.	11.2	30
5648	Electrolyte solvents for high voltage lithium ion batteries: ion correlation and specific anion effects in adiponitrile. <i>Physical Chemistry Chemical Physics</i> , 2018, 20, 25701-25715.	2.8	41
5649	Molecular Dynamics Simulations of Ether- and Ester-Linked Phospholipid Bilayers: A Comparative Study of Water Models. <i>Journal of Physical Chemistry B</i> , 2018, 122, 9399-9408.	2.6	6
5650	Free Energy Landscape for Alpha-Helix to Beta-Sheet Interconversion in Small Amyloid Forming Peptide under Nanoconfinement. <i>Journal of Physical Chemistry B</i> , 2018, 122, 9654-9664.	2.6	16
5651	Capturing Phase Behavior of Ternary Lipid Mixtures with a Refined Martini Coarse-Grained Force Field. <i>Journal of Chemical Theory and Computation</i> , 2018, 14, 6050-6062.	5.3	63
5652	Investigating the Influence of Arginine Dimethylation on Nucleosome Dynamics Using All-Atom Simulations and Kinetic Analysis. <i>Journal of Physical Chemistry B</i> , 2018, 122, 9625-9634.	2.6	11

#	ARTICLE	IF	CITATIONS
5653	Dispersion Correction Alleviates Dye Stacking of Single-Stranded DNA and RNA in Simulations of Single-Molecule Fluorescence Experiments. <i>Journal of Physical Chemistry B</i> , 2018, 122, 11626-11639.	2.6	21
5654	Stability and Structural Analysis of A <sub>6</sub> R Polypeptide Nanosheets: A Theoretical Study Using the Classical Molecular Dynamics Simulation. <i>Journal of Physical Chemistry C</i> , 2018, 122, 24445-24453.	3.1	18
5655	DNA Topoisomerase 1 Structure-BASED Design, Synthesis, Activity Evaluation and Molecular Simulations Study of New 7-Amide Camptothecin Derivatives Against <i>Spodoptera frugiperda</i> . <i>Frontiers in Chemistry</i> , 2018, 6, 456.	3.6	15
5656	A hybrid of mPEG-b-PCL and G1-PEA dendrimer for enhancing delivery of antibiotics. <i>Journal of Controlled Release</i> , 2018, 290, 112-128.	9.9	38
5657	Selective enhancement of auxeticity through changing a diameter of nanochannels in Yukawa systems. <i>Smart Materials and Structures</i> , 2018, 27, 115021.	3.5	11
5658	Hydration and Temperature Response of Water Mobility in Poly(diallyldimethylammonium)â€Poly(sodium 4-styrenesulfonate) Complexes. <i>Macromolecules</i> , 2018, 51, 8268-8277.	4.8	49
5659	Structural insights into the interaction of helicase and primase in <i>Mycobacterium tuberculosis</i> . <i>Biochemical Journal</i> , 2018, 475, 3493-3509.	3.7	5
5660	Mutational analysis of the conserved carboxylates of anion channelrhodopsin-2 (ACR2) expressed in <i>Escherichia coli</i> and their roles in anion transport. <i>Biophysics and Physicobiology</i> , 2018, 15, 179-188.	1.0	9
5661	Loop Motion in Triosephosphate Isomerase Is Not a Simple Open and Shut Case. <i>Journal of the American Chemical Society</i> , 2018, 140, 15889-15903.	13.7	63
5662	In-Situ Fractionation in Liquids-Rich Shales and its Implications for EOR: Experimental Verification and Modeling Study. , 2018, , .		4
5663	Novel Mechanism for Cyclic Dinucleotide Degradation Revealed by Structural Studies of <i>Vibrio</i> Phosphodiesterase V-cGAP3. <i>Journal of Molecular Biology</i> , 2018, 430, 5080-5093.	4.2	13
5664	The Impact of Using Single Atomistic Long-Range Cutoff Schemes with the GROMOS 54A7 Force Field. <i>Journal of Chemical Theory and Computation</i> , 2018, 14, 5823-5833.	5.3	33
5665	Engineering Salt Bridge Networks between Transmembrane Helices Confers Thermostability in G-Protein-Coupled Receptors. <i>Journal of Chemical Theory and Computation</i> , 2018, 14, 6574-6585.	5.3	10
5666	Role of Extracellular Loops and Membrane Lipids for Ligand Recognition in the Neuronal Adenosine Receptor Type 2A: An Enhanced Sampling Simulation Study. <i>Molecules</i> , 2018, 23, 2616.	3.8	13
5667	Exploring the PXR ligand binding mechanism with advanced Molecular Dynamics methods. <i>Scientific Reports</i> , 2018, 8, 16207.	3.3	27
5668	Bayesian calibration of force-fields from experimental data: TIP4P water. <i>Journal of Chemical Physics</i> , 2018, 149, 154110.	3.0	13
5669	Theoretical Study of Alkylsulfonic Acids: Force-Field Development and Molecular Dynamics Simulations. <i>Journal of Physical Chemistry B</i> , 2018, 122, 9747-9756.	2.6	1
5670	Baseline dasabuvir resistance in Hepatitis C virus from the genotypes 1, 2 and 3 and modeling of the NS5B-dasabuvir complex by their silicoapproach. <i>Infection Ecology and Epidemiology</i> , 2018, 8, 1528117.	0.8	5

#	ARTICLE	IF	CITATIONS
5671	<i>c</i> HCN1 <i>i</i> mutation spectrum: from neonatal epileptic encephalopathy to benign generalized epilepsy and beyond. <i>Brain</i> , 2018, 141, 3160-3178.	7.6	96
5672	Discovery of Novel, Drug-Like Ferroptosis Inhibitors with in Vivo Efficacy. <i>Journal of Medicinal Chemistry</i> , 2018, 61, 10126-10140.	6.4	80
5673	User-Tailored Metal-Organic Frameworks as Supports for Carbonic Anhydrase. <i>ACS Applied Materials &amp; Interfaces</i> , 2018, 10, 41326-41337.	8.0	49
5674	Intermolecular Voids in Lipid Bilayers in the Presence of Glycyrrhizic Acid. <i>Journal of Physical Chemistry B</i> , 2018, 122, 9938-9946.	2.6	14
5675	Statistical efficiency of methods for computing free energy of hydration. <i>Journal of Chemical Physics</i> , 2018, 149, 144111.	3.0	16
5676	Rational designing of 8-hydroxyquinolin-imidazolinone-based fluorescent protein mutants with dramatically red shifted emission: A computational study. <i>Journal of Computational Chemistry</i> , 2018, 39, 2307-2315.	3.3	2
5677	Role of thermal expansion heterogeneity in the cryogenic rejuvenation of metallic glasses. <i>JPhys Materials</i> , 2018, 1, 015001.	4.2	10
5678	Phospholipid-Cellulose Interactions: Insight from Atomistic Computer Simulations for Understanding the Impact of Cellulose-Based Materials on Plasma Membranes. <i>Journal of Physical Chemistry B</i> , 2018, 122, 9973-9981.	2.6	9
5679	A molecular dynamics approach towards evaluating osmotic and thermal stress in the extracellular environment. <i>International Journal of Hyperthermia</i> , 2018, 35, 559-567.	2.5	7
5680	Combinatorial Coarse-Graining of Molecular Dynamics Simulations for Detecting Relationships between Local Configurations and Overall Conformations. <i>Journal of Chemical Theory and Computation</i> , 2018, 14, 6026-6034.	5.3	5
5681	Patchy Particle Model of the Hierarchical Self-Assembly of $\pi$ -Conjugated Optoelectronic Peptides. <i>Journal of Physical Chemistry B</i> , 2018, 122, 10219-10236.	2.6	19
5682	Methionine 170 is an Environmentally Sensitive Membrane Anchor in the Disordered HVR of K-Ras4B. <i>Journal of Physical Chemistry B</i> , 2018, 122, 10086-10096.	2.6	22
5683	Folded Structure and Membrane Affinity of the N-Terminal Domain of the Three Human Isoforms of the Mitochondrial Voltage-Dependent Anion-Selective Channel. <i>ACS Omega</i> , 2018, 3, 11415-11425.	3.5	7
5684	Computational Insight Into Vitamin K1 $\gamma$ -Hydroxylation by Cytochrome P450 4F2. <i>Frontiers in Pharmacology</i> , 2018, 9, 1065.	3.5	8
5685	Does $\alpha$ -Tocopherol Flip-Flop Help to Protect Membranes Against Oxidation?. <i>Journal of Physical Chemistry B</i> , 2018, 122, 10362-10370.	2.6	22
5686	Confirmation of Bioinformatics Predictions of the Structural Domains in Honeybee Silk. <i>Polymers</i> , 2018, 10, 776.	4.5	4
5687	Atomistic simulation study of favored compositions of Ni-Nb-Al metallic glasses. <i>Science China Technological Sciences</i> , 2018, 61, 1829-1838.	4.0	6
5688	Comprehensive Understanding of Host- and Guest-Dependent Helix Inversion in Chiral Nematic Liquid Crystals: Experimental and Molecular Dynamics Simulation Study. <i>Journal of Physical Chemistry B</i> , 2018, 122, 10615-10626.	2.6	9

#	ARTICLE	IF	CITATIONS
5689	Intermetallic formation at deeply supercooled Ni/Al multilayer interfaces: A molecular dynamics study. <i>Journal of Applied Physics</i> , 2018, 124, .	2.5	11
5690	Contrasting Effects of Guanidinium Chloride and Urea on the Activity and Unfolding of Lysozyme. <i>ACS Omega</i> , 2018, 3, 14119-14126.	3.5	33
5691	Cryo-EM reveals two distinct serotonin-bound conformations of full-length 5-HT3A receptor. <i>Nature</i> , 2018, 563, 270-274.	27.8	98
5692	Uniaxial-deformation behavior of ice $I_h$ as described by the TIP4P/Ice and mW water models. <i>Journal of Chemical Physics</i> , 2018, 149, 164711.	3.0	11
5693	On the Applicability of Force Fields To Study the Aggregation of Amyloidogenic Peptides Using Molecular Dynamics Simulations. <i>Journal of Chemical Theory and Computation</i> , 2018, 14, 6063-6075.	5.3	68
5694	Evidence for a Partially Stalled $F_1$ Rotor in $F_1F_0$ -ATPase from Hydrogenâ€Deuterium Exchange Experiments and Molecular Dynamics Simulations. <i>Journal of the American Chemical Society</i> , 2018, 140, 14860-14869.	13.7	10
5695	Theoretical Study on Zearalenol Compounds Binding with Wild Type Zearalenone Hydrolase and V153H Mutant. <i>International Journal of Molecular Sciences</i> , 2018, 19, 2808.	4.1	12
5696	Overcoming Convergence Issues in Free-Energy Calculations of Amide-to-Ester Mutations in the Pin1-WW Domain. <i>Journal of Chemical Information and Modeling</i> , 2018, 58, 2305-2318.	5.4	2
5697	Facilitated and Non-Gaussian Diffusion of Cholesterol in Liquid Ordered Phase Bilayers Depends on the Flip-Flop and Spatial Arrangement of Cholesterol. <i>Journal of Physical Chemistry Letters</i> , 2018, 9, 6529-6535.	4.6	14
5698	On the phase diagram of Mackay icosahedra. <i>Journal of Chemical Physics</i> , 2018, 149, 134502.	3.0	1
5699	Lipid Architectonics for Superior Oral Bioavailability of Nelfinavir Mesylate: Comparative in vitro and in vivo Assessment. <i>AAPS PharmSciTech</i> , 2018, 19, 3584-3598.	3.3	9
5700	Self-organization into ferroelectric and antiferroelectric crystals via the interplay between particle shape and dipolar interaction. <i>Proceedings of the National Academy of Sciences of the United States of America</i> , 2018, 115, 9917-9922.	7.1	14
5701	Structural Prediction of the Dimeric Form of the Mammalian Translocator Membrane Protein TSPO: A Key Target for Brain Diagnostics. <i>International Journal of Molecular Sciences</i> , 2018, 19, 2588.	4.1	15
5702	Optimal Hydrophobicity and Reorientation of Amphiphilic Peptides Translocating through Membrane. <i>Biophysical Journal</i> , 2018, 115, 1045-1054.	0.5	29
5703	Selective reduction in glutaminase activity of Asparaginase by asparagine 248 to serine mutation: A combined computational and experimental effort in blood cancer treatment. <i>International Journal of Biological Macromolecules</i> , 2018, 120, 2448-2457.	7.5	21
5704	Glyceryl Monostearate: Probing the Self Assembly of a Lipid Amenable To Surface Modification for Hepatic Targeting. <i>Journal of Physical Chemistry C</i> , 2018, 122, 22160-22169.	3.1	4
5705	Percolation in supercritical water: Do the Widom and percolation lines coincide?. <i>Journal of Chemical Physics</i> , 2018, 149, 084504.	3.0	23
5706	A molecular dynamics study of adenylyl cyclase: The impact of ATP and G-protein binding. <i>PLoS ONE</i> , 2018, 13, e0196207.	2.5	19

#	ARTICLE	IF	CITATIONS
5707	Determination of Ionic Hydration Free Energies with Grand Canonical Monte Carlo/Molecular Dynamics Simulations in Explicit Water. <i>Journal of Chemical Theory and Computation</i> , 2018, 14, 5290-5302.	5.3	17
5708	Structure of the mechanosensitive OSCA channels. <i>Nature Structural and Molecular Biology</i> , 2018, 25, 850-858.	8.2	133
5709	An efficient Bayesian kinetic lumping algorithm to identify metastable conformational states via Gibbs sampling. <i>Journal of Chemical Physics</i> , 2018, 149, 072337.	3.0	25
5710	Guest Occupation Effects on the Transition of Crystalline Syndiotactic Polystyrene: Selection Criteria for Fundamental Structures $\beta$ and $\beta'$ . <i>Macromolecular Theory and Simulations</i> , 2018, 27, 1800039.	1.4	1
5711	Decoding the antineoplastic efficacy of Aplysin targeting Bcl-2: A de novo perspective. <i>Computational Biology and Chemistry</i> , 2018, 77, 390-401.	2.3	2
5712	A rationally designed JAZ subtype-selective agonist of jasmonate perception. <i>Nature Communications</i> , 2018, 9, 3654.	12.8	47
5713	The variation of mitochondrial NADH dehydrogenase subunit 4 (mtND4) and molecular dynamics simulation of SNPs among Iranian women with breast cancer. <i>Journal of Molecular Graphics and Modelling</i> , 2018, 85, 242-249.	2.4	3
5714	Structure, Dynamics, and Apparent Glass Transition of Stereoregular Poly(methyl) Tj ETQq1 1 0.784314 rgBT /Overlock 10 Tf 50 462 7d	4.8	31
5715	Thermodynamics of solid Sn and Pb Sn liquid mixtures using molecular dynamics simulations. <i>Acta Materialia</i> , 2018, 161, 320-330.	7.9	23
5716	Effect of late endosomal DOBMP lipid and traditional model lipids of electrophysiology on the anthrax toxin channel activity. <i>Biochimica Et Biophysica Acta - Biomembranes</i> , 2018, 1860, 2192-2203.	2.6	4
5717	FIH permits NAA10 to catalyze the oxygen-dependent lysyl-acetylation of HIF-1 $\alpha$ . <i>Redox Biology</i> , 2018, 19, 364-374.	9.0	22
5718	Molecular Insights into Human Hereditary Apolipoprotein A-I Amyloidosis Caused by the Glu34Lys Mutation. <i>Biochemistry</i> , 2018, 57, 5738-5747.	2.5	9
5719	Predicting polymorphism in molecular crystals using orientational entropy. <i>Proceedings of the National Academy of Sciences of the United States of America</i> , 2018, 115, 10251-10256.	7.1	57
5720	Assessment of mutation probabilities of KRAS G12 missense mutants and their long-timescale dynamics by atomistic molecular simulations and Markov state modeling. <i>PLoS Computational Biology</i> , 2018, 14, e1006458.	3.2	59
5721	Testing for physical validity in molecular simulations. <i>PLoS ONE</i> , 2018, 13, e0202764.	2.5	30
5722	Predicting Thermodynamic Properties of Alkanes by High-Throughput Force Field Simulation and Machine Learning. <i>Journal of Chemical Information and Modeling</i> , 2018, 58, 2502-2516.	5.4	23
5723	Monolayer Crystal Structure of the Organic Semiconductor 7-Decyl-2-phenyl[1]benzothieno[3,2- <i>b</i> ][1]benzothiophene. <i>Journal of Physical Chemistry C</i> , 2018, 122, 22225-22231.	3.1	18
5724	Conformations of Poly-L-lysine Molecules in Electrolyte Solutions: Modeling and Experimental Measurements. <i>Journal of Physical Chemistry C</i> , 2018, 122, 23180-23190.	3.1	23

#	ARTICLE	IF	CITATIONS
5725	Site-Mutation of Hydrophobic Core Residues Synchronically Poise Super Interleukin 2 for Signaling: Identifying Distant Structural Effects through Affordable Computations. International Journal of Molecular Sciences, 2018, 19, 916.	4.1	2
5726	Glucosylceramide modifies the LPS-induced inflammatory response in macrophages and the orientation of the LPS/TLR4 complex in silico. Scientific Reports, 2018, 8, 13600.	3.3	33
5727	Salt Bridge in Aqueous Solution: Strong Structural Motifs but Weak Enthalpic Effect. Scientific Reports, 2018, 8, 13626.	3.3	41
5728	Insights into the role of electrostatics in temperature adaptation: a comparative study of psychrophilic, mesophilic, and thermophilic subtilisin-like serine proteases. RSC Advances, 2018, 8, 29698-29713.	3.6	20
5729	<sup>195</sup> Pt NMR and Molecular Dynamics Simulation Study of the Solvation of [PtCl <sub>6</sub> ] <sup>2-</sup> in Water-Methanol and Water-Dimethoxyethane Binary Mixtures. Inorganic Chemistry, 2018, 57, 12025-12037.	4.0	6
5730	Biomolecular Simulations of Halogen Bonds with a GROMOS Force Field. Journal of Chemical Theory and Computation, 2018, 14, 5383-5392.	5.3	20
5731	Layer-Stacking-Driven Fluorescence in a Two-Dimensional Imine-Linked Covalent Organic Framework. Journal of the American Chemical Society, 2018, 140, 12922-12929.	13.7	147
5732	Mapping the Interface of a GPCR Dimer: A Structural Model of the A2A Adenosine and D2 Dopamine Receptor Heteromer. Frontiers in Pharmacology, 2018, 9, 829.	3.5	62
5733	Effect of Anionic Structure on the LCST Phase Behavior of Phosphonium Ionic Liquids in Water. Industrial & Engineering Chemistry Research, 2018, 57, 12935-12941.	3.7	19
5734	Amorphous silicon hexaboride: a first-principles study. Philosophical Magazine, 2018, 98, 2723-2733.	1.6	3
5735	A Luminal Loop of Wilson Disease Protein Binds Copper and Is Required for Protein Activity. Biophysical Journal, 2018, 115, 1007-1018.	0.5	3
5736	Disulfide bridge formation to increase thermostability of DFPase enzyme: A computational study. Computational Biology and Chemistry, 2018, 77, 272-278.	2.3	6
5737	Can Arginine Inhibit Insulin Aggregation? A Combined Protein Crystallography, Capillary Electrophoresis, and Molecular Simulation Study. Journal of Physical Chemistry B, 2018, 122, 10069-10076.	2.6	28
5738	Molecular dynamics study of the effect of inorganic salts on the monolayer of four surfactants at the oil/water interface. Journal of Dispersion Science and Technology, 2018, 39, 1758-1766.	2.4	10
5739	Understanding the antimicrobial activity of water soluble $\beta$ -cyclodextrin/alamethicin complex. Colloids and Surfaces B: Biointerfaces, 2018, 172, 451-458.	5.0	14
5740	Molecular dynamics modeling of <i>Pseudomonas aeruginosa</i> outer membranes. Physical Chemistry Chemical Physics, 2018, 20, 23635-23648.	2.8	27
5741	Influence of pH and Salts on Partial Molar Volume of Lysozyme and Bovine Serum Albumin in Aqueous Solutions. Chemical Engineering and Technology, 2018, 41, 2337-2345.	1.5	2
5742	Distribution of zwitter-ionic tryptophan between the micelles of 1-dodecyl-3-methyl imidazolium and aqueous medium from molecular dynamic simulation. Physical Chemistry Chemical Physics, 2018, 20, 23747-23753.	2.8	0



#	ARTICLE	IF	CITATIONS
5743	Modeling of solid-liquid interfaces using scaled charges: rutile (110) surfaces. <i>Physical Chemistry Chemical Physics</i> , 2018, 20, 23954-23966.	2.8	29
5744	Assessment and optimization of collective variables for protein conformational landscape: GB1 $\alpha$ -hairpin as a case study. <i>Journal of Chemical Physics</i> , 2018, 149, 094101.	3.0	26
5745	A Martini coarse-grained model of the calcein fluorescent dye. <i>Journal Physics D: Applied Physics</i> , 2018, 51, 384002.	2.8	20
5746	Monolayer and Bilayer Structures of Mixtures of Ceramide IIIb and c16-Alkyl Glucosides. <i>Bulletin of the Korean Chemical Society</i> , 2018, 39, 982-987.	1.9	0
5747	Abietane-Type Diterpenoids Inhibit Protein Tyrosine Phosphatases by Stabilizing an Inactive Enzyme Conformation. <i>Biochemistry</i> , 2018, 57, 5886-5896.	2.5	20
5748	Molecular Dynamics Study of an Atactic Poly(methyl methacrylate)-Carbon Nanotube Nanocomposite. <i>Journal of Physical Chemistry B</i> , 2018, 122, 9007-9021.	2.6	21
5749	K <sup>+</sup> binding and proton redistribution in the E2P state of the H <sup>+</sup> , K <sup>+</sup> -ATPase. <i>Scientific Reports</i> , 2018, 8, 12732.	3.3	13
5750	Binary mixtures of novel sulfoxides and water: intermolecular structure, dynamic properties, thermodynamics, and cluster analysis. <i>Physical Chemistry Chemical Physics</i> , 2018, 20, 23754-23761.	2.8	20
5751	<i>In silico</i> stress-strain measurements on self-assembled protein lattices. <i>Soft Matter</i> , 2018, 14, 8095-8104.	2.7	2
5752	Allosterism and signal transfer in DNA. <i>Nucleic Acids Research</i> , 2018, 46, 7554-7565.	14.5	30
5753	Structural Lipids Enable the Formation of Functional Oligomers of the Eukaryotic Purine Symporter UapA. <i>Cell Chemical Biology</i> , 2018, 25, 840-848.e4.	5.2	64
5754	Spreading and orientation of silver nano-drops over a flat graphene substrate: An atomistic investigation. <i>Carbon</i> , 2018, 138, 26-41.	10.3	10
5755	Multi experimental and computational studies for DNA and HSA interaction of new nano-scale ultrasound-assisted synthesized Pd(II) complex as a potent anticancer drug. <i>Journal of Molecular Liquids</i> , 2018, 264, 386-397.	4.9	14
5757	Rotational Dynamics of Proteins from Spin Relaxation Times and Molecular Dynamics Simulations. <i>Journal of Physical Chemistry B</i> , 2018, 122, 6559-6569.	2.6	26
5758	Mechanisms of Aggregation-Induced Emission and Photo/Thermal E/Z Isomerization of a Cyanostilbene Derivative: Theoretical Insights. <i>Journal of Physical Chemistry C</i> , 2018, 122, 12434-12440.	3.1	37
5759	Protein kinase C $\pm$ gain-of-function variant in Alzheimer's disease displays enhanced catalysis by a mechanism that evades down-regulation. <i>Proceedings of the National Academy of Sciences of the United States of America</i> , 2018, 115, E5497-E5505.	7.1	34
5760	A Dehydrogenase Dual Hydrogen Abstraction Mechanism Promotes Estrogen Biosynthesis: Can We Expand the Functional Annotation of the Aromatase Enzyme?. <i>Chemistry - A European Journal</i> , 2018, 24, 10840-10849.	3.3	31
5761	Computational discovery of potent drugs to improve the treatment of pyrazinamide resistant <i>Mycobacterium tuberculosis</i> mutants. <i>Journal of Cellular Biochemistry</i> , 2018, 119, 7328-7338.	2.6	3

#	ARTICLE	IF	CITATIONS
5762	Influence of the anion on the properties of ionic liquid mixtures: a molecular dynamics study. <i>Physical Chemistry Chemical Physics</i> , 2018, 20, 14899-14918.	2.8	40
5763	Mounting evidence validates Ursolic Acid directly activates SIRT1: A powerful STAC which mimic endogenous activator of SIRT1. <i>Archives of Biochemistry and Biophysics</i> , 2018, 650, 39-48.	3.0	14
5764	Escherichia coli AlkB and single-stranded DNA binding protein SSB interaction explored by Molecular Dynamics Simulation. <i>Journal of Molecular Graphics and Modelling</i> , 2018, 84, 29-35.	2.4	7
5765	Softly-confined water cluster between freestanding graphene sheets. <i>AIP Conference Proceedings</i> , 2018, , .	0.4	0
5766	Molecular dynamics simulation for desulphurization of hydrocarbon fuel using ionic liquids. <i>Journal of Molecular Liquids</i> , 2018, 264, 490-498.	4.9	16
5767	Exploring Cryptic Pockets Formation in Targets of Pharmaceutical Interest with SWISH. <i>Journal of Chemical Theory and Computation</i> , 2018, 14, 3321-3331.	5.3	45
5768	Effect of Cholesterol on Membrane Dipole Potential: Atomistic and Coarse-Grained Molecular Dynamics Simulations. <i>Journal of Chemical Theory and Computation</i> , 2018, 14, 3780-3795.	5.3	14
5769	Spontaneous insertion of GPI anchors into cholesterol-rich membrane domains. <i>AIP Advances</i> , 2018, 8, 055210.	1.3	4
5770	A rationally designed NRP1-independent superagonist SEMA3A mutant is an effective anticancer agent. <i>Science Translational Medicine</i> , 2018, 10, .	12.4	46
5771	Structural analysis, molecular docking and molecular dynamics of an edematogenic lectin from <i>Centrobium microchaete</i> seeds. <i>International Journal of Biological Macromolecules</i> , 2018, 117, 124-133.	7.5	12
5772	Distinct hydrophobicâ€“hydrophilic dual interactions occurring in the clathrate hydrates of 3,3-dimethyl-1-butanol with help gases. <i>Chemical Engineering Journal</i> , 2018, 348, 583-591.	12.7	11
5773	Compound CID 9998128 Is a Potential Multitarget Drug for Alzheimerâ€™s Disease. <i>ACS Chemical Neuroscience</i> , 2018, 9, 2588-2598.	3.5	17
5774	Ionâ€“ion interactions in the denatured state contribute to the stabilization of CutA1 proteins. <i>Scientific Reports</i> , 2018, 8, 7613.	3.3	6
5775	Membrane potential and dynamics in a ternary lipid mixture: insights from molecular dynamics simulations. <i>Physical Chemistry Chemical Physics</i> , 2018, 20, 15841-15851.	2.8	10
5776	Influence of loading directions on dislocation slip mechanism of nanotwinned Ni with void defect at the twin boundary. <i>Computational Materials Science</i> , 2018, 152, 1-11.	3.0	18
5777	Regulation of Shigella Effector Kinase OspG through Modulation of Its Dynamic Properties. <i>Journal of Molecular Biology</i> , 2018, 430, 2096-2112.	4.2	8
5778	Forward-flux sampling with jumpy order parameters. <i>Journal of Chemical Physics</i> , 2018, 149, 072303.	3.0	38
5779	Molecular dynamics simulations of liquid silica crystallization. <i>Proceedings of the National Academy of Sciences of the United States of America</i> , 2018, 115, 5348-5352.	7.1	78

#	ARTICLE	IF	CITATIONS
5780	Network analysis of a proposed exit pathway for protons to the P-side of cytochrome c oxidase. <i>Biochimica Et Biophysica Acta - Bioenergetics</i> , 2018, 1859, 997-1005.	1.0	35
5781	Consistent Prediction of Mutation Effect on Drug Binding in HIV-1 Protease Using Alchemical Calculations. <i>Journal of Chemical Theory and Computation</i> , 2018, 14, 3397-3408.	5.3	24
5782	Understanding the Role of Hydrophobic Terminal in the Hydrogen Bond Network of the Aqueous Mixture of 2,2,2-Trifluoroethanol: IR, Molecular Dynamics, Quantum Chemical as Well as Atoms in Molecules Studies. <i>Journal of Physical Chemistry B</i> , 2018, 122, 6616-6626.	2.6	10
5783	Intrinsically disordered protein-specific force field <sc>CHARMM</sc> 36 <sc>IDPSFF</sc>. <i>Chemical Biology and Drug Design</i> , 2018, 92, 1722-1735.	3.2	62
5784	Vibrational and thermoelastic properties of bcc iron from selected EAM potentials. <i>Computational Materials Science</i> , 2018, 152, 99-106.	3.0	8
5785	Direct observation of deformation twinning under stress gradient in body-centered cubic metals. <i>Acta Materialia</i> , 2018, 155, 56-68.	7.9	37
5786	Synthesis, crystal structure and antimicrobial potential of some fluorinated chalcone-1,2,3-triazole conjugates. <i>European Journal of Medicinal Chemistry</i> , 2018, 155, 263-274.	5.5	96
5787	Coarse-Grained Molecular Simulation and Nonlinear Manifold Learning of Archipelago Asphaltene Aggregation and Folding. <i>Journal of Physical Chemistry B</i> , 2018, 122, 6627-6647.	2.6	18
5788	On-the-Fly Specifications of Reaction Coordinates in Parallel Cascade Selection Molecular Dynamics Accelerate Conformational Transitions of Proteins. <i>Journal of Chemical Theory and Computation</i> , 2018, 14, 3332-3341.	5.3	9
5789	Faster Simulations with a 5 fs Time Step for Lipids in the CHARMM Force Field. <i>Journal of Chemical Theory and Computation</i> , 2018, 14, 3342-3350.	5.3	34
5790	Structural and biological evaluation of halogen derivatives of 1,9-pyrazoloanthrones towards the design of a specific potent inhibitor of c-Jun-N-terminal kinase (JNK). <i>New Journal of Chemistry</i> , 2018, 42, 10651-10660.	2.8	3
5791	Effect of alkaline metal cations on the ionic structure of cryolite melts: <i>Ab-initio</i> NpT MD study. <i>Journal of Chemical Physics</i> , 2018, 148, 064501.	3.0	8
5792	Exploring the effect of pendent side chain length on the structural and mechanical properties of hydrated perfluorosulfonic acid polymer membranes by molecular dynamics simulation. <i>Polymer</i> , 2018, 146, 53-62.	3.8	33
5793	Nitrobenzoxadiazole-Appended Cell Membrane Modifiers for Efficient Optoporation with Noncoherent Light. <i>Bioconjugate Chemistry</i> , 2018, 29, 2068-2073.	3.6	8
5794	Prediction of Binding Energy of Keap1 Interaction Motifs in the Nrf2 Antioxidant Pathway and Design of Potential High-Affinity Peptides. <i>Journal of Physical Chemistry B</i> , 2018, 122, 5851-5859.	2.6	17
5795	Hybrid Computational Strategy for Predicting CO<sub>2</sub> Solubilities in Reactive Ionic Liquids. <i>Journal of Physical Chemistry C</i> , 2018, 122, 14213-14221.	3.1	11
5796	Similarity Between Amorphous and Crystalline Phases: The Case of TiO<sub>2</sub>. <i>Journal of Physical Chemistry Letters</i> , 2018, 9, 2985-2990.	4.6	78
5797	SHS in Ni/Al Nanofolds: A Review of Experiments and Molecular Dynamics Simulations. <i>Advanced Engineering Materials</i> , 2018, 20, 1800091.	3.5	38

#	ARTICLE	IF	CITATIONS
5798	Temperature Transferability of Force Field Parameters for Dispersion Interactions. Journal of Chemical Theory and Computation, 2018, 14, 3595-3602.	5.3	14
5799	Activation of Toll-like receptors nucleates assembly of the MyDDosome signaling hub. ELife, 2018, 7, .	6.0	83
5800	Refined Alkali Metal Ion Parameters for the OPC Water Model. Bulletin of the Korean Chemical Society, 2018, 39, 931-935.	1.9	0
5801	The FapF Amyloid Secretion Transporter Possesses an Atypical Asymmetric Coiled Coil. Journal of Molecular Biology, 2018, 430, 3863-3871.	4.2	22
5802	The role of the jaw subdomain of peptidoglycan glycosyltransferases for lipid II polymerization. Cell Surface, 2018, 2, 54-66.	3.0	8
5803	Photoprogramming Allostery in Human Serum Albumin. Bioconjugate Chemistry, 2018, 29, 2215-2224.	3.6	3
5804	Investigating Polyoxometalate-Protein Interactions at Chemically Distinct Binding Sites. Journal of Physical Chemistry B, 2018, 122, 7219-7232.	2.6	27
5805	Transferable MARTINI Model of Poly(ethylene Oxide). Journal of Physical Chemistry B, 2018, 122, 7436-7449.	2.6	99
5806	Interaction between the barley allelochemical compounds gramine and hordenine and artificial lipid bilayers mimicking the plant plasma membrane. Scientific Reports, 2018, 8, 9784.	3.3	23
5807	Dynamics of loops at the substrate entry channel determine the specificity of iridoid synthases. FEBS Letters, 2018, 592, 2624-2635.	2.8	1
5808	Temperature-induced collapse of a disordered peptide observed by three sampling methods in molecular dynamics simulations. Journal of Chemical Physics, 2018, 149, 072313.	3.0	19
5809	Stress-stress fluctuation formula for elastic constants in the $\langle \text{mml:math xmlns:mml="http://www.w3.org/1998/Math/MathML">\langle \text{mml:mi mathvariant="italic">NPT}\langle \text{mml:mi}>\langle \text{mml:math}>\text{ensemble. Physical Review E, 2018, 97, 053002.}$	2.1	4
5810	Effect of Ca <sup>2+</sup> on the promiscuous target-protein binding of calmodulin. PLoS Computational Biology, 2018, 14, e1006072.	3.2	42
5811	Acyl chain asymmetry and polyunsaturation of brain phospholipids facilitate membrane vesiculation without leakage. ELife, 2018, 7, .	6.0	111
5812	Modulation of cellular membrane properties as a potential therapeutic strategy to counter lipointoxication in obstructive pulmonary diseases. Biochimica Et Biophysica Acta - Molecular Basis of Disease, 2018, 1864, 3069-3084.	3.8	12
5813	Formulation and Molecular Dynamics Simulations of a Fusidic Acid Nanosuspension for Simultaneously Enhancing Solubility and Antibacterial Activity. Molecular Pharmaceutics, 2018, 15, 3512-3526.	4.6	45
5814	Integration of external electric fields in molecular dynamics simulation models for resistive switching devices. Journal of Applied Physics, 2018, 123, .	2.5	13
5815	Structural Events in a Bacterial Uniporter Leading to Translocation of Glucose to the Cytosol. Journal of Molecular Biology, 2018, 430, 3337-3352.	4.2	7

#	ARTICLE	IF	CITATIONS
5816	Molecular dynamics simulations of a DMSO/water mixture using the AMBER force field. Journal of Molecular Modeling, 2018, 24, 174.	1.8	11
5817	Macroscopic Elastic Properties of Nonbonded Wavy Carbon Nanotube Composites. , 2018, , 479-501.		0
5818	Evolution of nanostructure and mechanical properties of silver nano-particle in the confined region between graphene sheets: An atomistic investigation. Computational Materials Science, 2018, 152, 393-407.	3.0	8
5819	Wettability and Structural Evolution of Gold over a Single-Walled Carbon Nanotube: An Atomistic Investigation. Journal of Physical Chemistry C, 2018, 122, 16346-16355.	3.1	2
5820	Fluorinated Copolymer Functionalized with Ethylene Oxide as Novel Water-Borne Binder for a High-Power Lithium Ion Battery: Synthesis, Mechanism, and Application. ACS Applied Energy Materials, 2018, 1, 3999-4008.	5.1	10
5821	A description of hydroquinone clathrates using molecular dynamics: Molecular model and crystalline structures for CH <sub>4</sub> and CO <sub>2</sub> guests. Journal of Chemical Physics, 2018, 148, 244502.	3.0	10
5822	First-principles study of the stability and edge stress of nitrogen-decorated graphene nanoribbons. Physical Review B, 2018, 97, .	3.2	4
5823	Fluid Phase Coexistence in Biological Membrane: Insights from Local Nonaffine Deformation of Lipids. Biophysical Journal, 2018, 115, 117-128.	0.5	16
5824	HIV-1 Env gp41 Transmembrane Domain Dynamics Are Modulated by Lipid, Water, and Ion Interactions. Biophysical Journal, 2018, 115, 84-94.	0.5	13
5825	Local low dose curcumin treatment improves functional recovery and remyelination in a rat model of sciatic nerve crush through inhibition of oxidative stress. Neuropharmacology, 2018, 139, 98-116.	4.1	51
5826	Covalency is Frustrating: La <sub>2</sub> Sn <sub>2</sub> O <sub>7</sub> and the Nature of Bonding in Pyrochlores under High Pressure–Temperature Conditions. Inorganic Chemistry, 2018, 57, 15051-15061.	4.0	10
5827	Dynamics and Thermodynamics of Transthyretin Association from Molecular Dynamics Simulations. BioMed Research International, 2018, 2018, 1-14.	1.9	9
5828	Specific ion effects for polyelectrolytes in aqueous and non-aqueous media: the importance of the ion solvation behavior. Soft Matter, 2018, 14, 6243-6255.	2.7	27
5829	Investigation of the effect of homocysteinylation of substance P on its binding to the NK1 receptor using molecular dynamics simulation. Journal of Molecular Modeling, 2018, 24, 177.	1.8	5
5830	A residue of motif III positions the helicase domains of motor subunit HsdR in restriction-modification enzyme EcoR124I. Journal of Molecular Modeling, 2018, 24, 176.	1.8	4
5831	Pharmacological characterization of the neurotrophic sesquiterpene jiadifenolide reveals a non-convulsant signature and potential for progression in neurodegenerative disease studies. Biochemical Pharmacology, 2018, 155, 61-70.	4.4	17
5832	Molecular Mechanism of Lipid Nanodisk Formation by Styrene-Maleic Acid Copolymers. Biophysical Journal, 2018, 115, 494-502.	0.5	64
5833	Synthesis of bismuth telluride nanotubes and their simulated thermal properties. Superlattices and Microstructures, 2018, 122, 587-595.	3.1	8

#	ARTICLE	IF	CITATIONS
5834	Molecular Insight into Drug-Loading Capacity of PEG-PLGA Nanoparticles for Itraconazole. <i>Journal of Physical Chemistry B</i> , 2018, 122, 7080-7090.	2.6	60
5835	Proline hydroxylation at different sites in hypoxia-inducible factor 1 $\alpha$ modulates its interactions with the von Hippel-Lindau tumor suppressor protein. <i>Physical Chemistry Chemical Physics</i> , 2018, 20, 18756-18765.	2.8	7
5836	Lipid extraction by boron nitride nanosheets from liquid-ordered and liquid-disordered nanodomains. <i>Nanoscale</i> , 2018, 10, 14073-14081.	5.6	6
5837	Generic parameters of trajectory-extending kinetic Monte Carlo for calculating diffusion coefficients. <i>AIP Advances</i> , 2018, 8, 065311.	1.3	3
5838	Force Field Benchmark of Amino Acids. 2. Partition Coefficients between Water and Organic Solvents. <i>Journal of Chemical Information and Modeling</i> , 2018, 58, 1669-1681.	5.4	33
5839	Damage characterization of (U,Pu)O <sub>2</sub> under irradiation by molecular dynamics simulations. <i>Journal of Nuclear Materials</i> , 2018, 512, 440-449.	2.7	27
5840	Molecular Dynamics Simulations to Study Drug Delivery Systems. , 0, , .		10
5841	A Multiscale Molecular Dynamics and Coupling with Nonlinear Finite Element Method. <i>Springer Proceedings in Mathematics and Statistics</i> , 2018, , 215-244.	0.2	1
5842	Changes in soybean trypsin inhibitor by varying pressure and temperature of processing: A molecular modeling study. <i>Innovative Food Science and Emerging Technologies</i> , 2018, 49, 31-40.	5.6	12
5843	Insights into the Mechanism of Antimicrobial Activity of Seven-Residue Peptides. <i>Journal of Medicinal Chemistry</i> , 2018, 61, 7614-7629.	6.4	19
5844	Temperature-Induced Collapse of Elastin-like Peptides Studied by 2DIR Spectroscopy. <i>Journal of Physical Chemistry B</i> , 2018, 122, 8243-8254.	2.6	12
5845	Nanometer-scale gradient atomic packing structure surrounding soft spots in metallic glasses. <i>Npj Computational Materials</i> , 2018, 4, .	8.7	37
5846	Molecular recognition of bio-active flavonoids quercetin and rutin by bovine hemoglobin: an overview of the binding mechanism, thermodynamics and structural aspects through multi-spectroscopic and molecular dynamics simulation studies. <i>Physical Chemistry Chemical Physics</i> , 2018, 20, 21668-21684.	2.8	76
5847	Membrane partition of bis-(3-hydroxy-4-pyridinonato) zinc(ii) complexes revealed by molecular dynamics simulations. <i>RSC Advances</i> , 2018, 8, 27081-27090.	3.6	4
5848	Computational methodology for solubility prediction: Application to sparingly soluble organic/inorganic materials. <i>Journal of Chemical Physics</i> , 2018, 149, 054102.	3.0	23
5849	Trehalose 6-phosphate phosphatases of <i>Pseudomonas aeruginosa</i> . <i>FASEB Journal</i> , 2018, 32, 5470-5482.	0.5	9
5850	GRAIL: GRids of phArmaphore Interaction fieldS. <i>Journal of Chemical Theory and Computation</i> , 2018, 14, 4958-4970.	5.3	15
5851	Dynamics with Explicit Solvation Reveals Formation of the Prereactive Dimer as Sole Determining Factor for the Efficiency of Ru(bda)L <sub>2</sub> Catalysts. <i>ACS Catalysis</i> , 2018, 8, 8642-8648.	11.2	30



#	ARTICLE	IF	CITATIONS
5852	Aromatic Rings Commonly Used in Medicinal Chemistry: Force Fields Comparison and Interactions With Water Toward the Design of New Chemical Entities. <i>Frontiers in Pharmacology</i> , 2018, 9, 395.	3.5	40
5853	PackMem: A Versatile Tool to Compute and Visualize Interfacial Packing Defects in Lipid Bilayers. <i>Biophysical Journal</i> , 2018, 115, 436-444.	0.5	57
5854	Spectroscopic and Molecular Dynamics Simulation Study of Lysozyme in the Aqueous Mixture of Ethanol: Insights into the Nonmonotonic Change of the Structure of Lysozyme. <i>Journal of Physical Chemistry B</i> , 2018, 122, 7811-7820.	2.6	9
5855	Biosolvation Nature of Ionic Liquids: Molecular Dynamics Simulation of Methylated Nucleobases in Hydrated 1-Ethyl-3-methylimidazolium Acetate. <i>ACS Omega</i> , 2018, 3, 8344-8354.	3.5	14
5856	In Vitro Antibacterial Activity of Teixobactin Derivatives on Clinically Relevant Bacterial Isolates. <i>Frontiers in Microbiology</i> , 2018, 9, 1535.	3.5	25
5857	Two-Dimensional Phosphorus Carbide Polymorphs: Influence of Structural Motifs on the Band Gap. <i>Physica Status Solidi (B): Basic Research</i> , 2018, 255, 1800192.	1.5	4
5858	A molecular dynamics framework to explore the structure and dynamics of layered double hydroxides. <i>Applied Clay Science</i> , 2018, 163, 164-177.	5.2	27
5859	Degradable Carbon Dots with Broad-Spectrum Antibacterial Activity. <i>ACS Applied Materials &amp; Interfaces</i> , 2018, 10, 26936-26946.	8.0	246
5860	Atomistic insights into the exothermic self-sustained alloying of Al-shell/Ni-core nanoparticle triggered by laser irradiation. <i>Physical Chemistry Chemical Physics</i> , 2018, 20, 20398-20405.	2.8	5
5861	Investigating the role of non-covalent interactions in conformation and assembly of triazine-based sequence-defined polymers. <i>Journal of Chemical Physics</i> , 2018, 149, 072330.	3.0	7
5862	A polarizable MARTINI model for monovalent ions in aqueous solution. <i>Journal of Chemical Physics</i> , 2018, 149, 163319.	3.0	32
5863	Interaction of the human erythrocyte Band 3 anion exchanger 1 (AE1, SLC4A1) with lipids and glycophorin A: Molecular organization of the Wright (Wr) blood group antigen. <i>PLoS Computational Biology</i> , 2018, 14, e1006284.	3.2	37
5864	Development and Validation of Quantum Mechanically Derived Force-Fields: Thermodynamic, Structural, and Vibrational Properties of Aromatic Heterocycles. <i>Journal of Chemical Theory and Computation</i> , 2018, 14, 4884-4900.	5.3	26
5865	Simulation of Mixed Self-Assembled Monolayers on Gold: Effect of Terminal Alkyl Anchor Chain and Monolayer Composition. <i>Journal of Physical Chemistry B</i> , 2018, 122, 7699-7710.	2.6	12
5866	A spin-1 representation for dual-funnel energy landscapes. <i>Journal of Chemical Physics</i> , 2018, 149, 035101.	3.0	2
5867	Crystal structure of the retroviral protease-like domain of a protozoal DNA damage-inducible 1 protein. <i>FEBS Open Bio</i> , 2018, 8, 1379-1394.	2.3	9
5868	Disorder guides domain rearrangement in elongation factor Tu. <i>Proteins: Structure, Function and Bioinformatics</i> , 2018, 86, 1037-1046.	2.6	16
5869	A coarse-grained approach to studying the interactions of the antimicrobial peptides aurein 1.2 and maculatin 1.1 with POPC/POPE lipid mixtures. <i>Journal of Molecular Modeling</i> , 2018, 24, 208.	1.8	12

#	ARTICLE	IF	CITATIONS
5870	Computational approach to unravel the impact of missense mutations of proteins (D2HGDH and IDH2) causing D-2-hydroxyglutaric aciduria 2. <i>Metabolic Brain Disease</i> , 2018, 33, 1699-1710.	2.9	38
5871	Large-scale ab initio simulations for periodic system. <i>Computer Physics Communications</i> , 2018, 233, 78-83.	7.5	23
5872	Physicochemical properties and formation mechanism of electrostatic complexes based on $\hat{\mu}$ -polylysine and whey protein: Experimental and molecular dynamics simulations study. <i>International Journal of Biological Macromolecules</i> , 2018, 118, 2208-2215.	7.5	22
5873	The effect of reactive oxygen and nitrogen species on the structure of cytoglobin: A potential tumor suppressor. <i>Redox Biology</i> , 2018, 19, 1-10.	9.0	31
5874	Carbamylation promotes amyloidogenesis and induces structural changes in Tau-core hexapeptide fibrils. <i>Biochimica Et Biophysica Acta - General Subjects</i> , 2018, 1862, 2590-2604.	2.4	24
5875	Substrate-Dependent Morphology and Its Effect on Electrical Mobility of Doped Poly(3,4-ethylenedioxythiophene) (PEDOT) Thin Films. <i>ACS Applied Materials &amp; Interfaces</i> , 2018, 10, 29115-29126.	8.0	34
5876	Mechanistic role of nucleobases in self-cleavage catalysis of hairpin ribozyme at ambient <i>versus</i> high-pressure conditions. <i>Physical Chemistry Chemical Physics</i> , 2018, 20, 20886-20898.	2.8	6
5877	The Effect of Alkaline Cations on the Intercalation of Carbon Dioxide in Sepiolite Minerals: A Molecular Dynamics Investigation. <i>Frontiers in Materials</i> , 2018, 5, .	2.4	2
5878	Cues to Opening Mechanisms From in Silico Electric Field Excitation of Cx26 Hemichannel and in Vitro Mutagenesis Studies in HeLa Transfectans. <i>Frontiers in Molecular Neuroscience</i> , 2018, 11, 170.	2.9	26
5879	Molecular dynamics study of TMPA mediated dissociation of Nur77-LKB1 complex. <i>Computational Biology and Chemistry</i> , 2018, 76, 67-78.	2.3	6
5880	Force-induced structural changes in non-sulfated carrageenan based oligosaccharides â€“ a theoretical study. <i>Soft Matter</i> , 2018, 14, 6264-6277.	2.7	9
5881	Ionic Liquids Treated within the Grand Canonical Adaptive Resolution Molecular Dynamics Technique. <i>Computation</i> , 2018, 6, 23.	2.0	3
5882	Interaction of Edge Dislocations with Graphene Nanosheets in Graphene/Fe Composites. <i>Crystals</i> , 2018, 8, 160.	2.2	24
5883	Direct observation of pseudocapacitive sodium storage behavior in molybdenum dioxide anodes. <i>Journal of Power Sources</i> , 2018, 397, 113-123.	7.8	10
5884	Understanding the indirect DNA read-out specificity of I-Crel Meganuclease. <i>Scientific Reports</i> , 2018, 8, 10286.	3.3	12
5885	Computational modelling approaches as a potential platform to understand the molecular genetics association between Parkinsonâ€™s and Gaucher diseases. <i>Metabolic Brain Disease</i> , 2018, 33, 1835-1847.	2.9	31
5886	Molecular dynamics study of racemic mixtures: Solutions of ibuprofen and $\hat{I}^2$ -cyclodextrin in methanol. <i>Journal of Molecular Liquids</i> , 2018, 265, 791-796.	4.9	6
5887	Atomistic Picture of Fluorescent Probes with Hydrocarbon Tails in Lipid Bilayer Membranes: An Investigation of Selective Affinities and Fluorescent Anisotropies in Different Environmental Phases. <i>Langmuir</i> , 2018, 34, 9072-9084.	3.5	15

#	ARTICLE	IF	CITATIONS
5888	Molecular dynamics simulation of human estrogen receptor free and bound to morpholine ether benzophenone inhibitor. Theoretical Chemistry Accounts, 2018, 137, 1.	1.4	5
5889	Synthesis and Self-Assembly of Amphiphilic Star/Linear“Dendritic Polymers: Effect of Core versus Peripheral Branching on Reverse Micelle Aggregation. Biomacromolecules, 2018, 19, 3177-3189.	5.4	12
5890	Electric-Field-Driven Translocation of ssDNA through Hydrophobic Nanopores. ACS Nano, 2018, 12, 8208-8213.	14.6	13
5891	Structural and functional characterization of suramin-bound MjTX-I from Bothrops moojeni suggests a particular myotoxic mechanism. Scientific Reports, 2018, 8, 10317.	3.3	26
5892	Bias-Exchange Metadynamics Simulation of Membrane Permeation of 20 Amino Acids. International Journal of Molecular Sciences, 2018, 19, 885.	4.1	14
5893	Importance of Hydrophilic Groups on Modulating the Structural, Mechanical, and Interfacial Properties of Bilayers: A Comparative Molecular Dynamics Study of Phosphatidylcholine and Ion Pair Amphiphile Membranes. International Journal of Molecular Sciences, 2018, 19, 1552.	4.1	7
5894	Anti-Correlation between the Dynamics of the Active Site Loop and C-Terminal Tail in Relation to the Homodimer Asymmetry of the Mouse Erythroid 5-Aminolevulinate Synthase. International Journal of Molecular Sciences, 2018, 19, 1899.	4.1	7
5895	The Mechanism for siRNA Transmembrane Assisted by PMAL. Molecules, 2018, 23, 1586.	3.8	2
5896	Possible Mechanism of Glucose Uptake Enhanced by Cold Atmospheric Plasma: Atomic Scale Simulations. Plasma, 2018, 1, 119-125.	1.8	3
5897	Interfacial Properties and Hopping Diffusion of Small Nanoparticle in Polymer/Nanoparticle Composite with Attractive Interaction on Side Group. Polymers, 2018, 10, 598.	4.5	7
5898	Novel Bacterial Topoisomerase Inhibitors Exploit Asp83 and the Intrinsic Flexibility of the DNA Gyrase Binding Site. International Journal of Molecular Sciences, 2018, 19, 453.	4.1	17
5899	Valid molecular dynamics simulations of human hemoglobin require a surprisingly large box size. ELife, 2018, 7, .	6.0	63
5900	A free energy landscape perspective on the nature of collective diffusion in amorphous solids. Acta Materialia, 2018, 157, 165-173.	7.9	33
5901	Dislocation mobility and Peierls stress of c-type screw dislocations in GaN from molecular dynamics. Computational Materials Science, 2018, 153, 409-416.	3.0	10
5902	On the Binding Free Energy and Molecular Origin of Sick Cell Hemoglobin Aggregation. Journal of Physical Chemistry B, 2018, 122, 7475-7483.	2.6	11
5903	Role of MDH2 pathogenic variant in pheochromocytoma and paraganglioma patients. Genetics in Medicine, 2018, 20, 1652-1662.	2.4	45
5904	Structural basis for endotoxin neutralisation and anti-inflammatory activity of thrombin-derived C-terminal peptides. Nature Communications, 2018, 9, 2762.	12.8	43
5905	Nonmonotonic Scission and Branching Free Energies as Functions of Hydrotrope Concentration for Charged Micelles. Physical Review Letters, 2018, 121, 038001.	7.8	18

#	ARTICLE	IF	CITATIONS
5906	Complete Coupled Binding–Folding Pathway of the Intrinsically Disordered Transcription Factor Protein Brinker Revealed by Molecular Dynamics Simulations and Markov State Modeling. <i>Biochemistry</i> , 2018, 57, 4404-4420.	2.5	15
5907	Oligomer Formation Propensities of Dimeric Bundle Peptides Correlate with Cell Penetration Abilities. <i>ACS Central Science</i> , 2018, 4, 885-893.	11.3	16
5908	Proactive response to tackle the threat of emerging drugs: Synthesis and toxicity evaluation of new cathinones. <i>Forensic Science International</i> , 2018, 290, 146-156.	2.2	28
5909	Determination of Dynamically Stable Electrenes toward Ultrafast Charging Battery Applications. <i>Journal of Physical Chemistry Letters</i> , 2018, 9, 4267-4274.	4.6	18
5910	Conformational and Dynamic Properties of Poly(ethylene oxide) in BMIM <sup>+</sup> BF <sub>4</sub> <sup>-</sup> : A Microsecond Computer Simulation Study Using ab Initio Force Fields. <i>Macromolecules</i> , 2018, 51, 5336-5345.	4.8	16
5911	Roles of PIP <sub>2</sub> in the membrane binding of MIM <sup>+</sup> BAR <sup>-</sup> : insights from molecular dynamics simulations. <i>FEBS Letters</i> , 2018, 592, 2533-2542.	2.8	13
5912	Importance of Solvents' Translational–Rotational Coupling for Translational Jump of a Small Hydrophobic Solute in Supercooled Water. <i>Journal of Physical Chemistry B</i> , 2018, 122, 7569-7583.	2.6	16
5913	Molecular Dynamics Simulation of Water-Based Fracturing Fluids in Kaolinite Slit Pores. <i>Journal of Physical Chemistry C</i> , 2018, 122, 17170-17183.	3.1	33
5914	Exploring the Therapeutic Ability of Fenugreek against Type 2 Diabetes and Breast Cancer Employing Molecular Docking and Molecular Dynamics Simulations. <i>Evidence-based Complementary and Alternative Medicine</i> , 2018, 2018, 1-12.	1.2	18
5915	Dynamics of Dystrophin's Actin-Binding Domain. <i>Biophysical Journal</i> , 2018, 115, 445-454.	0.5	8
5916	A Nonequilibrium Molecular Dynamics Study of Infrared Perturbed Electron Transfer. <i>Journal of Chemical Theory and Computation</i> , 2018, 14, 4818-4832.	5.3	1
5917	High-throughput Docking and Molecular Dynamics Simulations towards the Identification of Novel Peptidomimetic Inhibitors against CDC7. <i>Molecular Informatics</i> , 2018, 37, e1800022.	2.5	4
5918	Molecular and in silico analyses validates pathogenicity of homozygous mutations in the NPR2 gene underlying variable phenotypes of Acromesomelic dysplasia, type Maroteaux. <i>International Journal of Biochemistry and Cell Biology</i> , 2018, 102, 76-86.	2.8	14
5919	Solvent effect on the energetics of proton coupled electron transfer in guanine-cytosine pair in chloroform by mixed explicit and implicit solvation models. <i>Chemical Physics</i> , 2018, 515, 493-501.	1.9	4
5920	Implementation of isotension ensemble in molecular dynamics. <i>Computer Methods in Applied Mechanics and Engineering</i> , 2018, 342, 240-250.	6.6	2
5921	Molecular Dynamics of Lithium Ion Transport in a Model Solid Electrolyte Interphase. <i>Scientific Reports</i> , 2018, 8, 10736.	3.3	33
5922	Detection and characterization at nM concentration of oligomers formed by hIAPP, A $\beta$ (1–40) and their equimolar mixture using SERS and MD simulations. <i>Physical Chemistry Chemical Physics</i> , 2018, 20, 20588-20596.	2.8	22
5923	Role of atomic-scale chemical heterogeneities in improving the plasticity of Cu-Zr-Ag bulk amorphous alloys. <i>Acta Materialia</i> , 2018, 157, 209-217.	7.9	31

#	ARTICLE	IF	CITATIONS
5924	Structural Behavior of Isolated Asphaltene Molecules at the Oil–Water Interface. <i>Energy &amp; Fuels</i> , 2018, 32, 8259-8267.	5.1	22
5925	Binding Modes of a Glycopeptidomimetic Molecule on A $\beta$ Protofibrils: Implication for Its Inhibition Mechanism. <i>ACS Chemical Neuroscience</i> , 2018, 9, 2859-2869.	3.5	10
5926	Adaptive resolution molecular dynamics technique: Down to the essential. <i>Journal of Chemical Physics</i> , 2018, 149, 024104.	3.0	30
5927	Both reentrant loops of the sodium-coupled glutamate transporters contain molecular determinants of cation selectivity. <i>Journal of Biological Chemistry</i> , 2018, 293, 14200-14209.	3.4	3
5928	How to minimize dye-induced perturbations while studying biomembrane structure and dynamics: PEG linkers as a rational alternative. <i>Biochimica Et Biophysica Acta - Biomembranes</i> , 2018, 1860, 2436-2445.	2.6	31
5929	Sequence-dependent DNA condensation as a driving force of DNA phase separation. <i>Nucleic Acids Research</i> , 2018, 46, 9401-9413.	14.5	55
5930	Exploration for novel inhibitors showing back-to-front approach against VEGFR-2 kinase domain (4AG8) employing molecular docking mechanism and molecular dynamics simulations. <i>BMC Cancer</i> , 2018, 18, 264.	2.6	43
5931	Ginger ( <i>Zingiber officinale</i> ) phytochemicals—gingerenone-A and shogaol inhibit SaHPPK: molecular docking, molecular dynamics simulations and in vitro approaches. <i>Annals of Clinical Microbiology and Antimicrobials</i> , 2018, 17, 16.	3.8	33
5932	Molecular Dynamics Analysis of Cardiolipin and Monolysocardiolipin on Bilayer Properties. <i>Biophysical Journal</i> , 2018, 114, 2116-2127.	0.5	33
5933	Mechanism of Long-Chain Free Fatty Acid Protonation at the Membrane-Water Interface. <i>Biophysical Journal</i> , 2018, 114, 2142-2151.	0.5	57
5934	The influence of flexibility on the spectroscopic properties for organic molecules in solution: A theoretical study applied to A3R polypeptide. <i>Journal of Molecular Liquids</i> , 2018, 263, 334-341.	4.9	13
5935	Membrane-Induced pK <sub>a</sub> Shifts in wt-pHLIP and Its L16H Variant. <i>Journal of Chemical Theory and Computation</i> , 2018, 14, 3289-3297.	5.3	33
5936	Glycerol Solvates DPPC Headgroups and Localizes in the Interfacial Regions of Model Pulmonary Interfaces Altering Bilayer Structure. <i>Langmuir</i> , 2018, 34, 6941-6954.	3.5	25
5937	Computational analysis of the receptor binding specificity of novel influenza A/H7N9 viruses. <i>BMC Genomics</i> , 2018, 19, 88.	2.8	8
5938	Dissecting the conformational determinants of chitosan and chitlac oligomers. <i>Biopolymers</i> , 2018, 109, e23221.	2.4	8
5939	Machine learning and molecular design of self-assembling -conjugated oligopeptides. <i>Molecular Simulation</i> , 2018, 44, 930-945.	2.0	26
5940	A metadynamic approach to understand the recognition mechanism of the histone H3 tail with the ATRXADD domain. <i>Biochimica Et Biophysica Acta - Gene Regulatory Mechanisms</i> , 2018, 1861, 594-602.	1.9	4
5941	Structures of binary mixtures of ionic liquid 1-butyl-3-methylimidazolium bis(trifluoromethylsulfonyl)imide with primary alcohols: The role of hydrogen-bonding. <i>Journal of Molecular Liquids</i> , 2018, 261, 337-349.	4.9	17

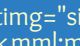
#	ARTICLE	IF	CITATIONS
5942	Molecular Investigation of the Initial Nucleation of Calcium Phosphate on TiO <sub>2</sub> Substrate: The Effects of Surface Nanotopographies. <i>Crystal Growth and Design</i> , 2018, 18, 3283-3290.	3.0	10
5943	Unraveling the molecular mechanisms of thermo-responsive properties of silk-elastin-like proteins by integrating multiscale modeling and experiment. <i>Journal of Materials Chemistry B</i> , 2018, 6, 3727-3734.	5.8	21
5944	Kinetic energy definition in velocity Verlet integration for accurate pressure evaluation. <i>Journal of Chemical Physics</i> , 2018, 148, 164109.	3.0	12
5945	Asymmetric nucleophilic fluorination under hydrogen bonding phase-transfer catalysis. <i>Science</i> , 2018, 360, 638-642.	12.6	137
5946	Investigation of Nonlinear Output-Input Microwave Power of DMSO-Ethanol Mixture by Molecular Dynamics Simulation. <i>Scientific Reports</i> , 2018, 8, 7186.	3.3	7
5947	Effects of area, aspect ratio and orientation of rectangular nanohole on the tensile strength of defective graphene – a molecular dynamics study. <i>RSC Advances</i> , 2018, 8, 17034-17043.	3.6	14
5948	Rotational Diffusion Depends on Box Size in Molecular Dynamics Simulations. <i>Journal of Physical Chemistry Letters</i> , 2018, 9, 2874-2878.	4.6	27
5949	Identification and characterization of smallest pore-forming protein in the cell wall of pathogenic <i>Corynebacterium urealyticum</i> DSM 7109. <i>BMC Biochemistry</i> , 2018, 19, 3.	4.4	7
5950	Determination of the Boundary Surface Between the Lipid Bilayer and Water. <i>Journal of Structural Chemistry</i> , 2018, 59, 96-105.	1.0	6
5951	A molecular dynamics simulation study on the conformational stability of amylose-linoleic acid complex in water. <i>Carbohydrate Polymers</i> , 2018, 196, 56-65.	10.2	67
5952	A critical assessment of force field accuracy against NMR data for cyclic peptides containing $\beta^2$ -amino acids. <i>Physical Chemistry Chemical Physics</i> , 2018, 20, 15807-15816.	2.8	9
5953	Formation of nanopores in DiynePCâ€“DPPC complex lipid bilayers triggered by on-demand photo-polymerization. <i>RSC Advances</i> , 2018, 8, 27988-27994.	3.6	6
5954	Optimizing Proteinâ€“Polymer Interactions in a Poly(ethylene glycol) Coarse-Grained Model. <i>Journal of Physical Chemistry B</i> , 2018, 122, 7997-8005.	2.6	19
5955	Atomic resolution mechanism of ligand binding to a solvent inaccessible cavity in T4 lysozyme. <i>PLoS Computational Biology</i> , 2018, 14, e1006180.	3.2	58
5956	A Novel Polar Core and Weakly Fixed C-Tail in Squid Arrestin Provide New Insight into Interaction with Rhodopsin. <i>Journal of Molecular Biology</i> , 2018, 430, 4102-4118.	4.2	7
5957	How Reactive are Druggable Cysteines in Protein Kinases?. <i>Journal of Chemical Information and Modeling</i> , 2018, 58, 1935-1946.	5.4	44
5958	Rational Design of Thermostable Carbonic Anhydrase Mutants Using Molecular Dynamics Simulations. <i>Journal of Physical Chemistry B</i> , 2018, 122, 8526-8536.	2.6	38
5959	Structures, dynamics, and hydrogen-bond interactions of antifreeze proteins in TIP4P/Ice water and their dependence on force fields. <i>PLoS ONE</i> , 2018, 13, e0198887.	2.5	20



#	ARTICLE	IF	CITATIONS
5960	Impact of Dispersion Coefficient on Simulations of Proteins and Organic Liquids. Journal of Physical Chemistry B, 2018, 122, 8018-8027.	2.6	16
5961	On the mechanistic studies of the growth of anisotropic particles (theory and simulation). , 2018, , 55-103.		0
5962	Structuring of Organic Solvents at Solid Interfaces and Ramifications for Antimalarial Adsorption on $\alpha$ -Hematin Crystals. ACS Applied Materials & Interfaces, 2018, 10, 29288-29298.	8.0	6
5963	Papain Loaded Poly( $\epsilon$ -Caprolactone) Nanoparticles: In-silico and In-Vitro Studies. Journal of Fluorescence, 2018, 28, 1127-1142.	2.5	14
5964	B-cell and T-cell epitope identification with stability analysis of Al-2 import ATP-binding cassette LsrA from <i>S. typhi</i> In silico approach. Microbial Pathogenesis, 2018, 123, 487-495.	2.9	3
5965	How Different Are the Characteristics of Aqueous Solutions of <i>tert</i> -Butyl Alcohol and Trimethylamine- <i>N</i> -Oxide? A Molecular Dynamics Simulation Study. Journal of Physical Chemistry B, 2018, 122, 8220-8232.	2.6	13
5966	Dynamics of Disordered Proteins under Confinement: Memory Effects and Internal Friction. Journal of Physical Chemistry B, 2018, 122, 9049-9060.	2.6	17
5967	Emergent Properties of Antiagglomerant Films Control Methane Transport: Implications for Hydrate Management. Langmuir, 2018, 34, 9701-9710.	3.5	26
5968	Engineering a Single-Agent Cytokine/Antibody Fusion That Selectively Expands Regulatory T Cells for Autoimmune Disease Therapy. Journal of Immunology, 2018, 201, 2094-2106.	0.8	58
5969	Identification of novel inhibitor against endonuclease subunit of Influenza pH1N1 polymerase: A combined molecular docking, molecular dynamics, MMPBSA, QMMM and ADME studies to combat influenza A viruses. Computational Biology and Chemistry, 2018, 77, 279-290.	2.3	8
5970	Membrane-Modulating Drugs can Affect the Size of Amyloid- $\beta$ 35 Aggregates in Anionic Membranes. Scientific Reports, 2018, 8, 12367.	3.3	8
5971	Aggregation behavior of dihexadecylviologen bistriflimide ionic liquid crystal in different solvents: influence of polarity and concentration. Physical Chemistry Chemical Physics, 2018, 20, 22730-22738.	2.8	8
5972	A revisit of the conformational dynamics of SNARE protein rYkt6. Biochemical and Biophysical Research Communications, 2018, 503, 2841-2847.	2.1	2
5973	Control of Peptide Aggregation and Fibrillation by Physical PEGylation. Biomacromolecules, 2018, 19, 3958-3969.	5.4	9
5974	Specific Ion Effects on Zwitterionic Micelles Are Independent of Interfacial Hydration Changes. Langmuir, 2018, 34, 11049-11057.	3.5	7
5975	Homology modeling, molecular docking, and dynamics of two $\alpha$ -methyl-d-mannoside-specific lectins from <i>Arachis</i> genus. Journal of Molecular Modeling, 2018, 24, 251.	1.8	5
5976	Hydrophobic gating in BK channels. Nature Communications, 2018, 9, 3408.	12.8	70
5977	Thermal neutron scattering cross sections of $^{238}\text{U}$ and $^{235}\text{U}$ in the $\beta$ phase. Journal of Physics Condensed Matter, 2018, 30, 415401.	1.8	4

#	ARTICLE	IF	CITATIONS
5978	Hydrogenated amorphous boron nitride: A first principles study. Journal of Non-Crystalline Solids, 2018, 502, 159-163.	3.1	5
5979	Cooperativity in Plant Plasma Membrane Intrinsic Proteins (PIPs): Mechanism of Increased Water Transport in Maize PIP1 Channels in Hetero-tetramers. Scientific Reports, 2018, 8, 12055.	3.3	22
5980	Non-equilibrium solvation dynamics in water-DMSO binary mixture: Composition dependence of non-linear relaxation. Journal of Chemical Physics, 2018, 149, 084501.	3.0	14
5981	Determining the molecular basis of voltage sensitivity in membrane proteins. Journal of General Physiology, 2018, 150, 1444-1458.	1.9	16
5982	Strongly correlated perovskite lithium ion shuttles. Proceedings of the National Academy of Sciences of the United States of America, 2018, 115, 9672-9677.	7.1	55
5983	Ligand binding and retention in snake gourd seed lectin (SGSL). A crystallographic, thermodynamic and molecular dynamics study. Glycobiology, 2018, 28, 968-977.	2.5	3
5984	Computational Design of Multi-Target Drugs Against Breast Cancer. Methods in Pharmacology and Toxicology, 2018, , 443-458.	0.2	2
5985	Molecular Dynamics Simulations of Furfural and 5-Hydroxymethylfurfural at Ambient and Hydrothermal Conditions. Journal of Physical Chemistry B, 2018, 122, 8416-8428.	2.6	7
5986	Boundary effects in discrete element method modeling of undrained cyclic triaxial and simple shear element tests. Granular Matter, 2018, 20, 1.	2.2	28
5987	Inhibition of the Exoglucanase Cel7A by a Douglas-Fir-Condensed Tannin. Journal of Physical Chemistry B, 2018, 122, 8665-8674.	2.6	2
5988	Protein Environment: A Crucial Triggering Factor in Josephin Domain Aggregation: The Role of 2,2,2-Trifluoroethanol. International Journal of Molecular Sciences, 2018, 19, 2151.	4.1	3
5989	Molecular property diagnostic suite for diabetes mellitus (MPDSDM): An integrated web portal for drug discovery and drug repurposing. Journal of Biomedical Informatics, 2018, 85, 114-125.	4.3	15
5990	Cation-Anion <sup>CO<sub>2</sub></sup> Interactions in Imidazolium-Based Ionic Liquid Sorbents. ChemPhysChem, 2018, 19, 2879-2884.	2.1	33
5991	Molecular insights into the interactions of GF $\epsilon$ 17 with the gram-negative and gram-positive bacterial lipid bilayers. Journal of Cellular Biochemistry, 2018, 119, 9205-9216.	2.6	11
5992	Molecular Simulation Studies of Cyanine-Based Chromonic Mesogens: Spontaneous Symmetry Breaking to Form Chiral Aggregates and the Formation of a Novel Lamellar Structure. Advanced Theory and Simulations, 2018, 1, 1800088.	2.8	5
5993	Diffusion Behavior of Methanol Molecules Confined in Cross-Linked Phenolic Resins Studied Using Neutron Scattering and Molecular Dynamics Simulations. Macromolecules, 2018, 51, 6334-6343.	4.8	12
5994	Local environment of organic dyes in an ionic liquid-water mixture: FCS and MD simulation. Journal of Chemical Physics, 2018, 149, 054501.	3.0	11
5995	How Does Friction Coefficient Affect the Conformational Sampling Efficiency of Parallel Cascade Selection Molecular Dynamics?. Chemistry Letters, 2018, 47, 1119-1122.	1.3	1

#	ARTICLE	IF	CITATIONS
5996	Temperature dependence of the Young's modulus of polymers calculated using a hybrid molecular mechanics-molecular dynamics method. <i>Journal of Physics Condensed Matter</i> , 2018, 30, 355901.	1.8	11
5997	Dynamics of DDB2-DDB1 complex under different naturally-occurring mutants in Xeroderma Pigmentosum disease. <i>Biochimica Et Biophysica Acta - General Subjects</i> , 2018, 1862, 2579-2589.	2.4	7
5998	Searching for improved mimetic peptides inhibitors preventing conformational transition of amyloid- $\beta$ 242 monomer. <i>Bioorganic Chemistry</i> , 2018, 81, 211-221.	4.1	7
5999	Rejuvenation by weakening the medium range order in Zr <sub>46</sub> Cu <sub>46</sub> Al <sub>8</sub> metallic glass with pressure preloading: A molecular dynamics simulation study. <i>Materials and Design</i> , 2018, 158, 248-255.	7.0	52
6000	Structural Dynamics of the PET-Degrading Cutinase-like Enzyme from <i>Saccharomonospora viridis</i> AHK190 in Substrate-Bound States Elucidates the Ca <sup>2+</sup> -Driven Catalytic Cycle. <i>Biochemistry</i> , 2018, 57, 5289-5300.	2.5	59
6001	Hydration Free Energies in the FreeSolv Database Calculated with Polarized Iterative Hirshfeld Charges. <i>Journal of Chemical Information and Modeling</i> , 2018, 58, 1779-1797.	5.4	31
6002	Molecular simulation of the high temperature phase behaviour of $\beta$ -unsubstituted sexithiophene. <i>Soft Matter</i> , 2018, 14, 8253-8266.	2.7	5
6003	Negatively Charged Gangliosides Promote Membrane Association of Amphipathic Neurotransmitters. <i>Neuroscience</i> , 2018, 384, 214-223.	2.3	17
6004	Influences of Cation Ratio, Anion Type, and Water Content on Polytypism of Layered Double Hydroxides. <i>Inorganic Chemistry</i> , 2018, 57, 7299-7313.	4.0	27
6005	New optimization scheme to obtain interaction potentials for oxide glasses. <i>Journal of Chemical Physics</i> , 2018, 148, 194504.	3.0	60
6006	Metronidazole within phosphatidylcholine lipid membranes: New insights to improve the design of imidazole derivatives. <i>European Journal of Pharmaceutics and Biopharmaceutics</i> , 2018, 129, 204-214.	4.3	13
6007	Predicting drug permeability through skin using molecular dynamics simulation. <i>Journal of Controlled Release</i> , 2018, 283, 269-279.	9.9	90
6008	Unravelling the Composition-Dependent Anomalies of Pair Hydrophobicity in Water-Ethanol Binary Mixtures. <i>Journal of Physical Chemistry B</i> , 2018, 122, 6801-6809.	2.6	19
6009	Molecular Dynamics Simulation of Salt Diffusion in Polyelectrolyte Assemblies. <i>Journal of Physical Chemistry B</i> , 2018, 122, 6656-6665.	2.6	11
6010	Insights into Membrane Translocation of Protegrin Antimicrobial Peptides by Multistep Molecular Dynamics Simulations. <i>ACS Omega</i> , 2018, 3, 6056-6065.	3.5	26
6011	How low-resolution structural data predict the conformational changes of a protein: a study on data-driven molecular dynamics simulations. <i>Physical Chemistry Chemical Physics</i> , 2018, 20, 17790-17798.	2.8	3
6012	PRODAN differentially influences its local environment. <i>Physical Chemistry Chemical Physics</i> , 2018, 20, 16060-16066.	2.8	13
6013	Analysis of three-phase equilibrium conditions for methane hydrate by isometric-isothermal molecular dynamics simulations. <i>Journal of Chemical Physics</i> , 2018, 148, 184501.	3.0	16

#	ARTICLE	IF	CITATIONS
6014	Redistribution of SERCA calcium pump conformers during intracellular calcium signaling. Journal of Biological Chemistry, 2018, 293, 10843-10856.	3.4	25
6015	Area Increase and Budding in Giant Vesicles Triggered by Light: Behind the Scene. Advanced Science, 2018, 5, 1800432.	11.2	37
6016	Designing effective anticancer-radiopeptides. A Molecular Dynamics study of their interaction with model tumor and healthy cell membranes. Biochimica Et Biophysica Acta - Biomembranes, 2018, 1860, 2348-2355.	2.6	8
6017	Atomistic simulations of superplasticity and amorphization of nanocrystalline anatase $\text{TiO}_2$ .  $\times 2$ . Extreme Mechanics Letters, 2018, 22, 131-137.	4.1	7
6018	Stability of Biological Membranes upon Mechanical Indentation. Journal of Physical Chemistry B, 2018, 122, 7073-7079.	2.6	3
6019	Heterogeneous Impacts of Protein-Stabilizing Osmolytes on Hydrophobic Interaction. Journal of Physical Chemistry B, 2018, 122, 6922-6930.	2.6	22
6020	Polyphenolic self-association accounts for redirecting a high-yielding amyloid aggregation. Journal of Molecular Liquids, 2018, 266, 291-298.	4.9	10
6021	Probing Additive Loading in the Lamellar Phase of a Nonionic Surfactant: Gibbs Ensemble Monte Carlo Simulations Using the SDK Force Field. Langmuir, 2018, 34, 8245-8254.	3.5	6
6022	Catanionic AOT/BDAC micelles on gold {111} surfaces. Colloid and Polymer Science, 2018, 296, 1301-1306.	2.1	6
6023	Direct Prediction of EPR Spectra from Lipid Bilayers: Understanding Structure and Dynamics in Biological Membranes. ChemPhysChem, 2018, 19, 2183-2193.	2.1	9
6024	Computational study of HIV gp120 as a target for polyanionic entry inhibitors: Exploiting the V3 loop region. PLoS ONE, 2018, 13, e0190658.	2.5	9
6025	A Funneled Conformational Landscape Governs Flavivirus Fusion Peptide Interaction with Lipid Membranes. Journal of Chemical Theory and Computation, 2018, 14, 3920-3932.	5.3	9
6026	Effect of Sodium Dodecyl Sulfate Surfactant on Methane Hydrate Formation: A Molecular Dynamics Study. Journal of Physical Chemistry B, 2018, 122, 6536-6542.	2.6	47
6027	Amorphous zirconia at high pressure. Journal of the American Ceramic Society, 2018, 101, 5411-5418.	3.8	1
6028	Molecular Insights into Variable Electron Transfer in Amphibian Cryptochrome. Biophysical Journal, 2018, 114, 2563-2572.	0.5	17
6029	Temperature-Shuffled Structural Dissimilarity Sampling Based on a Root-Mean-Square Deviation. Journal of Chemical Information and Modeling, 2018, 58, 1397-1405.	5.4	9
6030	Removal of Cs, Sr, U and Pu species from simulated nuclear waste effluent using graphene oxide. Journal of Radioanalytical and Nuclear Chemistry, 2018, 317, 93-102.	1.5	10
6031	Interactions of the EphA2 Kinase Domain with PIPs in Membranes: Implications for Receptor Function. Structure, 2018, 26, 1025-1034.e2.	3.3	33

#	ARTICLE	IF	CITATIONS
6032	Quantitatively Identifying the Roles of Interfacial Water and Solid Surface in Governing Peptide Adsorption. <i>Langmuir</i> , 2018, 34, 7932-7941.	3.5	21
6033	Structure and permeability of ionomers studied by atomistic molecular simulation combined with the theory of solutions in the energy representation. <i>Journal of Chemical Physics</i> , 2018, 148, 214903.	3.0	16
6034	A multiscale shear-transformation-zone (STZ) model and simulation of plasticity in amorphous solids. <i>Acta Materialia</i> , 2018, 155, 153-165.	7.9	31
6035	Influence of pH on the activity of thrombin-derived antimicrobial peptides. <i>Biochimica Et Biophysica Acta - Biomembranes</i> , 2018, 1860, 2374-2384.	2.6	25
6036	Interactions of a Bacterial Cu(I)-ATPase with a Complex Lipid Environment. <i>Biochemistry</i> , 2018, 57, 4063-4073.	2.5	6
6037	Variations of the Hydrogen Bonding and Hydrogen-Bonded Network in Ethanol-Water Mixtures on Cooling. <i>Journal of Physical Chemistry B</i> , 2018, 122, 6790-6800.	2.6	29
6038	Influence of Liquid Structure on Fickian Diffusion in Binary Mixtures of <i>n</i> -Hexane and Carbon Dioxide Probed by Dynamic Light Scattering, Raman Spectroscopy, and Molecular Dynamics Simulations. <i>Journal of Physical Chemistry B</i> , 2018, 122, 7122-7133.	2.6	39
6039	Different footprints of the Zika and dengue surface proteins on viral membranes. <i>Soft Matter</i> , 2018, 14, 5615-5621.	2.7	10
6040	Mechanical properties of drug loaded diblock copolymer bilayers: A molecular dynamics study. <i>Journal of Chemical Physics</i> , 2018, 148, 214901.	3.0	6
6041	Anticancer Agent Edelfosine Exhibits a High Affinity for Cholesterol and Disorganizes Liquid-Ordered Membrane Structures. <i>Langmuir</i> , 2018, 34, 8333-8346.	3.5	18
6042	Ligand-induced perturbation of the HIF-2 $\alpha$ :ARNT dimer dynamics. <i>PLoS Computational Biology</i> , 2018, 14, e1006021.	3.2	22
6043	Investigation of non-hydroxamate scaffolds against HDAC6 inhibition: A pharmacophore modeling, molecular docking, and molecular dynamics simulation approach. <i>Journal of Bioinformatics and Computational Biology</i> , 2018, 16, 1840015.	0.8	4
6044	Halogen-hydrogen bonds: A general synthetic approach for highly photoactive carbon nitride with tunable properties. <i>Applied Catalysis B: Environmental</i> , 2018, 237, 681-688.	20.2	44
6045	Structure of Aqueous Solutions of Trimethylaminoxide, Urea, and Their Mixture. <i>Journal of Structural Chemistry</i> , 2018, 59, 347-354.	1.0	6
6046	Amorphous magnesium silicide. <i>Journal of Non-Crystalline Solids</i> , 2018, 498, 118-124.	3.1	0
6047	A direct interaction of cholesterol with the dopamine transporter prevents its out-to-inward transition. <i>PLoS Computational Biology</i> , 2018, 14, e1005907.	3.2	81
6048	Computer simulations reveal changes in the conformational space of the transcriptional regulator MosR upon the formation of a disulphide bond and in the collective motions that regulate its DNA-binding affinity. <i>PLoS ONE</i> , 2018, 13, e0192826.	2.5	5
6049	Search for the Source of an Apparent Interfacial Resistance To Mass Transfer of CnEm Surfactants To the Water/Oil Interface. <i>Langmuir</i> , 2019, 35, 2898-2908.	3.5	7

#	ARTICLE	IF	CITATIONS
6050	Antimicrobial cell penetrating peptides with bacterial cell specificity: pharmacophore modelling, quantitative structure activity relationship and molecular dynamics simulation. Journal of Biomolecular Structure and Dynamics, 2019, 37, 2370-2380.	3.5	4
6051	In silico site-directed mutagenesis of neutralizing mAb 4C4 and analysis of its interaction with G-H loop of VP1 to explore its therapeutic applications against FMD. Journal of Biomolecular Structure and Dynamics, 2019, 37, 2641-2651.	3.5	1
6052	Computational simulations assessment of mutations impact on streptokinase (SK) from a group G streptococci with enhanced activity – insights into the functional roles of structural dynamics flexibility of SK and stabilization of SK <sup>1/4</sup> plasmin catalytic complex. Journal of Biomolecular Structure and Dynamics, 2019, 37, 1944-1955.	3.5	6
6053	Modeling dislocations and heat conduction in crystalline materials: atomistic/continuum coupling approaches. International Materials Reviews, 2019, 64, 407-438.	19.3	14
6054	Parallel Cascade Selection Molecular Dynamics Simulations for Transition Pathway Sampling of Biomolecules. Advances in Quantum Chemistry, 2019, , 129-147.	0.8	0
6055	Control of shear band dynamics in Cu50Zr50 metallic glass by introducing amorphous-crystalline interfaces. Journal of Alloys and Compounds, 2019, 770, 896-905.	5.5	38
6056	A comparison of different water models for melting point calculation of methane hydrate using molecular dynamics simulations. Chemical Physics, 2019, 516, 6-14.	1.9	25
6057	The contribution of lipid peroxidation to membrane permeability in electroporation: A molecular dynamics study. Bioelectrochemistry, 2019, 125, 46-57.	4.6	71
6058	Characterisation of a new nematic lyotropic liquid crystal with natural lipids from soybean. Molecular Physics, 2019, 117, 158-166.	1.7	1
6059	On the validity of using the Debye model to quantitatively correlate the shear modulus with vibrational properties in cubic metals. Scripta Materialia, 2019, 158, 34-37.	5.2	1
6060	Structural insights into the inhibitor binding and new inhibitor design to Polo-like kinase-1 Polo-box domain using computational studies. Journal of Biomolecular Structure and Dynamics, 2019, 37, 3410-3421.	3.5	2
6061	Spatial distribution of reservoir fluids in mature kerogen using molecular simulations. Fuel, 2019, 235, 448-459.	6.4	41
6062	Molecular dynamics simulations of CO <sub>2</sub> permeation through ionic liquids confined in $\gamma$ -alumina nanopores. Chemical Engineering Communications, 2019, 206, 301-317.	2.6	4
6063	Understanding the structural origin of intermediate glasses. Journal of the American Ceramic Society, 2019, 102, 1137-1149.	3.8	8
6064	Low-angle grain boundary structures and size effects of nickel nanolaminated structures. Journal of the Mechanics and Physics of Solids, 2019, 130, 280-296.	4.8	20
6065	How calcium ion binding induces the conformational transition of the calmodulin N-terminal domain – an atomic level characterization. Physical Chemistry Chemical Physics, 2019, 21, 19795-19804.	2.8	7
6066	Residue-Specialized Membrane Poration Kinetics of Melittin and Its Variants: Insight from Mechanistic Landscapes*. Communications in Theoretical Physics, 2019, 71, 887.	2.5	15
6067	Hydrogen Permeation in Hydrated Perfluorosulfonic Acid Polymer Membranes: Effect of Polymer Crystallinity and Equivalent Weight. Journal of Physical Chemistry C, 2019, 123, 20628-20638.	3.1	29



#	ARTICLE	IF	CITATIONS
6068	Membrane-Disrupting Nanofibrous Peptide Hydrogels. ACS Biomaterials Science and Engineering, 2019, 5, 4657-4670.	5.2	38
6069	Synergistic Effects of Melittin and Plasma Treatment: A Promising Approach for Cancer Therapy. Cancers, 2019, 11, 1109.	3.7	46
6070	Exploring the Multi-minima Behavior of Small Molecule Crystal Polymorphs at Finite Temperature. Crystal Growth and Design, 2019, 19, 5568-5580.	3.0	24
6071	Molecular Structure and Solubility Determination of Asphaltenes. Energy & Fuels, 2019, 33, 8259-8270.	5.1	22
6072	Quick temperature-sweep pure-shift NMR: the case of solvent effects in atorvastatin. Physical Chemistry Chemical Physics, 2019, 21, 19209-19215.	2.8	10
6073	Two distinct anionic phospholipid-dependent events involved in SecA-mediated protein translocation. Biochimica Et Biophysica Acta - Biomembranes, 2019, 1861, 183035.	2.6	16
6074	Effect of Cholesterol and 6-Ketocholestanol on Membrane Dipole Potential and Sterol Flip-Flop Motion in Bilayer Membranes. Langmuir, 2019, 35, 11232-11241.	3.5	5
6075	Pastâ€‘future information bottleneck for sampling molecular reaction coordinate simultaneously with thermodynamics and kinetics. Nature Communications, 2019, 10, 3573.	12.8	102
6076	Lysosomal integral membrane protein-2 (LIMP-2/SCARB2) is involved in lysosomal cholesterol export. Nature Communications, 2019, 10, 3521.	12.8	99
6077	Evaluation of second osmotic virial coefficients from molecular simulation following scaled-particle theory. Molecular Simulation, 2019, 45, 1403-1410.	2.0	1
6078	Molecular cloning, gene expression analysis, and in silico characterization of UDPâ€‘Nâ€‘acetylglucosamine pyrophosphorylase from Bombyx mori. Biotechnology and Applied Biochemistry, 2019, 66, 880-899.	3.1	7
6079	Temperature dependent GrÃ¼neisen parameter. Science China Technological Sciences, 2019, 62, 1565-1576.	4.0	15
6080	Hydantoin and Its Derivatives Reduce the Viscosity of Concentrated Antibody Formulations by Inhibiting Associations via Hydrophobic Amino Acid Residues. Industrial & Engineering Chemistry Research, 2019, 58, 16296-16306.	3.7	7
6081	Surface segregation of hydrogen in free-standing Pd-H alloy nanofilms. Science China Technological Sciences, 2019, 62, 1735-1746.	4.0	4
6082	Rationalizing the Phase Behavior of Triblock Copolymers through Experiments and Molecular Simulations. Journal of Physical Chemistry C, 2019, 123, 21224-21236.	3.1	33
6083	Structure and Dynamics of an Ionic Liquid Mixture Film Confined by Mica. Journal of Physical Chemistry C, 2019, 123, 20971-20979.	3.1	7
6084	Temperature dependent mechanical unfolding of calixarene nanocapsules studied by molecular dynamics simulations. Journal of Chemical Physics, 2019, 151, 045102.	3.0	1
6085	Phase behavior of empirical potentials of titanium dioxide. Journal of Chemical Physics, 2019, 151, .	3.0	7

#	ARTICLE	IF	CITATIONS
6086	Vibrational spectroscopy combined with molecular dynamics simulations as a tool for studying behavior of reactive aldehydes inserted in phospholipid bilayers. <i>Chemistry and Physics of Lipids</i> , 2019, 225, 104793.	3.2	3
6087	Influence of Single-Stranded DNA Coatings on the Interaction between Graphene Nanoflakes and Lipid Bilayers. <i>Journal of Physical Chemistry B</i> , 2019, 123, 7711-7721.	2.6	13
6088	Force Field Comparison of GM1 in a DOPC Bilayer Validated with AFM and FRET Experiments. <i>Journal of Physical Chemistry B</i> , 2019, 123, 7504-7517.	2.6	8
6089	Molecular Dynamics Simulation Studies of the Temperature-Dependent Structure and Dynamics of Isopropanol-Water Liquid Mixtures at Low Alcohol Content. <i>Journal of Physical Chemistry B</i> , 2019, 123, 7599-7610.	2.6	21
6090	Ice Crystallization in Shear Flows. <i>Journal of Physical Chemistry C</i> , 2019, 123, 21042-21049.	3.1	9
6091	Conformational Changes as Driving Force for Phase Recognition: The Case of Laurdan. <i>Langmuir</i> , 2019, 35, 11471-11481.	3.5	21
6092	Prediction of Partition Coefficients of Environmental Toxins Using Computational Chemistry Methods. <i>ACS Omega</i> , 2019, 4, 13772-13781.	3.5	24
6093	Characterization of H/D exchange in type 1 pili by proton-detected solid-state NMR and molecular dynamics simulations. <i>Journal of Biomolecular NMR</i> , 2019, 73, 281-291.	2.8	5
6094	Photophysics of BODIPY-Based Photosensitizer for Photodynamic Therapy: Surface Hopping and Classical Molecular Dynamics. <i>Journal of Chemical Theory and Computation</i> , 2019, 15, 5046-5057.	5.3	13
6095	Molecular dynamics simulation studies of the structure and antifouling performance of a gradient polyamide membrane. <i>Physical Chemistry Chemical Physics</i> , 2019, 21, 19995-20002.	2.8	16
6096	The air-water interface stabilizes $\alpha$ -helical conformations of the insulin B-chain. <i>Journal of Chemical Physics</i> , 2019, 151, 064706.	3.0	8
6097	Multiscale Investigation on Electrolyte Systems of [(Solvent + Additive) + LiPF <sub>6</sub> ] for Application in Lithium-Ion Batteries. <i>Journal of Physical Chemistry C</i> , 2019, 123, 21913-21930.	3.1	17
6098	If You Cannot Win Them, Join Them: Understanding New Ways to Target STAT3 by Small Molecules. <i>ACS Omega</i> , 2019, 4, 13913-13921.	3.5	7
6099	A [13]rotaxane assembled via a palladium molecular capsule. <i>Nature Communications</i> , 2019, 10, 3720.	12.8	19
6100	Computational study of the effect of protonation states of PSA protein zinc fingers on its DNA binding. <i>Journal of Physics: Conference Series</i> , 2019, 1274, 012002.	0.4	0
6101	Fat SIRAH: Coarse-Grained Phospholipids To Explore Membrane-Protein Dynamics. <i>Journal of Chemical Theory and Computation</i> , 2019, 15, 5674-5688.	5.3	36
6102	Dynamic properties of aqueous electrolyte solutions from non-polarisable, polarisable, and scaled-charge models. <i>Molecular Physics</i> , 2019, 117, 3538-3549.	1.7	30
6103	Ice growth rate: Temperature dependence and effect of heat dissipation. <i>Journal of Chemical Physics</i> , 2019, 151, 044509.	3.0	20

#	ARTICLE	IF	CITATIONS
6104	Lanosterol Disrupts the Aggregation of Amyloid- $\beta$ Peptides. ACS Chemical Neuroscience, 2019, 10, 4051-4060.	3.5	14
6105	Ceramide cross-linking leads to pore formation: Potential mechanism behind CAP enhancement of transdermal drug delivery. Plasma Processes and Polymers, 2019, 16, 1900122.	3.0	4
6106	Transient evaporation of water thin film over nanostructured graphene. Applied Surface Science, 2019, 495, 143545.	6.1	4
6107	Phase Behaviors of Ionic Liquids Heating from Different Crystal Polymorphs toward the Same Smectic-A Ionic Liquid Crystal by Molecular Dynamics Simulation. Crystals, 2019, 9, 26.	2.2	11
6108	Peptide-Based Subunit Vaccine Design of T- and B-Cells Multi-Epitopes against Zika Virus Using Immunoinformatics Approaches. Microorganisms, 2019, 7, 226.	3.6	25
6109	Pharmacophoric Site Identification and Inhibitor Design for Autotaxin. Molecules, 2019, 24, 2808.	3.8	6
6110	Atomistic Simulation Tools to Study Protein Self-Aggregation. Methods in Molecular Biology, 2019, 2039, 243-262.	0.9	2
6111	The H channel is not a proton transfer path in yeast cytochrome c oxidase. Biochimica Et Biophysica Acta - Bioenergetics, 2019, 1860, 717-723.	1.0	10
6112	Insight into the antimicrobial mechanism of action of $\beta$ -2-amino acid derivatives from molecular dynamics simulation: Dancing the can-can at the membrane surface. Biochimica Et Biophysica Acta - Biomembranes, 2019, 1861, 183028.	2.6	9
6113	Simulation-based protein engineering of R.Âerythropolis FMN oxidoreductase (DszD). Heliyon, 2019, 5, e02193.	3.2	2
6114	Toward Understanding the Impact of Dimerization Interfaces in Angiotensin II Type 1 Receptor. Journal of Chemical Information and Modeling, 2019, 59, 4314-4327.	5.4	13
6115	Compatibility of advanced water models with a united atom model of lipid in lipid bilayer simulation. Journal of Chemical Physics, 2019, 151, .	3.0	14
6116	Steering the Lipid Transfer To Unravel the Mechanism of Cholesteryl Ester Transfer Protein Inhibition. Biochemistry, 2019, 58, 3789-3801.	2.5	5
6117	How membrane lipids influence plasma delivery of reactive oxygen species into cells and subsequent DNA damage: an experimental and computational study. Physical Chemistry Chemical Physics, 2019, 21, 19327-19341.	2.8	28
6118	Physics-based oligomeric models of the yeast mitofusin Fzo1 at the molecular scale in the context of membrane docking. Mitochondrion, 2019, 49, 234-244.	3.4	12
6119	Tailoring the Chemical Modification of Chitosan Hydrogels to Fine-Tune the Release of a Synergistic Combination of Chemotherapeutics. Biomacromolecules, 2019, 20, 3126-3141.	5.4	25
6120	Molecular dynamics simulations on ROR $\beta$ : insights into its functional agonism and inverse agonism. Acta Pharmacologica Sinica, 2019, 40, 1480-1489.	6.1	9
6121	Biological relevance of charge transfer branching pathways in photolyases. Physical Chemistry Chemical Physics, 2019, 21, 17072-17081.	2.8	3

#	ARTICLE	IF	CITATIONS
6122	Effects of N-Glycosylation on the Structure, Function, and Stability of a Plant-Made Fc-Fusion Anthrax Decoy Protein. <i>Frontiers in Plant Science</i> , 2019, 10, 768.	3.6	29
6123	A Comparative Study on Interactions of Antimicrobial Peptides L- and D-phenylseptin with 1,2-dimyristoyl-sn-glycero-3-phosphocholine. <i>Applied Sciences (Switzerland)</i> , 2019, 9, 2601.	2.5	6
6124	Pressure-viscosity relation of 2,2,4-trimethylhexane predicted using all-atom TEAM force field. <i>Fluid Phase Equilibria</i> , 2019, 497, 64-70.	2.5	7
6125	Parallel cascade selection molecular dynamics to screen for protein complexes generated by rigid docking. <i>Journal of Molecular Graphics and Modelling</i> , 2019, 92, 94-99.	2.4	1
6126	On-the-fly machine learning force field generation: Application to melting points. <i>Physical Review B</i> , 2019, 100, .	3.2	233
6127	Using Small-Angle Scattering Data and Parametric Machine Learning to Optimize Force Field Parameters for Intrinsically Disordered Proteins. <i>Frontiers in Molecular Biosciences</i> , 2019, 6, 64.	3.5	22
6128	Multiple C2 domains and transmembrane region proteins ( <scp>MCTP</scp> s) tether membranes at plasmodesmata. <i>EMBO Reports</i> , 2019, 20, e47182.	4.5	92
6129	Rational design of a <i>Yarrowia lipolytica</i> derived lipase for improved thermostability. <i>International Journal of Biological Macromolecules</i> , 2019, 137, 1190-1198.	7.5	30
6130	New Insight into Cluster Aggregation Mechanism during Polymerization-Induced Self-Assembly by Molecular Dynamics Simulation. <i>Journal of Physical Chemistry B</i> , 2019, 123, 6609-6617.	2.6	24
6131	Development of Nonbonded Models for Metal Cations Using the Electronic Continuum Correction. <i>Journal of Computational Chemistry</i> , 2019, 40, 2464-2472.	3.3	15
6132	Nanobiocatalyst facilitated aglycosidic quercetin as a potent inhibitor of tau protein aggregation. <i>International Journal of Biological Macromolecules</i> , 2019, 138, 168-180.	7.5	21
6133	Structural and functional characterisation of a novel peptide from the Australian sea anemone <i>Actinia tenebrosa</i> . <i>Toxicon</i> , 2019, 168, 104-112.	1.6	11
6134	Evidence for ATP Interaction with Phosphatidylcholine Bilayers. <i>Langmuir</i> , 2019, 35, 9944-9953.	3.5	8
6135	A rippled defective phase of AOT lamella: A molecular dynamics study. <i>Colloids and Surfaces A: Physicochemical and Engineering Aspects</i> , 2019, 578, 123578.	4.7	4
6136	Formation of Strong Polycation (Poly[(3-allylamino-2-hydroxypropyl)trimethylammonium chloride]) Monolayers on Mica, Silica, and Gold Substrates: Modeling and Experimental Studies. <i>Journal of Physical Chemistry C</i> , 2019, 123, 19022-19032.	3.1	5
6137	Mutations in a conserved loop in the PSST subunit of respiratory complex I affect ubiquinone binding and dynamics. <i>Biochimica Et Biophysica Acta - Bioenergetics</i> , 2019, 1860, 573-581.	1.0	34
6138	Binding of quinazolinones to c-KIT G-quadruplex; an interplay between hydrogen bonding and $\pi$ - $\pi$ stacking. <i>Biophysical Chemistry</i> , 2019, 253, 106220.	2.8	11
6139	Molecular Simulation Studies on the Interactions of 2,4,6-Trinitrotoluene and Its Metabolites with Lipid Membranes. <i>Journal of Physical Chemistry B</i> , 2019, 123, 6481-6491.	2.6	14

#	ARTICLE	IF	CITATIONS
6140	Glycine Substitution Effects on the Supramolecular Morphology and Rigidity of Cell-Adhesive Amphiphilic Peptides. <i>Chemistry - A European Journal</i> , 2019, 25, 13523-13530.	3.3	19
6141	Loading and release of anticancer drug from phosphorene as a template material with high efficient carrier: From vacuum to cell membrane. <i>Journal of Molecular Liquids</i> , 2019, 291, 111346.	4.9	26
6142	Molecular Dynamics Simulations of Nanopolycrystals. , 2019, , 301-330.		1
6143	Inactivation of HeLa cells on nanoporous gold. <i>Materialia</i> , 2019, 7, 100370.	2.7	3
6144	Adenosine Triphosphate Templated Self-Assembly of Cationic Porphyrin into Chiral Double Superhelices and Enzyme-Mediated Disassembly. <i>Journal of the American Chemical Society</i> , 2019, 141, 12610-12618.	13.7	64
6145	Conformational modifications induced by internal tandem duplications on the FLT3 kinase and juxtamembrane domains. <i>Physical Chemistry Chemical Physics</i> , 2019, 21, 18467-18476.	2.8	9
6146	Insights Gained from Refined Force-Field for Pure and Aqueous Ethylene Glycol through Molecular Dynamics Simulations. <i>Journal of Physical Chemistry B</i> , 2019, 123, 6543-6553.	2.6	16
6147	LUF7244, an allosteric modulator/activator of $K_{v11.1}$ channels, counteracts dofetilide-induced torsades de pointes arrhythmia in the chronic atrioventricular block dog model. <i>British Journal of Pharmacology</i> , 2019, 176, 3871-3885.	5.4	16
6148	PIP2 Influences the Conformational Dynamics of Membrane-Bound KRAS4b. <i>Biochemistry</i> , 2019, 58, 3537-3545.	2.5	30
6149	<i>Ab initio</i> molecular dynamics simulation of Na-doped aluminosilicate glasses and glass-water interaction. <i>AIP Advances</i> , 2019, 9, .	1.3	14
6150	Interactions of Monovalent and Divalent Cations at Palmitoyl-Oleoyl-Phosphatidylcholine Interface. <i>Langmuir</i> , 2019, 35, 10522-10532.	3.5	10
6151	In Silico Prediction of the Thermodynamic Equilibrium of Solute Partition in Multiphase Complex Fluids: A Case Study of Oil-Water Microemulsion. <i>Langmuir</i> , 2019, 35, 10855-10865.	3.5	9
6152	Permeation of beta-defensin-3 encapsulated with polyethylene glycol in lung surfactant models at air-water interface. <i>Colloids and Surfaces B: Biointerfaces</i> , 2019, 182, 110357.	5.0	15
6153	Topological Water Network Analysis Around Amino Acids. <i>Molecules</i> , 2019, 24, 2653.	3.8	7
6154	Molecular simulation of $CH_4$ adsorption behavior in slit nanopores: Verification of simulation methods and models. <i>AIChE Journal</i> , 2019, 65, e16733.	3.6	22
6155	An atomistic physico-chemical description of acetonitrile/tricyanomethanide based electrolytes. <i>Journal of Molecular Liquids</i> , 2019, 292, 111439.	4.9	4
6156	Decoupling of Translational Diffusion from the Viscosity of Supercooled Water: Role of Translational Jump Diffusion. <i>Journal of Physical Chemistry B</i> , 2019, 123, 7178-7189.	2.6	36
6157	Surface Penetration without Enrichment: Simulations Show Ion Surface Propensities Consistent with Both Elevated Surface Tension and Surface Sensitive Spectroscopy. <i>Journal of Physical Chemistry B</i> , 2019, 123, 7197-7203.	2.6	6

#	ARTICLE	IF	CITATIONS
6158	Might a 2,2-Dimethylbutane Molecule Serve as a Site to Promote Gas Hydrate Nucleation?. Journal of Physical Chemistry C, 2019, 123, 20579-20586.	3.1	19
6159	Molecular dynamics simulation of $\pm$ -unsubstituted oligo-thiophenes: dependence of their high-temperature liquid-crystalline phase behaviour on molecular length. Journal of Materials Chemistry C, 2019, 7, 9984-9995.	5.5	3
6160	Replica exchange MD simulations of two-dimensional water in graphene nanocapillaries: rhombic versus square structures, proton ordering, and phase transitions. Physical Chemistry Chemical Physics, 2019, 21, 17640-17654.	2.8	11
6161	Histidine at position 462 determines the low quinine sensitivity of ether- $\text{A}_{\text{A}}$ - $\text{G}_{\text{G}}$ channel superfamily member K <sub>v</sub> 12.1. British Journal of Pharmacology, 2019, 176, 2708-2723.	5.4	2
6162	Molecular dynamics simulation of removal of heavy metals with sodium dodecyl sulfate micelle in water. Colloids and Surfaces A: Physicochemical and Engineering Aspects, 2019, 578, 123613.	4.7	5
6163	Investigating Drug-Target Residence Time in Kinases through Enhanced Sampling Simulations. Journal of Chemical Theory and Computation, 2019, 15, 4646-4659.	5.3	32
6164	White light emission in water through admixtures of donor-acceptor siblings: experiment and simulation. New Journal of Chemistry, 2019, 43, 11701-11709.	2.8	5
6165	Class polymorphism in TIP4P/2005 water: A description based on the potential energy landscape formalism. Journal of Chemical Physics, 2019, 150, 244506.	3.0	20
6166	Structural and interfacial properties of the CO <sub>2</sub> -in-water foams prepared with sodium dodecyl sulfate (SDS): A molecular dynamics simulation study. Colloids and Surfaces A: Physicochemical and Engineering Aspects, 2019, 578, 123615.	4.7	18
6167	Molecular Basis for Membrane Selectivity of Antimicrobial Peptide Pleurocidin in the Presence of Different Eukaryotic and Prokaryotic Model Membranes. Journal of Chemical Information and Modeling, 2019, 59, 3262-3276.	5.4	22
6168	Molecular Dynamics Simulation of Pure <i>n</i> -Alkanes and Their Mixtures at Elevated Temperatures Using Atomistic and Coarse-Grained Force Fields. Journal of Physical Chemistry B, 2019, 123, 6229-6243.	2.6	56
6169	Combined <i>in silico</i> and <i>in vitro</i> study of an aptasensor based on citrate-capped AuNPs for naked-eye detection of a critical biomarker of oxidative stress. RSC Advances, 2019, 9, 17592-17600.	3.6	11
6170	Combined Small-Angle X-ray and Neutron Scattering Restraints in Molecular Dynamics Simulations. Journal of Chemical Theory and Computation, 2019, 15, 4687-4698.	5.3	36
6171	Separation of water-alcohol mixtures using carbon nanotubes under an electric field. Physical Chemistry Chemical Physics, 2019, 21, 15431-15438.	2.8	4
6172	Mechanistic insight into E22Q-mutation-induced antiparallel-to-parallel $\beta$ -sheet transition of A $\beta$ <sub>16-22</sub> fibrils: an all-atom simulation study. Physical Chemistry Chemical Physics, 2019, 21, 15686-15694.	2.8	18
6173	On the coupling of protein and water dynamics in confinement: Spatially resolved molecular dynamics simulation studies. Journal of Chemical Physics, 2019, 150, 245101.	3.0	7
6174	Atomistic phase field chemomechanical modeling of dislocation-solute-precipitate interaction in Ni-Al-Co. Acta Materialia, 2019, 175, 250-261.	7.9	51
6175	Bisubstrate Inhibitors of Nicotinamide <i>N</i> -Methyltransferase (NNMT) with Enhanced Activity. Journal of Medicinal Chemistry, 2019, 62, 6597-6614.	6.4	54



#	ARTICLE	IF	CITATIONS
6176	Possible Proton Conduction Mechanism in Pseudo-Protic Ionic Liquids: A Concept of Specific Proton Conduction. <i>Journal of Physical Chemistry B</i> , 2019, 123, 6244-6252.	2.6	43
6177	Molecular Dynamics Simulations and Experimental Verification to Determine Mechanism of Cosolvents on Increased 5-Hydroxymethylfurfural Yield from Glucose. <i>ACS Sustainable Chemistry and Engineering</i> , 2019, 7, 12997-13003.	6.7	15
6178	Towards boosting the exciton lifetime and efficiency of near-infrared aggregation induced emitters with hybridized local and charge transfer excited states: a multiscale study. <i>Journal of Materials Chemistry C</i> , 2019, 7, 8874-8887.	5.5	35
6179	Discovery of a highly specific and efficacious inhibitor of human carboxylesterase 2 by large-scale screening. <i>International Journal of Biological Macromolecules</i> , 2019, 137, 261-269.	7.5	31
6180	Tuning deformation behavior of Cu <sub>0.5</sub> CoNiCrAl high-entropy alloy via cooling rate gradient: An atomistic study. <i>Intermetallics</i> , 2019, 112, 106553.	3.9	11
6181	Membrane Recognition and Binding by the Phosphatidylinositol Phosphate Kinase PIP5K1A: A Multiscale Simulation Study. <i>Structure</i> , 2019, 27, 1336-1346.e2.	3.3	22
6182	Molecular dynamics simulations of membrane properties affected by plasma ROS based on the GROMOS force field. <i>Biophysical Chemistry</i> , 2019, 253, 106214.	2.8	14
6183	Development of multi-epitope driven subunit vaccine against <i>Fasciola gigantica</i> using immunoinformatics approach. <i>International Journal of Biological Macromolecules</i> , 2019, 138, 224-233.	7.5	59
6184	Chalcogenide glasses as a playground for the application of first-principles molecular dynamics to disordered materials. <i>Solid State Sciences</i> , 2019, 95, 105925.	3.2	4
6185	Structural and dynamical heterogeneities at glutamine-water interfaces. <i>Physical Chemistry Chemical Physics</i> , 2019, 21, 16083-16094.	2.8	4
6186	Calculation of phase diagrams in the multithermal-multibaric ensemble. <i>Journal of Chemical Physics</i> , 2019, 150, 244119.	3.0	29
6187	Molecular dynamics study on fast diffusion of hydrogen molecules in filled ice II. <i>Journal of Molecular Liquids</i> , 2019, 292, 111316.	4.9	3
6188	Molecular dynamics simulations of a cyclotetramethylene tetra-nitramine/hydrazine 5,5'-bitetrazole-1,1'-diolate cocrystal. <i>RSC Advances</i> , 2019, 9, 19390-19396.	3.6	5
6189	Effects of Cholesterol on Water Permittivity of Biomimetic Ion Pair Amphiphile Bilayers: Interplay between Membrane Bending and Molecular Packing. <i>International Journal of Molecular Sciences</i> , 2019, 20, 3252.	4.1	6
6190	Surface Inhomogeneity of Graphene Oxide Influences Dissociation of A <sup>21</sup> Peptide Assembly. <i>Journal of Physical Chemistry B</i> , 2019, 123, 9098-9103.	2.6	13
6191	Deep Molecular Orbital Driven High-Temperature Hydrogen Tautomerization Switching. <i>Journal of Physical Chemistry Letters</i> , 2019, 10, 6755-6761.	4.6	12
6192	Unconventional Split Aptamers Cleaved at Functionally Essential Sites Preserve Biorecognition Capability. <i>Analytical Chemistry</i> , 2019, 91, 15811-15817.	6.5	29
6193	Residue-Specific Force Field Improving the Sample of Intrinsically Disordered Proteins and Folded Proteins. <i>Journal of Chemical Information and Modeling</i> , 2019, 59, 4793-4805.	5.4	39

#	ARTICLE	IF	CITATIONS
6194	Molecular dynamics simulations of mechanical stress on oxidized membranes. <i>Biophysical Chemistry</i> , 2019, 254, 106266.	2.8	6
6195	Molecular Mechanism for Gramicidin Dimerization and Dissociation in Bilayers of Different Thickness. <i>Biophysical Journal</i> , 2019, 117, 1831-1844.	0.5	15
6196	Exploring and Engineering the Conformational Landscape of Calmodulin through Specific Interactions. <i>Journal of Physical Chemistry B</i> , 2019, 123, 9321-9327.	2.6	4
6197	Fusion proteins with chromogenic and keratin binding modules. <i>Scientific Reports</i> , 2019, 9, 14044.	3.3	12
6198	Co-axially rotating carbon nanotubes: A novel mechanism for nanoscale pumping of fluids. <i>AIP Conference Proceedings</i> , 2019, , .	0.4	0
6199	Hydrogen Bonding Between Ions of Like Charge in Ionic Liquids Characterized by NMR Deuteron Quadrupole Coupling Constants—Comparison with Salt Bridges and Molecular Systems. <i>Angewandte Chemie</i> , 2019, 131, 18027-18035.	2.0	7
6200	Hydrogen Bonding Between Ions of Like Charge in Ionic Liquids Characterized by NMR Deuteron Quadrupole Coupling Constants—Comparison with Salt Bridges and Molecular Systems. <i>Angewandte Chemie - International Edition</i> , 2019, 58, 17863-17871.	13.8	41
6201	Shift of Creep Mechanism in Nanocrystalline NiAl Alloy. <i>Materials</i> , 2019, 12, 2508.	2.9	5
6202	Solution structure of the autophagy-related protein LC3C reveals a polyproline II motif on a mobile tether with phosphorylation site. <i>Scientific Reports</i> , 2019, 9, 14167.	3.3	15
6203	The Role of Charge Transfer in the Formation of Type I Deep Eutectic Solvent-Analogous Ionic Liquid Mixtures. <i>Molecules</i> , 2019, 24, 3687.	3.8	21
6204	Structural and functional insights into the tetrameric photosystem I from heterocyst-forming cyanobacteria. <i>Nature Plants</i> , 2019, 5, 1087-1097.	9.3	57
6205	Effects of solidification defects on nanoscale mechanical properties of rapid directionally solidified Al-Cu Alloy: A large scale molecular dynamics study. <i>Journal of Crystal Growth</i> , 2019, 527, 125255.	1.5	24
6206	Polyproline chains destabilize the Alzheimer's amyloid- $\beta$ protofibrils: A molecular dynamics simulation study. <i>Journal of Molecular Graphics and Modelling</i> , 2019, 93, 107456.	2.4	17
6207	Comparison of Carbohydrate Force Fields Using Gaussian Accelerated Molecular Dynamics Simulations and Development of Force Field Parameters for Heparin-Analogue Pentasaccharides. <i>Journal of Chemical Information and Modeling</i> , 2019, 59, 4855-4867.	5.4	20
6208	pH-Responsive Lipid-Dendrimer Hybrid Nanoparticles: An Approach To Target and Eliminate Intracellular Pathogens. <i>Molecular Pharmaceutics</i> , 2019, 16, 4594-4609.	4.6	52
6209	Toward the design of efficient transglycosidases: the case of the GH1 of <i>Thermus thermophilus</i> . <i>Protein Engineering, Design and Selection</i> , 2019, 32, 309-316.	2.1	5
6210	Structural basis for the docking of mTORC1 on the lysosomal surface. <i>Science</i> , 2019, 366, 468-475.	12.6	132
6211	Effect of oxidative stress on cystine transportation by xC $\text{â}^{\frac{3}{4}}$ antiporter. <i>Archives of Biochemistry and Biophysics</i> , 2019, 674, 108114.	3.0	7

#	ARTICLE	IF	CITATIONS
6212	Highly Miscible Hybrid Liquid-Crystal Systems Containing Fluorescent Excited-State Intramolecular Proton Transfer Molecules. <i>Langmuir</i> , 2019, 35, 14031-14041.	3.5	11
6213	Controlling Supramolecular Chirality in Peptide- $\pi$ -Peptide Networks by Variation of the Alkyl Spacer Length. <i>Langmuir</i> , 2019, 35, 14060-14073.	3.5	26
6214	Topology, landscapes, and biomolecular energy transport. <i>Nature Communications</i> , 2019, 10, 4662.	12.8	8
6215	Probing into Methylene Blue Interaction with Polyglutamic Acid: Spectroscopic and Molecular Dynamics Simulation Studies. <i>Asian Journal of Chemistry</i> , 2019, 31, 1949-1958.	0.3	1
6216	Serine Phosphorylation of L-Selectin Regulates ERM Binding, Clustering, and Monocyte Protrusion in Transendothelial Migration. <i>Frontiers in Immunology</i> , 2019, 10, 2227.	4.8	6
6217	Evaluating the strengths of salt bridges in the CutA1 protein using molecular dynamic simulations: a comparison of different force fields. <i>FEBS Open Bio</i> , 2019, 9, 1939-1956.	2.3	1
6218	Biocatalytic production of D-p-hydroxyphenylglycine by optimizing protein expression and cell wall engineering in <i>Escherichia coli</i> . <i>Applied Microbiology and Biotechnology</i> , 2019, 103, 8839-8851.	3.6	12
6219	Bias Correction of Gauge Data and its Effect on Precipitation Climatology over Mainland China. <i>Journal of Applied Meteorology and Climatology</i> , 2019, 58, 2177-2196.	1.5	16
6220	Molecular Simulation of Methane Adsorption Behavior in Kerogen Nanopores for Shale Gas Resource Assessment. , 2019, , .		7
6221	Transport Properties of Thermoplastic R-BAPB Polyimide: Molecular Dynamics Simulations and Experiment. <i>Polymers</i> , 2019, 11, 1775.	4.5	19
6222	Limiting distribution of translates of the orbit of a maximal $\mathbb{Q}$ -torus from identity on $\mathrm{SL}_N(\mathbb{R})/\mathrm{SL}_N(\mathbb{Z})$ . <i>Mathematische Annalen</i> , 2019, 375, 1231-1281.	1.4	2
6223	Self-Association of Antimicrobial Peptides: A Molecular Dynamics Simulation Study on Bombinin. <i>International Journal of Molecular Sciences</i> , 2019, 20, 5450.	4.1	17
6224	Effect of Kinase Inhibiting RNase Attenuator (KIRA) Compounds on the Formation of Face-to-Face Dimers of Inositol-Requiring Enzyme 1: Insights from Computational Modeling. <i>International Journal of Molecular Sciences</i> , 2019, 20, 5538.	4.1	6
6225	Magainin 2 and PGLa in Bacterial Membrane Mimics I: Peptide-Peptide and Lipid-Peptide Interactions. <i>Biophysical Journal</i> , 2019, 117, 1858-1869.	0.5	30
6226	Atomistic study of the physical properties of sulfonium-based ionic liquids as electrolyte for supercapacitors. <i>Journal of Molecular Liquids</i> , 2019, 296, 112065.	4.9	19
6227	Biochemical and Structural Insights Concerning Triclosan Resistance in a Novel YX7K Type Enoyl-Acyl Carrier Protein Reductase from Soil Metagenome. <i>Scientific Reports</i> , 2019, 9, 15401.	3.3	3
6228	Revealing the Sequence-Structure-Electronic Property Relation of Self-Assembling $\pi$ -Conjugated Oligopeptides by Molecular and Quantum Mechanical Modeling. <i>Langmuir</i> , 2019, 35, 15221-15231.	3.5	8
6229	Exploring the Conformational Space of Bcl-2 Protein Variants: Dynamic Contributions of the Flexible Loop Domain and Transmembrane Region. <i>Molecules</i> , 2019, 24, 3896.	3.8	9

#	ARTICLE	IF	CITATIONS
6230	Performance evaluation of molecular docking and free energy calculations protocols using the D3R Grand Challenge 4 dataset. <i>Journal of Computer-Aided Molecular Design</i> , 2019, 33, 1031-1043.	2.9	12
6231	Exploring the Free Energy Landscape To Predict the Surfactant Adsorption Isotherm at the Nanoparticleâ€“Water Interface. <i>ACS Central Science</i> , 2019, 5, 1804-1812.	11.3	19
6232	Computationally designed antibodyâ€“drug conjugates self-assembled via affinity ligands. <i>Nature Biomedical Engineering</i> , 2019, 3, 917-929.	22.5	19
6233	Understanding the Origin of the Breakdown of the Stokesâ€“Einstein Relation in Supercooled Water at Different Temperatureâ€“Pressure Conditions. <i>Journal of Physical Chemistry B</i> , 2019, 123, 10089-10099.	2.6	31
6234	Toward Predictive Molecular Dynamics Simulations of Asphaltenes in Toluene and Heptane. <i>ACS Omega</i> , 2019, 4, 20005-20014.	3.5	22
6235	South African Abietane Diterpenoids and Their Analogs as Potential Antimalarials: Novel Insights from Hybrid Computational Approaches. <i>Molecules</i> , 2019, 24, 4036.	3.8	6
6236	Effects of Sterols on the Interaction of SDS, Benzalkonium Chloride, and A Novel Compound, Kor105, with Membranes. <i>Biomolecules</i> , 2019, 9, 627.	4.0	10
6237	Multi-Target Chemometric Modelling, Fragment Analysis and Virtual Screening with ERK Inhibitors as Potential Anticancer Agents. <i>Molecules</i> , 2019, 24, 3909.	3.8	18
6238	Destabilization of Insulin Hexamer in Waterâ€“Ethanol Binary Mixture. <i>Journal of Physical Chemistry B</i> , 2019, 123, 10365-10375.	2.6	10
6239	Cholesteryl Hemisuccinate Is Not a Good Replacement for Cholesterol in Lipid Nanodiscs. <i>Journal of Physical Chemistry B</i> , 2019, 123, 9839-9845.	2.6	18
6240	Amino-Acid-Based Ionic Liquids for the Improvement in Stability and Activity of Cytochrome c: A Combined Experimental and Molecular Dynamics Study. <i>Journal of Physical Chemistry B</i> , 2019, 123, 10100-10109.	2.6	38
6241	Transport in Superconcentrated LiPF <sub>6</sub> and LiBF <sub>4</sub> /Propylene Carbonate Electrolytes. <i>ACS Energy Letters</i> , 2019, 4, 2843-2849.	17.4	71
6242	A suicide inhibitor of nematode trehalose-6-phosphate phosphatases. <i>Scientific Reports</i> , 2019, 9, 16165.	3.3	4
6243	Dynamical Rearrangement of Human Epidermal Growth Factor Receptor 2 upon Antibody Binding: Effects on the Dimerization. <i>Biomolecules</i> , 2019, 9, 706.	4.0	6
6244	Estimation of Proteinâ€“Ligand Unbinding Kinetics Using Non-Equilibrium Targeted Molecular Dynamics Simulations. <i>Journal of Chemical Information and Modeling</i> , 2019, 59, 5135-5147.	5.4	35
6245	Nontargeted Parallel Cascade Selection Molecular Dynamics Based on a Nonredundant Selection Rule for Initial Structures Enhances Conformational Sampling of Proteins. <i>Journal of Chemical Information and Modeling</i> , 2019, 59, 5198-5206.	5.4	5
6246	The Novel Serine/Threonine Protein Kinase LmjF.22.0810 from <i>Leishmania major</i> may be Involved in the Resistance to Drugs such as Paromomycin. <i>Biomolecules</i> , 2019, 9, 723.	4.0	8
6247	Disclosing the Impact of Carcinogenic SF3b Mutations on Pre-mRNA Recognition Via All-Atom Simulations. <i>Biomolecules</i> , 2019, 9, 633.	4.0	23

#	ARTICLE	IF	CITATIONS
6248	Molecular Dynamics Simulations of Crystal Nucleation from Solution at Constant Chemical Potential. <i>Journal of Chemical Theory and Computation</i> , 2019, 15, 6923-6930.	5.3	31
6249	Development of GROMOS-Compatible Parameter Set for Simulations of Chalcones and Flavonoids. <i>Journal of Physical Chemistry B</i> , 2019, 123, 994-1008.	2.6	7
6250	Polyethylenimineâ€“DNA Ratio Strongly Affects Their Nanoparticle Formation: A Large-Scale Coarse-Grained Molecular Dynamics Study. <i>Journal of Physical Chemistry B</i> , 2019, 123, 9629-9640.	2.6	14
6251	Hydrophobic Hydration of Fluoroalkyl (Câ€“F) is Distinctly Different from That of Its Hydrogenated Counterpart (Câ€“H), as Observed by Raman Difference with Simultaneous Curve Fitting Analysis. <i>Journal of Physical Chemistry C</i> , 2019, 123, 27012-27019.	3.1	25
6252	Pneumococcal VncR Strain-Specifically Regulates Capsule Polysaccharide Synthesis. <i>Frontiers in Microbiology</i> , 2019, 10, 2279.	3.5	3
6253	Obtaining Protein Association Energy Landscape for Integral Membrane Proteins. <i>Journal of Chemical Theory and Computation</i> , 2019, 15, 6444-6455.	5.3	17
6254	Van der Waals Integration of Bismuth Quantum Dotsâ€“Decorated Tellurium Nanotubes (Te@Bi) Heterojunctions and Plasmaâ€“Enhanced Optoelectronic Applications. <i>Small</i> , 2019, 15, e1903233.	10.0	45
6255	Improving the Vertical Thermal Conductivity of Carbon Fiber-Reinforced Epoxy Composites by Forming Layer-by-Layer Contact of Inorganic Crystals. <i>Materials</i> , 2019, 12, 3092.	2.9	19
6256	Fosfomycin Permeation through the Outer Membrane Porin OmpF. <i>Biophysical Journal</i> , 2019, 116, 258-269.	0.5	24
6257	Molecular Dynamics Simulations of Short-Chain Branched Bimodal Polyethylene: Topological Characteristics and Mechanical Behavior. <i>Macromolecules</i> , 2019, 52, 807-818.	4.8	42
6258	Molecular Insights into Destabilization of Alzheimerâ€™s A $\beta$ Protofibril by Arginine Containing Short Peptides: A Molecular Modeling Approach. <i>ACS Omega</i> , 2019, 4, 892-903.	3.5	38
6259	Comparing an All-Atom and a Coarse-Grained Description of Lipid Bilayers in Terms of Enthalpies and Entropies: From MD Simulations to 2D Lattice Models. <i>Journal of Chemical Theory and Computation</i> , 2019, 15, 6393-6402.	5.3	7
6260	Palmitoylation of Claudin-5 Proteins Influences Their Lipid Domain Affinity and Tight Junction Assembly at the Bloodâ€“Brain Barrier Interface. <i>Journal of Physical Chemistry B</i> , 2019, 123, 983-993.	2.6	27
6261	Controlled exploration of chemical space by machine learning of coarse-grained representations. <i>Physical Review E</i> , 2019, 100, 033302.	2.1	17
6262	Integration of multiscale molecular modeling approaches with the design and discovery of fusidic acid derivatives. <i>Future Medicinal Chemistry</i> , 2019, 11, 1427-1442.	2.3	10
6263	Molecular Dynamics and Metadynamics Insights of 1,4-Dioxane-Induced Structural Changes of Biomembrane Models. <i>Journal of Physical Chemistry B</i> , 2019, 123, 7869-7884.	2.6	7
6264	Molecular dynamics study of natural rubberâ€“fullerene composites: connecting microscopic properties to macroscopic behavior. <i>Physical Chemistry Chemical Physics</i> , 2019, 21, 19403-19413.	2.8	15
6265	Effects of Ether Linkage on Membrane Dipole Potential and Cholesterol Flip-Flop Motion in Lipid Bilayer Membranes. <i>Journal of Physical Chemistry B</i> , 2019, 123, 7818-7828.	2.6	7

#	ARTICLE	IF	CITATIONS
6266	Computational Study on Structure and Aggregation Pathway of A $\beta$ <sub>42</sub> Amyloid Protofibril. Journal of Physical Chemistry B, 2019, 123, 7859-7868.	2.6	4
6267	Enhancing Biomolecular Sampling with Reinforcement Learning: A Tree Search Molecular Dynamics Simulation Method. ACS Omega, 2019, 4, 13853-13862.	3.5	25
6268	In silico study of colchicine resistance molecular mechanisms caused by tubulin structural polymorphism. PLoS ONE, 2019, 14, e0221532.	2.5	12
6269	Covalent modification of phosphatidylethanolamine by 4-hydroxy-2-nonenal increases sodium permeability across phospholipid bilayer membranes. Free Radical Biology and Medicine, 2019, 143, 433-440.	2.9	13
6270	Anatomy of Microscopic Structure of Ethaline Deep Eutectic Solvent Decoded through Molecular Dynamics Simulations. Journal of Physical Chemistry B, 2019, 123, 8291-8299.	2.6	82
6271	Effects of Salinity and N-, S-, and O-Bearing Polar Components on Light Oil–Brine Interfacial Properties from Molecular Perspectives. Journal of Physical Chemistry C, 2019, 123, 23520-23528.	3.1	25
6272	The structural basis for membrane assembly of immunoreceptor signalling complexes. Journal of Molecular Modeling, 2019, 25, 277.	1.8	3
6273	Nontargeted Parallel Cascade Selection Molecular Dynamics Using Time-Localized Prediction of Conformational Transitions in Protein Dynamics. Journal of Chemical Theory and Computation, 2019, 15, 5144-5153.	5.3	12
6274	Pressure-Induced Miscibility Increase of CH <sub>4</sub> in H <sub>2</sub> O: A Computational Study Using Classical Potentials. Journal of Physical Chemistry B, 2019, 123, 8091-8095.	2.6	5
6275	Molecular Dynamics Study on the Mechanism of Graphene Oxide to Destabilize Oil/Water Emulsion. Journal of Physical Chemistry C, 2019, 123, 22989-22999.	3.1	34
6276	Spontaneously Forming Dendritic Voids in Liquid Water Can Host Small Polymers. Journal of Physical Chemistry Letters, 2019, 10, 5585-5591.	4.6	21
6277	Cytotoxicity of C <sub>2</sub> N Originating from Oxidative Stress Instead of Membrane Stress. ACS Applied Materials & Interfaces, 2019, 11, 34575-34585.	8.0	13
6278	Competitive double-switched self-assembled cyclic peptide nanotubes: a dual internal and external control. Physical Chemistry Chemical Physics, 2019, 21, 20750-20756.	2.8	11
6279	Non-linearity in dipolar solvation dynamics in water-ethanol mixture: Composition dependence of free energy landscape. Journal of Chemical Physics, 2019, 151, 084502.	3.0	6
6280	Localization model description of diffusion and structural relaxation in superionic crystalline UO <sub>2</sub> . Journal of Chemical Physics, 2019, 151, 071101.	3.0	18
6281	Insights into the Relationships Between Herbicide Activities, Molecular Structure and Membrane Interaction of Cinnamon and Citronella Essential Oils Components. International Journal of Molecular Sciences, 2019, 20, 4007.	4.1	42
6282	Investigating the solid-liquid extraction process of puerarin by molecular dynamics simulations. International Journal of Heat and Mass Transfer, 2019, 143, 118584.	4.8	8
6283	The Adaptive Path Collective Variable: A Versatile Biasing Approach to Compute the Average Transition Path and Free Energy of Molecular Transitions. Methods in Molecular Biology, 2019, 2022, 255-290.	0.9	8



#	ARTICLE	IF	CITATIONS
6284	Molecular Dynamics Simulation of Metal Matrix Composites Using BIOVIA Materials Studio, LAMMPS, and GROMACS. , 2019, , 101-140.		2
6285	An Integrated Markov State Model and Path Metadynamics Approach To Characterize Drug Binding Processes. Journal of Chemical Theory and Computation, 2019, 15, 5689-5702.	5.3	45
6286	Molecular Dynamics Simulations Reveal the Inhibitory Mechanism of Dopamine against Human Islet Amyloid Polypeptide (hIAPP) Aggregation and Its Destabilization Effect on hIAPP Protofibrils. ACS Chemical Neuroscience, 2019, 10, 4151-4159.	3.5	46
6287	Structural analysis of ionic liquids with symmetric and asymmetric fluorinated anions. Journal of Chemical Physics, 2019, 151, 074504.	3.0	20
6288	Amphiphilic peptide binding on crystalline vs. amorphous silica from molecular dynamics simulations. Molecular Physics, 2019, 117, 3642-3650.	1.7	11
6289	Combinatorial diversity of Syk recruitment driven by its multivalent engagement with FcÎµRIÎ³. Molecular Biology of the Cell, 2019, 30, 2331-2347.	2.1	11
6290	Achieving an Optimal <i>T</i><sub>g</sub> Change by Elucidating the Polymerâ€“Nanoparticle Interface: A Molecular Dynamics Simulation Study of the Poly(vinyl alcohol)â€“Silica Nanocomposite System. Journal of Physical Chemistry C, 2019, 123, 23995-24006.	3.1	18
6291	Molecular dynamics research on effect of doping defects on properties of PETN. Journal of Molecular Modeling, 2019, 25, 287.	1.8	5
6292	Structural dataset from microsecond-long simulations of yeast mitofusin Fzo1 in the context of membrane docking. Data in Brief, 2019, 26, 104460.	1.0	4
6293	Ligand-Dependent Sodium Ion Dynamics within the A<sub>2A</sub> Adenosine Receptor: A Molecular Dynamics Study. Journal of Physical Chemistry B, 2019, 123, 7947-7954.	2.6	4
6294	An electrostatic switching mechanism to control the lipid transfer activity of Osh6p. Nature Communications, 2019, 10, 3926.	12.8	32
6295	Superioniclike Diffusion in an Elemental Crystal: bcc Titanium. Physical Review Letters, 2019, 123, 105501.	7.8	28
6296	Insights into the EGFR SAR of N-phenylquinazolin-4-amine-derivatives using quantum mechanical pairwise-interaction energies. Journal of Computer-Aided Molecular Design, 2019, 33, 745-757.	2.9	5
6297	Natural compounds as potential Hsp90 inhibitors for breast cancer-Pharmacophore guided molecular modelling studies. Computational Biology and Chemistry, 2019, 83, 107113.	2.3	21
6298	Quantum Chemical Calculations of NMR Chemical Shifts in Phosphorylated Intrinsically Disordered Proteins. Journal of Chemical Theory and Computation, 2019, 15, 5642-5658.	5.3	6
6299	Enhancement of Adhesion Strength of Perfluoroalkylpolyethers on Rough Glassy Silica for Antismudge Coatings. ACS Applied Polymer Materials, 2019, 1, 2613-2621.	4.4	3
6300	Diffusion of tRNA inside the ribosome is position-dependent. Journal of Chemical Physics, 2019, 151, 085102.	3.0	31
6301	Mechanical properties of tubulin intra- and inter-dimer interfaces and their implications for microtubule dynamic instability. PLoS Computational Biology, 2019, 15, e1007327.	3.2	35

#	ARTICLE	IF	CITATIONS
6302	Antimicrobial peptide ROADâ€“1 triggers phase change in local membrane environment to execute its activity. <i>Journal of Molecular Modeling</i> , 2019, 25, 281.	1.8	0
6303	Soluble Regions of GlpG Influence Proteinâ€™Lipid Interactions and Lipid Distribution. <i>Journal of Physical Chemistry B</i> , 2019, 123, 7852-7858.	2.6	1
6304	Unsupervised Machine Learning for Analysis of Phase Separation in Ternary Lipid Mixture. <i>Journal of Chemical Theory and Computation</i> , 2019, 15, 6343-6357.	5.3	18
6305	Comparing water-mediated hydrogen-bonding in different polyelectrolyte complexes. <i>Soft Matter</i> , 2019, 15, 7823-7831.	2.7	31
6306	Molecular basis for functional diversity among microbial Nep1-like proteins. <i>PLoS Pathogens</i> , 2019, 15, e1007951.	4.7	39
6307	A Fragmenting Protocol with Explicit Hydration for Calculation of Binding Enthalpies of Target-Ligand Complexes at a Quantum Mechanical Level. <i>International Journal of Molecular Sciences</i> , 2019, 20, 4384.	4.1	11
6308	Pitfalls of the Martini Model. <i>Journal of Chemical Theory and Computation</i> , 2019, 15, 5448-5460.	5.3	159
6309	BioExcel Building Blocks, a software library for interoperable biomolecular simulation workflows. <i>Scientific Data</i> , 2019, 6, 169.	5.3	35
6310	Different platinum crystal surfaces show very distinct protein denaturation capabilities. <i>Nanoscale</i> , 2019, 11, 19352-19361.	5.6	3
6311	Biophysical Insight on the Membrane Insertion of an Arginine-Rich Cell-Penetrating Peptide. <i>International Journal of Molecular Sciences</i> , 2019, 20, 4441.	4.1	14
6312	Accurate Calculation of Barnase and SNase Folding Energetics Using Short Molecular Dynamics Simulations and an Atomistic Model of the Unfolded Ensemble: Evaluation of Force Fields and Water Models. <i>Journal of Chemical Information and Modeling</i> , 2019, 59, 4350-4360.	5.4	14
6313	MARK4 protein can explore the active-like conformations in its non-phosphorylated state. <i>Scientific Reports</i> , 2019, 9, 12967.	3.3	4
6314	Local accumulation of diacylglycerol alters membrane properties nonlinearly due to its transbilayer activity. <i>Communications Chemistry</i> , 2019, 2, .	4.5	37
6315	Diffusivities in 1-Alcohols Containing Dissolved H <sub>2</sub> , He, N <sub>2</sub> , CO, or CO <sub>2</sub> Close to Infinite Dilution. <i>Journal of Physical Chemistry B</i> , 2019, 123, 8777-8790.	2.6	36
6316	Molecular basis of dengue virus serotype 2 morphological switch from 29Â°C to 37Â°C. <i>PLoS Pathogens</i> , 2019, 15, e1007996.	4.7	25
6317	Mechanistic Aspects of Fungicide-Induced DNA Damage: Spectroscopic and Molecular Dynamics Simulation Studies. <i>Journal of Physical Chemistry B</i> , 2019, 123, 8653-8661.	2.6	16
6318	Osmolyte-Induced Macromolecular Aggregation Is Length-Scale Dependent. <i>Journal of Physical Chemistry B</i> , 2019, 123, 8697-8703.	2.6	8
6319	Why do G-quadruplexes dimerize through the 5â€™-ends? Driving forces for G4 DNA dimerization examined in atomic detail. <i>PLoS Computational Biology</i> , 2019, 15, e1007383.	3.2	26

#	ARTICLE	IF	CITATIONS
6320	Structure and thermodynamics of aqueous urea solutions from ambient to kilobar pressures: From thermodynamic modeling, experiments, and first principles simulations to an accurate force field description. <i>Biophysical Chemistry</i> , 2019, 254, 106260.	2.8	10
6321	Rattling Transport of Lithium Ion in the Cavities of Model Solid Electrolyte Interphase. <i>Journal of Physical Chemistry C</i> , 2019, 123, 25015-25024.	3.1	2
6322	Hybrid Atomistic and Coarse-Grained Model for Surfactants in Apolar Solvents. <i>ACS Omega</i> , 2019, 4, 15581-15592.	3.5	11
6323	Origin of Pyroelectricity in Ferroelectric HfO <sub>2</sub> . <i>Physical Review Applied</i> , 2019, 12, .	3.8	37
6324	Proton Control of Transitions in an Amino Acid Transporter. <i>Biophysical Journal</i> , 2019, 117, 1342-1351.	0.5	10
6325	Molecular Simulations of Intact Anion Exchanger 1 Reveal Specific Domain and Lipid Interactions. <i>Biophysical Journal</i> , 2019, 117, 1364-1379.	0.5	16
6326	Local Enrichment of Unsaturated Chains around the A <sub>2A</sub> Adenosine Receptor. <i>Biochemistry</i> , 2019, 58, 4096-4105.	2.5	9
6327	Dealing with Hydrogen Bonding on the Conformational Preference of 1,3-Aminopropanols: Experimental and Molecular Dynamics Approaches. <i>Journal of Physical Chemistry A</i> , 2019, 123, 8583-8594.	2.5	9
6328	Computational study of paroxetine-like inhibitors reveals new molecular insight to inhibit GRK2 with selectivity over ROCK1. <i>Scientific Reports</i> , 2019, 9, 13053.	3.3	21
6329	Extensive tests and evaluation of the CHARMM36IDPSFF force field for intrinsically disordered proteins and folded proteins. <i>Physical Chemistry Chemical Physics</i> , 2019, 21, 21918-21931.	2.8	37
6330	Investigation into Early Steps of Actin Recognition by the Intrinsically Disordered N-WASP Domain V. <i>International Journal of Molecular Sciences</i> , 2019, 20, 4493.	4.1	3
6331	Differential Dynamics Underlying the Gln27Glu Population Variant of the $\beta$ 2-Adrenergic Receptor. <i>Journal of Membrane Biology</i> , 2019, 252, 499-507.	2.1	11
6332	SDHA gain-of-function engages inflammatory mitochondrial retrograde signaling via KEAP1–Nrf2. <i>Nature Immunology</i> , 2019, 20, 1311-1321.	14.5	39
6333	Shape segregation in molecular organisation: a combined X-ray scattering and molecular dynamics study of smectic liquid crystals. <i>Soft Matter</i> , 2019, 15, 7722-7732.	2.7	8
6334	Phase stability of the ice XVII-based CO <sub>2</sub> chiral hydrate from molecular dynamics simulations. <i>Journal of Chemical Physics</i> , 2019, 151, 104502.	3.0	3
6335	Percolation Phase Transition from Ionic Liquids to Ionic Liquid Crystals. <i>Scientific Reports</i> , 2019, 9, 13169.	3.3	10
6336	Validation of the Generalized Force Fields GAFF, CGenFF, OPLS-AA, and PRODRGFF by Testing Against Experimental Osmotic Coefficient Data for Small Drug-Like Molecules. <i>Journal of Chemical Information and Modeling</i> , 2019, 59, 4239-4247.	5.4	26
6337	Standard Binding Free Energy of a SIM–SUMO Complex. <i>Journal of Chemical Theory and Computation</i> , 2019, 15, 6403-6410.	5.3	8

#	ARTICLE	IF	CITATIONS
6338	The dynamic behavior of gas hydrate dissociation by heating in tight sandy reservoirs: A molecular dynamics simulation study. <i>Fuel</i> , 2019, 258, 116106.	6.4	35
6339	Solubility of Polar and Nonpolar Aromatic Molecules in Subcritical Water: The Role of the Dielectric Constant. <i>Journal of Chemical Theory and Computation</i> , 2019, 15, 6277-6293.	5.3	18
6340	Molecular Model for the Self-Assembly of the Cyclic Lipodepsipeptide Pseudodesmin A. <i>Journal of Physical Chemistry B</i> , 2019, 123, 8916-8922.	2.6	2
6341	Fast healing of ionic bonds in tough hydrogels under an acoustic excitation. <i>Extreme Mechanics Letters</i> , 2019, 33, 100572.	4.1	13
6342	A force field of Li <sup>+</sup> , Na <sup>+</sup> , K <sup>+</sup> , Mg <sup>2+</sup> , Ca <sup>2+</sup> , Cl <sup>-</sup> , and SO <sub>4</sub> <sup>2-</sup> in aqueous solution based on the TIP4P/2005 water model and scaled charges for the ions. <i>Journal of Chemical Physics</i> , 2019, 151, 134504.	3.0	166
6343	Association of Both Inhibitory and Stimulatory G $\alpha$ Subunits Implies Adenylyl Cyclase 5 Deactivation. <i>Biochemistry</i> , 2019, 58, 4317-4324.	2.5	11
6344	Conformation and Domain Movement Analysis of Human Matrix Metalloproteinase-2: Role of Associated Zn <sup>2+</sup> and Ca <sup>2+</sup> Ions. <i>International Journal of Molecular Sciences</i> , 2019, 20, 4194.	4.1	5
6345	Study of the Lamellar and Micellar Phases of Pluronic F127: A Molecular Dynamics Approach. <i>Processes</i> , 2019, 7, 606.	2.8	3
6346	Molecular level insight into the counteraction of trehalose on the activity as well as denaturation of lysozyme induced by guanidinium chloride. <i>Chemical Physics</i> , 2019, 527, 110489.	1.9	6
6347	Effects of the Water Content on the Transport Properties of Ionic Liquids. <i>Industrial &amp; Engineering Chemistry Research</i> , 2019, 58, 19661-19669.	3.7	13
6348	Unraveling the Unbinding Pathways of Products Formed in Catalytic Reactions Involved in SIRT1 <sup>3</sup> : A Random Acceleration Molecular Dynamics Simulation Study. <i>Journal of Chemical Information and Modeling</i> , 2019, 59, 4100-4115.	5.4	10
6349	Quantitative Assessment of the Conformational Heterogeneity in Amylose across Force Fields. <i>Journal of Chemical Theory and Computation</i> , 2019, 15, 6203-6212.	5.3	15
6350	Controlled On/Off Switching of Tight-Binding Hydrogen Bonds between Model Cell Membranes and Acetylated Cellulose Surfaces. <i>Langmuir</i> , 2019, 35, 13753-13760.	3.5	6
6351	Methanol-ethanol $\epsilon$ -ideal mixtures as a test ground for the computation of Kirkwood-Buff integrals. <i>Journal of Molecular Liquids</i> , 2019, 293, 111447.	4.9	4
6352	Large-scale molecular dynamics simulation of perfluorosulfonic acid membranes: Remapping coarse-grained to all-atomistic simulations. <i>Polymer</i> , 2019, 181, 121766.	3.8	9
6353	Brazilin Inhibits $\beta$ -Synuclein Fibrillogenesis, Disrupts Mature Fibrils, and Protects against Amyloid-Induced Cytotoxicity. <i>Journal of Agricultural and Food Chemistry</i> , 2019, 67, 11769-11777.	5.2	31
6354	MemSurfer: A Tool for Robust Computation and Characterization of Curved Membranes. <i>Journal of Chemical Theory and Computation</i> , 2019, 15, 6411-6421.	5.3	36
6355	Relative Solvent Exposure of the Alpha-Helix and Beta-Sheet in Water Determines the Initial Stages of Urea and Guanidinium Chloride-Induced Denaturation of Alpha/Beta Proteins. <i>Journal of Physical Chemistry B</i> , 2019, 123, 8889-8900.	2.6	10

#	ARTICLE	IF	CITATIONS
6356	Overview of BIOVIA Materials Studio, LAMMPS, and GROMACS. , 2019, , 39-100.		10
6357	Membrane Remodeling by the Lytic Fragment of $\sigma$ -SticholysinIII: Implications for the Toroidal Pore Model. Biophysical Journal, 2019, 117, 1563-1576.	0.5	12
6358	Molecular Mechanism of S1P Binding and Activation of the S1P1 Receptor. Journal of Chemical Information and Modeling, 2019, 59, 4402-4412.	5.4	20
6359	Inhibition of Amyloid- $\beta$ Aggregation by Cobalt(III) Schiff Base Complexes: A Computational and Experimental Approach. Journal of the American Chemical Society, 2019, 141, 16685-16695.	13.7	50
6360	Conduction through a narrow inward-rectifier K <sup>+</sup> channel pore. Journal of General Physiology, 2019, 151, 1231-1246.	1.9	36
6361	PTP1B phosphatase as a novel target of oleuropein activity in MCF-7 breast cancer model. Toxicology in Vitro, 2019, 61, 104624.	2.4	15
6362	Lipid Acyl Chain <i>cis</i> Double Bond Position Modulates Membrane Domain Registration/Anti-Registration. Journal of the American Chemical Society, 2019, 141, 15884-15890.	13.7	36
6363	Decoding signatures of structure, bulk thermodynamics, and solvation in three-body angle distributions of rigid water models. Journal of Chemical Physics, 2019, 151, 094501.	3.0	16
6364	Coil-Globule Transition Thermodynamics of Poly( <i>N</i> -isopropylacrylamide). Journal of Physical Chemistry B, 2019, 123, 8838-8847.	2.6	45
6365	Understanding Interactions of Curcumin with Lipid Bilayers: A Coarse-Grained Molecular Dynamics Study. Journal of Chemical Information and Modeling, 2019, 59, 4413-4426.	5.4	13
6366	Generation of the configurational ensemble of an intrinsically disordered protein from unbiased molecular dynamics simulation. Proceedings of the National Academy of Sciences of the United States of America, 2019, 116, 20446-20452.	7.1	88
6367	Extension of the effective solid-fluid Steele potential for Mie force fields. Molecular Physics, 2019, 117, 3840-3851.	1.7	9
6368	Substrate conformational dynamics facilitate structure-specific recognition of gapped DNA by DNA polymerase. Nucleic Acids Research, 2019, 47, 10788-10800.	14.5	36
6369	Highly Efficient Solar-Driven Carbon Dioxide Reduction on Molybdenum Disulfide Catalyst Using Choline Chloride-Based Electrolyte. Advanced Energy Materials, 2019, 9, 1803536.	19.5	34
6370	Free Energy Calculation of Transmembrane Ion Permeation: Sample with a Single Reaction Coordinate and Analysis along Transition Path. Journal of Chemical Theory and Computation, 2019, 15, 1216-1225.	5.3	9
6371	Microsolvation of the Redox-Active Tyrosine-D in Photosystem II: Correlation of Energetics with EPR Spectroscopy and Oxidation-Induced Proton Transfer. Journal of the American Chemical Society, 2019, 141, 3217-3231.	13.7	14
6372	Molecular dynamics simulations of EPON-862/DETDA epoxy networks: structure, topology, elastic constants, and local dynamics. Soft Matter, 2019, 15, 721-733.	2.7	41
6373	Influence of glycerol on the cooling effect of pair hydrophobicity in water: relevance to proteins <sup>TM</sup> stabilization at low temperature. Physical Chemistry Chemical Physics, 2019, 21, 800-812.	2.8	14

#	ARTICLE	IF	CITATIONS
6374	Do water's electrons care about electrolytes?. Chemical Science, 2019, 10, 848-865.	7.4	31
6375	Homology modeling and <i>in vivo</i> functional characterization of the zinc permeation pathway in a heavy metal P-type ATPase. Journal of Experimental Botany, 2019, 70, 329-341.	4.8	25
6376	Elucidating the role of key structural motifs in antifreeze glycoproteins. Physical Chemistry Chemical Physics, 2019, 21, 3903-3917.	2.8	9
6377	Identification of Binding Sites for Efflux Pump Inhibitors of the AcrAB-TolC Component AcrA. Biophysical Journal, 2019, 116, 648-658.	0.5	27
6378	Possible Configurations of Apo-form Taste Receptor Type 1 (T1r) Studied by Microsecond-order Molecular Dynamics Simulation. Chemistry Letters, 2019, 48, 325-328.	1.3	1
6379	Chemisorption of carbon monoxide, carbon dioxide and $\alpha$ -methanephobia on the [0001] titanium surface. Applied Surface Science, 2019, 478, 128-133.	6.1	3
6380	Bennett acceptance ratio method to calculate the binding free energy of BACE1 inhibitors: Theoretical model and design of new ligands of the enzyme. Chemical Biology and Drug Design, 2019, 93, 1117-1128.	3.2	8
6381	Amorphous boron suboxide. Journal of the American Ceramic Society, 2019, 102, 4546-4554.	3.8	4
6382	Characterizing Solvent Density Fluctuations in Dynamical Observation Volumes. Journal of Physical Chemistry B, 2019, 123, 1650-1661.	2.6	12
6383	Alkali Metal Intercalation in MXene/Graphene Heterostructures: A New Platform for Ion Battery Applications. Journal of Physical Chemistry Letters, 2019, 10, 727-734.	4.6	88
6384	Investigation of reverse ionic diffusion in forward-osmosis-aided dewatering of microalgae: A molecular dynamics study. Bioresource Technology, 2019, 279, 181-188.	9.6	21
6385	Chiral Self-Assembly of Nanoparticles Induced by Polymers Synthesized <i>via</i> Reversible Addition-fragmentation Chain Transfer Polymerization. ACS Nano, 2019, 13, 1479-1489.	14.6	45
6386	Revisiting the structure-property relationship of metallic glasses: Common spatial correlation revealed as a hidden rule. Physical Review B, 2019, 99, .	3.2	50
6387	Flow-Arrest Transitions in Frictional Granular Matter. Physical Review Letters, 2019, 122, 048003.	7.8	23
6388	Mechanistic elucidation of amphetamine metabolism by tyramine oxidase from human gut microbiota using molecular dynamics simulations. Journal of Cellular Biochemistry, 2019, 120, 11206-11215.	2.6	4
6389	The catalytic activity of Abl1 single and compound mutations: Implications for the mechanism of drug resistance mutations in chronic myeloid leukaemia. Biochimica Et Biophysica Acta - General Subjects, 2019, 1863, 732-741.	2.4	18
6390	Ionic Liquid Mixture at the Vacuum Interface and the Peaks and Antipeaks Analysis of X-ray Reflectivity. Journal of Physical Chemistry C, 2019, 123, 4914-4925.	3.1	11
6391	Insight into the binding of ACE-inhibitory peptides to angiotensin-converting enzyme: a molecular simulation. Molecular Simulation, 2019, 45, 215-222.	2.0	18



#	ARTICLE	IF	CITATIONS
6392	Molecular simulation and experimental studies on the interfacial properties of a mixed surfactant SDS/C <sub>4</sub> mimBr. <i>Molecular Simulation</i> , 2019, 45, 223-229.	2.0	6
6393	Encapsulation driven conformational changes in n-alkanes inside a hydrogen-bonded supramolecular cavitand assembly. <i>Chemical Physics</i> , 2019, 521, 100-107.	1.9	7
6394	Location of Solvated Probe Molecules Within Nonionic Surfactant Micelles Using Molecular Dynamics. <i>Journal of Pharmaceutical Sciences</i> , 2019, 108, 205-213.	3.3	9
6395	Search for efficient inhibitors of myotoxic activity induced by ophidian phospholipase A2-like proteins using functional, structural and bioinformatics approaches. <i>Scientific Reports</i> , 2019, 9, 510.	3.3	24
6396	GAFF-IC: realistic viscosities for isocyanate molecules with a GAFF-based force field. <i>Molecular Simulation</i> , 2019, 45, 207-214.	2.0	9
6397	Predicting Asphaltene Aggregate Structure from Molecular Dynamics Simulation: Comparison to Neutron Total Scattering Data. <i>Energy &amp; Fuels</i> , 2019, 33, 3787-3795.	5.1	27
6398	Enhanced Li-ion dynamics in trivalently doped lithium phosphidosilicate Li <sub>2</sub> SiP <sub>2</sub> : a candidate material as a solid Li electrolyte. <i>Journal of Materials Chemistry A</i> , 2019, 7, 3953-3961.	10.3	8
6399	P152R Mutation Within MeCP2 Can Cause Loss of DNA-Binding Selectivity. <i>Interdisciplinary Sciences, Computational Life Sciences</i> , 2019, 11, 10-20.	3.6	1
6400	Curvature effect and stabilize ruptured membrane of BAX derived peptide studied by molecular dynamics simulations. <i>Journal of Molecular Graphics and Modelling</i> , 2019, 88, 152-159.	2.4	1
6401	Specific refolding pathway of viscumin A chain in membrane-like medium reveals a possible mechanism of toxin entry into cell. <i>Scientific Reports</i> , 2019, 9, 413.	3.3	3
6402	Semi-Empirical Force-Field Model for the Ti1~xAlxN (0 ≤ x ≤ 1) System. <i>Materials</i> , 2019, 12, 215.	2.9	22
6403	Theoretical investigations into effects of adulteration crystal defect on properties of HMX by molecular dynamics method. <i>Theoretical Chemistry Accounts</i> , 2019, 138, 1.	1.4	4
6404	Systematic Coarse-Grained Lipid Force Fields with Semiexplicit Solvation via Virtual Sites. <i>Journal of Chemical Theory and Computation</i> , 2019, 15, 2087-2100.	5.3	26
6405	New insights into GluT1 mechanics during glucose transfer. <i>Scientific Reports</i> , 2019, 9, 998.	3.3	60
6406	Molecular structure and vibrational spectra at water/poly(2-methoxyethylacrylate) and water/poly(methyl methacrylate) interfaces: A molecular dynamics simulation study. <i>Journal of Chemical Physics</i> , 2019, 150, 044707.	3.0	16
6407	Understanding Membrane Domain-Partitioning Thermodynamics of Transmembrane Domains with Potential of Mean Force Calculations. <i>Journal of Physical Chemistry B</i> , 2019, 123, 1009-1016.	2.6	15
6408	Modeling gas transport in polymer-grafted nanoparticle membranes. <i>Soft Matter</i> , 2019, 15, 424-432.	2.7	22
6409	Nucleation of pseudo hard-spheres and dumbbells at moderate metastability: appearance of A15 Frank-Kasper phase at intermediate elongations. <i>Physical Chemistry Chemical Physics</i> , 2019, 21, 1656-1670.	2.8	5

#	ARTICLE	IF	CITATIONS
6410	Destabilization of amyloid fibrils on interaction with MoS <sub>2</sub> -based nanomaterials. RSC Advances, 2019, 9, 1613-1624.	3.6	18
6411	Multiscale modeling of charge transfer in polymers with flexible backbones. Physical Chemistry Chemical Physics, 2019, 21, 1812-1819.	2.8	23
6412	Mineralization of phosphorylated cellulose: crucial role of surface structure and monovalent ions for optimizing calcium content. Physical Chemistry Chemical Physics, 2019, 21, 1067-1077.	2.8	7
6413	Assessing the transferability of common top-down and bottom-up coarse-grained molecular models for molecular mixtures. Physical Chemistry Chemical Physics, 2019, 21, 1912-1927.	2.8	44
6414	Probing the role of dispersion energy on structural transformation of double-stranded xylo- and ribo-nucleic acids. Physical Chemistry Chemical Physics, 2019, 21, 3842-3848.	2.8	6
6415	Does Preferential Adsorption Drive Cononsolvency?. Macromolecules, 2019, 52, 4131-4138.	4.8	29
6416	Essential Mycoplasma Glycolipid Synthase Adheres to the Cell Membrane by Means of an Amphipathic Helix. Scientific Reports, 2019, 9, 7085.	3.3	6
6417	Detecting early stage structural changes in wild type, pathogenic and non-pathogenic prion variants using Markov state model. RSC Advances, 2019, 9, 14567-14579.	3.6	6
6418	A comparison of peptide amphiphile nanofiber macromolecular assembly strategies. European Physical Journal E, 2019, 42, 63.	1.6	3
6419	Interaction of Antimicrobial Lipopeptides with Bacterial Lipid Bilayers. Journal of Membrane Biology, 2019, 252, 317-329.	2.1	20
6420	Interaction of SNARE Mimetic Peptides with Lipid bilayers: Effects of Secondary Structure, Bilayer Composition and Lipid Anchoring. Scientific Reports, 2019, 9, 7708.	3.3	9
6421	Permeabilities of CO <sub>2</sub> , H <sub>2</sub> S and CH <sub>4</sub> through Choline-Based Ionic Liquids: Atomistic-Scale Simulations. Molecules, 2019, 24, 214.	3.8	18
6422	Change in binding states between catabolite activating protein and DNA induced by ligand-binding: molecular dynamics and ab initio fragment molecular orbital calculations. Journal of Molecular Modeling, 2019, 25, 192.	1.8	5
6423	Sorption mechanism and dynamic behavior of graphene oxide as an effective adsorbent for the removal of chlorophenol based environmental-hormones: A DFT and MD simulation study. Chemical Engineering Journal, 2019, 375, 121964.	12.7	74
6424	Interference with Amyloid- $\beta$ Nucleation by Transient Ligand Interaction. Molecules, 2019, 24, 2129.	3.8	11
6425	Disassociation of $\beta$ 21- $\beta$ 1- $\beta$ 2 from the $\beta$ 2- $\beta$ 3 domain of prion protein (PrP) is a prerequisite for the conformational conversion of PrPC into PrPSc: Driven by the free energy landscape. International Journal of Biological Macromolecules, 2019, 136, 368-376.	7.5	5
6426	Prioritization of SNPs in $\gamma$ -LAT $\alpha$ 1 culpable of Lysinuric protein intolerance and their mutational impacts using protein-protein docking and molecular dynamics simulation studies. Journal of Cellular Biochemistry, 2019, 120, 18496-18508.	2.6	10
6427	Conformational coupling by trans-phosphorylation in calcium calmodulin dependent kinase II. PLoS Computational Biology, 2019, 15, e1006796.	3.2	5

#	ARTICLE	IF	CITATIONS
6428	Structural Basis of Protein Kinase R Autophosphorylation. <i>Biochemistry</i> , 2019, 58, 2967-2977.	2.5	22
6429	Structural, functional, and stability change predictions in human telomerase upon specific point mutations. <i>Scientific Reports</i> , 2019, 9, 8707.	3.3	23
6430	Amphiphilic copolymers change the nature of the ordered-to-disordered phase transition of lipid membranes from discontinuous to continuous. <i>Physical Chemistry Chemical Physics</i> , 2019, 21, 13746-13757.	2.8	6
6431	Relative entropy indicates an ideal concentration for structure-based coarse graining of binary mixtures. <i>Physical Review E</i> , 2019, 99, 053308.	2.1	3
6432	Temperature Dependence of Homogeneous Nucleation in Ice. <i>Physical Review Letters</i> , 2019, 122, 245501.	7.8	56
6433	Dynamical aspects of supercooled TIP3Pâ€“water in the grooves of DNA. <i>Journal of Chemical Physics</i> , 2019, 150, 235101.	3.0	11
6434	Revealing a Dual Role of Ganglioside Lipids in the Aggregation of Membrane-Associated Islet Amyloid Polypeptide. <i>Journal of Membrane Biology</i> , 2019, 252, 343-356.	2.1	8
6435	Molecular dynamics simulations of the interaction of Mouse and Torpedo acetylcholinesterase with covalent inhibitors explain their differential reactivity: Implications for drug design. <i>Chemico-Biological Interactions</i> , 2019, 310, 108715.	4.0	11
6436	Modeling of Specific Lipopolysaccharide Binding Sites on a Gram-Negative Porin. <i>Journal of Physical Chemistry B</i> , 2019, 123, 5700-5708.	2.6	11
6437	Local volume effects in the generalized pseudopotential theory. <i>Physical Review B</i> , 2019, 99, .	3.2	2
6438	Conformational change of L-phenylalanine in fluorinated alcohol-water mixed solvents studied by IR, NMR, and MD simulations. <i>Journal of Molecular Liquids</i> , 2019, 290, 111192.	4.9	5
6439	Rational design of novel fluorescent analogues of cholesterol: a â€œstep-by-stepâ€•computational study. <i>Physical Chemistry Chemical Physics</i> , 2019, 21, 15487-15503.	2.8	6
6440	Transport of Reactive Oxygen and Nitrogen Species across Aquaporin: A Molecular Level Picture. <i>Oxidative Medicine and Cellular Longevity</i> , 2019, 2019, 1-11.	4.0	32
6441	Specific Coordination Mode and Electrostatic Ion Atmosphere Effects of Divalent Cations Regulating Spatially Crossing Configurations of DNA Duplexes. <i>Journal of the Physical Society of Japan</i> , 2019, 88, 044801.	1.6	0
6442	Evidence for phospholipid export from the bacterial inner membrane by the Mla ABC transport system. <i>Nature Microbiology</i> , 2019, 4, 1692-1705.	13.3	88
6443	Probing the transition state in enzyme catalysis by high-pressure NMR dynamics. <i>Nature Catalysis</i> , 2019, 2, 726-734.	34.4	30
6444	Effect of ion concentration and multivalence on methane-brine interfacial tension and phenomena from molecular perspectives. <i>Fuel</i> , 2019, 254, 115657.	6.4	30
6445	Inverse hexagonal phase of poly-unsaturated monogalactolipid: A computer model and analysis. <i>Journal of Molecular Liquids</i> , 2019, 290, 111189.	4.9	3

#	ARTICLE	IF	CITATIONS
6446	Linear and Rationally Designed Stapled Peptides Abrogate TLR4 Pathway and Relieve Inflammatory Symptoms in Rheumatoid Arthritis Rat Model. <i>Journal of Medicinal Chemistry</i> , 2019, 62, 6495-6511.	6.4	27
6447	Molecular Insights into Dipole Relaxation Processes in Water-Lysine Mixtures. <i>Journal of Physical Chemistry B</i> , 2019, 123, 6056-6064.	2.6	3
6448	A heuristic derived from analysis of the ion channel structural proteome permits the rapid identification of hydrophobic gates. <i>Proceedings of the National Academy of Sciences of the United States of America</i> , 2019, 116, 13989-13995.	7.1	52
6449	Improvement of <i>Selenomonas ruminantium</i> $\beta$ -xylosidase thermal stability by replacing buried free cysteines via site directed mutagenesis. <i>International Journal of Biological Macromolecules</i> , 2019, 136, 352-358.	7.5	5
6450	Opposing Temperature Dependence of the Stretching Response of Single PEG and PNIPAM Polymers. <i>Journal of the American Chemical Society</i> , 2019, 141, 11603-11613.	13.7	53
6451	Atomistic Simulations of Membrane Ion Channel Conduction, Gating, and Modulation. <i>Chemical Reviews</i> , 2019, 119, 7737-7832.	47.7	87
6452	Low-diluted Phenacetinum disrupted the melanoma cancer cell migration. <i>Scientific Reports</i> , 2019, 9, 9109.	3.3	4
6453	Mesoscopic structural organization in fluorinated pyrrolidinium-based room temperature ionic liquids. <i>Journal of Molecular Liquids</i> , 2019, 289, 111110.	4.9	14
6454	Thermodynamic study of new antiepileptic compounds by combining chromatography on the phosphatidylcholine biomimetic stationary phase and differential scanning calorimetry. <i>Journal of Separation Science</i> , 2019, 42, 2628-2639.	2.5	8
6455	A functional substitution in the $\alpha$ -aromatic amino acid decarboxylase enzyme worsens somatic symptoms via a serotonergic pathway. <i>Annals of Neurology</i> , 2019, 86, 168-180.	5.3	9
6456	Erythromycin, Cethromycin and Solithromycin display similar binding affinities to the <i>E. coli</i> 's ribosome: A molecular simulation study. <i>Journal of Molecular Graphics and Modelling</i> , 2019, 91, 80-90.	2.4	4
6457	Structural and functional consequences of the STAT5B N642H driver mutation. <i>Nature Communications</i> , 2019, 10, 2517.	12.8	50
6458	Effect of mutations on binding of ligands to guanine riboswitch probed by free energy perturbation and molecular dynamics simulations. <i>Nucleic Acids Research</i> , 2019, 47, 6618-6631.	14.5	130
6459	Tau local structure shields an $\alpha$ -amyloid-forming motif and controls aggregation propensity. <i>Nature Communications</i> , 2019, 10, 2493.	12.8	124
6460	Structural Polymorphism of Actin. <i>Journal of Molecular Biology</i> , 2019, 431, 3217-3228.	4.2	22
6461	Mie 16-6 force field predicts viscosity with faster-than-exponential pressure dependence for 2,2,4-trimethylhexane. <i>Fluid Phase Equilibria</i> , 2019, 495, 76-85.	2.5	13
6462	Hydroxycinnamic acids in supercritical carbon dioxide. The dependence of cosolvent-induced solubility enhancement on the selective solvation. <i>Journal of Supercritical Fluids</i> , 2019, 150, 94-102.	3.2	4
6463	Understanding the stability of polypeptide membranes in ionic liquids: a theoretical molecular dynamics study. <i>New Journal of Chemistry</i> , 2019, 43, 10151-10161.	2.8	16

#	ARTICLE	IF	CITATIONS
6464	Effect of co-existing Co <sup>2+</sup> ions on the aggregation of humic acid in aquatic environment: Aggregation kinetics, dynamic properties and fluorescence spectroscopic study. <i>Science of the Total Environment</i> , 2019, 674, 544-553.	8.0	12
6465	Role of lipid composition on the structural and mechanical features of axonal membranes: a molecular simulation study. <i>Scientific Reports</i> , 2019, 9, 8000.	3.3	72
6466	Exploring the impact of proteins on the line tension of a phase-separating ternary lipid mixture. <i>Journal of Chemical Physics</i> , 2019, 150, 204702.	3.0	18
6467	A de novo substitution in BCL11B leads to loss of interaction with transcriptional complexes and craniosynostosis. <i>Human Molecular Genetics</i> , 2019, 28, 2501-2513.	2.9	23
6468	Phospholipid-Based Reverse Micelle Structures in Vegetable Oil Modified by Water Content, Free Fatty Acid, and Temperature. <i>Langmuir</i> , 2019, 35, 8373-8382.	3.5	10
6469	Curvature induction and membrane remodeling by FAM134B reticulon homology domain assist selective ER-phagy. <i>Nature Communications</i> , 2019, 10, 2370.	12.8	147
6470	Insights into the activation mechanism of human estrogen-related receptor $\beta$ by environmental endocrine disruptors. <i>Cellular and Molecular Life Sciences</i> , 2019, 76, 4769-4781.	5.4	16
6471	How do ribozymes accommodate additional water molecules upon hydrostatic compression deep into the kilobar pressure regime?. <i>Biophysical Chemistry</i> , 2019, 252, 106192.	2.8	6
6472	Molecular dynamics simulation of the adsorption of mung bean defensin VrD1 to a phospholipid bilayer. <i>Food Structure</i> , 2019, 21, 100117.	4.5	6
6473	Statistical geometry characterization of local structure of TMAO, TBA and urea aqueous solutions. <i>Journal of Molecular Liquids</i> , 2019, 286, 110870.	4.9	7
6474	The interplay between molecular flexibility and RNA chemical probing reactivities analyzed at the nucleotide level via an extensive molecular dynamics study. <i>Methods</i> , 2019, 162-163, 108-127.	3.8	15
6475	The Influence of Water on Choline-Based Ionic Liquids. <i>ACS Biomaterials Science and Engineering</i> , 2019, 5, 3645-3653.	5.2	42
6476	One century of ConA and 40 years of ConBr research: A structural review. <i>International Journal of Biological Macromolecules</i> , 2019, 134, 901-911.	7.5	26
6477	Structures of the otopetrin proton channels Otop1 and Otop3. <i>Nature Structural and Molecular Biology</i> , 2019, 26, 518-525.	8.2	48
6478	Inward-facing conformation of a multidrug resistance MATE family transporter. <i>Proceedings of the National Academy of Sciences of the United States of America</i> , 2019, 116, 12275-12284.	7.1	36
6479	Antimicrobial Zn-Based $\alpha$ -TSOL for Citrus Greening Management: Insights from Spectroscopy and Molecular Simulation. <i>Journal of Agricultural and Food Chemistry</i> , 2019, 67, 6970-6977.	5.2	6
6480	Molecular cloning and 3D model of a fatty-acid elongase in a carnivorous freshwater teleost, the European perch ( <i>Perca fluviatilis</i> ). <i>3 Biotech</i> , 2019, 9, 242.	2.2	4
6481	Phase Transitions of Hybrid Perovskites Simulated by Machine-Learning Force Fields Trained on the Fly with Bayesian Inference. <i>Physical Review Letters</i> , 2019, 122, 225701.	7.8	250

#	ARTICLE	IF	CITATIONS
6482	New insights into the tetrameric family of the Fur metalloregulators. <i>BioMetals</i> , 2019, 32, 501-519.	4.1	14
6483	Computational Identification of Novel Kir6 Channel Inhibitors. <i>Frontiers in Pharmacology</i> , 2019, 10, 549.	3.5	5
6484	Early impairment of epigenetic pattern in neurodegeneration: Additional mechanisms behind pyrethroid toxicity. <i>Experimental Gerontology</i> , 2019, 124, 110629.	2.8	27
6485	Theoretical design and experimental study of new aptamers with the improved target-affinity: New insights into the Pb <sup>2+</sup> -specific aptamers as a case study. <i>Journal of Molecular Liquids</i> , 2019, 289, 111159.	4.9	16
6486	Activation and Inactivation of the FLT3 Kinase: Pathway Intermediates and the Free Energy of Transition. <i>Journal of Physical Chemistry B</i> , 2019, 123, 5385-5394.	2.6	14
6487	Sodium Halide Adsorption and Water Structure at the $\gamma$ -Alumina(0001)/Water Interface. <i>Journal of Physical Chemistry C</i> , 2019, 123, 15618-15628.	3.1	19
6488	Novel analogs of sulfasalazine as system x <sub>c</sub> <sup>-</sup> antiporter inhibitors: Insights from the molecular modeling studies. <i>Drug Development Research</i> , 2019, 80, 758-777.	2.9	23
6489	Behavior of the DPH fluorescence probe in membranes perturbed by drugs. <i>Chemistry and Physics of Lipids</i> , 2019, 223, 104784.	3.2	47
6490	Trimethylamine N-oxide-derived zwitterionic polymers: A new class of ultralow fouling bioinspired materials. <i>Science Advances</i> , 2019, 5, eaaw9562.	10.3	149
6491	Rapid diffusion of cholesterol along polyunsaturated membranes <i>via</i> deep dives. <i>Physical Chemistry Chemical Physics</i> , 2019, 21, 11660-11669.	2.8	21
6492	Disease-associated missense variants in ZBTB18 disrupt DNA binding and impair the development of neurons within the embryonic cerebral cortex. <i>Human Mutation</i> , 2019, 40, 1841-1855.	2.5	10
6493	On the ubiquity of helical $\gamma$ -synuclein tetramers. <i>Physical Chemistry Chemical Physics</i> , 2019, 21, 12036-12043.	2.8	18
6494	Molecular modelling studies on the interactions of 7-methoxytacrine-4-pyridinealdoxime with VX-inhibited human acetylcholinesterase. A near attack approach to assess different spacer-lengths. <i>Chemico-Biological Interactions</i> , 2019, 307, 195-205.	4.0	5
6495	What accounts for the different functions in photolyases and cryptochromes: a computational study of proton transfers to FAD. <i>Physical Chemistry Chemical Physics</i> , 2019, 21, 11956-11966.	2.8	6
6496	Superionic UO <sub>2</sub> : A model anharmonic crystalline material. <i>Journal of Chemical Physics</i> , 2019, 150, 174506.	3.0	28
6497	Aqueous Mixtures of Room-Temperature Ionic Liquids: Entropy-Driven Accumulation of Water Molecules at Interfaces. <i>Journal of Physical Chemistry C</i> , 2019, 123, 13795-13803.	3.1	29
6498	From GROMACS to LAMMPS: GRO2LAM. <i>Journal of Molecular Modeling</i> , 2019, 25, 147.	1.8	29
6499	Configurational mapping significantly increases the efficiency of solid-solid phase coexistence calculations via molecular dynamics: Determining the FCC-HCP coexistence line of Lennard-Jones particles. <i>Journal of Chemical Physics</i> , 2019, 150, 164112.	3.0	3



#	ARTICLE	IF	CITATIONS
6500	Interactions in a Multi-scale Representation of Sparse Media: From Mechanics to Thermodynamics. <i>Journal of Elasticity</i> , 2019, 135, 91-115.	1.9	6
6501	Molecular Simulation Study on the Volume Swelling and the Viscosity Reduction of <i>n</i> -Alkane/CO <sub>2</sub> Systems. <i>Industrial &amp; Engineering Chemistry Research</i> , 2019, 58, 8871-8877.	3.7	26
6502	Structure and Conformation of Stereoregular Poly(methyl methacrylate) Chains Adsorbed on Graphene Oxide and Reduced Graphene Oxide via Atomistic Simulations. <i>Macromolecules</i> , 2019, 52, 3825-3838.	4.8	24
6503	Dynamic recrystallization initiated by direct grain reorientation at high-angle grain boundary in $\beta$ -titanium. <i>Journal of Materials Research</i> , 2019, 34, 1608-1621.	2.6	4
6504	Effects of Solvent Stabilization on Pharmaceutical Crystallization: Investigating Conformational Polymorphism of Probucol Using Combined Solid-State Density Functional Theory, Molecular Dynamics, and Terahertz Spectroscopy. <i>Journal of Physical Chemistry A</i> , 2019, 123, 6937-6947.	2.5	21
6505	Structural and free energy landscape of novel mutations in ribosomal protein S1 (rpsA) associated with pyrazinamide resistance. <i>Scientific Reports</i> , 2019, 9, 7482.	3.3	48
6506	An unexpected dynamic binding mode between coagulation factor X and Rivaroxaban reveals importance of flexibility in drug binding. <i>Chemical Biology and Drug Design</i> , 2019, 94, 1664-1671.	3.2	3
6507	Comparative assessment of the therapeutic drug targets of <i>C. botulinum</i> ATCC 3502 and <i>C. difficile</i> str. 630 using in silico subtractive proteomics approach. <i>Journal of Cellular Biochemistry</i> , 2019, 120, 16160-16184.	2.6	18
6508	Paclitaxel interaction with cucurbit [7]uril and acyclic Cucurbit[4]uril nanocontainers: A computational approach. <i>Journal of Molecular Graphics and Modelling</i> , 2019, 90, 210-218.	2.4	3
6509	A Three-Dimensional Model of Human Lysyl Oxidase, a Cross-Linking Enzyme. <i>ACS Omega</i> , 2019, 4, 8495-8505.	3.5	21
6510	Molecular dynamics simulation of tropomyosin bound to actins/myosin in the closed and open states. <i>Proteins: Structure, Function and Bioinformatics</i> , 2019, 87, 805-814.	2.6	0
6511	Molecular Dynamics of Polyrotaxane in Solution Investigated by Quasi-Elastic Neutron Scattering and Molecular Dynamics Simulation: Sliding Motion of Rings on Polymer. <i>Journal of the American Chemical Society</i> , 2019, 141, 9655-9663.	13.7	50
6512	Lysozyme-luteolin binding: molecular insights into the complexation process and the inhibitory effects of luteolin towards protein modification. <i>Physical Chemistry Chemical Physics</i> , 2019, 21, 12649-12666.	2.8	43
6513	Revisiting the Meyer-Overton rule for drug-membrane permeabilities. <i>Molecular Physics</i> , 2019, 117, 2900-2909.	1.7	10
6514	Phosphate-Functionalized Stabilized F127 Nanoparticles: Introduction of Discrete Surface Charges and Electrophoretic Determination of Aggregation Number. <i>Macromolecular Research</i> , 2019, 27, 657-662.	2.4	3
6515	$\beta$ 1 integrin is a sensor of blood flow direction. <i>Journal of Cell Science</i> , 2019, 132, .	2.0	41
6516	Hidden Aggregation Hot-Spots on Human Apolipoprotein E: A Structural Study. <i>International Journal of Molecular Sciences</i> , 2019, 20, 2274.	4.1	9
6517	Exploring Amyloid- $\beta$ Dimer Structure Using Molecular Dynamics Simulations. <i>Journal of Physical Chemistry A</i> , 2019, 123, 4658-4670.	2.5	13

#	ARTICLE	IF	CITATIONS
6518	Naphthalene crystal shape prediction from molecular dynamics simulations. CrystEngComm, 2019, 21, 3280-3288.	2.6	19
6519	Druggability assessment of mammalian Perâ€“Arntâ€“Sim [PAS] domains using computational approaches. MedChemComm, 2019, 10, 1126-1137.	3.4	10
6520	Different protonated states at the C-terminal of the amyloid-Î² peptide modulate the stability of S-shaped protofibril. Journal of Chemical Physics, 2019, 150, 185102.	3.0	3
6521	Molecular modeling studies on the interactions of 7-methoxytacrine-4-pyridinealdoxime, 4-PA, 2-PAM, and obidoxime with VX-inhibited human acetylcholinesterase: a near attack conformation approach. Journal of Enzyme Inhibition and Medicinal Chemistry, 2019, 34, 1018-1029.	5.2	18
6522	Control of anterior <scp>GR</scp> adient 2 ( <scp>AGR</scp> 2) dimerization links endoplasmic reticulum proteostasis to inflammation. EMBO Molecular Medicine, 2019, 11, .	6.9	48
6523	The Role of Structural Polymorphism in Driving the Mechanical Performance of the Alzheimer's Beta Amyloid Fibrils. Frontiers in Bioengineering and Biotechnology, 2019, 7, 83.	4.1	21
6524	Structural Investigation of Human Prolactin Receptor Transmembrane Domain Homodimerization in a Membrane Environment through Multiscale Simulations. Journal of Physical Chemistry B, 2019, 123, 4858-4866.	2.6	3
6525	Exploring New Crystal Structures of Glycine via Electric Field-Induced Structural Transformations with Molecular Dynamics Simulations. Processes, 2019, 7, 268.	2.8	9
6526	Structure and Dynamics of the Central Lipid Pool and Proteins of the Bacterial Holo-Translocon. Biophysical Journal, 2019, 116, 1931-1940.	0.5	22
6527	Coupling of Membrane Nanodomain Formation and Enhanced Electroporation near Phase Transition. Biophysical Journal, 2019, 116, 2131-2148.	0.5	33
6528	Asymmetric Spontaneous Intercalation of Lutein into a Phospholipid Bilayer, a Computational Study. Computational and Structural Biotechnology Journal, 2019, 17, 516-526.	4.1	11
6529	Osmolyte-Induced Collapse of a Charged Macromolecule. Journal of Physical Chemistry B, 2019, 123, 4636-4644.	2.6	12
6530	Anionic nanoparticle-lipid membrane interactions: the protonation of anionic ligands at the membrane surface reduces membrane disruption. RSC Advances, 2019, 9, 13992-13997.	3.6	17
6531	The Role of Temperature and Lipid Charge on Intake/Uptake of Cationic Gold Nanoparticles into Lipid Bilayers. Small, 2019, 15, e1805046.	10.0	35
6532	Dynamics of heroin molecule inside the lipid membrane: a molecular dynamics study. Journal of Molecular Modeling, 2019, 25, 121.	1.8	7
6533	Lipid Bilayer Composition Influences the Activity of the Antimicrobial Peptide Dermcidin Channel. Biophysical Journal, 2019, 116, 1658-1666.	0.5	20
6534	One-step annealing optimizes strength-ductility tradeoff in pearlitic steel wires. Materials Science & Engineering A: Structural Materials: Properties, Microstructure and Processing, 2019, 757, 1-13.	5.6	25
6535	Asphaltene Aggregation in Oil and Gas Mixtures: Insights from Molecular Simulation. Energy & Fuels, 2019, 33, 4721-4730.	5.1	23

#	ARTICLE	IF	CITATIONS
6536	First Step of the Transglutaminase Reaction Catalyzed by Activated Factor XIII Subunit A, Hybrid Quantum Chemistry/Molecular Mechanics Calculations. <i>Journal of Physical Chemistry B</i> , 2019, 123, 3887-3897.	2.6	2
6537	An experimentally validated approach to calculate the blood-brain barrier permeability of small molecules. <i>Scientific Reports</i> , 2019, 9, 6117.	3.3	39
6538	A screening platform to monitor RNA processing and protein-RNA interactions in ribonuclease P uncovers a small molecule inhibitor. <i>Nucleic Acids Research</i> , 2019, 47, 6425-6438.	14.5	11
6539	Tryptamine-Triazole Hybrid Compounds for Selective Butyrylcholinesterase Inhibition. <i>Bulletin of the Korean Chemical Society</i> , 2019, 40, 544-553.	1.9	4
6540	Molecular modeling of the effects of glycosylation on the structure and dynamics of human interferon-gamma. <i>Journal of Molecular Modeling</i> , 2019, 25, 127.	1.8	16
6541	Role of Structural Features in Oligomerization, Active-Site Integrity and Ligand Binding of Ribose-1,5-Bisphosphate Isomerase. <i>Computational and Structural Biotechnology Journal</i> , 2019, 17, 333-344.	4.1	5
6542	Free-energy analysis of the hydration and cosolvent effects on the $\beta$ -sheet aggregation through all-atom molecular dynamics simulation. <i>Journal of Chemical Physics</i> , 2019, 150, 145101.	3.0	14
6543	Extension of TEAM Force-Field Database to Ionic Liquids. <i>Journal of Chemical &amp; Engineering Data</i> , 2019, 64, 3718-3730.	1.9	10
6544	CO <sub>2</sub> and CH <sub>4</sub> Hydrates: Replacement or Cogrowth?. <i>Journal of Physical Chemistry C</i> , 2019, 123, 13401-13409.	3.1	27
6545	Insights into the Molecular Mechanisms of Eg5 Inhibition by (+)-Morelloflavone. <i>Pharmaceuticals</i> , 2019, 12, 58.	3.8	12
6546	Improved Temperature Behavior of PNIPAM in Water with a Modified OPLS Model. <i>Journal of Physical Chemistry B</i> , 2019, 123, 3875-3883.	2.6	28
6547	Dishevelled-3 conformation dynamics analyzed by FRET-based biosensors reveals a key role of casein kinase 1. <i>Nature Communications</i> , 2019, 10, 1804.	12.8	20
6548	Polarizable embedding for simulating redox potentials of biomolecules. <i>Physical Chemistry Chemical Physics</i> , 2019, 21, 11642-11650.	2.8	20
6549	Molecular Dynamics Simulations of Molecules in Uniform Flow. <i>Biophysical Journal</i> , 2019, 116, 1579-1585.	0.5	11
6550	An Atomistic Understanding of the Unusual Thermal Behavior of the Molecular Oxide Tc <sub>2</sub> O <sub>7</sub> . <i>Inorganic Chemistry</i> , 2019, 58, 5468-5475.	4.0	1
6551	Transferability of Local Density-Assisted Implicit Solvation Models for Homogeneous Fluid Mixtures. <i>Journal of Chemical Theory and Computation</i> , 2019, 15, 2881-2895.	5.3	19
6552	Interactions of Water and Alkanes: Modifying Additive Force Fields to Account for Polarization Effects. <i>Journal of Chemical Theory and Computation</i> , 2019, 15, 3854-3867.	5.3	25
6553	Evaluation of EGCG Loading Capacity in DMPC Membranes. <i>Langmuir</i> , 2019, 35, 6771-6781.	3.5	9

#	ARTICLE	IF	CITATIONS
6554	An Enzyme Cascade Synthesis of Vanillin. <i>Catalysts</i> , 2019, 9, 252.	3.5	16
6555	Bilirubin and its congeners: conformational analysis and chirality from metadynamics and related computational methods. <i>Monatshefte für Chemie</i> , 2019, 150, 801-812.	1.8	4
6556	Bilayer Membranes with Frequent Flip-Flops Have Tensionless Leaflets. <i>Nano Letters</i> , 2019, 19, 5011-5016.	9.1	60
6557	Computational Microscopy of PEDOT:PSS/Cellulose Composite Paper. <i>ACS Applied Energy Materials</i> , 2019, 2, 3568-3577.	5.1	28
6558	Conformational Stability Adaptation of a Double-Stranded RNA-Binding Domain to Transfer RNA Ligand. <i>Biochemistry</i> , 2019, 58, 2463-2473.	2.5	5
6559	Analysis of plastic strain-enhanced diffusivity in nanocrystalline iron by atomistic simulation. <i>Journal of Applied Physics</i> , 2019, 125, 135103.	2.5	8
6560	Aqueous Mixtures of Urea and Trimethylamine-N-oxide: Evidence for Kosmotropic or Chaotropic Behavior?. <i>Journal of Physical Chemistry B</i> , 2019, 123, 4415-4424.	2.6	26
6561	Structural basis for functional interactions in dimers of SLC26 transporters. <i>Nature Communications</i> , 2019, 10, 2032.	12.8	49
6562	Thermodynamic, structural and dynamic properties of ionic liquids [C4mim][CF3COO], [C4mim][Br] in the condensed phase, using molecular simulations. <i>RSC Advances</i> , 2019, 9, 13677-13695.	3.6	4
6563	Structural characterization and heterologous expression of a new cyt gene cloned from <i>Bacillus thuringiensis</i> . <i>Journal of Molecular Modeling</i> , 2019, 25, 136.	1.8	0
6564	Pharmacotherapeutics and Molecular Mechanism of Phytochemicals in Alleviating Hormone-Responsive Breast Cancer. <i>Oxidative Medicine and Cellular Longevity</i> , 2019, 2019, 1-14.	4.0	14
6565	Distinct Binding Dynamics, Sites and Interactions of Fullerene and Fullerenols with Amyloid- $\beta$ Peptides Revealed by Molecular Dynamics Simulations. <i>International Journal of Molecular Sciences</i> , 2019, 20, 2048.	4.1	28
6566	Structural and barrier properties of the skin ceramide lipid bilayer: a molecular dynamics simulation study. <i>Journal of Molecular Modeling</i> , 2019, 25, 140.	1.8	19
6567	Post-Translational Regulation of CYP450s Metabolism As Revealed by All-Atoms Simulations of the Aromatase Enzyme. <i>Journal of Chemical Information and Modeling</i> , 2019, 59, 2930-2940.	5.4	22
6568	Optimization and Evaluation of Site-Identification by Ligand Competitive Saturation (SILCS) as a Tool for Target-Based Ligand Optimization. <i>Journal of Chemical Information and Modeling</i> , 2019, 59, 3018-3035.	5.4	47
6569	Computational Simulations Identified Two Candidate Inhibitors of Cdk5/p25 to Abrogate Tau-associated Neurological Disorders. <i>Computational and Structural Biotechnology Journal</i> , 2019, 17, 579-590.	4.1	27
6570	Probing the Effect of NaCl Concentrations on a Model Asphaltene Adsorption onto Water Droplets of Different Sizes. <i>Energy &amp; Fuels</i> , 2019, 33, 3881-3890.	5.1	7
6571	Dopamine-Mediated Assembly of Citrate-Capped Plasmonic Nanoparticles into Stable Core-Shell Nanoworms for Intracellular Applications. <i>ACS Nano</i> , 2019, 13, 5864-5884.	14.6	57

#	ARTICLE	IF	CITATIONS
6572	Interface of Hydrated Perfluorosulfonic Acid Electrolyte and Platinum Catalyst: Construction of a Dissipative Particle Dynamics Simulation Model. <i>Journal of the Electrochemical Society</i> , 2019, 166, B3156-B3162.	2.9	1
6573	Synthesis, Biological Evaluation, and Molecular Modeling Studies of New Thiadiazole Derivatives as Potent P2X7 Receptor Inhibitors. <i>Frontiers in Chemistry</i> , 2019, 7, 261.	3.6	15
6574	NMR structure of CmPI-II, a non-classical Kazal protease inhibitor: Understanding its conformational dynamics and subtilisin A inhibition. <i>Journal of Structural Biology</i> , 2019, 206, 280-294.	2.8	10
6575	Potential blockade of the human voltage-dependent anion channel by MoS2 nanoflakes. <i>Physical Chemistry Chemical Physics</i> , 2019, 21, 9520-9530.	2.8	2
6576	Drug-induced activation of integrin alpha IIb beta 3 leads to minor localized structural changes. <i>PLoS ONE</i> , 2019, 14, e0214969.	2.5	6
6577	Structural origins for the generation of strength, ductility and toughness in bulk-metallic glasses using hydrogen microalloying. <i>Acta Materialia</i> , 2019, 171, 216-230.	7.9	47
6578	Solid Polymer Electrolytes for Lithium Metal Battery via Thermally Induced Cationic Ring-Opening Polymerization (CROP) with an Insight into the Reaction Mechanism. <i>Chemistry of Materials</i> , 2019, 31, 3118-3133.	6.7	51
6579	Spatially-Decomposed Free Energy of Solvation Based on the Endpoint Density-Functional Method. <i>Journal of Chemical Theory and Computation</i> , 2019, 15, 2896-2912.	5.3	12
6580	Complexation process of amylose under different concentrations of linoleic acid using molecular dynamics simulation. <i>Carbohydrate Polymers</i> , 2019, 216, 157-166.	10.2	35
6581	Discovery of selective activators of PRC2 mutant EED-I363M. <i>Scientific Reports</i> , 2019, 9, 6524.	3.3	12
6582	Allosteric effects in cyclophilin mutants may be explained by changes in nano-microsecond time scale motions. <i>Communications Chemistry</i> , 2019, 2, .	4.5	19
6583	The mechanism of RNA base fraying: Molecular dynamics simulations analyzed with core-set Markov state models. <i>Journal of Chemical Physics</i> , 2019, 150, 154123.	3.0	24
6584	Room-Temperature Metallic Fusion-Induced Layer-by-Layer Assembly for Highly Flexible Electrode Applications. <i>Advanced Functional Materials</i> , 2019, 29, 1806584.	14.9	23
6585	Structure of the human CIC-1 chloride channel. <i>PLoS Biology</i> , 2019, 17, e3000218.	5.6	66
6586	Chemical response of thioaldehydes to compression between magnesium oxide surfaces: A first-principles molecular dynamics study. <i>Surface Science</i> , 2019, 687, 7-16.	1.9	2
6587	Room temperature electrofreezing of water yields a missing dense ice phase in the phase diagram. <i>Nature Communications</i> , 2019, 10, 1925.	12.8	20
6588	Calculation of apparent pKa values of saturated fatty acids with different lengths in DOPC phospholipid bilayers. <i>Physical Chemistry Chemical Physics</i> , 2019, 21, 10052-10060.	2.8	16
6589	Water structure and mobility in acrylamide copolymer glycohydrogels with galactose and siloxane pendant groups. <i>Journal of Polymer Science, Part B: Polymer Physics</i> , 2019, 57, 584-597.	2.1	1

#	ARTICLE	IF	CITATIONS
6590	Multiconfigurational Coarse-Grained Molecular Dynamics. <i>Journal of Chemical Theory and Computation</i> , 2019, 15, 3306-3315.	5.3	22
6591	Dihydromyricetin Inhibits $\text{A}\beta$ -Synuclein Aggregation, Disrupts Preformed Fibrils, and Protects Neuronal Cells in Culture against Amyloid-Induced Cytotoxicity. <i>Journal of Agricultural and Food Chemistry</i> , 2019, 67, 3946-3955.	5.2	35
6592	Insights into structural and inhibitory mechanisms of low pH-induced conformational change of influenza HA2 protein: a computational approach. <i>Journal of Molecular Modeling</i> , 2019, 25, 99.	1.8	4
6593	In silico profiling the interaction mechanism of 2,5-diketopiperazine derivatives as oxytocin antagonists. <i>Journal of Molecular Graphics and Modelling</i> , 2019, 89, 178-191.	2.4	5
6594	Molecular Dynamics Investigation into the Effect of Zinc(II) on the Structure and Membrane Interactions of the Antimicrobial Peptide Clavanin A. <i>Journal of Physical Chemistry B</i> , 2019, 123, 3163-3176.	2.6	18
6595	Free energy analysis of membrane pore formation process in the presence of multiple melittin peptides. <i>Biochimica Et Biophysica Acta - Biomembranes</i> , 2019, 1861, 1409-1419.	2.6	25
6596	Effects of Selective Substitution of Cysteine Residues on the Conformational Properties of Chlorotoxin Explored by Molecular Dynamics Simulations. <i>International Journal of Molecular Sciences</i> , 2019, 20, 1261.	4.1	6
6597	Interfacial ordering of tristearin induced by glycerol monooleate and PGPR: A coarse-grained molecular dynamics study. <i>Colloids and Surfaces B: Biointerfaces</i> , 2019, 179, 107-113.	5.0	10
6598	Structure of Hydrated Kaolinite Edge Surfaces: DFT Results and Further Development of the ClayFF Classical Force Field with Metal- $\text{O}$ - $\text{H}$ Angle Bending Terms. <i>Journal of Physical Chemistry C</i> , 2019, 123, 11628-11638.	3.1	61
6599	Orientational distribution of DPH in lipid membranes: a comparison of molecular dynamics calculations and experimental time-resolved anisotropy experiments. <i>Physical Chemistry Chemical Physics</i> , 2019, 21, 7594-7604.	2.8	13
6600	Automated Markov state models for molecular dynamics simulations of aggregation and self-assembly. <i>Journal of Chemical Physics</i> , 2019, 150, 115101.	3.0	51
6601	First-principles characterization of reversible martensitic transformations. <i>Physical Review B</i> , 2019, 99, .	3.2	12
6602	How cardiolipin modulates the dynamics of respiratory complex I. <i>Science Advances</i> , 2019, 5, eaav1850.	10.3	56
6603	Defects in assembly explain reduced antiviral activity of the G249D polymorphism in human TRIM5 $\alpha$ . <i>PLoS ONE</i> , 2019, 14, e0212888.	2.5	0
6604	Solvation of $\text{Zn}^{2+}$ ion in 1-alkyl-3-methylimidazolium bis(trifluoromethylsulfonyl)imide ionic liquids: a molecular dynamics and X-ray absorption study. <i>Physical Chemistry Chemical Physics</i> , 2019, 21, 6958-6969.	2.8	21
6605	Discovery of natural product ovalicin sensitive type 1 methionine aminopeptidases: molecular and structural basis. <i>Biochemical Journal</i> , 2019, 476, 991-1003.	3.7	4
6606	Topologically disordered mesophase at the topmost surface layer of crystalline ice between 120 and 200 K. <i>Physical Review B</i> , 2019, 99, .	3.2	13
6607	Discovery of Novel Acetylcholinesterase Inhibitors as Potential Candidates for the Treatment of Alzheimer's Disease. <i>International Journal of Molecular Sciences</i> , 2019, 20, 1000.	4.1	28



#	ARTICLE	IF	CITATIONS
6608	Thermophysical properties of glycineâ€“water mixtures investigated by molecular modelling. <i>Physical Chemistry Chemical Physics</i> , 2019, 21, 6467-6476.	2.8	38
6609	Solubility of paracetamol in ethanol by molecular dynamics using the extended Einstein crystal method and experiments. <i>Journal of Chemical Physics</i> , 2019, 150, 094107.	3.0	19
6610	Unravelling the contribution of local structures to the anomalies of water: The synergistic action of several factors. <i>Journal of Chemical Physics</i> , 2019, 150, 094506.	3.0	52
6611	The disordered plant dehydrin Lti30 protects the membrane during water-related stress by cross-linking lipids. <i>Journal of Biological Chemistry</i> , 2019, 294, 6468-6482.	3.4	30
6612	Solvatochromism of Binary Mixtures of 2,2,2-Trifluoroethanol + Ionic Liquid [bmim][Tf <sub>2</sub> N]: A Comparative Study with Molecular Solvents. <i>Journal of Chemical &amp; Engineering Data</i> , 2019, 64, 1140-1154.	1.9	13
6613	Studying equilibria of polymers in solution by direct molecular dynamics simulations: poly(N-isopropylacrylamide) in water as a test case. <i>European Physical Journal: Special Topics</i> , 2019, 227, 1547-1558.	2.6	13
6614	Hydrogen storage on graphitic carbon nitride and its palladium nanocomposites: A multiscale computational approach. <i>International Journal of Hydrogen Energy</i> , 2019, 44, 8325-8340.	7.1	32
6615	Enterovirus particles expel capsid pentamers to enable genome release. <i>Nature Communications</i> , 2019, 10, 1138.	12.8	33
6616	Directing self-assembly in solution towards improved cooperativity in Fe( <sup>iii</sup> ) complexes with amphiphilic tridentate ligands. <i>Dalton Transactions</i> , 2019, 48, 4239-4247.	3.3	5
6617	Predicting the mechanism and rate of H-NS binding to AT-rich DNA. <i>PLoS Computational Biology</i> , 2019, 15, e1006845.	3.2	22
6618	Identification of a homozygous GFPT2 variant in a family with asthenozoospermia. <i>Gene</i> , 2019, 699, 16-23.	2.2	13
6619	Stabilizing osmolytes' effects on the structure, stability and function of tc-tenecteplase: A one peptide bond digested form of tenecteplase. <i>International Journal of Biological Macromolecules</i> , 2019, 130, 863-877.	7.5	4
6620	Polyurethanases: Three-dimensional structures and molecular dynamics simulations of enzymes that degrade polyurethane. <i>Journal of Molecular Graphics and Modelling</i> , 2019, 89, 82-95.	2.4	23
6621	Water in an electric field does not dance alone: The relation between equilibrium structure, time dependent viscosity and molecular motions. <i>Journal of Molecular Liquids</i> , 2019, 282, 303-315.	4.9	17
6622	NMR analysis of free and lipid nanodisc anchored CEACAM1 membrane proximal peptides with Ca <sup>2+</sup> /CaM. <i>Biochimica Et Biophysica Acta - Biomembranes</i> , 2019, 1861, 787-797.	2.6	5
6623	Molecular dynamics study on growth of carbon dioxide and methane hydrate from a seed crystal. <i>Chinese Journal of Chemical Engineering</i> , 2019, 27, 2074-2080.	3.5	20
6624	Binding of SV40â€™s Viral Capsid Protein VP1 to Its Glycosphingolipid Receptor GM1 Induces Negative Membrane Curvature: A Molecular Dynamics Study. <i>Langmuir</i> , 2019, 35, 3534-3544.	3.5	10
6625	Is it possible for short peptide composed of positively- and negatively-charged â€œhydrophilicâ€•amino acid residue-clusters to form metastable â€œhydrophobicâ€•packing?. <i>Physical Chemistry Chemical Physics</i> , 2019, 21, 9683-9693.	2.8	5

#	ARTICLE	IF	CITATIONS
6626	Different effects of cholesterol on membrane permeation of arginine and tryptophan revealed by bias-exchange metadynamics simulations. <i>Journal of Chemical Physics</i> , 2019, 150, 084106.	3.0	13
6627	Conformational sampling and polarization of Asp26 in pK <sub>a</sub> calculations of thioredoxin. <i>Proteins: Structure, Function and Bioinformatics</i> , 2019, 87, 467-477.	2.6	4
6628	Septin 9 has Two Polybasic Domains Critical to Septin Filament Assembly and Golgi Integrity. <i>IScience</i> , 2019, 13, 138-153.	4.1	31
6629	Binding Interaction of Juglone with Lysozyme: Spectroscopic Studies Aided by In Silico Calculations. <i>Journal of Photochemistry and Photobiology B: Biology</i> , 2019, 193, 89-99.	3.8	38
6630	Can All-Atom Molecular Dynamics Simulations Quantitatively Describe Homeodomainâ€‘DNA Binding Equilibria?. <i>Journal of Chemical Theory and Computation</i> , 2019, 15, 2635-2648.	5.3	8
6631	Solvent-Assisted Enhanced Emission of Cationic Perylene Diimide Supramolecular Assembly in Water: A Perspective from Experiment and Simulation. <i>Journal of Physical Chemistry C</i> , 2019, 123, 6241-6249.	3.1	9
6632	Glucose Can Protect Membranes against Dehydration Damage by Inducing a Glassy Membrane State at Low Hydrations. <i>Membranes</i> , 2019, 9, 15.	3.0	19
6633	Molecular Simulation of Methane Adsorption Behavior in Kerogen Nanopores for Shale Gas Resource Assessment. , 2019, , .		10
6634	Role of Second Quinone Binding Site in Proton Pumping by Respiratory Complex I. <i>Frontiers in Chemistry</i> , 2019, 7, 221.	3.6	36
6635	Proton leakage across lipid bilayers: Oxygen atoms of phospholipid ester linkers align water molecules into transmembrane water wires. <i>Biochimica Et Biophysica Acta - Bioenergetics</i> , 2019, 1860, 439-451.	1.0	14
6636	Structural modification of indomethacin toward selective inhibition of COX-2 with a significant increase in van der Waals contributions. <i>Bioorganic and Medicinal Chemistry</i> , 2019, 27, 1789-1794.	3.0	8
6637	Development of a hybrid biomimetic ligand with high selectivity and mild elution for antibody purification. <i>Chemical Engineering Journal</i> , 2019, 368, 678-686.	12.7	30
6638	Evolution of solidification defects in deformation of nano-polycrystalline aluminum. <i>Computational Materials Science</i> , 2019, 163, 176-185.	3.0	26
6639	Separation Efficiency of CO <sub>2</sub> in Ionic Liquids/Poly(vinylidene fluoride) Composite Membrane: A Molecular Dynamics Study. <i>Industrial &amp; Engineering Chemistry Research</i> , 2019, 58, 6887-6898.	3.7	18
6640	A pH Replica Exchange Scheme in the Stochastic Titration Constant-pH MD Method. <i>Journal of Chemical Theory and Computation</i> , 2019, 15, 3108-3116.	5.3	17
6641	Chasing the Full Free Energy Landscape of Neuroreceptor/Ligand Unbinding by Metadynamics Simulations. <i>Journal of Chemical Theory and Computation</i> , 2019, 15, 3354-3361.	5.3	53
6642	NMRâ€‘ and MD simulationâ€‘based structural characterization of the membrane-associating FATC domain of ataxia telangiectasia mutated. <i>Journal of Biological Chemistry</i> , 2019, 294, 7098-7112.	3.4	7
6643	Discovery of Small Molecules that Target Vascular Endothelial Growth Factor Receptor-2 Signalling Pathway Employing Molecular Modelling Studies. <i>Cells</i> , 2019, 8, 269.	4.1	14

#	ARTICLE	IF	CITATIONS
6644	Free Surface-Induced Glass-Transition Temperature Suppression of Simulated Polymer Chains. Journal of Physical Chemistry C, 2019, 123, 9237-9246.	3.1	16
6645	Molecular Modeling Investigation of the Interaction between <i>Humicola insolens</i> Cutinase and SDS Surfactant Suggests a Mechanism for Enzyme Inactivation. Journal of Chemical Information and Modeling, 2019, 59, 1977-1987.	5.4	14
6646	Outer Membrane Proteins OmpA, FhuA, OmpF, EstA, BtuB, and OmpX Have Unique Lipopolysaccharide Fingerprints. Journal of Chemical Theory and Computation, 2019, 15, 2608-2619.	5.3	34
6647	Organic-Free Interzeolite Transformation in the Absence of Common Building Units. Chemistry - A European Journal, 2019, 25, 5893-5898.	3.3	38
6648	Coagulation Factor XIIIa Inhibitor Tridegin: On the Role of Disulfide Bonds for Folding, Stability, and Function. Journal of Medicinal Chemistry, 2019, 62, 3513-3523.	6.4	7
6649	Coarse-Grained Simulation of Full-Length Integrin Activation. Biophysical Journal, 2019, 116, 1000-1010.	0.5	22
6650	Molecular dynamics simulations of novel electrolytes based on mixtures of protic and aprotic ionic liquids at the electrochemical interface: Structure and capacitance of the electric double layer. Electrochimica Acta, 2019, 305, 223-231.	5.2	16
6651	Designing Melittin-Graphene Hybrid Complexes for Enhanced Antibacterial Activity. Advanced Healthcare Materials, 2019, 8, e1801521.	7.6	36
6652	Specific Ion and Concentration Effects in Acetate Solutions with Na <sup>+</sup> , K <sup>+</sup> and Cs <sup>+</sup> . ChemPhysChem, 2019, 20, 1006-1010.	2.1	1
6653	Exploring the Dual Interaction of Natural Rhamnolipids with Plant and Fungal Biomimetic Plasma Membranes through Biophysical Studies. International Journal of Molecular Sciences, 2019, 20, 1009.	4.1	43
6654	Insights into water accessible pathways and the inactivation mechanism of proton translocation by the membrane-embedded domain of V-type ATPases. Biochimica Et Biophysica Acta - Biomembranes, 2019, 1861, 1004-1010.	2.6	10
6655	Structural Characterization of N-WASP Domain V Using MD Simulations with NMR and SAXS Data. Biophysical Journal, 2019, 116, 1216-1227.	0.5	18
6656	Molecular mechanism of material deformation and failure in butadiene rubber: Insight from all-atom molecular dynamics simulation using a bond breaking potential model. Polymer, 2019, 170, 113-119.	3.8	28
6657	Movement of Arginine through OprD: The Energetics of Permeation and the Role of Lipopolysaccharide in Directing Arginine to the Protein. Journal of Physical Chemistry B, 2019, 123, 2824-2832.	2.6	20
6658	Stimuli-Responsive Room-Temperature <i>N</i> -Heteroacene Liquid: In Situ Observation of the Self-Assembling Process and Its Multiple Properties. ACS Applied Materials & Interfaces, 2019, 11, 12053-12062.	8.0	28
6659	The IKK-binding domain of NEMO is an irregular coiled coil with a dynamic binding interface. Scientific Reports, 2019, 9, 2950.	3.3	20
6660	Insights into the dynamic nature of the dsRNA-bound TLR3 complex. Scientific Reports, 2019, 9, 3652.	3.3	39
6661	Details of hydrophobic entanglement between small molecules and Braun's lipoprotein within the cavity of the bacterial chaperone LolA. Scientific Reports, 2019, 9, 3717.	3.3	11

#	ARTICLE	IF	CITATIONS
6662	Mechanisms of phase separation in temperature-responsive acidic aqueous biphasic systems. <i>Physical Chemistry Chemical Physics</i> , 2019, 21, 7462-7473.	2.8	23
6663	Exploration of Catalytic Selectivity for Aminotransferase (BtrR) Based on Multiple Molecular Dynamics Simulations. <i>International Journal of Molecular Sciences</i> , 2019, 20, 1188.	4.1	5
6664	Poisson's Ratio of the f.c.c. Hard Sphere Crystals with Periodically Stacked (001)-Nanolayers of Hard Spheres of Another Diameter. <i>Materials</i> , 2019, 12, 700.	2.9	19
6665	Vasodilation Elicited by Isoxsuprine, Identified by High-Throughput Virtual Screening of Compound Libraries, Involves Activation of the NO/cGMP and H2S/KATP Pathways and Blockade of $\beta$ 1-Adrenoceptors and Calcium Channels. <i>Molecules</i> , 2019, 24, 987.	3.8	9
6666	Temperature Dependence of Intrinsically Disordered Proteins in Simulations: What are We Missing?. <i>Journal of Chemical Theory and Computation</i> , 2019, 15, 2672-2683.	5.3	55
6667	Interactions of human butyrylcholinesterase with phenylvalerate and acetylthiocholine as substrates and inhibitors: kinetic and molecular modeling approaches. <i>Archives of Toxicology</i> , 2019, 93, 1281-1296.	4.2	8
6668	Athermal mechanical analysis of Stone-Wales defects in two-dimensional silica. <i>Computational Materials Science</i> , 2019, 163, 301-307.	3.0	18
6669	EOR solvent-oil interaction in clay-hosted pores: Insights from molecular dynamics simulations. <i>Fuel</i> , 2019, 249, 233-251.	6.4	57
6670	Molecular Dynamics Simulations of the Allosteric Modulation of the Adenosine A2a Receptor by a Mini-G Protein. <i>Scientific Reports</i> , 2019, 9, 5495.	3.3	13
6671	Continuum Mechanics as a Computable Coarse-Grained Picture of Molecular Dynamics. <i>Journal of Elasticity</i> , 2019, 135, 183-235.	1.9	6
6672	Rad54 Phosphorylation Promotes Homologous Recombination by Balancing Rad54 Mobility and DNA Binding. <i>Biophysical Journal</i> , 2019, 116, 1406-1419.	0.5	5
6673	Study on the deformation and strength characteristics of hard rock under true triaxial stress state using bonded-particle model. <i>Computers and Geotechnics</i> , 2019, 112, 1-16.	4.7	27
6674	Nanotoxicity of Boron Nitride Nanosheet to Bacterial Membranes. <i>Langmuir</i> , 2019, 35, 6179-6187.	3.5	36
6675	Fluorinated Cyclic Phosphorus(III)-Based Electrolyte Additives for High Voltage Application in Lithium-Ion Batteries: Impact of Structure-Reactivity Relationships on CEI Formation and Cell Performance. <i>ACS Applied Materials &amp; Interfaces</i> , 2019, 11, 16605-16618.	8.0	27
6676	Physical origin underlying the prenucleation-cluster-mediated nonclassical nucleation pathways for calcium phosphate. <i>Physical Chemistry Chemical Physics</i> , 2019, 21, 14530-14540.	2.8	25
6677	Behavior of water molecules between molecular layers of by-products of dicumyl peroxide or surfactants in an external electric field: Computational insight. <i>Computational Materials Science</i> , 2019, 163, 134-140.	3.0	5
6678	Analyses of equilibrium water content and blood compatibility for Poly(2-methoxyethyl acrylate) by molecular dynamics simulation. <i>Polymer</i> , 2019, 170, 76-84.	3.8	19
6679	Fantastic Liquids and Where To Find Them: Optimizations of Discrete Chemical Space. <i>Journal of Chemical Information and Modeling</i> , 2019, 59, 2617-2625.	5.4	7

#	ARTICLE	IF	CITATIONS
6680	Effect of pH and Molecular Length on the Structure and Dynamics of Short Poly(acrylic acid) in Dilute Solution: Detailed Molecular Dynamics Study. <i>Journal of Physical Chemistry B</i> , 2019, 123, 4204-4219.	2.6	42
6681	Molecular Modifiers Suppress Nonclassical Pathways of Zeolite Crystallization. <i>Chemistry of Materials</i> , 2019, 31, 3228-3238.	6.7	39
6682	Mechanism of Trehalose-Induced Protein Stabilization from Neutron Scattering and Modeling. <i>Journal of Physical Chemistry B</i> , 2019, 123, 3679-3687.	2.6	28
6683	Time-Dependent Temperature and Time-Dependent Water Superposition Principles Applied to Poly(allylamine)/Poly(acrylic acid) Tj ETQq1.1.0.784314 rgBT (O) 4.8 61	4.8	61
6684	A review of current progress in multiscale simulations for fluid flow and heat transfer problems: The frameworks, coupling techniques and future perspectives. <i>International Journal of Heat and Mass Transfer</i> , 2019, 137, 1263-1289.	4.8	39
6685	Thermochemistry of Uracil, Thymine, Cytosine, and Adenine. <i>Journal of Physical Chemistry A</i> , 2019, 123, 4057-4067.	2.5	6
6686	Role of O-Antigen in Response to Mechanical Stress of the <i>E. coli</i> Outer Membrane: Insights from Coarse-Grained MD Simulations. <i>Journal of Physical Chemistry B</i> , 2019, 123, 3567-3575.	2.6	43
6687	How Fast Is Too Fast in Force-Probe Molecular Dynamics Simulations?. <i>Journal of Physical Chemistry B</i> , 2019, 123, 3658-3664.	2.6	17
6688	Molecular insights into ionic liquid/aqueous interface of phosphonium based phase-separable ionic liquids. <i>AIP Advances</i> , 2019, 9, 045115.	1.3	10
6689	Microscopic Structural and Dynamic Features in Triphasic Room Temperature Ionic Liquids. <i>Frontiers in Chemistry</i> , 2019, 7, 285.	3.6	25
6690	Ion-Specific and pH-Dependent Hydration of Mica-Electrolyte Interfaces. <i>Langmuir</i> , 2019, 35, 5737-5745.	3.5	49
6691	Role of $\alpha$ and $\beta$ relaxations in collapsing dynamics of a polymer chain in supercooled glass-forming liquid. <i>Journal of Chemical Physics</i> , 2019, 150, 114503.	3.0	4
6692	Determining selection free energetics from nucleotide pre-insertion to insertion in viral T7 RNA polymerase transcription fidelity control. <i>Nucleic Acids Research</i> , 2019, 47, 4721-4735.	14.5	12
6693	Modulation of solid-water-peptide interfacial properties towards surface adsorption/bioresistance. <i>Applied Surface Science</i> , 2019, 483, 373-382.	6.1	8
6694	Hydrodynamic volume of trehalose and its water uptake mechanism. <i>Biophysical Chemistry</i> , 2019, 249, 106145.	2.8	4
6695	Very low density amorphous phase of zircon. <i>Journal of Non-Crystalline Solids</i> , 2019, 513, 137-143.	3.1	4
6696	A Coarse-Grained Molecular Dynamics Approach to the Study of the Intrinsically Disordered Protein $\alpha$ -Synuclein. <i>Journal of Chemical Information and Modeling</i> , 2019, 59, 1458-1471.	5.4	44
6697	Pathways of amyloid-beta absorption and aggregation in a membranous environment. <i>Physical Chemistry Chemical Physics</i> , 2019, 21, 8559-8568.	2.8	16

#	ARTICLE	IF	CITATIONS
6698	Improving collective variables: The case of crystallization. <i>Journal of Chemical Physics</i> , 2019, 150, 094509.	3.0	38
6699	Unfolding of DNA by co-solutes: insights from Kirkwoodâ€“Buff integrals and transfer free energies. <i>European Physical Journal: Special Topics</i> , 2019, 227, 1665-1679.	2.6	18
6700	Steroidâ€“steroid interactions in biological membranes: Cholesterol and cortisone. <i>Chemistry and Physics of Lipids</i> , 2019, 221, 193-197.	3.2	5
6701	Nanoscrolls Formed from Two-Dimensional Covalent Organic Frameworks. <i>Chemistry of Materials</i> , 2019, 31, 3265-3273.	6.7	12
6702	Novel Intersubunit Interaction Critical for HIV-1 Core Assembly Defines a Potentially Targetable Inhibitor Binding Pocket. <i>MBio</i> , 2019, 10, .	4.1	13
6703	Interactions Between Natural Herbicides and Lipid Bilayers Mimicking the Plant Plasma Membrane. <i>Frontiers in Plant Science</i> , 2019, 10, 329.	3.6	18
6704	Complex Behavior of Phosphatidylcholineâ€“Phosphatidic Acid Bilayers and Monolayers: Effect of Acyl Chain Unsaturation. <i>Langmuir</i> , 2019, 35, 5944-5956.	3.5	27
6705	On the relevance of electrostatic interactions for the structural relaxation of ionic liquids: A molecular dynamics simulation study. <i>Journal of Chemical Physics</i> , 2019, 150, 124501.	3.0	14
6706	Molecular Dynamics Insights for Screening the Ability of Polymers to Remove Pesticides from Water. <i>ChemistryOpen</i> , 2019, 8, 438-446.	1.9	8
6707	Free energy calculations elucidate substrate binding, gating mechanism, and toleranceâ€“promoting mutations in herbicide target 4â€“hydroxyphenylpyruvate dioxygenase. <i>Protein Science</i> , 2019, 28, 1048-1058.	7.6	9
6708	Microscopic origin of the scattering pre-peak in aqueous propylamine mixtures: X-ray and neutron experiments <i>versus</i> simulations. <i>Physical Chemistry Chemical Physics</i> , 2019, 21, 9317-9325.	2.8	13
6709	Lipid Fingerprints and Cofactor Dynamics of Light-Harvesting Complex II in Different Membranes. <i>Biophysical Journal</i> , 2019, 116, 1446-1455.	0.5	31
6710	Design, computational studies, synthesis and biological evaluation of thiazole-based molecules as anticancer agents. <i>European Journal of Pharmaceutical Sciences</i> , 2019, 134, 20-30.	4.0	48
6711	Competition/Cooperation between Humic Acid and Graphene Oxide in Uranyl Adsorption Implicated by Molecular Dynamics Simulations. <i>Environmental Science &amp; Technology</i> , 2019, 53, 5102-5110.	10.0	53
6712	Oxidation destabilizes toxic amyloid beta peptide aggregation. <i>Scientific Reports</i> , 2019, 9, 5476.	3.3	33
6713	Anisotropic mechanical behavior and auxeticity of penta-graphene: Molecular statics/molecular dynamics studies. <i>Carbon</i> , 2019, 146, 572-587.	10.3	16
6714	Tailoring carbon nitride properties and photoactivity by interfacial engineering of hydrogen-bonded frameworks. <i>Nanoscale</i> , 2019, 11, 5564-5570.	5.6	21
6715	Equation of State of Fluid Methane from First Principles with Machine Learning Potentials. <i>Journal of Chemical Theory and Computation</i> , 2019, 15, 2574-2586.	5.3	40



#	ARTICLE	IF	CITATIONS
6716	<i>In Silico</i> Design and Characterization of Graphene Oxide Membranes with Variable Water Content and Flake Oxygen Content. ACS Nano, 2019, 13, 2995-3004.	14.6	32
6717	Double helical conformation and extreme rigidity in a rodlike polyelectrolyte. Nature Communications, 2019, 10, 801.	12.8	36
6718	Resolving solution conformations of the model semi-flexible polyelectrolyte homogalacturonan using molecular dynamics simulations and small-angle x-ray scattering. European Physical Journal E, 2019, 42, 19.	1.6	9
6719	9-Methylfascaplysin Is a More Potent A $\beta$ 2 Aggregation Inhibitor than the Marine-Derived Alkaloid, Fascaplysin, and Produces Nanomolar Neuroprotective Effects in SH-SY5Y Cells. Marine Drugs, 2019, 17, 121.	4.6	33
6720	The inhibitory mechanism of aurintricarboxylic acid targeting serine/threonine phosphatase Stp1 in Staphylococcus aureus: insights from molecular dynamics simulations. Acta Pharmacologica Sinica, 2019, 40, 850-858.	6.1	8
6721	All-atom structure ensembles of islet amyloid polypeptides determined by enhanced sampling and experiment data restraints. Proteins: Structure, Function and Bioinformatics, 2019, 87, 541-550.	2.6	10
6722	Systematic parameterization procedure to develop force fields for molecular fluids using explicit water. Fluid Phase Equilibria, 2019, 490, 1-12.	2.5	12
6723	Mechanics of the Formation, Interaction, and Evolution of Membrane Tubular Structures. Biophysical Journal, 2019, 116, 884-892.	0.5	6
6724	Structure of Outward-Facing PglK and Molecular Dynamics of Lipid-Linked Oligosaccharide Recognition and Translocation. Structure, 2019, 27, 669-678.e5.	3.3	29
6725	Self-Assembled Cationic $\beta$ -Cyclodextrin Nanostructures for siRNA Delivery. Molecular Pharmaceutics, 2019, 16, 1358-1366.	4.6	47
6726	Multithermal-Multibaric Molecular Simulations from a Variational Principle. Physical Review Letters, 2019, 122, 050601.	7.8	22
6727	Role of structural ions on the dynamics of the Pseudomonas fluorescens O7A metalloprotease. Food Chemistry, 2019, 286, 309-315.	8.2	10
6728	Binding from Both Sides: TolR and Full-Length OmpA Bind and Maintain the Local Structure of the E. Coli Cell Wall. Structure, 2019, 27, 713-724.e2.	3.3	42
6729	Binding and inhibitory effect of the food colorants Sunset Yellow and Ponceau 4R on amyloid fibrillation of lysozyme. New Journal of Chemistry, 2019, 43, 3956-3968.	2.8	28
6730	Two aspartate residues close to the lesion binding site of Agrobacterium ( $\epsilon$ ) photolyase are required for Mg <sup>2+</sup> stimulation of DNA repair. FEBS Journal, 2019, 286, 1765-1779.	4.7	15
6731	Structural basis for isoniazid resistance in KatG double mutants of Mycobacterium tuberculosis. Microbial Pathogenesis, 2019, 129, 152-160.	2.9	3
6732	Unbiased Atomistic Insight into the Mechanisms and Solvent Role for Globular Protein Dimer Dissociation. Journal of Physical Chemistry B, 2019, 123, 1883-1895.	2.6	10
6733	Aggregation Behavior of Model Asphaltene Revealed from Large-Scale Coarse-Grained Molecular Simulations. Journal of Physical Chemistry B, 2019, 123, 2380-2396.	2.6	29

#	ARTICLE	IF	CITATIONS
6734	A probe into underlying factors affecting ultrafast charge transfer at Donor/IDIC interface of all-small-molecule nonfullerene organic solar cells. <i>Journal of Photochemistry and Photobiology A: Chemistry</i> , 2019, 375, 1-8.	3.9	11
6735	Congenital myopathy-related mutations in tropomyosin disrupt regulatory function through altered actin affinity and tropomodulin binding. <i>FEBS Journal</i> , 2019, 286, 1877-1893.	4.7	14
6736	Effects of the PIWI/MID domain of Argonaute protein on the association of miRNA's seed base with the target. <i>Rna</i> , 2019, 25, 620-629.	3.5	6
6737	Effective Interactions between Calcium-Silicate-Hydrate Nanolayers. <i>Journal of Physical Chemistry C</i> , 2019, 123, 4755-4766.	3.1	54
6738	Transport of cystine across xCâ <sup>+</sup> antiporter. <i>Archives of Biochemistry and Biophysics</i> , 2019, 664, 117-126.	3.0	10
6739	Does glycation really distort the peptide Î±-helicity?. <i>International Journal of Biological Macromolecules</i> , 2019, 129, 254-266.	7.5	5
6740	Investigation on the intermolecular interactions in aliphatic isocyanurate liquids: revealing the importance of dispersion. <i>Journal of Molecular Liquids</i> , 2019, 280, 25-33.	4.9	7
6741	Improvement in the Predicted Partitioning of Alcohol and Polyethylene Oxide Groups Between Water and Octanol (logP) in Molecular Dynamics Simulations. <i>Journal of Pharmaceutical Sciences</i> , 2019, 108, 214-222.	3.3	7
6742	How Water Permutes the Structural Organization and Microscopic Dynamics of Cholinium Glycinate Biocompatible Ionic Liquid. <i>Journal of Physical Chemistry B</i> , 2019, 123, 2057-2069.	2.6	21
6743	Stability Effect of Quinary Interactions Reversed by Single Point Mutations. <i>Journal of the American Chemical Society</i> , 2019, 141, 4660-4669.	13.7	61
6744	An investigation into non-covalent functionalization of a single-walled carbon nanotube and a graphene sheet with protein G:A combined experimental and molecular dynamics study. <i>Scientific Reports</i> , 2019, 9, 1273.	3.3	22
6745	A molecular mechanism for transthyretin amyloidogenesis. <i>Nature Communications</i> , 2019, 10, 925.	12.8	92
6746	Effects of PI(4,5)P <sub>2</sub> concentration on the Fâ€BAR domain membrane binding as revealed by coarse-grained simulations. <i>Proteins: Structure, Function and Bioinformatics</i> , 2019, 87, 561-568.	2.6	2
6747	The SIRAH 2.0 Force Field: Altius, Fortius, Citius. <i>Journal of Chemical Theory and Computation</i> , 2019, 15, 2719-2733.	5.3	109
6748	Mobility Capillary Electrophoresis-Restrained Modeling Method for Protein Structure Analysis in Mixtures. <i>Journal of Physical Chemistry B</i> , 2019, 123, 2335-2341.	2.6	12
6749	Physical properties of model biological lipid bilayers: insights from all-atom molecular dynamics simulations. <i>Journal of Molecular Modeling</i> , 2019, 25, 76.	1.8	89
6750	Dynamic Docking of a Medium-Sized Molecule to Its Receptor by Multicanonical MD Simulations. <i>Journal of Physical Chemistry B</i> , 2019, 123, 2479-2490.	2.6	22
6751	Amyloid-Î²(29-42) Dimeric Conformations in Membranes Rich in Omega-3 and Omega-6 Polyunsaturated Fatty Acids. <i>Journal of Physical Chemistry B</i> , 2019, 123, 2687-2696.	2.6	14

#	ARTICLE	IF	CITATIONS
6752	Molecular Design of Microporous Polymer Membranes for the Upgrading of Natural Gas. Journal of Physical Chemistry C, 2019, 123, 6607-6615.	3.1	17
6753	A lipid gating mechanism for the channel-forming O antigen ABC transporter. Nature Communications, 2019, 10, 824.	12.8	44
6754	A pharmacological master key mechanism that unlocks the selectivity filter gate in K <sup>+</sup> channels. Science, 2019, 363, 875-880.	12.6	91
6755	Interaction of salt with ether- and ester-linked phospholipid bilayers. Biochimica Et Biophysica Acta - Biomembranes, 2019, 1861, 907-915.	2.6	2
6756	Non-equilibrium Markov state modeling of periodically driven biomolecules. Journal of Chemical Physics, 2019, 150, 054103.	3.0	10
6757	Relation between concentration fluctuations and dynamical heterogeneities in binary glass-forming liquids: A molecular dynamics simulation study. Journal of Chemical Physics, 2019, 150, 064502.	3.0	6
6758	Dietary flavonoids inhibit the glycation of lens proteins: implications in the management of diabetic cataract. 3 Biotech, 2019, 9, 47.	2.2	14
6759	NanoModeler: A Webserver for Molecular Simulations and Engineering of Nanoparticles. Journal of Chemical Theory and Computation, 2019, 15, 2022-2032.	5.3	26
6760	Open-Boundary Molecular Mechanics/Coarse-Grained Framework for Simulations of Low-Resolution G-Protein-Coupled Receptor–Ligand Complexes. Journal of Chemical Theory and Computation, 2019, 15, 2101-2109.	5.3	16
6761	Solvent organization around the noncanonical part of tyrosine modulates its fluorescence properties. Physical Chemistry Chemical Physics, 2019, 21, 6042-6050.	2.8	1
6762	Multi-scale approach for modeling stability, aggregation, and network formation of nanoparticles suspended in aqueous solutions. Nanoscale, 2019, 11, 3979-3992.	5.6	32
6763	Elastic constants of ice Ih as described by semi-empirical water models. Journal of Chemical Physics, 2019, 150, 044503.	3.0	10
6764	Selectivity of Carbon Nanotubes under An Electric Field on Transferring Water – Alcohol Mixtures. IOP Conference Series: Materials Science and Engineering, 2019, 494, 012099.	0.6	0
6765	Self-Assembly of Aldehyde Lipids in Water. IOP Conference Series: Materials Science and Engineering, 2019, 526, 012005.	0.6	0
6766	Effect of Nanoparticles and Surfactants on Oil/Water Interfacial Tension: A Coarse-Grained Molecular Dynamics Simulation Study. , 2019, , .		4
6767	Study on the Role of Solid Surface on Nanochannel Flow with Molecular Dynamics Simulation. , 2019, , .		1
6768	Size effect in molecular dynamics simulation of nucleation process during solidification of pure metals: investigating modified embedded atom method interatomic potentials. Modelling and Simulation in Materials Science and Engineering, 2019, 27, 085015.	2.0	17
6769	Deamidation disrupts native and transient contacts to weaken the interaction between UBC13 and RING-finger E3 ligases. ELife, 2019, 8, .	6.0	11

#	ARTICLE	IF	CITATIONS
6770	A Continuum-on-Atomistic Framework with Bi-Stable Elements for the Computation of Minimum Free Energy Paths. <i>Mechanics of Solids</i> , 2019, 54, 975-994.	0.7	0
6771	Confirmation of the formation of salt bridges in the denatured state of CutA1 protein using molecular dynamics simulations. <i>Biophysics and Physicobiology</i> , 2019, 16, 176-184.	1.0	1
6772	Rotational and Translational Diffusion of Proteins as a Function of Concentration. <i>ACS Omega</i> , 2019, 4, 20654-20664.	3.5	17
6773	Salt Bridges Regulate in Silico DimersFormation for Î²2-MicroglobulinAmyloidogenic Variants. <i>Journal of Self-Assembly and Molecular Electronics (SAME)</i> , 2019, 6, 35-60.	0.0	2
6774	Free energy profiles of lipid translocation across pure POPC and POPC/CHOL bilayer: all-atom molecular dynamics study. <i>Journal of Physics: Conference Series</i> , 2019, 1290, 012020.	0.4	1
6775	Computational evaluation of the effect of processing on the trypsin and alphaâ€œamylase inhibitor from Ragi (<scp><i>Eleusine coracana</i></scp>) seed. <i>Engineering Reports</i> , 2019, 1, e12064.	1.7	3
6776	Structural Influence and Interactive Binding Behavior of Dopamine and Norepinephrine on the Greek-Key-Like Core of Î±-Synuclein Protofibril Revealed by Molecular Dynamics Simulations. <i>Processes</i> , 2019, 7, 850.	2.8	3
6777	Clustering of atomic displacement parameters in bovine trypsin reveals a distributed lattice of atoms with shared chemical properties. <i>Scientific Reports</i> , 2019, 9, 19281.	3.3	7
6778	Effects of a remote mutation from the contact paratope on the structure of CDR-H3 in the anti-HIV neutralizing antibody PG16. <i>Scientific Reports</i> , 2019, 9, 19840.	3.3	4
6779	Molecular dynamics simulation of the nanosecond pulsed electric field effect on kinesin nanomotor. <i>Scientific Reports</i> , 2019, 9, 19721.	3.3	17
6780	&lt;p&gt;Characterization Of Bloodâ€œBrain Barrier Crossing And Tumor Homing Peptides By Molecular Dynamics Simulations&lt;p&gt;. <i>International Journal of Nanomedicine</i> , 2019, Volume 14, 10123-10136.	6.7	5
6781	Tensile Test Analysis of a Carbon Fiber Composite Material by Molecular Dynamics Simulation. <i>Journal of the Japan Society for Composite Materials</i> , 2019, 45, 19-25.	0.2	2
6782	Low temperature protein refolding suggested by molecular simulation. <i>Journal of Chemical Physics</i> , 2019, 151, 185101.	3.0	13
6783	Mechanism of synergistic actin filament pointed end depolymerization by cyclase-associated protein and cofilin. <i>Nature Communications</i> , 2019, 10, 5320.	12.8	76
6784	Fast surface dynamics enabled cold joining of metallic glasses. <i>Science Advances</i> , 2019, 5, eaax7256.	10.3	87
6785	Sequential activation of STIM1 links Ca <sup>2+</sup> with luminal domain unfolding. <i>Science Signaling</i> , 2019, 12, .	3.6	32
6786	Insights into the Effects of Cancer Associated Mutations at the UPF2 and ATP-Binding Sites of NMD Master Regulator: UPF1. <i>International Journal of Molecular Sciences</i> , 2019, 20, 5644.	4.1	13
6787	Evaluating Models of Varying Complexity of Crowded Intrinsically Disordered Protein Solutions Against SAXS. <i>Journal of Chemical Theory and Computation</i> , 2019, 15, 6968-6983.	5.3	15

6789	Identification of The Fipronil Resistance Associated Mutations in Nilaparvata lugens GABA Receptors by Molecular Modeling. <i>Molecules</i> , 2019, 24, 4116.	3.8	13
6790	Atomistic simulation of PDADMAC/PSS oligoelectrolyte multilayers: overall comparison of tri- and tetra-layer systems. <i>Soft Matter</i> , 2019, 15, 9437-9451.	2.7	5
6791	Investigation of Grignard Reagent as an Advanced Base for Aza-Claisen Rearrangement. <i>Molecules</i> , 2019, 24, 4597.	3.8	3
6792	Effect of Pore Size on the Ion Electrosorption and Hydrogen/Deuterium Electrosorption Using Sodium Chloride in $H_2O$ and $D_2O$ . <i>Journal of the Electrochemical Society</i> , 2019, 166, A4158-A4167.	2.9	8
6793	Dissecting $Ca^{2+}$ and $Na^{+}$ Interactions in Two Proteins Using a Combined Experimental and Computational Approach. <i>Scientific Reports</i> , 2019, 9, 20149.	3.3	27
6794	Molecular dynamics simulation of homogeneous nucleation of supersaturated potassium chloride (KCl) in aqueous solutions. <i>CrystEngComm</i> , 2019, 21, 7507-7518.	2.6	11
6795	Molecular mechanisms of 33-mer gliadin peptide oligomerisation. <i>Physical Chemistry Chemical Physics</i> , 2019, 21, 22539-22552.	2.8	13
6796	Insights into the adsorption mechanism and dynamic behavior of tetracycline antibiotics on reduced graphene oxide (RGO) and graphene oxide (GO) materials. <i>Environmental Science: Nano</i> , 2019, 6, 3336-3348.	4.3	93
6797	Interaction of the mononucleotide UMP with a fluid phospholipid bilayer. <i>Soft Matter</i> , 2019, 15, 8129-8136.	2.7	6
6798	Rational Coarse-Grained Molecular Dynamics Simulations of Supramolecular Anticancer Nanotubes. <i>Journal of Physical Chemistry B</i> , 2019, 123, 10582-10593.	2.6	9
6799	Sr-induced dipole scatter in $Ba_{1-x}Sr_x$ : Insights from a transferable-bond valence-based interatomic potential. <i>Physical Review B</i> , 2019, 100, .	3.2	18
6800	The conical shape of DIM lipids promotes <i>Mycobacterium tuberculosis</i> infection of macrophages. <i>Proceedings of the National Academy of Sciences of the United States of America</i> , 2019, 116, 25649-25658.	7.1	49
6801	Rational discovery of antimetastatic agents targeting the intrinsically disordered region of MBD2. <i>Science Advances</i> , 2019, 5, eaav9810.	10.3	21
6802	Details of the cooperative binding of piperlongumine with rat serum albumin obtained by spectroscopic and computational analyses. <i>Scientific Reports</i> , 2019, 9, 15667.	3.3	8
6803	Commensurate-incommensurate phase transition of dense potassium simulated by machine-learned interatomic potential. <i>Physical Review B</i> , 2019, 100, .	3.2	8
6804	Temperature Activates Contact Aging in Silica Nanocontacts. <i>Physical Review X</i> , 2019, 9, .	8.9	7
6805	Lipid Interactions of a Ciliary Membrane TRP Channel: Simulation and Structural Studies of Polycystin-2. <i>Structure</i> , 2020, 28, 169-184.e5.	3.3	37

#	ARTICLE	IF	CITATIONS
6806	A Molecular Dynamics Perspective To Identify Precursors to Aggregation in Human $\gamma$ S-Crystallin Unravels the Mechanism of Childhood Cataracts. <i>Journal of Physical Chemistry B</i> , 2019, 123, 10384-10393.	2.6	8
6807	Multimodal Interactions of Dopamine Hydrochloride with the Groove Region of DNA: A Key Factor in the Enhanced Stability of DNA. <i>Journal of Physical Chemistry B</i> , 2019, 123, 10700-10708.	2.6	14
6808	Crystallization of Morone Platelets using Cooperative Organic Structure-Directing Agents. <i>Journal of the American Chemical Society</i> , 2019, 141, 20155-20165.	13.7	42
6809	Approximating free energy and committor landscapes in standard transition path sampling using virtual interface exchange. <i>Journal of Chemical Physics</i> , 2019, 151, 174111.	3.0	17
6810	On the Nonaggregation of Normal Adult Hemoglobin and the Aggregation of Sick Cell Hemoglobin. <i>Journal of Physical Chemistry B</i> , 2019, 123, 10735-10745.	2.6	5
6811	Wetting Properties of the CO <sub>2</sub> -Water-Calcite System via Molecular Simulations: Shape and Size Effects. <i>Langmuir</i> , 2019, 35, 16669-16678.	3.5	36
6812	A Quantitative Molecular Atlas for Interactions Between Lignin and Cellulose. <i>ACS Sustainable Chemistry and Engineering</i> , 2019, 7, 19570-19583.	6.7	36
6813	Molecular mechanism of a potassium channel gating through activation gate-selectivity filter coupling. <i>Nature Communications</i> , 2019, 10, 5366.	12.8	83
6814	Functional and structural basis of E. coli enolase inhibition by SF2312: a mimic of the carbanion intermediate. <i>Scientific Reports</i> , 2019, 9, 17106.	3.3	9
6815	Structural basis for phospholipase A2-like toxin inhibition by the synthetic compound Varespladib (LY315920). <i>Scientific Reports</i> , 2019, 9, 17203.	3.3	49
6816	Molecular Dynamics Study of the Swelling of Poly(methyl methacrylate) in Supercritical Carbon Dioxide. <i>Materials</i> , 2019, 12, 3315.	2.9	15
6817	The Amphotericin B-Ergosterol Complex Spans a Lipid Bilayer as a Single-Length Assembly. <i>Biochemistry</i> , 2019, 58, 5188-5196.	2.5	21
6818	On the Stability of the Water-Soluble Chlorophyll-Binding Protein (WSCP) Studied by Molecular Dynamics Simulations. <i>Journal of Physical Chemistry B</i> , 2019, 123, 10594-10604.	2.6	8
6819	Structure and phase transition behaviors of water in carbon nanotube under the electric field and high pressure. <i>Materials Research Express</i> , 2019, 6, 1250a1.	1.6	2
6820	High-resolution cryo-EM structures of respiratory complex I: Mechanism, assembly, and disease. <i>Science Advances</i> , 2019, 5, eaax9484.	10.3	109
6821	An Integrated Pan-Cancer Analysis and Structure-Based Virtual Screening of GPR15. <i>International Journal of Molecular Sciences</i> , 2019, 20, 6226.	4.1	15
6822	Progressive Hydrophobicity of Fluorobenzenes. <i>Journal of Physical Chemistry B</i> , 2019, 123, 10083-10088.	2.6	6
6823	Mechanistic correlation between water infiltration and framework hydrophilicity in MFI zeolites. <i>Scientific Reports</i> , 2019, 9, 18429.	3.3	9



#	ARTICLE	IF	CITATIONS
6824	Predicting and designing therapeutics against the Nipah virus. PLoS Neglected Tropical Diseases, 2019, 13, e0007419.	3.0	24
6825	Does Sucrose Change Its Mechanism of Stabilization of Lipid Bilayers during Desiccation? Influences of Hydration and Concentration. Langmuir, 2019, 35, 15389-15400.	3.5	18
6826	Water Activity from Equilibrium Molecular Dynamics Simulations and Kirkwood-Buff Theory. Journal of Physical Chemistry B, 2019, 123, 10757-10768.	2.6	5
6827	Biofunctionalization of Silica Nanoparticles with Cell-Penetrating Peptides: Adsorption Mechanism and Binding Energy Estimation. Journal of Physical Chemistry B, 2019, 123, 10622-10630.	2.6	15
6828	Computational investigations of the binding mechanism of novel benzophenone imine inhibitors for the treatment of breast cancer. RSC Advances, 2019, 9, 35401-35416.	3.6	12
6829	Structural features of selected protic ionic liquids based on a super-strong base. Physical Chemistry Chemical Physics, 2019, 21, 25369-25378.	2.8	6
6830	The molecular mechanism of robust macrophage immune responses induced by PEGylated molybdenum disulfide. Nanoscale, 2019, 11, 22293-22304.	5.6	35
6831	Toward realistic computer modeling of paraffin-based composite materials: critical assessment of atomic-scale models of paraffins. RSC Advances, 2019, 9, 38834-38847.	3.6	39
6832	Collective absorption of 2,4,6-trinitrotoluene into lipid membranes and its effects on bilayer properties. A computational study. RSC Advances, 2019, 9, 39046-39054.	3.6	3
6833	Molecular dynamics investigation of wetting-dewetting behavior of model carbon material by 1-butyl-3-methylimidazolium acetate ionic liquid nanodroplet. Journal of Chemical Physics, 2019, 151, 244705.	3.0	5
6834	Assembly of Spinach Chloroplast ATP Synthase Rotor Ring Protein-Lipid Complex. Frontiers in Molecular Biosciences, 2019, 6, 135.	3.5	7
6835	Hydrogen embrittlement controlled by reaction of dislocation with grain boundary in alpha-iron. International Journal of Plasticity, 2019, 112, 206-219.	8.8	88
6836	Comparative molecular dynamic simulation study on the use of chitosan for temperature stabilization of interferon $\beta$ . Carbohydrate Polymers, 2019, 203, 52-59.	10.2	27
6837	Exploration and validation of diphosphate-based <i>Plasmodium</i> LytB inhibitors using computational approaches. Journal of Molecular Recognition, 2019, 32, e2762.	2.1	5
6838	In silico and in vitro study of magnetic niosomes for gene delivery: The effect of ergosterol and cholesterol. Materials Science and Engineering C, 2019, 94, 234-246.	7.3	73
6839	Modulation of aromatase by natural compounds—A pharmacophore guided molecular modelling simulations. South African Journal of Botany, 2019, 120, 230-240.	2.5	5
6840	Dispersion of graphene using surfactant mixtures: Experimental and molecular dynamics simulation studies. Applied Surface Science, 2019, 464, 440-450.	6.1	58
6841	The lipid environment determines the activity of the <i>Escherichia coli</i> ammonium transporter AmtB. FASEB Journal, 2019, 33, 1989-1999.	0.5	28

#	ARTICLE	IF	CITATIONS
6842	Predicting binding affinities of nitrogen-containing bisphosphonates on hydroxyapatite surface by molecular dynamics. Chemical Physics Letters, 2019, 716, 83-92.	2.6	12
6843	Helix-Switch Enables C99 Dimer Transition between the Multiple Conformations. Journal of Chemical Information and Modeling, 2019, 59, 339-350.	5.4	8
6844	Interplay between Membrane Curvature and Cholesterol: Role of Palmitoylated Caveolin-1. Biophysical Journal, 2019, 116, 69-78.	0.5	56
6845	Spectroscopic Ellipsometry of fluid and gel phase lipid bilayers in hydrated conditions. Colloids and Surfaces B: Biointerfaces, 2019, 176, 55-61.	5.0	7
6846	Genetic Mutations in the S-loop of Human Glutathione Synthetase: Links Between Substrate Binding, Active Site Structure and Allostery. Computational and Structural Biotechnology Journal, 2019, 17, 31-38.	4.1	7
6847	Derivation of micelle size-dependent free energies of aggregation for octyl phosphocholine from molecular dynamics simulation. Fluid Phase Equilibria, 2019, 485, 83-93.	2.5	8
6848	Protein G selects two binding sites for carbon nanotube with dissimilar behavior; a molecular dynamics study. Journal of Molecular Graphics and Modelling, 2019, 87, 257-267.	2.4	2

6849

#	ARTICLE	IF	CITATIONS
6860	Force spectroscopy of the thrombin-aptamer interaction: Comparison between AFM experiments and molecular dynamics simulations. <i>Applied Surface Science</i> , 2019, 475, 462-472.	6.1	6
6861	Highly tumor-specific DNA nanostructures discovered by in vivo screening of a nucleic acid cage library and their applications in tumor-targeted drug delivery. <i>Biomaterials</i> , 2019, 195, 1-12.	11.4	44
6862	The role of intermolecular interactions on the encapsulation of human insulin into the chitosan and cholesterol-grafted chitosan polymers. <i>Carbohydrate Polymers</i> , 2019, 208, 345-355.	10.2	17
6863	Hybrid thermal stabilization of Zr doped nanocrystalline Cu. <i>Materials and Design</i> , 2019, 164, 107564.	7.0	15
6864	Structural changes of a simple peptide "Trpzip-1" in aqueous solutions and the corresponding hydration phenomena under the influence of temperature. <i>Journal of Molecular Liquids</i> , 2019, 277, 532-540.	4.9	1
6865	Molecular Dynamics Study of Kinetic Hydrate Inhibitors: The Optimal Inhibitor Size and Effect of Guest Species. <i>Journal of Physical Chemistry C</i> , 2019, 123, 1806-1816.	3.1	40
6866	Effect of Familial Mutations on the Interconversion of $\alpha$ -Helix to $\beta$ -Sheet Structures in an Amyloid-Forming Peptide: Insight from Umbrella Sampling Simulations. <i>ACS Chemical Neuroscience</i> , 2019, 10, 1347-1354.	3.5	16
6867	3D structure of a <i>Brucella melitensis</i> porin: molecular modelling in lipid membranes. <i>Journal of Biomolecular Structure and Dynamics</i> , 2019, 37, 3923-3935.	3.5	6
6868	Linoleic and linolenic acid hydroperoxides interact differentially with biomimetic plant membranes in a lipid specific manner. <i>Colloids and Surfaces B: Biointerfaces</i> , 2019, 175, 384-391.	5.0	13
6869	A GROMOS Force Field for Furanose-Based Carbohydrates. <i>Journal of Chemical Theory and Computation</i> , 2019, 15, 1168-1186.	5.3	31
6870	Lipid Rafts: Buffers of Cell Membrane Physical Properties. <i>Journal of Physical Chemistry B</i> , 2019, 123, 2050-2056.	2.6	40
6871	Norepinephrine Inhibits Alzheimer's Amyloid- $\beta$ Peptide Aggregation and Destabilizes Amyloid- $\beta$ Protofibrils: A Molecular Dynamics Simulation Study. <i>ACS Chemical Neuroscience</i> , 2019, 10, 1585-1594.	3.5	83
6872	YB-1, an abundant core mRNA-binding protein, has the capacity to form an RNA nucleoprotein filament: a structural analysis. <i>Nucleic Acids Research</i> , 2019, 47, 3127-3141.	14.5	32
6873	Discovery of Potent Inhibitors for the Large Neutral Amino Acid Transporter 1 (LAT1) by Structure-Based Methods. <i>International Journal of Molecular Sciences</i> , 2019, 20, 27.	4.1	38
6874	Structural characterization and molecular dynamics simulations of the caprine and bovine solute carrier family 11 A1 (SLC11A1). <i>Journal of Computer-Aided Molecular Design</i> , 2019, 33, 265-285.	2.9	5
6875	An evaluation of in-silico methods for predicting solute partition in multiphase complex fluids "A case study of octanol/water partition coefficient. <i>Chemical Engineering Science</i> , 2019, 197, 150-158.	3.8	25
6876	The interaction of proteins with silica surfaces. Part II: Free energies of capped amino acids. <i>Computational and Theoretical Chemistry</i> , 2019, 1148, 38-43.	2.5	4
6877	In-vitro evaluation studies of 7-chloro-4-aminoquinoline Schiff bases and their copper complexes as cholinesterase inhibitors. <i>Journal of Inorganic Biochemistry</i> , 2019, 191, 183-193.	3.5	15

#	ARTICLE	IF	CITATIONS
6878	Bidirectional Control of Autophagy by BECN1 BARA Domain Dynamics. <i>Molecular Cell</i> , 2019, 73, 339-353.e6.	9.7	61
6879	Effect of general anesthetics on the properties of lipid membranes of various compositions. <i>Biochimica Et Biophysica Acta - Biomembranes</i> , 2019, 1861, 594-609.	2.6	13
6880	A conformational switch from a closed apo- to an open holo-form equips the acyl carrier protein for acyl chain accommodation. <i>Biochimica Et Biophysica Acta - Proteins and Proteomics</i> , 2019, 1867, 163-174.	2.3	6
6881	A molecular dynamics simulation study on the cavitation inception of water with dissolved gases. <i>Molecular Physics</i> , 2019, 117, 1894-1902.	1.7	7
6882	Thermal stability of single-domain antibodies estimated by molecular dynamics simulations. <i>Protein Science</i> , 2019, 28, 429-438.	7.6	38
6883	The lipid environment of Escherichia coli Aquaporin Z. <i>Biochimica Et Biophysica Acta - Biomembranes</i> , 2019, 1861, 431-440.	2.6	33
6884	Atomistic insights into cardiolipin binding sites of cytochrome c oxidase. <i>Biochimica Et Biophysica Acta - Bioenergetics</i> , 2019, 1860, 224-232.	1.0	15
6885	Molecular Self-Assembly Strategy for Encapsulation of an Amphipathic $\alpha$ -Helical Antimicrobial Peptide into the Different Polymeric and Copolymeric Nanoparticles. <i>Journal of Chemical Information and Modeling</i> , 2019, 59, 550-563.	5.4	26
6886	Dynamical and Environmental Effects on the Optical Properties of an Heteroleptic Ru(II)-Polypyridine Complex: A Multilevel Approach Combining Accurate Ground and Excited State QM-Derived Force Fields, MD and TD-DFT. <i>Journal of Chemical Theory and Computation</i> , 2019, 15, 529-545.	5.3	17
6887	Three-phase equilibrium curve shift for methane hydrate in oceanic conditions calculated from Molecular Dynamics simulations. <i>Journal of Molecular Liquids</i> , 2019, 274, 426-433.	4.9	26
6888	Structure-Based Drug Designing Recommends HDAC6 Inhibitors To Attenuate Microtubule-Associated Tau-Pathogenesis. <i>ACS Chemical Neuroscience</i> , 2019, 10, 1326-1335.	3.5	19
6889	Martini coarse-grained model for polyethylenimine. <i>Journal of Computational Chemistry</i> , 2019, 40, 607-618.	3.3	13
6890	Vibrio cholerae LMWPTP-2 display unique surface charge and grooves around the active site: Indicative of distinctive substrate specificity and scope to design specific inhibitor. <i>Biochimica Et Biophysica Acta - Proteins and Proteomics</i> , 2019, 1867, 114-124.	2.3	1
6891	Cavitation inception of water with solid nanoparticles: A molecular dynamics study. <i>Ultrasonics Sonochemistry</i> , 2019, 51, 120-128.	8.2	20
6892	Lipid composition and salt concentration as regulatory factors of the anion selectivity of VDAC studied by coarse-grained molecular dynamics simulations. <i>Chemistry and Physics of Lipids</i> , 2019, 220, 66-76.	3.2	6
6893	Interaction of the anticancer p28 peptide with p53-DBD as studied by fluorescence, FRET, docking and MD simulations. <i>Biochimica Et Biophysica Acta - General Subjects</i> , 2019, 1863, 342-350.	2.4	20
6894	Screening of novel histone deacetylase 7 inhibitors through molecular docking followed by a combination of molecular dynamics simulations and ligand-based approach. <i>Journal of Biomolecular Structure and Dynamics</i> , 2019, 37, 4092-4103.	3.5	15
6895	Characterization of Electrospray Ionization (ESI) Parameters on In-ESI Hydrogen/Deuterium Exchange of Carbohydrate-Metal Ion Adducts. <i>Journal of the American Society for Mass Spectrometry</i> , 2019, 30, 235-247.	2.8	22

#	ARTICLE	IF	CITATIONS
6896	Susceptibility of shear banding to chemical short-range order in metallic glasses. <i>Scripta Materialia</i> , 2019, 162, 141-145.	5.2	22
6897	Hybrid Cascade-Type Molecular Dynamics with a Markov State Model for Efficient Free Energy Calculations. <i>Journal of Chemical Theory and Computation</i> , 2019, 15, 680-687.	5.3	12
6898	Presence of Intra-helical Salt-Bridge in Loop E Half-Helix Can Influence the Transport Properties of AQP1 and GlpF Channels: Molecular Dynamics Simulations of In Silico Mutants. <i>Journal of Membrane Biology</i> , 2019, 252, 17-29.	2.1	4
6899	Molecular Mechanism of Spontaneous Nucleosome Unraveling. <i>Journal of Molecular Biology</i> , 2019, 431, 323-335.	4.2	63
6900	Comparative study of the binding mode between cytochrome P450 17A1 and prostate cancer drugs in the absence of haem iron. <i>Journal of Biomolecular Structure and Dynamics</i> , 2019, 37, 4161-4170.	3.5	7
6901	Mechanistic basis of vitamin B12 and cobinamide salvaging by the <i>Vibrio</i> species. <i>Biochimica Et Biophysica Acta - Proteins and Proteomics</i> , 2019, 1867, 140-151.	2.3	10
6902	Nematic-to-columnar mesophase transition by in situ supramolecular polymerization. <i>Science</i> , 2019, 363, 161-165.	12.6	69
6903	On identifying collective displacements in apo-proteins that reveal eventual binding pathways. <i>PLoS Computational Biology</i> , 2019, 15, e1006665.	3.2	11
6904	Environmental effects on the charge transfer properties of Graphene quantum dot based interfaces. <i>International Journal of Quantum Chemistry</i> , 2019, 119, e25882.	2.0	8
6905	Cryo-Cooling Effect on DHFR Crystal Studied by Replica-Exchange Molecular Dynamics Simulations. <i>Biophysical Journal</i> , 2019, 116, 395-405.	0.5	3
6906	Molecular Order Affects Interfacial Water Structure and Temperature-Dependent Hydrophobic Interactions between Nonpolar Self-Assembled Monolayers. <i>Langmuir</i> , 2019, 35, 2078-2088.	3.5	38
6907	Computational insights into the role of $\beta$ -strand/sheet in aggregation of $\beta$ -synuclein. <i>Scientific Reports</i> , 2019, 9, 59.	3.3	33
6908	Transferability of interatomic potentials in predicting the temperature dependency of elastic constants for titanium, zirconium and magnesium. <i>Modelling and Simulation in Materials Science and Engineering</i> , 2019, 27, 025005.	2.0	3
6909	tPA Point Mutation at Autolysis Loop Enhances Resistance to PAI-1 Inhibition and Catalytic Activity. <i>Thrombosis and Haemostasis</i> , 2019, 119, 077-086.	3.4	8
6910	Structural Parameter of Orientational Order to Predict the Boson Vibrational Anomaly in Glasses. <i>Physical Review Letters</i> , 2019, 122, 015501.	7.8	45
6911	Effects of hydrophobic and hydrogen-bond interactions on the binding affinity of antifreeze proteins to specific ice planes. <i>Journal of Molecular Graphics and Modelling</i> , 2019, 87, 48-55.	2.4	9
6912	Cross-talk between allosteric and orthosteric binding sites of $\beta^3$ -amino butyric acid type A receptors (GABA <sub>A</sub> -Rs): A computational study revealing the structural basis of selectivity. <i>Journal of Biomolecular Structure and Dynamics</i> , 2019, 37, 3065-3080.	3.5	5
6913	Structural Studies of Autophagy-Related Proteins. <i>Methods in Molecular Biology</i> , 2019, 1880, 17-56.	0.9	2

#	ARTICLE	IF	CITATIONS
6914	The effect of electric fields in methane hydrate growth and dissociation: A molecular dynamics simulation. Computational and Theoretical Chemistry, 2019, 1149, 57-68.	2.5	32
6915	Arabinose substitution effect on xylan rigidity and self-aggregation. Cellulose, 2019, 26, 2267-2278.	4.9	31
6916	Cholesterol Interaction Sites on the Transmembrane Domain of the Hedgehog Signal Transducer and Class F G Protein-Coupled Receptor Smoothed. Structure, 2019, 27, 549-559.e2.	3.3	77
6917	Factors Promoting the Formation of Clathrate-Like Ordering of Water in Biomolecular Structure at Ambient Temperature and Pressure. Journal of Physical Chemistry B, 2019, 123, 811-824.	2.6	18
6918	The human DNA topoisomerase I mutant Gly717Asp: Higher religation rate is not always associated with camptothecin resistance. Archives of Biochemistry and Biophysics, 2019, 663, 165-172.	3.0	1
6919	An In-Depth Look at DNA Crystals through the Prism of Molecular Dynamics Simulations. Chem, 2019, 5, 649-663.	11.7	11
6920	Governing the Inhibition of Reconstituted Collagen Type I Assemblies Mediated Through Noncovalent Forces of (Å±)-Î± Lipoic Acid. Langmuir, 2019, 35, 980-989.	3.5	5
6921	Alpha-Hederin Nanopore for Single Nucleotide Discrimination. ACS Nano, 2019, 13, 1719-1727.	14.6	11
6922	Structure and function prediction of arsenate reductase from Deinococcus indicus DR1. Journal of Molecular Modeling, 2019, 25, 15.	1.8	11
6923	Fatty Acids Compete with AÎ² in Binding to Serum Albumin by Quenching Its Conformational Flexibility. Biophysical Journal, 2019, 116, 248-257.	0.5	24
6924	Delivery of novel vancomycin nanoplexes for combating methicillin resistant Staphylococcus aureus (MRSA) infections. International Journal of Pharmaceutics, 2019, 558, 143-156.	5.2	34
6925	Combined molecular dynamics (MD) and small angle scattering (SAS) analysis of organization on a nanometer-scale in ternary solvent solutions containing a hydrotrope. Journal of Colloid and Interface Science, 2019, 540, 623-633.	9.4	23
6926	Conditional Reversible Work Coarse-Grained Models with Explicit Electrostatics” An Application to Butylmethylimidazolium Ionic Liquids. Journal of Chemical Theory and Computation, 2019, 15, 1187-1198.	5.3	7
6927	Role of Conformational Flexibility in Monte Carlo Simulations of Many-Protein Systems. Journal of Chemical Theory and Computation, 2019, 15, 1399-1408.	5.3	6
6928	Cholesterol Flip-Flop in Heterogeneous Membranes. Journal of Chemical Theory and Computation, 2019, 15, 2064-2070.	5.3	62
6929	Coarse-Grained Simulations of Peptide Nanoparticle Formation: Role of Local Structure and Nonbonded Interactions. Journal of Chemical Theory and Computation, 2019, 15, 1453-1462.	5.3	10
6930	AOT Bilayer Adsorption on Gold Surfaces: A Molecular Dynamics Study. Journal of Physical Chemistry B, 2019, 123, 948-953.	2.6	12
6931	Influence of Bilayer Size and Number in Multi-Bilayer DOPC Simulations at Full and Low Hydration. Langmuir, 2019, 35, 2399-2411.	3.5	16



#	ARTICLE	IF	CITATIONS
6932	Achieving Fast Kinetics and Enhanced Li Storage Capacity for Ti <sub>3</sub> C <sub>2</sub> O <sub>2</sub> by Intercalation of Quinone Molecules. <i>ACS Applied Energy Materials</i> , 2019, 2, 1251-1258.	5.1	19
6933	Drugâ€™Membrane Permeability across Chemical Space. <i>ACS Central Science</i> , 2019, 5, 290-298.	11.3	67
6934	De novo design of potent and selective mimics of IL-2 and IL-15. <i>Nature</i> , 2019, 565, 186-191.	27.8	362
6935	Phase transition of ZrN under pressure. <i>Philosophical Magazine</i> , 2019, 99, 942-955.	1.6	3
6936	Microswitches for the Activation of the Nociceptin Receptor Induced by Cebranopadol: Hints from Microsecond Molecular Dynamics. <i>Journal of Chemical Information and Modeling</i> , 2019, 59, 818-831.	5.4	4
6937	Dissociation Process of a MDM2/p53 Complex Investigated by Parallel Cascade Selection Molecular Dynamics and the Markov State Model. <i>Journal of Physical Chemistry B</i> , 2019, 123, 2469-2478.	2.6	36
6938	Designing an Aptasensor Based on Cysteamine-Capped AuNPs for 8-Oxo-dG Detection: A Molecular Dynamics Approach and Experimental Validation. <i>Journal of Physical Chemistry B</i> , 2019, 123, 1129-1138.	2.6	16
6939	Effects of CD4 Binding on Conformational Dynamics, Molecular Motions, and Thermodynamics of HIV-1 gp120. <i>International Journal of Molecular Sciences</i> , 2019, 20, 260.	4.1	10
6940	Conformational rearrangements in n-alkanes encapsulated within capsular self-assembly of capped carbon nanotubes. <i>Chemical Physics</i> , 2019, 517, 198-207.	1.9	4
6941	Thermally triggered nanorocket from double-walled carbon nanotube in water. <i>Molecular Simulation</i> , 2019, 45, 417-424.	2.0	9
6942	Atomistically motivated interface model to account for coupled plasticity and damage at grain boundaries. <i>Journal of the Mechanics and Physics of Solids</i> , 2019, 124, 325-349.	4.8	27
6943	Multiscale modeling of pressure-assisted sintering. <i>Computational Materials Science</i> , 2019, 156, 385-395.	3.0	14
6944	Designing the Optimal Formulation for Biopharmaceuticals: A New Approach Combining Molecular Dynamics and Experiments. <i>Journal of Pharmaceutical Sciences</i> , 2019, 108, 431-438.	3.3	16
6945	Pyrazinamide drug resistance in RpsA mutant (â††438A) of <i>Mycobacterium tuberculosis</i> : Dynamics of essential motions and freeâ€™energy landscape analysis. <i>Journal of Cellular Biochemistry</i> , 2019, 120, 7386-7402.	2.6	36
6946	An insight into the binding of 6-hydroxyflavone with hen egg white lysozyme: a combined approach of multi-spectroscopic and computational studies. <i>Journal of Biomolecular Structure and Dynamics</i> , 2019, 37, 4019-4034.	3.5	27
6947	Exploring the aggregation-prone regions from structural domains of human TDP-43. <i>Biochimica Et Biophysica Acta - Proteins and Proteomics</i> , 2019, 1867, 286-296.	2.3	27
6948	Identification of Novel Scaffolds with Dual Role as Antiepileptic and Anti-Breast Cancer. <i>IEEE/ACM Transactions on Computational Biology and Bioinformatics</i> , 2019, 16, 1663-1674.	3.0	5
6949	Using limiting activity coefficients to efficiently evaluate the ability of fixed-charge force fields to model miscible water plus cosolvent mixtures. <i>Molecular Simulation</i> , 2019, 45, 322-335.	2.0	8

#	ARTICLE	IF	CITATIONS
6950	Exploring Morin as an anti-quorum sensing agent (anti-QSA) against resistant strains of <i>Staphylococcus aureus</i> . <i>Microbial Pathogenesis</i> , 2019, 127, 304-315.	2.9	33
6951	Theoretical Evaluation of the Reaction Mechanism of Serine Hydroxymethyltransferase. <i>Journal of Physical Chemistry B</i> , 2019, 123, 407-418.	2.6	6
6952	Molecular Mechanism of Polycation-Induced Pore Formation in Biomembranes. <i>ACS Biomaterials Science and Engineering</i> , 2019, 5, 780-794.	5.2	27
6953	Salt Induced Structural Collapse, Swelling, and Signature of Aggregation of Two ssDNA Strands: Insights from Molecular Dynamics Simulation. <i>Journal of Physical Chemistry B</i> , 2019, 123, 47-56.	2.6	16
6954	Optimization and in-vitro/in-vivo evaluation of doxorubicin-loaded chitosan-alginate nanoparticles using a melanoma mouse model. <i>International Journal of Pharmaceutics</i> , 2019, 556, 1-8.	5.2	50
6955	Molecular dynamics simulation of linear polyethylene blends: Effect of molar mass bimodality on topological characteristics and mechanical behavior. <i>Polymer</i> , 2019, 161, 139-150.	3.8	50
6956	Novel approach to improve progesterone hydroxylation selectivity by CYP 106A2 via rational design of adrenodoxin binding. <i>FEBS Journal</i> , 2019, 286, 1240-1249.	4.7	11
6957	Amyloidogenicity and Cytotoxicity of a Recombinant C-Terminal His <sub>6</sub> -Tagged A $\beta$ <sub>42</sub> . <i>ACS Chemical Neuroscience</i> , 2019, 10, 1251-1262.	3.5	16
6958	SPICA Force Field for Lipid Membranes: Domain Formation Induced by Cholesterol. <i>Journal of Chemical Theory and Computation</i> , 2019, 15, 762-774.	5.3	65
6959	Duffy binding-like 1 $\pm$ adhesin from <i>Plasmodium falciparum</i> recognizes ABH histo-blood group saccharide in a type specific manner. <i>Carbohydrate Polymers</i> , 2019, 207, 266-275.	10.2	0
6960	Predicting Residence Time and Drug Unbinding Pathway through Scaled Molecular Dynamics. <i>Journal of Chemical Information and Modeling</i> , 2019, 59, 535-549.	5.4	64
6961	Application of the ChIMES Force Field to Nonreactive Molecular Systems: Water at Ambient Conditions. <i>Journal of Chemical Theory and Computation</i> , 2019, 15, 436-447.	5.3	23
6962	Discovery of potent and selective inhibitors of the <i>Escherichia coli</i> M1-aminopeptidase via multicomponent solid-phase synthesis of tetrazole-peptidomimetics. <i>European Journal of Medicinal Chemistry</i> , 2019, 163, 481-499.	5.5	29
6963	Computational Probing of Watson-Crick/Hoogsteen Breathing in a DNA Duplex Containing N1-Methylated Adenine. <i>Journal of Chemical Theory and Computation</i> , 2019, 15, 751-761.	5.3	14
6964	Highly Fluorescent Liquid Crystals from Excited-State Intramolecular Proton Transfer Molecules. <i>Advanced Optical Materials</i> , 2019, 7, 1801349.	7.3	27
6965	Pyrazinamide resistance and mutations L19R, R140H, and E144K in <i>Mycobacterium tuberculosis</i> . <i>Journal of Cellular Biochemistry</i> , 2019, 120, 7154-7166.	2.6	17
6966	Auxetic Properties of a f.c.c. Crystal of Hard Spheres with an Array of [001]-Nanochannels Filled by Hard Spheres of Another Diameter. <i>Physica Status Solidi (B): Basic Research</i> , 2019, 256, 1800611.	1.5	32
6967	Molecular insights into multilayer 18-crown-6-like graphene nanopores for K <sup>+</sup> /Na <sup>+</sup> separation: A molecular dynamics study. <i>Carbon</i> , 2019, 144, 32-42.	10.3	40

#	ARTICLE	IF	CITATIONS
6968	Solubilities of pyrene in organic solvents: Comparison between chemical potential calculations using a cavity-based method and direct coexistence simulations. Journal of Chemical Thermodynamics, 2019, 131, 620-629.	2.0	4
6969	Porous organic cages embedded in a lipid membrane for water desalination: A molecular simulation study. Journal of Membrane Science, 2019, 573, 177-183.	8.2	24
6970	Atomistic details on the mechanism of organophosphates resistance in insects: Insights from homology modeling, docking and molecular dynamic simulation. Journal of Molecular Liquids, 2019, 276, 59-66.	4.9	15
6971	Computational insights into pH dependence of structure and dynamics of pyrazinamidase: A comparison of wild type and mutants. Journal of Cellular Biochemistry, 2019, 120, 2502-2514.	2.6	3
6972	Accumulation behaviors of methane in the aqueous environment with organic matters. Fuel, 2019, 236, 836-842.	6.4	29
6973	Inhibitor binding studies of <i>Mycobacterium tuberculosis</i> MraY (Rv2156c): Insights from molecular modeling, docking, and simulation studies. Journal of Biomolecular Structure and Dynamics, 2019, 37, 3751-3763.	3.5	8
6974	Thermodynamic Characterization of the Dimerization of an Anionic Perylene Bisimide Dye Using Molecular Simulation. Journal of Physical Chemistry C, 2019, 123, 8027-8036.	3.1	2
6975	Atomistic mechanism of the constitutive activation of PDGFRA via its transmembrane domain. Biochimica Et Biophysica Acta - General Subjects, 2019, 1863, 82-95.	2.4	8
6976	Theoretical investigations into effects of adulteration crystal defect on properties of CL-20/TNT cocrystal explosive. Computational Materials Science, 2019, 156, 77-83.	3.0	24
6977	Computational fragment-based design of Wee1 kinase inhibitors with tricyclic core scaffolds. Structural Chemistry, 2019, 30, 213-226.	2.0	3
6978	A Parallel Multiscale Simulation Framework for Complex Polymerization: AB <sub>2</sub> Type Monomer Hyperbranched Polymerization as an Example. Advanced Theory and Simulations, 2019, 2, 1800102.	2.8	12
6979	A computational method to characterize the missense mutations in the catalytic domain of GAA protein causing Pompe disease. Journal of Cellular Biochemistry, 2019, 120, 3491-3505.	2.6	12
6980	Computational simulation of palm kernel oil-based esters nano-emulsions aggregation as a potential parenteral drug delivery system. Arabian Journal of Chemistry, 2019, 12, 2372-2383.	4.9	13
6981	Structural Characterization of the Trimerization of TRAF6 Protein Through Molecular Dynamics Simulations. Interdisciplinary Sciences, Computational Life Sciences, 2019, 11, 428-436.	3.6	1
6982	Nanoscale investigation of the influence of water on the elastic properties of C <sub>60</sub> -H gel by molecular simulation. Proceedings of the Institution of Mechanical Engineers, Part L: Journal of Materials: Design and Applications, 2019, 233, 1295-1306.	1.1	5
6983	Effects of low acyl and high acyl gellan gum on the thermal stability of purple sweet potato anthocyanins in the presence of ascorbic acid. Food Hydrocolloids, 2019, 86, 116-123.	10.7	59
6984	Screening of potential lead molecules against prioritised targets of multi-drug-resistant <i>Acinetobacter baumannii</i> insights from molecular docking, molecular dynamic simulations and <i>in vitro</i> assays. Journal of Biomolecular Structure and Dynamics, 2019, 37, 1146-1169.	3.5	34
6985	<i>In silico</i> development of new acetylcholinesterase inhibitors. Journal of Biomolecular Structure and Dynamics, 2019, 37, 1007-1021.	3.5	15

#	ARTICLE	IF	CITATIONS
6986	Investigating the selectivity of potential new inhibitors of dihydrofolate reductase from <i>Yersinia pestis</i> designed by molecular modeling. <i>Journal of Biomolecular Structure and Dynamics</i> , 2019, 37, 1170-1176.	3.5	4
6987	Computational study of solution behavior of magainin 2 monomers. <i>Journal of Biomolecular Structure and Dynamics</i> , 2019, 37, 1231-1240.	3.5	5
6988	The two mutations of actin-myosin interface and their effect on the dynamics, structures, and functions of skeletal muscle actin. <i>Journal of Biomolecular Structure and Dynamics</i> , 2019, 37, 372-382.	3.5	1
6989	The effect of the diameter of cyclic peptide nanotube on its chirality discrimination. <i>Journal of Biomolecular Structure and Dynamics</i> , 2019, 37, 691-701.	3.5	10
6990	Multiscale simulation of the interaction of calreticulin-thrombospondin-1 complex with a model membrane microdomain. <i>Journal of Biomolecular Structure and Dynamics</i> , 2019, 37, 811-822.	3.5	7
6991	Effects of Peutz-Jeghers syndrome (PJS) causing missense mutations L67P, L182P, G242V and R297S on the structural dynamics of LKB1 (Liver kinase B1) protein. <i>Journal of Biomolecular Structure and Dynamics</i> , 2019, 37, 796-810.	3.5	1
6992	Orthosteric and benzodiazepine cavities of the $\alpha 1\beta 2\gamma 2$ GABAA receptor: insights from experimentally validated in silico methods. <i>Journal of Biomolecular Structure and Dynamics</i> , 2019, 37, 1597-1615.	3.5	11
6993	Simulation of protein diffusion: a sensitive probe of protein-solvent interactions. <i>Journal of Biomolecular Structure and Dynamics</i> , 2019, 37, 1534-1544.	3.5	13
6994	The structure of galactoglucomannan impacts the degradation under alkaline conditions. <i>Cellulose</i> , 2019, 26, 2155-2175.	4.9	41
6995	Structure-Based Analysis of Single Nucleotide Variants in the Renin-Angiotensinogen Complex. <i>Global Heart</i> , 2017, 12, 121.	2.3	31
6996	3D-QSAR, docking, molecular dynamics simulation and free energy calculation studies of some pyrimidine derivatives as novel JAK3 inhibitors. <i>Arabian Journal of Chemistry</i> , 2020, 13, 1052-1078.	4.9	33
6997	The structuring in mixtures with acetone as the common solvent. <i>Physics and Chemistry of Liquids</i> , 2020, 58, 184-201.	1.2	5
6998	On the early events of the calcium-induced activation of coagulation factor XIII-A2 and tissue transglutaminase: an in silico study. <i>Journal of Biomolecular Structure and Dynamics</i> , 2020, 38, 152-167.	3.5	0
6999	An integrated <i>in silico</i> approach to understand protein-protein interactions: human meprin- $\beta^2$ with fetuin-A. <i>Journal of Biomolecular Structure and Dynamics</i> , 2020, 38, 2080-2092.	3.5	5
7000	Edaravone inhibits the conformational transition of amyloid- $\beta^{42}$ : insights from molecular dynamics simulations. <i>Journal of Biomolecular Structure and Dynamics</i> , 2020, 38, 2377-2388.	3.5	23
7001	Visualizing protein motion in Couette flow by all-atom molecular dynamics. <i>Biochimica Et Biophysica Acta - General Subjects</i> , 2020, 1864, 129383.	2.4	6
7002	Computational investigation on effect of mutations in PCNA resulting in structural perturbations and inhibition of mismatch repair pathway. <i>Journal of Biomolecular Structure and Dynamics</i> , 2020, 38, 1963-1974.	3.5	59
7003	Insights into resistance mechanism of hepatitis C virus nonstructural 3/4A protease mutant to boceprevir using umbrella sampling simulation study. <i>Journal of Biomolecular Structure and Dynamics</i> , 2020, 38, 1938-1945.	3.5	2

#	ARTICLE	IF	CITATIONS
7004	Region-Based Epitope Prediction, Docking and Dynamic Studies of OMP31 as a Dominant Antigen in Human and Sheep Brucella. International Journal of Peptide Research and Therapeutics, 2020, 26, 413-421.	1.9	4
7005	Disease-associated mutations alter the dynamic motion of the N-terminal domain of the human cardiac ryanodine receptor. Journal of Biomolecular Structure and Dynamics, 2020, 38, 1054-1070.	3.5	3
7006	Human LC3 and GABARAP subfamily members achieve functional specificity via specific structural modulations. Autophagy, 2020, 16, 239-255.	9.1	53
7007	Delineating the interaction of combretastatin A-4 with $\beta$ -tubulin isotypes present in drug resistant human lung carcinoma using a molecular modeling approach. Journal of Biomolecular Structure and Dynamics, 2020, 38, 426-438.	3.5	15
7008	Understanding ligands driven mechanism of wild and mutant aryl hydrocarbon receptor in presence of phytochemicals combating Parkinson's disease: an <i>in silico</i> and <i>in vivo</i> study. Journal of Biomolecular Structure and Dynamics, 2020, 38, 807-826.	3.5	8
7009	Comment on "Deficiencies in Molecular Dynamics Simulation-Based Prediction of Protein-DNA Binding Free Energy Landscapes". Journal of Physical Chemistry B, 2020, 124, 1115-1123.	2.6	4
7010	Integration of virtual screening and computational simulation identifies photodynamic therapeutics against human Protoporphyrinogen Oxidase IX (hPPO). Arabian Journal of Chemistry, 2020, 13, 2245-2256.	4.9	2
7011	Rejuvenated metallic glass strips produced via twin-roll casting. Journal of Materials Science and Technology, 2020, 38, 73-79.	10.7	26
7012	Designing new generation of potent inhibitors against membrane-type matrix metalloproteinase-2: a computational effort against multiple myeloma. Journal of Biomolecular Structure and Dynamics, 2020, 38, 3879-3891.	3.5	6
7013	Exploiting Cryo-EM Structural Information and All-Atom Simulations To Decrypt the Molecular Mechanism of Splicing Modulators. Journal of Chemical Information and Modeling, 2020, 60, 2510-2521.	5.4	24
7014	Understanding loading, diffusion and releasing of Doxorubicin and Paclitaxel dual delivery in graphene and graphene oxide carriers as highly efficient drug delivery systems. Applied Surface Science, 2020, 500, 144220.	6.1	88
7015	Tensile test analysis of carbon fiber composite material by molecular dynamics simulation. Advanced Composite Materials, 2020, 29, 179-190.	1.9	11
7016	Cyclodextrin solubilization and complexation of antiretroviral drug lopinavir: In silico prediction; Effects of derivatization, molar ratio and preparation method. Carbohydrate Polymers, 2020, 227, 115287.	10.2	29
7017	Structural analysis, molecular dynamics and docking calculations of skin protective tripeptide and design, characterization, cytotoxicity studies of its PLGA nanoparticles. Journal of Molecular Structure, 2020, 1200, 127046.	3.6	7
7018	Encapsulation of an endostatin peptide in liposomes: Stability, release, and cytotoxicity study. Colloids and Surfaces B: Biointerfaces, 2020, 185, 110552.	5.0	33
7019	The pathogenicity, structural and functional exploration of human HMGB1 single nucleotide polymorphisms using <i>in silico</i> study. Journal of Biomolecular Structure and Dynamics, 2020, 38, 4471-4482.	3.5	3
7020	Molecular description of the coil-to-globule transition of Poly(N-isopropylacrylamide) in water/ethanol mixture at low alcohol concentration. Journal of Molecular Liquids, 2020, 297, 111928.	4.9	27
7021	Transferable coarse-grained models for poly(ethylene oxide)/poly(methyl methacrylate) blends. Computational Materials Science, 2020, 172, 109346.	3.0	7

#	ARTICLE	IF	CITATIONS
7022	Absolute Protein Binding Free Energy Simulations for Ligands with Multiple Poses, a Thermodynamic Path That Avoids Exhaustive Enumeration of the Poses. <i>Journal of Computational Chemistry</i> , 2020, 41, 56-68.	3.3	16
7023	Comprehensive structural modeling and preparation of human 5-HT <sub>2A</sub> G-protein coupled receptor in functionally active form. <i>Biopolymers</i> , 2020, 111, e23329.	2.4	8
7024	Rationalising Supramolecular Hydrogelation of Bis-urea-Based Gelators through a Multiscale Approach. <i>ChemPlusChem</i> , 2020, 85, 267-276.	2.8	9
7025	Dynamic Vesicles Formed By Dissipative Self-Assembly. <i>ChemSystemsChem</i> , 2020, 2, e1900044.	2.6	53
7026	Glycerol induced stability enhancement and conformational changes of $\beta^2$ -lactoglobulin. <i>Food Chemistry</i> , 2020, 308, 125596.	8.2	12
7027	Pressure-induced amorphization, mechanical and electronic properties of zeolitic imidazolate framework (ZIF-8). <i>Materials Chemistry and Physics</i> , 2020, 240, 122222.	4.0	16
7028	Protein Nanotechnology. <i>Methods in Molecular Biology</i> , 2020, , .	0.9	4
7029	Interaction of naringin and naringenin with DPPC monolayer at the air-water interface. <i>Colloids and Surfaces A: Physicochemical and Engineering Aspects</i> , 2020, 584, 124024.	4.7	12
7030	Computational and experimental study of propeline: A choline chloride based deep eutectic solvent. <i>Journal of Molecular Liquids</i> , 2020, 298, 111978.	4.9	25
7031	Interfacial characterization of functionalized graphene-epoxy composites. <i>Journal of Composite Materials</i> , 2020, 54, 703-710.	2.4	13
7032	Identification potential inhibitors against the <i>Streptococcus</i> quorum-sensing signal pathway. <i>Journal of Biomolecular Structure and Dynamics</i> , 2020, 38, 2965-2975.	3.5	1
7033	In vitro and in silico studies on membrane interactions of diverse <i>Capsicum annuum</i> flower $\beta$ -thionin peptides. <i>Proteins: Structure, Function and Bioinformatics</i> , 2020, 88, 227-236.	2.6	8
7034	Potential novel inhibitors against emerging zoonotic pathogen <i>Nipah virus</i> : a virtual screening and molecular dynamics approach. <i>Journal of Biomolecular Structure and Dynamics</i> , 2020, 38, 3225-3234.	3.5	16
7035	Structure and dynamics of inactive and active MARK4: conformational switching through the activation process. <i>Journal of Biomolecular Structure and Dynamics</i> , 2020, 38, 2468-2481.	3.5	9
7036	Cyanine dyes with tail length asymmetry enhance photoselection: A multiscale study on DiD probes in a liquid disordered membrane. <i>Spectrochimica Acta - Part A: Molecular and Biomolecular Spectroscopy</i> , 2020, 224, 117329.	3.9	8
7037	Interaction of piroxicam with bovine serum albumin investigated by spectroscopic, calorimetric and computational molecular methods. <i>Journal of Biomolecular Structure and Dynamics</i> , 2020, 38, 2659-2671.	3.5	13
7038	F508del disturbs the dynamics of the nucleotide binding domains of CFTR before and after ATP hydrolysis. <i>Proteins: Structure, Function and Bioinformatics</i> , 2020, 88, 113-126.	2.6	20
7039	Modulation of p53 N-terminal transactivation domain 2 conformation ensemble and kinetics by phosphorylation. <i>Journal of Biomolecular Structure and Dynamics</i> , 2020, 38, 2613-2623.	3.5	9



#	ARTICLE	IF	CITATIONS
7040	Folding profiles of antimicrobial scorpion venom-derived peptides on hydrophobic surfaces: a molecular dynamics study. <i>Journal of Biomolecular Structure and Dynamics</i> , 2020, 38, 2928-2938.	3.5	1
7041	Structural dynamics behind variants in pyrazinamidase and pyrazinamide resistance. <i>Journal of Biomolecular Structure and Dynamics</i> , 2020, 38, 3003-3017.	3.5	7
7042	Computational basis for the design of PLK-2 inhibitors. <i>Structural Chemistry</i> , 2020, 31, 275-292.	2.0	1
7043	Discrete analyses of protein dynamics. <i>Journal of Biomolecular Structure and Dynamics</i> , 2020, 38, 2988-3002.	3.5	20
7044	The investigation of the G-quadruplex aptamer selectivity to Pb <sup>2+</sup> ion: a joint molecular dynamics simulation and density functional theory study. <i>Journal of Biomolecular Structure and Dynamics</i> , 2020, 38, 3659-3675.	3.5	11
7045	Deformation of copper particles upon impact: A molecular dynamics study of cold spray. <i>Computational Materials Science</i> , 2020, 171, 109219.	3.0	52
7046	Insights into membrane-bound presenilin 2 from all-atom molecular dynamics simulations. <i>Journal of Biomolecular Structure and Dynamics</i> , 2020, 38, 3196-3210.	3.5	24
7047	The Effect of Small Organic Cosolutes on Water Structure and Dynamics. <i>Journal of Chemical &amp; Engineering Data</i> , 2020, 65, 1197-1210.	1.9	17
7048	Thermal expansion mechanism of cordierite with titanium or germanium doping based on ab initio molecular dynamics simulation. <i>Journal of the American Ceramic Society</i> , 2020, 103, 531-540.	3.8	1
7049	Molecular dynamics study of membrane permeabilization by wild-type and mutant lytic peptides from the non-enveloped Flock House virus. <i>Biochimica Et Biophysica Acta - Biomembranes</i> , 2020, 1862, 183102.	2.6	8
7050	Biophysical characterization of the insertion of two potent antimicrobial peptides-Pin2 and its variant Pin2[GVG] in biological model membranes. <i>Biochimica Et Biophysica Acta - Biomembranes</i> , 2020, 1862, 183105.	2.6	13
7051	Molecular dynamics study of the behaviour of surfactant Triton X-100 in the extraction process of Cd <sup>2+</sup> . <i>Chemical Physics Letters</i> , 2020, 739, 136920.	2.6	3
7052	New steroidal oxazolines, benzoxazoles and benzimidazoles related to abiraterone and galeterone. <i>Steroids</i> , 2020, 153, 108534.	1.8	13
7053	Combined spectroscopic and molecular docking study on the pH dependence of molecular interactions between I <sup>2</sup> -lactoglobulin and ferulic acid. <i>Food Hydrocolloids</i> , 2020, 101, 105461.	10.7	56
7054	High pressure modifications in amorphous boron suboxide: An ab initio study. <i>Ceramics International</i> , 2020, 46, 5968-5975.	4.8	2
7055	Investigation on the efficiency and accuracy of methods for calculating melting temperature by molecular dynamics simulation. <i>Computational Materials Science</i> , 2020, 171, 109156.	3.0	29
7056	Pyridine-2,3-dicarboxylate, quinolinic acid, induces 1N4R Tau amyloid aggregation in vitro: Another evidence for the detrimental effect of the inescapable endogenous neurotoxin. <i>Chemico-Biological Interactions</i> , 2020, 315, 108884.	4.0	14
7057	Molecular dynamics simulations to the bidirectional adhesion signaling pathway of integrin $\alpha_5\beta_1$ . <i>Proteins: Structure, Function and Bioinformatics</i> , 2020, 88, 679-688.	2.6	17

#	ARTICLE	IF	CITATIONS
7058	Isolation and structural characterization of a Zn <sup>2+</sup> -bound single-domain antibody against NorC, a putative multidrug efflux transporter in bacteria. <i>Journal of Biological Chemistry</i> , 2020, 295, 55-68.	3.4	9
7059	Polymyxin B Loosens Lipopolysaccharide Bilayer but Stiffens Phospholipid Bilayer. <i>Biophysical Journal</i> , 2020, 118, 138-150.	0.5	40
7060	Protein adaptation to high hydrostatic pressure: Computational analysis of the structural proteome. <i>Proteins: Structure, Function and Bioinformatics</i> , 2020, 88, 584-592.	2.6	12
7061	Molecular basis of drug resistance in smoothened receptor: An in silico study of protein resistivity and specificity. <i>Proteins: Structure, Function and Bioinformatics</i> , 2020, 88, 514-526.	2.6	6
7062	Adsorption of ciprofloxacin on carbon nanotubes: Insights from molecular dynamics simulations. <i>Journal of Molecular Liquids</i> , 2020, 298, 111977.	4.9	46
7063	The relationship between viscosity and local structure in liquid zirconium via electromagnetic levitation and molecular dynamics simulations. <i>Journal of Molecular Liquids</i> , 2020, 298, 111992.	4.9	18
7064	Structural origin of the anomalous density maximum in silica and alkali silicate glasses. <i>Journal of the American Ceramic Society</i> , 2020, 103, 3942-3953.	3.8	6
7065	Wnt5a is involved in LOX $\alpha$ 1 and TLR4 induced host inflammatory response in peri $\alpha$ implantitis. <i>Journal of Periodontal Research</i> , 2020, 55, 199-208.	2.7	22
7066	Chemical $\alpha$ Shift Perturbations Reflect Bile Acid Binding to Norovirus Coat Protein: Recognition Comes in Different Flavors. <i>ChemBioChem</i> , 2020, 21, 1007-1021.	2.6	14
7067	Mechanism of $\frac{1}{4}$ -Opioid Receptor-Magnesium Interaction and Positive Allosteric Modulation. <i>Biophysical Journal</i> , 2020, 118, 909-921.	0.5	24
7068	Origin of Unusually High Fluorescence Anisotropy of 3-Hydroxyflavone in Water: Formation of Probe $\alpha$ Solvent Cage-like Cluster. <i>Journal of Physical Chemistry B</i> , 2020, 124, 173-180.	2.6	10
7069	Methane hydrate formation in the stacking of kaolinite particles with different surface contacts as nanoreactors: A molecular dynamics simulation study. <i>Applied Clay Science</i> , 2020, 186, 105439.	5.2	49
7070	Properties of Aqueous Trehalose Mixtures: Glass Transition and Hydrogen Bonding. <i>Journal of Chemical Theory and Computation</i> , 2020, 16, 1249-1262.	5.3	39
7071	Water Bridges in Clay Nanopores: Mechanisms of Formation and Impact on Hydrocarbon Transport. <i>Langmuir</i> , 2020, 36, 723-733.	3.5	47
7072	Molecular Dynamics Study of the Human Beta-defensins 2 and 3 Chimeric Peptides with the Cell Membrane Model of <i>Pseudomonas aeruginosa</i> . <i>International Journal of Peptide Research and Therapeutics</i> , 2020, 26, 2039-2056.	1.9	5
7073	Hydration of Fluorobenzenes: A Molecular Dynamics Simulation Investigation. <i>Journal of the Indian Institute of Science</i> , 2020, 100, 221-230.	1.9	1
7074	Dislocation nucleation and evolution at the ferrite-cementite interface under cyclic loadings. <i>Acta Materialia</i> , 2020, 186, 267-277.	7.9	30
7075	Quantum mechanics and molecular dynamics studies on the C $\alpha$ H interaction between small fullerenes (C <sub>36</sub> and C <sub>24</sub> ) and [M(H <sub>2</sub> O) <sub>6</sub> ] <sup>2+</sup> (M $\alpha$ = $\alpha$ Ca <sup>2+</sup> , Zn <sup>2+</sup> ) cations. <i>Journal of Molecular Liquids</i> , 2020, 301, 112339.	4.9	2

#	ARTICLE	IF	CITATIONS
7076	Critical nucleus of Greek-key-like core of $\beta$ -synuclein protofibril and its disruption by dopamine and norepinephrine. <i>Physical Chemistry Chemical Physics</i> , 2020, 22, 203-211.	2.8	22
7077	Characterization of $\beta^2$ -turns by electronic circular dichroism spectroscopy: a coupled molecular dynamics and time-dependent density functional theory computational study. <i>Physical Chemistry Chemical Physics</i> , 2020, 22, 1611-1623.	2.8	19
7078	Emergence of non-monotonic deep cavity cavitand assembly with increasing portal methylation. <i>Molecular Systems Design and Engineering</i> , 2020, 5, 656-665.	3.4	3
7079	A polyesteramide library from dicarboxylic acids and 2,2'-bis(2-oxazoline): synthesis, characterization, nanoparticle formulation and molecular dynamics simulations. <i>Polymer Chemistry</i> , 2020, 11, 112-124.	3.9	9
7080	Large scale relative protein ligand binding affinities using non-equilibrium alchemy. <i>Chemical Science</i> , 2020, 11, 1140-1152.	7.4	147
7081	Polarization Effects in Dynamic Interfaces of Platinum Electrodes and Ionic Liquid Phases: A Molecular Dynamics Study. <i>Journal of Physical Chemistry C</i> , 2020, 124, 2002-2007.	3.1	11
7082	Single-chain heteropolymers transport protons selectively and rapidly. <i>Nature</i> , 2020, 577, 216-220.	27.8	64
7083	Structural Basis of Teneurin-Latrophilin Interaction in Repulsive Guidance of Migrating Neurons. <i>Cell</i> , 2020, 180, 323-339.e19.	28.9	91
7084	Solubility and solvation free energy of a cardiovascular drug, LASSBio-294, in ionic liquids: A computational study. <i>Journal of Molecular Liquids</i> , 2020, 301, 112449.	4.9	32
7085	Insights into Novel Antimicrobial Based on Chitosan Nanoparticles: From a Computational and Experimental Perspective. <i>Engineering Materials</i> , 2020, , 107-143.	0.6	1
7086	Mechanistic study of the ATP hydrolysis reaction in dynein motor protein. <i>Physical Chemistry Chemical Physics</i> , 2020, 22, 1534-1542.	2.8	9
7087	Targeting the heme protein hemoglobin by ( $\alpha$ )-epigallocatechin gallate and the study of polyphenol-protein association using multi-spectroscopic and computational methods. <i>Physical Chemistry Chemical Physics</i> , 2020, 22, 2212-2228.	2.8	42
7088	The regulation mechanism of phosphorylation and mutations in intrinsically disordered protein 4E-BP2. <i>Physical Chemistry Chemical Physics</i> , 2020, 22, 2938-2948.	2.8	5
7089	The aggregation of striped nanoparticles in mixed phospholipid bilayers. <i>Nanoscale</i> , 2020, 12, 4868-4881.	5.6	8
7090	The role of electrostatic potential polarization in the translocation of graphene quantum dots across membranes. <i>Nanoscale</i> , 2020, 12, 2732-2739.	5.6	15
7091	Archaeal cyclopentane fragment in a surfactant's hydrophobic tail decreases the Krafft point. <i>Soft Matter</i> , 2020, 16, 1333-1341.	2.7	2
7092	Magainin 2 and PGLa in Bacterial Membrane Mimics II: Membrane Fusion and Sponge Phase Formation. <i>Biophysical Journal</i> , 2020, 118, 612-623.	0.5	25
7093	Is the E. coli Homolog of the Formate/Nitrite Transporter Family an Anion Channel? A Computational Study. <i>Biophysical Journal</i> , 2020, 118, 846-860.	0.5	3

#	ARTICLE	IF	CITATIONS
7094	In Situ Structure of an Intact Lipopolysaccharide-Bound Bacterial Surface Layer. <i>Cell</i> , 2020, 180, 348-358.e15.	28.9	79
7095	Effect of a dirhamnolipid biosurfactant on the structure and phase behaviour of dimyristoylphosphatidylserine model membranes. <i>Colloids and Surfaces B: Biointerfaces</i> , 2020, 185, 110576.	5.0	19
7096	Engineering shape-defined PLGA microPlates for the sustained release of anti-inflammatory molecules. <i>Journal of Controlled Release</i> , 2020, 319, 201-212.	9.9	27
7097	Molecular Dynamics Simulations of the Hypoxia-Inducible Factor PAS-B Domain Confirm That Internally Bound Water Molecules Function To Stabilize the Protein Core for Ligand Binding. <i>Biochemistry</i> , 2020, 59, 450-459.	2.5	5
7098	Computational Design of Biologically Active Anticancer Peptides and Their Interactions with Heterogeneous POPC/POPS Lipid Membranes. <i>Journal of Chemical Information and Modeling</i> , 2020, 60, 332-341.	5.4	14
7099	Toward a Structural View of hERG Activation by the Small-Molecule Activator ICA-105574. <i>Journal of Chemical Information and Modeling</i> , 2020, 60, 360-371.	5.4	12
7100	Dehydration Determines Hydrotropic Ion Affinity for Zwitterionic Micelles. <i>Journal of Chemical Information and Modeling</i> , 2020, 60, 604-610.	5.4	10
7101	Adiabatic-Molecular Dynamics Generalized Vertical Hessian Approach: A Mixed Quantum Classical Method To Compute Electronic Spectra of Flexible Molecules in the Condensed Phase. <i>Journal of Chemical Theory and Computation</i> , 2020, 16, 1215-1231.	5.3	50
7102	Modeling DNA Flexibility: Comparison of Force Fields from Atomistic to Multiscale Levels. <i>Journal of Physical Chemistry B</i> , 2020, 124, 38-49.	2.6	37
7103	Release of Carbohydrateâ€“Metal Adducts from Electrospray Droplets: Insight into Glycan Ionization by Electrospray. <i>Journal of Physical Chemistry B</i> , 2020, 124, 479-486.	2.6	18
7104	Structural Evolution of Ironâ€“Copper (Feâ€“Cu) Bimetallic Janus Nanoparticles during Solidification: An Atomistic Investigation. <i>Journal of Physical Chemistry C</i> , 2020, 124, 1053-1063.	3.1	18
7105	High-Density COH<sub>x</sub> Network Glass. <i>Journal of Physical Chemistry C</i> , 2020, 124, 107-114.	3.1	3
7106	Single Particle Dynamics at the Liquidâ€“Liquid Interface. Molecular Dynamics Simulation Study of the Water-CCl<sub>4</sub> System. <i>Journal of Physical Chemistry C</i> , 2020, 124, 2039-2049.	3.1	7
7107	Computational Analysis of the Silver Nanoparticleâ€“Human Serum Albumin Complex. <i>ACS Omega</i> , 2020, 5, 170-178.	3.5	42
7108	Toward Quantum Paraelectric, Paraelastic, and Paramagnetic 2D Materials. <i>Annalen Der Physik</i> , 2020, 532, 1900448.	2.4	2
7109	Enzyme Evolution: An Epistatic Ratchet versus a Smooth Reversible Transition. <i>Molecular Biology and Evolution</i> , 2020, 37, 1133-1147.	8.9	26
7110	Inhibition of pancreatic lipase by the constituents in St. John's Wort: In vitro and in silico investigations. <i>International Journal of Biological Macromolecules</i> , 2020, 145, 620-633.	7.5	40
7111	A computational study on the role of water and conformational fluctuations in Hsp90 in response to inhibitors. <i>Journal of Molecular Graphics and Modelling</i> , 2020, 96, 107510.	2.4	12

#	ARTICLE	IF	CITATIONS
7112	Atomistic Mechanism of the Nucleation of Methylammonium Lead Iodide Perovskite from Solution. <i>Chemistry of Materials</i> , 2020, 32, 529-536.	6.7	45
7113	Comparing the void space and long-range structure of an ionic liquid with a neutral mixture of similar sized molecules. <i>Journal of Molecular Liquids</i> , 2020, 299, 112121.	4.9	9
7114	Elucidating Molecular Design Principles for Charge-Alternating Peptides. <i>Biomacromolecules</i> , 2020, 21, 435-443.	5.4	14
7115	tRNA Dissociation from EF-Tu after GTP Hydrolysis: Primary Steps and Antibiotic Inhibition. <i>Biophysical Journal</i> , 2020, 118, 151-161.	0.5	19
7116	The role of fluorocarbon group in the hydrogen bond network, photophysical and solvation dynamics of fluorinated molecules. <i>Journal of Fluorine Chemistry</i> , 2020, 235, 109414.	1.7	2
7117	In-silico and in-vitro analysis of endocan interaction with statins. <i>International Journal of Biological Macromolecules</i> , 2020, 146, 1087-1099.	7.5	13
7118	Solvation of Co <sup>2+</sup> ion in 1-butyl-3-methylimidazolium bis(trifluoromethylsulfonyl)imide ionic liquid: A molecular dynamics and X-ray absorption study. <i>Journal of Molecular Liquids</i> , 2020, 299, 112120.	4.9	24
7119	Features of self-organization of sodium dodecyl sulfate in water-ethanol solutions: Theory and vibrational spectroscopy. <i>Journal of Molecular Liquids</i> , 2020, 298, 112053.	4.9	7
7120	Molecular insight into silk fibroin based delivery vehicle for amphiphilic drugs: Synthesis, characterization and molecular dynamics studies. <i>Journal of Molecular Liquids</i> , 2020, 299, 112156.	4.9	9
7121	“Digital Fluid Physics”: Prediction of phase equilibria for several mixtures of CO <sub>2</sub> with petroleum fluid systems. <i>Journal of Petroleum Science and Engineering</i> , 2020, 187, 106752.	4.2	5
7122	Combined Linear Interaction Energy and Alchemical Solvation Free-Energy Approach for Protein-Binding Affinity Computation. <i>Journal of Chemical Theory and Computation</i> , 2020, 16, 1300-1310.	5.3	12
7123	Solvate ionic liquids based on lithium bis(trifluoromethanesulfonyl)imide “glyme” systems: coordination in MD simulations with scaled charges. <i>Physical Chemistry Chemical Physics</i> , 2020, 22, 525-535.	2.8	22
7124	Impact of glutamate carboxylation in the adsorption of the Î±-1 domain of osteocalcin to hydroxyapatite and titania. <i>Molecular Systems Design and Engineering</i> , 2020, 5, 620-631.	3.4	8
7125	Influence of the ion size on the stability of the smectic phase of ionic liquid crystals. <i>Soft Matter</i> , 2020, 16, 411-420.	2.7	28
7126	Nafion Ionomer Dispersion in Mixtures of 1-Propanol and Water Based on the Martini Coarse-Grained Model. <i>Journal of Polymer Science</i> , 2020, 58, 487-499.	3.8	19
7127	Molecular dynamics and binding energy analysis of Vatairea guianensis lectin: a new tool for cancer studies. <i>Journal of Molecular Modeling</i> , 2020, 26, 22.	1.8	3
7128	A study of starch-urea-water mixtures with a combination of molecular dynamics simulation and traditional characterization methods. <i>International Journal of Biological Macromolecules</i> , 2020, 148, 121-128.	7.5	19
7129	Nonpolar solute cononsolvency in ethanol/water mixtures “Connections to solvent structure. <i>Journal of Molecular Liquids</i> , 2020, 298, 111944.	4.9	3

#	ARTICLE	IF	CITATIONS
7130	Syndecan-4 tunes cell mechanics by activating the kindlin-integrin-RhoA pathway. <i>Nature Materials</i> , 2020, 19, 669-678.	27.5	66
7131	On the ion coupling mechanism of the MATE transporter ClbM. <i>Biochimica Et Biophysica Acta - Biomembranes</i> , 2020, 1862, 183137.	2.6	16
7132	Quantum effects on elastic constants of diamond by path-integral Monte Carlo simulations. <i>Computational Materials Science</i> , 2020, 173, 109387.	3.0	8
7133	The Lazy Life of Lipid-Linked Oligosaccharides in All Life Domains. <i>Journal of Chemical Information and Modeling</i> , 2020, 60, 631-643.	5.4	4
7134	An atypical heterotrimeric G $\alpha$ protein has substantially reduced nucleotide binding but retains nucleotide-independent interactions with its cognate RGS protein and G $\beta\gamma$ dimer. <i>Journal of Biomolecular Structure and Dynamics</i> , 2020, 38, 5204-5218.	3.5	17
7135	Enhancing Water Solubility and Stability of Natamycin by Molecular Encapsulation in Methyl- $\beta$ -Cyclodextrin and its Mechanisms by Molecular Dynamics Simulations. <i>Food Biophysics</i> , 2020, 15, 188-195.	3.0	18
7136	Electrospun PVA-Dacarbazine nanofibers as a novel nano brain-implant for treatment of glioblastoma: in silico and in vitro characterization. <i>European Journal of Pharmaceutical Sciences</i> , 2020, 143, 105183.	4.0	32
7137	Post-Translational Modifications at the Coarse-Grained Level with the SIRAH Force Field. <i>Journal of Chemical Information and Modeling</i> , 2020, 60, 964-973.	5.4	12
7138	Growth Mechanism of Gold Nanorods: the Effect of Tip Surface Curvature As Revealed by Molecular Dynamics Simulations. <i>Langmuir</i> , 2020, 36, 257-263.	3.5	21
7139	Molecular modeling assisted identification and biological evaluation of potent cathepsin S inhibitors. <i>Journal of Molecular Graphics and Modelling</i> , 2020, 96, 107512.	2.4	9
7140	Dynamics of urea-water mixtures studied by molecular dynamics simulation. <i>Journal of Molecular Liquids</i> , 2020, 300, 112268.	4.9	14
7141	A Refined Open State of the Glycine Receptor Obtained via Molecular Dynamics Simulations. <i>Structure</i> , 2020, 28, 130-139.e2.	3.3	36
7142	Structural Basis for Glycerol Efflux and Selectivity of Human Aquaporin 7. <i>Structure</i> , 2020, 28, 215-222.e3.	3.3	43
7143	Off-Pocket Activity Cliffs: A Puzzling Facet of Molecular Recognition. <i>Journal of Chemical Information and Modeling</i> , 2020, 60, 152-161.	5.4	9
7144	Hierarchical Ensembles of Intrinsically Disordered Proteins at Atomic Resolution in Molecular Dynamics Simulations. <i>Journal of Chemical Theory and Computation</i> , 2020, 16, 725-737.	5.3	63
7145	Sequence specificity in DNA-drug intercalation: MD simulation and density functional theory approaches. <i>Journal of Computer-Aided Molecular Design</i> , 2020, 34, 83-95.	2.9	6
7146	Structure of an Unfolding Intermediate of an RRM Domain of ETR-3 Reveals Its Native-like Fold. <i>Biophysical Journal</i> , 2020, 118, 352-365.	0.5	1
7147	Making Soup: Preparing and Validating Models of the Bacterial Cytoplasm for Molecular Simulation. <i>Journal of Chemical Information and Modeling</i> , 2020, 60, 322-331.	5.4	17



#	ARTICLE	IF	CITATIONS
7148	Computing Spatially Resolved Rotational Hydration Entropies from Atomistic Simulations. <i>Journal of Chemical Theory and Computation</i> , 2020, 16, 108-118.	5.3	15
7149	Molecular insights into the effect of an apoptotic raft-like bilayer on the conformation and dynamics of calreticulin. <i>Biochimica Et Biophysica Acta - Biomembranes</i> , 2020, 1862, 183146.	2.6	2
7150	Supramolecular amphiphiles of Beta-cyclodextrin and Oleylamine for enhancement of vancomycin delivery. <i>International Journal of Pharmaceutics</i> , 2020, 574, 118881.	5.2	18
7151	Free Energy Calculations on the Water-Chain-Assisted and the Dehydration Mechanisms of Transmembrane Ion Permeation. <i>Journal of Chemical Theory and Computation</i> , 2020, 16, 700-710.	5.3	5
7152	Molecular dynamics simulations suggest conformational and hydration difference between zwitterionic poly (carboxybetaine methacrylate) and poly (ethylene glycol). <i>Chemical Physics</i> , 2020, 532, 110599.	1.9	8
7153	Microsecond simulation study on the replacement of methane in methane hydrate by carbon dioxide, nitrogen, and carbon dioxide-nitrogen mixtures. <i>Fuel</i> , 2020, 263, 116640.	6.4	35
7154	Molecular dynamics studies of hydrogen diffusion in tungsten at elevated temperature: Concentration dependence and defect effects. <i>International Journal of Hydrogen Energy</i> , 2020, 45, 822-834.	7.1	12
7155	Core effect of local atomic configuration and design principles in Al <sub>x</sub> CoCrFeNi high-entropy alloys. <i>Scripta Materialia</i> , 2020, 178, 181-186.	5.2	29
7156	Oriented attachment induces fivefold twins by forming and decomposing high-energy grain boundaries. <i>Science</i> , 2020, 367, 40-45.	12.6	136
7157	Alteration of the groove width of DNA induced by the multimodal hydrogen bonding of denaturants with DNA bases in its grooves affects their stability. <i>Biochimica Et Biophysica Acta - General Subjects</i> , 2020, 1864, 129498.	2.4	8
7158	Overbinding and Qualitative and Quantitative Changes Caused by Simple Na <sup>+</sup> and K <sup>+</sup> Ions in Polyelectrolyte Simulations: Comparison of Force Fields with and without NBFIX and ECC Corrections. <i>Journal of Chemical Theory and Computation</i> , 2020, 16, 677-687.	5.3	33
7159	Understanding the dual mechanism of bioactive peptides targeting the enzymes involved in Renin Angiotensin System (RAS): An <i>in-silico</i> approach. <i>Journal of Biomolecular Structure and Dynamics</i> , 2020, 38, 5044-5061.	3.5	8
7160	Elimination of bitter-off taste of stevioside through structure modification and computational interventions. <i>Journal of Theoretical Biology</i> , 2020, 486, 110094.	1.7	26
7161	Ligand Binding Thermodynamic Cycles: Hysteresis, the Locally Weighted Histogram Analysis Method, and the Overlapping States Matrix. <i>Journal of Chemical Theory and Computation</i> , 2020, 16, 67-79.	5.3	8
7162	pSPICA: A Coarse-Grained Force Field for Lipid Membranes Based on a Polar Water Model. <i>Journal of Chemical Theory and Computation</i> , 2020, 16, 782-793.	5.3	13
7163	Amorphous boron carbide from ab initio simulations. <i>Computational Materials Science</i> , 2020, 173, 109397.	3.0	6
7164	Atomistic simulations of Epoxy/Water/Aluminum systems using the ReaxFF method. <i>Computational Materials Science</i> , 2020, 173, 109424.	3.0	8
7165	Elucidation of interaction mechanism of hERG1 potassium channel with scorpion toxins BeKm-1 and BmTx3b. <i>Journal of Molecular Graphics and Modelling</i> , 2020, 96, 107504.	2.4	3

#	ARTICLE	IF	CITATIONS
7166	Arginine-259 of UGT2B7 Confers UDP-Sugar Selectivity. <i>Molecular Pharmacology</i> , 2020, 98, 710-718.	2.3	11
7167	Arginine 37 of Glycine Linker Dictates Regulatory Function of HapR. <i>Frontiers in Microbiology</i> , 2020, 11, 1949.	3.5	4
7168	Enhancing the thermostability of phospholipase D from <i>Streptomyces halstedii</i> by directed evolution and elucidating the mechanism of a key amino acid residue using molecular dynamics simulation. <i>International Journal of Biological Macromolecules</i> , 2020, 164, 3065-3074.	7.5	14
7169	Lysozyme Adsorption on Porous Organic Cages: A Molecular Simulation Study. <i>Langmuir</i> , 2020, 36, 12299-12308.	3.5	8
7170	The Surface and Hydration Properties of Lipid Droplets. <i>Biophysical Journal</i> , 2020, 119, 1958-1969.	0.5	20
7171	Disorder–Order Interplay of a Barnacle Cement Protein Triggered by Interactions with Calcium and Carbonate Ions: A Molecular Dynamics Study. <i>Chemistry of Materials</i> , 2020, 32, 8845-8859.	6.7	15
7172	Spontaneous Translocation of Single-Stranded DNA in Graphene–MoS <sub>2</sub> Heterostructure Nanopores: Shape Effect. <i>Journal of Physical Chemistry B</i> , 2020, 124, 9490-9496.	2.6	12
7173	Polycation–Anionic Lipid Membrane Interactions. <i>Langmuir</i> , 2020, 36, 12435-12450.	3.5	27
7174	Automated parameterization of quantum-mechanically derived force-fields including explicit sigma holes: A pathway to energetic and structural features of halogen bonds in gas and condensed phase. <i>Journal of Chemical Physics</i> , 2020, 153, 044106.	3.0	12
7175	Desmosome architecture derived from molecular dynamics simulations and cryo-electron tomography. <i>Proceedings of the National Academy of Sciences of the United States of America</i> , 2020, 117, 27132-27140.	7.1	28
7176	Oxidation degree of a cell membrane model and its response to structural changes, a coarse-grained molecular dynamics approach. <i>Journal of Biomolecular Structure and Dynamics</i> , 2022, 40, 1930-1941.	3.5	4
7177	Allosteric Priming of E. coli CheY by the Flagellar Motor Protein FlhM. <i>Biophysical Journal</i> , 2020, 119, 1108-1122.	0.5	9
7178	The Cytokine IL-1 $\beta$ and Piperine Complex Surveyed by Experimental and Computational Molecular Biophysics. <i>Biomolecules</i> , 2020, 10, 1337.	4.0	8
7179	Insights into the Microscopic Structure of RNF4-SIM-SUMO Complexes from MD Simulations. <i>Biophysical Journal</i> , 2020, 119, 1558-1567.	0.5	3
7180	The effect of the degree of substitution on the solubility of cellulose acetoacetates in water: A molecular dynamics simulation and density functional theory study. <i>Carbohydrate Research</i> , 2020, 496, 108134.	2.3	9
7181	Prediction of pKa in a system with high orthogonal barriers: Alchemical flying Gaussian method. <i>Chemical Physics Letters</i> , 2020, 760, 138012.	2.6	3
7182	On-site-coagulation gel polymer electrolytes with a high dielectric constant for lithium-ion batteries. <i>Journal of Power Sources</i> , 2020, 480, 228802.	7.8	16
7183	Simple corrections for the static dielectric constant of liquid mixtures from model force fields. <i>Physical Chemistry Chemical Physics</i> , 2020, 22, 21741-21749.	2.8	9

#	ARTICLE	IF	CITATIONS
7184	Predicting the Rate of Homogeneous Intermetallic Nucleation within Steep Composition Gradients. <i>Journal of Physical Chemistry C</i> , 2020, 124, 23807-23814.	3.1	3
7185	Novel formulation of antimicrobial peptides enhances antimicrobial activity against methicillin-resistant <i>Staphylococcus aureus</i> (MRSA). <i>Amino Acids</i> , 2020, 52, 1439-1457.	2.7	20
7186	Influence of lysosomal protease sensitivity in the immunogenicity of the antitumor biopharmaceutical asparaginase. <i>Biochemical Pharmacology</i> , 2020, 182, 114230.	4.4	6
7187	The effect of anion on aggregation of amino acid ionic liquid: Atomistic simulation. <i>Journal of Molecular Graphics and Modelling</i> , 2020, 101, 107733.	2.4	6
7188	Thermosensitive Hydration of Four Acrylamide-Based Polymers in Coil and Globule Conformations. <i>Journal of Physical Chemistry B</i> , 2020, 124, 9745-9756.	2.6	10
7189	Altering the Solubility of the Antibiotic Candidate Nisin—A Computational Study. <i>ACS Omega</i> , 2020, 5, 24854-24863.	3.5	9
7190	Influences of electric fields on the operation of Aqp1 aquaporin channels: a molecular dynamics study. <i>Physical Chemistry Chemical Physics</i> , 2020, 22, 25859-25868.	2.8	5
7191	Cholesterol sequestration by xenon nano bubbles leads to lipid raft destabilization. <i>Soft Matter</i> , 2020, 16, 9655-9661.	2.7	4
7192	Oxidative Stress-Induced STIM2 Cysteine Modifications Suppress Store-Operated Calcium Entry. <i>Cell Reports</i> , 2020, 33, 108292.	6.4	19
7193	Conserved Functions of Ether Lipids and Sphingolipids in the Early Secretory Pathway. <i>Current Biology</i> , 2020, 30, 3775-3787.e7.	3.9	59
7194	A study on the protease activity and structure of pepsin in the presence of atenolol and diltiazem. <i>International Journal of Biological Macromolecules</i> , 2020, 165, 2855-2868.	7.5	8
7195	Molecular Dynamics Simulations Suggest a Possible Role for NO in the Polyol Synthesis of Silver Nanostructures. <i>Journal of Physical Chemistry C</i> , 2020, 124, 24279-24288.	3.1	1
7196	Density functional and classical simulations of liquid and glassy selenium. <i>Physical Review B</i> , 2020, 102, .	3.2	4
7197	The dynamics of linear polyubiquitin. <i>Science Advances</i> , 2020, 6, .	10.3	38
7198	A Novel CCT5 Missense Variant Associated with Early Onset Motor Neuropathy. <i>International Journal of Molecular Sciences</i> , 2020, 21, 7631.	4.1	8
7199	Cooperative Aggregations of Nitrogen-Containing Perylene Diimides Driven by Rigid and Flexible Functional Groups. <i>Chemistry of Materials</i> , 2020, 32, 9115-9125.	6.7	14
7200	Potential therapeutic use of corticosteroids as SARS CoV-2 main protease inhibitors: a computational study. <i>Journal of Biomolecular Structure and Dynamics</i> , 2022, 40, 2053-2066.	3.5	14
7201	Sphingomyelinase Disables Inactivation in Endogenous PIEZO1 Channels. <i>Cell Reports</i> , 2020, 33, 108225.	6.4	47

#	ARTICLE	IF	CITATIONS
7202	Papain-like protease regulates SARS-CoV-2 viral spread and innate immunity. <i>Nature</i> , 2020, 587, 657-662.	27.8	818
7203	Pressure control using stochastic cell rescaling. <i>Journal of Chemical Physics</i> , 2020, 153, 114107.	3.0	113
7204	Molecular dynamics analysis predicts ritonavir and naloxegol strongly block the SARS-CoV-2 spike protein-hACE2 binding. <i>Journal of Biomolecular Structure and Dynamics</i> , 2022, 40, 1597-1606.	3.5	9
7205	Functional analysis and cryo-electron microscopy of <i>Campylobacter jejuni</i> serine protease HtrA. <i>Gut Microbes</i> , 2020, 12, 1810532.	9.8	12
7206	Are all-atom any better than united-atom force fields for the description of liquid properties of alkanes?. <i>Journal of Molecular Modeling</i> , 2020, 26, 296.	1.8	21
7207	Pulsed Electric Fields Can Create Pores in the Voltage Sensors of Voltage-Gated Ion Channels. <i>Biophysical Journal</i> , 2020, 119, 190-205.	0.5	43
7208	Raw nuclear magnetic resonance data of human linker histone H1x, lacking the C-terminal domain (NGH1x), and trajectory data of nanosecond molecular dynamics simulations of GH1x- and NGH1x-chromatosomes. <i>Data in Brief</i> , 2020, 31, 105865.	1.0	0
7209	Deformation nanomechanics and dislocation quantification at the atomic scale in nanocrystalline magnesium. <i>Journal of Magnesium and Alloys</i> , 2020, 8, 1296-1303.	11.9	33
7210	Understanding high pressure molecular hydrogen with a hierarchical machine-learned potential. <i>Nature Communications</i> , 2020, 11, 5014.	12.8	5
7211	Binding of divalent cations to acetate: molecular simulations guided by Raman spectroscopy. <i>Physical Chemistry Chemical Physics</i> , 2020, 22, 24014-24027.	2.8	28
7212	Correlated counterion effects on the solvation of proteins by ionic liquids. <i>Journal of Molecular Liquids</i> , 2020, 320, 114347.	4.9	10
7213	Elucidating the Key Role of the Cyano ( $\text{C}\equiv\text{N}$ ) Group to Construct Environmentally Friendly Fused-Ring Electron Acceptors. <i>Journal of Physical Chemistry C</i> , 2020, 124, 23059-23068.	3.1	28
7214	Dense packings of hard circular arcs. <i>Physical Review E</i> , 2020, 102, 042903.	2.1	6
7215	Blockage of Store-Operated $\text{Ca}^{2+}$ Influx by Synta66 is Mediated by Direct Inhibition of the $\text{Ca}^{2+}$ Selective Orai1 Pore. <i>Cancers</i> , 2020, 12, 2876.	3.7	30
7216	Biological evaluation and molecular modeling of peptidomimetic compounds as inhibitors for O-GlcNAc transferase (OGT). <i>European Journal of Pharmaceutical Sciences</i> , 2020, 154, 105510.	4.0	28
7217	Activation Microswitches in Adenosine Receptor $\text{A}_{2A}$ Function as Rheostats in the Cell Membrane. <i>Biochemistry</i> , 2020, 59, 4059-4071.	2.5	11
7218	Transport and Interfacial Properties of Mixed Molten Carbonate/Hydroxide Electrolytes by Molecular Dynamics Simulations. <i>Journal of Physical Chemistry C</i> , 2020, 124, 23532-23540.	3.1	7
7219	Asymmetric Hydrogen-Bonding Structure at a Water/Ice Interface. <i>Journal of Physical Chemistry C</i> , 2020, 124, 23287-23294.	3.1	5

#	ARTICLE	IF	CITATIONS
7220	Stability, deformation and rupture of Janus oligomer enabled self-emulsifying water-in-oil microemulsion droplets. <i>Physical Chemistry Chemical Physics</i> , 2020, 22, 24907-24916.	2.8	4
7221	Computer simulations of a heterogeneous membrane with enhanced sampling techniques. <i>Journal of Chemical Physics</i> , 2020, 153, 144110.	3.0	10
7222	The Effects of Resveratrol, Caffeine, $\beta$ -Carotene, and Epigallocatechin Gallate (EGCG) on Amyloid $\beta$ 25–35 Aggregation in Synthetic Brain Membranes. <i>Molecular Nutrition and Food Research</i> , 2020, 64, e2000632.	3.3	8
7223	Ordered Nanofibers Fabricated from Hierarchical Self-Assembling Processes of Designed $\alpha$ -Helical Peptides. <i>Small</i> , 2020, 16, e2003945.	10.0	11
7224	Impact of protein dynamics on secondary structure prediction. <i>Biochimie</i> , 2020, 179, 14-22.	2.6	7
7225	Membrane targeting antimicrobial cyclic peptide nanotubes – an experimental and computational study. <i>Colloids and Surfaces B: Biointerfaces</i> , 2020, 196, 111349.	5.0	16
7226	$\beta$ -Amyloid (1–42) peptide adsorbs but does not insert into ganglioside-containing phospholipid membranes in the liquid-disordered state: modelling and experimental studies. <i>International Journal of Biological Macromolecules</i> , 2020, 164, 2651-2658.	7.5	7
7227	The influence of polar and non-polar interactions on the self-assembly of peptide nanomembranes and their applications: An atomistic study using classical molecular dynamics. <i>Journal of Molecular Liquids</i> , 2020, 318, 114263.	4.9	15
7228	Exploring the Potential of Benzene-1,3,5-tricarboxamide Supramolecular Polymers as Biomaterials. <i>Biomacromolecules</i> , 2020, 21, 4105-4115.	5.4	21
7229	Molecular Dynamics Simulation of the Structures, Dynamics, and Aggregation of Dissolved Organic Matter. <i>Environmental Science &amp; Technology</i> , 2020, 54, 13527-13537.	10.0	36
7230	Mg <sup>2+</sup> Sensing by an RNA Fragment: Role of Mg <sup>2+</sup> -Coordinated Water Molecules. <i>Journal of Chemical Theory and Computation</i> , 2020, 16, 6702-6715.	5.3	9
7231	Optimization of Slipids Force Field Parameters Describing Headgroups of Phospholipids. <i>Journal of Physical Chemistry B</i> , 2020, 124, 8784-8793.	2.6	35
7232	Molecular View into the Cyclodextrin Cavity: Structure and Hydration. <i>ACS Omega</i> , 2020, 5, 25655-25667.	3.5	74
7233	Detailed Molecular Structure of Glassy Poly(phenylene oxide) (PPO) Studied by Molecular Dynamics Simulations. <i>Journal of Macromolecular Science - Physics</i> , 2020, 59, 796-820.	1.0	1
7234	Molecular dynamics simulation study on <i>Thermotoga maritima</i> EngA: GTP/GDP bound state of the second G-domain influences the domain–domain interface interactions. <i>Journal of Biomolecular Structure and Dynamics</i> , 2020, , 1-13.	3.5	3
7235	A coarse-grained model of dimethyl sulfoxide for molecular dynamics simulations with lipid membranes. <i>Journal of Chemical Physics</i> , 2020, 153, 035104.	3.0	8
7236	Temperature, Pressure, and Concentration Derivatives of Nonpolar Gas Hydration: Impact on the Heat Capacity, Temperature of Maximum Density, and Speed of Sound of Aqueous Mixtures. <i>Journal of Physical Chemistry B</i> , 2020, 124, 6924-6942.	2.6	9
7237	Simulation of Liquids with the Tight-Binding Density-Functional Approach and Improved Atomic Charges. <i>Journal of Physical Chemistry B</i> , 2020, 124, 7421-7432.	2.6	4

#	ARTICLE	IF	CITATIONS
7238	Conformations and Dynamics of Polymer Chains in Cis and Trans Polybutadiene/Silica Nanocomposites through Atomistic Simulations: From the Unentangled to the Entangled Regime. <i>Macromolecules</i> , 2020, 53, 6173-6189.	4.8	30
7239	Prospecting for new catechol- <i>O</i> -methyltransferase (COMT) inhibitors as a potential treatment for Parkinson's disease: a study by molecular dynamics and structure-based virtual screening. <i>Journal of Biomolecular Structure and Dynamics</i> , 2021, 39, 5872-5891.	3.5	1
7240	Enhanced Activity and Stability of <i>Acidothermus cellulolyticus</i> Endoglucanase 1 in Ionic Liquids via Engineering Active Site Residues and Non-Native Disulfide Bridges. <i>ACS Sustainable Chemistry and Engineering</i> , 2020, 8, 11299-11307.	6.7	12
7241	Molecular basis for the distinct functions of redox-active and FeS-transferring glutaredoxins. <i>Nature Communications</i> , 2020, 11, 3445.	12.8	47
7242	Oxygen intercalation in PVD graphene grown on copper substrates: A decoupling approach. <i>Applied Surface Science</i> , 2020, 529, 147100.	6.1	10
7243	Coupling between clay swelling/collapse and cationic partition. <i>Geochimica Et Cosmochimica Acta</i> , 2020, 285, 78-99.	3.9	29
7244	Structure of the Inhibited State of the Sec Translocon. <i>Molecular Cell</i> , 2020, 79, 406-415.e7.	9.7	44
7245	Insight into dynamic interaction of molten MgCl <sub>2</sub> -NaCl-KCl with impurity water via FPMD simulations. <i>Journal of Molecular Liquids</i> , 2020, 314, 113596.	4.9	20
7246	Structural ensemble and biological activity of DciA intrinsically disordered region. <i>Journal of Structural Biology</i> , 2020, 212, 107573.	2.8	11
7247	Xenon Dynamics in Ionic Liquids: A Combined NMR and MD Simulation Study. <i>Journal of Physical Chemistry B</i> , 2020, 124, 6617-6627.	2.6	12
7248	Electric Field Induced Wetting of a Hydrophobic Gate in a Model Nanopore Based on the 5-HT <sub>3</sub> Receptor Channel. <i>ACS Nano</i> , 2020, 14, 10480-10491.	14.6	30
7249	From monomer to fibril: Aβ amyloid binding to Aducanumab antibody studied by molecular dynamics simulation. <i>Proteins: Structure, Function and Bioinformatics</i> , 2020, 88, 1592-1606.	2.6	12
7250	Predicting the solvation structure and vehicular diffusion of hydroxide ion in an anion exchange membrane using nonreactive molecular dynamics simulation. <i>Chemical Physics Letters</i> , 2020, 755, 137802.	2.6	27
7251	Guanidinium binding to proteins: The intriguing effects on the D1 and D2 domains of <i>Thermotoga maritima</i> Arginine Binding Protein and a comprehensive analysis of the Protein Data Bank. <i>International Journal of Biological Macromolecules</i> , 2020, 163, 375-385.	7.5	6
7252	Inverse rule of mixtures at the nanoscale: Prediction of elastic properties of cellulose nanofibrils. <i>Composites Part A: Applied Science and Manufacturing</i> , 2020, 138, 106046.	7.6	12
7253	Atomic-Level Characterization of the Methadone-Stabilized Active Conformation of $\mu$ -Opioid Receptor. <i>Molecular Pharmacology</i> , 2020, 98, 475-486.	2.3	16
7254	Single-vesicle imaging quantifies calcium's regulation of nanoscale vesicle clustering mediated by $\beta$ -synuclein. <i>Microsystems and Nanoengineering</i> , 2020, 6, 38.	7.0	6
7255	Ultra-Fast High-Precision Metallic Nanoparticle Synthesis using Laser-Accelerated Protons. <i>Scientific Reports</i> , 2020, 10, 9570.	3.3	8



#	ARTICLE	IF	CITATIONS
7256	Solvent influence on molecular interactions in the bulk of fluorene copolymer films. RSC Advances, 2020, 10, 20772-20777.	3.6	3
7257	Molecular simulation of liquidâ€“vapor coexistence for NaCl: Full-charge vs scaled-charge interaction models. Journal of Chemical Physics, 2020, 153, 024501.	3.0	10
7258	Titrateable Martini model for constant pH simulations. Journal of Chemical Physics, 2020, 153, 024118.	3.0	57
7259	Balancing All-Atom Force Field for DNA Simulations Using Osmotic Pressure Data. Bulletin of the Korean Chemical Society, 2020, 41, 759-764.	1.9	1
7260	Exploring the physicochemical and morphological properties of peptideâ€“hybridized dendrimers (<sc>DendriPeps</sc>) and their aggregates. Journal of Polymer Science, 2020, 58, 2234-2247.	3.8	2
7261	Structure-based virtual screening, molecular docking and dynamics studies of natural product and classical inhibitors against human dihydrofolate reductase. Network Modeling Analysis in Health Informatics and Bioinformatics, 2020, 9, 1.	2.1	8
7262	Molecular dynamics simulations of two-dimensional materials. , 2020, , 125-148.		0
7263	Out of Sight, Out of Mind: The Effect of the Equilibration Protocol on the Structural Ensembles of Charged Glycolipid Bilayers. Molecules, 2020, 25, 5120.	3.8	7
7264	Self-Learning Molecular Design for High Lithium-Ion Conductive Ionic Liquids using Maze Game. Journal of Chemical Information and Modeling, 2020, 60, 4904-4911.	5.4	4
7265	Genetic Algorithm Approach for the Optimization of Protein Antifreeze Activity Using Molecular Simulations. Journal of Chemical Theory and Computation, 2020, 16, 7866-7873.	5.3	4
7266	Protein Denaturation, Zero Entropy Temperature, and the Structure of Water around Hydrophobic and Amphiphilic Solutes. Journal of Physical Chemistry B, 2020, 124, 10994-11006.	2.6	8
7267	Epigallocatechin Gallate Destabilizes Î±-Synuclein Fibril by Disrupting the E46â€“K80 Salt-Bridge and Inter-protofibril Interface. ACS Chemical Neuroscience, 2020, 11, 4351-4361.	3.5	25
7268	Stability of Protein Structure during Nanocarrier Encapsulation: Insights on Solvent Effects from Simulations and Spectroscopic Analysis. ACS Nano, 2020, 14, 16962-16972.	14.6	1
7269	The origins of binding specificity of a lanthanide ion binding peptide. Scientific Reports, 2020, 10, 19468.	3.3	8
7270	Unified Approach to Enhanced Sampling. Physical Review X, 2020, 10, .	8.9	43
7271	Interaction of Ionenes with Lipid Membrane: Unusual Impact of Charge Density. Langmuir, 2020, 36, 14717-14727.	3.5	6
7272	Development of parameters compatible with the CHARMM36 force field for [Fe<sub>4</sub>S<sub>4</sub>]<sup>2+</sup> clusters and molecular dynamics simulations of adenosine-5â€“phosphosulfate reductase in GROMACS 2019. Journal of Biomolecular Structure and Dynamics, 2022, 40, 3481-3491.	3.5	24
7273	Effect of pH on the Supramolecular Structure of Helicobacter pylori Urease by Molecular Dynamics Simulations. Polymers, 2020, 12, 2713.	4.5	8

#	ARTICLE	IF	CITATIONS
7274	Computational modeling of nanoparticles in inert environment. <i>Frontiers of Nanoscience</i> , 2020, 17, 5-26.	0.6	0
7275	Molecular simulation of osmometry in aqueous solutions of the BMIMCl ionic liquid: a potential route to force field parameterization of liquid mixtures. <i>Physical Chemistry Chemical Physics</i> , 2020, 22, 28325-28338.	2.8	3
7276	Aqueous solutions of binary ionic liquids: insight into structure, dynamics, and interface properties by molecular dynamics simulations and DFT methods. <i>Physical Chemistry Chemical Physics</i> , 2020, 22, 27882-27895.	2.8	8
7277	Development of Coarse-Grained Models for Poly(4-vinylphenol) and Poly(2-vinylpyridine): Polymer Chemistries with Hydrogen Bonding. <i>Polymers</i> , 2020, 12, 2764.	4.5	5
7278	Effect of external pressure on the release of methane through MFI zeolite nanochannels. <i>RSC Advances</i> , 2020, 10, 37507-37514.	3.6	2
7279	Essential role of accessory subunit LYRM6 in the mechanism of mitochondrial complex I. <i>Nature Communications</i> , 2020, 11, 6008.	12.8	25
7280	GClceNet: a graph convolutional network for accurate classification of water phases. <i>Physical Chemistry Chemical Physics</i> , 2020, 22, 26340-26350.	2.8	14
7281	Exploring the folding process of human $\beta$ 2-crystallin using multiscale molecular dynamics and the Markov state model. <i>Physical Chemistry Chemical Physics</i> , 2020, 22, 26753-26763.	2.8	5
7282	Three-Dimensional Molecular Mapping of Ionic Liquids at Electrified Interfaces. <i>ACS Nano</i> , 2020, 14, 17515-17523.	14.6	47
7283	Rapid and accurate determination of atomistic RNA dynamic ensemble models using NMR and structure prediction. <i>Nature Communications</i> , 2020, 11, 5531.	12.8	52
7284	DNA-binding mechanisms of human and mouse cGAS: a comparative MD and MM/GBSA study. <i>Physical Chemistry Chemical Physics</i> , 2020, 22, 26390-26401.	2.8	8
7285	Temperature-Induced Transition from Indirect to Direct Adsorption of Polycyclic Aromatic Hydrocarbons on Quartz: A Combined Theoretical and Experimental Study. <i>Industrial &amp; Engineering Chemistry Research</i> , 2020, 59, 18500-18509.	3.7	8
7286	Performance of Markov State Models and Transition Networks on Characterizing Amyloid Aggregation Pathways from MD Data. <i>Journal of Chemical Theory and Computation</i> , 2020, 16, 7825-7839.	5.3	24
7287	Tuning CO <sub>2</sub> Capture at the Gas/Amine Solution Interface by Changing the Solvent Polarity. <i>Journal of Physical Chemistry B</i> , 2020, 124, 10245-10256.	2.6	11
7288	Effect of Brønsted Acidity on Ion Conduction in Fluorinated Acetic Acid and N-Methylimidazole Equimolar Mixtures as Pseudo-protic Ionic Liquids. <i>Journal of Physical Chemistry B</i> , 2020, 124, 11157-11164.	2.6	13
7289	Double grain boundary configurations on graphite surfaces. <i>Carbon</i> , 2020, 170, 630-635.	10.3	2
7290	The SERCA residue Glu340 mediates interdomain communication that guides Ca <sup>2+</sup> transport. <i>Proceedings of the National Academy of Sciences of the United States of America</i> , 2020, 117, 31114-31122.	7.1	12
7291	Integrated Leaching and Separation of Metals Using Mixtures of Organic Acids and Ionic Liquids. <i>Molecules</i> , 2020, 25, 5570.	3.8	8

#	ARTICLE	IF	CITATIONS
7292	Protein Dynamics Enables Phosphorylation of Buried Residues in Cdk2/Cyclin-A-Bound p27. <i>Biophysical Journal</i> , 2020, 119, 2010-2018.	0.5	21
7293	Unveiling the local structure of 2-mercaptobenzothiazole intercalated in (Zn <sub>2</sub> Al) layered double hydroxides. <i>Applied Clay Science</i> , 2020, 198, 105842.	5.2	5
7294	In silico identification of Tretinoin as a SARS-CoV-2 envelope (E) protein ion channel inhibitor. <i>Computers in Biology and Medicine</i> , 2020, 127, 104063.	7.0	44
7295	Emergence of Barrel Motif in Amyloid-Î² Trimer: A Computational Study. <i>Journal of Physical Chemistry B</i> , 2020, 124, 10617-10631.	2.6	12
7296	mTORâ€“mLST8 interaction: hot spot identification through quantum biochemistry calculations. <i>New Journal of Chemistry</i> , 2020, 44, 20982-20992.	2.8	5
7297	Polarizable and non-polarizable force fields: Protein folding, unfolding, and misfolding. <i>Journal of Chemical Physics</i> , 2020, 153, 185102.	3.0	26
7298	Inhibition potential evaluation of two synthetic bis-indole compounds on amyloid fibrillation: a molecular simulation study. <i>Journal of Biomolecular Structure and Dynamics</i> , 2022, 40, 4051-4061.	3.5	3
7299	Characterisation of plasmodial transketolases and identification of potential inhibitors: an in silico study. <i>Malaria Journal</i> , 2020, 19, 442.	2.3	5
7300	In Silico Design of a Peptide Receptor for Dopamine Recognition. <i>Molecules</i> , 2020, 25, 5509.	3.8	3
7301	Ligand-Based Virtual Screening, Molecular Docking, Molecular Dynamics, and MM-PBSA Calculations towards the Identification of Potential Novel Ricin Inhibitors. <i>Toxins</i> , 2020, 12, 746.	3.4	17
7302	Thermal and Nonthermal Microwave Effects of Ethanol and Hexane-Mixed Solution as Revealed by In Situ Microwave Irradiation Nuclear Magnetic Resonance Spectroscopy and Molecular Dynamics Simulation. <i>Journal of Physical Chemistry B</i> , 2020, 124, 9615-9624.	2.6	14
7303	Concentration- and pH-Dependent Oligomerization of the Thrombin-Derived C-Terminal Peptide TCP-25. <i>Biomolecules</i> , 2020, 10, 1572.	4.0	9
7304	Deterring Effect of Resins on the Aggregation of Asphaltenes in <i>n</i> -Heptane. <i>Energy &amp; Fuels</i> , 2020, 34, 16081-16088.	5.1	15
7305	Computational guided identification of novel potent inhibitors of N-terminal domain of nucleocapsid protein of severe acute respiratory syndrome coronavirus 2. <i>Journal of Biomolecular Structure and Dynamics</i> , 2022, 40, 4084-4099.	3.5	31
7306	Lipid-Chaperone Hypothesis: A Common Molecular Mechanism of Membrane Disruption by Intrinsically Disordered Proteins. <i>ACS Chemical Neuroscience</i> , 2020, 11, 4336-4350.	3.5	101
7307	Laurdan and Di-4-ANEPPDHQ Influence the Properties of Lipid Membranes: A Classical Molecular Dynamics and Fluorescence Study. <i>Journal of Physical Chemistry B</i> , 2020, 124, 11419-11430.	2.6	20
7308	Molecular Dynamics Study on the Water Mobility and Side-Chain Flexibility of Hydrated Poly( <i>l</i> -methoxyalkyl acrylate)s. <i>ACS Biomaterials Science and Engineering</i> , 2020, 6, 6690-6700.	5.2	10
7309	Polarization of acetonitrile under thermal fields via non-equilibrium molecular dynamics simulations. <i>Journal of Chemical Physics</i> , 2020, 153, 204503.	3.0	6

#	ARTICLE	IF	CITATIONS
7310	Molecular Cartography of A1 and A2 Asphaltene Subfractions from Classical Molecular Dynamics Simulations. <i>Energy &amp; Fuels</i> , 2020, 34, 13954-13965.	5.1	15
7311	Tacticity Effects on the Bulk Modulus of Poly(methyl methacrylate) Explored by Coarse-Grained Simulations. <i>Journal of Physical Chemistry B</i> , 2020, 124, 10811-10821.	2.6	5
7312	Breakdown of the Stokes-Einstein Relation in Supercooled Water/Methanol Binary Mixtures: Explanation Using the Translational Jump-Diffusion Approach. <i>Journal of Physical Chemistry B</i> , 2020, 124, 10398-10408.	2.6	18
7313	Coplanar <i>versus</i> Noncoplanar Carboxyl Groups: The Influence of Sterically Enforced Noncoplanarity on the 2D Mixing Behavior of Benzene Tricarboxylic Acids. <i>Journal of Physical Chemistry C</i> , 2020, 124, 24874-24882.	3.1	9
7314	Epitope-Based Potential Vaccine Candidate for Humoral and Cell-Mediated Immunity to Combat Severe Acute Respiratory Syndrome Coronavirus 2 Pandemic. <i>Journal of Physical Chemistry Letters</i> , 2020, 11, 9920-9930.	4.6	12
7315	An $\alpha$ -helix mimetic oligopyridylamide, ADH-31, modulates $A\beta_{42}$ monomer aggregation and destabilizes protofibril structures: insights from molecular dynamics simulations. <i>Physical Chemistry Chemical Physics</i> , 2020, 22, 28055-28073.	2.8	12
7316	Different Force Fields Give Rise to Different Amyloid Aggregation Pathways in Molecular Dynamics Simulations. <i>Journal of Chemical Information and Modeling</i> , 2020, 60, 6462-6475.	5.4	82
7317	Injectable Single-Component Peptide Depot: Autonomously Rechargeable Tumor Photosensitization for Repeated Photodynamic Therapy. <i>ACS Nano</i> , 2020, 14, 15793-15805.	14.6	22
7318	Refined Force Field for Liquid Sulfolane with Particular Emphasis to Its Transport Characteristics. <i>ACS Omega</i> , 2020, 5, 28285-28295.	3.5	12
7319	Molecular Sizes and Antibacterial Performance Relationships of Flexible Ionic Liquid Derivatives. <i>Journal of the American Chemical Society</i> , 2020, 142, 20257-20269.	13.7	128
7320	Modulation of the binding affinity of naproxen to bovine serum albumin by conversion of the drug into amino acid ester salts. <i>Journal of Molecular Liquids</i> , 2020, 319, 114283.	4.9	8
7321	Cryo vs Thermo: Duality of Ethylene Glycol on the Stability of Proteins. <i>Journal of Physical Chemistry B</i> , 2020, 124, 10077-10088.	2.6	11
7322	Supramolecular Functionalization for Improving Thermoelectric Properties of Single-Walled Carbon Nanotubes-Small Organic Molecule Hybrids. <i>ACS Applied Materials &amp; Interfaces</i> , 2020, 12, 51387-51396.	8.0	13
7323	Control over the fibrillization yield by varying the oligomeric nucleation propensities of self-assembling peptides. <i>Communications Chemistry</i> , 2020, 3, .	4.5	7
7324	In silico characterisation of olive phenolic compounds as potential cyclooxygenase modulators. Part 1. <i>Journal of Molecular Graphics and Modelling</i> , 2020, 101, 107719.	2.4	3
7325	Structural Fluctuations of Aromatic Residues in an Apo-Form Reveal Cryptic Binding Sites: Implications for Fragment-Based Drug Design. <i>Journal of Physical Chemistry B</i> , 2020, 124, 9977-9986.	2.6	10
7326	The Post-Translational Modifications, Localization, and Mode of Attachment of Non-Covalently Bound Glucanolytransglycosylases of Yeast Cell Wall as a Key to Understanding their Functioning. <i>International Journal of Molecular Sciences</i> , 2020, 21, 8304.	4.1	4
7327	Chromium carbide micro-whiskers: Preparation and strengthening effects in extreme conditions with experiments and molecular dynamics simulations. <i>Journal of Solid State Chemistry</i> , 2020, 291, 121598.	2.9	14

#	ARTICLE	IF	CITATIONS
7328	Morphology and dynamics of self-assembled structures in mixed surfactant systems (SDS+CAPB) in the context of methane hydrate growth. <i>Journal of Molecular Liquids</i> , 2020, 319, 114296.	4.9	10
7329	Membrane Perturbation and Lipid Flip-Flop Mediated by Graphene Nanosheet. <i>Journal of Physical Chemistry B</i> , 2020, 124, 10632-10640.	2.6	8
7330	Theoretical insights into the effect of size and substitution patterns of azobenzene derivatives on the DNA G-quadruplex. <i>Physical Chemistry Chemical Physics</i> , 2020, 22, 26944-26954.	2.8	8
7331	Computational Studies of SARS-CoV-2 3CLpro: Insights from MD Simulations. <i>International Journal of Molecular Sciences</i> , 2020, 21, 5346.	4.1	48
7332	New Insights into the Effect of Residue Mutations on the Rotavirus VP1 Function Using Molecular Dynamic Simulations. <i>Journal of Chemical Information and Modeling</i> , 2020, 60, 5011-5025.	5.4	4
7333	Identification of polyphenols from <i>Broussonetia papyrifera</i> as SARS CoV-2 main protease inhibitors using <i>in silico</i> docking and molecular dynamics simulation approaches. <i>Journal of Biomolecular Structure and Dynamics</i> , 2021, 39, 6747-6760.	3.5	54
7334	Combining Machine Learning and Molecular Dynamics to Predict P-Glycoprotein Substrates. <i>Journal of Chemical Information and Modeling</i> , 2020, 60, 4730-4749.	5.4	30
7335	Computer-aided engineering of adipyl-CoA synthetase for enhancing adipic acid synthesis. <i>Biotechnology Letters</i> , 2020, 42, 2693-2701.	2.2	4
7336	Ion-induced free energy landscapes of A $\beta$ 42 peptide dimer in wet ionic liquids. <i>Journal of Molecular Liquids</i> , 2020, 318, 114026.	4.9	4
7338	PAMAM dendrimer in a phosphate solution: An atomistic simulation study. <i>Polymer</i> , 2020, 206, 122881.	3.8	2
7339	Unifying the Contrasting Mechanisms of Protein-Stabilizing Osmolytes. <i>Journal of Physical Chemistry B</i> , 2020, 124, 6565-6574.	2.6	26
7340	Equation of state modeling and force field-based molecular dynamics simulations of supercritical polyethylene+ hexane+ ethylene systems. <i>Journal of Molecular Graphics and Modelling</i> , 2020, 100, 107709.	2.4	0
7341	Triacylglycerols sequester monotopic membrane proteins to lipid droplets. <i>Nature Communications</i> , 2020, 11, 3944.	12.8	46
7342	Solubilization power of surfactant-free microemulsions. <i>Physical Chemistry Chemical Physics</i> , 2020, 22, 22185-22189.	2.8	9
7343	Role of Tyr-39 for the Structural Features of $\beta$ -Synuclein and for the Interaction with a Strong Modulator of Its Amyloid Assembly. <i>International Journal of Molecular Sciences</i> , 2020, 21, 5061.	4.1	4
7344	Complexity of seemingly simple lipid nanodiscs. <i>Biochimica Et Biophysica Acta - Biomembranes</i> , 2020, 1862, 183420.	2.6	22
7345	Modulating A $\beta$ aggregation by tyrosol-based ligands: The crucial role of the catechol moiety. <i>Biophysical Chemistry</i> , 2020, 265, 106434.	2.8	19
7346	Mesophilic Pyrophosphatase Function at High Temperature: A Molecular Dynamics Simulation Study. <i>Biophysical Journal</i> , 2020, 119, 142-150.	0.5	3

#	ARTICLE	IF	CITATIONS
7347	Confinement in Nanodiscs Anisotropically Modifies Lipid Bilayer Elastic Properties. Journal of Physical Chemistry B, 2020, 124, 7166-7175.	2.6	26
7348	Identification of a potential SARS-CoV2 inhibitor via molecular dynamics simulations and amino acid decomposition analysis. Journal of Biomolecular Structure and Dynamics, 2020, 39, 1-16.	3.5	23
7349	Composition-dependent microstructure evolution in liquid MgCl <sub>2</sub> -KCl: A first-principles molecular dynamics study. Journal of Molecular Liquids, 2020, 309, 113131.	4.9	27
7350	Characterizing the Hydration Properties of Proton Binding Sites in the ATP Synthase c-Rings of <i>Bacillus</i> Species. Journal of Physical Chemistry B, 2020, 124, 7176-7183.	2.6	5
7351	Simulations of Asymmetric Membranes Illustrate Cooperative Leaflet Coupling and Lipid Adaptability. Frontiers in Cell and Developmental Biology, 2020, 8, 575.	3.7	26
7352	Unravelling the Interactions between Surface-Active Ionic Liquids and Triblock Copolymers for the Design of Thermal Responsive Systems. Journal of Physical Chemistry B, 2020, 124, 7046-7058.	2.6	12
7353	Studies of Dynamic Binding of Amino Acids to TiO <sub>2</sub> Nanoparticle Surfaces by Solution NMR and Molecular Dynamics Simulations. Langmuir, 2020, 36, 10341-10350.	3.5	19
7354	Molecular Dynamics Simulation of the Diffusion Dynamics of Linear DNA Fragments in Dilute Solution with the Parmbsc1 Force Field and Comparison with Experimental Data and Theoretical Models. Macromolecules, 2020, 53, 6135-6150.	4.8	1
7355	Study on effects of co-solvents on the structure of DhaA by molecular dynamics simulation. Journal of Biomolecular Structure and Dynamics, 2021, 39, 5999-6007.	3.5	0
7356	Permeation of Biopolymers Across the Cell Membrane: A Computational Comparative Study on Polylactic Acid and Polyhydroxyalkanoate. Frontiers in Bioengineering and Biotechnology, 2020, 8, 718.	4.1	4
7357	Effects of Bubble Size and Gas Density on the Shock-induced Collapse of Nanoscale Cavitation Bubble. Multiscale Science and Engineering, 2020, 2, 127-134.	1.7	4
7358	ddcMD: A fully GPU-accelerated molecular dynamics program for the Martini force field. Journal of Chemical Physics, 2020, 153, 045103.	3.0	18
7359	The phase transition of rapidly super-cooled Tungsten under 100 GPa. Chemical Physics Letters, 2020, 755, 137789.	2.6	2
7360	Experimental and computational studies on the solubility of carbon dioxide in protic ammonium-based ionic liquids. Journal of the Taiwan Institute of Chemical Engineers, 2020, 112, 152-161.	5.3	14
7361	Molecular dynamics study on temperature and strain rate dependences of mechanical properties of single crystal Al under uniaxial loading. AIP Advances, 2020, 10, .	1.3	20
7362	Molecular basis for the inhibitory effects of 5-hydroxycyclopencillone on the conformational transition of Al <sup>240</sup> monomer. Journal of Biomolecular Structure and Dynamics, 2020, 39, 1-12.	3.5	2
7363	Comparison of Structure and Local Dynamics of Two Peptide Dendrimers with the Same Backbone but with Different Side Groups in Their Spacers. Polymers, 2020, 12, 1657.	4.5	9
7364	Mesoscale model of the synthesis of periodic mesoporous benzene-silica. Journal of Molecular Liquids, 2020, 316, 113861.	4.9	3



#	ARTICLE	IF	CITATIONS
7365	Can CHARMM36 atomic charges described correctly the interaction between amino acid and water molecules by molecular dynamics simulations?. Journal of Molecular Liquids, 2020, 317, 113919.	4.9	18
7366	Functional 3D architecture in an intrinsically disordered E3 ligase domain facilitates ubiquitin transfer. Nature Communications, 2020, 11, 3807.	12.8	11
7367	Optimal estimates of self-diffusion coefficients from molecular dynamics simulations. Journal of Chemical Physics, 2020, 153, 024116.	3.0	44
7368	Characterizing Polymer Hydration Shell Compressibilities with the Small-System Method. Nanomaterials, 2020, 10, 1460.	4.1	7
7369	Determinants of Endoplasmic Reticulum-to-Lipid Droplet Protein Targeting. Developmental Cell, 2020, 54, 471-487.e7.	7.0	42
7370	Thermomechanical properties of zero thermal expansion materials from theory and experiments. Physical Chemistry Chemical Physics, 2020, 22, 18518-18525.	2.8	3
7371	Prediction of Mycobacterium tuberculosis pyrazinamidase function based on structural stability, physicochemical and geometrical descriptors. PLoS ONE, 2020, 15, e0235643.	2.5	0
7372	E487K-Induced Disorder in Functionally Relevant Dynamics of Mitochondrial Aldehyde Dehydrogenase 2. Biophysical Journal, 2020, 119, 628-637.	0.5	4
7373	Peptide Inhibitors of Bacterial Protein Synthesis with Broad Spectrum and SbmA-Independent Bactericidal Activity against Clinical Pathogens. Journal of Medicinal Chemistry, 2020, 63, 9590-9602.	6.4	24
7374	Caught in the Act: Mechanistic Insight into Supramolecular Polymerization-Driven Self-Replication from Real-Time Visualization. Journal of the American Chemical Society, 2020, 142, 13709-13717.	13.7	44
7375	Unravelling the structural complexity and photophysical properties of adamantyl-based layered hybrid perovskites. Journal of Materials Chemistry A, 2020, 8, 17732-17740.	10.3	14
7376	Conserved internal hydration motifs in protein kinases. Proteins: Structure, Function and Bioinformatics, 2020, 88, 1578-1591.	2.6	6
7377	Prediction of thermodynamic properties of organic mixtures: Combining molecular simulations with classical thermodynamics. Fluid Phase Equilibria, 2020, 523, 112759.	2.5	7
7378	Molecular level insight into stability, activity, and structure of Laccase in aqueous ionic liquid and organic solvents: An experimental and computational research. Journal of Molecular Liquids, 2020, 317, 113925.	4.9	13
7379	Does SARS-CoV-2 Bind to Human ACE2 More Strongly Than Does SARS-CoV?. Journal of Physical Chemistry B, 2020, 124, 7336-7347.	2.6	108
7380	Enhanced Binding of SARS-CoV-2 Spike Protein to Receptor by Distal Polybasic Cleavage Sites. ACS Nano, 2020, 14, 10616-10623.	14.6	89
7381	Modelling and structural investigation of a new DNA Origami based flexible bio-nano joint. Molecular Simulation, 2020, 46, 994-1003.	2.0	5
7382	Effect of Glycyrrhizic Acid and Arabinogalactan on the Membrane Potential of Rat Thymocytes Studied by Potential-Sensitive Fluorescent Probe. Journal of Membrane Biology, 2020, 253, 343-356.	2.1	10

#	ARTICLE	IF	CITATIONS
7383	Machine-learned interatomic potentials by active learning: amorphous and liquid hafnium dioxide. Npj Computational Materials, 2020, 6, .	8.7	100
7384	Atomistic Modeling of Grain Boundary Migration in Nickel. Advanced Engineering Materials, 2020, 22, 2000115.	3.5	3
7385	A Computational and Modeling Study of the Reaction Mechanism of <i>Staphylococcus aureus</i> Monoglycosyltransferase Reveals New Insights on the GT51 Family of Enzymes. Journal of Chemical Information and Modeling, 2020, 60, 5513-5528.	5.4	3
7386	Transport Properties of Ionic Liquid and Sodium Salt Mixtures for Sodium-Ion Battery Electrolytes from Molecular Dynamics Simulation with a Self-Consistent Atomic Charge Determination. Journal of Physical Chemistry B, 2020, 124, 7291-7305.	2.6	22
7387	Identification of potential drug candidates to combat COVID-19: a structural study using the main protease (mpro) of SARS-CoV-2. Journal of Biomolecular Structure and Dynamics, 2021, 39, 6649-6659.	3.5	25
7388	Insights into the synergistic mechanism of target resistance: A case study of N. lugens RDL-GABA receptors and fipronil. Biophysical Chemistry, 2020, 265, 106426.	2.8	4
7389	A novel approach to calculate protein adsorption isotherms by molecular dynamics simulations. Journal of Chromatography A, 2020, 1620, 460940.	3.7	4
7390	GlyT1 encephalopathy: Characterization of presumably disease causing GlyT1 mutations. Neurochemistry International, 2020, 139, 104813.	3.8	7
7391	Pattern and Dynamics of FLT3 Duplications. Journal of Chemical Information and Modeling, 2020, 60, 4005-4020.	5.4	8
7392	Structural Characterization of Sphingomonas sp. KT-1 PahZ1-Catalyzed Biodegradation of Thermally Synthesized Poly(aspartic acid). ACS Sustainable Chemistry and Engineering, 2020, , .	6.7	1
7393	Structural dynamics of the GluK3-kainate receptor neurotransmitter binding domains revealed by cryo-EM. International Journal of Biological Macromolecules, 2020, 149, 1051-1058.	7.5	11
7394	A6H polypeptide membranes: Molecular dynamics simulation, GIAO-DFT-NMR and TD-DFT spectroscopy analysis. Journal of Molecular Liquids, 2020, 316, 113850.	4.9	19
7395	Versatile Dimerisation Process of Translocator Protein (TSPO) Revealed by an Extensive Sampling Based on a Coarse-Grained Dynamics Study. Journal of Chemical Information and Modeling, 2020, 60, 3944-3957.	5.4	7
7396	Dueling Backbones: Comparing Peptoid and Peptide Analogues of a Mussel Adhesive Protein. Macromolecules, 2020, 53, 6767-6779.	4.8	16
7397	Mechanism of Cell Penetration by Permeabilization of Late Endosomes: Interplay between a Multivalent TAT Peptide and Bis(monoacylglycero)phosphate. Cell Chemical Biology, 2020, 27, 1296-1307.e5.	5.2	23
7398	Discovery of Membrane-Permeating Cyclic Peptides via mRNA Display. Bioconjugate Chemistry, 2020, 31, 2325-2338.	3.6	9
7399	Genetic Algorithm Driven Force Field Parameterization for Molten Alkali-Metal Carbonate and Hydroxide Salts. Journal of Chemical Theory and Computation, 2020, 16, 5736-5746.	5.3	12
7400	<sc>d</sc>-Retro Inverso Amylin and the Stability of Amylin Fibrils. Journal of Chemical Theory and Computation, 2020, 16, 5358-5368.	5.3	13

#	ARTICLE	IF	CITATIONS
7401	Mechanisms of Ion Transport in Lithium Salt-Doped Polymeric Ionic Liquid Electrolytes. <i>Macromolecules</i> , 2020, 53, 6995-7008.	4.8	24
7402	Dual mechanism of ionic liquid-induced protein unfolding. <i>Physical Chemistry Chemical Physics</i> , 2020, 22, 19779-19786.	2.8	17
7403	Construction of the R17L mutant of MtC1LPMO for improved lignocellulosic biomass conversion by rational point mutation and investigation of the mechanism by molecular dynamics simulations. <i>Bioresource Technology</i> , 2020, 317, 124024.	9.6	23
7404	Efficient Conformational Sampling of Collective Motions of Proteins with Principal Component Analysis-Based Parallel Cascade Selection Molecular Dynamics. <i>Journal of Chemical Information and Modeling</i> , 2020, 60, 4021-4029.	5.4	10
7405	MARTINI-Compatible Coarse-Grained Model for the Mesoscale Simulation of Peptoids. <i>Journal of Physical Chemistry B</i> , 2020, 124, 7745-7764.	2.6	28
7406	Mechanisms of activation and desensitization of full-length glycine receptor in lipid nanodiscs. <i>Nature Communications</i> , 2020, 11, 3752.	12.8	74
7407	Theoretical spectroscopy of isotopically dilute water and hydrophobicity. <i>Journal of Chemical Physics</i> , 2020, 153, 094501.	3.0	4
7408	Granular packings with sliding, rolling, and twisting friction. <i>Physical Review E</i> , 2020, 102, 032903.	2.1	31
7409	Conformation of ultra-long-chain fatty acid in lipid bilayer: Molecular dynamics study. <i>Journal of Chemical Physics</i> , 2020, 153, 165101.	3.0	5
7410	Machine learning driven simulated deposition of carbon films: From low-density to diamondlike amorphous carbon. <i>Physical Review B</i> , 2020, 102, .	3.2	44
7411	K <sub>2P</sub> channel C-type gating involves asymmetric selectivity filter order-disorder transitions. <i>Science Advances</i> , 2020, 6, .	10.3	52
7412	Understanding High-Salt and Cold Adaptation of a Polyextremophilic Enzyme. <i>Microorganisms</i> , 2020, 8, 1594.	3.6	30
7413	Identification of promising molecules against MurD ligase from <i>Acinetobacter baumannii</i> : insights from comparative protein modelling, virtual screening, molecular dynamics simulations and MM/PBSA analysis. <i>Journal of Molecular Modeling</i> , 2020, 26, 304.	1.8	11
7414	Tuning the hydrophobicity of a coarse grained model of 1,2-dipalmitoyl-sn-glycero-3-phosphatidylcholine using the experimental octanol-water partition coefficient. <i>Journal of Molecular Liquids</i> , 2020, 319, 114132.	4.9	13
7415	Ultrafast Aqueous Dynamics in Concentrated Electrolytic Solutions of Lithium Salt and Ionic Liquid. <i>Journal of Physical Chemistry B</i> , 2020, 124, 9898-9912.	2.6	12
7416	Discovery of Potential Chemical Probe as Inhibitors of CXCL12 Using Ligand-Based Virtual Screening and Molecular Dynamic Simulation. <i>Molecules</i> , 2020, 25, 4829.	3.8	7
7417	A computer-simulated mechanism of familial Alzheimer's disease: Mutations enhance thermal dynamics and favor looser substrate-binding to $\beta$ -secretase. <i>Journal of Structural Biology</i> , 2020, 212, 107648.	2.8	18
7418	High-Level Antibiotic Tolerance of a Clinically Isolated <i>Enterococcus faecalis</i> Strain. <i>Applied and Environmental Microbiology</i> , 2020, 87, .	3.1	2

#	ARTICLE	IF	CITATIONS
7419	Molecular Dynamics Simulations of the Full-Length Prion Protein. Lobachevskii Journal of Mathematics, 2020, 41, 1502-1508.	0.9	2
7420	New insights on human IRE1 tetramer structures based on molecular modeling. Scientific Reports, 2020, 10, 17490.	3.3	5
7421	The structure of the antimicrobial human cathelicidin LL-37 shows oligomerization and channel formation in the presence of membrane mimics. Scientific Reports, 2020, 10, 17356.	3.3	54
7422	Critical Sequence Hotspots for Binding of Novel Coronavirus to Angiotensin Converter Enzyme as Evaluated by Molecular Simulations. Journal of Physical Chemistry B, 2020, 124, 10034-10047.	2.6	54
7423	Allosteric regulation of glutamate dehydrogenase deamination activity. Scientific Reports, 2020, 10, 16523.	3.3	8
7424	Using coarse-grained molecular dynamics to rationalize biomolecule solubilization mechanisms in ionic liquid-based colloidal systems. Physical Chemistry Chemical Physics, 2020, 22, 24771-24783.	2.8	9
7425	An able-cryoprotectant and a moderate denaturant: distinctive character of ethylene glycol on protein stability. Journal of Biomolecular Structure and Dynamics, 2020, , 1-13.	3.5	1
7426	A general-purpose machine-learning force field for bulk and nanostructured phosphorus. Nature Communications, 2020, 11, 5461.	12.8	72
7427	An allosteric interaction controls the activation mechanism of SHP2 tyrosine phosphatase. Scientific Reports, 2020, 10, 18530.	3.3	23
7428	Molecular dynamics investigation of wetting&ldquo;dewetting behavior of reline DES nanodroplet at model carbon material. Journal of Chemical Physics, 2020, 153, 164704.	3.0	11
7429	<i>Uncaria tomentosa</i> (cat&supm;s claw): a promising herbal medicine against SARS-CoV-2/ACE-2 junction and SARS-CoV-2 spike protein based on molecular modeling. Journal of Biomolecular Structure and Dynamics, 2022, 40, 2227-2243.	3.5	29
7430	How do nitrated lipids affect the properties of phospholipid membranes?. Archives of Biochemistry and Biophysics, 2020, 695, 108548.	3.0	10
7431	Polymorphism in a Nonsensitive-High-Energy Material: Discovery of a New Polymorph and Crystal Structure of 4,4&sup2,5,5&sup2-Tetranitro-1<i>H</i>,1&sup2<i>H</i>-[2,2&sup2-biimidazole]-1,1&sup2-diamine. Crystal Growth and Design, 2020, 20, 8005-8014.	3.0	20
7432	Dispersion state phase diagram of citrate-coated metallic nanoparticles in saline solutions. Nature Communications, 2020, 11, 5422.	12.8	47
7433	Ketohexokinase-A acts as a nuclear protein kinase that mediates fructose-induced metastasis in breast cancer. Nature Communications, 2020, 11, 5436.	12.8	38
7434	Making biological membrane resistant to the toxicity of misfolded protein oligomers: a lesson from trodusquemine. Nanoscale, 2020, 12, 22596-22614.	5.6	16
7435	Anti-inflammatory, antiallergic and COVID-19 protease inhibitory activities of phytochemicals from the Jordanian hawksbeard: identification, structure&ldquo;activity relationships, molecular modeling and impact on its folk medicinal uses. RSC Advances, 2020, 10, 38128-38141.	3.6	23
7436	<i>In silico</i> analysis of the interactions of certain flavonoids with the receptor-binding domain of 2019 novel coronavirus and cellular proteases and their pharmacokinetic properties. Journal of Biomolecular Structure and Dynamics, 2022, 40, 2460-2474.	3.5	22

#	ARTICLE	IF	CITATIONS
7437	Molecular Dynamics Study of Lipid and Cholesterol Reorganization Due to Membrane Binding and Pore Formation by Listeriolysin O. <i>Journal of Membrane Biology</i> , 2020, 253, 535-550.	2.1	20
7438	Ultrasonic plasticity of metallic glass near room temperature. <i>Applied Materials Today</i> , 2020, 21, 100866.	4.3	15
7439	Time-Resolved Fluorescence and Essential Dynamics Study on the Structural Heterogeneity of p53DBD Bound to the Anticancer p28 Peptide. <i>Journal of Physical Chemistry B</i> , 2020, 124, 9820-9828.	2.6	3
7440	Accounting for Vibronic Features through a Mixed Quantum-Classical Scheme: Structure, Dynamics, and Absorption Spectra of a Perylene Diimide Dye in Solution. <i>Journal of Chemical Theory and Computation</i> , 2020, 16, 7061-7077.	5.3	17
7441	The allosteric activation mechanism of a phospholipase A2-like toxin from <i>Bothrops jararacussu</i> venom: a dynamic description. <i>Scientific Reports</i> , 2020, 10, 16252.	3.3	14
7442	Mechanistic insights into the loss-of-function mechanisms of rare human D-amino acid oxidase variants implicated in amyotrophic lateral sclerosis. <i>Scientific Reports</i> , 2020, 10, 17146.	3.3	8
7443	Polyol and sugar osmolytes can shorten protein hydrogen bonds to modulate function. <i>Communications Biology</i> , 2020, 3, 528.	4.4	20
7444	Effective mass path integral simulations of quasiparticles in condensed phases. <i>Journal of Chemical Physics</i> , 2020, 153, 121104.	3.0	8
7445	Localization model description of the interfacial dynamics of crystalline Cu and Cu <sub>64</sub> Zr <sub>36</sub> metallic glass films. <i>Journal of Chemical Physics</i> , 2020, 153, 124508.	3.0	16
7446	Computational Study of the Ion and Water Permeation and Transport Mechanisms of the SARS-CoV-2 Pentameric E Protein Channel. <i>Frontiers in Molecular Biosciences</i> , 2020, 7, 565797.	3.5	26
7447	Design, synthesis and biological evaluation of anticholinesterase peptides: Fragment-based vs. template-based peptide design. <i>Bioorganic Chemistry</i> , 2020, 105, 104351.	4.1	4
7448	Effects of sodium and calcium chloride ionic stresses on model yeast membranes revealed by molecular dynamics simulation. <i>Chemistry and Physics of Lipids</i> , 2020, 233, 104980.	3.2	4
7449	In silico characterisation of olive phenolic compounds as potential cyclooxygenase modulators. Part 2. <i>Journal of Molecular Graphics and Modelling</i> , 2020, 101, 107743.	2.4	1
7450	Cryo-EM structure of the complete and ligand-saturated insulin receptor ectodomain. <i>Journal of Cell Biology</i> , 2020, 219, .	5.2	84
7451	Development of Charge-Augmented Three-Point Water Model (CAIP3P) for Accurate Simulations of Intrinsically Disordered Proteins. <i>International Journal of Molecular Sciences</i> , 2020, 21, 6166.	4.1	5
7452	On the X-ray Scattering Pre-peak of Linear Mono-ols and the Related Microstructure from Computer Simulations. <i>Journal of Physical Chemistry B</i> , 2020, 124, 8358-8371.	2.6	27
7453	Assessment of Sulfur-Functionalized MXenes for Li-Ion Battery Applications. <i>Journal of Physical Chemistry C</i> , 2020, 124, 21293-21304.	3.1	22
7454	Preferential Orientations and Anomalous Interfacial Tensions in Aqueous Solutions of Alcohols. <i>Journal of Physical Chemistry B</i> , 2020, 124, 8388-8401.	2.6	3

#	ARTICLE	IF	CITATIONS
7455	Insights into Salinity Variations for Waterfloods, Frac-Fluids and Drilling Mud in Clay-Hosted Pores using Molecular Simulations. , 2020, , .		1
7456	The Role of APOSTART in Switching between Sexuality and Apomixis in <i>Poa pratensis</i> . <i>Genes</i> , 2020, 11, 941.	2.4	7
7457	Modeling the Role of a Flexible Loop and Active Site Side Chains in Hydride Transfer Catalyzed by Glycerol-3-phosphate Dehydrogenase. <i>ACS Catalysis</i> , 2020, 10, 11253-11267.	11.2	14
7458	Outer Membranes of Polymyxin-Resistant <i>Acinetobacter baumannii</i> with Phosphoethanolamine-Modified Lipid A and Lipopolysaccharide Loss Display Different Atomic-Scale Interactions with Polymyxins. <i>ACS Infectious Diseases</i> , 2020, 6, 2698-2708.	3.8	19
7459	Molecular Bases of the Membrane Association Mechanism Potentiating Antibiotic Resistance by New Delhi Metallo- $\beta$ -lactamase 1. <i>ACS Infectious Diseases</i> , 2020, 6, 2719-2731.	3.8	11
7460	EOR in Clay-Hosted Pores: Effects of Brine Salinity, Water Saturation, Pore Surface Chemistry and Pore Width. , 2020, , .		0
7461	Phase Boundary and Salt Partitioning in Coacervate Complexes Formed between Poly(acrylic acid) and Poly( <i>N,N</i> -dimethylaminoethyl methacrylate) from Detailed Atomistic Simulations Combined with Free Energy Perturbation and Thermodynamic Integration Calculations. <i>Macromolecules</i> , 2020, 53, 7618-7634.	4.8	7
7462	Free-energy landscape of polymer-crystal polymorphism. <i>Soft Matter</i> , 2020, 16, 9683-9692.	2.7	9
7463	Molecular insight into the anion effect and free volume effect of CO <sub>2</sub> solubility in multivalent ionic liquids. <i>Physical Chemistry Chemical Physics</i> , 2020, 22, 20618-20633.	2.8	27
7464	An insight into de Vries behaviour of smectic liquid crystals from atomistic molecular dynamics simulations. <i>Journal of Materials Chemistry C</i> , 2020, 8, 13040-13052.	5.5	6
7465	Reconstitution of autophagosome nucleation defines Atg9 vesicles as seeds for membrane formation. <i>Science</i> , 2020, 369, .	12.6	159
7466	Estimating the accuracy of the MARTINI model towards the investigation of peripheral protein-membrane interactions. <i>Faraday Discussions</i> , 2021, 232, 131-148.	3.2	25
7467	Orchestrated actin nucleation by the <i>Candida albicans</i> polarisome complex enables filamentous growth. <i>Journal of Biological Chemistry</i> , 2020, 295, 14840-14854.	3.4	16
7468	Characterizing the binding and function of TARP $\beta$ -selective AMPA receptor modulators. <i>Journal of Biological Chemistry</i> , 2020, 295, 14565-14577.	3.4	19
7469	The role of disulfide bonds in a <i>Solanum tuberosum</i> saposin-like protein investigated using molecular dynamics. <i>PLoS ONE</i> , 2020, 15, e0237884.	2.5	4
7470	An Unusual Amino Acid Substitution Within Hummingbird Cytochrome <i>c</i> Oxidase Alters a Key Proton-Conducting Channel. <i>G3: Genes, Genomes, Genetics</i> , 2020, 10, 2477-2485.	1.8	4
7471	Enhanced Conformational Sampling Method Based on Anomaly Detection Parallel Cascade Selection Molecular Dynamics: ad-PaCS-MD. <i>Journal of Chemical Theory and Computation</i> , 2020, 16, 6716-6725.	5.3	2
7472	Cholesterol Localization around the Metabotropic Glutamate Receptor 2. <i>Journal of Physical Chemistry B</i> , 2020, 124, 9061-9078.	2.6	3



#	ARTICLE	IF	CITATIONS
7473	Stabilization of Lipid Membranes through Partitioning of the Blood Bag Plasticizer Di-2-ethylhexyl phthalate (DEHP). <i>Langmuir</i> , 2020, 36, 11899-11907.	3.5	15
7474	Water-Assisted Increase of Ionic Conductivity of Lithium Poly(acrylic acid)-Based Aqueous Polymer Electrolyte. <i>ACS Applied Energy Materials</i> , 2020, 3, 10119-10130.	5.1	19
7475	Effect of surface chemistry on islet amyloid polypeptide conformation. <i>Biointerphases</i> , 2020, 15, 051001.	1.6	7
7476	The Product of Matrix Metalloproteinase Cleavage of Doxorubicin Conjugate for Anticancer Drug Delivery: Calorimetric, Spectroscopic, and Molecular Dynamics Studies on Peptideâ€“Doxorubicin Binding to DNA. <i>International Journal of Molecular Sciences</i> , 2020, 21, 6923.	4.1	7
7477	Interfacial Water Structure at Zwitterionic Membrane/Water Interface: The Importance of Interactions between Water and Lipid Carbonyl Groups. <i>ACS Omega</i> , 2020, 5, 18080-18090.	3.5	7
7478	Ensemble-based enzyme design can recapitulate the effects of laboratory directed evolution in silico. <i>Nature Communications</i> , 2020, 11, 4808.	12.8	67
7479	Comparative analysis of ethanol dynamics in aqueous and non-aqueous solutions. <i>Physical Chemistry Chemical Physics</i> , 2020, 22, 23856-23868.	2.8	8
7480	Molecular modeling and dynamic simulation of chicken Mx protein with the S631N polymorphism. <i>Journal of Biomolecular Structure and Dynamics</i> , 2022, 40, 612-621.	3.5	4
7481	Repurposing of the approved small molecule drugs in order to inhibit SARS-CoV-2â€™S protein and human ACE2 interaction through virtual screening approaches. <i>Journal of Biomolecular Structure and Dynamics</i> , 2022, 40, 1299-1315.	3.5	38
7482	Allosteric Inhibition of Adenylyl Cyclase Type 5 by G-Protein: A Molecular Dynamics Study. <i>Biomolecules</i> , 2020, 10, 1330.	4.0	6
7483	Elucidation of molecular interaction of bioactive flavonoid luteolin with human serum albumin and its glycosylated analogue using multi-spectroscopic and computational studies. <i>Journal of Molecular Liquids</i> , 2020, 318, 114147.	4.9	38
7484	Molecular Dynamics Simulation of Molecular Crystals under Anisotropic Compression: Bulk and Directional Effects in Anthracene and Paracetamol. <i>Crystal Growth and Design</i> , 2020, 20, 7421-7428.	3.0	6
7485	Amphiphilic gold nanoparticles perturb phase separation in multidomain lipid membranes. <i>Nanoscale</i> , 2020, 12, 19746-19759.	5.6	23
7486	Experimental and Theoretical Study of Emodin Interaction with Phospholipid Bilayer and Linoleic Acid. <i>Applied Magnetic Resonance</i> , 2020, 51, 951-960.	1.2	6
7487	Molecular Dynamics Simulation on Creep Behavior of Nanocrystalline TiAl Alloy. <i>Nanomaterials</i> , 2020, 10, 1693.	4.1	12
7488	Structure of the Plasmodium falciparum PfSERA5 pseudoâ€“zymogen. <i>Protein Science</i> , 2020, 29, 2245-2258.	7.6	3
7489	Unraveling Molecular Interactions in Liquidâ€“Liquid Phase Separation of Disordered Proteins by Atomistic Simulations. <i>Journal of Physical Chemistry B</i> , 2020, 124, 9009-9016.	2.6	103
7490	A Benzene-Mapping Approach for Uncovering Cryptic Pockets in Membrane-Bound Proteins. <i>Journal of Chemical Theory and Computation</i> , 2020, 16, 5948-5959.	5.3	6

#	ARTICLE	IF	CITATIONS
7491	Discovering Protein Conformational Flexibility through Artificial-Intelligence-Aided Molecular Dynamics. <i>Journal of Physical Chemistry B</i> , 2020, 124, 8221-8229.	2.6	22
7492	Structural basis for antibiotic action of the B1 antivitamin 2- $\epsilon$ -methoxy-thiamine. <i>Nature Chemical Biology</i> , 2020, 16, 1237-1245.	8.0	13
7493	Fluorescence-Labeled Amyloid Beta Monomer: A Molecular Dynamical Study. <i>Molecules</i> , 2020, 25, 3524.	3.8	3
7494	On the Correlation between Pair Hydrophobicity and Mixing Enthalpies in Water-Alcohol Binary Mixtures. <i>Journal of Physical Chemistry B</i> , 2020, 124, 8023-8031.	2.6	7
7495	A potential for molecular simulation of compounds with linear moieties. <i>Journal of Chemical Physics</i> , 2020, 153, 084503.	3.0	5
7496	Tracking the motion of the K V 1.2 voltage sensor reveals the molecular perturbations caused by a de novo mutation in a case of epilepsy. <i>Journal of Physiology</i> , 2020, 598, 5245-5269.	2.9	7
7497	Differential Stability of Aurein 1.2 Pores in Model Membranes of Two Probiotic Strains. <i>Journal of Chemical Information and Modeling</i> , 2020, 60, 5142-5152.	5.4	5
7498	Liquid-Liquid Phase Separation of Viologen Bistriflimide/Benzene Mixtures: Role of the Dual Ionic and Organic Nature of Ionic Liquids. <i>Journal of Physical Chemistry B</i> , 2020, 124, 7929-7937.	2.6	9
7499	Effects of Solvent Polarity on Li-ion Diffusion in Polymer Electrolytes: An All-Atom Molecular Dynamics Study with Charge Scaling. <i>Journal of Physical Chemistry B</i> , 2020, 124, 8124-8131.	2.6	35
7500	Enhancing intracellular accumulation and target engagement of PROTACs with reversible covalent chemistry. <i>Nature Communications</i> , 2020, 11, 4268.	12.8	112
7501	In Silico Identification of Potential Natural Product Inhibitors of Human Proteases Key to SARS-CoV-2 Infection. <i>Molecules</i> , 2020, 25, 3822.	3.8	51
7502	Tail-Oxidized Cholesterol Enhances Membrane Permeability for Small Solutes. <i>Langmuir</i> , 2020, 36, 10438-10447.	3.5	24
7503	The effect of surfactants on hydrate particle agglomeration in liquid hydrocarbon continuous systems: a molecular dynamics simulation study. <i>RSC Advances</i> , 2020, 10, 31027-31038.	3.6	21
7504	Mechanism for H <sub>2</sub> diffusion in sII hydrates by molecular dynamics simulations. <i>Journal of Chemical Physics</i> , 2020, 153, 054706.	3.0	8
7505	Accurate Estimation of Membrane Capacitance from Atomistic Molecular Dynamics Simulations of Zwitterionic Lipid Bilayers. <i>Journal of Physical Chemistry B</i> , 2020, 124, 8278-8286.	2.6	11
7506	Targeting homologous recombination (HR) repair mechanism for cancer treatment: discovery of new potential UCHL-3 inhibitors via virtual screening, molecular dynamics and binding mode analysis. <i>Journal of Biomolecular Structure and Dynamics</i> , 2022, 40, 276-289.	3.5	4
7507	Functional Impact of the G279S Substitution in the Adenosine A <sub>1</sub> -Receptor (A <sub>1</sub> -R-G279S <sup>7.44</sup> ), a Mutation Associated with Parkinson's Disease. <i>Molecular Pharmacology</i> , 2020, 98, 250-266.	2.3	2
7508	Molecular Dynamics Simulation of Amorphous Poly(3-hexylthiophene). <i>Macromolecules</i> , 2020, 53, 7810-7824.	4.8	13

#	ARTICLE	IF	CITATIONS
7509	Adduct of the blistering warfare agent sesquimustard with human serum albumin and its mass spectrometric identification for biomedical verification of exposure. <i>Analytical and Bioanalytical Chemistry</i> , 2020, 412, 7723-7737.	3.7	14
7510	Rigorous Computational Study Reveals What Docking Overlooks: Double Trouble from Membrane Association in Protein Kinase C Modulators. <i>Journal of Chemical Information and Modeling</i> , 2020, 60, 5624-5633.	5.4	6
7511	BAK core dimers bind lipids and can be bridged by them. <i>Nature Structural and Molecular Biology</i> , 2020, 27, 1024-1031.	8.2	49
7512	Simulations of octapeptinâ€‘outer membrane interactions reveal conformational flexibility is linked to antimicrobial potency. <i>Journal of Biological Chemistry</i> , 2020, 295, 15902-15912.	3.4	13
7513	Molecular modelling study on pyrrolo[2,3- <i>b</i> ]pyridine derivatives as c-Met kinase inhibitors: a combined approach using molecular docking, 3D-QSAR modelling and molecular dynamics simulation. <i>Molecular Simulation</i> , 2020, 46, 1265-1280.	2.0	6
7514	Measles Virus Hemagglutinin Protein Establishes a Specific Interaction With the Extreme N-Terminal Region of Human Signaling Lymphocytic Activation Molecule to Enhance Infection. <i>Frontiers in Microbiology</i> , 2020, 11, 1830.	3.5	4
7515	Cooperative Effects of an Antifungal Moiety and DMSO on Pore Formation over Lipid Membranes Revealed by Free Energy Calculations. <i>Journal of Physical Chemistry B</i> , 2020, 124, 8811-8821.	2.6	6
7516	Statistical Inference of Transport Mechanisms and Long Time Scale Behavior from Time Series of Solute Trajectories in Nanostructured Membranes. <i>Journal of Physical Chemistry B</i> , 2020, 124, 8110-8123.	2.6	7
7517	Structures of the stator complex that drives rotation of the bacterial flagellum. <i>Nature Microbiology</i> , 2020, 5, 1553-1564.	13.3	131
7518	Conformational dynamics of amyloid-Î² (16â€‘22) peptide in aqueous ionic liquids. <i>RSC Advances</i> , 2020, 10, 33248-33260.	3.6	5
7519	Attenuated total reflectance far-ultraviolet and deep-ultraviolet spectroscopy analysis of the electronic structure of a dicyanamide-based ionic liquid with Li <sup>+</sup> . <i>Physical Chemistry Chemical Physics</i> , 2020, 22, 21768-21775.	2.8	7
7520	Diffusivities in Binary Mixtures of [AMIM][NTf <sub>2</sub> ] Ionic Liquids with the Dissolved Gases H <sub>2</sub> , He, N <sub>2</sub> , CO, CO <sub>2</sub> , or Kr Close to Infinite Dilution. <i>Journal of Chemical &amp; Engineering Data</i> , 2020, 65, 4116-4129.	1.9	21
7521	Impregnation of Poly(methyl methacrylate) with Carbamazepine in Supercritical Carbon Dioxide: Molecular Dynamics Simulation. <i>Journal of Physical Chemistry B</i> , 2020, 124, 8410-8417.	2.6	12
7522	Martini coarse-grained models of imidazolium-based ionic liquids: from nanostructural organization to liquidâ€‘liquid extraction. <i>Green Chemistry</i> , 2020, 22, 7376-7386.	9.0	45
7523	Effects of masking titanium with a one-atom-thick carbon layer on the adsorption of nitrogen monoxide, nitrogen dioxide, ozone, and formaldehyde. <i>Journal of Materials Science</i> , 2020, 55, 17000-17018.	3.7	2
7524	Transmembrane potential of physiologically relevant model membranes: Effects of membrane asymmetry. <i>Journal of Chemical Physics</i> , 2020, 153, 105103.	3.0	5
7525	Morphing of Amphipathic Helices to Explore the Activity and Selectivity of Membranolytic Antimicrobial Peptides. <i>Biochemistry</i> , 2020, 59, 3772-3781.	2.5	4
7526	Chirality Effects in Biomolecular Systems: Calculation of the Relative Free Energies by Molecular Dynamics Simulations. <i>Journal of Chemical Information and Modeling</i> , 2020, 60, 5424-5436.	5.4	2

#	ARTICLE	IF	CITATIONS
7527	<i>In silico</i> investigation of spice molecules as potent inhibitor of SARS-CoV-2. Journal of Biomolecular Structure and Dynamics, 2022, 40, 860-874.	3.5	35
7528	Phosphorylation regulates the binding of intrinsically disordered proteins via a flexible conformation selection mechanism. Communications Chemistry, 2020, 3, .	4.5	25
7529	Mapping the Structural and Dynamic Determinants of pH-Sensitive Heparin Binding to Granulocyte Macrophage Colony Stimulating Factor. Biochemistry, 2020, 59, 3541-3553.	2.5	4
7530	Experimentally Consistent Simulation of $\text{Al}^{2+}$ Peptides with a Minimal NMR Bias. Journal of Physical Chemistry B, 2020, 124, 8266-8277.	2.6	2
7531	Microsecond scale sampling of Egr-1 conformational landscape to decipher the impact of its disorder regions on structure–function relationship. Molecular Simulation, 2020, 46, 1255-1264.	2.0	2
7532	Microtubule instability driven by longitudinal and lateral strain propagation. PLoS Computational Biology, 2020, 16, e1008132.	3.2	15
7533	Mechanistic Insight Into the Antifungal Effects of a Fatty Acid Derivative Against Drug-Resistant Fungal Infections. Frontiers in Microbiology, 2020, 11, 2116.	3.5	16
7534	Molecular-Scale Strategies to Achieve High Efficiency and Low Efficiency Roll-Off in Simplified Solution-Processed Organic Light-Emitting Diodes. Advanced Functional Materials, 2020, 30, 2005292.	14.9	21
7535	Connection between liquid and non-crystalline solid phases in water. Journal of Chemical Physics, 2020, 153, 104503.	3.0	25
7536	Repurposing of FDA-Approved Toremifene to Treat COVID-19 by Blocking the Spike Glycoprotein and NSP14 of SARS-CoV-2. Journal of Proteome Research, 2020, 19, 4670-4677.	3.7	55
7537	Dissipative particle dynamics model of homogalacturonan based on molecular dynamics simulations. Scientific Reports, 2020, 10, 14691.	3.3	17
7538	Cryo-EM structure of human Cx31.3/GJC3 connexin hemichannel. Science Advances, 2020, 6, eaba4996.	10.3	46
7539	Targeting the Initiator Protease of the Classical Pathway of Complement Using Fragment-Based Drug Discovery. Molecules, 2020, 25, 4016.	3.8	9
7540	Solvent-induced membrane stress in biofuel production: molecular insights from small-angle scattering and all-atom molecular dynamics simulations. Green Chemistry, 2020, 22, 8278-8288.	9.0	9
7541	Orientation and Conformation of Proteins at the Air–Water Interface Determined from Integrative Molecular Dynamics Simulations and Sum Frequency Generation Spectroscopy. Langmuir, 2020, 36, 11855-11865.	3.5	30
7542	Molecular dynamics simulations informed by membrane lipidomics reveal the structure–interaction relationship of polymyxins with the lipid A-based outer membrane of <i>Acinetobacter baumannii</i> . Journal of Antimicrobial Chemotherapy, 2020, 75, 3534-3543.	3.0	25
7543	Enhancing cellulosic ethanol production through coevolution of multiple enzymatic characteristics of $\beta$ -glucosidase from <i>Penicillium oxalicum</i> 16. Applied Microbiology and Biotechnology, 2020, 104, 8299-8308.	3.6	10
7544	Self-assembly and mesophase formation in a non-ionic chromonic liquid crystal: insights from bottom-up and top-down coarse-grained simulation models. Soft Matter, 2020, 16, 9488-9498.	2.7	16

#	ARTICLE	IF	CITATIONS
7545	ADD Force Field for Sugars and Polyols: Predicting the Additivity of Proteinâ€“Osmolyte Interaction. Journal of Physical Chemistry B, 2020, 124, 7779-7790.	2.6	11
7546	Capturing Biologically Complex Tissue-Specific Membranes at Different Levels of Compositional Complexity. Journal of Physical Chemistry B, 2020, 124, 7819-7829.	2.6	47
7547	In situ structural analysis of SARS-CoV-2 spike reveals flexibility mediated by three hinges. Science, 2020, 370, 203-208.	12.6	531
7548	Improved GROMOS 54A7 Charge Sets for Phosphorylated Tyr, Ser, and Thr to Deal with pH-Dependent Binding Phenomena. Journal of Chemical Theory and Computation, 2020, 16, 6368-6376.	5.3	12
7549	Low-Frequency Spectra of 1-Methyl-3-octylimidazolium Tetrafluoroborate Mixtures with Methanol, Acetonitrile, and Dimethyl Sulfoxide: A Combined Study of Femtosecond Raman-Induced Kerr Effect Spectroscopy and Molecular Dynamics Simulations. Journal of Physical Chemistry B, 2020, 124, 7857-7871.	2.6	9
7550	Entropyâ€“Enthalpy Compensation in Peptide Adsorption on Solid Surfaces: Dependence on Surface Hydration. Langmuir, 2020, 36, 10822-10829.	3.5	15
7551	Alkyl-Substituted Selenium-Bridged V-Shaped Organic Semiconductors Exhibiting High Hole Mobility and Unusual Aggregation Behavior. Journal of the American Chemical Society, 2020, 142, 14974-14984.	13.7	25
7552	Stereochemical Effects on the Self-Assembly of Pyrenylalanine-Phenylalanine Dipeptide. Bulletin of the Chemical Society of Japan, 2020, 93, 969-977.	3.2	8
7553	Evidence for Disruption of Mg <sup>2+</sup> Pair as a Resistance Mechanism Against HIV-1 Integrase Strand Transfer Inhibitors. Frontiers in Molecular Biosciences, 2020, 7, 170.	3.5	2
7554	Putative SARS-CoV-2 Mpro Inhibitors from an In-House Library of Natural and Nature-Inspired Products: A Virtual Screening and Molecular Docking Study. Molecules, 2020, 25, 3745.	3.8	29
7555	Factors Responsible for the Aggregation of Poly(vinyl alcohol) in Aqueous Solution as Revealed by Molecular Dynamics Simulations. Industrial & Engineering Chemistry Research, 2020, 59, 16099-16111.	3.7	6
7556	Comparison and Evaluation of Force Fields for Intrinsically Disordered Proteins. Journal of Chemical Information and Modeling, 2020, 60, 4912-4923.	5.4	55
7557	Terminal Capping of an Amyloidogenic Tau Fragment Modulates Its Fibrillation Propensity. Journal of Physical Chemistry B, 2020, 124, 8772-8783.	2.6	17
7558	Downhill (Un)Folding Coupled to Binding as a Mechanism for Engineering Broadband Protein Conformational Transducers. ACS Synthetic Biology, 2020, 9, 2427-2439.	3.8	3
7559	An Alternative HIV-1 Non-Nucleoside Reverse Transcriptase Inhibition Mechanism: Targeting the p51 Subunit. Molecules, 2020, 25, 5902.	3.8	5
7560	Solidâ€“solid phase transition of tungsten induced by high pressure: A molecular dynamics simulation. Transactions of Nonferrous Metals Society of China, 2020, 30, 2980-2993.	4.2	11
7561	Probing relaxation models by means of Fast Field-Cycling relaxometry, NMR spectroscopy and molecular dynamics simulations: Detailed insight into the translational and rotational dynamics of a protic ionic liquid. Journal of Molecular Liquids, 2020, 319, 114207.	4.9	12
7562	Molecular Perspective on Water Vapor Accommodation into Ice and Its Dependence on Temperature. Journal of Physical Chemistry A, 2020, 124, 10879-10889.	2.5	3

#	ARTICLE	IF	CITATIONS
7563	Uptake of monoaromatic hydrocarbons during biodegradation by FadL channel-mediated lateral diffusion. <i>Nature Communications</i> , 2020, 11, 6331.	12.8	10
7564	Specifically bound BZIP transcription factors modulate DNA supercoiling transitions. <i>Scientific Reports</i> , 2020, 10, 18795.	3.3	22
7565	Effect of pH on the influenza fusion peptide properties unveiled by constant-pH molecular dynamics simulations combined with experiment. <i>Scientific Reports</i> , 2020, 10, 20082.	3.3	14
7566	Evaluating inositol phospholipid interactions with inward rectifier potassium channels and characterising their role in disease. <i>Communications Chemistry</i> , 2020, 3, .	4.5	23
7567	A cosolvent surfactant mechanism affects polymer collapse in miscible good solvents. <i>Communications Chemistry</i> , 2020, 3, .	4.5	14
7568	A multiscale coarse-grained model to predict the molecular architecture and drug transport properties of modified chitosan hydrogels. <i>Soft Matter</i> , 2020, 16, 10591-10610.	2.7	13
7569	Effect of ligand conjugation site on the micellization of Bio-Targeted PLGA-Based nanohybrids: A computational biology approach. <i>Journal of Biomolecular Structure and Dynamics</i> , 2020, , 1-10.	3.5	3
7570	Molecular determinant of substrate binding and specificity of cytochrome P450 2J2. <i>Scientific Reports</i> , 2020, 10, 22267.	3.3	9
7571	Deep neural network modeling based virtual screening and prediction of potential inhibitors for renin protein. <i>Journal of Biomolecular Structure and Dynamics</i> , 2020, , 1-14.	3.5	2
7572	Insights Into the Binding Mechanism of GC7 to Deoxyhypusine Synthase in <i>Sulfolobus solfataricus</i> : A Thermophilic Model for the Design of New Hypusination Inhibitors. <i>Frontiers in Chemistry</i> , 2020, 8, 609942.	3.6	8
7573	Detailed Characterization of the Cooperative Binding of Piperine with Heat Shock Protein 70 by Molecular Biophysical Approaches. <i>Biomedicines</i> , 2020, 8, 629.	3.2	3
7574	Deciphering the Structure of the Gramicidin A Channel in the Presence of AOT Reverse Micelles in Pentane Using Molecular Dynamics Simulations. <i>Journal of Physical Chemistry B</i> , 2020, 124, 11802-11818.	2.6	3
7575	Activation barriers in Class F G protein-coupled receptors revealed by umbrella sampling simulations. <i>Organic and Biomolecular Chemistry</i> , 2020, 18, 9816-9825.	2.8	3
7576	Influence of Different Aromatic Hydrophobic Residues on the Antimicrobial Activity and Membrane Selectivity of BRBR-NH <sub>2</sub> Tetrapeptide. <i>Langmuir</i> , 2020, 36, 15331-15342.	3.5	6
7577	Distortion of the bilayer and dynamics of the BAM complex in lipid nanodiscs. <i>Communications Biology</i> , 2020, 3, 766.	4.4	32
7578	Multitarget in silico studies of <i>Ocimum menthiifolium</i> , family Lamiaceae against SARS-CoV-2 supported by molecular dynamics simulation. <i>Journal of Biomolecular Structure and Dynamics</i> , 2020, , 1-11.	3.5	16
7579	How to calculate pH-dependent binding rates for receptor–ligand systems based on thermodynamic simulations with different binding motifs. <i>Molecular Simulation</i> , 2020, 46, 1443-1452.	2.0	7
7580	Spontaneous Membrane Nanodomain Formation in the Absence or Presence of the Neurotransmitter Serotonin. <i>Frontiers in Cell and Developmental Biology</i> , 2020, 8, 601145.	3.7	17



#	ARTICLE	IF	CITATIONS
7581	Design, Screening, and Testing of Non-Rational Peptide Libraries with Antimicrobial Activity: In Silico and Experimental Approaches. <i>Antibiotics</i> , 2020, 9, 854.	3.7	20
7582	Long-range dynamic correlations regulate the catalytic activity of the bacterial tyrosine kinase Wzc. <i>Science Advances</i> , 2020, 6, .	10.3	10
7583	Structure-based dynamic analysis of the glycine cleavage system suggests key residues for control of a key reaction step. <i>Communications Biology</i> , 2020, 3, 756.	4.4	13
7584	Analyzing the weak dimerization of a cellulose binding module by analytical ultracentrifugation. <i>International Journal of Biological Macromolecules</i> , 2020, 163, 1995-2004.	7.5	10
7585	Molecular dynamics simulation for the quantitative prediction of experimental tensile strength of a polymer material. <i>Composites Part C: Open Access</i> , 2020, 2, 100041.	3.2	9
7586	Fluorine induced conformational switching and modulation in photophysical properties of 7-fluorotryptophan: Spectroscopic, quantum chemical calculation and molecular dynamics simulation studies. <i>Journal of Photochemistry and Photobiology</i> , 2020, 3-4, 100011.	2.5	5
7587	Interleaflet Decoupling in a Lipid Bilayer at Excess Cholesterol Probed by Spectroscopic Ellipsometry and Simulations. <i>Journal of Membrane Biology</i> , 2020, 253, 647-659.	2.1	0
7588	Supercomputer-Based Ensemble Docking Drug Discovery Pipeline with Application to Covid-19. <i>Journal of Chemical Information and Modeling</i> , 2020, 60, 5832-5852.	5.4	134
7589	Remdesivir Strongly Binds to Both RNA-Dependent RNA Polymerase and Main Protease of SARS-CoV-2: Evidence from Molecular Simulations. <i>Journal of Physical Chemistry B</i> , 2020, 124, 11337-11348.	2.6	71
7590	Depicting the inhibitory potential of polyphenols from <i>Isatis indigotica</i> root against the main protease of SARS CoV-2 using computational approaches. <i>Journal of Biomolecular Structure and Dynamics</i> , 2020, , 1-12.	3.5	21
7591	Weak scaling of the contact distance between two fluctuating interfaces with system size. <i>Physical Review E</i> , 2020, 102, 062801.	2.1	3
7592	Understanding the pH-Directed Self-Assembly of a Four-Arm Block Copolymer. <i>Macromolecules</i> , 2020, 53, 11065-11076.	4.8	10
7593	A hydrophobic ratchet entrenches molecular complexes. <i>Nature</i> , 2020, 588, 503-508.	27.8	75
7594	Computer-based identification of potential compounds from <i>Salviae miltiorrhizae</i> against Neirisaral adhesion A regulatory protein. <i>Journal of Biomolecular Structure and Dynamics</i> , 2020, , 1-13.	3.5	13
7595	Calmodulin acts as a state-dependent switch to control a cardiac potassium channel opening. <i>Science Advances</i> , 2020, 6, .	10.3	38
7596	TBK1-mediated phosphorylation of LC3C and GABARAP-2 controls autophagosome shedding by ATG4 protease. <i>EMBO Reports</i> , 2020, 21, e48317.	4.5	58
7597	Deciphering the Role of Filamin B Calponin-Homology Domain in Causing the Larsen Syndrome, Boomerang Dysplasia, and Atelosteogenesis Type I Spectrum Disorders via a Computational Approach. <i>Molecules</i> , 2020, 25, 5543.	3.8	10
7598	Intrinsic water layering next to soft, solid, hydrophobic, and hydrophilic substrates. <i>Journal of Chemical Physics</i> , 2020, 153, 224702.	3.0	1

#	ARTICLE	IF	CITATIONS
7599	Bottom-up derived flexible water model with dipole and quadrupole moments for coarse-grained molecular simulations. <i>Physical Chemistry Chemical Physics</i> , 2020, 22, 27394-27412.	2.8	3
7600	Structural Basis of Inhibition of the Pioneer Transcription Factor NF-Y by Suramin. <i>Cells</i> , 2020, 9, 2370.	4.1	8
7601	Revealing the Growth of H <sub>2</sub> + THF Binary Hydrate through Molecular Simulations. <i>Energy &amp; Fuels</i> , 2020, 34, 15004-15010.	5.1	13
7602	X-ray Structure, Bioinformatics Analysis, and Substrate Specificity of a 6-Phospho-Î <sup>2</sup> -glucosidase Glycoside Hydrolase 1 Enzyme from <i>Bacillus licheniformis</i> . <i>Journal of Chemical Information and Modeling</i> , 2020, 60, 6392-6407.	5.4	5
7603	Voronoi Polyhedra as a Tool for the Characterization of Inhomogeneous Distribution in 1-Butyl-3-methylimidazolium Cation-Based Ionic Liquids. <i>Journal of Physical Chemistry B</i> , 2020, 124, 10419-10434.	2.6	6
7604	Surface modification effects on nanocellulose “ molecular dynamics simulations using umbrella sampling and computational alchemy. <i>Journal of Materials Chemistry A</i> , 2020, 8, 23617-23627.	10.3	24
7605	QSAR Implementation for HIC Retention Time Prediction of mAbs Using Fab Structure: A Comparison between Structural Representations. <i>International Journal of Molecular Sciences</i> , 2020, 21, 8037.	4.1	6
7606	Stacking Interactions of Poly Para-Phenylene Vinylene Oligomers with Graphene and Single-Walled Carbon Nanotubes: A Molecular Dynamics Approach. <i>Molecules</i> , 2020, 25, 4812.	3.8	1
7607	Computational Design of BH3-Mimetic Peptide Inhibitors That Can Bind Specifically to Mcl-1 or Bcl-X <sub>L</sub> : Role of Non-Hot Spot Residues. <i>Biochemistry</i> , 2020, 59, 4379-4394.	2.5	8
7608	Examination of the Role of Mg <sup>2+</sup> in the Mechanism of Nucleotide Binding to the Monomeric YME1L AAA+ Domain. <i>Biochemistry</i> , 2020, 59, 4303-4320.	2.5	3
7609	Impact of Cholesterol Concentration and Lipid Phase on Structure and Fluctuation of Amyloid Precursor Protein. <i>Journal of Physical Chemistry B</i> , 2020, 124, 10173-10185.	2.6	9
7610	Heterogeneous Structures of Ionic Liquids as Probed by CO Rotation with Nuclear Magnetic Resonance Relaxation Analysis and Molecular Dynamics Simulations. <i>Journal of Physical Chemistry B</i> , 2020, 124, 10465-10476.	2.6	8
7611	Computer aided identification of potential SARS CoV-2 main protease inhibitors from diterpenoids and biflavonoids of <i>Torreya nucifera</i> leaves. <i>Journal of Biomolecular Structure and Dynamics</i> , 2022, 40, 2647-2662.	3.5	34
7612	Effect of chemical structure on complexation efficiency of aromatic drugs with cyclodextrins: The example of dibenzazepine derivatives. <i>Carbohydrate Polymers</i> , 2020, 250, 116957.	10.2	5
7613	Bilayer compositional asymmetry influences the nanoscopic to macroscopic phase domain size transition. <i>Chemistry and Physics of Lipids</i> , 2020, 232, 104972.	3.2	6
7614	Drug-loading capacity of polylactide-based micro- and nanoparticles “ Experimental and molecular modeling study. <i>International Journal of Pharmaceutics</i> , 2020, 591, 120031.	5.2	13
7615	Solvent Nuances Modulate the Decreasing Effect of a Model Asphaltene on Interfacial Tension. <i>Energy &amp; Fuels</i> , 2020, 34, 13862-13870.	5.1	2
7616	Molecular Insights into Guest and Composition Dependence of Mixed Hydrate Nucleation. <i>Journal of Physical Chemistry C</i> , 2020, 124, 25078-25086.	3.1	20

#	ARTICLE	IF	CITATIONS
7617	Multi-conformational frame from molecular dynamics as a structure-based pharmacophore model for mapping, screening and identifying ligands against PPAR- $\gamma$ : a new protocol to develop promising candidates. <i>Journal of Biomolecular Structure and Dynamics</i> , 2022, 40, 2663-2673.	3.5	5
7618	Small-molecule sequestration of amyloid- $\beta$ as a drug discovery strategy for Alzheimer's disease. <i>Science Advances</i> , 2020, 6, .	10.3	95
7619	Identification of New Antimicrobial Peptides from Mediterranean Medical Plant <i>Charybdis pancratium</i> (Steinh.) Speta. <i>Antibiotics</i> , 2020, 9, 747.	3.7	10
7620	Insights into the structural and thermodynamic properties of fullerols [C <sub>60</sub> (OH) <sub>n</sub> , n=12, 14, 16, 18, 20, 22, 24] in aqueous media. <i>Fluid Phase Equilibria</i> , 2020, 525, 112805.	2.5	4
7621	Protein disorder-to-order transition enhances the nucleosome-binding affinity of H1. <i>Nucleic Acids Research</i> , 2020, 48, 5318-5331.	14.5	19
7622	Lubricated friction around nanodefects. <i>Science Advances</i> , 2020, 6, eaaz3673.	10.3	20
7623	Robust, high-performance n-type organic semiconductors. <i>Science Advances</i> , 2020, 6, eaaz0632.	10.3	135
7624	Comparative Study of the Biphasic Behavior of Cyanex301 and Its Two Analogs by Molecular Dynamics Simulations. <i>Advanced Theory and Simulations</i> , 2020, 3, 1900242.	2.8	1
7625	Microtubule Simulations Provide Insight into the Molecular Mechanism Underlying Dynamic Instability. <i>Biophysical Journal</i> , 2020, 118, 2938-2951.	0.5	22
7626	Molecular dynamics simulation on Na <sup>+</sup> ion-pair association from ambient to supercritical water. <i>Fluid Phase Equilibria</i> , 2020, 516, 112615.	2.5	3
7627	Spontaneous lid closure and substrate-induced lid opening dynamics of human pancreatic lipase-related protein 2: A computational study. <i>Journal of Molecular Structure</i> , 2020, 1217, 128365.	3.6	6
7628	Modeling the Hydration-Induced Structural Transitions of the SAPO-34 Zeolite and Their Impact on the Water's Sorbed Phase Equilibrium and Dynamics. <i>Journal of Physical Chemistry C</i> , 2020, 124, 11480-11489.	3.1	4
7629	Hofmeister Series for Metal-Cation-RNA Interactions: The Interplay of Binding Affinity and Exchange Kinetics. <i>Langmuir</i> , 2020, 36, 5979-5989.	3.5	36
7630	Combining native and omics mass spectrometry to identify endogenous ligands bound to membrane proteins. <i>Nature Methods</i> , 2020, 17, 505-508.	19.0	111
7631	Structural investigations of molecular solutes within nanostructured ionic liquids. <i>Physical Chemistry Chemical Physics</i> , 2020, 22, 11593-11608.	2.8	7
7632	Molecular Dynamics Simulations of the Elusive Matrix-Open State of Mitochondrial ADP/ATP Carrier. <i>Israel Journal of Chemistry</i> , 2020, 60, 735-743.	2.3	11
7633	Role of Alcohol as a Cosurfactant at the Brine-Oil Interface under a Typical Reservoir Condition. <i>Langmuir</i> , 2020, 36, 5198-5207.	3.5	16
7634	Structural basis for divergent and convergent evolution of catalytic machineries in plant aromatic amino acid decarboxylase proteins. <i>Proceedings of the National Academy of Sciences of the United States of America</i> , 2020, 117, 10806-10817.	7.1	34

#	ARTICLE	IF	CITATIONS
7635	To be ionized or not to be ionized: the vital role of physicochemical properties of galbanic acid derivatives in AChE assay. <i>Journal of Biomolecular Structure and Dynamics</i> , 2021, 39, 1-9.	3.5	4
7636	Structure and functional analysis of the <i>Legionella pneumophila</i> chitinase ChiA reveals a novel mechanism of metal-dependent mucin degradation. <i>PLoS Pathogens</i> , 2020, 16, e1008342.	4.7	29
7637	Atomistic Simulations on Interactions between Amphiphilic Janus Nanoparticles and Lipid Bilayers: Effects of Lipid Ordering and Leaflet Asymmetry. <i>Journal of Physical Chemistry B</i> , 2020, 124, 4466-4475.	2.6	12
7638	Molecular Dynamics Simulations of the Structural Arrangement and Density of Alkylamine Surfactants on Copper Surfaces: Implications for Anisotropic Growth of Copper Nanowires. <i>ACS Applied Nano Materials</i> , 2020, 3, 5343-5350.	5.0	12
7639	Water dynamics affects thermal transport at the surface of hydrophobic and hydrophilic irradiated nanoparticles. <i>Nanoscale Advances</i> , 2020, 2, 3181-3190.	4.6	11
7640	Effect of Twin Boundary Motion and Dislocation-Twin Interaction on Mechanical Behavior in Fcc Metals. <i>Materials</i> , 2020, 13, 2238.	2.9	5
7641	Hybrid Screening Approach for Very Small Fragments: X-ray and Computational Screening on FKBP51. <i>Journal of Medicinal Chemistry</i> , 2020, 63, 5856-5864.	6.4	11
7642	Spontaneous drying of non-polar deep-cavity cavitand pockets in aqueous solution. <i>Nature Chemistry</i> , 2020, 12, 589-594.	13.6	45
7643	Assessing the extent of the structural and dynamic modulation of membrane lipids due to pore forming toxins: insights from molecular dynamics simulations. <i>Soft Matter</i> , 2020, 16, 4840-4857.	2.7	13
7644	Conformation and Diffusivity of Ring and Linear Polyethylene Oxide in Aqueous Solution: Molecular Topology Dependent Concentration Effects and Comparison with Experimental Data. <i>Macromolecular Theory and Simulations</i> , 2020, 29, 2000016.	1.4	6
7645	Binary Mixtures of Aromatic Compounds ( <i>n</i> -Propylbenzene, 1,3,5-Trimethylbenzene, and) Tj ETQq0 0 0 rgBT /Overlock 10 Tf 50 3 Moduli, Surface Tensions, and Flash Points at 0.1 MPa. <i>Journal of Chemical &amp; Engineering Data</i> , 2020, 65, 2625-2641.	1.9	13
7646	Solvent Effects and Aggregation Phenomena Studied by Vibrational Optical Activity and Molecular Dynamics: The Case of Pantolactone. <i>Journal of Physical Chemistry B</i> , 2020, 124, 4512-4526.	2.6	24
7647	Identification of Structural Calcium Binding Sites in Membrane-Bound Presenilin 1 and 2. <i>Journal of Physical Chemistry B</i> , 2020, 124, 4697-4711.	2.6	6
7648	Insights into the Polyhexamethylene Biguanide (PHMB) Mechanism of Action on Bacterial Membrane and DNA: A Molecular Dynamics Study. <i>Journal of Physical Chemistry B</i> , 2020, 124, 4487-4497.	2.6	48
7649	Pyramid-Shaped PEG-PCL-PEG Polymeric-Based Model Systems for Site-Specific Drug Delivery of Vancomycin with Enhance Antibacterial Efficacy. <i>ACS Omega</i> , 2020, 5, 11935-11945.	3.5	39
7650	Molecular-weight dependence of simulated glass transition temperature for isolated poly(ethylene) Tj ETQq1 1 0.784314 rgBT /Overlock 10 Tf 50 3	2.0	6
7651	Highly Conserved Homotrimer Cavity Formed by the SARS-CoV-2 Spike Glycoprotein: A Novel Binding Site. <i>Journal of Clinical Medicine</i> , 2020, 9, 1473.	2.4	73
7652	Solvation Free Energy of Self-Assembled Complexes: Using Molecular Dynamics to Understand the Separation of ssDNA-Wrapped Single-Walled Carbon Nanotubes. <i>Journal of Physical Chemistry C</i> , 2020, 124, 13127-13140.	3.1	3

#	ARTICLE	IF	CITATIONS
7653	Oil–water transport in clay-hosted nanopores: Effects of long-range electrostatic forces. <i>AIChE Journal</i> , 2020, 66, e16276.	3.6	18
7654	The Influence of the Soft Yukawa Potential and Hard Core Interactions on Auxeticity of the Face Centered Cubic Crystal of Hard-Core Repulsive Yukawa Particles. <i>Physica Status Solidi (B): Basic Research</i> , 2020, 257, 2000194.	1.5	12
7655	Designing a vaccine for fascioliasis using immunogenic 24 kDa mu-class glutathione s-transferase. <i>Infection, Genetics and Evolution</i> , 2020, 83, 104352.	2.3	7
7656	From Order to Disorder: Computational Design of Triblock Amphiphiles with 1 nm Domains. <i>Journal of the American Chemical Society</i> , 2020, 142, 9352-9362.	13.7	9
7657	Structural and functional insights into oligopeptide acquisition by the RagAB transporter from <i>Porphyromonas gingivalis</i> . <i>Nature Microbiology</i> , 2020, 5, 1016-1025.	13.3	46
7658	Common mechanism of thermostability in small $\alpha$ - and $\beta$ -proteins studied by molecular dynamics. <i>Proteins: Structure, Function and Bioinformatics</i> , 2020, 88, 1233-1250.	2.6	4
7659	Structural analyses and force fields comparison for NACore (68–78) and SubNACore (69–77) fibril segments of Parkinson's disease. <i>Journal of Molecular Modeling</i> , 2020, 26, 132.	1.8	3
7660	Coarse-Grained Molecular Model for the Glycosylphosphatidylinositol Anchor with and without Protein. <i>Journal of Chemical Theory and Computation</i> , 2020, 16, 3889-3903.	5.3	10
7661	Predicting the Miscibility and Rigidity of Poly(lactic-co-glycolic acid)/Polyethylene Glycol Blends via Molecular Dynamics Simulations. <i>Macromolecules</i> , 2020, 53, 3643-3654.	4.8	21
7662	Mechanoradicals in tensed tendon collagen as a source of oxidative stress. <i>Nature Communications</i> , 2020, 11, 2315.	12.8	26
7663	Btk SH2-kinase interface is critical for allosteric kinase activation and its targeting inhibits B-cell neoplasms. <i>Nature Communications</i> , 2020, 11, 2319.	12.8	23
7664	Propane and Water: The Cooperativity of Unlikely Molecules to Form Clathrate Structures. <i>Journal of Physical Chemistry B</i> , 2020, 124, 4661-4671.	2.6	20
7665	Flexibility of intrinsically disordered degrons in AUX/IAA proteins reinforces auxin co-receptor assemblies. <i>Nature Communications</i> , 2020, 11, 2277.	12.8	38
7666	Identification of bioactive molecules from tea plant as SARS-CoV-2 main protease inhibitors. <i>Journal of Biomolecular Structure and Dynamics</i> , 2021, 39, 3449-3458.	3.5	216
7667	Impact of anion shape on $\text{Li}^+$ solvation and on transport properties for lithium–air batteries: a molecular dynamics study. <i>Physical Chemistry Chemical Physics</i> , 2020, 22, 15842-15852.	2.8	19
7668	Serine 298 Phosphorylation in Linker 2 of UHRF1 Regulates Ligand-Binding Property of Its Tandem Tudor Domain. <i>Journal of Molecular Biology</i> , 2020, 432, 4061-4075.	4.2	8
7669	Identification of potential natural inhibitors of SARS-CoV2 main protease by molecular docking and simulation studies. <i>Journal of Biomolecular Structure and Dynamics</i> , 2021, 39, 4334-4345.	3.5	129
7670	Theoretical studies and NMR assay of coumarins and neoflavanones derivatives as potential inhibitors of acetylcholinesterase. <i>Computational Biology and Chemistry</i> , 2020, 87, 107293.	2.3	5

#	ARTICLE	IF	CITATIONS
7671	Trimethyl chitosan nanoparticles for ocular baicalein delivery: Preparation, optimization, in vitro evaluation, in vivo pharmacokinetic study and molecular dynamics simulation. International Journal of Biological Macromolecules, 2020, 156, 749-761.	7.5	30
7672	Interactions of a Bacterial RND Transporter with a Transmembrane Small Protein in a Lipid Environment. Structure, 2020, 28, 625-634.e6.	3.3	47
7673	Sphingomyelin Effects in Caveolin-1 Mediated Membrane Curvature. Journal of Physical Chemistry B, 2020, 124, 5177-5185.	2.6	15
7674	Two-step mechanism of J-domain action in driving Hsp70 function. PLoS Computational Biology, 2020, 16, e1007913.	3.2	18
7675	Affibody-Binding Ligands. International Journal of Molecular Sciences, 2020, 21, 3769.	4.1	23
7676	How Good is Jarzynski's Equality for Computer-Aided Drug Design?. Journal of Physical Chemistry B, 2020, 124, 5338-5349.	2.6	12
7677	Origin of Unusual Acidity and Li <sup>+</sup> Diffusivity in a Series of Water-in-Salt Electrolytes. Journal of Physical Chemistry B, 2020, 124, 5284-5291.	2.6	26
7678	Dataset of molecular dynamics simulation trajectories of amino-acid solutions with various force fields, water models and modified force field parameters. Data in Brief, 2020, 30, 105483.	1.0	3
7679	The importance of chain context in assessing small nucleotide variants in titin: <i>in silico</i> case study of the I10-I11 tandem and its arrhythmic right ventricular cardiomyopathy linked position T2580. Journal of Biomolecular Structure and Dynamics, 2021, 39, 3480-3490.	3.5	5
7680	X-Ray Structure and Molecular Dynamics Study of Uridine Phosphorylase from <i>Vibrio cholerae</i> in Complex with 2,2'-Anhydrouridine. Crystallography Reports, 2020, 65, 269-277.	0.6	3
7681	Structure-Based Optimization of 10-DEBC Derivatives as Potent and Selective Pim-1 Kinase Inhibitors. Journal of Chemical Information and Modeling, 2020, 60, 3287-3294.	5.4	10
7682	Thermodynamic, structural and dynamic properties of selected non-associative neat liquids. Journal of Physics Condensed Matter, 2020, 32, 405101.	1.8	2
7683	Selectivity of 18-crown-6 ether to alkali ions by density functional theory and molecular dynamics simulation. Journal of Molecular Liquids, 2020, 311, 113305.	4.9	18
7684	Role of Viscosity in Deviations from the Nernst-Einstein Relation. Journal of Physical Chemistry B, 2020, 124, 4774-4780.	2.6	22
7685	Biophysical and computational view on the <i>in vitro</i> combination between an anticancer drug, saracatinib and human serum albumin. Journal of Biomolecular Structure and Dynamics, 2021, 39, 3565-3575.	3.5	7
7686	Predicting Solubility of Small Molecules in Macromolecular Compounds for Nanomedicine Application from Atomistic Simulations. Advanced Theory and Simulations, 2020, 3, 2000001.	2.8	11
7687	In silico identification of new inhibitors for Î²eta-2-glycoprotein I as a major antigen in antiphospholipid antibody syndrome. Journal of Molecular Modeling, 2020, 26, 156.	1.8	6
7688	3D reconstruction and flexibility of the hybrid engine <i>Acetobacterium woodii</i> F-ATP synthase. Biochemical and Biophysical Research Communications, 2020, 527, 518-524.	2.1	1



#	ARTICLE	IF	CITATIONS
7689	Interfacial kinetics induced phase separation enhancing low-temperature performance of lithium-ion batteries. <i>Nano Energy</i> , 2020, 75, 104977.	16.0	11
7690	Ionic Dynamics of Hydroxylammonium Ionic Liquids: A Classical Molecular Dynamics Simulation Study. <i>Journal of Physical Chemistry B</i> , 2020, 124, 4960-4974.	2.6	11
7691	Cavity Particle in Aqueous Solution with a Hydrophobic Solute: Structure, Energetics, and Functionals. <i>Journal of Physical Chemistry B</i> , 2020, 124, 5220-5237.	2.6	1
7692	Atomic scale investigation of the volume phase transition in concentrated PNIPAM microgels. <i>Journal of Chemical Physics</i> , 2020, 152, 204904.	3.0	7
7693	Phase equilibrium of liquid water and hexagonal ice from enhanced sampling molecular dynamics simulations. <i>Journal of Chemical Physics</i> , 2020, 152, 204116.	3.0	15
7694	Molecular dynamics study of functionally relevant interdomain and active site interactions in the autotransporter esterase EstA from <i>Pseudomonas aeruginosa</i> . <i>Molecular Simulation</i> , 2020, 46, 743-756.	2.0	0
7695	A concurrent multiscale study of dynamic fracture. <i>Computer Methods in Applied Mechanics and Engineering</i> , 2020, 366, 113075.	6.6	30
7696	Disruption of conserved polar interactions causes a sequential release of Bim mutants from the canonical binding groove of Mcl1. <i>International Journal of Biological Macromolecules</i> , 2020, 158, 364-374.	7.5	6
7697	Ab initio phase diagram and nucleation of gallium. <i>Nature Communications</i> , 2020, 11, 2654.	12.8	102
7698	Sequence specificity, energetics and mechanism of mismatch recognition by DNA damage sensing protein Rad4/XPC. <i>Nucleic Acids Research</i> , 2020, 48, 2246-2257.	14.5	11
7699	Pivotal Role of Interdigitation in Interleaflet Interactions: Implications from Molecular Dynamics Simulations. <i>Journal of Physical Chemistry Letters</i> , 2020, 11, 5171-5176.	4.6	17
7700	Force Response of Polypeptide Chains from Water-Explicit MD Simulations. <i>Macromolecules</i> , 2020, 53, 4618-4629.	4.8	3
7701	A synthetic ion channel with anisotropic ligand response. <i>Nature Communications</i> , 2020, 11, 2924.	12.8	36
7702	A composition transferable and time-scale consistent coarse-grained model for cis-polyisoprene and vinyl-polybutadiene oligomeric blends. <i>JPhys Materials</i> , 2020, 3, 034007.	4.2	10
7703	A shift of dynamic equilibrium between the $\text{K}^{\text{IT}}$ active and inactive states causes drug resistance. <i>Proteins: Structure, Function and Bioinformatics</i> , 2020, 88, 1434-1446.	2.6	0
7704	Plausible compounds drawn from plants as curative agents for neurodegeneration: An in-silico approach. <i>Journal of Computer-Aided Molecular Design</i> , 2020, 34, 1003-1011.	2.9	0
7705	1D hypo-crystals: A novel concept for the crystallization of stereo-irregular polymers. <i>Materials Today</i> , 2020, 40, 26-37.	14.2	13
7706	Tracking $\text{Ca}^{2+}$ ATPase intermediates in real time by x-ray solution scattering. <i>Science Advances</i> , 2020, 6, eaaz0981.	10.3	29

#	ARTICLE	IF	CITATIONS
7707	Membrane-Ion Interactions Modify the Lipid Flip-Flop Dynamics of Biological Membranes: A Molecular Dynamics Study. <i>Journal of Physical Chemistry B</i> , 2020, 124, 5156-5162.	2.6	8
7708	Membrane-Dependent Binding and Entry Mechanism of Dopamine into Its Receptor. <i>ACS Chemical Neuroscience</i> , 2020, 11, 1914-1924.	3.5	21
7709	Cryo-EM structure of islet amyloid polypeptide fibrils reveals similarities with amyloid- $\beta$ fibrils. <i>Nature Structural and Molecular Biology</i> , 2020, 27, 660-667.	8.2	120
7710	Numerical calculation of free-energy barriers for entangled polymer nucleation. <i>Journal of Chemical Physics</i> , 2020, 152, 224904.	3.0	6
7711	A boosted unbiased molecular dynamics method for predicting ligands binding mechanisms: probing the binding pathway of dasatinib to Src-kinase. <i>Bioinformatics</i> , 2020, 36, 4714-4720.	4.1	10
7712	Ligand-protein interactions in lysozyme investigated through a dual-resolution model. <i>Proteins: Structure, Function and Bioinformatics</i> , 2020, 88, 1351-1360.	2.6	8
7713	$\beta$ -Turn mimetic synthetic peptides as amyloid- $\beta$ aggregation inhibitors. <i>Bioorganic Chemistry</i> , 2020, 101, 104012.	4.1	18
7714	Two-Dimensional Nature and the Meaning of the Density of States in Redox Monolayers. <i>Journal of Physical Chemistry C</i> , 2020, 124, 14918-14927.	3.1	6
7715	Individual Roles of Peptides PGLa and Magainin 2 in Synergistic Membrane Poration. <i>Langmuir</i> , 2020, 36, 7190-7199.	3.5	24
7716	CX3CL1 homo-oligomerization drives cell-to-cell adherence. <i>Scientific Reports</i> , 2020, 10, 9069.	3.3	13
7717	Polymer principles behind solubilizing lignin with organic cosolvents for bioenergy. <i>Green Chemistry</i> , 2020, 22, 4331-4340.	9.0	13
7718	Reliability of molecular dynamics interatomic potentials for modeling of titanium in additive manufacturing processes. <i>Computational Materials Science</i> , 2020, 184, 109883.	3.0	7
7719	Hydrogen-bonded complexes protocatechualdehyde - acetone in carbon tetrachloride: NMR-spectroscopy and molecular dynamics simulation. <i>Journal of Molecular Liquids</i> , 2020, 309, 113124.	4.9	4
7720	How Does the Mono-Triazole Derivative Modulate $\beta$ Aggregation and Disrupt a Protofibril Structure: Insights from Molecular Dynamics Simulations. <i>ACS Omega</i> , 2020, 5, 15606-15619.	3.5	10
7721	Descriptors representing two- and three-body atomic distributions and their effects on the accuracy of machine-learned inter-atomic potentials. <i>Journal of Chemical Physics</i> , 2020, 152, 234102.	3.0	71
7722	The temperature of maximum density for amino acid aqueous solutions. An experimental and molecular dynamics study. <i>Fluid Phase Equilibria</i> , 2020, 521, 112703.	2.5	9
7723	Cholesterol Interaction with the Trimeric HIV Fusion Protein gp41 in Lipid Bilayers Investigated by Solid-State NMR Spectroscopy and Molecular Dynamics Simulations. <i>Journal of Molecular Biology</i> , 2020, 432, 4705-4721.	4.2	21
7724	Protein docking and steered molecular dynamics suggest alternative phospholamban-binding sites on the SERCA calcium transporter. <i>Journal of Biological Chemistry</i> , 2020, 295, 11262-11274.	3.4	15

#	ARTICLE	IF	CITATIONS
7725	Influence of Calcium Binding on Conformations and Motions of Anionic Polyamino Acids. Effect of Side Chain Length. <i>Polymers</i> , 2020, 12, 1279.	4.5	6
7726	The Glycosphingolipid GM3 Modulates Conformational Dynamics of the Glucagon Receptor. <i>Biophysical Journal</i> , 2020, 119, 300-313.	0.5	23
7727	Solvent influence on imidazolium based ionic liquid contact pairs. <i>Journal of Molecular Liquids</i> , 2020, 315, 113615.	4.9	2
7728	Photoinduced reconfiguration to control the protein-binding affinity of azobenzene-cyclized peptides. <i>Journal of Materials Chemistry B</i> , 2020, 8, 7413-7427.	5.8	17
7729	Computationally Guided Tuning of Amino Acid Configuration Influences the Chiroptical Properties of Supramolecular Peptide- $\pi$ -Peptide Nanostructures. <i>Langmuir</i> , 2020, 36, 6782-6792.	3.5	8
7730	Planar graphene/h-BN/graphene heterostructures for protein stretching and confinement. <i>Nanoscale</i> , 2020, 12, 13822-13828.	5.6	15
7731	Equilibrium and Transport Distributions of a DNA Dodecamer in Hydrophilic Nanopores. <i>Materials Today: Proceedings</i> , 2020, 20, 249-264.	1.8	0
7732	Effect of Protein Flexibility from Coarse-Grained Elastic Network Parameterizations on the Calculation of Free Energy Profiles of Ligand Binding. <i>Journal of Chemical Theory and Computation</i> , 2020, 16, 4734-4743.	5.3	5
7733	Physicochemical-guided design of cathelicidin-derived peptides generates membrane active variants with therapeutic potential. <i>Scientific Reports</i> , 2020, 10, 9127.	3.3	14
7734	Atomistic mechanism of transmembrane helix association. <i>PLoS Computational Biology</i> , 2020, 16, e1007919.	3.2	16
7735	Delivery of Alpha-Mangostin Using Cyclodextrins through a Biological Membrane: Molecular Dynamics Simulation. <i>Molecules</i> , 2020, 25, 2532.	3.8	8
7736	Fullerene-intercalated graphene nanocontainers for gas storage and sustained release. <i>Journal of Molecular Modeling</i> , 2020, 26, 166.	1.8	7
7737	Computational Insights Into Voltage Dependence of Polyamine Block in a Strong Inwardly Rectifying K <sup>+</sup> Channel. <i>Frontiers in Pharmacology</i> , 2020, 11, 721.	3.5	11
7738	Molecular simulation of the structure and elastic properties of ettringite and monosulfoaluminate. <i>Cement and Concrete Research</i> , 2020, 135, 106126.	11.0	30
7739	Atomistic insight into the aggregation of [Au <sub>25</sub> (SR) <sub>18</sub> ] <sup>q</sup> nanoclusters. <i>Nanoscale Advances</i> , 2020, 2, 2842-2852.	4.6	6
7740	Effect of dissolved salt on the anomalies of water at negative pressure. <i>Journal of Chemical Physics</i> , 2020, 152, 194501.	3.0	4
7741	Allosteric Communications between Domains Modulate the Activity of Matrix Metalloprotease-1. <i>Biophysical Journal</i> , 2020, 119, 360-374.	0.5	13
7742	Insight into structural properties of polyethylene glycol monolaurate in water and alcohols from molecular dynamics studies. <i>RSC Advances</i> , 2020, 10, 21760-21771.	3.6	8

#	ARTICLE	IF	CITATIONS
7743	Structural Basis of Ca <sup>2+</sup> -Dependent Self-Processing Activity of Repeat-in-Toxin Proteins. MBio, 2020, 11, .	4.1	5
7744	Improved Parameterization of Protein-DNA Interactions for Molecular Dynamics Simulations of PCNA Diffusion on DNA. Journal of Chemical Theory and Computation, 2020, 16, 4006-4013.	5.3	23
7745	Molecular Mechanism of Gas Solubility in Liquid: Constant Chemical Potential Molecular Dynamics Simulations. Journal of Chemical Theory and Computation, 2020, 16, 5279-5286.	5.3	7
7746	Botulinum Endopeptidase: SAXS Experiments and MD Simulations Reveal Extended Solution Structures That Account for Its Biochemical Properties. Journal of Physical Chemistry B, 2020, 124, 5801-5812.	2.6	5
7747	Solvation Induced Ring Puckering Effect in Fluorinated Prolines and Its Inclusion in Classical Force Fields. Journal of Physical Chemistry B, 2020, 124, 5899-5906.	2.6	3
7748	Investigating dual Ca <sup>2+</sup> modulation of the ryanodine receptor 1 by molecular dynamics simulation. Proteins: Structure, Function and Bioinformatics, 2020, 88, 1528-1539.	2.6	4
7749	Elucidating the Feature of Intermediate Water in Hydrated Poly( $\alpha$ -methoxyalkyl acrylate)s by Molecular Dynamics Simulation and Differential Scanning Calorimetry Measurement. ACS Biomaterials Science and Engineering, 2020, 6, 3915-3924.	5.2	17
7750	Dimerization of A $\beta$ 40 inside dipalmitoylphosphatidylcholine bilayer and its effect on bilayer integrity: Atomistic simulation at three temperatures. Proteins: Structure, Function and Bioinformatics, 2020, 88, 1540-1552.	2.6	8
7752	Nanoscale Interplay of Membrane Composition and Amyloid Self-Assembly. Journal of Physical Chemistry B, 2020, 124, 5837-5846.	2.6	8
7753	Developing a Fully Glycosylated Full-Length SARS-CoV-2 Spike Protein Model in a Viral Membrane. Journal of Physical Chemistry B, 2020, 124, 7128-7137.	2.6	240
7754	Hydrogen bonding of ionic liquids in the groove region of DNA controls the extent of its stabilization: synthesis, spectroscopic and simulation studies. Physical Chemistry Chemical Physics, 2020, 22, 15582-15591.	2.8	10
7755	S92 phosphorylation induces structural changes in the N-terminus domain of human mitochondrial calcium uniporter. Scientific Reports, 2020, 10, 9131.	3.3	10
7756	Influence of the molecular motifs of mannan and xylan populations on their recalcitrance and organization in spruce softwoods. Green Chemistry, 2020, 22, 3956-3970.	9.0	26
7757	Solvation structures of Na <sup>+</sup> Cl <sup>-</sup> ion pair in DMF-water and DMF-methanol mixtures. Molecular Simulation, 2020, 46, 766-776.	2.0	3
7758	Dynamical Fracture in Ice Ih as Modeled by TIP4P/Ice and mW Water Potentials. Annalen Der Physik, 2020, 532, 1900587.	2.4	2
7759	Determining Free-Energy Differences Through Variationally Derived Intermediates. Journal of Chemical Theory and Computation, 2020, 16, 3504-3512.	5.3	15
7760	Functional Heterologous Expression of Mature Lipase LipA from Pseudomonas aeruginosa PSA01 in Escherichia coli SHuffle and BL21 (DE3): Effect of the Expression Host on Thermal Stability and Solvent Tolerance of the Enzyme Produced. International Journal of Molecular Sciences, 2020, 21, 3925.	4.1	7
7761	Insulin Dissociates by Diverse Mechanisms of Coupled Unfolding and Unbinding. Journal of Physical Chemistry B, 2020, 124, 5571-5587.	2.6	35

#	ARTICLE	IF	CITATIONS
7762	Physicochemical and structural properties of lunasin revealed by spectroscopic, chromatographic and molecular dynamics approaches. <i>Biochimica Et Biophysica Acta - Proteins and Proteomics</i> , 2020, 1868, 140440.	2.3	5
7763	Utilisation of the OliveNet <sup>®</sup> Library to investigate phenolic compounds using molecular modelling studies in the context of Alzheimer's disease. <i>Computational Biology and Chemistry</i> , 2020, 87, 107271.	2.3	4
7764	Novel venom-based peptides (P13 and its derivative M6) to maintain self-renewal of human embryonic stem cells by activating FGF and TGF $\beta$ signaling pathways. <i>Stem Cell Research and Therapy</i> , 2020, 11, 243.	5.5	4
7765	Interplay of hydrophobic and hydrophilic interactions in sequence-dependent cell penetration of spontaneous membrane-translocating peptides revealed by bias-exchange metadynamics simulations. <i>Biochimica Et Biophysica Acta - Biomembranes</i> , 2020, 1862, 183402.	2.6	10
7766	Acetylation and Sugar Composition Influence the (In)Solubility of Plant $\beta$ -Mannans and Their Interaction with Cellulose Surfaces. <i>ACS Sustainable Chemistry and Engineering</i> , 2020, 8, 10027-10040.	6.7	25
7767	Conformationally constrained peptides for drug delivery. <i>Journal of Peptide Science</i> , 2020, 26, e3244.	1.4	10
7768	Entropic Origin of the Attenuated Width of the Ice-Water Interface. <i>Journal of Physical Chemistry C</i> , 2020, 124, 7334-7340.	3.1	13
7769	Decoupling copolymer, lipid and carbon nanotube interactions in hybrid, biomimetic vesicles. <i>Nanoscale</i> , 2020, 12, 6545-6555.	5.6	5
7770	Structure, dynamics and immunogenicity of a catalytically inactive CXC chemokine-degrading protease SpyCEP from <i>Streptococcus pyogenes</i> . <i>Computational and Structural Biotechnology Journal</i> , 2020, 18, 650-660.	4.1	19
7771	Performance of Mixed Quantum-Classical Approaches on Modeling the Crossover from Hopping to Bandlike Charge Transport in Organic Semiconductors. <i>Journal of Chemical Theory and Computation</i> , 2020, 16, 2071-2084.	5.3	21
7772	Proximal charge effects on guest binding to a non-polar pocket. <i>Chemical Science</i> , 2020, 11, 3656-3663.	7.4	21
7773	Capturing Deuteration Effects in a Molecular Mechanics Force Field: Deuterated THF and the THF-Water Miscibility Gap. <i>Journal of Chemical Theory and Computation</i> , 2020, 16, 2529-2540.	5.3	9
7774	Discovery of Self-Assembling $\beta$ -Conjugated Peptides by Active Learning-Directed Coarse-Grained Molecular Simulation. <i>Journal of Physical Chemistry B</i> , 2020, 124, 3873-3891.	2.6	76
7775	pH-Induced Changes in Polypeptide Conformation: Force-Field Comparison with Experimental Validation. <i>Journal of Physical Chemistry B</i> , 2020, 124, 2961-2972.	2.6	29
7776	Thermodynamic Investigation of the Mechanism of Heat Production During Membrane Depolarization. <i>Journal of Physical Chemistry B</i> , 2020, 124, 2815-2822.	2.6	1
7777	Lipid-specific interactions determine the organization and dynamics of membrane-active peptide melittin. <i>Soft Matter</i> , 2020, 16, 3498-3504.	2.7	15
7778	Impact of electronic polarizability on protein-functional group interactions. <i>Physical Chemistry Chemical Physics</i> , 2020, 22, 6848-6860.	2.8	16
7779	Local structure in water and its comparison with hexagonal ice from molecular dynamics simulations of TIP4P/2005 water model. <i>Molecular Simulation</i> , 2020, 46, 557-564.	2.0	1

#	ARTICLE	IF	CITATIONS
7780	Genomic Signature of Shifts in Selection in a Subalpine Ant and Its Physiological Adaptations. <i>Molecular Biology and Evolution</i> , 2020, 37, 2211-2227.	8.9	14
7781	Computational Investigation of Voltage-Gated Sodium Channel $\beta$ 3 Subunit Dynamics. <i>Frontiers in Molecular Biosciences</i> , 2020, 7, 40.	3.5	4
7782	Non-Flammable Fluorinated Phosphorus(III)-Based Electrolytes for Advanced Lithium-Ion Battery Performance. <i>ChemElectroChem</i> , 2020, 7, 1499-1508.	3.4	13
7783	Brine-Oil Interfacial Tension Modeling: Assessment of Machine Learning Techniques Combined with Molecular Dynamics. <i>ACS Applied Materials &amp; Interfaces</i> , 2020, 12, 15837-15843.	8.0	19
7784	The lipoprotein Pal stabilises the bacterial outer membrane during constriction by a mobilisation-and-capture mechanism. <i>Nature Communications</i> , 2020, 11, 1305.	12.8	50
7785	The Impact of Natural Compounds on S-Shaped A $\beta$ 42 Fibril: From Molecular Docking to Biophysical Characterization. <i>International Journal of Molecular Sciences</i> , 2020, 21, 2017.	4.1	18
7786	Increasing the Affinity of an O-Antigen Polysaccharide Binding Site in <i>Shigella flexneri</i> Bacteriophage Sf6 Tailspike Protein. <i>Chemistry - A European Journal</i> , 2020, 26, 7263-7273.	3.3	9
7787	Evaluation the synergistic antitumor effect of methotrexate-camptothecin codelivery prodrug from self-assembly process to acid-catalyzed both drugs release: A comprehensive theoretical study. <i>Journal of Computational Chemistry</i> , 2020, 41, 1486-1496.	3.3	11
7788	Stacking geometry between two sheared Watson-Crick basepairs: Computational chemistry and bioinformatics based prediction. <i>Biochimica Et Biophysica Acta - General Subjects</i> , 2020, 1864, 129600.	2.4	3
7789	High-content imaging and structure-based predictions reveal functional differences between Niemann-Pick C1 variants. <i>Traffic</i> , 2020, 21, 386-397.	2.7	14
7790	Adsorption of impurities in vegetable oil: A molecular modelling study. <i>Journal of Colloid and Interface Science</i> , 2020, 571, 55-65.	9.4	12
7791	How Ligand Binding Affects the Dynamical Transition Temperature in Proteins. <i>ChemPhysChem</i> , 2020, 21, 916-926.	2.1	3
7792	Scaled charges at work: Salting out and interfacial tension of methane with electrolyte solutions from computer simulations. <i>Fluid Phase Equilibria</i> , 2020, 513, 112548.	2.5	33
7793	Substrate Specificity of OXA-48 after $\beta$ 5 $\alpha$ - $\beta$ 6 Loop Replacement. <i>ACS Infectious Diseases</i> , 2020, 6, 1032-1043.	3.8	10
7794	Application of the 2PT model to understanding entropy change in molecular coarse-graining. <i>Soft Materials</i> , 2020, 18, 274-289.	1.7	8
7795	The effect of chitosan and PEG polymers on stabilization of GF-17 structure: A molecular dynamics study. <i>Carbohydrate Polymers</i> , 2020, 237, 116124.	10.2	17
7796	Ultrafast Formation of the Charge Transfer State of Prodan Reveals Unique Aspects of the Chromophore Environment. <i>Journal of Physical Chemistry B</i> , 2020, 124, 2643-2651.	2.6	11
7797	Conformational Insight on WT- and Mutated-EGFR Receptor Activation and Inhibition by Epigallocatechin-3-Gallate: Over a Rational Basis for the Design of Selective Non-Small-Cell Lung Anticancer Agents. <i>International Journal of Molecular Sciences</i> , 2020, 21, 1721.	4.1	31



#	ARTICLE	IF	CITATIONS
7798	The role of hydroxyl and carboxyl functional groups in adsorption of copper by carbon nanotube and hybrid graphene-carbon nanotube: insights from molecular dynamic simulation. <i>Adsorption</i> , 2020, 26, 397-405.	3.0	18
7799	Principal component analysis highlights the influence of temperature, curvature and cholesterol on conformational dynamics of lipids. <i>Biochimica Et Biophysica Acta - Biomembranes</i> , 2020, 1862, 183253.	2.6	5
7800	Amorphous silicon triboride: A first principles study. <i>Journal of Non-Crystalline Solids</i> , 2020, 536, 119995.	3.1	1
7801	Molecular Modeling Study of Uncharged Oximes Compared to HI-6 and 2-PAM Inside Human AChE Sarin and VX Conjugates. <i>ACS Omega</i> , 2020, 5, 4490-4500.	3.5	12
7802	Electrostatic Interactions Govern Extreme Nascent Protein Ejection Times from Ribosomes and Can Delay Ribosome Recycling. <i>Journal of the American Chemical Society</i> , 2020, 142, 6103-6110.	13.7	39
7803	Full-length human GLP-1 receptor structure without orthosteric ligands. <i>Nature Communications</i> , 2020, 11, 1272.	12.8	83
7804	Effect of Cations (Na <sup>+</sup> , K <sup>+</sup> , and Ca <sup>2+</sup> ) on Methane Hydrate Formation on the External Surface of Montmorillonite: Insights from Molecular Dynamics Simulation. <i>ACS Earth and Space Chemistry</i> , 2020, 4, 572-582.	2.7	32
7805	Probing the Accuracy of Explicit Solvent Constant pH Molecular Dynamics Simulations for Peptides. <i>Journal of Chemical Theory and Computation</i> , 2020, 16, 2561-2569.	5.3	13
7806	Examining Tail and Headgroup Effects on Binary and Ternary Gel-Phase Lipid Bilayer Structure. <i>Journal of Physical Chemistry B</i> , 2020, 124, 3043-3053.	2.6	3
7807	Group 3 LEA Protein Model Peptides Suppress Heat-Induced Lysozyme Aggregation. Elucidation of the Underlying Mechanism Using Coarse-Grained Molecular Simulations. <i>Journal of Physical Chemistry B</i> , 2020, 124, 2747-2759.	2.6	7
7808	Low-temperature paddlewheel effect in glassy solid electrolytes. <i>Nature Communications</i> , 2020, 11, 1483.	12.8	102
7809	Green method for preparation of cellulose nanocrystals using deep eutectic solvent. <i>Cellulose</i> , 2020, 27, 4305-4317.	4.9	40
7810	Classification of VUS and unclassified variants in BRCA1 BRCT repeats by molecular dynamics simulation. <i>Computational and Structural Biotechnology Journal</i> , 2020, 18, 723-736.	4.1	63
7811	Proton motive function of the terminal antiporter-like subunit in respiratory complex I. <i>Biochimica Et Biophysica Acta - Bioenergetics</i> , 2020, 1861, 148185.	1.0	12
7812	Effects of Low-level Lipid Peroxidation on the Permeability of Nitroaromatic Molecules across a Membrane: A Computational Study. <i>ACS Omega</i> , 2020, 5, 4798-4806.	3.5	11
7813	Coarse-graining of polyisoprene melts using inverse Monte Carlo and local density potentials. <i>Journal of Chemical Physics</i> , 2020, 152, 124902.	3.0	27
7814	Evolution of internal granular structure at the flow-arrest transition. <i>Granular Matter</i> , 2020, 22, 1.	2.2	5
7815	Probing conformational transitions of PIN1 from L. major during chemical and thermal denaturation. <i>International Journal of Biological Macromolecules</i> , 2020, 154, 904-915.	7.5	7

#	ARTICLE	IF	CITATIONS
7816	Theoretical Investigation of Dissolution and Decomposition Mechanisms of a Cellulose Fiber in Ionic Liquids. <i>Journal of Physical Chemistry B</i> , 2020, 124, 3090-3102.	2.6	14
7817	Molecular Dynamics Analysis of a Rationally Designed Aldehyde Dehydrogenase Gives Insights into Improved Activity for the Non-Native Cofactor NAD <sup>+</sup> . <i>ACS Synthetic Biology</i> , 2020, 9, 920-929.	3.8	13
7818	Molecular mechanism of the skin permeation enhancing effect of ethanol: a molecular dynamics study. <i>RSC Advances</i> , 2020, 10, 12234-12248.	3.6	35
7819	Two Novel Cases of Resistance to Thyroid Hormone Due to <i>THRA</i> Mutation. <i>Thyroid</i> , 2020, 30, 1217-1221.	4.5	16
7820	Quercetin and Baicalein Act as Potent Anti-amyloidogenic and Fibril Destabilizing Agents for SOD1 Fibrils. <i>ACS Chemical Neuroscience</i> , 2020, 11, 1129-1138.	3.5	36
7821	The Na,K-ATPase acts upstream of phosphoinositide PI(4,5)P <sub>2</sub> facilitating unconventional secretion of Fibroblast Growth Factor 2. <i>Communications Biology</i> , 2020, 3, 141.	4.4	21
7822	Amorphous silicon hexaboride at high pressure. <i>Philosophical Magazine</i> , 2020, 100, 1818-1833.	1.6	5
7823	Novel potential inhibitor discovery against tyrosyl-tRNA synthetase from <i>Staphylococcus aureus</i> by virtual screening, molecular dynamics, MMPBSA and QMMM simulations. <i>Molecular Simulation</i> , 2020, 46, 507-520.	2.0	13
7824	Octopus, a computational framework for exploring light-driven phenomena and quantum dynamics in extended and finite systems. <i>Journal of Chemical Physics</i> , 2020, 152, 124119.	3.0	210
7825	Molecular dynamics based descriptors for predicting supramolecular gelation. <i>Chemical Science</i> , 2020, 11, 4226-4238.	7.4	29
7826	Exploring Conformational Dynamics of the Extracellular <i>Venus flytrap</i> Domain of the GABA <sub>B</sub> Receptor: A Path-Metadynamics Study. <i>Journal of Chemical Information and Modeling</i> , 2020, 60, 2294-2303.	5.4	5
7827	Binuclear and tetranuclear Zn( <sup>II</sup> ) complexes with thiosemicarbazones: synthesis, X-ray crystal structures, ATP-sensing, DNA-binding, phosphatase activity and theoretical calculations. <i>RSC Advances</i> , 2020, 10, 12735-12746.	3.6	9
7828	Rings, Hexagons, Petals, and Dipolar Moment Sink-Sources: The Fanciful Behavior of Water around Cyclodextrin Complexes. <i>Biomolecules</i> , 2020, 10, 431.	4.0	14
7829	Development and Characterization of the Shortest Anti-Adhesion Peptide Analogue of B49Mod1. <i>Molecules</i> , 2020, 25, 1188.	3.8	5
7830	Contribution of the two liquid phases to the interfacial tension at various water-organic liquid-liquid interfaces. <i>Journal of Molecular Liquids</i> , 2020, 306, 112872.	4.9	8
7831	Exploration of Free Energy Surfaces Across a Membrane Channel Using Metadynamics and Umbrella Sampling. <i>Journal of Chemical Theory and Computation</i> , 2020, 16, 2751-2765.	5.3	26
7832	Bioluminescent Nanoluciferase-Furimamide Complex: A Theoretical Study on Different Protonation States. <i>Journal of Physical Chemistry B</i> , 2020, 124, 2539-2548.	2.6	5
7833	Molecular simulation of the shape deformation of a polymersome. <i>Soft Matter</i> , 2020, 16, 3234-3244.	2.7	18

#	ARTICLE	IF	CITATIONS
7834	Confinement and Diffusion of Small Molecules in a Molecular-Scale Tunnel. <i>Journal of the Electrochemical Society</i> , 2020, 167, 023505.	2.9	3
7835	Heightened Cold-Denaturation of Proteins at the Ice–Water Interface. <i>Journal of the American Chemical Society</i> , 2020, 142, 5722-5730.	13.7	59
7836	Purification, Characterization and Mechanistic Evaluation of Angiotensin Converting Enzyme Inhibitory Peptides Derived from <i>Zizyphus Jujuba</i> Fruit. <i>Scientific Reports</i> , 2020, 10, 3976.	3.3	18
7837	Cyclopentane rings in hydrophobic chains of a phospholipid enhance the bilayer stability to electric breakdown. <i>Soft Matter</i> , 2020, 16, 3216-3223.	2.7	3
7838	Self-assembly of small molecules at hydrophobic interfaces using group effect. <i>Nanoscale</i> , 2020, 12, 5452-5463.	5.6	27
7839	Symmetry-breaking transitions in the early steps of protein self-assembly. <i>European Biophysics Journal</i> , 2020, 49, 175-191.	2.2	28
7840	SAMPL6 Octanol–water partition coefficients from alchemical free energy calculations with MBIS atomic charges. <i>Journal of Computer-Aided Molecular Design</i> , 2020, 34, 327-334.	2.9	5
7841	Pulmonary Surfactant Lipid Reorganization Induced by the Adsorption of the Oligomeric Surfactant Protein B Complex. <i>Journal of Molecular Biology</i> , 2020, 432, 3251-3268.	4.2	29
7842	On the microscopic origin of the cryoprotective effect in lysine solutions. <i>Physical Chemistry Chemical Physics</i> , 2020, 22, 6919-6927.	2.8	7
7843	Polymyxins Bind to the Cell Surface of Unculturable <i>Acinetobacter baumannii</i> and Cause Unique Dependent Resistance. <i>Advanced Science</i> , 2020, 7, 2000704.	11.2	31
7844	Visualizing group II intron dynamics between the first and second steps of splicing. <i>Nature Communications</i> , 2020, 11, 2837.	12.8	31
7845	Uncovering the effects of interface-induced ordering of liquid on crystal growth using machine learning. <i>Nature Communications</i> , 2020, 11, 3260.	12.8	32
7846	Computational investigation on the effects of pharmaceutical polymers on the structure and dynamics of interleukin2 in heat stress. <i>Journal of Biomolecular Structure and Dynamics</i> , 2020, 39, 1-11.	3.5	3
7847	Structural Analysis of Nonapeptides Derived from Elastin. <i>Biophysical Journal</i> , 2020, 118, 2755-2768.	0.5	2
7848	The cation effect on the solubility of glycylglycine and N-acetylglycine in aqueous solution: Experimental and molecular dynamics studies. <i>Journal of Molecular Liquids</i> , 2020, 310, 113044.	4.9	2
7849	On Calculating the Bending Modulus of Lipid Bilayer Membranes from Buckling Simulations. <i>Journal of Physical Chemistry B</i> , 2020, 124, 6299-6311.	2.6	42
7850	Mechanism of $\beta^2$ -arrestin recruitment by the $\beta^4$ -opioid G protein-coupled receptor. <i>Proceedings of the National Academy of Sciences of the United States of America</i> , 2020, 117, 16346-16355.	7.1	40
7851	Unusual activated processes controlling dislocation motion in body-centered-cubic high-entropy alloys. <i>Proceedings of the National Academy of Sciences of the United States of America</i> , 2020, 117, 16199-16206.	7.1	117

#	ARTICLE	IF	CITATIONS
7852	Disulfide Bond Replacement with 1,4- and 1,5-disubstituted [1,2,3]-triazole on CXCR4 Chemokine Receptor Type 4 (CXCR4) Peptide Ligands: Small Changes that Make Big Differences. Chemistry - A European Journal, 2020, 26, 10113-10125.	3.3	10
7853	Structure and Dynamics of a Thermostable Alcohol Dehydrogenase from the Antarctic Psychrophile <i>Moraxella</i> sp. TAE123. ACS Omega, 2020, 5, 14523-14534.	3.5	12
7854	Molecular profiling of lamellar ichthyosis pathogenic missense mutations on the structural and stability aspects of TGM1 protein. Journal of Biomolecular Structure and Dynamics, 2021, 39, 4962-4972.	3.5	6
7855	How Anionic Lipids Affect Spatiotemporal Properties of KRAS4B on Model Membranes. Journal of Physical Chemistry B, 2020, 124, 5434-5453.	2.6	18
7856	Effect of Helical Kink on Peptide Translocation across Phospholipid Membranes. Journal of Physical Chemistry B, 2020, 124, 5940-5947.	2.6	13
7857	Assessing Barriers for Antimicrobial Penetration in Complex Asymmetric Bacterial Membranes: A Case Study with Thymol. Langmuir, 2020, 36, 8800-8814.	3.5	29
7858	On interactions of P-glycoprotein with various anti-tumor drugs by binding free energy calculations. Journal of Biomolecular Structure and Dynamics, 2020, 39, 1-13.	3.5	2
7859	Effect of chain length on the near edge X-ray absorption fine structure spectra of liquid n-Alkanes. Chemical Physics Letters, 2020, 752, 137564.	2.6	4
7860	Pressure, Peptides, and a Piezolyte: Structural Analysis of the Effects of Pressure and Trimethylamine- <i>N</i> -oxide on the Peptide Solvation Shell. Journal of Physical Chemistry B, 2020, 124, 6508-6519.	2.6	8
7861	Can Polarity-Inverted Surfactants Self-Assemble in Nonpolar Solvents?. Journal of Physical Chemistry B, 2020, 124, 6448-6458.	2.6	8
7862	The molecular basis of selective DNA binding by the BRG1 AT-hook and bromodomain. Biochimica Et Biophysica Acta - Gene Regulatory Mechanisms, 2020, 1863, 194566.	1.9	13
7863	Molecular dynamic simulations of full-length human purinergic receptor subtype P2X7 bonded to potent inhibitors. European Journal of Pharmaceutical Sciences, 2020, 152, 105454.	4.0	11
7864	Developing a Coarse-Grained Model for Bacterial Cell Walls: Evaluating Mechanical Properties and Free Energy Barriers. Journal of Chemical Theory and Computation, 2020, 16, 5369-5384.	5.3	31
7865	Ether-Functionalized Sulfonium Ionic Liquid and Its Binary Mixtures with Acetonitrile as Electrolyte for Electrochemical Double Layer Capacitors: A Molecular Dynamics Study. Journal of Physical Chemistry B, 2020, 124, 6679-6689.	2.6	20
7866	On the advantages of exploiting memory in Markov state models for biomolecular dynamics. Journal of Chemical Physics, 2020, 153, 014105.	3.0	37
7867	Identification of inhibitor binding hotspots in <i>Acinetobacter baumannii</i> Î <sup>2</sup> -ketoacyl acyl carrier protein synthase III using molecular dynamics simulation. Journal of Molecular Graphics and Modelling, 2020, 100, 107669.	2.4	3
7868	Breakage of Hydrophobic Contacts Limits the Rate of Passive Lipid Exchange between Membranes. Journal of Physical Chemistry B, 2020, 124, 5884-5898.	2.6	15
7869	In silico analysis: structural insights about inter-protofilaments interactions for Î±-synuclein (50-57) fibrils and its familial mutation. Molecular Simulation, 2020, 46, 867-878.	2.0	5

#	ARTICLE	IF	CITATIONS
7870	Molecular and clinical profile of congenital fibrinogen disorders in Iran, identification of two novel mutations. <i>International Journal of Laboratory Hematology</i> , 2020, 42, 619-627.	1.3	6
7871	Functional impact of the G279S substitution in the adenosine A1-receptor (A1R-G279S), a mutation associated with Parkinson's disease. <i>Molecular Pharmacology</i> , 2020, 98, MOLPHARM-AR-2020-000003.	2.3	12
7872	Molecular Dynamics Simulations to Investigate How PZM21 Affects the Conformational State of the $\mu$ -Opioid Receptor Upon Activation. <i>International Journal of Molecular Sciences</i> , 2020, 21, 4699.	4.1	8
7873	Iron's Wake: The Performance of Quantum Mechanical-Derived Versus General-Purpose Force Fields Tested on a Luminescent Iron Complex. <i>Molecules</i> , 2020, 25, 3084.	3.8	8
7874	Desaturase specificity is controlled by the physicochemical properties of a single amino acid residue in the substrate binding tunnel. <i>Computational and Structural Biotechnology Journal</i> , 2020, 18, 1202-1209.	4.1	8
7875	Insights into the mechanism of inhibition of phospholipase A2 by resveratrol: An extensive molecular dynamics simulation and binding free energy calculation. <i>Journal of Molecular Graphics and Modelling</i> , 2020, 100, 107649.	2.4	10
7876	Connecting Correlated and Uncorrelated Transport to Dynamics of Ionic Interactions in Cyclic Ammonium-Based Ionic Liquids. <i>Journal of Physical Chemistry B</i> , 2020, 124, 6813-6824.	2.6	9
7877	Polymer-coated gold nanoparticles and polymeric nanoparticles as nanocarrier of the BP100 antimicrobial peptide through a lung surfactant model. <i>Journal of Molecular Liquids</i> , 2020, 314, 113661.	4.9	16
7878	Structural plasticity of SARS-CoV-2 3CL Mpro active site cavity revealed by room temperature X-ray crystallography. <i>Nature Communications</i> , 2020, 11, 3202.	12.8	334
7879	The hydrolytic water molecule of Class A $\beta$ -lactamase relies on the acyl-enzyme intermediate ES* for proper coordination and catalysis. <i>Scientific Reports</i> , 2020, 10, 10205.	3.3	13
7880	Slow-, Tight-Binding Inhibition of CYP17A1 by Abiraterone Redefines Its Kinetic Selectivity and Dosing Regimen. <i>Journal of Pharmacology and Experimental Therapeutics</i> , 2020, 374, 438-451.	2.5	16
7881	Development and application of coarse-grained MARTINI model of skin lipid ceramide [AP]. <i>Journal of Molecular Modeling</i> , 2020, 26, 182.	1.8	4
7882	Co-evolution of $\beta$ -glucosidase activity and product tolerance for increasing cellulosic ethanol yield. <i>Biotechnology Letters</i> , 2020, 42, 2239-2250.	2.2	8
7883	Multispectroscopic analysis, atomic force microscopy, molecular docking and molecular dynamic simulation studies of the interaction between [SnMe <sub>2</sub> Cl <sub>2</sub> (Me <sub>2</sub> phen)] complex and ct-DNA in the presence of glucose. <i>Journal of Biomolecular Structure and Dynamics</i> , 2021, 39, 5068-5082.	3.5	4
7884	Cryo-EM, X-ray diffraction, and atomistic simulations reveal determinants for the formation of a supramolecular myelin-like proteolipid lattice. <i>Journal of Biological Chemistry</i> , 2020, 295, 8692-8705.	3.4	15
7885	Cholesterol Alters the Orientation and Activity of the Influenza Virus M2 Amphipathic Helix in the Membrane. <i>Journal of Physical Chemistry B</i> , 2020, 124, 6738-6747.	2.6	22
7886	Thermal Molecular Motion Can Amplify Intermolecular Magnetic Interactions. <i>Journal of Physical Chemistry B</i> , 2020, 124, 6175-6180.	2.6	4
7887	Conformational and Dynamic Properties of Short DNA Minicircles in Aqueous Solution from Atomistic Molecular Dynamics Simulations. <i>Macromolecules</i> , 2020, 53, 5903-5918.	4.8	8

#	ARTICLE	IF	CITATIONS
7888	Filgrastim loading in PLGA and SLN nanoparticulate system: a bioinformatics approach. Drug Development and Industrial Pharmacy, 2020, 46, 1354-1361.	2.0	13
7889	Molecular dynamics simulations on interaction of ssDNA-causing DM1 with carbon and boron nitride nanotubes to inhibit the formation of CTG repeat secondary structures. Applied Surface Science, 2020, 524, 146572.	6.1	13
7890	Acquired Functional Capsid Structures in Metazoan Totivirus-like dsRNA Virus. Structure, 2020, 28, 888-896.e3.	3.3	12
7891	Functional effect of nobiletin as a food-derived allosteric modulator of mouse CRFR2 $\hat{1}$ 2 in skeletal muscle. Biochemical and Biophysical Research Communications, 2020, 529, 328-334.	2.1	0
7892	Calcium-Lipid Interactions Observed with Isotope-Edited Infrared Spectroscopy. Biophysical Journal, 2020, 118, 2694-2702.	0.5	9
7893	Shock wave induced exfoliation of molybdenum disulfide (MoS2) in various solvents: All-atom molecular dynamics simulation. Journal of Molecular Liquids, 2020, 314, 113671.	4.9	8
7894	Assessing the DOPC-cholesterol interactions and their influence on fullerene C60 partitioning in lipid bilayers. Journal of Molecular Liquids, 2020, 315, 113698.	4.9	15
7895	From the vapor-liquid equilibrium to the supercritical condition. Molecular dynamics modeling of 1,3-butadiene. Journal of Molecular Liquids, 2020, 315, 113702.	4.9	4
7896	Computational modeling on mitochondrial channel nanotoxicity. Nano Today, 2020, 34, 100913.	11.9	7
7897	Phenotypic and molecular characteristics of CF patients carrying the I1234V mutation. Respiratory Medicine, 2020, 170, 106027.	2.9	1
7898	Studying O2 pathways in [NiFe]- and [NiFeSe]-hydrogenases. Scientific Reports, 2020, 10, 10540.	3.3	5
7899	Controlling ion transport in a C<sub>2</sub>-N-based nanochannel with tunable interlayer spacing. Physical Chemistry Chemical Physics, 2020, 22, 16855-16861.	2.8	10
7900	Effect of novel leukemia mutations (K75E & E222K) on interferon regulatory factor 1 and its interaction with DNA: insights from molecular dynamics simulations and docking studies. Journal of Biomolecular Structure and Dynamics, 2021, 39, 5235-5247.	3.5	23
7901	Theoretical insights on helix repacking as the origin of P-glycoprotein promiscuity. Scientific Reports, 2020, 10, 9823.	3.3	15
7902	The Dynamics of S-adenosyl-methionine and S-adenosyl-homocysteine in Mouse Dnmt1 is Driven by Their Structural Flexibilities. Chemistry Letters, 2020, 49, 785-788.	1.3	1
7903	In Silico Study of the Mechanism of Binding of the N-Terminal Region of $\hat{1}$ ± Synuclein to Synaptic-Like Membranes. Life, 2020, 10, 98.	2.4	7
7904	Heterogeneous Rotational Dynamics of Imidazolium-Based Organic Ionic Plastic Crystals. Journal of Physical Chemistry B, 2020, 124, 6894-6904.	2.6	18
7905	Structureâ€Interaction Relationship of Polymyxins with the Membrane of Human Kidney Proximal Tubular Cells. ACS Infectious Diseases, 2020, 6, 2110-2119.	3.8	18



#	ARTICLE	IF	CITATIONS
7906	Deciphering the Binding of Salicylic Acid to Arabidopsis thaliana Chloroplastic GAPDH-A1. International Journal of Molecular Sciences, 2020, 21, 4678.	4.1	9
7907	Free energy of proton transfer at the water–TiO <sub>2</sub> interface from <i>ab initio</i> deep potential molecular dynamics. Chemical Science, 2020, 11, 2335-2341.	7.4	134
7908	Probing remote residues important for catalysis in Escherichia coli ornithine transcarbamoylase. PLoS ONE, 2020, 15, e0228487.	2.5	4
7909	Dependence of amino-acid dielectric relaxation on solute-water interaction: Molecular dynamics study. Journal of Molecular Liquids, 2020, 303, 112613.	4.9	3
7910	7-Methoxytacrine and 2-Aminobenzothiazole Heterodimers: Structure–Mechanism Relationship of Amyloid Inhibitors Based on Rational Design. ACS Chemical Neuroscience, 2020, 11, 715-729.	3.5	10
7911	Role of the porphyrins and demulsifiers in the aggregation process of asphaltenes at water/oil interfaces under desalting conditions: a molecular dynamics study. Petroleum Science, 2020, 17, 797-810.	4.9	17
7912	Structural evaluation and deformation features of polycrystalline BCC Fe with carbides during creep process. Journal of Materials Research and Technology, 2020, 9, 2969-2982.	5.8	3
7913	Biophysical and in silico investigations of the molecular association between a potent RNA polymerase inhibitor, thiolutin and human serum albumin. Journal of Molecular Liquids, 2020, 303, 112648.	4.9	10
7914	Solvation structure of supercritical CO <sub>2</sub> and brine mixture for CO <sub>2</sub> plume geothermal applications: A molecular dynamics study. Journal of Supercritical Fluids, 2020, 159, 104783.	3.2	1
7915	Insights into the Emerging Networks of Voids in Simulated Supercooled Water. Journal of Physical Chemistry B, 2020, 124, 2180-2190.	2.6	14
7916	A Thermolabile Phospholipase B from Talaromyces marneffe GD-0079: Biochemical Characterization and Structure Dynamics Study. Biomolecules, 2020, 10, 231.	4.0	15
7917	Mixing states of imidazolium-based ionic liquid, [C <sub>4</sub> mim][TFSI], with cycloethers studied by SANS, IR, and NMR experiments and MD simulations. Physical Chemistry Chemical Physics, 2020, 22, 5332-5346.	2.8	4
7918	Structural Features of $\beta$ -Cyclodextrin Solvation in the Deep Eutectic Solvent, Reline. Journal of Physical Chemistry B, 2020, 124, 2652-2660.	2.6	23
7919	Capturing Choline–Aromatics Cation– $\pi$ Interactions in the MARTINI Force Field. Journal of Chemical Theory and Computation, 2020, 16, 2550-2560.	5.3	35
7920	Cholesterol Reduces Partitioning of Antifungal Drug Itraconazole into Lipid Bilayers. Journal of Physical Chemistry B, 2020, 124, 2139-2148.	2.6	12
7921	Molecular and Coarse-Grained Modeling to Characterize and Optimize Dendrimer-Based Nanocarriers for Short Interfering RNA Delivery. ACS Omega, 2020, 5, 2978-2986.	3.5	10
7922	Biophysical Characterization of Epigallocatechin-3-Gallate Effect on the Cardiac Sodium Channel Nav1.5. Molecules, 2020, 25, 902.	3.8	3
7923	Relaxation dynamics and power spectra of liquid water: a molecular dynamics simulation study. Molecular Physics, 2020, 118, e1733117.	1.7	0

#	ARTICLE	IF	CITATIONS
7924	Investigation of a Direct Interaction between miR4749 and the Tumor Suppressor p53 by Fluorescence, FRET and Molecular Modeling. <i>Biomolecules</i> , 2020, 10, 346.	4.0	8
7925	Kinetics of pH-dependent interactions between PD-1 and PD-L1 immune checkpoint proteins from molecular dynamics. <i>Proteins: Structure, Function and Bioinformatics</i> , 2020, 88, 1162-1168.	2.6	4
7926	Effects of Layer-Charge Distribution of 2:1 Clay Minerals on Methane Hydrate Formation: A Molecular Dynamics Simulation Study. <i>Langmuir</i> , 2020, 36, 3323-3335.	3.5	39
7927	In Silico Insights into Protein-Protein Interaction Disruptive Mutations in the PCSK9-LDLR Complex. <i>International Journal of Molecular Sciences</i> , 2020, 21, 1550.	4.1	13
7928	Single-channel properties of skeletal muscle ryanodine receptor pore Î²4923FF4924 in two brothers with a lethal form of fetal akinesia. <i>Cell Calcium</i> , 2020, 87, 102182.	2.4	6
7929	Molecular dynamics simulations reveal distinct differences in conformational dynamics and thermodynamics between the unliganded and CD4-bound states of HIV-1 gp120. <i>Physical Chemistry Chemical Physics</i> , 2020, 22, 5548-5560.	2.8	12
7930	Effects of pH and electrolytes on the sheet-to-sheet aggregation mode of graphene oxide in aqueous solutions. <i>Environmental Science: Nano</i> , 2020, 7, 984-995.	4.3	13
7931	Not all therapeutic antibody isotypes are equal: the case of IgM versus IgG in Pertuzumab and Trastuzumab. <i>Chemical Science</i> , 2020, 11, 2843-2854.	7.4	23
7932	Charge-dependent interactions of monomeric and filamentous actin with lipid bilayers. <i>Proceedings of the National Academy of Sciences of the United States of America</i> , 2020, 117, 5861-5872.	7.1	35
7933	Hexagonal arrangement of phospholipids in bilayer membranes*. <i>Chinese Physics B</i> , 2020, 29, 030505.	1.4	2
7934	Overcharging of the Zinc Ion in the Structure of the Zinc-Finger Protein Is Needed for DNA Binding Stability. <i>Biochemistry</i> , 2020, 59, 1378-1390.	2.5	13
7935	Conversion of chemical to mechanical energy by the nucleotide binding domains of ABCB1. <i>Scientific Reports</i> , 2020, 10, 2589.	3.3	6
7936	Diverse effects of aqueous polar co-solvents on Candida antarctica lipase B. <i>International Journal of Biological Macromolecules</i> , 2020, 150, 930-940.	7.5	23
7937	The self-assembly and microscopic interfacial properties of a supercritical CO2 microemulsion having hydrotropes: Atom-level observation from molecular dynamics simulation. <i>Journal of CO2 Utilization</i> , 2020, 38, 77-87.	6.8	6
7938	Characterizing Membrane Association and Periplasmic Transfer of Bacterial Lipoproteins through Molecular Dynamics Simulations. <i>Structure</i> , 2020, 28, 475-487.e3.	3.3	15
7939	Phosphorylation of a Disordered Peptide-Structural Effects and Force Field Inconsistencies. <i>Journal of Chemical Theory and Computation</i> , 2020, 16, 1924-1935.	5.3	21
7940	The Catalytic Acid-Base in GH109 Resides in a Conserved GGHGG Loop and Allows for Comparable Î±-Retaining and Î²-Inverting Activity in an <i>N</i> -Acetylgalactosaminidase from <i>Akkermansia muciniphila</i> . <i>ACS Catalysis</i> , 2020, 10, 3809-3819.	11.2	15
7941	Cyanidin-3-O-glucoside inhibits AÎ²40 fibrillogenesis, disintegrates preformed fibrils, and reduces amyloid cytotoxicity. <i>Food and Function</i> , 2020, 11, 2573-2587.	4.6	26

#	ARTICLE	IF	CITATIONS
7942	SAMPL6 hostâ€“guest binding affinities and binding poses from spherical-coordinates-biased simulations. <i>Journal of Computer-Aided Molecular Design</i> , 2020, 34, 589-600.	2.9	23
7943	Response Theory for Static and Dynamic Solvation of Ionic and Dipolar Solutes in Water. <i>Journal of Statistical Physics</i> , 2020, 180, 721-738.	1.2	6
7944	New insights on the role of ROS in the mechanisms of sonoporation-mediated gene delivery. <i>Ultrasonics Sonochemistry</i> , 2020, 64, 104998.	8.2	16
7945	Polysaccharide Structures in the Outer Mucilage of <i>Arabidopsis</i> Seeds Visualized by AFM. <i>Biomacromolecules</i> , 2020, 21, 1450-1459.	5.4	17
7946	The Ca <sup>2+</sup> permeation mechanism of the ryanodine receptor revealed by a multi-site ion model. <i>Nature Communications</i> , 2020, 11, 922.	12.8	33
7947	Improvement in predicting drug sensitivity changes associated with protein mutations using a molecular dynamics based alchemical mutation method. <i>Scientific Reports</i> , 2020, 10, 2161.	3.3	7
7948	Localized Axolemma Deformations Suggest Mechanoporation as Axonal Injury Trigger. <i>Frontiers in Neurology</i> , 2020, 11, 25.	2.4	16
7949	Inhibition of quorum sensingâ€“associated virulence factors and biofilm formation in <i>Pseudomonas aeruginosa</i> PAO1 by <i>Mycoleptodiscus indicus</i> PUTY1. <i>Brazilian Journal of Microbiology</i> , 2020, 51, 467-487.	2.0	14
7950	Structural Dynamics of Neighboring Water Molecules of N-Isopropylacrylamide Pentamer. <i>ACS Omega</i> , 2020, 5, 1408-1413.	3.5	10
7951	High- $\chi$ alternating copolymers for accessing sub-5 nm domains via simulations. <i>Physical Chemistry Chemical Physics</i> , 2020, 22, 5577-5583.	2.8	12
7952	Protein unfolding by SDS: the microscopic mechanisms and the properties of the SDS-protein assembly. <i>Nanoscale</i> , 2020, 12, 5422-5434.	5.6	34
7953	Statistical complexity of potential energy landscape as a dynamic signature of the glass transition. <i>Physical Review B</i> , 2020, 101, .	3.2	12
7954	Stress-Measure Dependence of Phase Transformation Criterion under Finite Strains: Hierarchy of Crystal Lattice Instabilities for Homogeneous and Heterogeneous Transformations. <i>Physical Review Letters</i> , 2020, 124, 075701.	7.8	8
7955	Multiple lipid binding sites determine the affinity of PH domains for phosphoinositide-containing membranes. <i>Science Advances</i> , 2020, 6, eaay5736.	10.3	44
7956	Novel Sequence Feature of SecA Translocase Protein Unique to the Thermophilic Bacteria: Bioinformatics Analyses to Investigate Their Potential Roles. <i>Microorganisms</i> , 2020, 8, 59.	3.6	6
7957	Inserting Small Molecules across Membrane Mixtures: Insight from the Potential of Mean Force. <i>Biophysical Journal</i> , 2020, 118, 1321-1332.	0.5	15
7958	Exploring the interaction of bioactive kaempferol with serum albumin, lysozyme and hemoglobin: A biophysical investigation using multi-spectroscopic, docking and molecular dynamics simulation studies. <i>Journal of Photochemistry and Photobiology B: Biology</i> , 2020, 205, 111825.	3.8	70
7959	Folding intermediate states of the parallel human telomeric G-quadruplex DNA explored using Well-Tempered Metadynamics. <i>Scientific Reports</i> , 2020, 10, 3176.	3.3	21

#	ARTICLE	IF	CITATIONS
7960	Molecular dynamics simulations of alkaline earth metal ions binding to DNA reveal ion size and hydration effects. <i>Physical Chemistry Chemical Physics</i> , 2020, 22, 5584-5596.	2.8	20
7961	Oversized ubiquinones as molecular probes for structural dynamics of the ubiquinone reaction site in mitochondrial respiratory complex I. <i>Journal of Biological Chemistry</i> , 2020, 295, 2449-2463.	3.4	17
7962	Molecular dynamics simulation on the dissolution process of Kaempferol cluster. <i>Journal of Molecular Liquids</i> , 2020, 304, 112779.	4.9	2
7963	Mutual and Thermal Diffusivities as well as Fluid-Phase Equilibria of Mixtures of 1-Hexanol and Carbon Dioxide. <i>Journal of Physical Chemistry B</i> , 2020, 124, 2482-2494.	2.6	32
7964	Interfacial structure in the liquid-liquid extraction of rare earth elements by phosphoric acid ligands: a molecular dynamics study. <i>Physical Chemistry Chemical Physics</i> , 2020, 22, 4177-4192.	2.8	9
7965	Saccharide Insertion in Carbon Nanotube: Molecular Dynamics Simulation Studies. <i>Bulletin of the Korean Chemical Society</i> , 2020, 41, 439-443.	1.9	2
7966	Performing solvation free energy calculations in LAMMPS using the decoupling approach. <i>Journal of Computer-Aided Molecular Design</i> , 2020, 34, 641-646.	2.9	10
7967	Choice of Force Field for Proteins Containing Structured and Intrinsically Disordered Regions. <i>Biophysical Journal</i> , 2020, 118, 1621-1633.	0.5	28
7968	High temperature induced structural changes of apo-lactoferrin and interactions with $\beta$ 2-lactoglobulin and $\beta$ 1-lactalbumin for potential encapsulation strategies. <i>Food Hydrocolloids</i> , 2020, 105, 105817.	10.7	15
7969	Determination of Protein Structural Ensembles by Hybrid-Resolution SAXS Restrained Molecular Dynamics. <i>Journal of Chemical Theory and Computation</i> , 2020, 16, 2825-2834.	5.3	33
7970	Thermodynamics of <i>N</i> -Isopropylacrylamide in Water: Insight from Experiments, Simulations, and Kirkwood-Buff Analysis Teamwork. <i>Journal of Physical Chemistry B</i> , 2020, 124, 2495-2504.	2.6	13
7971	Protein-Mutation-Induced Conformational Changes of the DNA and Nuclease Domain in CRISPR/Cas9 Systems by Molecular Dynamics Simulations. <i>Journal of Physical Chemistry B</i> , 2020, 124, 2168-2179.	2.6	10
7972	How Hydration Affects the Microscopic Structural Morphology in a Deep Eutectic Solvent. <i>Journal of Physical Chemistry B</i> , 2020, 124, 2230-2237.	2.6	75
7973	Molecular Dynamics Simulation Study of the Plastic/Ferroelectric Crystal Quinuclidinium Perrhenate. <i>Journal of Physical Chemistry C</i> , 2020, 124, 2171-2177.	3.1	10
7974	The relation between lignin sequence and its 3D structure. <i>Biochimica Et Biophysica Acta - General Subjects</i> , 2020, 1864, 129547.	2.4	17
7975	Structural Basis for Lipid Binding and Function by an Evolutionarily Conserved Protein, Serum Amyloid A. <i>Journal of Molecular Biology</i> , 2020, 432, 1978-1995.	4.2	16
7976	Key Factors Determining Efficiency of Liquid-Liquid Extraction: Implications from Molecular Dynamics Simulations of Biphasic Behaviors of CyMe <sub>4</sub> -BTPPhen and Its Am(III) Complexes. <i>Journal of Physical Chemistry B</i> , 2020, 124, 1751-1766.	2.6	8
7977	Predicting Partition Coefficients of Neutral and Charged Solutes in the Mixed SLES-Fatty Acid Micellar System. <i>Journal of Physical Chemistry B</i> , 2020, 124, 1653-1664.	2.6	5

#	ARTICLE	IF	CITATIONS
7978	Comparing the Hinge-Type Mobility of Natural and Designed Intermolecular Bi-disulfide Domains. <i>Frontiers in Chemistry</i> , 2020, 8, 25.	3.6	5
7979	Probing Carbon Utilization of <i>Cordyceps militaris</i> by Sugar Transportome and Protein Structural Analysis. <i>Cells</i> , 2020, 9, 401.	4.1	13
7980	Molecular dynamics trajectories for 630 coarse-grained drug-membrane permeations. <i>Scientific Data</i> , 2020, 7, 51.	5.3	23
7981	A novel artificial intelligence protocol for finding potential inhibitors of acute myeloid leukemia. <i>Journal of Materials Chemistry B</i> , 2020, 8, 2063-2081.	5.8	12
7982	How Flexibility of the Nanoscale Solvophobic Confining Material Promotes Capillary Evaporation of Ionic Liquids. <i>Journal of Physical Chemistry C</i> , 2020, 124, 4899-4906.	3.1	5
7983	Charge transfer as a ubiquitous mechanism in determining the negative charge at hydrophobic interfaces. <i>Nature Communications</i> , 2020, 11, 901.	12.8	68
7984	Salt effect on thermodynamics and kinetics of a single RNA base pair. <i>Rna</i> , 2020, 26, 470-480.	3.5	14
7985	Elucidating the Effect of Static Electric Field on Amyloid Beta 1â€“42 Supramolecular Assembly. <i>Journal of Molecular Graphics and Modelling</i> , 2020, 96, 107535.	2.4	14
7986	Comparing Alchemical Free Energy Estimates to Experimental Values Based on the Ben-Naim Formula: How Much Agreement Can We Expect?. <i>Journal of Physical Chemistry B</i> , 2020, 124, 840-847.	2.6	2
7987	Recruiting Mechanism and Functional Role of a Third Metal Ion in the Enzymatic Activity of 5â€“ <sup>2</sup> Structure-Specific Nucleases. <i>Journal of the American Chemical Society</i> , 2020, 142, 2823-2834.	13.7	13
7988	Elucidating the preference of dimeric over monomeric form for thermal stability of <i>Thermus thermophilus</i> isopropylmalate dehydrogenase: A molecular dynamics perspective. <i>Journal of Molecular Graphics and Modelling</i> , 2020, 96, 107530.	2.4	3
7989	Anion Effect on Gas Absorption in Imidazolium-Based Ionic Liquids. <i>Journal of Chemical Information and Modeling</i> , 2020, 60, 661-666.	5.4	15
7990	Simulation of Raman and Raman optical activity of saccharides in solution. <i>Physical Chemistry Chemical Physics</i> , 2020, 22, 1983-1993.	2.8	29
7991	Choline Chloride as a Nanoâ€“Crowder Protects HPâ€“36 from Ureaâ€“Induced Denaturation: Insights from Solvent Dynamics and Proteinâ€“Solvent Interactions. <i>ChemPhysChem</i> , 2020, 21, 552-567.	2.1	25
7992	A spontaneous mitonuclear epistasis converging on Rieske Fe-S protein exacerbates complex III deficiency in mice. <i>Nature Communications</i> , 2020, 11, 322.	12.8	17
7993	Structural instability and divergence from conserved residues underlie intracellular retention of mammalian odorant receptors. <i>Proceedings of the National Academy of Sciences of the United States of America</i> , 2020, 117, 2957-2967.	7.1	27
7994	Influence of osmolytes and ionic liquids on the Bacteriorhodopsin structure in the absence and presence of oxidative stress: A combined experimental and computational study. <i>International Journal of Biological Macromolecules</i> , 2020, 148, 657-665.	7.5	13
7995	A structural entropy index to analyse local conformations in intrinsically disordered proteins. <i>Journal of Structural Biology</i> , 2020, 210, 107464.	2.8	13

#	ARTICLE	IF	CITATIONS
7996	Retained Stability of the RNA Structure in DNA Packaging Motor with a Single Mg <sup>2+</sup> Ion Bound at the Double Mg-Clamp Structure. <i>Journal of Physical Chemistry B</i> , 2020, 124, 701-707.	2.6	4
7997	Cryo-Electron Microscopy Structure of the Î±IIbÎ²3-Abciximab Complex. <i>Arteriosclerosis, Thrombosis, and Vascular Biology</i> , 2020, 40, 624-637.	2.4	12
7998	In Silico design of AVP (4â€“5) peptide and synthesis, characterization and in vitro activity of chitosan nanoparticles. <i>DARU, Journal of Pharmaceutical Sciences</i> , 2020, 28, 139-157.	2.0	6
7999	A Structural Basis for Restricted Codon Recognition Mediated by 2-thiocytidine in tRNA Containing a Wobble Position Inosine. <i>Journal of Molecular Biology</i> , 2020, 432, 913-929.	4.2	12
8000	Conformational equilibria of pharmaceuticals in supercritical CO <sub>2</sub> , IR spectroscopy and quantum chemical calculations. <i>Spectrochimica Acta - Part A: Molecular and Biomolecular Spectroscopy</i> , 2020, 230, 118072.	3.9	18
8001	Cryo-temperature effects on membrane protein structure and dynamics. <i>Physical Chemistry Chemical Physics</i> , 2020, 22, 5427-5438.	2.8	35
8002	Hup-Type Hydrogenases of Purple Bacteria: Homology Modeling and Computational Assessment of Biotechnological Potential. <i>International Journal of Molecular Sciences</i> , 2020, 21, 366.	4.1	4
8003	Site Directed Disulfide PEGylation of Interferon-Î²-1b with Fork Peptide Linker. <i>Bioconjugate Chemistry</i> , 2020, 31, 708-720.	3.6	0
8004	Molecular Insight into the Interaction between Camptothecin and Acyclic Cucurbit[4]urils as Efficient Nanocontainers in Comparison with Cucurbit[7]uril: Molecular Docking and Molecular Dynamics Simulation. <i>Journal of Chemical Information and Modeling</i> , 2020, 60, 1791-1803.	5.4	10
8005	Size and Diffusivity of Polymer Rings in Linear Polymer Matrices: The Key Role of Threading Events. <i>Macromolecules</i> , 2020, 53, 803-820.	4.8	26
8006	Insights into the Gas Adsorption Mechanisms in Metalâ€“Organic Frameworks from Classical Molecular Simulations. <i>Topics in Current Chemistry</i> , 2020, 378, 14.	5.8	16
8007	Molecular Dynamics. , 2020, , 573-594.		6
8008	Mechanical Unfolding of Spectrin Repeats Induces Water-Molecule Ordering. <i>Biophysical Journal</i> , 2020, 118, 1076-1089.	0.5	3
8009	Liquidâ€“Liquid Phase Behavior of Solutions of 1,3-Diethylimidazolium Bis((trifluoromethyl)sulfonyl)amide in <i>n</i>-Alkyl Alcohols. <i>Journal of Chemical &amp; Engineering Data</i> , 2020, 65, 1345-1357.	1.9	6
8010	Determination of the Free Energies of Mixing of Organic Solutions through a Combined Molecular Dynamics and Bayesian Statistics Approach. <i>Journal of Chemical Information and Modeling</i> , 2020, 60, 1424-1431.	5.4	6
8011	Role of Oxidized Gly25, Gly29, and Gly33 Residues on the Interactions of AÎ² <sub>42</sub> with Lipid Membranes. <i>ACS Chemical Neuroscience</i> , 2020, 11, 535-548.	3.5	9
8012	Ion transport mechanisms in saltâ€“doped polymerized zwitterionic electrolytes. <i>Journal of Polymer Science</i> , 2020, 58, 578-588.	3.8	11
8013	Prediction of octanol-water partition coefficients for the SAMPL6-\$\$\$ molecules using molecular dynamics simulations with OPLS-AA, AMBER and CHARMM force fields. <i>Journal of Computer-Aided Molecular Design</i> , 2020, 34, 543-560.	2.9	30



#	ARTICLE	IF	CITATIONS
8014	A new insight into protein-protein interactions and the effect of conformational alterations in PCNA. International Journal of Biological Macromolecules, 2020, 148, 999-1009.	7.5	49
8015	Structure and assembly of calcium homeostasis modulator proteins. Nature Structural and Molecular Biology, 2020, 27, 150-159.	8.2	55
8016	Expanding the structural diversity of peptide assemblies by coassembling dipeptides with diphenylalanine. Nanoscale, 2020, 12, 3038-3049.	5.6	14
8017	Design and analysis of polypeptide nanofiber using full atomistic Molecular Dynamic. Journal of Molecular Liquids, 2020, 302, 112610.	4.9	14
8018	Structural Bioinformatics. Methods in Molecular Biology, 2020, , .	0.9	5
8019	Molecular Dynamics Simulations of Hydrophobic Nanoparticle Effects on Gas Hydrate Formation. Journal of Physical Chemistry C, 2020, 124, 4162-4171.	3.1	29
8020	Combined Force-Frequency Sampling for Simulation of Systems Having Rugged Free Energy Landscapes. Journal of Chemical Theory and Computation, 2020, 16, 1448-1455.	5.3	14
8021	Current Status of Carbohydrates Information in the Protein Data Bank. Journal of Chemical Information and Modeling, 2020, 60, 684-699.	5.4	24
8022	Impact of hydrogen microalloying on the mechanical behavior of Zr-bearing metallic glasses: A molecular dynamics study. Journal of Materials Science and Technology, 2020, 45, 198-206.	10.7	16
8023	Phase Separation in Atomistic Simulations of Model Membranes. Journal of the American Chemical Society, 2020, 142, 2844-2856.	13.7	57
8024	In Silico Identification of a Key Residue for Substrate Recognition of the Riboflavin Membrane Transporter RFVT3. Journal of Chemical Information and Modeling, 2020, 60, 1368-1375.	5.4	4
8025	Properties of Lipid Models of Lung Surfactant Containing Cholesterol and Oxidized Lipids: A Mixed Experimental and Computational Study. Langmuir, 2020, 36, 1023-1033.	3.5	12
8026	Optimization of hydrophobic nanoparticles to better target lipid rafts with molecular dynamics simulations. Nanoscale, 2020, 12, 4101-4109.	5.6	23
8027	Deciphering the molecular mechanism of FLT3 resistance mutations. FEBS Journal, 2020, 287, 3200-3220.	4.7	16
8028	Supramolecular Protein Assembly Retains Its Structural Integrity at Liquid-Liquid Interface. Advanced Materials Interfaces, 2020, 7, 1901674.	3.7	4
8029	Transit of Procaspase-9 towards its activation. New mechanistic insights from molecular dynamics simulations. Journal of Molecular Modeling, 2020, 26, 24.	1.8	2
8030	Comparative modeling of the disregistry and Peierls stress for dissociated edge and screw dislocations in Al. International Journal of Plasticity, 2020, 129, 102689.	8.8	38
8031	Protein Preferential Solvation in Water:Glycerol Mixtures. Journal of Physical Chemistry B, 2020, 124, 1424-1437.	2.6	18

#	ARTICLE	IF	CITATIONS
8032	Multiscale model of the role of grain boundary structures in the dynamic intergranular failure of polycrystal aggregates. <i>Computer Methods in Applied Mechanics and Engineering</i> , 2020, 362, 112868.	6.6	7
8033	Flexible bond and angle, FBA/Ĵ model of water. <i>Journal of Molecular Liquids</i> , 2020, 303, 112598.	4.9	7
8034	Lipophilicity of Coarse-Grained Cholesterol Models. <i>Journal of Chemical Information and Modeling</i> , 2020, 60, 569-577.	5.4	17
8035	A Polarization-Consistent Model for Alcohols to Predict Solvation Free Energies. <i>Journal of Chemical Information and Modeling</i> , 2020, 60, 1352-1367.	5.4	14
8036	Cutting antiparallel DNA strands in a single active site. <i>Nature Structural and Molecular Biology</i> , 2020, 27, 119-126.	8.2	25
8037	Molecular Simulation of Mechanical Properties and Membrane Activities of the ESCRT-III Complexes. <i>Biophysical Journal</i> , 2020, 118, 1333-1343.	0.5	14
8038	Effects of Nanoparticle Electrostatics and Protein-Protein Interactions on Corona Formation: Conformation and Hydrodynamics. <i>Small</i> , 2020, 16, e1906598.	10.0	37
8039	Functional analysis and screening small molecules to RpfF protein in <i>Xanthomonas oryzae</i> involved in rice bacterial blight disease. <i>Journal of Integrative Agriculture</i> , 2020, 19, 735-747.	3.5	9
8040	Lignin solvation by ionic liquids: The role of cation. <i>Journal of Molecular Liquids</i> , 2020, 303, 112588.	4.9	17
8041	Structural basis of proton-coupled potassium transport in the KUP family. <i>Nature Communications</i> , 2020, 11, 626.	12.8	60
8042	Mechanism of homodimeric cytokine receptor activation and dysregulation by oncogenic mutations. <i>Science</i> , 2020, 367, 643-652.	12.6	123
8043	Raman Optical Activity of Glucose and Sorbose in Extended Wavenumber Range. <i>ChemPhysChem</i> , 2020, 21, 1272-1279.	2.1	9
8044	Variance of Atomic Coordinates as a Dynamical Metric to Distinguish Proteins and Protein-Protein Interactions in Molecular Dynamics Simulations. <i>Journal of Physical Chemistry B</i> , 2020, 124, 4247-4262.	2.6	4
8045	Elucidating the Molecular Interactions between Uremic Toxins and the Sudlow II Binding Site of Human Serum Albumin. <i>Journal of Physical Chemistry B</i> , 2020, 124, 3922-3930.	2.6	5
8046	Dispersion of Nafion Ionomer Aggregates in 1-Propanol/Water Solutions: Effects of Ionomer Concentration, Alcohol Content, and Salt Addition. <i>Macromolecules</i> , 2020, 53, 3273-3283.	4.8	34
8047	Insights into Hydrophobic Ion Pairing from Molecular Simulation and Experiment. <i>ACS Nano</i> , 2020, 14, 6097-6106.	14.6	18
8048	Study of the aggregation behaviour of three primary reactive dyes via molecular dynamics simulations. <i>Molecular Simulation</i> , 2020, 46, 627-637.	2.0	8
8049	Formation of aggregates, icosahedral structures and percolation clusters of fullerenes in lipids bilayers: The key role of lipid saturation. <i>Biochimica Et Biophysica Acta - Biomembranes</i> , 2020, 1862, 183328.	2.6	9

#	ARTICLE	IF	CITATIONS
8050	Cavitation in lipid bilayers poses strict negative pressure stability limit in biological liquids. Proceedings of the National Academy of Sciences of the United States of America, 2020, 117, 10733-10739.	7.1	16
8051	Conformational Changes in Tyrosine 11 of Neurotensin Are Required to Activate the Neurotensin Receptor 1. ACS Pharmacology and Translational Science, 2020, 3, 690-705.	4.9	16
8052	Induced Polarization in Molecular Dynamics Simulations of the 5-HT <sub>3</sub> Receptor Channel. Journal of the American Chemical Society, 2020, 142, 9415-9427.	13.7	38
8053	Inter-domain dynamics in the chaperone SurA and multi-site binding to its outer membrane protein clients. Nature Communications, 2020, 11, 2155.	12.8	48
8054	Mining the Cambridge Database for theoretical chemistry. Mi-LJC: a new set of Lennard-Jones+“Coulomb atom+“atom potentials for the computer simulation of organic condensed matter. CrystEngComm, 2020, 22, 7350-7360.	2.6	17
8055	Single+Molecule Study of Peptides with the Same Amino Acid Composition but Different Sequences by Using an Aerolysin Nanopore. ChemBioChem, 2020, 21, 2467-2473.	2.6	14
8056	+MkVsites+ : A tool for creating +GROMACS+ virtual sites parameters to increase performance in all+atom molecular dynamics simulations. Journal of Computational Chemistry, 2020, 41, 1564-1569.	3.3	15
8057	Exhaustive search of the configurational space of heat+shock protein 90 with its inhibitor by multicanonical molecular dynamics based dynamic docking. Journal of Computational Chemistry, 2020, 41, 1606-1615.	3.3	20
8058	Voltage-induced structural modifications on M2 muscarinic receptor and their functional implications when interacting with the superagonist iperovo. Biochemical Pharmacology, 2020, 177, 113961.	4.4	7
8059	Lipid coating and end functionalization govern the formation and stability of transmembrane carbon nanotube porins. Carbon, 2020, 164, 391-397.	10.3	15
8060	Atomistic insights into the effects of carbonyl oxygens in functionalized graphene nanopores on Ca <sup>2+</sup> /Na <sup>+</sup> sieving. Carbon, 2020, 164, 305-316.	10.3	12
8061	Two-scale simulation of plasticity in molybdenum: Combination of atomistic simulation and dislocation dynamics with non-linear mobility function. Computational Materials Science, 2020, 179, 109585.	3.0	8
8062	Molecular insights into the inhibitory mechanisms of gallate moiety on the A $\beta$ 1-40 amyloid aggregation: A molecular dynamics simulation study. International Journal of Biological Macromolecules, 2020, 156, 40-50.	7.5	13
8063	Tension-Compression asymmetry of single-crystalline and nanocrystalline NiTi shape memory alloy: An atomic scale study. Mechanics of Materials, 2020, 145, 103402.	3.2	33
8064	Water in confinement of epoxy layer and hydroxylated (001) $\gamma$ -alumina: An atomistic simulation view. Journal of Molecular Liquids, 2020, 307, 112976.	4.9	2
8065	Quantitative Prediction of the Structure and Viscosity of Aqueous Micellar Solutions of Ionic Surfactants: A Combined Approach Based on Coarse-Grained MARTINI Simulations Followed by Reverse-Mapped All-Atom Molecular Dynamics Simulations. Journal of Chemical Theory and Computation, 2020, 16, 3363-3372.	5.3	17
8066	Interactions between Band 3 Anion Exchanger and Lipid Nanodomains in Ternary Lipid Bilayers: Atomistic Simulations. Journal of Physical Chemistry B, 2020, 124, 3054-3064.	2.6	9
8067	Site-Specific Interactions with Copper Promote Amyloid Fibril Formation for $\beta$ galL2-R24G. ACS Omega, 2020, 5, 7085-7095.	3.5	5

#	ARTICLE	IF	CITATIONS
8068	Structural insights into tetraspanin CD9 function. <i>Nature Communications</i> , 2020, 11, 1606.	12.8	114
8069	Membrane mediated toppling mechanism of the folate energy coupling factor transporter. <i>Nature Communications</i> , 2020, 11, 1763.	12.8	21
8070	A relationship between membrane permeation and partitioning of nitroaromatic explosives and their functional groups. A computational study. <i>Physical Chemistry Chemical Physics</i> , 2020, 22, 8791-8799.	2.8	6
8071	The interfacial structure and dynamics in a polymer nanocomposite containing small attractive nanoparticles: a full atomistic molecular dynamics simulation study. <i>Physical Chemistry Chemical Physics</i> , 2020, 22, 11400-11408.	2.8	11
8072	Unexpected electrochemical behavior of an anolyte redoxmer in flow battery electrolytes: solvating cations help to fight against the thermodynamicâ€“kinetic dilemma. <i>Journal of Materials Chemistry A</i> , 2020, 8, 13470-13479.	10.3	17
8073	Towards molecular simulations that are transparent, reproducible, usable by others, and extensible (TRUE). <i>Molecular Physics</i> , 2020, 118, e1742938.	1.7	22
8074	The mutation L69P in the PAS domain of the hERG potassium channel results in LQTS by trafficking deficiency. <i>Channels</i> , 2020, 14, 163-174.	2.8	1
8075	LUF7244 plus Dofetilide Rescues Aberrant Kv11.1 Trafficking and Produces Functional IKv11.1. <i>Molecular Pharmacology</i> , 2020, 97, 355-364.	2.3	10
8076	Physicochemical Characterisation of KEIFâ€“The Intrinsically Disordered N-Terminal Region of Magnesium Transporter A. <i>Biomolecules</i> , 2020, 10, 623.	4.0	5
8077	Molecular Dynamics Simulations Reveal Canonical Conformations in Different pMHC/TCR Interactions. <i>Cells</i> , 2020, 9, 942.	4.1	18
8078	Structural Characterization of Carbonic Anhydrase VIII and Effects of Missense Single Nucleotide Variations to Protein Structure and Function. <i>International Journal of Molecular Sciences</i> , 2020, 21, 2764.	4.1	11
8079	PDADMAC/PSS Oligoelectrolyte Multilayers: Internal Structure and Hydration Properties at Early Growth Stages from Atomistic Simulations. <i>Molecules</i> , 2020, 25, 1848.	3.8	5
8080	Synthesis, antifungal activity and potential mechanism of fusidic acid derivatives possessing amino-terminal groups. <i>Future Medicinal Chemistry</i> , 2020, 12, 763-774.	2.3	8
8081	Binding Dynamics of siRNA with Selected Lipopeptides: A Computer-Aided Study of the Effect of Lipopeptidesâ€™ Functional Groups and Stereoisomerism. <i>Journal of Chemical Theory and Computation</i> , 2020, 16, 3842-3855.	5.3	4
8082	Block Copolymers Composed of PEO and Polyesteramides Based on Glycolic Acid, L-Valine, and L-Isoleucine. <i>Macromolecules</i> , 2020, 53, 3580-3590.	4.8	12
8083	Competing Dissolution Pathways and Ligand Passivation-Enhanced Interfacial Stability of Hybrid Perovskites with Liquid Water. <i>ACS Applied Materials &amp; Interfaces</i> , 2020, 12, 23584-23594.	8.0	16
8084	Push/Pull Effect as Driving Force for Different Optical Responses of Azobenzene in a Biological Environment. <i>Journal of Physical Chemistry C</i> , 2020, 124, 8310-8322.	3.1	11
8085	Effect of Core Oligomer Length on the Phase Behavior and Assembly of Î¶-Conjugated Peptides. <i>ACS Applied Materials &amp; Interfaces</i> , 2020, 12, 20722-20732.	8.0	6

#	ARTICLE	IF	CITATIONS
8086	Sodium-salt adduct fullerenes prevent self-association and amyloid $\beta^2$ fibril formation: molecular dynamics approach. <i>Soft Materials</i> , 2020, 18, 335-347.	1.7	3
8087	Atomistic Simulation of Nanoindentation of Ice $\text{I}_{\text{h}}$ . <i>Journal of Physical Chemistry C</i> , 2020, 124, 9329-9336.	3.1	7
8088	Investigation of Initial Static Shear Stress Effects on Liquefaction Resistance Using Discrete Element Method Simulations. <i>International Journal of Geomechanics</i> , 2020, 20, .	2.7	9
8089	Pressure-temperature diagram of wetting and dewetting in a hydrophobic grain boundary and the liquidlike to icelike transition of monolayer water. <i>Physical Review B</i> , 2020, 101, .	3.2	3
8090	Adaptive hard and tough mechanical response in single-crystal B1 VN <sub>x</sub> ceramics via control of anion vacancies. <i>Acta Materialia</i> , 2020, 192, 78-88.	7.9	46
8091	Conformational properties of inulin, levan and arabinan studied by molecular dynamics simulations. <i>Carbohydrate Polymers</i> , 2020, 240, 116266.	10.2	4
8092	Role of allosteric switches and adaptor domains in long-distance cross-talk and transient tunnel formation. <i>Science Advances</i> , 2020, 6, eaay7919.	10.3	10
8093	Defining the mobility range of a hinge-type connection using molecular dynamics and metadynamics. <i>PLoS ONE</i> , 2020, 15, e0230962.	2.5	3
8094	Unrevealing the thermophysical properties and microstructural evolution of MgCl <sub>2</sub> -NaCl-KCl eutectic: FPMD simulations and experimental measurements. <i>Solar Energy Materials and Solar Cells</i> , 2020, 210, 110504.	6.2	32
8095	Force-dependent folding pathways in mechanically interlocked calixarene dimers via atomistic force quench simulations. <i>Molecular Physics</i> , 2020, 118, e1743886.	1.7	0
8096	A Novel Approach to Atomistic Molecular Dynamics Simulation of Phenolic Resins Using Symthons. <i>Polymers</i> , 2020, 12, 926.	4.5	3
8097	Complexation with $\beta^2$ -cyclodextrin enhances apoptosis-mediated cytotoxic effect of harman in chemoresistant BRAF-mutated melanoma cells. <i>European Journal of Pharmaceutical Sciences</i> , 2020, 150, 105353.	4.0	7
8098	Structural and molecular insight into the pH-induced low-permeability of the voltage-gated potassium channel Kv1.2 through dewetting of the water cavity. <i>PLoS Computational Biology</i> , 2020, 16, e1007405.	3.2	7
8099	Glycyrrhizin-induced changes in phospholipid dynamics studied by <sup>1</sup> H NMR and MD simulation. <i>Archives of Biochemistry and Biophysics</i> , 2020, 686, 108368.	3.0	21
8100	Size-dependent aggregation of hydrophobic nanoparticles in lipid membranes. <i>Nanoscale</i> , 2020, 12, 9452-9461.	5.6	13
8101	Computer-Aided aptamer design for sulfadimethoxine antibiotic: step by step mutation based on MD simulation approach. <i>Journal of Biomolecular Structure and Dynamics</i> , 2021, 39, 1-9.	3.5	9
8102	Temperature and molecular crowding effects on the sensitivity of T30695 aptamer toward Pb <sup>2+</sup> ion: a joint molecular dynamics simulation and experimental study. <i>Molecular Simulation</i> , 2020, 46, 592-603.	2.0	9
8103	Structural basis of ER-associated protein degradation mediated by the Hrd1 ubiquitin ligase complex. <i>Science</i> , 2020, 368, .	12.6	143

#	ARTICLE	IF	CITATIONS
8104	Dynamic Heterogeneity in Ring-Linear Polymer Blends. <i>Polymers</i> , 2020, 12, 752.	4.5	15
8105	Atomistic investigation on effect of Ca doping ratio on mechanical behaviors of nanocrystalline Mg-Ca alloys. <i>Journal of Molecular Modeling</i> , 2020, 26, 103.	1.8	3
8106	Molecular dynamics simulations in photosynthesis. <i>Photosynthesis Research</i> , 2020, 144, 273-295.	2.9	50
8107	Heterodimer and pore formation of magainin 2 and PGLa: The anchoring and tilting of peptides in lipid bilayers. <i>Biochimica Et Biophysica Acta - Biomembranes</i> , 2020, 1862, 183305.	2.6	6
8108	Small Conformational Changes Underlie Evolution of Resistance to NNRTI in HIV Reverse Transcriptase. <i>Biophysical Journal</i> , 2020, 118, 2489-2501.	0.5	3
8109	Improved coarse-grain model to unravel the phase behavior of 1-alkyl-3-methylimidazolium-based ionic liquids through molecular dynamics simulations. <i>Journal of Colloid and Interface Science</i> , 2020, 574, 324-336.	9.4	28
8110	pH-Dependent adsorption of aromatic compounds on graphene oxide: An experimental, molecular dynamics simulation and density functional theory investigation. <i>Journal of Hazardous Materials</i> , 2020, 395, 122680.	12.4	48
8111	Microsecond molecular dynamics simulation of the adsorption and penetration of oil droplets on cellular membrane. <i>Journal of Hazardous Materials</i> , 2020, 397, 122683.	12.4	18
8112	Molecular dynamics simulations of two double-helical hexamer fragments of iota-carrageenan in aqueous solution. <i>Journal of Molecular Graphics and Modelling</i> , 2020, 98, 107588.	2.4	7
8113	The effect of individual elements of alkali aluminosilicate glass on scratch characteristics: A molecular dynamics study. <i>Journal of Non-Crystalline Solids</i> , 2020, 536, 119840.	3.1	3
8114	On the Thermal Stability of O <sup>6</sup> -Methylguanine-DNA Methyltransferase from <i>Archaeon Pyrococcus kodakaraensis</i> by Molecular Dynamics Simulations. <i>Journal of Chemical Information and Modeling</i> , 2020, 60, 2138-2154.	5.4	8
8115	Investigation of the Dissociation Mechanism of Single-Walled Carbon Nanotube on Mature Amyloid- $\beta^2$ Fibrils at Single Nanotube Level. <i>Journal of Physical Chemistry B</i> , 2020, 124, 3459-3468.	2.6	13
8116	Microscopic Understanding of the Effect of Ionic Liquid on Protein from Molecular Simulation Studies. <i>Journal of Physical Chemistry B</i> , 2020, 124, 3909-3921.	2.6	20
8117	Peptide Side-COOH Groups Have Two Distinct Conformations under Biorelevant Conditions. <i>Journal of Physical Chemistry Letters</i> , 2020, 11, 3466-3472.	4.6	7
8118	Effects of the Hydrophobicity of Key Residues on the Characteristics and Stability of Glucose Oxidase on a Graphene Surface. <i>ACS Biomaterials Science and Engineering</i> , 2020, 6, 1899-1908.	5.2	10
8119	Molecular recognition and specificity of biomolecules to titanium dioxide from molecular dynamics simulations. <i>Npj Computational Materials</i> , 2020, 6, .	8.7	8
8120	Novel $\alpha$ -ruthenium cyclopentadienyl- $\beta$ -peptide conjugate complexes against human FGFR(+) breast cancer. <i>Dalton Transactions</i> , 2020, 49, 5974-5987.	3.3	9
8121	The quasi-irreversible inactivation of cytochrome P450 enzymes by paroxetine: a computational approach. <i>Organic and Biomolecular Chemistry</i> , 2020, 18, 3334-3345.	2.8	16



#	ARTICLE	IF	CITATIONS
8122	Structure-mechanics statistical learning unravels the linkage between local rigidity and global flexibility in nucleic acids. Chemical Science, 2020, 11, 4969-4979.	7.4	10
8123	Phosphorylation-dependent conformational changes of arrestin in the rhodopsin–arrestin complex. Physical Chemistry Chemical Physics, 2020, 22, 9330-9338.	2.8	1
8124	The accuracy of force fields on the simulation of intrinsically disordered proteins: A benchmark test on the human p53 tumor suppressor. Journal of Theoretical and Computational Chemistry, 2020, 19, 2050011.	1.8	3
8125	Recognition Dynamics of Cancer Mutations on the ERp57-Tapasin Interface. Cancers, 2020, 12, 737.	3.7	8
8126	Primary Radiation Damage Formation in Solids. , 2020, , 620-662.		10
8127	Exploring the interaction of Peloruside-A with drug resistant $\beta$ -II and $\beta$ -III tubulin isotypes in human ovarian carcinoma using a molecular modeling approach. Journal of Biomolecular Structure and Dynamics, 2021, 39, 1990-2002.	3.5	8
8128	A molecular dynamics investigation on transporting mechanism of glucose through a cyclic peptide nanotube. Journal of Biomolecular Structure and Dynamics, 2021, 39, 2230-2241.	3.5	3
8129	Protein dynamics and molecular motions study in relation to molecular interaction between proteins from sulfur oxidizing proteobacteria Allochromatium vinosum. Journal of Biomolecular Structure and Dynamics, 2021, 39, 2771-2787.	3.5	1
8130	Structural dynamics of inosine triphosphate pyrophosphatase (ITPA) protein and two clinically relevant mutants: molecular dynamics simulations. Journal of Biomolecular Structure and Dynamics, 2021, 39, 1236-1247.	3.5	5
8131	In silico design of peptide inhibitors of tubulin: amyloid- $\beta$ as a lead compound. Journal of Biomolecular Structure and Dynamics, 2021, 39, 2189-2198.	3.5	3
8132	Molecular dynamics simulations of human $\alpha$ -thrombin in different structural contexts: evidence for an aptamer-guided cooperation between the two exosites. Journal of Biomolecular Structure and Dynamics, 2021, 39, 2199-2209.	3.5	9
8133	<i>In silico</i> screening of FDA approved drugs on AXL kinase and validation for breast cancer cell line. Journal of Biomolecular Structure and Dynamics, 2021, 39, 2056-2070.	3.5	4
8134	Multiscale computational prediction of $\beta$ -sheet peptide self-assembly morphology. Molecular Simulation, 2021, 47, 428-438.	2.0	3
8135	Oil-in-water nanoemulsions comprising Berberine in olive oil: biological activities, binding mechanisms to human serum albumin or holo-transferrin and QMMD simulations. Journal of Biomolecular Structure and Dynamics, 2021, 39, 1029-1043.	3.5	194
8136	Molecular Dynamics Simulation of Biomolecular Interactions. , 2021, , 182-189.		9
8137	Atomistic and coarse-grained simulations of membrane proteins: A practical guide. Methods, 2021, 185, 15-27.	3.8	14
8138	Structural and molecular bases of angiotensin-converting enzyme inhibition by bovine casein-derived peptides: an <i>in silico</i> molecular dynamics approach. Journal of Biomolecular Structure and Dynamics, 2021, 39, 1386-1403.	3.5	4
8139	Atomistic study of metallurgical bonding upon the high velocity impact of fcc core-shell particles. Computational Materials Science, 2021, 186, 110045.	3.0	14

#	ARTICLE	IF	CITATIONS
8140	Effect of imidazolium based ionic liquids on CO-association dynamics and thermodynamic stability of Ferrocycochrome c. Biophysical Chemistry, 2021, 268, 106497.	2.8	2
8141	Structural evolution of arsenopyrite and dearsenification by mechanical activation. Journal of Environmental Chemical Engineering, 2021, 9, 104682.	6.7	4
8142	Toward Biotherapeutics Formulation Composition Engineering using Site-Identification by Ligand Competitive Saturation (SILCS). Journal of Pharmaceutical Sciences, 2021, 110, 1103-1110.	3.3	9
8143	Adsorption kinetic of myoglobin on mica and silica " Role of electrostatic interactions. Colloids and Surfaces B: Biointerfaces, 2021, 198, 111436.	5.0	6
8144	Ultrahigh coulombic efficiency electrolyte enables Li   SPAN batteries with superior cycling performance. Materials Today, 2021, 42, 17-28.	14.2	50
8145	Quantum dots functionalised artificial peptides bioinspired to the D1 protein from the Photosystem II of Chlamydomonas reinhardtii for endocrine disruptor optosensing. Talanta, 2021, 224, 121854.	5.5	1
8146	Molecular characterization of carbon dioxide, methane, and water adsorption in micropore space of kerogen matrix. Fuel, 2021, 283, 119254.	6.4	40
8147	Rational development of molecular imprinted carbon paste electrode for Furazolidone detection: theoretical and experimental approach. Sensors and Actuators B: Chemical, 2021, 329, 129112.	7.8	43
8148	Structural insights into the membrane receptor ShuA in DDM micelles and in a model of gram-negative bacteria outer membrane as seen by SAXS and MD simulations. Biochimica Et Biophysica Acta - Biomembranes, 2021, 1863, 183504.	2.6	3
8149	Morphology of bile salts micelles and mixed micelles with lipolysis products, from scattering techniques and atomistic simulations. Journal of Colloid and Interface Science, 2021, 587, 522-537.	9.4	25
8150	From Venom to AChE Inhibitor: Design, Molecular Modeling, and Synthesis of a Peptidic Inhibitor of AChE. International Journal of Peptide Research and Therapeutics, 2021, 27, 463-474.	1.9	3
8151	Irinotecan and vandetanib create synergies for treatment of pancreatic cancer patients with concomitant TP53 and KRAS mutations. Briefings in Bioinformatics, 2021, 22, .	6.5	19
8152	Annexin A4 trimers are recruited by high membrane curvatures in giant plasma membrane vesicles. Soft Matter, 2021, 17, 308-318.	2.7	28
8153	Evaluation of interface properties of carbon fiber/resin using the full atomistic model considering the electric charge state. Advanced Composite Materials, 2021, 30, 164-175.	1.9	23
8154	Predicting chemical reaction equilibria in molten carbonate fuel cells via molecular simulations. AIChE Journal, 2021, 67, e16988.	3.6	8
8155	Multiscale Molecular Modelling of ATP-Fueled Supramolecular Polymerisation and Depolymerisation**. ChemSystemsChem, 2021, 3, e2000038.	2.6	8
8156	Passive Internalization of Bioactive $\beta$ -Casein Peptides into Phospholipid (POPC) Bilayers. Free Energy Landscapes from Unbiased Equilibrium MD Simulations at $\mu$ s-Time Scale. Food Biophysics, 2021, 16, 70-83.	3.0	0
8157	An MD study of the polymer-polymer adhesion via connector chains: some aspects of the competition between bulk dissipation in the interphase and pull-out of interface-connecting molecules. Computational Materials Science, 2021, 186, 110048.	3.0	3

#	ARTICLE	IF	CITATIONS
8158	Crystal binding effects on neutron scattering and criticality in U <sup>235</sup> Mo fuels. Journal of Nuclear Materials, 2021, 543, 152570.	2.7	2
8159	Atomistic insights into metal hardening. Nature Materials, 2021, 20, 315-320.	27.5	59
8160	Structure, Dynamics, and Interactions of GPI-Anchored Human Glypican-1 with Heparan Sulfates in a Membrane. Glycobiology, 2021, 31, 593-602.	2.5	6
8161	Topological analysis of single-stranded DNA with an alpha-hederin nanopore. Biosensors and Bioelectronics, 2021, 171, 112711.	10.1	3
8162	The effect of grain boundary structures on crack nucleation in nickel nanolaminated structure: A molecular dynamics study. Computational Materials Science, 2021, 186, 110019.	3.0	3
8163	Sequence specific hydrogen bond of DNA with denaturants affects its stability: Spectroscopic and simulation studies. Biochimica Et Biophysica Acta - General Subjects, 2021, 1865, 129735.	2.4	10
8164	Discovery and in silico evaluation of aminoarylbenzosuberene molecules as novel checkpoint kinase 1 inhibitor determinants. Genomics, 2021, 113, 707-715.	2.9	58
8165	In vitro identification of imidazo[1,2-a]pyrazine-based antileishmanial agents and evaluation of L-tyrosine casein kinase 1 inhibition. European Journal of Medicinal Chemistry, 2021, 210, 112956.	5.5	14
8166	Why Does the Novel Coronavirus Spike Protein Interact so Strongly with the Human ACE2? A Thermodynamic Answer. ChemBioChem, 2021, 22, 865-875.	2.6	31
8167	Signaling Mechanism of Phytochromes in Solution. Structure, 2021, 29, 151-160.e3.	3.3	14
8168	A first principles study of amorphous and crystalline silicon tetraboride. Materials Chemistry and Physics, 2021, 258, 123928.	4.0	2
8169	Understanding the breakup mechanism of a droplet under a DC electric field with molecular dynamics simulations and weak interaction analysis. Journal of Molecular Liquids, 2021, 321, 114475.	4.9	25
8170	Diffusivity of $\alpha$ -, $\beta$ -, $\gamma$ -cyclodextrin and the inclusion complex of $\beta$ -cyclodextrin: Ibuprofen in aqueous solutions; A molecular dynamics simulation study. Fluid Phase Equilibria, 2021, 528, 112842.	2.5	30
8171	Effects of amino acid modifications on the permeability of the pentameric sarcolipin channel. Proteins: Structure, Function and Bioinformatics, 2021, 89, 427-435.	2.6	4
8172	Evaluation of acridinedione analogs as potential SARS-CoV-2 main protease inhibitors and their comparison with repurposed anti-viral drugs. Computers in Biology and Medicine, 2021, 128, 104117.	7.0	90
8173	The molecular insight into the $\alpha$ -Zeolite-ice as hydrogen storage material. Energy, 2021, 217, 119406.	8.8	7
8174	Insights into quaternary ammonium-based ionic liquids series with tetrafluoroborate anion for CO <sub>2</sub> capture. Journal of Molecular Liquids, 2021, 327, 114857.	4.9	12
8175	Green tea extract EGCG plays a dual role in A $\beta$ 42 protofibril disruption and membrane protection: A molecular dynamic study. Chemistry and Physics of Lipids, 2021, 234, 105024.	3.2	19

#	ARTICLE	IF	CITATIONS
8176	Structure of the class D GPCR Ste2 dimer coupled to two G proteins. <i>Nature</i> , 2021, 589, 148-153.	27.8	55
8177	Analysis of Atomistic Potentials for Poly(ethylene glycol) Ethers. <i>Journal of Chemical Theory and Computation</i> , 2021, 17, 315-321.	5.3	3
8178	Selective 5-hydroxymethylfurfural production from cellulose formate in DMSO-H <sub>2</sub> O media. <i>Applied Catalysis B: Environmental</i> , 2021, 285, 119799.	20.2	30
8179	Confined Ru-catalysts in a Two-phase Heptane/Ionic Liquid Solution: Modeling Aspects. <i>ChemCatChem</i> , 2021, 13, 739-746.	3.7	2
8180	Novel complexes with ONNO tetradentate coumarin schiff-base donor ligands: x-ray structures, DFT calculations, molecular dynamics and potential anticarcinogenic activity. <i>BioMetals</i> , 2021, 34, 119-140.	4.1	9
8181	Insight into the behavior at the hygroscopicity and interface of the hydrophobic imidazolium-based ionic liquids. <i>Chinese Journal of Chemical Engineering</i> , 2021, 31, 42-55.	3.5	27
8182	Structural and dynamical insights into the PH domain of p62 in human TFIIH. <i>Nucleic Acids Research</i> , 2021, 49, 2916-2930.	14.5	10
8183	A molecular dynamics study of the binding effectiveness between undoped conjugated polymer binders and tetra-sulfides in lithium-sulfur batteries. <i>Composites Part B: Engineering</i> , 2021, 206, 108531.	12.0	9
8184	LSPR biosensing for the early-stage prostate cancer detection using hydrogen bonds between PSA and antibody: Molecular dynamic and experimental study. <i>Journal of Molecular Liquids</i> , 2021, 324, 114736.	4.9	20
8185	Study on staged work hardening mechanism of nickel-based single crystal alloy during atomic and close-to-atomic scale cutting. <i>Precision Engineering</i> , 2021, 68, 35-56.	3.4	27
8186	Elastic moduli of lipid membranes: Reproducibility of AFM measures. <i>Chemistry and Physics of Lipids</i> , 2021, 234, 105011.	3.2	15
8187	Computational design of small molecular modulators of <scp>protein-protein</scp> interactions with a novel thermodynamic cycle: Allosteric inhibitors of <scp>HIV</scp> integrase. <i>Protein Science</i> , 2021, 30, 438-447.	7.6	6
8188	Purple passion fruit seeds ( <i>Passiflora edulis</i> f. <i>edulis</i> Sims) as a promising source of skin anti-aging agents: Enzymatic, antioxidant and multi-level computational studies. <i>Arabian Journal of Chemistry</i> , 2021, 14, 102905.	4.9	21
8189	Non-equilibrium molecular dynamics and continuum modelling of transient freezing of atomistic solids. <i>International Journal of Heat and Mass Transfer</i> , 2021, 164, 120601.	4.8	4
8190	A novel amino cellulose derivative using ATRP method: Preparation, characterization, and investigation of its antibacterial activity. <i>Bioorganic Chemistry</i> , 2021, 106, 104355.	4.1	8
8191	The influence of binary mixtures' structuring on the calculation of Kirkwood-Buff integrals: A molecular dynamics study. <i>Journal of Molecular Liquids</i> , 2021, 324, 114773.	4.9	3
8192	Viscometric flow of dense granular materials under controlled pressure and shear stress. <i>Journal of Fluid Mechanics</i> , 2021, 907, .	3.4	13
8193	In vitro and in silico studies of 8(17),12E,14-labdatrien-18-oic acid in airways smooth muscle relaxation: new molecular insights about its mechanism of action. <i>Naunyn-Schmiedeberg's Archives of Pharmacology</i> , 2021, 394, 885-902.	3.0	0

#	ARTICLE	IF	CITATIONS
8194	Enzymatic characterization, molecular dynamics simulation, and application of a novel <i>Bacillus licheniformis</i> laccase. <i>International Journal of Biological Macromolecules</i> , 2021, 167, 1393-1405.	7.5	16
8195	Comparative Study of Influence of Ethanol and 2,2,2-Trifluoroethanol on Thermophysical Properties of 1-Ethyl-3-methylimidazolium Dicyanamide in Binary Mixtures: Experimental and MD Simulations. <i>Journal of Chemical &amp; Engineering Data</i> , 2021, 66, 101-115.	1.9	13
8196	Update of CHARMM36's atomic charges for aromatic amino acids in water solution simulations and spectroscopy analysis via sequential molecular dynamics and DFT calculations. <i>Journal of Molecular Liquids</i> , 2021, 321, 114739.	4.9	12
8197	Molecular Dynamics Simulations Reveal Membrane Interactions for Poorly Water-Soluble Drugs: Impact of Bile Solubilization and Drug Aggregation. <i>Journal of Pharmaceutical Sciences</i> , 2021, 110, 176-185.	3.3	16
8198	Imidazolium-based Multiblock Amphiphile as Transmembrane Anion Transporter. <i>Chemistry - an Asian Journal</i> , 2021, 16, 147-157.	3.3	9
8199	A comparison of the location in membranes of curcumin and curcumin-derived bivalent compounds with potential neuroprotective capacity for Alzheimer's disease. <i>Colloids and Surfaces B: Biointerfaces</i> , 2021, 199, 111525.	5.0	12
8200	Structural and dynamical properties of water in surfactant-like peptide-based nanotubes: Effect of pore size, tube length and charge. <i>Journal of Molecular Liquids</i> , 2021, 323, 115033.	4.9	7
8201	Simultaneous doxorubicin encapsulation and in-situ microfluidic micellization of bio-targeted polymeric nanohybrids using dichalcogenide monolayers: A molecular in-silico study. <i>Materials Today Communications</i> , 2021, 26, 101948.	1.9	19
8202	SARS-CoV-2 spike protein binds to bacterial lipopolysaccharide and boosts proinflammatory activity. <i>Journal of Molecular Cell Biology</i> , 2021, 12, 916-932.	3.3	121
8203	Capsid Structure of <i>Leishmania</i> RNA Virus 1. <i>Journal of Virology</i> , 2021, 95, .	3.4	10
8204	Further thermostabilization of thermophilic rhodopsin from <i>Thermus thermophilus</i> JLC18 through engineering in extramembrane regions. <i>Proteins: Structure, Function and Bioinformatics</i> , 2021, 89, 301-310.	2.6	6
8205	A second shell residue modulates a conserved ATP-binding site with radically different affinities for ATP. <i>Biochimica Et Biophysica Acta - General Subjects</i> , 2021, 1865, 129766.	2.4	4
8206	Interplay of cholesterol, membrane bilayers and the AT1R: A cholesterol consensus motif on AT1R is revealed. <i>Computational and Structural Biotechnology Journal</i> , 2021, 19, 110-120.	4.1	7
8207	Computational Probing of Temperature-Dependent Unfolding of a Small Globular Protein: From Cold to Heat Denaturation. <i>Journal of Chemical Theory and Computation</i> , 2021, 17, 515-524.	5.3	7
8208	Molecular-weight and cooling-rate dependence of polymer thermodynamics in molecular dynamics simulation. <i>Polymer Journal</i> , 2021, 53, 455-462.	2.7	5
8209	Kinetic and thermodynamic analysis defines roles for two metal ions in DNA polymerase specificity and catalysis. <i>Journal of Biological Chemistry</i> , 2021, 296, 100184.	3.4	11
8210	Inhibition of Silica Nanoparticle Adhesion to Poly(vinyl alcohol) Surfaces by Ammonia-Mediated Hydration: Implications for Effective Post-Chemical Mechanical Planarization Cleaning. <i>ACS Applied Nano Materials</i> , 2021, 4, 71-83.	5.0	7
8211	Identification of molecular scaffolds from Caatinga Brazilian biome with potential against <i>Aedes aegypti</i> by molecular docking and molecular dynamics simulations. <i>Journal of Molecular Structure</i> , 2021, 1229, 129621.	3.6	0

#	ARTICLE	IF	CITATIONS
8212	Using coarse-grained models to examine structure-property relationships of diblock-arm star polymers. <i>European Polymer Journal</i> , 2021, 142, 110149.	5.4	2
8213	Insight on the stability of polycrystalline natural gas hydrates by molecular dynamics simulations. <i>Fuel</i> , 2021, 289, 119946.	6.4	23
8214	Cu <sup>2+</sup> , Ca <sup>2+</sup> , and methionine oxidation expose the hydrophobic $\beta$ -synuclein NAC domain. <i>International Journal of Biological Macromolecules</i> , 2021, 169, 251-263.	7.5	8
8215	Structural dynamics of double-stranded DNA with epigenome modification. <i>Nucleic Acids Research</i> , 2021, 49, 1152-1162.	14.5	8
8216	Molecular dynamic simulations, $^{15}\text{N}$ -NMR and TD-DFT spectroscopy analyze for zwitterionic isoleucine ( $\text{N}^+\text{H}_3^+$ ), $^{15}\text{N}$ -NMR, in water solutions. <i>Journal of Computational Chemistry</i> , 2021, 42, 344-357.	3.6	0
8217	Identification of FDA approved drugs and nucleoside analogues as potential SARS-CoV-2 A1pp domain inhibitor: An in silico study. <i>Computers in Biology and Medicine</i> , 2021, 130, 104185.	7.0	36
8218	Aqueous phase behavior of the PEO-containing non-ionic surfactant C12E6: A molecular dynamics simulation study. <i>Journal of Colloid and Interface Science</i> , 2021, 588, 257-268.	9.4	12
8219	Properties of DNA- and Protein-Scaffolded Lipid Nanodiscs. <i>ACS Nano</i> , 2021, 15, 751-764.	14.6	17
8220	Effect of dimethyl carbonate on the behavior of water confined in carbon nanotube. <i>Chinese Journal of Chemical Engineering</i> , 2021, 31, 177-185.	3.5	2
8221	Interactions of a DNA G-quadruplex with TMAO and urea: a molecular dynamics study on co-solute compensation mechanisms. <i>Physical Chemistry Chemical Physics</i> , 2021, 23, 1254-1264.	2.8	14
8222	A physics-informed operator regression framework for extracting data-driven continuum models. <i>Computer Methods in Applied Mechanics and Engineering</i> , 2021, 373, 113500.	6.6	43
8223	Molecular Reorganization during the Formation of the Human Skin Barrier Studied In Situ. <i>Journal of Investigative Dermatology</i> , 2021, 141, 1243-1253.e6.	0.7	16
8224	Structure and intermolecular interactions in spheroidal high-density lipoprotein subpopulations. <i>Journal of Structural Biology: X</i> , 2021, 5, 100042.	1.3	5
8225	Insight into the Microcosm of the Human Growth Hormone and Its Interactions with Polymers and Copolymers: A Molecular Dynamics Perspective. <i>Langmuir</i> , 2021, 37, 90-104.	3.5	1
8226	Location and Conformation of the LK14 Peptide in Water/Ethanol Mixtures. <i>Langmuir</i> , 2021, 37, 469-477.	3.5	3
8227	Antidepressant drugs act by directly binding to TRKB neurotrophin receptors. <i>Cell</i> , 2021, 184, 1299-1313.e19.	28.9	347
8228	First-principles based simulation of electron and hole transfer in PET oligmer. <i>Electronics and Communications in Japan</i> , 2021, 104, 10-17.	0.5	0
8229	Non-equilibrium approach for binding free energies in cyclodextrins in SAMPL7: force fields and software. <i>Journal of Computer-Aided Molecular Design</i> , 2021, 35, 49-61.	2.9	23



#	ARTICLE	IF	CITATIONS
8230	Interface microstructure and bonding energy of layered bimetallic ZCuSn6Pb6Zn3/Steel coupling with temperature and pressure. Tribology International, 2021, 155, 106754.	5.9	8
8231	Simulation of FUS Protein Condensates with an Adapted Coarse-Grained Model. Journal of Chemical Theory and Computation, 2021, 17, 525-537.	5.3	118
8232	Molecular dynamics simulations of aqueous solutions of short chain alcohols. Excess properties and the temperature of maximum density. Fluid Phase Equilibria, 2021, 528, 112840.	2.5	13
8233	Molecular dynamics study on TOTO-based ionic liquids with different cations. Fluid Phase Equilibria, 2021, 529, 112870.	2.5	0
8234	Effects of paraffin, fatty acid and long alkyl chain phenol on the solidification of n-hexadecane under harsh subcooling condition: A molecular dynamics simulation study. Fuel, 2021, 285, 119029.	6.4	5
8236	Experimental and computational investigation of polylactic acid/silver@NPANanocomposite with antimicrobial activity prepared by plasma in liquid. Plasma Processes and Polymers, 2021, 18, 2000169.	3.0	12
8237	QM/MM Studies of Light-responsive Biological Systems. Challenges and Advances in Computational Chemistry and Physics, 2021, , .	0.6	7
8238	Structural and dynamical effects of targeted mutations on $\beta$ 4O-Conotoxin MfVIA: Molecular simulation studies. Journal of Molecular Graphics and Modelling, 2021, 102, 107777.	2.4	3
8239	Effect of the lipid composition and cholesterol on the membrane selectivity of low generations PAMAM dendrimers: A molecular dynamics simulation study. Applied Surface Science, 2021, 540, 148274.	6.1	7
8240	Exploring the role of hydrophilic amino acids in unfolding of protein in aqueous ethanol solution. Proteins: Structure, Function and Bioinformatics, 2021, 89, 116-125.	2.6	9
8241	Targeting 14-3-3 $\mu$ activates apoptotic signaling to prevent cutaneous squamous cell carcinoma. Carcinogenesis, 2021, 42, 232-242.	2.8	6
8242	Self-assembly of the surfactant mixtures on graphene in the presence of electrolyte: a molecular simulation study. Adsorption, 2021, 27, 69-79.	3.0	3
8243	SAMPL7 TrimerTrip host-guest binding poses and binding affinities from spherical-coordinates-biased simulations. Journal of Computer-Aided Molecular Design, 2021, 35, 105-115.	2.9	20
8245	Exploring the conformational dynamics of $\langle \text{scp} \rangle \text{PD1} \langle / \text{scp} \rangle$ in complex with different ligands: What we can learn for designing novel $\langle \text{scp} \rangle \text{PD1} \langle / \text{scp} \rangle$ signaling blockers?. Proteins: Structure, Function and Bioinformatics, 2021, 89, 141-148.	2.6	5
8246	Mechanical Properties of Soot Particles: The Impact of Crosslinked Polycyclic Aromatic Hydrocarbons. Combustion Science and Technology, 2021, 193, 643-663.	2.3	14
8247	Liposomes with pH responsive $\text{on}$ and $\text{off}^{\text{TM}}$ switches for targeted and intracellular delivery of antibiotics. Journal of Liposome Research, 2021, 31, 45-63.	3.3	20
8248	Non-enzymatic glycation of human serum albumin modulates its binding efficacy towards bioactive flavonoid chrysin: A detailed study using multi-spectroscopic and computational methods. Journal of Biomolecular Structure and Dynamics, 2021, 39, 476-492.	3.5	13
8249	Predicting interfacial hot-spot residues that stabilize protein-protein interfaces in oligomeric membrane-toxin pores through hydrogen bonds and salt bridges. Journal of Biomolecular Structure and Dynamics, 2021, 39, 20-34.	3.5	6

#	ARTICLE	IF	CITATIONS
8250	Identification of potential inhibitors against pathogenic missense mutations of PMM2 using a structure-based virtual screening approach. Journal of Biomolecular Structure and Dynamics, 2021, 39, 171-187.	3.5	14
8251	Identifying the key residues instrumental in imparting stability to amyloid beta protofibrils â€” a comparative study using MD simulations of 17â€”42 residues. Journal of Biomolecular Structure and Dynamics, 2021, 39, 431-456.	3.5	9
8252	<i>In-silico</i> profiling and structural insights into the impact of nSNPs in the <i>P. falciparum</i> acetyl-CoA transporter</i> gene to understand the mechanism of drug resistance in malaria. Journal of Biomolecular Structure and Dynamics, 2021, 39, 558-569.	3.5	2
8253	Molecular modeling studies of pyrrolo[2,3-d]pyrimidin-4-amine derivatives as JAK1 inhibitors based on 3D-QSAR, molecular docking, molecular dynamics (MD) and MM-PBSA calculations. Journal of Biomolecular Structure and Dynamics, 2021, 39, 753-765.	3.5	18
8254	Atomistic insights into the structure and elasticity of densified 45S5 bioactive glasses. Physical Chemistry Chemical Physics, 2021, 23, 15292-15301.	2.8	13
8255	Continuous Constant pH Molecular Dynamics Simulations of Transmembrane Proteins. Methods in Molecular Biology, 2021, 2302, 275-287.	0.9	11
8256	Coarse-Grained Molecular Dynamics Simulations of Membrane Proteins: A Practical Guide. Methods in Molecular Biology, 2021, 2302, 253-273.	0.9	3
8257	Computational design of SARS-CoV-2 spike glycoproteins to increase immunogenicity by T cell epitope engineering. Computational and Structural Biotechnology Journal, 2021, 19, 518-529.	4.1	19
8258	Coarse-Grained Force Fields Built on Atomistic Force Fields. Molecular Modeling and Simulation, 2021,, 143-180.	0.2	0
8259	Translocation of flexible and tensioned ssDNA through <i>in silico</i> designed hydrophobic nanopores with two constrictions. Nanoscale, 2021, 13, 1673-1679.	5.6	1
8260	Molecular Basis of the Anticancer and Antibacterial Properties of CecropinXJ Peptide: An In Silico Study. International Journal of Molecular Sciences, 2021, 22, 691.	4.1	12
8261	A computational approach to analyse the amino acid variants of GLB1 protein causing GM1 Gangliosidosis. Metabolic Brain Disease, 2021, 36, 499-508.	2.9	4
8262	Phosphorylation-induced changes in the PDZ domain of Dishevelled 3. Scientific Reports, 2021, 11, 1484.	3.3	2
8265	<i>In silico</i> design of novel FAK inhibitors using integrated molecular docking, 3D-QSAR and molecular dynamics simulation studies. Journal of Biomolecular Structure and Dynamics, 2022, 40, 5965-5982.	3.5	9
8266	Molecular mechanisms underlying the role of the puckered surface in the biocompatibility of black phosphorus. Nanoscale, 2021, 13, 3790-3799.	5.6	9
8267	Molecular Dynamics Simulation Studies of the CL-20/DNB Co-crystal Based PBX with HTPB. Journal of Physics: Conference Series, 2021, 1721, 012010.	0.4	4
8268	Effect of water nanoconfinement on the dynamic properties of paramagnetic colloidal complexes. Physical Chemistry Chemical Physics, 2021, 23, 16948-16957.	2.8	1
8269	Kinetic and thermodynamic stability comparison for the fibrillar form of small amyloid-Î²(1â€”42) oligomers using scaled molecular dynamics. Physical Chemistry Chemical Physics, 2021, 23, 16897-16908.	2.8	3

#	ARTICLE	IF	CITATIONS
8270	Mechanisms of melatonin binding and destabilizing the protofilament and filament of tau R3â€“R4 domains revealed by molecular dynamics simulation. Physical Chemistry Chemical Physics, 2021, 23, 20615-20626.	2.8	18
8271	<i>In silico</i> mutational analyses reveal different ligand-binding abilities of double pockets of medaka fish taste receptor type 1 essential for efficient taste recognition. Physical Chemistry Chemical Physics, 2021, 23, 20398-20405.	2.8	0
8272	Glycanâ€“protein interactions determine kinetics of <i>N</i> -glycan remodeling. RSC Chemical Biology, 2021, 2, 917-931.	4.1	16
8273	Sequence-selective recognition of cationic amphipathic tripeptides with similar structures in aqueous solutions by cucurbit[7]uril. Physical Chemistry Chemical Physics, 2021, 23, 13724-13733.	2.8	4
8274	Entropy of stapled peptide inhibitors in free state is the major contributor to the improvement of binding affinity with the GK domain. RSC Chemical Biology, 2021, 2, 1274-1284.	4.1	8
8275	Structure and noncovalent interactions in ionic liquids mixtures and deep eutectic solvents. , 2021, , 105-157.		3
8276	Adsorption of metallic ions from aqueous solution on surfactant aggregates: a molecular dynamics study. Condensed Matter Physics, 2021, 24, 23601.	0.7	1
8277	<i>In silico</i> study of the interactions of <i>Pilocarpus microphyllus</i> imidazolic alkaloids with the main protease (M <sup>pro</sup> ) of SARS-CoV-2. Molecular Simulation, 2021, 47, 74-87.	2.0	6
8278	Nanocapsule designs for antimicrobial resistance. Nanoscale, 2021, 13, 10342-10355.	5.6	7
8279	Solvent extraction in extended hydrogen bonded fluids â€“ separation of Pt( <i>iv</i> ) from Pd( <i>ii</i> ) using TOPO-based type V DES. Green Chemistry, 2021, 23, 4540-4550.	9.0	16
8280	Linker residues regulate the activity and stability of hexokinase 2, a promising anticancer target. Journal of Biological Chemistry, 2021, 296, 100071.	3.4	7
8281	Identification of Pan-Assay INterference compounds (PAINS) Using an MD-Based Protocol. Methods in Molecular Biology, 2021, 2315, 263-271.	0.9	6
8282	Long chain sphingomyelin depletes cholesterol from the cytoplasmic leaflet in asymmetric lipid membranes. RSC Advances, 2021, 11, 22677-22682.	3.6	5
8283	Molecular dynamics study of wetting of alkanes on water: from high temperature to the supercooled region and the influence of second inflection points of interfacial tensions. Physical Chemistry Chemical Physics, 2021, 23, 14465-14476.	2.8	4
8284	Molecular Dynamics Simulation to Uncover the Mechanisms of Protein Instability During Freezing. Journal of Pharmaceutical Sciences, 2021, 110, 2457-2471.	3.3	22
8285	Structural insights and inhibition mechanism of TMPRSS2 by experimentally known inhibitors Camostat mesylate, Nafamostat and Bromhexine hydrochloride to control SARS-coronavirus-2: A molecular modeling approach. Informatics in Medicine Unlocked, 2021, 24, 100597.	3.4	32
8286	Evaluation of drug repositioning by molecular docking of pharmaceutical resources available in the Brazilian healthcare system against SARS-CoV-2. Informatics in Medicine Unlocked, 2021, 23, 100539.	3.4	15
8288	Chirality affects cholesterol-oxysterol association in water, a computational study. Computational and Structural Biotechnology Journal, 2021, 19, 4319-4335.	4.1	2

#	ARTICLE	IF	CITATIONS
8289	Structural investigation of three distinct amorphous forms of Ar hydrate. RSC Advances, 2021, 11, 30744-30754.	3.6	5
8290	Distinct kinetic mechanisms of H3K4 methylation catalyzed by MLL3 and MLL4 core complexes. Journal of Biological Chemistry, 2021, 296, 100635.	3.4	6
8291	Molecular dynamics simulation of lithium fluoride in aqueous solutions at different temperatures 300 K – 360 K. E3S Web of Conferences, 2021, 229, 01045.	0.5	1
8292	Updating atomic charge parameters of aliphatic amino acids: a quest to improve the performance of molecular modeling via sequential molecular dynamics and DFT-GIAO-NMR calculations. Physical Chemistry Chemical Physics, 2021, 23, 8413-8425.	2.8	12
8293	Phenolic compounds alter the ion permeability of phospholipid bilayers via specific lipid interactions. Physical Chemistry Chemical Physics, 2021, 23, 22352-22366.	2.8	14
8294	G11 inhibition mechanism of ATP-bound adenylyl cyclase type 5. PLoS ONE, 2021, 16, e0245197.	2.5	5
8295	RNA dependent RNA polymerase (RdRp) as a drug target for SARS-CoV2. Journal of Biomolecular Structure and Dynamics, 2022, 40, 6039-6051.	3.5	29
8296	Identification and characterisation of putative drug binding sites in human ATP-binding cassette B5 (ABCB5) transporter. Computational and Structural Biotechnology Journal, 2021, 19, 691-704.	4.1	5
8297	Membrane Binding of Antimicrobial Peptides Is Modulated by Lipid Charge Modification. Journal of Chemical Theory and Computation, 2021, 17, 1218-1228.	5.3	10
8298	Phosphotyrosine couples peptide binding and SHP2 activation via a dynamic allosteric network. Computational and Structural Biotechnology Journal, 2021, 19, 2398-2415.	4.1	28
8299	On the association of frustrated Lewis pairs in ionic liquids: a molecular dynamics simulation study. Physical Chemistry Chemical Physics, 2021, 23, 12541-12548.	2.8	2
8300	Asymmetric dynamics of dimeric SARS-CoV-2 and SARS-CoV main proteases in an apo form: Molecular dynamics study on fluctuations of active site, catalytic dyad, and hydration water. BBA Advances, 2021, 1, 100016.	1.6	4
8301	Polyphenols Weaken Pea Protein Gel by Formation of Large Aggregates with Diminished Noncovalent Interactions. Biomacromolecules, 2021, 22, 1001-1014.	5.4	33
8302	Identification of novel potential ricin inhibitors by virtual screening, molecular docking, molecular dynamics and MM-PBSA calculations: a drug repurposing approach. Journal of Biomolecular Structure and Dynamics, 2022, 40, 5309-5319.	3.5	4
8303	Using multiscale molecular dynamics simulations to obtain insights into pore forming toxin mechanisms. Methods in Enzymology, 2021, 649, 461-502.	1.0	9
8304	MD simulations of charged binary mixtures reveal a generic relation between high- and low-temperature behavior. Journal of Chemical Physics, 2021, 154, 024501.	3.0	2
8306	Uncovering the interactions driving carotenoid binding in light-harvesting complexes. Chemical Science, 2021, 12, 5113-5122.	7.4	18
8307	Relevance of hydrogen bonded associates to the transport properties and nanoscale dynamics of liquid and supercooled 2-propanol. Physical Chemistry Chemical Physics, 2021, 23, 7220-7232.	2.8	5

#	ARTICLE	IF	CITATIONS
8308	Fullerene translocation through peroxidized lipid membranes. RSC Advances, 2021, 11, 7575-7586.	3.6	3
8309	Tautomers of <i>N</i> -acetyl- <i>D</i> -allosamine: an NMR and computational chemistry study. Organic and Biomolecular Chemistry, 2021, 19, 7190-7201.	2.8	10
8310	Specificity of Molecular Fragments Binding to S100B versus S100A1 as Identified by NMR and Site Identification by Ligand Competitive Saturation (SILCS). Molecules, 2021, 26, 381.	3.8	6
8311	The redox potential of a heme cofactor in <i>Nitrosomonas europaea</i> cytochrome <i>c</i> peroxidase: a polarizable QM/MM study. Physical Chemistry Chemical Physics, 2021, 23, 16506-16515.	2.8	8
8313	Thermodynamics and kinetics of the amyloid- $\beta^2$ peptide revealed by Markov state models based on MD data in agreement with experiment. Chemical Science, 2021, 12, 6652-6669.	7.4	46
8314	Transformation-induced plasticity in omega titanium. Journal of Applied Physics, 2021, 129, .	2.5	10
8315	Aggregation of the Dipeptide Leu-Gly in Alcohol-Water Binary Solvents Elucidated from the Solvation Structure for Each Moiety. Journal of Physical Chemistry B, 2021, 125, 240-252.	2.6	2
8316	Spontaneous NaCl-doped ices $I_h$ , $I_c$ , III, V and VI. Understanding the mechanism of ion inclusion and its dependence on the crystalline structure of ice. Physical Chemistry Chemical Physics, 2021, 23, 22897-22911.	2.8	7
8317	Corilagin and 1,3,6-Tri-O-galloyl- $\beta$ -D-glucose: potential inhibitors of SARS-CoV-2 variants. Physical Chemistry Chemical Physics, 2021, 23, 14873-14888.	2.8	12
8318	Using coarse-grained molecular dynamics to understand the effect of ionic liquids on the aggregation of Pluronic copolymer solutions. Physical Chemistry Chemical Physics, 2021, 23, 5824-5833.	2.8	17
8319	An efficient approach to study membrane nano-inclusions: from the complex biological world to a simple representation. RSC Advances, 2021, 11, 10962-10974.	3.6	4
8320	Dimeric phosphorylation of glyoxalase I alters its symmetry and substrate binding mechanism: simulation studies. Journal of Biomolecular Structure and Dynamics, 2021, , 1-15.	3.5	0
8321	Searching for potential drugs against SARS-CoV-2 through virtual screening on several molecular targets. Journal of Biomolecular Structure and Dynamics, 2021, , 1-14.	3.5	5
8322	Coarse-grained molecular dynamics study of the self-assembly of polyphilic bolaamphiphiles using the SAFT- $\Gamma^3$ Mie force field. Molecular Systems Design and Engineering, 2021, 6, 594-608.	3.4	11
8323	The polyphenolic phytoalexin polydatin inhibits amyloid aggregation of recombinant human prion protein. RSC Advances, 2021, 11, 25901-25911.	3.6	4
8324	Proline isomerization effects in the amyloidogenic protein $\beta^2$ -microglobulin. Physical Chemistry Chemical Physics, 2021, 23, 356-367.	2.8	8
8325	Grain-Boundary Sliding in Ice $I_h$ : Tribology and Rheology at the Nanoscale. Journal of Physical Chemistry C, 2021, 125, 627-634.	3.1	9
8326	Tailoring the phase diagram of discotic mesogens. Soft Matter, 2021, 17, 8693-8704.	2.7	1

#	ARTICLE	IF	CITATIONS
8327	Atomistic simulation studies of ionic cyanine dyes: self-assembly and aggregate formation in aqueous solution. <i>Physical Chemistry Chemical Physics</i> , 2021, 23, 6408-6421.	2.8	10
8328	Coarse-Grained Force Fields from the Perspective of Statistical Mechanics: Better Understanding of the Origins of a MARTINI Hangover. <i>Journal of Chemical Theory and Computation</i> , 2021, 17, 1170-1180.	5.3	46
8329	Dissecting the role of glutamine in seeding peptide aggregation. <i>Computational and Structural Biotechnology Journal</i> , 2021, 19, 1595-1602.	4.1	15
8330	Electric Field-Mediated Fibronectin-Hydroxyapatite Interaction: A Molecular Insight. <i>Journal of Physical Chemistry B</i> , 2021, 125, 3-16.	2.6	14
8331	Dynamic Docking Using Multicanonical Molecular Dynamics: Simulating Complex Formation at the Atomistic Level. <i>Methods in Molecular Biology</i> , 2021, 2266, 187-202.	0.9	8
8332	Heterogeneity in hydrophobic deep eutectic solvents: SAXS prepeak and local environments. <i>Physical Chemistry Chemical Physics</i> , 2021, 23, 3915-3924.	2.8	29
8333	Structural and dynamical properties simulations of potassium fluoride aqueous system at various temperatures from 298.15 K to 358.15 K. <i>E3S Web of Conferences</i> , 2021, 297, 01009.	0.5	2
8334	The stress deformation response influenced by the chain rigidity for mesostructures in diblock copolymers. <i>Physical Chemistry Chemical Physics</i> , 2021, 23, 22992-23004.	2.8	1
8335	Descriptor selection for predicting interfacial thermal resistance by machine learning methods. <i>Scientific Reports</i> , 2021, 11, 739.	3.3	5
8336	Lanthanide-dependent coordination interactions in lanmodulin: a 2D IR and molecular dynamics simulations study. <i>Physical Chemistry Chemical Physics</i> , 2021, 23, 21690-21700.	2.8	8
8337	Origins of structural and electronic transitions in disordered silicon. <i>Nature</i> , 2021, 589, 59-64.	27.8	192
8338	Probing remdesivir nucleotide analogue insertion to SARS-CoV-2 RNA dependent RNA polymerase in viral replication. <i>Molecular Systems Design and Engineering</i> , 2021, 6, 888-902.	3.4	11
8339	Cancer associated talin point mutations disorganise cell adhesion and migration. <i>Scientific Reports</i> , 2021, 11, 347.	3.3	18
8341	Effect of Nanocellulose on Water-Oil Interfacial Tension. <i>Key Engineering Materials</i> , 0, 874, 13-19.	0.4	1
8342	Simultaneous binding mechanism of multiple substrates for multidrug resistance transporter P-glycoprotein. <i>Physical Chemistry Chemical Physics</i> , 2021, 23, 4530-4543.	2.8	10
8343	An octanol hinge opens the door to water transport. <i>Chemical Science</i> , 2021, 12, 2294-2303.	7.4	4
8344	A theoretical investigation into the cooperativity effect on the TNT melting point under external electric field. <i>Journal of Molecular Modeling</i> , 2021, 27, 4.	1.8	4
8346	A combined experimental and molecular dynamics study of the relation between the limiting molar conductivities and self-diffusion coefficients of acetonitrile solution. <i>Chemical Physics Letters</i> , 2021, 763, 138246.	2.6	0



#	ARTICLE	IF	CITATIONS
8347	Gold( <i>scp</i> ) bridged dimeric and trimeric heterometallic {Cr <sub>7</sub> Ni}-based qubit systems and their characterization. Dalton Transactions, 2021, 50, 4390-4395.	3.3	2
8348	Molecular interactions of the M and E integral membrane proteins of SARS-CoV-2. Faraday Discussions, 2021, 232, 49-67.	3.2	19
8349	Substrate-independent three-dimensional polymer nanosheets induced by solution casting. Chemical Science, 2021, 12, 11748-11755.	7.4	1
8350	Solute-adsorption enhanced heterogeneous nucleation: the effect of Cu adsorption on $\pm$ -Al nucleation at the sapphire substrate. Physical Chemistry Chemical Physics, 2021, 23, 5270-5282.	2.8	12
8351	Repurposing FDA-approved drugs to fight COVID-19 using in silico methods: Targeting SARS-CoV-2 RdRp enzyme and host cell receptors (ACE2, CD147) through virtual screening and molecular dynamic simulations. Informatics in Medicine Unlocked, 2021, 23, 100541.	3.4	24
8352	Physico-chemical properties of 4-(methylnitrosamino)-1-(3-pyridyl)-1-butanone (NNK) diazonium ion: a theoretical investigation. RSC Advances, 2021, 11, 26750-26762.	3.6	0
8353	<i>In silico</i> and <i>in vitro</i> design of cordycepin encapsulation in liposomes for colon cancer treatment. RSC Advances, 2021, 11, 8475-8484.	3.6	7
8354	Coacervate formation studied by explicit solvent coarse-grain molecular dynamics with the Martini model. Chemical Science, 2021, 12, 8521-8530.	7.4	37
8355	Surface ligand rigidity modulates lipid raft affinity of ultra-small hydrophobic nanoparticles: insights from molecular dynamics simulations. Nanoscale, 2021, 13, 9825-9833.	5.6	3
8356	Water-mediated structural rearrangement establishes active conformation of caspases for apoptosis and inflammation. Journal of Biomolecular Structure and Dynamics, 2021, , 1-14.	3.5	0
8357	In Silico Disulfide Bond Engineering to Improve Human LEPTIN Stability. Journal of Renewable Materials, 2021, 9, 1843-1857.	2.2	2
8358	Chain ordering of phospholipids in membranes containing cholesterol: what matters?. Soft Matter, 2021, 17, 6098-6108.	2.7	4
8359	Simulation of Crystallization of Pentacene and Its Derivatives from Solution. Journal of Physical Chemistry C, 2021, 125, 2257-2263.	3.1	4
8360	Contact Ion Pairs in the Bulk Affect Anion Interactions with Poly( <i>N</i> -isopropylacrylamide). Journal of Physical Chemistry B, 2021, 125, 680-688.	2.6	9
8361	Determination of intermediate state structures in the opening pathway of SARS-CoV-2 spike using cryo-electron microscopy. Chemical Science, 2021, 12, 9168-9175.	7.4	25
8362	Dynamics and electrostatics define an allosteric druggable site within the receptor-binding domain of SARS-CoV-2 spike protein. FEBS Letters, 2021, 595, 442-451.	2.8	9
8363	The G protein-first activation mechanism of opioid receptors by Gi protein and agonists. QRB Discovery, 2021, 2, .	1.6	7
8364	Synthesis and molecular dynamics simulation of CuS@GO-CS hydrogel for enhanced photothermal antibacterial effect. New Journal of Chemistry, 2021, 45, 6895-6903.	2.8	13

#	ARTICLE	IF	CITATIONS
8365	pK a Calculations in Membrane Proteins from Molecular Dynamics Simulations. <i>Methods in Molecular Biology</i> , 2021, 2315, 185-195.	0.9	2
8366	From point particles to body points. <i>Mathematics in Engineering</i> , 2021, 4, 1-29.	0.9	5
8367	High-throughput molecular simulations reveal the origin of ion free energy barriers in graphene oxide membranes. <i>Nanoscale</i> , 2021, 13, 13693-13702.	5.6	12
8368	Influence of diluent concentration in localized high concentration electrolytes: elucidation of hidden diluent-Li <sup>+</sup> interactions and Li <sup>+</sup> transport mechanism. <i>Journal of Materials Chemistry A</i> , 2021, 9, 17459-17473.	10.3	28
8369	Physisorption of bio oil nitrogen compounds onto montmorillonite. <i>Physical Chemistry Chemical Physics</i> , 2021, 23, 21840-21851.	2.8	9
8370	Enhancing the peroxidase-mimicking activity of hemin by covalent immobilization in polymer nanogels. <i>Polymer Chemistry</i> , 2021, 12, 858-866.	3.9	18
8371	Stabilization of DPPC Lipid Bilayers in the Presence of Co-Solutes: Molecular Mechanisms and Interaction Patterns. <i>Physical Chemistry Chemical Physics</i> , 2021, 23, 22936-22946.	2.8	2
8372	Restricted binding of a model protein on C <sub>3</sub> N <sub>4</sub> nanosheets suggests an adequate biocompatibility of the nanomaterial. <i>RSC Advances</i> , 2021, 11, 7417-7425.	3.6	7
8373	Structure-guided evolution of a ketoreductase for efficient and stereoselective bioreduction of bulky 1- $\alpha$ -amino 1 <sup>2</sup> -keto esters. <i>Catalysis Science and Technology</i> , 2021, 11, 6755-6769.	4.1	8
8374	Experimental and Computational Observations of Immunogenic Cobalt Porphyrin Lipid Bilayers: Nanodomain-Enhanced Antigen Association. <i>Pharmaceutics</i> , 2021, 13, 98.	4.5	12
8375	Effects of lipid heterogeneity on model human brain lipid membranes. <i>Soft Matter</i> , 2021, 17, 126-135.	2.7	14
8376	Predictive Rules of Efflux Inhibition and Avoidance in <i>Pseudomonas aeruginosa</i> . <i>MBio</i> , 2021, 12, .	4.1	28
8377	On the chirality-dependent adsorption behavior of volatile organic compounds on carbon nanotubes. <i>Physical Chemistry Chemical Physics</i> , 2021, 23, 21941-21950.	2.8	10
8378	The molecular basis for the pH-dependent calcium affinity of the pattern recognition receptor langerin. <i>Journal of Biological Chemistry</i> , 2021, 296, 100718.	3.4	11
8379	Unexpected inverse correlations and cooperativity in ion-pair phase transfer. <i>Chemical Science</i> , 2021, 12, 13930-13939.	7.4	2
8380	Molecular dynamics simulation of nanocellulose-oil-water interaction in enhanced oil recovery application. <i>IOP Conference Series: Materials Science and Engineering</i> , 2020, 980, 012008.	0.6	2
8381	How to control interactions of cellulose-based biomaterials with skin: the role of acidity in the contact area. <i>Soft Matter</i> , 2021, 17, 6507-6518.	2.7	3
8382	USING VORONOI DIAGRAMS TO INTERPRET BULK PROPERTIES OF SOLUTIONS. <i>Journal of Structural Chemistry</i> , 2021, 62, 58-69.	1.0	6

#	ARTICLE	IF	CITATIONS
8383	The Role of Entropy in the Structural Transitions in Zeolitic Imidazolate Frameworks. Molecular Modeling and Simulation, 2021, , 25-35.	0.2	1
8384	Investigating the structural properties of hydrophobic solvent-rich lipid bilayers. Soft Matter, 2021, 17, 5329-5335.	2.7	8
8385	<i>In silico</i> screening of drug candidates for thermoresponsive liposome formulations. Molecular Systems Design and Engineering, 2021, 6, 368-380.	3.4	4
8386	Theoretical and Experimental Study of Monofunctional Vinyl Cyclopropanes Bearing Hydrogen Bond Enabling Side Chains. Macromolecules, 2021, 54, 11-21.	4.8	2
8387	The mechanism of the selective binding ability between opiate metabolites and acyclic cucurbit[4]uril: an MD/DFT study. Physical Chemistry Chemical Physics, 2021, 23, 2186-2192.	2.8	1
8389	A theoretical study on the signal transduction process of bacterial photoreceptor PpSB1 based on the Markov state model. Physical Chemistry Chemical Physics, 2021, 23, 2398-2405.	2.8	2
8390	Partridge and embryonated partridge egg as new preclinical models for candidiasis. Scientific Reports, 2021, 11, 2072.	3.3	3
8391	Physical mechanism analysis of cholesterol concentration effect on asymmetric phospholipid membrane. European Physical Journal Plus, 2021, 136, 1.	2.6	3
8392	Molecular Dynamic Simulation of Intrinsically Disordered Proteins and Relevant Forcefields. , 2021, , 317-333.		1
8393	Transmembrane penetration mechanism of cyclic pollutants inspected by molecular dynamics and metadynamics: the case of morpholine, phenol, 1,4-dioxane and oxane. Physical Chemistry Chemical Physics, 2021, 23, 15338-15351.	2.8	4
8394	Kinase inhibitors allosterically disrupt a regulatory interaction to enhance PKC $\zeta$ membrane translocation. Journal of Biological Chemistry, 2021, 296, 100339.	3.4	2
8395	The impact of Gag non-cleavage site mutations on HIV-1 viral fitness from integrative modelling and simulations. Computational and Structural Biotechnology Journal, 2021, 19, 330-342.	4.1	7
8396	Spontaneous binding of potential COVID-19 drugs (Camostat and Nafamostat) to human serine protease TMPRSS2. Computational and Structural Biotechnology Journal, 2021, 19, 467-476.	4.1	25
8398	<i>In vivo</i> / <i>in silico</i> insight into the effect of titanium dioxide nanoparticle on serum paraoxonase 1 activity in rat. Journal of Biomolecular Structure and Dynamics, 2022, 40, 4961-4971.	3.5	3
8399	Lanosterol reduces the aggregation propensity of ultraviolet-damaged human $\beta$ -crystallins: a molecular dynamics study. Physical Chemistry Chemical Physics, 2021, 23, 13696-13704.	2.8	1
8400	On the role of water in the hydrogen bond network in DESs: an ab initio molecular dynamics and quantum mechanical study on the urea $\beta$ -betaine system. Physical Chemistry Chemical Physics, 2021, 23, 1994-2004.	2.8	6
8401	NMR and MD simulations reveal the impact of the V23D mutation on the function of yeast oligosaccharyltransferase subunit Ost4. Glycobiology, 2021, 31, 838-850.	2.5	2
8402	Molecular Simulations and Markov State Modeling Reveal Inactive Form of Quorum Sensing Regulator SdiA of <i>Escherichia Coli</i> . IEEE/ACM Transactions on Computational Biology and Bioinformatics, 2021, 18, 2835-2840.	3.0	4

#	ARTICLE	IF	CITATIONS
8403	Molecular level understanding of CO <sub>2</sub> capture in ionic liquid/polyimide composite membrane. <i>Frontiers of Chemical Science and Engineering</i> , 2022, 16, 141-151.	4.4	9
8405	Thermodynamics of DNA Hybridization from Atomistic Simulations. <i>Journal of Physical Chemistry B</i> , 2021, 125, 771-779.	2.6	15
8406	Adsorption of Organic Molecules and Surfactants on Graphene: A Coarse-Grained Study. <i>Journal of Physical Chemistry A</i> , 2021, 125, 700-711.	2.5	2
8407	Predicting stable binding modes from simulated dimers of the D76N mutant of $\alpha$ 2-microglobulin. <i>Computational and Structural Biotechnology Journal</i> , 2021, 19, 5160-5169.	4.1	2
8408	Quantum-mechanical exploration of the phase diagram of water. <i>Nature Communications</i> , 2021, 12, 588.	12.8	32
8409	Wide-angle X-ray scattering and molecular dynamics simulations of supercooled protein hydration water. <i>Physical Chemistry Chemical Physics</i> , 2021, 23, 18308-18313.	2.8	5
8410	Lipid-Composition-Mediated Forces Can Stabilize Tubular Assemblies of I-BAR Proteins. <i>Biophysical Journal</i> , 2021, 120, 46-54.	0.5	18
8411	Heparin remodels the microtubule-binding repeat R3 of Tau protein towards fibril-prone conformations. <i>Physical Chemistry Chemical Physics</i> , 2021, 23, 20406-20418.	2.8	16
8412	Translocation of silica nanospheres through giant unilamellar vesicles (GUVs) induced by a high frequency electromagnetic field. <i>RSC Advances</i> , 2021, 11, 31408-31420.	3.6	3
8413	A structural view onto disease-linked mutations in the human neutral amino acid exchanger ASCT1. <i>Computational and Structural Biotechnology Journal</i> , 2021, 19, 5246-5254.	4.1	9
8414	Covalent and non-covalent binding free energy calculations for peptidomimetic inhibitors of SARS-CoV-2 main protease. <i>Physical Chemistry Chemical Physics</i> , 2021, 23, 6746-6757.	2.8	30
8415	Effects of lateral-chain thiophene fluorination on morphology and charge transport of BDT-T based small molecule donors: a study with multiscale simulations. <i>Journal of Materials Chemistry C</i> , 2021, 9, 14637-14647.	5.5	5
8416	Release of methane from nanochannels through displacement using CO <sub>2</sub> . <i>RSC Advances</i> , 2021, 11, 15457-15466.	3.6	4
8417	Tuning the transdermal transport by application of external continuous electric field: a coarse-grained molecular dynamics study. <i>Physical Chemistry Chemical Physics</i> , 2021, 23, 8273-8281.	2.8	4
8418	Universal features in the lifetime distribution of clusters in hydrogen-bonding liquids. <i>Physical Chemistry Chemical Physics</i> , 2021, 23, 19537-19546.	2.8	10
8419	Capsid opening enables genome release of iflaviruses. <i>Science Advances</i> , 2021, 7, .	10.3	13
8420	<i>In silico</i> study of the inhibition of SARS-COV-2 viral cell entry by neem tree extracts. <i>RSC Advances</i> , 2021, 11, 26524-26533.	3.6	7
8421	Coarse-Grained Molecular Dynamics Simulation of Perfluorosulfonic Acid Polymer in Water/Ethanol Mixtures. <i>Macromolecules</i> , 2021, 54, 609-620.	4.8	17

#	ARTICLE	IF	CITATIONS
8423	A new equation for period vectors of crystals under external stress and temperature in statistical physics: mechanical equilibrium condition and equation of state. <i>European Physical Journal Plus</i> , 2021, 136, 1.	2.6	0
8424	The Interplay of Cholesterol and Ligand Binding in hTSP0 from Classical Molecular Dynamics Simulations. <i>Molecules</i> , 2021, 26, 1250.	3.8	5
8425	Multivalent Display of SARS-CoV-2 Spike (RBD Domain) of COVID-19 to Nanomaterial, Protein Ferritin Nanocages. <i>Biomolecules</i> , 2021, 11, 297.	4.0	20
8426	Molecular understanding of the LCST phase behaviour of P(MEO <sub>2</sub> MA-b-OEGMA) block copolymers. <i>Molecular Simulation</i> , 2021, 47, 299-305.	2.0	2
8427	Modeling solvation effects on absorption and fluorescence spectra of indole in aqueous solution. <i>Journal of Chemical Physics</i> , 2021, 154, 064104.	3.0	9
8428	Extraordinary negative thermal expansion of two-dimensional nitrides: A comparative <i>ab initio</i> study of quasiharmonic approximation and molecular dynamics simulations. <i>Physical Review B</i> , 2021, 103, .	3.2	12
8429	Rabdosianone I, a Bitter Diterpene from an Oriental Herb, Suppresses Thymidylate Synthase Expression by Directly Binding to ANT2 and PHB2. <i>Cancers</i> , 2021, 13, 982.	3.7	4
8430	Atomistic Simulation of Severely Adhesive Wear on a Rough Aluminum Substrate. , 0, , .		0
8432	Cholesterols Work as a Molecular Regulator of the Antimicrobial Peptide-Membrane Interactions. <i>Frontiers in Molecular Biosciences</i> , 2021, 8, 638988.	3.5	5
8433	pH-Sensitive Glycyrrhizin Based Vesicles for Nifedipine Delivery. <i>Molecules</i> , 2021, 26, 1270.	3.8	11
8434	Folding nucleus and unfolding dynamics of protein 2GB1*. <i>Chinese Physics B</i> , 2021, 30, 028703.	1.4	1
8435	Ectopic positioning of the cell division plane is associated with single amino acid substitutions in the FtsZ-recruiting SsgB in <i>Streptomyces</i> . <i>Open Biology</i> , 2021, 11, 200409.	3.6	6
8436	Optimizing GÅ•MARTINI Coarse-Grained Model for F-BAR Protein on Lipid Membrane. <i>Frontiers in Molecular Biosciences</i> , 2021, 8, 619381.	3.5	32
8437	Molecular dynamics simulations of stretchâ€induced crystallization in layered polyethylene. <i>Polymer Crystallization</i> , 2021, 4, e10172.	0.8	1
8438	Antibody affinity versus dengue morphology influences neutralization. <i>PLoS Pathogens</i> , 2021, 17, e1009331.	4.7	8
8439	NaCl aggregation in water at elevated temperatures and pressures: Comparison of classical force fields. <i>Journal of Chemical Physics</i> , 2021, 154, 064503.	3.0	10
8440	Organoselenium Compounds as Acetylcholinesterase Inhibitors: Evidence and Mechanism of Mixed Inhibition. <i>Journal of Physical Chemistry B</i> , 2021, 125, 1531-1541.	2.6	16
8441	Albumin Alters the Conformational Ensemble of Amyloid-Î² by Promiscuous Interactions: Implications for Amyloid Inhibition. <i>Frontiers in Molecular Biosciences</i> , 2020, 7, 629520.	3.5	13

#	ARTICLE	IF	CITATIONS
8442	Cooperativity between the orthosteric and allosteric ligand binding sites of ROR $\beta$ t. Proceedings of the National Academy of Sciences of the United States of America, 2021, 118, .	7.1	26
8443	Assembly of [Ni(Schiff)] Films on an Inert Surface: A Multiscale Computational Study. Journal of Physical Chemistry C, 2021, 125, 2926-2937.	3.1	4
8444	Pushing and Pulling: A Dual pH Trigger Controlled by Varying the Alkyl Tail Length in Heme Coordinating Peptide Amphiphiles. Journal of Physical Chemistry B, 2021, 125, 1317-1330.	2.6	5
8445	Screening of Yeast Display Libraries of Enzymatically Treated Peptides to Discover Macrocyclic Peptide Ligands. International Journal of Molecular Sciences, 2021, 22, 1634.	4.1	14
8446	Serotonin and Melatonin Show Different Modes of Action on A $\beta$ <sub>42</sub> Protofibril Destabilization. ACS Chemical Neuroscience, 2021, 12, 799-809.	3.5	24
8447	Polyunsaturated Fatty Acid Modulates Membrane-Bound Monomeric $\tau$ -Synuclein by Modulating Membrane Microenvironment through Preferential Interactions. ACS Chemical Neuroscience, 2021, 12, 675-688.	3.5	8
8448	Fe elementindeki $\text{Fe}^{2+}$ Kat $\pm$ -Kat $\pm$ Faz Ge $\ddot{A}$ si $\ddot{A}$ yl $\ddot{A}$ lerinin Molek $\ddot{A}$ ler Dinamik Benzetimi ile $\ddot{A}$ ncelenmesi. F $\ddot{A}$ rat $\ddot{A}$ eniversitesi M $\ddot{A}$ hendislik Bilimleri Dergisi, 2021, 33, 275-282.	0.5	0
8449	Effect of N-terminal modification on the mode of action between the Xyn11A and Xylotetraose. International Journal of Biological Macromolecules, 2021, 170, 240-247.	7.5	3
8450	Insights into the Thermal Response of a Poly(ethylene oxide)-poly(propylene oxide)-poly(ethylene) Tj ETQq0 0 0 rgBTJ/Overlock 10 Tf 50	2.6	1
8451	Molecular dynamics simulation and in-situ MRI observation of organic exclusion during CO <sub>2</sub> hydrate growth. Chemical Physics Letters, 2021, 764, 138287.	2.6	16
8452	Quantitative linear dichroism imaging of molecular processes in living cells made simple by open software tools. Communications Biology, 2021, 4, 189.	4.4	4
8453	C-Terminal Amination of a Cationic Anti-Inflammatory Peptide Improves Bioavailability and Inhibitory Activity Against LPS-Induced Inflammation. Frontiers in Immunology, 2020, 11, 618312.	4.8	7
8455	SARS-CoV-2 S protein:ACE2 interaction reveals novel allosteric targets. ELife, 2021, 10, .	6.0	100
8456	Direct Observation of Cholesterol Dimers and Tetramers in Lipid Bilayers. Journal of Physical Chemistry B, 2021, 125, 1825-1837.	2.6	25
8457	Influence of the Environment on Shaping the Absorption of Monomeric Infrared Fluorescent Proteins. Journal of Physical Chemistry B, 2021, 125, 2231-2240.	2.6	1
8458	Potential Unwinding of Double-Stranded DNA upon Binding to a Carbon Nitride Polyaniline (C <sub>3</sub> N) Nanosheet. Journal of Physical Chemistry B, 2021, 125, 2258-2265.	2.6	5
8459	Strategic aromatic residues in the catalytic cleft of the xyloglucanase MtXgh74 modifying thermostability, mode of enzyme action, and viscosity reduction ability. Applied Microbiology and Biotechnology, 2021, 105, 1461-1476.	3.6	2
8460	Structure and Transport of Solvent Ligated Octahedral Mg-Ion in an Aqueous Battery Electrolyte. Journal of Chemical & Engineering Data, 2021, 66, 1543-1554.	1.9	4



#	ARTICLE	IF	CITATIONS
8461	Machine learning metadynamics simulation of reconstructive phase transition. <i>Physical Review B</i> , 2021, 103, .	3.2	15
8462	Fast green FCF inhibits A $\beta$ 2 fibrillogenesis, disintegrates mature fibrils, reduces the cytotoxicity, and attenuates A $\beta$ 2-induced cognitive impairment in mice. <i>International Journal of Biological Macromolecules</i> , 2021, 170, 33-41.	7.5	9
8463	On the stability of proteinâ€DNA complexes in molecular dynamics simulations using the CUFIX corrections. <i>Journal of the Korean Physical Society</i> , 2021, 78, 461-466.	0.7	6
8464	Experimental and theoretical evidence of enhanced catalytic performance of lipase B from <i>Candida antarctica</i> acquired by the chemical modification with amino acid ionic liquids. <i>Molecular Catalysis</i> , 2021, 501, 111355.	2.0	9
8465	Intermolecular interactions in composites of organically-modified silica aerogels and polymers: A molecular simulation study. <i>Microporous and Mesoporous Materials</i> , 2021, 314, 110838.	4.4	10
8466	The potential utilization of lecithin as natural gas hydrate decomposition inhibitor in oil well cement at low temperatures. <i>Construction and Building Materials</i> , 2021, 269, 121274.	7.2	18
8467	Resolving the Equal Number Density Puzzle: Molecular Picture from Simulations of LiCl(aq) and NaCl(aq). <i>Journal of Physical Chemistry B</i> , 2021, 125, 3153-3162.	2.6	12
8468	Exploring the Cold-Adaptation Mechanism of Serine Hydroxymethyltransferase by Comparative Molecular Dynamics Simulations. <i>International Journal of Molecular Sciences</i> , 2021, 22, 1781.	4.1	10
8469	Relations between thermodynamics, structures, and dynamics for modified water models in their supercooled regimes. <i>Journal of Chemical Physics</i> , 2021, 154, 054502.	3.0	5
8470	Monolayer Structures of Supramolecular Antagonistic Salt Aggregates. <i>Journal of Physical Chemistry B</i> , 2021, 125, 2351-2359.	2.6	3
8471	Full structural ensembles of intrinsically disordered proteins from unbiased molecular dynamics simulations. <i>Communications Biology</i> , 2021, 4, 243.	4.4	52
8472	The atomistic details of the ice recrystallisation inhibition activity of PVA. <i>Nature Communications</i> , 2021, 12, 1323.	12.8	62
8473	Fast dynamics in a model metallic glass-forming material. <i>Journal of Chemical Physics</i> , 2021, 154, 084505.	3.0	32
8474	Sensitivity of Binding Free Energy Calculations to Initial Protein Crystal Structure. <i>Journal of Chemical Theory and Computation</i> , 2021, 17, 1806-1821.	5.3	13
8475	Diethylstilbestrol Modifies the Structure of Model Membranes and Is Localized Close to the First Carbons of the Fatty Acyl Chains. <i>Biomolecules</i> , 2021, 11, 220.	4.0	3
8476	Computational Modulation of the V3 Region of Glycoprotein gp125 of HIV-2. <i>International Journal of Molecular Sciences</i> , 2021, 22, 1948.	4.1	3
8477	State-dependent protein-lipid interactions of a pentameric ligand-gated ion channel in a neuronal membrane. <i>PLoS Computational Biology</i> , 2021, 17, e1007856.	3.2	18
8478	Investigation of the stability and the helix-tail interaction of sCT and its various charged mutants based on comparative molecular dynamics simulations. <i>Chemical Physics</i> , 2021, 542, 111057.	1.9	1

#	ARTICLE	IF	CITATIONS
8479	<i>Ar</i> omaphilicity Index of Amino Acids: Molecular Dynamics Simulations of the Protein Binding Affinity for Carbon Nanomaterials. ACS Applied Nano Materials, 2021, 4, 2486-2495.	5.0	29
8480	Visualization of the mechanosensitive ion channel MscS under membrane tension. Nature, 2021, 590, 509-514.	27.8	77
8482	Curvature Energetics Determined by Alchemical Simulation on Four Topologically Distinct Lipid Phases. Journal of Physical Chemistry B, 2021, 125, 1815-1824.	2.6	5
8483	Evaluating the Performance of Water Models with Host-Guest Force Fields in Binding Enthalpy Calculations for Cucurbit[7]uril-Guest Systems. Journal of Physical Chemistry B, 2021, 125, 1558-1567.	2.6	6
8484	Computational Analysis Reveals a Critical Point Mutation in the N-Terminal Region of the Signaling Lymphocytic Activation Molecule Responsible for the Cross-Species Infection with Canine Distemper Virus. Molecules, 2021, 26, 1262.	3.8	4
8485	Quasi-Universal Solubility Behavior of Light Gases in Imidazolium-Based Ionic Liquids with Varying Anions: A Molecular Dynamics Simulation Study. Journal of Physical Chemistry B, 2021, 125, 1647-1659.	2.6	15
8486	Hofmeister versus Neuberg: is ATP really a biological hydrotrope?. Cell Reports Physical Science, 2021, 2, 100343.	5.6	40
8487	Mechanistic Insights into the Co-Aggregation of A $\beta$ 2 and hIAPP: An All-Atom Molecular Dynamic Study. Journal of Physical Chemistry B, 2021, 125, 2050-2060.	2.6	23
8488	Hedgehog proteins create a dynamic cholesterol interface. PLoS ONE, 2021, 16, e0246814.	2.5	8
8489	Comparing the Ion-Conducting Polymers with Sulfonate and Ether Moieties as Cathode Binders for High-Power Lithium-Ion Batteries. ACS Applied Materials & Interfaces, 2021, 13, 9846-9855.	8.0	16
8490	Pressure-Dependent Structure of Methanol-Water Mixtures up to 1.2 GPa: Neutron Diffraction Experiments and Molecular Dynamics Simulations. Molecules, 2021, 26, 1218.	3.8	2
8492	Development and Validation of a DFT-Based Force Field for a Hydrated Homoalanine Polypeptide. Journal of Physical Chemistry B, 2021, 125, 1568-1581.	2.6	6
8493	Relation between glycosidic linkage, structure and dynamics of $\alpha$ - and $\beta$ -glucans in water. Biopolymers, 2021, 112, e23423.	2.4	11
8494	Specific domain V reduction of beta-2-glycoprotein I induces protein flexibility and alters pathogenic antibody binding. Scientific Reports, 2021, 11, 4542.	3.3	3
8495	Metastable solid phase diagrams derived from polymorphic solidification kinetics. Proceedings of the National Academy of Sciences of the United States of America, 2021, 118, .	7.1	11
8496	Role of Calcium in Modulating the Conformational Landscape and Peptide Binding Induced Closing of Calmodulin. Journal of Physical Chemistry B, 2021, 125, 2317-2327.	2.6	9
8497	Quantum Simulations of Hydrogen Bonding Effects in Glycerol Carbonate Electrolyte Solutions. Journal of Physical Chemistry B, 2021, 125, 2157-2166.	2.6	7
8498	Extraction of protein dynamics information from cryo-EM maps using deep learning. Nature Machine Intelligence, 2021, 3, 153-160.	16.0	57

#	ARTICLE	IF	CITATIONS
8499	Molecular dynamics simulation of lentinan and its interaction with the innate receptor dectin-1. International Journal of Biological Macromolecules, 2021, 171, 527-538.	7.5	27
8500	Ionic Liquid for PEDOT:PSS Treatment. Ion Binding Free Energy in Water Revealing the Importance of Anion Hydrophobicity. Journal of Physical Chemistry B, 2021, 125, 1916-1923.	2.6	25
8501	Molecular dynamics study of hydrogen diffusion in the C2 Hydrogen Hydrates. Journal of Physics: Conference Series, 2021, 1816, 012084.	0.4	0
8503	Design and Immunological Evaluation of a Hybrid Peptide as a Potent TLR2 Agonist by Structure-Based Virtual Screening. Frontiers in Cell and Developmental Biology, 2021, 9, 620370.	3.7	3
8504	Fluorinated Triazole Foldamers: Folded or Extended Conformational Preferences. ChemPlusChem, 2021, 86, 241-251.	2.8	3
8505	Silencing of the tRNA Modification Enzyme Cdkal1 Effects Functional Insulin Synthesis in NIT-1 Cells: tRNALys3 Lacking ms2- (ms2t6A37) is Unable to Establish Sufficient Anticodon:Codon Interactions to Decode the Wobble Codon AAG. Frontiers in Molecular Biosciences, 2020, 7, 584228.	3.5	2
8506	Effect of palmitoylation on the dimer formation of the human dopamine transporter. Scientific Reports, 2021, 11, 4164.	3.3	8
8508	Molecular Modeling of Subsurface Phenomena Related to Petroleum Engineering. Energy & Fuels, 2021, 35, 2851-2869.	5.1	12
8509	Molecular Origin of Carbonâ€“Oxygenâ€“Bridge Isomerization Induced Reverse Aggregation Ability in Acceptorâ€“Donorâ€“Acceptor Electron Acceptors for Organic Solar Cells. Solar Rrl, 2021, 5, 2000780.	5.8	5
8510	Spontaneous rearrangement of acetylated xylan on hydrophilic cellulose surfaces. Cellulose, 2021, 28, 3327-3345.	4.9	14
8511	Quaternary ammonium cellulose promoted synthesis of hollow nano-sized ZSM-5 zeolite as stable catalyst for benzene alkylation with ethanol. Journal of Materials Science, 2021, 56, 8461-8478.	3.7	11
8512	Thermal Conductivity of B-DNA. Journal of Physical Chemistry B, 2021, 125, 1363-1368.	2.6	1
8513	Molecular Dynamics Simulation of the <i>n</i>-Octacosaneâ€“Water Mixture Confined in Graphene Mesopores: Comparison of Atomistic and Coarse-Grained Calculations and the Effect of Catalyst Nanoparticle. Energy & Fuels, 2021, 35, 4313-4332.	5.1	5
8514	Selecting Collective Variables and Free-Energy Methods for Peptide Translocation across Membranes. Journal of Chemical Information and Modeling, 2021, 61, 819-830.	5.4	22
8515	Pre-existing bilayer stresses modulate triglyceride accumulation in the ER versus lipid droplets. ELife, 2021, 10, .	6.0	55
8516	Dynamics and Rheology of Polymer Melts <i>via</i> Hierarchical Atomistic, Coarse-Grained, and Slip-Spring Simulations. Macromolecules, 2021, 54, 2740-2762.	4.8	40
8517	Flavin-Conjugated Nanobombs: Key Structural Requirements Governing Their Self-Assembliesâ€™ Morphologies. Bioconjugate Chemistry, 2021, 32, 553-562.	3.6	10
8518	Impact of dimerization and N3 binding on molecular dynamics of SARS-CoV and SARS-CoV-2 main proteases. Journal of Biomolecular Structure and Dynamics, 2022, 40, 6243-6254.	3.5	15

#	ARTICLE	IF	CITATIONS
8519	Specific PIP2 binding promotes calcium activation of TMEM16A chloride channels. <i>Communications Biology</i> , 2021, 4, 259.	4.4	21
8520	Structural phase transition in monolayer gold(I) telluride: From a room-temperature topological insulator to an auxetic semiconductor. <i>Physical Review B</i> , 2021, 103, .	3.2	10
8521	In silico analysis of resveratrol induced PD-L1 dimerisation. <i>Journal of the Belarusian State University Biology</i> , 2021, , 39-47.	0.2	0
8522	Theoretical insights into molecular mechanism and energy criteria of PARP $\alpha$ 2 enzyme inhibition by benzimidazole analogues. <i>Proteins: Structure, Function and Bioinformatics</i> , 2021, 89, 988-1004.	2.6	6
8524	ANT1 Activation and Inhibition Patterns Support the Fatty Acid Cycling Mechanism for Proton Transport. <i>International Journal of Molecular Sciences</i> , 2021, 22, 2490.	4.1	25
8525	Localization model description of the interfacial dynamics of crystalline Cu and $\text{Cu}_{64}\text{Zr}_{36}$ metallic glass nanoparticles. <i>European Physical Journal E</i> , 2021, 44, 33.	1.6	6
8526	Nanoscale heterogeneity, hydrogen bonding and their temperature dependence in cholinium phenylalaninate bio-ionic liquid. <i>Journal of Molecular Liquids</i> , 2021, 326, 115329.	4.9	6
8527	Unraveling the mechanism of arbidol binding and inhibition of SARS-CoV-2: Insights from atomistic simulations. <i>European Journal of Pharmacology</i> , 2021, 894, 173836.	3.5	51
8528	Determining the atomic charge of calcium ion requires the information of its coordination geometry in an EF-hand motif. <i>Journal of Chemical Physics</i> , 2021, 154, 124104.	3.0	6
8529	Binding and inhibitory effect of ravidasvir on 3CL <sup>pro</sup> of SARS-CoV $\alpha$ 2: a molecular docking, molecular dynamics and MM/PBSA approach. <i>Journal of Biomolecular Structure and Dynamics</i> , 2022, 40, 7303-7310.	3.5	15
8530	Structure-based modeling and dynamics of MurM, a <i>Streptococcus pneumoniae</i> penicillin resistance determinant present at the cytoplasmic membrane. <i>Structure</i> , 2021, 29, 731-742.e6.	3.3	7
8531	Insights into the Solubility of Poly(vinylphenothiazine) in Carbonate-Based Battery Electrolytes. <i>ACS Applied Materials &amp; Interfaces</i> , 2021, 13, 12442-12453.	8.0	23
8532	Effect of Protein Corona on Nanoparticleâ€“Lipid Membrane Binding: The Binding Strength and Dynamics. <i>Langmuir</i> , 2021, 37, 3751-3760.	3.5	8
8533	Collective variables for the study of crystallisation. <i>Molecular Physics</i> , 2021, 119, .	1.7	25
8534	Cryptic-site binding mechanism of medium-sized Bcl-xL inhibiting compounds elucidated by McMD-based dynamic docking simulations. <i>Scientific Reports</i> , 2021, 11, 5046.	3.3	11
8535	Insight Into Seeded Tau Fibril Growth From Molecular Dynamics Simulation of the Alzheimerâ€™s Disease Protofibril Core. <i>Frontiers in Molecular Biosciences</i> , 2021, 8, 624302.	3.5	17
8537	Comparison of Carbohydrate Force Fields in Molecular Dynamics Simulations of Proteinâ€“Carbohydrate Complexes. <i>Journal of Chemical Theory and Computation</i> , 2021, 17, 2575-2585.	5.3	23
8538	Molecular Study of Ultrasound-Triggered Release of Fluorescein from Liposomes. <i>Langmuir</i> , 2021, 37, 3868-3881.	3.5	7

#	ARTICLE	IF	CITATIONS
8539	High Li-ion conductivity in tetragonal LGPO: A comparative first-principles study against known LISICON and LGPS phases. <i>Physical Review Materials</i> , 2021, 5, .	2.4	8
8540	Identification and evaluation of immunogenic MHC-I and MHC-II binding peptides from <i>Mycobacterium tuberculosis</i> . <i>Computers in Biology and Medicine</i> , 2021, 130, 104203.	7.0	6
8541	All-Atom Simulations and Free-Energy Calculations of Antibodies Bound to the Spike Protein of SARS-CoV-2: The Binding Strength and Multivalent Hydrogen-Bond Interactions. <i>Advanced Theory and Simulations</i> , 2021, 4, 2100012.	2.8	2
8542	A weakened interface in the P182L variant of HSP27 associated with severe Charcot-Marie-Tooth neuropathy causes aberrant binding to interacting proteins. <i>EMBO Journal</i> , 2021, 40, e103811.	7.8	14
8543	Specific inhibition of the Survivin-CRM1 interaction by peptide-modified molecular tweezers. <i>Nature Communications</i> , 2021, 12, 1505.	12.8	18
8545	A computational drug repurposing approach in identifying the cephalosporin antibiotic and anti-hepatitis C drug derivatives for COVID-19 treatment. <i>Computers in Biology and Medicine</i> , 2021, 130, 104186.	7.0	26
8546	Molecular Dynamics Simulations of a Catalytic Multivalent Peptide-Nanoparticle Complex. <i>International Journal of Molecular Sciences</i> , 2021, 22, 3624.	4.1	13
8547	Determining the hydration free energies of selected small molecules with MP2 and local MP2 through adaptive force matching. <i>Journal of Chemical Physics</i> , 2021, 154, 104113.	3.0	2
8548	N-Glycosylation can selectively block or foster different receptor-ligand binding modes. <i>Scientific Reports</i> , 2021, 11, 5239.	3.3	18
8549	Benchmarking of Molecular Dynamics Force Fields for Solid-Liquid and Solid-Solid Phase Transitions in Alkanes. <i>Journal of Physical Chemistry B</i> , 2021, 125, 5145-5159.	2.6	29
8550	Prioritization of candidate genes for a South African family with Parkinson's disease using in-silico tools. <i>PLoS ONE</i> , 2021, 16, e0249324.	2.5	9
8551	A rational design of a multi-epitope vaccine against SARS-CoV-2 which accounts for the glycan shield of the spike glycoprotein. <i>Journal of Biomolecular Structure and Dynamics</i> , 2022, 40, 7099-7113.	3.5	15
8552	Microscopic Kinetics Pathway of Salt Crystallization in Graphene Nanocapillaries. <i>Physical Review Letters</i> , 2021, 126, 136001.	7.8	22
8553	Shear deformations in crystalline alkali-silica reaction products at the molecular scale: anisotropy and role of specific ion effects. <i>Materials and Structures/Materiaux Et Constructions</i> , 2021, 54, 1.	3.1	2
8555	Azobioisosteres of Curcumin with Pronounced Activity against Amyloid Aggregation, Intracellular Oxidative Stress, and Neuroinflammation. <i>Chemistry - A European Journal</i> , 2021, 27, 6015-6027.	3.3	4
8557	NMR refinement and peptide folding using the GROMACS software. <i>Journal of Biomolecular NMR</i> , 2021, 75, 143-149.	2.8	9
8558	Insights into the interaction dynamics between volatile anesthetics and tubulin through computational molecular modelling. <i>Journal of Biomolecular Structure and Dynamics</i> , 2022, 40, 7324-7338.	3.5	4
8559	Reconstruction of ARNT PAS-B Unfolding Pathways by Steered Molecular Dynamics and Artificial Neural Networks. <i>Journal of Chemical Theory and Computation</i> , 2021, 17, 2080-2089.	5.3	14

#	ARTICLE	IF	CITATIONS
8560	Structural Insights into gp16 ATPase in the Bacteriophage $\phi$ 29 DNA Packaging Motor. <i>Biochemistry</i> , 2021, 60, 886-897.	2.5	7
8561	Differential Effects of IL2R $\alpha$ and IL15R $\alpha$ over the Stability of the Common Beta-Gamma Signaling Subunits of the IL2 and IL15 Receptors. <i>Journal of Chemical Information and Modeling</i> , 2021, 61, 1913-1920.	5.4	3
8562	Mixing of Surfactin, an Anionic Biosurfactant, with Alkylbenzene Sulfonate, a Chemically Synthesized Anionic Surfactant, at the <sc><i>n</i></sc>-Decane</sc>/Water Interface. <i>Journal of Surfactants and Detergents</i> , 2021, 24, 445-457.	2.1	6
8563	Flavonoids as potential therapeutics against novel coronavirus disease-2019 (nCOVID-19). <i>Journal of Biomolecular Structure and Dynamics</i> , 2022, 40, 6989-7001.	3.5	13
8564	Crystal orientation and grain boundary effects on plastic deformation of FCC particles under high velocity impacts. <i>Materialia</i> , 2021, 15, 101004.	2.7	11
8565	Extended Lifetime of Molecules Adsorbed onto Excipients Drives Nucleation in Heterogeneous Crystallization. <i>Crystal Growth and Design</i> , 2021, 21, 2101-2112.	3.0	4
8566	Thermodynamic and sequential characteristics of phase separation and droplet formation for an intrinsically disordered region/protein ensemble. <i>PLoS Computational Biology</i> , 2021, 17, e1008672.	3.2	15
8567	Water orientation and dynamics in the closed and open influenza B virus M2 proton channels. <i>Communications Biology</i> , 2021, 4, 338.	4.4	20
8568	Lipid regulation of hERG1 channel function. <i>Nature Communications</i> , 2021, 12, 1409.	12.8	9
8571	Temperature Dependence of Internal Friction of Peptides. <i>Journal of Physical Chemistry B</i> , 2021, 125, 2821-2832.	2.6	2
8572	Interfacial Polarization and Ionic Structure at the Ionic Liquid-Metal Interface Studied by Vibrational Spectroscopy and Molecular Dynamics Simulations. <i>Journal of Physical Chemistry B</i> , 2021, 125, 2741-2753.	2.6	9
8573	Thermodynamic and structural aspects of molecular recognition in mannose-binding protein complexes: a theoretical study over HRP-ArtinM association. <i>Journal of Molecular Modeling</i> , 2021, 27, 107.	1.8	1
8575	The structure of Prp2 bound to RNA and ADP-BeF <sub>3</sub> <sup>-</sup> reveals structural features important for RNA unwinding by DEAH-box ATPases. <i>Acta Crystallographica Section D: Structural Biology</i> , 2021, 77, 496-509.	2.3	9
8576	In silico screening and analysis of nonsynonymous SNPs in human CYP1A2 to assess possible associations with pathogenicity and cancer susceptibility. <i>Scientific Reports</i> , 2021, 11, 4977.	3.3	12
8577	Influence of the number and type of functional groups on self-diffusion of some aromatic compounds in acetone: Nuclear magnetic resonance and molecular dynamics simulations. <i>Journal of Molecular Liquids</i> , 2021, 326, 115230.	4.9	4
8579	Free Energy Cost of Interdigitation of Lamellar Bilayers of Fatty Alcohols with Cationic Surfactants from Molecular Dynamics Simulations. <i>Journal of Physical Chemistry B</i> , 2021, 125, 2389-2397.	2.6	2
8580	The influences of surface polar unit density on the water dispersity of nanoparticles. <i>Journal of Molecular Liquids</i> , 2021, 325, 115241.	4.9	2
8581	Computational drug repurposing study elucidating simultaneous inhibition of entry and replication of novel corona virus by Grazoprevir. <i>Scientific Reports</i> , 2021, 11, 7307.	3.3	27



#	ARTICLE	IF	CITATIONS
8582	Choice of fluorophore affects dynamic DNA nanostructures. <i>Nucleic Acids Research</i> , 2021, 49, 4186-4195.	14.5	20
8583	Per   Mut: Spatially Resolved Hydration Entropies from Atomistic Simulations. <i>Journal of Chemical Theory and Computation</i> , 2021, 17, 2090-2098.	5.3	13
8584	How does Sec63 affect the conformation of Sec61 in yeast?. <i>PLoS Computational Biology</i> , 2021, 17, e1008855.	3.2	13
8585	Effect of Water Models on Transmembrane Self-Assembled Cyclic Peptide Nanotubes. <i>ACS Nano</i> , 2021, 15, 7053-7064.	14.6	12
8586	Positive allosteric modulators of lecithin: Cholesterol acyltransferase adjust the orientation of the membrane-binding domain and alter its spatial free energy profile. <i>PLoS Computational Biology</i> , 2021, 17, e1008426.	3.2	2
8587	Designing a natural inhibitor against human kynurenine aminotransferase type II and a comparison with PF-04859989: a computational effort against schizophrenia. <i>Journal of Biomolecular Structure and Dynamics</i> , 2022, 40, 7038-7051.	3.5	9
8588	<i>in silico</i> exploration of hydroxylated polychlorinated biphenyls as estrogen receptor $\beta$ ligands by 3D-QSAR, molecular docking and molecular dynamics simulations. <i>Journal of Biomolecular Structure and Dynamics</i> , 2022, 40, 6798-6809.	3.5	3
8589	Characterization of a <i>Bacillus megaterium</i> strain with metal bioremediation potential and <i>in silico</i> discovery of novel cadmium binding motifs in the regulator, CadC. <i>Applied Microbiology and Biotechnology</i> , 2021, 105, 2573-2586.	3.6	16
8590	Implementing and Assessing an Alchemical Method for Calculating Protein-Protein Binding Free Energy. <i>Journal of Chemical Theory and Computation</i> , 2021, 17, 2457-2464.	5.3	16
8591	Effect of oxidation on cellulose and water structure: a molecular dynamics simulation study. <i>Cellulose</i> , 2021, 28, 3917-3933.	4.9	16
8592	Decelerated aging in metallic glasses by low temperature thermal cycling. <i>Physical Review Research</i> , 2021, 3, .	3.6	12
8593	Mechanistic differences in the effects of sucrose and sucralose on the phase stability of lysozyme solutions. <i>Journal of Molecular Liquids</i> , 2021, 326, 115245.	4.9	11
8594	Coarse-Grained Simulations on Interactions between Spectrins and Phase-Separated Lipid Bilayers. <i>Chinese Physics B</i> , 0, , .	1.4	0
8595	Marine-Derived Natural Products as ATP-Competitive mTOR Kinase Inhibitors for Cancer Therapeutics. <i>Pharmaceuticals</i> , 2021, 14, 282.	3.8	16
8596	Assessment of Amyloid Forming Tendency of Peptide Sequences from Amyloid Beta and Tau Proteins Using Force-Field, Semi-Empirical, and Density Functional Theory Calculations. <i>International Journal of Molecular Sciences</i> , 2021, 22, 3244.	4.1	3
8597	Lead and mercury removal from aqueous solution using Sodium Dodecyl Sulfate micelles: A molecular dynamics study. <i>Chemical Physics Letters</i> , 2021, 767, 138340.	2.6	3
8598	Molecular dynamics simulations vs field-cycling NMR relaxometry: Structural relaxation mechanisms in the glass-former glycerol revisited. <i>Journal of Chemical Physics</i> , 2021, 154, 124503.	3.0	15
8599	A phenylalanine dynamic switch controls the interfacial activation of <i>Rhizopus chinensis</i> lipase. <i>International Journal of Biological Macromolecules</i> , 2021, 173, 1-12.	7.5	27

#	ARTICLE	IF	CITATIONS
8600	Predicting lipid and ligand binding sites in TRPV1 channel by molecular dynamics simulation and machine learning. <i>Proteins: Structure, Function and Bioinformatics</i> , 2021, 89, 966-977.	2.6	1
8601	The role of plasmalogens, Forssman lipids, and sphingolipid hydroxylation in modulating the biophysical properties of the epithelial plasma membrane. <i>Journal of Chemical Physics</i> , 2021, 154, 095101.	3.0	12
8603	Spatial-Decomposition Analysis of Electrical Conductivity in Mixtures of Ionic Liquid and Sodium Salt for Sodium-Ion Battery Electrolytes. <i>Journal of Physical Chemistry B</i> , 2021, 125, 3374-3385.	2.6	6
8604	Computational evidence for nitro derivatives of quinoline and quinoline N-oxide as low-cost alternative for the treatment of SARS-CoV-2 infection. <i>Scientific Reports</i> , 2021, 11, 6397.	3.3	11
8605	Insight into the properties and structures of vapor-liquid interface for imidazolium-based ionic liquids by molecular dynamics simulations. <i>Journal of Molecular Liquids</i> , 2021, 326, 115295.	4.9	11
8607	Polyacrylamide adsorption on (1 0 1) quartz surfaces in saltwater for a range of pH values by molecular dynamics simulations. <i>Minerals Engineering</i> , 2021, 162, 106741.	4.3	23
8609	Structure based analysis of KATP channel with a DEND syndrome mutation in murine skeletal muscle. <i>Scientific Reports</i> , 2021, 11, 6668.	3.3	4
8611	Unveiling Carbon Dioxide and Ethanol Diffusion in Carbonated Water-Ethanol Mixtures by Molecular Dynamics Simulations. <i>Molecules</i> , 2021, 26, 1711.	3.8	2
8615	On the vibrational free energy of hydrated proteins. <i>Physical Biology</i> , 2021, 18, 036003.	1.8	0
8616	Allosteric Kinase Inhibitors Reshape MEK1 Kinase Activity Conformations in Cells and In Silico. <i>Biomolecules</i> , 2021, 11, 518.	4.0	4
8617	CENP-A Nucleosome is a Sensitive Allosteric Scaffold for DNA and Chromatin Factors. <i>Journal of Molecular Biology</i> , 2021, 433, 166789.	4.2	5
8618	The "hidden side" of spin labelled oligonucleotides: Molecular dynamics study focusing on the EPR-silent components of base pairing. <i>Journal of Magnetic Resonance</i> , 2021, 324, 106924.	2.1	2
8619	First-principles hydration free energies of oxygenated species at water-platinum interfaces. <i>Journal of Chemical Physics</i> , 2021, 154, 094107.	3.0	11
8620	Structure and dynamics of water plastic crystals from computer simulations. <i>Journal of Chemical Physics</i> , 2021, 154, 104501.	3.0	9
8621	Molecular simulation of zwitterionic polypeptides on protecting glucagon-like peptide-1 (GLP-1). <i>International Journal of Biological Macromolecules</i> , 2021, 174, 519-526.	7.5	5
8622	Understanding the binding affinities between SFRP1CRD, SFRP1Netrin, Wnt5B and frizzled receptors 2, 3 and 7 using MD simulations. <i>Journal of Biomolecular Structure and Dynamics</i> , 2021, , 1-14.	3.5	3
8624	Analyzing the Long Time-Scale Dynamics of Uremic Toxins Bound to Sudlow Site II in Human Serum Albumin. <i>Journal of Physical Chemistry B</i> , 2021, 125, 2910-2920.	2.6	4
8625	Structure, Dynamics, Receptor Binding, and Antibody Binding of the Fully Glycosylated Full-Length SARS-CoV-2 Spike Protein in a Viral Membrane. <i>Journal of Chemical Theory and Computation</i> , 2021, 17, 2479-2487.	5.3	62

#	ARTICLE	IF	CITATIONS
8626	Protein Dynamics Influence the Enzymatic Activity of Phospholipase A/Acyltransferases 3 and 4. <i>Biochemistry</i> , 2021, 60, 1178-1190.	2.5	6
8627	Membrane Interactions of Î±-Synuclein Revealed by Multiscale Molecular Dynamics Simulations, Markov State Models, and NMR. <i>Journal of Physical Chemistry B</i> , 2021, 125, 2929-2941.	2.6	17
8628	First-principles calculations of equilibrium nitrogen isotope fractionations among aqueous ammonium, silicate minerals and salts. <i>Geochimica Et Cosmochimica Acta</i> , 2021, 297, 220-232.	3.9	17
8629	Martini 3: a general purpose force field for coarse-grained molecular dynamics. <i>Nature Methods</i> , 2021, 18, 382-388.	19.0	557
8630	Lin28, a major translation reprogramming factor, gains access to YB-1-packaged mRNA through its cold-shock domain. <i>Communications Biology</i> , 2021, 4, 359.	4.4	13
8631	A potential interaction between the SARS-CoV-2 spike protein and nicotinic acetylcholine receptors. <i>Biophysical Journal</i> , 2021, 120, 983-993.	0.5	43
8632	Investigation of interactions between zein and natamycin by fluorescence spectroscopy and molecular dynamics simulation. <i>Journal of Molecular Liquids</i> , 2021, 327, 114873.	4.9	23
8633	Revised Atomic Charges for OPLS Force Field Model of Poly(Ethylene Oxide): Benchmarks and Applications in Polymer Electrolyte. <i>Polymers</i> , 2021, 13, 1131.	4.5	18
8638	Moving toward generalizable NZ-1 labeling for 3D structure determination with optimized epitope-tag insertion. <i>Acta Crystallographica Section D: Structural Biology</i> , 2021, 77, 645-662.	2.3	18
8639	Thermodynamic and kinetic properties of a single base pair in A-DNA and B-DNA. <i>Physical Review E</i> , 2021, 103, 042409.	2.1	9
8640	Relationship of structure and mechanical property of silica with enhanced sampling and machine learning. <i>Journal of the American Ceramic Society</i> , 2021, 104, 3910-3920.	3.8	4
8641	An interplay of excluded-volume and polymerâ€™(co)solvent attractive interactions regulates polymer collapse in mixed solvents. <i>Journal of Chemical Physics</i> , 2021, 154, 134903.	3.0	16
8642	Coarse-grained model of a nanoscale-segregated ionic liquid for simulations of low-temperature structure and dynamics. <i>Journal of Physics Condensed Matter</i> , 2021, 33, 204002.	1.8	6
8643	Conformational Plasticity-Rigidity Axis of the Coagulation Factor VII Zymogen Elucidated by Atomistic Simulations of the N-Terminally Truncated Factor VIIa Protease Domain. <i>Biomolecules</i> , 2021, 11, 549.	4.0	7
8644	Mechanism of CH <sub>4</sub> Sorption onto a Shale Surface in the Presence of Cationic Surfactant. <i>Energy &amp; Fuels</i> , 2021, 35, 7943-7955.	5.1	13
8646	Solvent effects on host-guest residence time and kinetics: further insights from metadynamics simulation of Toussaintine-A unbinding from chitosan nanoparticle. <i>Journal of Molecular Modeling</i> , 2021, 27, 127.	1.8	1
8647	Interaction of Peptides Containing CRAC Motifs with Lipids in Membranes of Various Composition. <i>Biochemistry (Moscow) Supplement Series A: Membrane and Cell Biology</i> , 2021, 15, 120-129.	0.6	1
8648	Molecular Mechanism of the Intercalation of the SOX-4 Protein into DNA Inducing Bends and Kinks. <i>Journal of Physical Chemistry B</i> , 2021, 125, 3752-3762.	2.6	4

8650	Molecular dynamics simulations reveal the destabilization mechanism of Alzheimer's disease-related tau R3-R4 Protofilament by norepinephrine. Biophysical Chemistry, 2021, 271, 106541.	2.8	13
8651	The RIT1 C-terminus associates with lipid bilayers via charge complementarity. Computational Biology and Chemistry, 2021, 91, 107437.	2.3	6
8652	The antibiotic darobactin mimics a Î²-strand to inhibit outer membrane insertase. Nature, 2021, 593, 125-129.	27.8	112
8653	Cluster Identification Using Modularity Optimization to Uncover Chemical Heterogeneity in Complex Solutions. Journal of Physical Chemistry A, 2021, 125, 3986-3993.	2.5	6
8654	Prevention of SARS-CoV-2 Proliferation with a Novel and Potent Main Protease Inhibitor by Docking, ADMET, MM-PBSA, and Molecular Dynamics Simulation. Journal of Computational Biophysics and Chemistry, 2021, 20, 305-322.	1.7	8
8655	Informing NMR experiments with molecular dynamics simulations to characterize the dominant activated state of the KcsA ion channel. Journal of Chemical Physics, 2021, 154, 165102.	3.0	11
8657	Effect of Stapling on the Thermodynamics of mdm2â€“p53 Binding. Journal of Chemical Information and Modeling, 2021, 61, 1989-2000.	5.4	8
8658	Switching the O-O Bond Formation Pathways of Ru-pda Water Oxidation Catalyst by Third Coordination Sphere Engineering. Research, 2021, 2021, 9851231.	5.7	7
8660	Biotransformation of rare earth oxide nanoparticles eliciting microbiota imbalance. Particle and Fibre Toxicology, 2021, 18, 17.	6.2	14
8661	Comparing the effects of polymer binders on Li+ transport near the liquid electrolyte/LiFePO4 interfaces: A molecular dynamics simulation study. Electrochimica Acta, 2021, 375, 137915.	5.2	11
8662	Formation of contraction twins in titanium through reversible martensitic phase transformation. Scripta Materialia, 2021, 195, 113694.	10.2	10
8663	Origins of Clustering of Metalateâ€“Extractant Complexes in Liquidâ€“Liquid Extraction. ACS Applied Materials & Interfaces, 2021, 13, 24194-24206.	8.0	27
8664	Modeling of full-length Piezo1 suggests importance of the proximal N-terminus for dome structure. Biophysical Journal, 2021, 120, 1343-1356.	0.5	23
8665	Antimicrobial Bombinin-like Peptide 3 Selectively Recognizes and Inserts into Bacterial Biomimetic Bilayers in Multiple Steps. Journal of Medicinal Chemistry, 2021, 64, 5185-5197.	6.4	5
8667	A combined molecular dynamics and experimental study of two-step process enabling low-temperature formation of phase-pure Î±-FAPbI3. Science Advances, 2021, 7, .	10.3	49
8668	Macroion molecule properties from slender body hydrodynamics. Polymers for Advanced Technologies, 2021, 32, 3900-3908.	3.2	4
8669	Computational Simulations Identified Marine-Derived Natural Bioactive Compounds as Replication Inhibitors of SARS-CoV-2. Frontiers in Microbiology, 2021, 12, 647295.	3.5	24

#	ARTICLE	IF	CITATIONS
8670	Molecular determinants of binding of non-oxime bispyridinium nerve agent antidote compounds to the adult muscle nAChR. <i>Toxicology Letters</i> , 2021, 340, 114-122.	0.8	8
8672	Investigating 3,4-bis(3-nitrofurazan-4-yl)furoxan detonation with a rapidly tuned density functional tight binding model. <i>Journal of Chemical Physics</i> , 2021, 154, 164115.	3.0	12
8673	Polyunsaturated Phospholipids Increase Cell Resilience to Mechanical Constraints. <i>Cells</i> , 2021, 10, 937.	4.1	5
8674	Deciphering molecular details of the RACâ€“ribosome interaction by EPR spectroscopy. <i>Scientific Reports</i> , 2021, 11, 8681.	3.3	5
8675	Phase Equilibrium of Water with Hexagonal and Cubic Ice Using the SCAN Functional. <i>Journal of Chemical Theory and Computation</i> , 2021, 17, 3065-3077.	5.3	37
8676	Study on the Influence of Factors on the Structure and Mechanical Properties of Amorphous Aluminium by Molecular Dynamics Method. <i>Advances in Materials Science and Engineering</i> , 2021, 2021, 1-10.	1.8	3
8677	Estimating the Directional Flexibility of Proteins from Equilibrium Thermal Fluctuations. <i>Journal of Chemical Theory and Computation</i> , 2021, 17, 3103-3118.	5.3	4
8678	A universal allosteric mechanism for G protein activation. <i>Molecular Cell</i> , 2021, 81, 1384-1396.e6.	9.7	33
8679	Tauroursodeoxycholic Acid (TUDCA)â€™Lipid Interactions and Antioxidant Properties of TUDCA Studied in Model of Photoreceptor Membranes. <i>Membranes</i> , 2021, 11, 327.	3.0	3
8680	Design of new drug delivery platform based on surface functionalization of black phosphorus nanosheet with a smart polymer for enhancing the efficiency of doxorubicin in the treatment of cancer. <i>Journal of Biomedical Materials Research - Part A</i> , 2021, 109, 1912-1921.	4.0	9
8682	Automated Development of Molten Salt Machine Learning Potentials: Application to LiCl. <i>Journal of Physical Chemistry Letters</i> , 2021, 12, 4278-4285.	4.6	26
8683	Structural Model for Recruitment of RIT1 to the LZTR1 E3 Ligase: Evidences from an Integrated Computational Approach. <i>Journal of Chemical Information and Modeling</i> , 2021, 61, 1875-1888.	5.4	1
8684	Asymmetric CorA Gating Mechanism as Observed by Molecular Dynamics Simulations. <i>Journal of Chemical Information and Modeling</i> , 2021, 61, 2407-2417.	5.4	10
8685	Theoretical Investigation of the Na<sup>+</sup> Transport Mechanism and the Performance of Ionic Liquid-Based Electrolytes in Sodium-Ion Batteries. <i>ACS Applied Energy Materials</i> , 2021, 4, 4444-4458.	5.1	27
8686	Effects of surface modification of Nano-SiO2 imbedded in organic matrix on interfacial accumulation of water molecules: an atomistic simulation study. <i>Surfaces and Interfaces</i> , 2021, 23, 100942.	3.0	1
8687	Atomistic Mechanism Underlying the $\text{Si}(\text{OH})_4$ Nucleation: $\text{H}_2\text{O}$ and $\text{H}_2\text{O}_2$ Molecules. <i>Journal of Chemical Theory and Computation</i> , 2021, 17, 3103-3118.	7.8	12
8688	D936Y and Other Mutations in the Fusion Core of the SARS-CoV-2 Spike Protein Heptad Repeat 1: Frequency, Geographical Distribution, and Structural Effect. <i>Molecules</i> , 2021, 26, 2622.	3.8	21
8689	Experimentally Driven Automated Machine-Learned Interatomic Potential for a Refractory Oxide. <i>Physical Review Letters</i> , 2021, 126, 156002.	7.8	28

#	ARTICLE	IF	CITATIONS
8690	Monoubiquitination of KRAS at Lysine104 and Lysine147 Modulates Its Dynamics and Interaction with Partner Proteins. <i>Journal of Physical Chemistry B</i> , 2021, 125, 4681-4691.	2.6	3
8691	Evaluating the Efficiency of the Martini Force Field to Study Protein Dimerization in Aqueous and Membrane Environments. <i>Journal of Chemical Theory and Computation</i> , 2021, 17, 3088-3102.	5.3	42
8692	Differences in interactions between transmembrane domains tune the activation of metabotropic glutamate receptors. <i>ELife</i> , 2021, 10, .	6.0	18
8693	Glycan-Induced Protein Dynamics in Human Norovirus P Dimers Depend on Virus Strain and Deamidation Status. <i>Molecules</i> , 2021, 26, 2125.	3.8	13
8695	The structural plasticity of nucleic acid duplexes revealed by WAXS and MD. <i>Science Advances</i> , 2021, 7, .	10.3	25
8697	Structural and functional impact of clinically relevant E1± variants causing pyruvate dehydrogenase complex deficiency. <i>Biochimie</i> , 2021, 183, 78-88.	2.6	10
8700	The loops of the N-SH2 binding cleft do not serve as allosteric switch in SHP2 activation. <i>Proceedings of the National Academy of Sciences of the United States of America</i> , 2021, 118, .	7.1	11
8701	Understanding the molecular interactions of inhibitors against Bla1 beta-lactamase towards unraveling the mechanism of antimicrobial resistance. <i>International Journal of Biological Macromolecules</i> , 2021, 177, 337-350.	7.5	4
8702	Sequence-dependent nanomolar binding of tripeptides containing N-terminal phenylalanine by Cucurbit[7]uril: A theoretical study. <i>Journal of Molecular Liquids</i> , 2021, 328, 115479.	4.9	12
8703	Diffusivities in Binary Mixtures of $n$ -Hexane or 1-Hexanol with Dissolved $CH_4$ , Ne, Kr, R143a, $SF_6$ , or R236fa Close to Infinite Dilution. <i>Journal of Chemical &amp; Engineering Data</i> , 2021, 66, 2218-2232.	1.9	14
8705	g_elpot: A Tool for Quantifying Biomolecular Electrostatics from Molecular Dynamics Trajectories. <i>Journal of Chemical Theory and Computation</i> , 2021, 17, 3157-3167.	5.3	6
8706	Dynamic heterogeneity, cooperative motion, and Johariâ€“Goldstein $\beta$ -relaxation in a metallic glass-forming material exhibiting a fragile-to-strong transition. <i>European Physical Journal E</i> , 2021, 44, 56.	1.6	24
8708	Heavy Water Models for Classical Molecular Dynamics: Effective Inclusion of Nuclear Quantum Effects. <i>Journal of Physical Chemistry B</i> , 2021, 125, 4514-4519.	2.6	6
8709	Unsupervised Learning Unravels the Structure of Four-Arm and Linear Block Copolymer Micelles. <i>Macromolecules</i> , 2021, 54, 3755-3768.	4.8	12
8710	Balance Between Contact and Solvent-Separated Ion Pairs in Mixtures of the Protic Ionic Liquid $[Et_3NH][MeSO_3]$ with Water Controlled by Water Content and Temperature. <i>Journal of Physical Chemistry B</i> , 2021, 125, 4476-4488.	2.6	9
8711	Hydrogen storage in sH binary hydrate: Insights from molecular dynamics simulation. <i>International Journal of Hydrogen Energy</i> , 2021, 46, 15748-15760.	7.1	22
8712	Molecular simulation study of 3,4-dihydroxyphenylalanine in the context of underwater adhesive design. <i>Journal of Chemical Physics</i> , 2021, 154, 144702.	3.0	3
8713	Computer-Aided Drug Discovery Identifies Alkaloid Inhibitors of Parkinsonâ€™s Disease Associated Protein, Prolyl Oligopeptidase. <i>Evidence-based Complementary and Alternative Medicine</i> , 2021, 2021, 1-10.	1.2	3



#	ARTICLE	IF	CITATIONS
8714	Behavior of Chemokine Receptor 6 (CXCR6) in Complex with CXCL16 Soluble form Chemokine by Molecular Dynamic Simulations: General Protein-Ligand Interaction Model and 3D-QSAR Studies of Synthetic Antagonists. <i>Life</i> , 2021, 11, 346.	2.4	4
8715	Inhibition of SARS-CoV-2 main protease: a repurposing study that targets the dimer interface of the protein. <i>Journal of Biomolecular Structure and Dynamics</i> , 2022, 40, 7167-7182.	3.5	5
8716	Effect of sodium chloride on the behaviour of the lactose in aqueous solution studied from diffusion experiments and molecular dynamics simulations. <i>Journal of Chemical Thermodynamics</i> , 2021, 155, 106370.	2.0	3
8717	Passive Diffusion of Ciprofloxacin and its Metalloantibiotic: A Computational and Experimental study. <i>Journal of Molecular Biology</i> , 2021, 433, 166911.	4.2	9
8718	Identifying Conformational Isomers of Organic Molecules in Solution via Unsupervised Clustering. <i>Journal of Chemical Information and Modeling</i> , 2021, 61, 2263-2273.	5.4	3
8719	From virus to diabetes therapy: Characterization of a specific insulin-degrading enzyme inhibitor for diabetes treatment. <i>FASEB Journal</i> , 2021, 35, e21374.	0.5	7
8720	Effect of interfacial bonding on dislocation strengthening in graphene nanosheet reinforced iron composite: A molecular dynamics study. <i>Computational Materials Science</i> , 2021, 191, 110309.	3.0	11
8721	Synergy and allostery in ligand binding by HIV-1 Nef. <i>Biochemical Journal</i> , 2021, 478, 1525-1545.	3.7	4
8722	Atomistic dynamics of a viral infection process: Release of membrane lytic peptides from a non-enveloped virus. <i>Science Advances</i> , 2021, 7, .	10.3	6
8723	Histone dynamics mediate DNA unwrapping and sliding in nucleosomes. <i>Nature Communications</i> , 2021, 12, 2387.	12.8	70
8724	Viscosity, Interfacial Tension, and Density of Binary-Liquid Mixtures of <i>n</i> -Hexadecane with <i>n</i> -Octacosane, 2,2,4,4,6,8,8-Heptamethylnonane, or 1-Hexadecanol at Temperatures between 298.15 and 573.15 K by Surface Light Scattering and Equilibrium Molecular Dynamics Simulations. <i>Journal of Chemical &amp; Engineering Data</i> , 2021, 66, 2264-2280.	1.9	12
8725	Encapsulation of Curcumin in Polystyrene-Based Nanoparticles—Drug Loading Capacity and Cytotoxicity. <i>ACS Omega</i> , 2021, 6, 12168-12178.	3.5	18
8726	Biocomputational Screening of Natural Compounds against Acetylcholinesterase. <i>Molecules</i> , 2021, 26, 2641.	3.8	10
8727	Entropy drives the adsorption of xyloglucan to cellulose surfaces – A molecular dynamics study. <i>Journal of Colloid and Interface Science</i> , 2021, 588, 485-493.	9.4	47
8728	Loss of a water-mediated network results in reduced agonist affinity in a $\beta$ 2-adrenergic receptor clinical variant. <i>Biochimica Et Biophysica Acta - Proteins and Proteomics</i> , 2021, 1869, 140605.	2.3	7
8729	Pyrazole[3,4-d]pyrimidine derivatives loaded into halloysite as potential CDK inhibitors. <i>International Journal of Pharmaceutics</i> , 2021, 599, 120281.	5.2	14
8730	Delineating the conformational landscape of the adenosine A2A receptor during G protein coupling. <i>Cell</i> , 2021, 184, 1884-1894.e14.	28.9	97
8731	Cryo-EM Structures of CusA Reveal a Mechanism of Metal-Ion Export. <i>MBio</i> , 2021, 12, .	4.1	15

#	ARTICLE	IF	CITATIONS
8732	Computing inelastic neutron scattering spectra from molecular dynamics trajectories. Scientific Reports, 2021, 11, 7938.	3.3	7
8733	Molecular Dynamics Simulation for Evaluating Fracture Entropy of a Polymer Material under Various Combined Stress States. Materials, 2021, 14, 1884.	2.9	11
8734	The Effect of Cholesterol on Membrane-Bound Islet Amyloid Polypeptide. Frontiers in Molecular Biosciences, 2021, 8, 657946.	3.5	7
8735	Biomolecular interaction mechanism of an anticancer drug, pazopanib with human serum albumin: a multi-spectroscopic and computational approach. Journal of Biomolecular Structure and Dynamics, 2022, 40, 8312-8323.	3.5	3
8737	Molecular dynamics simulations of Piezo1 channel opening by increases in membrane tension. Biophysical Journal, 2021, 120, 1510-1521.	0.5	33
8738	Functional Group Distributions, Partition Coefficients, and Resistance Factors in Lipid Bilayers Using Site Identification by Ligand Competitive Saturation. Journal of Chemical Theory and Computation, 2021, 17, 3188-3202.	5.3	6
8739	Association of sigma-1 receptor with dopamine transporter attenuates the binding of methamphetamine via distinct helix-helix interactions. Chemical Biology and Drug Design, 2021, 97, 1194-1209.	3.2	5
8741	Dual nature of human ACE2 glycosylation in binding to SARS-CoV-2 spike. Proceedings of the National Academy of Sciences of the United States of America, 2021, 118, .	7.1	131
8742	Multiscale Molecular Dynamics Studies Reveal Different Modes of Receptor Clustering by Gb3-Binding Lectins. Journal of Chemical Theory and Computation, 2021, 17, 2488-2501.	5.3	15
8743	Why Lithium Ions Stick to Some Anions and Not Others. Journal of Physical Chemistry B, 2021, 125, 4447-4455.	2.6	8
8744	Length-scale-dependent elasticity in DNA from coarse-grained and all-atom models. Physical Review E, 2021, 103, 042408.	2.1	16
8745	Exploring the Conformational Landscape of the Neh4 and Neh5 Domains of Nrf2 Using Two Different Force Fields and Circular Dichroism. Journal of Chemical Theory and Computation, 2021, 17, 3145-3156.	5.3	11
8746	Cannabidiol inhibits the skeletal muscle Nav1.4 by blocking its pore and by altering membrane elasticity. Journal of General Physiology, 2021, 153, .	1.9	38
8747	Understanding Hypervelocity Sampling of Biosignatures in Space Missions. Astrobiology, 2021, 21, 421-442.	3.0	31
8748	CHARMM-GUI Polymer Builder for Modeling and Simulation of Synthetic Polymers. Journal of Chemical Theory and Computation, 2021, 17, 2431-2443.	5.3	58
8749	The hitchhiker's guide to the periplasm: Unexpected molecular interactions of polymyxin B1 in E. coli. Structure, 2021, 29, 444-456.e2.	3.3	20
8750	Yielding in an amorphous solid subject to constant stress at finite temperatures. Physical Review E, 2021, 103, 052604.	2.1	2
8752	Synergistic strengthening mechanisms of rhenium in nickel-based single crystal superalloys. Intermetallics, 2021, 132, 107133.	3.9	15

#	ARTICLE	IF	CITATIONS
8753	Parkinson Hastalıkları ile ilişkiliendirilen PreNAC Fibril Kesiti ve Onun A53C, A53E, A53G, A53T, A53V Mutasyonların Yapısal Kararlılığı Araştırılması. SDU Journal of Science, 0, , 66-76.	0.3	0
8754	Identification of PUFA interaction sites on the cardiac potassium channel KCNQ1. Journal of General Physiology, 2021, 153, .	1.9	22
8755	Molecular mechanisms of ion conduction and ion selectivity in TMEM16 lipid scramblases. Nature Communications, 2021, 12, 2826.	12.8	14
8756	Cholesterol recognition motifs in the transmembrane domain of the tyrosine kinase receptor family: The case of TRKB. European Journal of Neuroscience, 2021, 53, 3311-3322.	2.6	15
8757	Site-specific identification and validation of hepatic histone nitration in vivo: Implications for alcohol-induced liver injury. Journal of Mass Spectrometry, 2021, 56, e4713.	1.6	4
8758	Moving pictures: Reassessing docking experiments with a dynamic view of protein interfaces. Proteins: Structure, Function and Bioinformatics, 2021, 89, 1315-1323.	2.6	7
8759	Protein-protein interaction and in silico mutagenesis studies on IL17A and its peptide inhibitor. 3 Biotech, 2021, 11, 305.	2.2	0
8760	Computational Approaches to Discover Novel Natural Compounds for SARS-CoV-2 Therapeutics. ChemistryOpen, 2021, 10, 593-599.	1.9	7
8761	High-resolution structural profile of hylaseptin-4: Aggregation, membrane topology and pH dependence of overall membrane binding process. Biochimica Et Biophysica Acta - Biomembranes, 2021, 1863, 183581.	2.6	5
8762	Free electron to electrone transition in dense liquid potassium. Nature Physics, 2021, 17, 955-960.	16.7	15
8763	Stressed Lipid Droplets: How Neutral Lipids Relieve Surface Tension and Membrane Expansion Drives Protein Association. Journal of Physical Chemistry B, 2021, 125, 5572-5586.	2.6	18
8764	Molecular Simulation of High-Salinity Brines in Contact with Diisopropylamine and Tripropylamine Solvents. Industrial & Engineering Chemistry Research, 2021, 60, 7917-7925.	3.7	10
8765	Toward Physics-Based Solubility Computation for Pharmaceuticals to Rival Informatics. Journal of Chemical Theory and Computation, 2021, 17, 3700-3709.	5.3	15
8766	Nanocomposites of 2D-MoS <sub>2</sub> Exfoliated in Thermotropic Liquid Crystals. , 2021, 3, 704-712.		9
8767	Electrical conductivity variations of aqueous NaCl solutions with microwave field: A molecular dynamics study. Chemical Physics, 2021, 545, 111134.	1.9	6
8768	KEAP1 Cancer Mutants: A Large-Scale Molecular Dynamics Study of Protein Stability. International Journal of Molecular Sciences, 2021, 22, 5408.	4.1	7
8770	Topology and complexity of the hydrogen bond network in classical models of water. Journal of Molecular Liquids, 2021, 329, 115530.	4.9	20
8771	Ion effects on the extraction of cesium (I) by 1,3-Diisopropoxycalix [4] arenecrown-6(BPC6) and the highly efficient extraction under neutral conditions. Solvent Extraction and Ion Exchange, 2022, 40, 333-348.	2.0	2

#	ARTICLE	IF	CITATIONS
8772	How to Determine Accurate Conformational Ensembles by Metadynamics Metainference: A Chignolin Study Case. <i>Frontiers in Molecular Biosciences</i> , 2021, 8, 694130.	3.5	5
8773	Attacking COVID-19 Progression Using Multi-Drug Therapy for Synergetic Target Engagement. <i>Biomolecules</i> , 2021, 11, 787.	4.0	14
8774	Importance of glutamine 189 flexibility in SARS-CoV-2 main protease: Lesson learned from in silico virtual screening of ChEMBL database and molecular dynamics. <i>European Journal of Pharmaceutical Sciences</i> , 2021, 160, 105744.	4.0	13
8775	Structural (dis)order and dynamic propensity in a mildly undercooled glass-forming liquid: Spatial correlations and the role of crystalline environments. <i>Physica A: Statistical Mechanics and Its Applications</i> , 2021, 569, 125764.	2.6	1
8777	Energetic Arguments on the Microstructural Analysis in Ionic Liquids. <i>Advanced Theory and Simulations</i> , 2021, 4, 2100114.	2.8	2
8778	Molecular engineering of piezoelectricity in collagen-mimicking peptide assemblies. <i>Nature Communications</i> , 2021, 12, 2634.	12.8	68
8779	Structural Basis for Selective Oxidation of Phosphorylated Ethylphenols by Cytochrome P450 Monooxygenase CreJ. <i>Applied and Environmental Microbiology</i> , 2021, 87, .	3.1	2
8780	Three- and four-site models for heavy water: SPC/E-HW, TIP3P-HW, and TIP4P/2005-HW. <i>Journal of Chemical Physics</i> , 2021, 154, 194501.	3.0	18
8781	Individual Contributions of Adsorbed and Free Chains to Microscopic Dynamics of Unentangled poly(ethylene Glycol)/Silica Nanocomposite Melts and the Important Role of End Groups: Theory and Simulation. <i>Macromolecules</i> , 2021, 54, 4470-4487.	4.8	14
8782	Diffusion coefficients of CO <sub>2</sub> and SO <sub>2</sub> in water and CO <sub>2</sub> and N <sub>2</sub> in water systems and their impact on the CO <sub>2</sub> sequestration process: Molecular dynamics and dissolution process simulations. , 2021, 11, 764-779.		10
8783	Unraveling the unbinding pathways of SARS-CoV-2 Papain-like proteinase known inhibitors by Supervised Molecular Dynamics simulation. <i>PLoS ONE</i> , 2021, 16, e0251910.	2.5	10
8784	Effects of Amino Acid Side-Chain Length and Chemical Structure on Anionic Polyglutamic and Polyaspartic Acid Cellulose-Based Polyelectrolyte Brushes. <i>Polymers</i> , 2021, 13, 1789.	4.5	1
8785	Structures of <scp>MERSâ€CoV</scp> macro domain in aqueous solution with dynamics: Impacts of parallel tempering simulation techniques and <scp>CHARMM36m</scp> and <scp>AMBER99SB</scp> force field parameters. <i>Proteins: Structure, Function and Bioinformatics</i> , 2021, 89, 1289-1299.	2.6	2
8786	A Multiscale Simulation Study of Influence of Morphology on Ion Transport in Block Copolymeric Ionic Liquids. <i>Macromolecules</i> , 2021, 54, 4997-5010.	4.8	16
8787	Exploring ligand binding pathways on proteins using hypersound-accelerated molecular dynamics. <i>Nature Communications</i> , 2021, 12, 2793.	12.8	24
8789	Conformational plasticity and dynamic interactions of the N-terminal domain of the chemokine receptor CXCR1. <i>PLoS Computational Biology</i> , 2021, 17, e1008593.	3.2	15
8790	Predicting Hugoniot equation of state in erythritol with ab initio and reactive molecular dynamics. <i>Journal of Applied Physics</i> , 2021, 129, 195106.	2.5	0
8791	Membrane fusion and drug delivery with carbon nanotube porins. <i>Proceedings of the National Academy of Sciences of the United States of America</i> , 2021, 118, .	7.1	25

#	ARTICLE	IF	CITATIONS
8792	Antimicrobial PEGtides: A Modular Poly(ethylene glycol)-Based Peptidomimetic Approach to Combat Bacteria. <i>ACS Nano</i> , 2021, 15, 9143-9153.	14.6	15
8793	Efficient isotropic water desalination in anisotropic lamellar nano-channels formed by layered black phosphorus membrane. <i>Desalination</i> , 2021, 504, 114962.	8.2	16
8794	Evaluation of the effects of isoniazid and rifampin on the structure and activity of pepsin enzyme by multi spectroscopy and molecular modeling methods. <i>Spectrochimica Acta - Part A: Molecular and Biomolecular Spectroscopy</i> , 2021, 253, 119523.	3.9	12
8796	Structural basis of antifolate recognition and transport by PCFT. <i>Nature</i> , 2021, 595, 130-134.	27.8	36
8797	Atomistic understanding of creep and relaxation mechanisms of Cu <sub>64</sub> Zr <sub>36</sub> metallic glass at different temperatures and stress levels. <i>Journal of Non-Crystalline Solids</i> , 2021, 559, 120676.	3.1	12
8798	Construction of dimeric hTSP0 protein model using homology modeling and molecular dynamics. <i>Journal of Physics: Conference Series</i> , 2021, 1932, 012016.	0.4	1
8799	Coordination of Substrate Binding and Protonation in the <i>N</i> -Agonorrhoeae MtrD Efflux Pump Controls the Functionally Rotating Transport Mechanism. <i>ACS Infectious Diseases</i> , 2021, 7, 1833-1847.	3.8	5
8800	Structure, Dynamics, and Ligand Recognition of Human-Specific CHRFAM7A (Dup $\pm$ 7) Nicotinic Receptor Linked to Neuropsychiatric Disorders. <i>International Journal of Molecular Sciences</i> , 2021, 22, 5466.	4.1	3
8801	Improving the specificity of organophosphorus hydrolase to acephate by mutagenesis at its binding site: a computational study. <i>Journal of Molecular Modeling</i> , 2021, 27, 164.	1.8	0
8802	Modelling of an autonomous Nav1.5 channel system as a part of in silico pharmacology study. <i>Journal of Molecular Modeling</i> , 2021, 27, 182.	1.8	3
8803	Thermodynamics and Rheology of Imidazolium-Based Ionic Liquidâ€“Oil Mixtures: A Molecular Simulation Study. <i>Journal of Physical Chemistry B</i> , 2021, 125, 5897-5908.	2.6	3
8804	Halting the Spread of Herpes Simplex Virus-1: The Discovery of an Effective Dual $\beta$ / $\gamma$ Integrin Ligand. <i>Journal of Medicinal Chemistry</i> , 2021, 64, 6972-6984.	6.4	9
8805	Effects of Trehalose on Lipid Membranes under Rapid Cooling using All-Atom and Coarse-Grained Molecular Simulations. <i>Journal of Physical Chemistry B</i> , 2021, 125, 5346-5357.	2.6	3
8806	Atomic-Level Features for Kinetic Monte Carlo Models of Complex Chemistry from Molecular Dynamics Simulations. <i>Journal of Physical Chemistry A</i> , 2021, 125, 4233-4244.	2.5	4
8807	Two Fascinating Polysaccharides: Chitosan and Starch. Some Prominent Characterizations for Applying as Eco-Friendly Food Packaging and Pollutant Remover in Aqueous Medium. Progress in Recent Years: A Review. <i>Polymers</i> , 2021, 13, 1737.	4.5	8
8808	General Protocol for Constructing Molecular Models of Nanodiscs. <i>Journal of Chemical Information and Modeling</i> , 2021, 61, 2869-2883.	5.4	11
8809	Distinct pathways of solid-to-solid phase transitions induced by defects: the case of $\alpha$ -DL-methionine. <i>IUCr</i> , 2021, 8, 584-594.	2.2	13
8811	Reconciling conformational heterogeneity and substrate recognition in cytochrome P450. <i>Biophysical Journal</i> , 2021, 120, 1732-1745.	0.5	7

#	ARTICLE	IF	CITATIONS
8812	EfgA is a conserved formaldehyde sensor that leads to bacterial growth arrest in response to elevated formaldehyde. <i>PLoS Biology</i> , 2021, 19, e3001208.	5.6	13
8813	Helix-coil transition and conformational deformity in $\alpha$ -42 <sup>+</sup> -monomer: a case study using the Zn <sup>2+</sup> cation. <i>Journal of Biomolecular Structure and Dynamics</i> , 2022, 40, 8949-8960.	3.5	1
8814	Structural characterization of cassava linamarase-linamarin enzyme complex: an integrated computational approach. <i>Journal of Biomolecular Structure and Dynamics</i> , 2022, 40, 9270-9278.	3.5	2
8815	Chain and Solvent Dynamics in Polymer Membrane Films Supported on a Polymeric Substrate. <i>ACS Applied Polymer Materials</i> , 2021, 3, 3164-3174.	4.4	1
8816	Fick Diffusion Coefficient in Binary Mixtures of [HMIM][NTf <sub>2</sub> ] and Carbon Dioxide by Dynamic Light Scattering and Molecular Dynamics Simulations. <i>Journal of Physical Chemistry B</i> , 2021, 125, 5100-5113.	2.6	14
8817	Engineered MATE multidrug transporters reveal two functionally distinct ion-coupling pathways in NorM from <i>Vibrio cholerae</i> . <i>Communications Biology</i> , 2021, 4, 558.	4.4	3
8818	Concentrated brines in aqueous methanolic solutions in supercritical conditions: Effect of concentration and composition from molecular dynamics simulations. <i>Fluid Phase Equilibria</i> , 2021, 536, 112978.	2.5	2
8821	Effects of Side-Chain Spacing and Length on Hydration States of Poly(2-methoxyethyl acrylate) Analogues: A Molecular Dynamics Study. <i>ACS Biomaterials Science and Engineering</i> , 2021, 7, 2383-2391.	5.2	7
8823	In-silico screening and identification of potential inhibitors against 2Cys peroxiredoxin of <i>Candidatus Liberibacter asiaticus</i> . <i>Journal of Biomolecular Structure and Dynamics</i> , 2022, 40, 8725-8739.	3.5	10
8824	Combined Use of Structure Analysis, Studies of Molecular Association in Solution, and Molecular Modelling to Understand the Different Propensities of Dihydroxybenzoic Acids to Form Solid Phases. <i>Pharmaceutics</i> , 2021, 13, 734.	4.5	3
8825	Sintering mechanism of copper nanoparticle sphere-plate of crystal misalignment: A study by molecular dynamics simulations. <i>Journal of Materials Research and Technology</i> , 2021, 12, 668-678.	5.8	13
8826	Binding Mechanisms of Amyloid-like Peptides to Lipid Bilayers and Effects of Divalent Cations. <i>ACS Chemical Neuroscience</i> , 2021, 12, 2027-2035.	3.5	19
8827	Morphological Stability of Organic Photovoltaics: Coarse-grained Molecular Dynamics Simulation Studies. <i>Bulletin of the Korean Chemical Society</i> , 2021, 42, 988-993.	1.9	2
8829	Benchmarking binding energy calculations for organic structure-directing agents in pure-silica zeolites. <i>Journal of Chemical Physics</i> , 2021, 154, 174109.	3.0	26
8830	Cooperative DNA looping by PRC2 complexes. <i>Nucleic Acids Research</i> , 2021, 49, 6238-6248.	14.5	19
8833	Distributed charge models of liquid methane and ethane for dielectric effects and solvation. <i>Molecular Physics</i> , 2021, 119, .	1.7	3
8834	Characterizing the Interplay between Polymer Solvation and Conformation. <i>Journal of Physical Chemistry B</i> , 2021, 125, 5434-5442.	2.6	9
8835	Lysozyme Adsorption on Different Functionalized MXenes: A Multiscale Simulation Study. <i>Langmuir</i> , 2021, 37, 5932-5942.	3.5	6



#	ARTICLE	IF	CITATIONS
8836	Microbially Guided Discovery and Biosynthesis of Biologically Active Natural Products. <i>ACS Synthetic Biology</i> , 2021, 10, 1505-1519.	3.8	11
8837	Structural analysis of EhPSP in complex with 3-phosphoglyceric acid from <i>Entamoeba histolytica</i> reveals a basis for its lack of phosphoglycerate mutase activity. <i>International Journal of Biological Macromolecules</i> , 2021, 178, 1-10.	7.5	3
8838	Arginine multivalency stabilizes protein/RNA condensates. <i>Protein Science</i> , 2021, 30, 1418-1426.	7.6	18
8839	Distinct EH domains of the endocytic TPLATE complex confer lipid and protein binding. <i>Nature Communications</i> , 2021, 12, 3050.	12.8	23
8841	Engineering Next Generation Cyclized Peptide Ligands for Light-Controlled Capture and Release of Therapeutic Proteins. <i>Advanced Functional Materials</i> , 2021, 31, 2101410.	14.9	15
8842	Hydrogen bonding and percolation in propan-2-ol + Water liquid mixtures: X-ray diffraction experiments and computer simulations. <i>Journal of Molecular Liquids</i> , 2021, 329, 115592.	4.9	11
8843	Spectroscopic and Simulation Studies of the Sequence-Dependent DNA Destabilization by a Fungicide. <i>ACS Omega</i> , 2021, 6, 14371-14378.	3.5	4
8844	Molecular Structure of Cefuroxime Axetil Complexes with $\beta$ -, $\gamma$ -, $\delta$ -, and 2-Hydroxypropyl- $\beta$ -Cyclodextrins: Molecular Simulations and Raman Spectroscopic and Imaging Studies. <i>International Journal of Molecular Sciences</i> , 2021, 22, 5238.	4.1	11
8845	Activation of G-protein-coupled receptors is thermodynamically linked to lipid solvation. <i>Biophysical Journal</i> , 2021, 120, 1777-1787.	0.5	10
8846	Accurate absolute free energies for ligand-protein binding based on non-equilibrium approaches. <i>Communications Chemistry</i> , 2021, 4, .	4.5	49
8847	Investigating the Mechanism of Sodium Binding to SERT Using Direct Simulations. <i>Frontiers in Cellular Neuroscience</i> , 2021, 15, 673782.	3.7	9
8848	Design and development of polymeric micelles as nanocarriers for anti-cancer Ribociclib drug. <i>Journal of Molecular Liquids</i> , 2021, 329, 115574.	4.9	26
8849	Structure and Dynamics of Interfacial Water on Muscovite Surface under Different Temperature Conditions (298 K to 673 K): Molecular Dynamics Investigation. <i>Water (Switzerland)</i> , 2021, 13, 1320.	2.7	8
8850	Can molecular dynamics simulations improve the structural accuracy and virtual screening performance of GPCR models?. <i>PLoS Computational Biology</i> , 2021, 17, e1008936.	3.2	16
8851	Order from disorder in the sarcomere: FATZ forms a fuzzy but tight complex and phase-separated condensates with $\beta$ -actinin. <i>Science Advances</i> , 2021, 7, .	10.3	15
8852	Synthesis of new 2-aminothiazolyl/benzothiazolyl-based 3,4-dihydropyrimidinones and evaluation of their effects on adenocarcinoma gastric cell migration. <i>Molecular Diversity</i> , 2022, 26, 1039-1051.	3.9	1
8853	Mechanistic insights into the inhibitory activity of FDA approved ivermectin against SARS-CoV-2: old drug with new implications. <i>Journal of Biomolecular Structure and Dynamics</i> , 2022, 40, 8100-8111.	3.5	3
8854	Effect of alkyl chain length of protic ionic liquids on dynamic and static properties of alkylammonium nitrate/water mixtures. <i>Journal of Molecular Liquids</i> , 2021, 329, 115610.	4.9	1

#	ARTICLE	IF	CITATIONS
8855	Rational design of hyper-glycosylated human follicle-stimulating hormone analogs (a bioinformatics) Tj ETQq0 0 0 rgBT /Overlck 10 Tf 5	8.5	4
8856	Transient Excursions to Membrane Core as Determinants of Influenza Virus Fusion Peptide Activity. International Journal of Molecular Sciences, 2021, 22, 5301.	4.1	5
8857	ATP hydrolysis and nucleotide exit enhance maltose translocation in the MalFGK2E importer. Scientific Reports, 2021, 11, 10591.	3.3	1
8858	Discovery of a Potent and Selective Chikungunya Virus Envelope Protein Inhibitor through Computer-Aided Drug Design. ACS Infectious Diseases, 2021, 7, 1503-1518.	3.8	9
8859	The Effects of Different Glycosaminoglycans on the Structure and Aggregation of the Amyloid- $\beta$ (16-22) Peptide. Journal of Physical Chemistry B, 2021, 125, 5511-5525.	2.6	3
8860	Hydrogen Bond Kinetics, Ionic Dynamics, and Voids in the Binary Mixtures of Protic Ionic Liquids with Alkanolamines. Journal of Physical Chemistry B, 2021, 125, 5587-5600.	2.6	7
8862	Altered Local Interactions and Long-Range Communications in UK Variant (B.1.1.7) Spike Glycoprotein. International Journal of Molecular Sciences, 2021, 22, 5464.	4.1	9
8863	Theoretical analyses of pressure induced glass transition in water: Signatures of surprising diffusion-entropy scaling across the transition. Molecular Physics, 0, , e1930222.	1.7	3
8864	Modifying the catalytic preference of $\alpha$ -amylase toward $n$ -alkanes for bioremediation purposes using <i>in silico</i> strategies. Journal of Computational Chemistry, 2021, 42, 1540-1551.	3.3	2
8865	Autism-associated SHANK3 missense point mutations impact conformational fluctuations and protein turnover at synapses. ELife, 2021, 10, .	6.0	14
8866	Conformational Reorganization of Apolipoprotein E Triggered by Phospholipid Assembly. Journal of Physical Chemistry B, 2021, 125, 5285-5295.	2.6	4
8867	Structural Characterization and Drug Delivery System of Natural Growth-Modulating Peptide Against Glioblastoma Cancer. International Journal of Peptide Research and Therapeutics, 2021, 27, 2015-2028.	1.9	9
8868	The Role of Cyclodextrins against Interface-Induced Denaturation in Pharmaceutical Formulations: A Molecular Dynamics Approach. Molecular Pharmaceutics, 2021, 18, 2322-2333.	4.6	18
8869	Dissecting the Conformational Free Energy of a Small Peptide in Solution. Journal of Physical Chemistry B, 2021, 125, 4634-4644.	2.6	11
8870	Implementation of the Freely Jointed Chain Model to Assess Kinetics and Thermodynamics of Thermosensitive Coil-Globule Transition by Markov States. Journal of Physical Chemistry B, 2021, 125, 4898-4909.	2.6	4
8871	Repurposing potential of Ayurvedic medicinal plants derived active principles against SARS-CoV-2 associated target proteins revealed by molecular docking, molecular dynamics and MM-PBSA studies. Biomedicine and Pharmacotherapy, 2021, 137, 111356.	5.6	38
8872	The accelerated weight histogram method for alchemical free energy calculations. Journal of Chemical Physics, 2021, 154, 204103.	3.0	15
8873	Computational Investigation Identified Potential Chemical Scaffolds for Heparanase as Anticancer Therapeutics. International Journal of Molecular Sciences, 2021, 22, 5311.	4.1	12

#	ARTICLE	IF	CITATIONS
8874	Anomalous dislocation core structure in shock compressed bcc high-entropy alloys. <i>Acta Materialia</i> , 2021, 209, 116801.	7.9	42
8875	Enhanced translocation of amphiphilic peptides across membranes by transmembrane proteins. <i>Biophysical Journal</i> , 2021, 120, 2296-2305.	0.5	7
8876	Force Field Benchmark of Amino Acids. 3. Hydration with Scaled Lennard-Jones Interactions. <i>Journal of Chemical Information and Modeling</i> , 2021, 61, 3571-3582.	5.4	15
8877	Neat and Aqueous Polyelectrolytes under a Steady-Shear Flow. <i>Journal of Physical Chemistry B</i> , 2021, 125, 6930-6944.	2.6	4
8878	Macrochirality of Self-Assembled and Co-assembled Supramolecular Structures of a Pair of Enantiomeric Peptides. <i>Frontiers in Molecular Biosciences</i> , 2021, 8, 700964.	3.5	5
8879	Efficient Parametrization of Force Field for the Quantitative Prediction of the Physical Properties of Ionic Liquid Electrolytes. <i>Journal of Chemical Theory and Computation</i> , 2021, 17, 4274-4290.	5.3	11
8880	Molecular dynamics simulations of phospholipid bilayer mechanoporation under different strain states—a comparison between GROMACS and LAMMPS. <i>Modelling and Simulation in Materials Science and Engineering</i> , 2021, 29, 055015.	2.0	4
8881	Formulation matters! A spectroscopic and molecular dynamics investigation on the peptide CIGB552 as itself and in its therapeutical formulation. <i>Journal of Peptide Science</i> , 2022, 28, e3356.	1.4	1
8882	Fe Elementinin Kristal ve Camı Faza Dönüşümünün Hidrostatik Basınç Altındaki İncelenmesi: Moleküler Dinamik Benzetim Analizi. <i>Bilecik Şeyh Edebali Üniversitesi Fen Bilimleri Dergisi</i> , 0, , .	0.6	0
8883	Entropy-based distance cutoff for protein internal contact networks. <i>Proteins: Structure, Function and Bioinformatics</i> , 2021, 89, 1333-1339.	2.6	2
8884	Spike protein fusion loop controls SARS-CoV-2 fusogenicity and infectivity. <i>Journal of Structural Biology</i> , 2021, 213, 107713.	2.8	11
8885	Computational Discovery of SARS-CoV-2 NSP 16 Drug Candidates Based on Pharmacophore Modeling and Molecular Dynamics Simulation. <i>Journal of Computational Biophysics and Chemistry</i> , 2021, 20, 377-390.	1.7	1
8886	Developing and Assessing Nonbonded Dummy Models of Magnesium Ion with Different Hydration Free Energy References. <i>Journal of Chemical Information and Modeling</i> , 2021, 61, 2981-2997.	5.4	5
8887	Interaction mechanism of kafirin with ferulic acid and tetramethyl pyrazine: Multiple spectroscopic and molecular modeling studies. <i>Food Chemistry</i> , 2021, 363, 130298.	8.2	24
8888	Rational design of antimicrobial peptides targeting Gram-negative bacteria. <i>Computational Biology and Chemistry</i> , 2021, 92, 107475.	2.3	4
8889	Lipid Oxidation: Role of Membrane Phase-Separated Domains. <i>Journal of Chemical Information and Modeling</i> , 2021, 61, 2857-2868.	5.4	12
8890	Why Should Metformin Not Be Given in Advanced Kidney Disease? Potential Leads from Computer Simulations. <i>ACS Omega</i> , 2021, 6, 15382-15391.	3.5	2
8891	Mutation of a conserved glutamine residue does not abolish desensitization of acid-sensing ion channel 1. <i>Journal of General Physiology</i> , 2021, 153, .	1.9	9

#	ARTICLE	IF	CITATIONS
8892	Interpretations on the Interaction between Protein Tyrosine Phosphatase and E7 Oncoproteins of High and Low-Risk HPV: A Computational Perception. <i>ACS Omega</i> , 2021, 6, 16472-16487.	3.5	7
8893	Molecular Insights into Pore Formation Mechanism, Membrane Perturbation, and Water Permeation by the Antimicrobial Peptide Pleurocidin: A Combined All-Atom and Coarse-Grained Molecular Dynamics Simulation Study. <i>Journal of Physical Chemistry B</i> , 2021, 125, 7163-7176.	2.6	14
8894	Computation of the Thermal Expansion Coefficient of Graphene with Gaussian Approximation Potentials. <i>Journal of Physical Chemistry C</i> , 2021, 125, 14409-14415.	3.1	7
8895	Glycine rich segments adopt polyproline II helices: Implications for biomolecular condensate formation. <i>Archives of Biochemistry and Biophysics</i> , 2021, 704, 108867.	3.0	4
8896	Multifaceted Regulation of Potassium-Ion Channels by Graphene Quantum Dots. <i>ACS Applied Materials &amp; Interfaces</i> , 2021, 13, 27784-27795.	8.0	4
8898	Effect of quercetin on lipid membrane rigidity: assessment by atomic force microscopy and molecular dynamics simulations. <i>BBA Advances</i> , 2021, 1, 100018.	1.6	10
8899	Membrane Insertion of MoS2 Nanosheets: Fresh vs. Aged. <i>Frontiers in Chemistry</i> , 2021, 9, 706917.	3.6	6
8900	Integrated docking and enhanced sampling-based selection of repurposing drugs for SARS-CoV-2 by targeting host dependent factors. <i>Journal of Biomolecular Structure and Dynamics</i> , 2022, 40, 9897-9908.	3.5	7
8903	CHIMs are versatile cholesterol analogs mimicking and visualizing cholesterol behavior in lipid bilayers and cells. <i>Communications Biology</i> , 2021, 4, 720.	4.4	13
8904	Structural and functional analysis of the simultaneous binding of two duplex/quadruplex aptamers to human $\beta$ -thrombin. <i>International Journal of Biological Macromolecules</i> , 2021, 181, 858-867.	7.5	8
8905	The oxidoreductase PYROXD1 uses NAD(P) <sup>+</sup> as an antioxidant to sustain tRNA ligase activity in pre-tRNA splicing and unfolded protein response. <i>Molecular Cell</i> , 2021, 81, 2520-2532.e16.	9.7	21
8906	Metadynamics-Based Approaches for Modeling the Hypoxia-Inducible Factor 2 $\alpha$ Ligand Binding Process. <i>Journal of Chemical Theory and Computation</i> , 2021, 17, 3841-3851.	5.3	12
8907	Automated Parameterization of Quantum Mechanically Derived Force Fields for Soft Materials and Complex Fluids: Development and Validation. <i>Journal of Chemical Theory and Computation</i> , 2021, 17, 4449-4464.	5.3	11
8908	Association Mechanism of Peptide-Coated Metal Nanoparticles with Model Membranes: A Coarse-Grained Study. <i>Journal of Chemical Theory and Computation</i> , 2021, 17, 4512-4523.	5.3	13
8909	Structural and dynamical heterogeneity of water trapped inside Na <sup>+</sup> -pumping KR2 rhodopsin in the dark state. <i>Journal of Chemical Physics</i> , 2021, 154, 215101.	3.0	2
8910	Xanthine Oxidase Inhibitory Activity of <i>Euphorbia peplus</i> L. Phenolics. <i>Combinatorial Chemistry and High Throughput Screening</i> , 2022, 25, 1336-1344.	1.1	3
8911	Evolutionary selectivity of amino acid is inspired from the enhanced structural stability and flexibility of the folded protein. <i>Life Sciences</i> , 2021, 281, 119774.	4.3	7
8912	TRIM7 inhibits enterovirus replication and promotes emergence of a viral variant with increased pathogenicity. <i>Cell</i> , 2021, 184, 3410-3425.e17.	28.9	35

#	ARTICLE	IF	CITATIONS
8913	Destabilization of the Alzheimer's amyloid- $\beta^2$ protofibrils by THC: A molecular dynamics simulation study. <i>Journal of Molecular Graphics and Modelling</i> , 2021, 105, 107889.	2.4	8
8914	HnRNPA2 <sup>TM</sup> in LC(286-291) Domain Fibrili ve Onun D290V Mutasyonu Hakkında Teorik Bir Çalışma. <i>Journal of the Institute of Science and Technology</i> , 0, , 1080-1089.	0.9	0
8915	DFT and force-field based MD simulations of formamide intercalation in LDH and its exfoliated form. <i>Applied Surface Science</i> , 2021, 552, 149450.	6.1	5
8916	Identification of viable TCDD access pathways to human AhR PAS-B ligand binding domain. <i>Journal of Molecular Graphics and Modelling</i> , 2021, 105, 107886.	2.4	5
8917	Improving the activity and stability of <i>Bacillus clausii</i> alkaline protease using directed evolution and molecular dynamics simulation. <i>Enzyme and Microbial Technology</i> , 2021, 147, 109787.	3.2	17
8918	Binding of Ca <sup>2+</sup> -independent C2 domains to lipid membranes: A multi-scale molecular dynamics study. <i>Structure</i> , 2021, 29, 1200-1213.e2.	3.3	19
8920	Simulations of the Upper Critical Solution Temperature Behavior of Poly(ornithine-co-citrulline)s Using MARTINI-Based Coarse-Grained Force Fields. <i>Journal of Chemical Theory and Computation</i> , 2021, 17, 4499-4511.	5.3	2
8921	Ionic contrast across a lipid membrane for Debye length extension: towards an ultimate bioelectronic transducer. <i>Nature Communications</i> , 2021, 12, 3741.	12.8	13
8922	Molecular Basis for the Interactions of Human Thioredoxins with Their Respective Reductases. <i>Oxidative Medicine and Cellular Longevity</i> , 2021, 2021, 1-17.	4.0	6
8923	Molecular simulation of the morphology and viscosity of aqueous micellar solutions of sodium lauryl ether sulfate (SLEnS). <i>JPhys Materials</i> , 2021, 4, 044001.	4.2	4
8924	Pressure and Temperature Phase Diagram for Liquid-Liquid Phase Separation of the RNA-Binding Protein Fused in Sarcoma. <i>Journal of Physical Chemistry B</i> , 2021, 125, 6821-6829.	2.6	30
8925	Steric and Electrostatic Effects on the Diffusion of CH <sub>4</sub> /CH <sub>3</sub> OH in Copper-Exchanged Zeolites: Insights from Enhanced Sampling Molecular Dynamics and Free Energy Calculations. <i>Langmuir</i> , 2021, 37, 8014-8023.	3.5	1
8926	Unraveling the Allosteric Cross-Talk between the Coactivator Peptide and the Ligand-Binding Site in the Glucocorticoid Receptor. <i>Journal of Chemical Information and Modeling</i> , 2021, 61, 3667-3680.	5.4	10
8927	Multipronged Regulatory Functions of Serum Albumin in Early Stages of Amyloid- $\beta^2$ Aggregation. <i>ACS Chemical Neuroscience</i> , 2021, 12, 2409-2420.	3.5	10
8928	Physical Characterization of Triolein and Implications for Its Role in Lipid Droplet Biogenesis. <i>Journal of Physical Chemistry B</i> , 2021, 125, 6874-6888.	2.6	13
8929	Mechanistic Insight into How PEGylation Reduces the Efficacy of pH-Sensitive Liposomes from Molecular Dynamics Simulations. <i>Molecular Pharmaceutics</i> , 2021, 18, 2612-2621.	4.6	8
8930	Targeting the NS2B-NS3 protease of tick-borne encephalitis virus with pan-flaviviral protease inhibitors. <i>Antiviral Research</i> , 2021, 190, 105074.	4.1	12
8931	A molecular dynamics study of a fully zwitterionic copolymer/ionic liquid-based electrolyte: Li <sup>+</sup> transport mechanisms and ionic interactions. <i>Journal of Computational Chemistry</i> , 2021, 42, 1689-1703.	3.3	6

#	ARTICLE	IF	CITATIONS
8932	Potential phytochemical inhibitors of SARS-CoV-2 helicase Nsp13: a molecular docking and dynamic simulation study. <i>Molecular Diversity</i> , 2022, 26, 429-442.	3.9	27
8933	Crystallization behavior of Fe <sub>70</sub> Ni <sub>10</sub> Cr <sub>20</sub> during rapid solidification under different cooling rates. <i>Materials Today Communications</i> , 2021, 27, 102255.	1.9	4
8934	Quantitative predictions from molecular simulations using explicit or implicit interactions. <i>Wiley Interdisciplinary Reviews: Computational Molecular Science</i> , 2022, 12, e1560.	14.6	14
8935	Residue 6.43 defines receptor function in class F GPCRs. <i>Nature Communications</i> , 2021, 12, 3919.	12.8	14
8936	Order and disorder—An integrative structure of the full-length human growth hormone receptor. <i>Science Advances</i> , 2021, 7, .	10.3	25
8937	Structural and functional role of invariant water molecules in matrix metalloproteinases: a data-mining approach. <i>Journal of Biomolecular Structure and Dynamics</i> , 2022, 40, 10074-10085.	3.5	3
8938	Structural Basis of the Function of Yariv Reagent—An Important Tool to Study Arabinogalactan Proteins. <i>Frontiers in Molecular Biosciences</i> , 2021, 8, 682858.	3.5	7
8939	Cryo-EM structure of the photosynthetic RC-LH1-PufX supercomplex at 2.8-Å... resolution. <i>Science Advances</i> , 2021, 7, .	10.3	29
8940	Groove Switching of Hydroxychloroquine Modulates the Efficacy of Binding and Induced Stability to DNA. <i>Journal of Physical Chemistry B</i> , 2021, 125, 6889-6896.	2.6	10
8941	Atomistic Modeling of PEDOT:PSS Complexes II: Force Field Parameterization. <i>Macromolecules</i> , 2021, 54, 5354-5365.	4.8	9
8942	Layer-by-Layer Assembly-Based Electrocatalytic Fibril Electrodes Enabling Extremely Low Overpotentials and Stable Operation at 100 mA cm <sup>-2</sup> in Water-Splitting Reaction. <i>Advanced Functional Materials</i> , 2021, 31, 2102530.	14.9	15
8943	Identification of potential inhibitors for LLM of <i>Staphylococcus aureus</i> : structure-based pharmacophore modeling, molecular dynamics, and binding free energy studies. <i>Journal of Biomolecular Structure and Dynamics</i> , 2022, 40, 9833-9847.	3.5	28
8944	Evolution of the Free Energy Landscapes of n-Alkane Guests Bound within Supramolecular Complexes. <i>Journal of Physical Chemistry B</i> , 2021, 125, 7299-7310.	2.6	4
8945	Distinguishing Weak and Strong Hydrogen Bonds in Liquid Water—A Potential of Mean Force-Based Approach. <i>Journal of Physical Chemistry B</i> , 2021, 125, 7187-7198.	2.6	18
8947	Periodic boundary conditions for arbitrary deformations in molecular dynamics simulations. <i>Journal of Computational Physics</i> , 2021, 435, 110238.	3.8	16
8948	Cancellation of Auxetic Properties in F.C.C. Hard Sphere Crystals by Hybrid Layer-Channel Nano-inclusions Filled by Hard Spheres of Another Diameter. <i>Materials</i> , 2021, 14, 3008.	2.9	8
8949	In Silico Approach Using Free Software to Optimize the Antiproliferative Activity and Predict the Potential Mechanism of Action of Pyrrolizine-Based Schiff Bases. <i>Molecules</i> , 2021, 26, 4002.	3.8	9
8950	Specific and nondisruptive interaction of guanidium-functionalized gold nanoparticles with neutral phospholipid bilayers. <i>Communications Chemistry</i> , 2021, 4, .	4.5	8



#	ARTICLE	IF	CITATIONS
8952	Identification of 13 Guanidinobenzoyl- or Aminidinobenzoyl-Containing Drugs to Potentially Inhibit TMPRSS2 for COVID-19 Treatment. <i>International Journal of Molecular Sciences</i> , 2021, 22, 7060.	4.1	10
8954	Temperature-dependent elastic properties of binary and multicomponent high-entropy refractory carbides. <i>Materials and Design</i> , 2021, 204, 109634.	7.0	26
8955	Transcriptional processing of an unnatural base pair by eukaryotic RNA polymerase II. <i>Nature Chemical Biology</i> , 2021, 17, 906-914.	8.0	16
8956	Structure and lipid dynamics in the maintenance of lipid asymmetry inner membrane complex of <i>A. baumannii</i> . <i>Communications Biology</i> , 2021, 4, 817.	4.4	31
8957	Extended JAZ degron sequence for plant hormone binding in jasmonate co-receptor of tomato SICO1-SIJAZ. <i>Scientific Reports</i> , 2021, 11, 13612.	3.3	11
8958	Reweighting of molecular simulations with explicit-solvent SAXS restraints elucidates ion-dependent RNA ensembles. <i>Nucleic Acids Research</i> , 2021, 49, e84-e84.	14.5	25
8960	Hydrocarbon Self-Diffusion and Assessing the Validity of Graham's Law under Nanoporous Confinement in Shales. <i>Energy &amp; Fuels</i> , 2021, 35, 10512-10518.	5.1	4
8961	Evaluating Coarse-Grained MARTINI Force-Fields for Capturing the Ripple Phase of Lipid Membranes. <i>Journal of Physical Chemistry B</i> , 2021, 125, 6587-6599.	2.6	6
8962	Mechanism of Vitamin D Receptor Ligand-Binding Domain Regulation Studied by gREST Simulations. <i>Journal of Chemical Information and Modeling</i> , 2021, 61, 3625-3637.	5.4	3
8963	Amorphous zircon at high pressure. <i>Journal of Physics and Chemistry of Solids</i> , 2021, 153, 109991.	4.0	0
8964	Toward the Identification of Potential $\alpha$ -Ketoamide Covalent Inhibitors for SARS-CoV-2 Main Protease: Fragment-Based Drug Design and MM-PBSA Calculations. <i>Processes</i> , 2021, 9, 1004.	2.8	21
8965	Tight docking of membranes before fusion represents a metastable state with unique properties. <i>Nature Communications</i> , 2021, 12, 3606.	12.8	20
8966	Binding of <i>Foeniculum vulgare</i> essential oil and its major compounds to double-stranded DNA: In silico and in vitro studies. <i>Food Bioscience</i> , 2021, 41, 100972.	4.4	6
8971	Liquid structure of a choline chloride-water natural deep eutectic solvent: A molecular dynamics characterization. <i>Journal of Molecular Liquids</i> , 2021, 331, 115750.	4.9	37
8972	Structure-based mimicking of hydroxylated biphenyl congeners (OHPCBs) for human transthyretin, an important enzyme of thyroid hormone system. <i>Journal of Molecular Graphics and Modelling</i> , 2021, 105, 107870.	2.4	29
8973	EXPRORER: Rational Cosolvent Set Construction Method for Cosolvent Molecular Dynamics Using Large-Scale Computation. <i>Journal of Chemical Information and Modeling</i> , 2021, 61, 2744-2753.	5.4	6
8974	A $\text{HNO}_3$ -Responsive Aqueous Biphasic System for Metal Separation: Application towards $\text{Ce}^{IV}$ Recovery. <i>ChemSusChem</i> , 2021, 14, 3018-3026.	6.8	8
8975	Geological storage of $\text{CO}_2$ - $\text{N}_2$ - $\text{O}_2$ mixtures produced by membrane-based direct air capture (DAC)., 2021, 11, 610-618.		17

#	ARTICLE	IF	CITATIONS
8976	Molecular insight into COF monolayers for urea sorption in artificial kidneys. Scientific Reports, 2021, 11, 12085.	3.3	14
8977	Quantum polyamorphism in compressed distinguishable helium-4. Journal of Chemical Physics, 2021, 154, 224503.	3.0	2
8978	Sub-nanometer confinement enables facile condensation of gas electrolyte for low-temperature batteries. Nature Communications, 2021, 12, 3395.	12.8	42
8980	Elucidating Axonal Injuries Through Molecular Modelling of Myelin Sheaths and Nodes of Ranvier. Frontiers in Molecular Biosciences, 2021, 8, 669897.	3.5	5
8981	The role of the envelope protein in the stability of a coronavirus model membrane against an ethanolic disinfectant. Journal of Chemical Physics, 2021, 154, 245101.	3.0	4
8982	Controlling Peptide Function by Directed Assembly Formation: Mechanistic Insights Using Multiscale Modeling on an Antimicrobial Peptideâ€“Drugâ€“Membrane System. ACS Omega, 2021, 6, 15756-15769.	3.5	4
8983	Ceramide structure dictates glycosphingolipid nanodomain assembly and function. Nature Communications, 2021, 12, 3675.	12.8	27
8984	Atomic scale modeling of the coherent strain field surrounding Ni <sub>4</sub> Ti <sub>3</sub> precipitate and its effects on thermally-induced martensitic transformation in a NiTi alloy. Acta Materialia, 2021, 211, 116883.	7.9	27
8985	Effect of water models on structure and dynamics of lignin in solution. AIP Advances, 2021, 11, .	1.3	10
8986	Optimized Halogen Atomic Radii for PBSA Calculations Using Off-Center Point Charges. Journal of Chemical Information and Modeling, 2021, 61, 3361-3375.	5.4	4
8987	Sphingomonas sp. KT-1 PahZ2 Structure Reveals a Role for Conformational Dynamics in Peptide Bond Hydrolysis. Journal of Physical Chemistry B, 2021, 125, 5722-5739.	2.6	1
8988	Unveiling Interfacial Li-Ion Dynamics in Li <sub>7</sub> La <sub>3</sub> Zr <sub>2</sub> O <sub>12</sub> /PEO(LiTFSI) Composite Polymer-Ceramic Solid Electrolytes for All-Solid-State Lithium Batteries. ACS Applied Materials & Interfaces, 2021, 13, 30653-30667.	8.0	25
8989	Exploring the Conformational Changes Induced by Nanosecond Pulsed Electric Fields on the Voltage Sensing Domain of a Ca <sup>2+</sup> Channel. Membranes, 2021, 11, 473.	3.0	12
8990	Enhancing the binding of the Î²-sheet breaker peptide LPFFD to the amyloid-Î² fibrils by aromatic modifications: A molecular dynamics simulation study. Computational Biology and Chemistry, 2021, 92, 107471.	2.3	12
8991	Improved Protocol to Tackle the pH Effects on Membrane-Inserting Peptides. Journal of Chemical Theory and Computation, 2021, 17, 3830-3840.	5.3	12
8992	Molecular Dynamics Study of Conformational Changes of Tankyrase 2 Binding Subsites upon Ligand Binding. ACS Omega, 2021, 6, 17609-17620.	3.5	14
8993	Classical nucleation theory of ice nucleation: Second-order corrections to thermodynamic parameters. Journal of Chemical Physics, 2021, 154, 234503.	3.0	9
8994	Nanoscale architecture of a VAP-A-OSBP tethering complex at membrane contact sites. Nature Communications, 2021, 12, 3459.	12.8	29

#	ARTICLE	IF	CITATIONS
8995	Ensemble-based screening of natural products and FDA-approved drugs identified potent inhibitors of SARS-CoV-2 that work with two distinct mechanisms. <i>Journal of Molecular Graphics and Modelling</i> , 2021, 105, 107871.	2.4	7
8996	An in-silico evaluation of different bioactive molecules of tea for their inhibition potency against non structural protein-15 of SARS-CoV-2. <i>Food Chemistry</i> , 2021, 346, 128933.	8.2	125
8997	Molecular Dynamics Simulations of Nanostructures Formed by Hydrophobins and Oil in Seawater. <i>Journal of Physical Chemistry B</i> , 2021, 125, 7886-7899.	2.6	4
8998	Nanomechanical Stability of Al <sup>2+</sup> Tetramers and Fibril-like Structures: Molecular Dynamics Simulations. <i>Journal of Physical Chemistry B</i> , 2021, 125, 7628-7637.	2.6	9
8999	Molecular Dynamics Simulations of Complexation of Am(III) with a Preorganized Dicationic Ligand in an Ionic Liquid. <i>Journal of Physical Chemistry B</i> , 2021, 125, 8532-8538.	2.6	7
9000	Computationally Designed Crystal Structures of the Supertetrahedral Ga <sub>4</sub> C and Ga <sub>4</sub> Si Solids. <i>Journal of Physical Chemistry A</i> , 2021, 125, 6556-6561.	2.5	1
9001	An <i>in silico</i> molecular dynamics simulation study on the inhibitors of SARS-CoV-2 proteases (3CL <sup>pro</sup> and PL <sup>pro</sup> ) to combat COVID-19. <i>Molecular Simulation</i> , 2021, 47, 1168-1184.	2.0	10
9002	Site-Specific Steric Control of SARS-CoV-2 Spike Glycosylation. <i>Biochemistry</i> , 2021, 60, 2153-2169.	2.5	54
9003	Influence of the gallate moiety on the interactions between green tea polyphenols and lipid membranes elucidated by molecular dynamics simulations. <i>Biophysical Chemistry</i> , 2021, 274, 106592.	2.8	9
9004	Lipoprotein-Induced Increases in Cholesterol and 7-Ketocholesterol Result in Opposite Molecular-Scale Biophysical Effects on Membrane Structure. <i>Frontiers in Cardiovascular Medicine</i> , 2021, 8, 715932.	2.4	8
9005	Calorimetric, spectroscopic and computational investigation of morin binding effect on bovine serum albumin stability. <i>Journal of Molecular Liquids</i> , 2021, 333, 115953.	4.9	10
9006	Comparison and Validation of Force Fields for Deep Eutectic Solvents in Combination with Water and Alcohol Dehydrogenase. <i>Journal of Chemical Theory and Computation</i> , 2021, 17, 5322-5341.	5.3	17
9007	A Bayesian approach to extracting free-energy profiles from cryo-electron microscopy experiments. <i>Scientific Reports</i> , 2021, 11, 13657.	3.3	27
9008	Gating movements and ion permeation in HCN4 pacemaker channels. <i>Molecular Cell</i> , 2021, 81, 2929-2943.e6.	9.7	41
9009	Ionic conductance oscillations in sub-nanometer pores probed by optoelectronic control. <i>Matter</i> , 2021, 4, 2378-2391.	10.0	13
9010	Rosmarinic Acid Potently Detoxifies Amylin Amyloid and Ameliorates Diabetic Pathology in a Transgenic Rat Model of Type 2 Diabetes. <i>ACS Pharmacology and Translational Science</i> , 2021, 4, 1322-1337.	4.9	14
9011	Atomic Scale Interactions between RNA and DNA Aptamers with the TNF- $\alpha$ Protein. <i>BioMed Research International</i> , 2021, 2021, 1-11.	1.9	6
9013	A computational study of the interface interaction between SARS-CoV-2 RBD and ACE2 from human, cat, dog, and ferret. <i>Transboundary and Emerging Diseases</i> , 2022, 69, 2287-2295.	3.0	4

#	ARTICLE	IF	CITATIONS
9014	Comparison of potential inhibitors and targeting fat mass and obesity-associated protein causing diabetes through docking and molecular dynamics strategies. <i>Journal of Cellular Biochemistry</i> , 2021, 122, 1625-1638.	2.6	8
9015	Performing Molecular Dynamics Simulations and Computing Hydration Free Energies on the B3LYP-D3(BJ) Potential Energy Surface with Adaptive Force Matching: A Benchmark Study with Seven Alcohols and One Amine. <i>ACS Physical Chemistry Au</i> , 2021, 1, 14-24.	4.0	9
9016	Mutation-Dependent Refolding of Prion Protein Unveils Amyloidogenic-Related Structural Ramifications: Insights from Molecular Dynamics Simulations. <i>ACS Chemical Neuroscience</i> , 2021, 12, 2810-2819.	3.5	5
9017	$\beta$ -tubulin tail modifications regulate microtubule stability through selective effector recruitment, not changes in intrinsic polymer dynamics. <i>Developmental Cell</i> , 2021, 56, 2016-2028.e4.	7.0	55
9018	On the Metal-Aided Catalytic Mechanism for Phosphodiester Bond Cleavage Performed by Nanozymes. <i>ACS Catalysis</i> , 2021, 11, 8736-8748.	11.2	20
9019	Two Bacterial Small Heat Shock Proteins, IbpA and IbpB, Form a Functional Heterodimer. <i>Journal of Molecular Biology</i> , 2021, 433, 167054.	4.2	12
9020	Molecular thermodynamic and dynamic insights into gas dehydration with imidazolium-based ionic liquids. <i>Chemical Engineering Journal</i> , 2021, 416, 129168.	12.7	27
9021	Effect of magnesium sulfate in oxidized lipid bilayers properties by using molecular dynamics. <i>Biochemistry and Biophysics Reports</i> , 2021, 26, 100998.	1.3	1
9022	Binding analysis of the curcumin-based synthetic $\alpha$ -glucosidase inhibitors to beta-lactoglobulin as potential vehicle carrier for antidiabetic drugs. <i>Journal of the Iranian Chemical Society</i> , 2022, 19, 489-503.	2.2	3
9023	Solubility Prediction of Organic Molecules with Molecular Dynamics Simulations. <i>Crystal Growth and Design</i> , 2021, 21, 5198-5205.	3.0	14
9024	Bridging Gaussian Density Fluctuations from Microscopic to Macroscopic Volumes: Applications to Non-Polar Solute Hydration Thermodynamics. <i>Journal of Physical Chemistry B</i> , 2021, 125, 8152-8164.	2.6	5
9025	Force Field Parameterization for the Description of the Interactions between Hydroxypropyl- $\beta$ -Cyclodextrin and Proteins. <i>Journal of Physical Chemistry B</i> , 2021, 125, 7397-7405.	2.6	9
9026	Investigating Crosstalk Among PTMs Provides Novel Insight Into the Structural Basis Underlying the Differential Effects of Nt17 PTMs on Mutant Httex1 Aggregation. <i>Frontiers in Molecular Biosciences</i> , 2021, 8, 686086.	3.5	8
9027	Formulation and Efficacy of Catalase-Loaded Nanoparticles for the Treatment of Neonatal Hypoxic-Ischemic Encephalopathy. <i>Pharmaceutics</i> , 2021, 13, 1131.	4.5	6
9028	Förster Resonance Energy Transfer in Linear DNA Multifluorophore Photonic Wires: Comparing Dual versus Split Rail Building Block Designs. <i>Advanced Optical Materials</i> , 2021, 9, 2100884.	7.3	5
9029	HL-7 and HL-10 Peptides Stimulate Insulin Secretion in the INS-1 Insulinoma Cell Line through Incretin-Dependent Pathway and Increasing the Glucose Uptake in L6 Myoblast. <i>International Journal of Peptide Research and Therapeutics</i> , 0, 1.	1.9	3
9030	Structural origin of thermal shrinkage in soda-lime silicate glass below the glass transition temperature: A theoretical investigation by microsecond timescale molecular dynamics simulations. <i>Journal of Chemical Physics</i> , 2021, 155, 044501.	3.0	6
9031	In silico identification of potential Hsp90 inhibitors via ensemble docking, DFT and molecular dynamics simulations. <i>Journal of Biomolecular Structure and Dynamics</i> , 2022, 40, 10665-10676.	3.5	5

#	ARTICLE	IF	CITATIONS
9032	Definition of the immune evasion-replication interface of rabies virus P protein. PLoS Pathogens, 2021, 17, e1009729.	4.7	10
9033	Speciation of Substituted Benzoic Acids in Solution: Evaluation of Spectroscopic and Computational Methods for the Identification of Associates and Their Role in Crystallization. Crystal Growth and Design, 2021, 21, 4823-4836.	3.0	5
9034	An Enhanced Scheme for Multiscale Modeling of Thermomechanical Properties of Polymer Bulks. Journal of Physical Chemistry B, 2021, 125, 8612-8626.	2.6	3
9035	Atomic and Electronic Structure of Pilus from Geobacter sulfurreducens through QM/MM Calculations: Evidence for Hole Transfer in Aromatic Residues. Journal of Physical Chemistry B, 2021, 125, 8305-8312.	2.6	8
9036	Dimethyl sulfoxide reduces the stability but enhances catalytic activity of the main SARS-CoV-2 protease 3CLpro. FASEB Journal, 2021, 35, e21774.	0.5	13
9037	Identification of ACK1 inhibitors as anticancer agents by using computer-aided drug designing. Journal of Molecular Structure, 2021, 1235, 130200.	3.6	13
9038	Flexible pivoting of dynamin pleckstrin homology domain catalyzes fission: insights into molecular degrees of freedom. Molecular Biology of the Cell, 2021, 32, 1306-1319.	2.1	11
9039	Asphaltenes as novel thermal conductivity enhancers for liquid paraffin: Insight from in silico modeling. Journal of Molecular Liquids, 2021, , 117112.	4.9	8
9040	Guanidine-II aptamer conformations and ligand binding modes through the lens of molecular simulation. Nucleic Acids Research, 2021, 49, 7954-7965.	14.5	6
9041	Coordination and Thermophysical Properties of Transition Metal Chlorocomplexes in LiCl-KCl Eutectic. Journal of Physical Chemistry B, 2021, 125, 8876-8887.	2.6	13
9042	Competition between the Photothermal Effect and Emission in Potential Phototherapy Agents. Journal of Physical Chemistry B, 2021, 125, 8733-8741.	2.6	7
9043	New insights into adsorption equilibrium of organic pollutant on MnO <sub>2</sub> nanorods: Experimental and computational studies. Journal of Molecular Liquids, 2022, 345, 117016.	4.9	6
9044	Structural and Binding Effects of Chemical Modifications on Thrombin Binding Aptamer (TBA). Molecules, 2021, 26, 4620.	3.8	4
9046	Computational study of DMPC liposomes loaded with the N-(2-Hydroxyphenyl)-2-propylpentanamide (HO-AAVPA) and determination of its antiproliferative activity <i>in vitro</i> in NIH-3T3 cells. Journal of Biomolecular Structure and Dynamics, 2022, 40, 11448-11459.	3.5	2
9047	In Silico Identification of Cholesterol Binding Motifs in the Chemokine Receptor CCR3. Membranes, 2021, 11, 570.	3.0	14
9048	Membrane interactions of Ocellatins. Where do antimicrobial gaps stem from?. Amino Acids, 2021, 53, 1241-1256.	2.7	1
9050	Simulations of Promising Indolizidine <sup>†</sup> ±6- <sup>†</sup> 2 Nicotinic Acetylcholine Receptor Complexes. International Journal of Molecular Sciences, 2021, 22, 7934.	4.1	1
9053	Rational Design of Nonbonded Point Charge Models for Divalent Metal Cations with Lennard-Jones 12-6 Potential. Journal of Chemical Information and Modeling, 2021, 61, 4031-4044.	5.4	13

#	ARTICLE	IF	CITATIONS
9054	Effect of electric field strength on deformation and breakup behaviors of droplet in oil phase: A molecular dynamics study. <i>Journal of Molecular Liquids</i> , 2021, 333, 115995.	4.9	36
9055	The synthetic varespladib molecule is a multi-functional inhibitor for PLA2 and PLA2-like ophidic toxins. <i>Biochimica Et Biophysica Acta - General Subjects</i> , 2021, 1865, 129913.	2.4	20
9056	Allosteric activation of T $\beta$ cell antigen receptor signaling by quaternary structure relaxation. <i>Cell Reports</i> , 2021, 36, 109375.	6.4	23
9057	Precise force-field-based calculations of octanol-water partition coefficients for the SAMPL7 molecules. <i>Journal of Computer-Aided Molecular Design</i> , 2021, 35, 853-870.	2.9	5
9058	Molecular dynamics study on the stability of foot-and-mouth disease virus particle in salt solution. <i>Molecular Simulation</i> , 2021, 47, 1104-1111.	2.0	1
9059	Mechanistic Insights on ATP's Role as a Hydrotrope. <i>Journal of Physical Chemistry B</i> , 2021, 125, 7717-7731.	2.6	21
9060	Donor-acceptor structure and dynamics: Molecular dynamics simulation study of TIP4P/2005 water model. <i>Chemical Physics Letters</i> , 2021, 775, 138581.	2.6	0
9061	Computationally Guided Tuning of Peptide-Conjugated Perylene Diimide Self-Assembly. <i>Langmuir</i> , 2021, 37, 8594-8606.	3.5	9
9062	Probe into the Molecular Mechanism of Ibuprofen Interaction with Warfarin Bound to Human Serum Albumin in Comparison to Ascorbic and Salicylic Acids: Allosteric Inhibition of Anticoagulant Release. <i>Journal of Chemical Information and Modeling</i> , 2021, 61, 4045-4057.	5.4	9
9064	Zinc binding alters the conformational dynamics and drives the transport cycle of the cation diffusion facilitator YfiP. <i>Journal of General Physiology</i> , 2021, 153, .	1.9	14
9065	Shear response in crystalline models of poly(p-phenylene terephthalamide). <i>Molecular Physics</i> , 0, , e1948122.	1.7	3
9066	The Structural Effect of FLT3 Mutations at 835th Position and Their Interaction with Acute Myeloid Leukemia Inhibitors: In Silico Approach. <i>International Journal of Molecular Sciences</i> , 2021, 22, 7602.	4.1	19
9067	Maintenance of complex I and its supercomplexes by NDUF-11 is essential for mitochondrial structure, function and health. <i>Journal of Cell Science</i> , 2021, 134, .	2.0	17
9068	Elaborating the high thermal storage and conductivity of molten NaCl-KCl-NaF eutectic from microstructures by FPMD simulations. <i>Journal of Molecular Liquids</i> , 2022, 346, 117054.	4.9	4
9069	Identification of effective and specific serotonin1B receptor ligands by structure-based virtual screening and molecular dynamics. <i>Journal of Proteins and Proteomics</i> , 2021, 12, 213-226.	1.5	0
9070	Aggregation Behavior of Asphalt on the Natural Gas Hydrate Surface with Different Surfactant Coverages. <i>Journal of Physical Chemistry C</i> , 2021, 125, 16378-16390.	3.1	28
9071	The molecular dynamics of possible inhibitors for SARS-CoV-2. <i>Journal of Biomolecular Structure and Dynamics</i> , 2021, , 1-10.	3.5	5
9072	Hydrogen Bonding and the Structural Properties of Glycerol-Water Mixtures with a Microwave Field: a Molecular Dynamics Study. <i>Journal of Physical Chemistry B</i> , 2021, 125, 8099-8106.	2.6	9



#	ARTICLE	IF	CITATIONS
9073	Effect of the single mutation N9Y on the catalytical properties of xylanase Xyn11A from <i>Cellulomonas uda</i> : a biochemical and molecular dynamic simulation analysis. <i>Bioscience, Biotechnology and Biochemistry</i> , 2021, 85, 1971-1985.	1.3	2
9074	Energy-entropy method using multiscale cell correlation to calculate binding free energies in the SAMPL8 host-guest challenge. <i>Journal of Computer-Aided Molecular Design</i> , 2021, 35, 911-921.	2.9	11
9075	Structural Compactness in Hen Egg White Lysozyme Induced by Bisphenol-S: Spectroscopic and Molecular Dynamics Simulation Approach. <i>ChemPhysChem</i> , 2021, 22, 1745-1753.	2.1	10
9077	Interaction of epoxy-based hydrogels and water: A molecular dynamics simulation study. <i>Journal of Molecular Graphics and Modelling</i> , 2021, 106, 107915.	2.4	9
9078	Investigation of Inhibition Effect of Nicotine and Dopamine on Alpha-synuclein. <i>Journal of Computational Biophysics and Chemistry</i> , 2021, 20, 477-494.	1.7	0
9079	Effect of Cholesterol Versus Ergosterol on DPPC Bilayer Properties: Insights from Atomistic Simulations. <i>Journal of Physical Chemistry B</i> , 2021, 125, 7679-7690.	2.6	8
9080	Using Molecular Simulations to Understand the Effect of Dodecyl Sulfate on the Calcium-Binding Ability of Polystyrene Sulfonate. <i>Journal of Physical Chemistry B</i> , 2021, 125, 7919-7931.	2.6	2
9082	Modulation of Phospholipid Bilayer Properties by Simvastatin. <i>Journal of Physical Chemistry B</i> , 2021, 125, 8406-8418.	2.6	5
9083	New (Iso)quinolinyl-pyridine-2,6-dicarboxamide G-Quadruplex Stabilizers. A Structure-Activity Relationship Study. <i>Pharmaceuticals</i> , 2021, 14, 669.	3.8	7
9084	Structural basis of the effect of activating mutations on the EGF receptor. <i>ELife</i> , 2021, 10, .	6.0	24
9085	Identification of potential ZIKV NS2B-NS3 protease inhibitors from <i>Andrographis paniculata</i> : An insilico approach. <i>Journal of Biomolecular Structure and Dynamics</i> , 2022, 40, 11203-11215.	3.5	6
9086	Temperature, Pressure, and Length-Scale Dependence of Solvation in Water-like Solvents. II. Large Solvophobic Solutes. <i>Journal of Physical Chemistry B</i> , 2021, 125, 8175-8184.	2.6	2
9087	On the Structure and Flip-flop of Free Docosahexaenoic Acid in a Model Human Brain Membrane. <i>Journal of Physical Chemistry B</i> , 2021, 125, 8038-8047.	2.6	4
9088	Atomistic molecular dynamics simulations of tubulin heterodimers explain the motion of a microtubule. <i>European Biophysics Journal</i> , 2021, 50, 927-940.	2.2	2
9089	Electrostatic Interactions Explain the Higher Binding Affinity of the CR3022 Antibody for SARS-CoV-2 than the 4A8 Antibody. <i>Journal of Physical Chemistry B</i> , 2021, 125, 7368-7379.	2.6	25
9090	Plasma treatment causes structural modifications in lysozyme, and increases cytotoxicity towards cancer cells. <i>International Journal of Biological Macromolecules</i> , 2021, 182, 1724-1736.	7.5	21
9091	Facilitating SARS CoV-2 RNA-Dependent RNA polymerase (RdRp) drug discovery by the aid of HCV NS5B palm subdomain binders: In silico approaches and benchmarking. <i>Computers in Biology and Medicine</i> , 2021, 134, 104468.	7.0	15
9092	Computation and volumetric insight into (p,T) effect on aqueous guanidinium chloride. <i>Journal of Chemical Thermodynamics</i> , 2021, 158, 106450.	2.0	5

#	ARTICLE	IF	CITATIONS
9093	Identification of 3D motifs based on sequences and structures for binding to CFIâ€400945, and deep screeningâ€based design of new lead molecules for PLKâ€4. Chemical Biology and Drug Design, 2021, 98, 522-538.	3.2	2
9094	Effects of changes in glycan composition on glycoprotein dynamics: example of N-glycans on insulin receptor. Glycobiology, 2021, 31, 1121-1133.	2.5	2
9095	The impacts of net charge on the water dispersity of nanoparticles. Journal of Molecular Liquids, 2021, , 117105.	4.9	2
9096	Transmembrane Self-Assembled Cyclic Peptide Nanotubes Based on Î±â€Residues and Cyclic Î±â€Amino Acids: A Computational Study. Frontiers in Chemistry, 2021, 9, 704160.	3.6	3
9097	Biophysical analysis of an HCN1 epilepsy variant suggests a critical role for S5 helix Met-305 in voltage sensor to pore domain coupling. Progress in Biophysics and Molecular Biology, 2021, 166, 156-172.	2.9	16
9098	Cysteine cross-linking in native membranes establishes the transmembrane architecture of Ire1. Journal of Cell Biology, 2021, 220, .	5.2	8
9100	Structure and Dynamics of Curcumin Encapsulated Lecithin Micelles: A Molecular Dynamics Simulation Study. Science and Technology Indonesia, 2021, 6, 113-120.	0.8	0
9101	Temperature-Dependent Properties of Molten Li<sub>2</sub>BeF<sub>4</sub> Salt Using <i>Ab Initio</i> Molecular Dynamics. ACS Omega, 2021, 6, 19822-19835.	3.5	17
9102	Insights into the orientation and hydrogen bond influence on thermophysical and transport properties in choline-based deep eutectic solvents and methanol. Journal of Molecular Liquids, 2022, 345, 117019.	4.9	13
9103	Atomistic modelling of thermal-cycling rejuvenation in metallic glasses. Acta Materialia, 2021, 213, 116952.	7.9	32
9104	Structural and mechanistic basis for translation inhibition by macrolide and ketolide antibiotics. Nature Communications, 2021, 12, 4466.	12.8	43
9105	Effect of nanoparticles on interfacial mass transfer characteristics and mechanisms in liquid-liquid extraction by molecular dynamics simulation. International Journal of Heat and Mass Transfer, 2021, 173, 121236.	4.8	8
9106	How a crosslinker agent interacts with the Î²-glucosidase enzyme surface in an aqueous solution: Insight from quantum mechanics calculations and molecular dynamics simulations. Colloids and Surfaces B: Biointerfaces, 2021, 203, 111761.	5.0	4
9107	Luteolin: a blocker of SARS-CoV-2 cell entry based on relaxed complex scheme, molecular dynamics simulation, and metadynamics. Journal of Molecular Modeling, 2021, 27, 221.	1.8	17
9108	Machine Learning and Enhanced Sampling Simulations for Computing the Potential of Mean Force and Standard Binding Free Energy. Journal of Chemical Theory and Computation, 2021, 17, 5287-5300.	5.3	23
9109	A method to apply Piola-Kirchhoff stress in molecular statics simulation. Computational Materials Science, 2021, 195, 110496.	3.0	3
9110	Determination of Ligand Binding Modes in Hydrated Viral Ion Channels to Foster Drug Design and Repositioning. Journal of Chemical Information and Modeling, 2021, 61, 4011-4022.	5.4	10
9111	Dye-Sensitized Solar Cells Based on Deep Eutectic Solvent Electrolytes: Insights from Experiment and Simulation. Journal of Physical Chemistry C, 2021, 125, 15155-15165.	3.1	12

#	ARTICLE	IF	CITATIONS
9112	Multi-scale simulations of the T cell receptor reveal its lipid interactions, dynamics and the arrangement of its cytoplasmic region. <i>PLoS Computational Biology</i> , 2021, 17, e1009232.	3.2	13
9114	Deformation response of high entropy alloy nanowires. <i>Journal of Materials Science</i> , 2021, 56, 16447-16462.	3.7	13
9115	Viscosity and Interfacial Tension of Binary Mixtures of <i>n</i> -Hexadecane with Dissolved Gases Using Surface Light Scattering and Equilibrium Molecular Dynamics Simulations. <i>Journal of Chemical &amp; Engineering Data</i> , 2021, 66, 3205-3218.	1.9	17
9116	The N-terminal Tails of Histones H2A and H2B Adopt Two Distinct Conformations in the Nucleosome with Contact and Reduced Contact to DNA. <i>Journal of Molecular Biology</i> , 2021, 433, 167110.	4.2	16
9117	Hydrophobic Interactions of Ru-bda-Type Catalysts for Promoting Water Oxidation Activity. <i>Energy &amp; Fuels</i> , 2021, 35, 19096-19103.	5.1	7
9118	Molecular Dynamics of PEDOT:PSS Treated with Ionic Liquids. Origin of Anion Dependence Leading to Cation Design Principles. <i>Journal of Physical Chemistry B</i> , 2021, 125, 8601-8611.	2.6	17
9119	Mechanical models and numerical simulations in nanomechanics: A review across the scales. <i>Engineering Analysis With Boundary Elements</i> , 2021, 128, 149-170.	3.7	19
9122	Interaction mechanism between resveratrol and ovalbumin based on fluorescence spectroscopy and molecular dynamic simulation. <i>LWT - Food Science and Technology</i> , 2021, 146, 111455.	5.2	24
9123	Boron nitride nanosheets elicit significant hemolytic activity via destruction of red blood cell membranes. <i>Colloids and Surfaces B: Biointerfaces</i> , 2021, 203, 111765.	5.0	16
9124	Ionic-Group Dependence of Polyelectrolyte Coacervate Phase Behavior. <i>Macromolecules</i> , 2021, 54, 7572-7581.	4.8	10
9125	Exploring dynamics and network analysis of spike glycoprotein of SARS-COV-2. <i>Biophysical Journal</i> , 2021, 120, 2902-2913.	0.5	22
9126	The structural, functional, and dynamic effect of Tau tubulin kinase1 upon a mutation: A neurodegenerative hotspot. <i>Journal of Cellular Biochemistry</i> , 2021, 122, 1653-1664.	2.6	11
9128	Ion-solvent chemistry in lithium battery electrolytes: From mono-solvent to multi-solvent complexes. <i>Fundamental Research</i> , 2021, 1, 393-398.	3.3	50
9129	Design, synthesis, and molecular dynamics simulation studies of quinoline derivatives as protease inhibitors against SARS-CoV-2. <i>Journal of Biomolecular Structure and Dynamics</i> , 2022, 40, 10519-10542.	3.5	17
9130	An Intracellular Pathway Controlled by the N-terminus of the Pump Subunit Inhibits the Bacterial KdpFABC Ion Pump in High K <sup>+</sup> Conditions. <i>Journal of Molecular Biology</i> , 2021, 433, 167008.	4.2	3
9131	Design of Linearly Substituted Fullerene Bis-Adducts with High Dielectric Constants Based on Theoretical Calculations. <i>Bulletin of the Chemical Society of Japan</i> , 2021, 94, 1833-1839.	3.2	4
9133	Molecular Dynamics of Decane Solubilization and Diffusion of Aggregates Consisting of Surfactant and Decane Molecules in Aqueous Solutions. <i>Colloid Journal</i> , 2021, 83, 406-417.	1.3	2
9134	Design and proof of concept for targeted phage-based COVID-19 vaccination strategies with a streamlined cold-free supply chain. <i>Proceedings of the National Academy of Sciences of the United States of America</i> , 2021, 118, .	7.1	35

9136	Atomistic molecular dynamics study on the influence of high temperatures on the structure of peptide nanomembranes candidates for organic supercapacitor electrode. Journal of Molecular Liquids, 2021, 334, 116126.	4.9	15
9137	Structure and dynamics of the quaternary hunchback mRNA translation repression complex. Nucleic Acids Research, 2021, 49, 8866-8885.	14.5	4
9138	Binding of SARS-CoV-2 Fusion Peptide to Host Endosome and Plasma Membrane. Journal of Physical Chemistry B, 2021, 125, 7732-7741.	2.6	32
9139	Intermolecular interactions in tetrabutylammonium chloride based deep eutectic solvents: Classical molecular dynamics studies. Journal of Molecular Liquids, 2021, 335, 116139.	4.9	16
9140	In silico studies of semi-synthetic benzo[a]phenazines as inhibitors of dihydrofolate reductase from Plasmodium falciparum. Journal of Molecular Structure, 2021, 1237, 130404.	3.6	0
9141	Highly Heterogeneous Polarization and Solvation of Gold Nanoparticles in Aqueous Electrolytes. ACS Nano, 2021, 15, 13155-13165.	14.6	9
9142	Contrasting Local and Macroscopic Effects of Collagen Hydroxylation. International Journal of Molecular Sciences, 2021, 22, 9068.	4.1	3
9145	Determining structure and action mechanism of LBF14 by molecular simulation. Journal of Biomolecular Structure and Dynamics, 2021, , 1-12.	3.5	2
9146	Simulative Analysis of a Family of DNA Tetrahedrons Produced by Changing the Twisting Number of Each Double Helix. Journal of Computational Biophysics and Chemistry, 2021, 20, 529-537.	1.7	2
9147	Ion Valency and Concentration Effect on the Structural and Thermodynamic Properties of Brine-Decane Interfaces with Anionic Surfactant (SDS). Journal of Physical Chemistry B, 2021, 125, 9610-9620.	2.6	12
9149	Normal mode calculation and infrared spectroscopy of proteins in water solution: Relationship between amide I transition dipole strength and secondary structure. International Journal of Biological Macromolecules, 2021, 185, 369-376.	7.5	4
9150	Cardiolipin-Containing Lipid Membranes Attract the Bacterial Cell Division Protein DivIVA. International Journal of Molecular Sciences, 2021, 22, 8350.	4.1	5
9151	Structure of the human signal peptidase complex reveals the determinants for signal peptide cleavage. Molecular Cell, 2021, 81, 3934-3948.e11.	9.7	51
9152	Functional cross-talk between phosphorylation and disease-causing mutations in the cardiac sodium channel Na <sub>v</sub> 1.5. Proceedings of the National Academy of Sciences of the United States of America, 2021, 118, .	7.1	15
9153	Transforming iodoquinol into broad spectrum anti-tumor leads: Repurposing to modulate redox homeostasis. Bioorganic Chemistry, 2021, 113, 105035.	4.1	4
9154	A Unique Sequence Is Essential for Efficient Multidrug Efflux Function of the MtrD Protein of Neisseria gonorrhoeae. MBio, 2021, 12, e0167521.	4.1	1
9155	Nucleating a Different Coordination in a Crystal under Pressure: A Study of the $B_{1+1}^{\infty}$ Transition in NaCl by Metadynamics. Physical Review Letters, 2021, 127, 105701	7.8	11

#	ARTICLE	IF	CITATIONS
9156	Molecular dynamic study of alcohol-based deep eutectic solvents. Journal of Chemical Physics, 2021, 155, 064506.	3.0	15
9157	ATP Can Efficiently Stabilize Protein through a Unique Mechanism. JACS, 2021, 143, 1766-1777.	7.9	24
9158	Molecular Dynamics of Hemoglobin Reveals Structural Alterations and Explains the Interactions Driving Sickle Cell Fibrillation. Journal of Physical Chemistry B, 2021, 125, 9921-9933.	2.6	5
9159	Quaternary Structure Transitions of Human Hemoglobin: An Atomic-Level View of the Functional Intermediate States. Journal of Chemical Information and Modeling, 2021, 61, 3988-3999.	5.4	4
9160	Unraveling the Influence of Osmolytes on Water Hydrogen-Bond Network: From Local Structure to Graph Theory Analysis. Journal of Chemical Information and Modeling, 2021, 61, 3927-3944.	5.4	15
9161	Nonconverged Constraints Cause Artificial Temperature Gradients in Lipid Bilayer Simulations. Journal of Physical Chemistry B, 2021, 125, 9537-9546.	2.6	28
9162	Roles of the Coupling Agent and Surfactant in Droplet Structure in Sizing Emulsions: A Molecular Dynamics Simulations Study. Langmuir, 2021, 37, 10183-10190.	3.5	1
9163	Mitochondrial Uncoupling Proteins (UCP1-UCP3) and Adenine Nucleotide Translocase (ANT1) Enhance the Protonophoric Action of 2,4-Dinitrophenol in Mitochondria and Planar Bilayer Membranes. Biomolecules, 2021, 11, 1178.	4.0	16
9164	Remdesivir interactions with sulphobutylether- $\beta$ -cyclodextrins: A case study using selected substitution patterns. Journal of Molecular Liquids, 2022, 346, 117157.	4.9	9
9165	Pyrophyllite dissolution at elevated pressure conditions: An ab initio study. Geochimica Et Cosmochimica Acta, 2021, 307, 42-55.	3.9	6
9166	Membrane perturbation of fullerene and graphene oxide distinguished by pore-forming peptide melittin. Carbon, 2021, 180, 67-76.	10.3	12
9167	The formation and growth model of a CO <sub>2</sub> hydrate layer based on molecular dynamics. AIChE Journal, 2021, 67, e17406.	3.6	2
9168	NEDD8 Deamidation Inhibits Cullin RING Ligase Dynamics. Frontiers in Immunology, 2021, 12, 695331.	4.8	5
9169	Understanding the role of mTOR-mLst8 binding through coarse-grained simulation approaches. Molecular Simulation, 2021, 47, 1198-1207.	2.0	0
9170	On the molecular origins of the ferroelectric splay nematic phase. Nature Communications, 2021, 12, 4962.	12.8	61
9171	Discovery of potent thieno[2,3-d]pyrimidine VEGFR-2 inhibitors: Design, synthesis and enzyme inhibitory evaluation supported by molecular dynamics simulations. Bioorganic Chemistry, 2021, 113, 105019.	4.1	29
9172	Electron Transfer Coupled to Conformational Dynamics in Cell Respiration. Frontiers in Molecular Biosciences, 2021, 8, 711436.	3.5	4
9174	N-Glycosylation Enhances Conformational Flexibility of Protein Disulfide Isomerase Revealed by Microsecond Molecular Dynamics and Markov State Modeling. Journal of Physical Chemistry B, 2021, 125, 9467-9479.	2.6	16

#	ARTICLE	IF	CITATIONS
9175	Protein-induced membrane curvature in coarse-grained simulations. <i>Biophysical Journal</i> , 2021, 120, 3211-3221.	0.5	16
9176	SUMOylation Regulates TDP-43 Splicing Activity and Nucleocytoplasmic Distribution. <i>Molecular Neurobiology</i> , 2021, 58, 5682-5702.	4.0	19
9177	DNA-MBF1 study using molecular dynamics simulations. <i>European Biophysics Journal</i> , 2021, 50, 1055-1067.	2.2	2
9179	Tunable inhibition of $\beta^2$ -amyloid peptides by fast green molecules*. <i>Chinese Physics B</i> , 2021, 30, 088701.	1.4	1
9180	Anticorrelated position fluctuation of lipids in forming membrane water pores: molecular dynamics simulations study with dengue virus capsid protein. <i>Journal of Biomolecular Structure and Dynamics</i> , 2022, 40, 11395-11404.	3.5	1
9181	PIP2-induced membrane binding of the Vinculin tail competes with its other binding partners. <i>Biophysical Journal</i> , 2021, 120, 4608-4622.	0.5	3
9182	Competing Roles of Ca <sup>2+</sup> and Nonmuscle Myosin IIA on the Dynamics of the Metastasis-Associated Protein S100A4. <i>Journal of Physical Chemistry B</i> , 2021, 125, 10059-10071.	2.6	2
9183	Unraveling the Allosteric Mechanism of Four Cancer-related Mutations in the Disruption of p53-DNA Interaction. <i>Journal of Physical Chemistry B</i> , 2021, 125, 10138-10148.	2.6	10
9184	<scp>Water-mediated</scp> interactions destabilize proteins. <i>Protein Science</i> , 2021, 30, 2132-2143.	7.6	11
9185	Iron coordination to pyochelin siderophore influences dynamics of FptA receptor from <i>Pseudomonas aeruginosa</i> : a molecular dynamics simulation study. <i>BioMetals</i> , 2021, 34, 1099-1119.	4.1	2
9186	The two redox states of the human NEET proteins' [2Fe-2S] clusters. <i>Journal of Biological Inorganic Chemistry</i> , 2021, 26, 763-774.	2.6	6
9187	An $\alpha$ -oriented methionine-aromatic structural motif in SUMO is critical for its stability and activity. <i>Journal of Biological Chemistry</i> , 2021, 297, 100970.	3.4	4
9188	Regulation of a pentameric ligand-gated ion channel by a semiconserved cationic lipid-binding site. <i>Journal of Biological Chemistry</i> , 2021, 297, 100899.	3.4	15
9190	Reaction Mechanism of MHETase, a PET Degrading Enzyme. <i>ACS Catalysis</i> , 2021, 11, 10416-10428.	11.2	36
9192	Solvent Effects in the Ultraviolet and X-ray Absorption Spectra of Pyridazine in Aqueous Solution. <i>Journal of Physical Chemistry A</i> , 2021, 125, 7198-7206.	2.5	7
9193	Microwave Heating of Liquid Crystals and Ethanol-Hexane Mixed Solution and Its Features (Review). , 0, , .		0
9194	An integrated computational pipeline for designing high-affinity nanobodies with expanded genetic codes. <i>Briefings in Bioinformatics</i> , 2021, 22, .	6.5	4
9195	Biphasic Proton Transport Mechanism for Uncoupling Proteins. <i>Journal of Physical Chemistry B</i> , 2021, 125, 9130-9144.	2.6	8



#	ARTICLE	IF	CITATIONS
9196	Contrasting Effects of Ionic Liquids of Varying Degree of Hydrophilicity on the Conformational and Interfacial Properties of a Globular Protein. <i>Journal of Physical Chemistry B</i> , 2021, 125, 9441-9453.	2.6	6
9197	Research on homogeneous nucleation and microstructure evolution of aluminium alloy melt. <i>Royal Society Open Science</i> , 2021, 8, 210501.	2.4	2
9198	A comprehensive characterization of novel CYP-BM3 homolog (CYP-BA) from <i>Bacillus aryabhatai</i> . <i>Enzyme and Microbial Technology</i> , 2021, 148, 109806.	3.2	0
9199	The structural basis of bacterial manganese import. <i>Science Advances</i> , 2021, 7, .	10.3	17
9200	Targeting the EGFR in cancer cells by fusion protein consisting of arazyme and third loop of TGF- $\alpha$ : an in silico study. <i>Journal of Biomolecular Structure and Dynamics</i> , 2022, 40, 11744-11757.	3.5	4
9201	A multiscale approach for bridging the gap between potency, efficacy, and safety of small molecules directed at membrane proteins. <i>Scientific Reports</i> , 2021, 11, 16580.	3.3	10
9202	Computational analysis of protein conformational heterogeneity. <i>Journal of Biomolecular Structure and Dynamics</i> , 2021, , 1-6.	3.5	0
9203	Differences in Gluco and Galacto Substrate-Binding Interactions in a Dual 6Pi <sup>2</sup> -Glucosidase/6Pi <sup>2</sup> -Galactosidase Glycoside Hydrolase 1 Enzyme from <i>Bacillus licheniformis</i> . <i>Journal of Chemical Information and Modeling</i> , 2021, 61, 4554-4570.	5.4	2
9204	Detection and Characterization of VIM-52, a New Variant of VIM-1 from a <i>Klebsiella pneumoniae</i> Clinical Isolate. <i>Antimicrobial Agents and Chemotherapy</i> , 2021, 65, e0266020.	3.2	2
9205	Hydrogen bonding rearrangement by a mitochondrial disease mutation in cytochrome <i>bc<sub>L</sub></i> perturbs heme <i>b<sub>L</sub></i> redox potential and spin state. <i>Proceedings of the National Academy of Sciences of the United States of America</i> , 2021, 118, .	7.1	4
9206	Allosteric regulation in CRISPR/Cas1-Cas2 protospacer acquisition mediated by DNA and Cas2. <i>Biophysical Journal</i> , 2021, 120, 3126-3137.	0.5	1
9208	Antimicrobial peptide induced colloidal transformations in bacteria-mimetic vesicles: Combining in silico tools and experimental methods. <i>Journal of Colloid and Interface Science</i> , 2021, 596, 352-363.	9.4	13
9209	Fusion pores with low conductance are cation selective. <i>Cell Reports</i> , 2021, 36, 109580.	6.4	3
9210	Identification and assessment of cardiolipin interactions with <i>E. coli</i> inner membrane proteins. <i>Science Advances</i> , 2021, 7, .	10.3	49
9211	<i>In Situ</i> Characterization of Dehydration during Ion Transport in Polymeric Nanochannels. <i>Journal of the American Chemical Society</i> , 2021, 143, 14242-14252.	13.7	89
9212	One-shot identification of SARS-CoV-2 RBD escape mutants using yeast screening. <i>Cell Reports</i> , 2021, 36, 109627.	6.4	35
9213	Inelastic contact behaviors of nanosized single-asperity and multi-asperity on $\hat{1}\pm$ -Fe surface: Molecular dynamic simulations. <i>International Journal of Mechanical Sciences</i> , 2021, 204, 106569.	6.7	12
9214	Water Dissolved in a Variety of Polymers Studied by Molecular Dynamics Simulation and a Theory of Solutions. <i>Journal of Physical Chemistry B</i> , 2021, 125, 9357-9371.	2.6	10

#	ARTICLE	IF	CITATIONS
9216	Machine-learning integrated glassy defect from an intricate configurational-thermodynamic-dynamic space. <i>Physical Review B</i> , 2021, 104, .	3.2	15
9217	Presence of a SARS-CoV-2 Protein Enhances Amyloid Formation of Serum Amyloid A. <i>Journal of Physical Chemistry B</i> , 2021, 125, 9155-9167.	2.6	27
9218	Molecular modeling and dynamics simulation of alcohol dehydrogenase enzyme from high efficacy cellulosic ethanol-producing yeast mutant strain <i>Pichia kudriavzevii</i> BGY1- $\Delta$ 3m. <i>Journal of Biomolecular Structure and Dynamics</i> , 2022, 40, 12022-12036.	3.5	4
9219	Investigating the property and strength of intermolecular interaction in saturated and unsaturated cyclic cations constructed ionic liquids. <i>Journal of Molecular Liquids</i> , 2021, 335, 116253.	4.9	5
9220	Unravelling the therapeutic potential of marine drugs as SARS-CoV-2 inhibitors: An insight from essential dynamics and free energy landscape. <i>Computers in Biology and Medicine</i> , 2021, 135, 104525.	7.0	7
9222	Molecular modeling prediction of albumin-based nanoparticles and experimental preparation, characterization, and in-vitro release kinetics of prednisolone from the nanoparticles. <i>Journal of Drug Delivery Science and Technology</i> , 2021, 64, 102588.	3.0	6
9223	The identification of novel inhibitors of human angiotensin-converting enzyme 2 and main protease of Sars-Cov-2: A combination of in silico methods for treatment of COVID-19. <i>Journal of Molecular Structure</i> , 2021, 1237, 130409.	3.6	11
9225	An alternate covalent form of platelet $\alpha$ IIb $\beta$ 3 integrin that resides in focal adhesions and has altered function. <i>Blood</i> , 2021, 138, 1359-1372.	1.4	8
9226	Binding of SEP-363856 within TAAR1 and the 5HT1A receptor: implications for the design of novel antipsychotic drugs. <i>Molecular Psychiatry</i> , 2022, 27, 88-94.	7.9	15
9227	Molecular mechanisms by which tetrahydrofuran affects CO <sub>2</sub> hydrate Growth: Implications for carbon storage. <i>Chemical Engineering Journal</i> , 2021, 418, 129423.	12.7	36
9228	Ethanol Blending to Improve Reverse Micelle Dispersivity in Supercritical CO <sub>2</sub> : A Molecular Dynamics Study. <i>Journal of Physical Chemistry B</i> , 2021, 125, 9621-9628.	2.6	9
9229	Highly selective carbon capture by novel graphene-carbon nanotube hybrids. <i>Molecular Simulation</i> , 2021, 47, 1326-1334.	2.0	2
9231	Factors underlying asymmetric pore dynamics of disaggregase and microtubule-severing AAA+ machines. <i>Biophysical Journal</i> , 2021, 120, 3437-3454.	0.5	12
9232	Spatially resolved free-energy contributions of $\Delta$ native fold and molten-globule-like Crambin. <i>Biophysical Journal</i> , 2021, 120, 3470-3482.	0.5	10
9233	Somatic genetic rescue of a germline ribosome assembly defect. <i>Nature Communications</i> , 2021, 12, 5044.	12.8	44
9234	Cryo-EM structure of PepT2 reveals structural basis for proton-coupled peptide and prodrug transport in mammals. <i>Science Advances</i> , 2021, 7, .	10.3	37
9236	Antitumor drugs effect on the stability of double-stranded DNA: steered molecular dynamics analysis. <i>Journal of Biomolecular Structure and Dynamics</i> , 2021, , 1-10.	3.5	0
9237	MD simulation and MM/PBSA identifies phytochemicals as bifunctional inhibitors of SARS-CoV-2. <i>Journal of Biomolecular Structure and Dynamics</i> , 2022, 40, 12048-12061.	3.5	5

#	ARTICLE	IF	CITATIONS
9238	Effects of Weak Nonspecific Interactions with ATP on Proteins. <i>Journal of the American Chemical Society</i> , 2021, 143, 11982-11993.	13.7	40
9239	Simulating PIP2-Induced Gating Transitions in Kir6.2 Channels. <i>Frontiers in Molecular Biosciences</i> , 2021, 8, 711975.	3.5	6
9240	Intramolecular hydrogen bonds in a single macromolecule: Strength in high vacuum versus liquid environments. <i>Nano Research</i> , 2022, 15, 1517-1523.	10.4	16
9241	Large-Scale Molecular Dynamics Simulations Reveal New Insights Into the Phase Transition Mechanisms in MIL-53(Al). <i>Frontiers in Chemistry</i> , 2021, 9, 718920.	3.6	15
9243	Two intermediate incommensurate phases in the molecular dissociation process of solid iodine under high pressure. <i>Physical Review Research</i> , 2021, 3, .	3.6	4
9244	Deciphering ion transport and ATPase coupling in the intersubunit tunnel of KdpFABC. <i>Nature Communications</i> , 2021, 12, 5098.	12.8	10
9245	Molecular dynamics simulations of the permeation and distribution of plasma ROS in aquaporin-1. <i>Physics of Plasmas</i> , 2021, 28, .	1.9	7
9246	Design of peptides with strong binding affinity to poly(methyl methacrylate) resin by use of molecular simulation-based materials informatics. <i>Polymer Journal</i> , 2021, 53, 1439-1449.	2.7	7
9247	Identification of Natural Inhibitors Against SARS-CoV-2 Drugable Targets Using Molecular Docking, Molecular Dynamics Simulation, and MM-PBSA Approach. <i>Frontiers in Cellular and Infection Microbiology</i> , 2021, 11, 730288.	3.9	46
9248	Context-dependent Cryptic Roles of Specific Residues in Substrate Selectivity of the UapA Purine Transporter. <i>Journal of Molecular Biology</i> , 2021, 433, 166814.	4.2	7
9249	Time-Lagged Independent Component Analysis of Random Walks and Protein Dynamics. <i>Journal of Chemical Theory and Computation</i> , 2021, 17, 5766-5776.	5.3	27
9251	Effect of Sodium Chloride on Internal Quasi-Liquid Layers in Ice I <sub>h</sub> . <i>Journal of Physical Chemistry C</i> , 2021, 125, 18526-18535.	3.1	5
9252	Large scale model lipid membrane movement induced by a cation switch. <i>Journal of Colloid and Interface Science</i> , 2021, 596, 297-311.	9.4	7
9253	Molecular Dynamics Study of Ion Transport in Polymer Electrolytes of All-Solid-State Li-Ion Batteries. <i>Micromachines</i> , 2021, 12, 1012.	2.9	8
9254	Pseudopotentials for coarse-grained cross-link-assisted modeling of protein structures. <i>Journal of Computational Chemistry</i> , 2021, 42, 2054-2067.	3.3	4
9255	Phytochemicals present in Indian ginseng possess potential to inhibit SARS-CoV-2 virulence: A molecular docking and MD simulation study. <i>Microbial Pathogenesis</i> , 2021, 157, 104954.	2.9	33
9256	Unveiling the inhibitory mechanism of peptidomimetic inhibitor against A $\beta$ 42 aggregation and protofibril disaggregation by molecular dynamics. <i>Journal of Molecular Liquids</i> , 2021, 335, 116474.	4.9	5
9257	Diffusion of silver in titanium nitride: Insights from density functional theory and molecular dynamics. <i>Applied Surface Science</i> , 2021, 556, 149738.	6.1	10

#	ARTICLE	IF	CITATIONS
9258	Independent Nontargeted Parallel Cascade Selection Molecular Dynamics (Ino-PaCS-MD) to Enhance the Conformational Sampling of Proteins. <i>Journal of Chemical Theory and Computation</i> , 2021, 17, 5933-5943.	5.3	2
9259	Ion dynamics and selectivity of Nav channels from molecular dynamics simulation. <i>Chemical Physics</i> , 2021, 548, 111245.	1.9	19
9262	New Force-Field for Organosilicon Molecules in the Liquid Phase. <i>ACS Physical Chemistry Au</i> , 2021, 1, 54-69.	4.0	5
9263	Guiding the Immune Response to a Conserved Epitope in MSP2, an Intrinsically Disordered Malaria Vaccine Candidate. <i>Vaccines</i> , 2021, 9, 855.	4.4	2
9265	Lysine Deacetylase Substrate Selectivity: A Dynamic Ionic Interaction Specific to KDAC8. <i>Biochemistry</i> , 2021, 60, 2524-2536.	2.5	6
9266	Liquid-Liquid Critical Point in Phosphorus. <i>Physical Review Letters</i> , 2021, 127, 080603.	7.8	28
9267	Signatures in SARS-CoV-2 spike protein conferring escape to neutralizing antibodies. <i>PLoS Pathogens</i> , 2021, 17, e1009772.	4.7	74
9268	Phase Behavior of Pure PSPC and PEGylated Multicomponent Lipid and Their Interaction with Paclitaxel: An All-Atom MD Study. <i>Langmuir</i> , 2021, 37, 10259-10271.	3.5	1
9269	Phenothiazines alter plasma membrane properties and sensitize cancer cells to injury by inhibiting annexin-mediated repair. <i>Journal of Biological Chemistry</i> , 2021, 297, 101012.	3.4	16
9270	Solvent-mediated forces in protein dielectrophoresis. <i>Electrophoresis</i> , 2021, 42, 2060-2069.	2.4	3
9271	Machine Learning Directed Optimization of Classical Molecular Modeling Force Fields. <i>Journal of Chemical Information and Modeling</i> , 2021, 61, 4400-4414.	5.4	29
9272	Complete reconstruction of dasatinib unbinding pathway from c-Src kinase by supervised molecular dynamics simulation method; assessing efficiency and trustworthiness of the method. <i>Journal of Biomolecular Structure and Dynamics</i> , 2022, 40, 12535-12545.	3.5	2
9273	Solvent-Assisted Li-Ion Transport and Structural Heterogeneity in Fluorinated Battery Electrolytes. <i>Journal of Physical Chemistry B</i> , 2021, 125, 10551-10561.	2.6	4
9274	The cryo-EM structure of the bd oxidase from <i>M. tuberculosis</i> reveals a unique structural framework and enables rational drug design to combat TB. <i>Nature Communications</i> , 2021, 12, 5236.	12.8	29
9275	Membrane-binding mechanism of the EEA1 FYVE domain revealed by multi-scale molecular dynamics simulations. <i>PLoS Computational Biology</i> , 2021, 17, e1008807.	3.2	9
9276	Interfacial Interactions in a Model Composite Material: Insights into the Phase Transition of the Magnetite Reinforced Poly(Vinylidene Fluoride) Systems by All-Atom Molecular Dynamics Simulation. <i>Journal of Physical Chemistry C</i> , 2021, 125, 21635-21644.	3.1	11
9277	The molecular-level understanding of the uptake of PFOS and its alternatives (6:2 Cl-PFESA and OBS) into phospholipid bilayers. <i>Journal of Hazardous Materials</i> , 2021, 417, 125991.	12.4	18
9279	Closer look into the structures of tetrabutylammonium bromide-glycerol-based deep eutectic solvents and their mixtures with water. <i>Journal of Molecular Liquids</i> , 2021, 338, 116676.	4.9	13

#	ARTICLE	IF	CITATIONS
9281	Dielectric relaxations of molten acetamide: dependence on the model interaction potentials and the effects of system size. <i>Journal of Chemical Sciences</i> , 2021, 133, 1.	1.5	5
9282	Structural basis for the hyperthermostability of an archaeal enzyme induced by succinimide formation. <i>Biophysical Journal</i> , 2021, 120, 3732-3746.	0.5	5
9283	Relaxation Times of Solid-like Polyelectrolyte Complexes of Varying pH and Water Content. <i>Macromolecules</i> , 2021, 54, 7765-7776.	4.8	14
9284	A Molecular Dynamics Simulations Study of the Influence of Prestrain on the Pop-In Behavior and Indentation Size Effect in Cu Single Crystals. <i>Materials</i> , 2021, 14, 5220.	2.9	10
9285	Interaction of DNA-Complexed Boron Nitride Nanotubes and Cosolvents Impacts Dispersion and Length Characteristics. <i>Langmuir</i> , 2021, 37, 10934-10944.	3.5	12
9286	Spontaneous transmembrane pore formation by short-chain synthetic peptide. <i>Biophysical Journal</i> , 2021, 120, 4557-4574.	0.5	6
9287	Specific Protein-Membrane Interactions Promote Packaging of Metallo- $\beta$ -Lactamases into Outer Membrane Vesicles. <i>Antimicrobial Agents and Chemotherapy</i> , 2021, 65, e0050721.	3.2	10
9289	Controlling the Substrate Specificity of an Enzyme through Structural Flexibility by Varying the Salt-Bridge Density. <i>Molecules</i> , 2021, 26, 5693.	3.8	3
9290	Structural and functional interactions between the $\text{Ca}^{2+}$ -, $\text{ATP}$ -, and caffeine-binding sites of skeletal muscle ryanodine receptor (RyR1). <i>Journal of Biological Chemistry</i> , 2021, 297, 101040.	3.4	13
9291	Boosting the conformational sampling by combining replica exchange with solute tempering and $\omega$ -sliced metadynamics. <i>Journal of Computational Chemistry</i> , 2021, 42, 2233-2240.	3.3	7
9292	Effects of Micellization Behavior on the Interfacial Adsorption in Binary Anionic/Nonionic Surfactant Systems: A Molecular Simulation Study. <i>Langmuir</i> , 2021, 37, 11835-11843.	3.5	6
9293	Adsorption of Phosphate Ions on the Basal and Edge Surfaces of Kaolinite in Low Salt Aqueous Solutions Using Molecular Dynamics Simulations. <i>Journal of Physical Chemistry C</i> , 2021, 125, 21179-21190.	3.1	17
9294	Impact of Lipid Peroxidation on the Response of Cell Membranes to High-Speed Equibiaxial Stretching: A Computational Study. <i>Journal of Physical Chemistry B</i> , 2021, 125, 10736-10747.	2.6	3
9295	Delving into controversial dichotomy of direct and indirect mechanisms of Trehalose: In search of unanimous consensus. <i>Journal of Molecular Liquids</i> , 2021, 338, 116656.	4.9	5
9296	A Comprehensive Insight into the Mechanisms of Dopamine in Disrupting $\text{A}\beta$ Protofibrils and Inhibiting $\text{A}\beta$ Aggregation. <i>ACS Chemical Neuroscience</i> , 2021, 12, 4007-4019.	3.5	28
9298	Impact of Reactive Oxygen and Nitrogen Species Produced by Plasma on Mdm2-p53 Complex. <i>International Journal of Molecular Sciences</i> , 2021, 22, 9585.	4.1	5
9299	Predicting octanol/water partition coefficients using molecular simulation for the SAMPL7 challenge: comparing the use of neat and water saturated 1-octanol. <i>Journal of Computer-Aided Molecular Design</i> , 2021, 35, 1009-1024.	2.9	5
9300	Allosteric Inhibition of the Tumor-Promoting Interaction between AIMP2-DX2 and HSP70. <i>Journal of Pharmacology and Experimental Therapeutics</i> , 2021, 379, JPET-AR-2021-000766.	2.5	1

#	ARTICLE	IF	CITATIONS
9302	Phosphorylation of luminal region of the SUN-domain protein Mps3 promotes nuclear envelope localization during meiosis. <i>ELife</i> , 2021, 10, .	6.0	9
9303	TD-DFT absorption spectrum of (poly)threonine in water: A study combining molecular dynamics and quantum mechanics calculations. <i>Chemical Physics Letters</i> , 2021, 779, 138876.	2.6	4
9304	Effect of the Force Field on Molecular Dynamics Simulations of the Multidrug Efflux Protein P-Glycoprotein. <i>Journal of Chemical Theory and Computation</i> , 2021, 17, 6491-6508.	5.3	17
9305	The milk-derived lactoferrin inhibits V-ATPase activity by targeting its V1 domain. <i>International Journal of Biological Macromolecules</i> , 2021, 186, 54-70.	7.5	7
9306	Temperature Modulation of the DBDp53 Structure as Monitored by Static and Time-Resolved Fluorescence Combined with Molecular Dynamics Simulations. <i>Journal of Physical Chemistry B</i> , 2021, 125, 10166-10173.	2.6	2
9307	Comparing state-of-the-art approaches to back-calculate SAXS spectra from atomistic molecular dynamics simulations. <i>European Physical Journal B</i> , 2021, 94, 1.	1.5	12
9308	Membrane hydrophobicity determines the activation free energy of passive lipid transport. <i>Biophysical Journal</i> , 2021, 120, 3718-3731.	0.5	13
9310	ColBuilder: A server to build collagen fibril models. <i>Biophysical Journal</i> , 2021, 120, 3544-3549.	0.5	10
9311	Force Field Effects in Simulations of Flexible Peptides with Varying Polyproline II Propensity. <i>Journal of Chemical Theory and Computation</i> , 2021, 17, 6634-6646.	5.3	24
9312	Protein hydration shell formation: Dynamics of water in biological systems exhibiting nanoscopic cavities. <i>Journal of Molecular Liquids</i> , 2021, 337, 116584.	4.9	7
9313	Flexible model of water based on the dielectric and electromagnetic spectrum properties: TIP4P/ <math xmlns:mml="http://www.w3.org/1998/Math/MathML" altimg="si140.svg"><mml:mrow><mml:msub><mml:mrow><mml:mi>â~Š</mml:mi></mml:mrow><mml:mrow><mml:mi>mathvariant="italic">Flex</mml:mi></mml:mrow></mml:msub></mml:mrow></mml:math>. <i>Journal of Molecular Liquids</i> , 2021, 338, 116770.	4.9	3
9314	Molecular Insights on Successful Reconstitution of Freeze-Dried Nanofibrillated Cellulose Hydrogel. <i>ACS Applied Bio Materials</i> , 2021, 4, 7157-7167.	4.6	7
9315	Influence of external electric fields and temperature on the behavior of water and acetophenone molecules in C12OH242 chains: A molecular dynamics study. <i>Materials Today Communications</i> , 2021, 28, 102514.	1.9	0
9316	Molecular Simulation Studies on the Interactions of Bilirubin at Different States with a Lipid Bilayer. <i>Langmuir</i> , 2021, 37, 11707-11715.	3.5	4
9317	Conformational Fluctuations in GTP-Bound K-Ras: A Metadynamics Perspective with Harmonic Linear Discriminant Analysis. <i>Journal of Chemical Information and Modeling</i> , 2021, 61, 5212-5222.	5.4	13
9319	Peptide based nano-drug candidate for cancer treatment: Preparation, characterization, in vitro and in silico evaluation. <i>Journal of Molecular Structure</i> , 2021, 1240, 130573.	3.6	4
9320	A comparison of three DFT exchangeâ€“correlation functionals and two basis sets for the prediction of the conformation distribution of hydrated polyglycine. <i>Journal of Chemical Physics</i> , 2021, 155, 094104.	3.0	6
9321	Role of intercalated water in calcium hydroxide interlayers for carbonation reaction. <i>Chemical Engineering Journal</i> , 2021, 420, 130422.	12.7	8



#	ARTICLE	IF	CITATIONS
9322	The role of SAXS and molecular simulations in 3D structure elucidation of a DNA aptamer against lung cancer. <i>Molecular Therapy - Nucleic Acids</i> , 2021, 25, 316-327.	5.1	14
9323	Synthesis, in vitro biological investigation, and molecular dynamics simulations of thiazolopyrimidine based compounds as corticotrophin releasing factor receptor-1 antagonists. <i>Bioorganic Chemistry</i> , 2021, 114, 105079.	4.1	2
9324	Molecular Basis of Artemisinin Derivatives Inhibition of Myeloid Differentiation Protein 2 by Combined in Silico and Experimental Study. <i>Molecules</i> , 2021, 26, 5698.	3.8	2
9325	Endothelial TRP channels and cannabinoid receptors are involved in affinin-induced vasodilation. <i>FÄ-toterapÄ-Ä¢</i> , 2021, 153, 104985.	2.2	3
9326	Epistatic interactions promote persistence of NS3-Q80K inÄHCV infection by compensating for protein folding instability. <i>Journal of Biological Chemistry</i> , 2021, 297, 101031.	3.4	2
9327	Rational Design of Nonbonded Point Charge Models for Highly Charged Metal Cations with Lennard-Jones 12-6 Potential. <i>Journal of Chemical Information and Modeling</i> , 2021, 61, 4613-4629.	5.4	5
9328	Noncovalent Interactions with PAMAM and PPI Dendrimers Promote the Cellular Uptake and Photodynamic Activity of Rose Bengal: The Role of the Dendrimer Structure. <i>Journal of Medicinal Chemistry</i> , 2021, 64, 15758-15771.	6.4	11
9330	Cyclodextrin dimers: A versatile approach to optimizing encapsulation and their application to therapeutic extraction of toxic oxysterols. <i>International Journal of Pharmaceutics</i> , 2021, 606, 120522.	5.2	10
9331	Cooperative Oxide-Ion Transport in Pyrochlore $Y_{2-x}Ti_{2-x}O_{7-x}$ : A First-Principles Molecular Dynamics Study. <i>Journal of Physical Chemistry C</i> , 2021, 125, 20460-20467.	3.1	3
9332	Cation isomerism effect on micellization of pyridinium based surface-active ionic liquids. <i>Journal of Molecular Liquids</i> , 2021, 337, 116353.	4.9	8
9333	ChargeÄ€Transfer Effects of Organic Ligands on Energy Storage Performance of Oxide NanoparticleÄ€Based Electrodes. <i>Advanced Functional Materials</i> , 2022, 32, 2106438.	14.9	9
9334	How Long are Polymer Chains in Poly(3,4-ethylenedioxythiophene):Tosylate Films? An Insight from Molecular Dynamics Simulations. <i>Journal of Physical Chemistry B</i> , 2021, 125, 10324-10334.	2.6	10
9335	Structure-based virtual screening and molecular dynamics simulation for the identification of sphingosine kinase-2 inhibitors as potential analgesics. <i>Journal of Biomolecular Structure and Dynamics</i> , 2022, 40, 12472-12490.	3.5	8
9336	Identification of CDK7 Inhibitors from Natural Sources Using Pharmacoinformatics and Molecular Dynamics Simulations. <i>Biomedicines</i> , 2021, 9, 1197.	3.2	10
9337	Combination of molecular dynamics simulation, COSMO-RS, and experimental study to understand extraction of naphthenic acid. <i>Separation and Purification Technology</i> , 2022, 280, 119810.	7.9	20
9338	Exploring the factors that affect the themostability of barley limit dextrinase Ä€ Inhibitor complex. <i>Journal of Molecular Graphics and Modelling</i> , 2021, 109, 108043.	2.4	3
9339	Plasma membrane phospholipid signature recruits the plant exocyst complex via the EXO70A1 subunit. <i>Proceedings of the National Academy of Sciences of the United States of America</i> , 2021, 118, .	7.1	40
9340	Thermal transport and phase transitions of zirconia by on-the-fly machine-learned interatomic potentials. <i>Npj Computational Materials</i> , 2021, 7, .	8.7	57

#	ARTICLE	IF	CITATIONS
9341	Acrylic Paints: An Atomistic View of Polymer Structure and Effects of Environmental Pollutants. Journal of Physical Chemistry B, 2021, 125, 10854-10865.	2.6	11
9342	Effect of pH and temperature on the aggregation behaviour of dirhamnolipid biosurfactant. An experimental and molecular dynamics study. Journal of Colloid and Interface Science, 2021, 597, 160-170.	9.4	8
9343	Identification of potential plant bioactive as SARS-CoV-2 Spike protein and human ACE2 fusion inhibitors. Computers in Biology and Medicine, 2021, 136, 104631.	7.0	75
9344	Understanding the molecular interaction of SARS-CoV-2 spike mutants with ACE2 (angiotensin) Tj ETQq1 1 0.784314 rgBT /Qyerlock 10	3.5	19
9346	Comparative analysis of the unbinding pathways of antiviral drug Indinavir from HIV and HTLV1 proteases by supervised molecular dynamics simulation. PLoS ONE, 2021, 16, e0257916.	2.5	4
9347	Structure and dynamics of liquid linear and cyclic alkanes: a molecular dynamics study. Fluid Phase Equilibria, 2021, , 113237.	2.5	5
9349	How phosphorylation of peptides affects their interaction with 14â€³â€³<i>Î</i> domains. Proteins: Structure, Function and Bioinformatics, 2022, 90, 351-362.	2.6	5
9350	A molecular insight into poly(methyl methacrylate) impregnation with mefenamic acid in supercritical carbon dioxide: A computational simulation. Journal of Molecular Liquids, 2021, 337, 116424.	4.9	4
9351	Evidence that specific interactions play a role in the cholesterol sensitivity of G protein-coupled receptors. Biochimica Et Biophysica Acta - Biomembranes, 2021, 1863, 183557.	2.6	9
9352	Interplay of lipid and surfactant: Impact on nanoparticle structure. Journal of Colloid and Interface Science, 2021, 597, 278-288.	9.4	12
9353	Conformational changes and binding property of the periplasmic binding protein BtuF during vitamin B12 transport revealed by collision-induced unfolding, hydrogen-deuterium exchange mass spectrometry and molecular dynamic simulation. International Journal of Biological Macromolecules, 2021, 187, 350-360.	7.5	2
9355	Exploring EZH2-Proteasome Dual-Targeting Drug Discovery through a Computational Strategy to Fight Multiple Myeloma. Molecules, 2021, 26, 5574.	3.8	2
9356	Methylammonium Triiodide for Defect Engineering of High-Efficiency Perovskite Solar Cells. ACS Energy Letters, 2021, 6, 3650-3660.	17.4	28
9357	Accurate Binding Configuration Prediction of a G-Protein-Coupled Receptor to Its Antagonist Using Multicanonical Molecular Dynamics-Based Dynamic Docking. Journal of Chemical Information and Modeling, 2021, 61, 5161-5171.	5.4	10
9358	Conformational Properties of Glycosaminoglycan Disaccharides: A Molecular Dynamics Study. Journal of Physical Chemistry B, 2021, 125, 10900-10916.	2.6	14
9359	Coarseâ€³Grained Molecular Simulation of Polymers Supported by the Use of the SAFTâ€³\$gamma\$ Mie Equation of State. Macromolecular Theory and Simulations, 2022, 31, 2100031.	1.4	7
9360	Accurate and Transferable Reactive Molecular Dynamics Models from Constrained Density Functional Theory. Journal of Physical Chemistry B, 2021, 125, 10471-10480.	2.6	11
9361	Rational design of hyperstable antibacterial peptides for food preservation. Npj Science of Food, 2021, 5, 26.	5.5	21

#	ARTICLE	IF	CITATIONS
9362	Role of cholesterol flip-flop in oxidized lipid bilayers. Biophysical Journal, 2021, 120, 4525-4535.	0.5	5
9363	Extracting free energies of counterion binding to polyelectrolytes by molecular dynamics simulations. Journal of Chemical Physics, 2021, 155, 114902.	3.0	3
9364	Identification of a small molecule splicing inhibitor targeting UHM domains. FEBS Journal, 2022, 289, 682-698.	4.7	8
9365	Hidden electrostatic energy contributions define dynamic allosteric communications within p53 during molecular recognition. Biophysical Journal, 2021, 120, 4512-4524.	0.5	5
9366	Interactions of Truncated Menaquinones in Lipid Monolayers and Bilayers. International Journal of Molecular Sciences, 2021, 22, 9755.	4.1	3
9367	Identification of potential antileishmanial agents via structure-based molecular simulations. Journal of Molecular Graphics and Modelling, 2021, 110, 108039.	2.4	3
9369	Predicted Structure of Fully Activated Tas1R3/1R3 <sup>2</sup> Homodimer Bound to G Protein and Natural Sugars: Structural Insights into G Protein Activation by a Class C Sweet Taste Homodimer with Natural Sugars. Journal of the American Chemical Society, 2021, 143, 16824-16838.	13.7	6
9370	Temperature-Dependent Conformational Evolution of SARS CoV-2 RNA Genome Using Network Analysis. Journal of Physical Chemistry B, 2021, 125, 10672-10681.	2.6	3
9371	Influence of water models on water movement through AQP1. Journal of Chemical Physics, 2021, 155, 154502.	3.0	6
9372	Î2-Hairpin Peptide Mimics Decrease Human Islet Amyloid Polypeptide (hIAPP) Aggregation. Frontiers in Cell and Developmental Biology, 2021, 9, 729001.	3.7	6
9374	Unraveling the permeation of reactive species across nitrated membranes by computer simulations. Computers in Biology and Medicine, 2021, 136, 104768.	7.0	7
9375	Phase separation and toxicity of C9orf72 poly(PR) depends on alternate distribution of arginine. Journal of Cell Biology, 2021, 220, .	5.2	21
9376	In silico study of levodopa in hydrated lipid bilayers at the atomistic level. Journal of Molecular Graphics and Modelling, 2021, 107, 107972.	2.4	4
9378	Abrogating the nsp10 <sup>1</sup> –nsp16 switching mechanisms in SARS-CoV-2 by phytochemicals from Withania somnifera: a molecular dynamics study. Molecular Simulation, 0, , 1-9.	2.0	1
9379	Electronic transport through odd-even methylenic spacers connected to an aromatic ring. Computational Materials Science, 2021, 197, 110596.	3.0	2
9380	Automated Coarse-Grained Mapping Algorithm for the Martini Force Field and Benchmarks for Membrane–Water Partitioning. Journal of Chemical Theory and Computation, 2021, 17, 5777-5791.	5.3	35
9381	Fenugreek steroidal saponins hinder osteoclastogenic bone resorption by targeting CSF-1R which diminishes the RANKL/OPG ratio. International Journal of Biological Macromolecules, 2021, 186, 351-364.	7.5	17
9382	pH-Dependent Conformations of an Antimicrobial Spider Venom Peptide, Cupiennin 1a, from Unbiased HREMD Simulations. ACS Omega, 2021, 6, 24166-24175.	3.5	2

#	ARTICLE	IF	CITATIONS
9383	Effects of surface nanostructure and wettability on pool boiling: A molecular dynamics study. International Journal of Thermal Sciences, 2021, 167, 106980.	4.9	36
9384	Computational and biochemical analysis of type IV pilus dynamics and stability. Structure, 2021, 29, 1397-1409.e6.	3.3	5
9385	Molecular Dynamics Simulations and Experimental Results Provide Insight into Clinical Performance Differences between Sandimmune® and Neoral® Lipid-Based Formulations. Pharmaceutical Research, 2021, 38, 1531-1547.	3.5	3
9386	Different connection models of icosahedral structures in TiAl alloy caused by the cooling rates. Physica Status Solidi (B): Basic Research, 0, , 2100083.	1.5	0
9387	Integrin-based mechanosensing through conformational deformation. Biophysical Journal, 2021, 120, 4349-4359.	0.5	10
9389	Adsorption of industrial dyes on functionalized and nonfunctionalized asphaltene: A combined molecular dynamics and quantum mechanics study. Journal of Molecular Liquids, 2021, 337, 116433.	4.9	20
9390	Spontaneously formed nanostructures in double perovskite rare-earth tantalates for thermal barrier coatings. Acta Materialia, 2021, 216, 117152.	7.9	13
9391	Stimuli-Responsive Self-Assembly of $\pi$ -Conjugated Liquids Triggers Circularly Polarized Luminescence. ACS Applied Materials & Interfaces, 2021, 13, 47127-47133.	8.0	10
9392	Deciphering the competitive inhibition of dihydropteroate synthase by 8 mercaptoguanine analogs: enhanced potency in phenylsulfonyl fragments. Journal of Biomolecular Structure and Dynamics, 2021, , 1-20.	3.5	3
9393	Subdiffusive-Brownian crossover in membrane proteins: a Generalized Langevin Equation-based approach. Biophysical Journal, 2021, 120, 4722-4737.	0.5	6
9394	Regulatory Approved Monoclonal Antibodies Contain Framework Mutations Predicted From Human Antibody Repertoires. Frontiers in Immunology, 2021, 12, 728694.	4.8	7
9395	Atypical kinetics of cytochrome P450 2J2: Epoxidation of arachidonic acid and reversible inhibition by xenobiotic inhibitors. European Journal of Pharmaceutical Sciences, 2021, 164, 105889.	4.0	9
9396	Boosted activity by engineering the enzyme microenvironment in cascade reaction: A molecular understanding. Synthetic and Systems Biotechnology, 2021, 6, 163-172.	3.7	6
9397	Dynamic Interactions of Fully Glycosylated SARS-CoV-2 Spike Protein with Various Antibodies. Journal of Chemical Theory and Computation, 2021, 17, 6559-6569.	5.3	13
9398	Multifunctional inhibitors of SARS-CoV-2 by MM/PBSA, essential dynamics, and molecular dynamic investigations. Journal of Molecular Graphics and Modelling, 2021, 107, 107969.	2.4	21
9399	Direct Calculation of Entropic Components in Cohesive Interaction Free Energies. Journal of Physical Chemistry B, 2021, 125, 11026-11035.	2.6	2
9400	Penetration of Chitosan into the Single Walled Armchair Carbon Nanotubes: Atomic Scale Insight. Crystals, 2021, 11, 1174.	2.2	4
9401	Molecular mechanism of ATP and RNA binding to Zika virus NS3 helicase and identification of repurposed drugs using molecular dynamics simulations. Journal of Biomolecular Structure and Dynamics, 2022, 40, 12642-12659.	3.5	3

#	ARTICLE	IF	CITATIONS
9402	Relative Affinities of Proteinâ€“Cholesterol Interactions from Equilibrium Molecular Dynamics Simulations. <i>Journal of Chemical Theory and Computation</i> , 2021, 17, 6548-6558.	5.3	21
9404	CG2AT2: an Enhanced Fragment-Based Approach for Serial Multi-scale Molecular Dynamics Simulations. <i>Journal of Chemical Theory and Computation</i> , 2021, 17, 6472-6482.	5.3	64
9405	Probing allosteric regulations with coevolution-driven molecular simulations. <i>Science Advances</i> , 2021, 7, eabj0786.	10.3	8
9406	Structural significance of Neprylsin from <i>Streptococcus suis</i> GZ1 in the degradation of AÎ² peptides, a causative agent in Alzheimer's disease. <i>Computers in Biology and Medicine</i> , 2021, 136, 104691.	7.0	7
9407	The cooperative binding of TDP-43 to GU-rich RNA repeats antagonizes TDP-43 aggregation. <i>ELife</i> , 2021, 10, .	6.0	35
9409	Water molecules in CNTâ€“Si3N4 membrane: Properties and the separation effect for waterâ€“alcohol solution. <i>Journal of Chemical Physics</i> , 2021, 155, 104701.	3.0	1
9411	Investigation of water-mediated intermolecular interactions with the adaptive resolution simulation technique. <i>Journal of Physics Condensed Matter</i> , 2022, 34, 115101.	1.8	3
9412	Using Neural Network Force Fields to Ascertain the Quality of <i>Ab Initio</i> Simulations of Liquid Water. <i>Journal of Physical Chemistry B</i> , 2021, 125, 10772-10778.	2.6	13
9413	Molecular dynamics study on the shear strain induced martensite-like transformation between rutile and Î±-PbO2 phase of titanium dioxide. <i>Journal of Alloys and Compounds</i> , 2021, 878, 160452.	5.5	1
9414	Novel cytotoxic amphiphilic nitro-compounds derived from a synthetic route for paraconic acids. <i>Colloids and Surfaces A: Physicochemical and Engineering Aspects</i> , 2021, 626, 126984.	4.7	6
9415	Free energy convergence in short- and long-length hydrophobic hydration. <i>Journal of Molecular Liquids</i> , 2021, 339, 116699.	4.9	10
9416	Physalin pool from <i>Physalis angulata</i> L. leaves and physalin D inhibit P2X7 receptor function in vitro and acute lung injury in vivo. <i>Biomedicine and Pharmacotherapy</i> , 2021, 142, 112006.	5.6	12
9417	Machine learning atomic-scale stiffness in metallic glass. <i>Extreme Mechanics Letters</i> , 2021, 48, 101446.	4.1	19
9418	Classical molecular dynamics simulations of the deformation of metals under uniaxial monotonic loading: A review. <i>Computers and Structures</i> , 2021, 254, 106614.	4.4	23
9419	A molecular dynamics simulations study of the ionic liquid effect on the Î²-glucosidase active site interactions with a flavonoid glycoside. <i>Journal of Molecular Liquids</i> , 2021, 340, 117115.	4.9	5
9420	FPMD studies on the microstructures and transport properties of molten MgCl2-NaCl-KCl with addition of active metals. <i>Solar Energy Materials and Solar Cells</i> , 2021, 232, 111351.	6.2	5
9421	Inhomogeneity of polylysine adsorption layers on lipid membranes revealed by theoretical analysis of electrokinetic data and molecular dynamics simulations. <i>Bioelectrochemistry</i> , 2021, 141, 107828.	4.6	3
9422	Spectroscopic and computational insight into the conformational dynamics of hemoglobin in the presence of vitamin B12. <i>International Journal of Biological Macromolecules</i> , 2021, 189, 306-315.	7.5	12

#	ARTICLE	IF	CITATIONS
9423	Diffusion Behavior of Methane in 3D Kerogen Models. Energy & Fuels, 0, , .	5.1	10
9424	Calculation of diffusion coefficients of pesticides by employing molecular dynamics simulations. Journal of Molecular Liquids, 2021, 340, 117106.	4.9	10
9425	Interactions of chlorogenic acid and isochlorogenic acid A with model lipid bilayer membranes: Insights from molecular dynamics simulations. Chemistry and Physics of Lipids, 2021, 240, 105136.	3.2	3
9426	Role of hydrogen bonding in wheat gluten protein systems plasticized with glycerol and water. Polymer, 2021, 232, 124149.	3.8	24
9427	Effects of Distal Mutations on Ligand-Binding Affinity in <i>E. coli</i> Dihydrofolate Reductase. ACS Omega, 2021, 6, 26065-26076.	3.5	2
9428	Molecular dynamics of fluoromethane type I hydrates. Journal of Molecular Liquids, 2021, 339, 116720.	4.9	6
9429	Hydroxylic, sulfur-containing and amidic amino acids in water solution: Atomic charges parameters for computational modeling using molecular dynamics simulation and DFT calculations. Journal of Molecular Liquids, 2021, 339, 116815.	4.9	6
9430	Prioritization of potential vaccine candidates and designing a multiepitope-based subunit vaccine against multidrug-resistant Salmonella Typhi str. CT18: A subtractive proteomics and immunoinformatics approach. Microbial Pathogenesis, 2021, 159, 105150.	2.9	15
9431	Computational and experimental characterization of isomers of escin-induced renal cytotoxicity by inhibiting heat shock proteins. European Journal of Pharmacology, 2021, 908, 174372.	3.5	4
9432	Integrating electronic properties of Prodan by parameterization: Combining theory with experimentation. Journal of Molecular Structure, 2021, 1241, 130639.	3.6	1
9433	Surfactant desorption and scission free energies for cylindrical and spherical micelles from umbrella-sampling molecular dynamics simulations. Journal of Colloid and Interface Science, 2021, 599, 773-784.	9.4	12
9434	Cellulose-hemicellulose interactions - A nanoscale view. Carbohydrate Polymers, 2021, 270, 118364.	10.2	41
9435	Amorphous boron phosphide: An ab initio investigation. Journal of Non-Crystalline Solids, 2021, 570, 121006.	3.1	2
9436	Effects of hydrophobic solute on water normal modes. Chemical Physics, 2021, 550, 111303.	1.9	2
9437	Structural and functional variation of chitin-binding domains of a lytic polysaccharide monooxygenase from <i>Cellvibrio japonicus</i> . Journal of Biological Chemistry, 2021, 297, 101084.	3.4	16
9438	Molecular dynamics simulations of the effects of lipid oxidation on the permeability of cell membranes. Bioelectrochemistry, 2021, 141, 107869.	4.6	23
9439	Design and synthesis of polyacrylic acid/deoxycholic acid-modified chitosan copolymer and a close inspection of human growth hormone-copolymer interactions: An experimental and computational study. Colloids and Surfaces B: Biointerfaces, 2021, 206, 111956.	5.0	4
9440	Structural Basis for Silicic Acid Uptake by Higher Plants. Journal of Molecular Biology, 2021, 433, 167226.	4.2	18



#	ARTICLE	IF	CITATIONS
9441	Computational investigation of novel farnesyltransferase inhibitors using 3D-QSAR pharmacophore modeling, virtual screening, molecular docking and molecular dynamics simulation studies: A new insight into cancer treatment. <i>Journal of Molecular Structure</i> , 2021, 1241, 130667.	3.6	12
9442	Insights into the Molecular-Level details of betaine interactions with Laccase under various thermal conditions. <i>Journal of Molecular Liquids</i> , 2021, 339, 116832.	4.9	6
9443	The cooperative effect between cyclic naphthenic acids and surfactant enhances the separation efficiency. <i>Journal of Molecular Liquids</i> , 2021, 342, 117577.	4.9	4
9444	Revertant mutation V48G alters conformational dynamics of highly drug resistant HIV protease PRS17. <i>Journal of Molecular Graphics and Modelling</i> , 2021, 108, 108005.	2.4	1
9445	Cholesterol plays a decisive role in tetraspanin assemblies during bilayer deformations. <i>BioSystems</i> , 2021, 209, 104505.	2.0	4
9446	Study of lipid heterogeneity on bilayer membranes using molecular dynamics simulations. <i>Journal of Molecular Graphics and Modelling</i> , 2021, 108, 108000.	2.4	5
9447	Dissimilar action of tamoxifen and 4-hydroxytamoxifen on phosphatidylcholine model membranes. <i>Biophysical Chemistry</i> , 2021, 278, 106681.	2.8	1
9448	Molecular simulation of separation of gadolinium ions from aqueous waste using directional solvent extraction. <i>Journal of Molecular Liquids</i> , 2021, 341, 117330.	4.9	5
9449	High-salinity brine desalination with amine-based temperature swing solvent extraction: A molecular dynamics study. <i>Journal of Molecular Liquids</i> , 2021, 341, 117359.	4.9	14
9450	Laminar peptide structure: Energetic and structural evaluation using molecular dynamics. <i>Journal of Molecular Liquids</i> , 2021, 341, 117261.	4.9	4
9451	Expression, solubility monitoring, and purification of the co-folded LUBAC LTM domain by structure-guided tandem folding in autoinducing cultures. <i>Protein Expression and Purification</i> , 2021, 187, 105953.	1.3	3
9452	Thermodynamic and structural description of relative solubility of the flavonoid rutin by DFT calculations and molecular dynamics simulations. <i>Journal of Molecular Liquids</i> , 2021, 341, 117214.	4.9	8
9453	Interplay between human islet amyloid polypeptide aggregates and micro-heterogeneous membranes. <i>Biochimica Et Biophysica Acta - Biomembranes</i> , 2021, 1863, 183691.	2.6	3
9454	Molecular dynamics simulations support the hypothesis that the brGDGT paleothermometer is based on homeoviscous adaptation. <i>Geochimica Et Cosmochimica Acta</i> , 2021, 312, 44-56.	3.9	28
9455	Design and analysis of interactions in ionic liquids based on procaine and pharmaceutically active anions. <i>European Journal of Pharmaceutical Sciences</i> , 2021, 166, 105966.	4.0	9
9456	Structural and functional changes of catalase through interaction with Erlotinib hydrochloride. Use of Chou's 5-steps rule to study mechanisms. <i>Spectrochimica Acta - Part A: Molecular and Biomolecular Spectroscopy</i> , 2021, 260, 119940.	3.9	16
9457	Development of a molecular imprinted electrochemiluminescence sensor for amitriptyline detection: From MD simulations to experimental implementation. <i>Electrochimica Acta</i> , 2021, 397, 139273.	5.2	8
9458	Heavy radiation damage in alpha zirconium at cryogenic temperature: A computational study. <i>Journal of Nuclear Materials</i> , 2021, 555, 153159.	2.7	10

#	ARTICLE	IF	CITATIONS
9459	Assessment of the classical nucleation theory in supercooled nickel by molecular dynamics. <i>Materials Chemistry and Physics</i> , 2021, 272, 125011.	4.0	5
9460	Ripple-like instability in the simulated gel phase of finite size phosphocholine bilayers. <i>Biochimica Et Biophysica Acta - Biomembranes</i> , 2021, 1863, 183714.	2.6	6
9461	Receptor based virtual screening of potential novel inhibitors of tigar [TP53 (tumour protein) Tj ETQq0 0 0 rgBT /Overlock 10 Tf 50 662	1.5	1
9462	Evaluation of chloroquine and hydroxychloroquine as ACE-2 Inhibitors By In Silico Approaches: Cardiac Arrhythmia Cause?. <i>Journal of Molecular Structure</i> , 2021, 1244, 130946.	3.6	3
9463	Comparative analysis of non structural protein 1 of SARS-CoV2 with SARS-CoV1 and MERS-CoV: An in silico study. <i>Journal of Molecular Structure</i> , 2021, 1243, 130854.	3.6	10
9464	Identification of new alpha-synuclein fibrillogenesis inhibitor using in silico structure-based virtual screening. <i>Journal of Molecular Graphics and Modelling</i> , 2021, 108, 108010.	2.4	8
9465	Enhancing plasticity in high-entropy refractory ceramics via tailoring valence electron concentration. <i>Materials and Design</i> , 2021, 209, 109932.	7.0	32
9466	Carrageenan molecule conformations and electrokinetic properties in electrolyte solutions: Modeling and experimental measurements. <i>Food Hydrocolloids</i> , 2021, 121, 107033.	10.7	5
9467	Computational design of a minimal "protein-like" conjugate for potent membrane poration. <i>Giant</i> , 2021, 8, 100071.	5.1	4
9468	Effect of B2O3 on the structure of CaO-Al2O3-B2O3 ternary melts: A molecular dynamics simulation. <i>Journal of Non-Crystalline Solids</i> , 2021, 574, 121141.	3.1	11
9469	3CLpro and PLpro affinity, a docking study to fight COVID19 based on 900 compounds from PubChem and literature. Are there new drugs to be found?. <i>Journal of Molecular Structure</i> , 2021, 1245, 130968.	3.6	15
9470	From virtual screening hits targeting a cryptic pocket in BACE-1 to a nontoxic brain permeable multitarget anti-Alzheimer lead with disease-modifying and cognition-enhancing effects. <i>European Journal of Medicinal Chemistry</i> , 2021, 225, 113779.	5.5	7
9471	Biochemical and biophysical characterization of the RVB-1/RVB-2 protein complex, the RuvBL/RVB homologues in <i>Neurospora crassa</i> . <i>Biochimie</i> , 2021, 191, 11-26.	2.6	1
9472	Tuning force field parameters of ionic liquids using machine learning techniques. <i>Computational Materials Science</i> , 2021, 200, 110759.	3.0	5
9473	Formation of a very high-density amorphous phase of carbon and its crystallization into a simple cubic structure at high pressure. <i>Computational Materials Science</i> , 2021, 200, 110822.	3.0	1
9474	Removal of phenazopyridine as a pharmacological contaminant using nanoporous metal/covalent-organic frameworks (MOF/COF) adsorbent. <i>Applied Materials Today</i> , 2021, 25, 101196.	4.3	8
9475	Aggregation versus inclusion complexes to solubilize drugs with cyclodextrins. A case study using sulphobutylether- $\beta$ -cyclodextrins and remdesivir. <i>Journal of Molecular Liquids</i> , 2021, 343, 117588.	4.9	12
9476	Interaction of multicomponent anionic liposomes with cationic pyridylphenylene dendrimer: Does the complex behavior depend on the liposome composition?. <i>Biochimica Et Biophysica Acta - Biomembranes</i> , 2021, 1863, 183761.	2.6	5

#	ARTICLE	IF	CITATIONS
9477	Modelling peptide adsorption energies on gold surfaces with an effective implicit solvent and surface model. <i>Journal of Colloid and Interface Science</i> , 2022, 605, 493-499.	9.4	3
9478	Effect of Rosa Roxburghii juice on starch digestibility: A focus on the binding of polyphenols to amylose and porcine pancreatic Î±-amylase by molecular modeling. <i>Food Hydrocolloids</i> , 2022, 123, 106966.	10.7	21
9479	Molecular aspects of temperature swing solvent extraction for brine desalination using imidazole-based solvents. <i>Chemical Engineering Science</i> , 2022, 247, 116866.	3.8	12
9480	Molecular behavior of CO2 hydrate growth in the presence of dissolvable ionic organics. <i>Chemical Engineering Journal</i> , 2022, 428, 131176.	12.7	36
9481	Polystyrene perturbs the structure, dynamics, and mechanical properties of DPPC membranes: An experimental and computational study. <i>Journal of Colloid and Interface Science</i> , 2022, 605, 110-119.	9.4	15
9482	Modelling the adsorption of proteins to nanoparticles at the solid-liquid interface. <i>Journal of Colloid and Interface Science</i> , 2022, 605, 286-295.	9.4	9
9483	Molecular dynamics study of droplet electrocoalescence in the oil phase and the gas phase. <i>Separation and Purification Technology</i> , 2021, 278, 119622.	7.9	17
9484	Comparative Study of Interactions between Human cGAS and Inhibitors: Insights from Molecular Dynamics and MM/PBSA Studies. <i>International Journal of Molecular Sciences</i> , 2021, 22, 1164.	4.1	3
9486	Molecular Dynamics Simulations of Î±-FLAG-hIFNÎ³ Fusion Glycoproteins. <i>Studies in Computational Intelligence</i> , 2021, , 256-267.	0.9	0
9487	Investigating the lipid fingerprint of SLC6 neurotransmitter transporters: a comparison of dDAT, hDAT, hSERT, and GlyT2. <i>BBA Advances</i> , 2021, 1, 100010.	1.6	9
9488	Energy-dependent protein folding: modeling how a protein folding machine may work. <i>F1000Research</i> , 2021, 10, 3.	1.6	4
9489	Discovery of beta-lactamase CMY-10 inhibitors for combination therapy against multi-drug resistant Enterobacteriaceae. <i>PLoS ONE</i> , 2021, 16, e0244967.	2.5	19
9490	The food additive fast green FCF inhibits Î±-synuclein aggregation, disassembles mature fibrils and protects against amyloid-induced neurotoxicity. <i>Food and Function</i> , 2021, 12, 5465-5477.	4.6	14
9491	Shaking the Î²-Bulges. <i>IEEE/ACM Transactions on Computational Biology and Bioinformatics</i> , 2022, 19, 14-18.	3.0	3
9492	Aqueous TMAO solution under high hydrostatic pressure. <i>Physical Chemistry Chemical Physics</i> , 2021, 23, 11355-11365.	2.8	3
9493	SHP2 Nuclear/Cytoplasmic Trafficking in Granulosa Cells Is Essential for Oocyte Meiotic Resumption and Maturation. <i>Frontiers in Cell and Developmental Biology</i> , 2020, 8, 611503.	3.7	10
9494	Unveiling the phase behavior of C <sub>i</sub> E <sub>j</sub> non-ionic surfactants in water through coarse-grained molecular dynamics simulations. <i>Soft Matter</i> , 2021, 17, 5183-5196.	2.7	8
9495	Extending the timescale of molecular simulations by using time-temperature superposition: rheology of ionic liquids. <i>Soft Matter</i> , 2021, 17, 7210-7220.	2.7	8

#	ARTICLE	IF	CITATIONS
9496	Structural basis of trehalose recognition by the mycobacterial LpqY-SugABC transporter. <i>Journal of Biological Chemistry</i> , 2021, 296, 100307.	3.4	13
9497	Identification of multiple substrate binding sites in SLC4 transporters in the outward-facing conformation: Insights into the transport mechanism. <i>Journal of Biological Chemistry</i> , 2021, 296, 100724.	3.4	15
9498	<i>In silico</i> analysis of antiviral phytochemicals efficacy against Epstein-Barr virus glycoprotein H. <i>Journal of Biomolecular Structure and Dynamics</i> , 2022, 40, 5372-5385.	3.5	21
9499	Determining Partial Atomic Charges for Liquid Water: Assessing Electronic Structure and Charge Models. <i>Journal of Chemical Theory and Computation</i> , 2021, 17, 889-901.	5.3	15
9500	Enhanced Adsorption of Anionic Polymer on Montmorillonite by Divalent Cations and the Effect of Salinity. <i>Journal of Physical Chemistry A</i> , 2021, 125, 1025-1035.	2.5	9
9501	Molecular Resolution into the Nucleation and Crystal Growth of Clathrate Hydrates Formed from Methane and Propane Mixtures. <i>Crystal Growth and Design</i> , 2021, 21, 960-973.	3.0	14
9502	Fluid-Fluid Interfacial Effects in Multiphase Flow during Carbonated Waterflooding in Sandstone: Application of X-ray Microcomputed Tomography and Molecular Dynamics. <i>ACS Applied Materials &amp; Interfaces</i> , 2021, 13, 5731-5740.	8.0	7
9503	Mechanisms for $\sim 100\times$ interstitial dislocation loops to diffuse in BCC iron. <i>Nature Communications</i> , 2021, 12, 225.	12.8	22
9504	The importance of intramolecular hydrogen bonds on the translocation of the small drug piracetam through a lipid bilayer. <i>RSC Advances</i> , 2021, 11, 899-908.	3.6	39
9505	An Implementation of Replica Exchange with Dynamical Scaling for Efficient Large-Scale Simulations. <i>Journal of Chemical Information and Modeling</i> , 2021, 61, 810-818.	5.4	5
9506	Seipin traps triacylglycerols to facilitate their nanoscale clustering in the endoplasmic reticulum membrane. <i>PLoS Biology</i> , 2021, 19, e3000998.	5.6	54
9507	Multiscale modelling of charge transport in P3HT:DIPBI bulk heterojunction organic solar cells. <i>Physical Chemistry Chemical Physics</i> , 2021, 23, 12233-12250.	2.8	4
9508	Alchemical absolute protein-ligand binding free energies for drug design. <i>Chemical Science</i> , 2021, 12, 13958-13971.	7.4	48
9509	Inhibitor binding influences the protonation states of histidines in SARS-CoV-2 main protease. <i>Chemical Science</i> , 2021, 12, 1513-1527.	7.4	47
9510	Concentration effects on the self-assembly of tyrosine molecules. <i>Physical Chemistry Chemical Physics</i> , 2021, 23, 22620-22628.	2.8	5
9511	A generic force field for simulating native protein structures using dissipative particle dynamics. <i>Soft Matter</i> , 2021, 17, 9772-9785.	2.7	6
9512	Molecular Dynamics Simulation of the Stability Behavior of Graphene in Glycerol/Urea Solvents in Liquid-Phase Exfoliation. <i>Acta Chimica Sinica</i> , 2021, 79, 530.	1.4	1
9513	Unique and generic structural features of cholinium amino acid-based biocompatible ionic liquids. <i>Physical Chemistry Chemical Physics</i> , 2021, 23, 10662-10669.	2.8	14

#	ARTICLE	IF	CITATIONS
9514	Molecular Dynamics Applications in Packaging. , 2021, , 537-554.		0
9515	Transfer learning of memory kernels for transferable coarse-graining of polymer dynamics. Soft Matter, 2021, 17, 5864-5877.	2.7	15
9516	Extension of the CAVS model to the simulation of helical peptides in a membrane environment. Physical Chemistry Chemical Physics, 2021, 23, 12850-12863.	2.8	1
9517	Structural insights and molecular dynamics into the inhibitory mechanism of a Kunitz-type trypsin inhibitor from <i>Tamarindus indica</i> L. Journal of Enzyme Inhibition and Medicinal Chemistry, 2021, 36, 480-490.	5.2	9
9518	Computational studies of polyurethanases from <i>Pseudomonas</i> . Journal of Molecular Modeling, 2021, 27, 46.	1.8	4
9519	Surface modification of polyamide reverse osmosis membranes with small-molecule zwitterions for enhanced fouling resistance: a molecular simulation study. Physical Chemistry Chemical Physics, 2021, 23, 6623-6631.	2.8	7
9520	Inherent Dipole Layer Formation Driven by Surface Energy at Nonplanar Dielectric Interface. IEEE Transactions on Electron Devices, 2021, 68, 294-298.	3.0	1
9521	Methods of Computer Simulation. Soft and Biological Matter, 2021, , 131-193.	0.3	0
9522	Coarse-grained simulations uncover Gram-negative bacterial defense against polymyxins by the outer membrane. Computational and Structural Biotechnology Journal, 2021, 19, 3885-3891.	4.1	13
9523	NMR-Based Structural Characterization of a Two-Disulfide-Bonded Analogue of the FXIIIa Inhibitor Tridegin: New Insights into Structure–Activity Relationships. International Journal of Molecular Sciences, 2021, 22, 880.	4.1	4
9524	Block-copolymer-like self-assembly behavior of mobile-ligand grafted ultra-small nanoparticles. Soft Matter, 2021, 17, 5897-5906.	2.7	5
9525	Scrutiny of the mechanism of $\beta$ 2-amyloid protein captures HSV-2 to protect the brain infection. E3S Web of Conferences, 2021, 261, 02069.	0.5	0
9526	Computational studies of membrane pore formation induced by Pin2. Journal of Biomolecular Structure and Dynamics, 2022, 40, 5060-5068.	3.5	2
9527	Effects of surface contamination on the interfacial properties of CO <sub>2</sub> /water/calcite systems. Physical Chemistry Chemical Physics, 2021, 23, 18885-18892.	2.8	9
9528	Role of structural rigidity and collective behaviour in the molecular design of gas hydrate anti-agglomerants. Molecular Systems Design and Engineering, 2021, 6, 713-721.	3.4	11
9529	Native-like membrane models of <i>E. coli</i> polar lipid extract shed light on the importance of lipid composition complexity. BMC Biology, 2021, 19, 4.	3.8	33
9530	A novel chemical biology and computational approach to expedite the discovery of new-generation polymyxins against life-threatening <i>Acinetobacter baumannii</i> . Chemical Science, 2021, 12, 12211-12220.	7.4	13
9531	Computational prediction of the supramolecular self-assembling properties of organic molecules: the role of conformational flexibility of amide moieties. Physical Chemistry Chemical Physics, 2021, 23, 20453-20465.	2.8	2

#	ARTICLE	IF	CITATIONS
9532	Non-Ideality in Thymol + Menthol Type V Deep Eutectic Solvents. ACS Sustainable Chemistry and Engineering, 2021, 9, 2203-2211.	6.7	72
9533	Ligand Affinities within the Open-Boundary Molecular Mechanics/Coarse-Grained Framework (I): Alchemical Transformations within the Hamiltonian Adaptive Resolution Scheme. Journal of Physical Chemistry B, 2021, 125, 789-797.	2.6	2
9534	Self-Assembly of Silk-like Protein into Nanoscale Bicontinuous Networks under Phase-Separation Conditions. Biomacromolecules, 2021, 22, 690-700.	5.4	10
9535	In silico analysis of novel dipeptidyl peptidase-IV inhibitory peptides released from Macadamia integrifolia antimicrobial protein 2 (MiAMP2) and the possible pathways involved in diabetes protection. Current Research in Food Science, 2021, 4, 603-611.	5.8	20
9536	Ligand-decoration determines the translational and rotational dynamics of nanoparticles on a lipid bilayer membrane. Physical Chemistry Chemical Physics, 2021, 23, 9158-9165.	2.8	2
9537	Molecular Dynamics Simulations of Mitochondrial Uncoupling Protein 2. International Journal of Molecular Sciences, 2021, 22, 1214.	4.1	8
9538	Rapid and accurate estimation of protein-ligand relative binding affinities using site-identification by ligand competitive saturation. Chemical Science, 2021, 12, 8844-8858.	7.4	18
9539	Modulating the thermal and structural stability of gallene <i>via</i> variation of atomistic thickness. Nanoscale Advances, 2021, 3, 499-507.	4.6	10
9540	How stereochemistry of lipid components can affect lipid organization and the route of liposome internalization into cells. Nanoscale, 2021, 13, 11976-11993.	5.6	8
9541	Conformers, Properties of the Anticancer Drug Plocabulin, and its Binding Mechanism with p-Glycoprotein: DFT and MD Studies. Australian Journal of Chemistry, 2021, 74, 529.	0.9	0
9542	Aromatic side-chain flips orchestrate the conformational sampling of functional loops in human histone deacetylase 8. Chemical Science, 2021, 12, 9318-9327.	7.4	5
9543	Host-guest interaction-induced emission enhancement of amphiphilic AIEgens: a computational study. Materials Chemistry Frontiers, 2021, 5, 1806-1816.	5.9	16
9544	Coarse-Grained Parameterization of Nucleotide Cofactors and Metabolites: Protonation Constants, Partition Coefficients, and Model Topologies. Journal of Chemical Information and Modeling, 2021, 61, 335-346.	5.4	9
9545	Computational simulations reveal the binding dynamics between human ACE2 and the receptor binding domain of SARS-CoV-2 spike protein. Quantitative Biology, 2021, 9, 61-72.	0.5	15
9546	Wrapping Up Viruses at Multiscale Resolution: Optimizing PACKMOL and SIRAH Execution for Simulating the Zika Virus. Journal of Chemical Information and Modeling, 2021, 61, 408-422.	5.4	18
9547	Artificial stabilization of the fusion pore by intra-organelle styrene-maleic acid copolymers. Soft Matter, 2021, 17, 8314-8321.	2.7	4
9548	Mechanism of recognition of parallel G-quadruplexes by DEAH/RHAU helicase DHX36 explored by molecular dynamics simulations. Computational and Structural Biotechnology Journal, 2021, 19, 2526-2536.	4.1	12
9549	The role of size and nature in nanoparticle binding to a model lung membrane: an atomistic study. Nanoscale Advances, 2021, 3, 6635-6648.	4.6	9



#	ARTICLE	IF	CITATIONS
9550	QM/MM and molecular dynamics investigation of the mechanism of covalent inhibition of TAK1 kinase. Organic and Biomolecular Chemistry, 2021, 19, 1412-1425.	2.8	5
9551	Biological evaluation of new TEM1 targeting recombinant antibodies for radioimmunotherapy: In vitro, in vivo and in silico studies. European Journal of Pharmaceutics and Biopharmaceutics, 2021, 158, 233-244.	4.3	3
9552	A combination of solid-state NMR and MD simulations reveals the binding mode of a rhomboid protease inhibitor. Chemical Science, 2021, 12, 12754-12762.	7.4	4
9553	Inhibition of non-enzymatic glycation by capsaicin: targeting AGE-induced diabetic complications. New Journal of Chemistry, 2021, 45, 16048-16058.	2.8	1
9554	Microscopic structural features of water in aqueousâ€“relne mixtures of varying compositions. Physical Chemistry Chemical Physics, 2021, 23, 3779-3793.	2.8	17
9555	Molecular mechanism of inhibition of COVID-19 main protease by Î²-adrenoceptor agonists and adenosine deaminase inhibitors using <i>in silico</i> methods. Journal of Biomolecular Structure and Dynamics, 2022, 40, 5112-5127.	3.5	5
9556	Molecular perspective on charge-tunable adsorption of volatile organic compounds on carbon nanotubes. Physical Chemistry Chemical Physics, 2021, 23, 2972-2980.	2.8	14
9557	Alginate gels crosslinked with chitosan oligomers â€“ a systematic investigation into alginate block structure and chitosan oligomer interaction. RSC Advances, 2021, 11, 13780-13798.	3.6	16
9559	Intracellular Pathways Involved in Bone Regeneration Triggered by Recombinant Silkâ€“Silica Chimeras. Advanced Functional Materials, 2018, 28, 1702570.	14.9	31
9560	The evolutionary background and functional consequences of the rs2071307 polymorphism in human tropoelastin. Biopolymers, 2021, 112, e23414.	2.4	4
9561	Alchemical free energy calculations via metadynamics: Application to the <scp>theophyllineâ€“RNA</scp> aptamer complex. Journal of Computational Chemistry, 2020, 41, 1804-1819.	3.3	10
9562	Supercell Methods for Defect Calculations. Topics in Applied Physics, 0, , 29-68.	0.8	10
9563	Microscopic Elasticity of Complex Systems. Lecture Notes in Physics, 2006, , 287-307.	0.7	6
9564	Theory and Simulation of Friction and Lubrication. , 2006, , 65-104.		15
9566	Nanoindentation in Nanocrystalline Metallic Layers: A Molecular Dynamics Study on Size Effects. Nanostructure Science and Technology, 2006, , 109-142.	0.1	5
9567	Integrating Molecular Simulation and Experimental Data: A Bayesian/Maximum Entropy Reweighting Approach. Methods in Molecular Biology, 2020, 2112, 219-240.	0.9	129
9568	Protocol for Simulations of PEGylated Proteins with Martini 3. Methods in Molecular Biology, 2021, 2199, 315-335.	0.9	10
9569	Computational High Pressure Science. , 2004, , 179-198.		2

#	ARTICLE	IF	CITATIONS
9570	Atomistic Visualization. , 2005, , 1051-1068.		9
9571	Elastic Stability Criteria and Structural Bifurcations in Crystals Under Load. , 2005, , 1223-1279.		3
9572	Atomistic Studies of the Elastic Properties of Metallic BCC Nanowires and Films. IUTAM Symposium on Cellular, Molecular and Tissue Mechanics, 2009, , 221-230.	0.2	3
9573	Microscopic Mechanisms of Tribological and Wear Processes: Molecular Dynamics Simulations. , 1988, , 159-166.		5
9574	Classical and First Principles Molecular Dynamics Simulations in Material Science: Application to Structural and Dynamical Properties of Free and Supported Clusters. NATO ASI Series Series B: Physics, 1996, , 295-324.	0.2	1
9575	The Martensitic Transformation in Iron-Nickel Alloys: A Molecular Dynamics Study. , 1997, , 95-100.		4
9576	Molecular Dynamics for Reactions of Heterogeneous Catalysis. NATO ASI Series Series B: Physics, 1991, , 133-144.	0.2	1
9577	Time Scales of Lipid Dynamics and Molecular Dynamics. , 1996, , 3-29.		21
9578	Computer Simulations of Phase Transitions in Liquid Crystals. NATO ASI Series Series B: Physics, 1992, , 67-95.	0.2	8
9579	Molecular Dynamics Simulations. Methods in Molecular Biology, 2015, 1215, 3-26.	0.9	41
9580	Coarse-Grained Force Fields for Molecular Simulations. Methods in Molecular Biology, 2015, 1215, 125-149.	0.9	18
9581	In Silico Design of Antimicrobial Peptides. Methods in Molecular Biology, 2015, 1268, 195-219.	0.9	20
9582	Molecular Dynamics Simulation of Proteins. Methods in Molecular Biology, 2020, 2073, 311-327.	0.9	47
9583	First-Principles Modeling of Binary Chalcogenides: Recent Accomplishments and New Achievements. Springer Series in Materials Science, 2015, , 313-344.	0.6	3
9584	CALYPSO Method for Structure Prediction and Its Applications to Materials Discovery. , 2020, , 2729-2756.		3
9585	Molecular Dynamics Study of the Solution Behaviour of Antimicrobial Peptide Indolicidin. Studies in Computational Intelligence, 2019, , 257-265.	0.9	4
9586	The Development of Molecular Dynamics Simulations in the 1980s. Springer Series in Solid-state Sciences, 1992, , 11-19.	0.3	1
9587	Molecular Dynamics Simulations in Material Science and Condensed Matter Physics. Springer Proceedings in Physics, 1988, , 108-123.	0.2	6

#	ARTICLE	IF	CITATIONS
9588	Deterministic Methods. , 1986, , 13-55.		1
9589	Introduction to Damage Mechanics. , 2000, , 1-15.		6
9590	On (Andersenâ€™)Parrinelloâ€™Rahman Molecular Dynamics, the Related Metadynamics, and the Use of the Cauchyâ€™Born Rule. , 2010, , 145-153.		1
9591	On the Calculation of the Dielectric Properties of Liquid Ionic Systems. NATO Science for Peace and Security Series B: Physics and Biophysics, 2013, , 103-122.	0.3	12
9592	Coarse-Grained Molecular Dynamics Provides Insight into the Interactions of Lipids and Cholesterol with Rhodopsin. Advances in Experimental Medicine and Biology, 2014, 796, 75-94.	1.6	27
9593	Simulation of Interfaces at the Atomic Scale. , 1996, , 163-187.		2
9594	Monte Carlo Simulations. , 1990, , 83-123.		11
9595	Molecular Dynamics Simulations in the Solid State Sciences. , 1988, , 501-590.		6
9596	Numerical Techniques to Study Complex Liquids. , 1995, , 357-419.		5
9597	Molecular Dynamics Studies of High Pressure Transformations and Structures. , 1999, , 59-85.		1
9598	Molecular Dynamics Methods and Large-Scale Simulations of Amorphous Materials. , 1997, , 151-213.		26
9599	NEW CRYSTAL STRUCTURES OF SiO2 PREDICTED BY MOLECULAR DYNAMICS STUDY. , 1991, , 381-384.		3
9600	Synergetic adsorption of polymers on montmorillonite: Insights from molecular dynamics simulations. Applied Clay Science, 2020, 193, 105654.	5.2	24
9601	Structural based study to identify new potential inhibitors for dual specificity tyrosine-phosphorylation- regulated kinase. Computer Methods and Programs in Biomedicine, 2020, 194, 105494.	4.7	54
9602	Determining the unbinding events and conserved motions associated with the pyrazinamide release due to resistance mutations of Mycobacterium tuberculosis pyrazinamidase. Computational and Structural Biotechnology Journal, 2020, 18, 1103-1120.	4.1	13
9603	Combining Ramachandran plot and molecular dynamics simulation for structural-based variant classification: Using TP53 variants as model. Computational and Structural Biotechnology Journal, 2020, 18, 4033-4039.	4.1	31
9604	Binding studies of crocin to Î²-Lactoglobulin and its impacts on both components. Food Hydrocolloids, 2020, 108, 106003.	10.7	24
9605	Structural modification of NADPH oxidase activator (Noxa 1) by oxidative stress: An experimental and computational study. International Journal of Biological Macromolecules, 2020, 163, 2405-2414.	7.5	19

#	ARTICLE	IF	CITATIONS
9606	Mechanism of the antimicrobial activity of whey protein- $\beta$ -polylysine complexes against <i>Escherichia coli</i> and its application in sauced duck products. <i>International Journal of Food Microbiology</i> , 2020, 328, 108663.	4.7	34
9607	Statistical geometry characterization of global structure of TMAO and TBA aqueous solutions. <i>Journal of Molecular Liquids</i> , 2017, 245, 35-41.	4.9	12
9608	Elucidating NH <sub>2</sub> -I3V3A3G3K3-COOH and NH <sub>2</sub> -K3G3A3V3I3-COOH polypeptide membranes: A classical molecular dynamics study. <i>Journal of Molecular Liquids</i> , 2019, 279, 740-749.	4.9	20
9609	The effect of water/ethanol solvent mixtures on interactions of an antibody selective for wild-type alpha-1-antitrypsin in complex with its antigen. <i>Journal of Molecular Liquids</i> , 2020, 312, 113437.	4.9	4
9610	Interactions of human islet amyloid polypeptide with lipid structure of different curvatures. <i>Theoretical and Applied Mechanics Letters</i> , 2020, 10, 412-418.	2.8	5
9612	Stepwise Insertion of Cobra Cardiotoxin CT2 into a Lipid Bilayer Occurs as an Interplay of Protein and Membrane "Dynamic Molecular Portraits". <i>Journal of Chemical Information and Modeling</i> , 2021, 61, 385-399.	5.4	6
9613	Dimerization and Structural Stability of Amyloid Precursor Proteins Affected by the Membrane Microenvironments. <i>Journal of Chemical Information and Modeling</i> , 2017, 57, 1375-1387.	5.4	23
9614	Residue "Residue Mutual Work Analysis of Retinal" Opsin Interaction in Rhodopsin: Implications for Protein "Ligand Binding. <i>Journal of Chemical Theory and Computation</i> , 2020, 16, 1834-1842.	5.3	5
9615	A New Lipid Force Field (FUJI). <i>Journal of Chemical Theory and Computation</i> , 2020, 16, 3664-3676.	5.3	7
9616	Solvation Structures of Tetraethylammonium Bromide and Tetrafluoroborate in Aqueous Binary Solvents with Ethanol, Trifluoroethanol, and Acetonitrile. <i>Journal of Physical Chemistry B</i> , 2020, 124, 5009-5020.	2.6	4
9617	Assessing the Effect of Hofmeister Anions on the Hydrogen-Bonding Strength of Water via Nitrile Stretching Frequency Shift. <i>Journal of Physical Chemistry B</i> , 2020, 124, 11783-11792.	2.6	7
9618	Molecular Dynamics Study of the Interaction between the N-terminal of $\beta$ -Synuclein and a Lipid Bilayer Mimicking Synaptic Vesicles. <i>Journal of Physical Chemistry B</i> , 2021, 125, 1036-1048.	2.6	9
9619	Functional Oligomeric Forms of Uncoupling Protein 2: Strong Evidence for Asymmetry in Protein and Lipid Bilayer Systems. <i>Journal of Physical Chemistry B</i> , 2021, 125, 169-183.	2.6	11
9620	Temperature, Pressure, and Length-Scale Dependence of Solvation in Water-like Solvents. I. Small Solvophobic Solutes. <i>Journal of Physical Chemistry B</i> , 2021, 125, 297-306.	2.6	4
9621	The Effects of Chain Length on the Structural Properties of Intrinsically Disordered Proteins in Concentrated Solutions. <i>Journal of Physical Chemistry B</i> , 2020, 124, 11843-11853.	2.6	19
9622	Can a DNA Origami Structure Constrain the Position and Orientation of an Attached Dye Molecule?. <i>Journal of Physical Chemistry C</i> , 2021, 125, 1509-1522.	3.1	26
9623	Structural Properties of Inverted Hexagonal Phase: A Hybrid Computational and Experimental Approach. <i>Langmuir</i> , 2020, 36, 6668-6680.	3.5	9
9624	Hydrophobic/Hydrophilic Directionality Affects the Mechanism of Ru-Catalyzed Water Oxidation Reaction. <i>ACS Catalysis</i> , 2020, 10, 13364-13370.	11.2	15

#	ARTICLE	IF	CITATIONS
9625	Green Tea Extracts EGCG and EGC Display Distinct Mechanisms in Disrupting A $\beta$ <sub>42</sub> Protofibril. ACS Chemical Neuroscience, 2020, 11, 1841-1851.	3.5	73
9626	Molecular Dynamics Simulation of the Interaction of Two Linear Battacin Analogs with Model Gram-Positive and Gram-Negative Bacterial Cell Membranes. ACS Omega, 2021, 6, 388-400.	3.5	19
9627	Dependence of fullerene aggregation on lipid saturation due to a balance between entropy and enthalpy. Scientific Reports, 2019, 9, 1037.	3.3	14
9628	A conserved histidine in switch-II of EF-G moderates release of inorganic phosphate. Scientific Reports, 2015, 5, 12970.	3.3	21
9629	Tuning of the Na,K-ATPase by the beta subunit. Scientific Reports, 2016, 6, 20442.	3.3	37
9630	Chapter 2. Molecular Dynamics Computer Simulations of Biological Systems. Chemical Biology, 0, , 39-68.	0.2	1
9631	Computer Simulation Studies of Heat Capacity Effects Associated with Hydrophobic Effects. , 2010, , 436-456.		7
9632	Ion association in concentrated NaCl brines from ambient to supercritical conditions: results from classical molecular dynamics simulations. Geochemical Transactions, 2002, 3, 102.	0.7	3
9633	Predicting selectivity of paracellular pores for biomimetic applications. Molecular Systems Design and Engineering, 2020, 5, 686-696.	3.4	7
9634	Can the roles of polar and non-polar moieties be reversed in non-polar solvents?. Physical Chemistry Chemical Physics, 2020, 22, 25848-25858.	2.8	9
9635	Myoglobin molecule charging in electrolyte solutions. Physical Chemistry Chemical Physics, 2020, 22, 26764-26775.	2.8	6
9636	An insight into the role of riboflavin ligand in the self-assembly of poly(lactic-co-glycolic) Tj ETQq1 1 0.784314 rgBT /Overlock 10 5250-5260.	2.7	17
9637	Biochemical and structural characterization of murine GBP7, a guanylate binding protein with an elongated C-terminal tail. Biochemical Journal, 2019, 476, 3161-3182.	3.7	8
9638	<i>Prevotella intermedia</i> produces two proteins homologous to <i>Porphyromonas gingivalis</i> HmuY but with different heme coordination mode. Biochemical Journal, 2020, 477, 381-405.	3.7	21
9639	Biophysical characterization of p53 core domain aggregates. Biochemical Journal, 2020, 477, 111-120.	3.7	17
9640	Characterization of a naturally occurring mutation V368M in the human glucagon receptor and its association with metabolic disorders. Biochemical Journal, 2020, 477, 2581-2594.	3.7	6
9641	Design a protein gripper to capture a hydrophobic cargo. IET Nanobiotechnology, 2019, 13, 546-552.	3.8	4
9642	A general purpose model for the condensed phases of water: TIP4P/2005. , 0, .		1

#	ARTICLE	IF	CITATIONS
9643	Ion transport in backbone-embedded polymerized ionic liquids. Journal of Chemical Physics, 2019, 151, 124902.	3.0	18
9644	Large scale and linear scaling DFT with the CONQUEST code. Journal of Chemical Physics, 2020, 152, 164112.	3.0	55
9645	Accurate MP2-based force fields predict hydration free energies for simple alkanes and alcohols in good agreement with experiments. Journal of Chemical Physics, 2020, 153, 244505.	3.0	5
9646	The role played by two parallel free surfaces in the deformation mechanism of nanocrystalline metals: a molecular dynamics simulation. Philosophical Magazine A: Physics of Condensed Matter, Structure, Defects and Mechanical Properties, 2002, 82, 1-15.	0.6	4
9647	Targeting the protein-protein interface pocket of Aurora-A-TPX2 complex: rational drug design and validation. Journal of Biomolecular Structure and Dynamics, 2021, 39, 3882-3891.	3.5	80
9648	In-silico identification of new inhibitors for Low-density lipoprotein receptor-related protein6 (LRP6). Journal of Biomolecular Structure and Dynamics, 2022, 40, 4440-4450.	3.5	51
9649	Atomistic simulations of gold surface functionalization for nanoscale biosensors applications. Nanotechnology, 2021, 32, 095702.	2.6	9
9650	Structural and dynamical mechanisms of a naturally occurring variant of the human prion protein in preventing prion conversion. Chinese Physics B, 2020, 29, 108710.	1.4	5
9651	Tail-structure regulated phase behaviors of a lipid bilayer*. Chinese Physics B, 2020, 29, 128701.	1.4	6
9652	Suppression of helium bubble nucleation in beryllium exposed tungsten surfaces. Nuclear Fusion, 2020, 60, 126018.	3.5	8
9753	Viscoelasticity of liquid water investigated using molecular dynamics simulations. Physical Review Fluids, 2019, 4, .	2.5	13
9754	Confinement and hydrophilicity effects on geologically relevant fluids in silica nanopores. Physical Review Fluids, 2020, 5, .	2.5	3
9755	Molecular interpretation of the non-Newtonian viscoelastic behavior of liquid water at high frequencies. Physical Review Fluids, 2020, 5, .	2.5	11
9756	Irradiation-driven amorphous-to-glassy transition in quartz: The crucial role of the medium-range order in crystallization. Physical Review Materials, 2017, 1, .	2.4	27
9757	Achieving DFT accuracy with a machine-learning interatomic potential: Thermomechanics and defects in bcc ferromagnetic iron. Physical Review Materials, 2018, 2, .	2.4	175
9758	Migration mechanisms of a faceted grain boundary. Physical Review Materials, 2018, 2, .	2.4	14
9759	Aggregation of poly( $Tj$ ETQq0 0 0 rgBT /Overlock 10 Tf 50 107 Td (xmlns:mml="http://www.w3.org/1998/Math/MathML">	2.4	5
9760	Temperature-induced phase transition and Li self-diffusion in $C_2$ : A first-principles study. Physical Review Materials, 2019, 3, .	2.4	3



#	ARTICLE	IF	CITATIONS
9761	Overscreening and crowding in electrochemical ionic liquid systems. <i>Physical Review Materials</i> , 2019, 3, .	2.4	14
9762	Electrically driven ferroelastic domain walls, domain wall interactions, and moving needle domains. <i>Physical Review Materials</i> , 2019, 3, .	2.4	21
9763	Pattern formation during deformation of metallic nanolaminates. <i>Physical Review Materials</i> , 2020, 4, .	2.4	7
9764	Neural-network interatomic potential for grain boundary structures and their energetics in silicon. <i>Physical Review Materials</i> , 2020, 4, .	2.4	21
9765	Strength, transformation toughening, and fracture dynamics of rock salt structure $T_{\text{c}}$ $\sim 1$ $\times 10^4$ K. <i>Physical Review Letters</i> , 2020, 125, 125701.	2.4	12
9766	Water as a catalyst for ion transport across the electrical double layer in ionic liquids. <i>Physical Review Materials</i> , 2020, 4, .	2.4	5
9767	Enhanced piezoelectricity in twinned ferroelastics with nanocavities. <i>Physical Review Materials</i> , 2020, 4, .	2.4	10
9768	Wrinkle patterns in active viscoelastic thin sheets. <i>Physical Review Research</i> , 2020, 2, .	3.6	12
9769	Propagation of uncertainty in physicochemical data to force field predictions. <i>Physical Review Research</i> , 2020, 2, .	3.6	4
9770	The structure of a potassium-selective ion channel reveals a hydrophobic gate regulating ion permeation. <i>IUCr</i> , 2020, 7, 835-843.	2.2	8
9771	Crystal structure of ( <i>S</i> )-3- <i>O</i> -geranylgeranyl glycerol phosphate synthase from <i>Thermoplasma acidophilum</i> in complex with the substrate <i>sn</i> -glycerol 1-phosphate. <i>Acta Crystallographica Section F: Structural Biology Communications</i> , 2019, 75, 470-479.	0.8	3
9772	Influence of the presence of the heme cofactor on the JK-loop structure in indoleamine 2,3-dioxygenase 1. <i>Acta Crystallographica Section D: Structural Biology</i> , 2020, 76, 1211-1221.	2.3	12
9773	Effect of the air-water interface on the conformation of amyloid beta. <i>Biointerphases</i> , 2020, 15, 061011.	1.6	9
9774	Ceramide chain length-dependent protein sorting into selective endoplasmic reticulum exit sites. <i>Science Advances</i> , 2020, 6, .	10.3	38
9775	Vapor-assisted deposition of highly efficient, stable black-phase FAPbI <sub>3</sub> perovskite solar cells. <i>Science</i> , 2020, 370, .	12.6	530
9776	Oxidative hotspots on actin promote skeletal muscle weakness in rheumatoid arthritis. <i>JCI Insight</i> , 2019, 4, .	5.0	23
9777	Ab initio theory of phase transitions and thermoelasticity of minerals. , 0, , 83-170.		23
9778	Single-File Water Flux Through Two-Dimensional Nanoporous Membranes. <i>Nanoscale Research Letters</i> , 2020, 15, 204.	5.7	7

#	ARTICLE	IF	CITATIONS
9779	Challenges in the use of atomistic simulations to predict solubilities of drug-like molecules. F1000Research, 2018, 7, 686.	1.6	6
9780	Challenges in the use of atomistic simulations to predict solubilities of drug-like molecules. F1000Research, 2018, 7, 686.	1.6	6
9781	Interaction of N-3-oxododecanoyl homoserine lactone with transcriptional regulator LasR of <i>Pseudomonas aeruginosa</i> : Insights from molecular docking and dynamics simulations. F1000Research, 2018, 7, 324.	1.6	7
9782	Calculation of Free Volume in Computer Generated Grain Boundaries. Acta Physica Polonica A, 2005, 107, 769-775.	0.5	6
9783	Method of Planes Normal Pressure for Slit Geometries in Molecular Dynamics Simulations,. Computational Methods in Science and Technology, 2013, 19, 167-173.	0.3	1
9785	Keys to Lipid Selection in Fatty Acid Amide Hydrolase Catalysis: Structural Flexibility, Gating Residues and Multiple Binding Pockets. PLoS Computational Biology, 2015, 11, e1004231.	3.2	31
9786	Markov State Models Reveal a Two-Step Mechanism of miRNA Loading into the Human Argonaute Protein: Selective Binding followed by Structural Re-arrangement. PLoS Computational Biology, 2015, 11, e1004404.	3.2	56
9787	The Structural Basis for Activation and Inhibition of ZAP-70 Kinase Domain. PLoS Computational Biology, 2015, 11, e1004560.	3.2	12
9788	The Molecular Basis of Polyunsaturated Fatty Acid Interactions with the Shaker Voltage-Gated Potassium Channel. PLoS Computational Biology, 2016, 12, e1004704.	3.2	47
9789	Sequence determinants of protein phase behavior from a coarse-grained model. PLoS Computational Biology, 2018, 14, e1005941.	3.2	427
9790	Predicting peak spectral sensitivities of vertebrate cone visual pigments using atomistic molecular simulations. PLoS Computational Biology, 2018, 14, e1005974.	3.2	15
9791	Closely related, yet unique: Distinct homo- and heterodimerization patterns of G protein coupled chemokine receptors and their fine-tuning by cholesterol. PLoS Computational Biology, 2018, 14, e1006062.	3.2	33
9792	Cholesterol binding to the sterol-sensing region of Niemann Pick C1 protein confines dynamics of its N-terminal domain. PLoS Computational Biology, 2020, 16, e1007554.	3.2	12
9793	Structural Heterogeneity and Quantitative FRET Efficiency Distributions of Polyprolines through a Hybrid Atomistic Simulation and Monte Carlo Approach. PLoS ONE, 2011, 6, e19791.	2.5	108
9794	Unprocessed Viral DNA Could Be the Primary Target of the HIV-1 Integrase Inhibitor Raltegravir. PLoS ONE, 2012, 7, e40223.	2.5	8
9795	Structure and Dynamics of Amyloid-Î² Segmental Polymorphisms. PLoS ONE, 2012, 7, e41479.	2.5	72
9796	The Structural Dynamics of the Flavivirus Fusion Peptide-Membrane Interaction. PLoS ONE, 2012, 7, e47596.	2.5	23
9797	Effects of Molecular Crowding on the Dynamics of Intrinsically Disordered Proteins. PLoS ONE, 2012, 7, e49876.	2.5	85

#	ARTICLE	IF	CITATIONS
9798	The Influence of 150-Cavity Binders on the Dynamics of Influenza A Neuraminidases as Revealed by Molecular Dynamics Simulations and Combined Clustering. PLoS ONE, 2013, 8, e59873.	2.5	19
9799	Replacement of the Human Topoisomerase Linker Domain with the Plasmodial Counterpart Renders the Enzyme Camptothecin Resistant. PLoS ONE, 2013, 8, e68404.	2.5	13
9800	Insight into the Intermolecular Recognition Mechanism between Keap1 and IKK $\beta$ Combining Homology Modelling, Protein-Protein Docking, Molecular Dynamics Simulations and Virtual Alanine Mutation. PLoS ONE, 2013, 8, e75076.	2.5	42
9801	Binding Mode Analyses and Pharmacophore Model Development for Stilbene Derivatives as a Novel and Competitive Class of $\beta$ -Glucosidase Inhibitors. PLoS ONE, 2014, 9, e85827.	2.5	26
9802	Human Lactate Dehydrogenase A Inhibitors: A Molecular Dynamics Investigation. PLoS ONE, 2014, 9, e86365.	2.5	31
9803	Ligand Photo-Isomerization Triggers Conformational Changes in iGluR2 Ligand Binding Domain. PLoS ONE, 2014, 9, e92716.	2.5	8
9804	Comparative Computational Study of Interaction of C60-Fullerene and Tris-Malonyl-C60-Fullerene Isomers with Lipid Bilayer: Relation to Their Antioxidant Effect. PLoS ONE, 2014, 9, e102487.	2.5	30
9805	In Silico Insights into Protein-Protein Interactions and Folding Dynamics of the Saposin-Like Domain of Solanum tuberosum Aspartic Protease. PLoS ONE, 2014, 9, e104315.	2.5	19
9806	Viscous Friction between Crystalline and Amorphous Phase of Dragline Silk. PLoS ONE, 2014, 9, e104832.	2.5	16
9807	How Modification of Accessible Lysines to Phenylalanine Modulates the Structural and Functional Properties of Horseradish Peroxidase: A Simulation Study. PLoS ONE, 2014, 9, e109062.	2.5	5
9808	In Silico Screening, Genotyping, Molecular Dynamics Simulation and Activity Studies of SNPs in Pyruvate Kinase M2. PLoS ONE, 2015, 10, e0120469.	2.5	19
9809	Dynamics of the Peripheral Membrane Protein P2 from Human Myelin Measured by Neutron Scattering—A Comparison between Wild-Type Protein and a Hinge Mutant. PLoS ONE, 2015, 10, e0128954.	2.5	17
9810	Secondary Structure of Rat and Human Amylin across Force Fields. PLoS ONE, 2015, 10, e0134091.	2.5	47
9811	Polar Desolvation and Position 226 of Pancreatic and Neutrophil Elastases Are Crucial to their Affinity for the Kunitz-Type Inhibitors ShPI-1 and ShPI-1/K13L. PLoS ONE, 2015, 10, e0137787.	2.5	4
9812	Phosphorylation Regulates the Bound Structure of an Intrinsically Disordered Protein: The p53-TAZ2 Case. PLoS ONE, 2016, 11, e0144284.	2.5	16
9813	How Intrinsic Molecular Dynamics Control Intramolecular Communication in Signal Transducers and Activators of Transcription Factor STAT5. PLoS ONE, 2015, 10, e0145142.	2.5	7
9814	DNA Repair Gene (XRCC1) Polymorphism (Arg399Gln) Associated with Schizophrenia in South Indian Population: A Genotypic and Molecular Dynamics Study. PLoS ONE, 2016, 11, e0147348.	2.5	16
9815	Ion Concentration- and Voltage-Dependent Push and Pull Mechanisms of Potassium Channel Ion Conduction. PLoS ONE, 2016, 11, e0150716.	2.5	5

#	ARTICLE	IF	CITATIONS
9816	SRPK1 and Akt Protein Kinases Phosphorylate the RS Domain of Lamin B Receptor with Distinct Specificity: A Combined Biochemical and In Silico Approach. PLoS ONE, 2016, 11, e0154198.	2.5	16
9817	G-Protein/ $\beta^2$ -Arrestin-Linked Fluctuating Network of G-Protein-Coupled Receptors for Predicting Drug Efficacy and Bias Using Short-Term Molecular Dynamics Simulation. PLoS ONE, 2016, 11, e0155816.	2.5	9
9818	Functional and Structural Analyses of CYP1B1 Variants Linked to Congenital and Adult-Onset Glaucoma to Investigate the Molecular Basis of These Diseases. PLoS ONE, 2016, 11, e0156252.	2.5	26
9819	Molecular Dynamics Simulations and Structural Analysis to Decipher Functional Impact of a Twenty Residue Insert in the Ternary Complex of Mus musculus TdT Isoform. PLoS ONE, 2016, 11, e0157286.	2.5	9
9820	Molecular Dynamics Driven Design of pH-Stabilized Mutants of MNEI, a Sweet Protein. PLoS ONE, 2016, 11, e0158372.	2.5	28
9821	Structural Dynamics Investigation of Human Family 1 & 2 Cystatin-Cathepsin L1 Interaction: A Comparison of Binding Modes. PLoS ONE, 2016, 11, e0164970.	2.5	11
9822	Sox10 contributes to the balance of fate choice in dorsal root ganglion progenitors. PLoS ONE, 2017, 12, e0172947.	2.5	24
9823	Transient helicity in intrinsically disordered Axin-1 studied by NMR spectroscopy and molecular dynamics simulations. PLoS ONE, 2017, 12, e0174337.	2.5	7
9824	Molecular simulations and Markov state modeling reveal the structural diversity and dynamics of a theophylline-binding RNA aptamer in its unbound state. PLoS ONE, 2017, 12, e0176229.	2.5	29
9825	The structural basis of a high affinity ATP binding $\hat{\mu}$ subunit from a bacterial ATP synthase. PLoS ONE, 2017, 12, e0177907.	2.5	13
9826	Dynamics and asymmetry in the dimer of the norovirus major capsid protein. PLoS ONE, 2017, 12, e0182056.	2.5	9
9827	Excessive aggregation of membrane proteins in the Martini model. PLoS ONE, 2017, 12, e0187936.	2.5	147
9828	Structural analysis of human glycoprotein butyrylcholinesterase using atomistic molecular dynamics: The importance of glycosylation site ASN241. PLoS ONE, 2017, 12, e0187994.	2.5	15
9830	Structure and elevator mechanism of the mammalian sodium/proton exchanger NHE9. EMBO Journal, 2020, 39, 4541-4559.	7.8	31
9831	Grain-Boundary Diffusion of Hydrogen Atoms in the $\alpha$ -Iron. Metallofizika i Noveishie Tekhnologii, 2016, 36, 1399-1410.	0.5	6
9832	Molecular Dynamics Simulation of the Effect of Interfaces in Melting and Solid-State Amorphization. Materials Research Society Symposia Proceedings, 1991, 230, 3.	0.1	7
9833	Orientation of lutein in a lipid bilayer - revisited.. Acta Biochimica Polonica, 2012, 59, .	0.5	11
9834	Genetic identification and molecular modeling characterization reveal a novel <i>PROM1</i> mutation in Stargardt4-like macular dystrophy. Oncotarget, 2018, 9, 122-141.	1.8	32

#	ARTICLE	IF	CITATIONS
9835	In Vitro Holdase Activity of E. coli Small Heat-Shock Proteins IbpA, IbpB and IbpAB: A Biophysical Study with Some Unconventional Techniques. Protein and Peptide Letters, 2014, 21, 564-571.	0.9	9
9836	Use of Molecular Dynamics Simulations in Structure-Based Drug Discovery. Current Pharmaceutical Design, 2019, 25, 3339-3349.	1.9	36
9837	Mechanism of A pH-induced Peptide Inserting into a POPC Bilayer: A Molecular Dynamic Study. Current Pharmaceutical Biotechnology, 2014, 15, 814-822.	1.6	2
9838	Molecular Dynamics Simulations of Glycyrrhizic Acid Aggregates as Drug-Carriers for Paclitaxel. Current Drug Delivery, 2019, 16, 618-627.	1.6	10
9839	Molecular Docking and Dynamics Simulation Analysis of Thymoquinone and Thymol Compounds from Nigella sativa L. that Inhibits P38 Protein: Probable Remedies for Hepatocellular Carcinoma. Medicinal Chemistry, 2020, 16, 350-357.	1.5	9
9840	Computational Outlook of Marine Compounds as Anti-Cancer Representatives Targeting BCL-2 and Survivin. Current Computer-Aided Drug Design, 2019, 15, 265-276.	1.2	2
9841	Density Functional Theory Calculations on Interface Structures and Adsorption Properties of Graphenes: A Review. The Open Nanoscience Journal, 2009, 3, 34-55.	1.8	9
9842	Molecular Dynamics Simulation Studies of the CL-20/DNB Co-crystal. Central European Journal of Energetic Materials, 2016, 13, 677-693.	0.4	8
9843	Soft Phonon Mode and Elastic Instabilities in Stress-Induced Phase Transformation. Nippon Kinzoku Gakkaishi/Journal of the Japan Institute of Metals, 1997, 61, 696-701.	0.4	3
9844	Title is missing!. Materia Japan, 2006, 45, 670-676.	0.1	2
9845	Effect of Fluorine on Melt Structure for $\text{CaO-SiO}_2\text{-CaF}_2$ and $\text{CaO-Al}_2\text{O}_3\text{-O}_3\text{-CaF}_2$ by Molecular Dynamics Simulations. ISIJ International, 2020, 60, 2176-2182.	1.4	15
9846	Molecular Dynamics Simulations. Definitions of Elastic Constants.. Zairyo/Journal of the Society of Materials Science, Japan, 1997, 46, 218-227.	0.2	1
9847	Molecular Dynamics Simulations. Molecular Dynamic Study on Strength of Coincidence Grain Boundaries.. Zairyo/Journal of the Society of Materials Science, Japan, 1997, 46, 238-243.	0.2	2
9848	Recent Advances and Multi-Hierarchical Perspectives in Plasticity Theory. VII: Simulation of Plastic Deformation by Using Molecular Dynamics.. Zairyo/Journal of the Society of Materials Science, Japan, 1999, 48, 1328-1334.	0.2	2
9853	Molecular Docking and Molecular Dynamics Studies of L-Glycyl-L-Glutamic Acid Dipeptide. Bilge International Journal of Science and Technology Research, 2019, 3, 1-9.	0.5	11
9854	Modeling PrPSc Generation Through Deformed Templating. Frontiers in Bioengineering and Biotechnology, 2020, 8, 590501.	4.1	12
9855	Atomic-Approach to Predict the Energetically Favored Composition Region and to Characterize the Short-, Medium-, and Extended-Range Structures of the Ti-Nb-Al Ternary Metallic Glasses. Materials, 2019, 12, 432.	2.9	1
9856	Complexation of Alkali and Alkaline-Earth Metal Cations at Spodumene-Saltwater Interfaces by Molecular Simulation: Impact on Oleate Adsorption. Minerals (Basel, Switzerland), 2021, 11, 12.	2.0	11

#	ARTICLE	IF	CITATIONS
9857	Profiling the Structural Determinants of Aryl Benzamide Derivatives as Negative Allosteric Modulators of mGluR5 by In Silico Study. <i>Molecules</i> , 2020, 25, 406.	3.8	9
9858	Computational Study of C-X-C Chemokine Receptor (CXCR)3 Binding with Its Natural Agonists Chemokine (C-X-C Motif) Ligand (CXCL)9, 10 and 11 and with Synthetic Antagonists: Insights of Receptor Activation towards Drug Design for Vitiligo. <i>Molecules</i> , 2020, 25, 4413.	3.8	5
9859	Antimicrobial Peptide K11 Selectively Recognizes Bacterial Biomimetic Membranes and Acts by Twisting Their Bilayers. <i>Pharmaceuticals</i> , 2021, 14, 1.	3.8	54
9860	Some Factors Affected on Structure, Mechanical of Ni Bulk. <i>Advances in Materials Physics and Chemistry</i> , 2018, 08, 177-192.	0.7	1
9861	Impact of Mutations on K-Ras-p120GAP Interaction. <i>Computational Molecular Bioscience</i> , 2013, 03, 9-17.	0.4	11
9862	Computational and Experimental Analyses of Detachment Force at the Interface between Carbon Fibers and Epoxy Resin. <i>Open Journal of Composite Materials</i> , 2017, 07, 179-184.	0.8	10
9863	Molecular Dynamics Simulations of the Structure and the Analyses of Detachment Force at the Interface between Graphene and Epoxy Resin. <i>Seikei-Kakou</i> , 2018, 30, 251-256.	0.0	3
9864	An Amber Force Field for S-Nitrosoethanethiol That Is Transferable to S-Nitrosocysteine. <i>Bulletin of the Korean Chemical Society</i> , 2010, 31, 2903-2908.	1.9	2
9865	Molecular Dynamics Simulation Study for Ionic Strength Dependence of RNA-host factor Interaction in <i>Staphylococcus aureus</i> Hfq. <i>Bulletin of the Korean Chemical Society</i> , 2010, 31, 1519-1526.	1.9	8
9866	Molecular Dynamics Simulation of Sorbitan Monooleate Bilayers. <i>Bulletin of the Korean Chemical Society</i> , 2013, 34, 946-948.	1.9	13
9867	Applications of Al Modified Graphene on Gas Sensors and Hydrogen Storage. , 0, , .		3
9868	Simulations of Deformation Processes in Energetic Materials. , 0, , .		6
9869	Understanding Rifampicin Resistance in Tuberculosis through a Computational Approach. <i>Genomics and Informatics</i> , 2014, 12, 276.	0.8	25
9870	Simulation studies on the influence of nanofilm thickness on the elastic properties of B2-NiAl. <i>Wuli Xuebao/Acta Physica Sinica</i> , 2015, 64, 016803.	0.5	2
9871	Bonding nature of the amorphous structure studied by a combination of cutoff and electronic localization function. <i>Wuli Xuebao/Acta Physica Sinica</i> , 2016, 65, 173101.	0.5	3
9872	Molecular dynamics simulations on DNA flexibility: a comparative study of Amber bsc1 and bsc0 force fields. <i>Wuli Xuebao/Acta Physica Sinica</i> , 2018, 67, 108701.	0.5	4
9873	Molecular simulation of interaction between charged nanoparticles and phase-separated biomembranes containing charged lipids. <i>Wuli Xuebao/Acta Physica Sinica</i> , 2019, 68, 028701.	0.5	6
9874	Allosteric signalling in the outer membrane translocation domain of PapC usher. <i>ELife</i> , 2014, 3, .	6.0	18



#	ARTICLE	IF	CITATIONS
9875	The <i>Caenorhabditis elegans</i> protein SAS-5 forms large oligomeric assemblies critical for centriole formation. <i>ELife</i> , 2015, 4, e07410.	6.0	37
9876	Molecular basis for multimerization in the activation of the epidermal growth factor receptor. <i>ELife</i> , 2016, 5, .	6.0	144
9877	v-SNARE transmembrane domains function as catalysts for vesicle fusion. <i>ELife</i> , 2016, 5, .	6.0	50
9878	Proton currents constrain structural models of voltage sensor activation. <i>ELife</i> , 2016, 5, .	6.0	32
9879	Mechanism of allosteric regulation of $\beta_2$ -adrenergic receptor by cholesterol. <i>ELife</i> , 2016, 5, .	6.0	115
9880	Changes in the free-energy landscape of p38 $\beta$ MAP kinase through its canonical activation and binding events as studied by enhanced molecular dynamics simulations. <i>ELife</i> , 2017, 6, .	6.0	65
9881	Modeling Hsp70/Hsp40 interaction by multi-scale molecular simulations and coevolutionary sequence analysis. <i>ELife</i> , 2017, 6, .	6.0	48
9882	Helical jackknives control the gates of the double-pore K <sup>+</sup> uptake system KtrAB. <i>ELife</i> , 2017, 6, .	6.0	23
9883	The liquid structure of elastin. <i>ELife</i> , 2017, 6, .	6.0	137
9884	Single methyl groups can act as toggle switches to specify transmembrane Protein-protein interactions. <i>ELife</i> , 2017, 6, .	6.0	14
9885	Key steps in unconventional secretion of fibroblast growth factor 2 reconstituted with purified components. <i>ELife</i> , 2017, 6, .	6.0	63
9886	Microtubule assembly governed by tubulin allosteric gain in flexibility and lattice induced fit. <i>ELife</i> , 2018, 7, .	6.0	42
9887	Mechano-redox control of integrin de-adhesion. <i>ELife</i> , 2018, 7, .	6.0	47
9888	Simulation of spontaneous G protein activation reveals a new intermediate driving GDP unbinding. <i>ELife</i> , 2018, 7, .	6.0	39
9889	ATP-induced asymmetric pre-protein folding as a driver of protein translocation through the Sec machinery. <i>ELife</i> , 2019, 8, .	6.0	32
9890	Comment on 'Valid molecular dynamics simulations of human hemoglobin require a surprisingly large box size'. <i>ELife</i> , 2019, 8, .	6.0	35
9891	A single K <sup>+</sup> -binding site in the crystal structure of the gastric proton pump. <i>ELife</i> , 2019, 8, .	6.0	22
9892	Effect of helical kink in antimicrobial peptides on membrane pore formation. <i>ELife</i> , 2020, 9, .	6.0	39

#	ARTICLE	IF	CITATIONS
9893	Î²11-12 linker isomerization governs acid-sensing ion channel desensitization and recovery. <i>ELife</i> , 2020, 9, .	6.0	30
9894	Structure of a mitochondrial ATP synthase with bound native cardiolipin. <i>ELife</i> , 2019, 8, .	6.0	69
9895	A molecular view on the escape of lipoplexed DNA from the endosome. <i>ELife</i> , 2020, 9, .	6.0	46
9896	Helix breaking transition in the S4 of HCN channel is critical for hyperpolarization-dependent gating. <i>ELife</i> , 2019, 8, .	6.0	49
9897	Local frustration determines loop opening during the catalytic cycle of an oxidoreductase. <i>ELife</i> , 2020, 9, .	6.0	13
9898	Dynamics at the serine loop underlie differential affinity of cryptochromes for CLOCK:BMAL1 to control circadian timing. <i>ELife</i> , 2020, 9, .	6.0	50
9899	On the importance of statistics in molecular simulations for thermodynamics, kinetics and simulation box size. <i>ELife</i> , 2020, 9, .	6.0	34
9900	Bacterial OTU deubiquitinases regulate substrate ubiquitination upon <i>Legionella</i> infection. <i>ELife</i> , 2020, 9, .	6.0	23
9901	Binding mechanism of the matrix domain of HIV-1 gag on lipid membranes. <i>ELife</i> , 2020, 9, .	6.0	21
9902	Structural ordering of the <i>Plasmodium berghei</i> circumsporozoite protein repeats by inhibitory antibody 3D11. <i>ELife</i> , 2020, 9, .	6.0	15
9903	Peroxisredoxin promotes longevity and H <sub>2</sub> O <sub>2</sub> -resistance in yeast through redox-modulation of protein kinase A. <i>ELife</i> , 2020, 9, .	6.0	20
9904	The helical domain of the EcoR124I motor subunit participates in ATPase activity and dsDNA translocation. <i>PeerJ</i> , 2017, 5, e2887.	2.0	2
9905	Novel NAC-loaded poly(lactide-co-glycolide acid) nanoparticles for cataract treatment: preparation, characterization, evaluation of structure, cytotoxicity, and molecular docking studies. <i>PeerJ</i> , 2018, 6, e4270.	2.0	13
9906	How well do force fields capture the strength of salt bridges in proteins?. <i>PeerJ</i> , 2018, 6, e4967.	2.0	58
9907	NMR structure of the C-terminal domain of TonB protein from <i>Pseudomonas aeruginosa</i> . <i>PeerJ</i> , 2018, 6, e5412.	2.0	13
9908	Single mutations in the Îµ subunit from thermophilic <i>Bacillus</i> PS3 generate a high binding affinity site for ATP. <i>PeerJ</i> , 2018, 6, e5505.	2.0	3
9909	A conserved Neurite Outgrowth and Guidance motif with biomimetic potential in neuronal Cell Adhesion Molecules. <i>Computational and Structural Biotechnology Journal</i> , 2021, 19, 5622-5636.	4.1	3
9910	Anharmonic lattice dynamics of superionic lithium nitride. <i>Journal of Materials Chemistry A</i> , 2022, 10, 2295-2304.	10.3	9

#	ARTICLE	IF	CITATIONS
9911	Exciton energy transfer and bi-exciton annihilation in the emitting layers of thermally activated delayed fluorescence-based OLEDs. <i>Journal of Materials Chemistry C</i> , 2021, 9, 15141-15149.	5.5	4
9912	Designing amphiphilic Janus nanoparticles with tunable lipid raft affinity <i>via</i> molecular dynamics simulation. <i>Biomaterials Science</i> , 2021, 9, 8249-8258.	5.4	1
9913	The combined action of cations and anions of ionic liquids modulates the formation and stability of G-quadruplex DNA. <i>Physical Chemistry Chemical Physics</i> , 2021, 23, 24497-24504.	2.8	8
9914	Allosteric pockets and dynamic residue network hubs of falcipain 2 in mutations including those linked to artemisinin resistance. <i>Computational and Structural Biotechnology Journal</i> , 2021, 19, 5647-5666.	4.1	13
9915	Cation-π interactions drive hydrophobic self-assembly and aggregation of niclosamide in water. <i>RSC Advances</i> , 2021, 11, 33136-33147.	3.6	5
9916	Isomeric effects in structure formation and dielectric dynamics of different octanols. <i>Physical Chemistry Chemical Physics</i> , 2021, 23, 24211-24221.	2.8	9
9917	Ultrasensitive two-dimensional material-based MCF-7 cancer cell sensor driven by perturbation processes. <i>Nanoscale Advances</i> , 2021, 3, 6974-6983.	4.6	10
9918	The effect of S427F mutation on RXRα activity depends on its dimeric partner. <i>Chemical Science</i> , 2021, 12, 14700-14710.	7.4	2
9919	DNA sequence and methylation prescribe the inside-out conformational dynamics and bending energetics of DNA minicircles. <i>Nucleic Acids Research</i> , 2021, 49, 11459-11475.	14.5	11
9920	Docking and Molecular Dynamic Simulations of Cholecalciferol (Vitamin D3) as a Promising Inhibitor of Main Protease of Coronavirus to Prevent COVID-19 Infection. , 2021, , .		0
9921	Crystallization in Microgravity and the Atomic-Resolution Structure of Uridine Phosphorylase from <i>Vibrio cholerae</i> . <i>Crystallography Reports</i> , 2021, 66, 777-785.	0.6	3
9922	Analysis of the Structure-Function-Dynamics Relationships of GALT Enzyme and of Its Pathogenic Mutant p.Q188R: A Molecular Dynamics Simulation Study in Different Experimental Conditions. <i>Molecules</i> , 2021, 26, 5941.	3.8	5
9923	Supramolecular Complexes of Tetrapeptides Capable of Inducing the Human α2-Lactalbumin α2-Domain Conformational Transitions. <i>Crystallography Reports</i> , 2021, 66, 840-845.	0.6	0
9924	Study of GroEL Conformational Mobility by Cryo-Electron Microscopy and Molecular Dynamics. <i>Crystallography Reports</i> , 2021, 66, 846-853.	0.6	1
9928	Site of Cholesterol Oxidation Impacts Its Localization and Domain Formation in the Neuronal Plasma Membrane. <i>ACS Chemical Neuroscience</i> , 2021, 12, 3873-3884.	3.5	4
9929	Generalized Method for Charge-Transfer Equilibration in Reactive Molecular Dynamics. <i>Journal of Chemical Theory and Computation</i> , 2021, 17, 6691-6704.	5.3	7
9930	Potential efficacy of existing drug molecules against severe fever with thrombocytopenia syndrome virus: an in silico study. <i>Scientific Reports</i> , 2021, 11, 20857.	3.3	3
9932	Activation of Abl1 Kinase Explored Using Well-Tempered Metadynamics Simulations on an Essential Dynamics Sampled Path. <i>Journal of Chemical Theory and Computation</i> , 2021, 17, 7260-7270.	5.3	11

#	ARTICLE	IF	CITATIONS
9933	Impact of deep eutectic solvents and their constituents on the aqueous solubility of phloroglucinol dihydrate. <i>Journal of Molecular Liquids</i> , 2021, 344, 117932.	4.9	15
9934	Kinetics of Phenol Escape from the Insulin R <sub>6</sub> Hexamer. <i>Journal of Physical Chemistry B</i> , 2021, 125, 11637-11649.	2.6	5
9935	Thermophysical properties of liquid (U, Zr)O <sub>2</sub> by molecular dynamics. <i>Molecular Simulation</i> , 2021, 47, 1502-1508.	2.0	1
9936	Drug delivery by SiC nanotubes as nanocarriers for anti-cancer drugs: investigation of drug encapsulation and system stability using molecular dynamics simulation. <i>Materials Research Express</i> , 2021, 8, 105012.	1.6	8
9937	Molecular Dynamics Simulations of the Breathing Phase Transition of MOF Nanocrystallites II: Explicitly Modeling the Pressure Medium. <i>Frontiers in Chemistry</i> , 2021, 9, 757680.	3.6	8
9938	Dicationic-Type Quaternary Ammonium Salts as Candidates of Desiccants for an Air-Conditioning System. <i>ACS Sustainable Chemistry and Engineering</i> , 2021, 9, 14502-14514.	6.7	4
9939	Mutation in the Plasmodium falciparum BTB/POZ Domain of K13 Protein Confers Artemisinin Resistance. <i>Antimicrobial Agents and Chemotherapy</i> , 2022, 66, AAC0132021.	3.2	14
9941	Identifying the natural compound Catechin from tropical mangrove plants as a potential lead candidate against 3CL <sup>pro</sup> from SARS-CoV-2: An integrated <i>in silico</i> approach. <i>Journal of Biomolecular Structure and Dynamics</i> , 2022, 40, 13392-13411.	3.5	6
9942	Supramolecular Organization of Polymer Prodrug Nanoparticles Revealed by Coarse-Grained Simulations. <i>Journal of the American Chemical Society</i> , 2021, 143, 17412-17423.	13.7	18
9943	Lutein and Zeaxanthin in the Lipid Bilayer—Similarities and Differences Revealed by Computational Studies. <i>Frontiers in Molecular Biosciences</i> , 2021, 8, 768449.	3.5	5
9944	Structural Ensemble of the Insulin Monomer. <i>Biochemistry</i> , 2021, 60, 3125-3136.	2.5	5
9945	Revisiting OD-stretching dynamics of methanol-d <sub>4</sub> , ethanol-d <sub>6</sub> and dilute HOD/H <sub>2</sub> O mixture with predefined potentials and wavelet transform spectra. <i>Chemical Physics</i> , 2022, 553, 111385.	1.9	7
9946	A simple strategy for signal enhancement in lateral flow assays using superabsorbent polymers. <i>Mikrochimica Acta</i> , 2021, 188, 364.	5.0	1
9947	Sequential Voxel-Based Leaflet Segmentation of Complex Lipid Morphologies. <i>Journal of Chemical Theory and Computation</i> , 2021, 17, 7873-7885.	5.3	8
9949	Identification of New Specificity Determinants in Bacterial Purine Nucleobase Transporters based on an Ancestral Sequence Reconstruction Approach. <i>Journal of Molecular Biology</i> , 2021, 433, 167329.	4.2	4
9950	Influence of Monovalent Salts on $\alpha$ -Glycine Crystal Growth from Aqueous Solution: Molecular Dynamics Simulations at Constant Supersaturation Conditions. <i>Journal of Physical Chemistry B</i> , 2021, 125, 11732-11741.	2.6	1
9951	Molecular Dynamics Study of the Conformation, Ion Adsorption, Diffusion, and Water Structure of Soluble Polymers in Saline Solutions. <i>Polymers</i> , 2021, 13, 3550.	4.5	11
9952	Molecular Mechanism of Phosphate Steering for DNA Binding, Cleavage Localization, and Substrate Release in Nucleases. <i>ACS Catalysis</i> , 2021, 11, 13244-13254.	11.2	1

#	ARTICLE	IF	CITATIONS
9953	Predicting plastic events and quantifying the local yield surface in 3D model glasses. <i>Journal of the Mechanics and Physics of Solids</i> , 2022, 158, 104671.	4.8	10
9954	A Modeling-Based Design to Engineering Protein Hydrogels with Random Copolymers. <i>ACS Nano</i> , 2021, 15, 16139-16148.	14.6	13
9955	Structural Stability of Insulin Oligomers and Protein Association–Dissociation Processes: Free Energy Landscape and Universal Role of Water. <i>Journal of Physical Chemistry B</i> , 2021, 125, 11793-11811.	2.6	11
9956	Mechanism of lipid droplet formation by the yeast Sei1/Ldb16 Seipin complex. <i>Nature Communications</i> , 2021, 12, 5892.	12.8	40
9957	Effect of urea on the hydration and aggregation of hydrophobic and amphiphilic solute models: Implications to protein aggregation. <i>Journal of Chemical Physics</i> , 2021, 155, 144501.	3.0	5
9958	Simulation of the Interactions of Arginine with Wild-Type GALT Enzyme and the Classic Galactosemia-Related Mutant p.Q188R by a Computational Approach. <i>Molecules</i> , 2021, 26, 6061.	3.8	3
9959	Solvent Structure and Dynamics near the Surfaces of $\text{H}^2$ -Hematin Crystals. <i>Journal of Physical Chemistry B</i> , 2021, 125, 11264-11274.	2.6	2
9960	The Effect of Multisite Phosphorylation on the Conformational Properties of Intrinsically Disordered Proteins. <i>International Journal of Molecular Sciences</i> , 2021, 22, 11058.	4.1	9
9961	Binding of $\text{L}$ -lipoic acid to human serum albumin: spectroscopic and molecular modeling studies. <i>Monatshefte für Chemie</i> , 2021, 152, 1589-1602.	1.8	2
9962	Markov state models of proton- and pore-dependent activation in a pentameric ligand-gated ion channel. <i>ELife</i> , 2021, 10, .	6.0	9
9963	Deformation and breakup mechanism of water droplet in acidic crude oil emulsion under uniform electric field: A molecular dynamics study. <i>Colloids and Surfaces A: Physicochemical and Engineering Aspects</i> , 2022, 632, 127746.	4.7	21
9964	Structural Aspects of the Superionic Transition in AX <sub>2</sub> Compounds With the Fluorite Structure. <i>Frontiers in Chemistry</i> , 2021, 9, 723507.	3.6	7
9966	Quantum mechanical, virtual screening, molecular docking, molecular dynamics, ADME and antimicrobial activity studies of some new indole-hydrazone derivatives as potent agents against <i>E. faecalis</i> . <i>Journal of Biomolecular Structure and Dynamics</i> , 2022, 40, 8112-8126.	3.5	2
9967	Threshold of heteroplasmic truncating MT-ATP6 mutation in reprogramming, Notch hyperactivation and motor neuron metabolism. <i>Human Molecular Genetics</i> , 2022, 31, 958-974.	2.9	9
9969	Rippling Ferroic Phase Transition and Domain Switching In 2D Materials. <i>Advanced Materials</i> , 2021, 33, e2103469.	21.0	14
9970	Investigating the Molecular Mechanism of H3B-8800: A Splicing Modulator Inducing Preferential Lethality in Spliceosome-Mutant Cancers. <i>International Journal of Molecular Sciences</i> , 2021, 22, 11222.	4.1	9
9971	Thermodynamically consistent physics-informed neural networks for hyperbolic systems. <i>Journal of Computational Physics</i> , 2022, 449, 110754.	3.8	49
9972	Insights from molecular dynamics on CO <sub>2</sub> diffusion coefficient in saline water over a wide range of temperatures, pressures, and salinity: CO <sub>2</sub> geological storage implications. <i>Journal of Molecular Liquids</i> , 2022, 345, 117868.	4.9	17

#	ARTICLE	IF	CITATIONS
9973	DINC-COVID: A webserver for ensemble docking with flexible SARS-CoV-2 proteins. Computers in Biology and Medicine, 2021, 139, 104943.	7.0	8
9974	Cardiolipin prevents pore formation in phosphatidylglycerol bacterial membrane models. FEBS Letters, 2021, 595, 2701-2714.	2.8	9
9975	Computational Insights into the Aggregation Pathway of Self-Assembled Nanotubules. Journal of Physical Chemistry B, 2021, 125, 12082-12094.	2.6	0
9976	In silico identification of noncompetitive inhibitors targeting an uncharacterized allosteric site of falcipain-2. Journal of Computer-Aided Molecular Design, 2021, 35, 1067-1079.	2.9	5
9977	Structure of High-Pressure Supercooled and Glassy Water. Physical Review Letters, 2021, 127, 175502.	7.8	13
9978	Ribosome Elongation Kinetics of Consecutively Charged Residues Are Coupled to Electrostatic Force. Biochemistry, 2021, 60, 3223-3235.	2.5	18
9980	Structure Based Engineering of an Anti-angiogenic scFv Antibody for Soluble Production in E. Coli without Loss of Activity. Biotechnology and Applied Biochemistry, 2021, , .	3.1	4
9981	Cooperation of Conical and Polyunsaturated Lipids to Regulate Initiation and Processing of Membrane Fusion. Frontiers in Molecular Biosciences, 2021, 8, 763115.	3.5	11
9982	Molecular dynamics simulations elucidate oligosaccharide recognition pathways by galectin-3 at atomic resolution. Journal of Biological Chemistry, 2021, 297, 101271.	3.4	3
9983	SHANK3 conformation regulates direct actin binding and crosstalk with Rap1 signaling. Current Biology, 2021, 31, 4956-4970.e9.	3.9	14
9984	Comprehensive Identification of Deleterious TP53 Missense VUS Variants Based on Their Impact on TP53 Structural Stability. International Journal of Molecular Sciences, 2021, 22, 11345.	4.1	5
9986	Structure and Formation Mechanism of Antimicrobial Peptides Temporin B- and L-Induced Tubular Membrane Protrusion. International Journal of Molecular Sciences, 2021, 22, 11015.	4.1	7
9988	A Systematic Approach: Molecular Dynamics Study and Parametrisation of Gemini Type Cationic Surfactants. International Journal of Molecular Sciences, 2021, 22, 10939.	4.1	2
9989	Molecular Mechanism of the Anti-Inflammatory Action of Heparin. International Journal of Molecular Sciences, 2021, 22, 10730.	4.1	20
9990	The Influences of Sulphation, Salt Type, and Salt Concentration on the Structural Heterogeneity of Glycosaminoglycans. International Journal of Molecular Sciences, 2021, 22, 11529.	4.1	13
9991	Domain Formation in Charged Polymer Vesicles. Macromolecules, 2021, 54, 9258-9267.	4.8	5
9993	Molecular docking and simulation studies of phytocompounds derived from Centella asiatica and Andrographis paniculata against hexokinase II as mitocan agents. Mitochondrion, 2021, 61, 138-146.	3.4	12
9994	Molecular modelling of the FOXO4-TP53 interaction to design senolytic peptides for the elimination of senescent cancer cells. EBioMedicine, 2021, 73, 103646.	6.1	21



#	ARTICLE	IF	CITATIONS
9995	Identification of Berberine, Oxyacanthine and Rutin from Berberis asiatica as anti-SARS-CoV-2 compounds: An in silico study. Journal of Molecular Graphics and Modelling, 2021, 109, 108028.	2.4	10
9996	Role of molecular dynamics in optimising ligand discovery: Case study with novel inhibitor search for peptidyl t-RNA hydrolase. Chemical Physics Impact, 2021, 3, 100048.	3.5	3
9997	Dissolving power of the binary solvent carbon tetrachloride & methanol. Solubility of caffeine: Experiment, ASL model, and MD simulation. Journal of Molecular Liquids, 2021, 344, 117736.	4.9	5
9998	In-silico behavior of dissolved prolamins under electric field effect applied by electrospinning process using molecular dynamics simulation. Journal of Molecular Liquids, 2021, 344, 117778.	4.9	11
9999	Conformational dynamics of myoglobin in the presence of vitamin B12: A spectroscopic and in silico investigation. International Journal of Biological Macromolecules, 2021, 192, 564-573.	7.5	9
10000	Designing new antitubercular isoniazid derivatives with improved reactivity and membrane trafficking abilities. Biomedicine and Pharmacotherapy, 2021, 144, 112362.	5.6	11
10001	First-Principles Investigation of Unknown Structures and Properties of Materials under Pressure.. Review of High Pressure Science and Technology/Koatsuryoku No Kagaku To Gijutsu, 2000, 10, 134-141.	0.0	1
10002	On the Effects of Roughness on Structures, Solvation Forces and Shear of Molecular Films in a Nano-Confinement. , 2001, , 583-605.		1
10003	Essential damage mechanics&quot;Bridging the scales. , 2002, , 17-47.		0
10005	Computer Simulations. , 2003, , 145-159.		0
10006	Exploration of coarse free energy surfaces templated on continuum numerical methods. Lecture Notes in Computational Science and Engineering, 2004, , 81-91.	0.3	0
10007	Connffessit. , 2004, , .		1
10009	Multiscale Modeling of Stress Localization and Fracture in Nanocrystalline Metallic Materials. , 2005, , .		0
10010	Development of a general purpose molecular simulation system from microscopic to mesoscopic scales. The KIPS Transactions PartD, 2005, 12D, 921-930.	0.2	0
10012	Phases and crystal structures. , 2007, , 3-86.		0
10013	Energetic Study on Defect Structures in Nanocrystalline Aluminum and Copper by Atomic Simulations. Zairoy/Journal of the Society of Materials Science, Japan, 2007, 56, 1068-1075.	0.2	2
10014	Numerical simulation of residual stresses at the grain and sub-grain length scale using atomistic modeling<sup>â—</sup>. HTM - Journal of Heat Treatment and Materials, 2007, 62, 85-90.	0.2	0
10015	Petascale Special-Purpose Computer for Molecular Dynamics Simulations. Chapman & Hall/CRC Computational Science, 2007, , 183-209.	0.5	0

#	ARTICLE	IF	CITATIONS
10016	Atomistic Formation Mechanism of Multiple Shear Bands in Amorphous Metals. Zaiyo/Journal of the Society of Materials Science, Japan, 2008, 57, 119-125.	0.2	6
10017	Monte Carlo Simulations of a Coarse-Grain Model for Block Copolymer Systems. , 2008, , 361-377.		0
10018	Multiscale Materials. , 2009, , 481-513.		0
10019	An atomistic simulation on melting and breaking relaxation characteristics of Ag nanorods at high temperature. Wuli Xuebao/Acta Physica Sinica, 2010, 59, 6377.	0.5	1
10020	Construction of metallic nanocrystalline samples by molecular dynamics simulation. Wuli Xuebao/Acta Physica Sinica, 2010, 59, 4781.	0.5	6
10021	N-Body Computational Methods. , 2011, , 1259-1268.		0
10022	Molecular dynamics simulation for the impact of hydrazine on the water of pressurized water reactors. Wuli Xuebao/Acta Physica Sinica, 2011, 60, 032802.	0.5	1
10023	Effect of Substituted Aluminum in Magnesium Tension Twin. , 2011, , 325-329.		0
10024	Strength in Atomic Components. , 2011, , 217-270.		0
10025	Influence of Yttrium on Creep Behavior in Nano-Crystalline Magnesium Using Molecular Dynamics Simulation. , 2013, , 21-26.		0
10028	Influence Factors for Brittle-to-Ductile Transition in Twinned Copper. , 2014, , 487-494.		0
10029	Molecular-Dynamic Simulations of Many-Particle Systems: New Faces on Old Problems. , 1985, , 521-563.		0
10031	Computer Simulation of Nonequilibrium Processes. , 1986, , 37-49.		1
10032	Calculation of Elastic Constants Using Molecular Dynamics. , 1987, , 41-50.		0
10033	Computer Simulation of Quasi Two-Dimensional Phases. , 1987, , 73-107.		0
10034	Molecular Dynamics Studies of Glass Transitions: Vitrification and Amortization. , 1987, , 1-7.		0
10035	Current Movements in Molecular Dynamics Study with Regard to Its Application to Materials Science and Engineering. Tetsu-To-Hagane/Journal of the Iron and Steel Institute of Japan, 1988, 74, 753-763.	0.4	3
10036	Molecular Dynamics Simulations of Materials: Beyond Pair Interactions. , 1989, , 443-459.		0

#	ARTICLE	IF	CITATIONS
10037	Molecular Dynamics. Mechanics and Physics of Discrete Systems, 1990, 2, 141-171.	0.0	0
10038	Molecular Dynamics. , 1990, , 55-82.		0
10039	Interatomic Potentials. Mechanics and Physics of Discrete Systems, 1990, , 37-64.	0.0	0
10040	Monte Carlo Methods in Classical Statistical Mechanics. , 1990, , 195-228.		0
10041	Computer Simulation Algorithms. , 1990, , 121-168.		2
10042	Molecular Dynamics Simulation of Silica with a First-Principles Interatomic Potential. , 1990, , 1-21.		1
10043	Applications of molecular dynamics simulation in materials research.. Zairyo/Journal of the Society of Materials Science, Japan, 1991, 40, 509-518.	0.2	2
10044	The Application of Computer Simulations to Mineralogy.. Journal of the Mineralogical Society of Japan, 1992, 21, 69-78.	0.2	0
10045	MD Simulation of Crystal Structures, Physical Properties, and Phase Transitions.. Journal of the Mineralogical Society of Japan, 1992, 21, 205-209.	0.2	0
10046	Monte-Carlo Simulations in Adiabatic Ensembles. Springer Proceedings in Physics, 1993, , 155-161.	0.2	0
10047	Modeling materials for microelectronics – The old and the new challenges. , 1993, , 1575-1580.		0
10048	Computer Simulation of the Structural and Physical Properties of Minerals in the Earth's Deep-Interior.. Nihon Kessho Gakkaishi, 1993, 35, 190-197.	0.0	0
10049	A short random walk through polymer material behavior. The IMA Volumes in Mathematics and Its Applications, 1995, , 186-197.	0.5	0
10050	MOLECULAR DYNAMICS STUDY OF DEFORMATION MECHANISM AND DAMAGE IN SINGLE-COMPONENT AMORPHOUS. , 1996, , 489-494.		1
10051	Molecular Dynamics Simulation of Silica with a First-principles Interatomic Potential. Topics in Molecular Organization and Engineering, 1997, , 201-226.	0.1	2
10052	Molecular Dynamics Simulations. Molecular Dynamics Simulation of Ni Crystals under Uniaxial Deformation.. Zairyo/Journal of the Society of Materials Science, Japan, 1997, 46, 228-231.	0.2	0
10053	Large-Scale Simulations of Melting in Two-Dimensional Lennard-Jones Systems: Evidence for a Metastable Hexatic Phase. Springer Proceedings in Physics, 1997, , 31-42.	0.2	0
10054	Accelerated Molecular Dynamics Method. Advances in Materials Research, 1998, , 229-238.	0.2	0

#	ARTICLE	IF	CITATIONS
10055	Instability Analyses of Stress-Induced Phase Transformation. Advances in Materials Research, 1998, , 100-110.	0.2	0
10056	Analysis on Structure and Formation Energy of Junction of Grain Boundary and Surface in Aluminum by Molecular Dynamics.. Zairyo/Journal of the Society of Materials Science, Japan, 1999, 48, 991-996.	0.2	0
10057	Molecular Dynamics Simulations of Plastic Damage in Metals. , 2015, , 453-486.		2
10059	Computer Simulation Study of the Molecular Dynamics in Homocysteine Systems. Springer Proceedings in Physics, 2015, , 365-386.	0.2	0
10060	Anisotropy of melting of Ag nanocrystal with different crystallographic planes at high temperature. Wuli Xuebao/Acta Physica Sinica, 2015, 64, 106101.	0.5	1
10061	Temperature dependent electronic properties of bulk Aluminium system. Bitlis Eren University Journal of Science and Technology, 2013, 3, 39-39.	0.8	0
10062	Prediction of Lysine Acetylation Sites in Porcine Pancreas Lipase Modified by the Ionic Liquids Using Molecular Dynamics Simulations. Lecture Notes in Electrical Engineering, 2015, , 365-379.	0.4	0
10063	Creation of the ab initio theoretical high-pressure mineral physics. Ganseki Kobutsu Kagaku, 2015, 44, 10-24.	0.1	0
10064	Structural and Material Perturbations of Lipid Bilayers Due to HIV-1 Tat Peptide. Springer Theses, 2015, , 9-63.	0.1	0
10065	Molecular dynamics simulation of crystallization of amorphous aluminium modelled with EAM. Bitlis Eren University Journal of Science and Technology, 2012, 2, 44-44.	0.8	2
10066	FLEXIBILITY ANALYSIS OF NATIVE PYRIDOXAL KINASE AND ITS COMPLEXES WITH ATP AND ADP: A MOLECULAR DYNAMICS SIMULATION STUDY. International Journal for Computational Biology, 2015, 5, 13.	0.1	0
10067	Inhibitory Effect of Bridged Nucleosides on Thermus aquaticus DNA Polymerase and Insight into the Binding Interactions. PLoS ONE, 2016, 11, e0147234.	2.5	1
10068	NOVEL APPROACH TO MAKE HUGONOT PREDICTIONS: QUANTUM MECHANICS/MOLECULAR DYNAMICS CALCULATIONS. International Journal of Energetic Materials and Chemical Propulsion, 2016, 15, 89-111.	0.3	0
10069	Molecular Dynamics Simulations and Comparison of Two New and High Selective Imprinted Xerogels. , 2016, , 339-361.		0
10072	A Molecular Dynamics Simulation Study of Hydroxyls in Dioctahedral Phyllosilicates. Journal of the Mineralogical Society of Korea, 2016, 29, 209-220.	0.2	0
10074	Molecular Dynamics Simulation of Membrane Free Energy Profiles Using Accurate Force Field for Ionic Liquids. , 2017, , 265-284.		0
10075	Quantum Chemical Studies of Hole Transfer in Liquid Hexane. IEEJ Transactions on Fundamentals and Materials, 2017, 137, 435-441.	0.2	1
10076	Molecular dynamic simulations of glycine amino acid association with potassium and sodium ions in explicit solvent. F1000Research, 0, 6, 74.	1.6	1

#	ARTICLE	IF	CITATIONS
10095	Atomistic simulation of microvoid formation and its influence on crack nucleation in hexagonal titanium. Wuli Xuebao/Acta Physica Sinica, 2018, 67, 050203.	0.5	0
10112	Hidrojen depolama malzemeleri için MgH <sub>2</sub> 'nin yapısı ve elektronik özellikleri. Gazi Üniversitesi Fen Bilimleri Dergisi, 0, , 451-461.	0.6	1
10132	Criteria of instability of copper and aluminium perfect crystals subjected to elastic deformation in the temperature range 0â€‰%â€‰â€‰400Â°K. Letters on Materials, 2019, 9, 265-269.	0.7	1
10135	In Silico Molecular Modelling: Key Technologies in the Drug Discovery Process to Combat Multidrug Resistance. , 2019, , 213-238.		0
10140	Molecular Dynamics Simulation and Quantum Chemical Calculations of Surfactant Having Suppression Effect on Water Trees. IEEJ Transactions on Fundamentals and Materials, 2019, 139, 92-98.	0.2	3
10161	The Thermodynamic and Lattice Vibrational Properties of CuPd Alloy Under Hydrostatic Pressure. Anadolu University Journal of Sciences & Technology, 0, , .	0.2	0
10188	Suppression of Electrical and Water Tree by Additive Molecules: A Computational Insight. Lecture Notes in Electrical Engineering, 2020, , 12-21.	0.4	0
10195	Molecular Dynamics Study of the Hydrogen and Carbon Effect on Mobility of Grain Boundaries in $\alpha$ -Fe. Metallofizika i Noveishie Tekhnologii, 2019, 41, 1187-1203.	0.5	0
10204	A Universal Allosteric Mechanism for G Protein Activation. SSRN Electronic Journal, 0, , .	0.4	0
10205	Enhanced Molecular Dynamics Simulations of Intrinsically Disordered Proteins. Methods in Molecular Biology, 2020, 2141, 391-411.	0.9	8
10212	Molecular Dynamics Simulation, Characterization and In Vitro Drug Release of Isoniazid Loaded Poly- $\epsilon$ -caprolactone Magnetite Nanocomposite. Pharmaceutical Sciences, 2020, 26, 406-413.	0.2	0
10223	Polyelectrolyte in Electric Field: Disparate Conformational Behavior along an Aminopolysaccharide Chain. ACS Omega, 2020, 5, 12016-12026.	3.5	11
10225	Embedded Mean-Field Theory for Solution-Phase Transition-Metal Polyolefin Catalysis. Journal of Chemical Theory and Computation, 2020, 16, 4226-4237.	5.3	3
10230	Molecular dynamics simulation of the heart type fatty acid binding protein in a crystal environment. Journal of Biomolecular Structure and Dynamics, 2021, 39, 3459-3468.	3.5	2
10247	One-dimensional nature of protein low-energy vibrations. Physical Review Research, 2020, 2, .	3.6	7
10248	Molecular Simulations Guidelines for Biological Nanomaterials: From Peptides to Membranes. Methods in Molecular Biology, 2021, 2208, 81-100.	0.9	0
10253	First-principles Based Simulation of Electron and Hole Transfer in PET Oligomer. IEEJ Transactions on Fundamentals and Materials, 2020, 140, 425-431.	0.2	0
10254	Molecular dynamics simulation of mass transfer characteristics of DMSO at the hexane/water interface in the presence of amphiphilic Janus nanoparticles. Chemical Engineering Science, 2022, 248, 117231.	3.8	4

#	ARTICLE	IF	CITATIONS
10255	Structure and vibrational features of the protic ionic liquid 1,8-diazabicyclo[5.4.0]-undec-7-ene-8-ium bis(trifluoromethanesulfonyl)amide, [DBUH][TFSI]. Journal of Molecular Liquids, 2022, 347, 117981.	4.9	2
10257	Screening and Identification of Potential iNOS Inhibitors to Curtail Cervical Cancer Progression: an In Silico Drug Repurposing Approach. Applied Biochemistry and Biotechnology, 2022, 194, 570-586.	2.9	10
10258	Phospholipids dock SARS-CoV-2 spike protein via hydrophobic interactions: a minimal in-silico study of lecithin nasal spray therapy. European Physical Journal E, 2021, 44, 132.	1.6	2
10259	Aggregation properties of a therapeutic peptide for rheumatoid arthritis: A spectroscopic and molecular dynamics study. ChemPhysMater, 2021, 1, 62-62.	2.8	2
10261	Glycosylation and Serological Reactivity of an Expression-enhanced SARS-CoV-2 Viral Spike Mimetic. Journal of Molecular Biology, 2022, 434, 167332.	4.2	22
10263	A combined molecular docking and molecular dynamics simulation approach to probing the host-guest interactions of Ataluren with natural and modified cyclodextrins. Molecular Simulation, 2022, 48, 108-119.	2.0	6
10264	Structural Insights into the Human Mitochondrial Pyruvate Carrier Complexes. Journal of Chemical Information and Modeling, 2021, 61, 5614-5625.	5.4	5
10265	Size and Structure of Empty and Filled Nanocontainer Based on Peptide Dendrimer with Histidine Spacers at Different pH. Molecules, 2021, 26, 6552.	3.8	6
10266	Genetic, cellular, and structural characterization of the membrane potential-dependent cell-penetrating peptide translocation pore. ELife, 2021, 10, .	6.0	31
10267	Structural basis of polyamine transport by human ATP13A2 (PARK9). Molecular Cell, 2021, 81, 4635-4649.e8.	9.7	22
10268	Investigation of Antidepressant Properties of Yohimbine by Employing Structure-Based Computational Assessments. Current Issues in Molecular Biology, 2021, 43, 1805-1827.	2.4	18
10269	Tailored Parameterization of the LIE Method for Calculating the Binding Free Energy of Vps34-Inhibitor Complexes. ACS Omega, 2021, 6, 29525-29536.	3.5	4
10270	Pharmacological chaperones improve intra-domain stability and inter-domain assembly via distinct binding sites to rescue misfolded CFTR. Cellular and Molecular Life Sciences, 2021, 78, 7813-7829.	5.4	36
10273	O-Methylation in Carbohydrates: An NMR and MD Simulation Study with Application to Methylcellulose. Journal of Physical Chemistry B, 2021, 125, 11967-11979.	2.6	7
10274	Structure and Mechanical Stabilities of the Three-Way Junction Motifs in Prohead RNA. Journal of Physical Chemistry B, 2021, 125, 12125-12134.	2.6	2
10275	Computational spectroscopy of complex systems. Journal of Chemical Physics, 2021, 155, 170901.	3.0	27
10276	Enabling Magnesium Anodes by Tuning the Electrode/Electrolyte Interfacial Structure. ACS Applied Materials & Interfaces, 2021, 13, 52461-52468.	8.0	13
10277	Experimental and Simulation Study of the Solvent Effects on the Intrinsic Properties of Spherical Lignin Nanoparticles. Journal of Physical Chemistry B, 2021, 125, 12315-12328.	2.6	21



#	ARTICLE	IF	CITATIONS
10278	The Impact of Mutation L138F/L210F on the Orai Channel: A Molecular Dynamics Simulation Study. <i>Frontiers in Molecular Biosciences</i> , 2021, 8, 755247.	3.5	4
10279	Weakly hydrated anions bind to polymers but not monomers in aqueous solutions. <i>Nature Chemistry</i> , 2022, 14, 40-45.	13.6	57
10280	Systematic Search for a Predictor for the Clinical Observables of Alzheimer's Disease. <i>Journal of Physical Chemistry B</i> , 2021, 125, 12177-12186.	2.6	2
10281	Potential of turmeric-derived compounds against RNA-dependent RNA polymerase of SARS-CoV-2: An in-silico approach. <i>Computers in Biology and Medicine</i> , 2021, 139, 104965.	7.0	54
10286	Development and Testing of Force Field Parameters for Phenylalanine and Tyrosine Derivatives. <i>Frontiers in Molecular Biosciences</i> , 2020, 7, 608931.	3.5	2
10287	Origin of subdiffusions in proteins: Insight from peptide systems. <i>Physical Review E</i> , 2020, 102, 062424.	2.1	5
10288	Free energy calculations of the functional selectivity of 5-HT2B G protein-coupled receptor. <i>PLoS ONE</i> , 2020, 15, e0243313.	2.5	2
10290	Update on Performance Analysis of Different Computational Architectures: Molecular Dynamics in Application to Protein-Protein Interactions. <i>Supercomputing Frontiers and Innovations</i> , 2020, 7, .	0.4	1
10291	Effect of Cosolvent Ethanol on Solubilization of Ionic Liquids in Supercritical CO <sub>2</sub> Microemulsions: Experiments and Simulations. <i>Journal of Chemical &amp; Engineering Data</i> , 2021, 66, 347-359.	1.9	2
10292	Unraveling microstrain-promoted structural evolution and thermally driven phase transition in $\text{O}_3\text{C}$ nanocrystals at high pressure. <i>Physical Review B</i> , 2020, 102, .		
10295	Interactions of Gallic Acid with Porcine Hemoglobin: Effect on the Redox State and Structure of Hemoglobin. <i>Journal of Agricultural and Food Chemistry</i> , 2021, 69, 397-403.	5.2	19
10298	Ab Initio QM/MM Simulation of Ferrocene Homogeneous Electron-Transfer Reaction. <i>Journal of Physical Chemistry A</i> , 2021, 125, 25-33.	2.5	7
10299	Why the Orientational Mobility in Arginine and Lysine Spacers of Peptide Dendrimers Designed for Gene Delivery Is Different?. <i>International Journal of Molecular Sciences</i> , 2020, 21, 9749.	4.1	7
10301	Water/oil interfacial tension reduction is an interfacial entropy driven process. <i>Physical Chemistry Chemical Physics</i> , 2021, 23, 25075-25085.	2.8	17
10302	On the transport and dynamics of disaccharides: H-bonding effect in sucrose and sucralose. <i>Journal of Molecular Liquids</i> , 2022, 345, 117855.	4.9	8
10303	Efficient anisotropic desalination by layer-stacked black phosphorus carbide ( $\text{I}\pm\text{PC}$ ) membrane. <i>Desalination</i> , 2022, 522, 115422.	8.2	9
10304	The stressed life of a lipid in the Zika virus membrane. <i>Biochimica Et Biophysica Acta - Biomembranes</i> , 2022, 1864, 183804.	2.6	6
10305	The role of water coordination in the pH-dependent gating of hAQP10. <i>Biochimica Et Biophysica Acta - Biomembranes</i> , 2022, 1864, 183809.	2.6	3

#	ARTICLE	IF	CITATIONS
10306	Structure analysis of aqueous Mg(NO <sub>3</sub> ) <sub>2</sub> solutions. Spectrochimica Acta - Part A: Molecular and Biomolecular Spectroscopy, 2022, 267, 120478.	3.9	5
10307	Insights into the mechanism during viscosity reduction process of heavy oil through molecule simulation. Fuel, 2022, 310, 122270.	6.4	27
10308	Chemical short-range order strengthening mechanism in CoCrNi medium-entropy alloy under nanoindentation. Scripta Materialia, 2022, 209, 114364.	5.2	48
10309	Study on simultaneous binding of resveratrol and curcumin to $\beta$ -lactoglobulin: Multi-spectroscopic, molecular docking and molecular dynamics simulation approaches. Food Hydrocolloids, 2022, 124, 107331.	10.7	46
10310	Correlation between the topologically close-packed structure and the deformation behavior of metallic Cu <sub>64.5</sub> Zr <sub>35.5</sub> . Physical Chemistry Chemical Physics, 2021, 23, 25933-25943.	2.8	8
10311	Rearrangement of protein structures on a gold nanoparticle surface is regulated by ligand adsorption modes. Nanoscale, 2021, 13, 20425-20436.	5.6	7
10312	Distinct Roles of Graphene and Graphene Oxide Nanosheets in Regulating Phospholipid Flip-Flopcover Letter. SSRN Electronic Journal, 0, , .	0.4	0
10316	Molecular Dynamics Performance Evaluation with Modern Computer Architecture. Lecture Notes in Computer Science, 2020, , 322-329.	1.3	0
10318	In Silico Study on the Structure of Novel Natural Bioactive Peptides. Lecture Notes in Computer Science, 2020, , 332-339.	1.3	0
10319	Insights on Solidification of Mg and Mg-Al Alloys by Large Scale Atomistic Simulations. Minerals, Metals and Materials Series, 2020, , 51-53.	0.4	0
10322	Effects of Water Molecules on Metal Complexes of Hydroxyoxime and Carboxylic Acid Extractants. Solvent Extraction Research and Development, 2020, 27, 25-38.	0.4	1
10329	A buried glutamate in the cross- $\beta$ core renders $\beta$ -endorphin fibrils reversible. Nanoscale, 2021, 13, 19593-19603.	5.6	4
10330	Homogeneous nucleation of NaCl in supersaturated solutions. Physical Chemistry Chemical Physics, 2021, 23, 26843-26852.	2.8	20
10331	Potential interference of graphene nanosheets in immune response <i>via</i> disrupting the recognition of HLA-presented KK10 by TCR: a molecular dynamics simulation study. Nanoscale, 2021, 13, 19255-19263.	5.6	4
10336	In silico Analysis of Sulpiride, Synthesis, Characterization and In vitro Studies of its Nanoparticle for the Treatment of Schizophrenia. Current Computer-Aided Drug Design, 2020, 16, 104-121.	1.2	9
10338	Introduction to molecular dynamics and its application to mechanical behaviors. Keikinzoku/Journal of Japan Institute of Light Metals, 2020, 70, 107-112.	0.4	0
10344	Molecular Structure and Vibrational Spectra of Water Molecules Sorbed in Poly(2-methoxyethylacrylate) Revealed by Molecular Dynamics Simulation. Journal of Physical Chemistry B, 2021, 125, 12095-12103.	2.6	6
10345	Engineering of Cytolethal Distending Toxin B by Its Reducing Immunogenicity and Maintaining Stability as a New Drug Candidate for Tumor Therapy; an In Silico Study. Toxins, 2021, 13, 785.	3.4	5

#	ARTICLE	IF	CITATIONS
10346	Maturation of siRNA by strand separation: Steered molecular dynamics study. <i>Journal of Biomolecular Structure and Dynamics</i> , 2022, 40, 13682-13692.	3.5	2
10347	Molecular recognition of two bioactive coumarin derivatives 7-hydroxycoumarin and 4-methyl-7-hydroxycoumarin by hen egg white lysozyme: Exploring the binding mechanism, thermodynamic parameters and structural changes using multispectroscopic and computational approaches. <i>Journal of Biomolecular Structure and Dynamics</i> , 2022, 40, 13872-13888.	3.5	2
10348	Computational insights into differential interaction of mammalian angiotensin-converting enzyme 2 with the SARS-CoV-2 spike receptor binding domain. <i>Computers in Biology and Medicine</i> , 2022, 141, 105017.	7.0	11
10349	Zn(II) binding causes interdomain changes in the structure and flexibility of the human prion protein. <i>Scientific Reports</i> , 2021, 11, 21703.	3.3	8
10351	Finding the First Potential Inhibitors of Shikimate Kinase from Methicillin Resistant <i>Staphylococcus aureus</i> through Computer-Assisted Drug Design. <i>Molecules</i> , 2021, 26, 6736.	3.8	2
10352	Local Structural Dynamics at the Metal-Centered Catalytic Site of Polymerases is Critical for Fidelity. <i>ACS Catalysis</i> , 2021, 11, 14110-14121.	11.2	7
10353	Progress toward SHAPE Constrained Computational Prediction of Tertiary Interactions in RNA Structure. <i>Non-coding RNA</i> , 2021, 7, 71.	2.6	6
10354	Relaxed complex scheme and molecular dynamics simulation suggests small molecule inhibitor of human TMPRSS2 for combating COVID-19. <i>Journal of Biomolecular Structure and Dynamics</i> , 2021, , 1-11.	3.5	1
10355	The TAR binding dynamics and its implication in Tat degradation mechanism. <i>Biophysical Journal</i> , 2021, 120, 5158-5168.	0.5	8
10356	Molecular Simulations of Vaporâ€“Liquid Equilibrium of Isocyanates. <i>Journal of Physical Chemistry B</i> , 2021, 125, 12528-12538.	2.6	2
10357	Cholesterol-Mediated Clustering of the HIV Fusion Protein gp41 in Lipid Bilayers. <i>Journal of Molecular Biology</i> , 2022, 434, 167345.	4.2	4
10358	Liquid Structure of a Water-in-Salt Electrolyte with a Remarkably Asymmetric Anion. <i>Journal of Physical Chemistry B</i> , 2021, 125, 12500-12517.	2.6	11
10359	Sitosterol and glucosylceramide cooperative transversal and lateral uneven distribution in plant membranes. <i>Scientific Reports</i> , 2021, 11, 21618.	3.3	3
10361	Origin of Apparent Slow Solvent Dynamics in Concentrated Polymer Solutions. <i>Macromolecules</i> , 2021, 54, 10340-10349.	4.8	10
10362	Novel Insights into the Self-assembly Behaviors of Cationic Surfactant and Bivalent Acid: Effects of Group Positions in Bivalent Acid. <i>Journal of Molecular Liquids</i> , 2021, , 118012.	4.9	0
10363	Phenylethanoid glycosides as a possible COVID-19 protease inhibitor: a virtual screening approach. <i>Journal of Molecular Modeling</i> , 2021, 27, 341.	1.8	10
10364	Fullerene C60 spectroscopy in [BMIM][PF6] ionic liquid: Molecular dynamics study using polarization effects. <i>Journal of Molecular Structure</i> , 2022, 1250, 131887.	3.6	5
10365	Identification and comparison of plant-derived scaffolds as selective CDK5 inhibitors against standard molecules: Insights from umbrella sampling simulations. <i>Journal of Molecular Liquids</i> , 2022, 348, 118015.	4.9	11

#	ARTICLE	IF	CITATIONS
10366	Improving the self-assembly of bioresponsive nanocarriers by engineering doped nanocarbons: a computational atomistic insight. <i>Scientific Reports</i> , 2021, 11, 21538.	3.3	5
10368	Biological Evaluation and Molecular Modeling of 3,4-dihydropyrimidine- 2(1H)-one Derivatives as Cytotoxic Agents on Breast Cancer In Vitro. <i>Letters in Drug Design and Discovery</i> , 2020, 17, 983-992.	0.7	0
10376	Alpha-synucleinâ€™™ in PreNAC(46-56) Fibril Bâ€™™tâ€™™n Molekâ€™™ler Dinamik Simâ€™™lasyon Yâ€™™ntemi ile Konformasyonel Deâ€™™erlendirmesi. <i>Kahramanmaraâ€™™ Sâ€™™tâ€™™nâ€™™mâ€™™m âœ“niversitesi Tarâ€™™m Ve Doâ€™™a Dergisi</i> , 0, , .	0.7	1
10378	Studying the Effect of Amino Acid Substitutions in the M2 Ion Channel of the Influenza Virus on the Antiviral Activity of the Aminoadamantane Derivative<i>In Vitro</i> and<i>In Silico</i>. <i>Advanced Pharmaceutical Bulletin</i> , 2020, 11, 700-711.	1.4	5
10379	Atomistic Visualization. , 2005, , 1051-1068.		1
10380	Multiscale modeling of intergranular fracture in metals. , 2007, , 343-367.		0
10381	The Interaction of Ile-Phe Dipeptide with Phosphatidylinositide 3-Kinase (PI3K): Molecular Dynamics and Molecular Docking Studies. <i>Natural and Engineering Sciences</i> , 2020, 5, 18-29.	0.3	0
10382	Short-wavelength-sensitive 2 (Sws2) visual photopigment models combined with atomistic molecular simulations to predict spectral peaks of absorbance. <i>PLoS Computational Biology</i> , 2020, 16, e1008212.	3.2	3
10392	Polarizable Embedding as a Tool to Address Light-Responsive Biological Systems. Challenges and Advances in Computational Chemistry and Physics, 2021, , 143-195.	0.6	3
10393	Targeting 14-3-3â€™™-CDC25A interactions to trigger apoptotic cell death in skin cancer. <i>Oncotarget</i> , 2020, 11, 3267-3278.	1.8	8
10398	Universal relationship of boson peak with Debye level and Debye-Waller factor in disordered materials. <i>Physical Review Materials</i> , 2020, 4, .	2.4	5
10399	Reconstruction of protein structures from single-molecule time series. <i>Journal of Chemical Physics</i> , 2020, 153, 194102.	3.0	6
10406	Effect of Intramolecular Disulfide Bonds of Bovine Serum Albumin on Its Binding and Pseudo-Esterase Activity According To Computer Modeling Data. , 0, , .		0
10407	Non-fullerene electron acceptors constructed by four strong electron-withdrawing end groups: Potential to improve the photoelectric performance of organic solar cells by theoretical investigations. <i>Dyes and Pigments</i> , 2020, 181, 108542.	3.7	7
10408	Molecular dynamics, MM/PBSA and inâ€™™vitro validation of a novel quinazoline-based EGFR tyrosine kinase inhibitor identified using structure-based in silico screening. <i>Journal of Molecular Graphics and Modelling</i> , 2020, 99, 107639.	2.4	6
10409	Structure of anisole derivatives by total neutron and X-ray scattering: Evidences of weak C Hâ€™™O and C Hâ€™™â€™™ interactions in the liquid state. <i>Journal of Molecular Liquids</i> , 2020, 314, 113795.	4.9	6
10410	Scaffold-based Screening and Molecular Dynamics Simulation Study to Identify Two Structurally Related Phenolic Compounds as Potent MMP1 Inhibitors. <i>Combinatorial Chemistry and High Throughput Screening</i> , 2020, 23, 757-774.	1.1	1
10411	Substitution of distal and active site residues reduces product inhibition of E1 from <i>Acidothermus Cellulolyticus</i>. <i>Protein Engineering, Design and Selection</i> , 2021, 34, .	2.1	2

#	ARTICLE	IF	CITATIONS
10412	Towards a predictive model for polymer solubility using the noncovalent interaction index: polyethylene as a case study. <i>Physical Chemistry Chemical Physics</i> , 2021, 23, 25374-25387.	2.8	6
10413	Structural and dynamic insights into Mn <sub>4</sub> Ca cluster-depleted Photosystem II. <i>Physical Chemistry Chemical Physics</i> , 2021, 23, 27428-27436.	2.8	3
10414	Atomistic Mechanisms Underlying Plasticity and Crack Growth in Ceramics: A Case Study of AlN/Tin Superlattices. <i>SSRN Electronic Journal</i> , 0, , .	0.4	0
10415	Investigation of the anti-inflammatory and analgesic activities of promising pyrazole derivative. <i>European Journal of Pharmaceutical Sciences</i> , 2022, 168, 106080.	4.0	25
10416	Disulfide Bonds Play a Critical Role in the Structure and Function of the Receptor-binding Domain of the SARS-CoV-2 Spike Antigen. <i>Journal of Molecular Biology</i> , 2022, 434, 167357.	4.2	43
10417	Molecular basis of the anticancer, apoptotic and antibacterial activities of Bombyx mori Cecropin A. <i>Archives of Biochemistry and Biophysics</i> , 2022, 715, 109095.	3.0	9
10418	Nucleation and dissociation of carbon dioxide hydrate in the inter- and intra-particle pores of dioctahedral smectite: Mechanistic insights from molecular dynamics simulations. <i>Applied Clay Science</i> , 2022, 216, 106344.	5.2	16
10419	Molecular insights into the uptake of SiO <sub>2</sub> nanoparticles on phospholipid membrane: Effect of surface properties and particle size. <i>Colloids and Surfaces B: Biointerfaces</i> , 2022, 210, 112250.	5.0	10
10420	Molecular mechanism for methane hydrate nucleation on corroded iron surface. <i>Chemical Engineering Science</i> , 2022, 249, 117303.	3.8	6
10421	Conformational exploration of RbgA using molecular dynamics: Possible implications in ribosome maturation and GTPase activity in different nucleotide bound states. <i>Journal of Molecular Graphics and Modelling</i> , 2022, 111, 108087.	2.4	1
10422	The role of temperature in the binding of the disordered epitope region of human thrombopoietin to antibody: A molecular dynamics simulations study. <i>Journal of Molecular Graphics and Modelling</i> , 2022, 111, 108098.	2.4	1
10425	Investigation of Marine-Derived Natural Products as Raf Kinase Inhibitory Protein (RKIP)-Binding Ligands. <i>Marine Drugs</i> , 2021, 19, 581.	4.6	5
10426	A general theoretical framework to design base editors with reduced bystander effects. <i>Nature Communications</i> , 2021, 12, 6529.	12.8	10
10427	Computational Insights into the Unfolding of a Destabilized Superoxide Dismutase 1 Mutant. <i>Biology</i> , 2021, 10, 1240.	2.8	1
10428	The structure of the <i>Aquifex aeolicus</i> MATE family multidrug resistance transporter and sequence comparisons suggest the existence of a new subfamily. <i>Proceedings of the National Academy of Sciences of the United States of America</i> , 2021, 118, .	7.1	5
10429	AMPA GluA2 subunit competitive inhibitors for PICK1 PDZ domain: Pharmacophore-based virtual screening, molecular docking, molecular dynamics simulation, and ADME studies. <i>Journal of Biomolecular Structure and Dynamics</i> , 2023, 41, 336-351.	3.5	1
10430	The initiation of shear band formation in deformed metallic glasses from soft localized domains. <i>Journal of Chemical Physics</i> , 2021, 155, 204504.	3.0	13
10431	How Does <i>Dc</i> AFP, a Plant Antifreeze Protein, Control Ice Inhibition through the Kelvin Effect?. <i>Industrial &amp; Engineering Chemistry Research</i> , 2021, 60, 18230-18242.	3.7	3

#	ARTICLE	IF	CITATIONS
10432	Do non-thermal effects exist in microwave heating of glucose aqueous solutions? Evidence from molecular dynamics simulations. Food Chemistry, 2022, 375, 131677.	8.2	9
10433	Gating of Substrate Access and Long-Range Proton Transfer in <i>Escherichia coli</i> Nitrate Reductase A: The Essential Role of a Remote Glutamate Residue. ACS Catalysis, 2021, 11, 14303-14318.	11.2	8
10434	New insights on the mechanism of polyethylenimine transfection and their implications on gene therapy and DNA vaccines. Colloids and Surfaces B: Biointerfaces, 2022, 210, 112219.	5.0	23
10435	Molecular simulation studies of self-assembly for a chromonic perylene dye: All-atom studies and new approaches to coarse-graining. Journal of Molecular Liquids, 2022, 345, 118210.	4.9	6
10436	Molecular dynamics study of hydrogen bond in peptide membrane at 150–300 ÅK. Journal of Molecular Liquids, 2022, 349, 118165.	4.9	4
10437	High-resolution structure and dynamics of mitochondrial complex I—Insights into the proton pumping mechanism. Science Advances, 2021, 7, eabj3221.	10.3	65
10438	Local Orientational Mobility of Collapsed Dendrimers. Macromolecules, 2021, 54, 11083-11092.	4.8	4
10439	Structure of the hexameric fungal plasma membrane proton pump in its autoinhibited state. Science Advances, 2021, 7, eabj5255.	10.3	20
10440	Mechanisms of ion transport in lithium salt-doped polymeric ionic liquid electrolytes at higher salt concentrations. Journal of Polymer Science, 2022, 60, 199-213.	3.8	5
10441	Tracking the ATP-binding response in adenylate kinase in real time. Science Advances, 2021, 7, eabi5514.	10.3	18
10443	Efficient protein incorporation and release by a jigsaw-shaped self-assembling peptide hydrogel for injured brain regeneration. Nature Communications, 2021, 12, 6623.	12.8	26
10445	Molecular Simulations of Intrinsically Disordered Proteins and Their Binding Mechanisms. Methods in Molecular Biology, 2022, 2376, 343-362.	0.9	3
10447	Immunoinformatics-Based Designing of a Multi-Epitope Chimeric Vaccine From Multi-Domain Outer Surface Antigens of Leptospira. Frontiers in Immunology, 2021, 12, 735373.	4.8	11
10448	Combinatorial screening of ionic liquid extractant for removal of methanol from methylal. Chemical Engineering Science, 2022, 249, 117317.	3.8	17
10450	Toward Automated Sampling of Polymorph Nucleation and Free Energies with the SGOOP and Metadynamics. Journal of Physical Chemistry B, 2021, 125, 13049-13056.	2.6	9
10451	Structure, dynamics, and function of SrrR, a transcription factor for nickel-dependent gene expression. Metallomics, 2021, 13, .	2.4	4
10452	A systematic drug repurposing approach to identify promising inhibitors from FDA-approved drugs against Nsp4 protein of SARS-CoV-2. Journal of Biomolecular Structure and Dynamics, 2023, 41, 550-559.	3.5	5
10453	Approaching isotropic charge transport of n-type organic semiconductors with bulky substituents. Communications Chemistry, 2021, 4, .	4.5	10



#	ARTICLE	IF	CITATIONS
10454	Destabilization of the Alzheimer's amyloid- $\beta$ peptide by a proline-rich $\beta$ -sheet breaker peptide: a molecular dynamics simulation study. <i>Journal of Molecular Modeling</i> , 2021, 27, 356.	1.8	8
10455	Effect of Surface Coverage of Water Molecules on Methane Adsorption on Muscovite and Pyrophyllite: Molecular Dynamics Study. <i>Energy &amp; Fuels</i> , 2021, 35, 19986-19999.	5.1	6
10456	In Silico Elucidation of Molecular Picture of Water-Choline Chloride Mixture. <i>Journal of Physical Chemistry B</i> , 2021, 125, 13212-13228.	2.6	10
10457	Evaluation on performance of MM/PBSA in nucleic acid-protein systems. <i>Chinese Physics B</i> , 2022, 31, 048701.	1.4	2
10458	Reconsidering the Roles of Noncovalent Intramolecular $\pi$ -Locks in $\pi$ -Conjugated Molecules. <i>Chemistry of Materials</i> , 2021, 33, 9139-9151.	6.7	8
10459	The impact of phosphatidylserine exposure on cancer cell membranes on the activity of the anticancer peptide HB43. <i>FEBS Journal</i> , 2022, 289, 1984-2003.	4.7	6
10460	High-resolution mapping of metal ions reveals principles of surface layer assembly in <i>Caulobacter crescentus</i> cells. <i>Structure</i> , 2022, 30, 215-228.e5.	3.3	12
10461	Temperature-Dependent Dielectric Relaxation in Ionic Acetamide Deep Eutectics: Partial Viscosity Decoupling and Explanations from the Simulated Single-Particle Reorientation Dynamics and Hydrogen-Bond Fluctuations. <i>Journal of Physical Chemistry B</i> , 2021, 125, 12552-12567.	2.6	7
10463	Molecular Investigation of Chicken Acid-Sensing Ion Channel 1 $\beta$ 11-12 Linker Isomerization and Channel Kinetics. <i>Frontiers in Cellular Neuroscience</i> , 2021, 15, 761813.	3.7	3
10464	Evaluation of transport mechanism of ascorbic acid through cyclic peptide-based nanotubes: A molecular dynamics study. <i>Journal of Molecular Liquids</i> , 2022, 349, 118136.	4.9	3
10465	The interaction between citronellol and bovine serum albumin: Spectroscopic, computational and thermal imaging studies. <i>Journal of Molecular Structure</i> , 2021, 1251, 131986.	3.6	3
10466	Calcium Ion Binding at the Lipid-Water Interface Alters the Ion Permeability of Phospholipid Bilayers. <i>Langmuir</i> , 2021, 37, 14026-14033.	3.5	9
10467	Water Nanoconfined in a Hydrophobic Pore: Molecular Dynamics Simulations of Transmembrane Protein 175 and the Influence of Water Models. <i>ACS Nano</i> , 2021, 15, 19098-19108.	14.6	14
10468	Correlation in Domain Fluctuations Navigates Target Search of a Viral Peptide along RNA. <i>Journal of Physical Chemistry B</i> , 2021, 125, 12678-12689.	2.6	2
10469	Enhanced Sampling Approach to the Induced-Fit Docking Problem in Protein-Ligand Binding: The Case of Mono-ADP-Ribosylation Hydrolase Inhibitors. <i>Journal of Chemical Theory and Computation</i> , 2021, 17, 7899-7911.	5.3	17
10470	A teamwork promotion of formin-mediated actin nucleation by Bud6 and Aip5 in <i>Saccharomyces cerevisiae</i> . <i>Molecular Biology of the Cell</i> , 2022, 33, mbcE21060285.	2.1	2
10471	Planar Boronic Graphene and Nitrogenized Graphene Heterostructure for Protein Stretch and Confinement. <i>Biomolecules</i> , 2021, 11, 1756.	4.0	1
10472	Investigation of the intermolecular voids at the dissolution of CO <sub>2</sub> in ionic liquids. <i>Journal of Molecular Liquids</i> , 2022, 349, 118127.	4.9	8

#	ARTICLE	IF	CITATIONS
10473	Computational and Experimental Models of Type III Lipid-Based Formulations of Loratadine Containing Complex Nonionic Surfactants. <i>Molecular Pharmaceutics</i> , 2021, 18, 4354-4370.	4.6	3
10475	Understanding creep in TiAl alloys on the nanosecond scale by molecular dynamics simulations. <i>Materials and Design</i> , 2021, 212, 110282.	7.0	5
10476	Histone H3 Inhibits Ubiquitin-Ubiquitin Intermolecular Interactions to Enhance Binding to DNA Methyl Transferase 1. <i>Journal of Molecular Biology</i> , 2022, 434, 167371.	4.2	1
10477	Frenkel Line in Nitrogen Terminates at the Triple Point. <i>Journal of Physical Chemistry Letters</i> , 2021, 12, 11609-11615.	4.6	5
10478	In-silico Study of Seaweed Secondary Metabolites as AXL Kinase Inhibitors. <i>Saudi Journal of Biological Sciences</i> , 2021, 29, 689-701.	3.8	1
10479	The Role of Posttranslational Acetylation in the Association of Autophagy Protein ATG8 with Microtubules in Plant Cells. <i>Cytology and Genetics</i> , 2021, 55, 510-518.	0.5	2
10480	Icosahedral silicon boride: A potential hybrid photovoltaic-thermoelectric for energy harvesting. <i>Physical Review Materials</i> , 2021, 5, .	2.4	4
10481	Fused aromatic networks as a new class of gas hydrate inhibitors. <i>Chemical Engineering Journal</i> , 2022, 433, 133691.	12.7	7
10482	Frizzled BRET sensors based on bioorthogonal labeling of unnatural amino acids reveal WNT-induced dynamics of the cysteine-rich domain. <i>Science Advances</i> , 2021, 7, eabj7917.	10.3	15
10484	Novel dynamic residue network analysis approaches to study allosteric modulation: SARS-CoV-2 Mpro and its evolutionary mutations as a case study. <i>Computational and Structural Biotechnology Journal</i> , 2021, 19, 6431-6455.	4.1	14
10485	Study on the dispersion mechanism of the polycarboxylic acid dispersant for disperse dyes. <i>Journal of Molecular Liquids</i> , 2022, 349, 118140.	4.9	14
10486	Theoretical Design and Experimental Study of New Aptamers with the Enhanced Binding Affinity Relying on Colorimetric Assay for Tetracycline Detection. <i>Journal of Molecular Liquids</i> , 2021, 349, 118196.	4.9	4
10487	Screening of Severe Acute Respiratory Syndrome Coronavirus 2 RNA-Dependent RNA Polymerase Inhibitors Using Computational Approach. <i>Journal of Computational Biology</i> , 2021, 28, 1228-1247.	1.6	13
10489	Nanocomposite of Fullerenes and Natural Rubbers: MARTINI Force Field Molecular Dynamics Simulations. <i>Polymers</i> , 2021, 13, 4044.	4.5	6
10490	A General Picture of Cucurbit[8]uril Host-Guest Binding. <i>Journal of Chemical Information and Modeling</i> , 2021, 61, 6107-6134.	5.4	35
10491	Mechanism of Thermal Protein Aggregation: Experiments and Molecular Dynamics Simulations on the High-Temperature Behavior of Myoglobin. <i>Journal of Physical Chemistry B</i> , 2021, 125, 13099-13110.	2.6	8
10492	Docking and molecular dynamics simulation for therapeutic repurposing in small cell lung cancer (SCLC) patients infected with COVID-19. <i>Journal of Biomolecular Structure and Dynamics</i> , 2023, 41, 16-25.	3.5	10
10493	Atomistic insights into the performance of thermodynamic inhibitors in the nucleation of methane hydrate. <i>Chemical Engineering Journal</i> , 2022, 431, 133479.	12.7	9

#	ARTICLE	IF	CITATIONS
10494	Alkali metal chlorides in DMSO–methanol binary mixtures: insights into the structural properties through molecular dynamics simulations. Theoretical Chemistry Accounts, 2021, 140, 1.	1.4	2
10495	Structural and Computational Study of the GroEL–Prion Protein Complex. Biomedicines, 2021, 9, 1649.	3.2	6
10496	Low-frequency collective motion of <sc>DNA</sc>–binding domain defines p53 function. Proteins: Structure, Function and Bioinformatics, 2022, 90, 881-888.	2.6	1
10497	In Silico and In Vitro Evaluation of the Antimicrobial Potential of Bacillus cereus Isolated from Apis dorsata Gut against Neisseria gonorrhoeae. Antibiotics, 2021, 10, 1401.	3.7	12
10498	The role of TCP structures in glass formation of Ni50Ag50 alloys. Journal of Alloys and Compounds, 2022, 897, 162743.	5.5	8
10499	Structural and dynamic studies of the human RNA binding protein RBM3 reveals the molecular basis of its oligomerization and RNA recognition. FEBS Journal, 2022, 289, 2847-2864.	4.7	4
10500	Acyl-chain saturation regulates the order of phosphatidylinositol 4,5-bisphosphate nanodomains. Communications Chemistry, 2021, 4, .	4.5	4
10501	Investigation of microcystin conformation and binding towards PPP1 by molecular dynamics simulation. Chemico-Biological Interactions, 2022, 351, 109766.	4.0	5
10502	Molecular Determinants and Specificity of mRNA with Alternatively-Spliced UPF1 Isoforms, Influenced by an Insertion in the –Regulatory Loop–™. International Journal of Molecular Sciences, 2021, 22, 12744.	4.1	7
10503	Critical role of backbone coordination in the mRNA recognition by RNA induced silencing complex. Communications Biology, 2021, 4, 1345.	4.4	13
10504	Elucidation of the interaction mechanism of olmutinib with human $\alpha$ -1 acid glycoprotein: insights from spectroscopic and molecular modeling studies. Journal of Biomolecular Structure and Dynamics, 2023, 41, 525-537.	3.5	9
10505	In Situ Fabricated Quasi–Solid Polymer Electrolyte for High–Energy–Density Lithium Metal Battery Capable of Subzero Operation. Advanced Energy Materials, 2022, 12, 2102932.	19.5	69
10506	Nonequilibrium molecular dynamics method based on coarse-graining formalism: Application to a nonuniform temperature field system. Physical Review E, 2021, 104, 065301.	2.1	3
10507	Structural and dynamic insights into the HNH nuclease of divergent Cas9 species. Journal of Structural Biology, 2022, 214, 107814.	2.8	8
10508	Identification of Anti–Cancer Agents Targeting Aldo–Keto Reductase (AKR) 1C3 Protein by–Pharmacophore Modeling, Virtual Screening and Molecular Docking. ChemistrySelect, 2021, 6, 12820-12833.	1.5	2
10509	Transient exposure of a buried phosphorylation site in an autoinhibited protein. Biophysical Journal, 2022, 121, 91-101.	0.5	8
10510	N-Terminal-Driven Binding Mechanism of an Antigen Peptide to Human Leukocyte Antigen-A*2402 Elucidated by Multicanonical Molecular Dynamic-Based Dynamic Docking and Path Sampling Simulations. Journal of Physical Chemistry B, 2021, 125, 13376-13384.	2.6	7
10511	Assessing the Intestinal Permeability of Small Molecule Drugs via Diffusion Motion on a Multidimensional Free Energy Surface. Journal of Chemical Theory and Computation, 2022, 18, 503-515.	5.3	10

#	ARTICLE	IF	CITATIONS
10512	Reconstruction of the binding pathway of an anti-HIV drug, Indinavir, in complex with the HTLV-1 protease using unaggregated unbiased molecular dynamics simulation. Computational Biology and Chemistry, 2022, 96, 107616.	2.3	2
10513	The role of the N-terminal amphipathic helix in bacterial YidC: Insights from functional studies, the crystal structure and molecular dynamics simulations. Biochimica Et Biophysica Acta - Biomembranes, 2022, 1864, 183825.	2.6	10
10514	Hydrogen bonding in liquid water at 1 GPa : Molecular dynamics simulation study of TIP4P/2005 water model. Computational and Theoretical Chemistry, 2022, 1208, 113527.	2.5	1
10515	Mitigation of methanol inactivation of lipases by reaction medium engineering with glycine betaine for enzymatic biodiesel synthesis. Fuel, 2022, 313, 122637.	6.4	8
10516	Volumetric properties, conductivity and computation analysis of selected imidazolium chloride ionic liquids in ethylene glycol. Journal of Molecular Liquids, 2021, 345, 118178.	4.9	9
10517	Recharging your fats: CHARMM36 parameters for neutral lipids triacylglycerol and diacylglycerol. Biophysical Reports, 2021, 1, 100034.	1.2	10
10518	Molecular insights on Ca <sup>2+</sup> /Na <sup>+</sup> separation via graphene-based nanopores: The role of electrostatic interactions to ionic dehydration. Chinese Journal of Chemical Engineering, 2022, 41, 220-229.	3.5	3
10519	Communication pathways bridge local and global conformations in an IgG4 antibody. Scientific Reports, 2021, 11, 23197.	3.3	5
10521	Structural Elucidation of Inter-CARD Interfaces involved in NOD2 Tandem CARD Association and RIP2 Recognition. Journal of Physical Chemistry B, 2021, 125, 13349-13365.	2.6	4
10522	ACE2 Peptide Fragment Interaction with Different S1 Protein Sites. International Journal of Peptide Research and Therapeutics, 2022, 28, 7.	1.9	7
10523	Molecular Dynamics Simulation Study of Covalently Bound Hybrid Coagulants (CBHyC): Molecular Structure and Coagulation Mechanisms. SSRN Electronic Journal, 0, , .	0.4	0
10524	Kinetic coherence underlies the dynamics of disordered proteins. RSC Advances, 2021, 11, 36242-36249.	3.6	0
10525	Molecular simulations on the stability and dynamics of bulk nanobubbles in aqueous environments. Physical Chemistry Chemical Physics, 2021, 23, 27533-27542.	2.8	18
10527	A rigorous framework for detecting SARS-CoV-2 spike protein mutational ensemble from genomic and structural features. Current Research in Structural Biology, 2021, 3, 290-300.	2.2	17
10529	Experimental and theoretical study on converting myoglobin into a stable domain-swapped dimer by utilizing a tight hydrogen bond network at the hinge region. RSC Advances, 2021, 11, 37604-37611.	3.6	2
10530	The dynamic simulation of aggregate chemical systems: Use and misuse of long lists of numbers. Theoretical and Computational Chemistry, 2021, 20, 231-265.	0.4	0
10531	A Random Batch Ewald Method for Charged Particles in the Isothermal-Isobaric Ensemble. SSRN Electronic Journal, 0, , .	0.4	0
10532	Stability of adsorption of Mg and Na on sulfur-functionalized MXenes. Physical Chemistry Chemical Physics, 2021, 23, 25424-25433.	2.8	8

10534	The impact of borate on the structure of antifreeze glycoproteins. Chinese Journal of Chemical Physics, 0, , .	1.3	2
10535	Small-to-large length scale transition of TMAO interaction with hydrophobic solutes. Physical Chemistry Chemical Physics, 2022, 24, 2080-2087.	2.8	5
10536	Longitudinal strand ordering leads to shear thinning in Nafion. Physical Chemistry Chemical Physics, 2021, 23, 25901-25910.	2.8	6
10537	Evaluation of all-atom force fields in viral capsid simulations and properties. RSC Advances, 2021, 12, 216-220.	3.6	0
10538	Thermodynamic solubility of celecoxib in organic solvents. CrystEngComm, 0, , .	2.6	0
10539	A hybrid coarse-grained model for structure, solvation and assembly of lipid-like peptides. Physical Chemistry Chemical Physics, 2022, 24, 1553-1568.	2.8	4
10540	Investigating natural compounds against oncogenic RET tyrosine kinase using pharmacoinformatic approaches for cancer therapeutics. RSC Advances, 2021, 12, 1194-1207.	3.6	10
10541	Temperature-Transferable Coarse-Grained Model for Poly(propylene oxide) to Study Thermo-Responsive Behavior of Triblock Copolymers. Journal of Physical Chemistry B, 2022, 126, 292-307.	2.6	6
10542	Small Amphiphilic Peptides: Activity Against a Broad Range of Drug-Resistant Bacteria and Structural Insight into Membranolytic Properties. Journal of Medicinal Chemistry, 2022, 65, 665-687.	6.4	8
10543	Pharmacophore screening to identify natural origin compounds to target RNA-dependent RNA polymerase (RdRp) of SARS-CoV2. Molecular Diversity, 2022, 26, 2613-2629.	3.9	4
10544	High-Voltage Aqueous Mg-Ion Batteries Enabled by Solvation Structure Reorganization. Advanced Functional Materials, 2022, 32, 2110674.	14.9	38
10545	Pocket delipidation induced by membrane tension or modification leads to a structurally analogous mechanosensitive channel state. Structure, 2022, 30, 608-622.e5.	3.3	16
10546	Integrated approach to functional analysis of an ERBB2 variant of unknown significance detected by a cancer gene panel test. Cellular Oncology (Dordrecht), 2022, 45, 121.	4.4	1
10547	Fruit Bromelain-Derived Peptide Potentially Restrains the Attachment of SARS-CoV-2 Variants to hACE2: A Pharmacoinformatics Approach. Molecules, 2022, 27, 260.	3.8	21
10548	Phosphorylation tunes elongation propensity and cohesiveness of INCENP's intrinsically disordered region. Journal of Molecular Biology, 2022, 434, 167387.	4.2	7
10549	Molecular dynamics studies of $\langle \mathbf{a} \cdot \mathbf{b} \rangle$ -type screw dislocation core structure polymorphism in titanium. Physical Review Materials, 2022, 6, .	2.1	1
10550	Interface effects from moisture in nanocomposites of 2D graphene oxide in cellulose nanofiber (CNF) matrix – A molecular dynamics study. Journal of Materials Chemistry A, 2022, 10, 2122-2132.	10.3	18

#	ARTICLE	IF	CITATIONS
10551	Following the crystal growth of anthradithiophenes through atomistic molecular dynamics simulations and graph characterization. <i>Molecular Systems Design and Engineering</i> , 0, , .	3.4	0
10552	The Systems of Naringenin with Solubilizers Expand Its Capability to Prevent Neurodegenerative Diseases. <i>International Journal of Molecular Sciences</i> , 2022, 23, 755.	4.1	12
10553	Using all-atom simulations in explicit solvent to study aggregation of amphipathic peptides into amyloid-like fibrils. <i>Journal of Molecular Liquids</i> , 2022, 347, 118283.	4.9	15
10554	A systematic and critical review of application of molecular dynamics simulation in low salinity water injection. <i>Advances in Colloid and Interface Science</i> , 2022, 300, 102594.	14.7	21
10555	Quantification of CO <sub>2</sub> Replacement in Methane Gas Hydrates: A Molecular Dynamics Perspective. <i>Journal of Natural Gas Science and Engineering</i> , 2022, 98, 104396.	4.4	11
10556	Introducing the potency of new boron-based heterocyclic anion receptor additives to regulate the solvation and transport properties of Li-ions in ethylene carbonate electrolyte of Li-ion battery: An atomistic molecular dynamics study. <i>Journal of Power Sources</i> , 2022, 521, 230962.	7.8	5
10557	Pharmaceutical profiling and molecular dynamics simulations reveal crystallization effects in amorphous formulations. <i>International Journal of Pharmaceutics</i> , 2022, 613, 121360.	5.2	8
10558	A molecular dynamics investigation of La <sup>3+</sup> and Lu <sup>3+</sup> -ligand speciation in aqueous solution. <i>Journal of Molecular Liquids</i> , 2022, 347, 118367.	4.9	4
10559	Conformational dynamics of polymers in ethylammonium nitrate from advanced sampling methods. <i>Computational Materials Science</i> , 2022, 203, 111072.	3.0	3
10560	Efficient dual-function inhibitors for prevention of gas hydrate formation and CO <sub>2</sub> /H <sub>2</sub> S corrosion inside oil and gas pipelines. <i>Chemical Engineering Journal</i> , 2022, 431, 134098.	12.7	25
10561	Exploring the permeation of fluoroquinolone metalloantibiotics across outer membrane porins by combining molecular dynamics simulations and a porin-mimetic in vitro model. <i>Biochimica Et Biophysica Acta - Biomembranes</i> , 2022, 1864, 183838.	2.6	2
10562	Novel imidazopyrimidines-based molecules induce tetramerization of tumor pyruvate kinase M2 and exhibit potent antiproliferative profile. <i>European Journal of Pharmaceutical Sciences</i> , 2022, 170, 106112.	4.0	20
10563	Interactions between polymyxin B and various bacterial membrane mimics: A molecular dynamics study. <i>Colloids and Surfaces B: Biointerfaces</i> , 2022, 211, 112288.	5.0	6
10564	Morphology of MoS <sub>2</sub> nanosheets and its influence on water/oil interfacial tension: A molecular dynamics study. <i>Fuel</i> , 2022, 312, 122938.	6.4	7
10565	The effect of external salts on the aggregation of the multiheaded surfactants: All-atom molecular dynamics studies. <i>Journal of Molecular Graphics and Modelling</i> , 2022, 111, 108110.	2.4	1
10566	Alanine scanning mutagenesis in Cys-His boxes of human immunodeficiency virus type 1 Nucleocapsid protein P7: Insight from an in silico investigation. <i>Chemical Data Collections</i> , 2022, 38, 100828.	2.3	0
10567	Molecular dynamics simulations of the flexibility and inhibition of SARS-CoV-2 NSP 13 helicase. <i>Journal of Molecular Graphics and Modelling</i> , 2022, 112, 108122.	2.4	3
10568	Potential inhibitors for peroxiredoxin 6 of <i>W. bancrofti</i> : A combined study of modelling, structure-based drug design and MD simulation. <i>Journal of Molecular Graphics and Modelling</i> , 2022, 112, 108115.	2.4	6



#	ARTICLE	IF	CITATIONS
10569	Experimental and computational investigation of hydrophilic monomeric substances as novel CO <sub>2</sub> hydrate inhibitors and potential synergists. <i>Energy</i> , 2022, 244, 123136.	8.8	10
10572	Volumetric Properties for the Binding of 1,4-Dioxane to Amide Naphthotubes in Water. <i>Journal of Physical Chemistry B</i> , 2020, 124, 9175-9181.	2.6	5
10574	Evaluation of Interface Properties of Carbon Fiber/Resin Using the Full Atomistic Model Considering the Electric Charge State. <i>Journal of the Japan Society for Composite Materials</i> , 2020, 46, 265-271.	0.2	0
10575	Atomistic Insights on the Adsorption of Long-Chain Undecane Molecules on Hydroxyl-Functionalized Carbon Nanotubes. <i>SSRN Electronic Journal</i> , 0, , .	0.4	0
10576	Effects of the N-Terminal Dynamics on the Conformational States of Human Dopamine Transporter. <i>SSRN Electronic Journal</i> , 0, , .	0.4	0
10577	How does excess phenylalanine affect the packing density and fluidity of a lipid membrane?. <i>Physical Chemistry Chemical Physics</i> , 2021, 23, 27294-27303.	2.8	4
10578	Atomistic level characterisation of ssDNA translocation through the E. coli proteins CsgG and CsgF for nanopore sequencing. <i>Computational and Structural Biotechnology Journal</i> , 2021, 19, 6417-6430.	4.1	1
10579	Atomistic Simulations of the Human Proteasome Inhibited by a Covalent Ligand. , 2021, , 47-57.		0
10580	On the Adsorption of Volatile Organic Compounds on Hydroxyl-Functionalized Carbon Nanotubes in Aqueous Solution. <i>SSRN Electronic Journal</i> , 0, , .	0.4	0
10581	Understanding the Mechanism of Nitrogen Transport in the Perfluorinated Sulfonic-Acid Hydrated Membranes <i>Via</i> Molecular Dynamics Simulations. <i>SSRN Electronic Journal</i> , 0, , .	0.4	0
10583	Molecular Dynamic Simulation of Uniaxial Stress Strain Applied to $\hat{\pm}$ -Fe Nanowire. <i>Turkish Journal of Engineering</i> , 0, , .	1.2	0
10584	Unraveling the Influence of K280 Acetylation on the Conformational Features of Tau Core Fragment: A Molecular Dynamics Simulation Study. <i>Frontiers in Molecular Biosciences</i> , 2021, 8, 801577.	3.5	8
10585	Anchoring of Amyloid- $\beta^2$ onto Polyunsaturated Phospholipid Membranes. <i>Journal of Biomolecular Structure and Dynamics</i> , 2021, , 1-11.	3.5	0
10586	The Role of Triazole and Glucose Moieties in Alkali Metal Cation Complexation by Lower-Rim Tertiary-Amide Calix[4]arene Derivatives. <i>Molecules</i> , 2022, 27, 470.	3.8	4
10587	The Role of Copper Salts and O<sub>2</sub> in the Mechanism of C $\hat{\alpha}$ -N Bond Activation for Facilitating Nitrogen Transfer Reactions**. <i>Angewandte Chemie</i> , 2022, 134, .	2.0	0
10588	Molecular dynamics simulation of rhenium effects on creep behavior of Ni-based single crystal superalloys. <i>Progress in Natural Science: Materials International</i> , 2022, 32, 259-266.	4.4	15
10589	Molecular dynamics study of effects of point defects on thermal conductivity in cubic silicon carbide. <i>Wuli Xuebao/Acta Physica Sinica</i> , 2022, 71, 036501.	0.5	3
10590	Computational Investigations of the Reactivity of Metalloporphyrins for Ammonia Oxidation. <i>Topics in Catalysis</i> , 2022, 65, 341-353.	2.8	4

#	ARTICLE	IF	CITATIONS
10592	Size-Dependent Order–Disorder Crossover in Hydrophobic Hydration: Comparison between Spherical Solutes and Linear Alcohols. ACS Omega, 2022, 7, 2671-2678.	3.5	9
10593	Occlusion of the human serotonin transporter is mediated by serotonin-induced conformational changes in the bundle domain. Journal of Biological Chemistry, 2022, 298, 101613.	3.4	13
10594	Naturally occurring anthraquinones as potential inhibitors of SARS-CoV-2 main protease: an integrated computational study. Biologia (Poland), 2022, 77, 1121-1134.	1.5	5
10595	Impact of deep eutectic solvents (DESSs) and individual DES components on alcohol dehydrogenase catalysis: connecting experimental data and molecular dynamics simulations. Green Chemistry, 2022, 24, 1120-1131.	9.0	37
10596	Modeling mRNA-based vaccine YFV.E1988 against yellow fever virus E-protein using immuno-informatics and reverse vaccinology approach. Journal of Biomolecular Structure and Dynamics, 2023, 41, 1617-1638.	3.5	3
10597	Key Factors Governing Initial Stages of Lipid Droplet Formation. Journal of Physical Chemistry B, 2022, 126, 453-462.	2.6	15
10598	Atomistic mechanism of leptin and leptin-receptor association. Journal of Biomolecular Structure and Dynamics, 2023, 41, 2231-2248.	3.5	2
10599	An encapsulating lithium-polysulfide electrolyte for practical lithium–sulfur batteries. Chem, 2022, 8, 1083-1098.	11.7	77
10600	Computational techniques to study protein dynamics and conformations. , 2022, , 199-212.		0
10601	Correlation between vibrational anomalies and emergent anharmonicity of the local potential energy landscape in metallic glasses. Physical Review B, 2022, 105, .	3.2	12
10602	Multi-stage structure-based virtual screening approach towards identification of potential SARS-CoV-2 NSP13 helicase inhibitors. Journal of Enzyme Inhibition and Medicinal Chemistry, 2022, 37, 563-572.	5.2	15
10603	The Molecular Mechanism of Human Voltage-Dependent Anion Channel 1 Blockade by the Metallofullerenol Gd@C82(OH)22: An In Silico Study. Biomolecules, 2022, 12, 123.	4.0	1
10604	Structure–and Interaction–Based Design of Anti–SARS–CoV–2 Aptamers. Chemistry - A European Journal, 2022, 28, .	3.3	9
10605	Discovery of small molecular inhibitors for interleukin-33/ST2 protein–protein interaction: a virtual screening, molecular dynamics simulations and binding free energy calculations. Molecular Diversity, 2022, 26, 2659-2678.	3.9	10
10606	Molecular modeling of indazole-3-carboxylic acid and its metal complexes (Zn, Ni, Co, Fe and Mn) as NO synthase inhibitors: DFT calculations, docking studies and molecular dynamics simulations. Inorganic Chemistry Communication, 2022, 135, 109120.	3.9	5
10607	Molecular dynamics and functional characterization of I37R-CFTR lasso mutation provide insights into channel gating activity. IScience, 2022, 25, 103710.	4.1	6
10608	Joint neutron/molecular dynamics vibrational spectroscopy reveals softening of HIV-1 protease upon binding of a tight inhibitor. Physical Chemistry Chemical Physics, 2022, 24, 3586-3597.	2.8	3
10609	Membrane Structure Obtained in an Experimental Evolution Process. Life, 2022, 12, 145.	2.4	4

#	ARTICLE	IF	CITATIONS
10610	Molecular simulations of zwitterlation-induced conformation and dynamics variation of glucagon-like peptide-1 and insulin. <i>Journal of Materials Chemistry B</i> , 2022, 10, 2490-2496.	5.8	3
10611	A Possibility for Quantitative Detection of Mechanically-Induced Invisible Damage by Thermal Property Measurement via Entropy Generation for a Polymer Material. <i>Materials</i> , 2022, 15, 737.	2.9	12
10612	SuPepMem: A database of innate immune system peptides and their cell membrane interactions. <i>Computational and Structural Biotechnology Journal</i> , 2022, 20, 874-881.	4.1	4
10613	Folding of VemP into translation-arresting secondary structure is driven by the ribosome exit tunnel. <i>Nucleic Acids Research</i> , 2022, 50, 2258-2269.	14.5	8
10614	NOG-Derived Peptides Can Restore Neuritogenesis on a CRASH Syndrome Cell Model. <i>Biomedicines</i> , 2022, 10, 102.	3.2	3
10615	Slow liquid dynamics near solid surfaces: Insights from site-resolved studies of ionic liquids in silica confinement. <i>Journal of Chemical Physics</i> , 2022, 156, 074501.	3.0	5
10616	How to Characterize Amorphous Shapes: The Tale of a Reverse Micelle. <i>Journal of Physical Chemistry B</i> , 2022, 126, 953-963.	2.6	4
10617	Effect of conductivity, viscosity, and density of water-in-salt electrolytes on the electrochemical behavior of supercapacitors: molecular dynamics simulations and <i>in situ</i> characterization studies. <i>Materials Advances</i> , 2022, 3, 611-623.	5.4	23
10618	Conformational dynamics promotes disordered regions from function-dispensable to essential in evolved site-specific DNA recombinases. <i>Computational and Structural Biotechnology Journal</i> , 2022, 20, 989-1001.	4.1	4
10619	Scission energy and topology of micelles controlled by the molecular structure of additives. <i>Soft Matter</i> , 2022, 18, 1678-1687.	2.7	3
10620	Elucidating the Structural Features of ABCA1 in its Heterogeneous Membrane Environment. <i>Frontiers in Molecular Biosciences</i> , 2021, 8, 803078.	3.5	4
10621	Discovery and Characterization of a Cryptic Secondary Binding Site in the Molecular Chaperone HSP70. <i>Molecules</i> , 2022, 27, 817.	3.8	1
10622	Penetration of $C_{60}$ into lung surfactant membranes: Molecular dynamics simulation studies. <i>Bulletin of the Korean Chemical Society</i> , 2022, 43, 364-368.	1.9	2
10623	Hierarchical Self-Assembly Pathways of Peptoid Helices and Sheets. <i>Biomacromolecules</i> , 2022, 23, 992-1008.	5.4	19
10624	Understanding the mechanism of nitrogen transport in the perfluorinated sulfonic-acid hydrated membranes via molecular dynamics simulations. <i>Journal of Membrane Science</i> , 2022, 648, 120328.	8.2	9
10625	Computational Studies of $MoS_2$ Nanotubes for Hydrosulfurization. <i>ACS Applied Nano Materials</i> , 2022, 5, 2029-2037.	5.0	3
10626	Oil Occurrence States in Shale Mixed Inorganic Matter Nanopores. <i>Frontiers in Earth Science</i> , 2022, 9, .	1.8	5
10627	Ion currents through Kir potassium channels are gated by anionic lipids. <i>Nature Communications</i> , 2022, 13, 490.	12.8	9

#	ARTICLE	IF	CITATIONS
10628	Route to a direct-gap silicon allotrope Si <sub>32</sub> . Journal of Physics Condensed Matter, 2022, 34, 154006.	1.8	1
10629	Molecular dynamics of liquidâ€“liquid equilibrium and interfacial properties of aqueous solutions of methyl esters. Physical Chemistry Chemical Physics, 2022, 24, 5371-5382.	2.8	1
10630	Expulsion of Hydroxide Ions from Methyl Hydration Shells. Journal of Physical Chemistry B, 2022, 126, 869-877.	2.6	0
10631	Inhibition-mediated changes in prolyl oligopeptidase dynamics possibly related to Î±-synuclein aggregation. Physical Chemistry Chemical Physics, 2022, 24, 4366-4373.	2.8	2
10632	Salt-in-water and water-in-salt electrolytes: the effects of the asymmetry in cation and anion valence on their properties. Physical Chemistry Chemical Physics, 2021, 24, 336-346.	2.8	8
10633	<i>In silico</i> screening and <i>in vitro</i> validation of phytochemicals as multidrug efflux pump inhibitor against <i>E. coli</i> . Journal of Biomolecular Structure and Dynamics, 2023, 41, 2189-2201.	3.5	13
10634	Thymosin Î²4 Is an Endogenous Iron Chelator and Molecular Switcher of Ferroptosis. International Journal of Molecular Sciences, 2022, 23, 551.	4.1	15
10635	Development of IKATP Ion Channel Blockers Targeting Sulfonylurea Resistant Mutant KIR6.2 Based Channels for Treating DEND Syndrome. Frontiers in Pharmacology, 2021, 12, 814066.	3.5	2
10636	The interaction of DNMT1 and DNMT3A epigenetic enzymes with phthalates and perfluoroalkyl substances: an <i>in silico</i> approach. Journal of Biomolecular Structure and Dynamics, 2022, , 1-17.	3.5	1
10638	Effect of the degree of hydrogenation on the viscosity, surface tension, and density of the liquid organic hydrogen carrier system based on diphenylmethane. International Journal of Hydrogen Energy, 2022, 47, 6111-6130.	7.1	19
10639	Molecular dynamics simulations of radiation damage in YBa <sub>2</sub> Cu <sub>3</sub> O <sub>7</sub> . Superconductor Science and Technology, 2022, 35, 035010.	3.5	6
10640	Binding free energies for the SAMPL8 CB8 â€œDrugs of Abuseâ€•challenge from umbrella sampling combined with Hamiltonian replica exchange. Journal of Computer-Aided Molecular Design, 2022, 36, 1-9.	2.9	2
10641	Critical structural invariant during high-pressure solidification of copper. MRS Communications, 2022, 12, 45-50.	1.8	2
10642	Accurate prediction of grain boundary structures and energetics in CdTe: a machine-learning potential approach. Physical Chemistry Chemical Physics, 2022, 24, 1620-1629.	2.8	11
10643	Mechanistic Insights into the Ligand-Induced Unfolding of an RNA G-Quadruplex. Journal of the American Chemical Society, 2022, 144, 935-950.	13.7	21
10644	â€œC-typeâ€™ closed state and gating mechanisms of K2P channels revealed by conformational changes of the TREK-1 channel. Journal of Molecular Cell Biology, 2022, 14, .	3.3	9
10645	Insect RDL Receptor Models for Virtual Screening: Impact of the Template Conformational State in Pentameric Ligand-Gated Ion Channels. ACS Omega, 2022, 7, 1988-2001.	3.5	2
10646	Understanding the Effect of pH on the Solubility and Aggregation Extent of Humic Acid in Solution by Combining Simulation and the Experiment. Environmental Science & Technology, 2022, 56, 917-927.	10.0	35

#	ARTICLE	IF	CITATIONS
10647	Computational investigations on the potential role of hygrophorones as quorum sensing inhibitors against LasR protein of <i>Pseudomonas aeruginosa</i> . Journal of Biomolecular Structure and Dynamics, 2023, 41, 2249-2259.	3.5	3
10648	A Gain-of-Function Mutation on BCKDK Gene and Its Possible Pathogenic Role in Branched-Chain Amino Acid Metabolism. Genes, 2022, 13, 233.	2.4	3
10649	Sub-layer rationale of anomalous layer-shrinkage from atomistic simulations of a fluorinated mesogen. Materials Advances, 2022, 3, 1212-1223.	5.4	1
10650	Molecular simulations: past, present, and future (a Topical Issue in EPJB). European Physical Journal B, 2022, 95, 1.	1.5	20
10651	Unravelling the mechanism of glucose binding in a protein-based fluorescence probe: molecular dynamics simulation with a tailor-made charge model. Physical Chemistry Chemical Physics, 2022, 24, 2441-2453.	2.8	2
10652	Molecular Architecture of the Antiophidic Protein DM64 and its Binding Specificity to Myotoxin II From Bothrops asper Venom. Frontiers in Molecular Biosciences, 2021, 8, 787368.	3.5	2
10653	The importance of the compact disordered state in the fuzzy interactions between intrinsically disordered proteins. Chemical Science, 2022, 13, 2363-2377.	7.4	7
10654	Aggregation of DNA-Grafted Nanoparticles in Water: The Critical Role of Sequence-Dependent Conformation of DNA Coating. Journal of Physical Chemistry B, 2022, 126, 847-857.	2.6	6
10655	DNA methylation cues in nucleosome geometry, stability and unwrapping. Nucleic Acids Research, 2022, 50, 1864-1874.	14.5	25
10656	Slipknot or Crystallographic Error: A Computational Analysis of the Plasmodium falciparum DHFR Structural Folds. International Journal of Molecular Sciences, 2022, 23, 1514.	4.1	3
10657	Switching promotor recognition of phage RNA polymerase in silico along lab-directed evolution path. Biophysical Journal, 2022, 121, 582-595.	0.5	0
10658	Loading of DOX into a tetrahedral DNA nanostructure: the corner does matter. Nanoscale Advances, 2022, 4, 754-760.	4.6	12
10659	Bridging atomistic simulations and thermodynamic hydration models of aqueous electrolyte solutions. Journal of Chemical Physics, 2022, 156, 024502.	3.0	1
10661	Immunoinformatics guided modeling of CCHF_GN728, an mRNA-based universal vaccine against Crimean-Congo hemorrhagic fever virus. Computers in Biology and Medicine, 2022, 140, 105098.	7.0	7
10662	Computational Medicinal Chemistry to Target GPCRs. , 2022, , 84-114.		3
10663	Integrated <i>in silico</i> – <i>in vitro</i> strategy for the discovery of potential xanthine oxidase inhibitors from Egyptian propolis and their synergistic effect with allopurinol and febuxostat. RSC Advances, 2022, 12, 2843-2872.	3.6	17
10664	Complex nanoemulsion for vitamin delivery: droplet organization and interaction with skin membranes. Nanoscale, 2022, 14, 506-514.	5.6	19
10665	An open state of a voltage-gated sodium channel involving a $\alpha$ -helix and conserved pore-facing asparagine. Biophysical Journal, 2022, 121, 11-22.	0.5	8

#	ARTICLE	IF	CITATIONS
10666	Breviarium de Motu Simulato Ad Atomos Pertinenti. Israel Journal of Chemistry, 2022, 62, .	2.3	3
10667	The phase behaviour of cetyltrimethylammonium chloride surfactant aqueous solutions at high concentrations: an all-atom molecular dynamics simulation study. Soft Matter, 2022, , .	2.7	4
10668	Changes in the Local Conformational States Caused by Simple Na <sup>+</sup> and K <sup>+</sup> Ions in Polyelectrolyte Simulations: Comparison of Seven Force Fields with and without NBFIX and ECC Corrections. Polymers, 2022, 14, 252.	4.5	4
10669	Can two wrongs make a right? F508del-CFTR ion channel rescue by second-site mutations in its transmembrane domains. Journal of Biological Chemistry, 2022, 298, 101615.	3.4	4
10670	A bioactivated in vivo assembly nanotechnology fabricated NIR probe for small pancreatic tumor intraoperative imaging. Nature Communications, 2022, 13, 418.	12.8	28
10671	How well does molecular simulation reproduce environment-specific conformations of the intrinsically disordered peptides PLP, TP2 and ONEG?. Chemical Science, 2022, 13, 1957-1971.	7.4	7
10672	Interaction between miR4749 and Human Serum Albumin as Revealed by Fluorescence, FRET, Atomic Force Spectroscopy and Computational Modelling. International Journal of Molecular Sciences, 2022, 23, 1291.	4.1	4
10673	Local Electronic Charge Transfer in the Helical Induction of Cis-Transoid Poly(4-carboxyphenyl)acetylene by Chiral Amines. Journal of Chemical Information and Modeling, 2022, , .	5.4	1
10674	The effects of molecular weight and orientation on the membrane permeation and partitioning of polycyclic aromatic hydrocarbons: a computational study. Physical Chemistry Chemical Physics, 2022, 24, 2158-2166.	2.8	2
10676	Highly Similar Sequence and Structure Yet Different Biophysical Behavior: A Computational Study of Two Triosephosphate Isomerases. Journal of Chemical Information and Modeling, 2022, 62, 668-677.	5.4	1
10677	SIRT1 activation by Taurine: in vitro evaluation, molecular docking and molecular dynamics simulation studies. Journal of Nutritional Biochemistry, 2022, 102, 108948.	4.2	12
10678	Heterogeneous Effect of Organic Matter on Accumulation Behaviors of Shale Gas in Water. Energy & Fuels, 2022, 36, 1507-1514.	5.1	3
10680	Substrate-bound and substrate-free outward-facing structures of a multidrug ABC exporter. Science Advances, 2022, 8, eabg9215.	10.3	27
10681	Sodium Binding Stabilizes the Outward-Open State of SERT by Limiting Bundle Domain Motions. Cells, 2022, 11, 255.	4.1	7
10683	The Madrid-2019 force field for electrolytes in water using TIP4P/2005 and scaled charges: Extension to the ions Fâ <sup>-</sup> , Brâ <sup>-</sup> , Iâ <sup>-</sup> , Rb <sup>+</sup> , and Cs <sup>+</sup> . Journal of Chemical Physics, 2022, 156, 044505.	3.0	36
10684	The use of in silico models for the rationalization of molecularly imprinted polymer synthesis. European Polymer Journal, 2022, 166, 111024.	5.4	9
10685	Molecular Dynamics of Solids at Constant Pressure and Stress Using Anisotropic Stochastic Cell Rescaling. Applied Sciences (Switzerland), 2022, 12, 1139.	2.5	1
10686	Membrane-Bound Configuration and Lipid Perturbing Effects of Hemagglutinin Subunit 2 N-Terminus Investigated by Computer Simulations. Frontiers in Molecular Biosciences, 2022, 9, 826366.	3.5	2



#	ARTICLE	IF	CITATIONS
10687	Fluorinated graphene nanomaterial causes potential mechanical perturbations to a biomembrane. Journal of Molecular Modeling, 2022, 28, 49.	1.8	0
10688	Mutations on RBD of SARS-CoV-2 Omicron variant result in stronger binding to human ACE2 receptor. Biochemical and Biophysical Research Communications, 2022, 590, 34-41.	2.1	178
10689	The T850D Phosphomimetic Mutation in the Androgen Receptor Ligand Binding Domain Enhances Recruitment at Activation Function 2. International Journal of Molecular Sciences, 2022, 23, 1557.	4.1	3
10690	Analysis of Fluctuation in the Heme-Binding Pocket and Heme Distortion in Hemoglobin and Myoglobin. Life, 2022, 12, 210.	2.4	7
10691	The Role of Copper Salts and O <sub>2</sub> in the Mechanism of C≡N Bond Activation for Facilitating Nitrogen Transfer Reactions**. Angewandte Chemie - International Edition, 2022, , .	13.8	2
10692	Structural basis of Plasmodium vivax inhibition by antibodies binding to the circumsporozoite protein repeats. ELife, 2022, 11, .	6.0	5
10693	Understanding excited state properties of host materials in OLEDs: simulation of absorption spectrum of amorphous 4,4-bis(carbazol-9-yl)-2,2-biphenyl (CBP). Physical Chemistry Chemical Physics, 2022, , .	2.8	2
10694	Spontaneous local membrane curvature induced by transmembrane proteins. Biophysical Journal, 2022, 121, 671-683.	0.5	15
10695	Molecular dynamics simulations of structural and dynamical aspects of DNA hydration water. Journal of Physics Condensed Matter, 2022, 34, 164002.	1.8	1
10696	A novel leishmanial copper P-type ATPase plays a vital role in parasite infection and intracellular survival. Journal of Biological Chemistry, 2022, 298, 101539.	3.4	5
10697	Mechanistic investigation of cellulose formate to 5-hydroxymethylfurfural conversion in DMSO-H <sub>2</sub> O. Journal of Molecular Liquids, 2022, 348, 118471.	4.9	3
10698	Mechanical force can enhance c-Src kinase activity by impairing autoinhibition. Biophysical Journal, 2022, 121, 684-691.	0.5	5
10699	Identification of novel leads as potent inhibitors of HDAC3 using ligand-based pharmacophore modeling and MD simulation. Scientific Reports, 2022, 12, 1712.	3.3	15
10700	How to quantify and avoid finite size effects in computational studies of crystal nucleation: The case of homogeneous crystal nucleation. Journal of Chemical Physics, 2022, 156, 054503.	3.0	10
10701	How clay delamination supports aseismic slip. American Mineralogist, 2023, 108, 87-99.	1.9	2
10702	Chemical modification for improving catalytic performance of lipase B from Candida antarctica with hydrophobic proline ionic liquid. Bioprocess and Biosystems Engineering, 2022, 45, 749-759.	3.4	6
10703	Molecular Dynamics Insight into the Role of Water Molecules in Ionic Liquid Mixtures of 1-Butyl-3-methylimidazolium Iodide and Ethylammonium Nitrate. Journal of Physical Chemistry B, 2022, 126, 1115-1124.	2.6	6
10704	Effects of various temperature and pressure initial conditions to predict the thermal conductivity and phase alteration duration of water based carbon hybrid nanofluids via MD approach. Journal of Molecular Liquids, 2022, 351, 118654.	4.9	25

#	ARTICLE	IF	CITATIONS
10705	Disease-linked TDP43 hyperphosphorylation suppresses TDP43 condensation and aggregation. <i>EMBO Journal</i> , 2022, 41, e108443.	7.8	68
10706	Effects of Salt Aggregation in Perfluoroether Electrolytes. <i>Journal of the Electrochemical Society</i> , 2022, 169, 020506.	2.9	2
10707	Protein dynamics and lipid affinity of monomeric, zeaxanthin-binding LHCII in thylakoid membranes. <i>Biophysical Journal</i> , 2022, 121, 396-409.	0.5	9
10709	Adsorption Kinetics and Self-Assembled Structures of <i>Aspergillus oryzae</i> Hydrophobin RolA on Hydrophobic and Charged Solid Surfaces. <i>Applied and Environmental Microbiology</i> , 2022, 88, AEM0208721.	3.1	3
10710	Removing Auxetic Properties in f.c.c. Hard Sphere Crystals by Orthogonal Nanochannels with Hard Spheres of Another Diameter. <i>Materials</i> , 2022, 15, 1134.	2.9	11
10711	How Far Is "Bulk Water" from Interfaces? Depends on the Nature of the Surface and What We Measure. <i>Journal of Physical Chemistry B</i> , 2022, 126, 1125-1135.	2.6	9
10712	Distribution of lipid aldehydes in phase-separated membranes: A molecular dynamics study. <i>Archives of Biochemistry and Biophysics</i> , 2022, 717, 109136.	3.0	2
10713	Molecular simulations of proteins: From simplified physical interactions to complex biological phenomena. <i>Biochimica Et Biophysica Acta - Proteins and Proteomics</i> , 2022, 1870, 140757.	2.3	11
10714	Effective and efficient transport mechanism of CO <sub>2</sub> in subnano-porous crystalline membrane of syndiotactic polystyrene. <i>Journal of Membrane Science</i> , 2022, 646, 120202.	8.2	3
10715	Systematic comparison of activity and mechanism of antimicrobial peptides against nosocomial pathogens. <i>European Journal of Medicinal Chemistry</i> , 2022, 231, 114135.	5.5	26
10716	Exploring tuning phenomena of THF-H <sub>2</sub> hydrates via molecular dynamics simulations. <i>Journal of Molecular Liquids</i> , 2022, 349, 118490.	4.9	13
10717	Identification of novel bioactive compounds from <i>Olea europaea</i> by evaluation of chemical compounds in the OliveNet <sub>2.0</sub> library: in silico bioactivity and molecular modelling, and in vitro validation of hERG activity. <i>Computers in Biology and Medicine</i> , 2022, 142, 105247.	7.0	5
10718	Ascorbate-and iron-driven redox activity of Dp44mT and Emodin facilitates peroxidation of micelles and bicelles. <i>Biochimica Et Biophysica Acta - General Subjects</i> , 2022, 1866, 130078.	2.4	7
10719	Molecular dynamics simulations reveal single-stranded DNA (ssDNA) forms ordered structures upon adsorbing onto single-walled carbon nanotubes (SWCNT). <i>Colloids and Surfaces B: Biointerfaces</i> , 2022, 212, 112343.	5.0	2
10720	Effects of the N-terminal dynamics on the conformational states of human dopamine transporter. <i>Biophysical Chemistry</i> , 2022, 283, 106765.	2.8	3
10721	Genetic and molecular Omp25 analyses from worldwide <i>Brucella canis</i> strains: Possible mutational influences in protein function. <i>Gene</i> , 2022, 817, 146175.	2.2	0
10722	Optimizing Lennard-Jones parameters by coupling single molecule and ensemble target data. <i>Computer Physics Communications</i> , 2022, 274, 108285.	7.5	1
10723	Mechanistic study of the adsorption and penetration of modified SiO <sub>2</sub> nanoparticles on cellular membrane. <i>Chemosphere</i> , 2022, 294, 133793.	8.2	7

#	ARTICLE	IF	CITATIONS
10724	Electrochemical and theoretical investigation on the behavior of the Co <sup>2+</sup> ion in three eutectic solvents. Journal of Molecular Graphics and Modelling, 2022, 112, 108137.	2.4	4
10725	Structural-based virtual screening and identification of novel potent antimicrobial compounds against YsxC of Staphylococcus aureus. Journal of Molecular Structure, 2022, 1255, 132476.	3.6	29
10726	Excipient-free prodrug-based three-in-one nanoparticles co-deliver diversified agents to amplify tumor therapy. Chemical Engineering Journal, 2022, 435, 134880.	12.7	9
10727	Thermodynamic and kinetic corrosion behavior of alloys in molten MgCl <sub>2</sub> -NaCl eutectic: FPMD simulations and electrochemical technologies. Solar Energy Materials and Solar Cells, 2022, 238, 111624.	6.2	6
10728	Unconventional deformation mechanism in nanocrystalline metals?. International Journal of Materials Research, 2022, 94, 1106-1110.	0.3	4
10729	Control techniques of molecular dynamics simulation. , 2022, , 67-96.		3
10730	A system for artificial light signal transduction via molecular translocation in a lipid membrane. Chemical Science, 2022, 13, 2487-2494.	7.4	4
10731	A proximity-based in silico approach to identify redox-labile disulfide bonds: The example of FVIII. PLoS ONE, 2022, 17, e0262409.	2.5	1
10732	Physical Chemistry of a Single tRNA-Modified Nucleoside Regulates Decoding of the Synonymous Lysine Wobble Codon and Affects Type 2 Diabetes. Journal of Physical Chemistry B, 2022, 126, 1168-1177.	2.6	6
10733	First-Principles Calculations about Elastic and Li <sup>+</sup> Transport Properties of Lithium Superoxides under High Pressure and High Temperature. Chinese Physics Letters, 2022, 39, 026101.	3.3	2
10734	From Protein Design to the Energy Landscape of a Cold Unfolding Protein. Journal of Physical Chemistry B, 2022, 126, 1212-1231.	2.6	3
10735	Insights into Sorption and Molecular Transport of Aqueous Glucose into Zeolite Nanopores. Journal of Physical Chemistry B, 2022, 126, 1352-1364.	2.6	1
10736	Mg <sup>2+</sup> -dependent conformational equilibria in CorA and an integrated view on transport regulation. ELife, 2022, 11, .	6.0	10
10737	Early aggregation mechanism of Aβ <sup>1-42</sup> revealed by Markov state models. International Journal of Biological Macromolecules, 2022, 204, 606-616.	7.5	5
10738	A highly distorted ultraelastic chemically complex Elinvar alloy. Nature, 2022, 602, 251-257.	27.8	75
10739	Structure and dynamics of the SARS-CoV-2 envelope protein monomer. Proteins: Structure, Function and Bioinformatics, 2022, 90, 1102-1114.	2.6	18
10740	Ion permeation, selectivity, and electronic polarization in fluoride channels. Biophysical Journal, 2022, 121, 1336-1347.	0.5	12
10741	Computational prediction of the effect of mutations in the receptor-binding domain on the interaction between SARS-CoV-2 and human ACE2. Molecular Diversity, 2022, 26, 3309-3324.	3.9	17

#	ARTICLE	IF	CITATIONS
10742	Molecular docking studies of YKT tripeptide and drug delivery system with poly( $\epsilon$ -caprolactone) nanoparticles. <i>Archiv Der Pharmazie</i> , 2022, 355, e2100437.	4.1	3
10743	Structural Characteristics of Glycocins: Unraveling the Role of S-Linked Carbohydrates and Other Structural Elements. <i>Journal of Chemical Information and Modeling</i> , 2022, 62, 927-935.	5.4	4
10744	Molecular insights into the primary nucleation of polymorphic amyloid $\beta$ dimers in <sc>DOPC</sc> lipid bilayer membrane. <i>Protein Science</i> , 2022, 31, .	7.6	17
10745	Mechanisms underlying TARP modulation of the GluA1/2- $\beta$ 8 AMPA receptor. <i>Nature Communications</i> , 2022, 13, 734.	12.8	15
10746	Pharmacophore modeling, Virtual screening, Molecular docking and dynamics studies for the discovery of HER2-tyrosine kinase inhibitors: An in-silico approach. <i>Journal of Molecular Structure</i> , 2022, , 132531.	3.6	8
10747	Inherent conformational plasticity in dsRBDs enables interaction with topologically distinct RNAs. <i>Biophysical Journal</i> , 2022, , .	0.5	2
10748	Reconstruction of the unbinding pathways of noncovalent SARS-CoV and SARS-CoV-2 3CLpro inhibitors using unbiased molecular dynamics simulations. <i>PLoS ONE</i> , 2022, 17, e0263251.	2.5	2
10749	Mechanistic insight into the impact of a bivalent ligand on the structure and dynamics of a GPCR oligomer. <i>Computational and Structural Biotechnology Journal</i> , 2022, 20, 925-936.	4.1	6
10750	Structures of human pannexin-1 in nanodiscs reveal gating mediated by dynamic movement of the N terminus and phospholipids. <i>Science Signaling</i> , 2022, 15, eabg6941.	3.6	34
10751	Dynamic regulation of O-GlcNAcylation and phosphorylation on STAT3 under hypoxia-induced EMT. <i>Cellular Signalling</i> , 2022, , 110277.	3.6	3
10752	Computational study of nanoscale mechanical properties of Fe-Cr-Ni alloy. <i>Molecular Simulation</i> , 2022, 48, 551-567.	2.0	6
10753	Counterintuitive Electrostatics upon Metal Ion Coordination to a Receptor with Two Homotopic Binding Sites. <i>Journal of the American Chemical Society</i> , 2022, 144, 2921-2932.	13.7	3
10754	SPCS1-Dependent E2-p7 processing determines HCV Assembly efficiency. <i>PLoS Pathogens</i> , 2022, 18, e1010310.	4.7	2
10755	Computational investigation of the alkaloids of <i>Pilocarpus microphyllus</i> species as phytopharmaceuticals for the inhibition of sterol 14 $\alpha$ -demethylase protease of <i>Trypanosoma cruzi</i> . <i>Journal of Biomolecular Structure and Dynamics</i> , 2023, 41, 2555-2573.	3.5	1
10757	Can Urea and Trimethylamine-N-oxide Prevent the Pressure-Induced Phase Transition of Lipid Membrane?. <i>Journal of Physical Chemistry B</i> , 2022, , .	2.6	8
10758	Chemically realistic coarse-grained models for polyelectrolyte solutions. <i>Journal of Chemical Physics</i> , 2022, 156, 094902.	3.0	1
10759	Multiscale Computational Study of the Conformation of the Full-Length Intrinsically Disordered Protein MeCP2. <i>Journal of Chemical Information and Modeling</i> , 2022, 62, 958-970.	5.4	3
10760	Hard-Cation-Soft-Anion Ionic Liquids for PEDOT:PSS Treatment. <i>Journal of Physical Chemistry B</i> , 2022, 126, 1615-1624.	2.6	9

#	ARTICLE	IF	CITATIONS
10762	The Role of Hydrogen Bonds and Electrostatic Interactions in Enhancing Two-Photon Absorption in Green and Yellow Fluorescent Proteins. <i>ChemPhysChem</i> , 2022, 23, .	2.1	4
10763	Indocyanine Green Performance Enhanced System for Potent Photothermal Treatment of Bacterial Infection. <i>Molecular Pharmaceutics</i> , 2022, 19, 4527-4537.	4.6	5
10765	Coarse-grained molecular dynamics study of elasticity of block copolymers with cubic symmetrical morphology. <i>Polymer</i> , 2022, 243, 124624.	3.8	5
10766	Magainin 2 and PGLa in Bacterial Membrane Mimics III: Membrane Fusion and Disruption. <i>Biophysical Journal</i> , 2022, , .	0.5	4
10767	The complexin C-terminal amphipathic helix stabilizes the fusion pore open state by sculpting membranes. <i>Nature Structural and Molecular Biology</i> , 2022, 29, 97-107.	8.2	15
10768	Permeation of Fosfomycin through the Phosphate-Specific Channels OprP and OprO of <i>Pseudomonas aeruginosa</i> . <i>Journal of Physical Chemistry B</i> , 2022, 126, 1388-1403.	2.6	7
10769	Charge scaling parameter evaluation for multivalent ionic liquids with fixed point charge force fields. <i>Journal of Ionic Liquids</i> , 2022, 2, 100020.	2.7	8
10770	Mechanisms of Interaction of Small Hydroxylated Cryosolvents with Dehydrated Model Cell Membranes: Stabilization vs Destruction. <i>Journal of Physical Chemistry B</i> , 2022, 126, 197-216.	2.6	5
10771	Dynamical Manifestations of Supercooling in Amyloid Hydration. <i>Journal of Physical Chemistry B</i> , 2022, 126, 44-53.	2.6	3
10772	Model Folded Hydrophobic Polymers Reside in Highly Branched Voids. <i>Journal of Physical Chemistry Letters</i> , 2022, 13, 183-189.	4.6	5
10773	Structural Insights into Self-Assembled Aerosol-OT Aggregates in Aqueous Media Using Atomistic Molecular Dynamics. <i>Journal of Physical Chemistry B</i> , 2021, 125, 13789-13803.	2.6	1
10774	Screening cyclooxygenase-2 inhibitors from <i>Allium sativum</i> L. compounds: in silico approach. <i>Journal of Molecular Modeling</i> , 2022, 28, 24.	1.8	20
10775	Adaptive Recombinant Nanoworms from Genetically Encodable Star Amphiphiles. <i>Biomacromolecules</i> , 2022, 23, 863-876.	5.4	4
10776	Martini 3 Coarse-Grained Model for Type III Deep Eutectic Solvents: Thermodynamic, Structural, and Extraction Properties. <i>ACS Sustainable Chemistry and Engineering</i> , 2021, 9, 17338-17350.	6.7	20
10777	Molecular basis for redox control by the human cystine/glutamate antiporter system xc <sup>+</sup> . <i>Nature Communications</i> , 2021, 12, 7147.	12.8	65
10778	Efficient sampling of high-dimensional free energy landscapes using adaptive reinforced dynamics. <i>Nature Computational Science</i> , 2022, 2, 20-29.	8.0	18
10781	Structure-guided glyco-engineering of ACE2 for improved potency as soluble SARS-CoV-2 decoy receptor. <i>ELife</i> , 2021, 10, .	6.0	29
10782	Insights into the Adsorption Mechanism of Tetracycline on Hierarchically Porous Carbon and the Effect of Nanoporous Geometry. <i>SSRN Electronic Journal</i> , 0, , .	0.4	0

#	ARTICLE	IF	CITATIONS
10783	Thermodynamically consistent physics-informed neural networks for hyperbolic systems.. , 2021, , .		1
10784	Molecular insights into the resistance of phospholipid heads to the membrane penetration of graphene nanosheets. <i>Nanoscale</i> , 2022, 14, 5384-5391.	5.6	6
10785	Permeation Process of Metal Complexes with Hydroxyoxime and Carboxylic Acid Extractants through Organic-Aqueous Interface. <i>Solvent Extraction Research and Development</i> , 2022, 29, 21-29.	0.4	0
10786	Role of density and electrostatic interactions in the viscosity and non-newtonian behavior of ionic liquids â€“ a molecular dynamics study. <i>Physical Chemistry Chemical Physics</i> , 2022, 24, 6866-6879.	2.8	9
10787	Molecular simulation of glycerol-derived triether podands for lithium ion solvation. <i>Physical Chemistry Chemical Physics</i> , 2022, 24, 9459-9466.	2.8	4
10788	Efficient Separation of Co2/Ch4 by Ionic Liquids Confined in Graphene Oxide: A Molecular Dynamics Simulation. <i>SSRN Electronic Journal</i> , 0, , .	0.4	0
10789	Synaptotagmin-1 C2B domains cooperatively stabilize the fusion stalk <i>via</i> a master-servant mechanism. <i>Chemical Science</i> , 2022, 13, 3437-3446.	7.4	11
10790	Modifying Amyloid Motif Aggregation Through Local Structure. <i>Methods in Molecular Biology</i> , 2022, 2340, 343-356.	0.9	1
10791	All-atom simulations of bent liquid crystal dimers: the twist-bend nematic phase and insights into conformational chirality. <i>Soft Matter</i> , 2022, 18, 3087-3096.	2.7	11
10792	The auto-inhibition mechanism of transcription factor Ets-1 induced by phosphorylation on the intrinsically disordered region. <i>Computational and Structural Biotechnology Journal</i> , 2022, 20, 1132-1141.	4.1	3
10793	Computational and Experimental Study of Different Brines in Temperature Swing Solvent Extraction Desalination with Amine Solvents. <i>SSRN Electronic Journal</i> , 0, , .	0.4	0
10794	Conserved Î-Helix-3 is Crucial for Structure and Functions of Rad6 E2 Ubiquitin-Conjugating Enzymes. <i>SSRN Electronic Journal</i> , 0, , .	0.4	0
10795	Computational discovery of high charge mobility self-assembling Î€-conjugated peptides. <i>Molecular Systems Design and Engineering</i> , 2022, 7, 447-459.	3.4	8
10796	Molecular behavior of hybrid gas hydrate nucleation: separation of soluble H<sub>2</sub>S from mixed gas. <i>Physical Chemistry Chemical Physics</i> , 2022, 24, 9509-9520.	2.8	5
10797	A coarse-grained model for capturing the helical behavior of isotactic polypropylene. <i>Soft Matter</i> , 2022, , .	2.7	1
10798	Molecular Dynamics Simulations of Protein Aggregation: Protocols for Simulation Setup and Analysis with Markov State Models and Transition Networks. <i>Methods in Molecular Biology</i> , 2022, 2340, 235-279.	0.9	9
10799	Single nucleobase identification for transversally-confined ssDNA using longitudinal ionic currents. <i>Nanoscale</i> , 2022, , .	5.6	0
10800	Investigation of the pH-dependent aggregation mechanisms of GCSF using low resolution protein characterization techniques and advanced molecular dynamics simulations. <i>Computational and Structural Biotechnology Journal</i> , 2022, 20, 1439-1455.	4.1	4



#	ARTICLE	IF	CITATIONS
10801	Controlling Li <sup>+</sup> transport in ionic liquid electrolytes through salt content and anion asymmetry: a mechanistic understanding gained from molecular dynamics simulations. <i>Physical Chemistry Chemical Physics</i> , 2022, 24, 6072-6086.	2.8	8
10802	Toward Unveiling Structure and Property Relationships from Ionic Ordering in Li/S Battery Electrolytes: Neutron Total Scattering and Molecular Dynamics Simulations. <i>SSRN Electronic Journal</i> , 0, , .	0.4	0
10803	Application of molecular dynamics simulations for shale gas systems. , 2022, , 323-343.		0
10804	Predictive Modeling of Neurotoxic Î±-Synuclein Polymorphs. <i>Methods in Molecular Biology</i> , 2022, 2340, 379-399.	0.9	1
10805	Virtual screening of phytochemicals from Indian medicinal plants against the endonuclease domain of SFTS virus L polymerase. <i>RSC Advances</i> , 2022, 12, 6234-6247.	3.6	10
10806	Molecular Dynamics Simulation Study of Covalently Bound Hybrid Coagulants (Cbhyc): Molecular Structure and Coagulation Mechanisms. <i>SSRN Electronic Journal</i> , 0, , .	0.4	0
10807	Hydrophobic association and solvation of neopentane in urea, TMAO and urea+TMAO solutions. <i>Physical Chemistry Chemical Physics</i> , 2022, 24, 6941-6957.	2.8	3
10808	Designing and screening of fluoroquinolone substitutes using combined <i>in silico</i> approaches: biological metabolism+bioconcentration bilateral selection and their mechanism analyses. <i>Green Chemistry</i> , 2022, 24, 3778-3793.	9.0	25
10809	The role of pressure and defects in the wurtzite to rock salt transition in cadmium selenide. <i>Physical Chemistry Chemical Physics</i> , 2022, 24, 8378-8386.	2.8	1
10810	Molecular Dynamics Simulations of Plastic Damage in Metals. , 2022, , 1335-1369.		0
10811	Recovery of enzyme structure and activity following rehydration from ionic liquid. <i>Physical Chemistry Chemical Physics</i> , 2022, , .	2.8	2
10812	Polar/apolar interfaces modulate the conformational behavior of cyclic peptides with impact on their passive membrane permeability. <i>RSC Advances</i> , 2022, 12, 5782-5796.	3.6	10
10813	Bridging the N-terminal and middle domains in FlhG of the flagellar rotor. <i>Current Research in Structural Biology</i> , 2022, 4, 59-67.	2.2	2
10814	Mutations in G6PC2 gene with increased risk for development of type 2 diabetes: Understanding via computational approach. <i>Advances in Protein Chemistry and Structural Biology</i> , 2022, 130, 351-373.	2.3	6
10815	Human IL-2RÉ' subunit binding modulation of IL-2 through a decline in electrostatic interactions: A computational and experimental approach. <i>PLoS ONE</i> , 2022, 17, e0264353.	2.5	9
10816	Can the jigsaw puzzle model of protein folding reassemble a hydrophobic core?. <i>Proteins: Structure, Function and Bioinformatics</i> , 2022, 90, 1390-1412.	2.6	6
10817	Approach to Study pH-Dependent Protein Association Using Constant-pH Molecular Dynamics: Application to the Dimerization of Î²-Lactoglobulin. <i>Journal of Chemical Theory and Computation</i> , 2022, 18, 1982-2001.	5.3	7
10818	Coarse-Grained Model of Thiol+Epoxy-Based Alternating Copolymers in Explicit Solvents. <i>Journal of Physical Chemistry B</i> , 2022, 126, 1830-1841.	2.6	1

#	ARTICLE	IF	CITATIONS
10819	Unraveling a Conserved Conformation of the FG Loop upon the Binding of Natural Ligands to the Human and Murine PD1. <i>Journal of Physical Chemistry B</i> , 2022, 126, 1441-1446.	2.6	1
10820	Deciphering Ethanol-Driven Swelling, Rupturing, Aggregation, and Fusion of Lipid Vesicles Using Coarse-Grained Molecular Dynamics Simulations. <i>Langmuir</i> , 2022, 38, 2445-2459.	3.5	9
10821	Dynamics of Ultrafast Phase Transitions in (001) Si on the Shock-Wave Front. <i>International Journal of Molecular Sciences</i> , 2022, 23, 2115.	4.1	3
10822	Leveraging the multivalent p53 peptide-MdmX interaction to guide the improvement of small molecule inhibitors. <i>Nature Communications</i> , 2022, 13, 1087.	12.8	9
10823	Structural insights into the Venus flytrap mechanosensitive ion channel Flycatcher1. <i>Nature Communications</i> , 2022, 13, 850.	12.8	13
10824	Role of Ionic Strength in the Formation of Stable Supramolecular Nanoparticle-Protein Conjugates for Biosensing. <i>International Journal of Molecular Sciences</i> , 2022, 23, 2368.	4.1	5
10825	Direct Detection of Bound Ammonium Ions in the Selectivity Filter of Ion Channels by Solid-State NMR. <i>Journal of the American Chemical Society</i> , 2022, 144, 4147-4157.	13.7	7
10827	Free Energy and Stacking of Eumelanin Nanoaggregates. <i>Journal of Physical Chemistry B</i> , 2022, 126, 1805-1818.	2.6	8
10828	Multiscale Study of the Charge Transport Properties of Silicone Rubber Oligomers. <i>Journal of Physical Chemistry A</i> , 2022, 126, 1369-1377.	2.5	4
10830	HNF1A POU Domain Mutations Found in Japanese Liver Cancer Patients Cause Downregulation of HNF4A Promoter Activity with Possible Disruption in Transcription Networks. <i>Genes</i> , 2022, 13, 413.	2.4	3
10831	Understanding the Energetic Components Influencing the Thermodynamic Quantities of Carbonic Anhydrase Protein upon Ligand Binding. <i>ChemistrySelect</i> , 2022, 7, .	1.5	0
10832	A Molecular Investigation of the Solvent Influence on Inter- and Intra-Molecular Hydrogen Bond Interaction of Linamarin. <i>Processes</i> , 2022, 10, 352.	2.8	2
10833	Visualizing RNA Structures by SAXS-Driven MD Simulations. <i>Frontiers in Bioinformatics</i> , 2022, 2, .	2.1	12
10834	Evidence for a trap-and-flip mechanism in a proton-dependent lipid transporter. <i>Nature Communications</i> , 2022, 13, 1022.	12.8	10
10835	A Method for Detection of Water Permeation Events in Molecular Dynamics Simulations of Lipid Bilayers. <i>Brazilian Journal of Physics</i> , 2022, 52, 1.	1.4	3
10836	Conformational Dynamics of the Soluble and Membrane-Bound Forms of Interleukin-1 Receptor Type-1: Insights into Linker Flexibility and Domain Orientation. <i>International Journal of Molecular Sciences</i> , 2022, 23, 2599.	4.1	2
10838	Computational Investigation of Structural Basis for Enhanced Binding of Isoflavone Analogues with Mitochondrial Aldehyde Dehydrogenase. <i>ACS Omega</i> , 2022, 7, 8115-8127.	3.5	6
10839	Molecular Interactions of Tannic Acid with Proteins Associated with SARS-CoV-2 Infectivity. <i>International Journal of Molecular Sciences</i> , 2022, 23, 2643.	4.1	21

#	ARTICLE	IF	CITATIONS
10841	Identification of electroporation sites in the complex lipid organization of the plasma membrane. <i>ELife</i> , 2022, 11, .	6.0	11
10843	Interaction of Docetaxel with Phosphatidylcholine Membranes: A Combined Experimental and Computational Study. <i>Journal of Membrane Biology</i> , 2022, 255, 277-291.	2.1	4
10844	Capturing Free-Radical Polymerization by Synergetic <i>Ab Initio</i> Calculations and Topological Reactive Molecular Dynamics. <i>Macromolecules</i> , 2022, 55, 1474-1486.	4.8	3
10845	Capturing a Crucial "Disorder-to-Order Transition" at the Heart of the Coronavirus Molecular Pathology" Triggered by Highly Persistent, Interchangeable Salt-Bridges. <i>Vaccines</i> , 2022, 10, 301.	4.4	5
10846	Ligand Binding Path Sampling Based on Parallel Cascade Selection Molecular Dynamics: LB-PaCS-MD. <i>Materials</i> , 2022, 15, 1490.	2.9	1
10847	Structural basis of neuropeptide Y signaling through Y1 receptor. <i>Nature Communications</i> , 2022, 13, 853.	12.8	20
10848	Computational Simulations Highlight the IL2R Binding Potential of Polyphenol Stilbenes from Fenugreek. <i>Molecules</i> , 2022, 27, 1215.	3.8	2
10849	Molecular modelling studies and identification of novel phytochemical inhibitor of DLL3. <i>Journal of Biomolecular Structure and Dynamics</i> , 2023, 41, 3089-3109.	3.5	0
10850	The Full Model of the pMHC-TCR-CD3 Complex: A Structural and Dynamical Characterization of Bound and Unbound States. <i>Cells</i> , 2022, 11, 668.	4.1	2
10851	Caging Polycations: Effect of Increasing Confinement on the Modes of Interaction of Spermidine <sup>3+</sup> With DNA Double Helices. <i>Frontiers in Chemistry</i> , 2022, 10, 836994.	3.6	2
10852	High-Dimensional Parameter Search Method to Determine Force Field Mixing Terms in Molecular Simulations. <i>Langmuir</i> , 2022, 38, 2840-2851.	3.5	5
10853	Molecular Mechanism of Dual Intercalation in Sac7 DNA Complexation. <i>Journal of Physical Chemistry B</i> , 2022, 126, 1682-1690.	2.6	1
10854	Modeling the Structure and Interactions of Intrinsically Disordered Peptides with Multiple Replica, Metadynamics-Based Sampling Methods and Force-Field Combinations. <i>Journal of Chemical Theory and Computation</i> , 2022, 18, 1915-1928.	5.3	7
10855	Discovery and Characterization of a New Crustin Antimicrobial Peptide from <i>Amphibalanus amphitrite</i> . <i>Pharmaceutics</i> , 2022, 14, 413.	4.5	8
10856	Photoinduced Oxidation of Lipid Membranes in the Presence of the Nonsteroidal Anti-Inflammatory Drug Ketoprofen. <i>Membranes</i> , 2022, 12, 251.	3.0	7
10857	Structure, mechanism and lipid-mediated remodeling of the mammalian Na <sup>+</sup> /H <sup>+</sup> exchanger NHA2. <i>Nature Structural and Molecular Biology</i> , 2022, 29, 108-120.	8.2	27
10858	Stress-induced tyrosine phosphorylation of RtcB modulates IRE1 activity and signaling outputs. <i>Life Science Alliance</i> , 2022, 5, e202201379.	2.8	8
10859	Paired Simulations and Experimental Investigations into the Calcium-Dependent Conformation of Albumin. <i>Journal of Chemical Information and Modeling</i> , 2022, 62, 1282-1293.	5.4	7

#	ARTICLE	IF	CITATIONS
10860	Probing the Molecular Basis of Cofactor Affinity and Conformational Dynamics of <i>Mycobacterium tuberculosis</i> Elongation Factor Tu: An Integrated Approach Employing Steered Molecular Dynamics and Umbrella Sampling Simulations. <i>Journal of Physical Chemistry B</i> , 2022, 126, 1447-1461.	2.6	5
10861	Salt Destabilization of Cationic Colistin Complexation within Polyanionic Microgels. <i>Macromolecules</i> , 2022, 55, 1736-1746.	4.8	4
10862	Atomistic Simulation of Lysozyme in Solutions Crowded by Tetraethylene Glycol: Force Field Dependence. <i>Molecules</i> , 2022, 27, 2110.	3.8	1
10863	In silico discovery of potential azole-containing mPGES-1 inhibitors by virtual screening, pharmacophore modeling and molecular dynamics simulations. <i>Structural Chemistry</i> , 0, , 1.	2.0	1
10864	Poly-L-Arginine Molecule Properties in Simple Electrolytes: Molecular Dynamic Modeling and Experiments. <i>International Journal of Environmental Research and Public Health</i> , 2022, 19, 3588.	2.6	10
10865	Mechanistic Pathway of Lipid Phase-Dependent Lipid Corona Formation on Phenylalanine-Functionalized Gold Nanoparticles: A Combined Experimental and Molecular Dynamics Simulation Study. <i>Journal of Physical Chemistry B</i> , 2022, 126, 2241-2255.	2.6	7
10866	Rigorous expressions for thermodynamic properties in the $\langle i \rangle NpH \langle i \rangle$ ensemble. <i>Physical Review E</i> , 2022, 105, 035301.	2.1	7
10867	Identification of potential <i>Staphylococcus aureus</i> dihydrofolate reductase inhibitors using QSAR, molecular docking, dynamics simulations and free energy calculation. <i>Journal of Biomolecular Structure and Dynamics</i> , 2023, 41, 3835-3846.	3.5	2
10868	The electrical double layer revisited. <i>Natural Sciences</i> , 2022, 2, .	2.1	8
10869	Partially Auxetic Properties of Face-Centered Cubic Hard-Sphere Crystals with Nanochannels of Different Sizes, Parallel to [001] Direction and Filled by Other Hard Spheres. <i>Physica Status Solidi (B): Basic Research</i> , 0, , 2200006.	1.5	7
10870	Inhibition of the hexamerization of SARS-CoV-2 endoribonuclease and modeling of RNA structures bound to the hexamer. <i>Scientific Reports</i> , 2022, 12, 3860.	3.3	5
10871	Linking Alzheimer's Disease and Type 2 Diabetes: Characterization and Inhibition of Cytotoxic A $\beta$ 2 and IAPP Hetero-Aggregates. <i>Frontiers in Molecular Biosciences</i> , 2022, 9, 842582.	3.5	6
10872	Sphingolipids with 2-hydroxy fatty acids aid in plasma membrane nanodomain organization and oxidative burst. <i>Plant Physiology</i> , 2022, 189, 839-857.	4.8	13
10875	Spliced isoforms of the cardiac Nav1.5 channel modify channel activation by distinct structural mechanisms. <i>Journal of General Physiology</i> , 2022, 154, .	1.9	1
10876	The increment of the temperature of maximum density of water by addition of small amounts of <i>tert</i> -butanol: Experimental data and microscopic description revisited. <i>Journal of Chemical Physics</i> , 2022, 156, 104502.	3.0	5
10877	Interaction between PET tracer and the specific residues around the gate of the open form of Monoamine Oxidase B (MAO-B). <i>Journal of Physics: Conference Series</i> , 2022, 2207, 012025.	0.4	0
10878	Designing specific inhibitors against dihydrofolate reductase of <i>W. bancrofti</i> towards drug discovery for lymphatic filariasis. <i>Structural Chemistry</i> , 2022, 33, 935-947.	2.0	3
10879	Response of Terahertz Protein Vibrations to Ligand Binding: Calmodulin-Peptide Complexes as a Case Study. <i>Journal of Chemical Information and Modeling</i> , 2022, 62, 1669-1679.	5.4	2

#	ARTICLE	IF	CITATIONS
10880	Redefining the Molecular Interplay between Dimethyl Sulfoxide, Lipid Bilayers, and Dehydration. <i>Journal of Physical Chemistry B</i> , 2022, 126, 2513-2529.	2.6	4
10881	Synthesis and Profiling of Highly Selective Inhibitors of Methyltransferase DOT1L Based on Carbocyclic C-Nucleosides. <i>Journal of Medicinal Chemistry</i> , 2022, 65, 5701-5723.	6.4	5
10882	Computational studies suggest compounds restoring function of p53 cancer mutants can bind SARS-CoV-2 spike protein. <i>Journal of Biomolecular Structure and Dynamics</i> , 2022, , 1-14.	3.5	0
10883	Supramolecular Engineering of Alkylated, Fluorinated, and Mixed Amphiphiles. <i>Macromolecular Rapid Communications</i> , 2022, 43, e2100914.	3.9	7
10884	Crack-path bifurcation, arrest, and renucleation in porous 3C-SiC. <i>Journal of Applied Physics</i> , 2022, 131, 115105.	2.5	2
10886	Cation-Ligand Interactions Dictate Salt Partitioning and Diffusivity in Ligand-Functionalized Polymer Membranes. <i>Macromolecules</i> , 2022, 55, 2260-2270.	4.8	11
10887	Molecular Insight into Dye-Surfactant Interaction at Premicellar Concentrations: A Combined Two-Photon Absorption and Molecular Dynamics Simulation Study. <i>Langmuir</i> , 2022, 38, 3105-3112.	3.5	7
10888	In silico evidence for prednisone and progesterone efficacy in recurrent implantation failure treatment. <i>Journal of Molecular Modeling</i> , 2022, 28, 105.	1.8	3
10889	<sc>l</sc>- to <sc>d</sc>-Amino Acid Substitution in the Immunodominant LCMV-Derived Epitope gp33 Highlights the Sensitivity of the TCR Recognition Mechanism for the MHC/Peptide Structure and Dynamics. <i>ACS Omega</i> , 2022, 7, 9622-9635.	3.5	1
10890	Biomolecular engineering of drugs loading in Riboflavin-targeted polymeric devices: simulation and experimental. <i>Scientific Reports</i> , 2022, 12, 5119.	3.3	11
10891	Structural and dynamic properties of eutectic mixtures based on menthol and fatty acids derived from coconut oil: a MD simulation study. <i>Scientific Reports</i> , 2022, 12, 5153.	3.3	9
10892	Ergodic Structural Diversity Predicts Dynamics in Amorphous Materials. <i>Frontiers in Materials</i> , 2022, 9, .	2.4	0
10893	Investigation of the structural and dynamic basis of kinesin dissociation from microtubule by atomistic molecular dynamics simulations. <i>Chinese Physics B</i> , 2022, 31, 058702.	1.4	2
10894	Molecular Dynamics Simulations of Transmembrane Cyclic Peptide Nanotubes Using Classical Force Fields, Hydrogen Mass Repartitioning, and Hydrogen Isotope Exchange Methods: A Critical Comparison. <i>International Journal of Molecular Sciences</i> , 2022, 23, 3158.	4.1	1
10895	Alteration of lipid bilayer mechanics by volatile anesthetics: Insights from 1/4s-long molecular dynamics simulations. <i>IScience</i> , 2022, 25, 103946.	4.1	7
10896	Phase Transformation in TiNi Nano-Wafers for Nanomechanical Devices with Shape Memory Effect. <i>Nanomaterials</i> , 2022, 12, 1107.	4.1	2
10897	Structure of the BAK-activating antibody 7D10 bound to BAK reveals an unexpected role for the 1-2 loop in BAK activation. <i>Cell Death and Differentiation</i> , 2022, 29, 1757-1768.	11.2	4
10898	Oxygen Quenching-Resistant Nanoaggregates with Aggregation-Induced Delayed Fluorescence for Time-Resolved Mapping of Intracellular Microviscosity. <i>ACS Nano</i> , 2022, 16, 6176-6184.	14.6	7

#	ARTICLE	IF	CITATIONS
10899	Correction Schemes for Absolute Binding Free Energies Involving Lipid Bilayers. <i>Journal of Chemical Theory and Computation</i> , 2022, 18, 2657-2672.	5.3	2
10900	Green lubricants production from Nile tilapia waste and prediction of physical properties through molecular dynamics simulations. <i>JAOCs, Journal of the American Oil Chemists' Society</i> , 2022, 99, 341-352.	1.9	1
10901	Binary Matrix Method to Enumerate, Hierarchically Order, and Structurally Classify Peptide Aggregation. <i>Journal of Chemical Information and Modeling</i> , 2022, 62, 1585-1594.	5.4	0
10903	Changes in elastin structure and extensibility induced by hypercalcemia and hyperglycemia. <i>Acta Biomaterialia</i> , 2023, 163, 131-145.	8.3	3
10904	Novel Detection Method for Evaluating the Activity of an Alkaline Serine Protease from <i>Bacillus clausii</i> . <i>Journal of Agricultural and Food Chemistry</i> , 2022, 70, 3765-3774.	5.2	3
10905	Exploring the Effect of Enhanced Sampling on Protein Stability Prediction. <i>Journal of Chemical Theory and Computation</i> , 2022, 18, 2569-2583.	5.3	8
10906	Ligand-Dependent Modulation of the Dynamics of Intracellular Loops Dictates Functional Selectivity of 5-HT <sub>2A</sub> R. <i>Journal of Chemical Information and Modeling</i> , 2022, 62, 2522-2537.	5.4	5
10907	Activation mechanism of the class D fungal GPCR dimer Ste2. <i>Nature</i> , 2022, 603, 743-748.	27.8	13
10908	A molecular dynamics study on the mechanical properties of defective CNT/epoxy nanocomposites using static and dynamic deformation approaches. <i>International Polymer Processing</i> , 2022, 37, 176-190.	0.5	6
10909	Membrane contact probability: An essential and predictive character for the structural and functional studies of membrane proteins. <i>PLoS Computational Biology</i> , 2022, 18, e1009972.	3.2	8
10911	Structure and Dynamic Properties of a Glycerol-Betaine Deep Eutectic Solvent: When Does a DES Become an Aqueous Solution?. <i>ACS Sustainable Chemistry and Engineering</i> , 2022, 10, 3501-3512.	6.7	13
10912	Molecular dynamics study of interfacial strength and debonding in SiC/SiC nanocomposite. <i>MRS Advances</i> , 0, , 1.	0.9	0
10913	Densities of the Standard Amino Acids in Aqueous Solutions via Molecular Dynamics Simulations. <i>Journal of Chemical &amp; Engineering Data</i> , 2022, 67, 797-808.	1.9	0
10914	Kinase domain autophosphorylation rewires the activity and substrate specificity of CK1 enzymes. <i>Molecular Cell</i> , 2022, 82, 2006-2020.e8.	9.7	12
10915	Atomistic Insights into the Droplet Size Evolution during Self-Microemulsification. <i>Langmuir</i> , 2022, 38, 3129-3138.	3.5	3
10916	Mesoscopic Modeling of a Highly-Ordered Sanidic Polymer Mesophase and Comparison With Experimental Data. <i>Journal of Physical Chemistry B</i> , 2022, 126, 2285-2298.	2.6	2
10917	Novel Loss-of-Function Mutations in NPR2 Cause Acromesomelic Dysplasia, Maroteaux Type. <i>Frontiers in Genetics</i> , 2022, 13, 823861.	2.3	5
10918	An atomistic view on the uptake of aromatic compounds by cyclodextrin immobilized on mesoporous silica. <i>Adsorption</i> , 2022, 28, 125-136.	3.0	1



#	ARTICLE	IF	CITATIONS
10919	Effects of cryo-EM cooling on structural ensembles. <i>Nature Communications</i> , 2022, 13, 1709.	12.8	33
10920	The role of <scp>ATP</scp> in solubilizing <scp>RNA</scp>â€binding protein fused in sarcoma. <i>Proteins: Structure, Function and Bioinformatics</i> , 2022, 90, 1606-1612.	2.6	11
10921	Camel back shaped Kirkwoodâ€Buff integrals. <i>Journal of Chemical Physics</i> , 2022, 156, 124503.	3.0	2
10922	Demulsification of Heavy Oil-in-Water Emulsion by a Novel Janus Graphene Oxide Nanosheet: Experiments and Molecular Dynamic Simulations. <i>Molecules</i> , 2022, 27, 2191.	3.8	3
10923	Stimuli-Responsive Adaptive Nanotoxin to Directly Penetrate the Cellular Membrane by Molecular Folding and Unfolding. <i>Journal of the American Chemical Society</i> , 2022, 144, 5503-5516.	13.7	8
10924	Cryo-EM structure of the heptameric calcium homeostasis modulator 1 channel. <i>Journal of Biological Chemistry</i> , 2022, 298, 101838.	3.4	6
10925	Drug Resistance Mechanism of M46I-Mutation-Induced Saquinavir Resistance in HIV-1 Protease Using Molecular Dynamics Simulation and Binding Energy Calculation. <i>Viruses</i> , 2022, 14, 697.	3.3	14
10926	Blockage of the Monoamine Oxidase by a Natural Compound to Overcome Parkinsonâ€™s Disease via Computational Biology. <i>Journal of Computational Biophysics and Chemistry</i> , 2022, 21, 373-387.	1.7	7
10927	Modeling of Poly(3-hexylthiophene) and Its Oligomerâ€™s Structure and Thermal Behavior with Different Force Fields: Insights into the Phase Transitions of Semiconducting Polymers. <i>Macromolecules</i> , 0, , .	4.8	3
10928	Multiadducts of C60 Modulate Amyloid-Î² Fibrillation with Dual Acetylcholinesterase Inhibition and Antioxidant Properties: In Vitro and In Silico Studies. <i>Journal of Alzheimer's Disease</i> , 2022, 87, 741-759.	2.6	1
10929	Bending-torsional elasticity and energetics of the plus-end microtubule tip. <i>Proceedings of the National Academy of Sciences of the United States of America</i> , 2022, 119, e2115516119.	7.1	7
10930	Structural characteristics of low-density environments in liquid water. <i>Physical Review E</i> , 2022, 105, 034604.	2.1	13
10931	Computational studies on the design of NCI natural products as inhibitors to SARS-CoV-2 main protease. <i>Journal of Biomolecular Structure and Dynamics</i> , 2023, 41, 3741-3751.	3.5	3
10932	Membrane thickness, lipid phase and sterol type are determining factors in the permeability of membranes to small solutes. <i>Nature Communications</i> , 2022, 13, 1605.	12.8	81
10933	Inflammasome NLRP3 activation induced by Convulxin, a C-type lectin-like isolated from <i>Crotalus durissus terrificus</i> snake venom. <i>Scientific Reports</i> , 2022, 12, 4706.	3.3	43
10934	A molecular switch controls the impact of cholesterol on a Kir channel. <i>Proceedings of the National Academy of Sciences of the United States of America</i> , 2022, 119, e2109431119.	7.1	9
10935	Understanding the Interactions between Triolein and Cosolvent Binary Mixtures Using Molecular Dynamics Simulations. <i>ACS Omega</i> , 2022, 7, 10212-10224.	3.5	2
10936	Assessing models of force-dependent unbinding rates via infrequent metadynamics. <i>Journal of Chemical Physics</i> , 2022, 156, 125102.	3.0	12

#	ARTICLE	IF	CITATIONS
10938	Tug-of-War between Internal and External Frictions and Viscosity Dependence of Rate in Biological Reactions. <i>Physical Review Letters</i> , 2022, 128, 108101.	7.8	14
10939	Solubility of Gases in Choline Chloride-Based Deep Eutectic Solvents from Molecular Dynamics Simulation. <i>Industrial &amp; Engineering Chemistry Research</i> , 2022, 61, 4659-4671.	3.7	9
10940	Vibrational spectroscopy by means of first-principles molecular dynamics simulations. <i>Wiley Interdisciplinary Reviews: Computational Molecular Science</i> , 2022, 12, .	14.6	29
10941	Coarse-Grained Molecular Dynamics Simulations of Paclitaxel-Loaded Polymeric Micelles. <i>Molecular Pharmaceutics</i> , 2022, 19, 1117-1134.	4.6	6
10942	Structure, substrate recognition and initiation of hyaluronan synthase. <i>Nature</i> , 2022, 604, 195-201.	27.8	53
10943	Structures of the Wild-Type and S59L Mutant CHCHD10 Proteins Important in Amyotrophic Lateral Sclerosis—Frontotemporal Dementia. <i>ACS Chemical Neuroscience</i> , 2022, 13, 1273-1280.	3.5	6
10944	Molecular Insight into the High Thermal Stability of Metalloprotein Azurin. <i>Journal of Physical Chemistry B</i> , 2022, 126, 2496-2506.	2.6	2
10945	Translational Jump-Diffusion of Hydroxide Ion in Anion Exchange Membrane: Deciphering the Nature of Vehicular Diffusion. <i>Journal of Physical Chemistry B</i> , 2022, 126, 2430-2440.	2.6	6
10948	Construction of Al-Mg-Zn Interatomic Potential and the Prediction of Favored Glass Formation Compositions and Associated Driving Forces. <i>Materials</i> , 2022, 15, 2062.	2.9	3
10950	Rad5 HIRAN domain: Structural insights into its interaction with ssDNA through molecular modeling approaches. <i>Journal of Biomolecular Structure and Dynamics</i> , 2023, 41, 3062-3075.	3.5	0
10951	Triamcinolone as a Potential Inhibitor of SARS-CoV-2 Main Protease and Cytokine Storm: An In silico Study. <i>Letters in Drug Design and Discovery</i> , 2023, 20, 1230-1242.	0.7	1
10952	The importance of atomic partial charges in the reproduction of intermolecular interactions for the triacetin - a model of glycerol backbone. <i>Chemistry and Physics of Lipids</i> , 2022, , 105203.	3.2	0
10953	Structural basis of lipopolysaccharide maturation by the O-antigen ligase. <i>Nature</i> , 2022, 604, 371-376.	27.8	25
10954	Docking and molecular simulations reveal a quinone-binding site on the surface of respiratory complex I. <i>FEBS Letters</i> , 2022, 596, 1133-1146.	2.8	4
10955	Engineering the Aggregation of Dyes on Ligand-Shell Protected Gold Nanoparticles to Promote Plexcitons Formation. <i>Nanomaterials</i> , 2022, 12, 1180.	4.1	7
10956	Amorphous Inclusion Complexes: Molecular Interactions of Hesperidin and Hesperetin with HP- $\beta$ -CD and Their Biological Effects. <i>International Journal of Molecular Sciences</i> , 2022, 23, 4000.	4.1	21
10958	Temperature and pressure driven spin transitions and piezochromism in a Mn-based hybrid perovskite. <i>Physical Review Materials</i> , 2022, 6, .	2.4	3
10959	Atomistic insights into the mixed-alkali effect in phosphosilicate glasses. <i>Physical Review B</i> , 2022, 105, .	3.2	14

#	ARTICLE	IF	CITATIONS
10960	Novel angiotensinâ€converting enzyme ( <scp>ACE</scp> ) inhibitory mechanism of peptides from <i>Macadamia integrifolia</i> antimicrobial protein 2 ( <scp>MiAMP2</scp> ). Journal of Food Biochemistry, 2022, 46, e14168.	2.9	6
10961	A Newtonian algorithm for constant pressure molecular dynamics with periodic boundary conditions. Molecular Physics, 2022, 120, .	1.7	0
10963	Poly lactide nanoparticle impregnation with carbamazepine in supercritical media and its subsequent release in liquid solvents: insights from molecular simulation. Journal of Molecular Liquids, 2022, 352, 118758.	4.9	4
10964	Molecular Modeling of Subtype-Specific Tat Protein Signatures to Predict Tat-TAR Interactions That May Be Involved in HIV-Associated Neurocognitive Disorders. Frontiers in Microbiology, 2022, 13, 866611.	3.5	7
10965	A Database of Solution Additives Promoting Mg<sup>2+</sup> Dehydration and the Onset of MgCO<sub>3</sub> Nucleation. Crystal Growth and Design, 2022, 22, 3080-3089.	3.0	5
10966	Insight into the self-aggregation behavior of lignite and anthracite in water: Atomic-level research using experiments and molecular dynamics simulations. Journal of Molecular Liquids, 2022, 357, 119099.	4.9	3
10967	Modeling sizing emulsion droplet deposition onto silica using all-atom molecular dynamics simulations. Composites Part B: Engineering, 2022, 235, 109712.	12.0	1
10968	Design and Analysis of a Mutant form of the Ice-Binding Protein from Choristoneura fumiferana. Protein Journal, 2022, 41, 304-314.	1.6	2
10970	Nek1-inhibitor and temozolomide-loaded microfibers as a co-therapy strategy for glioblastoma treatment. International Journal of Pharmaceutics, 2022, 617, 121584.	5.2	4
10971	Solvation Shell Thermodynamics of Extended Hydrophobic Solutes in Mixed Solvents. Journal of Chemical Physics, 2022, 156, 164901.	3.0	0
10972	Atomistic Insight into the Hydration States of Layered Double Hydroxides. ACS Omega, 2022, 7, 12412-12423.	3.5	9
10973	Alpha-cadinol as a potential ACE-inhibitory volatile compound identified from Phaseolus vulgaris L. through inÂvitro and in silico analysis. Journal of Biomolecular Structure and Dynamics, 2023, 41, 3847-3861.	3.5	3
10974	HIF-1-Dependent Induction of Î²3 Adrenoceptor: Evidence from the Mouse Retina. Cells, 2022, 11, 1271.	4.1	9
10977	Structure-based screening of natural product libraries in search of potential antiviral drug-leads as first-line treatment to COVID-19 infection. Microbial Pathogenesis, 2022, 165, 105497.	2.9	11
10978	Freezing point depression of salt aqueous solutions using the Madrid-2019 model. Journal of Chemical Physics, 2022, 156, 134503.	3.0	21
10979	Bridging the gap between mesoscopic and molecular models of solid/liquid interfaces out-of-equilibrium. Chemical Engineering Research and Design, 2022, 180, 285-295.	5.6	5
10980	The potential of antifungal peptide Sesquin as natural food preservative. Biochimie, 2022, 203, 51-64.	2.6	6
10981	Data-centric framework for crystal structure identification in atomistic simulations using machine learning. Physical Review Materials, 2022, 6, .	2.4	5

#	ARTICLE	IF	CITATIONS
10983	Ginger ( <i>Zingiber officinale</i> ) components as alternative for inhibition of the human dopamine receptor D2: a computational approach. <i>Molecular Simulation</i> , 0, , 1-15.	2.0	1
10984	Development of the poly(l-histidine) grafted carbon nanotube as a possible smart drug delivery vehicle. <i>Computers in Biology and Medicine</i> , 2022, 143, 105336.	7.0	9
10985	Mechanistic Origin of Different Binding Affinities of SARS-CoV and SARS-CoV-2 Spike RBDs to Human ACE2. <i>Cells</i> , 2022, 11, 1274.	4.1	8
10987	Functional control of a 0.5 MDa TET aminopeptidase by a flexible loop revealed by MAS NMR. <i>Nature Communications</i> , 2022, 13, 1927.	12.8	11
10988	Deciphering Isoniazid Drug Resistance Mechanisms on Dimeric <i>Mycobacterium tuberculosis</i> KatG via Post-molecular Dynamics Analyses Including Combined Dynamic Residue Network Metrics. <i>ACS Omega</i> , 2022, 7, 13313-13332.	3.5	9
10989	Single-Walled Zeolitic Nanotubes Reject Diffusive Permeation of Aqueous NaCl. <i>Journal of Physical Chemistry C</i> , 2022, 126, 6803-6808.	3.1	0
10990	Theoretical investigations on a novel CL-20/LLM-105 cocrystal explosive by molecular dynamics method. <i>Theoretical Chemistry Accounts</i> , 2022, 141, .	1.4	5
10991	Insight into the dual effect of water on lignin dissolution in ionic liquids. <i>International Journal of Biological Macromolecules</i> , 2022, 205, 178-184.	7.5	13
10992	Improving Martini 3 for Disordered and Multidomain Proteins. <i>Journal of Chemical Theory and Computation</i> , 2022, 18, 2033-2041.	5.3	54
10993	On the adsorption of volatile organic compounds on hydroxyl-functionalized carbon nanotubes in aqueous solution. <i>Diamond and Related Materials</i> , 2022, 125, 108994.	3.9	7
10994	Effect of water behaviour on the oil transport in illite nanopores: Insights from a molecular dynamics study. <i>Journal of Molecular Liquids</i> , 2022, 354, 118854.	4.9	12
10995	Understanding ion-ion and ion-solvent interactions in aqueous solutions of morpholinium ionic liquids with N-acetyl-L-alaninate anion through partial molar properties and molecular dynamics simulations. <i>Journal of Molecular Liquids</i> , 2022, 354, 118876.	4.9	2
10996	Characteristic mechanism for fast $H^+$ conduction in $LaH_{2.5}O_{0.25}$ . <i>Journal of Molecular Liquids</i> , 2022, 353, 118749.	7.9	8
10997	Efficient separation of CO <sub>2</sub> /CH <sub>4</sub> by ionic liquids confined in graphene oxide: A molecular dynamics simulation. <i>Separation and Purification Technology</i> , 2022, 289, 120736.	7.9	10
10998	Mechanistic behavior and subtle key events during DNA clamp opening and closing in T4 bacteriophage. <i>International Journal of Biological Macromolecules</i> , 2022, 208, 11-19.	7.5	54
10999	Allosteric modulation of the chemokine receptor-chemokine CXCR4-CXCL12 complex by tyrosine sulfation. <i>International Journal of Biological Macromolecules</i> , 2022, 206, 812-822.	7.5	4
11000	Atomistic mechanisms underlying plasticity and crack growth in ceramics: a case study of AlN/TiN superlattices. <i>Acta Materialia</i> , 2022, 229, 117809.	7.9	29
11001	The behaviour of aluminium ions in artificial saliva and the impact of the chlorhexidine digluconate on its removal – A diffusion model. <i>Journal of Molecular Liquids</i> , 2022, 353, 118749.	4.9	1

#	ARTICLE	IF	CITATIONS
11002	Drug repurposing through virtual screening and in vitro validation identifies tigecycline as a novel putative HCV polymerase inhibitor. <i>Virology</i> , 2022, 570, 9-17.	2.4	1
11003	Tetrabutylammonium based ionic liquids (ILs) inhibit the amyloid aggregation of superoxide dismutase 1 (SOD1). <i>Journal of Molecular Liquids</i> , 2022, 353, 118761.	4.9	8
11004	Analysis of the behavior of Sn <sup>2+</sup> and In <sup>3+</sup> ions in DES and in water: A theoretical approach. <i>Journal of Molecular Liquids</i> , 2022, 353, 118774.	4.9	2
11005	Mapping relationships between cation-F bonds and the heat capacity, thermal conductivity, viscosity of molten NaF-BeF <sub>2</sub> . <i>Journal of Molecular Liquids</i> , 2022, 354, 118915.	4.9	2
11006	Microscopic mechanism for electrocoalescence of water droplets in water-in-oil emulsions containing surfactant: A molecular dynamics study. <i>Separation and Purification Technology</i> , 2022, 289, 120756.	7.9	28
11007	A hyaluronic acid-based nanogel for the co-delivery of nitric oxide (NO) and a novel antimicrobial peptide (AMP) against bacterial biofilms. <i>International Journal of Biological Macromolecules</i> , 2022, 206, 381-397.	7.5	13
11008	Are all-atom any better than united-atom force fields for the description of liquid properties of alkanes? 2. A systematic study considering different chain lengths. <i>Journal of Molecular Liquids</i> , 2022, 354, 118829.	4.9	5
11009	Experimental and molecular dynamic insights on the thermophysical properties for MWCNT-Phosphonium based eutectic thermal media. <i>Journal of Molecular Liquids</i> , 2022, 354, 118892.	4.9	4
11010	Motional clustering in supra- $\langle \text{mml:math xmlns:mml="http://www.w3.org/1998/Math/MathML" altimg="si29.svg">\langle \text{mml:mrow}>\langle \text{mml:msub}>\langle \text{mml:mrow}>\langle \text{mml:mi}>\text{I},\langle \text{mml:mi}>\langle \text{mml:mrow}>\langle \text{mml:mi} \text{mathvariant="normal"}>\text{c}\langle \text{mml:mi}>\langle \text{mml:mrow}>\langle \text{mml:msub}>\langle \text{mml:mrow}>\langle \text{mml:math}>$ conformational exchange influences NOE cross-relaxation rate. <i>Journal of Magnetic Resonance</i> , 2022, 338, 107196.	2.1	4
11011	Influence mechanism of Na <sub>2</sub> O on the network structure depolymerization of ZD coal ash silicate under high temperature. <i>Journal of Non-Crystalline Solids</i> , 2022, 584, 121507.	3.1	4
11012	Non-equilibrium free-energy calculation of phase-boundaries using LAMMPS. <i>Computational Materials Science</i> , 2022, 207, 111275.	3.0	3
11013	Timescales for convergence in all-atom molecular dynamics simulations of hydrated amorphous xylan. <i>Carbohydrate Polymers</i> , 2022, 286, 119263.	10.2	0
11014	QSAR modeling, molecular docking, ADMET prediction and molecular dynamics simulations of some 6-arylquinazolin-4-amine derivatives as DYRK1A inhibitors. <i>Journal of Molecular Structure</i> , 2022, 1258, 132659.	3.6	14
11015	Crystallization insights revealed by simulation solidification study of Fe <sub>63</sub> Ni <sub>33</sub> Co <sub>4</sub> alloy melt at subcritical cooling rate. <i>Journal of Non-Crystalline Solids</i> , 2022, 586, 121557.	3.1	3
11016	Circular dichroism spectroscopic assessment of structural changes upon protein thermal unfolding at contrasting pH: Comparison with molecular dynamics simulations. <i>Spectrochimica Acta - Part A: Molecular and Biomolecular Spectroscopy</i> , 2022, 274, 121039.	3.9	1
11017	Interfacial tension reduction mechanism by alkaline-surfactant-polymer at oil-water interface from experimental and molecular dynamics approaches. <i>Journal of Molecular Liquids</i> , 2022, 356, 119006.	4.9	13
11018	The process of L-asparaginase encapsulation by poly (lactic-co-glycolic acid) and methoxy poly (ethylene glycol): A molecular dynamics simulation study. <i>Materials Today Communications</i> , 2022, 31, 103435.	1.9	1
11019	In silico design, synthesis and anti-HIV activity of quinoline derivatives as non-nucleoside reverse transcriptase inhibitors (NNRTIs). <i>Computational Biology and Chemistry</i> , 2022, 98, 107675.	2.3	6

#	ARTICLE	IF	CITATIONS
11020	Xylan adsorption on cellulose: Preferred alignment and local surface immobilizing effect. Carbohydrate Polymers, 2022, 285, 119221.	10.2	7
11021	Glycosylation is key for enhancing drug recognition into spike glycoprotein of SARS-CoV-2. Computational Biology and Chemistry, 2022, 98, 107668.	2.3	0
11022	Incommensurate lamellar phase from long chain Mannosides: Investigation by X-Ray scattering and replica exchange molecular dynamics (REMD). Journal of Molecular Liquids, 2022, 356, 119027.	4.9	6
11023	Facilitating gas hydrate dissociation kinetics and gas migration in clay interlayer by surface cations shielding effects. Fuel, 2022, 318, 123576.	6.4	18
11024	Mutation in Eth A protein of Mycobacterium tuberculosis conferred drug tolerance against enthinoamide in Mycobacterium smegmatis mc2155. Computational Biology and Chemistry, 2022, 98, 107677.	2.3	4
11025	NSAID solubilisation promotes morphological transitions in Triton X-114 surfactant micelles. Journal of Molecular Liquids, 2022, 356, 119050.	4.9	5
11026	Ameliorative effect of pioglitazone on glucose induced glycation of I $\alpha$ -crystallin: Management of complications associated with diabetic retinopathy. International Journal of Biological Macromolecules, 2022, 209, 107-116.	7.5	4
11027	The dipole moment of alcohols in the liquid phase and in solution. Journal of Molecular Liquids, 2022, 356, 119033.	4.9	9
11028	Modelling the transport mechanism of organic molecules into cell membranes: The role of organic solvents. Computational Biology and Chemistry, 2022, 98, 107663.	2.3	0
11029	Design and various in silico studies of the novel curcumin derivatives as potential candidates against COVID-19 -associated main enzymes. Computational Biology and Chemistry, 2022, 98, 107657.	2.3	9
11030	The mechanism of flip-flops in a AOT lamella: A molecular dynamics study. Colloids and Surfaces A: Physicochemical and Engineering Aspects, 2022, 642, 128681.	4.7	3
11031	Structure, dynamics and conductivities of ionic liquid-alcohol mixtures. Journal of Molecular Liquids, 2022, 355, 118955.	4.9	9
11032	Molecular dynamics investigation of non-ionic deep eutectic solvents. Journal of Molecular Graphics and Modelling, 2022, 113, 108152.	2.4	11
11033	Insights into the adsorption mechanism of tetracycline on hierarchically porous carbon and the effect of nanoporous geometry. Chemical Engineering Journal, 2022, 437, 135454.	12.7	28
11034	Vibrational spectral dynamics and ion-probe interactions of the hydrogen-bonded liquids in 1-ethyl-3-methylimidazolium bis(trifluoromethylsulfonyl)imide. Chemical Physics, 2022, 559, 111519.	1.9	5
11035	Understanding fluorine-free electrolytes via small-angle X-ray scattering. Journal of Energy Chemistry, 2022, 70, 340-346.	12.9	10
11036	Dynamics of the Acinetobacter baumannii inner membrane under exogenous polyunsaturated fatty acid stress. Biochimica Et Biophysica Acta - Biomembranes, 2022, 1864, 183908.	2.6	3
11037	Molecular dynamics study of fluid-fluid and solid-fluid interactions in mixed-wet shale pores. Fuel, 2022, 319, 123587.	6.4	15



#	ARTICLE	IF	CITATIONS
11038	Characterization and interaction mechanism of selective protein separation by epsilon-polylysine: The role of hydrophobic attraction. <i>Food Hydrocolloids</i> , 2022, 130, 107710.	10.7	5
11039	Atomistic simulation on the generation of defects in Cu/SiC composites during cooling. <i>Journal of Materials Science and Technology</i> , 2022, 123, 1-12.	10.7	6
11040	In Situ Coupled Electrochemical-Goniometry as a Tool to Reveal Conformational Changes of Charged Peptides. <i>Advanced Materials Interfaces</i> , 2022, 9, .	3.7	6
11041	Unravelling the Interaction of Piperlongumine with the Nucleotide-Binding Domain of HSP70: A Spectroscopic and In Silico Study. <i>Pharmaceuticals</i> , 2021, 14, 1298.	3.8	1
11042	In Silico Screening and In Vitro Assessment of Natural Products with Anti-Virulence Activity against <i>Helicobacter pylori</i> . <i>Molecules</i> , 2022, 27, 20.	3.8	7
11043	Probing Interplays between Human XBP1u Translational Arrest Peptide and 80S Ribosome. <i>Journal of Chemical Theory and Computation</i> , 2022, 18, 1905-1914.	5.3	5
11044	Wavefunction-Based Electrostatic-Embedding QM/MM Using CFOUR through MiMiC. <i>Journal of Chemical Theory and Computation</i> , 2022, 18, 13-24.	5.3	2
11045	Atomistic Model of Solute Transport across the Blood-Brain Barrier. <i>ACS Omega</i> , 2022, 7, 1100-1112.	3.5	7
11046	Improved Parameterization of Phosphatidylinositide Lipid Headgroups for the Martini 3 Coarse-Grain Force Field. <i>Journal of Chemical Theory and Computation</i> , 2022, 18, 357-373.	5.3	24
11047	Predicting Ion Channel Conductance via Dissipation-Corrected Targeted Molecular Dynamics and Langevin Equation Simulations. <i>Journal of Chemical Theory and Computation</i> , 2022, 18, 494-502.	5.3	7
11048	Evaluation of Constrained and Restrained Molecular Dynamics Simulation Methods for Predicting Skin Lipid Permeability. <i>ACS Omega</i> , 2021, 6, 35363-35374.	3.5	2
11049	Multifaceted 3D-QSAR analysis for the identification of pharmacophoric features of biphenyl analogues as aromatase inhibitors. <i>Journal of Biomolecular Structure and Dynamics</i> , 2023, 41, 1322-1341.	3.5	4
11051	Identifying the Hot Spot Residues of the SARS-CoV-2 Main Protease Using MM-PBSA and Multiple Force Fields. <i>Life</i> , 2022, 12, 54.	2.4	3
11054	Novel 1,3,5-Triazinyl Aminobenzenesulfonamides Incorporating Aminoalcohol, Aminochalcone and Aminostilbene Structural Motifs as Potent Anti-VRE Agents, and Carbonic Anhydrases I, II, VII, IX, and XII Inhibitors. <i>International Journal of Molecular Sciences</i> , 2022, 23, 231.	4.1	5
11055	Facile Synthesis of Zn <sup>2+</sup> -Based Hybrid Nanoparticles as a New Paradigm for the Treatment of Internal Bacterial Infections. <i>Advanced Functional Materials</i> , 2022, 32, .	14.9	17
11056	Thermal Unfolding of the Human Serotonin Transporter: Differential Effect by Stabilizing and Destabilizing Mutations and Cholesterol on Thermodynamic and Kinetic Stability. <i>Molecular Pharmacology</i> , 2022, 101, 95-105.	2.3	9
11057	Anion Effects on the Mixing States of 1-Methyl-3-octylimidazolium Tetrafluoroborate and Bis(trifluoromethylsulfonyl)amide with Methanol, Acetonitrile, and Dimethyl Sulfoxide on the Meso- and Microscopic Scales. <i>Journal of Physical Chemistry B</i> , 2021, 125, 13896-13907.	2.6	2
11058	Knowledge-Based Atomic Polarizabilities Used to Model Circular Dichroism Spectra of Proteins. <i>Journal of Physical Chemistry B</i> , 2022, 126, 80-92.	2.6	0

#	ARTICLE	IF	CITATIONS
11059	Ethanol Dehydration with Ionic Liquids from Molecular Insights to Process Intensification. ACS Sustainable Chemistry and Engineering, 2022, 10, 441-455.	6.7	8
11060	Amorphous $\text{Bi}_2\text{Te}_{3-x}\text{S}_x$ thin films: structural, electronic, and topological nature from first principles. Physical Review B, 2021, 104, .	3.2	1
11061	2-Arylquinolines as novel anticancer agents with dual EGFR/FAK kinase inhibitory activity: synthesis, biological evaluation, and molecular modelling insights. Journal of Enzyme Inhibition and Medicinal Chemistry, 2022, 37, 355-378.	5.2	15
11062	Molecular Simulation of Methane Sorption onto Kerogen Surface of Shale in Presence of Surfactant. , 2021, , .		1
11063	Binding site hotspot map of PI3K $\alpha$ and mTOR in the presence of selective and dual ATP-competitive inhibitors. Journal of Biomolecular Structure and Dynamics, 2023, 41, 1085-1097.	3.5	1
11064	Redox Potentials of Disulfide Bonds in LOXL2 Studied by Nonequilibrium Alchemical Simulation. Frontiers in Chemistry, 2021, 9, 797036.	3.6	0
11065	RBD Double Mutations of SARS-CoV-2 Strains Increase Transmissibility through Enhanced Interaction between RBD and ACE2 Receptor. Viruses, 2022, 14, 1.	3.3	23
11067	Explicit-pH Coarse-Grained Molecular Dynamics Simulations Enable Insights into Restructuring of Intestinal Colloidal Aggregates with Permeation Enhancers. Processes, 2022, 10, 29.	2.8	8
11068	Distinctive Formation of PEG-Lipid Nanopatches onto Solid Polymer Surfaces Interfacing Solvents from Atomistic Simulation. Journal of Physical Chemistry B, 2022, 126, 1598-1608.	2.6	1
11070	<i>In silico</i> modeling revealed new insights into the mechanism of action of enzyme 2'-5'-oligoadenylate synthetase in cattle. Journal of Biomolecular Structure and Dynamics, 2021, , 1-14.	3.5	2
11071	Persister control by leveraging dormancy associated reduction of antibiotic efflux. PLoS Pathogens, 2021, 17, e1010144.	4.7	10
11072	Computational investigation of potent inhibitors against YsxC: structure-based pharmacophore modeling, molecular docking, molecular dynamics, and binding free energy. Journal of Biomolecular Structure and Dynamics, 2023, 41, 930-941.	3.5	15
11073	Molecular dynamics simulation study of doxorubicin adsorption on functionalized carbon nanotubes with folic acid and tryptophan. Scientific Reports, 2021, 11, 24210.	3.3	9
11074	pH-Dependent Behavior of Ionizable Cationic Lipids in mRNA-Carrying Lipoplexes Investigated by Molecular Dynamics Simulations. Macromolecular Rapid Communications, 2022, 43, e2100683.	3.9	12
11075	Assembly and Analysis of Cell-Scale Membrane Envelopes. Journal of Chemical Information and Modeling, 2022, 62, 602-617.	5.4	17
11076	Polybutadiene Copolymers via Atomistic and Systematic Coarse-Grained Simulations. Macromolecules, 2022, 55, 224-240.	4.8	5
11077	Exploration of Neuroprotective Properties of a Naturally Inspired Multifunctional Molecule (F24) against Oxidative Stress and Amyloid $\text{A}\beta$ Induced Neurotoxicity in Alzheimer's Disease Models. ACS Chemical Neuroscience, 2022, 13, 27-42.	3.5	12
11079	Martini Coarse-Grained Model for Poly(alkylimidazolium) Ionenenes and Applications in Aromatic Compound Extraction. Macromolecules, 2022, 55, 26-34.	4.8	3

#	ARTICLE	IF	CITATIONS
11080	DNA-Based Gold Nanoparticle Sensor for Bladder Cancer Detection. ACS Applied Nano Materials, 2022, 5, 985-995.	5.0	1
11081	Exploring High-Pressure Transformations in Low-Z (H <sub>2</sub> , Ne) Hydrates at Low Temperatures. Crystals, 2022, 12, 9.	2.2	2
11082	Enhanced specificity mutations perturb allosteric signaling in CRISPR-Cas9. ELife, 2021, 10, .	6.0	27
11084	Martini 3 Coarse-Grained Force Field: Small Molecules. Advanced Theory and Simulations, 2022, 5, .	2.8	72
11085	The Role of Key Amino Acids in the Antimicrobial Mechanism of a Bacteriocin Model Revealed by Molecular Simulations. Journal of Chemical Information and Modeling, 2021, 61, 6066-6078.	5.4	4
11086	Specific Ion Solvation and Pairing Effects in Glycerol Carbonate. Journal of Physical Chemistry B, 2021, 125, 13635-13643.	2.6	4
11087	A Structural Ensemble of a Tau-Microtubule Complex Reveals Regulatory Tau Phosphorylation and Acetylation Mechanisms. ACS Central Science, 2021, 7, 1986-1995.	11.3	29
11088	In Silico-Based Experiments on Mechanistic Interactions between Several Intestinal Permeation Enhancers with a Lipid Bilayer Model. Molecular Pharmaceutics, 2022, 19, 124-137.	4.6	10
11091	2D-QSAR and molecular docking studies of carbamate derivatives to discover novel potent anti-acetylcholinesterase agents for Alzheimer's disease treatment. Bulletin of the Korean Chemical Society, 2022, 43, 277-292.	1.9	22
11092	The Monoclonal Antibody Pembrolizumab Alters Dynamics of the Human Programmed Cell Death Receptor 1 (PD-1). , 2021, , .		2
11093	Assessing Differential Binding of Aggregation-Induced Emission-Based Luminogens to Host Interacting Surface Proteins of SARS-CoV-2 and Influenza Virus-An in silico Approach. Frontiers in Microbiology, 2021, 12, 766351.	3.5	2
11094	Structure and ion-release mechanism of PIB-4-type ATPases. ELife, 2021, 10, .	6.0	8
11095	Synthesis, Structural Characterization, and In Vitro and In Silico Antifungal Evaluation of Azo-Azomethine Pyrazoles (PhN <sub>2</sub> (PhOH)CHN(C <sub>3</sub> N <sub>2</sub> (CH <sub>3</sub> ) <sub>3</sub> )PhR, R = H or NO <sub>2</sub> ). Molecules, 2021, 26, 7435.	3.8	6
11096	Posttreatment Effects on the Crystal Structure and Superconductivity of Ca-Free Double-Layered Cuprate Sr <sub>2</sub> SrCu <sub>2</sub> O <sub>4+y</sub> F <sub>2</sub> . Chemistry of Materials, 2021, 33, 9690-9697.	6.7	1
11097	A Computational Study of RNA Tetraloop Thermodynamics, Including Misfolded States. Journal of Physical Chemistry B, 2021, 125, 13685-13695.	2.6	5
11098	Molecular Dynamics Studies on the Bacterial Membrane Pore Formation by Small Molecule Antimicrobial Agents. Journal of Chemical Information and Modeling, 2022, 62, 40-48.	5.4	7
11099	finDr: A web server for in silico D-peptide ligand identification. Synthetic and Systems Biotechnology, 2021, 6, 402-413.	3.7	5
11102	Taking the Monte Carlo gamble: How not to buckle under the pressure!. Journal of Computational Chemistry, 2022, 43, 431-434.	3.3	6

#	ARTICLE	IF	CITATIONS
11103	Uygulanan Äžekme Deformasyonu AltÄ±nda Niyobyum Nano Telinin Mekanik Äzelliklerinin Molek¼ler Dinamik Benzetimi ile Äncelenmesi. Journal of the Institute of Science and Technology, 0, , 2758-2771.	0.9	0
11104	Elucidation of SARS-Cov-2 Budding Mechanisms through Molecular Dynamics Simulations of M and E Protein Complexes. Journal of Physical Chemistry Letters, 2021, 12, 12249-12255.	4.6	16
11105	Structure-Based Design of an RNase Chimera for Antimicrobial Therapy. International Journal of Molecular Sciences, 2022, 23, 95.	4.1	4
11106	Optical Configuration Effect on the Structure and Reactivity of Diastereomers Revealed by Spin Effects and Molecular Dynamics Calculations. International Journal of Molecular Sciences, 2022, 23, 38.	4.1	3
11107	Computational study of the <sc> <i>pK</i> <sub> <i>a</i></sub> </sc> values of a modified GÄ-C base pair in duplex <sc>DNA</sc>. Bulletin of the Korean Chemical Society, 2022, 43, 201-209.	1.9	0
11108	Effect of Cysteine Oxidation in SARS-CoV-2 Receptor-Binding Domain on Its Interaction with Two Cell Receptors: Insights from Atomistic Simulations. Journal of Chemical Information and Modeling, 2022, 62, 129-141.	5.4	9
11109	Repositioning Food and Drug Administration-Approved Drugs for Inhibiting Biliverdin IXÎ² Reductase B as a Novel Thrombocytopenia Therapeutic Target. Journal of Medicinal Chemistry, 2022, 65, 2548-2557.	6.4	1
11110	Rational Design of Nonbonded Point Charge Models for Monovalent Ions with Lennard-Jones 12â€6 Potential. Journal of Physical Chemistry B, 2021, 125, 13502-13518.	2.6	10
11111	Novel Aurora A and Protein Kinase C (Î±, Î²1, Î²2, and Î³) Multitarget Inhibitors: Impact of Selenium Atoms on the Potency and Selectivity. Journal of Medicinal Chemistry, 2022, 65, 3134-3150.	6.4	8
11112	Role of polyplex charge density in lipopolyplex. Nanoscale, 2022, 14, 7174-7180.	5.6	0
11113	Understanding of Bulk and Interfacial Structures Ternary and Binary Deep Eutectic Solvents with a Constant Potential Method: A Molecular Dynamics Study. Physical Chemistry Chemical Physics, 2022, , .	2.8	3
11114	Short-chain branched sulfosuccinate as missing link between surfactants and hydrotropes. Physical Chemistry Chemical Physics, 2022, , .	2.8	0
11115	Martini 3 coarse-grained force field for poly(<i>para</i>-phenylene ethynylene)s. Physical Chemistry Chemical Physics, 2022, 24, 9998-10010.	2.8	7
11116	Differences in the local anaesthesia effect by lidocaine and bupivacaine based on free energy analysis. Molecular Simulation, 0, , 1-7.	2.0	0
11117	Atomistic mechanisms of human TRPA1 activation by electrophile irritants through molecular dynamics simulation and mutual information analysis. Scientific Reports, 2022, 12, 4929.	3.3	8
11118	Machine learning-based predictive models for identifying high active compounds against HIV-1 integrase. SAR and QSAR in Environmental Research, 2022, , 1-16.	2.2	1
11119	Structural insight into PRMT5 inhibitors through amalgamating pharmacophore-based virtual screening, ADME toxicity, and binding energy studies to identify new inhibitors by molecular docking. Structural Chemistry, 2022, 33, 1223-1239.	2.0	1
11121	Effects of cholesterol on the mechanism of fengycin, a biofungicide. Biophysical Journal, 2022, 121, 1963-1974.	0.5	5

#	ARTICLE	IF	CITATIONS
11122	Novel Hydrazone Derivatives of 3-Bromopyruvate: Synthesis, Evaluation of the Cytotoxic Effects, Molecular Docking and ADME Studies. Chemistry and Biodiversity, 2022, 19, .	2.1	5
11123	Distinct lipid membrane interaction and uptake of differentially charged nanoplastics in bacteria. Journal of Nanobiotechnology, 2022, 20, 191.	9.1	30
11126	Alchemical Design of Pharmacological Chaperones with Higher Affinity for Phenylalanine Hydroxylase. International Journal of Molecular Sciences, 2022, 23, 4502.	4.1	1
11127	Molecular Dynamics Studies on Effective Surface-Active Additives: Toward Hard Water-Resistant Chemical Flooding for Enhanced Oil Recovery. Langmuir, 2022, 38, 4802-4811.	3.5	5
11128	Identification of potent inhibitors of NEK7 protein using a comprehensive computational approach. Scientific Reports, 2022, 12, 6404.	3.3	48
11129	Computational design of stapled peptide inhibitor against SARS-CoV-2 receptor binding domain. Peptide Science, 2022, 114, e24267.	1.8	8
11130	Effect of Ethanol and Urea as Solvent Additives on PSS-PDADMA Polyelectrolyte Complexation. Macromolecules, 2022, 55, 3140-3150.	4.8	11
11131	SPICA Force Field for Proteins and Peptides. Journal of Chemical Theory and Computation, 2022, 18, 3204-3217.	5.3	21
11133	Practical guide to replica exchange transition interface sampling and forward flux sampling. Journal of Chemical Physics, 2022, 156, .	3.0	9
11134	Influence of the Nonprotein Amino Acid Mimosine in Peptide Conformational Propensities from Novel Amber Force Field Parameters. Journal of Physical Chemistry B, 2022, , .	2.6	0
11135	Hydroxychloroquine Does Not Function as a Direct Zinc Ionophore. Pharmaceutics, 2022, 14, 899.	4.5	3
11136	Maximum in density of electrolyte solutions: Learning about ion-water interactions and testing the Madrid-2019 force field. Journal of Chemical Physics, 2022, 156, 154502.	3.0	13
11138	Structural dynamics shape the fitness window of alanine:glyoxylate aminotransferase. Protein Science, 2022, 31, e4303.	7.6	6
11139	Structural basis for the assembly and quinone transport mechanisms of the dimeric photosynthetic RC-LH1 supercomplex. Nature Communications, 2022, 13, 1977.	12.8	22
11140	Changes in Salt Concentration Modify the Translocation of Neutral Molecules through a CymA Nanopore in a Non-monotonic Manner. ACS Nano, 2022, 16, 7701-7712.	14.6	6
11141	Cyclohexanodecyl-Assisted Interfacial Engineering for Robust and High-Performance Zinc Metal Anode. Nano-Micro Letters, 2022, 14, 110.	27.0	42
11142	Novel US-CpHMD Protocol to Study the Protonation-Dependent Mechanism of the ATP/ADP Carrier. Journal of Chemical Information and Modeling, 2022, , .	5.4	10
11143	Atomistic and Coarse-Grained Simulations of Bulk Amorphous Amylose Above and Below the Glass Transition. Macromolecules, 0, , .	4.8	2

#	ARTICLE	IF	CITATIONS
11144	Structural Basis for Reduced Dynamics of Three Engineered HNH Endonuclease Lys-to-Ala Mutants for the Clustered Regularly Interspaced Short Palindromic Repeat (CRISPR)-Associated 9 (CRISPR/Cas9) Enzyme. <i>Biochemistry</i> , 2022, 61, 785-794.	2.5	12
11145	Microfluidic Engineering of RGD<sup>[1]</sup>-Terminated Nanocarriers Micellization and Inâ€Situ Docetaxel Encapsulation: An Atomistic Insight. <i>ChemistrySelect</i> , 2022, 7, .	1.5	7
11146	Cocktail of REGN Antibodies Binds More Strongly to SARS-CoV-2 Than Its Components, but the Omicron Variant Reduces Its Neutralizing Ability. <i>Journal of Physical Chemistry B</i> , 2022, 126, 2812-2823.	2.6	11
11147	A Multi-Scale Simulation Study of Irradiation Swelling of Silicon Carbide. <i>Materials</i> , 2022, 15, 3008.	2.9	0
11148	A selectivity filter mutation provides insights into gating regulation of a K <sup>+</sup> channel. <i>Communications Biology</i> , 2022, 5, 345.	4.4	2
11149	Fragmentation Method for Computing Quantum Mechanics and Molecular Mechanics Gradients for Force Matching: Validation with Hydration Free Energy Predictions Using Adaptive Force Matching. <i>Journal of Physical Chemistry A</i> , 2022, 126, 2609-2617.	2.5	2
11150	Two Consecutive Prolines in the Fusion Peptide of Murine Î²-Coronavirus Spike Protein Predominantly Determine Fusogenicity and May Be Essential but Not Sufficient to Cause Demyelination. <i>Viruses</i> , 2022, 14, 834.	3.3	1
11151	AKT mutant allele-specific activation dictates pharmacologic sensitivities. <i>Nature Communications</i> , 2022, 13, 2111.	12.8	10
11152	Finite-deformation phase-field microelasticity with application to dislocation core and reaction modeling in fcc crystals. <i>Journal of the Mechanics and Physics of Solids</i> , 2022, , 104897.	4.8	1
11153	Nanoindentation in Nanocrystalline Metallic Layers: A Molecular Dynamics Study on Size Effects. , 0, , 109-142.		0
11154	Atomistic Methods for Structure-Property Correlations. , 2005, , 1931-1951.		0
11155	Ensembles and Computer Simulation Calculation of Response Functions. , 2005, , 729-743.		0
11156	Elastic Stability Criteria and Structural Bifurcations in Crystals Under Load. , 2005, , 1223-1279.		0
11254	Anisaxins, helical antimicrobial peptides from marine parasites, kill resistant bacteria by lipid extraction and membrane disruption. <i>Acta Biomaterialia</i> , 2022, 146, 131-144.	8.3	15
11255	Revealing the Anticorrelation Behavior Mechanism between the Grotthuss and Vehicular Diffusions for Proton Transport in Concentrated Acid Solutions. <i>Journal of Physical Chemistry B</i> , 2022, 126, 3319-3326.	2.6	3
11256	Lipid-Mediated Association of the Slg1 Transmembrane Domains in Yeast Plasma Membranes. <i>Journal of Physical Chemistry B</i> , 2022, 126, 3240-3256.	2.6	4
11257	Dependence of Vibrational Energy Transfer on Distance in a Four-Helix Bundle Protein: Equidistant Increments with the Periodicity of Î± Helices. <i>Journal of Physical Chemistry B</i> , 2022, 126, 3283-3290.	2.6	3
11258	Tuning Contact Angles of Aqueous Droplets on Hydrophilic and Hydrophobic Surfaces by Surfactants. <i>Journal of Physical Chemistry B</i> , 2022, 126, 3374-3384.	2.6	18



#	ARTICLE	IF	CITATIONS
11259	Effect of pH on the Surface Layer of Molecular Crystals at the Solidâ€“Liquid Interface. <i>Molecular Pharmaceutics</i> , 2022, 19, 1598-1603.	4.6	2
11260	Ion-bridges and lipids drive aggregation of same-charge nanoparticles on lipid membranes. <i>Nanoscale</i> , 2022, 14, 6912-6921.	5.6	9
11261	PEGDA hydrogel structure from semi-dilute concentrations: insights from experiments and molecular simulations. <i>Soft Matter</i> , 2022, 18, 3565-3574.	2.7	9
11262	Evaluation of phytoconstituents of <i>Tinospora cordifolia</i> against K417N and N501Y mutant spike glycoprotein and main protease of SARS-CoV-2- an in silico study. <i>Journal of Biomolecular Structure and Dynamics</i> , 2023, 41, 4106-4123.	3.5	1
11263	Cholecalciferol complexation with hydroxypropyl- $\beta$ -cyclodextrin (HPBCD) and its molecular dynamics simulation. <i>Pharmaceutical Development and Technology</i> , 2022, 27, 389-398.	2.4	5
11264	Molecular dynamics simulations reveal the selectivity mechanism of structurally similar agonists to TLR7 and TLR8. <i>PLoS ONE</i> , 2022, 17, e0260565.	2.5	7
11265	Bacterial Membranes Are More Perturbed by the Asymmetric Versus Symmetric Loading of Amphiphilic Molecules. <i>Membranes</i> , 2022, 12, 350.	3.0	2
11266	<i>Mycobacterium bovis</i> PknG R242P Mutation Results in Structural Changes with Enhanced Virulence in the Mouse Model of Infection. <i>Microorganisms</i> , 2022, 10, 673.	3.6	2
11267	Using molecular dynamics simulations to interrogate T cell receptor non-equilibrium kinetics. <i>Computational and Structural Biotechnology Journal</i> , 2022, 20, 2124-2133.	4.1	9
11268	Hydrogen bond redistribution effects in mixtures of protic ionic liquids sharing the same cation: non-ideal mixing with large negative mixing enthalpies. <i>Physical Chemistry Chemical Physics</i> , 2022, 24, 14740-14750.	2.8	2
11269	Identification of the probable structure of the sAPP $\beta$ -GABA <sub>B</sub> R1a complex and theoretical solutions for such cases. <i>Physical Chemistry Chemical Physics</i> , 2022, 24, 12267-12280.	2.8	6
11270	Tuning aprotic solvent properties with long alkyl chain ionic liquid for lithium-based electrolytes. <i>Journal of Materials Chemistry A</i> , 2022, 10, 11684-11701.	10.3	9
11271	Molecular screening of ionic liquids for CO <sub>2</sub> absorption and molecular dynamic simulation. <i>Open Chemistry</i> , 2022, 20, 379-387.	1.9	2
11272	Weak Cation Selectivity in HCN Channels Results From K <sup>+</sup> -Mediated Release of Na <sup>+</sup> From Selectivity Filter Binding Sites. <i>Function</i> , 2022, 3, .	2.3	3
11273	Functional and molecular characterization of a cold-active lipase from <i>Psychrobacter celer</i> PU3 with potential antibiofilm property. <i>International Journal of Biological Macromolecules</i> , 2022, 211, 741-753.	7.5	8
11276	A lesson for the maestro of the replication fork: Targeting the proteinâ€“binding interface of proliferating cell nuclear antigen for anticancer therapy. <i>Journal of Cellular Biochemistry</i> , 2022, 123, 1091-1102.	2.6	50
11277	Insights into Carbon Dioxide Hydrate Nucleation on the External Basal Surface of Clay Minerals from Molecular Dynamics Simulations. <i>ACS Sustainable Chemistry and Engineering</i> , 2022, 10, 6358-6369.	6.7	14
11278	Can molecular simulations reliably compare homogeneous and heterogeneous ice nucleation?. <i>Journal of Chemical Physics</i> , 2022, 156, 164501.	3.0	3

#	ARTICLE	IF	CITATIONS
11279	Ring mechanism of fast $\text{Na}^+$ ion transport in $\text{H}_2\text{O}$ : Insight from molecular dynamics simulation. <i>Physical Review Materials</i> , 2022, 6, .	2.4	2
11280	Molecular Dynamics Simulation of Privileged Biflavonoids as SARS-CoV2 3CLpro Targeting Agents. <i>Journal of Computational Biophysics and Chemistry</i> , 2022, 21, 569-582.	1.7	2
11281	In silico investigation of phytoconstituents from Cameroonian medicinal plants towards COVID-19 treatment. <i>Structural Chemistry</i> , 2022, 33, 1799-1813.	2.0	15
11282	Enthalpic and entropic contributions to interleaflet coupling drive domain registration and antiregistration in biological membrane. <i>Physical Review E</i> , 2022, 105, 044408.	2.1	3
11283	Direct free energy evaluation of classical and quantum many-body systems via field-theoretic simulation. <i>Proceedings of the National Academy of Sciences of the United States of America</i> , 2022, 119, e2201804119.	7.1	13
11284	AlphaFold2: A Role for Disordered Protein/Region Prediction?. <i>International Journal of Molecular Sciences</i> , 2022, 23, 4591.	4.1	72
11285	Multiple Poses and Thermodynamics of Ligands Targeting Protein Surfaces: The Case of Furosemide Binding to mitoNEET in Aqueous Solution. <i>Frontiers in Cell and Developmental Biology</i> , 2022, 10, 886568.	3.7	3
11286	Chromene Derivatives as Selective TERRA G-Quadruplex RNA Binders with Antiproliferative Properties. <i>Pharmaceuticals</i> , 2022, 15, 548.	3.8	7
11287	Autonomous Search for Polymers with High Thermal Conductivity Using a Rapid Greenâ€Kubo Estimation. <i>Macromolecules</i> , 2022, 55, 3384-3395.	4.8	6
11288	Heparin-Assisted Amyloidogenesis Uncovered through Molecular Dynamics Simulations. <i>ACS Omega</i> , 2022, 7, 15132-15144.	3.5	7
11289	Nanoporous SiOx plasma polymer films as carrier for liquidâ€infused surfaces. <i>Plasma Processes and Polymers</i> , 2022, 19, .	3.0	4
11290	Fullerenesâ€™ Interactions with Plasma Membranes: Insight from the MD Simulations. <i>Biomolecules</i> , 2022, 12, 639.	4.0	1
11291	Study of the dynamic behavior of the cruzain enzyme in free and complexed forms with competitive and noncovalent benzimidazole inhibitors. <i>Journal of Biomolecular Structure and Dynamics</i> , 2023, 41, 4368-4382.	3.5	1
11292	Inverse Mixed-Solvent Molecular Dynamics for Visualization of the Residue Interaction Profile of Molecular Probes. <i>International Journal of Molecular Sciences</i> , 2022, 23, 4749.	4.1	0
11293	Ion Migration Mechanisms in the Sodium Sulfide Solid Electrolyte $\text{Na}_3\text{SbW}_4\text{S}_4$ . <i>Chemistry of Materials</i> , 2022, 34, 4166-4171.	6.7	6
11294	Sequence Analysis and Molecule Docking of Collagenase Inhibitory Peptides from the Peptic Hydrolysate of Flounder Skin. <i>Journal of the Korean Society of Food Science and Nutrition</i> , 2022, 51, 322-333.	0.9	1
11295	Investigating the Role of Solvent in the Formation of Vacancies on Ibuprofen Crystal Facets. <i>Crystal Growth and Design</i> , 2022, 22, 3034-3041.	3.0	0
11296	Dimerization of the pulmonary surfactant protein C in a membrane environment. <i>PLoS ONE</i> , 2022, 17, e0267155.	2.5	5

#	ARTICLE	IF	CITATIONS
11297	Stereoselectivity of Interaction of Nonsteroidal Anti-Inflammatory Drug S-Ketoprofen with L/D-Tryptophan in Phospholipid Membranes. <i>Membranes</i> , 2022, 12, 460.	3.0	6
11298	Peptidoglycan biosynthesis is driven by lipid transfer along enzyme-substrate affinity gradients. <i>Nature Communications</i> , 2022, 13, 2278.	12.8	20
11299	A machine-learned interatomic potential for silica and its relation to empirical models. <i>Npj Computational Materials</i> , 2022, 8, .	8.7	36
11300	Molecular Dynamics of DHHC20 Acyltransferase Suggests Principles of Lipid and Protein Substrate Selectivity. <i>International Journal of Molecular Sciences</i> , 2022, 23, 5091.	4.1	6
11301	Molecular modeling of lactoferrin for food and nutraceutical applications: insights from <i>in silico</i> techniques. <i>Critical Reviews in Food Science and Nutrition</i> , 2023, 63, 9074-9097.	10.3	2
11302	Non-Newtonian shear viscosity of confined water in forsterite nanoslits: insights from molecular dynamics simulations. <i>Molecular Simulation</i> , 0, , 1-11.	2.0	0
11303	Absorption of Volatile Organic Compounds Toluene and Acetaldehyde in Choline Chloride-Based Deep Eutectic Solvents. <i>Journal of Physical Chemistry B</i> , 2022, 126, 3705-3716.	2.6	10
11304	Effect of succinonitrile on ion transport in PEO-based lithium-ion battery electrolytes. <i>Journal of Chemical Physics</i> , 2022, 156, .	3.0	7
11305	Simulation of the carbon dioxide hydrate-water interfacial energy. <i>Journal of Colloid and Interface Science</i> , 2022, 623, 354-367.	9.4	9
11306	Probing the Link between Pancratistatin and Mitochondrial Apoptosis through Changes in the Membrane Dynamics on the Nanoscale. <i>Molecular Pharmaceutics</i> , 2022, 19, 1839-1852.	4.6	4
11307	Finding alternatives to 5-fluorouracil: application of ensemble-based virtual screening for drug repositioning against human thymidylate synthase. <i>Journal of Biomolecular Structure and Dynamics</i> , 2022, , 1-17.	3.5	3
11309	Enthalpy of solvation of alkali metal salts in a protic ionic liquid: Effect of cation charge and size. <i>Journal of Molecular Liquids</i> , 2022, 360, 119228.	4.9	6
11310	Identifying signatures of proteolytic stability and monomeric propensity in O-glycosylated insulin using molecular simulation. <i>Journal of Computer-Aided Molecular Design</i> , 2022, 36, 313-328.	2.9	2
11311	Virtual screening of PEBP1 inhibitors by combining 2D/3D-QSAR analysis, hologram QSAR, homology modeling, molecular docking analysis, and molecular dynamic simulations. <i>Journal of Molecular Modeling</i> , 2022, 28, 145.	1.8	0
11312	Design, synthesis, molecular modeling and DNA-binding studies of new barbituric acid derivatives. <i>Journal of the Iranian Chemical Society</i> , 2022, 19, 3887-3898.	2.2	3
11313	Simulations of cross-amyloid aggregation of amyloid- $\beta^2$ and islet amyloid polypeptide fragments. <i>Biophysical Journal</i> , 2022, 121, 2002-2013.	0.5	4
11314	Magic mushroom extracts in lipid membranes. <i>Biochimica Et Biophysica Acta - Biomembranes</i> , 2022, 1864, 183957.	2.6	5
11315	Mechanistic insights of key host proteins and potential repurposed inhibitors regulating SARS-CoV-2 pathway. <i>Journal of Computational Chemistry</i> , 2022, 43, 1237-1250.	3.3	4

#	ARTICLE	IF	CITATIONS
11316	Molecular basis of cross-interactions between A $\beta$ 2 and Tau protofibrils probed by molecular simulations. <i>Chinese Journal of Chemical Engineering</i> , 2023, 55, 173-180.	3.5	2
11317	Molecular View on the Impact of DHA Molecules on the Physical Properties of a Model Cell Membrane. <i>Journal of Chemical Information and Modeling</i> , 2022, 62, 2421-2431.	5.4	7
11318	Promising antivirals for PLpro of SARS-CoV-2 using virtual screening, molecular docking, dynamics, and MMPBSA. <i>Journal of Biomolecular Structure and Dynamics</i> , 2023, 41, 4650-4666.	3.5	18
11319	Accurate and efficient molecular dynamics based on machine learning and non von Neumann architecture. <i>Npj Computational Materials</i> , 2022, 8, .	8.7	11
11320	Class III Peroxidases PRX01, PRX44, and PRX73 Control Root Hair Growth in <i>Arabidopsis thaliana</i> . <i>International Journal of Molecular Sciences</i> , 2022, 23, 5375.	4.1	15
11321	Li-Ion Permeability of Holey Graphene in Solid State Batteries: A Particle Dynamics Study. <i>ACS Applied Materials &amp; Interfaces</i> , 2022, 14, 21363-21370.	8.0	1
11322	AIMP2-DX2 provides therapeutic interface to control KRAS-driven tumorigenesis. <i>Nature Communications</i> , 2022, 13, 2572.	12.8	3
11323	Simulation studies of polypeptoids using replica exchange with dynamical scaling and dihedral biasing. <i>Journal of Computational Chemistry</i> , 2022, 43, 1229-1236.	3.3	4
11324	Divergent effects of cholesterol on the structure and fluidity of liposome and cationic vesicle membranes. <i>FEBS Letters</i> , 2022, 596, 1827-1838.	2.8	2
11325	Anomalous Viscosity of a Racemate: A Simple Experiment Demonstrating Chirally Induced Spin Selectivity. <i>Journal of Physical Chemistry Letters</i> , 2022, 13, 4215-4219.	4.6	2
11326	Antibiotic-Like Activity of Atomic Layer Boron Nitride for Combating Resistant Bacteria. <i>ACS Nano</i> , 2022, 16, 7674-7688.	14.6	25
11327	Molecular insights into binding dynamics of tandem RNA recognition motifs (tRRMs) of human antigen R (HuR) with mRNA and the effect of point mutations in impaired HuR-mRNA recognition. <i>Journal of Biomolecular Structure and Dynamics</i> , 2022, , 1-17.	3.5	2
11328	Insights into the behavior of unsaturated diacylglycerols in mixed lipid bilayers in relation to protein kinase C activation—A molecular dynamics simulation study. <i>Biochimica Et Biophysica Acta - Biomembranes</i> , 2022, 1864, 183961.	2.6	4
11329	The Val34Met, Thr164Ile and Ser220Cys Polymorphisms of the $\beta$ 2-Adrenergic Receptor and Their Consequences on the Receptor Conformational Features: A Molecular Dynamics Simulation Study. <i>International Journal of Molecular Sciences</i> , 2022, 23, 5449.	4.1	1
11330	3,4,5-Trimethoxybenzoate of Catechin, an Anticarcinogenic Semisynthetic Catechin, Modulates the Physical Properties of Anionic Phospholipid Membranes. <i>Molecules</i> , 2022, 27, 2910.	3.8	2
11331	Determination of Multidirectional Pathways for Ligand Release from the Receptor: A New Approach Based on Differential Evolution. <i>Journal of Chemical Theory and Computation</i> , 2022, 18, 3860-3872.	5.3	3
11332	Unexpected Dynamic Binding May Rescue the Binding Affinity of Rivaroxaban in a Mutant of Coagulation Factor X. <i>Frontiers in Molecular Biosciences</i> , 2022, 9, .	3.5	0
11333	Load-Bearing Nanostructures in Composites of Chitosan with Anionic Surfactants: Implications for Programmable Mechanomaterials. <i>ACS Applied Nano Materials</i> , 2022, 5, 6463-6473.	5.0	7

#	ARTICLE	IF	CITATIONS
11334	Conformational dynamics of the membrane enzyme LspA upon antibiotic and substrate binding. <i>Biophysical Journal</i> , 2022, 121, 2078-2083.	0.5	4
11335	Molecular dynamic simulations reveal anti-SARS-CoV-2 activity of mitocurcumin by potentially blocking innate immune evasion proteins NSP3 and NSP16. <i>Molecular Diversity</i> , 2023, 27, 635-649.	3.9	2
11336	Curvature-based sorting of eight lipid types in asymmetric buckled plasma membrane models. <i>Biophysical Journal</i> , 2022, 121, 2060-2068.	0.5	8
11337	Gasdermin-A3 pore formation propagates along variable pathways. <i>Nature Communications</i> , 2022, 13, 2609.	12.8	25
11338	Temperature induced change of TMAO effects on hydrophobic hydration. <i>Journal of Chemical Physics</i> , 2022, 156, 184501.	3.0	1
11339	The structure and molecular dynamics of prolyl oligopeptidase from <i>Microbulbifer arenaceus</i> provide insights into catalytic and regulatory mechanisms. <i>Acta Crystallographica Section D: Structural Biology</i> , 2022, 78, 735-751.	2.3	2
11340	Discovery of first-in-class nanomolar inhibitors of heptosyltransferase I reveals a new aminoglycoside target and potential alternative mechanism of action. <i>Scientific Reports</i> , 2022, 12, 7302.	3.3	5
11341	Molecular dynamics simulations of ultralow hysteretic behavior in super-elastic shape memory alloys. <i>Acta Materialia</i> , 2022, 232, 117973.	7.9	4
11342	Cyclic and tensile deformations of Gold-Silver core shell systems using newly parameterized MEAM potential. <i>Mechanics of Materials</i> , 2022, 169, 104304.	3.2	2
11343	Molecular dynamics simulation of grain size effect on mechanism of twin martensite transformation of nanocrystalline NiTi shape memory alloys. <i>Computational Materials Science</i> , 2022, 210, 111451.	3.0	7
11344	At least three xenon binding sites in the glycine binding domain of the N-methyl D-aspartate receptor. <i>Archives of Biochemistry and Biophysics</i> , 2022, 724, 109265.	3.0	0
11345	Investigation of the structural and dynamical properties of human uncoupling protein 2 through molecular dynamics simulations. <i>Journal of Molecular Graphics and Modelling</i> , 2022, 114, 108203.	2.4	2
11346	Removal of tetracycline by aerobic granular sludge from marine aquaculture wastewater: A molecular dynamics investigation. <i>Bioresource Technology</i> , 2022, 355, 127286.	9.6	23
11347	Theoretical insights into the uptake of sulfonamides onto phospholipid bilayers: Mechanisms, interaction and toxicity evaluation. <i>Journal of Hazardous Materials</i> , 2022, 435, 129033.	12.4	10
11348	Benchmarking the ability of novel compounds to inhibit SARS-CoV-2 main protease using steered molecular dynamics simulations. <i>Computers in Biology and Medicine</i> , 2022, 146, 105572.	7.0	28
11349	Investigation of a high-sensitive electrochemical DNA biosensor for determination of Idarubicin and studies of DNA-binding properties. <i>Microchemical Journal</i> , 2022, 179, 107546.	4.5	49
11350	The effect of pressure-promoted thermal rejuvenation on the fracture energy of metallic glasses. <i>Journal of Non-Crystalline Solids</i> , 2022, 590, 121674.	3.1	6
11351	Structural dynamics of Smoothed (SMO) in the ciliary membrane and its interaction with membrane lipids. <i>Biochimica Et Biophysica Acta - Biomembranes</i> , 2022, 1864, 183946.	2.6	5

#	ARTICLE	IF	CITATIONS
11352	Statistical and energetic analysis of hydrogen bonds in short and long peptide nanotapes/nanofibers using molecular dynamics simulations. <i>Journal of Molecular Liquids</i> , 2022, 359, 119308.	4.9	4
11353	Cooperative antimicrobial action of melittin on lipid membranes: A coarse-grained molecular dynamics study. <i>Biochimica Et Biophysica Acta - Biomembranes</i> , 2022, 1864, 183955.	2.6	10
11354	Structural phase transitions in $\text{SrTiO}_3$ from deep potential molecular dynamics. <i>Physical Review B</i> , 2022, 105, .	3.2	25
11355	Betulinic acid and 3-o-acetyl-betulinic acid interactions with external and internal surface of boron-nitride nanotubes: A DFT and MD investigation. <i>Computational and Theoretical Chemistry</i> , 2022, , 113738.	2.5	1
11356	A chemoproteoinformatics approach demonstrates that aspirin increases sensitivity to MEK inhibition by directly binding to RPS5. , 0, , .		1
11357	Computational studies evidenced the potential of steroidal lactone to disrupt surface interaction of SARS-CoV-2 spike protein and hACE2. <i>Computers in Biology and Medicine</i> , 2022, 146, 105598.	7.0	3
11358	Novel All-Nitrogen Molecular Crystals Composed of Tetragonal N4 Molecules. <i>International Journal of Molecular Sciences</i> , 2022, 23, 5503.	4.1	2
11359	Molecular dynamics study of electric field enhanced hydrate growth for gas storage. <i>Journal of Natural Gas Science and Engineering</i> , 2022, 103, 104617.	4.4	10
11360	Reverse vaccinology-based prediction of a multi-epitope SARS-CoV-2 vaccine and its tailoring to new coronavirus variants. <i>Journal of Biomolecular Structure and Dynamics</i> , 2022, , 1-22.	3.5	4
11361	Understanding the different cross-membrane transport kinetics of two charged molecules on the DOPG lipid surface with second harmonic generation and MD simulation. <i>Soft Matter</i> , 2022, 18, 4305-4314.	2.7	4
11363	A Bottom-Up Coarse-Grained Model for Nucleosome–Nucleosome Interactions with Explicit Ions. <i>Journal of Chemical Theory and Computation</i> , 2022, 18, 3948-3960.	5.3	12
11364	Deciphering the role of the two conserved motifs of the ECF41 family $\sigma$ factor in the autoregulation of its own promoter in <i>Azospirillum brasilense</i> Sp245. <i>Proteins: Structure, Function and Bioinformatics</i> , 2022, , .	2.6	0
11365	Amyloid $\text{I}^2$ Dodecamer Disrupts the Neuronal Membrane More Strongly than the Mature Fibril: Understanding the Role of Oligomers in Neurotoxicity. <i>Journal of Physical Chemistry B</i> , 2022, 126, 3659-3672.	2.6	9
11366	AlphaFold-predicted Protein Structure vs Experimentally Obtained Protein Structure: An Emphasis on the Side Chains. <i>Journal of the Physical Society of Japan</i> , 2022, 91, .	1.6	2
11367	Enhancing Ligand and Protein Sampling Using Sequential Monte Carlo. <i>Journal of Chemical Theory and Computation</i> , 2022, , .	5.3	5
11368	Molecular Dynamics Simulations Indicate Aromaticity as a Key Factor in the Inhibition of IAPP <sub>(20–29)</sub> Aggregation. <i>ACS Chemical Neuroscience</i> , 2022, 13, 1615-1626.	3.5	6
11369	Interaction of Therapeutic $\alpha$ -Peptides with $\text{Al}^{242}$ Monomers, Thermodynamics, and Binding Analysis. <i>ACS Chemical Neuroscience</i> , 2022, 13, 1638-1650.	3.5	7
11370	Highly Ion-Permselective Porous Organic Cage Membranes with Hierarchical Channels. <i>Journal of the American Chemical Society</i> , 2022, 144, 10220-10229.	13.7	67



#	ARTICLE	IF	CITATION
11371	Differences in ligand-induced protein dynamics extracted from an unsupervised deep learning approach correlate with proteinâ€™ligand binding affinities. Communications Biology, 2022, 5, 481.	4.4	13
11372	Molecular evolution and structural analyses of the spike glycoprotein from Brazilian SARS-CoV-2 genomes: the impact of selected mutations. Journal of Biomolecular Structure and Dynamics, 2023, 41, 3110-3128.	3.5	1
11373	Seipin transmembrane segments critically function in triglyceride nucleation and lipid droplet budding from the membrane. ELife, 2022, 11, .	6.0	22
11374	Forecasting molecular dynamics energetics of polymers in solution from supervised machine learning. Chemical Science, 2022, 13, 7021-7033.	7.4	5
11375	Ultralong recovery time in nanosecond electroporation systems enabled by orientational-disordering processes. Nanoscale, 2022, 14, 7934-7942.	5.6	4
11376	â€œTiAlâ€•é†‘â‚Ž«é€Ÿâ†šâ€•è‚ž†ç“ä;æ<“æ%‰‘âˆ†â†ç”“æž„çš„æ¼ƒ”â€œCE–ç%‰¹â³¼• Scientia Sinica: Physica, Mechanica Et Astronomica, 2022,	3.5	4
11377	The Impact of Chromate on Pseudomonas aeruginosa Molybdenum Homeostasis. Frontiers in Microbiology, 2022, 13, .	2.6	1
11378	Consistent Picture of Phosphateâ€™Divalent Cation Binding from Models with Implicit and Explicit Electronic Polarization. Journal of Physical Chemistry B, 0, , .	9.4	3
11379	Not so rigid capsids based on cyclodextrin complexes: Keys to design. Journal of Colloid and Interface Science, 2022, 623, 938-946.	3.5	5
11380	Aggregation of a Parkinsonâ€™s Disease-Related Peptide: When Does Urea Weaken Hydrophobic Interactions?. ACS Chemical Neuroscience, 2022, 13, 1769-1781.	7.6	11
11383	Topological dynamics of an intrinsically disordered Nâ€™terminal domain of the human androgen receptor. Protein Science, 2022, 31, .	2.4	2
11384	Effect of biphosphate salt on d <sc>lpalmitoylphosphatidylcholine</sc> bilayer deformation by Tat polypeptide. Biopolymers, 0, , .	5.3	0
11385	How Peptides Bind to PSD-95/Discs-Large/ZO-1 Domains. Journal of Chemical Theory and Computation, 2022, 18, 3845-3859.	3.2	10
11387	Quantum chemical calculations, spectroscopic studies and molecular docking investigations of the anti-cancer drug quercitrin with B-RAF inhibitor. Heliyon, 2022, 8, e09539.	4.1	3
11389	Unravelling hierarchical levels of structure in lipid membranes. Computational and Structural Biotechnology Journal, 2022, 20, 2798-2806.	3.5	3
11390	Ultrasensitive Detection of MCF-7 Cells with a Carbon Nanotube-Based Optoelectronic-Pulse Sensor Framework. ACS Omega, 2022, 7, 18459-18470.	1.4	0
11391	<i>In silico</i> folding of hydrophobic peptides that form Î²â€™hairpin structures in solution. Journal of Peptide Science, 0, , .	3.0	6
11392	The â€™good,â€™the â€™bad,â€™and the â€™hiddenâ€™in neutron scattering and molecular dynamics of ionic aqueous solutions. Journal of Chemical Physics, 2022, 156, .		

#	ARTICLE	IF	CITATIONS
11394	Small-molecule fulvic acid with strong hydration ability for non-vitreous cellular cryopreservation. IScience, 2022, 25, 104423.	4.1	3
11395	Self-derived peptides from the SARS-CoV-2 spike glycoprotein disrupting shaping and stability of the homotrimer unit. Biomedicine and Pharmacotherapy, 2022, 151, 113190.	5.6	0
11396	Insilico structure based drug design approach to find potential hits in ventilator-associated pneumonia caused by Pseudomonas aeruginosa. Computers in Biology and Medicine, 2022, 146, 105597.	7.0	0
11397	Binding behavior of ibuprofen-based ionic liquids with bovine serum albumin: Thermodynamic and molecular modeling studies. Journal of Molecular Liquids, 2022, 360, 119367.	4.9	4
11398	A quantum-chemistry and molecular-dynamics study of non-covalent interactions between tri-n-butyl phosphate and 1-butyl-3-methylimidazolium bis(trifluoromethylsulfonyl)imide. Journal of Molecular Liquids, 2022, 360, 119430.	4.9	8
11399	Computational and experimental study of different brines in temperature swing solvent extraction desalination with amine solvents. Desalination, 2022, 537, 115863.	8.2	12
11400	Human serum albumin adsorption on cellulose nanocrystal: A spectroscopy and molecular dynamics simulation research. Applied Surface Science, 2022, 597, 153749.	6.1	2
11401	Membrane binding of pore-forming $\beta$ -hemolysin components studied at different lipid compositions. Biochimica Et Biophysica Acta - Biomembranes, 2022, 1864, 183970.	2.6	5
11402	Theoretical Study on the Stability Mechanism of a High Energy System Composed of Molecules Containing C-O-C or -N3 Groups and Aluminum Hydride. SSRN Electronic Journal, 0, , .	0.4	0
11403	Molecular dynamics simulations of proton conducting media containing phosphoric acid. Physical Chemistry Chemical Physics, 2022, 24, 15522-15531.	2.8	7
11404	Influence Mechanism of Different Organic Solvents on Api Solvation Behaviors: Molecular Dynamics Simulations. SSRN Electronic Journal, 0, , .	0.4	0
11405	Molecular Dynamics Simulations of Amyloid- $\beta$ Protein in KCl Salt Solution. , 2022, , .		0
11406	Structural and functional insights into the DNA damage-inducible protein 1 (Ddi1) from protozoa. Current Research in Structural Biology, 2022, 4, 175-191.	2.2	0
11407	Dilithium Phthalocyanine as Electrolyte Additive for the Regulation of Ion Solvation and Transport Towards Dendrite-Free Li Metal Anodes. SSRN Electronic Journal, 0, , .	0.4	0
11408	Dipeptides as Environmentally Friendly CH <sub>4</sub> Hydrate Inhibitors: Experimental and Computational Approaches. SSRN Electronic Journal, 0, , .	0.4	0
11409	Mechanical properties of nucleic acids and the non-local twistable wormlike chain model. Journal of Chemical Physics, 2022, 156, .	3.0	6
11410	Stabilizing a Double Gyroid Network Phase with 2 nm Feature Size by Blending of Lamellar and Cylindrical Forming Block Oligomers. JACS Au, 2022, 2, 1405-1416.	7.9	5
11411	Structural insights into binding of therapeutic channel blockers in NMDA receptors. Nature Structural and Molecular Biology, 2022, 29, 507-518.	8.2	21

#	ARTICLE	IF	CITATIONS
11412	Allosteric Binding Sites of A $\beta$ 2 Peptides on the Acetylcholine Synthesizing Enzyme ChAT as Deduced by In Silico Molecular Modeling. International Journal of Molecular Sciences, 2022, 23, 6073.	4.1	21
11413	Space Charge Behavior in Epoxy-Based Dielectrics: Progress and Perspective. Advanced Electronic Materials, 2022, 8, .	5.1	15
11414	Evaluation of Colchicine's interaction with the ATP-binding region of mice NLRP3-NACHT domain using molecular docking and dynamics simulation. Journal of Physics: Conference Series, 2022, 2269, 012012.	0.4	2
11415	Sequence dependence of transient Hoogsteen base pairing in DNA. PLoS Computational Biology, 2022, 18, e1010113.	3.2	6
11416	Atomistic Assessment of Melting Point Depression and Enhanced Interfacial Diffusion of Cu in Confinement with AlN. ACS Applied Materials & Interfaces, 2022, 14, 26099-26115.	8.0	5
11417	Conformational Entropy as a Potential Liability of Computationally Designed Antibodies. Biomolecules, 2022, 12, 718.	4.0	8
11418	Dielectric constant of aqueous solutions of proteins and organic polymers from molecular dynamics simulations. Journal of Chemical Physics, 2022, 156, .	3.0	1
11421	All-atom molecular simulation study of cellulose acetate: amorphous structure and the dissolution of small molecule. Cellulose, 2022, 29, 5463-5478.	4.9	1
11422	Computational Modelling and Sustainable Synthesis of a Highly Selective Electrochemical MIP-Based Sensor for Citalopram Detection. Molecules, 2022, 27, 3315.	3.8	5
11423	GenNBPSeg: Online Web Server to Generate Never Born Protein Sequences Using Toeplitz Matrix Approach with Structure Analysis. Current Bioinformatics, 2022, 17, 565-577.	1.5	2
11424	Transition between conformational states of the TREK-1 K2P channel promoted by interaction with PIP2. Biophysical Journal, 2022, 121, 2380-2388.	0.5	3
11425	Mitochondrial uncouplers induce proton leak by activating AAC and UCP1. Nature, 2022, 606, 180-187.	27.8	48
11426	Macrocyclic Cavitand $\beta$ -Cyclodextrin Inhibits the Alcohol-Induced Trypsin Aggregation. ChemPhysChem, 2022, 23, .	2.1	1
11427	Diverse reaction behaviors of artificial ubiquinones in mitochondrial respiratory complex I. Journal of Biological Chemistry, 2022, 298, 102075.	3.4	3
11428	Probing structural basis for enhanced binding of SARS-CoV-2 P.1 variant spike protein with the human ACE2 receptor. Journal of Cellular Biochemistry, 2022, 123, 1207-1221.	2.6	3
11430	An Insight Based on Computational Analysis of the Interaction between the Receptor-Binding Domain of the Omicron Variants and Human Angiotensin-Converting Enzyme 2. Biology, 2022, 11, 797.	2.8	10
11431	Designing of high-performance dye-sensitized solar cells by using a new electrolyte based on deep eutectic solvents. International Journal of Energy Research, 2022, 46, 14546-14557.	4.5	10
11432	Negative Effects of Inorganic Salt Invasion on the Dissociation Kinetics of Silica-Confined Gas Hydrate via Thermal Stimulation. Energy & Fuels, 2022, 36, 6216-6228.	5.1	8

#	ARTICLE	IF	CITATIONS
11433	Influence of Ion Specificity and Concentration on the Conformational Transition of Intrinsically Disordered Sheep Prion Peptide. <i>ChemPhysChem</i> , 2022, 23, .	2.1	3
11435	The Influence of Short Motifs on the Anticancer Activity of HB43 Peptide. <i>Pharmaceutics</i> , 2022, 14, 1089.	4.5	3
11436	Proton coupling and the multiscale kinetic mechanism of a peptide transporter. <i>Biophysical Journal</i> , 2022, 121, 2266-2278.	0.5	9
11438	Data-Driven and Multiscale Modeling of DNA-Templated Dye Aggregates. <i>Molecules</i> , 2022, 27, 3456.	3.8	6
11439	Chitosan characteristics in electrolyte solutions: Combined molecular dynamics modeling and slender body hydrodynamics. <i>Carbohydrate Polymers</i> , 2022, 292, 119676.	10.2	7
11441	Modified Poisson-Boltzmann theory for polyelectrolytes in monovalent salt solutions with finite-size ions. <i>Journal of Chemical Physics</i> , 2022, 156, .	3.0	4
11445	Molecular Docking, Dynamics Simulation and Physicochemical Analysis of Some Phytochemicals as Antiplatelet Agents. <i>Letters in Drug Design and Discovery</i> , 2022, 19, .	0.7	0
11447	Subtype-specific responses of hKv7.4 and hKv7.5 channels to polyunsaturated fatty acids reveal an unconventional modulatory site and mechanism. <i>ELife</i> , 0, 11, .	6.0	5
11448	Patched 1 regulates Smoothed by controlling sterol binding to its extracellular cysteine-rich domain. <i>Science Advances</i> , 2022, 8, .	10.3	19
11450	Lifetime distribution of clusters in binary mixtures involving hydrogen bonding liquids. <i>Scientific Reports</i> , 2022, 12, .	3.3	10
11451	Uncovering cryptic pockets in the SARS-CoV-2 spike glycoprotein. <i>Structure</i> , 2022, 30, 1062-1074.e4.	3.3	21
11452	Biphasic Behaviors of Nd <sup>3+</sup> Bound with Cyanex272, Cyanex301, and Cyanex302: A Molecular Dynamics Simulation Study. <i>Inorganic Chemistry</i> , 2022, 61, 8920-8929.	4.0	0
11453	Enhanced steric effect and desolvation process on organic solvent nanofiltration: A mechanism study for removing anionic dyes. <i>Chemical Engineering Journal</i> , 2022, 446, 137360.	12.7	4
11454	Molecular engineering and activity improvement of acetylcholinesterase inhibitors: Insights from 3D-QSAR, docking, and molecular dynamics simulation studies. <i>Journal of Molecular Graphics and Modelling</i> , 2022, 116, 108239.	2.4	4
11458	Adsorption Energetics of Amino Acid Analogs on Polymer/Water Interfaces Studied by All-Atom Molecular Dynamics Simulation and a Theory of Solutions. <i>Journal of Physical Chemistry B</i> , 2022, 126, 4389-4400.	2.6	4
11459	Structural, Functional and Computational Studies of Membrane Recognition by Plasmodium Perforin-Like Proteins 1 and 2. <i>Journal of Molecular Biology</i> , 2022, 434, 167642.	4.2	0
11460	Molecular dynamics simulations of microstructural evolution of irradiated (U,Pu)O <sub>2</sub> studied via simulated XRD patterns. <i>Journal of Nuclear Materials</i> , 2022, 567, 153834.	2.7	5
11461	Molecular dynamics simulation on $\beta$ -CL-20 based PBXs with chain-extended poly(3,3-bis(azidomethyl)oxetane). <i>Computational and Theoretical Chemistry</i> , 2022, 1214, 113762.	2.5	3

#	ARTICLE	IF	CITATIONS
11462	The investigation of deep eutectic electrolyte based on Choline Chloride: Ethylene glycol in 1:3ÅM ratio and lithium hexafluorophosphate salt for application in Lithium-Ion batteries. Journal of Molecular Liquids, 2022, 360, 119476.	4.9	4
11463	Binding of bioactive esculin and esculetin with hen egg white lysozyme: Spectroscopic and computational methods to comprehensively elucidate the binding affinities, interacting forces, and conformational alterations at molecular level. Journal of Molecular Liquids, 2022, 360, 119423.	4.9	7
11464	Evaluation of hydrogen storage ability of hydroquinone clathrates using molecular simulations. Journal of Molecular Liquids, 2022, 360, 119487.	4.9	5
11465	Simulation and theoretical analysis of the origin of the temperature of maximum density of water. Fluid Phase Equilibria, 2022, 560, 113515.	2.5	5
11466	Synthesis and investigations of reactive properties, photophysical properties and biological activities of a pyrazole-triazole hybrid molecule. Journal of Molecular Structure, 2022, 1265, 133363.	3.6	11
11467	Rational design, molecular docking, dynamic simulation, synthesis, PPAR-Î³ competitive binding and transcription analysis of novel glitazones. Journal of Molecular Structure, 2022, 1265, 133354.	3.6	4
11469	CLiB â€“ a novel cardiolipin-binder isolated <i>via</i> data-driven and <i>in vitro</i> screening. RSC Chemical Biology, 0, , .	4.1	1
11470	ALS-associated A315E and A315pT variants exhibit distinct mechanisms in inducing irreversible aggregation of TDP-43<sub>312</sub>â€“317</sub> peptides. Physical Chemistry Chemical Physics, 2022, 24, 16263-16273.	2.8	6
11471	Homologous basic helixâ€“loopâ€“helix transcription factors induce distinct deformations of torsionally-stressed DNA: a potential transcription regulation mechanism. QRB Discovery, 2022, 3, .	1.6	0
11472	Molecular Dynamics Simulation of Solidification Epitaxial Growth in Nano-Scale Molten Pool. SSRN Electronic Journal, 0, , .	0.4	0
11473	Coacervation of poly-electrolytes in the presence of lipid bilayers: mutual alteration of structure and morphology. Chemical Science, 2022, 13, 7933-7946.	7.4	16
11474	Refining details of the structural and electronic properties of the Cu<sub>B</sub> site in pMMO enzyme through sequential molecular dynamics/CPKS-EPR calculations. Physical Chemistry Chemical Physics, 0, , .	2.8	0
11475	Effect of N-glycosylation on horseradish peroxidase structural and dynamical properties. Computational and Structural Biotechnology Journal, 2022, 20, 3096-3105.	4.1	6
11476	Probing the distribution of ionic liquid mixtures at charged and neutral interfaces via simulations and lattice-gas theory. Physical Chemistry Chemical Physics, 0, , .	2.8	0
11477	Impacts of targeting different hydration free energy references in the development of ion potentials. Physical Chemistry Chemical Physics, 0, , .	2.8	0
11478	Analysis of the galactomannan binding ability of Î²-mannosidases, BtMan2A and CmMan5A, regarding their activity and synergism with a Î²-mannanase. Computational and Structural Biotechnology Journal, 2022, 20, 3140-3150.	4.1	1
11480	Hybrid computationalâ€“experimental data-driven design of self-assembling Îµ-conjugated peptides. , 2022, 1, 448-462.		7
11481	Rational Design of Amphiphilic Fluorinated Peptides: Evaluation of Self-Assembly Properties and Hydrogel Formation. Nanoscale, 0, , .	5.6	9

#	ARTICLE	IF	CITATIONS
11482	Dual functional amphiphilic sugar-coated AIE-active fluorescent organic nanoparticles for the monitoring and inhibition of insulin amyloid fibrillation based on carbohydrateâ€“protein interactions. <i>Journal of Materials Chemistry B</i> , 2022, 10, 5602-5611.	5.8	3
11486	Molecular Dynamics Simulations Reveal Structural Interconnections within Sec14-PH Bipartite Domain from Human Neurofibromin. <i>International Journal of Molecular Sciences</i> , 2022, 23, 5707.	4.1	0
11488	Using PD-L1 full-length structure, enhanced induced fit docking and molecular dynamics simulations for structural insights into inhibition of PD-1/PD-L1 interaction by small-molecule ligands. <i>Molecular Simulation</i> , 2022, 48, 1269-1283.	2.0	2
11491	Hydrophobic Ï€-Ï€ stacking interactions and hydrogen bonds drive self-aggregation of luteolin in water. <i>Journal of Molecular Graphics and Modelling</i> , 2022, 116, 108243.	2.4	6
11492	The regulatory role of the <i>Aspergillus flavus</i> core retromer complex in aflatoxin metabolism. <i>Journal of Biological Chemistry</i> , 2022, 298, 102120.	3.4	3
11494	Targeting SARS-CoV-2 non-structural protein 13 via helicase-inhibitor-repurposing and non-structural protein 16 through pharmacophore-based screening. <i>Molecular Diversity</i> , 2023, 27, 1067-1085.	3.9	6
11495	Amphotericin B assembles into seven-molecule ion channels: An NMR and molecular dynamics study. <i>Science Advances</i> , 2022, 8, .	10.3	20
11496	All-atom molecular dynamics simulations of Synaptotagmin-SNARE-complexin complexes bridging a vesicle and a flat lipid bilayer. <i>ELife</i> , 0, 11, .	6.0	22
11497	Determinants of Selectivity for the Formation of Monocyclic and Bicyclic Products in Monoterpene Synthases. <i>ACS Catalysis</i> , 2022, 12, 7453-7469.	11.2	6
11498	Mapping the deformability of natural and designed cellulosomes in solution. , 2022, 15, .		4
11499	Melting points of water models: Current situation. <i>Journal of Chemical Physics</i> , 2022, 156, .	3.0	14
11500	Enhanced BRAF engagement by NRAS mutants capable of promoting melanoma initiation. <i>Nature Communications</i> , 2022, 13, .	12.8	11
11503	Phosphorylation Induced Conformational Transitions in DNA Polymerase Î². <i>Frontiers in Molecular Biosciences</i> , 0, 9, .	3.5	2
11504	MERTK activation drives osimertinib resistance in EGFR-mutant nonâ€“small cell lung cancer. <i>Journal of Clinical Investigation</i> , 2022, 132, .	8.2	12
11505	The Amyloidogenic Peptide Amyloid Beta(16â€“22) Displays Facet Dependent Conformation on Metal Surfaces. <i>Biophysica</i> , 2022, 2, 135-153.	1.4	1
11506	Efficient Quantification of Lipid Packing Defect Sensing by Amphipathic Peptides: Comparing Martini 2 and 3 with CHARMM36. <i>Journal of Chemical Theory and Computation</i> , 2022, 18, 4503-4514.	5.3	9
11507	Mechanistic Insight on General Protein-Binding Ability of ATP and the Impacts of Arginine Residues. <i>Journal of Physical Chemistry B</i> , 2022, 126, 4647-4658.	2.6	5
11508	Differential Activation of TRPM8 by the Stereoisomers of Menthol. <i>Frontiers in Pharmacology</i> , 0, 13, .	3.5	1



#	ARTICLE	IF	CITATIONS
11509	Liquidâ€“liquid criticality in the WAIL water model. <i>Journal of Chemical Physics</i> , 2022, 157, .	3.0	20
11511	Binding of DEP domain to phospholipid membranes: More than just electrostatics. <i>Biochimica Et Biophysica Acta - Biomembranes</i> , 2022, 1864, 183983.	2.6	1
11513	Small ionic radii limit time step in Martini 3 molecular dynamics simulations. <i>Journal of Chemical Physics</i> , 2022, 157, .	3.0	6
11514	A new hypothesis for cavitation nucleation in gas saturated solutions: Clustering of gas molecules lowers significantly the surface tension. <i>Chinese Journal of Chemical Engineering</i> , 2022, 50, 347-351.	3.5	4
11515	A computational algorithm to assess the physiochemical determinants of T cell receptor dissociation kinetics. <i>Computational and Structural Biotechnology Journal</i> , 2022, 20, 3473-3481.	4.1	1
11516	Exploring TRPC3 Interaction with Cholesterol through Coarse-Grained Molecular Dynamics Simulations. <i>Biomolecules</i> , 2022, 12, 890.	4.0	1
11519	Spider Toxin SNX-482 Gating Modifier Spontaneously Partitions in the Membrane Guided by Electrostatic Interactions. <i>Membranes</i> , 2022, 12, 595.	3.0	1
11521	An L-theanine derivative targets against SARS-CoV-2 and its Delta and Omicron variants. <i>Heliyon</i> , 2022, 8, e09660.	3.2	1
11522	Collective Variable for Metadynamics Derived From AlphaFold Output. <i>Frontiers in Molecular Biosciences</i> , 0, 9, .	3.5	5
11523	Multiscale Simulation of Ternary Stratum Corneum Lipid Mixtures: Effects of Cholesterol Composition. <i>Langmuir</i> , 2022, 38, 7496-7511.	3.5	7
11524	Stabilization of CDK6 by ribosomal protein uS7, a target protein of the natural product fucoxanthinol. <i>Communications Biology</i> , 2022, 5, .	4.4	1
11525	Relating the Degree of Nanofiller Functionality to the Glass Transition Temperature and Structure in a Polymerâ€“Polyhedral Oligomeric Silsesquioxane Nanocomposite. <i>Macromolecules</i> , 2022, 55, 4891-4898.	4.8	4
11526	Stability of high-temperature salty ice suggests electrolyte permeability in water-rich exoplanet icy mantles. <i>Nature Communications</i> , 2022, 13, .	12.8	13
11527	Plasticity of Membrane Binding by the Central Region of Î±-Synuclein. <i>Frontiers in Molecular Biosciences</i> , 0, 9, .	3.5	5
11528	Is Lipid Specificity Key to the Potential Antiviral Activity of Mouthwash Reagent Chlorhexidine against SARS-CoV-2?. <i>Membranes</i> , 2022, 12, 616.	3.0	2
11529	Exploring structure and dynamics of the polylacticâ€“glycolic acidâ€“polyethylene glycol copolymer and its homopolymer constituents in various solvents using allâ€“atom molecular dynamics. <i>Journal of Applied Polymer Science</i> , 2022, 139, .	2.6	3
11531	Steady-like topology of the dynamical hydrogen bond network in supercooled water. , 2022, 1, .		7
11532	Activated chemical bonds in nanoporous and amorphous iridium oxides favor low overpotential for oxygen evolution reaction. <i>Nature Communications</i> , 2022, 13, .	12.8	31

#	ARTICLE	IF	CITATIONS
11533	Understanding Metal-Organic Framework Nucleation from a Solution with Evolving Graphs. <i>Journal of the American Chemical Society</i> , 2022, 144, 11099-11109.	13.7	19
11534	Different Binding Modes of SARS-CoV-1 and SARS-CoV-2 Fusion Peptides to Cell Membranes: The Influence of Peptide Helix Length. <i>Journal of Physical Chemistry B</i> , 2022, 126, 4261-4271.	2.6	6
11535	Insights into the Atomistic Mechanisms of Phosphorylation in Disrupting Liquid-Liquid Phase Separation and Aggregation of the FUS Low-Complexity Domain. <i>Journal of Chemical Information and Modeling</i> , 2022, 62, 3227-3238.	5.4	18
11536	Computational identification of bioactive compounds from <i>Cydonia oblonga</i> Mill. against hepatocellular carcinoma by targeting pTEN and HBx-interacting protein. <i>Journal of Molecular Modeling</i> , 2022, 28, .	1.8	0
11537	Protein-modified SEI formation and evolution in Li metal batteries. <i>Journal of Energy Chemistry</i> , 2022, 73, 248-258.	12.9	16
11538	Controlling the Ion Transport Number in Solvent-in-Salt Solutions. <i>Journal of Physical Chemistry B</i> , 2022, 126, 4572-4583.	2.6	5
11539	A Transfer Free Energy Based Implicit Solvent Model for Protein Simulations in Solvent Mixtures: Urea-Induced Denaturation as a Case Study. <i>Journal of Physical Chemistry B</i> , 2022, 126, 4472-4482.	2.6	3
11540	Oncogenic KRAS G12C: Kinetic and redox characterization of covalent inhibition. <i>Journal of Biological Chemistry</i> , 2022, 298, 102186.	3.4	5
11541	Molecular mechanism of CD44 homodimerization modulated by palmitoylation and membrane environments. <i>Biophysical Journal</i> , 2022, 121, 2671-2683.	0.5	6
11542	Efficiently Computing NMR <sup>1</sup> H and <sup>13</sup> C Chemical Shifts of Saccharides in Aqueous Environment. <i>Journal of Chemical Theory and Computation</i> , 2022, 18, 4373-4386.	5.3	6
11543	Optimization of an <i>in Silico</i> Protocol Using Probe Permeabilities to Identify Membrane Pan-Assay Interference Compounds. <i>Journal of Chemical Information and Modeling</i> , 2022, 62, 3034-3042.	5.4	5
11545	Toward the Noninvasive Diagnosis of Alzheimer's Disease: Molecular Basis for the Specificity of Curcumin for Fibrillar Amyloid- $\beta$ . <i>ACS Omega</i> , 2022, 7, 22032-22038.	3.5	3
11546	Molecular dynamics simulation of hydrogen diffusion in water-saturated clay minerals; implications for Underground Hydrogen Storage (UHS). <i>International Journal of Hydrogen Energy</i> , 2022, 47, 24871-24885.	7.1	27
11547	Antibacterial and Anti-Inflammatory Effects of Apolipoprotein E. <i>Biomedicines</i> , 2022, 10, 1430.	3.2	8
11548	Diffusional isotope fractionation of singly and doubly substituted isotopologues of H <sub>2</sub> , N <sub>2</sub> and O <sub>2</sub> during air-water gas transfer. <i>Geochimica Et Cosmochimica Acta</i> , 2022, 332, 78-87.	3.9	1
11549	Discovery of Phenylcarbamoylazinane-1,2,4-Triazole Amides Derivatives as the Potential Inhibitors of Aldo-Keto Reductases (AKR1B1 & AKR1B10): Potential Lead Molecules for Treatment of Colon Cancer. <i>Molecules</i> , 2022, 27, 3981.	3.8	7
11550	Characterization of the membrane interactions of phospholipase C $\beta$ reveals key features of the active enzyme. <i>Science Advances</i> , 2022, 8, .	10.3	7
11552	Computational Insights into the Role of Cholesterol in Inverted Hexagonal Phase Stabilization and Endosomal Drug Release. <i>Langmuir</i> , 2022, 38, 7462-7471.	3.5	11

#	ARTICLE	IF	CITATIONS
11553	Removal of Pharmaceutical Pollutants from Wastewater Using 2D Covalent Organic Frameworks (COFs): An In Silico Engineering Study. Industrial & Engineering Chemistry Research, 2022, 61, 8809-8820.	3.7	13
11554	Effect of Tetrabutylammonium on Methylene Blue Adsorption. Journal of Physics: Conference Series, 2022, 2243, 012078.	0.4	0
11555	Computational discovery of small drug-like compounds as potential inhibitors of PD-1/PD-L1 interactions. Journal of Biomolecular Structure and Dynamics, 0, , 1-17.	3.5	1
11556	Immunoinformatics Aided Design and In-Vivo Validation of a Cross-Reactive Peptide Based Multi-Epitope Vaccine Targeting Multiple Serotypes of Dengue Virus. Frontiers in Immunology, 0, 13, .	4.8	19
11557	Designing of potent anti-diabetic molecules by targeting SIK2 using computational approaches. Molecular Diversity, 2023, 27, 1101-1121.	3.9	3
11558	SARS-CoV-2 Omicron Variant Binds to Human Cells More Strongly than the Wild Type: Evidence from Molecular Dynamics Simulation. Journal of Physical Chemistry B, 2022, 126, 4669-4678.	2.6	25
11559	<scp>PcoB</scp> is a defense outer membrane protein that facilitates cellular uptake of copper. Protein Science, 2022, 31, .	7.6	5
11560	Hidden spatiotemporal sequence in transition to shear band in amorphous solids. Physical Review Research, 2022, 4, .	3.6	10
11561	A cholesterol analog stabilizes the human $\beta_2$ -adrenergic receptor nonlinearly with temperature. Science Signaling, 2022, 15, .	3.6	8
11564	Nonmonotonic Relationship between the Oxidation State of Graphene-Based Materials and Its Cell Membrane Damage Effects. ACS Applied Materials & Interfaces, 2022, 14, 30306-30314.	8.0	4
11566	The guidance and adhesion protein FLRT2 dimerizes in cis via dual small-X3-small transmembrane motifs. Structure, 2022, 30, 1354-1365.e5.	3.3	4
11568	Electronic Structure of de Novo Peptide ACC-Hex from First Principles. Journal of Physical Chemistry B, 2022, 126, 4289-4298.	2.6	2
11571	Molecular Dynamics Simulations of the Effects of Entanglement on Polymer Crystal Nucleation. Macromolecules, 2022, 55, 4899-4906.	4.8	14
11572	Discovery of GSK3 $\beta$ Inhibitors through In Silico Prediction-and-Experiment Cycling Strategy, and Biological Evaluation. Molecules, 2022, 27, 3825.	3.8	3
11573	Quercetin and luteolin are single-digit micromolar inhibitors of the SARS-CoV-2 RNA-dependent RNA polymerase. Scientific Reports, 2022, 12, .	3.3	31
11574	Theoretical methods for structural phase transitions in elemental solids at extreme conditions: statics and dynamics. Journal of Physics Condensed Matter, 2022, 34, 363001.	1.8	1
11575	Are the current commercially available oximes capable of reactivating acetylcholinesterase inhibited by the nerve agents of the A-series?. Archives of Toxicology, 2022, 96, 2559-2572.	4.2	10
11576	Gas Adsorption and Diffusion Behaviors in Interfacial Systems Composed of a Polymer of Intrinsic Microporosity and Amorphous Silica: A Molecular Simulation Study. Langmuir, 2022, 38, 7567-7579.	3.5	4

#	ARTICLE	IF	CITATIONS
11577	Interaction of Phthalates with Lipid Bilayer Membranes. <i>Journal of Physical Chemistry B</i> , 2022, 126, 4679-4688.	2.6	3
11578	Identification of flexible Pif1â€DNA interactions and their impacts on enzymatic activities. <i>Nucleic Acids Research</i> , 2022, 50, 7002-7012.	14.5	2
11579	Nonpolarizable Force Fields through the Self-Consistent Modeling Scheme with MD and DFT Methods: From Ionic Liquids to Self-Assembled Ionic Liquid Crystals. <i>Journal of Physical Chemistry B</i> , 2022, 126, 4611-4622.	2.6	6
11580	Dynamical Ion Association and Transport Properties in PEOâLiTFSI Electrolytes: Effect of Salt Concentration. <i>Journal of Physical Chemistry B</i> , 2022, 126, 4531-4542.	2.6	10
11581	Mechanistic Insight into Permeation of Plasma-Generated Species from Vacuum into Water Bulk. <i>International Journal of Molecular Sciences</i> , 2022, 23, 6330.	4.1	5
11582	Symmetric Molecular Dynamics. <i>Journal of Chemical Theory and Computation</i> , 2022, 18, 4077-4081.	5.3	1
11583	Structural basis of Omicron immune evasion: A comparative computational study. <i>Computers in Biology and Medicine</i> , 2022, 147, 105758.	7.0	6
11584	Exploring the phytochemicals of <i>Platycodon grandiflorus</i> for TMPRSS2 inhibition in the search for SARS-CoV-2 entry inhibitors. <i>Journal of King Saud University - Science</i> , 2022, 34, 102155.	3.5	3
11585	Computational repurposing approach for targeting the critical spike mutations in B.1.617.2 (delta), AY.1 (delta plus) and C.37 (lambda) SARS-CoV-2 variants using exhaustive structure-based virtual screening, molecular dynamic simulations and MM-PBSA methods. <i>Computers in Biology and Medicine</i> , 2022, 147, 105709.	7.0	3
11586	Foreseeing the future of green Technology. Molecular dynamic investigation on passive membrane penetration by the products of the CO2 and 1,3-butadiene reaction. <i>Journal of Molecular Liquids</i> , 2022, 361, 119581.	4.9	0
11587	Molecular insights into the very early steps of AÎ²1-42 pentameric protofibril disassembly by PGG: A molecular dynamics simulation study. <i>Journal of Molecular Liquids</i> , 2022, 361, 119638.	4.9	5
11588	Towards the correct microscopic structure of aqueous CsCl solutions with a comparison of classical interatomic potential models. <i>Journal of Molecular Liquids</i> , 2022, 361, 119660.	4.9	2
11589	Bovine hemoglobin thermal stability in the presence of naringenin: Calorimetric, spectroscopic and molecular modeling studies. <i>Journal of Molecular Liquids</i> , 2022, 361, 119617.	4.9	5
11590	Cytostatic effects of structurally different ginsenosides on yeast cells with altered sterol biosynthesis and transport. <i>Biochimica Et Biophysica Acta - Biomembranes</i> , 2022, 1864, 183993.	2.6	4
11591	Probing effects of the SARS-CoV-2 E protein on membrane curvature and intracellular calcium. <i>Biochimica Et Biophysica Acta - Biomembranes</i> , 2022, 1864, 183994.	2.6	11
11592	Exploring competitive inhibition of a family 10 xylanase derived from Hu sheep rumen microbiota by <i>Oryza sativa</i> xylanase inhibitor protein: In vitro and in silico perspectives. <i>Enzyme and Microbial Technology</i> , 2022, 160, 110082.	3.2	5
11593	Machine learning potentials of kaolinite based on the potential energy surfaces of GGA and meta-GGA density functional theory. <i>Applied Clay Science</i> , 2022, 228, 106596.	5.2	6
11594	Interaction of mancozeb with human hemoglobin: Spectroscopic, molecular docking and molecular dynamic simulation studies. <i>Spectrochimica Acta - Part A: Molecular and Biomolecular Spectroscopy</i> , 2022, 280, 121503.	3.9	22

#	ARTICLE	IF	CITATIONS
11595	Spectroscopic, electronic structure, molecular docking, and molecular dynamics simulation study of 7-Trifluoromethyl-1H-indole-2-carboxylic acid as an aromatase inhibitor. <i>Spectrochimica Acta - Part A: Molecular and Biomolecular Spectroscopy</i> , 2022, 280, 121530.	3.9	3
11596	AI-based structure prediction empowers integrative structural analysis of human nuclear pores. <i>Science</i> , 2022, 376, .	12.6	136
11597	Ultrafast Förster resonance energy transfer between tyrosine and tryptophan: potential contributions to proteinâ€“water dynamics measurements. <i>Physical Chemistry Chemical Physics</i> , 2022, 24, 18055-18066.	2.8	4
11598	Hybrid composites with shape memory alloys and piezoelectric thin layers. , 2022, , 225-265.		1
11599	Simulation study of domain formation in a model bacterial membrane. <i>Physical Chemistry Chemical Physics</i> , 0, , .	2.8	4
11600	Breakthrough pressure of oil displacement by water through the ultra-narrow kerogen pore throat from the Youngâ€“Laplace equation and molecular dynamic simulations. <i>Physical Chemistry Chemical Physics</i> , 2022, 24, 17195-17209.	2.8	9
11601	Stability and Conformational Memory of Electrosprayed and Rehydrated Bacteriophage Ms2 Virus Coat Proteins. <i>SSRN Electronic Journal</i> , 0, , .	0.4	0
11602	Coupling of acceptor-substituted diazo compounds and tertiary thioamides: synthesis of enamino carbonyl compounds and their pharmacological evaluation. <i>RSC Advances</i> , 2022, 12, 19431-19444.	3.6	1
11603	Association of Lasioglossin-III Antimicrobial Peptide with Model Lipid Bilayers. <i>Biophysics (Russian)</i> Tj ETQq0 0 0 rgBT /Overlock 10 Tf 50 0.7		1
11604	Exploring the Conformational Impact of Glycine Receptor TM1-2 Mutations Through Coarse-Grained Analysis and Atomistic Simulations. <i>Frontiers in Molecular Biosciences</i> , 0, 9, .	3.5	2
11606	Toward Bottom-Up Understanding of Transport in Concentrated Battery Electrolytes. <i>ACS Central Science</i> , 2022, 8, 880-890.	11.3	14
11608	Molecular Dynamics Simulations of the Tau Amyloid Fibril Core Dimer at the Surface of a Lipid Bilayer Model: I. In <i>Alzheimerâ€™s Disease</i> . <i>Journal of Physical Chemistry B</i> , 2022, 126, 4849-4856.	2.6	10
11609	Enhanced Expansion and Reduced Kiss-and-Run Events in Fusion Pores Steered by Synaptotagmin-1 C2B Domains. <i>Journal of Chemical Theory and Computation</i> , 2022, 18, 4544-4554.	5.3	5
11610	Loosely-packed dynamical structures with partially-melted surface being the key for thermophilic argonaute proteins achieving high DNA-cleavage activity. <i>Nucleic Acids Research</i> , 2022, 50, 7529-7544.	14.5	9
11611	On the mechanism for the highly sensitive response of cellulose nanofiber hydrogels to the presence of ionic solutes. <i>Cellulose</i> , 2022, 29, 6109-6121.	4.9	10
11612	Molecular Modeling of Ionic Liquids: Forceâ€“Field Validation and Thermodynamic Perspective from Largeâ€“Scale Fastâ€“Growth Solvation Free Energy Calculations. <i>Advanced Theory and Simulations</i> , 2022, 5, .	2.8	6
11613	A molecular dynamics investigation of N-glycosylation effects on T-cell receptor kinetics. <i>Journal of Biomolecular Structure and Dynamics</i> , 2023, 41, 5614-5623.	3.5	1
11615	Modeling the Electronic Absorption Spectra of the Indocarbocyanine Cy3. <i>Molecules</i> , 2022, 27, 4062.	3.8	8

#	ARTICLE	IF	CITATIONS
11616	Effect of Functionalization with Potassium Atoms on the Electronic Properties of a 3D Glass-like Nanomaterial Reinforced with Carbon Nanotubes: In Silico Study. <i>Journal of Composites Science</i> , 2022, 6, 186.	3.0	1
11618	Scan-Find-Scan-Model: Discrete Site-Targeted Suppressor Design Strategy for Amyloid-Î². <i>ACS Chemical Neuroscience</i> , 2022, 13, 2191-2208.	3.5	2
11619	Molecular dynamics simulations of ovalbumin adsorption at squalene/water interface. <i>Chinese Journal of Chemical Engineering</i> , 2022, 50, 369-378.	3.5	1
11620	Antibody–nanobody combination increases their neutralizing activity against SARS-CoV-2 and nanobody H11-H4 is effective against Alpha, Kappa and Delta variants. <i>Scientific Reports</i> , 2022, 12, .	3.3	2
11621	Structural and electrophysiological basis for the modulation of KCNQ1 channel currents by ML277. <i>Nature Communications</i> , 2022, 13, .	12.8	15
11622	Atomistic insight into the luminal allosteric regulation of vesicular glutamate transporter 2 by chloride and protons: An <i>all-atom</i> molecular dynamics simulation study. <i>Proteins: Structure, Function and Bioinformatics</i> , 2022, 90, 2045-2057.	2.6	2
11623	Membrane fluidity, composition, and charge affect the activity and selectivity of the AMP ascapfin-8. <i>Biophysical Journal</i> , 2022, 121, 3034-3048.	0.5	2
11624	Surface segregation and relaxation in free-standing <i>Ni<sub>1-x</sub>Cu<sub>x</sub></i> alloy nanofilms. <i>Journal of Applied Physics</i> , 2022, 132, 035303.	2.5	1
11626	Highly efficient separation of benzene + cyclohexane mixtures by extraction combined extractive distillation using imidazolium-based dicationic ionic liquids. <i>Green Chemical Engineering</i> , 2023, 4, 312-323.	6.3	8
11627	A new approach used in docking study for predicting the combination drug efficacy in EML4-ALK target of NSCLC. <i>Journal of Biomolecular Structure and Dynamics</i> , 2023, 41, 5597-5613.	3.5	2
11628	Revealing the growth mechanism of sH hydrate by molecular simulations. <i>Journal of Molecular Liquids</i> , 2022, 363, 119873.	4.9	3
11629	Crystal structure of the Rubella virus protease reveals a unique papain-like protease fold. <i>Journal of Biological Chemistry</i> , 2022, 298, 102250.	3.4	4
11630	Biochemical characterization and structure-based <i>in silico</i> screening of potent inhibitor molecules against the 1 cys peroxiredoxin of bacterioferritin comigratory protein family from <i>Candidatus Liberibacter asiaticus</i> . <i>Journal of Biomolecular Structure and Dynamics</i> , 2023, 41, 5776-5788.	3.5	4
11631	Chemical and Morphological Structure of Transgenic Switchgrass Organosolv Lignin Extracted by Ethanol, Tetrahydrofuran, and Î³-Valerolactone Pretreatments. <i>ACS Sustainable Chemistry and Engineering</i> , 2022, 10, 9041-9052.	6.7	10
11632	The structural role of SARS-CoV-2 genetic background in the emergence and success of spike mutations: The case of the spike A222V mutation. <i>PLoS Pathogens</i> , 2022, 18, e1010631.	4.7	11
11633	Does an Ionomer Penetrate a Carbon Mesopore? Free-Energy Analysis Using Molecular Dynamics Simulations. <i>Journal of Physical Chemistry C</i> , 2022, 126, 11518-11528.	3.1	5
11634	TatA and TatB generate a hydrophobic mismatch important for the function and assembly of the Tat translocon in <i>Escherichia coli</i> . <i>Journal of Biological Chemistry</i> , 2022, 298, 102236.	3.4	4
11635	Andrographolide induces anti-SARS-CoV-2 response through host-directed mechanism: an <i>in silico</i> study. <i>Future Virology</i> , 2022, 17, 651-673.	1.8	13



#	ARTICLE	IF	CITATIONS
11636	Physical insight into the entropy-driven ion association. <i>Journal of Computational Chemistry</i> , 0, , .	3.3	1
11637	Phase diagram of the TIP4P/Ice water model by enhanced sampling simulations. <i>Journal of Chemical Physics</i> , 2022, 157, .	3.0	8
11638	In silico screening of some compounds derived from the desert medicinal plant <i>Rhazya stricta</i> for the potential treatment of COVID-19. <i>Scientific Reports</i> , 2022, 12, .	3.3	3
11639	Crystal Growth of Urea and Its Modulation by Additives as Analyzed by All-Atom MD Simulation and Solution Theory. <i>Journal of Physical Chemistry B</i> , 2022, 126, 5274-5290.	2.6	2
11641	Decoding the Effect of Hydrostatic Pressure on TRPV1 Lower-Gate Conformation by Molecular-Dynamics Simulation. <i>International Journal of Molecular Sciences</i> , 2022, 23, 7366.	4.1	3
11642	On the force field optimisation of $\beta$ -lactam cores using the force field Toolkit. <i>Journal of Computer-Aided Molecular Design</i> , 0, , .	2.9	0
11643	Molecular Dynamics in the Light of Non-equilibrium Thermodynamics. <i>Journal of the Physical Society of Japan</i> , 2022, 91, .	1.6	2
11645	Fragment-based inhibitor design for SARS-CoV2 main protease. <i>Structural Chemistry</i> , 2022, 33, 1467-1487.	2.0	1
11646	Polymer-ion interactions in PVDF@ionic liquid polymer electrolytes: A combined experimental and computational study. <i>Electrochimica Acta</i> , 2022, 427, 140831.	5.2	9
11648	Insights into the mechanism on the high-temperature activity of transglutaminase from <i>Bacillus clausii</i> and its crosslinked mode at protein level. <i>Biochemical Engineering Journal</i> , 2022, 185, 108544.	3.6	2
11649	Strategies for Controlling the Spatial Orientation of Single Molecules Tethered on DNA Origami Templates Physisorbed on Glass Substrates: Intercalation and Stretching. <i>International Journal of Molecular Sciences</i> , 2022, 23, 7690.	4.1	11
11650	How Shockwaves Open Tight Junctions of Blood-Brain Barrier: Comparison of Three Biomechanical Effects. <i>Journal of Physical Chemistry B</i> , 2022, 126, 5094-5102.	2.6	3
11651	CaMKII binds both substrates and activators at the active site. <i>Cell Reports</i> , 2022, 40, 111064.	6.4	15
11652	Interactions of boron nitride nanosheet with amino acids of differential polarity. <i>Scientific Reports</i> , 2022, 12, .	3.3	5
11656	Spectroscopic and Molecular Dynamics Aspect of Antimalarial Drug Hydroxychloroquine Binding with Human Telomeric G-Quadruplex. <i>Journal of Physical Chemistry B</i> , 2022, 126, 5241-5249.	2.6	7
11657	Highly Efficient Dye-Sensitized Solar Cells Based on Electrolyte Solutions Containing Choline Chloride/Ethylene Glycol Deep Eutectic Solvent: Electrolyte Optimization. <i>Industrial &amp; Engineering Chemistry Research</i> , 2022, 61, 11464-11473.	3.7	5
11658	Solubility of Organic Salts in Solvent-Antisolvent Mixtures: A Combined Experimental and Molecular Dynamics Simulations Approach. <i>Journal of Chemical Theory and Computation</i> , 2022, 18, 4952-4959.	5.3	3
11659	Autism-associated mutation in Hevin/Sparcl1 induces endoplasmic reticulum stress through structural instability. <i>Scientific Reports</i> , 2022, 12, .	3.3	8

#	ARTICLE	IF	CITATIONS
11660	Toward unveiling structure and property relationships from ionic ordering in Li/S battery electrolytes: Neutron total scattering and molecular dynamics simulations. <i>Energy Storage Materials</i> , 2022, 52, 85-93.	18.0	2
11661	A monomeric mycobacteriophage immunity repressor utilizes two domains to recognize an asymmetric DNA sequence. <i>Nature Communications</i> , 2022, 13, .	12.8	5
11662	Structure and Orientation of Water and Choline Chloride Molecules around a Methane Hydrophobe: A Computer Simulation Study. <i>ChemPhysChem</i> , 2022, 23, .	2.1	3
11663	Hydrophilic But Not Hydrophobic Surfactant Protein Genetic Variants Are Associated With Severe Acute Respiratory Syncytial Virus Infection in Children. <i>Frontiers in Immunology</i> , 0, 13, .	4.8	1
11664	Interrogating the substrate specificity landscape of UvrC reveals novel insights into its non-canonical function. <i>Biophysical Journal</i> , 2022, 121, 3103-3125.	0.5	4
11665	Heterogeneity and Nanostructure of Superconcentrated LiTFSI/EmimTFSI Hybrid Aqueous Electrolytes: Beyond the 21 m Limit of Water-in-Salt Electrolyte. <i>Journal of Physical Chemistry B</i> , 2022, 126, 5291-5304.	2.6	8
11666	Coarse-Grained Model Incorporating Short- and Long-Range Effective Potentials for the Fast Simulation of Micelle Formation in Solutions of Ionic Surfactants. <i>Journal of Physical Chemistry B</i> , 2022, 126, 5555-5569.	2.6	2
11667	Structural insight into the activation mechanism of MrgD with heterotrimeric Gi-protein revealed by cryo-EM. <i>Communications Biology</i> , 2022, 5, .	4.4	8
11668	Theoretical investigation on properties of CL-20/HMX cocrystal explosive with crystal defect by molecular dynamics method. <i>Theoretical Chemistry Accounts</i> , 2022, 141, .	1.4	1
11669	Ionic Liquid Decelerates Single-Stranded DNA Transport through Molybdenum Disulfide Nanopores. <i>ACS Applied Materials &amp; Interfaces</i> , 2022, 14, 32618-32624.	8.0	3
11670	Protein aggregation rate depends on mechanical stability of fibrillar structure. <i>Journal of Chemical Physics</i> , 2022, 157, .	3.0	6
11673	In Search of a Dynamical Vocabulary: A Pipeline to Construct a Basis of Shared Traits in Large-Scale Motions of Proteins. <i>Applied Sciences (Switzerland)</i> , 2022, 12, 7157.	2.5	1
11674	Modulation of global stability, ligand binding and catalytic properties of trypsin by anions. <i>Biophysical Chemistry</i> , 2022, 288, 106856.	2.8	3
11675	Cryo-EM structure of the human Kv3.1 channel reveals gating control by the cytoplasmic T1 domain. <i>Nature Communications</i> , 2022, 13, .	12.8	16
11676	Correlation between the binding affinity and the conformational entropy of nanobody SARS-CoV-2 spike protein complexes. <i>Proceedings of the National Academy of Sciences of the United States of America</i> , 2022, 119, .	7.1	11
11678	Comparative study of the unbinding process of some HTLV-1 protease inhibitors using unbiased molecular dynamics simulations. <i>PLoS ONE</i> , 2022, 17, e0263200.	2.5	1
11679	Interaction between Antimicrobial Peptide Magainin 2 and Nonlipid Components in the Bacterial Outer Envelope. <i>Journal of Physical Chemistry B</i> , 2022, 126, 5473-5480.	2.6	2
11680	Allosteric enhancement of the BCR-Abl1 kinase inhibition activity of nilotinib by cobinding of asciminib. <i>Journal of Biological Chemistry</i> , 2022, 298, 102238.	3.4	13

#	ARTICLE	IF	CITATIONS
11681	Modeling Gd <sup>3+</sup> Complexes for Molecular Dynamics Simulations: Toward a Rational Optimization of MRI Contrast Agents. <i>Inorganic Chemistry</i> , 2022, 61, 11837-11858.	4.0	3
11682	Effect of Cholesterol on C99 Dimerization: Revealed by Molecular Dynamics Simulations. <i>Frontiers in Molecular Biosciences</i> , 0, 9, .	3.5	2
11683	Bombyx mori Cecropin D could trigger cancer cell apoptosis by interacting with mitochondrial cardiolipin. <i>Biochimica Et Biophysica Acta - Biomembranes</i> , 2022, 1864, 184003.	2.6	7
11684	An Intelligent Strategy with All-Atom Molecular Dynamics Simulations for the Design of Lipopeptides against Multidrug-Resistant <i>Pseudomonas aeruginosa</i> . <i>Journal of Medicinal Chemistry</i> , 2022, 65, 10001-10013.	6.4	6
11685	Experimental and Computational Investigation of Clustering Behavior of Cyclodextrin-Perfluorocarbon Inclusion Complexes as Effective Histotripsy Agents. <i>Molecular Pharmaceutics</i> , 2022, 19, 2907-2921.	4.6	1
11686	Effect of hydrophile-lipophile balance of the linker in Gal/GalNAc ligands on high-affinity binding of galactosylated liposomes by the asialoglycoprotein receptor. <i>International Journal of Pharmaceutics</i> , 2022, 624, 121967.	5.2	5
11687	Induction of 2-hydroxycatecholestrogens O-methylation: A missing puzzle piece in diagnostics and treatment of lung cancer. <i>Redox Biology</i> , 2022, 55, 102395.	9.0	5
11688	Umbrella sampling with machine learning potentials applied for solid phase transition of GeSbTe. <i>Chemical Physics Letters</i> , 2022, 803, 139813.	2.6	2
11689	A second nearest-neighbor modified embedded-atom method combined with a charge equilibration interatomic potential for the Li-Ni-O ternary system and Li diffusion in lithium-ion battery cathode structure. <i>Journal of Power Sources</i> , 2022, 542, 231790.	7.8	2
11690	Evaluation of interaction between Ponceau 4R (P4R) and trypsin using kinetic, spectroscopic, and molecular dynamics simulation methods. <i>Journal of Molecular Liquids</i> , 2022, 362, 119761.	4.9	3
11691	Molecular simulation of methane hydrate growth confined into a silica pore. <i>Journal of Molecular Liquids</i> , 2022, 362, 119698.	4.9	4
11692	Molecular basis of the anchoring and stabilization of human islet amyloid polypeptide in lipid hydroperoxidized bilayers. <i>Biochimica Et Biophysica Acta - General Subjects</i> , 2022, 1866, 130200.	2.4	4
11693	Molecular simulation study on the stability of methane hydrate confined in slit-shaped pores. <i>Energy</i> , 2022, 257, 124738.	8.8	12
11694	Rationalizing the activity of a hybrid biocatalyst for ethanol oxidation. <i>Journal of Molecular Structure</i> , 2022, 1268, 133682.	3.6	1
11695	An efficient TSA catalyzed synthesis of some new substituted 5-hydroxy-3-phenylisoxazola-4-yl)-1,3-dimethyl-1H-chromeno[2,3-d]pyrimidine-2,4(3H,5H)-dione/3,3'-bipyridine-4,4'-dicarboxylic acid derivatives and evaluation of their pharmacological and computational investigations. <i>Journal of Molecular Structure</i> , 2022, 1267, 133587.	3.6	7
11696	In-silico functional and structural annotation of hypothetical protein from <i>Klebsiella pneumonia</i> : A potential drug target. <i>Journal of Molecular Graphics and Modelling</i> , 2022, 116, 108262.	2.4	23
11697	Exploring the multiple conformational states of RNA genome through interhelical dynamics and network analysis. <i>Journal of Molecular Graphics and Modelling</i> , 2022, 116, 108264.	2.4	1
11698	Dilithium phthalocyanine as electrolyte additive for the regulation of ion solvation and transport towards dendrite-free Li metal anodes. <i>Chemical Engineering Journal</i> , 2022, 450, 138112.	12.7	3

#	ARTICLE	IF	CITATIONS
11699	Structural requirements and interaction mechanisms of ACE inhibitory peptides: molecular simulation and thermodynamics studies on LAPYK and its modified peptides. Food Science and Human Wellness, 2022, 11, 1623-1630.	4.9	19
11700	Enhanced thermal stability of nanocrystalline Cu-Al alloy by nanotwin and nanoprecipitate. Journal of Alloys and Compounds, 2022, 922, 166273.	5.5	2
11701	CO2 storage behavior via forming hydrate from N2/CO2 gas mixtures in the presence of initial SI CO2 hydrate seeds. Chemical Engineering Journal, 2022, 450, 138001.	12.7	7
11702	Effect of Date Palm (Phoenix dactylifera) Phytochemicals on A $\beta$ 1-40 Amyloid Formation: An in-silico Analysis. Frontiers in Neuroscience, 0, 16, .	2.8	2
11703	Structural Basis of Mutation-Dependent p53 Tetramerization Deficiency. International Journal of Molecular Sciences, 2022, 23, 7960.	4.1	1
11704	Folate-Targeted Curcumin-Loaded Niosomes for Site-Specific Delivery in Breast Cancer Treatment: In Silico and In Vitro Study. Molecules, 2022, 27, 4634.	3.8	36
11706	Predicted Adsorption Affinity for Enteric Microbial Metabolites to Metal and Carbon Nanomaterials. Journal of Chemical Information and Modeling, 2022, 62, 3589-3603.	5.4	4
11709	Contrasting Effect of Salts on the Binding of Antimalarial Drug Hydroxychloroquine with Different Sequences of Duplex DNA. Journal of Physical Chemistry B, 2022, 126, 5605-5612.	2.6	2
11710	Effects of Lipid Shape and Interactions on the Conformation, Dynamics, and Curvature of Ultrasound-Responsive Liposomes. Pharmaceutics, 2022, 14, 1512.	4.5	2
11711	Free Energy Landscapes, Diffusion Coefficients, and Kinetic Rates from Transition Paths. Journal of Chemical Theory and Computation, 2022, 18, 4639-4648.	5.3	6
11713	Systematic simulation of the interactions of pleckstrin homology domains with membranes. Science Advances, 2022, 8, .	10.3	12
11714	Strain Sensitivity of $\text{Li}^+$ -ion Conductivity in $\text{PS}^3$ Electrolyte. , 2022, 1, .		4
11715	The Effect of Hydrogen Bonding on Polymerization Behavior of Monofunctional Vinyl Cyclopropane- $\alpha$ -Amides with Different Side Chains. Macromolecular Chemistry and Physics, 2022, 223, .	2.2	0
11718	Talin variant P229S compromises integrin activation and associates with multifaceted clinical symptoms. Human Molecular Genetics, 0, , .	2.9	2
11719	Structure-Function Relationships in Temperature Effects on Bacterial Luciferases: Nothing Is Perfect. International Journal of Molecular Sciences, 2022, 23, 8119.	4.1	2
11720	Ionic liquid solvation of proteins in native and denatured states. Journal of Molecular Liquids, 2022, 363, 119953.	4.9	5
11721	Preliminary Discovery of Small Molecule Inhibitors of Epidermal Growth Factor Receptor (EGFR) That Bind to the Extracellular Domain. Cancers, 2022, 14, 3647.	3.7	2
11722	Effects of interdiffusion on shear response of semi-coherent {111} interfaces in Ni/Cu. International Journal of Plasticity, 2022, 157, 103393.	8.8	5

#	ARTICLE	IF	CITATIONS
11723	Effect of Surface Hydrophobicity on the Adsorption of a Pilus-Derived Adhesin-like Peptide. <i>Langmuir</i> , 2022, 38, 9257-9265.	3.5	6
11724	Effect of hydration on intermolecular interactions in tetrabutylammonium chloride based deep eutectic solvents. <i>Journal of Molecular Liquids</i> , 2022, 363, 119959.	4.9	5
11725	Polymer affinity with quartz (1 0 1) surface in saline solutions: A molecular dynamics study. <i>Minerals Engineering</i> , 2022, 186, 107750.	4.3	3
11726	Insights of cationic diffusion in nickel-based honeycomb layered tellurates using molecular dynamics simulation. <i>Solid State Ionics</i> , 2022, 383, 115982.	2.7	0
11727	Understanding the role of water on temperature-dependent structural modifications of SARS CoV-2 main protease binding sites. <i>Journal of Molecular Liquids</i> , 2022, 363, 119867.	4.9	1
11728	A lateral electric field inhibits gel-to-fluid transition in lipid bilayers. <i>Soft Matter</i> , 2022, 18, 6437-6442.	2.7	2
11729	Photostabilization of ketoprofen by inclusion in glycyrrhizin micelles and gel nanoparticles. <i>New Journal of Chemistry</i> , 2022, 46, 17865-17873.	2.8	1
11730	Decoding regioselective reaction mechanism of gentisic acid catalyzed by the gentisate 1,2-dioxygenase enzyme. <i>Catalysis Science and Technology</i> , 2022, 12, 5742-5751.	4.1	1
11731	Conformational Analysis of Tyrosyl-Lysyl-Threonine Tripeptide Using MM, MD and QM Methods and Its Hyperpolarizability Study. <i>Sakarya University Journal of Science</i> , 0, , .	0.7	0
11732	Human TMPRSS2 non-catalytic ectodomain and SARS-CoV-2 S2' subunit interaction mediated SARS-CoV-2 endocytosis: a model proposal with virtual screening for potential drug molecules to inhibit this interaction. <i>Journal of Biomolecular Structure and Dynamics</i> , 0, , 1-12.	3.5	0
11734	Modeling Adsorption, Conformation, and Orientation of the Fis1 Tail Anchor at the Mitochondrial Outer Membrane. <i>Membranes</i> , 2022, 12, 752.	3.0	1
11735	Anomalous Infrared Absorbance of Sâ••O: A Perturbation Study of Î±-Câ••H/D. <i>Journal of Physical Chemistry B</i> , 2022, 126, 5490-5496.	2.6	2
11736	Synthesis of aminochalcones and <i>in silico</i> evaluation of their antiparasitic potential against <i>Leishmania</i>. <i>Journal of Biomolecular Structure and Dynamics</i> , 0, , 1-8.	3.5	2
11737	Extending the Martini 3 Coarse-Grained Force Field to Carbohydrates. <i>Journal of Chemical Theory and Computation</i> , 2022, 18, 5089-5107.	5.3	14
11738	Kinetic Characterization and Computational Modeling of <i>Escherichia coli</i> Heptosyltransferase II: Exploring the Role of Protein Dynamics in Catalysis for GT-B Glycosyltransferase. <i>Biochemistry</i> , 2022, 61, 1572-1584.	2.5	2
11739	A Computationalâ••Experimental Investigation of the Molecular Mechanism of Interleukin-6-Piperine Interaction. <i>International Journal of Molecular Sciences</i> , 2022, 23, 7994.	4.1	1
11740	Molecular dynamics study of hydroxide ion diffusion in polymer electrolytes. <i>Electrochemistry Communications</i> , 2022, 140, 107334.	4.7	3
11741	Composition-transferable machine learning potential for LiCl-KCl molten salts validated by high-energy x-ray diffraction. <i>Physical Review B</i> , 2022, 106, .	3.2	3

#	ARTICLE	IF	CITATIONS
11742	Finite-Size Effects in Simulations of Peptide/Lipid Assembly. <i>Journal of Membrane Biology</i> , 2022, 255, 437-449.	2.1	3
11743	Anti-apoptotic Bcl-2 protein in apo and holo conformation anchored to the membrane: comparative molecular dynamics simulations. <i>Journal of Biomolecular Structure and Dynamics</i> , 2023, 41, 6074-6088.	3.5	3
11744	Role of Enzyme and Active Site Conformational Dynamics in the Catalysis by Î±-Amylase Explored with QM/MM Molecular Dynamics. <i>Journal of Chemical Information and Modeling</i> , 2022, 62, 3638-3650.	5.4	7
11745	Molecular docking and molecular dynamic simulations of apoptosis proteins with potential anticancer compounds present in <i>Clinacanthus nutans</i> extract using gas chromatographyâ€“mass spectrometry. <i>Journal of Biomolecular Structure and Dynamics</i> , 2023, 41, 6104-6120.	3.5	2
11746	Assessing the effect of a liquid water layer on the adsorption of hydrate anti-agglomerants using molecular simulations. <i>Journal of Chemical Physics</i> , 2022, 157, .	3.0	2
11747	Water-Controlled Ketoâ€“Enol Tautomerization of a Prebiotic Nucleobase. <i>Journal of Physical Chemistry B</i> , 2022, 126, 5735-5743.	2.6	1
11748	Differences in ion-RNA binding modes due to charge density variations explain the stability of RNA in monovalent salts. <i>Science Advances</i> , 2022, 8, .	10.3	10
11749	Solvent Organization and Electrostatics Tuned by Solute Electronic Structure: Amide versus Non-Amide Carbonyls. <i>Journal of Physical Chemistry B</i> , 2022, 126, 5876-5886.	2.6	3
11750	Redox-Transition from Irreversible to Reversible Vitamin C by Pore Confinement in Microporous Carbon Network. <i>ACS Applied Materials &amp; Interfaces</i> , 2022, 14, 36557-36569.	8.0	5
11751	Conformer Selection Upon Dilution with Water: The Fascinating Case of Liquid Ethylene Glycol Studied via Molecular Dynamics Simulations**. <i>ChemistryOpen</i> , 2023, 12, .	1.9	2
11753	Polymyxins induce lipid scrambling and disrupt the homeostasis of Gram-negative bacteria membrane. <i>Biophysical Journal</i> , 2022, 121, 3486-3498.	0.5	7
11754	Insights into aggregation dynamics of <scp>NACore</scp> peptides from coarseâ€“grained simulations. <i>Proteins: Structure, Function and Bioinformatics</i> , 2023, 91, 16-21.	2.6	1
11755	Insight into the mechanism of DNA synthesis by human terminal deoxynucleotidyltransferase. <i>Life Science Alliance</i> , 2022, 5, e202201428.	2.8	1
11756	Coordination polymer design for fast proton conduction: hybrid atomistic approach based on kinetic Monte Carlo and molecular dynamics methods. <i>Materials and Design</i> , 2022, , 111094.	7.0	4
11757	Molecular modelling of antiproliferative inhibitors based on SMILES descriptors using Monte-Carlo method, docking, MD simulations and ADME/Tox studies. <i>Molecular Simulation</i> , 2022, 48, 1575-1591.	2.0	12
11758	Binding Models of AÎ²42 Peptide with Membranes Explored by Molecular Simulations. <i>Journal of Chemical Information and Modeling</i> , 2022, 62, 6482-6493.	5.4	6
11759	Unveiling the G4-PAMAM capacity to bind and protect Ang-(1-7) bioactive peptide by molecular dynamics simulations. <i>Journal of Computer-Aided Molecular Design</i> , 0, , .	2.9	3
11761	Mechanistic insight toward EGFR activation induced by ATP: role of mutations and water in ATP binding patterns. <i>Journal of Biomolecular Structure and Dynamics</i> , 2023, 41, 6492-6501.	3.5	4



#	ARTICLE	IF	CITATIONS
11762	Structural and dynamic mechanisms of GABAA receptor modulators with opposing activities. <i>Nature Communications</i> , 2022, 13, .	12.8	31
11763	Vacuum Interfacial Structure and X-ray Reflectivity of Imidazolium-Based Ionic Liquids with Perfluorinated Anions from a Theory and Simulations Perspective. <i>Journal of Physical Chemistry C</i> , 2022, 126, 13936-13945.	3.1	1
11765	Absolute binding free energies of mucroporin and its analog mucroporin-M1 with the heptad repeat 1 domain and RNA-dependent RNA polymerase of SARS-CoV-2. <i>Journal of Biomolecular Structure and Dynamics</i> , 2023, 41, 6957-6968.	3.5	1
11766	Molecular Dynamics of CYFIP2 Protein and Its R87C Variant Related to Early Infantile Epileptic Encephalopathy. <i>International Journal of Molecular Sciences</i> , 2022, 23, 8708.	4.1	2
11767	Effect of Solvent Quality on Structure and Dynamics of Lignin in Solution. <i>Journal of Physical Chemistry B</i> , 2022, 126, 5752-5764.	2.6	6
11768	Biodegradable Block Copolymerâ€™Tannic Acid Glue. <i>Jacs Au</i> , 2022, 2, 1978-1988.	7.9	4
11769	Phospholipid Monolayer/Graphene Interfaces: Curvature Effect on Lipid Morphology and Dynamics. <i>Journal of Physical Chemistry B</i> , 2022, 126, 6261-6270.	2.6	1
11770	Impact of Polydopamine Nanoparticle Surface Pattern and Roughness on Interactions with Poly(ethylene glycol) in Aqueous Solution: A Multiscale Modeling and Simulation Study. <i>Journal of Physical Chemistry B</i> , 2022, 126, 6301-6313.	2.6	1
11771	Identifying inhibitors of NSP16-NSP10 of SARS-CoV-2 from large databases. <i>Journal of Biomolecular Structure and Dynamics</i> , 2023, 41, 7045-7054.	3.5	2
11772	Effect of natural deep eutectic solvents of non-eutectic compositions on enzyme stability. <i>Journal of Molecular Liquids</i> , 2022, 366, 120180.	4.9	14
11774	Molecular dynamics insight into phase separation and transport in anion-exchange membranes: Effect of hydrophobicity of backbones. <i>Journal of Membrane Science</i> , 2022, 661, 120922.	8.2	28
11775	Identification of Novel AXL Kinase Inhibitors Using Ligand-Based Pharmacophore Screening and Molecular Dynamics Simulations. <i>Crystals</i> , 2022, 12, 1158.	2.2	1
11776	Phenol sensing in nature is modulated via a conformational switch governed by dynamic allostery. <i>Journal of Biological Chemistry</i> , 2022, 298, 102399.	3.4	4
11777	Free-Energy Landscape Analysis of Protein-Ligand Binding: The Case of Human Glutathione Transferase A1. <i>Applied Sciences (Switzerland)</i> , 2022, 12, 8196.	2.5	4
11778	Influence of Asphaltene Modification on Structure of P3HT/Asphaltene Blends: Molecular Dynamics Simulations. <i>Nanomaterials</i> , 2022, 12, 2867.	4.1	2
11779	Temperature- and pressure-dependence of the hydrogen bond network in plastic ice VII. <i>Journal of Chemical Physics</i> , 2022, 157, .	3.0	6
11780	Understanding the Stabilizing Effect of Histidine on mAb Aggregation: A Molecular Dynamics Study. <i>Molecular Pharmaceutics</i> , 2022, 19, 3288-3303.	4.6	18
11781	Antibacterial Activity and Mechanism of Action of Whey Protein-Îµ-Polylysine Complexes against <i>Staphylococcus aureus</i> and <i>Bacillus subtilis</i> . <i>Foods</i> , 2022, 11, 2311.	4.3	6

#	ARTICLE	IF	CITATIONS
11782	A Uniquely Stable Trimeric Model of SARS-CoV-2 Spike Transmembrane Domain. International Journal of Molecular Sciences, 2022, 23, 9221.	4.1	1
11783	Multiple Ensembles of the Hydrogen-Bonded Network in Ethylammonium Nitrate versus Water from Vibrational Spectral Dynamics of SCN-Probe. ChemPhysChem, 0, , .	2.1	0
11785	Unexpected structures formed by the kinase RET C634R mutant extracellular domain suggest potential oncogenic mechanisms in MEN2A. Journal of Biological Chemistry, 2022, 298, 102380.	3.4	0
11786	Impact of A2T and D23N mutations on C99 homodimer conformations. Journal of Chemical Physics, 2022, 157, 085102.	3.0	0
11787	Structure of a fully assembled tumor-specific T cell receptor ligated by pMHC. Cell, 2022, 185, 3201-3213.e19.	28.9	40
11788	Structure of SARS-CoV-2 membrane protein essential for virus assembly. Nature Communications, 2022, 13, .	12.8	70
11789	Well-Tempered Metadynamics Simulations Predict the Structural and Dynamic Properties of a Chiral 24-Atom Macrocyclic in Solution. ACS Omega, 2022, 7, 30291-30296.	3.5	9
11790	Lipid/water interface of galactolipid bilayers in different lyotropic liquid-crystalline phases. Frontiers in Molecular Biosciences, 0, 9, .	3.5	2
11791	G protein coupling and activation of the metabotropic GABAB heterodimer. Nature Communications, 2022, 13, .	12.8	7
11792	Discovery of promising cholinesterase inhibitors for Alzheimer's disease treatment through DFT, docking, and molecular dynamics studies of eugenol derivatives. Journal of the Chinese Chemical Society, 2022, 69, 1534-1551.	1.4	11
11793	Immunoinformatics-Aided Design and <i>In Vivo</i> Validation of a Peptide-Based Multiepitope Vaccine Targeting Canine Circovirus. ACS Pharmacology and Translational Science, 2022, 5, 679-691.	4.9	18
11794	Development of peptide ligands for the purification of $\alpha$ -1 antitrypsin from cell culture fluids. Journal of Chromatography A, 2022, 1679, 463363.	3.7	6
11795	Xenon and Krypton Dissolved in Water Form Nanoblobbs: No Evidence for Nanobubbles. Physical Review Letters, 2022, 129, .	7.8	3
11796	Exploring the Energy Landscape of Riboswitches Using Collective Variables Based on Tertiary Contacts. Journal of Molecular Biology, 2022, 434, 167788.	4.2	2
11797	Seasonal variation of the composition of essential oils from <i>Piper cernuum</i> Vell and <i>Piper rivinoides</i> Kunth, ADMET study, DFT calculations, molecular docking and dynamics studies of major components as potent inhibitors of the heterodimer methyltransferase complex NSP16-NSP10 SARS COV-2 protein. Journal of Biomolecular Structure and Dynamics, 2023, 41, 6326-6344.	3.5	4
11798	Exploring the binding kinetics and behaviors of self-aggregated beta-amyloid oligomers to phase-separated lipid rafts with or without ganglioside-clusters. Biophysical Chemistry, 2022, 290, 106874.	2.8	15
11800	Molecular Dynamics Modeling Based Investigation of the Effect of Freezing Rate on Lysozyme Stability. Pharmaceutical Research, 2022, 39, 2585-2596.	3.5	1
11801	ABCA1 is an extracellular phospholipid translocase. Nature Communications, 2022, 13, .	12.8	17

#	ARTICLE	IF	CITATIONS
11802	Refinement of the Optimized Potentials for Liquid Simulations Force Field for Thermodynamics and Dynamics of Liquid Alkanes. <i>Journal of Physical Chemistry B</i> , 2022, 126, 5896-5907.	2.6	6
11803	The effect of lipid composition on the dynamics of tau fibrils. <i>Proteins: Structure, Function and Bioinformatics</i> , 2022, 90, 2103-2115.	2.6	8
11804	The dynamics of metal nanoparticles on a supporting interacting substrate. <i>Journal of Chemical Physics</i> , 2022, 157, .	3.0	2
11805	The volume changes of unfolding of dsDNA. <i>Biophysical Journal</i> , 2022, , .	0.5	2
11806	Cationic lithium polysulfides in lithium–sulfur batteries. <i>Chem</i> , 2022, 8, 3031-3050.	11.7	42
11807	Molecular dynamics study on the role of Ar ions in the sputter deposition of Al thin films. <i>Journal of Applied Physics</i> , 2022, 132, 063302.	2.5	4
11808	In Vitro Evaluation of In Silico Screening Approaches in Search for Selective ACE2 Binding Chemical Probes. <i>Molecules</i> , 2022, 27, 5400.	3.8	1
11809	Molecular Simulations Matching Denaturation Experiments for N <sup>6</sup> -Methyladenosine. <i>ACS Central Science</i> , 2022, 8, 1218-1228.	11.3	3
11810	Synthesis, antileishmanial activity and molecular modeling of new 1-aryl/alkyl-3-benzoyl/cyclopropanoyl thiourea derivatives. <i>Molecular Diversity</i> , 0, , .	3.9	0
11812	The effect of heating rate on sintering mechanism of alumina nanoparticles. <i>Journal of the American Ceramic Society</i> , 2022, 105, 7149-7158.	3.8	4
11813	Coarse-Grained Molecular Dynamics Simulation of Cobalt Nanoparticle in the n-Octacosane–Water Mixture: The Effect of Water Concentration and Nanoparticle Size. <i>Journal of Physical Chemistry C</i> , 2022, 126, 13975-13985.	3.1	1
11814	Critical Thicknesses of Free-Standing Thin Films of Molten Polymers: A Multiscale Simulation Study. <i>Journal of Physical Chemistry B</i> , 2022, 126, 6500-6510.	2.6	3
11815	Structural basis for cannabinoid-induced potentiation of alpha1-glycine receptors in lipid nanodiscs. <i>Nature Communications</i> , 2022, 13, .	12.8	3
11816	Spectrin: an alternate target for cytoskeletal drugs. <i>Journal of Biomolecular Structure and Dynamics</i> , 2023, 41, 6534-6545.	3.5	1
11817	Activation of TMEM16F by inner gate charged mutations and possible lipid/ion permeation mechanisms. <i>Biophysical Journal</i> , 2022, 121, 3445-3457.	0.5	1
11818	Modeling of MT. P495, an mRNA-based vaccine against the phosphate-binding protein PstS1 of <i>Mycobacterium tuberculosis</i> . <i>Molecular Diversity</i> , 2023, 27, 1613-1632.	3.9	4
11819	Can Ammonia Be Used To Enhance the CO <sub>2</sub> Sequestration in Methane Hydrates: A Molecular Dynamics Perspective. <i>Energy &amp; Fuels</i> , 2022, 36, 10583-10590.	5.1	2
11820	The Flexible, Extended Coil of the PDZ-Binding Motif of the Three Deadly Human Coronavirus E Proteins Plays a Role in Pathogenicity. <i>Viruses</i> , 2022, 14, 1707.	3.3	3

#	ARTICLE	IF	CITATIONS
11821	Analgesic $\hat{\pm}$ -Conotoxin Binding Site on the Human GABA <sub>B</sub> Receptor. <i>Molecular Pharmacology</i> , 2022, 102, 196-208.	2.3	3
11822	Structural Evolution of Delta (B.1.617.2) and Omicron (BA.1) Spike Glycoproteins. <i>International Journal of Molecular Sciences</i> , 2022, 23, 8680.	4.1	7
11823	Des3PI: a fragment-based approach to design cyclic peptides targeting protein-protein interactions. <i>Journal of Computer-Aided Molecular Design</i> , 2022, 36, 605-621.	2.9	5
11824	Atomic-Level View of the Functional Transition in Vertebrate Hemoglobins: The Case of Antarctic Fish Hbs. <i>Journal of Chemical Information and Modeling</i> , 2022, 62, 3874-3884.	5.4	0
11825	Insight on the interaction between the scorpion toxin blocker Discrepin on potassium voltage-gated channel Kv4.3 by molecular dynamics simulations. <i>Journal of Biomolecular Structure and Dynamics</i> , 2023, 41, 6272-6281.	3.5	1
11827	A Molecular Dynamics Study of Antimicrobial Peptide Interactions with the Lipopolysaccharides of the Outer Bacterial Membrane. <i>Journal of Membrane Biology</i> , 2022, 255, 665-675.	2.1	10
11829	The Effects of Cholesterol Oxidation on Erythrocyte Plasma Membranes: A Monolayer Study. <i>Membranes</i> , 2022, 12, 828.	3.0	4
11830	Substrate spectrum of PPM1D in the cellular response to DNA double-strand breaks. <i>IScience</i> , 2022, 25, 104892.	4.1	4
11831	Monitoring lipid phase transition temperatures using fluorescent probes and temperature-dependent fluorescence spectroscopy. <i>Dyes and Pigments</i> , 2022, 206, 110621.	3.7	2
11832	Computational approach for building QSAR models for inhibition of HIF-1A. <i>Journal of the Indian Chemical Society</i> , 2022, 99, 100687.	2.8	1
11833	The use of 1-ethyl-3-methylimidazolium iodide ionic liquid in dye sensitized solar cells: A joint experimental and computational perspective. <i>Journal of Molecular Liquids</i> , 2022, 364, 119982.	4.9	4
11834	Impact of arginine modified SNARE peptides on interactions with phospholipid bilayers and coiled-coil formation: A molecular dynamics study. <i>Journal of Molecular Liquids</i> , 2022, 364, 119972.	4.9	0
11835	Single-asperity failure mechanism driven by morphology and multiaxial loading using molecular dynamics simulation. <i>Computational Materials Science</i> , 2022, 213, 111671.	3.0	1
11836	The effect of collectors on froth stability of frother: Atomic-scale study by experiments and molecular dynamics simulations. <i>Journal of Molecular Liquids</i> , 2022, 364, 120035.	4.9	5
11837	Siamenflavones A-C, three undescribed biflavonoids from <i>Selaginella siamensis</i> Hieron. and biflavonoids from spike mosses as EGFR inhibitor. <i>Phytochemistry</i> , 2022, 203, 113374.	2.9	5
11838	Molecular dynamics simulation study of covalently bound hybrid coagulants (CBHyC): Molecular structure and coagulation mechanisms. <i>Chemosphere</i> , 2022, 307, 135863.	8.2	1
11839	X-ray scattering and molecular dynamics simulations reveal the secondary structure of $\hat{\pm}$ -carrageenan in the solution state. <i>Carbohydrate Polymers</i> , 2022, 296, 119958.	10.2	4
11840	Baicalein exhibits differential effects and mechanisms towards disruption of $\hat{\pm}$ -synuclein fibrils with different polymorphs. <i>International Journal of Biological Macromolecules</i> , 2022, 220, 316-325.	7.5	11

#	ARTICLE	IF	CITATIONS
11841	Nano-sized single-asperity friction behavior: Insight from molecular dynamics simulations. <i>European Journal of Mechanics, A/Solids</i> , 2022, 96, 104760.	3.7	4
11842	Molecular-level solvation and selectivity behavior of Na <sup>+</sup> , K <sup>+</sup> , and Li <sup>+</sup> within glycerol-derived solvents. <i>Chemical Engineering Science</i> , 2022, 262, 117992.	3.8	1
11843	Anionic lipids induce a fold-unfold transition in the membrane-translocating Engrailed homeodomain. <i>Biochimica Et Biophysica Acta - Biomembranes</i> , 2022, 1864, 184030.	2.6	1
11844	Effects of thermostats/barostats on physical properties of liquids by molecular dynamics simulations. <i>Journal of Molecular Liquids</i> , 2022, 365, 120116.	4.9	67
11845	Effect of molecular structure and ionization state on aggregation of carboxymethyl chitosan: A molecular dynamics study. <i>Carbohydrate Polymers</i> , 2022, 297, 119993.	10.2	7
11846	Computational study of the conformational ensemble of CX3C chemokine receptor 1 (CX3CR1) and its interactions with antagonist and agonist ligands. <i>Journal of Molecular Graphics and Modelling</i> , 2022, 117, 108278.	2.4	1
11847	Molecular insights into the self-assembly of hydrophobically modified chondroitin sulfate in aqueous media. <i>Carbohydrate Polymers</i> , 2022, 297, 119999.	10.2	5
11848	Dipeptides as environmentally friendly CH <sub>4</sub> hydrate inhibitors: Experimental and computational approaches. <i>Fuel</i> , 2022, 329, 125479.	6.4	6
11849	Theoretical study on the stability mechanism of a high energy system composed of molecules containing C O C or N <sub>3</sub> groups and aluminum hydride. <i>Applied Surface Science</i> , 2022, 604, 154509.	6.1	1
11850	Molecular modelling of ionic liquids: General guidelines on fixed-charge force fields for balanced descriptions. <i>Journal of Ionic Liquids</i> , 2022, 2, 100043.	2.7	13
11851	Molecular dynamics simulations to study the role of biphenylalanine in promoting the antibacterial activity of ultrashort peptides. <i>Journal of Molecular Graphics and Modelling</i> , 2022, 117, 108282.	2.4	0
11852	Identification of new anti-cancer agents against CENTERIN: Structure-based virtual screening, AutoDock and binding free energy studies. <i>Journal of Molecular Structure</i> , 2022, 1270, 133952.	3.6	2
11853	4-Dimethylamino-beta-nitrostyrene, a fluorescent solvatochromic probe to estimate the apparent dielectric constant in serum albumin: Experimental and molecular dynamics studies. <i>Journal of Photochemistry and Photobiology A: Chemistry</i> , 2022, 433, 114197.	3.9	3
11854	Towards predicting liquid fuel physicochemical properties using molecular dynamics guided machine learning models. <i>Fuel</i> , 2022, 329, 125415.	6.4	8
11855	Molecular simulations of fluoxetine in hydrated lipid bilayers, as well as in aqueous solutions containing $\beta$ -cyclodextrin. <i>Journal of Molecular Graphics and Modelling</i> , 2022, 117, 108305.	2.4	2
11856	The fate of aggregated graphene oxide upon the increasing of pH: An experimental and molecular dynamic study. <i>Science of the Total Environment</i> , 2022, 851, 157954.	8.0	2
11857	Superhydrophilicity of $\gamma$ -alumina surfaces results from tight binding of interfacial waters to specific aluminols. <i>Journal of Colloid and Interface Science</i> , 2022, 628, 943-954.	9.4	7
11858	A colloidal aqueous electrolyte modulated by oleic acid for durable zinc metal anode. <i>Chemical Engineering Journal</i> , 2023, 451, 138589.	12.7	25

#	ARTICLE	IF	CITATIONS
11859	Iterative Landmark-Based Umbrella Sampling (ILBUS) Protocol for Sampling of Conformational Space of Biomolecules. Journal of Chemical Information and Modeling, 2022, 62, 4783-4798.	5.4	2
11861	Molecular modelling, DFT, molecular dynamics simulations, synthesis and antimicrobial potential studies of heterocyclic nucleoside mimetics. Journal of Molecular Structure, 2022, , 134071.	3.6	2
11862	Photoswitchable, Waterâ€Soluble Bisazobenzene Crossâ€Linkers with Enhanced Properties for Biological Applications. ChemPhotoChem, 2022, 6, .	3.0	2
11863	Dialkyl carbonates enforce energy storage as new dielectric liquids. Journal of Molecular Liquids, 2022, 367, 120454.	4.9	3
11864	Understanding the effect of nitrosylation on dynamics of human epidermal growth factor: a Âµs simulation study. Journal Physics D: Applied Physics, 2022, 55, 475201.	2.8	4
11865	Virtual screening and molecular dynamic study of potential new binders to mTOR. Journal of Molecular Modeling, 2022, 28, .	1.8	1
11866	Calix[4]areneâ€Based Sensitizers for Hostâ€Guest Supramolecular Dyads for Solar Energy Conversion in Photoelectrochemical Cells.. European Journal of Organic Chemistry, 2022, 2022, .	2.4	4
11868	Calculation of Heat Capacity Changes in Enzyme Catalysis and Ligand Binding. Journal of Chemical Theory and Computation, 2022, 18, 6345-6353.	5.3	7
11869	<scp>SARSâ€CoV</scp>â€2 spike protein aggregation is triggered by bacterial lipopolysaccharide. FEBS Letters, 2022, 596, 2566-2575.	2.8	7
11870	Observation of H<sub>2</sub> Evolution and Electrolyte Diffusion on MoS<sub>2</sub> Monolayer by In Situ Liquidâ€Phase Transmission Electron Microscopy. Advanced Materials, 2022, 34, .	21.0	16
11871	Anticancer drugs tamoxifen and 4hydroxytamoxifen as effectors of phosphatidylethanolamine lipid polymorphism. Chemistry and Physics of Lipids, 2022, 248, 105239.	3.2	1
11872	Computational exploration of the dual role of the phytochemical fortunellin: Antiviral activities against SARS-CoV-2 and immunomodulatory abilities against the host. Computers in Biology and Medicine, 2022, 149, 106049.	7.0	3
11873	Structures of Streptococcus pyogenes class A sortase in complex with substrate and product mimics provide key details of target recognition. Journal of Biological Chemistry, 2022, 298, 102446.	3.4	8
11874	Effect of electric field intensity on electrophoretic migration and deformation of oil droplets in O/W emulsion under DC electric field: A molecular dynamics study. Chemical Engineering Science, 2022, 262, 118034.	3.8	9
11875	Trifluoroethanol direct interactions with protein backbones destabilize Î±-helices. Journal of Molecular Liquids, 2022, 365, 120209.	4.9	4
11876	Disjoining pressure of room temperature ionic liquid in charged slit carbon nanopore: Molecular dynamics study. Journal of Molecular Liquids, 2022, 366, 120307.	4.9	6
11877	Site selective analysis of water in hydrogen bond network of aqueous dimethyl sulfoxide solutions by oxygen K-edge X-ray absorption spectroscopy. Journal of Molecular Liquids, 2022, 366, 120310.	4.9	1
11878	On the structure and stability of novel cationic DPPC liposomes doped with gemini surfactants. Journal of Molecular Liquids, 2022, 366, 120230.	4.9	5



#	ARTICLE	IF	CITATIONS
11879	On the role of alkanethiol Au complex in the formation of gold deposits; an in-silico approach. <i>Chemical Geology</i> , 2022, 610, 121101.	3.3	2
11880	Distinct mode of membrane interaction and disintegration by diverse class of antimicrobial peptides. <i>Biochimica Et Biophysica Acta - Biomembranes</i> , 2022, 1864, 184047.	2.6	2
11881	The effect of Ni content on phase transformation behavior of NiTi alloys: An atomistic modeling study. <i>Computational Materials Science</i> , 2022, 215, 111804.	3.0	7
11882	HIV-1 protease with 10 lopinavir and darunavir resistance mutations exhibits altered inhibition, structural rearrangements and extreme dynamics. <i>Journal of Molecular Graphics and Modelling</i> , 2022, 117, 108315.	2.4	2
11883	The concealed solid-solid structural phase transition of Fe70Ni10Cr20 under high pressure. <i>Materials Today Communications</i> , 2022, 33, 104499.	1.9	1
11884	First-principles calculations study of TiS2/Ti2CS2 heterostructure as an anode material for Li/Na/K-ion batteries. <i>Computational Materials Science</i> , 2022, 215, 111784.	3.0	6
11885	Molecular dynamics simulation of model asphaltenes between surfaces of varying polarity. <i>Fuel</i> , 2023, 331, 125842.	6.4	9
11886	GenEvaPa: A generic evaporation package for modeling evaporation in molecular dynamics simulations. <i>Computer Physics Communications</i> , 2023, 282, 108539.	7.5	2
11887	Computational and structural investigation of Palmitoyl-Protein Thioesterase 1 (PPT1) protein causing Neuronal Ceroid Lipofuscinoses (NCL). <i>Advances in Protein Chemistry and Structural Biology</i> , 2022, , 89-109.	2.3	2
11888	Unveiling molecular details behind improved activity at neutral to alkaline pH of an engineered DyP-type peroxidase. <i>Computational and Structural Biotechnology Journal</i> , 2022, 20, 3899-3910.	4.1	5
11889	Estimating the binding energetics of reversible covalent inhibitors of the SARS-CoV-2 main protease: an <i>in silico</i> study. <i>Physical Chemistry Chemical Physics</i> , 2022, 24, 23391-23401.	2.8	2
11890	Energy landscapes in inorganic chemistry. , 2023, , 262-392.		2
11891	Molecular Mechanisms of Ph-Tunable Stability and Surface Coverage of Polypeptide Films. <i>SSRN Electronic Journal</i> , 0, , .	0.4	0
11892	Tailoring the interaction between a gold nanocluster and a fluorescent dye by cluster size: creating a toolbox of range-adjustable pH sensors. <i>Nanoscale Advances</i> , 2022, 4, 4579-4588.	4.6	6
11893	Determination of specific and non-specific proteinâ€“protein interactions for beta-lactoglobulin by analytical ultracentrifugation and membrane osmometry experiments. <i>Soft Matter</i> , 2022, 18, 6739-6756.	2.7	2
11894	Computational design and characterization of a multiepitope vaccine against carbapenemase-producing <i>Klebsiella pneumoniae</i> strains, derived from antigens identified through reverse vaccinology. <i>Computational and Structural Biotechnology Journal</i> , 2022, 20, 4446-4463.	4.1	6
11895	Information-theoretical measures identify accurate low-resolution representations of protein configurational space. <i>Soft Matter</i> , 2022, 18, 7064-7074.	2.7	3
11896	Dynamic effects of the spine of hydrated magnesium on viral RNA pseudoknot structure. <i>Physical Chemistry Chemical Physics</i> , 2022, 24, 24570-24581.	2.8	5

#	ARTICLE	IF	CITATIONS
11897	Computational modeling of potential milciclib derivatives inhibitor-CDK2 binding through global docking and accelerated molecular dynamics simulations. Informatics in Medicine Unlocked, 2022, 33, 101069.	3.4	4
11898	A predicted orthogonal semimetallic carbon with negative thermal expansion and compressibility. Physical Chemistry Chemical Physics, 2022, 24, 23497-23506.	2.8	2
11899	Interaction between two polyelectrolytes in monovalent aqueous salt solutions. Physical Chemistry Chemical Physics, 2022, 24, 21112-21121.	2.8	2
11900	Non-monotonic composition dependence of the breakdown of Stokes-Einstein relation for water in aqueous solutions of ethanol and 1-propanol: explanation using translational jump-diffusion approach. Physical Chemistry Chemical Physics, 2022, 24, 18738-18750.	2.8	10
11901	Morphology of conducting polymer blends at the interface of conducting and insulating phases: insight from PEDOT:PSS atomistic simulations. Journal of Materials Chemistry C, 2022, 10, 16126-16137.	5.5	8
11902	Assessing the impact of valence asymmetry in ionic solutions and its consequences on the performance of supercapacitors. Physical Chemistry Chemical Physics, 2022, 24, 20445-20453.	2.8	0
11903	Structure and diffusive dynamics of aspartate $\pm$ -decarboxylase (ADC) liganded with $\alpha$ -serine in aqueous solution. Physical Chemistry Chemical Physics, 2022, 24, 20336-20347.	2.8	1
11904	Mechanistic regulation of $\beta$ -secretase by their substrates. Physical Chemistry Chemical Physics, 2022, 24, 19223-19232.	2.8	1
11905	Mechanistic insights into the mitigation of $A\beta$ aggregation and protofibril destabilization by $\alpha$ -enantiomeric decapeptide rk10. Physical Chemistry Chemical Physics, 2022, 24, 21975-21994.	2.8	8
11906	Molecular dynamics simulations of cyanine dimers attached to DNA Holliday junctions. RSC Advances, 2022, 12, 28063-28078.	3.6	6
11907	The destructive mechanism of $A\beta_{1-42}$ protofibrils by norepinephrine revealed via molecular dynamics simulations. Physical Chemistry Chemical Physics, 2022, 24, 19827-19836.	2.8	6
11908	Atomistic Simulation of Shear Deformation at Bcc-Fe Grain Boundary and Precipitation Strengthening by Cr23c6. SSRN Electronic Journal, 0, , .	0.4	0
11909	Slag Structure of High Alumina Blast Furnace Slag. , 2022, , 43-76.		0
11910	Molecular dynamics analysis of the structural properties of the transglutaminases of Kutzneria albida and Streptomyces mobaraensis. Computational and Structural Biotechnology Journal, 2022, 20, 3924-3934.	4.1	3
11911	Deciphering the origin of the melting profile of unilamellar phosphatidylcholine liposomes by measuring the turbidity of its suspensions. Soft Matter, 2022, 18, 6703-6715.	2.7	9
11912	Liposome Deformation Induced by Random Coil and $\pm$ -Helical Peptides. SSRN Electronic Journal, 0, , .	0.4	0
11913	Understanding the structure-band gap relationship in $SrZrS_3$ at elevated temperatures: a detailed NPT MD study. Journal of Materials Chemistry C, 2022, 10, 12032-12042.	5.5	5
11914	Finite temperature string method with umbrella sampling using path collective variables: application to secondary structure change in a protein. Soft Matter, 2022, 18, 7593-7603.	2.7	7

#	ARTICLE	IF	CITATIONS
11915	Molecular dynamics simulation study of adsorption of anionic/nonionic surfactants at oil/water interfaces. RSC Advances, 2022, 12, 27330-27343.	3.6	6
11916	Does the inclusion of electronic polarisability lead to a better modelling of peptide aggregation?. RSC Advances, 2022, 12, 20829-20837.	3.6	3
11917	Site-specific water dynamics in the first hydration layer of an anti-freeze glyco-protein: a simulation study. Physical Chemistry Chemical Physics, 2022, 24, 21165-21177.	2.8	2
11918	Ligand-based pharmacophore modeling, molecular docking, and molecular dynamic studies of HMG-CoA reductase inhibitors. Informatics in Medicine Unlocked, 2022, 32, 101063.	3.4	0
11919	Mechanistic insight into the disruption of Tau R3/R4 protofibrils by curcumin and epinephrine: an all-atom molecular dynamics study. Physical Chemistry Chemical Physics, 2022, 24, 20454-20465.	2.8	13
11920	Binding properties of the anti-TB drugs bedaquiline and TBAJ-876 to a mycobacterial F-ATP synthase. Current Research in Structural Biology, 2022, 4, 278-284.	2.2	6
11921	Investigation of the binding behavior of bioactive 7-methoxyflavone to human serum albumin by coupling multi-spectroscopic with computational approaches. Spectrochimica Acta - Part A: Molecular and Biomolecular Spectroscopy, 2023, 285, 121920.	3.9	0
11922	Molecular dynamics simulations of CH <sub>4</sub> /CO <sub>2</sub> hydrates nucleation in kaolinite particles. Applied Surface Science, 2023, 607, 154911.	6.1	8
11923	Molecular dynamic simulations of methane hydrate formation between solid surfaces: Implications for methane storage. Energy, 2023, 262, 125511.	8.8	13
11924	Molecular dynamics simulation and machine learning for predicting hydrogen solubility in water: Effects of temperature, pressure, finite system size and choice of molecular force fields. Chemical Physics, 2023, 564, 111725.	1.9	4
11925	Structure of POPC Lipid Bilayers in OPLS3e Force Field. Journal of Chemical Information and Modeling, 2022, 62, 6462-6474.	5.4	13
11926	Computational Assessment of Xanthenes from African Medicinal Plants as Aldose Reductase Inhibitors. Computation, 2022, 10, 146.	2.0	5
11928	QM/MM Simulations for the Broken-Symmetry Catalytic Reaction Mechanism of Human Arginase I. ACS Omega, 2022, 7, 32536-32548.	3.5	0
11930	Structural basis of ion uptake in copper-transporting P1B-type ATPases. Nature Communications, 2022, 13, .	12.8	6
11931	All-Atom Simulations Elucidate the Impact of U2AF2 Cancer-Associated Mutations on Pre-mRNA Recognition. Journal of Chemical Information and Modeling, 2022, 62, 6691-6703.	5.4	9
11932	Applications of Molecular Dynamics Simulation in Protein Study. Membranes, 2022, 12, 844.	3.0	18
11933	MDO: A Computational Protocol for Prediction of Flexible Enzyme-Ligand Binding Mode. Current Computer-Aided Drug Design, 2022, 18, .	1.2	0
11934	New pyrazolylpyrazoline derivatives as dual acting antimalarial-antileishmanial agents: synthesis, biological evaluation and molecular modelling simulations. Journal of Enzyme Inhibition and Medicinal Chemistry, 2022, 37, 2320-2333.	5.2	12

#	ARTICLE	IF	CITATIONS
11935	Lipid Modulation of a Class B GPCR: Elucidating the Modulatory Role of PI(4,5)P <sub>2</sub> Lipids. Journal of Chemical Information and Modeling, 2022, 62, 6788-6802.	5.4	9
11936	The Transport Properties of Semi-Crystalline Polyetherimide BPDA-P3 in Amorphous and Ordered States: Computer Simulations. Membranes, 2022, 12, 856.	3.0	4
11937	Local Structure of DMF-Water Mixtures, as Seen from Computer Simulations and Voronoi Analysis. Journal of Physical Chemistry B, 2022, 126, 6964-6978.	2.6	4
11938	mRNA lipid nanoparticle phase transition. Biophysical Journal, 2022, 121, 3927-3939.	0.5	17
11939	Comparative Interaction Studies of Quercetin with 2-Hydroxyl-propyl- $\beta$ -cyclodextrin and 2,6-Methylated- $\beta$ -cyclodextrin. Molecules, 2022, 27, 5490.	3.8	7
11940	Teixobactin kills bacteria by a two-pronged attack on the cell envelope. Nature, 2022, 608, 390-396.	27.8	60
11941	Acarbose potentially binds to the type I peptide deformylase catalytic site and inhibits bacterial growth: An in silico and in vitro study. Current Pharmaceutical Design, 2022, 28, .	1.9	2
11942	Molecular insights into the interaction of apo-lactoferrin with the receptor binding domain of the SARS-CoV-2 spike protein: a molecular dynamics simulation study. Journal of Biomolecular Structure and Dynamics, 2023, 41, 7372-7385.	3.5	0
11943	Water regulates the residence time of Benzamidine in Trypsin. Nature Communications, 2022, 13, .	12.8	19
11944	The clinical drug candidate anle138b binds in a cavity of lipidic $\beta$ -synuclein fibrils. Nature Communications, 2022, 13, .	12.8	17
11945	Synthesis of pH-responsive dimethylglycine surface-modified branched lipids for targeted delivery of antibiotics. Chemistry and Physics of Lipids, 2022, 249, 105241.	3.2	1
11947	Characterisation of HOIP RBR E3 ligase conformational dynamics using integrative modelling. Scientific Reports, 2022, 12, .	3.3	0
11948	Charged Small Molecule Binding to Membranes in MD Simulations Evaluated against NMR Experiments. Journal of Physical Chemistry B, 2022, 126, 6955-6963.	2.6	3
11949	Formation Mechanism of Inter-Crosslink in DNA by Nitrogen Oxides Pollutants through A Diazonium Intermediate. International Journal of Molecular Sciences, 2022, 23, 10621.	4.1	1
11950	Identification of Potential Allosteric Site Binders of Indoleamine 2,3-Dioxygenase 1 from Plants: A Virtual and Molecular Dynamics Investigation. Pharmaceuticals, 2022, 15, 1099.	3.8	0
11951	Quantum Biochemistry and MM-PBSA Description of the ZIKV NS2B-NS3 Protease: Insights into the Binding Interactions beyond the Catalytic Triad Pocket. International Journal of Molecular Sciences, 2022, 23, 10088.	4.1	3
11952	Computational Analysis of Natural Compounds as Potential Isocitrate Dehydrogenase 1 Inhibitor for the Treatment of Ovarian Cancer. Springer Protocols, 2023, , 427-442.	0.3	0
11953	Hybrid <i>in vitro/in silico</i> analysis of low-affinity protein-protein interactions that regulate signal transduction by <i>Sema6D</i> . Protein Science, 0, , .	7.6	3

#	ARTICLE	IF	CITATIONS
11954	All-Atom Simulations Uncover Structural and Dynamical Properties of STING Proteins in the Membrane System. <i>Journal of Chemical Information and Modeling</i> , 2022, 62, 4486-4499.	5.4	2
11955	Study of tyramine-binding mechanism and insecticidal activity of oil extracted from Eucalyptus against <i>Sitophilus oryzae</i> . <i>Frontiers in Chemistry</i> , 0, 10, .	3.6	3
11956	Thermokinetic stabilisation of nanocrystalline Cu by ternary approach. <i>Philosophical Magazine</i> , 0, , 1-16.	1.6	0
11957	The Structures of Heterogeneous Membranes and Their Interactions with an Anticancer Peptide: A Molecular Dynamics Study. <i>Life</i> , 2022, 12, 1473.	2.4	4
11958	Effectiveness of Remdesivir in Comparison with Five Approved Antiviral Drugs for Inhibition of RdRp in Combat with SARS-CoV-2. <i>Iranian Journal of Science and Technology, Transaction A: Science</i> , 0, , .	1.5	0
11959	Fine adjustments of thermo-vibrations between residues surrounding the active center in protein using dual artificial intelligence approaches and computer simulations. <i>AIP Advances</i> , 2022, 12, .	1.3	1
11960	Benchmarking coarse-grained models of organic semiconductors via deep backmapping. <i>Frontiers in Chemistry</i> , 0, 10, .	3.6	3
11961	Prediction of Aptamerâ€“Small-Molecule Interactions Using Metastable States from Multiple Independent Molecular Dynamics Simulations. <i>Journal of Chemical Information and Modeling</i> , 2022, 62, 4799-4809.	5.4	3
11962	Scalable Constant pH Molecular Dynamics in GROMACS. <i>Journal of Chemical Theory and Computation</i> , 2022, 18, 6148-6160.	5.3	40
11963	Multiconfigurational SCF and Short-Range DFT Combined with Polarizable Density Embedding: Comparison of Linear-Response and State-Specific Solvatochromic Shifts of Acrolein and <i>p</i> -nitrophenolate in Water. <i>Journal of Chemical Theory and Computation</i> , 2022, 18, 6231-6239.	5.3	2
11964	Identifying the Template for Oligomer to Fibril Conversion for Amyloidâ€“ $\beta$ (1â€“42) Oligomers using Hamiltonian Replica Exchange Molecular Dynamics. <i>ChemPhysChem</i> , 0, , .	2.1	0
11966	Gene expression profile analysis unravelled the systems level association of renal cell carcinoma with diabetic nephropathy and Matrix-metalloproteinase-9 as a potential therapeutic target. <i>Journal of Biomolecular Structure and Dynamics</i> , 2023, 41, 7535-7550.	3.5	0
11967	Erythro-PmBs: A Selective Polymyxin B Delivery System Using Antibody-Conjugated Hybrid Erythrocyte Liposomes. <i>ACS Infectious Diseases</i> , 2022, 8, 2059-2072.	3.8	8
11969	Conformational Heterogeneity and Interchain Percolation Revealed in an Amorphous Conjugated Polymer. <i>ACS Nano</i> , 2022, 16, 14432-14442.	14.6	4
11970	Phytochemical Investigation of Egyptian Spinach Leaves, a Potential Source for Antileukemic Metabolites: In Vitro and In Silico Study. <i>Revista Brasileira De Farmacognosia</i> , 2022, 32, 774-785.	1.4	1
11971	Capturing the Liquid-Crystalline Phase Transformation: Implications for Protein Targeting to Sterol Ester-Rich Lipid Droplets. <i>Membranes</i> , 2022, 12, 949.	3.0	2
11973	Role of an Ice Surface in the Photoreaction of Coumarins. <i>Langmuir</i> , 2022, 38, 11346-11353.	3.5	3
11974	Best Practices in Constant pH MD Simulations: Accuracy and Sampling. <i>Journal of Chemical Theory and Computation</i> , 2022, 18, 6134-6147.	5.3	14

#	ARTICLE	IF	CITATIONS
11975	Ultralight supertetrahedral aluminum: Stability at various temperatures. MRS Bulletin, 0, ,	3.5	0
11976	Copper binding leads to increased dynamics in the regulatory N-terminal domain of full-length human copper transporter ATP7B. PLoS Computational Biology, 2022, 18, e1010074.	3.2	3
11977	A novel phenolic derivative inhibits AHL-dependent quorum sensing signaling in Pseudomonas aeruginosa. Frontiers in Pharmacology, 0, 13, .	3.5	6
11978	Atomic Insights into Amyloid-Induced Membrane Damage. ACS Chemical Neuroscience, 2022, 13, 2766-2777.	3.5	5
11980	Accurate p <i>K<sub>a</sub></i> Calculations in Proteins with Reactive Molecular Dynamics Provide Physical Insight Into the Electrostatic Origins of Their Values. Journal of Physical Chemistry B, 2022, 126, 7321-7330.	2.6	2
11981	Melatonin Inhibits hIAPP Oligomerization by Preventing $\beta$ -Sheet and Hydrogen Bond Formation of the Amyloidogenic Region Revealed by Replica-Exchange Molecular Dynamics Simulation. International Journal of Molecular Sciences, 2022, 23, 10264.	4.1	7
11982	The EDN1 Missense Variant rs5370G & T Regulates Adaptation and Maladaptation under Hypobaric Hypoxia. International Journal of Environmental Research and Public Health, 2022, 19, 11174.	2.6	2
11983	Phosphorylation of FAM134C by CK2 controls starvation-induced ER-phagy. Science Advances, 2022, 8, .	10.3	16
11984	Promising antibacterials for LLM of <i>Staphylococcus aureus</i> using virtual screening, molecular docking, dynamics, and MMPBSA. Journal of Biomolecular Structure and Dynamics, 2023, 41, 7277-7289.	3.5	2
11985	Effect of Tacticity and Degree of Sulfonation of Polystyrene Sulfonate on Calcium-Binding Behavior in the Presence of Dodecyl Sulfate. Industrial & Engineering Chemistry Research, 2022, 61, 13442-13452.	3.7	3
11986	Deciphering the QR Code of the CRISPR-Cas9 System: Synergy between Gln768 (Q) and Arg976 (R). ACS Physical Chemistry Au, 2022, 2, 496-505.	4.0	1
11988	Dissecting the Inhibitory Mechanism of the $\beta$ -Crystallin Domain against $A\beta_{42}$ Aggregation and Its Effect on $A\beta_{42}$ Protofibrils: A Molecular Dynamics Simulation Study. ACS Chemical Neuroscience, 2022, 13, 2842-2851.	3.5	3
11989	The dynamic interplay of PIP <sub>2</sub> and ATP in the regulation of the K <sub>ATP</sub> channel. Journal of Physiology, 2022, 600, 4503-4519.	2.9	7
11990	Chemical Space Exploration with Active Learning and Alchemical Free Energies. Journal of Chemical Theory and Computation, 2022, 18, 6259-6270.	5.3	24
11991	Mutations of Rad6 E2 ubiquitin-conjugating enzymes at alanine-126 in helix-3 affect ubiquitination activity and decrease enzyme stability. Journal of Biological Chemistry, 2022, 298, 102524.	3.4	9
11992	Glycosylated Flavonoid Compounds as Potent CYP121 Inhibitors of Mycobacterium tuberculosis. Biomolecules, 2022, 12, 1356.	4.0	8
11993	Gradient of mechanical properties in polymer nanocomposites: From atomistic scale to the strain gradient effective continuum. International Journal of Solids and Structures, 2022, 256, 111977.	2.7	6
11994	A molecular dynamics simulation study to investigate the effect of C60 on thermo- mechanical and elastic properties of DGEBA/DETA nanocomposites. , 2022, 32, 32-42.		0



#	ARTICLE	IF	CITATIONS
11995	Ligand Unbinding Pathway and Mechanism Analysis Assisted by Machine Learning and Graph Methods. Journal of Chemical Information and Modeling, 2022, 62, 4591-4604.	5.4	8
11996	SARS-CoV-2 VOCs, Mutational diversity and clinical outcome: Are they modulating drug efficacy by altered binding strength?. Genomics, 2022, 114, 110466.	2.9	18
11997	Ionic Strength and Solution Composition Dictate the Adsorption of Cell-Penetrating Peptides onto Phosphatidylcholine Membranes. Langmuir, 2022, 38, 11284-11295.	3.5	12
11998	In silico elucidation of the interactions of thymoquinone analogues with phosphatase and tensin homolog (PTEN). Journal of Molecular Modeling, 2022, 28, .	1.8	0
11999	A comparative study of receptor interactions between SARS-CoV and SARS-CoV-2 from molecular modeling. Journal of Molecular Modeling, 2022, 28, .	1.8	3
12001	Stabilizing Mechanisms of Î²-Lactoglobulin in Amorphous Solid Dispersions of Indomethacin. Molecular Pharmaceutics, 2022, 19, 3922-3933.	4.6	7
12002	Simulation Study of the Effect of Antimicrobial Peptide Associations on the Mechanism of Action with Bacterial and Eukaryotic Membranes. Membranes, 2022, 12, 891.	3.0	4
12003	Bell-Evans model and steered molecular dynamics in uncovering the dissociation kinetics of ligands targeting G-protein-coupled receptors. Scientific Reports, 2022, 12, .	3.3	4
12004	A Molecular Dynamics Simulation of Polymersâ€™ Interactions with Kaolinite (010) Surfaces in Saline Solutions. Polymers, 2022, 14, 3851.	4.5	2
12005	Energetically unfavorable protein angles: Exploration of a conserved dihedral angle in triosephosphate isomerase. Biopolymers, 0, , .	2.4	1
12006	Mechanistic Insights into the Activation of Lecithinâ€™Cholesterol Acyltransferase in Therapeutic Nanodiscs Composed of Apolipoprotein A-I Mimetic Peptides and Phospholipids. Molecular Pharmaceutics, 2022, 19, 4135-4148.	4.6	4
12007	Systematic structure guided clustering of chemical lead compounds targeting RdRp of SARS-CoV-2. Minerva Biotechnology and Biomolecular Research, 2022, 34, .	0.5	5
12008	H2A-H2B Histone Dimer Plasticity and Its Functional Implications. Cells, 2022, 11, 2837.	4.1	3
12009	The influence of antibody humanization on shark variable domain (VNAR) binding site ensembles. Frontiers in Immunology, 0, 13, .	4.8	7
12011	Graphdiyne oxide nanosheets display selective anti-leukemia efficacy against DNMT3A-mutant AML cells. Nature Communications, 2022, 13, .	12.8	20
12012	Thinâ€™plate superstructures of the immunogenic 33â€™mer gliadin peptide. ChemBioChem, 0, , .	2.6	2
12013	Novel Calcium-Binding Ablating Mutations Induce Constitutive RET Activity and Drive Tumorigenesis. Cancer Research, 2022, 82, 3751-3762.	0.9	0
12014	Evaluating the use of absolute binding free energy in the fragment optimisation process. Communications Chemistry, 2022, 5, .	4.5	11

#	ARTICLE	IF	CITATIONS
12015	Mechanistic insight into impact of phosphorylation on the enzymatic steps of farnesyltransferase. Protein Science, 2022, 31, .	7.6	2
12016	Ionic Dynamics of the Charge Carrier in Layered Solid Materials for Mg Rechargeable Batteries. Chemistry of Materials, 2022, 34, 8769-8776.	6.7	3
12019	Immunoinformatics Approach to Design Novel Subunit Vaccine against the Epstein-Barr Virus. Microbiology Spectrum, 2022, 10, .	3.0	10
12020	Cholesterol promotes clustering of PI(4,5)P2 driving unconventional secretion of FGF2. Journal of Cell Biology, 2022, 221, .	5.2	7
12021	Self-Assembly of Chiral Optical Materials from Nonchiral Oligothiophene-Porphyrin Derivatives and Random Coil Synthetic Peptides. ChemPlusChem, 0, , .	2.8	2
12022	Mechanical Behavior of Polymer Nanocomposites via Atomistic Simulations: Conformational Heterogeneity and the Role of Strain Rate. Journal of Physical Chemistry B, 2022, 126, 7429-7444.	2.6	2
12023	<i>In silico</i> approach identified benzoylguanidines as SARS-CoV-2 main protease ( $M^{pro}$ ) potential inhibitors. Journal of Biomolecular Structure and Dynamics, 2023, 41, 7686-7699.	3.5	2
12024	Accessing a Forbidden Disordered State of a Zeolitic Imidazolate Framework with Higher Stiffness and Toughness through Irradiation. Chemistry of Materials, 2022, 34, 8749-8759.	6.7	7
12025	A computer-aided drug design approach to explore novel type II inhibitors of c-Met receptor tyrosine kinase for cancer therapy: QSAR, molecular docking, ADMET and molecular dynamics simulations. Journal of Biomolecular Structure and Dynamics, 2023, 41, 7768-7785.	3.5	20
12027	Dislocation glide driven interstitial shuffling of oxygen interstitials in titanium. Physical Review Materials, 2022, 6, .	2.4	1
12028	Probing Factor Xa Protein-Ligand Interactions: Accurate Free Energy Calculations and Experimental Validations of Two Series of High-Affinity Ligands. Journal of Medicinal Chemistry, 2022, 65, 13013-13028.	6.4	1
12029	Single-chain insulin analogs threaded by the insulin receptor $\beta$ CT domain. Biophysical Journal, 2022, 121, 4063-4077.	0.5	2
12030	Dissecting the mechanisms of environment sensitivity of smart probes for quantitative assessment of membrane properties. Open Biology, 2022, 12, .	3.6	8
12031	A Novel Cryptic Clostridial Peptide That Kills Bacteria by a Cell Membrane Permeabilization Mechanism. Microbiology Spectrum, 2022, 10, .	3.0	4
12033	Shear and cooling induced regulation of mechanical properties and glass transition temperature of isotactic polypropylene. Materials Today: Proceedings, 2022, , .	1.8	2
12034	Rutin Potentially Binds the Gamma Secretase Catalytic Site, Down Regulates the Notch Signaling Pathway and Reduces Sphere Formation in Colonospheres. Metabolites, 2022, 12, 926.	2.9	9
12035	New insights into adsorption structure and hydration of polymer at oil-water interface obtained by molecular dynamics simulations: Isotactic poly(methacrylic acid). Polymer, 2022, 260, 125378.	3.8	8
12036	Directed Self-Assembly of Conducting Polymer Nanofilms on Single-Crystalline Ice Facets. Macromolecular Research, 0, , .	2.4	3

#	ARTICLE	IF	CITATIONS
12038	Connecting Non-Gaussian Water Density Fluctuations to the Lengthscale Dependent Crossover in Hydrophobic Hydration. <i>Journal of Physical Chemistry B</i> , 2022, 126, 7604-7614.	2.6	4
12039	Molecular Insights on Bioactive Compounds against Covid-19: A Network Pharmacological and Computational Study. <i>Current Computer-Aided Drug Design</i> , 2022, 18, 425-439.	1.2	1
12040	Investigation of strain rate effects on the mechanical behavior of polymer nanocomposites with and without defects in nanotubes. <i>Polymer Bulletin</i> , 2023, 80, 8877-8898.	3.3	1
12041	LAWS: Local alignment for water sitesâ€”Tracking ordered water in simulations. <i>Biophysical Journal</i> , 2023, 122, 2871-2883.	0.5	1
12042	Dynamics of Polymer Chains in Poly(ethylene oxide)/Silica Nanocomposites via a Combined Computational and Experimental Approach. <i>Journal of Physical Chemistry B</i> , 2022, 126, 7745-7760.	2.6	4
12044	Size-dependent ferroic phase transformations in GeSe nanoribbons. <i>Applied Physics Letters</i> , 2022, 121, .	3.3	6
12045	Martini 3 model of surface modified cellulose nanocrystals: investigation of aqueous colloidal stability. <i>Cellulose</i> , 2022, 29, 9493-9509.	4.9	3
12046	A mechanism for SARS-CoV-2 RNA capping and its inhibition by nucleotide analog inhibitors. <i>Cell</i> , 2022, 185, 4347-4360.e17.	28.9	21
12047	Dissolution of nitrones in alkylphosphates: a structural study. <i>Journal of Molecular Liquids</i> , 2022, , 120517.	4.9	0
12048	Inhibition of nonstructural protein 15 of SARSâ€”CoVâ€”2 by golden spice: A computational insight. <i>Cell Biochemistry and Function</i> , 2022, 40, 926-934.	2.9	28
12049	Alkyl chain length-dependent protein nonadsorption and adsorption properties of crystalline alkyl Î²-celluloside assemblies. <i>Colloids and Surfaces B: Biointerfaces</i> , 2022, 220, 112898.	5.0	4
12050	Influence of DPPE surface undulations on melting temperature determination: UV/Vis spectroscopic and MD study. <i>Biochimica Et Biophysica Acta - Biomembranes</i> , 2023, 1865, 184072.	2.6	4
12051	Computational Modeling of TP63â€”TP53 Interaction and Rational Design of Inhibitors: Implications for Therapeutics. <i>Molecular Cancer Therapeutics</i> , 2022, 21, 1846-1856.	4.1	1
12052	Discovery of Small Molecule Agonist of Gonadotropin-Releasing Hormone Receptor (GnRH1R). <i>Journal of Chemical Information and Modeling</i> , 2022, 62, 5009-5022.	5.4	4
12053	Usefulness of higher-order system-size correction for macromolecule diffusion coefficients: A molecular dynamics study. <i>Chemical Physics Letters</i> , 2022, , 140096.	2.6	0
12054	Revealing hydrogen bond dynamics between ion pairs in binary and reciprocal ionic liquid mixtures. <i>Journal of Molecular Liquids</i> , 2022, 368, 120515.	4.9	3
12055	Alchemical Free-Energy Calculations of Watsonâ€”Crick and Hoogsteen Base Pairing Interconversion in DNA. <i>Journal of Chemical Theory and Computation</i> , 2022, 18, 6966-6973.	5.3	3
12056	Influence of force field choice on the conformational landscape of rat and human islet amyloid polypeptide. <i>Proteins: Structure, Function and Bioinformatics</i> , 2023, 91, 338-353.	2.6	6

#	ARTICLE	IF	CITATIONS
12057	Near-infrared fluorophores with absolute aggregation-caused quenching and negligible fluorescence re-illumination for in vivo bioimaging of nanocarriers. <i>Aggregate</i> , 2023, 4, .	9.9	10
12058	Pterostilbene-isothiocyanate impedes RANK/TRAF6 interaction to inhibit osteoclastogenesis, promoting osteogenesis in vitro and alleviating glucocorticoid induced osteoporosis in rats. <i>Biochemical Pharmacology</i> , 2022, 206, 115284.	4.4	3
12059	Molecular dynamics identifies semi-rigid domains in the PD-1 checkpoint receptor bound to its natural ligand PD-L1. <i>Frontiers in Bioengineering and Biotechnology</i> , 0, 10, .	4.1	2
12060	Ionic liquids with hydrogenated and perfluorinated chains: Structural study of the [P6,6,6,14][FnCOO] <sup>n</sup> n=7, 9, 11. Checking the existence of polar “hydrogenated” perfluorinated triphilic continuity. <i>Journal of Molecular Liquids</i> , 2022, 367, 120506.	4.9	6
12061	SARS-CoV-2 variants impact RBD conformational dynamics and ACE2 accessibility. <i>Frontiers in Medical Technology</i> , 0, 4, .	2.5	6
12062	Organizations of melittin peptides after spontaneous penetration into cell membranes. <i>Biophysical Journal</i> , 2022, 121, 4368-4381.	0.5	4
12063	Targeting human thymidylate synthase: Ensemble-based virtual screening for drug repositioning and the role of water. <i>Journal of Molecular Graphics and Modelling</i> , 2023, 118, 108348.	2.4	2
12064	Markov state modelling reveals heterogeneous drug-inhibition mechanism of Calmodulin. <i>PLoS Computational Biology</i> , 2022, 18, e1010583.	3.2	1
12065	Extending the Stochastic Titration CpHMD to CHARMM36m. <i>Journal of Physical Chemistry B</i> , 2022, 126, 7870-7882.	2.6	5
12066	A dynamical view of protein-protein complexes: Studies by molecular dynamics simulations. <i>Frontiers in Molecular Biosciences</i> , 0, 9, .	3.5	7
12067	Influence of dissolved hydrogen on the viscosity and interfacial tension of the liquid organic hydrogen carrier system based on diphenylmethane by surface light scattering and molecular dynamics simulations. <i>International Journal of Hydrogen Energy</i> , 2022, 47, 39163-39178.	7.1	4
12068	Repurposing FDA-approved anti-diabetic drug to target <i>H. pylori</i> peptidyl deformylase using computer-based drug discovery approach. <i>Molecular Simulation</i> , 0, , 1-9.	2.0	1
12069	Simulation of the CO <sub>2</sub> hydrate-water interfacial energy: The mold integration “guest methodology. <i>Journal of Chemical Physics</i> , 2022, 157, 134709.	3.0	5
12070	Hydrogen-bonds mediate liquid-liquid phase separation of mussel derived adhesive peptides. <i>Nature Communications</i> , 2022, 13, .	12.8	29
12071	Predicting the structural basis of targeted protein degradation by integrating molecular dynamics simulations with structural mass spectrometry. <i>Nature Communications</i> , 2022, 13, .	12.8	27
12073	Drug repurposing against galectin-3 using simulation-based studies. <i>Journal of Biomolecular Structure and Dynamics</i> , 0, , 1-8.	3.5	1
12074	Effect of Disulfide Bridge on the Binding of SARS-CoV-2 Fusion Peptide to Cell Membrane: A Coarse-Grained Study. <i>ACS Omega</i> , 0, , .	3.5	2
12075	Topologically close-packed structure characteristics of the plastic deformation regions of amorphous Cu <sub>64.5</sub> Zr <sub>35.5</sub> . <i>Journal of Materials Research and Technology</i> , 2022, 21, 749-760.	5.8	4

#	ARTICLE	IF	CITATIONS
12076	Molecular simulation of the structural and thermodynamic properties of n-alkane/brine interfacial systems with nonionic surfactants. <i>Colloids and Surfaces A: Physicochemical and Engineering Aspects</i> , 2022, 655, 130301.	4.7	2
12077	An atomistic entropy based finite element multiscale method for modeling amorphous materials. <i>International Journal of Solids and Structures</i> , 2022, 256, 111983.	2.7	1
12078	Liquid-liquid extraction of polyaromatic compounds with ionic liquid. A theoretical and experimental approach. <i>Separation and Purification Technology</i> , 2022, 303, 122160.	7.9	5
12079	Molecular modelling of ionic liquids: Physical properties of species with extremely long aliphatic chains from a near-optimal regime. <i>Journal of Molecular Liquids</i> , 2022, 367, 120492.	4.9	9
12080	The role of mechanical loading in bcc-hcp phase transition: tension-compression asymmetry and twin formation. <i>Acta Materialia</i> , 2022, 241, 118377.	7.9	4
12081	Modeling, energetic and structural analysis of peptide membranes formed by arginine and phenylalanine (R2F4R2) using fully atomistic molecular dynamics. <i>Journal of Molecular Liquids</i> , 2022, 367, 120498.	4.9	1
12082	An experimental and computational study of a low-temperature electrolyte design utilizing iodide-based ionic liquid and butyronitrile. <i>Molecular Systems Design and Engineering</i> , 0, , .	3.4	0
12083	Monovalent ion-mediated charge-charge interactions drive aggregation of surface-functionalized gold nanoparticles. <i>Nanoscale</i> , 2022, 14, 15181-15192.	5.6	3
12084	Molecular dynamics simulations and solid-state nuclear magnetic resonance spectroscopy measurements of C-H bond order parameters and effective correlation times in a POPC-GM3 bilayer. <i>Physical Chemistry Chemical Physics</i> , 2022, 24, 25588-25601.	2.8	4
12085	A computational study on strontium ion modified hydroxyapatite-fibronectin interactions. <i>Physical Chemistry Chemical Physics</i> , 2022, 24, 27989-28002.	2.8	2
12086	Osmolyte effect on enzymatic stability and reaction equilibrium of formate dehydrogenase. <i>Physical Chemistry Chemical Physics</i> , 2022, 24, 27930-27939.	2.8	7
12087	Cardiolipin, and not monolysocardiolipin, preferentially binds to the interface of complexes III and IV. <i>Chemical Science</i> , 2022, 13, 13489-13498.	7.4	3
12088	MoS <sub>2</sub> nanosheets effectively bind to the receptor binding domain of the SARS-CoV-2 spike protein and destabilize the spike-human ACE2 receptor interactions. <i>Soft Matter</i> , 2022, 18, 8961-8973.	2.7	4
12089	Development of a transferable coarse-grained model of polydimethylsiloxane. <i>Soft Matter</i> , 2022, 18, 7887-7896.	2.7	4
12090	How lignin sticks to cellulose—insights from atomic force microscopy enhanced by machine-learning analysis and molecular dynamics simulations. <i>Nanoscale</i> , 2022, 14, 17561-17570.	5.6	3
12091	Self-assembly of an <i>in silico</i> designed dipeptide derivative to obtain photo-responsive vesicles. <i>Physical Chemistry Chemical Physics</i> , 2022, 24, 27751-27758.	2.8	1
12092	Identification of Diosmin and Flavin Adenine Dinucleotide as Repurposing Treatments for Monkeypox Virus: A Computational Study. <i>International Journal of Molecular Sciences</i> , 2022, 23, 11570.	4.1	11
12093	Computational study of the structural ensemble of CC chemokine receptor type 5 (CCR5) and its interactions with different ligands. <i>PLoS ONE</i> , 2022, 17, e0275269.	2.5	0

#	ARTICLE	IF	CITATIONS
12094	In vivo developmental studies of <i>Helicoverpa armigera</i> and in silico molecular interactions with trypsin reveal the bio-insecticidal potential of trypsin inhibitor (SSTI) isolated from <i>Solanum surattense</i> . <i>International Journal of Biological Macromolecules</i> , 2022, 223, 335-345.	7.5	1
12095	Conformational Preferences of Pyridone Adenine Dinucleotides from Molecular Dynamics Simulations. <i>International Journal of Molecular Sciences</i> , 2022, 23, 11866.	4.1	3
12096	High-performance electrified hydrogel actuators based on wrinkled nanomembrane electrodes for untethered insect-scale soft aquabots. <i>Science Robotics</i> , 2022, 7, .	17.6	24
12097	Modeling the Effect of Hydrophobicity on the Passive Permeation of Solutes across a Bacterial Model Membrane. <i>Journal of Chemical Information and Modeling</i> , 2022, 62, 5023-5033.	5.4	6
12098	Membrane-Specific Binding of 4 nm Lipid Nanoparticles Mediated by an Entropy-Driven Interaction Mechanism. <i>ACS Nano</i> , 2022, 16, 18090-18100.	14.6	11
12099	Characterization of the Interaction of Polymeric Micelles with siRNA: A Combined Experimental and Molecular Dynamics Study. <i>Polymers</i> , 2022, 14, 4409.	4.5	1
12100	Structural insights into light-driven anion pumping in cyanobacteria. <i>Nature Communications</i> , 2022, 13, .	12.8	4
12101	Evidence and Impacts of Nanoplastic Accumulation on Crop Grains. <i>Advanced Science</i> , 2022, 9, .	11.2	19
12103	In Silico Characterization of African Swine Fever Virus Nucleoprotein p10 Interaction with DNA. <i>Viruses</i> , 2022, 14, 2348.	3.3	2
12104	RNA Captures More Cations than DNA: Insights from Molecular Dynamics Simulations. <i>Journal of Physical Chemistry B</i> , 2022, 126, 8646-8654.	2.6	17
12105	Analysis of 1-Aroyl-3-[3-chloro-2-methylphenyl] Thiourea Hybrids as Potent Urease Inhibitors: Synthesis, Biochemical Evaluation and Computational Approach. <i>International Journal of Molecular Sciences</i> , 2022, 23, 11646.	4.1	13
12106	Advances in micro-mechanical modeling using a bonded-particle model and periodic homogenization within discrete element framework applied to heterogeneous ceramics. <i>Journal of the European Ceramic Society</i> , 2022, , .	5.7	0
12107	The Ion-Dipole Correction of the 3DRISM Solvation Model to Accurately Compute Water Distributions around Negatively Charged Biomolecules. <i>Journal of Physical Chemistry B</i> , 2022, 126, 8632-8645.	2.6	5
12108	Dimer-parity-dependent odd-even effects in photoinduced transitions to cholesteric and twist grain boundary smectic- $C$ experiments and simulations. <i>Physical Review E</i> , 2022, 106, .	2.1	1
12109	Discovery of putative inhibitors against main drivers of SARS-CoV-2 infection: Insight from quantum mechanical evaluation and molecular modeling. <i>Frontiers in Chemistry</i> , 0, 10, .	3.6	3
12110	Structural basis for recognition of antihistamine drug by human histamine receptor. <i>Nature Communications</i> , 2022, 13, .	12.8	17
12111	Towards commonality between shear banding and glass-liquid transition in metallic glasses. <i>Physical Review Materials</i> , 2022, 6, .	2.4	1
12112	Impact of Conjugated Polymer Addition on the Properties of Paraffin-Asphaltene Blends for Heat Storage Applications: Insight from Computer Modeling and Experiment. <i>Journal of Chemical Physics</i> , 0, , .	3.0	2



#	ARTICLE	IF	CITATIONS
12113	Solubility of Methane in Water: Some Useful Results for Hydrate Nucleation. Journal of Physical Chemistry B, 2022, 126, 8553-8570.	2.6	15
12114	Toward the design and development of $\alpha$ -peptidomimetic inhibitors of the Ataxin-1 aggregation pathway. Biophysical Journal, 2022, , .	0.5	2
12115	Tuning the ionic character of sodium dodecyl sulphate via counter-ion binding: An experimental and computational study. Frontiers in Materials, 0, 9, .	2.4	2
12116	The Spike Mutants Website: A Worldwide Used Resource against SARS-CoV-2. International Journal of Molecular Sciences, 2022, 23, 13082.	4.1	7
12117	Free energy perturbation calculations of tetrahydroquinolines complexed to the first bromodomain of BRD4. Molecular Physics, 0, , .	1.7	0
12118	Conformational Heterogeneity and Frustration of the Tumor Suppressor p53 as Tuned by Punctual Mutations. International Journal of Molecular Sciences, 2022, 23, 12636.	4.1	0
12122	A Coarse-Grained Molecular Dynamics Description of Docetaxel-Conjugate Release from PLGA Matrices. Biomacromolecules, 2022, 23, 4678-4686.	5.4	3
12123	DNA opening during transcription initiation by RNA polymerase II in atomic detail. Biophysical Journal, 2022, , .	0.5	1
12126	Asymmetric reduction of conjugated C C bonds by immobilized fusion of old yellow enzyme and glucose dehydrogenase. Green Synthesis and Catalysis, 2022, , .	6.8	1
12127	Dynamic HIV-1 spike motion creates vulnerability for its membrane-bound tripod to antibody attack. Nature Communications, 2022, 13, .	12.8	6
12128	Intrinsic lipolysis rate for systematic design of lipid-based formulations. Drug Delivery and Translational Research, 2023, 13, 1288-1304.	5.8	2
12129	Hydrophobicity Determines the Bacterial Killing Rate of $\alpha$ -Helical Antimicrobial Peptides and Influences the Bacterial Resistance Development. Journal of Medicinal Chemistry, 2022, 65, 14701-14720.	6.4	18
12130	The determination of the effect(s) of solute carrier family 22-member 2 (SLC22A2) haplotype variants on drug binding via molecular dynamic simulation systems. Scientific Reports, 2022, 12, .	3.3	0
12131	Role of Anions in $\alpha$ -Hydroxymethylfurfural Solvation in Ionic Liquids from Molecular Dynamics Simulations. Advanced Theory and Simulations, 2022, 5, .	2.8	2
12132	Inhibited KdpFABC transitions into an E1 off-cycle state. ELife, 0, 11, .	6.0	5
12134	Accurate Quantum-Mechanically Derived Force-Fields through a Fragment-Based Approach: Balancing Specificity and Transferability in the Prediction of Self-Assembly in Soft Matter. Journal of Chemical Theory and Computation, 2022, 18, 6905-6919.	5.3	4
12135	Governing dynamics and preferential binding of the $\alpha$ AXH domain influence the aggregation pathway of Ataxin-1. Proteins: Structure, Function and Bioinformatics, 2023, 91, 380-394.	2.6	0
12136	Substantial Effect of Terminal Groups in <i>cis</i> -Polyisoprene: A Multiscale Molecular Dynamics Simulation Study. Macromolecules, 2022, 55, 9650-9662.	4.8	7

#	ARTICLE	IF	CITATIONS
12137	Molecular doping of nucleic acids into light emitting crystals driven by multisite-intermolecular interaction. <i>Nature Communications</i> , 2022, 13, .	12.8	4
12138	Polystyrene-modified carbon nanotubes: Promising carriers in targeted drug delivery. <i>Biophysical Journal</i> , 2022, 121, 4271-4279.	0.5	3
12140	Activated I-BAR IRSp53 clustering controls the formation of VASP-actin-based membrane protrusions. <i>Science Advances</i> , 2022, 8, .	10.3	18
12141	Lateral fenestrations in the extracellular domain of the glycine receptor contribute to the main chloride permeation pathway. <i>Science Advances</i> , 2022, 8, .	10.3	2
12142	Quantum-based machine learning and AI models to generate force field parameters for drug-like small molecules. <i>Frontiers in Molecular Biosciences</i> , 0, 9, .	3.5	2
12145	<i>In silico</i> structural elucidation of Nipah virus L protein and targeting RNA-dependent RNA polymerase domain by nucleoside analogs. <i>Journal of Biomolecular Structure and Dynamics</i> , 2023, 41, 8215-8229.	3.5	6
12146	Deciphering the Molecular Mechanism of Inhibition of $\beta$ -Secretase (BACE1) Activity by a 2-Aminoimidazole-4-one Derivative. <i>ChemistrySelect</i> , 2022, 7, .	1.5	1
12147	Arginine-based surfactants alter the rheological and in-plane structural properties of stratum corneum model membranes. <i>Journal of Colloid and Interface Science</i> , 2022, , .	9.4	1
12148	Effects of membrane lipids on phospholamban pentameric channel structure and ion transportation mechanisms. <i>International Journal of Biological Macromolecules</i> , 2023, 224, 766-775.	7.5	2
12149	Modeling the partitioning of amphiphilic molecules and co-solvents in biomembranes. <i>Journal of Applied Crystallography</i> , 2022, 55, 1401-1412.	4.5	2
12150	Computational identification and experimental validation of anti-filarial lead molecules targeting metal binding/substrate channel residues of Cu/Zn SOD1 from <i>Wuchereria bancrofti</i> . <i>Journal of Biomolecular Structure and Dynamics</i> , 2023, 41, 8715-8728.	3.5	2
12151	On the Use of a Non-Constant Non-Affine or Slip Parameter in Polymer Rheology Constitutive Modeling. <i>Dynamics</i> , 2022, 2, 380-398.	1.2	2
12152	Molecular Simulation-Guided Spectroscopy of Imidazolium-Based Ionic Liquids and Effects of Methylation on Ion-Cage and -Pair Dynamics. <i>Journal of Physical Chemistry B</i> , 2022, 126, 8838-8850.	2.6	1
12153	A random batch Ewald method for charged particles in the isothermal-isobaric ensemble. <i>Journal of Chemical Physics</i> , 2022, 157, .	3.0	3
12154	Structural impact of pathogenic SNPs on $\beta$ -tubulin using molecular dynamics study. <i>Journal of Biomolecular Structure and Dynamics</i> , 0, , 1-11.	3.5	0
12158	Hesperidin potentially interacts with the catalytic site of gamma-secretase and modifies notch sensitive genes and cancer stemness marker expression in colon cancer cells and colonosphere. <i>Journal of Biomolecular Structure and Dynamics</i> , 2023, 41, 8432-8444.	3.5	7
12160	Effects of the Na <sup>+</sup> /Ca <sup>2+</sup> Ratio and Cation Type in the Montmorillonite Interlayer on the Intercalated Methane Hydrate Formation: Insights from Molecular Dynamics Simulations. <i>ACS Earth and Space Chemistry</i> , 2022, 6, 2745-2754.	2.7	6
12162	Molecular Mechanism of Hydrotropic Properties of GTP and ATP. <i>Journal of Physical Chemistry B</i> , 2022, 126, 8486-8494.	2.6	4

#	ARTICLE	IF	CITATIONS
12163	Magainin 2 and PGLa in bacterial membrane mimics IV: Membrane curvature and partitioning. Biophysical Journal, 2022, 121, 4689-4701.	0.5	1
12164	Anisotropic Microgels by Supramolecular Assembly and Precipitation Polymerization of Pyrazole-Modified Monomers. Advanced Science, 2022, 9, .	11.2	4
12165	Energy Transport and Its Function in Heptahelical Transmembrane Proteins. Journal of Physical Chemistry B, 2022, 126, 8735-8746.	2.6	3
12166	Structure and Dynamics of Human Chemokine CCL16—Implications for Biological Activity. Biomolecules, 2022, 12, 1588.	4.0	0
12167	An inducible amphipathic $\alpha$ -helix mediates subcellular targeting and membrane binding of RPE65. Life Science Alliance, 2023, 6, e202201546.	2.8	3
12168	The ABC transporter MsbA adopts the wide inward-open conformation in <i>E. coli</i> cells. Science Advances, 2022, 8, .	10.3	27
12169	An N-glycan on the C2 domain of JAGGED1 is important for Notch activation. Science Signaling, 2022, 15, .	3.6	3
12170	Synergistic Membrane Disturbance Improves the Antibacterial Performance of Polymyxin B. Polymers, 2022, 14, 4316.	4.5	0
12171	Mulberroside A could serve as a pan inhibitor for the tyrosine kinase domains of the HER family. F1000Research, 0, 11, 1201.	1.6	0
12173	Exploiting Ligand-binding Domain Dimerization for Development of Novel Androgen Receptor Inhibitors. Molecular Cancer Therapeutics, 2022, 21, 1823-1834.	4.1	5
12175	GPC3-Unc5 receptor complex structure and role in cell migration. Cell, 2022, 185, 3931-3949.e26.	28.9	10
12176	Ion transfer mechanisms in Mrp-type antiporters from high resolution cryoEM and molecular dynamics simulations. Nature Communications, 2022, 13, .	12.8	6
12177	Novel <i>Eubacterium rectale</i> inhibitor from <i>Coriandrum sativum</i> L. for possible prevention of colorectal cancer: a computational approach. Journal of Biomolecular Structure and Dynamics, 2023, 41, 8402-8416.	3.5	5
12178	A new Molecular Insight in Effects of Alcohol Co-solvents on Miscibility of Anhydrous Ethanol/Diesel Blends. Journal of Energy Resources Technology, Transactions of the ASME, 0, , 1-27.	2.3	0
12179	Immunoinformatics-Aided Design of a Peptide Based Multiepitope Vaccine Targeting Glycoproteins and Membrane Proteins against Monkeypox Virus. Viruses, 2022, 14, 2374.	3.3	24
12180	Molecular Dynamics Simulation Study on the Effect of Mn on the Tensile Behavior of a Ferrite/Austenite Iron Bicrystal. Journal of Materials Engineering and Performance, 2023, 32, 6810-6820.	2.5	2
12181	SAR exploration of the nonimidazole histamine H <sub>3</sub> receptor ligand ZELH16 reveals potent inverse agonism. Archiv Der Pharmazie, 0, , .	4.1	0
12182	Influence of TMAO and Pressure on the Folding Equilibrium of TrpCage. Journal of Physical Chemistry B, 2022, 126, 8374-8380.	2.6	0

#	ARTICLE	IF	CITATIONS
12183	Identification of potential mutational hotspots in serratiopeptidase to address its poor pH tolerance issue. <i>Journal of Biomolecular Structure and Dynamics</i> , 2023, 41, 8831-8843.	3.5	19
12185	Peptide-DNA origami as a cryoprotectant for cell preservation. <i>Science Advances</i> , 2022, 8, .	10.3	8
12186	Prospecting <i>in silico</i> antibacterial activity of a peptide from trypsin inhibitor isolated from tamarind seed. <i>Journal of Enzyme Inhibition and Medicinal Chemistry</i> , 2023, 38, 67-83.	5.2	2
12187	Recognition of the ligand-induced spatiotemporal residue pair pattern of $\beta^2$ -adrenergic receptors using 3-D residual networks trained by the time series of protein distance maps. <i>Computational and Structural Biotechnology Journal</i> , 2022, 20, 6360-6374.	4.1	1
12188	Experimental and simulation study on the delayed release of CO in the initial stage of the low-temperature oxidation of coal. <i>Scientific Reports</i> , 2022, 12, .	3.3	0
12190	Compounds Isolated from <i>Lawsonia inermis</i> L. Collected in Vietnam and Evaluation of Their Potential Activity Against the Main Protease of SARS-CoV-2 Using <i>In silico</i> Molecular Docking and Molecular Dynamic Simulation. <i>Natural Product Communications</i> , 2022, 17, 1934578X2211251.	0.5	1
12191	Structure of SARS-CoV-2 M protein in lipid nanodiscs. <i>ELife</i> , 0, 11, .	6.0	31
12192	Structural basis for host recognition and superinfection exclusion by bacteriophage T5. <i>Proceedings of the National Academy of Sciences of the United States of America</i> , 2022, 119, .	7.1	14
12193	Isothermal and adiabatic elastic constants from virial fluctuations. <i>Physical Review E</i> , 2022, 106, .	2.1	0
12194	Preliminary Structure-Activity Relationship Study of the MMV Pathogen Box Compound MMV675968 (2,4-Diaminoquinazoline) Unveils Novel Inhibitors of <i>Trypanosoma brucei brucei</i> . <i>Molecules</i> , 2022, 27, 6574.	3.8	5
12195	Structural and spectroscopic details of polysaccharide-bile acid composites from molecular dynamics simulations. <i>Journal of Biomolecular Structure and Dynamics</i> , 0, , 1-13.	3.5	0
12196	Lipids mediate supramolecular outer membrane protein assembly in bacteria. <i>Science Advances</i> , 2022, 8, .	10.3	25
12197	Assessment of two-dimensional materials on the biological membrane permeability of Epirubicin anti-cancer drug. <i>Applied Surface Science</i> , 2023, 610, 155557.	6.1	1
12198	Infrared Spectroscopy of $\text{Li}^+$ Solvation in $\text{EmimBF}_4$ and in Propylene Carbonate: Ab Initio Molecular Dynamics and Experiment. <i>Journal of Physical Chemistry B</i> , 2022, 126, 9643-9662.	2.6	4
12199	Synergistic Effects of IMX-104 Components in Membrane Absorption: A Computational Study. <i>ACS Omega</i> , 0, , .	3.5	0
12200	A 3D-Predicted Structure of the Amine Oxidase Domain of Lysyl Oxidase-Like 2. <i>International Journal of Molecular Sciences</i> , 2022, 23, 13385.	4.1	7
12201	The Role of Electrostatic Interactions in IFIT5-RNA Complexes Predicted by the UBDB+EPMM Method. <i>Journal of Physical Chemistry B</i> , 2022, 126, 9152-9167.	2.6	2
12204	High-Throughput Molecular Dynamics-Based Alchemical Free Energy Calculations for Predicting the Binding Free Energy Change Associated with the Selected Omicron Mutations in the Spike Receptor-Binding Domain of SARS-CoV-2. <i>Biomedicines</i> , 2022, 10, 2779.	3.2	2

#	ARTICLE	IF	CITATIONS
12205	A Core-Shell Approach for Systematically Coarsening Nanoparticle-Membrane Interactions: Application to Silver Nanoparticles. <i>Nanomaterials</i> , 2022, 12, 3859.	4.1	1
12206	A conserved function of Human DLC3 and Drosophila Cvc in testis development. <i>ELife</i> , 0, 11, .	6.0	1
12207	Janus regulation of ice growth by hyperbranched polyglycerols generating dynamic hydrogen bonding. <i>Nature Communications</i> , 2022, 13, .	12.8	5
12208	Organic solvents aggregating and shaping structural folding of protein, a case study of the protease enzyme. <i>Biophysical Chemistry</i> , 2022, 291, 106909.	2.8	2
12209	Identification of a novel nitroflavone-based scaffold for designing mutant-selective EGFR tyrosine kinase inhibitors targeting T790M and C797S resistance in advanced NSCLC. <i>Bioorganic Chemistry</i> , 2022, 129, 106219.	4.1	5
12210	Effect of inorganic salt concentration and types on electrophoretic migration of oil droplets in oil-in-water emulsion: A molecular dynamics study. <i>Journal of Molecular Liquids</i> , 2022, 367, 120549.	4.9	5
12211	Computational investigations of indanedione and indanone derivatives in drug discovery: Indanone derivatives inhibits cereblon, an E3 ubiquitin ligase component. <i>Computational Biology and Chemistry</i> , 2022, 101, 107776.	2.3	3
12212	Insight into the effect of anions on cycloaddition of CO <sub>2</sub> catalyzed by carboxylate anion-based ionic liquids: A theoretical study by QM and MD. <i>Journal of Molecular Liquids</i> , 2022, 368, 120629.	4.9	1
12213	Quantum effects on the elastic properties of cubic boron nitride by path-integral Monte Carlo simulation. <i>Computational Condensed Matter</i> , 2022, 33, e00759.	2.1	0
12214	Mechanism and thermodynamics of adsorption of diclofenac on graphene-based nanomaterials. <i>Journal of Environmental Chemical Engineering</i> , 2022, 10, 108789.	6.7	13
12215	Selective absorption of H <sub>2</sub> S and CO <sub>2</sub> by azole based protic ionic liquids: A combined density functional theory and molecular dynamics study. <i>Journal of Molecular Liquids</i> , 2022, 367, 120558.	4.9	20
12216	Atomistic simulation of shear deformation at bcc-Fe grain boundary and precipitation strengthening by Cr <sub>23</sub> C <sub>6</sub> . <i>Materials Today Communications</i> , 2022, 33, 104711.	1.9	0
12217	EF4K bola-amphiphilic peptide nanomembrane: structural, energetic and dynamic properties using molecular dynamics. <i>Journal of Molecular Liquids</i> , 2022, 368, 120651.	4.9	1
12218	Lycopene, but not zeaxanthin, serves as a skeleton for the formation of an orthorhombic organization of intercellular lipids within the lamellae in the stratum corneum: Molecular dynamics simulations of the hydrated ceramide NS bilayer model. <i>Biochimica Et Biophysica Acta - Biomembranes</i> , 2023, 1865, 184081.	2.6	3
12219	New family of Type V eutectic solvents based on 1,10-phenanthroline and their application in metal extraction. <i>Hydrometallurgy</i> , 2023, 215, 105971.	4.3	3
12220	Understanding the mechanism of amylin aggregation: From identifying crucial segments to tracing dominant sequential events to modeling potential aggregation suppressors. <i>Biochimica Et Biophysica Acta - Proteins and Proteomics</i> , 2023, 1871, 140866.	2.3	3
12221	Free energy reconstruction/decomposition from WHAM, force integration and free energy perturbation for an umbrella sampling simulation. <i>Chemical Physics</i> , 2023, 565, 111736.	1.9	3
12222	The influence mechanism of pH and hydrothermal processing on the interaction between cyanidin-3-O-glucoside and starch. <i>Food Hydrocolloids</i> , 2023, 136, 108234.	10.7	1

#	ARTICLE	IF	CITATIONS
12223	Solid state synthesis of bispyridyl-ferrocene conjugates with unusual site selective 1,4-Michael addition, as potential inhibitor and electrochemical probe for fibrillation in amyloidogenic protein. Journal of Molecular Structure, 2023, 1273, 134362.	3.6	4
12224	Basket-type G-quadruplex with two tetrads in the presence of TMAO and urea: A molecular dynamics study. Journal of Molecular Structure, 2023, 1274, 134375.	3.6	3
12225	Assessment of a host-guest interaction in a bilayer membrane model. RSC Advances, 2022, 12, 32046-32055.	3.6	1
12226	Recognition motifs for importin 4 [(L)PPRS(G/P)P] and importin 5 [KP(K/Y)LV] binding, identified by bio-informatic simulation and experimental in vitro validation. Computational and Structural Biotechnology Journal, 2022, 20, 5952-5961.	4.1	2
12227	Slower diffusion and anomalous association of R453W lamin A protein alter nuclear architecture in AD-EDMD. RSC Advances, 2022, 12, 32129-32141.	3.6	2
12228	3D Modeling of Non-coding RNA Interactions. Advances in Experimental Medicine and Biology, 2022, , 281-317.	1.6	2
12229	New multienzymatic complex formed between human cathepsin D and snake venom phospholipase A2. Journal of Venomous Animals and Toxins Including Tropical Diseases, 0, 28, .	1.4	0
12230	Characterization of kaolinite-3-aminopropyltriethoxysilane intercalation complexes. Applied Clay Science, 2023, 231, 106753.	5.2	2
12231	Identification and in-vitro analysis of potential proteasome inhibitors targeting PSM $\alpha$ 25 for multiple myeloma. Biomedicine and Pharmacotherapy, 2023, 157, 113963.	5.6	5
12232	The impact of lipid polyunsaturation on the physical and mechanical properties of lipid membranes. Biochimica Et Biophysica Acta - Biomembranes, 2023, 1865, 184084.	2.6	11
12233	Importance of the lysine cluster in the translocation of anions through the pyrophosphate specific channel OprO. Biochimica Et Biophysica Acta - Biomembranes, 2023, 1865, 184086.	2.6	2
12234	Biopolymer recovery from waste activated sludge toward self-healing mortar crack. Science of the Total Environment, 2023, 858, 160107.	8.0	3
12235	Analysis of Ion Atmosphere Around Nucleosomes Using Supercomputer MD Simulations. Supercomputing Frontiers and Innovations, 2022, 9, .	0.4	0
12236	Predicting Binding Free Energies for DPS Protein-DNA Complexes and Crystals Using Molecular Dynamics. Supercomputing Frontiers and Innovations, 2022, 9, .	0.4	1
12237	Glutamate Permeability of Chicken Best1. Experimental Neurobiology, 2022, 31, 277-288.	1.6	1
12238	In silico identification of potential inhibitors of vital monkeypox virus proteins from FDA approved drugs. Molecular Diversity, 2023, 27, 2169-2184.	3.9	17
12239	Lipid-mediated activation of plasma membrane-localized deubiquitylating enzymes modulate endosomal trafficking. Nature Communications, 2022, 13, .	12.8	6
12240	Martini 3 Coarse-Grained Force Field for Carbohydrates. Journal of Chemical Theory and Computation, 2022, 18, 7555-7569.	5.3	25



#	ARTICLE	IF	CITATIONS
12242	An insight from computational approach to explore novel, high-affinity phosphodiesterase 10A inhibitors for neurological disorders. <i>Journal of Biomolecular Structure and Dynamics</i> , 2023, 41, 9424-9436.	3.5	14
12243	Influence of Selective Extraction/Isolation of Heme/Hemoglobin with Hydrophobic Imidazolium Ionic Liquids on the Precision and Accuracy of Cotinine ELISA Test. <i>International Journal of Molecular Sciences</i> , 2022, 23, 13692.	4.1	0
12244	Thermal Stability Estimation of Single Domain Antibodies Using Molecular Dynamics Simulations. <i>Methods in Molecular Biology</i> , 2023, , 151-163.	0.9	3
12245	The use of machine learning modeling, virtual screening, molecular docking, and molecular dynamics simulations to identify potential VEGFR2 kinase inhibitors. <i>Scientific Reports</i> , 2022, 12, .	3.3	9
12246	Molecular dynamics simulations of cancer cell membrane electroporation under the plasma electric field effect. <i>Plasma Processes and Polymers</i> , 2023, 20, .	3.0	1
12247	Screening and Identification of Natural Productâ€Like Compounds as Potential Antibacterial Agents Targeting FemC of <i>Staphylococcus aureus</i> : An inâ€Silico Approach. <i>ChemistrySelect</i> , 2022, 7, .	1.5	15
12248	Theoretical research on performances of CL-20/HMX cocrystal explosive and its based polymer bonded explosives (PBXs) by molecular dynamics method. <i>Journal of Molecular Modeling</i> , 2022, 28, .	1.8	2
12249	Stability and conformational memory of electrosprayed and rehydrated bacteriophage MS2 virus coat proteins. <i>Current Research in Structural Biology</i> , 2022, 4, 338-348.	2.2	4
12250	Sublytic gasdermin-D pores captured in atomistic molecular simulations. <i>ELife</i> , 0, 11, .	6.0	15
12251	Selectively Targeting STAT3 Using a Small Molecule Inhibitor is a Potential Therapeutic Strategy for Pancreatic Cancer. <i>Clinical Cancer Research</i> , 2023, 29, 815-830.	7.0	12
12252	pH Regulates Ligand Binding to an Enzyme Active Site by Modulating Intermediate Populations. <i>Journal of Physical Chemistry B</i> , 2022, 126, 9759-9770.	2.6	1
12253	Cyclin-Dependent Kinase 5 Regulates cPLA2 Activity and Neuroinflammation in Parkinsonâ€™s Disease. <i>ENeuro</i> , 2022, 9, ENEURO.0180-22.2022.	1.9	4
12254	Mechanical Unfolding and Refolding of NanoLuc via Single-Molecule Force Spectroscopy and Computer Simulations. <i>Biomacromolecules</i> , 2022, 23, 5164-5178.	5.4	1
12255	Cryo-EM structure of the agonist-bound Hsp90-XAP2-AHR cytosolic complex. <i>Nature Communications</i> , 2022, 13, .	12.8	46
12257	The armadillo-repeat domain of Plakophilin 1 binds to human enzyme PADI4. <i>Biochimica Et Biophysica Acta - Proteins and Proteomics</i> , 2023, 1871, 140868.	2.3	3
12258	Computational investigation of conformational fluctuations of AÎ²42 monomers in aqueous ionic liquid mixtures. <i>Journal of Molecular Liquids</i> , 2022, 368, 120779.	4.9	2
12260	Assembling Biocompatible Polymers on Gold Nanoparticles: Toward a Rational Design of Particle Shape by Molecular Dynamics. <i>ACS Omega</i> , 2022, 7, 42292-42303.	3.5	4
12261	Computational design, synthesis and biological evaluation of PDE5 inhibitors based on N2,N4-diaminoquinazoline and N2,N6-diaminopurine scaffolds. <i>Bioorganic and Medicinal Chemistry</i> , 2022, 76, 117092.	3.0	2

#	ARTICLE	IF	CITATIONS
12262	Effect of the CER[NP]:CER[AP] a ratio on the structure of a stratum corneum model lipid matrix - a molecular dynamics study. Chemistry and Physics of Lipids, 2022, , 105259.	3.2	0
12263	Structure and Transport Properties of Poly(ethylene oxide)-Based Cross-Linked Polymer Electrolytesâ”€A Molecular Dynamics Simulations Study. Macromolecules, 2022, 55, 10229-10242.	4.8	2
12264	On the diffusion of ketoprofen and ibuprofen in water: An experimental and theoretical approach. Journal of Chemical Thermodynamics, 2023, 178, 106955.	2.0	2
12265	Binary Salt Structure Classification with Convolutional Neural Networks:Application to Crystal Nucleation and Melting Point Calculations. Journal of Chemical Physics, 0, , .	3.0	0
12266	Betaine Attenuates Chronic Constriction Injury-Induced Neuropathic Pain in Rats by Inhibiting KIF17-Mediated Nociception. ACS Chemical Neuroscience, 2022, 13, 3362-3377.	3.5	3
12267	Conserved Water Networks Identification for Drug Design Using Density Clustering Approaches on Positional and Orientational Data. Journal of Chemical Information and Modeling, 2022, 62, 6105-6117.	5.4	5
12269	Analyzing the potential of selected plant extracts and their structurally diverse secondary metabolites for $\alpha$ -glucosidase inhibitory activity: <i>in vitro</i> and <i>in silico</i> approach. Journal of Biomolecular Structure and Dynamics, 2023, 41, 9523-9538.	3.5	1
12270	Practical Design of 3,6-Di- <i>tert</i> -butyldiphenyldibenzofulvene Derivatives with Enhanced Aggregation-Induced Emission. , 2023, 1, 340-353.		2
12271	Noscapineâ”€Amino Acid Conjugates Suppress the Progression of Cancer Cells. ACS Pharmacology and Translational Science, 0, , .	4.9	3
12272	Partition of the Reactive Species of the Suzukiâ”€Miyaura Reaction between Aqueous and Micellar Environments. Journal of Physical Chemistry B, 2022, 126, 9408-9416.	2.6	7
12273	An allosteric modulator activates BK channels by perturbing coupling between Ca <sup>2+</sup> binding and pore opening. Nature Communications, 2022, 13, .	12.8	7
12274	In Vitro Membrane Platform for the Visualization of Water Impermeability across the Liquid-Ordered Phase under Hypertonic Conditions. Journal of the American Chemical Society, 2022, 144, 21887-21896.	13.7	4
12275	Ethnicâ”€specificity, evolution origin and deleteriousness of Asian <i>BRCA</i> variation revealed by over 7500 <i>BRCA</i> variants derived from Asian population. International Journal of Cancer, 2023, 152, 1159-1173.	5.1	6
12276	Genomic analysis of <i>Paenibacillus</i> sp. MDMC362 from the Merzouga desert leads to the identification of a potentially thermostable catalase. Antonie Van Leeuwenhoek, 2023, 116, 21-38.	1.7	1
12277	Hydrophobicity Effects of $\beta$ -Glutamyl Transpeptidase-Responsive Polymers on the Catalytic Activity and Transcytosis Efficacy. Bioconjugate Chemistry, 2022, 33, 2132-2142.	3.6	4
12278	Dynamic Dissociation Behaviors of sII Hydrates in Liquid Water by Heating: A Molecular Dynamics Simulation Approach. ACS Omega, 2022, 7, 42774-42782.	3.5	1
12279	Molecular study on the behavior of CO <sub>2</sub> hydrate growth promoted by the electric field. Journal of Petroleum Science and Engineering, 2023, 221, 111261.	4.2	5
12280	Absorption Spectra of Flexible Fluorescent Probes by a Combined Computational Approach: Molecular Dynamics Simulations and Time-Dependent Density Functional Theory. Journal of Physical Chemistry A, 2022, 126, 8809-8817.	2.5	2

#	ARTICLE	IF	CITATIONS
12281	<i>In silico</i> designed microtubule-stabilizer drugs against tauopathy in Alzheimer's disease. Journal of Biomolecular Structure and Dynamics, 2023, 41, 8992-9012.	3.5	0
12282	Manifestations of the structural origin of supercooled water's anomalies in the heterogeneous relaxation on the potential energy landscape. Journal of Chemical Physics, 2022, 157, .	3.0	3
12283	Bioactive Nonthermal Biocompatible Plasma Enhances Migration on Human Gingival Fibroblasts. Advanced Healthcare Materials, 2023, 12, .	7.6	3
12284	Binding of the peptide deformylase on the ribosome surface modulates the exit tunnel interior. Biophysical Journal, 2022, , .	0.5	1
12285	Modeling Peptide Nucleic Acid Binding Enthalpies Using MM-GBSA. Journal of Physical Chemistry B, 0, , .	2.6	0
12286	Conformations of Three Types of Ultra-Long-Chain Fatty Acids in Multicomponent Lipid Bilayers. Journal of Physical Chemistry B, 2022, 126, 9316-9324.	2.6	0
12288	Examining the Effect of Polymer Extension on Protein-Polymer Interactions That Occur during Formulation of Protein-Loaded Poly(lactic acid-co-glycolic acid)-polyethylene Glycol Nanoparticles. Polymers, 2022, 14, 4730.	4.5	0
12289	Connection between empty volume and solubility of light gases in [CnMIM][NTf2] ionic liquids. Journal of Molecular Liquids, 2022, 368, 120740.	4.9	1
12290	Defect-characterized phase transition kinetics. Applied Physics Reviews, 2022, 9, .	11.3	14
12291	Deciphering antiviral efficacy of malaria box compounds against malaria exacerbating viral pathogens-Epstein Barr virus and SARS-CoV-2, an in silico study. Medicine in Drug Discovery, 2022, 16, 100146.	4.5	13
12292	Concerted enhanced-sampling simulations to elucidate the helix-fibril transition pathway of intrinsically disordered I $\alpha$ -Synuclein. International Journal of Biological Macromolecules, 2022, 223, 1024-1041.	7.5	3
12293	On the influence of increasing the concentration of Au <sup>144</sup> (SRCOO <sup>1-</sup> ) <sub>60</sub> nanoparticles in water/Na <sup>1+</sup> solution using molecular dynamics simulations. Journal of Molecular Liquids, 2022, 368, 120776.	4.9	0
12294	Anticarcinogenic trimethoxybenzoate of catechin stabilizes the liquid crystalline bilayer phase in phosphatidylethanolamine membranes. Journal of Molecular Liquids, 2022, 368, 120774.	4.9	0
12295	Nucleation Rate Theory for Coordination Number: Elucidating Water-Mediated Formation of a Zigzag Na <sub>2</sub> SO <sub>4</sub> Morphology. ACS Applied Materials & Interfaces, 2022, 14, 53213-53227.	8.0	0
12296	Structural basis of the myotoxic inhibition of the Bothrops pirajai PrTX-I by the synthetic varespladib. Biochimie, 2023, 207, 1-10.	2.6	5
12297	Quantifying the Effect of Spatial Confinement on the Diffusion and Nuclear Magnetic Resonance Relaxation of Water/Hydrocarbon Mixtures: A Molecular Dynamics Simulation Study. Langmuir, 2022, 38, 14540-14549.	3.5	6
12298	Activation and signaling mechanism revealed by GPR119-Gs complex structures. Nature Communications, 2022, 13, .	12.8	6
12299	Quantitative and structural analysis of water association in water-lithium bromide-1,3-dimethylimidazolium chloride mixtures. Journal of Molecular Liquids, 2022, 368, 120828.	4.9	1

#	ARTICLE	IF	CITATIONS
12302	Temperature Extrapolation of Molecular Dynamics Simulations of Complex Chemistry to Microsecond Timescales Using Kinetic Models: Applications to Hydrocarbon Pyrolysis. <i>Journal of Chemical Theory and Computation</i> , 2022, 18, 7496-7509.	5.3	1
12303	Coordinating Anions to the Rescue of the Lithium Ion Mobility in Ternary Solid Polymer Electrolytes Plasticized With Ionic Liquids. <i>Advanced Energy Materials</i> , 2023, 13, .	19.5	25
12304	Molecular Dynamics Model to Explore the Initial Stages of Anion Exchange involving Layered Double Hydroxide Particles. <i>Nanomaterials</i> , 2022, 12, 4039.	4.1	1
12305	What makes 1,3-dioxolane an efficient sil hydrate former?. <i>Fuel</i> , 2023, 334, 126714.	6.4	3
12306	Experimental and computational physics of fullerenes and their nanocomposites: Synthesis, thermo-mechanical characteristics and nanomedicine applications. <i>Physics Reports</i> , 2023, 996, 1-116.	25.6	10
12307	A comprehensive in vitro exploration into the interaction mechanism of coumarin derivatives with bovine hemoglobin: Spectroscopic and computational methods. <i>Journal of Photochemistry and Photobiology A: Chemistry</i> , 2023, 436, 114425.	3.9	8
12309	Discovery of oxindole-based FLT3 inhibitors as a promising therapeutic lead for acute myeloid leukemia carrying the oncogenic ITD mutation. <i>Archiv Der Pharmazie</i> , 2023, 356, .	4.1	12
12310	Understanding the transformations of nanoplastic onto phospholipid bilayers: Mechanism, microscopic interaction and cytotoxicity assessment. <i>Science of the Total Environment</i> , 2023, 859, 160388.	8.0	7
12311	SAFT- $\langle \text{mml:mrow} \langle \text{mml:mi} \rangle \text{I}^3 \langle \text{mml:mi} \rangle \langle \text{mml:mrow} \rangle \langle \text{mml:math} \rangle$ force field for the simulation of molecular fluids 9: Coarse-grained models for polyaromatic hydrocarbons describing thermodynamic, interfacial, structural, and transport properties. <i>Journal of Molecular Liquids</i> , 2023, 369, 120827.	4.9	1
12312	Medium-entropy ceramic aerogels for robust thermal sealing. <i>Journal of Materials Chemistry A</i> , 2023, 11, 742-752.	10.3	2
12313	Insight into molecular mechanism of human insulin encapsulation into the polyacrylic acid/deoxycholic acid-modified chitosan nanogel: An experimental and molecular dynamics investigation. <i>Journal of Molecular Liquids</i> , 2023, 369, 120850.	4.9	2
12314	High-entropy Fe-Cr-Ni-Co-(Cu) coatings produced by vacuum electro-spark deposition for marine and coastal applications. <i>Surface and Coatings Technology</i> , 2023, 453, 129136.	4.8	9
12315	Basics of Quantum Chemical Calculation. , 2022, , 217-241.		0
12316	Biophysical investigation of the interaction between NSAID ibuprofen and cationic biodegradable Cm-E2O2-Cm gemini surfactants. <i>Journal of Molecular Liquids</i> , 2023, 370, 120972.	4.9	6
12317	Molecular dynamics study of the environmental stress cracking agent assisted cavitation in linear and branched polyethylene. <i>Polymer</i> , 2023, 264, 125542.	3.8	2
12318	Neuroprotective potential of cinnamoyl derivatives against Parkinson's disease indicators in <i>Drosophila melanogaster</i> and in silico models. <i>NeuroToxicology</i> , 2023, 94, 147-157.	3.0	2
12319	Oleochemical carbonates: A comprehensive characterization of an emerging class of organic compounds. <i>Journal of Molecular Liquids</i> , 2023, 369, 120854.	4.9	3
12320	Evolutionary and structural aspects of Solanaceae RNases T2. <i>Genetics and Molecular Biology</i> , 2023, 46, .	1.3	1

#	ARTICLE	IF	CITATIONS
12321	Deep learning models for the estimation of free energy of permeation of small molecules across lipid membranes. , 2023, 2, 189-201.		0
12322	Molecular guest exchange and subsequent structural transformation in CH <sub>4</sub> ↔ CO <sub>2</sub> replacement occurring in sH hydrates as revealed by <sup>13</sup> C NMR spectroscopy and molecular dynamic simulations. Chemical Engineering Journal, 2023, 455, 140937.	12.7	6
12323	On the not so anomalous water-induced structural transformations of choline chloride↔urea (reline) deep eutectic system. Physical Chemistry Chemical Physics, 2022, 25, 439-454.	2.8	4
12324	Capturing coacervate formation and protein partition by molecular dynamics simulation. Chemical Science, 0, , .	7.4	1
12325	Investigation of structure and properties of polymerizable deep eutectic solvent based on choline chloride and acrylic acid. Journal of Molecular Liquids, 2023, 370, 121030.	4.9	3
12326	Development of peptide affinity ligands for the purification of polyclonal and monoclonal Fabs from recombinant fluids. Journal of Chromatography A, 2023, 1687, 463701.	3.7	5
12327	Molecular dynamics simulations and kinetic measurements provide insights into the structural requirements of substrate size-dependent specificity of oligogalacturonide oxidase 1 (OGOX1). Plant Physiology and Biochemistry, 2023, 194, 315-325.	5.8	4
12328	Assessment of inconsistencies in the solvent-accessible surfaces of proteins between crystal structures and solution structures observed by LC-MS. Biochemical and Biophysical Research Communications, 2023, 640, 97-104.	2.1	1
12329	The impact of bilayer composition on the dimerization properties of the Slg1 stress sensor TMD from a multiscale analysis. Physical Chemistry Chemical Physics, 0, , .	2.8	0
12330	Insight into poly(1,3-dioxolane)-based polymer electrolytes and their interfaces with lithium Metal: Effect of electrolyte compositions. Chemical Engineering Journal, 2023, 455, 140931.	12.7	2
12331	Alanine rich amphiphilic peptides as green substitutes for hydrate inhibitors: A molecular simulation study. Journal of Molecular Liquids, 2023, 370, 121008.	4.9	22
12332	Novel biosurfactants: Rationally designed surface-active peptides and in silico evaluation at the decane-water interface. Process Biochemistry, 2023, 125, 84-95.	3.7	1
12333	Understanding the role of host-guest interactions in enhancing oil recovery through Î²-cyclodextrin and adamantane modified copolymer. Journal of Molecular Liquids, 2023, 369, 120841.	4.9	8
12334	Molecular dynamics simulations and X-ray scattering show the Î³-carrageenan disorder-to-order transition to be the formation of double-helices. Carbohydrate Polymers, 2023, 302, 120417.	10.2	6
12335	Study of potential inhibition of the estrogen receptor Î± by cannabinoids using an in silico approach: Agonist vs antagonist mechanism. Computers in Biology and Medicine, 2023, 152, 106403.	7.0	0
12336	In silico study of selective inhibition mechanism of S-adenosyl-L-methionine analogs for human DNA methyltransferase 3A. Computational Biology and Chemistry, 2023, 102, 107796.	2.3	0
12337	A synergistic effect of NH <sub>3</sub> BH <sub>3</sub> and H <sub>2</sub> on their pressurization metallization: An Ab initio molecular dynamics study. Computational Materials Science, 2023, 218, 111972.	3.0	0
12338	Temperature-dependent effect of cooling rate on the melt-quenching process of metallic glasses. Computational Materials Science, 2023, 218, 111930.	3.0	5

#	ARTICLE	IF	CITATIONS
12339	Determination of hydrophobicity and hydrophilicity ratio in the synergistic effect between cationic surfactants using coarse-grained MD simulation. <i>Colloids and Surfaces A: Physicochemical and Engineering Aspects</i> , 2023, 659, 130779.	4.7	1
12340	Ag <sup>+</sup> ion in choline chloride and glycerol mixture: Evaluation of electrochemical properties and molecular modelling approaches. <i>Journal of Molecular Liquids</i> , 2023, 371, 121053.	4.9	4
12341	Atomic structures of grain boundaries for Si and Ge: A simulated annealing method with artificial-neural-network interatomic potentials. <i>Journal of Physics and Chemistry of Solids</i> , 2023, 173, 111114.	4.0	3
12342	Ligand-receptor interaction in the specific targeting of biomimetic peptide nanoparticles to lysophosphatidylcholine. <i>International Journal of Biological Macromolecules</i> , 2023, 227, 193-202.	7.5	4
12343	Glycation restrains open-closed conformation of Insulin. <i>Computational Biology and Chemistry</i> , 2023, 102, 107803.	2.3	1
12344	Characterization of Climbazoleâ€“Bovine serum albumin interaction by experimental and in silico approaches. <i>Spectrochimica Acta - Part A: Molecular and Biomolecular Spectroscopy</i> , 2023, 288, 122197.	3.9	5
12345	Identification of possible binding modes of SARS-CoV-2 spike N-terminal domain for ganglioside GM1. <i>Chemical Physics Letters</i> , 2023, 812, 140260.	2.6	3
12346	Effects of inert gas CO <sub>2</sub> /N <sub>2</sub> injection on coal low-temperature oxidation characteristic: Experiments and simulations. <i>Arabian Journal of Chemistry</i> , 2023, 16, 104510.	4.9	11
12347	An in-silico study to gain a comprehensive understanding of the effects of glucosylation on quercetin properties. <i>Computational and Theoretical Chemistry</i> , 2023, 1220, 113981.	2.5	2
12348	Carbon dioxide capture and its electrochemical reduction study in deep eutectic solvent (DES) via experimental and molecular simulation approaches. <i>Journal of CO<sub>2</sub> Utilization</i> , 2023, 68, 102349.	6.8	8
12349	Molecular level insight into the different interaction intensity between microplastics and aromatic hydrocarbon in pure water and seawater. <i>Science of the Total Environment</i> , 2023, 862, 160786.	8.0	9
12350	Design of elevated temperature phase change materials of carbonate-villiaumite eutectic mixtures: Method, validation, and application. <i>Solar Energy Materials and Solar Cells</i> , 2023, 251, 112155.	6.2	1
12351	Tunnel dynamics of quinone derivatives and its coupling to protein conformational rearrangements in respiratory complex I. <i>Biochimica Et Biophysica Acta - Bioenergetics</i> , 2023, 1864, 148951.	1.0	1
12352	Abnormal methylation in the <i>NDUFA13</i> gene promoter of breast cancer cells breaks the cooperative DNA recognition by transcription factors. <i>QRB Discovery</i> , 2022, 3, .	1.6	2
12353	Drug and Anti-Viral Peptide Design to Inhibit the Monkeypox Virus by Restricting A36R Protein. <i>Bioinformatics and Biology Insights</i> , 2022, 16, 117793222211411.	2.0	2
12354	Shape Memory Alloys â€“ Frontier Developments. , 2023, , 610-679.		0
12355	Solvent effects on catechol's binding affinity: investigating the role of the intra-molecular hydrogen bond through a multi-level computational approach. <i>Physical Chemistry Chemical Physics</i> , 2023, 25, 2523-2536.	2.8	1
12358	Densities, Viscosities, Thermal Expansivities, and Isothermal Compressibilities of Carbonated Hydroalcoholic Solutions for Applications in Sparkling Beverages. <i>Journal of Physical Chemistry B</i> , 2022, 126, 10194-10205.	2.6	1



#	ARTICLE	IF	CITATIONS
12359	Analysis and Identification of Bioactive Compounds of Cannabinoids in Silico for Inhibition of SARS-CoV-2 and SARS-CoV. <i>Biomolecules</i> , 2022, 12, 1729.	4.0	2
12361	Molecular dynamics simulation study on <i>Bacillus subtilis</i> EngA: the presence of Mg <sup>2+</sup> at the active-sites promotes the functionally important conformation. <i>Journal of Biomolecular Structure and Dynamics</i> , 2023, 41, 9219-9231.	3.5	0
12363	The Mechanism of Selective Recognition of Lipid Substrate by hDHH20 Enzyme. <i>International Journal of Molecular Sciences</i> , 2022, 23, 14791.	4.1	1
12364	Electrostatic Interactions Are the Primary Determinant of the Binding Affinity of SARS-CoV-2 Spike RBD to ACE2: A Computational Case Study of Omicron Variants. <i>International Journal of Molecular Sciences</i> , 2022, 23, 14796.	4.1	14
12366	Poisson's Ratio of f.c.c. Hard-Sphere Crystals with Cubic Supercells Containing Four Nanochannels Filled by Hard Spheres of Another Diameter. <i>Physica Status Solidi (B): Basic Research</i> , 2022, 259, .	1.5	4
12367	Encapsulation Dynamics of Neuromuscular Blocking Drugs by Sugammadex. <i>Anesthesiology</i> , 2023, 138, 152-163.	2.5	7
12370	The Role of Host Cell Glycans on Virus Infectivity: The SARS-CoV-2 Case. <i>Advanced Science</i> , 2023, 10, .	11.2	4
12372	Spiro heterocycles bearing piperidine moiety as potential scaffold for antileishmanial activity: synthesis, biological evaluation, and <i>in silico</i> studies. <i>Journal of Enzyme Inhibition and Medicinal Chemistry</i> , 2023, 38, 330-342.	5.2	7
12373	Protein Structure Validation Derives a Smart Conformational Search in a Physically Relevant Configurational Subspace. <i>Journal of Chemical Information and Modeling</i> , 2022, 62, 6217-6227.	5.4	0
12374	Effect of Alcohol Tail Length on Aggregate Behavior of Alcohol and AOT at the Water-scCO <sub>2</sub> Interface: MD Simulation Study. <i>ACS Symposium Series</i> , 0, , 263-288.	0.5	0
12375	Molecular mechanism of drug transport and release through zeolitic imidazole framework nanospheres for versatile drug delivery applications. <i>Journal of Molecular Liquids</i> , 2023, 371, 120822.	4.9	2
12376	Cooling-Rate Computer Simulations for the Description of Crystallization of Organic Phase-Change Materials. <i>International Journal of Molecular Sciences</i> , 2022, 23, 14576.	4.1	5
12377	Water Network in the Binding Pocket of Fluorinated BPTI–Trypsin Complexes—Insights from Simulation and Experiment. <i>Journal of Physical Chemistry B</i> , 2022, 126, 9985-9999.	2.6	2
12378	Kinetics of Drug Release from Clay Using Enhanced Sampling Methods. <i>Pharmaceutics</i> , 2022, 14, 2586.	4.5	2
12379	Hierarchical Coarse-Grained Strategy for Macromolecular Self-Assembly: Application to Hepatitis B Virus-Like Particles. <i>International Journal of Molecular Sciences</i> , 2022, 23, 14699.	4.1	2
12380	Computational Study of Helicase from SARS-CoV-2 in RNA-Free and Engaged Form. <i>International Journal of Molecular Sciences</i> , 2022, 23, 14721.	4.1	3
12381	Osmotic Contribution of Synthesized Betaine by Choline Dehydrogenase Using In Vivo and In Vitro Models of Post-traumatic Syringomyelia. <i>Cellular and Molecular Bioengineering</i> , 2023, 16, 41-54.	2.1	2
12382	Differentiating interactions of antimicrobials with Gram-negative and Gram-positive bacterial cell walls using molecular dynamics simulations. <i>Biointerphases</i> , 2022, 17, .	1.6	7

#	ARTICLE	IF	CITATIONS
12384	Hydration Structures and Dynamics of the Sodium Fluoride Aqueous Solutions at Various Temperatures: Molecular Dynamics Simulations. <i>Journal of Solution Chemistry</i> , 2023, 52, 176-186.	1.2	1
12385	SARS-CoV-2 Delta Variant: Interplay between Individual Mutations and Their Allosteric Synergy. <i>Biomolecules</i> , 2022, 12, 1742.	4.0	6
12386	Path Sampling Simulations Reveal How the Q61L Mutation Alters the Dynamics of KRas. <i>Journal of Physical Chemistry B</i> , 2022, 126, 10034-10044.	2.6	0
12387	SARS-CoV-2 accessory protein 7b forms homotetramers in detergent. <i>Virology Journal</i> , 2022, 19, .	3.4	1
12388	SIMPLE METHOD TO MODIFY FORCE FIELDS FOR THE MOLECULAR DYNAMICS SIMULATION OF AQUEOUS ALCOHOL SOLUTIONS. <i>Journal of Structural Chemistry</i> , 2022, 63, 1802-1810.	1.0	1
12389	A Comparison of Methods for Computing Relative Anhydrousâ€Hydrate Stability with Molecular Simulation. <i>Crystal Growth and Design</i> , 2023, 23, 142-167.	3.0	5
12390	Membrane Lipid Reshaping Underlies Oxidative Stress Sensing by the Mitochondrial Proteins UCP1 and ANT1. <i>Antioxidants</i> , 2022, 11, 2314.	5.1	2
12391	Fluorescence Turnâ€on of Tetraphenylethylene Derivative by Transfer from Cyclodextrin to Liposomes, HeLa Cells, and <i>E. coli</i> . <i>Chemistry - A European Journal</i> , 2023, 29, .	3.3	3
12392	Intrinsically disordered ectodomain modulates ion permeation through a metal transporter. <i>Proceedings of the National Academy of Sciences of the United States of America</i> , 2022, 119, .	7.1	0
12393	Elucidating lipid conformations in the ripple phase: Machine learning reveals four lipid populations. <i>Biophysical Journal</i> , 2023, 122, 442-450.	0.5	4
12399	Uptake mechanism of iron-phytosiderophore from the soil based on the structure of yellow stripe transporter. <i>Nature Communications</i> , 2022, 13, .	12.8	5
12400	Intercalation of argon in honeycomb structures towards promising strategy for rechargeable Li-ion batteries. <i>Journal of Physics Condensed Matter</i> , 2023, 35, 085301.	1.8	0
12401	Molecular and thermodynamic insights into interfacial interactions between collagen and cellulose investigated by molecular dynamics simulation and umbrella sampling. <i>Journal of Computer-Aided Molecular Design</i> , 2023, 37, 39-51.	2.9	3
12402	Membrane curvature sensing and stabilization by the autophagic LC3 lipidation machinery. <i>Science Advances</i> , 2022, 8, .	10.3	24
12403	Molecular Dynamics and Nuclear Magnetic Resonance Studies of Supercritical CO2 Sorption in Poly(Methyl Methacrylate). <i>Polymers</i> , 2022, 14, 5332.	4.5	5
12404	Orientational Preferences of GPI-Anchored Ly6/uPAR Proteins. <i>International Journal of Molecular Sciences</i> , 2023, 24, 11.	4.1	3
12406	Multilayered allosteric modulation of coupled folding and binding by phosphorylation, peptidyl-prolyl <i>cis</i> / <i>trans</i> isomerization, and diversity of interaction partners. <i>Journal of Chemical Physics</i> , 2022, 157, .	3.0	2
12407	Towards a rational design of natural deep eutectic solvents for the extraction of polyphenols from <i>Luma apiculata</i> . <i>Journal of Molecular Liquids</i> , 2023, 372, 121155.	4.9	3

#	ARTICLE	IF	CITATIONS
12408	Dynamical Interaction Analysis of Proteins by a Random Forest-Fragment Molecular Orbital (RF-FMO) Method and Application to Src Tyrosine Kinase. Bulletin of the Chemical Society of Japan, 2023, 96, 42-47.	3.2	6
12409	Understanding the Molecular-Level Structure and Dynamics of Sodium Ions in Water in Ionic Liquid Electrolytes by Molecular Dynamics Simulations. Journal of Chemical & Engineering Data, 2023, 68, 162-172.	1.9	2
12410	Dual aromatase-steroid sulfatase inhibitors (DASI's) for the treatment of breast cancer: a structure guided ligand based designing approach. Journal of Biomolecular Structure and Dynamics, 2023, 41, 10604-10626.	3.5	0
12411	(-)-Epigallocatechin-3-gallate Directly Binds Cyclophilin D: A Potential Mechanism for Mitochondrial Protection. Molecules, 2022, 27, 8661.	3.8	1
12412	Thermal conductivity and conductance of protein in aqueous solution: Effects of geometrical shape. Journal of Computational Chemistry, 2023, 44, 857-868.	3.3	6
12413	Knowledge-driven design and optimization of potent symmetric anticancer molecules: A case study on PKM2 activators. Computers in Biology and Medicine, 2022, 151, 106313.	7.0	0
12414	In vitro and computational studies of the $\beta$ -lactamase inhibition and $\beta$ -lactam potentiating properties of plant secondary metabolites. Journal of Biomolecular Structure and Dynamics, 2023, 41, 10326-10346.	3.5	1
12416	Molecular simulation of the adsorption of the hydration inhibitor		

#	ARTICLE	IF	CITATIONS
12432	Designing a multi-epitope candidate vaccine by employing immunoinformatics approaches to control African swine fever spread. <i>Journal of Biomolecular Structure and Dynamics</i> , 2023, 41, 10214-10229.	3.5	6
12433	Elasticity and Viscosity of hcp Iron at Earth's Inner Core Conditions From Machine Learningâ€Based Largeâ€Scale Atomistic Simulations. <i>Geophysical Research Letters</i> , 2022, 49, .	4.0	2
12434	Unraveling the Structural Changes in the DNA-Binding Region of Tumor Protein p53 (TP53) upon Hotspot Mutation p53 Arg248 by Comparative Computational Approach. <i>International Journal of Molecular Sciences</i> , 2022, 23, 15499.	4.1	3
12435	Molecular Dynamics Simulation of Methane Hydrate Formation on Pipeline Surface in the Presence of Corrosion Inhibitors. <i>Energy &amp; Fuels</i> , 2023, 37, 301-309.	5.1	2
12437	Visualizing the transiently populated closed-state of human HSP90 ATP binding domain. <i>Nature Communications</i> , 2022, 13, .	12.8	4
12438	Amentoflavone and methyl hesperidin, novel lead molecules targeting epitranscriptomic modulator in acute myeloid leukemia: in silico drug screening and molecular dynamics simulation approach. <i>Journal of Molecular Modeling</i> , 2023, 29, .	1.8	11
12439	Structural basis for Y2 receptor-mediated neuropeptide Y and peptide YY signaling. <i>Structure</i> , 2023, 31, 44-57.e6.	3.3	2
12440	Hard-disk pressure computationsâ€a historic perspective. <i>Journal of Chemical Physics</i> , 2022, 157, .	3.0	5
12441	Synthesis of Carrier-Free Paclitaxelâ€Curcumin Nanoparticles: The Role of Curcuminoids. <i>Bioengineering</i> , 2022, 9, 815.	3.5	1
12442	Microsecond-long simulation reveals the molecular mechanism for the dual inhibition of falcipain-2 and falcipain-3 by antimalarial lead compounds. <i>Frontiers in Molecular Biosciences</i> , 0, 9, .	3.5	3
12443	Calculation of Free Energy of Binding for Widely Specific Pyrimidine-Nucleoside Phosphorylase and Suspected Inhibitors. <i>Russian Journal of Bioorganic Chemistry</i> , 2022, 48, 1262-1272.	1.0	0
12446	Influence mechanism of different organic solvents on API solvation behaviors: Molecular dynamics simulations. <i>Fluid Phase Equilibria</i> , 2023, 567, 113708.	2.5	4
12447	Personal Precise Force Field for Intrinsically Disordered and Ordered Proteins Based on Deep Learning. <i>Journal of Chemical Information and Modeling</i> , 2023, 63, 362-374.	5.4	6
12448	Bioactive compounds from <i>Pandanous fascicularis</i> as potential therapeutic candidate to tackle hepatitis a inhibition: Docking and molecular dynamics simulation study. <i>Journal of Biomolecular Structure and Dynamics</i> , 2023, 41, 10478-10494.	3.5	4
12449	Global Analysis of Plasmodium falciparum Dihydropteroate Synthase Variants Associated with Sulfadoxine Resistance Reveals Variant Distribution and Mechanisms of Resistance:A Computational-Based Study. <i>Molecules</i> , 2023, 28, 145.	3.8	0
12450	Integrin Î±IIbÎ²3 intermediates: From molecular dynamics to adhesion assembly. <i>Biophysical Journal</i> , 2023, 122, 533-543.	0.5	4
12451	The effect of various partial atomic charges on the bulk and liquid/vacuum interface properties of iodobenzene derivatives at their melting points. <i>Journal of Molecular Graphics and Modelling</i> , 2023, 119, 108400.	2.4	2
12452	Correlated Fluctuations of Structural Indicators Close to the Liquidâ€Liquid Transition in Supercooled Water. <i>Journal of Physical Chemistry B</i> , 2023, 127, 378-386.	2.6	10

#	ARTICLE	IF	CITATIONS
12453	Proton Transfers to DNA in Native Electrospray Ionization Mass Spectrometry: A Quantum Mechanics/Molecular Mechanics Study. <i>Journal of Physical Chemistry Letters</i> , 0, , 12004-12010.	4.6	1
12454	Liquid structure of a water-based, hydrophobic and natural deep eutectic solvent: The case of thymol-water. A Molecular Dynamics study. <i>Journal of Molecular Liquids</i> , 2023, 372, 121151.	4.9	5
12455	Conformation and energy investigation of microtubule longitudinal dynamic instability induced by natural products. <i>Chemical Biology and Drug Design</i> , 0, , .	3.2	0
12456	Fragment screening using biolayer interferometry reveals ligands targeting the SHP-motif binding site of the AAA+ATPase p97. <i>Communications Chemistry</i> , 2022, 5, .	4.5	2
12457	Computational Exploration of Anti-cancer Potential of Flavonoids against Cyclin-Dependent Kinase 8: An <i>In Silico</i> Molecular Docking and Dynamic Approach. <i>ACS Omega</i> , 2023, 8, 391-409.	3.5	19
12458	Thermally Controlled Exciplex Fluorescence in a Dynamic Homo[2]catenane. <i>Journal of the American Chemical Society</i> , 2022, 144, 23551-23559.	13.7	12
12459	Molecular dynamics studies of $\langle \text{CED} \rangle^{\text{E4}} \langle \text{CED} \rangle^{\text{E9}} \langle \text{EGL} \rangle^{\text{E1}}$ ternary complex reveal $\langle \text{CED} \rangle^{\text{E4}}$ release mechanism in the linear apoptotic pathway of <i>Caenorhabditis elegans</i> . <i>Proteins: Structure, Function and Bioinformatics</i> , 2023, 91, 679-693.	2.6	0
12460	Absolute binding free energies of the antiviral peptide ATN-161 with protein targets of SARS-CoV-2. <i>Journal of Biomolecular Structure and Dynamics</i> , 2023, 41, 10546-10557.	3.5	2
12461	Blue Fluorescence of Cyano-tryptophan Predicts Local Electrostatics and Hydrogen Bonding in Biomolecules. <i>Journal of Physical Chemistry B</i> , 2022, 126, 10732-10740.	2.6	4
12462	Study on the dislocation mechanism of $\text{Ni}_{47}\text{Co}_{53}$ alloy during rapid solidification. <i>Chinese Physics B</i> , 0, , .	1.4	0
12463	Carbonyl-Containing Solid Polymer Electrolyte Host Materials: Conduction and Coordination in Polyketone, Polyester, and Polycarbonate Systems. <i>Macromolecules</i> , 2022, 55, 10940-10949.	4.8	12
12464	An $\text{I}^{\text{S}} \rightarrow \text{I}^{\text{E}}$ transition in S6 shapes the conformational cycle of the bacterial sodium channel NavAb. <i>Journal of General Physiology</i> , 2023, 155, .	1.9	2
12465	Does Supramolecular Gelation Require an External Trigger?. <i>Gels</i> , 2022, 8, 813.	4.5	2
12466	A Biologically Active Chromone from <i>Bomarea setacea</i> ( <i>Alstroemeriaceae</i> ): Leishmanicidal, Antioxidant and Multilevel Computational Studies. <i>ChemistrySelect</i> , 2022, 7, .	1.5	2
12467	Building Quantitative Bridges between Dynamics and Sequences of SARS-CoV-2 Main Protease and a Diverse Set of Thirty-Two Proteins. <i>Journal of Chemical Information and Modeling</i> , 2023, 63, 9-19.	5.4	0
12468	Conformational Dynamics of the Receptor-Binding Domain of the SARS-CoV-2 Spike Protein. <i>Biomedicines</i> , 2022, 10, 3233.	3.2	0
12469	Structural Investigation of DHICA Eumelanin Using Density Functional Theory and Classical Molecular Dynamics Simulations. <i>Molecules</i> , 2022, 27, 8417.	3.8	0
12470	Combined computational approaches for developing new anti-Alzheimer drug candidates: 3D-QSAR, molecular docking and molecular dynamics studies of liquiritigenin derivatives. <i>Heliyon</i> , 2022, 8, e11991.	3.2	27

#	ARTICLE	IF	CITATIONS
12471	<i>Protic</i> Ionic Liquids for Intrinsically Stretchable Conductive Polymers. ACS Applied Materials & Interfaces, 2023, 15, 3202-3213.	8.0	3
12474	Potential inhibitors of FemC to combat <i>Staphylococcus aureus</i>: virtual screening, molecular docking, dynamics simulation, and MM-PBSA analysis. Journal of Biomolecular Structure and Dynamics, 0, , 1-12.	3.5	1
12475	Structural insights into the mechanism of the sodium/iodide symporter. Nature, 2022, 612, 795-801.	27.8	15
12476	Synthesis, Characterization, DFT Mechanistic Study, Antimicrobial Activity, Molecular Modeling, and ADMET Properties of Novel Pyrazole-isoxazoline Hybrids. ACS Omega, 2022, 7, 46731-46744.	3.5	15
12478	Microtubule Severing Enzymes Oligomerization and Allostery: A Tale of Two Domains. Journal of Physical Chemistry B, 2022, 126, 10569-10586.	2.6	3
12479	Csk Î±C Helix: A Computational Analysis of an Essential Region for Conformational Transitions. Journal of Physical Chemistry B, 2022, 126, 10587-10596.	2.6	5
12480	Assisting role of water molecules in ionic recognition by 18-crown-6 ether in aqueous solutions. Journal of Molecular Liquids, 2023, 371, 121127.	4.9	4
12481	Guide for determination of protein structural ensembles by combining <scp>cryoâ€EM</scp> data with metadynamics. FEBS Open Bio, 0, , .	2.3	0
12482	<i>In Vitro</i> Screening and MD Simulations of Thiourea Derivatives against SARS-CoV-2 in Association with Multidrug Resistance ABCB1 Transporter. ACS Omega, 2022, 7, 47671-47679.	3.5	2
12483	Molecular characterization of glutor-GLUT interaction and prediction of glutorâ€™s drug-likeness: implications for its utility as an antineoplastic agent. Journal of Biomolecular Structure and Dynamics, 2023, 41, 11262-11273.	3.5	0
12484	Carbon K-edge x-ray absorption spectra of liquid alcohols from quantum chemical calculations of liquid structures obtained by molecular dynamics simulations. Journal of Chemical Physics, 2023, 158, .	3.0	2
12485	<i>In silico</i> study revealed the inhibitory activity of selected phytomolecules of <i>C. rotundus</i> against VacA implicated in gastric ulcer. Journal of Biomolecular Structure and Dynamics, 2023, 41, 10713-10724.	3.5	2
12486	Free energy calculations and unbiased molecular dynamics targeting the liquidâ€™liquid transition in water no manâ€™s land. Journal of Chemical Physics, 2023, 158, .	3.0	3
12488	The Role of the Extrafibrillar Volume on the Mechanical Properties of Molecular Models of Mineralized Bone Microfibrils. ACS Biomaterials Science and Engineering, 2023, 9, 230-245.	5.2	2
12489	Interference of malvidin and its mono- and di-glucosides on the membrane â€™ Combined in vitro and computational chemistry study. Journal of Functional Foods, 2022, 99, 105340.	3.4	4
12490	Force-tuned avidity of spike variant-ACE2 interactions viewed on the single-molecule level. Nature Communications, 2022, 13, .	12.8	20
12493	Investigation of human Î²-defensins 1, 2 and 3 in human saliva by molecular dynamics. European Physical Journal E, 2022, 45, .	1.6	0
12494	Evaluation of action of steroid molecules on SARS-CoV-2 by inhibiting NSP-15, an endoribonuclease. Molecular Diversity, 0, , .	3.9	1



#	ARTICLE	IF	CITATIONS
12497	Potential binding modes of the gut bacterial metabolite, 5-hydroxyindole, to the intestinal L-type calcium channels and its impact on the microbiota in rats. <i>Gut Microbes</i> , 2023, 15, .	9.8	3
12499	In silico and inÂvitro studies of potential inhibitors against Dengue viral protein NS5 Methyl Transferase from Ginseng and Notoginseng. <i>Journal of Traditional and Complementary Medicine</i> , 2023, 13, 1-10.	2.7	6
12500	Studies on the Interaction between Model Proteins and Fluorinated Ionic Liquids. <i>Pharmaceutics</i> , 2023, 15, 157.	4.5	4
12502	Coenzyme corona formation on carbon nanotubes leads to disruption of the redox balance in metabolic reactions. <i>Nanoscale</i> , 2023, 15, 2340-2353.	5.6	2
12503	Discovery of TP0597850: A Selective, Chemically Stable, and Slow Tight-Binding Matrix Metalloproteinase-2 Inhibitor with a Phenylbenzamideâ€“Pentapeptide Hybrid Scaffold. <i>Journal of Medicinal Chemistry</i> , 2023, 66, 822-836.	6.4	4
12504	Modeling the molecular fingerprint of protein-lipid interactions of MLKL on complex bilayers. <i>Frontiers in Chemistry</i> , 0, 10, .	3.6	5
12505	Mechanistic insights and importance of hydrophobicity in cationic polymers for cancer therapy. <i>Journal of Materials Chemistry B</i> , 2023, 11, 1456-1468.	5.8	1
12506	Atomistic Insights into the Inhibitory Mechanism of Tyrosine Phosphorylation against the Aggregation of Human Tau Fragment PHF6. <i>Journal of Physical Chemistry B</i> , 2023, 127, 335-345.	2.6	4
12507	Peptideâ€“Membrane Binding: Effects of the Amino Acid Sequence. <i>Journal of Physical Chemistry B</i> , 2023, 127, 912-920.	2.6	3
12508	Theoretical Study on the Swelling Mechanism and Structural Stability of Ni<sub>3</sub>Al-LDH Based on Molecular Dynamics. <i>ACS Omega</i> , 2023, 8, 3286-3297.	3.5	2
12510	SHP-1 tyrosine phosphatase binding to c-Src kinase phosphor-dependent conformations: A comparative structural framework. <i>PLoS ONE</i> , 2023, 18, e0278448.	2.5	0
12511	The specificity of pectate lyase VdPelB from <i>Verticillium dahliae</i> is highlighted by structural, dynamical and biochemical characterizations. <i>International Journal of Biological Macromolecules</i> , 2023, 231, 123137.	7.5	1
12512	Molecular Dynamics Simulation of NiTi Shape Memory Alloys Produced by Laser Powder Bed Fusion: Laser Parameters on Phase Transformation Behavior. <i>Materials</i> , 2023, 16, 409.	2.9	4
12513	Molecular Modelling of Ionic Liquids: Situations When Charge Scaling Seems Insufficient. <i>Molecules</i> , 2023, 28, 800.	3.8	5
12516	Theoretical Study on the Regulating Mechanism of the Transition Between the Open-closed State of hCtBP2: A Combined Molecular Dynamics and Quantum Mechanical Interaction Analysis. <i>Chemistry Letters</i> , 2023, 52, 120-123.	1.3	2
12517	Rational design of potent ultrashort antimicrobial peptides with programmable assembly into nanostructured hydrogels. <i>Frontiers in Chemistry</i> , 0, 10, .	3.6	3
12518	Discovery of new inhibitors of <i>Mycobacterium tuberculosis</i> EPSP synthase - A computational study. <i>Journal of Molecular Graphics and Modelling</i> , 2023, , 108404.	2.4	1
12519	Molecular Insights into Substrate Binding of the Outer Membrane Enzyme OmpT. <i>Catalysts</i> , 2023, 13, 214.	3.5	1

#	ARTICLE	IF	CITATIONS
12520	Atomistic Insights into Organization of RNA-Loaded Lipid Nanoparticles. <i>Journal of Physical Chemistry B</i> , 2023, 127, 1158-1166.	2.6	4
12521	Citrus, Milk Thistle, and Propolis Extracts Improved the Intestinal Permeability of Curcuminoids from Turmeric Extractâ€”An <i>In Silico</i> and <i>In Vitro</i> Permeability Caco-2 Cells Approach. <i>ACS Food Science &amp; Technology</i> , 2023, 3, 113-122.	2.7	2
12522	Reentrant 2D Nanostructured Liquid Crystals by Competition between Molecular Packing and Conformation: Potential Design for Multistep Switching of Ionic Conductivity. <i>ChemPhysChem</i> , 2023, 24, .	2.1	2
12523	Electronic Origin of Laser-Induced Ferroelectricity in SrTiO <sub>3</sub> . <i>Journal of Physical Chemistry Letters</i> , 2023, 14, 576-583.	4.6	5
12524	Molecular mechanism of LIP05 derived from <i>Monascus purpureus</i> YJX-8 for synthesizing fatty acid ethyl esters under aqueous phase. <i>Frontiers in Microbiology</i> , 0, 13, .	3.5	8
12525	Butein Inhibits the Glycation of Î±-Crystallin: An Approach in Prevention of Retinopathy. <i>Journal of Fluorescence</i> , 2023, 33, 1347-1358.	2.5	1
12527	Physical Properties and Low-Frequency Polarizability Anisotropy and Dipole Responses of Phosphonium Bis(fluorosulfonyl)amide Ionic Liquids with Pentyl, Ethoxyethyl, or 2-(Ethylthio)ethyl Group. <i>Journal of Physical Chemistry B</i> , 2023, 127, 542-556.	2.6	4
12528	Effects of the Jokela type of spinal muscular atrophyâ€”related <i>scp</i> >G66V</scp> mutation on the structural ensemble characteristics of <i>scp</i> >CHCHD10</scp>. <i>Proteins: Structure, Function and Bioinformatics</i> , 2023, 91, 739-749.	2.6	1
12529	A structure-based virtual high-throughput screening, molecular docking, molecular dynamics and MM/PBSA study identified novel putative drug-like dual inhibitors of trypanosomal cruzain and rhodesain cysteine proteases. <i>Molecular Diversity</i> , 0, , .	3.9	0
12530	Brute Force Virtual Drug Screening with Molecular Dynamics Simulation and MM/PBSA to Find Potent Inhibitors of METTL16. <i>IEEE/ACM Transactions on Computational Biology and Bioinformatics</i> , 2023, 20, 2356-2361.	3.0	4
12531	A Molecular Insight into the Dehydration of a Metalâ€”Organic Framework and its Impact on the CO <sub>2</sub> Capture. <i>Chemistry - A European Journal</i> , 2023, 29, .	3.3	2
12532	Physical mechanisms of the Soret effect in binary Lennard-Jones liquids elucidated with thermal-response calculations. <i>Journal of Chemical Physics</i> , 2023, 158, .	3.0	1
12533	Ab initio study of boronâ€”rich amorphous boron carbides. <i>Journal of the American Ceramic Society</i> , 2023, 106, 2862-2874.	3.8	1
12534	A novel fold for acyltransferase-3 (AT3) proteins provides a framework for transmembrane acyl-group transfer. <i>ELife</i> , 0, 12, .	6.0	1
12535	Effects of a Semisynthetic Catechin on Phosphatidylglycerol Membranes: A Mixed Experimental and Simulation Study. <i>Molecules</i> , 2023, 28, 422.	3.8	1
12537	Predictions of the Poses and Affinity of a Ligand over the Entire Surface of a NEET Protein: The Case of Human MitoNEET. <i>Journal of Chemical Information and Modeling</i> , 2023, 63, 643-654.	5.4	2
12539	4-Cyanotryptophan as a Sensitive Fluorescence Probe of Local Electric Field of Proteins. <i>Journal of Physical Chemistry B</i> , 2023, 127, 514-519.	2.6	2
12540	Increasing the calcium sensitivity of muscle using trifluoperazine-induced manipulations in silico, in vitro and in vivo systems. <i>Archives of Biochemistry and Biophysics</i> , 2023, , 109521.	3.0	0

#	ARTICLE	IF	CITATIONS
12541	Microfluidicsâ€Based Force Spectroscopy Enables Highâ€Throughput Force Experiments with Subâ€Nanometer Resolution and Subâ€Piconewton Sensitivity. <i>Small</i> , 2023, 19, .	10.0	1
12542	On the Propensity of Excess Hydroxide Ions at the Alcohol Monolayerâ€Water Interface. <i>Journal of Physical Chemistry B</i> , 2023, 127, 783-793.	2.6	0
12543	Martini 3 Coarse-Grained Model for Second-Generation Unidirectional Molecular Motors and Switches. <i>Journal of Chemical Theory and Computation</i> , 2023, 19, 596-604.	5.3	2
12544	How acidic amino acid residues facilitate DNA target site selection. <i>Proceedings of the National Academy of Sciences of the United States of America</i> , 2023, 120, .	7.1	1
12545	Fully Atomistic Molecular Dynamics Simulation of a TIPS-Pentacene:Polystyrene Mixed Film Obtained via the Solution Process. <i>Nanomaterials</i> , 2023, 13, 312.	4.1	1
12546	Probing DNA structural heterogeneity by identifying conformational subensembles of a bicovalently bound cyanine dye. <i>Journal of Chemical Physics</i> , 2023, 158, .	3.0	2
12547	The pathogenic effect of SNPs on structure and function of human TLR4 using a computational approach. <i>Journal of Biomolecular Structure and Dynamics</i> , 2023, 41, 12387-12400.	3.5	1
12548	Determining interchromophore effects for energy transport in molecular networks using machine-learning algorithms. <i>Physical Chemistry Chemical Physics</i> , 2023, 25, 3651-3665.	2.8	2
12549	Molecular dynamics simulation of solidification epitaxial growth in a nanoscale molten pool. <i>Nanoscale Advances</i> , 0, , .	4.6	1
12550	Mechanisms by Which Small Molecules of Diverse Chemotypes Arrest Sec14 Lipid Transfer Activity. <i>Journal of Biological Chemistry</i> , 2023, , 102861.	3.4	1
12551	Softening by charging: how collective modes of ionic association in concentrated redoxmer/electrolyte solutions define the structural and dynamic properties in different states of charge. <i>Physical Chemistry Chemical Physics</i> , 2023, 25, 4243-4254.	2.8	1
12553	Suppression of Lung Cancer Malignancy by Micellized siRNA through Cell Cycle Arrest. <i>Advanced Healthcare Materials</i> , 2023, 12, .	7.6	2
12554	Diameter-Selective Sorting of Single-Walled Carbon Nanotubes Using Ė-Molecular Tweezers for Energy Materials. <i>ACS Applied Nano Materials</i> , 2023, 6, 1919-1926.	5.0	4
12556	Redispersion mechanisms of 2D nanosheets: combined role of intersheet contact and surface chemistry. <i>Nanoscale</i> , 2023, 15, 3159-3168.	5.6	1
12557	Interaction of Chondroitin and Hyaluronan Glycosaminoglycans with Surfaces of Carboxylated Carbon Nanotubes Studied Using Molecular Dynamics Simulations. <i>Molecules</i> , 2023, 28, 826.	3.8	0
12558	Conformational dynamics and putative substrate extrusion pathways of the N-glycosylated outer membrane factor CmeC from <i>Campylobacter jejuni</i> . <i>PLoS Computational Biology</i> , 2023, 19, e1010841.	3.2	1
12559	Multiscale molecular dynamics simulations predict arachidonic acid binding sites in human ASIC1a and ASIC3 transmembrane domains. <i>Journal of General Physiology</i> , 2023, 155, .	1.9	1
12560	Lamellarity-Driven Differences in Surface Structural Features of DPPS Lipids: Spectroscopic, Calorimetric and Computational Study. <i>Membranes</i> , 2023, 13, 83.	3.0	7

#	ARTICLE	IF	CITATIONS
12561	Ability of ionic liquids to inhibit the formation of methane hydrate: Insights from molecular dynamics simulations. , 2023, , 204878.		1
12563	Targeting RNA:protein interactions with an integrative approach leads to the identification of potent YBX1 inhibitors. ELife, 0, 12, .	6.0	3
12564	Amphiphilic Co-Solvents Modulate the Structure of Membrane Domains. ACS Sustainable Chemistry and Engineering, 0, , .	6.7	1
12565	Hydrophobic Hydration: A Theoretical Investigation of Structure and Dynamics. Journal of Chemical Sciences, 2023, 135, .	1.5	0
12566	Silibinin chronic treatment in a rat model of Parkinson disease: A comprehensive in-vivo evaluation and in silico molecular modeling. European Journal of Pharmacology, 2023, , 175517.	3.5	3
12567	Discovery of All- $\alpha$ -Peptide Inhibitors of SARS-CoV-2 3C-like Protease. ACS Chemical Biology, 2023, 18, 315-330.	3.4	5
12568	Discovery of Natural Bisbenzylisoquinoline Analogs from the Library of Thai Traditional Plants as SARS-CoV-2 3CL <sup>Pro</sup> Inhibitors: <i>In Silico</i> Molecular Docking, Molecular Dynamics, and <i>In Vitro</i> Enzymatic Activity. Journal of Chemical Information and Modeling, 2023, 63, 2104-2121.	5.4	12
12569	Hydrate Nucleation in Water Nanodroplets: Key Factors and Molecular Mechanisms. Energy & Fuels, 2023, 37, 1044-1056.	5.1	3
12570	The Interaction of Anthracycline Based Quinone-Chelators with Model Lipid Membranes: 1H NMR and MD Study. Membranes, 2023, 13, 61.	3.0	4
12571	Sequence and structural similarities of ACCase protein of Phalaris minor and wheat: An insight to explain herbicide selectivity. Frontiers in Plant Science, 0, 13, .	3.6	4
12572	Diffusion and dynamics of noble gases in hydroquinone clathrate channels. Journal of Chemical Physics, 2023, 158, .	3.0	6
12573	New amidine-benzenesulfonamides as iNOS inhibitors for the therapy of the triple negative breast cancer. European Journal of Medicinal Chemistry, 2023, 248, 115112.	5.5	2
12574	Molecular mechanisms of integrin $\alpha_2\beta_1$ activation regulated by graphene, boron nitride and black phosphorus nanosheets. Colloids and Surfaces B: Biointerfaces, 2023, 222, 113139.	5.0	2
12575	Diffusivities of ketones and aldehydes in liquid ethanol by molecular dynamics simulations. Journal of Molecular Liquids, 2023, 371, 121068.	4.9	2
12576	Effect of microwave electric field on asphaltene aggregation in a heavy oil system: MD and DFT investigation. Journal of Molecular Liquids, 2023, 372, 121212.	4.9	1
12577	3D printing of complicated GelMA-coated Alginate/Tri-calcium silicate scaffold for accelerated bone regeneration. International Journal of Biological Macromolecules, 2023, 229, 636-653.	7.5	13
12578	Theoretical investigations of TTR derived aggregation-prone peptidesâ€™ potential to biochemically attenuate the amyloidogenic propensities of V30A TTR amyloid fibrils. Journal of the Indian Chemical Society, 2023, 100, 100892.	2.8	0
12579	Emergent failure transition of pearlitic steel at extremely high strain rates. Computational Materials Science, 2023, 219, 112005.	3.0	1

#	ARTICLE	IF	CITATIONS
12580	Interaction of psychedelic tryptamine derivatives with a lipid bilayer. Chemistry and Physics of Lipids, 2023, 251, 105279.	3.2	7
12581	EGCG attenuates $\beta$ -synuclein protofibril-membrane interactions and disrupts the protofibril. International Journal of Biological Macromolecules, 2023, 230, 123194.	7.5	12
12582	Fundamental links between shear transformation, $\langle \text{mml:math xmlns:mml="http://www.w3.org/1998/Math/MathML" altimg="si58.svg" display="inline" id="d1e288">\langle \text{mml:mi}>\hat{1}^2\langle \text{mml:mi}>\langle \text{mml:math}>$ relaxation, and string-like motion in metallic glasses. Acta Materialia, 2023, 246, 118701.	7.9	8
12583	Molecular mechanisms of pH-tunable stability and surface coverage of polypeptide films. Applied Surface Science, 2023, 615, 156331.	6.1	5
12584	Effect of tryptophan mutation on the structure of LOV1 domain of phototropin1 protein of <i>Ostreococcus tauri</i> : A combined molecular dynamics simulation and biophysical approach. Biochimica Et Biophysica Acta - General Subjects, 2023, 1867, 130304.	2.4	2
12585	Interfacial tension of carbon dioxide - water under conditions of CO <sub>2</sub> geological storage and enhanced geothermal systems: A molecular dynamics study on the effect of temperature. Fuel, 2023, 337, 127219.	6.4	7
12586	Replica-exchange optimization of antibody fragments. Computational Biology and Chemistry, 2023, 103, 107819.	2.3	1
12587	Kinetic enhanced separation of praseodymium and neodymium induced by specific ion effect. Separation and Purification Technology, 2023, 310, 123157.	7.9	2
12588	<i>in silico</i> identification of potential $\beta$ -secretase inhibitor of marine-algal origin: an anticancer intervention. Molecular Simulation, 0, , 1-10.	2.0	0
12589	High-Throughput Prediction of the Impact of Genetic Variability on Drug Sensitivity and Resistance Patterns for Clinically Relevant Epidermal Growth Factor Receptor Mutations from Atomistic Simulations. Journal of Chemical Information and Modeling, 2023, 63, 321-334.	5.4	1
12590	Effect of the shell thickness on the mechanical properties of arrays composed of hybrid core-shell Si/SiC nanoparticles with overlapped shells. Ceramics International, 2023, 49, 24280-24292.	4.8	1
12591	Sequence Tendency for the Interaction between Low-Complexity Intrinsically Disordered Proteins. JACS Au, 2023, 3, 93-104.	7.9	5
12592	The Formation of RNA Pre-Polymers in the Presence of Different Prebiotic Mineral Surfaces Studied by Molecular Dynamics Simulations. Life, 2023, 13, 112.	2.4	0
12593	Elucidation of pH-Induced Protein Structural Changes: A Combined 2D IR and Computational Approach. Biochemistry, 2023, 62, 451-461.	2.5	0
12594	A comprehensive computer simulation insight into inhibitory mechanisms of EGCG and NQTrp ligands on amyloid-beta assemblies as the Alzheimer's disease insignia. Journal of Biomolecular Structure and Dynamics, 2023, 41, 10830-10839.	3.5	4
12596	Modelling the Transitioning of SARS-CoV-2 nsp3 and nsp4 Luminal Regions towards a More Stable State on Complex Formation. International Journal of Molecular Sciences, 2023, 24, 720.	4.1	7
12597	Double Paddle-Wheel Enhanced Sodium Ion Conduction in an Antiperovskite Solid Electrolyte. Advanced Energy Materials, 2023, 13, .	19.5	11
12598	Polyelectrolyte Influence on Beta-Hairpin Peptide Stability: A Simulation Study. Journal of Physical Chemistry B, 2023, 127, 359-370.	2.6	0

#	ARTICLE	IF	CITATIONS
12599	Effect of Local Stress on Accurate Modeling of Bacterial Outer Membranes Using All-Atom Molecular Dynamics. <i>Journal of Chemical Theory and Computation</i> , 2023, 19, 363-372.	5.3	3
12600	Effects of the Cations Li+, Na+, K+, Mg2+, or Ca2+ on Physicochemical Properties of Xanthan Gum in Aqueous Medium – A view from Computational Molecular Dynamics Calculations. <i>Food Biophysics</i> , 2023, 18, 32-47.	3.0	3
12601	Free-Energy Profiles for Membrane Permeation of Compounds Calculated Using Rare-Event Sampling Methods. <i>Journal of Chemical Information and Modeling</i> , 2023, 63, 259-269.	5.4	4
12602	Interfacial Characteristics of Graphene-Reinforced Iron Composites: A Molecular Dynamics Study. <i>Crystals</i> , 2023, 13, 27.	2.2	0
12603	Temperature-induced structural change of integrin $\alpha_5\beta_1$ receptor and its interaction with the $\alpha$ 5GPD peptide ligand. <i>Peptide Science</i> , 2023, 115, .	1.8	2
12604	Citrus nutraceutical eriocitrin and its metabolites are partial agonists of peroxisome proliferator-activated receptor gamma (PPAR $\gamma$ ): a molecular docking and molecular dynamics study. <i>Journal of Biomolecular Structure and Dynamics</i> , 2023, 41, 11373-11393.	3.5	1
12605	Direct Correlation between Short-Range Vibrational Spectral Diffusion and Localized Ion-Cage Dynamics of Water-in-Salt Electrolytes. <i>Journal of Physical Chemistry B</i> , 2023, 127, 236-248.	2.6	1
12606	Structure and elasticity of model disordered, polydisperse, and defect-free polymer networks. <i>Journal of Chemical Physics</i> , 2023, 158, .	3.0	3
12610	A computational framework for evaluating molecular dynamics potential parameters employing quantum mechanics. <i>Molecular Systems Design and Engineering</i> , 2023, 8, 632-646.	3.4	3
12611	State-specific morphological deformations of the lipid bilayer explain mechanosensitive gating of MscS ion channels. <i>ELife</i> , 0, 12, .	6.0	10
12612	Resistance to a tyrosine kinase inhibitor mediated by changes to the conformation space of the kinase. <i>Physical Chemistry Chemical Physics</i> , 2023, 25, 6175-6183.	2.8	1
12613	In Silico Targeting of Fascin Protein for Cancer Therapy: Benchmarking, Virtual Screening and Molecular Dynamics Approaches. <i>Molecules</i> , 2023, 28, 1296.	3.8	2
12614	Drug specificity and affinity are encoded in the probability of cryptic pocket opening in myosin motor domains. <i>ELife</i> , 0, 12, .	6.0	16
12615	What Drives Chorismate Mutase to Top Performance? Insights from a Combined <i>In Silico</i> and <i>In Vitro</i> Study. <i>Biochemistry</i> , 2023, 62, 782-796.	2.5	3
12617	Comparative Protein Structural Network Analysis Reveals C-Terminal Tail Phosphorylation Structural Communication Fingerprint in PTEN-Associated Mutations in Autism and Cancer. <i>Journal of Physical Chemistry B</i> , 2023, 127, 634-647.	2.6	1
12618	Polypropylene carbonate-based electrolytes as model for a different approach towards improved ion transport properties for novel electrolytes. <i>Physical Chemistry Chemical Physics</i> , 2023, 25, 4810-4823.	2.8	6
12620	<i>In Silico</i> Identification of Triclosan Derivatives as Potential Inhibitors of Mutant <i>Mycobacterium tuberculosis</i> InhA. <i>Journal of Computational Biophysics and Chemistry</i> , 2023, 22, 473-487.	1.7	2
12621	Multidirectional Polarization Impacts on Microwave Heating Efficiency: A Molecular Dynamics Research of Microwave Heating of Common Solvents. <i>Journal of Physical Chemistry B</i> , 2023, 127, 970-979.	2.6	4



#	ARTICLE	IF	CITATIONS
12622	Assessment of Different Parameters on the Accuracy of Computational Alanine Scanning of Protein-Protein Complexes with the Molecular Mechanics/Generalized Born Surface Area Method. Journal of Physical Chemistry B, 2023, 127, 944-954.	2.6	6
12623	Synthesis, Molecular Dynamics Simulation, and In-vitro Antitumor Activity of Quinazoline-2,4,6-triamine Derivatives as Novel EGFR Tyrosine Kinase Inhibitors. Iranian Journal of Pharmaceutical Research, 2023, 21, .	0.5	2
12624	A top-down and bottom-up combined strategy for parameterization of coarse-grained force fields for phospholipids. Physical Chemistry Chemical Physics, 2023, 25, 6757-6767.	2.8	2
12625	Impacts of external electric fields on the permeation of glycerol and water molecules through aquaglyceroporin-7: molecular dynamics simulation approach. European Physical Journal E, 2023, 46, .	1.6	0
12626	Upstream of N-Ras C-terminal cold shock domains mediate poly(A) specificity in a novel RNA recognition mode and bind poly(A) binding protein. Nucleic Acids Research, 2023, 51, 1895-1913.	14.5	2
12627	Molecular interaction of di-ester bonded cationic Gemini surfactants with pepsin: <i>in vitro</i> and <i>in silico</i> perspectives. Journal of Biomolecular Structure and Dynamics, 0, , 1-16.	3.5	1
12629	Rigid Base Biasing in Molecular Dynamics Enables Enhanced Sampling of DNA Conformations. Journal of Chemical Theory and Computation, 2023, 19, 902-909.	5.3	2
12631	Discovery of differentially expressed novel miRNAs in breast normal cells and their putative targets. Molecular and Cellular Biochemistry, 2023, 478, 2361-2378.	3.1	2
12632	Interaction of Tryptophan- and Arginine-Rich Antimicrobial Peptide with E. coli Outer Membrane-A Molecular Simulation Approach. International Journal of Molecular Sciences, 2023, 24, 2005.	4.1	6
12633	Impact of an Ionic Liquid on Amino Acid Side Chains: A Perspective from Molecular Simulation Studies. Journal of Chemical Information and Modeling, 2023, 63, 959-972.	5.4	2
12634	Molecular Engineering of Cyclic Azobenzene-Peptide Hybrid Ligands for the Purification of Human Blood Factor VIII via Photo-Affinity Chromatography. Advanced Functional Materials, 2023, 33, .	14.9	4
12635	Molecular Simulation on Hydrate Nucleation in the Presence of Initial Ice and Nanobubble. Energy & Fuels, 2023, 37, 3307-3313.	5.1	2
12636	In silico investigation of cytochrome bc1 molecular inhibition mechanism against Trypanosoma cruzi. PLoS Neglected Tropical Diseases, 2023, 17, e0010545.	3.0	2
12637	Atomistic molecular modeling methods. , 2023, , 37-73.		0
12639	Effect of Charge State on the Equilibrium and Kinetic Properties of Mechanically Interlocked [5]Rotaxane: A Molecular Dynamics Study. Journal of Physical Chemistry B, 2023, 127, 1254-1263.	2.6	1
12642	Molecular dynamics investigation of the asphaltene-kaolinite interactions in water, toluene, and water-toluene mixtures. Physical Chemistry Chemical Physics, 2023, 25, 5638-5647.	2.8	2
12643	Supramolecular organization and dynamics of mannosylated phosphatidylinositol lipids in the mycobacterial plasma membrane. Proceedings of the National Academy of Sciences of the United States of America, 2023, 120, .	7.1	9
12644	Molecular Dynamics Simulations of Asphaltene Aggregation: Machine-Learning Identification of Representative Molecules, Molecular Polydispersity, and Inhibitor Performance. ACS Omega, 2023, 8, 4862-4877.	3.5	3

#	ARTICLE	IF	CITATIONS
12645	Solids that are also liquids: elastic tensors of superionic materials. Npj Computational Materials, 2023, 9, .	8.7	2
12647	Experimental and Computational Study of Microstructure of Al <sub>2</sub> FeCoNiCu High-Entropy Alloy. Journal of Phase Equilibria and Diffusion, 0, , .	1.4	0
12648	Coacervate Formation of Elastin-like Polypeptides in Explicit Aqueous Solution Using Coarse-Grained Molecular Dynamics Simulations. Macromolecules, 2023, 56, 794-805.	4.8	0
12649	A comparative analysis of the influence of hydrofluoroethers as diluents on solvation structure and electrochemical performance in non-flammable electrolytes. Journal of Materials Chemistry A, 2023, 11, 4111-4125.	10.3	8
12651	Selective Action of Antimalarial Hydroxychloroquine on the Packing of Phospholipids and Interfacial Water Associated with Lysosomal Model Membranes: A Vibrational Sum Frequency Generation Study. Langmuir, 2023, 39, 2435-2443.	3.5	0
12652	Surface viscosities of lipid bilayers determined from equilibrium molecular dynamics simulations. Biophysical Journal, 2023, 122, 1094-1104.	0.5	5
12653	Aggregation of Asphaltene Subfractions A1 and A2 in Different Solvents from the Perspective of Molecular Dynamics Simulations. Energy & Fuels, 2023, 37, 2681-2691.	5.1	6
12654	Biophysical evaluation of the oligomerization and conformational properties of the N-terminal domain of TDP-43. Archives of Biochemistry and Biophysics, 2023, 737, 109533.	3.0	0
12656	Impact and structure of water in aqueous octanol mixtures: Hz-GHz dielectric relaxation measurements and computer simulations. Journal of Photochemistry and Photobiology A: Chemistry, 2023, 439, 114600.	3.9	2
12657	Distinct roles of graphene and graphene oxide nanosheets in regulating phospholipid flip-flop. Journal of Colloid and Interface Science, 2023, 637, 112-122.	9.4	3
12658	Computational assessment of hexadecane freezing by equilibrium atomistic molecular dynamics simulations. Journal of Colloid and Interface Science, 2023, 638, 743-757.	9.4	8
12659	Carboxyl PEGylation of magnetic nanoparticles as antithrombotic and thrombolytic agents by calcium binding. Journal of Colloid and Interface Science, 2023, 638, 672-685.	9.4	5
12660	A molecular dynamics study on nanobubble formation and dynamics via methane hydrate dissociation. Fuel, 2023, 341, 127650.	6.4	3
12661	Mechanical and Electronic Properties of a Carbon-Composite 3D Nanomaterial with an Island-Type Topology. Nanobiotechnology Reports, 2022, 17, S9-S14.	0.6	0
12662	Role of Cation Size on Order-Disorder Phase Transition Temperature and Cation Hopping Mechanism based on LiCB <sub>11</sub> H <sub>12</sub> . Materials Advances, 0, , .	5.4	0
12663	Energetic vs. entropic stabilization between a Remdesivir analogue and cognate ATP upon binding and insertion into the active site of SARS-CoV-2 RNA dependent RNA polymerase. Physical Chemistry Chemical Physics, 2023, 25, 13508-13520.	2.8	3
12664	The Effect of Cholesterol in SOPC Lipid Bilayers at Low Temperatures. Membranes, 2023, 13, 275.	3.0	2
12665	Structural water in amorphous carbonate minerals: <i>ab initio</i> molecular dynamics simulations of X-ray pair distribution experiments. Physical Chemistry Chemical Physics, 2023, 25, 6768-6779.	2.8	1

#	ARTICLE	IF	CITATIONS
12666	Synthesis, Biological Evaluation and <i>in Silico</i> Study of <i>N</i> -(2- <i>tert</i> -butyl-6-( <i>pyridin-2-yl</i> )benzamido)- <i>N</i> -(2- <i>tert</i> -butyl-6-( <i>pyridin-2-yl</i> )benzamido)- <i>N</i> -(2- <i>tert</i> -butyl-6-( <i>pyridin-2-yl</i> )benzamido) Derivatives as Quorum Sensing Inhibitors against <i>Pseudomonas aeruginosa</i> . Chemistry and Biodiversity, 2023, 20, .	2.1	0
12667	Characterization of a TatA/TatB binding site on the TatC component of the Escherichia coli twin arginine translocase. Microbiology (United Kingdom), 2023, 169, .	1.8	2
12668	Molecular Dynamics Simulation of Ti Metal Cutting Using a TiN:Ag Self-Lubricating Coated Tool. Materials, 2023, 16, 1344.	2.9	2
12669	The effect of rhamnolipids on fungal membrane models as described by their interactions with phospholipids and sterols: An <i>in silico</i> study. Frontiers in Chemistry, 0, 11, .	3.6	3
12670	Stability and structural evolution of double-stranded DNA molecules under high pressures: A molecular dynamics study. Frontiers in Physics, 0, 11, .	2.1	1
12671	Salinity Effect on the Interfacial Tension of CO <sub>2</sub> -Brine: Estimation and Investigation by Molecular Dynamics Simulations. , 2023, , .		0
12672	Gold Nanorods Inhibit Tumor Metastasis by Regulating MMP-9 Activity: Implications for Radiotherapy. ACS Applied Materials & Interfaces, 0, , .	8.0	1
12673	Metabolite-induced <i>in vivo</i> fabrication of substrate-free organic bioelectronics. Science, 2023, 379, 795-802.	12.6	36
12674	Structural basis for bacterial energy extraction from atmospheric hydrogen. Nature, 2023, 615, 541-547.	27.8	19
12677	Structural basis for TRIM72 oligomerization during membrane damage repair. Nature Communications, 2023, 14, .	12.8	4
12678	Experimental and computational studies on the ion dissociation states of 1-butyl-3-methylimidazolium tetrafluoroborate in water and alcohols. Journal of Molecular Liquids, 2023, 375, 121370.	4.9	0
12679	<i>In silico</i> design of photoresponsive peptide-based hydrogel with controllable structural and rheological properties. Colloids and Surfaces A: Physicochemical and Engineering Aspects, 2023, 663, 131020.	4.7	4
12680	Bias-force guided simulations combined with experimental validations towards GPR17 modulators identification. Biomedicine and Pharmacotherapy, 2023, 160, 114320.	5.6	7
12681	Application of molecular dynamics simulation for exploring the roles of plant biomolecules in promoting environmental health. Science of the Total Environment, 2023, 869, 161871.	8.0	4
12682	Contribution of air-water interface in removing PFAS from drinking water: Adsorption, stability, interaction and machine learning studies. Water Research, 2023, 236, 119947.	11.3	5
12683	The effects of adsorbed benzo(a)pyrene on dynamic behavior of polystyrene nanoplastics through phospholipid membrane: A molecular simulation study. Colloids and Surfaces B: Biointerfaces, 2023, 224, 113211.	5.0	3
12684	Effect of temperature and salt addition on the structural properties of Triton X-100. Physica A: Statistical Mechanics and Its Applications, 2023, 615, 128614.	2.6	0
12685	Unique structure of ozoralizumab, a trivalent anti-TNF $\alpha$ NANOBODY <sup>®</sup> compound, offers the potential advantage of mitigating the risk of immune complex-induced inflammation. Frontiers in Immunology, 0, 14, .	4.8	4

#	ARTICLE	IF	CITATIONS
12686	Leveraging Advanced In Silico Techniques in Early Drug Discovery: A Study of Potent Small-Molecule YAP-TEAD PPI Disruptors. <i>Journal of Chemical Information and Modeling</i> , 2023, 63, 2520-2531.	5.4	1
12688	An implementation of the Martini coarse-grained force field in OpenMM. <i>Biophysical Journal</i> , 2023, 122, 2864-2870.	0.5	4
12689	Embedding Beyond Electrostatics: The Extended Polarizable Density Embedding Model. <i>Journal of Physical Chemistry B</i> , 2023, 127, 3248-3256.	2.6	1
12690	Gamma-Hemolysin Components: Computational Strategies for LukF-Hlg2 Dimer Reconstruction on a Model Membrane. <i>International Journal of Molecular Sciences</i> , 2023, 24, 7113.	4.1	0
12691	Molecular dynamics investigation on the vapor-liquid interface behavior of long-chain alkanes, alcohols, and their mixtures. <i>Journal of Molecular Liquids</i> , 2023, 375, 121283.	4.9	3
12692	Engineering a membrane-binding protein to trimerize and induce high membrane curvature. <i>Biophysical Journal</i> , 2023, 122, 3008-3017.	0.5	1
12693	Silica In Silico: A Molecular Dynamics Characterization of the Early Stages of Protein Embedding for Atom Probe Tomography. <i>Biophysica</i> , 2023, 3, 276-287.	1.4	1
12694	Unusual heating effect of the elliptically polarized microwave electric field on sodium chloride solution: A molecular dynamics simulation. <i>Chemical Physics</i> , 2023, 569, 111856.	1.9	0
12695	Room for improvement in the initial martini 3 parameterization of peptide interactions. <i>Chemical Physics Letters</i> , 2023, 819, 140436.	2.6	7
12696	In silico repurposing of CNS drugs for multiple sclerosis. <i>Multiple Sclerosis and Related Disorders</i> , 2023, 73, 104622.	2.0	1
12697	Rational design of a polysaccharide-based viral mimicry nanocomplex for potent gene silencing in inflammatory tissues. <i>Journal of Controlled Release</i> , 2023, 357, 120-132.	9.9	2
12698	Conformational stability of the deamidated and mutated human $\beta$ 2B2-crystallin. <i>Biophysical Chemistry</i> , 2023, 296, 106986.	2.8	1
12699	Can sodium 1-alkylsulfonates participate in the sodium dodecyl sulfate micelle formation?. <i>Journal of Molecular Liquids</i> , 2023, 377, 121568.	4.9	2
12700	Computational design of cyclic peptides to inhibit protein-peptide interactions. <i>Biophysical Chemistry</i> , 2023, 296, 106987.	2.8	2
12701	Building a Hofmeister-like series for the maximum in density temperature of aqueous electrolyte solutions. <i>Journal of Molecular Liquids</i> , 2023, 377, 121433.	4.9	4
12702	Identification of alkaloid compounds as potent inhibitors of <i>Mycobacterium tuberculosis</i> NadD using computational strategies. <i>Computers in Biology and Medicine</i> , 2023, 158, 106863.	7.0	2
12703	Water-Mediated attraction between Like-charged species involved in calcium phosphate nucleation. <i>Journal of Molecular Liquids</i> , 2023, 378, 121585.	4.9	1
12704	Atomic-scale deformation mechanisms of nano-polycrystalline Cu/Al layered composites: a molecular dynamics simulation. <i>Journal of Materials Research and Technology</i> , 2023, 24, 1177-1189.	5.8	6

#	ARTICLE	IF	CITATIONS
12705	Atomic and electronic structure of grain boundaries in $\alpha$ -Al <sub>2</sub> O <sub>3</sub> : A combination of machine learning, first-principles calculation and electron microscopy. <i>Scripta Materialia</i> , 2023, 229, 115368.	5.2	3
12706	Whether carbon nanotubes are suitable for delivering small drugs with aromatic rings through non-covalent adsorption?. <i>Journal of Molecular Liquids</i> , 2023, 378, 121595.	4.9	1
12707	Molecular modelling of ionic liquids: Perfluorinated anionic species with enlarged halogen substitutions. <i>Journal of Molecular Liquids</i> , 2023, 378, 121599.	4.9	3
12708	Aqueous solutions of chiral ionic liquids based on (â€“)â€“)-menthol: An experimental and computational study of volumetric and transport properties. <i>Journal of Molecular Liquids</i> , 2023, 378, 121591.	4.9	0
12709	Assessing the inhibition of glycation of Î²-crystallin by thymoquinone: A mechanistic approach using experimental and computational methods. <i>Journal of Molecular Liquids</i> , 2023, 380, 121750.	4.9	1
12710	Machine learning insight into h-BN growth on Pt(111) from atomic states. <i>Applied Surface Science</i> , 2023, 621, 156893.	6.1	4
12711	A comparative study on inclusion complex formation between formononetin and Î²-cyclodextrin derivatives through multiscale classical and umbrella sampling simulations. <i>Carbohydrate Polymers</i> , 2023, 310, 120729.	10.2	14
12712	Helical micelle of an achiral surfactant from the template interaction with dendrimer. <i>Giant</i> , 2023, 14, 100147.	5.1	0
12713	GAP positions catalytic H-Ras residue Q61 for GTP hydrolysis in molecular dynamics simulations, complicating chemical rescue of Ras deactivation. <i>Computational Biology and Chemistry</i> , 2023, 104, 107835.	2.3	0
12714	Molecular insights into the inhibition mechanism of harringtonine against essential proteins associated with SARS-CoV-2 entry. <i>International Journal of Biological Macromolecules</i> , 2023, 240, 124352.	7.5	3
12715	Computational identification of drug-like marine natural products as potential RNA polymerase inhibitors against Nipah virus. <i>Computational Biology and Chemistry</i> , 2023, 104, 107850.	2.3	4
12716	In silico characterization of the psilocybin biosynthesis pathway. <i>Computational Biology and Chemistry</i> , 2023, 104, 107854.	2.3	1
12717	Use of computational and wet lab techniques to examine the molecular association between a potent hepatitis C virus inhibitor, PSI-6206 and human serum albumin. <i>Spectrochimica Acta - Part A: Molecular and Biomolecular Spectroscopy</i> , 2023, 294, 122543.	3.9	2
12718	Molecular dynamics simulation of phase transformation and wear behavior of Ni <sub>35</sub> Al <sub>30</sub> Co <sub>35</sub> high temperature shape memory alloy. <i>Wear</i> , 2023, 522, 204849.	3.1	2
12719	Multicomponent Petasis reaction for the identification of pyrazine based multi-target directed anti-Alzheimer's agents: In-silico design, synthesis, and characterization. <i>European Journal of Medicinal Chemistry</i> , 2023, 254, 115354.	5.5	5
12720	New insights into the pH dependence of anthocyanin-protein interactions by a case study of cyanidin-3-O-glucoside and bovine serum albumin. <i>Food Hydrocolloids</i> , 2023, 140, 108649.	10.7	8
12721	Comparing supercapacitors with graphene/graphyne electrodes and [Bmim][PF <sub>6</sub> ], [Emim][BF <sub>4</sub> ], [Ch][Gly] and [Pyr][Tfsi] ionic liquids using molecular dynamics. <i>Journal of Molecular Liquids</i> , 2023, 379, 121703.	4.9	4
12722	Effects of nanobubbles on methane hydrate dissociation: A molecular simulation study. <i>Fuel</i> , 2023, 345, 128230.	6.4	8

#	ARTICLE	IF	CITATIONS
12723	A computational study of cellulose regeneration: Coarse-grained molecular dynamics simulations. Carbohydrate Polymers, 2023, 313, 120853.	10.2	6
12724	Transfer or blockage: Unraveling the interaction between deformation twinning and grain boundary in tantalum under shock loading with molecular dynamics. Journal of Materials Science and Technology, 2023, 156, 118-128.	10.7	8
12726	Mechano-Redox Control of Mac-1 De-Adhesion by PDI Promotes Directional Movement Under Flow. Circulation Research, 2023, 132, .	4.5	5
12727	Miscibility of Phosphatidylcholines in Bilayers: Effect of Acyl Chain Unsaturation. Membranes, 2023, 13, 411.	3.0	1
12728	Numerical simulation of peristalsis to study co-localization and intestinal distribution of a macromolecular drug and permeation enhancer. International Journal of Biological Macromolecules, 2023, 240, 124388.	7.5	2
12729	Accurate and efficient constrained molecular dynamics of polymers using Newton's method and special purpose code. Computer Physics Communications, 2023, 288, 108742.	7.5	2
12730	The temperature of maximum density of diluted aqueous solutions of non-polar solutes: A molecular simulation study using TIP4P/2005 water and LJ point solutes. Journal of Molecular Liquids, 2023, 381, 121815.	4.9	1
12731	The molecular basis of the antidepressant action of the magic mushroom extract, psilocin. Biochimica Et Biophysica Acta - Proteins and Proteomics, 2023, 1871, 140914.	2.3	1
12732	Uncovering the mechanisms of cyclic peptide self-assembly in membranes with the chirality-aware MA(R/S)TINI forcefield. Journal of Colloid and Interface Science, 2023, 642, 84-99.	9.4	1
12733	Surface-induced demixing of self-assembled isomeric mixtures of citral. Journal of Molecular Liquids, 2023, 381, 121803.	4.9	2
12736	Molecular dynamics simulations of the calmodulin-induced $\alpha$ -helix in the SK2 calcium-gated potassium ion channel. Journal of Biological Chemistry, 2023, 299, 102850.	3.4	0
12737	Fracture universality in amorphous nanowires. Journal of the Mechanics and Physics of Solids, 2023, 173, 105210.	4.8	5
12738	Boron-rich amorphous boron oxides from ab initio simulations. Journal of Non-Crystalline Solids, 2023, 604, 122130.	3.1	0
12739	Deciphering the interactions of genistein with $\beta$ -cyclodextrin derivatives through experimental and microsecond timescale umbrella sampling simulations. Journal of Molecular Liquids, 2023, 374, 121295.	4.9	11
12740	Atomistic insights on the adsorption of long-chain undecane molecules on carbon nanotubes: Roles of chirality and surface hydroxylation. Diamond and Related Materials, 2023, 133, 109706.	3.9	2
12741	Computational analysis of protein-ligand interaction by targeting a cell cycle restrainer. Computer Methods and Programs in Biomedicine, 2023, 231, 107367.	4.7	18
12742	Quantifying defect production in solids at finite temperatures: Thermally-activated correlated defect recombination corrections to DPA (CRC-DPA). Journal of Nuclear Materials, 2023, 577, 154292.	2.7	5
12743	The role of conformational change and key glutamic acid residues in the CIC-ec1 antiporter. Biophysical Journal, 2023, 122, 1068-1085.	0.5	1



#	ARTICLE	IF	CITATIONS
12744	On the Behavior of the Ethylene Glycol Components of Polydisperse Polyethylene Glycol PEG200. Journal of Physical Chemistry B, 2023, 127, 1178-1196.	2.6	3
12745	Explicit molecular dynamics simulation studies to discover novel natural compound analogues as Mycobacterium tuberculosis inhibitors. Heliyon, 2023, 9, e13324.	3.2	8
12747	Effects of Water Deuteration on Thermodynamic and Structural Properties of Proteins and Biomembranes. Journal of Physical Chemistry B, 2023, 127, 1138-1143.	2.6	7
12748	Long-time-step molecular dynamics can retard simulation of protein-ligand recognition process. Biophysical Journal, 2023, 122, 802-816.	0.5	3
12749	Liposome Deformation Induced by Membrane-Binding Peptides. Micromachines, 2023, 14, 373.	2.9	2
12750	Dispersion Free Energy of Carbon Nanotubes in Water Systems. Chemistry Letters, 2023, 52, 156-159.	1.3	0
12751	Phosphate aggregation, diffusion, and adsorption on kaolinite in saline solutions by molecular dynamics simulation. Applied Clay Science, 2023, 233, 106844.	5.2	3
12752	Simulation of AOT reverse micelles with polyethylenimine in hexane. Colloid and Polymer Science, 2023, 301, 283-291.	2.1	0
12753	Structural Basis for Agonistic Activity and Selectivity toward Melatonin Receptors hMT1 and hMT2. International Journal of Molecular Sciences, 2023, 24, 2863.	4.1	3
12754	Unveiling New Druggable Pockets in Influenza Non-Structural Protein 1: NS1â€™Host Interactions as Antiviral Targets for Flu. International Journal of Molecular Sciences, 2023, 24, 2977.	4.1	0
12755	Integration of deep learning with Ramachandran plot molecular dynamics simulation for genetic variant classification. IScience, 2023, 26, 106122.	4.1	2
12756	Multiâ€™Hydration Induced Zwitterionic Hydrogel with Open Environment Stability for Chemical Sensing. , 2023, 2, .		0
12757	The Structural Basis of African Swine Fever Virus pS273R Protease Binding to E64 through Molecular Dynamics Simulations. Molecules, 2023, 28, 1435.	3.8	1
12758	Fast, Accurate, and System-Specific Variable-Resolution Modeling of Proteins. Journal of Chemical Information and Modeling, 2023, 63, 1260-1275.	5.4	1
12759	Interaction of guanidinium and ammonium cations with phosphatidylcholine and phosphatidylserine lipid bilayers â€™ Calorimetric, spectroscopic and molecular dynamics simulations study. Biochimica Et Biophysica Acta - Biomembranes, 2023, 1865, 184122.	2.6	4
12761	The effects of size and surface functionalization of polystyrene nanoplastics on stratum corneum model membranes: An experimental and computational study. Journal of Colloid and Interface Science, 2023, 638, 778-787.	9.4	5
12762	The origin of pigment-binding differences in CP29 and LHCII: the role of protein structure and dynamics. Photochemical and Photobiological Sciences, 0, , .	2.9	0
12763	HPV and molecular mimicry in systemic lupus erythematosus and an impact of compiling B-cell epitopes and MHC-class II binding profiles with <i>in silico</i> evidence. Journal of Biomolecular Structure and Dynamics, 0, , 1-9.	3.5	0

#	ARTICLE	IF	CITATIONS
12764	Critical Role of Position 10 Residue in the Polymyxin Antimicrobial Activity. <i>Journal of Medicinal Chemistry</i> , 2023, 66, 2865-2876.	6.4	1
12765	Secreted Aspartyl Proteinases Targeted Multi-Epitope Vaccine Design for <i>Candida dubliniensis</i> Using Immunoinformatics. <i>Vaccines</i> , 2023, 11, 364.	4.4	14
12766	Ubiquitylation of BBSome is required for ciliary assembly and signaling. <i>EMBO Reports</i> , 2023, 24, .	4.5	8
12767	Integrated use of ligand and structure-based virtual screening, molecular dynamics, free energy calculation and ADME prediction for the identification of potential PTP1B inhibitors. <i>Molecular Diversity</i> , 0, , .	3.9	1
12768	Computational modeling of cyanobacterial phytoconstituents against toll-like receptors of skin cancer. <i>Journal of Biomolecular Structure and Dynamics</i> , 0, , 1-13.	3.5	0
12769	Thermal site energy fluctuations in photosystem I: new insights from MD/QM/MM calculations. <i>Chemical Science</i> , 2023, 14, 3117-3131.	7.4	1
12770	High-pressure properties of type V Natural Deep Eutectic Solvents: The case of menthol: thymol. <i>Journal of Molecular Liquids</i> , 2023, 376, 121398.	4.9	0
12771	Molecular Mechanism in the Disruption of Chronic Traumatic Encephalopathy-Related R3â€“R4 Tau Protofibril by Quercetin and Gallic Acid: Similarities and Differences. <i>ACS Chemical Neuroscience</i> , 2023, 14, 897-908.	3.5	5
12772	Structural Insights into ATP-Sensitive Potassium Channel Mechanics: A Role of Intrinsically Disordered Regions. <i>Journal of Chemical Information and Modeling</i> , 2023, 63, 1806-1818.	5.4	2
12773	Dynamic molecular ordering in multiphasic nanoconfined ionic liquids detected with time-resolved diffusion NMR. <i>Communications Materials</i> , 2023, 4, .	6.9	1
12774	Thermodynamics and kinetics of an A-U RNA base pair under force studied by molecular dynamics simulations. <i>Physical Review E</i> , 2023, 107, .	2.1	0
12775	Evaluation of free radical quenching, anti-inflammatory activity together with anticancer potential of <i>Lychnis coronaria</i> and characterization of novel molecules from its extract through high resolution-liquid chromatography mass spectrometry coupled to structural biochemistry approach. <i>Journal of Biomolecular Structure and Dynamics</i> , 2023, 41, 13041-13055.	3.5	1
12776	Scaled charges for ions: An improvement but not the final word for modeling electrolytes in water. <i>Journal of Chemical Physics</i> , 2023, 158, .	3.0	16
12777	Systematic investigation of the multi-scale mechanisms of herbal medicine on treating ventricular remodeling: Theoretical and experimental studies. <i>Phytomedicine</i> , 2023, 112, 154706.	5.3	2
12779	An S-Shaped AÎ²42 Cross-Î² Hexamer Embedded into a Lipid Bilayer Reveals Membrane Disruption and Permeability. <i>ACS Chemical Neuroscience</i> , 2023, 14, 936-946.	3.5	4
12780	Lipidation Alters the Structure and Hydration of Myristoylated Intrinsically Disordered Proteins. <i>Biomacromolecules</i> , 2023, 24, 1244-1257.	5.4	3
12781	Driving and characterizing nucleation of urea and glycine polymorphs in water. <i>Proceedings of the National Academy of Sciences of the United States of America</i> , 2023, 120, .	7.1	9
12782	Structural Insights into the Antiparallel G-Quadruplex in the Presence of K <sup>+</sup> and Mg <sup>2+</sup> Ions. <i>Journal of Physical Chemistry B</i> , 2023, 127, 1499-1512.	2.6	1

#	ARTICLE	IF	CITATIONS
12783	Computational multi-target approach to target essential enzymes of <i>Leishmania donovani</i> using comparative molecular dynamic simulations and MMPBSA analysis. <i>Phytochemical Analysis</i> , 2023, 34, 842-854.	2.4	10
12784	Lessons for Oral Bioavailability: How Conformationally Flexible Cyclic Peptides Enter and Cross Lipid Membranes. <i>Journal of Medicinal Chemistry</i> , 2023, 66, 2773-2788.	6.4	11
12785	Rationalizing the Design of Pluronics-Surfactant Mixed Micelles through Molecular Simulations and Experiments. <i>Langmuir</i> , 2023, 39, 2692-2709.	3.5	4
12786	Discovery of AcrAB-TolC pump inhibitors: Virtual screening and molecular dynamics simulation approach. <i>Journal of Biomolecular Structure and Dynamics</i> , 2023, 41, 12503-12520.	3.5	4
12787	Histone variant H2A.Z modulates nucleosome dynamics to promote DNA accessibility. <i>Nature Communications</i> , 2023, 14, .	12.8	13
12789	The Evolution of Hydrogen Bond Network in Nafion via Molecular Dynamics Simulation. <i>Macromolecules</i> , 2023, 56, 1688-1703.	4.8	5
12791	Rheological Performance of High-Temperature-Resistant, Salt-Resistant Fracturing Fluid Gel Based on Organic-Zirconium-Crosslinked HPAM. <i>Gels</i> , 2023, 9, 151.	4.5	3
12792	Pseudouridimycin-A Potent Nucleoside Inhibitor of the RNA Polymerase Beta Prime Subunit of <i>Streptococcus pyogenes</i> . <i>ACS Omega</i> , 2023, 8, 7989-8000.	3.5	2
12793	The combination of polyphenols and phospholipids as an efficient platform for delivery of natural products. <i>Scientific Reports</i> , 2023, 13, .	3.3	5
12794	Anionic phospholipids control mechanisms of GPCR-G protein recognition. <i>Nature Communications</i> , 2023, 14, .	12.8	18
12795	Effect of Organic Ions on The Formation and Collapse of Nanometric Bubbles in Ionic Liquid/Water Solutions: A Molecular Dynamics Study. <i>Journal of Physical Chemistry B</i> , 2023, 127, 1628-1644.	2.6	1
12796	Hexamethylenetetramine additive with zincophilic head and hydrophobic tail for realizing ultra-stable Zn anode. <i>Chemical Engineering Journal</i> , 2023, 460, 141902.	12.7	22
12797	Catalytic site mutations confer multiple states of G protein activation. <i>Science Signaling</i> , 2023, 16, .	3.6	3
12798	Predicting Reaction Barriers in Solid-State Systems Under Stress via Second-Order Energy Expansion. <i>Canadian Journal of Chemistry</i> , 0, , .	1.1	0
12799	Novel Inhibitory Role of Fenofibric Acid by Targeting Cryptic Site on the RBD of SARS-CoV-2. <i>Biomolecules</i> , 2023, 13, 359.	4.0	2
12800	Cytocompatibility of Ti <sub>3</sub> C <sub>2</sub> T <sub>x</sub> MXene with Red Blood Cells and Human Umbilical Vein Endothelial Cells and the Underlying Mechanisms. <i>Chemical Research in Toxicology</i> , 2023, 36, 347-359.	3.3	2
12801	Gatekeeper mutations activate FGF receptor tyrosine kinases by destabilizing the autoinhibited state. <i>Proceedings of the National Academy of Sciences of the United States of America</i> , 2023, 120, .	7.1	5
12803	Conformational ensemble of the NSP1 CTD in SARS-CoV-2: Perspectives from the free energy landscape. <i>Biophysical Journal</i> , 2023, 122, 2948-2959.	0.5	1

#	ARTICLE	IF	CITATIONS
12804	How Do Cyclopropane Fatty Acids Protect the Cell Membrane of <i>Escherichia coli</i> in Cold Shock?. Journal of Physical Chemistry B, 2023, 127, 1607-1617.	2.6	5
12805	Study on host-guest interaction of aroma compounds/ $\beta$ -cyclodextrin inclusion complexes. LWT - Food Science and Technology, 2023, 178, 114589.	5.2	5
12806	Inferring Pathways of Oxidative Folding from Prefolding Free Energy Landscapes of Disulfide-Rich Toxins. Journal of Physical Chemistry B, 2023, 127, 1689-1703.	2.6	1
12807	Unravelling the destabilization potential of ellagic acid on $\alpha$ -synuclein fibrils using molecular dynamics simulations. Physical Chemistry Chemical Physics, 2023, 25, 8128-8143.	2.8	1
12808	Thermodynamics and transport properties of valine and cysteine peptides in water. Journal of Molecular Liquids, 2023, 376, 121472.	4.9	0
12809	Inhibition of 3-Hydroxykynurenine Transaminase from <i>Aedes aegypti</i> and <i>Anopheles gambiae</i> : A Mosquito-Specific Target to Combat the Transmission of Arboviruses. ACS Bio & Med Chem Au, 2023, 3, 211-222.	3.7	0
12810	NanoModeler CG: A Tool for Modeling and Engineering Functional Nanoparticles at a Coarse-Grained Resolution. Journal of Chemical Theory and Computation, 2023, 19, 1582-1591.	5.3	4
12811	Differences in protein distribution, conformation, and dynamics in hard and soft coronas: dependence on protein and particle electrostatics. Physical Chemistry Chemical Physics, 2023, 25, 7496-7507.	2.8	1
12812	Molecular dynamics simulations reveal the importance of amyloid-beta oligomer $\beta$ -sheet edge conformations in membrane permeabilization. Journal of Biological Chemistry, 2023, 299, 103034.	3.4	6
12813	Understanding native defect induced photoluminescence in $\text{ZnMn}_2\text{O}_7$ . Physical Review B, 2023, 107, .		
12814	Elucidating activation and deactivation dynamics of VEGFR-2 transmembrane domain with coarse-grained molecular dynamics simulations. PLoS ONE, 2023, 18, e0281781.	2.5	1
12815	Systematic investigation of the mechanism of herbal medicines for the treatment of prostate cancer. Aging, 0, , .	3.1	0
12816	Discovery of potent inhibitors targeting Glutathione S-transferase of <i>Wuchereria bancrofti</i> : a step toward the development of effective anti-filariasis drugs. Molecular Diversity, 0, , .	3.9	0
12817	Functional Imaging and Inhibitor Screening of Human Pancreatic Lipase by a Resorufin-Based Fluorescent Probe. Biosensors, 2023, 13, 283.	4.7	2
12818	Optimal Bond Constraint Topology for Molecular Dynamics Simulations of Cholesterol. Journal of Chemical Theory and Computation, 2023, 19, 1592-1601.	5.3	5
12819	Impact of Hydrogen Bonds on $\text{CO}_2$ Binding in Eutectic Solvents: An Experimental and Computational Study toward Sorbent Design for $\text{CO}_2$ Capture. ACS Sustainable Chemistry and Engineering, 2023, 11, 3740-3749.	6.7	11
12820	Cholesterol esters form supercooled lipid droplets whose nucleation is facilitated by triacylglycerols. Nature Communications, 2023, 14, .	12.8	12
12821	Unraveling topoisomerase IA gate dynamics in presence of PPEF and its preclinical evaluation against multidrug-resistant pathogens. Communications Biology, 2023, 6, .	4.4	1

#	ARTICLE	IF	CITATIONS
12822	Molecular dynamics simulations of the Li-ion diffusion in the amorphous solid electrolyte interphase. Chinese Chemical Letters, 2023, 34, 108242.	9.0	2
12823	Conformational changes in the human Cx43/GJA1 gap junction channel visualized using cryo-EM. Nature Communications, 2023, 14, .	12.8	13
12824	Theoretical prediction of nanomolar and sequence-selective binding of synthetic supramolecular cucurbit[7]uril to N-terminal Leu-containing tripeptides. Physical Chemistry Chemical Physics, 2023, 25, 7893-7900.	2.8	0
12825	A review on shale oil and gas characteristics and molecular dynamics simulation for the fluid behavior in shale pore. Journal of Molecular Liquids, 2023, 376, 121507.	4.9	17
12826	Molecular Dynamics Simulation of the Complex of PDE5 and Evodiamine. Life, 2023, 13, 578.	2.4	1
12827	Phosphorylation-Competent Metastable State of <i>Escherichia coli</i> Toxin HipA. Biochemistry, 2023, 62, 989-999.	2.5	1
12828	Free energy change in the complete transport of all water molecules through a carbon nanotube. Physical Chemistry Chemical Physics, 2023, 25, 7032-7046.	2.8	2
12830	Self-Organization of Mobile, Polyelectrolytic Dendrons on Stable, Amphiphile-Based Spherical Surfaces. Langmuir, 2023, 39, 3439-3449.	3.5	1
12831	Study on molecular mechanisms of CD4 dependency and independency of HIV-1 gp120. RSC Advances, 2023, 13, 6274-6286.	3.6	0
12833	Genomic, transcriptomic, and metabolomic analysis of <i>Oldenlandia corymbosa</i> reveals the biosynthesis and mode of action of anti-cancer metabolites. Journal of Integrative Plant Biology, 2023, 65, 1442-1466.	8.5	7
12834	Identification of and Mechanistic Insights into SARS-CoV-2 Main Protease Non-Covalent Inhibitors: An In-Silico Study. International Journal of Molecular Sciences, 2023, 24, 4237.	4.1	1
12835	AI-Accelerated Design of Targeted Covalent Inhibitors for SARS-CoV-2. Journal of Chemical Information and Modeling, 2023, 63, 1438-1453.	5.4	4
12836	Mechanism of external K <sup>+</sup> sensitivity of KCNQ1 channels. Journal of General Physiology, 2023, 155, .	1.9	3
12837	Intrinsically disordered region of talin <sup>TM</sup> s FERM domain functions as an initial PIP2 recognition site. Biophysical Journal, 2023, 122, 1277-1286.	0.5	2
12838	Molecular rotations trigger a glass-to-plastic fcc heterogeneous crystallization in high-pressure water. Journal of Chemical Physics, 2023, 158, .	3.0	5
12839	FERM domains recruit ample PI(4,5)P2s to form extensive protein-membrane attachments. Biophysical Journal, 2023, 122, 1325-1333.	0.5	3
12840	Influence of Cholesterol on the Membrane Binding and Conformation of $\beta$ -Synuclein. Journal of Physical Chemistry B, 2023, 127, 1956-1964.	2.6	1
12841	Characterization of the coupling mechanism of scorpion $\beta$ -neurotoxins on the voltage-gated sodium channel hNav1.6. Journal of Biomolecular Structure and Dynamics, 2023, 41, 14419-14427.	3.5	0

#	ARTICLE	IF	CITATIONS
12842	Coâ€Assembly of Carbon Nanotube Porins into Biomimetic Peptoid Membranes. Small, 2023, 19, .	10.0	3
12843	Hierarchical Aggregation in a Complex Fluidâ€The Role of Isomeric Interconversion. Journal of Physical Chemistry B, 2023, 127, 2052-2065.	2.6	0
12844	Common framework mutations impact antibody interfacial dynamics and flexibility. Frontiers in Immunology, 0, 14, .	4.8	1
12845	Anastrozole-mediated modulation of mitochondrial activity by inhibition of mitochondrial permeability transition pore opening: an initial perspective. Journal of Biomolecular Structure and Dynamics, 2023, 41, 14063-14079.	3.5	0
12846	Scaling Proteinâ€Water Interactions in the Martini 3 Coarse-Grained Force Field to Simulate Transmembrane Helix Dimers in Different Lipid Environments. Journal of Chemical Theory and Computation, 2023, 19, 2109-2119.	5.3	10
12847	Structure of human NaV1.6 channel reveals Na <sup>+</sup> selectivity and pore blockade by 4,9-anhydro-tetrodotoxin. Nature Communications, 2023, 14, .	12.8	8
12848	Continuum mechanics from molecular dynamics via adiabatic time and length scale separation. Letters in Mathematical Physics, 2023, 113, .	1.1	1
12849	Repurposing of phyto-ligand molecules from the honey bee products for Alzheimerâ€™s disease as novel inhibitors of BACE-1: small molecule bioinformatics strategies as amyloid-based therapy. Environmental Science and Pollution Research, 2023, 30, 51143-51169.	5.3	2
12851	Understanding the Reaction Kinetics and Microdynamics between Methylimidazole and Alkyl Thiocyanate for Ionic Liquid Synthesis through Experiments and Theoretical Calculation. Industrial & Engineering Chemistry Research, 2023, 62, 3889-3897.	3.7	1
12852	Molecular effects of site-specific phosphate-methylated primer on the structure and motions of Taq DNA polymerase. Computational and Structural Biotechnology Journal, 2023, 21, 1820-1827.	4.1	2
12854	Tween-80 on Water/Oil Interface: Structure and Interfacial Tension by Molecular Dynamics Simulations. Langmuir, 2023, 39, 3255-3265.	3.5	6
12855	What is the Optimal Dipole Moment for Nonpolarizable Models of Liquids?. Journal of Chemical Theory and Computation, 2023, 19, 1790-1804.	5.3	5
12856	In silico target specific design of potential quinazoline-based anti-NSCLC agents. Journal of Biomolecular Structure and Dynamics, 2023, 41, 10725-10736.	3.5	0
12857	GAFF-AIC: reoptimisation of the GAFF force field for realistic densities and viscosities in aromatic isocyanates. Molecular Simulation, 2023, 49, 576-588.	2.0	1
12858	Influence of <sc>ALS</sc>â€linked <sc>M337V</sc> mutation on the conformational ensembles of <sc>TDPâ€43<sub>321â€340</sub></sc> peptide monomer and dimer. Proteins: Structure, Function and Bioinformatics, 0, , .	2.6	3
12859	The Mechanism of Action of SAAP-148 Antimicrobial Peptide as Studied with NMR and Molecular Dynamics Simulations. Pharmaceutics, 2023, 15, 761.	4.5	3
12860	Effect of macrocyclization and tetramethylrhodamine labeling on chemokine binding peptides. Journal of Peptide Science, 0, , .	1.4	0
12861	Effects of flexibility in coarse-grained models for bovine serum albumin and immunoglobulin G. Journal of Chemical Physics, 2023, 158, 084112.	3.0	0



#	ARTICLE	IF	CITATIONS
12862	The Atomistic Understanding of the Ice Recrystallization Inhibition Activity of Antifreeze Glycoproteins. <i>Crystals</i> , 2023, 13, 405.	2.2	1
12863	Revealing the Key Packing Features Determining the Stability of Peptide Bilayer Membrane. <i>ACS Applied Bio Materials</i> , 2024, 7, 564-578.	4.6	2
12864	ATP binding by an F1Fo ATP synthase $\hat{\mu}$ subunit is pH dependent, suggesting a diversity of $\hat{\mu}$ subunit functional regulation in bacteria. <i>Frontiers in Molecular Biosciences</i> , 0, 10, .	3.5	4
12865	An in silico approach to determine interâ€subunit affinities in human septin complexes. <i>Cytoskeleton</i> , 2023, 80, 141-152.	2.0	7
12866	Reversible Zinc Electrodeposition at $\hat{\sim}$ 60 $\hat{\text{A}}^{\circ}\text{C}$ Using a Deep Eutectic Electrolyte for Low-Temperature Zinc Metal Batteries. <i>Journal of Physical Chemistry Letters</i> , 2023, 14, 2378-2386.	4.6	3
12867	Dipole Cooperativity and Polarization Frustration Determine the Secondary Structure Distribution of Short Alanine Peptides in Water. <i>Journal of Physical Chemistry B</i> , 2023, 127, 3126-3138.	2.6	2
12868	Designing and property prediction of a novel three-component CL-20/HMX/TNAD energetic cocrystal explosive by MD method. <i>Journal of Molecular Modeling</i> , 2023, 29, .	1.8	3
12869	Dual photoisomerization mechanism of azobenzene embedded in a lipid membrane. <i>Journal of Materials Chemistry B</i> , 2023, 11, 2518-2529.	5.8	2
12870	Effect of Glycone Diversity on the Interaction of Triterpenoid Saponins and Lipid Bilayers. <i>ACS Applied Bio Materials</i> , 2024, 7, 553-563.	4.6	2
12871	Mechanical Behavior and Physical Properties of Mg Binary Alloys via Y-doping: Molecular Dynamic Study. <i>Journal of Materials Engineering and Performance</i> , 2023, 32, 6738-6746.	2.5	0
12873	Fluorescent Probes cis- and trans-Parinaric Acids in Fluid and Gel Lipid Bilayers: A Molecular Dynamics Study. <i>Molecules</i> , 2023, 28, 2241.	3.8	3
12874	Alchemical Metadynamics: Adding Alchemical Variables to Metadynamics to Enhance Sampling in Free Energy Calculations. <i>Journal of Chemical Theory and Computation</i> , 2023, 19, 1805-1817.	5.3	5
12875	Investigation of the Impact of Lipid Acyl Chain Saturation on Fusion Peptide Interactions with Lipid Bilayers. <i>Biophysica</i> , 2023, 3, 121-138.	1.4	2
12876	Predicting locations of cryptic pockets from single protein structures using the PocketMiner graph neural network. <i>Nature Communications</i> , 2023, 14, .	12.8	27
12877	On the Mechanism of Membrane Permeabilization by Tamoxifen and 4-Hydroxytamoxifen. <i>Membranes</i> , 2023, 13, 292.	3.0	1
12878	Singlet fission as a polarized spin generator for dynamic nuclear polarization. <i>Nature Communications</i> , 2023, 14, .	12.8	11
12879	Strongly Solvating Ether Electrolytes for High-Voltage Lithium Metal Batteries. <i>ACS Applied Materials &amp; Interfaces</i> , 2023, 15, 13155-13164.	8.0	5
12880	Molecular recognition of bio-active triterpenoids from <i>Swertia chirayita</i> towards hepatitis Delta antigen: a mechanism through docking, dynamics simulation, Gibbs free energy landscape. <i>Journal of Biomolecular Structure and Dynamics</i> , 2023, 41, 14651-14664.	3.5	4

#	ARTICLE	IF	CITATIONS
12881	Conformational and oligomeric states of SPOP from small-angle X-ray scattering and molecular dynamics simulations. <i>ELife</i> , 0, 12, .	6.0	2
12882	Long-range communication between transmembrane- and nucleotide-binding domains does not depend on drug binding to mutant P-glycoprotein. <i>Journal of Biomolecular Structure and Dynamics</i> , 0, , 1-10.	3.5	0
12883	Highlyâ€Selective Harvesting of (6,4) SWCNTs Using the Aqueous Twoâ€Phase Extraction Method and Nonionic Surfactants. <i>Advanced Science</i> , 2023, 10, .	11.2	10
12884	Mechanistic Insight into the Amyloid Fibrillation Inhibition of Hen Egg White Lysozyme by Three Different Bile Acids. <i>Journal of Physical Chemistry B</i> , 2023, 127, 2198-2213.	2.6	3
12885	Effects of representative point mutations on dynamic behavior of the DISC1â€Ndel1 complex: a molecular dynamics study. <i>Journal of Biomolecular Structure and Dynamics</i> , 2023, 41, 13228-13234.	3.5	0
12886	Extension of the TraPPE Force Field for Battery Electrolyte Solvents. <i>Journal of Physical Chemistry B</i> , 2023, 127, 2224-2236.	2.6	1
12887	Probing Redox Properties of Extreme Concentrations Relevant for Nonaqueous Redox-Flow Batteries. <i>ACS Applied Energy Materials</i> , 2023, 6, 2819-2831.	5.1	2
12889	Atomistic origins of biomass recalcitrance in organosolv pretreatment. <i>Chemical Engineering Science</i> , 2023, 272, 118587.	3.8	2
12890	Rational Computational Approaches in Drug Discovery: Potential Inhibitors for Allosteric Regulation of Mutant Isocitrate Dehydrogenase-1 Enzyme in Cancers. <i>Molecules</i> , 2023, 28, 2315.	3.8	2
12891	Composition-dependent fracture energy in metallic glasses. <i>Physical Review Materials</i> , 2023, 7, .	2.4	1
12892	Microscopic Understanding of the Conformational Stability of the Aggregated Nonamyloid Î² Components of Î±-Synuclein. <i>Journal of Chemical Information and Modeling</i> , 2023, 63, 1542-1555.	5.4	0
12895	Structural and Dynamical Properties of Elastin-Like Peptides near Their Lower Critical Solution Temperature. <i>Biomacromolecules</i> , 2023, 24, 1912-1923.	5.4	2
12896	Phosphorylation of LKB1 by PDK1 Inhibits Cell Proliferation and Organ Growth by Decreased Activation of AMPK. <i>Cells</i> , 2023, 12, 812.	4.1	2
12898	Estimation of bubble cavitation rates in a symmetrical Lennard-Jones mixture by <i>NVT</i> seeding simulations. <i>Journal of Chemical Physics</i> , 2023, 158, 124109.	3.0	3
12899	Coarse-Grained Force Field for Polyethylene Oxide and Polyethylene Glycol Aqueous Solutions Based on a Polarizable Water Model. <i>Journal of Chemical Theory and Computation</i> , 2023, 19, 1864-1874.	5.3	2
12900	Allosteric communication in the gating mechanism for controlled protein degradation by the bacterial ClpP peptidase. <i>Journal of Chemical Physics</i> , 2023, 158, .	3.0	4
12901	ALS-Linked A315T and A315E Mutations Enhance Î²-Barrel Formation of the TDP-43<sub>307â€319</sub> Hexamer: A REST2 Simulation Study. <i>ACS Chemical Neuroscience</i> , 2023, 14, 1310-1320.	3.5	2
12903	Autoregulation of GPCR signalling through the third intracellular loop. <i>Nature</i> , 2023, 615, 734-741.	27.8	19

#	ARTICLE	IF	CITATIONS
12904	Efficient Purification of Cowpea Chlorotic Mottle Virus by a Novel Peptide Aptamer. <i>Viruses</i> , 2023, 15, 697.	3.3	1
12905	IDP Force Fields Applied to Model PP11-Rich 33-mer Gliadin Peptides. <i>Journal of Physical Chemistry B</i> , 2023, 127, 2407-2417.	2.6	0
12907	Exploration of potent antiviral phytomedicines from Lauraceae family plants against SARS-CoV-2 RNA-dependent RNA polymerase. <i>Journal of Biomolecular Structure and Dynamics</i> , 2023, 41, 15085-15105.	3.5	1
12908	Unsupervised Data-Driven Reconstruction of Molecular Motifs in Simple to Complex Dynamic Micelles. <i>Journal of Physical Chemistry B</i> , 2023, 127, 2595-2608.	2.6	3
12909	Molybdenum disulfide under extreme conditions: An <i>ab initio</i> study on its melting. <i>Journal of Applied Physics</i> , 2023, 133, .	2.5	1
12910	How NaFTA salt affects the structural landscape and transport properties of Pyr1,3FTA ionic liquid. <i>Journal of Chemical Physics</i> , 2023, 158, .	3.0	1
12911	Lipid Bicelles in the Study of Biomembrane Characteristics. <i>Journal of Chemical Theory and Computation</i> , 2023, 19, 1908-1921.	5.3	4
12912	Possible boron-rich amorphous silicon borides from <i>ab initio</i> simulations. <i>Journal of Molecular Modeling</i> , 2023, 29, .	1.8	0
12913	Combining machine learning and structure-based approaches to develop oncogene PIM kinase inhibitors. <i>Frontiers in Chemistry</i> , 0, 11, .	3.6	0
12914	Implementation of probe rheology simulation technique in atomistically detailed molecular dynamics simulations. <i>Journal of Computational Chemistry</i> , 2023, 44, 1484-1492.	3.3	0
12915	Cryo-EM structures of human Cx36/GJD2 neuronal gap junction channel. <i>Nature Communications</i> , 2023, 14, .	12.8	11
12916	Computational insight into structural basis of human ELOVL1 inhibition. <i>Computers in Biology and Medicine</i> , 2023, 157, 106786.	7.0	1
12917	HuR modulation counteracts lipopolysaccharide response in murine macrophages. <i>DMM Disease Models and Mechanisms</i> , 2023, 16, .	2.4	1
12919	The motion and growth behaviors of nucleuses in Al melt solidified under supergravity condition—molecular dynamics simulation. <i>Materials Research Express</i> , 2023, 10, 036510.	1.6	0
12921	Structural basis of odorant recognition by a human odorant receptor. <i>Nature</i> , 2023, 615, 742-749.	27.8	31
12922	Direct Calculation of the Interfacial Free Energy between NaCl Crystal and Its Aqueous Solution at the Solubility Limit. <i>Physical Review Letters</i> , 2023, 130, .	7.8	0
12923	B-cell epitope discovery: The first protein flexibility-based algorithm—Zika virus conserved epitope demonstration. <i>PLoS ONE</i> , 2023, 18, e0262321.	2.5	1
12924	Theoretical Spectroscopy Aided Validation of the Hydration Structure of Trimethylamine <i>N</i> -Oxide (TMAO). <i>Journal of Physical Chemistry B</i> , 2023, 127, 2774-2783.	2.6	2

#	ARTICLE	IF	CITATIONS
12925	Aggregation of chlorophylls on plant thylakoid membranes using coarse-grained simulations. <i>Physical Chemistry Chemical Physics</i> , 2023, 25, 11356-11367.	2.8	2
12926	Mutagenic analysis of actin reveals the mechanism of His161 flipping that triggers ATP hydrolysis. <i>Frontiers in Cell and Developmental Biology</i> , 0, 11, .	3.7	0
12927	Creatinase: Using Increased Entropy to Improve the Activity and Thermostability. <i>Journal of Physical Chemistry B</i> , 2023, 127, 2671-2682.	2.6	2
12928	Free Energy Differences from Molecular Simulations: Exact Confidence Intervals from Transition Counts. <i>Journal of Chemical Theory and Computation</i> , 2023, 19, 2102-2108.	5.3	1
12930	Dynamic play between human N- $\epsilon$ -acetyltransferase D and H4-mutant histones: Molecular dynamics study. <i>Current Protein and Peptide Science</i> , 2023, 24, .	1.4	0
12931	In Silico Prediction of Stratum Corneum Partition Coefficients via COSMOmic and Molecular Dynamics Simulations. <i>Journal of Physical Chemistry B</i> , 2023, 127, 2719-2728.	2.6	1
12932	The pH Response of a Peptoid Oligomer. <i>Journal of Physical Chemistry B</i> , 2023, 127, 2872-2878.	2.6	2
12933	Elemental zoning enhances mass transport in zeolite catalysts for methanol to hydrocarbons. <i>Nature Catalysis</i> , 2023, 6, 254-265.	34.4	11
12934	Homogeneous nucleation rate of methane hydrate formation under experimental conditions from seeding simulations. <i>Journal of Chemical Physics</i> , 2023, 158, .	3.0	8
12935	The architecture of transmembrane and cytoplasmic juxtamembrane regions of Toll-like receptors. <i>Nature Communications</i> , 2023, 14, .	12.8	5
12936	Targeting high symmetry in structure predictions by biasing the potential energy surface. <i>Physical Review Research</i> , 2023, 5, .	3.6	5
12937	Identifying promising druggable binding sites and their flexibility to target the receptor-binding domain of SARS-CoV-2 spike protein. <i>Computational and Structural Biotechnology Journal</i> , 2023, 21, 2339-2351.	4.1	5
12938	Ultraviolet irradiation confers titanium oxide oleophilicity. <i>Journal of Materials Science</i> , 2023, 58, 5258-5268.	3.7	0
12939	Sappanin-type homoisoflavonoids from <i>Scilla nervosa</i> inhibits acetylcholinesterase enzyme: a combined in silico and in vitro approach. <i>Journal of Biomolecular Structure and Dynamics</i> , 2023, 41, 10957-10968.	3.5	1
12941	Insights into targeting SARS-CoV-2: design, synthesis, in silico studies and antiviral evaluation of new dimethylxanthine derivatives. <i>RSC Medicinal Chemistry</i> , 2023, 14, 899-920.	3.9	1
12942	A cooperative knock-on mechanism underpins Ca <sup>2+</sup> -selective cation permeation in TRPV channels. <i>Journal of General Physiology</i> , 2023, 155, .	1.9	5
12945	Human Pol <sup>II</sup> Natural Polymorphic Variants G118V and R149I Affects Substate Binding and Catalysis. <i>International Journal of Molecular Sciences</i> , 2023, 24, 5892.	4.1	3
12946	Temperature-dependent UV-Vis dielectric functions of BaTiO <sub>3</sub> across ferroelectric-paraelectric phase transition. <i>Optics Express</i> , 2023, 31, 12357.	3.4	1

#	ARTICLE	IF	CITATIONS
12947	Accelerating Cryptic Pocket Discovery Using AlphaFold. Journal of Chemical Theory and Computation, 2023, 19, 4355-4363.	5.3	19
12948	Rutin impedes human low-density lipoprotein from non-enzymatic glycation: A mechanistic insight against diabetes-related disorders. International Journal of Biological Macromolecules, 2023, 238, 124151.	7.5	3
12949	Mechanistic insights into the inhibition of amyloid- $\beta^2$ aggregation by chitosan. Physical Chemistry Chemical Physics, 2023, 25, 10113-10120.	2.8	1
12950	Structural basis of mitochondrial membrane bending by the $\text{F}_1\text{F}_0$ V2 supercomplex. Nature, 2023, 615, 934-938.	27.8	30
12951	Using the SAFT- $\Gamma^3$ -Mie to Generate Coarse-Grained Force Fields Useable in Molecular Dynamics Simulations: Describing the Micellar Phases of Polyalkylglycols in Aqueous Solutions. Industrial & Engineering Chemistry Research, 2023, 62, 5658-5667.	3.7	0
12952	Investigation of Solid Formation Enthalpy and Molecular Mechanics Energies of Amino Acids via Force Field Approach. Bitlis Eren $\ddot{A}$ eniversitesi Fen Bilimleri Dergisi, 2023, 12, 10-16.	0.5	0
12953	Structural and functional characterization of novel $\text{F7}$ mutations identified in Chinese factor VII $\text{scp}$ deficient patients. British Journal of Haematology, 0, , .	2.5	2
12954	Nanoscale friction of biomimetic hair surfaces. Nanoscale, 2023, 15, 7086-7104.	5.6	2
12955	Unraveling the Aquaporin-3 Inhibitory Effect of Rottlerin by Experimental and Computational Approaches. International Journal of Molecular Sciences, 2023, 24, 6004.	4.1	1
12956	FTD-tau S320F mutation stabilizes local structure and allosterically promotes amyloid motif-dependent aggregation. Nature Communications, 2023, 14, .	12.8	5
12957	Synthesis, molecular docking and dynamics studies of pyridazino[4,5- $b$ ]quinoxalin-1(2- $H$ ) Tj ETQq0 0 0 rgBT /Overlock 10 0	3.5	0
12958	Distinct structure and gating mechanism in diverse NMDA receptors with GluN2C and GluN2D subunits. Nature Structural and Molecular Biology, 2023, 30, 629-639.	8.2	7
12959	Human Amylin in the Presence of SARS-COV-2 Protein Fragments. ACS Omega, 2023, 8, 12501-12511.	3.5	4
12962	Molecular Docking Identifies 1,8-Cineole (Eucalyptol) as A Novel PPAR $\beta^3$ Agonist That Alleviates Colon Inflammation. International Journal of Molecular Sciences, 2023, 24, 6160.	4.1	7
12963	Computational Modelling of MOF Mechanics: From Elastic Behaviour to Phase Transformations. , 2023, , 113-204.		0
12964	Effective Molecular Dynamics from Neural Network-Based Structure Prediction Models. Journal of Chemical Theory and Computation, 2023, 19, 1965-1975.	5.3	10
12965	The water cavitation line as predicted by the TIP4P/2005 model. Journal of Chemical Physics, 2023, 158, .	3.0	4
12968	Physicochemical Properties and Route of Systemic Delivery Control the In Vivo Dynamics and Breakdown of Radiolabeled Gold Nanostars. Small, 2023, 19, .	10.0	4

#	ARTICLE	IF	CITATIONS
12969	Conformational transitions and allosteric modulation in a heteromeric glycine receptor. <i>Nature Communications</i> , 2023, 14, .	12.8	5
12972	The Mechanism Underlying the Amylose-Zein Complexation Process and the Stability of the Molecular Conformation of Amylose-Zein Complexes in Water Based on Molecular Dynamics Simulation. <i>Foods</i> , 2023, 12, 1418.	4.3	2
12973	Internal Normal Mode Analysis Applied to RNA Flexibility and Conformational Changes. <i>Journal of Chemical Information and Modeling</i> , 0, , .	5.4	0
12974	Exploring biogenic chalcones as DprE1 inhibitors for antitubercular activity via in silico approach. <i>Journal of Molecular Modeling</i> , 2023, 29, .	1.8	9
12975	Effects of pH and NaCl on the Spatial Structure and Conformation of Myofibrillar Proteins and the Emulsion Gel System—Insights from Computational Molecular Dynamics on Myosin of Golden Pompano. <i>Gels</i> , 2023, 9, 270.	4.5	1
12976	Factors controlling heteroepitaxial phase formation at intermetallic-Al <sub>3</sub> Sc/liquid interfaces. <i>Journal of Applied Physics</i> , 2023, 133, 124902.	2.5	0
12977	Effect of Electric Field on $\alpha$ -Synuclein Fibrils: Revealed by Molecular Dynamics Simulations. <i>International Journal of Molecular Sciences</i> , 2023, 24, 6312.	4.1	4
12978	Investigation of the Entry Pathway and Molecular Nature of $\beta$ 1 Receptor Ligands. <i>International Journal of Molecular Sciences</i> , 2023, 24, 6367.	4.1	0
12979	The path towards type V deep eutectic solvents: inductive effects and steric hindrance in the system <i>tert</i> -butanol + perfluoro <i>tert</i> -butanol. <i>Physical Chemistry Chemical Physics</i> , 2023, 25, 11227-11236.	2.8	2
12980	Unraveling the molecular mechanism of novel leukemia mutations on NTRK2 (A203T & R458G) and NTRK3 (E176D & L449F) genes using molecular dynamics simulations approach. <i>F1000Research</i> , 0, 12, 345.	1.6	2
12982	Discovery and Binding Mechanism of Pyrazoloisoquinoline-Based Novel $\beta$ -Arrestin Inverse Agonists of the Kappa-Opioid Receptor. <i>Journal of Medicinal Chemistry</i> , 2023, 66, 5154-5170.	6.4	0
12983	The Effect of Interatomic Potentials on the Nature of Nanohole Propagation in Single-Crystal Nickel: A Molecular Dynamics Simulation Study. <i>Crystals</i> , 2023, 13, 585.	2.2	1
12985	Characterization of the role of Kunitz-type protease inhibitor domain in dimerization of amyloid precursor protein. <i>Journal of Computational Chemistry</i> , 2023, 44, 1437-1445.	3.3	1
12986	Crystal Structure of Bright Fluorescent Protein BrUSLEE with Subnanosecond Fluorescence Lifetime; Electric and Dynamic Properties. <i>International Journal of Molecular Sciences</i> , 2023, 24, 6403.	4.1	0
12987	In Silico Analyses of a Promising Drug Candidate for the Treatment of Amyotrophic Lateral Sclerosis Targeting Superoxide Dismutase I Protein. <i>Pharmaceutics</i> , 2023, 15, 1095.	4.5	2
12988	Effect of temperature on hepatitis a virus and exploration of binding mode mechanism of phytochemicals from <i>C. tinospora cordifolia</i> : an insight into molecular docking, MM/GBSA, and molecular dynamics simulation study. <i>Journal of Biomolecular Structure and Dynamics</i> , 2024, 42, 598-614.	3.5	3
12989	Developing a comprehensive solution aimed to disrupt LARS1/RagD protein-protein interaction. <i>Journal of Biomolecular Structure and Dynamics</i> , 2024, 42, 747-758.	3.5	0
12990	A General Picture of Cucurbit[8]uril Host-Guest Binding: Recalibrating Bonded Interactions. <i>Molecules</i> , 2023, 28, 3124.	3.8	5



#	ARTICLE	IF	CITATIONS
12991	Mechanistic Insights into the Binding of Different Positron Emission Tomography Tracers to Chronic Traumatic Encephalopathy Tau Protofibrils. ACS Chemical Neuroscience, 0, , .	3.5	2
12992	Metadynamics simulations for the investigation of drug loading on functionalized inorganic nanoparticles. Nanoscale, 0, , .	5.6	2
12993	IFITM3 blocks influenza virus entry by sorting lipids and stabilizing hemifusion. Cell Host and Microbe, 2023, 31, 616-633.e20.	11.0	14
12994	Partial Denaturation of Double-Stranded DNA on Pristine Graphene under Physiological-like Conditions. Liquids, 2023, 3, 168-186.	2.5	0
12995	Mutation in glutamate transporter homologue GltTk provides insights into pathologic mechanism of episodic ataxia 6. Nature Communications, 2023, 14, .	12.8	3
12997	How SGLT2 inhibitors interact with metformin? A molecular dynamics study. Molecular Simulation, 2023, 49, 867-876.	2.0	0
12998	The targeted next-generation sequence revealed SMAD4, AKT1, and TP53 mutations from circulating cell-free DNA of breast cancer and its effect on protein structure “ A computational approach. Journal of Biomolecular Structure and Dynamics, 2023, 41, 15584-15597.	3.5	0
12999	Structural and molecular insights into tacrine-benzofuran hybrid induced inhibition of amyloid- $\beta^2$ peptide aggregation and BACE1 activity. Journal of Biomolecular Structure and Dynamics, 2023, 41, 13211-13227.	3.5	0
13000	pH-Sensitive Liposomes with Embedded 3-(isobutylamino)cholan-24-oic Acid: What Is the Possible Mechanism of Fast Cargo Release?. Membranes, 2023, 13, 407.	3.0	1
13001	Effect of Force Field Resolution on Membrane Mechanical Response and Mechanoporation Damage under Deformation Simulations. Molecular Biotechnology, 0, , .	2.4	2
13002	1-Benzyl-5-bromo-3-hydrazonoindolin-2-ones as Novel Anticancer Agents: Synthesis, Biological Evaluation and Molecular Modeling Insights. Molecules, 2023, 28, 3203.	3.8	1
13003	Single-molecule fingerprinting of protein-drug interaction using a funneled biological nanopore. Nature Communications, 2023, 14, .	12.8	6
13004	A Computational Biology Study on the Structure and Dynamics Determinants of Thermal Stability of the Chitosanase from Aspergillus fumigatus. International Journal of Molecular Sciences, 2023, 24, 6671.	4.1	0
13005	Structural and regulatory insights into the glideosome-associated connector from Toxoplasma gondii. ELife, 0, 12, .	6.0	4
13006	Inorganic Anion Recognition in Aqueous Solution by Coupling Nearby Highly Hydrophilic and Hydrophobic Moieties in a Macrocyclic Receptor. Dalton Transactions, 0, , .	3.3	2
13007	An Affordable Topography-Based Protocol for Assigning a Residue’s Character on a Hydrophathy (PARCH) Scale. Journal of Chemical Theory and Computation, 2024, 20, 1656-1672.	5.3	4
13008	Influence of Core Topologies on Poly-<sc>l</sc>-lysine Dendrimer Structures. Journal of Physical Chemistry B, 2023, 127, 3364-3371.	2.6	0
13009	The Role of C2 Domains in Two Different Phosphatases: PTEN and SHIP2. Membranes, 2023, 13, 408.	3.0	2

#	ARTICLE	IF	CITATIONS
13010	Proton Transport in Perfluorinated Ionomer Simulated by Machine-Learned Interatomic Potential. <i>Journal of Physical Chemistry Letters</i> , 2023, 14, 3581-3588.	4.6	5
13011	Novel Strategy of Machine Learning for Predicting Henry's Law Constants of CO <sub>2</sub> in Ionic Liquids. <i>ACS Sustainable Chemistry and Engineering</i> , 2023, 11, 6090-6099.	6.7	1
13012	Surfactin-like lipopeptides from <i>Bacillus clausii</i> efficiently bind to spike glycoprotein of SARS-CoV-2. <i>Journal of Biomolecular Structure and Dynamics</i> , 0, , 1-12.	3.5	2
13013	Deep Eutectic Solvents for the Enzymatic Synthesis of Sugar Esters: A Generalizable Strategy?. <i>ACS Sustainable Chemistry and Engineering</i> , 2023, 11, 5926-5936.	6.7	9
13015	Sodium is a negative allosteric regulator of the ghrelin receptor. <i>Cell Reports</i> , 2023, 42, 112320.	6.4	3
13016	Identification of a 1, 8-naphthyridine-containing compound endowed with the inhibition of p53-MDM2/X interaction signaling: a computational perspective. <i>Molecular Diversity</i> , 0, , .	3.9	2
13017	Continuous millisecond conformational cycle of a DEAH box helicase reveals control of domain motions by atomic-scale transitions. <i>Communications Biology</i> , 2023, 6, .	4.4	3
13018	Mechanism of Nucleation Pathway Selection in Binary Lennard-Jones Solution: A Combined Study of Molecular Dynamics Simulation and Free Energy Analysis. <i>Journal of Physical Chemistry B</i> , 2023, 127, 3524-3533.	2.6	4
13019	Coarse-Grained MD Simulations of Opioid Interactions with the $\mu$ -Opioid Receptor and the Surrounding Lipid Membrane. <i>Biophysica</i> , 2023, 3, 263-275.	1.4	0
13020	Enhancement of neutrophil chemotaxis by trans-anethole-treated <i>Staphylococcus aureus</i> strains. <i>PLoS ONE</i> , 2023, 18, e0284042.	2.5	1
13021	Novel hits for autosomal dominated polycystic kidney disease (ADPKD) targeting derived by <i>in silico</i> screening on ZINC-15 natural product database. <i>Journal of Biomolecular Structure and Dynamics</i> , 2024, 42, 885-902.	3.5	1
13022	G $\beta$ 's slow conformational transition upon GTP binding and a novel G $\beta$ 's regulator. <i>IScience</i> , 2023, 26, 106603.	4.1	3
13023	Rehydration Post-orientation: Investigating Field-Induced Structural Changes via Computational Rehydration. <i>Protein Journal</i> , 2023, 42, 205-218.	1.6	2
13024	Molecular origin of the two-step mechanism of gellan aggregation. <i>Science Advances</i> , 2023, 9, .	10.3	5
13025	In silico investigation of the structural stability as the origin of the pathogenicity of $\alpha$ -synuclein protofibrils. <i>Journal of Biomolecular Structure and Dynamics</i> , 2023, 41, 14103-14115.	3.5	1
13026	Comparative molecular dynamics simulations of pathogenic and non-pathogenic huntingtin protein monomers and dimers. <i>Frontiers in Molecular Biosciences</i> , 0, 10, .	3.5	3
13027	Impact of solvent sulfolane in enhancing methanol selectivity during methane partial oxidation on Fe-ZSM5 catalyst with H <sub>2</sub> O <sub>2</sub> as an oxidant. <i>Reaction Chemistry and Engineering</i> , 2023, 8, 1260-1269.	3.7	1
13028	Ceramide-1-phosphate transfer protein enhances lipid transport by disrupting hydrophobic lipid-membrane contacts. <i>PLoS Computational Biology</i> , 2023, 19, e1010992.	3.2	1

#	ARTICLE	IF	CITATIONS
13029	Ion Conduction Mechanisms in Potassium Channels Revealed by Permeation Cycles. Journal of Chemical Theory and Computation, 2023, 19, 2574-2589.	5.3	4
13030	Improving the activity of horseradish peroxidase in betaine-based natural deep eutectic systems. , 2023, 1, 886-897.		3
13031	Water-Soluble Cellulose As a New Class of Green CH <sub>4</sub> Hydrate Inhibitors: Insights from Experiments and Molecular Dynamics Simulations. ACS Sustainable Chemistry and Engineering, 2023, 11, 6153-6162.	6.7	5
13032	Magnetic Polaron States in Photoluminescent Carbon Dots Enable Hydrogen Peroxide Photoproduction. Small, 2023, 19, .	10.0	2
13033	Triazole-“Peptide Conjugate as a Modulator of A $\beta$ -Aggregation, Metal-Mediated A $\beta$ -Aggregation, and Cytotoxicity. ACS Chemical Neuroscience, 2023, 14, 1631-1645.	3.5	3
13034	Nucleobase Specific Understanding about the Interaction of Antimalarial Drug Chloroquine with Duplex DNA. Journal of Physical Chemistry B, 2023, 127, 3341-3351.	2.6	0
13035	HRMAS-NMR and simulation study of self-assembly of surfactants on carbon nanotubes. Physical Chemistry Chemical Physics, 0, , .	2.8	1
13036	Optimizing the Martini 3 Force Field Reveals the Effects of the Intricate Balance between Protein-Water Interaction Strength and Salt Concentration on Biomolecular Condensate Formation. Journal of Chemical Theory and Computation, 2024, 20, 1646-1655.	5.3	5
13038	A Unified Description of the Liquid Structure, Static and Dynamic Anomalies, and Criticality of TIP4P/2005 Water by a Hierarchical Two-State Model. Journal of Physical Chemistry B, 2023, 127, 3452-3462.	2.6	3
13039	Collagen breaks at weak sacrificial bonds taming its mechanoradicals. Nature Communications, 2023, 14, .	12.8	8
13040	Disulfide bond reduction and exchange in C4 domain of von Willebrand factor undermines platelet binding. Journal of Thrombosis and Haemostasis, 2023, 21, 2089-2100.	3.8	1
13041	Modular development of deep potential for complex solid solutions. Physical Review B, 2023, 107, .	3.2	4
13044	Detecting Liquid-Liquid Phase Separations Using Molecular Dynamics Simulations and Spectral Clustering. Journal of Physical Chemistry B, 2023, 127, 3682-3689.	2.6	2
13046	Coarse-Grained Modeling of Polystyrene-Modified CNTs and Their Interactions with Lipid Bilayers. Biophysical Journal, 2023, , .	0.5	1
13047	The Interaction Mechanism of Intramuscular Gene Delivery Materials with Cell Membranes. Journal of Functional Biomaterials, 2023, 14, 219.	4.4	0
13048	In-silico approaches for identification of compounds inhibiting SARS-CoV-2 3CL protease. PLoS ONE, 2023, 18, e0284301.	2.5	2
13049	Studying the Mechanism of Interaction of Doxofylline with Human Lysozyme: A Biophysical and In Silico Approach. Molecules, 2023, 28, 3462.	3.8	1
13050	Energy coupling and stoichiometry of Zn <sup>2+</sup> /H <sup>+</sup> antiport by the prokaryotic cation diffusion facilitator YiiP. ELife, 0, 12, .	6.0	1

#	ARTICLE	IF	CITATIONS
13051	Predicting liposome formulations by the integrated machine learning and molecular modeling approaches. <i>Asian Journal of Pharmaceutical Sciences</i> , 2023, , 100811.	9.1	2
13052	Structure and stability of nitrogen hydrate in a single-walled carbon nanotube under external electric fields. <i>Chinese Physics B</i> , 2023, 32, 076402.	1.4	1
13053	Profiling the disintegration of BRPs released by massive wasp stings using serratiopeptidase: An in-silico insight. <i>Computers in Biology and Medicine</i> , 2023, 159, 106951.	7.0	3
13054	Influence of Ethanol Parametrization on Diffusion Coefficients Using OPLS-AA Force Field. <i>International Journal of Molecular Sciences</i> , 2023, 24, 7316.	4.1	1
13055	Development of a coarse-grained model for surface-functionalized gold nanoparticles: towards an accurate description of their aggregation behavior. <i>Soft Matter</i> , 2023, 19, 3290-3300.	2.7	1
13056	Targeting multidrug resistant <i>Staphylococcus aureus</i> with cationic chlorpromazine-peptide conjugates. <i>Chemistry - an Asian Journal</i> , 2023, 18, .	3.3	1
13057	Domain- and state-specific shape of the electric field tunes voltage sensing in voltage-gated sodium channels. <i>Biophysical Journal</i> , 2023, 122, 1807-1821.	0.5	2
13059	Discovery of a cryptic pocket in the AI-predicted structure of PPM1D phosphatase explains the binding site and potency of its allosteric inhibitors. <i>Frontiers in Molecular Biosciences</i> , 0, 10, .	3.5	4
13060	Structural and Dynamic Characterization of Ionic Liquid Electrolyte Solutions for Application in Li-Ion Batteries: A Molecular Dynamics Approach. <i>Batteries</i> , 2023, 9, 234.	4.5	1
13061	Phase Transition and Phase Separation in Realistic Thylakoid Lipid Membrane of Marine Algae in All-Atom Simulations. <i>Journal of Chemical Information and Modeling</i> , 2023, 63, 3328-3339.	5.4	4
13062	Molecular modeling and DFT studies on the antioxidant activity of <i>Centaurea scoparia</i> flavonoids and molecular dynamics simulation of their interaction with $\beta$ -lactoglobulin. <i>RSC Advances</i> , 2023, 13, 12361-12374.	3.6	5
13063	Discovery of seven-membered ring berberine analogues as highly potent and specific hCES2A inhibitors. <i>Chemico-Biological Interactions</i> , 2023, 378, 110501.	4.0	3
13064	Structure and dynamics of a glucose-based cryoprotectant mixture: a computer simulation study. <i>Theoretical Chemistry Accounts</i> , 2023, 142, .	1.4	0
13065	Acidity reduction using ionic liquids: Extraction, kinetic, and theoretical study. <i>Journal of Molecular Liquids</i> , 2023, 382, 121870.	4.9	1
13066	In silico EsxG EsxH rational epitope selection: Candidate epitopes for vaccine design against pulmonary tuberculosis. <i>PLoS ONE</i> , 2023, 18, e0284264.	2.5	1
13067	Thermodynamic response functions and Stokes-Einstein breakdown in superheated water under gigapascal pressure. <i>Theoretical Chemistry Accounts</i> , 2023, 142, .	1.4	1
13068	Modified electrochemical aptasensor for ultrasensitive detection of tetracycline: In silico and in vitro studies. <i>Food Chemistry</i> , 2023, 421, 136195.	8.2	7
13069	O-GlcNAcylation promotes the cytosolic localization of the m6A reader YTHDF1 and colorectal cancer tumorigenesis. <i>Journal of Biological Chemistry</i> , 2023, 299, 104738.	3.4	7

#	ARTICLE	IF	CITATIONS
13072	Effect of Pressure on the Dynamics of Iodide Defects in Methylammonium Lead Iodide: An Atomistic Simulation. <i>Journal of Physical Chemistry C</i> , 2023, 127, 7938-7943.	3.1	2
13073	Interactions between amphiphilic nanoparticles coated with striped hydrophilic/hydrophobic ligands and a lipid bilayer. <i>Communications in Theoretical Physics</i> , 2023, 75, 065601.	2.5	2
13074	Interaction of the tau fibrils with the neuronal membrane. <i>Biophysical Chemistry</i> , 2023, 298, 107024.	2.8	1
13075	The Ebola virus VP40 matrix layer undergoes endosomal disassembly essential for membrane fusion. <i>EMBO Journal</i> , 2023, 42, .	7.8	11
13077	Investigation of the inhibitory behavior of XFE and mitoxantrone molecules in interaction with AKT1 protein: a molecular dynamics simulation study. <i>Journal of Molecular Modeling</i> , 2023, 29, .	1.8	1
13078	On a mechanistic impact of transmembrane tetramerization in the pathological activation of RTKs. <i>Computational and Structural Biotechnology Journal</i> , 2023, 21, 2837-2844.	4.1	1
13079	Seipin concentrates distinct neutral lipids via interactions with their acyl chain carboxyl esters. <i>Journal of Cell Biology</i> , 2022, 221, .	5.2	10
13080	The geometry of calix[3]pyrrole and the formation of the calix[3]pyrrole- $\text{F}^{\text{+}}$ complex in solution. <i>Theoretical Chemistry Accounts</i> , 2023, 142, .	1.4	0
13081	Investigating structural features of dimeric SARS-CoV-2 Mpro catalytic site with bound covalent ligands at physiological temperature. <i>Journal of Physics: Conference Series</i> , 2023, 2485, 012006.	0.4	0
13082	Visualizing the Residue Interaction Landscape of Proteins by Temporal Network Embedding. <i>Journal of Chemical Theory and Computation</i> , 2023, 19, 2985-2995.	5.3	4
13083	Fundamentals of Crystalline Evolution and Properties of Carbon Nanotube-Reinforced Polyether Ether Ketone Nanocomposites in Fused Filament Fabrication. <i>ACS Applied Materials &amp; Interfaces</i> , 2023, 15, 22506-22523.	8.0	1
13084	Visualizing the disordered nuclear transport machinery in situ. <i>Nature</i> , 2023, 617, 162-169.	27.8	31
13085	Spontaneous Hybrid Nano- $\text{D}$ Domain Behavior of the Organic-Inorganic Hybrid Perovskites. <i>Advanced Functional Materials</i> , 2023, 33, .	14.9	4
13086	Structural insights into SARS-CoV-2 main protease conformational plasticity. <i>Journal of Cellular Biochemistry</i> , 2023, 124, 861-876.	2.6	3
13087	Non-equilibrium virus particle dynamics: Microsecond MD simulations of the complete Flock House virus capsid under different conditions. <i>Journal of Structural Biology</i> , 2023, 215, 107964.	2.8	1
13088	DNA Detection Using a Single-Layer Phosphorene Nanopore. <i>ACS Applied Nano Materials</i> , 2023, 6, 7814-7820.	5.0	2
13089	Paradoxical effect of $\text{Al}^{2+}$ on protein levels of ABCA1 in astrocytes, microglia, and neurons isolated from C57BL/6 mice: an in vitro and in silico study to elucidate the effect of $\text{Al}^{2+}$ on ABCA1 in the brain cells. <i>Journal of Biomolecular Structure and Dynamics</i> , 2024, 42, 274-287.	3.5	4
13090	Exploration of natural compounds against the human mpox virus DNA-dependent RNA polymerase in silico. <i>Journal of Infection and Public Health</i> , 2023, 16, 996-1003.	4.1	5

#	ARTICLE	IF	CITATIONS
13092	Ab Initio Molecular Dynamics: A Guide to Applications. , 2024, , 493-517.		0
13093	Exploring the structure of halomethanes with xenon: An NMR and MD investigation. Journal of Molecular Liquids, 2023, 382, 122011.	4.9	1
13094	Efficient purification of biogas using ionic liquid as absorbent: Molecular thermodynamics, dynamics and experiment. Journal of Environmental Chemical Engineering, 2023, 11, 110083.	6.7	0
13095	Isatin-pyrimidine hybrid derivatives as enoyl acyl carrier protein reductase (InhA) inhibitors against Mycobacterium tuberculosis. Bioorganic Chemistry, 2023, 138, 106591.	4.1	2
13096	Interaction between microplastics and humic acid and its effect on their properties as revealed by molecular dynamics simulations. Journal of Hazardous Materials, 2023, 455, 131636.	12.4	4
13097	Entropic contribution of ACE2 glycans to RBD binding. Biophysical Journal, 2023, 122, 2506-2517.	0.5	3
13099	Markov State Models Reconcile Conformational Plasticity of GTPase with Its Substrate Binding Event. JACS, 2023, 3, 1728-1741.	7.9	1
13100	Curvature Matters: Modeling Calcium Binding to Neutral and Anionic Phospholipid Bilayers. Journal of Physical Chemistry B, 2023, 127, 4523-4531.	2.6	4
13102	A coarse-grained molecular dynamics investigation on spontaneous binding of A $\beta$ 1-40 fibrils with cholesterol-mixed DPPC bilayers. Computational and Structural Biotechnology Journal, 2023, 21, 2688-2695.	4.1	7
13103	Probing the combination of erlotinib hydrochloride, an anticancer drug, and human serum albumin: Spectroscopic, molecular docking, and molecular dynamic analyses. Luminescence, 2023, 38, 772-782.	2.9	7
13104	Probing the general base for DNA polymerization in telomerase: a molecular dynamics investigation. Physical Chemistry Chemical Physics, 2023, 25, 14147-14157.	2.8	0
13105	<i>SCOMAP-XD</i>: atomistic deuterium contrast matching for small-angle neutron scattering in biology. Acta Crystallographica Section D: Structural Biology, 2023, 79, 420-434.	2.3	2
13106	Liquidâ€“Liquid Criticality in TIP4P/2005 and Three-State Models of Water. Journal of Physical Chemistry B, 2023, 127, 3902-3910.	2.6	0
13107	Theoretical studies on the quercetin interactions in the oil-in-water F127 microemulsion: A DFT and MD investigation. Journal of Molecular Liquids, 2023, 383, 122037.	4.9	2
13108	Functional insight into <i>Cordyceps militaris</i> sugar transporters by structure modeling, network analysis and allosteric regulation. Physical Chemistry Chemical Physics, 2023, 25, 14311-14323.	2.8	2
13110	A Deep Potential model for liquidâ€“vapor equilibrium and cavitation rates of water. Journal of Chemical Physics, 2023, 158, .	3.0	6
13111	A Systems Biology Approach Reveals the Endocrine Disrupting Potential of Aflatoxin B1. Exposure and Health, 2024, 16, 321-340.	4.9	0
13112	Solubility of carbon dioxide in water: Some useful results for hydrate nucleation. Journal of Chemical Physics, 2023, 158, .	3.0	5



#	ARTICLE	IF	CITATIONS
13113	One- and Two- Electron Reductions in MiniSOG and their Implication in Catalysis. ChemPhysChem, 0, , .	2.1	0
13114	Tyrosine kinases compete for growth hormone receptor binding and regulate receptor mobility and degradation. Cell Reports, 2023, 42, 112490.	6.4	4
13116	Structure and elasticity of healthy and Alzheimer's disease cell membranes revealed by molecular dynamics simulations. Proteins: Structure, Function and Bioinformatics, 0, , .	2.6	1
13117	Exploring structural and dynamical properties of polymer-ionic liquid ternary electrolytes for sodium ion batteries. Electrochimica Acta, 2023, 461, 142635.	5.2	1
13118	Molecular insights into the inhibition of early stages of A $\beta$ peptide aggregation and destabilization of Alzheimer's A $\beta$ protofibril by dipeptide D-Trp-Aib: A molecular modelling approach. International Journal of Biological Macromolecules, 2023, 242, 124880.	7.5	3
13119	PACAP key interactions with PAC1, VPAC1, and VPAC2 identified by molecular dynamics simulations. Journal of Biomolecular Structure and Dynamics, 0, , 1-17.	3.5	0
13120	Y225A induces long-range conformational changes in human prion protein that are protective in Drosophila. Journal of Biological Chemistry, 2023, 299, 104881.	3.4	2
13121	Phase transformation behavior of aluminum under high hydrostatic pressure: A molecular dynamics study. Materials Today Communications, 2023, 35, 106199.	1.9	0
13122	The effect of water-soluble polymers on the dynamics of carbon dioxide sorption by lime sorbents. Kataliz V Promyshlennosti, 2023, 23, 6-14.	0.3	0
13123	Switching from Aromatase Inhibitors to Dual Targeting Flavonoid-Based Compounds for Breast Cancer Treatment. Molecules, 2023, 28, 3047.	3.8	2
13124	<sc>GPU-specific</sc> algorithms for improved solute sampling in grand canonical Monte Carlo simulations. Journal of Computational Chemistry, 2023, 44, 1719-1732.	3.3	3
13125	Exploring the Microscopic Aspects of 1-Methyl-3-octylimidazolium Tetrafluoroborate Mixtures with Formamide, <i>N</i>-Methylformamide, and <i>N</i>-Dimethylformamide by Multiple Spectroscopic Techniques and Computations. Journal of Physical Chemistry B, 2023, 127, 3870-3887.	2.6	3
13126	Investigation of Macrocyclic mTOR Modulators of Rapamycin Binding Site via Pharmacoinformatics Approaches. Computational Biology and Chemistry, 2023, 104, 107875.	2.3	0
13127	Machine-guided path sampling to discover mechanisms of molecular self-organization. Nature Computational Science, 2023, 3, 334-345.	8.0	27
13128	Identification of novel potential hepatitis E virus inhibitors as seen from molecular docking, free energy landscape and molecular dynamics simulation studies. Molecular Simulation, 2023, 49, 967-981.	2.0	1
13129	Studying the Effect of Cross-Linking and Sulfonation on the Calcium-Binding Ability of Polystyrene Sulfonate in the Presence of Dodecyl Sulfate. Industrial & Engineering Chemistry Research, 2023, 62, 7017-7030.	3.7	2
13130	Discovery of lipid binding sites in a ligand-gated ion channel by integrating simulations and cryo-EM. ELife, 0, 12, .	6.0	1
13131	Crystallization behavior of polyvinylidene fluoride (PVDF) in NMP/DMF solvents: a molecular dynamics study. RSC Advances, 2023, 13, 12917-12924.	3.6	2

#	ARTICLE	IF	CITATIONS
13133	Mechanistic Insights into Polyphenolsâ€™ Aggregation Inhibition of Î±-Synuclein and Related Peptides. ACS Chemical Neuroscience, 2023, 14, 1905-1920.	3.5	3
13134	Choline based deep eutectic solvent for denitrogenation of liquid fuel: A molecular dynamics study. Journal of Molecular Liquids, 2023, 382, 121862.	4.9	1
13135	Molecular simulation of partially denatured Î²-lactoglobulin. Food Hydrocolloids, 2023, 142, 108811.	10.7	0
13136	Membrane Potential-Dependent Uptake of Cationic Oligoimidazolium Mediates Bacterial DNA Damage and Death. Antimicrobial Agents and Chemotherapy, 2023, 67, .	3.2	0
13137	Cholesterol Biases the Conformational Landscape of the Chemokine Receptor CCR3: A MAS SSNMR-Filtered Molecular Dynamics Study. Journal of Chemical Information and Modeling, 2023, 63, 3068-3085.	5.4	3
13138	Sulfonamide derived from anacardic acid as potential antichagasic: a theoretical approach based on molecular docking, molecular dynamics, and density functional theory calculations. Journal of Molecular Modeling, 2023, 29, .	1.8	0
13139	SARS-CoV-2 Omicron subvariant spike N405 unlikely to rapidly deamidate. Biochemical and Biophysical Research Communications, 2023, 666, 61-67.	2.1	1
13140	Identification of Catechinsâ€™ Binding Sites in Monomeric AÎ²42 through Ensemble Docking and MD Simulations. International Journal of Molecular Sciences, 2023, 24, 8161.	4.1	1
13142	Design and In-Silico Screening of Short Antimicrobial Peptides (Amps) as Anti-Tubercular Agents Targeting INHA. Current Bioinformatics, 2023, 18, .	1.5	0
13143	Coarse-grained molecular dynamics simulation of cation distribution profiles on negatively charged lipid membranes during phase separation. Soft Matter, 2023, 19, 3640-3651.	2.7	1
13144	Monovalent Ionic Atmosphere Modulates the Selection of Suboptimal RNA Sequences by Splicing Factorsâ€™ RNA Recognition Motifs. Journal of Chemical Information and Modeling, 2023, 63, 3086-3093.	5.4	4
13145	Computational and Experimental Determination of the Properties, Structure, and Stability of Peptoid Nanosheets and Nanotubes. Biomacromolecules, 2023, 24, 2618-2632.	5.4	2
13146	Dielectric relaxation and dielectric decrement in ionic acetamide deep eutectic solvents: Spectral decomposition and comparison with experiments. Journal of Chemical Physics, 2023, 158, .	3.0	2
13147	Evolution of large <sc>A</sc> Î²2</i>16â€“22 aggregates at atomic details and potential of mean force associated to peptide unbinding and fragmentation events. Proteins: Structure, Function and Bioinformatics, 2023, 91, 1152-1162.	2.6	3
13148	Influence of Lennardâ€“Jones Parameters in the Temperature Dependence of Real Gases Diffusion through Nanochannels. Nanomaterials, 2023, 13, 1534.	4.1	1
13150	Utilization of a kinetic isotope effect to decrease decomposition of ceftriaxone in a mixture of D2O/H2O. European Journal of Pharmaceutical Sciences, 2023, 187, 106461.	4.0	1
13151	Selective Non-toxic Inhibitors Targeting DHFR for Tuberculosis and Cancer Therapy: Pharmacophore Generation and Molecular Dynamics Simulation. Bioinformatics and Biology Insights, 2023, 17, 117793222311717.	2.0	0
13154	Dynamacophore model for breast cancer estrogen receptor alpha as an effective lead generation screening technique. Journal of Biomolecular Structure and Dynamics, 2023, 41, 13029-13040.	3.5	0

#	ARTICLE	IF	CITATIONS
13155	Atomistic analysis of the effect of cholesterol on cancerous membrane protein system: unfolding and associated resistance stresses under strain. <i>Molecular Simulation</i> , 2023, 49, 1019-1030.	2.0	0
13156	Relating Molecular Dynamics Simulations to Functional Activity for Gly-Rich Membranolytic Helical Kiadin Peptides. <i>Pharmaceutics</i> , 2023, 15, 1433.	4.5	1
13157	Non-Phenomenological Description of the Time-Resolved Emission in Solution with Quantumâ€“Classical Vibronic Approachesâ€“Application to Coumarin C153 in Methanol. <i>Molecules</i> , 2023, 28, 3910.	3.8	0
13158	<i>Escherichia coli</i> FtsZ molecular dynamics simulations. <i>Journal of Biomolecular Structure and Dynamics</i> , 2024, 42, 2653-2666.	3.5	1
13159	Dynamics of a methane hydrophobe in aqueous choline chloride solution: Insights from molecular dynamics simulations. <i>Chemical Physics Impact</i> , 2023, 6, 100223.	3.5	0
13160	Three phase equilibria of the methane hydrate in NaCl solutions: A simulation study. <i>Journal of Molecular Liquids</i> , 2023, 383, 122031.	4.9	7
13164	Discovery of AI-2 Quorum Sensing Inhibitors Targeting the LsrK/HPr Proteinâ€“Protein Interaction Site by Molecular Dynamics Simulation, Virtual Screening, and Bioassay Evaluation. <i>Pharmaceutics</i> , 2023, 16, 737.	3.8	1
13166	Frontotemporal Dementia-Related V57E Mutation Impairs Mitochondrial Function and Alters the Structural Properties of CHCHD10. <i>ACS Chemical Neuroscience</i> , 2023, 14, 2134-2145.	3.5	0
13167	Differential membrane curvature induced by distinct protein conformers. <i>Soft Matter</i> , 2023, 19, 4021-4028.	2.7	1
13168	Phase equilibrium, dynamics and rheology of phospholipidâ€“ethanol mixtures: a combined molecular dynamics, NMR and viscometry study. <i>Physical Chemistry Chemical Physics</i> , 2023, 25, 15905-15915.	2.8	0
13169	Polarization-consistent force field for ketones. <i>Journal of Molecular Liquids</i> , 2023, 383, 122070.	4.9	0
13170	The Missing Relationship between the Miscibility of Chiral Dopants and the Microscopic Dynamics of Solvent Liquid Crystals: A Molecular Dynamics Study. <i>Symmetry</i> , 2023, 15, 1092.	2.2	1
13171	Molecular Insights into the Binding Behavior of Imidazolium Ionic Liquids to the Receptor Binding Domain of the SARS-CoV-2 Spike Protein. <i>Journal of Physical Chemistry B</i> , 2023, 127, 4396-4405.	2.6	1
13172	<i>In vitro</i> and <i>in silico</i> analysis for elucidation of antioxidant potential of Djiboutian <i>Avicennia Marina</i> (Forsk.) Vierh. phytochemicals. <i>Journal of Biomolecular Structure and Dynamics</i> , 0, , 1-16.	3.5	1
13173	Molecular docking and dynamic simulations of quinoxaline 1,4-di-N-oxide as inhibitors for targets from <i>Trypanosoma cruzi</i> , <i>Trichomonas vaginalis</i> , and <i>Fasciola hepatica</i> . <i>Journal of Molecular Modeling</i> , 2023, 29, .	1.8	0
13174	NMR spectrum prediction for dynamic molecules by machine learning: A case study of trefoil knot molecule. <i>Journal of Chemical Physics</i> , 2023, 158, .	3.0	0
13175	Grain-boundary thermodynamics with artificial-neural-network potential: Its ability to predict the atomic structures, energetics, and lattice vibrational properties for Al. <i>Physical Review Materials</i> , 2023, 7, .	2.4	1
13176	Comparison of On-the-Fly Probability Enhanced Sampling and Parallel Tempering Combined with Metadynamics for Atomistic Simulations of RNA Tetraloop Folding. <i>Journal of Physical Chemistry B</i> , 2023, 127, 4722-4732.	2.6	3

#	ARTICLE	IF	CITATIONS
13177	Stereochemical engineering yields a multifunctional peptide macrocycle inhibitor of Akt2 by fine-tuning macrocycle-cell membrane interactions. <i>Communications Chemistry</i> , 2023, 6, .	4.5	0
13178	Alchemical Free Energy and Hamiltonian Replica Exchange Molecular Dynamics to Compute Hydrofluorocarbon Isotherms in Imidazolium-Based Ionic Liquids. <i>Journal of Chemical Theory and Computation</i> , 2023, 19, 3324-3335.	5.3	2
13179	Plant polygalacturonase structures specify enzyme dynamics and processivities to fine-tune cell wall pectins. <i>Plant Cell</i> , 2023, 35, 3073-3091.	6.6	6
13180	Classical Molecular Dynamics Simulation of Molecular Crystals and Materials: Old Lessons and New Perspectives. , 2024, , 777-803.		1
13181	Structural Insights into Phosphorylation-Mediated Polymerase Function Loss for DNA Polymerase $\beta$ Bound to Gapped DNA. <i>International Journal of Molecular Sciences</i> , 2023, 24, 8988.	4.1	0
13183	Destabilization of Human Islet Amyloid Polypeptide Fibrils by Charged Graphene Quantum Dots: A Molecular Dynamics Investigation with Implications for Nanomedicine. <i>ACS Applied Nano Materials</i> , 2023, 6, 9649-9656.	5.0	2
13184	Driving forces for ultrafast laser-induced sp <sup>2</sup> to sp <sup>3</sup> structural transformation in graphite. <i>Npj Computational Materials</i> , 2023, 9, .	8.7	2
13186	In Silico Interactome of a Room-Temperature Ferroelectric Nematic Material. <i>Crystals</i> , 2023, 13, 857.	2.2	2
13187	All-atoms molecular dynamics study to screen potent efflux pump inhibitors against KpnE protein of <i>Klebsiella pneumoniae</i> . <i>Journal of Biomolecular Structure and Dynamics</i> , 2024, 42, 3492-3506.	3.5	2
13188	Significance of Astragaloside IV from the Roots of <i>Astragalus mongholicus</i> as an Acetylcholinesterase Inhibitor—From the Computational and Biomimetic Analyses to the In Vitro and In Vivo Studies of Safety. <i>International Journal of Molecular Sciences</i> , 2023, 24, 9152.	4.1	3
13189	Machine learning and classical MD simulation to identify inhibitors against the P37 envelope protein of monkeypox virus. <i>Journal of Biomolecular Structure and Dynamics</i> , 0, , 1-14.	3.5	2
13190	Pressure Dependence of Solid Electrolyte Ionic Conductivity: A Particle Dynamics Study. <i>ACS Applied Materials &amp; Interfaces</i> , 2023, 15, 27243-27252.	8.0	1
13192	Local structural power exponent as an indicator of elastic heterogeneity in glasses. <i>Physical Review B</i> , 2023, 107, .	3.2	0
13193	On the possible locus of the liquid–liquid critical point in real water from studies of supercooled water using the TIP4P/Ice model. <i>Journal of Chemical Physics</i> , 2023, 158, .	3.0	3
13194	Adsorbate Organization Characterized by Sublevelset Persistent Homology. <i>Journal of Chemical Theory and Computation</i> , 2023, 19, 3303-3312.	5.3	0
13195	Differential toxicity and localization of arginine-rich C9ORF72 dipeptide repeat proteins depend on de-clustering of positive charges. <i>IScience</i> , 2023, 26, 106957.	4.1	3
13196	Utilization of DNA and 2D metal oxide interaction for an optical biosensor. <i>Physical Chemistry Chemical Physics</i> , 0, , .	2.8	0
13197	TCDD-Induced Allosteric Perturbation of the AhR:ARNT Binding to DNA. <i>International Journal of Molecular Sciences</i> , 2023, 24, 9339.	4.1	2

#	ARTICLE	IF	CITATIONS
13198	Effect of Cas9 Protein on the Seed-Target Base Pair of the sgRNA/DNA Hybrid Duplex. Journal of Physical Chemistry B, 2023, 127, 4989-4997.	2.6	0
13200	At the origin of the selectivity of the chlorophyll-binding sites in Light Harvesting Complex II (LHCII). International Journal of Biological Macromolecules, 2023, 243, 125069.	7.5	5
13201	Combination of molecular dynamics simulation and COSMO to understand asphaltenes aggregation. Molecular Simulation, 2023, 49, 1091-1103.	2.0	0
13202	<i>Bacteroides fragilis</i> expresses three proteins similar to <i>Porphyromonas gingivalis</i> HmuY: Hemophore-like proteins differentially evolved to participate in heme acquisition in oral and gut microbiomes. FASEB Journal, 2023, 37, .	0.5	3
13204	Spectroscopic, voltammetric and computational approaches shed light on the combination characteristics of an anticancer agent, bexarotene with human serum albumin. Journal of Photochemistry and Photobiology A: Chemistry, 2023, 443, 114881.	3.9	1
13205	Molecular simulation studies on a zwitterionic peptide-dendrimer conjugate for integrin $\alpha_5\beta_3$ binding. Biointerphases, 2023, 18, .	1.6	1
13206	Electrostatic Modulation of Intramolecular and Intermolecular Interactions during the Formation of an Amyloid-like Assembly. Biochemistry, 2023, 62, 1890-1905.	2.5	0
13207	Molecular simulations of DEAH-box helicases reveal control of domain flexibility by ligands: RNA, ATP, ADP, and G-patch proteins. Biological Chemistry, 2023, .	2.5	1
13209	Yielding under compression and the polyamorphic transition in silicon. Physical Review Materials, 2023, 7, .	2.4	2
13212	Activity modulation of the Escherichia coli F1FO ATP synthase by a designed antimicrobial peptide via cardiolipin sequestering. IScience, 2023, 26, 107004.	4.1	1
13213	Ordered domain unfolding of thermophilic isolated $\beta^2$ subunit ATP synthase. Protein Science, 2023, 32, .	7.6	0
13215	Disulfide bridge-dependent dimerization triggers FGF2 membrane translocation into the extracellular space. ELife, 0, 12, .	6.0	0
13216	Aurones: A Promising Scaffold to Inhibit SARS-CoV-2 Replication. Journal of Natural Products, 2023, 86, 1536-1549.	3.0	6
13217	Influence of Functionalization on the Crystallinity and Basic Thermodynamic Properties of Polyethylene. Macromolecules, 2023, 56, 3873-3883.	4.8	4
13219	Unwrapping NPT Simulations to Calculate Diffusion Coefficients. Journal of Chemical Theory and Computation, 2023, 19, 3406-3417.	5.3	3
13220	Q1291H-CFTR molecular dynamics simulations and ex vivo theratyping in nasal epithelial models and clinical response to elexacaftor/tezacaftor/ivacaftor in a Q1291H/F508del patient. Frontiers in Molecular Biosciences, 0, 10, .	3.5	1
13221	Investigating the Impact of the Glycolipid Content on Aurein 1.2 Pores in Prokaryotic Model Bilayers: A Coarse-Grain Molecular Dynamics Simulation Study. Journal of Physical Chemistry B, 2023, 127, 5190-5198.	2.6	1
13222	Mechanism of monovalent and divalent ion mobility in Nafion membrane: An atomistic simulation study. Journal of Chemical Physics, 2023, 158, .	3.0	1

#	ARTICLE	IF	CITATIONS
13223	Structural Impact of Selected Retinoids on Model Photoreceptor Membranes. <i>Membranes</i> , 2023, 13, 575.	3.0	2
13224	Interaction and binding mechanism of cyanidin-3-O-glucoside to lysozyme in varying pH conditions: Multi-spectroscopic, molecular docking and molecular dynamics simulation approaches. <i>Food Chemistry</i> , 2023, 425, 136509.	8.2	5
13225	Liquid Structure Scenario of the Archetypal Supramolecular Deep Eutectic Solvent: Heptakis(2,6-di- <i>o</i> -methyl)- $\beta$ -cyclodextrin/levulinic Acid. <i>ACS Sustainable Chemistry and Engineering</i> , 2023, 11, 9103-9110.	6.7	0
13227	Molecular dynamics simulation of CL20/DNDAP cocrystal-based PBXs. <i>Journal of Molecular Modeling</i> , 2023, 29, .	1.8	4
13228	Exploiting the potential of natural polyphenols as antivirals against monkeypox envelope protein F13 using machine learning and all-atoms MD simulations. <i>Computers in Biology and Medicine</i> , 2023, 162, 107116.	7.0	5
13230	Functional impact and molecular binding modes of drugs that target the PI3K isoform p110 $\beta$ . <i>Communications Biology</i> , 2023, 6, .	4.4	0
13231	Boron based podand molecule as an anion receptor additive in Li-ion battery electrolytes: A combined density functional theory and molecular dynamics study. <i>Journal of Molecular Liquids</i> , 2023, 384, 122236.	4.9	1
13232	Separation of furfuryl alcohol from water using hydrophobic deep eutectic solvents. <i>Journal of Molecular Liquids</i> , 2023, 384, 122232.	4.9	2
13233	DNA damage-induced YTHDC1 O-GlcNAcylation promotes homologous recombination by enhancing m6A binding. <i>Fundamental Research</i> , 2023, , .	3.3	1
13234	Fitting Force Field Parameters to NMR Relaxation Data. <i>Journal of Chemical Theory and Computation</i> , 2023, 19, 3741-3751.	5.3	3
13235	An Electrochemistry and Computational Study at an Electrified Liquid–Liquid Interface for Studying Beta-Amyloid Aggregation. <i>Membranes</i> , 2023, 13, 584.	3.0	0
13236	First-principles study of the distribution of excess intercalated lithium in Li <sub>3</sub> V <sub>2</sub> O <sub>5</sub> with a disordered rock-salt structure. <i>Journal of Materials Chemistry A</i> , 0, , .	10.3	0
13237	Molecular basis for the recognition of 24-(S)-hydroxycholesterol by integrin $\alpha$ $\beta$ 23. <i>Scientific Reports</i> , 2023, 13, .	3.3	2
13238	Systematic modification of functionality in disordered elastic networks through free energy surface tailoring. <i>Science Advances</i> , 2023, 9, .	10.3	2
13239	Analysis of Fe <sup>2+</sup> and Mn <sup>2+</sup> ions in DES and water: A theoretical study using molecular dynamic simulations, QTAIM and NCI-RDG. <i>Colloids and Surfaces A: Physicochemical and Engineering Aspects</i> , 2023, 674, 131818.	4.7	3
13240	Dynamical Nonequilibrium Molecular Dynamics Simulations Identify Allosteric Sites and Positions Associated with Drug Resistance in the SARS-CoV-2 Main Protease. <i>Jacs Au</i> , 2023, 3, 1767-1774.	7.9	7
13241	Comparative Study of Molecular Mechanics Force Fields for $\beta$ -Peptidic Foldamers: Folding and Self-Association. <i>Journal of Chemical Information and Modeling</i> , 2023, 63, 3799-3813.	5.4	1
13242	Tackling Hysteresis in Conformational Sampling: How to Be Forgetful with MEMENTO. <i>Journal of Chemical Theory and Computation</i> , 2023, 19, 3705-3720.	5.3	2



#	ARTICLE	IF	CITATIONS
13243	Synthesis, Spectroscopic Analysis, Molecular Docking, Molecular Dynamics Simulation of 5-(Adamantan-1-yl)-4-(3-Chlorophenyl)-2,4-Dihydro-3 <i>H</i> -1,2,4-Triazole-3-Thione, a Potential Anti-proliferative Agent. Polycyclic Aromatic Compounds, 0, , 1-23.	2.6	0
13244	Surface Effect on Phase Transformation of Single Crystal NiTi Shape Memory Alloys Studied by Molecular Dynamics Simulation. Advanced Engineering Materials, 0, , .	3.5	0
13245	Theoretical and experimental studies on the interaction of biphenyl ligands with human and murine PD-L1: Up-to-date clues for drug design. Computational and Structural Biotechnology Journal, 2023, 21, 3355-3368.	4.1	1
13246	Monitoring of breast cancer progression via aptamer-based detection of circulating tumor cells in clinical blood samples. Frontiers in Molecular Biosciences, 0, 10, .	3.5	4
13248	Molecular dynamics simulation of the effect of AQP1 on the transmembrane transport of plasma RONS across cancer cell membranes. Physics of Plasmas, 2023, 30, .	1.9	2
13249	Autophagosome membrane expansion is mediated by the N-terminus and cis-membrane association of human ATG8s. ELife, 0, 12, .	6.0	10
13251	Study of the weak interaction mechanism of ovalbumin and caffeic acid using fluorescence spectroscopy and molecular dynamics simulation. Spectrochimica Acta - Part A: Molecular and Biomolecular Spectroscopy, 2023, 301, 122966.	3.9	2
13252	Evolutional insights into the interaction between Rab7 and RILP in lysosome motility. IScience, 2023, 26, 107040.	4.1	1
13253	Computational analysis of sodium-dependent phosphate transporter SLC20A1/Pi1 gene identifies missense variations C573F, and T58A as high-risk deleterious SNPs. Journal of Biomolecular Structure and Dynamics, 0, , 1-15.	3.5	0
13254	Effect of cold atmospheric plasma induced electric field on aquaporin-5 structure and ROS transport. Results in Physics, 2023, 51, 106621.	4.1	1
13255	Molecular Dynamics Simulations with Grand-Canonical Reweighting Suggest Cooperativity Effects in RNA Structure Probing Experiments. Journal of Chemical Theory and Computation, 2023, 19, 3672-3685.	5.3	2
13256	A multicentric consortium study demonstrates that dimethylarginine dimethylaminohydrolase 2 is not a dimethylarginine dimethylaminohydrolase. Nature Communications, 2023, 14, .	12.8	6
13257	â€˜Computational studies on coumestrol-ArlR interaction to target ArlRS signaling cascade involved in MRSA virulenceâ€™. Journal of Biomolecular Structure and Dynamics, 0, , 1-19.	3.5	1
13258	Pyroglutamate-modified amyloid Î²(3â€˜42) monomer has more Î²-sheet content than the amyloid Î²(1â€˜42) monomer. Physical Chemistry Chemical Physics, 2023, 25, 16483-16491.	2.8	2
13259	Designing a bioadjuvant candidate vaccine targeting infectious bursal disease virus (IBDV) using viral VP2 fusion and chicken IL-2 antigenic epitope: A bioinformatics approach. Computers in Biology and Medicine, 2023, 163, 107087.	7.0	1
13260	Machine Learning-Enabled Development of Accurate Force Fields for Refrigerants. Journal of Chemical Theory and Computation, 2023, 19, 4546-4558.	5.3	1
13261	A Study of a Protein-Folding Machine: Transient Rotation of the Polypeptide Backbone Facilitates Rapid Folding of Protein Domains in All-Atom Molecular Dynamics Simulations. International Journal of Molecular Sciences, 2023, 24, 10049.	4.1	0
13262	Machine learning predictions of diffusion in bulk and confined ionic liquids using simple descriptors. Molecular Systems Design and Engineering, 2023, 8, 1257-1274.	3.4	1

#	ARTICLE	IF	CITATIONS
13265	Integrated data-driven and experimental approaches to accelerate lead optimization targeting SARS-CoV-2 main protease. <i>Journal of Computer-Aided Molecular Design</i> , 0, , .	2.9	0
13266	The structure of phosphatidylinositol remodeling MBOAT7 reveals its catalytic mechanism and enables inhibitor identification. <i>Nature Communications</i> , 2023, 14, .	12.8	5
13267	Simulation Study of Membrane Bending by Protein Crowding: A Case Study with the Epsin N-terminal Homology Domain. <i>Soft Matter</i> , 0, , .	2.7	2
13268	Extein residues regulate the catalytic function of <i>Spl</i> DnaX intein enzyme by restricting the near-attack conformations of the active-site residues. <i>Protein Science</i> , 2023, 32, .	7.6	2
13269	Molecular Latent Space Simulators for Distributed and Multimolecular Trajectories. <i>Journal of Physical Chemistry A</i> , 2023, 127, 5470-5490.	2.5	2
13270	Targeting RNA Structure to Inhibit Editing in Trypanosomes. <i>International Journal of Molecular Sciences</i> , 2023, 24, 10110.	4.1	0
13272	Mesoscale computer modeling of asphaltene aggregation in liquid paraffin. <i>Journal of Chemical Physics</i> , 2023, 158, .	3.0	0
13273	Unveiling How Hydroxytyrosol Destabilizes $\beta$ -Syn Oligomers Using Molecular Simulations. <i>Journal of Physical Chemistry B</i> , 2023, 127, 5620-5632.	2.6	0
13274	Analytic geometric gradients for the polarizable density embedding model. <i>International Journal of Quantum Chemistry</i> , 0, , .	2.0	0
13275	Bioactive molecules of <i>Triadica sebifera</i> as eco-friendly antifeedants against <i>Plutella xylostella</i> : A pest management approach. <i>Molecular Systems Design and Engineering</i> , 0, , .	3.4	0
13276	Using classifiers to understand coarse-grained models and their fidelity with the underlying all-atom systems. <i>Journal of Chemical Physics</i> , 2023, 158, .	3.0	0
13277	Robust Mechanical Destruction to the Cell Membrane of Carbon Nitride Polyaniline (C <sub>3</sub> N): A Molecular Dynamics Simulation Study. <i>Journal of Chemical Information and Modeling</i> , 0, , .	5.4	0
13278	Early blockage of Mycobacterium Tuberculosis Cell-wall Synthesis via EchA Inhibition to Overcome Resistance Strain: Insights from Umbrella Sampling Simulations. <i>Current Bioactive Compounds</i> , 2023, 19, .	0.5	0
13279	A locally activatable sensor for robust quantification of organellar glutathione. <i>Nature Chemistry</i> , 2023, 15, 1415-1421.	13.6	9
13280	A computational approach to design a polyvalent vaccine against human respiratory syncytial virus. <i>Scientific Reports</i> , 2023, 13, .	3.3	4
13281	Objective molecular dynamics study of cross slip under high-rate deformation. <i>Journal of the Mechanics and Physics of Solids</i> , 2023, 179, 105361.	4.8	0
13282	SAMHD1 impairs type I interferon induction through the MAVS, IKK $\mu$ , and IRF7 signaling axis during viral infection. <i>Journal of Biological Chemistry</i> , 2023, 299, 104925.	3.4	1
13283	pH dependence of the assembly mechanism and properties of poly(L-lysine) and poly(L-glutamic acid) complexes. <i>Physical Chemistry Chemical Physics</i> , 0, , .	2.8	0

#	ARTICLE	IF	CITATIONS
13284	Investigation of Zika virus methyl transferase inhibitors using steered molecular dynamics. <i>Journal of Biomolecular Structure and Dynamics</i> , 2024, 42, 1711-1724.	3.5	1
13285	Morphology and Dynamics in Hydrated Graphene Oxide/Branched Poly(ethyleneimine) Nanocomposites: An In Silico Investigation. <i>Nanomaterials</i> , 2023, 13, 1865.	4.1	1
13286	Impact on <i>S. aureus</i> and <i>E. coli</i> Membranes of Treatment with Chlorhexidine and Alcohol Solutions: Insights from Molecular Simulations and Nuclear Magnetic Resonance. <i>Journal of Molecular Biology</i> , 2023, 435, 167953.	4.2	4
13287	Reactive Martini: Chemical Reactions in Coarse-Grained Molecular Dynamics Simulations. <i>Journal of Chemical Theory and Computation</i> , 2023, 19, 4040-4046.	5.3	4
13290	Crystal structure of a variable region segment of <i>Leptospira</i> host-interacting outer surface protein, LigA, reveals the orientation of Ig-like domains. <i>International Journal of Biological Macromolecules</i> , 2023, 244, 125445.	7.5	0
13291	Observation of multiple protein temperature transitions dependent upon the chemical environment. <i>Journal of Molecular Liquids</i> , 2023, 385, 122348.	4.9	0
13292	Investigation of structural phase transformation of Al metallic glass under uniaxial compression strain by molecular dynamics simulation. <i>Applied Physics A: Materials Science and Processing</i> , 2023, 129, .	2.3	0
13293	Insights from molecular dynamics and DFT calculations into the interaction of 1,4-benzodiazepines with 2-hydroxypropyl- $\beta$ -CD in a theoretical study. <i>Scientific Reports</i> , 2023, 13, .	3.3	4
13294	Protein Modelling and Molecular Docking Analysis of <i>Fasciola hepatica</i> $\beta$ -Tubulin's Interaction Sites, with Triclabendazole, Triclabendazole Sulphoxide and Triclabendazole Sulphone. <i>Acta Parasitologica</i> , 0, , .	1.1	0
13296	Structure and dynamics of an archetypal DNA nanoarchitecture revealed via cryo-EM and molecular dynamics simulations. <i>Nature Communications</i> , 2023, 14, .	12.8	8
13298	Analysis of the binding modes and resistance mechanism of four methyl benzimidazole carbamates inhibitors fungicides with <i>Monilinia fructicola</i> $\beta$ -tubulin protein. <i>Journal of Molecular Structure</i> , 2023, 1291, 136057.	3.6	0
13299	Galangin for COVID-19 and Mucormycosis co-infection: a potential therapeutic strategy of targeting critical host signal pathways triggered by SARS-CoV-2 and Mucormycosis. <i>Network Modeling Analysis in Health Informatics and Bioinformatics</i> , 2023, 12, .	2.1	1
13300	Molecular dynamics simulation of the mechanical and thermal properties of phagraphene nanosheets and nanotubes: a review. <i>Journal of Materials Science</i> , 2023, 58, 10222-10260.	3.7	0
13301	Li intercalation, electronic and thermodynamic properties in H <sub>2</sub> Ti <sub>3</sub> O <sub>7</sub> bulk: A theoretical study. <i>Computational Materials Science</i> , 2023, 228, 112344.	3.0	0
13302	Comparative Performance of Computer Simulation Models of Intrinsically Disordered Proteins at Different Levels of Coarse-Graining. <i>Journal of Chemical Information and Modeling</i> , 2023, 63, 4079-4087.	5.4	3
13303	Limitations of non-polarizable force fields in describing anion binding poses in non-polar synthetic hosts. <i>Physical Chemistry Chemical Physics</i> , 0, , .	2.8	0
13304	Mixtures of ethylammonium nitrate and ethylene carbonate: Bulk and interfacial analysis. <i>Journal of Molecular Liquids</i> , 2023, 385, 122361.	4.9	1
13305	Interplay between VSD, pore, and membrane lipids in electromechanical coupling in HCN channels. <i>ELife</i> , 0, 12, .	6.0	1

#	ARTICLE	IF	CITATIONS
13306	Albumin Is a Component of the Esterase Status of Human Blood Plasma. International Journal of Molecular Sciences, 2023, 24, 10383.	4.1	6
13307	Role of Charge Ordering in the Dynamics of Cluster Formation in Associated Liquids. Journal of Physical Chemistry B, 2023, 127, 5645-5654.	2.6	4
13308	Cyclic di-AMP traps proton-coupled K <sup>+</sup> transporters of the KUP family in an inward-occluded conformation. Nature Communications, 2023, 14, .	12.8	5
13309	How soluble misfolded proteins bypass chaperones at the molecular level. Nature Communications, 2023, 14, .	12.8	2
13310	Exploitation of active site flexibility-low temperature activity relation for engineering broad range temperature active enzymes. Molecular Systems Design and Engineering, 0, , .	3.4	0
13311	Predicting a Stable Dimeric Form of the PD1-PDL1 Complex: Implications for Understanding the PD1 Activation Mechanism. Journal of Physical Chemistry B, 0, , .	2.6	0
13312	The limit of macroscopic homogeneous ice nucleation at the nanoscale. Faraday Discussions, 0, 249, 210-228.	3.2	0
13313	Effect of xenon, an apolar general anaesthetic on the properties of the DPPC bilayer. Journal of Molecular Liquids, 2023, 386, 122405.	4.9	2
13314	A C-type lectin induces NLRP3 inflammasome activation via TLR4 interaction in human peripheral blood mononuclear cells. Cellular and Molecular Life Sciences, 2023, 80, .	5.4	2
13315	Exploring the Heterogeneous Dynamical Environment at the Interface of AÎ <sup>2</sup> <sub>42</sub> Peptide in Aqueous Ionic Liquid Solution. Journal of Physical Chemistry B, 2023, 127, 5808-5820.	2.6	1
13316	A computational study of the R120G mutation in human Î±B-crystallin: implications for structural stability and functionality. Journal of Biomolecular Structure and Dynamics, 0, , 1-11.	3.5	1
13317	The impacts of the mitochondrial myopathy-associated G58R mutation on the dynamic structural properties of CHCHD10. Journal of Biomolecular Structure and Dynamics, 0, , 1-10.	3.5	0
13318	Identification of new pentapeptides as potential inhibitors of amyloidÎ² <sub>42</sub> aggregation using virtual screening and molecular dynamics simulations. Journal of Molecular Graphics and Modelling, 2023, 124, 108558.	2.4	2
13319	Modeling competitive adsorption and diffusion of CH <sub>4</sub> /CO <sub>2</sub> mixtures confined in mature type-II kerogen: Insights from molecular dynamics simulations. Fuel, 2023, 352, 129020.	6.4	4
13321	Development of sulfate-based smart water for improving the oil recovery from the calcite formation: New insights from molecular simulation. Journal of Molecular Liquids, 2023, 386, 122409.	4.9	0
13322	Molecular Insights on the Conformational Transitions and Activity Regulation of the c-Met Kinase Induced by Ligand Binding. Journal of Chemical Information and Modeling, 2023, 63, 4147-4157.	5.4	1
13323	Synergistic effect of chlorogenic acid and vitamin D3 (cholecalciferol) on in-vitro glycation may assist in prevention of Polycystic Ovarian Syndrome (PCOS) progression - A biophysical, biochemical and in-silico study. International Journal of Biological Macromolecules, 2023, 245, 125497.	7.5	3
13324	Structure of human CALHM1 reveals key locations for channel regulation and blockade by ruthenium red. Nature Communications, 2023, 14, .	12.8	3

#	ARTICLE	IF	CITATIONS
13325	Understanding the Molecular Mechanism of Anesthesia: Effect of General Anesthetics and Structurally Similar Non-Anesthetics on the Properties of Lipid Membranes. Journal of Physical Chemistry B, 2023, 127, 6078-6090.	2.6	3
13326	A dynamic biomimetic model of the membrane-bound CD4-CD3-TCR complex during pMHC disengagement. Biophysical Journal, 2023, 122, 3133-3145.	0.5	1
13327	Kinetics and Mechanism of $\hat{\Gamma}^3\text{-Al}_{2\text{O}_3}$ Solid Phase Epitaxy on c-Plane $\langle b \rangle \hat{\Gamma}^{\pm}\text{-Al}_{2\text{O}_3}$ . Journal of Physical Chemistry C, 0, , .	3.1	0
13328	Origins of Conformational Heterogeneity in Peptoid Helices Formed by Chiral $\langle i \rangle \text{N} \langle /i \rangle$ -1-Phenylethyl Sidechains. Journal of Physical Chemistry B, 2023, 127, 6163-6170.	2.6	4
13329	Identification of novel TACE inhibitors using DNN based- virtual screening, molecular dynamics and biological evaluation. Journal of Biomolecular Structure and Dynamics, 0, , 1-12.	3.5	0
13331	T cell epitope based vaccine design while targeting outer capsid proteins of rotavirus strains infecting neonates: an immunoinformatics approach. Journal of Biomolecular Structure and Dynamics, 0, , 1-19.	3.5	1
13332	Self-Association of ACE-2 with Different RBD Amounts: A Dynamic Simulation Perspective on SARS-CoV-2 Infection. Journal of Chemical Information and Modeling, 0, , .	5.4	0
13333	Identification of Mulberrofuran as a potent inhibitor of hepatitis A virus 3Cpro and RdRP enzymes through structure-based virtual screening, dynamics simulation, and DFT studies. Molecular Diversity, 0, , .	3.9	0
13334	Origin of structural and dynamic heterogeneity in thymol and coumarin-based hydrophobic deep eutectic solvents as revealed by molecular dynamics. Physical Chemistry Chemical Physics, 2023, 25, 19693-19705.	2.8	3
13335	Direct determination of oligomeric organization of integral membrane proteins and lipids from intact customizable bilayer. Nature Methods, 2023, 20, 891-897.	19.0	14
13336	Automated relative binding free energy calculations from SMILES to $\hat{\Gamma}^{\circ}\hat{\Gamma}^{\circ}\text{G}$ . Communications Chemistry, 2023, 6, .	4.5	3
13337	Effect of coarse graining in water models for the study of kinetics and mechanisms of clathrate hydrates nucleation and growth. Journal of Chemical Physics, 2023, 158, .	3.0	2
13338	Polymeric Unimolecular CO Dehydrogenase Mimic with both Inner and Outer Spheres for Enhanced Photocatalytic $\text{CO}_{2\text{O}}$ Reduction in Aqueous Solution. Chemistry - A European Journal, 2023, 29, .	3.3	1
13339	Dissecting how ALS-associated D290V mutation enhances pathogenic aggregation of hnRNPA2286â€“291 peptides: Dynamics and conformational ensembles. International Journal of Biological Macromolecules, 2023, 241, 124659.	7.5	3
13340	Computational investigation of the impact of potential AT $\text{O}_{2\text{O}}$ R polymorphism on small molecule binding. Journal of Biomolecular Structure and Dynamics, 2024, 42, 2231-2241.	3.5	0
13341	Melting process of lead-bismuth eutectic alloy from atomistic simulation. Physica B: Condensed Matter, 2023, 662, 414934.	2.7	0
13342	Integrated Covalent Drug Design Workflow Using Site Identification by Ligand Competitive Saturation. Journal of Chemical Theory and Computation, 2023, 19, 3007-3021.	5.3	1
13343	Role of Side-Chain Lengths on Hydronium Mobility in Sulfonated Poly(ether sulfone) Proton-Conducting Model Membranes. Journal of Physical Chemistry C, 2023, 127, 8462-8472.	3.1	2

#	ARTICLE	IF	CITATIONS
13344	Molecular dynamics simulation of the inhibition mechanism of factor XIa by Milvexian-like macrocyclic inhibitors. Computational and Theoretical Chemistry, 2023, 1225, 114131.	2.5	3
13345	Naphthoquinone–dopamine hybrids disrupt A $\beta$ -synuclein fibrils by their intramolecular synergistic interactions with fibrils and display a better effect on fibril disruption. Physical Chemistry Chemical Physics, 2023, 25, 14471-14483.	2.8	3
13346	Interaction of Two Commercial Azobenzene Food Dyes, Amaranth and New Coccine, with Human Serum Albumin: Biophysical Characterization. ACS Food Science & Technology, 2023, 3, 955-968.	2.7	14
13347	Revealing the hidden dynamics of confined water in acrylate polymers: Insights from hydrogen-bond lifetime analysis. Journal of Chemical Physics, 2023, 158, .	3.0	0
13348	Dissecting the Molecular Mechanisms of the Co-Aggregation of A $\beta$ <sup>240</sup> and A $\beta$ <sup>242</sup> Peptides: A REMD Simulation Study. Journal of Physical Chemistry B, 2023, 127, 4050-4060.	2.6	6
13349	Water Influence on the Physico-Chemical Properties and 3D Printability of Choline Acrylate–Bacterial Cellulose Inks. Polymers, 2023, 15, 2156.	4.5	5
13350	The electron–proton bottleneck of photosynthetic oxygen evolution. Nature, 2023, 617, 623-628.	27.8	31
13352	The Activity of Natural Polymorphic Variants of Human DNA Polymerase $\beta$ Having an Amino Acid Substitution in the Transferase Domain. Cells, 2023, 12, 1300.	4.1	1
13353	Elucidation of the key role of isomerization in the self-assembly and luminescence properties of AIEgens. Physical Chemistry Chemical Physics, 2023, 25, 14387-14399.	2.8	2
13355	Liquid–Liquid Phase Separation Modifies the Dynamic Properties of Intrinsically Disordered Proteins. Journal of the American Chemical Society, 2023, 145, 10548-10563.	13.7	17
13356	On the Binding Mode and Molecular Mechanism of Enzymatic Polyethylene Terephthalate Degradation. ACS Catalysis, 2023, 13, 6919-6933.	11.2	8
13357	Benzo(ghi)perylene (BgP) a black tattoo ingredient induced skin toxicity via direct and indirect mode of DNA damage under UVA irradiation. Chemico-Biological Interactions, 2023, 379, 110508.	4.0	4
13358	Multifunctional magnetoliposomes as drug delivery vehicles for the potential treatment of Parkinson’s disease. Frontiers in Bioengineering and Biotechnology, 0, 11, .	4.1	2
13359	Effect of Fluorinated Carboxylic Acid Ester on Lithium Solvation as an Additive in Electrolyte and Low-Temperature Insight on Battery Performance. Industrial & Engineering Chemistry Research, 2023, 62, 7682-7692.	3.7	0
13360	A pH-dependent cluster of charges in a conserved cryptic pocket on flaviviral envelopes. ELife, 0, 12, .	6.0	1
13361	Circulating tumor DNA reveals mechanisms of lorlatinib resistance in patients with relapsed/refractory ALK-driven neuroblastoma. Nature Communications, 2023, 14, .	12.8	5
13362	A Multilevel Study of Eupatorin and Scutellarein as Anti-Amyloid Agents in Alzheimer’s Disease. Biomedicines, 2023, 11, 1357.	3.2	0
13363	Drug cross-linking electrospun fiber for effective infected wound healing. Bioengineering and Translational Medicine, 2023, 8, .	7.1	1



#	ARTICLE	IF	CITATIONS
13364	GNN-assisted phase space integration with application to atomistics. <i>Mechanics of Materials</i> , 2023, 182, 104681.	3.2	1
13365	Effects of Coulomb and vdW modifiers on hydrogen-bonds, energy and structural properties of peptide nanomembranes: A study by Molecular Dynamics simulations. <i>Journal of Molecular Liquids</i> , 2023, 382, 122017.	4.9	1
13366	Transformation of non-screw super-dislocation dipoles in M3Al (M=Ni, Fe, Ti) intermetallics: High-throughput atomistic modeling. <i>Journal of Alloys and Compounds</i> , 2023, 958, 170437.	5.5	0
13367	Inhibiting gas generation to achieve ultralong-lifespan lithium-ion batteries at low temperatures. <i>Matter</i> , 2023, 6, 2274-2292.	10.0	18
13368	High-throughput screening and molecular dynamics simulations of natural products targeting LuxS/AI-2 system as a novel antibacterial strategy for antibiotic resistance in <i>Helicobacter pylori</i> . <i>Journal of Biomolecular Structure and Dynamics</i> , 0, , 1-16.	3.5	4
13369	Bound Phospholipids Assist Cholesteryl Ester Transfer in the Cholesteryl Ester Transfer Protein. <i>Journal of Chemical Information and Modeling</i> , 2023, 63, 3054-3067.	5.4	0
13370	Structural and functional insights into the flexible $\beta$ -hairpin of glycerol dehydrogenase. <i>FEBS Journal</i> , 0, , .	4.7	0
13371	DARVIC: Dihedral angle-reliant variant impact classifier for functional prediction of missense VUS. <i>Computer Methods and Programs in Biomedicine</i> , 2023, 238, 107596.	4.7	0
13372	Signal peptide mimicry primes Sec61 for client-selective inhibition. <i>Nature Chemical Biology</i> , 2023, 19, 1054-1062.	8.0	5
13373	Molecular insights into the behavior of the allosteric and ATP-competitive inhibitors in interaction with AKT1 protein: A molecular dynamics study. <i>International Journal of Biological Macromolecules</i> , 2023, 242, 124853.	7.5	2
13374	Conformation and Affinity Modulations by Multiple Phosphorylation Occurring in the BIN1 SH3 Domain Binding Site of the Tau Protein Proline-Rich Region. <i>Biochemistry</i> , 2023, 62, 1631-1642.	2.5	0
13375	Prion Protein Octarepeat Domain Forms Transient $\beta$ -Sheet Structures upon Residue-Specific Binding to Cu(II) and Zn(II) Ions. <i>Biochemistry</i> , 2023, 62, 1689-1705.	2.5	1
13377	Extraction of natural colorants using supramolecular solvents composed of Triton X-114 and ionic liquids. <i>Separation and Purification Technology</i> , 2023, 319, 124070.	7.9	0
13378	Structure-Kinetic Relationship for Drug Design Revealed by a PLS Model with Retrosynthesis-Based Pre-Trained Molecular Representation and Molecular Dynamics Simulation. <i>ACS Omega</i> , 2023, 8, 18312-18322.	3.5	1
13379	Oligomer Dynamics of LL37 Truncated Fragments Probed by $\alpha$ -Hemolysin Pore and Molecular Simulations. <i>Small</i> , 2023, 19, .	10.0	3
13380	Highly selective preparation of N-terminus Horseradish peroxidase-DNA conjugate with fully retained enzymatic activity: HRP-DNA structure-activity relation. <i>Enzyme and Microbial Technology</i> , 2023, 168, 110257.	3.2	1
13381	Structure and sucrose binding mechanism of the plant SUC1 sucrose transporter. <i>Nature Plants</i> , 2023, 9, 938-950.	9.3	4
13382	Analysis of Testosterone Binding with Cytochrome P450 11 $\beta$ -Hydroxylase and Its Variants Through Computational Approach. <i>Re:GEN Open</i> , 2023, 3, 21-33.	0.2	0

#	ARTICLE	IF	CITATIONS
13383	A deep encoder–decoder framework for identifying distinct ligand binding pathways. <i>Journal of Chemical Physics</i> , 2023, 158, .	3.0	1
13384	Effect of pressure on the carbon dioxide hydrate–water interfacial free energy along its dissociation line. <i>Journal of Chemical Physics</i> , 2023, 158, .	3.0	0
13385	Antimicrobial activity of photosensitizers: arrangement in bacterial membrane matters. <i>Frontiers in Molecular Biosciences</i> , 0, 10, .	3.5	1
13386	Neutron scattering study of polyamorphic THF·17(H <sub>2</sub> O) – toward a generalized picture of amorphous states and structures derived from clathrate hydrates. <i>Physical Chemistry Chemical Physics</i> , 2023, 25, 14981-14991.	2.8	0
13387	Micelle kinetics of photoswitchable surfactants: Self-assembly pathways and relaxation mechanisms. <i>Journal of Colloid and Interface Science</i> , 2023, 646, 883-899.	9.4	2
13388	A matrine-based supramolecular ionic salt that enhances the water solubility, transdermal delivery, and bioactivity of salicylic acid. <i>Chemical Engineering Journal</i> , 2023, 468, 143480.	12.7	3
13389	An exa-scale high-performance molecular dynamics simulation program: MODYLAS. <i>Journal of Chemical Physics</i> , 2023, 158, .	3.0	1
13390	Simple Coacervation of Guanidinium-Containing Polymers Induced by Monovalent Salt. <i>Macromolecules</i> , 2023, 56, 3989-3999.	4.8	1
13391	Molecular Dynamics of Drying-Induced Structural Transformations in a Single Nanocellulose. <i>Small</i> , 2023, 19, .	10.0	2
13392	Role of Metal Cofactor in Enhanced Thermal Stability of Azurin. <i>Journal of Physical Chemistry B</i> , 2023, 127, 4374-4385.	2.6	2
13393	Intrinsic Disorder in $\alpha$ -Synuclein Regulates the Exocytotic Fusion Pore Transition. <i>ACS Chemical Neuroscience</i> , 2023, 14, 2049-2059.	3.5	4
13394	Antimicrobial activity of Geranyl acetate against cell wall synthesis proteins of <i>P. aeruginosa</i> and <i>S. aureus</i> using molecular docking and simulation. <i>Journal of Biomolecular Structure and Dynamics</i> , 0, , 1-21.	3.5	0
13395	Extent of N-Terminus Folding of Semenogelin 1 Cleavage Product Determines Tendency to Amyloid Formation. <i>International Journal of Molecular Sciences</i> , 2023, 24, 8949.	4.1	0
13396	Contributions of nonconventional intramolecular hydrogen bond on the bioactivity of a series of substituted 6-amino, 4-phenyl, tetrahydroquinoline derivatives. <i>Journal of Molecular Liquids</i> , 2023, 383, 122055.	4.9	0
13397	Structural rationale for boson peak in metallic glass informed by an interpretable neural network model. <i>Physical Review Research</i> , 2023, 5, .	3.6	3
13398	Localizing Oleylamine Ligands on Amine–Halide Copassivated Indium Phosphide Nanocrystals. <i>Chemistry of Materials</i> , 2023, 35, 4393-4403.	6.7	4
13399	Molecular modeling study of natural products as potential bioactive compounds against SARS-CoV-2. <i>Journal of Molecular Modeling</i> , 2023, 29, .	1.8	1
13400	Molecular basis of PIP2-dependent conformational switching of phosphorylated CD44 in binding FERM. <i>Biophysical Journal</i> , 2023, 122, 2675-2685.	0.5	2

#	ARTICLE	IF	CITATIONS
13401	Inhibitive and Destructive Mechanisms of Chronic Traumatic Encephalopathy-Related R3-R4 Tau Peptide Chains and Protofibril by Epigallocatechin Gallate: Evidence from Molecular Dynamics Simulation. ACS Chemical Neuroscience, 2023, 14, 2098-2111.	3.5	3
13402	Dynamics of upstream ESCRT organization at the HIV-1 budding site. Biophysical Journal, 2023, 122, 2655-2674.	0.5	0
13403	Identification of potent anti-fibrinolytic compounds against plasminogen and tissue-type plasminogen activator employing <i>in silico</i> approaches. Journal of Biomolecular Structure and Dynamics, 0, , 1-19.	3.5	1
13404	The structural analysis of the periplasmic domain of <i>Sinorhizobium meliloti</i> chemoreceptor <scp>McpZ</scp> reveals a novel fold and suggests a complex mechanism of transmembrane signaling. Proteins: Structure, Function and Bioinformatics, 2023, 91, 1394-1406.	2.6	1
13405	How hydrogen bond donor acceptor ratio and water content impact heterogeneity in microstructure and dynamics of N,N-diisooctylacetamide and decanol based hydrophobic deep eutectic solvent. Journal of Molecular Liquids, 2023, 385, 122127.	4.9	4
13406	Interface Adsorption versus Bulk Micellization of Surfactants: Insights from Molecular Simulations. Journal of Chemical Theory and Computation, 2024, 20, 1568-1578.	5.3	0
13407	Diffusion coefficients in binary electrolyte mixtures by dynamic light scattering and molecular dynamics simulations. Electrochimica Acta, 2023, 462, 142637.	5.2	2
13408	Comparison of force fields to study the zinc-finger containing protein NPL4, a target for disulfiram in cancer therapy. Biochimica Et Biophysica Acta - Proteins and Proteomics, 2023, 1871, 140921.	2.3	2
13409	Unveiling the multifaceted properties of a 3d covalent-organic framework: Pressure-induced phase transition, negative linear compressibility and auxeticity. Computational Materials Science, 2023, 227, 112275.	3.0	2
13410	Virtual screeningâ€‘based discovery of AI-2 quorum sensing inhibitors that interact with an allosteric hydrophobic site of LsrK and their functional evaluation. Frontiers in Chemistry, 0, 11, .	3.6	0
13412	Ubiquitination regulates ER-phagy and remodelling of endoplasmic reticulum. Nature, 2023, 618, 394-401.	27.8	26
13413	Discovery of plant-based phytochemicals effective antivirals that target the non-structural protein C of the Nipah virus through computational methods. Journal of Biomolecular Structure and Dynamics, 0, , 1-11.	3.5	1
13414	Heteromeric clusters of ubiquitinated ER-shaping proteins drive ER-phagy. Nature, 2023, 618, 402-410.	27.8	9
13415	The structural basis of the multi-step allosteric activation of Aurora B kinase. ELife, 0, 12, .	6.0	0
13416	Structural basis for water modulating RNA duplex formation in the CUG repeats of myotonic dystrophy type 1. Journal of Biological Chemistry, 2023, 299, 104864.	3.4	0
13417	Two modes of fusogenic action for influenza virus fusion peptide. PLoS Computational Biology, 2023, 19, e1011174.	3.2	1
13418	The Effect of Oxygen Vacancies on the Diffusion Characteristics of Zn(II) Ions in the Perovskite SrTiO3 Layer: A Computational Study. Materials, 2023, 16, 3957.	2.9	1
13419	<i>In silico</i> and POM analysis for potential antimicrobial agents of thymidine analogs by using molecular docking, molecular dynamics and ADMET profiling. Nucleosides, Nucleotides and Nucleic Acids, 2023, 42, 877-918.	1.1	5

#	ARTICLE	IF	CITATIONS
13420	Computational and experimental validation of phthalocyanine and hypericin as effective SARS-CoV-2 fusion inhibitors. <i>Journal of Biomolecular Structure and Dynamics</i> , 0, , 1-15.	3.5	0
13421	Molecular Dynamics Simulations of HPr Proteins from a Thermophilic and a Mesophilic Organism: A Comparative Thermal Study. <i>International Journal of Molecular Sciences</i> , 2023, 24, 9557.	4.1	0
13422	Study of Speciation and Transport Properties for Different Compositions of Carbonates in $\text{Li}_{2\text{CO}_3}$ and $\text{Li}_2\text{CO}_3$ Binary Systems at High Temperature in Molten State. <i>Journal of Physical Chemistry C</i> , 2023, 127, 11186-11194.	3.1	1
13423	Hydrostatic pressure-induced transition in grain boundary segregation tendency in nanocrystalline metals. <i>Scripta Materialia</i> , 2023, 234, 115576.	5.2	1
13424	Conformational dynamics and mechanical properties of biomimetic RNA, DNA, and RNA-DNA hybrid nanotubes: an atomistic molecular dynamics study. <i>Physical Chemistry Chemical Physics</i> , 2023, 25, 16527-16549.	2.8	0
13425	Electric field-induced deformation and breakup of water droplets in polymer-flooding W/O emulsions: A simulation study. <i>Separation and Purification Technology</i> , 2023, 320, 124237.	7.9	3
13426	Destabilization mechanism of R3-R4 tau protofilament by purpurin: a molecular dynamics study. <i>Physical Chemistry Chemical Physics</i> , 2023, 25, 16856-16865.	2.8	1
13428	The dynamics of agonist- $\beta_2$ -adrenergic receptor activation induced by binding of GDP-bound Gs protein. <i>Nature Chemistry</i> , 2023, 15, 1127-1137.	13.6	3
13429	Revealing the key structural characteristics governing the glass forming ability in $\text{Ca}_{50}\text{Mg}_{50-x}\text{Zn}_x$ alloys. <i>Journal of Non-Crystalline Solids</i> , 2023, 616, 122442.	3.1	0
13430	Archaeal Hel308 suppresses recombination through a catalytic switch that controls DNA annealing. <i>Nucleic Acids Research</i> , 2023, 51, 8563-8574.	14.5	1
13431	Dynamic Solution Structures of Whole Human NAP1 Dimer Bound to One and Two Histone H2A-H2B Heterodimers Obtained by Integrative Methods. <i>Journal of Molecular Biology</i> , 2023, 435, 168189.	4.2	1
13433	Histidine Protonation and Conformational Switching in Diphtheria Toxin Translocation Domain. <i>Toxins</i> , 2023, 15, 410.	3.4	0
13434	A $\beta$ -( <i>Euterpe oleracea</i> Mart.) Seed Oil Exerts a Cytotoxic Role over Colorectal Cancer Cells: Insights of Annexin A2 Regulation and Molecular Modeling. <i>Metabolites</i> , 2023, 13, 789.	2.9	1
13435	Probing the Conformational Preference to $\beta$ -Strand during Peptide Self-Assembly. <i>Journal of Physical Chemistry B</i> , 2023, 127, 5821-5836.	2.6	0
13436	Design of a Synthetic Long Peptide Vaccine Targeting HPV-16 and -18 Using Immunoinformatic Methods. <i>Pharmaceutics</i> , 2023, 15, 1798.	4.5	2
13437	Molecular Dynamics of Carbon Sequestration via Forming $\text{CO}_2$ Hydrate in a Marine Environment. <i>Energy &amp; Fuels</i> , 2023, 37, 9309-9317.	5.1	0
13438	Effect of oxidation on POPC lipid bilayers: anionic carboxyl group plays a major role. <i>Physical Chemistry Chemical Physics</i> , 2023, 25, 18310-18321.	2.8	0
13439	Targeting DPP4-RBD interactions by sitagliptin and linagliptin delivers a potential host-directed therapy against pan-SARS-CoV-2 infections. <i>International Journal of Biological Macromolecules</i> , 2023, 245, 125444.	7.5	0

#	ARTICLE	IF	CITATIONS
13440	Interaction of Terahertz Waves with the RNA Hairpin. , 2023, , .		0
13441	Temperature-Derived Purification of Gold Nano-Bipyramids for Colorimetric Detection of Tannic Acid. ACS Applied Nano Materials, 2023, 6, 11572-11580.	5.0	2
13442	Structure-based virtual screening, molecular docking, and molecular dynamics simulation approaches for identification of new potential inhibitors of class a Î²-lactamase enzymes. Journal of Biomolecular Structure and Dynamics, 0, , 1-11.	3.5	0
13443	Conformational dynamics of complement protease C1r inhibitor proteins from Lyme diseaseâ€œcausing spirochetes. Journal of Biological Chemistry, 2023, 299, 104972.	3.4	1
13444	Characterizing Surface Ice-Philicity Using Molecular Simulations and Enhanced Sampling. Journal of Physical Chemistry B, 2023, 127, 6125-6135.	2.6	0
13445	The origin of deformation induced topological anisotropy in silica glass. Acta Materialia, 2023, 257, 119108.	7.9	3
13446	Molecular Dynamics Simulations Elucidate the Molecular Basis of Pre-mRNA Translocation by the Prp2 Spliceosomal Helicase. Journal of Chemical Information and Modeling, 2023, 63, 4180-4189.	5.4	2
13447	Approach to hyperuniformity in a metallic glass-forming material exhibiting a fragile to strong glass transition. European Physical Journal E, 2023, 46, .	1.6	4
13448	Molecular Dynamics Study of the Effect of Charge and Glycosyl on Superoxide Anion Distribution near Lipid Membrane. International Journal of Molecular Sciences, 2023, 24, 10926.	4.1	0
13449	Pyrazolo[4,3-e]tetrazolo[1,5-b][1,2,4]triazine Sulfonamides as an Important Scaffold for Anticancer Drug Discoveryâ€œIn Vitro and In Silico Evaluation. International Journal of Molecular Sciences, 2023, 24, 10959.	4.1	2
13450	Combining Molecular Dynamics Simulations and Biophysical Characterization to Investigate Protein-Specific Excipient Effects on Reteplase during Freeze Drying. Pharmaceutics, 2023, 15, 1854.	4.5	0
13451	Viscoelasticity. Lecture Notes in Physics, 2023, , 119-152.	0.7	0
13452	Interaction of Near-Infrared (NIR)-Light Responsive Probes with Lipid Membranes: A Combined Simulation and Experimental Study. Pharmaceutics, 2023, 15, 1853.	4.5	0
13453	Toward a Molecular Mechanism of Complementary RNA Duplexes Denaturation. Journal of Physical Chemistry B, 2023, 127, 6015-6028.	2.6	3
13454	Dispersion-corrected DFT calculations and umbrella sampling simulations to investigate stability of Chrysin-cyclodextrin inclusion complexes. Carbohydrate Polymers, 2023, 319, 121162.	10.2	9
13455	Evolution of the hydrogen-bonded network in methanol-water mixtures upon cooling. Journal of Molecular Liquids, 2023, 386, 122494.	4.9	1
13456	Structural displacement model of chitooligosaccharide transport through chitoporin. Journal of Biological Chemistry, 2023, 299, 105000.	3.4	0
13458	Condensed-Phase Molecular Representation to Link Structure and Thermodynamics in Molecular Dynamics. Journal of Chemical Theory and Computation, 2023, 19, 4770-4779.	5.3	0

#	ARTICLE	IF	CITATIONS
13461	Arginine Residues Modulate the Membrane Interactions of pHLIP Peptides. Journal of Chemical Information and Modeling, 2023, 63, 4433-4446.	5.4	2
13462	The Effect of Mechanical Elongation on the Thermal Conductivity of Amorphous and Semicrystalline Thermoplastic Polyimides: Atomistic Simulations. Polymers, 2023, 15, 2926.	4.5	3
13463	Synthesis of a glycan hairpin. Nature Chemistry, 2023, 15, 1461-1469.	13.6	6
13464	Umbelliferone modulates the quorum sensing and biofilm of Gram <sup>+</sup> bacteria: <i>in vitro</i> and <i>in silico</i> investigations. Journal of Biomolecular Structure and Dynamics, 0, , 1-14.	3.5	5
13465	Rigidity and Flexibility: Unraveling the Role of Fulvic Acid in Uranyl Sorption on Graphene Oxide Using Molecular Dynamics Simulations. Environmental Science & Technology, 2023, 57, 10339-10347.	10.0	2
13466	Engineered vitamin E-tethered non-immunogenic facial lipopeptide for developing improved siRNA based combination therapy against metastatic breast cancer. Chemical Science, 2023, 14, 7842-7866.	7.4	3
13467	<i>In vitro</i> interactions of esculin and esculetin with bovine hemoglobin alter its structure and inhibit aggregation: insights from spectroscopic and computational studies. New Journal of Chemistry, 0, , .	2.8	1
13468	Unravel the Tangle: Atomistic Insight into Ultrahigh Curcumin <sup>-</sup> Loaded Polymer Micelles. Small, 2023, 19, .	10.0	0
13469	Reconstructing the transport cycle in the sugar porter superfamily using coevolution-powered machine learning. ELife, 0, 12, .	6.0	6
13470	Interfacial structure of protic and aprotic ionic liquid-DMSO-Li salt mixtures near charged and neutral electrodes: A Molecular Dynamics study. Journal of Molecular Liquids, 2023, 386, 122492.	4.9	1
13472	Non-equilibrium transport of nanoparticles across the lipid membrane. Nanoscale, 2023, 15, 12307-12318.	5.6	1
13473	Conformational response to ligand binding of TMPRSS2, a protease involved in SARS-CoV-2 infection: Insights through computational modeling. Proteins: Structure, Function and Bioinformatics, 2023, 91, 1288-1297.	2.6	0
13474	Gefitinib derivatives and drug-resistance: A perspective from molecular dynamics simulations. Computers in Biology and Medicine, 2023, 163, 107204.	7.0	0
13475	Exploring the Anticancer Activity of Tamoxifen-Based Metal Complexes Targeting Mitochondria. Journal of Medicinal Chemistry, 2023, 66, 9823-9841.	6.4	6
13476	What Can We Learn about PEDOT:PSS Morphology from Molecular Dynamics Simulations of Ionic Diffusion?. Chemistry of Materials, 2023, 35, 5512-5523.	6.7	1
13477	SARS-COV-2 spike protein fragment eases amyloidogenesis of $\beta$ -synuclein. Journal of Chemical Physics, 2023, 159, .	3.0	2
13478	Heterogenised catalysts for the H-transfer reduction reaction of aldehydes: influence of solvent and solvation effects on reaction performances. Physical Chemistry Chemical Physics, 2023, 25, 21416-21427.	2.8	1
13480	Anharmonicity and the emergence of diffusive behavior in a lattice-solute model solid-state electrolyte. Computational Materials Science, 2023, 228, 112359.	3.0	0



#	ARTICLE	IF	CITATIONS
13481	Structural determinants underlying high-temperature adaptation of thermophilic xylanase from hot-spring microorganisms. <i>Frontiers in Microbiology</i> , 0, 14, .	3.5	0
13482	Lateral membrane organization as target of an antimicrobial peptidomimetic compound. <i>Nature Communications</i> , 2023, 14, .	12.8	3
13483	Microscopic understanding of the supramolecular interaction in enhanced oil recovery. <i>Journal of Molecular Liquids</i> , 2023, 386, 122546.	4.9	2
13484	Identification of a new Kir6 potassium channel and comparison of properties of Kir6 subtypes by structural modelling and molecular dynamics. <i>International Journal of Biological Macromolecules</i> , 2023, 247, 125771.	7.5	0
13485	Accurate modelling of pyrrolidinium ionic liquids with charge and vdW scaling. <i>Journal of Molecular Liquids</i> , 2023, 386, 122541.	4.9	0
13486	AL4GAP: Active learning workflow for generating DFT-SCAN accurate machine-learning potentials for combinatorial molten salt mixtures. <i>Journal of Chemical Physics</i> , 2023, 159, .	3.0	0
13487	Examining sialic acid derivatives as potential inhibitors of SARS-CoV-2 spike protein receptor binding domain. <i>Journal of Biomolecular Structure and Dynamics</i> , 0, , 1-17.	3.5	1
13489	Analytic elastic coefficients in molecular calculations: Finite strain, nonaffine displacements, and many-body interatomic potentials. <i>Physical Review Materials</i> , 2023, 7, .	2.4	1
13490	Effect of Isomeric Alcohols on the Thermophysical Properties of Cyano-Based Ionic Liquids: Experimental and Simulation Studies. <i>Journal of Chemical &amp; Engineering Data</i> , 0, , .	1.9	0
13491	Aggregation patterns of curcumin and piperine mixtures in different polar media. <i>Physical Chemistry Chemical Physics</i> , 2023, 25, 19899-19910.	2.8	0
13492	Structural Origins of Viscosity in Imidazolium and Pyrrolidinium Ionic Liquids Coupled with the NTf <sub>2</sub> <sup>+</sup> Anion. <i>Journal of Physical Chemistry B</i> , 2023, 127, 6342-6353.	2.6	3
13493	Toward a general neural network force field for protein simulations: Refining the intramolecular interaction in protein. <i>Journal of Chemical Physics</i> , 2023, 159, .	3.0	3
13494	Combining Experiments and Simulations to Examine the Temperature-Dependent Behavior of a Disordered Protein. <i>Journal of Physical Chemistry B</i> , 2023, 127, 6277-6286.	2.6	1
13495	SNAP25 disease mutations change the energy landscape for synaptic exocytosis due to aberrant SNARE interactions. <i>ELife</i> , 0, 12, .	6.0	1
13496	Peptide ligands for the affinity purification of adeno-associated viruses from HEK 293 cell lysates. <i>Biotechnology and Bioengineering</i> , 2023, 120, 2283-2300.	3.3	2
13498	Mechanistic Investigation of <i>tert</i> -Butanol's Impact on Biopharmaceutical Formulations: When Experiments Meet Molecular Dynamics. <i>Molecular Pharmaceutics</i> , 0, , .	4.6	1
13500	Introduction of constrained Trp analogs in RW9 modulates structure and partition in membrane models. <i>Bioorganic Chemistry</i> , 2023, 139, 106731.	4.1	0
13501	PLSCR1 is a cell-autonomous defence factor against SARS-CoV-2 infection. <i>Nature</i> , 2023, 619, 819-827.	27.8	7

#	ARTICLE	IF	CITATIONS
13503	Validity of the Onsagerâ€“Glarum relationship in a molecular coulomb fluid: investigation <i>via</i> temperature-dependent molecular dynamics simulations of a representative ionic liquid, [BMIM][PF <sub>6</sub> ]. New Journal of Chemistry, 0, , .	2.8	0
13504	Synergistic Inhibitory Effect of Quercetin and Cyanidin-3O-Sophoroside on ABCB1. International Journal of Molecular Sciences, 2023, 24, 11341.	4.1	0
13505	Strain Anisotropy Driven Spontaneous Formation of Nanoscrolls from 2D Janus Layers. Advanced Functional Materials, 2023, 33, .	14.9	2
13506	Clustering molecular dynamics conformations of the CCâ€™-loop of the PD-1 immuno-checkpoint receptor. Computational and Structural Biotechnology Journal, 2023, 21, 3920-3932.	4.1	0
13507	SARS-CoV-2 main protease cleaves MAGED2 to antagonize host antiviral defense. MBio, 0, , .	4.1	1
13508	Crosstalk between regulatory elements in disordered TRPV4 N-terminus modulates lipid-dependent channel activity. Nature Communications, 2023, 14, .	12.8	10
13509	Unveiling the Influence of Hydrated Deep Eutectic Solvents on the Dynamics of Waterâ€“Soluble Proteins. Journal of Physical Chemistry B, 2023, 127, 6487-6499.	2.6	4
13512	Structural and Transport Properties of Norbornene-Functionalized Poly(vinyl alcohol) â€“Clickâ€“Hydrogel: A Molecular Dynamics Study. ACS Sustainable Chemistry and Engineering, 2023, 11, 10812-10824.	6.7	0
13513	Development, validation and analysis of a human profurin 3D model using comparative modeling and molecular dynamics simulations. Journal of Biomolecular Structure and Dynamics, 0, , 1-19.	3.5	0
13514	Protein-Mediated Electroporation in a Cardiac Voltage-Sensing Domain Due to an nsPEF Stimulus. International Journal of Molecular Sciences, 2023, 24, 11397.	4.1	0
13515	NH <sub>3</sub> production from absorbed NO with synergistic catalysis of Pd/C and functionalized ionic liquids. Green Chemistry, 0, , .	9.0	0
13516	Individual Contributions of Amido Acid Residues Tyr122, Ile168, and Asp173 to the Activity and Substrate Specificity of Human DNA Dioxygenase ABH2. Cells, 2023, 12, 1839.	4.1	0
13517	Relaxation dynamics of water in the vicinity of cellulose nanocrystals. Cellulose, 2023, 30, 8051-8061.	4.9	0
13518	Exploring the 1,3-benzoxazine chemotype for cannabinoid receptor 2 as a promising anti-cancer therapeutic. European Journal of Medicinal Chemistry, 2023, 259, 115647.	5.5	3
13519	Investigation of the therapeutic role of native plant compounds against colorectal cancer based on system biology and virtual screening. Scientific Reports, 2023, 13, .	3.3	1
13520	pH-dependence of the Plasmodium falciparum chloroquine resistance transporter is linked to the transport cycle. Nature Communications, 2023, 14, .	12.8	0
13521	Effect of preprocessing and simulation parameters on the performance of molecular docking studies. Journal of Molecular Modeling, 2023, 29, .	1.8	1
13522	Self-diffusion of aromatic compounds in the carbon tetrachloride â€“ acetone binary system. NMR experiment and MD simulation. Journal of Molecular Liquids, 2023, 387, 122604.	4.9	0

#	ARTICLE	IF	CITATIONS
13523	Proteinâ€‘protein association properties of human <sc>Î²2</sc>â€‘crystallins. Proteins: Structure, Function and Bioinformatics, 0, , .	2.6	0
13524	Anisotropic Collective Variables with Machine Learning Potential for <i>Ab Initio</i> Crystallization of Complex Ceramics. ACS Nano, 2023, 17, 14099-14113.	14.6	1
13525	Conformational variation of site specific glycated albumin: A Molecular dynamics approach. Computers in Biology and Medicine, 2023, 164, 107276.	7.0	2
13527	Structure and interaction of therapeutic proteins in solution: a combined simulation and experimental study. Molecular Physics, 2023, 121, .	1.7	2
13528	Complexity of Guanine Quadruplex Unfolding Pathways Revealed by Atomistic Pulling Simulations. Journal of Chemical Information and Modeling, 2023, 63, 4716-4731.	5.4	1
13532	Allosteric activation of vinculin by talin. Nature Communications, 2023, 14, .	12.8	5
13533	The role of electrostatic potential in the translocation of triangulene across membranes. RSC Advances, 2023, 13, 21545-21549.	3.6	0
13534	Probing the influence of defects and Si-doping in graphene sheet as an efficacious carrier for drug delivery system in gas and aqua phases - Combined DFT and classical MD simulation. Journal of Physics and Chemistry of Solids, 2023, 181, 111562.	4.0	2
13535	Repurposing Anti-Dengue Compounds against Monkeypox Virus Targeting Core Cysteine Protease. Biomedicines, 2023, 11, 2025.	3.2	2
13536	Multiepitope glycan based laser assisted fluorescent nanocomposite with dual functionality for sensing and ablation of Pseudomonas aeruginosa. Nanoscale, 0, , .	5.6	1
13537	Human aromatic amino acid decarboxylase is an asymmetric and flexible enzyme: implication in <sc>AADC</sc> deficiency. Protein Science, 0, , .	7.6	1
13538	Thermodynamic Modeling and Experimental Data Reveal That Sugars Stabilize Proteins According to an Excluded Volume Mechanism. Journal of the American Chemical Society, 2023, 145, 16678-16690.	13.7	2
13539	Extreme dynamics in a biomolecular condensate. Nature, 2023, 619, 876-883.	27.8	42
13540	Molecular dynamics simulations identify the topological weak spots of a protease CN2S8A. Journal of Molecular Graphics and Modelling, 2023, 124, 108571.	2.4	0
13541	Short hydrocarbon stapled ApoC2-mimetic peptides activate lipoprotein lipase and lower plasma triglycerides in mice. Frontiers in Cardiovascular Medicine, 0, 10, .	2.4	1
13542	Molecular Dynamics in various ensembles. , 2023, , 233-260.		0
13544	<i>In silico</i> exploration of promising heterocyclic molecules against both acetylcholinesterase and butyrylcholinesterase enzymes. Journal of Biomolecular Structure and Dynamics, 0, , 1-22.	3.5	0
13545	Unravelling the structural and dynamical properties of concentrated aqueous ammonium nitrate solutions: MD simulation studies. Molecular Simulation, 2023, 49, 1413-1430.	2.0	1

#	ARTICLE	IF	CITATIONS
13547	Does supercooled water retain its universal nucleation behavior under shear at high pressure?. Physical Chemistry Chemical Physics, 0, , .	2.8	1
13548	Decoupling of Interactions between Model-Charged Peptides Reveals Key Factors Responsible for Liquid-Liquid Phase Separation. Journal of Physical Chemistry B, 0, , .	2.6	0
13549	Synthesis and thermophysical property determination of NaCl-PuCl <sub>3</sub> salts. Journal of Molecular Liquids, 2023, 387, 122636.	4.9	2
13551	Computational prediction of phytochemical inhibitors against the cap-binding domain of Rift Valley fever virus. Molecular Diversity, 0, , .	3.9	0
13553	Deciphering the role of fucoidan from brown macroalgae in inhibiting SARS-CoV-2 by targeting its main protease and receptor binding domain: Invitro and insilico approach. International Journal of Biological Macromolecules, 2023, 248, 125950.	7.5	2
13554	Adsorption/Desorption of Cationic-Hydrophobic Peptides on Zwitterionic Lipid Bilayer Is Associated with the Possibility of Proton Transfer. Antibiotics, 2023, 12, 1216.	3.7	1
13555	Atomistic characterization of multi nano-crystal formation process in Fe-Cr-Ni alloy during directional solidification: Perspective to the additive manufacturing. Materials Chemistry and Physics, 2023, 308, 128242.	4.0	4
13556	The effect of chemical constitution on polyisoprene dynamics. Journal of Chemical Physics, 2023, 159, .	3.0	1
13557	E46K Mutation of $\beta$ -Synuclein Preorganizes the Intramolecular Interactions Crucial for Aggregation. Journal of Chemical Information and Modeling, 0, , .	5.4	0
13558	Expulsion mechanism of the substrate-translocating subunit in ECF transporters. Nature Communications, 2023, 14, .	12.8	3
13559	Efficient variable cell shape geometry optimization. Journal of Computational Physics: X, 2023, 17, 100131.	0.7	1
13560	Structural basis of human Slo2.2 channel gating and modulation. Cell Reports, 2023, 42, 112858.	6.4	1
13561	A FRET-Based Assay for the Identification of PCNA Inhibitors. International Journal of Molecular Sciences, 2023, 24, 11858.	4.1	0
13562	Discovery of novel $\alpha$ -TRPV1 modulators through machine learning-based molecular docking and molecular similarity searching. Chemical Biology and Drug Design, 2023, 102, 409-423.	3.2	0
13563	Drastic differences between the release kinetics of two highly related porphyrins in liposomal membranes: mTHPP and pTHPP. Journal of Colloid and Interface Science, 2023, 651, 750-759.	9.4	0
13564	Densest-known packings and phase behavior of hard spherical capsids. Journal of Chemical Physics, 2023, 159, .	3.0	2
13566	Phase Behaviors of Dialkyldimethylammonium Bromide Bilayers. Langmuir, 0, , .	3.5	0
13567	Solvation thermodynamics from cavity shapes of amino acids. , 2023, 2, .		1

#	ARTICLE	IF	CITATIONS
13568	Insights into the Interaction Mechanism of Boceprevir with SARS-CoV-2 Main Protease. <i>ChemistrySelect</i> , 2023, 8, .	1.5	0
13570	Prediction of Superionic State in $\text{LiH}_{2\text{O}}$ at Conditions Enroute to Nuclear Fusion. <i>Chinese Physics B</i> , 0, , .	1.4	0
13571	Effective Interactions between Double-Stranded DNA Molecules in Aqueous Electrolyte Solutions: Effects of Molecular Architecture and Counterion Valency. <i>Journal of Physical Chemistry B</i> , 2023, 127, 6969-6981.	2.6	2
13573	How the Temperature and Composition Govern the Structure and Band Gap of Zr-Based Chalcogenide Perovskites: Insights from ML Accelerated AIMD. <i>Inorganic Chemistry</i> , 2023, 62, 12480-12492.	4.0	1
13574	P176S Mutation Rewires Electrostatic Interactions That Alter Maspin Functionality. <i>ACS Omega</i> , 0, , .	3.5	0
13575	Morphological Changes of Polymer-Grafted Nanocellulose during a Drying Process. <i>Biomacromolecules</i> , 0, , .	5.4	0
13576	Binding characteristics and conformational changes in alpha-2-macroglobulin by the dietary flavanone naringenin: biophysical and computational approach. <i>Journal of Biomolecular Structure and Dynamics</i> , 0, , 1-16.	3.5	0
13577	Computational Framework Combining Quantum Mechanics, Molecular Dynamics, and Deep Neural Networks to Evaluate the Intrinsic Properties of Materials. <i>Journal of Physical Chemistry A</i> , 2023, 127, 6603-6613.	2.5	1
13578	Ion selectivity and rotor coupling of the <i>Vibrio</i> flagellar sodium-driven stator unit. <i>Nature Communications</i> , 2023, 14, .	12.8	6
13579	Theoretical verification on adsorptive removal of caffeine by carbon and nitrogen-based surfaces: Role of charge transfer, $\pi$ electron occupancy, and temperature. <i>Chemosphere</i> , 2023, 339, 139667.	8.2	2
13580	Alkali metal cations modulate the geometry of different binding sites in HCN4 selectivity filter for permeation or block. <i>Journal of General Physiology</i> , 2023, 155, .	1.9	0
13582	Axial Diffusion in Liquid-Saturated Cylindrical Silica Pore Models. <i>Journal of Physical Chemistry C</i> , 2023, 127, 14374-14388.	3.1	0
13583	Essence into the kinetic enhanced extraction induced by Marangoni convection on the surface of freely rising oil droplets. <i>Chemical Engineering Science</i> , 2023, 281, 119101.	3.8	0
13584	Lipid exchange in crystal-confined fatty acid binding proteins: X-ray evidence and molecular dynamics explanation. <i>Proteins: Structure, Function and Bioinformatics</i> , 2023, 91, 1525-1534.	2.6	0
13586	Computation of Electrical Conductivities of Aqueous Electrolyte Solutions: Two Surfaces, One Property. <i>Journal of Chemical Theory and Computation</i> , 2023, 19, 5380-5393.	5.3	5
13587	ãfãf²ã,ãfãf¬ãf³ã«ãšãä,«æ™,é–“â€“æ,©ã° æ•ç®—ã%ãã°ç¾4è±ã®èš£æ~Ž. <i>Journal of the Japan Society for Composite Materials</i> , 2023, 53, 1-10.	0.1	0
13588	Strategy for building training set for neural-network potentials for ionic diffusion in solids: example for hydride-ion diffusion in LaHO. <i>Science and Technology of Advanced Materials Methods</i> , 2023, 3, .	1.3	1
13589	Reconstruction of the unbinding pathways of new inhibitors of the SARS-CoV-2 papain-like protease using molecular dynamics simulation. <i>Journal of Biomolecular Structure and Dynamics</i> , 0, , 1-14.	3.5	0

#	ARTICLE	IF	CITATIONS
13590	A single antiviral for a triple epidemic: is it possible?. <i>Future Virology</i> , 2023, 18, 633-642.	1.8	0
13591	Pathway selectivity in Frizzleds is achieved by conserved micro-switches defining pathway-determining, active conformations. <i>Nature Communications</i> , 2023, 14, .	12.8	2
13592	Wetting of native and acetylated cellulose by water and organic liquids from atomistic simulations. <i>Cellulose</i> , 2023, 30, 8089-8106.	4.9	1
13593	Frequency-Selective Anharmonic Mode Analysis of Thermally Excited Vibrations in Proteins. <i>Journal of Chemical Theory and Computation</i> , 2023, 19, 5481-5490.	5.3	2
13594	AI-based AlphaFold2 significantly expands the structural space of the autophagy pathway. <i>Autophagy</i> , 0, , 1-20.	9.1	0
13595	A Comprehensive Study on the Binding of Anti-cancer Drug (Floxuridine) with Human Serum Albumin. , 2023, 47, 1155-1167.		1
13596	Melting of atomic materials under high pressures using computer simulations. <i>Advances in Physics: X</i> , 2023, 8, .	4.1	0
13597	Comparison and Possible Binding Orientations of SARS-CoV-2 Spike N-Terminal Domain for Gangliosides GM3 and GM1. <i>Journal of Physical Chemistry B</i> , 2023, 127, 6940-6948.	2.6	0
13598	Side Groups Convert the Î±7 Nicotinic Receptor Agonist Ether Quinuclidine into a Type I Positive Allosteric Modulator. <i>ACS Chemical Neuroscience</i> , 2023, 14, 2876-2887.	3.5	0
13599	Chloride Insertion Enhances the Electrochemical Oxidation of Iron Hydroxide Double-Layer Hydroxide into Oxyhydroxide in Alkaline Iron Batteries. <i>Chemistry of Materials</i> , 2023, 35, 6517-6526.	6.7	1
13600	Conformation and hydration property of low-acetyl gellan gum under microwave irradiation: Experiments and molecular dynamics simulations. <i>Food Hydrocolloids</i> , 2023, 145, 109140.	10.7	4
13603	Nature of the Amorphousâ€“Amorphous Interfaces in Solid-State Batteries Revealed Using Machine-Learned Interatomic Potentials. <i>Chemistry of Materials</i> , 2023, 35, 6346-6356.	6.7	1
13604	Influence of dexamethasone on the interaction between glucocorticoid receptor and SOX9: A molecular dynamics study. <i>Journal of Molecular Graphics and Modelling</i> , 2023, 125, 108587.	2.4	0
13605	Effects of surfactant with different injection times on asphaltene adsorption behaviors on the kaolinite surfaces: A molecular simulation study. <i>Applied Surface Science</i> , 2023, 639, 158167.	6.1	1
13607	Nucleosideâ€“Driven Specificity of DNA Methyltransferase**. <i>ChemBioChem</i> , 2023, 24, .	2.6	1
13609	Uracil/H+ Symport by FurE Refines Aspects of the Rocking-bundle Mechanism of APC-type Transporters. <i>Journal of Molecular Biology</i> , 2023, 435, 168226.	4.2	1
13610	Insights into the self-assembly of water reverse micelles and solubilization process in liquid and supercritical solvents: A molecular dynamics study. <i>Colloids and Surfaces A: Physicochemical and Engineering Aspects</i> , 2023, 676, 132200.	4.7	0
13611	Structural insights into anion selectivity and activation mechanism of LRRC8 volume-regulated anion channels. <i>Cell Reports</i> , 2023, 42, 112926.	6.4	2



#	ARTICLE	IF	CITATIONS
13612	Ion clustering, aggregation and diffusion in amide based deep eutectic solvents: A microstructural investigation using various NMR spectroscopic techniques and molecular dynamics simulation. Journal of Molecular Liquids, 2023, 388, 122761.	4.9	0
13613	Effect of static electric fields on liquid water, its structure, dynamics, and hydrogen bond asymmetry: A molecular dynamics simulation study of TIP4P/2005 water model. Journal of Chemical Physics, 2023, 159, .	3.0	2
13614	Structural conservation of antibiotic interaction with ribosomes. Nature Structural and Molecular Biology, 2023, 30, 1380-1392.	8.2	8
13615	Optimal Reaction Coordinates and Kinetic Rates from the Projected Dynamics of Transition Paths. Journal of Chemical Theory and Computation, 2023, 19, 5701-5711.	5.3	3
13616	Non-Markov models of single-molecule dynamics from information-theoretical analysis of trajectories. Journal of Chemical Physics, 2023, 159, .	3.0	0
13617	Host Dynamics under General-Purpose Force Fields. Molecules, 2023, 28, 5940.	3.8	1
13618	Growth rate of CO <sub>2</sub> and CH <sub>4</sub> hydrates by means of molecular dynamics simulations. Journal of Chemical Physics, 2023, 159, .	3.0	2
13619	Structure and Dynamics of a Polybutadiene Melt Confined between Alumina Substrates. Macromolecules, 2023, 56, 6552-6564.	4.8	2
13620	A Hairpin Motif in the Amyloid- $\beta$ Peptide Is Important for Formation of Disease-Related Oligomers. Journal of the American Chemical Society, 2023, 145, 18340-18354.	13.7	12
13621	The protease associated (PA) domain in ScpA from Streptococcus pyogenes plays a role in substrate recruitment. Biochimica Et Biophysica Acta - Proteins and Proteomics, 2023, 1871, 140946.	2.3	2
13622	Coarse-Grained Molecular Dynamics Simulation of Thermostable Starch Branching Enzyme. , 2023, , .		0
13623	Disorder enhanced dynamical heterogeneity in strain glass alloys. Journal of Physics Condensed Matter, 2023, 35, 465402.	1.8	0
13624	Model-Dependent Solvation of the K-18 Domain of the Intrinsically Disordered Protein Tau. Journal of Physical Chemistry B, 2023, 127, 7220-7230.	2.6	0
13625	Ensemble-based virtual screening of African natural products to target human thymidylate synthase. Journal of Molecular Graphics and Modelling, 2023, 125, 108568.	2.4	0
13626	Molecular Simulations of Understanding Separation of Cadmium and Lead Ions from Aqueous Waste Water Using Directional Solvent Extraction. Industrial & Engineering Chemistry Research, 2023, 62, 13096-13106.	3.7	0
13627	An anchorâ€‘tether â€‘hinderedâ€‘™ HCN1 inhibitor is antihyperalgesic in a rat spared nerve injury neuropathic pain model. British Journal of Anaesthesia, 2023, , .	3.4	0
13628	Converging PMF Calculations of Antibiotic Permeation across an Outer Membrane Porin with Subkilocalorie per Mole Accuracy. Journal of Chemical Information and Modeling, 2023, 63, 5319-5330.	5.4	1
13629	Terahertz waves regulate the mechanical unfolding of tau pre-mRNA hairpins. IScience, 2023, 26, 107572.	4.1	1

#	ARTICLE	IF	CITATIONS
13630	Assessing the Performance of Non-Equilibrium Thermodynamic Integration in Flavodoxin Redox Potential Estimation. <i>Molecules</i> , 2023, 28, 6016.	3.8	0
13631	A molecular simulation study of ethoxylated surfactant effects on bulk and water/crude-oil interfacial asphaltenes. <i>Fluid Phase Equilibria</i> , 2023, 575, 113925.	2.5	2
13632	Membrane Domain Anti-Registration Induces an Intrinsic Transmembrane Potential. <i>Langmuir</i> , 2023, 39, 11621-11627.	3.5	0
13633	Probing the coalescence mechanism of water droplet and Oil/Water interface in demulsification process under DC electric field. <i>Separation and Purification Technology</i> , 2023, 326, 124798.	7.9	3
13635	Thiadiazine-thiones as inhibitors of leishmania pteridine reductase (PTR1) target: investigations and in silico approach. <i>Journal of Biomolecular Structure and Dynamics</i> , 0, , 1-10.	3.5	2
13636	Computational insights into the role of structurally diverse plant secondary metabolites as inhibitors against Imidazole Glycerol Phosphate Dehydratase of <i>Mycobacterium tuberculosis</i> . <i>Journal of Biomolecular Structure and Dynamics</i> , 0, , 1-13.	3.5	0
13638	Structural insights on the deformations induced by various mutations on cholesteryl ester transfer protein. <i>Biophysical Chemistry</i> , 2023, 301, 107093.	2.8	0
13639	Cheminformatics Strategies Unlock Marburg Virus VP35 Inhibitors from Natural Compound Library. <i>Viruses</i> , 2023, 15, 1739.	3.3	7
13640	Designing of neoepitopes based vaccine against breast cancer using integrated immuno and bioinformatics approach. <i>Journal of Biomolecular Structure and Dynamics</i> , 0, , 1-14.	3.5	0
13642	Lipid composition modulates interactions of p7 viroporin during membrane insertion. <i>Journal of Structural Biology</i> , 2023, 215, 108013.	2.8	0
13643	Deciphering the Inhibitory Mechanism of Naphthoquinoneâ€Dopamine on the Aggregation of Tau Core Fragments PHF6* and PHF6. <i>ACS Chemical Neuroscience</i> , 0, , .	3.5	0
13646	Phase Separation and Ion Diffusion in Ionic Liquid, Organic Solvent, and Lithium Salt Electrolyte Mixtures. <i>Journal of Physical Chemistry B</i> , 2023, 127, 7531-7541.	2.6	0
13647	Atomistic Molecular Insights into Angiotensin-(1-7) Interpeptide Interactions. <i>Journal of Chemical Information and Modeling</i> , 2023, 63, 5331-5340.	5.4	0
13649	Investigating the molecular-level thermodynamics and adsorption properties of per- and poly-fluoroalkyl substances. <i>Journal of Molecular Liquids</i> , 2023, 389, 122826.	4.9	1
13650	Identification of CXCR4 inhibitors as a key therapeutic small molecule in renal fibrosis. <i>Journal of Biomolecular Structure and Dynamics</i> , 0, , 1-13.	3.5	1
13651	Design, synthesis, biological evaluation and in silico studies of N-(pyridin-2-yl)-benzamides derivatives as quorum sensing inhibitors. <i>Journal of the Indian Chemical Society</i> , 2023, 100, 101082.	2.8	0
13652	Kinetic and thermodynamic allostery in the Ras protein family. <i>Biophysical Journal</i> , 2023, 122, 3882-3893.	0.5	1
13653	Mechanisms of ssDNA aptamer binding to Cd2+ in aqueous solution: A molecular dynamics study. <i>International Journal of Biological Macromolecules</i> , 2023, 251, 126412.	7.5	2

#	ARTICLE	IF	CITATIONS
13655	Molecular analysis of hydrogen-propane hydrate formation mechanism and its influencing factors for hydrogen storage. International Journal of Hydrogen Energy, 2023, , .	7.1	0
13656	Rationalizing Na-ion solvation structure by weakening carbonate solvent coordination ability for high-voltage sodium metal batteries. Journal of Energy Chemistry, 2023, 87, 105-113.	12.9	4
13657	The energetics and ion coupling of cholesterol transport through Patched1. Science Advances, 2023, 9, .	10.3	2
13658	Structure based exploration of potential lead molecules against the extracellular cysteine protease (EcpA) of <i>Staphylococcus epidermidis</i> : a therapeutic halt. Journal of Biomolecular Structure and Dynamics, 0, , 1-17.	3.5	1
13659	Structural basis of peptidoglycan synthesis by E. coli RodA-PBP2 complex. Nature Communications, 2023, 14, .	12.8	1
13661	Oxygen plasma-treated graphite sheet electrodes: A sensitive and disposable sensor for methamphetamines. Electrochimica Acta, 2023, 467, 143089.	5.2	1
13663	Optimization of a small molecule inhibitor of secondary nucleation in $\beta$ -synuclein aggregation. Frontiers in Molecular Biosciences, 0, 10, .	3.5	1
13664	Effect of flavonoids on the destabilization of $\beta$ -synuclein fibrils and their conversion to amorphous aggregate: A molecular dynamics simulation and experimental study. Biochimica Et Biophysica Acta - Proteins and Proteomics, 2023, 1871, 140951.	2.3	0
13665	Molecular docking and molecular dynamics simulation analysis of bioactive compounds of <i>Cichorium intybus</i> L. seed against hepatocellular carcinoma. Journal of Biomolecular Structure and Dynamics, 0, , 1-12.	3.5	0
13666	Synergistic "Anchor-Capture"-Enabled by Amino and Carboxyl for Constructing Robust Interface of Zn Anode. Nano-Micro Letters, 2023, 15, .	27.0	7
13667	Equation of state predictions for ScF3 and CaZrF6 with neural network-driven molecular dynamics. Journal of Chemical Physics, 2023, 159, .	3.0	0
13668	Formation of modified chitosan/carrageenan multilayers at silica: Molecular dynamics modeling and experiments. Food Hydrocolloids, 2023, , 109222.	10.7	1
13669	Mechanical Codes of Chemical-Scale Specificity in DNA Motifs. Chemical Science, 0, , .	7.4	0
13670	Insight into the Factors for Separation of Lignin and Cellulose by Ionic Liquids Based on Molecular Simulation. Industrial & Engineering Chemistry Research, 0, , .	3.7	0
13671	Towards targeting EGFR and COX-2 inhibitors: comprehensive computational studies on the role of chlorine group in novel thienyl-pyrazoline derivative. Journal of Biomolecular Structure and Dynamics, 0, , 1-16.	3.5	0
13672	Neural potentials of proteins extrapolate beyond training data. Journal of Chemical Physics, 2023, 159, .	3.0	3
13673	Dynamozones are the most obvious sign of the evolution of conformational dynamics in HIV-1 protease. Scientific Reports, 2023, 13, .	3.3	3
13674	Benchmarking of force fields to characterize the intrinsically disordered R2-FUS-LC region. Scientific Reports, 2023, 13, .	3.3	0

#	ARTICLE	IF	CITATIONS
13676	Structure of the Hexadecane Rotator Phase: Combination of X-ray Spectra and Molecular Dynamics Simulation. Journal of Physical Chemistry B, 2023, 127, 7772-7784.	2.6	2
13677	Structure-based virtual screening of natural compounds against wild and mutant (R1155K, A1156T and) Tj ETQq1 1.0.784314 rgBT /Qv	3.5	2
13678	Promising kinetic gas hydrate inhibitors for developing sour gas reservoirs. Energy, 2023, 282, 128979.	8.8	2
13679	Atomistic Perspective of the Crystallization of Naphthodithiophene in Two Hydrocarbon Solvents. Chemistry of Materials, 0, , .	6.7	0
13680	Neuroprotective Properties of Oleanolic Acidâ€”Computational-Driven Molecular Research Combined with In Vitro and In Vivo Experiments. Pharmaceuticals, 2023, 16, 1234.	3.8	0
13681	Solvation behavior of phenolic pollutants in aqueous solutions of imidazolium-based ionic liquids: A molecular dynamics simulations study. Computational and Theoretical Chemistry, 2023, 1228, 114304.	2.5	0
13682	Efficient Simulations of Solvent Asymmetry Across Lipid Membranes Using Flat-Bottom Restraints. Journal of Chemical Theory and Computation, 0, , .	5.3	0
13683	Interfacial Tensionâ€”Temperatureâ€”Pressureâ€”Salinity Relationship for the Hydrogenâ€”Brine System under Reservoir Conditions: Integration of Molecular Dynamics and Machine Learning. Langmuir, 2023, 39, 12680-12691.	3.5	8
13684	New Approach to the Study of Association in Solutions. Journal of Structural Chemistry, 2023, 64, 1380-1390.	1.0	2
13685	Turning gas hydrate nucleation with oxygen-containing groups on size-selected graphene oxide flakes. Journal of Energy Chemistry, 2023, 87, 351-358.	12.9	1
13686	Photomanipulation of Minimal Synthetic Cells: Area Increase, Softening, and Interleaflet Coupling of Membrane Models Doped with Azobenzeneâ€”Lipid Photoswitches. Advanced Science, 2023, 10, .	11.2	2
13687	Characterizing the transmembrane domains of ADAM10 and BACE1 and the impact of membrane composition. Biophysical Journal, 2023, , .	0.5	0
13688	Modelling approach applied to SnIn coatings from choline chloride/ethylene glycol deep eutectic solvent. Journal of Molecular Liquids, 2023, , 122973.	4.9	0
13689	Interhelical E@<i>g</i>â€”N@<i>a</i> interactions modulate coiled coil stability within a de novo set of orthogonal peptide heterodimers. Journal of Peptide Science, 2024, 30, .	1.4	0
13690	Design and synthesis of novel 1,2,3,<sc>4â€”tetrazines</sc> as new antiâ€”leukemia cancer agents. Chemical Biology and Drug Design, 2023, 102, 1186-1201.	3.2	0
13691	Coupled Electrostatic and Hydrophobic Destabilisation of the Gelsolin-Actin Complex Enables Facile Detection of Ovarian Cancer Biomarker Lysophosphatidic Acid. Biomolecules, 2023, 13, 1426.	4.0	0
13692	Toward a structural identification of metastable molecular conformations. Journal of Chemical Physics, 2023, 159, .	3.0	0
13693	Membrane manipulation by free fatty acids improves microbial plant polyphenol synthesis. Nature Communications, 2023, 14, .	12.8	2

#	ARTICLE	IF	CITATIONS
13694	Computational Peptide Design Cotargeting Glucagon and Glucagon-like Peptide-1 Receptors. <i>Journal of Chemical Information and Modeling</i> , 2023, 63, 4934-4947.	5.4	0
13695	Malonyl-CoA is a conserved endogenous ATP-competitive mTORC1 inhibitor. <i>Nature Cell Biology</i> , 2023, 25, 1303-1318.	10.3	4
13696	Structural Phenomena in a Vesicle Membrane Obtained through an Evolution Experiment: A Study Based on MD Simulations. <i>Life</i> , 2023, 13, 1735.	2.4	0
13697	Structural and thermodynamic properties of bulk triglycerides and triglyceride/water mixtures reproduced using a polarizable coarse-grained model. <i>Physical Chemistry Chemical Physics</i> , 2023, 25, 22232-22243.	2.8	0
13698	Effect of Al <sub>2</sub> Cu constituent layer thickness discrepancy on the tensile mechanical behavior of Cu/Al <sub>2</sub> Cu/Al layered composites: a molecular dynamics simulation. <i>Nanotechnology</i> , 2023, 34, 445702.	2.6	0
13699	Conformational flexibility of the disaccharide Î <sup>2</sup> -Fuc <sub>1</sub> -(1→4)-Î <sup>4</sup> -Glc <sub>1</sub> -OMe as deduced from NMR spectroscopy experiments and computer simulations. <i>Organic and Biomolecular Chemistry</i> , 2023, 21, 6979-6994.	2.8	4
13700	The dilatable membrane of oleosomes (lipid droplets) allows their <i>in vitro</i> resizing and triggered release of lipids. <i>Soft Matter</i> , 2023, 19, 6355-6367.	2.7	1
13701	Structural evolution of water-in-propylene carbonate mixtures revealed by polarized Raman spectroscopy and molecular dynamics. <i>Physical Chemistry Chemical Physics</i> , 2023, 25, 23963-23976.	2.8	0
13702	Binding of synthetic nanobodies to the SARS-CoV-2 receptor-binding domain: the importance of salt bridges. <i>Physical Chemistry Chemical Physics</i> , 2023, 25, 24129-24142.	2.8	0
13703	Dynamic geometry design of cyclic peptide architectures for RNA structure. <i>Physical Chemistry Chemical Physics</i> , 2023, 25, 27967-27980.	2.8	1
13704	Fighting Celiac Disease: Improvement of pH Stability of Cathepsin L In Vitro by Computational Design. <i>International Journal of Molecular Sciences</i> , 2023, 24, 12369.	4.1	0
13705	Effects of Stress State, Crackâ€™s Phase Interface Relative Locations and Orientations on the Deformation and Crack Propagation Behaviors of the Ni-Based Superalloyâ€™A Molecular Dynamics Study. <i>Crystals</i> , 2023, 13, 1446.	2.2	0
13706	<i>In Vitro</i> and <i>in silico</i> studies to explore potent antidiabetic inhibitor against human pancreatic alpha-amylase from the methanolic extract of the green microalga <i>Chlorella vulgaris</i> . <i>Journal of Biomolecular Structure and Dynamics</i> , 0, , 1-11.	3.5	2
13707	Comprehensive views toward the biomolecular recognition of an anticancer drug, leflunomide with human serum albumin. <i>Journal of Biomolecular Structure and Dynamics</i> , 0, , 1-15.	3.5	2
13708	In Silico Strategies to Predict Anti-aging Features of Whey Peptides. <i>Molecular Biotechnology</i> , 0, , .	2.4	1
13709	Conformational Fluctuations in Î <sup>2</sup> -Microglobulin Using Markov State Modeling and Molecular Dynamics. <i>Journal of Physical Chemistry B</i> , 2023, 127, 6887-6895.	2.6	1
13710	The influence of counterion structure identity on conductivity, dynamical correlations, and ion transport mechanisms in polymerized ionic liquids. <i>Journal of Chemical Physics</i> , 2023, 159, .	3.0	1
13711	Strengthening mechanism of Niâ€™Cu nanotwins with void under different tensile directions based on Molecular Dynamics simulation. <i>Physica B: Condensed Matter</i> , 2023, 668, 415259.	2.7	0

#	ARTICLE	IF	CITATIONS
13712	The tensile and compressive deformation mechanisms of the Cu/Al <sub>2</sub> Cu/Al-layered composites via molecular dynamics simulation. <i>Applied Physics A: Materials Science and Processing</i> , 2023, 129, .	2.3	0
13713	Design of Acetylcholinesterase Inhibitors as Promising Anti-Alzheimer's Agents Based on QSAR, Molecular Docking, and Molecular Dynamics Studies of Liquiritigenin Derivatives. <i>ChemistrySelect</i> , 2023, 8, .	1.5	5
13714	Uncertainties in Markov State Models of Small Proteins. <i>Journal of Chemical Theory and Computation</i> , 2023, 19, 5516-5524.	5.3	2
13715	Mutational analyses, pharmacophore-based inhibitor design and in silico validation for Zika virus NS3-helicase. <i>Journal of Biomolecular Structure and Dynamics</i> , 0, , 1-19.	3.5	0
13716	O-methyltransferase-like enzyme catalyzed diazo installation in polyketide biosynthesis. <i>Nature Communications</i> , 2023, 14, .	12.8	1
13717	Anisotropy in Near-Spherical Colloidal Nanoparticles. <i>ACS Nano</i> , 2023, 17, 17873-17883.	14.6	1
13718	Self-play reinforcement learning guides protein engineering. <i>Nature Machine Intelligence</i> , 2023, 5, 845-860.	16.0	4
13719	Atomic visualization of flipped-back conformations of high mannose glycans interacting with cargo lectins: An MD simulation perspective. <i>Proteins: Structure, Function and Bioinformatics</i> , 0, , .	2.6	0
13720	Molecular dynamics simulation of bilayer core-shell structure of CL-20 surface-modified by polydopamine coated with polymer binder. <i>Materials Today Communications</i> , 2023, 37, 107099.	1.9	0
13721	Anticholinesterase and Serotonergic Evaluation of Benzimidazole-Carboxamides as Potential Multifunctional Agents for the Treatment of Alzheimer's Disease. <i>Pharmaceutics</i> , 2023, 15, 2159.	4.5	1
13722	Engineering salt-tolerant Cas12f1 variants for gene-editing applications. <i>Journal of Biomolecular Structure and Dynamics</i> , 0, , 1-11.	3.5	0
13723	All-Atom Molecular Dynamics Simulations of Poly(2,6-dimethyl-1,4-phenylene) Oxide: Validation of OPLS-AA Force Field for Conformational Behaviour in Vacuum and in Carbon Tetrachloride. <i>Macromolecular Chemistry and Physics</i> , 2023, 224, .	2.2	0
13724	The H163A mutation unravels an oxidized conformation of the SARS-CoV-2 main protease. <i>Nature Communications</i> , 2023, 14, .	12.8	0
13725	Atomistic molecular simulations of $\text{Zn}^{2+}$ conformational ensembles. <i>Proteins: Structure, Function and Bioinformatics</i> , 2024, 92, 134-144.	2.6	0
13726	Why do polyarginines adsorb at neutral phospholipid bilayers and polylysines do not? An insight from density functional theory calculations and molecular dynamics simulations. <i>Physical Chemistry Chemical Physics</i> , 2023, 25, 27204-27214.	2.8	0
13727	Driving forces behind phase separation of the carboxy-terminal domain of RNA polymerase II. <i>Nature Communications</i> , 2023, 14, .	12.8	8
13728	Reaction Kinetics and Microenvironments between Alkylimidazole and Methylthiocyanate for the Synthesis of Ionic Liquids. <i>Industrial &amp; Engineering Chemistry Research</i> , 2023, 62, 14963-14972.	3.7	0
13729	Role of concentration and hydrophobic nature of weak polyelectrolytes on adsorption structure and thermodynamics at oil-water interface: Study of several carboxylate polymers. <i>Polymer</i> , 2023, 285, 126315.	3.8	1



#	ARTICLE	IF	CITATIONS
13730	Cryo-EM structures of human organic anion transporting polypeptide OATP1B1. <i>Cell Research</i> , 2023, 33, 940-951.	12.0	6
13731	Molecular mechanisms of inorganic-phosphate release from the core and barbed end of actin filaments. <i>Nature Structural and Molecular Biology</i> , 2023, 30, 1774-1785.	8.2	3
13732	Structural basis of hydroxycarboxylic acid receptor signaling mechanisms through ligand binding. <i>Nature Communications</i> , 2023, 14, .	12.8	1
13733	OneOPES, a Combined Enhanced Sampling Method to Rule Them All. <i>Journal of Chemical Theory and Computation</i> , 2023, 19, 5731-5742.	5.3	1
13734	AhR diminishes the efficacy of chemotherapy via suppressing STING dependent type-I interferon in bladder cancer. <i>Nature Communications</i> , 2023, 14, .	12.8	4
13735	Design, synthesis, biological evaluation and molecular dynamics of some novel 3-phenylpyrazolo[1,5- <i>a</i> ]pyrimidine-2,7(1 <i>H</i> -,4 <i>H</i> -)-dione based compounds as anti-tubercular agents. <i>Journal of Biomolecular Structure and Dynamics</i> , 0, , 1-19.	3.5	0
13736	The World of GPCR dimers – Mapping dopamine receptor D2 homodimers in different activation states and configuration arrangements. <i>Computational and Structural Biotechnology Journal</i> , 2023, 21, 4336-4353.	4.1	0
13737	C3N nanodots inhibits A $\beta$ 2 peptides aggregation pathogenic path in Alzheimer’s disease. <i>Nature Communications</i> , 2023, 14, .	12.8	3
13738	Identification of candidate target genes of oral squamous cell carcinoma using high-throughput RNA-Seq data and <i>in silico</i> studies of their interaction with naturally occurring bioactive compounds. <i>Journal of Biomolecular Structure and Dynamics</i> , 0, , 1-21.	3.5	0
13739	Protein–lipid charge interactions control the folding of outer membrane proteins into asymmetric membranes. <i>Nature Chemistry</i> , 2023, 15, 1754-1764.	13.6	2
13740	Effect of water and hydrogen bond acceptor on the density and viscosity of glycol-based eutectic solvents. <i>Journal of Molecular Liquids</i> , 2023, 389, 122856.	4.9	5
13741	Effect of Water Models on The Stability of RNA: Role of Counter-Ions. <i>Chemical Physics Impact</i> , 2023, 7, 100313.	3.5	1
13742	Cholesterol catalyzes unfolding in membrane-inserted motifs of the pore forming protein cytolysinA. <i>Biophysical Journal</i> , 2023, 122, 4068-4081.	0.5	1
13743	Reducing the assemblies of amyloid-beta multimers by sodium dodecyl sulfate surfactant at concentrations lower than critical micelle concentration: molecular dynamics simulation exploration. <i>Journal of Biomolecular Structure and Dynamics</i> , 0, , 1-15.	3.5	2
13744	Effects of C-Terminal Lys-Arg Residue of AapA1 Protein on Toxicity and Structural Mechanism. <i>Toxins</i> , 2023, 15, 542.	3.4	0
13745	Influence of Protonation on the Norepinephrine Inhibiting $\beta$ -Synuclein 71–82 Oligomerization. <i>Journal of Physical Chemistry B</i> , 2023, 127, 7848-7857.	2.6	1
13746	Fluorescent protein lifetimes report densities and phases of nuclear condensates during embryonic stem-cell differentiation. <i>Nature Communications</i> , 2023, 14, .	12.8	5
13747	Host–guest interactions of Crizotinib with natural and modified cyclodextrins: a combined molecular docking and molecular dynamics simulation approaches. <i>Molecular Simulation</i> , 2023, 49, 1684-1697.	2.0	0

#	ARTICLE	IF	CITATIONS
13748	Design of light-responsive amphiphilic self-assemblies: A novel application of the photosensitive diazirine moiety. <i>Journal of Colloid and Interface Science</i> , 2024, 653, 1792-1804.	9.4	0
13749	Pentagalloyl Glucose-Targeted Inhibition of P-Glycoprotein and Re-Sensitization of Multidrug-Resistant Leukemic Cells (K562/ADR) to Doxorubicin: In Silico and Functional Studies. <i>Pharmaceuticals</i> , 2023, 16, 1192.	3.8	2
13750	Percolation of Low-Dimensional Water at Crystalline Interfaces Mediates Fluid Migration in Subducting Slabs. <i>Journal of Geophysical Research: Solid Earth</i> , 2023, 128, .	3.4	0
13751	DFT calculations of copper complexes mimicking superoxide dismutase and docking studies and molecular dynamics of the transition metal complex binding to serum albumin. <i>Journal of Biomolecular Structure and Dynamics</i> , 0, , 1-11.	3.5	1
13752	Viscosity Prediction of High-Concentration Antibody Solutions with Atomistic Simulations. <i>Journal of Chemical Information and Modeling</i> , 2023, 63, 6129-6140.	5.4	5
13753	Computed Protein-Protein Enthalpy Signatures as a Tool for Identifying Conformation Sampling Problems. <i>Journal of Chemical Information and Modeling</i> , 2023, 63, 6095-6108.	5.4	0
13754	Understanding the free-energy landscape of phase separation in lipid bilayers using molecular dynamics. <i>Biophysical Journal</i> , 2023, , .	0.5	0
13755	FA Sliding as the Mechanism for the ANT1-Mediated Fatty Acid Anion Transport in Lipid Bilayers. <i>International Journal of Molecular Sciences</i> , 2023, 24, 13701.	4.1	3
13756	Molecular simulations of understanding the Na <sup>+</sup> ion structure, dynamic and thermodynamic behavior in ionic liquids: Butyl ammonium hydrogen bisulfate and tri-butyl ammonium hydrogen bisulfate. <i>Journal of Molecular Graphics and Modelling</i> , 2023, 125, 108610.	2.4	0
13757	Structure and Molecular Mechanism of Signaling for the Glucagon-like Peptide-1 Receptor Bound to Gs Protein and Exendin-P5 Biased Agonist. <i>Journal of the American Chemical Society</i> , 2023, 145, 20422-20431.	13.7	0
13758	Pathway for Water Transport through Breathable Nanocomposite Membranes of PEBAX with Ionic Liquid [C12C1im]Cl. <i>Membranes</i> , 2023, 13, 749.	3.0	0
13759	Effect of lipid oxidation on the channel properties of Cx26 hemichannels: A molecular dynamics study. <i>Archives of Biochemistry and Biophysics</i> , 2023, 746, 109741.	3.0	0
13760	Identification of hits as anti-obesity agents against human pancreatic lipase <i>via</i> docking, drug-likeness, <i>in-silico</i> ADME(T), pharmacophore, DFT, molecular dynamics, and MM/PB(GB)SA analysis. <i>Journal of Biomolecular Structure and Dynamics</i> , 0, , 1-23.	3.5	2
13761	Identification of Potential Hits against Fungal Lysine Deacetylase Rpd3 via Molecular Docking, Molecular Dynamics Simulation, DFT, In-Silico ADMET and Drug-Likeness Assessment. <i>Chemistry Africa</i> , 2024, 7, 1151-1164.	2.4	3
13762	QSAR, DFT studies, docking molecular and simulation dynamic molecular of 2-styrylquinoline derivatives through their anticancer activity. <i>Journal of Saudi Chemical Society</i> , 2023, 27, 101728.	5.2	0
13763	Parasitic Protozoans: Exploring the Potential of N,N <sup>TM</sup> -Bis[2-(5-bromo-7-azabenzimidazol-1-yl)-2-oxoethyl]ethylene-1,3-Diamine and Its Cyclohexyl-1,2-diamine Analogue as TryR and Pf-DHODH Inhibitors. <i>Acta Parasitologica</i> , 0, , .	1.1	1
13764	Aggregation of an Amyloidogenic Peptide on Gold Surfaces. <i>Biomolecules</i> , 2023, 13, 1261.	4.0	0
13765	A pH-responsive nanoparticle delivery system containing dihydralazine and doxorubicin-based prodrug for enhancing antitumor efficacy. <i>Aggregate</i> , 2024, 5, .	9.9	0

#	ARTICLE	IF	CITATIONS
13766	Role of Terminal Groups of <i>cis</i> -1,4-Polyisoprene Chains in the Formation of Physical Junction Points in Natural Rubber. <i>Biomacromolecules</i> , 2023, 24, 3589-3602.	5.4	4
13767	Molecular Signatures of Asphaltene Precipitation in a Depressurization Process. <i>Energy &amp; Fuels</i> , 2023, 37, 14688-14698.	5.1	0
13768	The impact of physiologically relevant temperatures on physical properties of thylakoid membranes: a molecular dynamics study. <i>Photosynthetica</i> , 0, , .	1.7	1
13769	Claudin-23 reshapes epithelial tight junction architecture to regulate barrier function. <i>Nature Communications</i> , 2023, 14, .	12.8	5
13770	Molecular Insights into Distinct Membrane-insertion Behaviors and Mechanisms of 20 Amino Acids: an All-atom MD Simulation Study. <i>Chemical Research in Chinese Universities</i> , 2023, 39, 829-839.	2.6	0
13771	Osmolytes as Cryoprotectants under Salt Stress. <i>ACS Biomaterials Science and Engineering</i> , 2023, 9, 5639-5652.	5.2	3
13772	Complex role of chemical nature and tacticity in the adsorption free energy of carboxylic acid polymers at the oil/water interface: molecular dynamics simulations. <i>Physical Chemistry Chemical Physics</i> , 2023, 25, 27783-27797.	2.8	0
13773	Molecular Dynamics Simulation Study of the Selective Inhibition of Coagulation Factor IXa over Factor Xa. <i>Molecules</i> , 2023, 28, 6909.	3.8	0
13774	Dynamical coarse-grained models of molecular liquids and their ideal and non-ideal mixtures. <i>Journal of Chemical Physics</i> , 2023, 159, .	3.0	1
13775	Phytoconstituents of Ashwagandha as potential inhibitors of human islet amyloid polypeptide (hIAPP): an <i>in silico</i> investigation. <i>Journal of Biomolecular Structure and Dynamics</i> , 0, , 1-17.	3.5	2
13776	Exploring the Barriers in the Aggregation of a Hexadecameric Human Prion Peptide through the Markov State Model. <i>ACS Chemical Neuroscience</i> , 2023, 14, 3622-3645.	3.5	0
13777	Computation of Absolute Binding Free Energies for Noncovalent Inhibitors with SARS-CoV-2 Main Protease. <i>Journal of Chemical Information and Modeling</i> , 2023, 63, 5309-5318.	5.4	1
13778	Dynamic structural analysis-based epitope prediction of Exendin-4 in aqueous solution. <i>Physical Review E</i> , 2023, 108, .	2.1	0
13779	Turning nanopowder into nanomaterial: Effect of continuous SiC coating on mechanical properties of Si nanoparticle arrays. <i>Materialia</i> , 2023, 32, 101906.	2.7	0
13780	Amylose complexation with diacylglycerols involves multiple intermolecular interaction mechanisms. <i>Food Hydrocolloids</i> , 2024, 146, 109251.	10.7	1
13781	Incorporating physics to overcome data scarcity in predictive modeling of protein function: A case study of BK channels. <i>PLoS Computational Biology</i> , 2023, 19, e1011460.	3.2	1
13782	Melt structure of calcium aluminate-based non-reactive mold flux: Molecular dynamics simulation and spectroscopic experimental verification. <i>Construction and Building Materials</i> , 2023, 406, 133363.	7.2	0
13783	Molecular Dynamics Study of Silica Nanoparticles and CO <sub>2</sub> -Switchable Surfactants at an Oil/Water Interface. <i>Langmuir</i> , 2023, 39, 11283-11293.	3.5	0

#	ARTICLE	IF	CITATIONS
13784	Cardiolipin occupancy profiles of YidC paralogs reveal the significance of respective TM2 helix residues in determining paralog-specific phenotypes. <i>Frontiers in Molecular Biosciences</i> , 0, 10, .	3.5	0
13785	Effect of Tacticity Sequence of the Poly( <i>N</i> -isopropylacrylamide) Oligomer on Phase Transition Behavior in Aqueous Solution. <i>Journal of Physical Chemistry B</i> , 2023, 127, 8660-8668.	2.6	0
13786	OpenMSCG: A Software Tool for Bottom-Up Coarse-Graining. <i>Journal of Physical Chemistry B</i> , 2023, 127, 8537-8550.	2.6	10
13787	Permeability of antioxidants through a lipid bilayer model with coarse-grained simulations. <i>Journal of Biomolecular Structure and Dynamics</i> , 0, , 1-19.	3.5	0
13788	Insights into the auxetic behavior of graphene: A study on the temperature dependence of Poisson's ratio and in-plane moduli. <i>Carbon</i> , 2023, 215, 118416.	10.3	0
13789	Using a novel structure/function approach to select diverse swine major histocompatibility complex 1 alleles to predict epitopes for vaccine development. <i>Bioinformatics</i> , 2023, 39, .	4.1	0
13790	Molecular mechanism of the common and opposing cosolvent effects of fluorinated alcohol and urea on a coiled coil protein. <i>Protein Science</i> , 2023, 32, .	7.6	0
13791	BtuB TonB-dependent transporters and BtuG surface lipoproteins form stable complexes for vitamin B12 uptake in gut <i>Bacteroides</i> . <i>Nature Communications</i> , 2023, 14, .	12.8	1
13792	Catalytic Reaction Mechanism of Bacterial GH92 Î±-D-Mannosidase: A QM/MM Metadynamics Study. <i>ChemPhysChem</i> , 2023, 24, .	2.1	0
13793	Thermodynamic Insights into Variation in Thermomechanical and Physical Properties of Isotactic Polypropylene: Effect of Shear and Cooling Rates. <i>ACS Omega</i> , 2023, 8, 36775-36788.	3.5	0
13794	Understanding the Behavior of Sodium Polyacrylate in Suspensions of Silica and Monovalent Salts. <i>Polymers</i> , 2023, 15, 3861.	4.5	0
13795	Strain-aided room-temperature second-order ferroelectric phase transition in monolayer PbTe: Deep potential molecular dynamics simulations. <i>Physical Review B</i> , 2023, 108, .	3.2	1
13796	Martini-3 Coarse-Grained Models for the Bacterial Lipopolysaccharide Outer Membrane of <i>Escherichia coli</i> . <i>Journal of Chemical Theory and Computation</i> , 2024, 20, 1704-1716.	5.3	3
13797	Supramolecular Polymerization of a Pyrene-Substituted Diamide and Its Ensemble of Kinetically Trapped Configurations. <i>Angewandte Chemie</i> , 2023, 135, .	2.0	0
13798	Supramolecular Polymerization of a Pyrene-Substituted Diamide and Its Ensemble of Kinetically Trapped Configurations. <i>Angewandte Chemie - International Edition</i> , 2023, 62, .	13.8	1
13799	Molecular dynamics simulation of vapor-liquid equilibrium in 1-alkanol unary systems: a study of surface tension, density, and vapor pressure of TraPPE-UA force field. <i>Fluid Phase Equilibria</i> , 2024, 577, 113967.	2.5	0
13800	ARL8B mediates lipid droplet contact and delivery to lysosomes for lipid remobilization. <i>Cell Reports</i> , 2023, 42, 113203.	6.4	1
13801	Mechanisms of <i>Listeria monocytogenes</i> Disinfection with Benzalkonium Chloride: From Molecular Dynamics to Kinetics of Time-Kill Curves. <i>International Journal of Molecular Sciences</i> , 2023, 24, 12132.	4.1	1

#	ARTICLE	IF	CITATIONS
13802	Exploring the non-monotonic DNA capture behavior in a charged graphene nanopore. <i>Physical Chemistry Chemical Physics</i> , 2023, 25, 28034-28042.	2.8	0
13803	The role of flow in the self-assembly of dragline spider silk proteins. <i>Biophysical Journal</i> , 2023, , .	0.5	0
13804	Elucidating binding mechanisms of caffeic acid and resveratrol by beta-lactoglobulin: Insights into hydrophobic interactions and complex formation. <i>Food Hydrocolloids</i> , 2024, 146, 109269.	10.7	1
13805	Exploring Fullerenol-C60(OH)24 interactions with lipid bilayers: Molecular dynamics study of agglomeration and surface deposition. <i>Journal of Molecular Liquids</i> , 2023, 391, 123205.	4.9	0
13806	Towards compartmentalized micelles: Mixed perfluorinated and hydrogenated ionic surfactants in aqueous solution. <i>Journal of Colloid and Interface Science</i> , 2023, , .	9.4	1
13807	Dynamics of molecular collisions in air and its mean free path. <i>Physics of Fluids</i> , 2023, 35, .	4.0	1
13808	Combined <i>In Silico</i> and <i>In Vitro</i> Study to Reveal the Structural Insights and Nucleotide-Binding Ability of the Transcriptional Regulator PehR from the Phytopathogen <i>Ralstonia solanacearum</i> . <i>ACS Omega</i> , 2023, 8, 34499-34515.	3.5	1
13809	Counteraction Effects of Ammonium-Based Ionic Liquids on Urea-Induced Denaturation of $\beta$ -Lactalbumin: A Comprehensive Molecular Simulation Study. <i>Journal of Physical Chemistry B</i> , 2023, 127, 7251-7265.	2.6	1
13810	<i>In silico</i> design and identification of new peptides for mitigating hIAPP aggregation in type 2 diabetes. <i>Journal of Biomolecular Structure and Dynamics</i> , 0, , 1-16.	3.5	1
13811	Molecular dynamics analysis of superoxide dismutase 1 mutations suggests decoupling between mechanisms underlying ALS onset and progression. <i>Computational and Structural Biotechnology Journal</i> , 2023, 21, 5296-5308.	4.1	1
13812	The Molecular Mechanism of PSM $\pm$ 3 Aggregation: A New View. <i>Journal of Physical Chemistry B</i> , 2023, 127, 8317-8330.	2.6	0
13813	Phosphorylation motif dictates GPCR C-terminal domain conformation and arrestin interaction. <i>Structure</i> , 2023, , .	3.3	1
13814	Multi-scale molecular simulation of random peptide phase separation and its extended-to-compact structure transition driven by hydrophobic interactions. <i>Soft Matter</i> , 2023, 19, 7944-7954.	2.7	0
13815	Free-Energy Landscape and Rate Estimation of the Aromatic Ring Flips in Basic Pancreatic Trypsin Inhibitors Using Metadynamics. <i>Journal of Chemical Theory and Computation</i> , 2023, 19, 6605-6618.	5.3	0
13816	Sensing their plasma membrane curvature allows migrating cells to circumvent obstacles. <i>Nature Communications</i> , 2023, 14, .	12.8	2
13817	Highly robust quantum mechanics and umbrella sampling studies on inclusion complexes of curcumin and $\beta$ -cyclodextrin. <i>Carbohydrate Polymers</i> , 2024, 323, 121432.	10.2	6
13818	Design, synthesis and antimicrobial activity of novel quinoline derivatives: an <i>in silico</i> and <i>in vitro</i> study. <i>Journal of Biomolecular Structure and Dynamics</i> , 0, , 1-21.	3.5	0
13820	Characterization and regulation of salt upregulated cyclophilin from a halotolerant strain of <i>Penicillium oxalicum</i> . <i>Scientific Reports</i> , 2023, 13, .	3.3	0

#	ARTICLE	IF	CITATIONS
13821	LptM promotes oxidative maturation of the lipopolysaccharide translocon by substrate binding mimicry. <i>Nature Communications</i> , 2023, 14, .	12.8	2
13822	Electrolyte Permeability in Plastic Ice VII. <i>Journal of Physical Chemistry B</i> , 2023, 127, 6734-6742.	2.6	0
13823	Cheminformatics and machine learning approaches for repurposing anti-viral compounds against monkeypox virus thymidylate kinase. <i>Molecular Diversity</i> , 0, , .	3.9	1
13824	Fluoride permeation mechanism of the Fluc channel in liposomes revealed by solid-state NMR. <i>Science Advances</i> , 2023, 9, .	10.3	3
13826	Enhanced electrochemical treatment of humic acids and metal ions in leachate concentrate: Experimental and molecular mechanism investigations. <i>Journal of Hazardous Materials</i> , 2024, 462, 132774.	12.4	1
13827	Transport Properties of NaCl in Aqueous Solution and Hydrogen Solubility in Brine. <i>Journal of Physical Chemistry B</i> , 2023, 127, 8900-8915.	2.6	2
13828	In silico study of the interaction of phenazines with tuberculostatic activity with known molecular targets of <i>Mycobacterium tuberculosis</i> . <i>Results in Chemistry</i> , 2023, 6, 101094.	2.0	0
13829	Docosahexaenoic acid promotes vesicle clustering mediated by alpha-Synuclein via electrostatic interaction. <i>European Physical Journal E</i> , 2023, 46, .	1.6	0
13830	Structuring of 2â€œoleodipalmitin at the air interface from allâ€œatom, unitedâ€œatom, and coarseâ€œgrained molecular dynamics simulations. <i>European Journal of Lipid Science and Technology</i> , 2023, 125, .	1.5	0
13831	Enhancing Giardicidal Activity and Aqueous Solubility through the Development of â€œRetroABZâ€œ, a Regioisomer of Albendazole: In Vitro, In Vivo, and In Silico Studies. <i>International Journal of Molecular Sciences</i> , 2023, 24, 14949.	4.1	0
13832	The opening dynamics of the lateral gate regulates the activity of rhomboid proteases. <i>Science Advances</i> , 2023, 9, .	10.3	1
13833	Viroporins of Mpox Virus. <i>International Journal of Molecular Sciences</i> , 2023, 24, 13828.	4.1	0
13834	The structure of a <i>Lactobacillus helveticus</i> chlorogenic acid esterase and the dynamics of its insertion domain provide insights into substrate binding. <i>FEBS Letters</i> , 2023, 597, 2946-2962.	2.8	0
13835	Dynamic lipid interactions in the plasma membrane Na <sup>+</sup> ,K <sup>+</sup> -ATPase. <i>Biochimica Et Biophysica Acta - Molecular Cell Research</i> , 2023, 1870, 119545.	4.1	0
13836	Arylcoumarin and novel biscoumarin derivatives as potent inhibitors of human glutathione S-transferase. <i>Journal of Biomolecular Structure and Dynamics</i> , 0, , 1-15.	3.5	1
13837	Effect of cations (Na <sup>+</sup> , Co <sup>2+</sup> , Fe <sup>3+</sup> ) contamination in Nafion membrane: A molecular simulations study. <i>International Journal of Hydrogen Energy</i> , 2024, 50, 635-649.	7.1	0
13838	Monte Carlo simulations in various ensembles. , 2023, , 181-232.		0
13839	Free-energy calculations. , 2023, , 263-321.		0



#	ARTICLE	IF	CITATIONS
13843	Melting curves of ice polymorphs in the vicinity of the liquid–liquid critical point. Journal of Chemical Physics, 2023, 159, .	3.0	1
13845	Estimating Gibbs free energies via isobaric-isothermal flows. Machine Learning: Science and Technology, 2023, 4, 035039.	5.0	0
13847	Conformational flexibility of spermidine <sup>3+</sup> interacting with DNA double helix. Journal of Molecular Liquids, 2023, 389, 122828.	4.9	0
13851	Finding Novel AMPs Secreted from the Human Microbiome as Potent Antibacterial and Antibiofilm Agents and Studying Their Synergistic Activity with Ag NCs. ACS Applied Bio Materials, 2023, 6, 3674-3682.	4.6	1
13853	A mechanistic insight for the biosynthesis of N,N-dimethyltryptamine: An ONIOM theoretical approach. Biochemical and Biophysical Research Communications, 2023, 678, 148-157.	2.1	0
13856	Twin-boundary and precipitate interaction in Mg–Al alloy: an MD study. Modelling and Simulation in Materials Science and Engineering, 2023, 31, 075007.	2.0	0
13857	Computational assessment of lipid facilitated membrane permeation of vancomycin using force-probe molecular dynamic simulation. Journal of Biomolecular Structure and Dynamics, 0, , 1-11.	3.5	0
13859	Quantum biochemistry description of PI3K $\gamma$ enzyme bound to selective inhibitors. Journal of Biomolecular Structure and Dynamics, 0, , 1-11.	3.5	0
13861	Interactions of the male contraceptive target EPPIN with semenogelin-1 and small organic ligands. Scientific Reports, 2023, 13, .	3.3	1
13863	Elucidation of binding mechanism, affinity, and complex structure between mWT1 tumor-associated antigen peptide and HLA-A*24:02. Protein Science, 2023, 32, .	7.6	1
13866	Systematic exploration of the interactions between anionic polyacrylamide and manganese peroxidase based on docking and molecular dynamics simulations. Catalysis Communications, 2023, 183, 106758.	3.3	0
13869	OrthoBoXY: A Simple Way to Compute True Self-Diffusion Coefficients from MD Simulations with Periodic Boundary Conditions without Prior Knowledge of the Viscosity. Journal of Physical Chemistry B, 2023, 127, 7983-7987.	2.6	4
13870	An immunoinformatics and extended molecular dynamics approach for designing a polyvalent vaccine against multiple strains of Human T-lymphotropic virus (HTLV). PLoS ONE, 2023, 18, e0287416.	2.5	1
13871	Molecular Dynamics Simulations of a Hexanitrohexaazaisowurtzitane/4-Amino-3,7-dinitro-1,2,4-triazolo[5,1-c][1,2,4]triazine Cocrystal. ChemistrySelect, 2023, 8, .	1.5	0
13872	Addressing the complexities in measuring cyclodextrin-sterol binding constants: A multidimensional study. Carbohydrate Polymers, 2024, 323, 121360.	10.2	3
13873	Stacks of monogalactolipid bilayers can transform into a lattice of water channels. IScience, 2023, 26, 107863.	4.1	0
13874	Bioactive Suture with Added Innate Defense Functionality for the Reduction of Bacterial Infection and Inflammation. Advanced Healthcare Materials, 2023, 12, .	7.6	1
13875	Preparation, Characterization, and Molecular Dynamic Simulation of Novel Coenzyme Q10 Loaded Nanostructured Lipid Carriers. Current Pharmaceutical Design, 2023, 29, 2177-2190.	1.9	0

#	ARTICLE	IF	CITATIONS
13876	Molecular dynamics simulation of apolipoprotein E3 lipid nanodiscs. <i>Biochimica Et Biophysica Acta - Biomembranes</i> , 2024, 1866, 184230.	2.6	1
13877	Reactive natural deep eutectic solvents increase selectivity and efficiency of lipase catalyzed esterification of carbohydrate polyols. <i>Catalysis Today</i> , 2024, 426, 114373.	4.4	4
13878	Coarse-Grained Modeling Using Neural Networks Trained on Structural Data. <i>Journal of Chemical Theory and Computation</i> , 2023, 19, 6704-6717.	5.3	0
13879	Deconstructing Electrostatics of Functionalized Metal Nanoparticles from Molecular Dynamics Simulations. <i>Journal of Physical Chemistry B</i> , 2023, 127, 8226-8241.	2.6	0
13886	Analysis of Reconstituted Tripartite Complex Supports Avidity-based Recruitment of Hsp70 by Substrate Bound J-domain Protein. <i>Journal of Molecular Biology</i> , 2023, 435, 168283.	4.2	1
13887	Identifying Selectivity Filters in Protein Biosensor for Ligand Screening. <i>Jacs Au</i> , 2023, 3, 2800-2812.	7.9	0
13888	Parametrization of embedded-atom method potential for liquid lithium and lead-lithium eutectic alloy. <i>Journal of Nuclear Materials</i> , 2023, 587, 154735.	2.7	0
13889	The effect of linker conformation on performance and stability of a two-domain lytic polysaccharide monooxygenase. <i>Journal of Biological Chemistry</i> , 2023, 299, 105262.	3.4	2
13890	Novel multi-objective affinity approach allows to identify pH-specific $\mu$ -opioid receptor agonists. <i>Journal of Cheminformatics</i> , 2023, 15, .	6.1	0
13892	<i>In silico</i> identification of novel heterocyclic compounds combats Alzheimer's disease through inhibition of butyrylcholinesterase enzymatic activity. <i>Journal of Biomolecular Structure and Dynamics</i> , 0, , 1-21.	3.5	0
13893	Dose-dependent binding behavior of anthraquinone derivative purpurin interacting with tau-derived peptide protofibril. <i>Physical Chemistry Chemical Physics</i> , 2023, 25, 26787-26796.	2.8	0
13894	Molecular insights into the structure destabilization effects of ECG and EC on the A $\beta$ 2 protofilament: An all-atom molecular dynamics simulation study. <i>International Journal of Biological Macromolecules</i> , 2023, 253, 127002.	7.5	0
13895	Operando FTIR-ATR with molecular dynamic simulations to understand the diffusion mechanism of waste tire-derived pyrolytic oil for asphalt self-healing. <i>Fuel</i> , 2024, 357, 129834.	6.4	6
13896	Methane hydrate formation in clay mineral suspensions containing glycine: Experimental study and molecular dynamics simulation. <i>Journal of Molecular Liquids</i> , 2023, 390, 123124.	4.9	2
13897	Antibacterial and anticancer activity of two NK-lysin-derived peptides from the Antarctic teleost <i>Trematomus bernacchii</i> . <i>Fish and Shellfish Immunology</i> , 2023, 142, 109099.	3.6	1
13898	Calcium binding and permeation in TRPV channels: Insights from molecular dynamics simulations. <i>Journal of General Physiology</i> , 2023, 155, .	1.9	1
13899	Self-assembly and structures of nanoscale double emulsion droplets through coarse-grained molecular dynamics simulations. <i>Soft Matter</i> , 2023, 19, 7731-7743.	2.7	0
13900	Spike Protein Mutation-Induced Changes in the Kinetic and Thermodynamic Behavior of Its Receptor Binding Domains Explain Their Higher Propensity to Attain Open States in SARS-CoV-2 Variants of Concern. <i>ACS Central Science</i> , 2023, 9, 1894-1904.	11.3	2

#	ARTICLE	IF	CITATIONS
13901	Molecular simulation of ensembles. , 2024, , 309-358.		0
13904	Biochemical and structural characterization of the RT domain of Leishmania sp. telomerase reverse transcriptase. Biochimica Et Biophysica Acta - General Subjects, 2023, 1867, 130451.	2.4	0
13906	Unveiling the interaction modes of Imiquimod with DNA: Biophysical and computational studies. Journal of Photochemistry and Photobiology A: Chemistry, 2024, 447, 115190.	3.9	0
13907	Decoding the dual recognition mechanism of the glucocorticoid receptor for DNA and RNA: sequence versus shape. Scientific Reports, 2023, 13, .	3.3	0
13908	Revealing the crystalline packing structure of Y6 in the active layer of organic solar cells: the critical role of solvent additives. Journal of Materials Chemistry A, 2023, 11, 21895-21907.	10.3	2
13909	Interfacing $\beta$ -casein "Phenolic compound interactions via molecular dynamics simulations with diffusion kinetics in delivery vehicles. Food Chemistry, 2024, 435, 137595.	8.2	0
13910	Lansoprazole as a potent HDAC2 inhibitor for treatment of colorectal cancer: An in-silico analysis and experimental validation. Computers in Biology and Medicine, 2023, 166, 107518.	7.0	3
13911	Riding the Wave: Unveiling the Conformational Waves from RBD of SARS-CoV-2 Spike Protein to ACE2. Journal of Physical Chemistry B, 2023, 127, 8525-8536.	2.6	0
13914	Hydrodynamic radius of dendrimers in solvents. Physical Chemistry Chemical Physics, 2023, 25, 28220-28229.	2.8	0
13915	Molecular Study on Carbon Dioxide Hydrate Formation in Salty Water. Crystal Growth and Design, 2023, 23, 8361-8369.	3.0	1
13916	Tailoring the adsorption behaviors of flucytosine on BnNn ( $n=12, 16, 20$ , and $24$ ) nanocage scaffolds: A computational insight on drug delivery applications. Colloids and Surfaces A: Physicochemical and Engineering Aspects, 2023, 678, 132481.	4.7	1
13917	Structural, Energetic and Dynamic Investigation of Poly(ethylene oxide) in Imidazolium-Based Ionic Liquids with Different Cationic Structures. Physical Chemistry Chemical Physics, 0, , .	2.8	0
13918	Grain boundary segregation of Y and Hf dopants in $\text{Al}_{0.2}\text{O}_{0.3}$ : A Monte Carlo simulation with artificial-neural-network potential and density-functional-theory calculation. Journal of the Ceramic Society of Japan, 2023, 131, 751-761.	1.1	0
13919	Screening of potential inhibitors against structural proteins from Monkeypox and related viruses of <i>Poxviridae</i> family via docking and molecular dynamics simulation. Journal of Biomolecular Structure and Dynamics, 0, , 1-16.	3.5	1
13921	Enhanced Photovoltaic Properties of Y6 Derivatives with Asymmetric Terminal Groups: A Theoretical Insight. International Journal of Molecular Sciences, 2023, 24, 14753.	4.1	0
13925	Solvent-Induced Lag Phase during the Formation of Lysozyme Amyloid Fibrils Triggered by Sodium Dodecyl Sulfate: Biophysical Experimental and In Silico Study of Solvent Effects. Molecules, 2023, 28, 6891.	3.8	0
13927	Functional Group-Dependent Proton Conductivity of Phosphoric Acid-Doped Ion-Pair Coordinated Polymer Electrolytes: A Molecular Dynamics Study. Journal of Physical Chemistry B, 2023, 127, 8993-8999.	2.6	0
13929	Deciphering the Catalytic Mechanism of Virginiamycin B Lyase with Multiscale Methods and Molecular Dynamics Simulations. Journal of Chemical Information and Modeling, 2023, 63, 6354-6365.	5.4	0

#	ARTICLE	IF	CITATIONS
13930	Characterization and molecular simulation of lignin in Cyrene pretreatment of switchgrass. <i>Green Chemistry</i> , 0, , .	9.0	0
13931	Martini 3 Coarse-Grained Force Field for Cholesterol. <i>Journal of Chemical Theory and Computation</i> , 2023, 19, 7387-7404.	5.3	3
13932	Molecular Dynamics Simulation of the Conformational Mobility of the Lipid-Binding Site in the Apolipoprotein E Isoforms $\mu$ 2, $\mu$ 3, and $\mu$ 4. <i>Moscow University Biological Sciences Bulletin</i> , 2023, 78, 59-65.	0.7	0
13933	The rise of FTIR spectroscopy in the characterization of asymmetric lipid membranes. <i>Spectrochimica Acta - Part A: Molecular and Biomolecular Spectroscopy</i> , 2024, 305, 123488.	3.9	0
13934	Tracing the substrate translocation mechanism in P-glycoprotein. <i>ELife</i> , 0, 12, .	6.0	2
13936	Mitochondrial membrane model: Lipids, elastic properties, and the changing curvature of cardiolipin. <i>Biophysical Journal</i> , 2023, 122, 4274-4287.	0.5	1
13937	Spectral characterization and binding dynamics of bioactive compounds from <i>Chlorella minutissima</i> against $\beta$ -glucosidase: An in vitro and in silico approach. <i>Algal Research</i> , 2023, 75, 103281.	4.6	1
13939	Analysis of temperature effect in the CO <sub>2</sub> absorption using a deep eutectic solvent: An in silico approach. <i>Journal of Molecular Graphics and Modelling</i> , 2024, 126, 108649.	2.4	1
13940	A Theoretical Study on the Underlying Factors of the Difference in Performance of Organic Solar Cells Based on ITIC and Its Isomers. <i>Molecules</i> , 2023, 28, 6968.	3.8	0
13942	Effect of different counterions on the self-assembly structures and properties of imidazole based ionic liquids surfactant: A molecular dynamics study. <i>Journal of Molecular Liquids</i> , 2023, 391, 123277.	4.9	0
13943	Comparative docking and molecular dynamics studies of molnupiravir (EIDD-2801): implications for novel mechanisms of action on influenza and SARS-CoV-2 protein targets. <i>Journal of Biomolecular Structure and Dynamics</i> , 0, , 1-13.	3.5	0
13944	Salt-Induced Coil $\rightarrow$ Globule Transition of Sulfonate-Modified HPAM is Affected by the Branched Chain Length. <i>Langmuir</i> , 2023, 39, 14969-14976.	3.5	0
13945	Identification of naturally occurring compounds as alternatives to radiation therapy for treatment of small cell lung cancer. <i>Journal of Biomolecular Structure and Dynamics</i> , 0, , 1-12.	3.5	0
13947	Identification of potential phytochemical inhibitors for the proven six chronic obstructive pulmonary disease biomarkers $\alpha$ A molecular dynamics study. <i>Journal of Biomolecular Structure and Dynamics</i> , 0, , 1-26.	3.5	0
13948	A morpheein equilibrium regulates catalysis in phosphoserine phosphatase SerB2 from <i>Mycobacterium tuberculosis</i> . <i>Communications Biology</i> , 2023, 6, .	4.4	0
13949	Computational Study on the Enzyme $\rightarrow$ Ligand Relationship between Cannabis Phytochemicals and Human Acetylcholinesterase: Implications in Alzheimer $\rightarrow$ s Disease. <i>Journal of Physical Chemistry B</i> , 2023, 127, 8780-8795.	2.6	1
13950	Accurately Predicting Protein $pK_a$ Values Using Nonequilibrium Alchemy. <i>Journal of Chemical Theory and Computation</i> , 2023, 19, 7833-7845.	5.3	2
13951	Infrared Spectroscopy of Li <sup>+</sup> Solvation in Diglyme: Ab Initio Molecular Dynamics and Experiment. <i>Journal of Physical Chemistry B</i> , 0, , .	2.6	0

#	ARTICLE	IF	CITATIONS
13952	<i>In-silico</i> prediction of $TGF\beta 1$ non-synonymous variants and their impact on binding affinity to Fresolimumab. <i>Journal of Biomolecular Structure and Dynamics</i> , 0, , 1-14.	3.5	1
13954	Thylakoid Composition Facilitates Chlorophyll a Dimerization through Stronger Interlipid Interactions. <i>Journal of Physical Chemistry B</i> , 0, , .	2.6	0
13955	Lessons on protein structure from interleukin $\alpha 4$ : All disulfides are not created equal. <i>Proteins: Structure, Function and Bioinformatics</i> , 2024, 92, 219-235.	2.6	0
13956	Cellular excitability and ns-pulsed electric fields: Potential involvement of lipid oxidation in the action potential activation. <i>Bioelectrochemistry</i> , 2024, 155, 108588.	4.6	1
13959	Polyfluoroalkyl Chain-Based Assemblies for Biomimetic Catalysis. <i>Chemistry - A European Journal</i> , 2024, 30, .	3.3	0
13960	Mass spectrometric assays monitoring the deubiquitinase activity of the SARS-CoV-2 papain-like protease inform on the basis of substrate selectivity and have utility for substrate identification. <i>Bioorganic and Medicinal Chemistry</i> , 2023, 95, 117498.	3.0	0
13962	Molecular Basis for Mambalgin-2 Interaction with Heterotrimeric $\alpha 1\beta 3$ -ENaC/ASIC1a Channels in Cancer Cells. <i>Toxins</i> , 2023, 15, 612.	3.4	0
13963	Palmitoylation modifies transmembrane adaptor protein PAC for ordered lipid environment: A molecular dynamics simulation study. <i>Biophysical Chemistry</i> , 2023, , 107124.	2.8	0
13964	Interactions of Nucleosomes with Acidic Patch-Binding Peptides: A Combined Structural Bioinformatics, Molecular Modeling, Fluorescence Polarization, and Single-Molecule FRET Study. <i>International Journal of Molecular Sciences</i> , 2023, 24, 15194.	4.1	0
13966	Water molecule ordering on the surface of an intrinsically disordered protein. <i>Biophysical Journal</i> , 2023, 122, 4326-4335.	0.5	0
13967	Particle Deformability Enables Control of Interactions between Membrane-Anchored Nanoparticles. <i>Journal of Chemical Theory and Computation</i> , 2024, 20, 1732-1739.	5.3	0
13968	Lithium dynamics at grain boundaries of $Li_3PS_4$ solid electrolyte. <i>Energy Advances</i> , 2023, 2, 2029-2041.	3.3	1
13969	Molecular dynamics simulations evidence the thermoresponsive behavior of PNIPAM and PDEA in glycerol solutions. <i>Frontiers in Nanotechnology</i> , 0, 5, .	4.8	0
13970	Investigating the Effects of the POPC Lipid Bilayer Composition on PAP248 $\alpha$ Binding Using CG Molecular Dynamics Simulations. <i>Journal of Physical Chemistry B</i> , 0, , .	2.6	0
13971	Myristoyl's dual role in allosterically regulating and localizing Abl kinase. <i>ELife</i> , 0, 12, .	6.0	0
13972	Classification of PTEN missense VUS through exascale simulations. <i>Briefings in Bioinformatics</i> , 2023, 24, .	6.5	0
13973	Integration of an LPAR1 Antagonist into Liposomes Enhances Their Internalization and Tumor Accumulation in an Animal Model of Human Metastatic Breast Cancer. <i>Molecular Pharmaceutics</i> , 0, , .	4.6	1
13974	Inhibition of LINGO1 as a therapeutic target to promote axonal regeneration and repair for neurological disorders. <i>3 Biotech</i> , 2023, 13, .	2.2	0

#	ARTICLE	IF	CITATIONS
13975	Mechanism Analysis and Property Prediction of Extended Surfactants Based on the Respectively Optimized Force Field. <i>Langmuir</i> , 2023, 39, 14859-14868.	3.5	1
13976	Strengthening-softening transition and maximum strength in Schwarz nanocrystals. <i>Nano Materials Science</i> , 2023, , .	8.8	1
13977	Hardening of fcc hard-sphere crystals by introducing nanochannels: Auxetic aspects. <i>Physical Review E</i> , 2023, 108, .	2.1	2
13978	Polymorphic structure of $\alpha$ -type screw dislocation cores in $\alpha$ -Ti. <i>Physical Review Materials</i> , 2023, 7, .	2.4	0
13979	Multiscale simulations reveal TDP-43 molecular-level interactions driving condensation. <i>Biophysical Journal</i> , 2023, 122, 4370-4381.	0.5	4
13980	Computational Modelling of Wettability in Calcite-Oil-Water Systems. , 2023, , .		0
13981	Serine/threonine kinase of Mpox virus: computational modeling and structural analysis. <i>Journal of Biomolecular Structure and Dynamics</i> , 0, , 1-12.	3.5	0
13983	Treatment-Emergent Cilgavimab Resistance Was Uncommon in Vaccinated Omicron BA.4/5 Outpatients. <i>Biomolecules</i> , 2023, 13, 1538.	4.0	0
13984	Mechanism of Fluoride Ion Encapsulation by Magnesium Ions in a Bacterial Riboswitch. <i>Journal of Physical Chemistry B</i> , 2023, 127, 9267-9281.	2.6	2
13985	Photodynamic inactivation of bacteria: Why it is not enough to excite a photosensitizer. <i>Photodiagnosis and Photodynamic Therapy</i> , 2023, 44, 103853.	2.6	0
13986	Identifying therapeutic antibacterial peptides against <i>Vibrio cholerae</i> to inhibit the function of Na(+)-translocating NADH-quinone reductase. <i>Journal of Biomolecular Structure and Dynamics</i> , 0, , 1-16.	3.5	0
13988	Correlations between Molecular Structure, Solvation Topology, and Transport Properties of Aqueous Organic Flow Battery Electrolyte Solutions. , 0, , 3050-3057.		0
13989	Multi-targeted Virtual Screening of Phytocompounds of <i>Rauwolfia serpentina</i> Against Caspase-8, BACE, and AChE for the Treatment of Neurodegenerative Diseases. , 2023, 2, .		0
13990	Molecular dynamics investigation of the interaction between volatile organic compounds and deep eutectic solvents. <i>Molecular Simulation</i> , 2024, 50, 9-19.	2.0	0
13991	Methane hydrate formation in slit-shaped pores: Impacts of surface hydrophilicity. <i>Energy</i> , 2023, 285, 129414.	8.8	4
13993	Malic acid-based deep eutectic solvent and its application in Insulin's structural stability. <i>Results in Engineering</i> , 2023, 20, 101529.	5.1	0
13995	The molecular basis of dapsone activation of CYP2C9-catalyzed non-steroidal anti-inflammatory drug (NSAID) oxidation. <i>Journal of Biological Chemistry</i> , 2023, , 105368.	3.4	0
13997	Combining molecular dynamics simulations and x-ray scattering techniques for the accurate treatment of protonation degree and packing of ionizable lipids in monolayers. <i>Journal of Chemical Physics</i> , 2023, 159, .	3.0	1



#	ARTICLE	IF	CITATIONS
13998	Computational assessment of the reactivity and pharmaceutical potential of novel triazole derivatives: An approach combining DFT calculations, molecular dynamics simulations, and molecular docking. <i>Arabian Journal of Chemistry</i> , 2024, 17, 105376.	4.9	3
13999	State-dependent dynamics of extramembrane domains in the $\alpha_2\beta_2$ -adrenergic receptor. <i>Proteins: Structure, Function and Bioinformatics</i> , 2024, 92, 317-328.	2.6	1
14000	Diversity of rhodopsin cyclases in zoospore-forming fungi. <i>Proceedings of the National Academy of Sciences of the United States of America</i> , 2023, 120, .	7.1	1
14001	Activating Mutations Drive Human MEK1 Kinase Using a Gear-Shifting Mechanism. <i>Biochemical Journal</i> , 0, , .	3.7	1
14002	An Enhanced Sampling Approach for Computing the Free Energy of Solid Surface and Solid-Liquid Interface. <i>Advanced Theory and Simulations</i> , 2024, 7, .	2.8	0
14003	Studies on the selectivity of the SARS-CoV-2 papain-like protease reveal the importance of the P2 <sup>2</sup> proline of the viral polyprotein. <i>RSC Chemical Biology</i> , 2024, 5, 117-130.	4.1	0
14004	Biochemical, structural and dynamical characterizations of the lactate dehydrogenase from <i>Selenomonas ruminantium</i> provide information about an intermediate evolutionary step prior to complete allosteric regulation acquisition in the super family of lactate and malate dehydrogenases. <i>Journal of Structural Biology</i> , 2023, 215, 108039.	2.8	0
14006	Development of Robust Cationic Light-Activated Thermosensitive Liposomes: Choosing the Right Lipids. <i>Molecular Pharmaceutics</i> , 0, , .	4.6	0
14007	Origin of the nonlinear structural and mechanical properties in oppositely curved lipid mixtures. <i>Journal of Chemical Physics</i> , 2023, 159, .	3.0	0
14008	Putative Role of Cholesterol in Shaping the Structural and Functional Dynamics of Smoothened (SMO). <i>Journal of Physical Chemistry B</i> , 2023, 127, 9476-9495.	2.6	1
14009	Understanding the Mechanical Properties of Ultradeformable Liposomes Using Molecular Dynamics Simulations. <i>Journal of Physical Chemistry B</i> , 2023, 127, 9496-9512.	2.6	2
14013	Adsorbing DNA to Mica by Cations: Influence of Valency and Ion Type. <i>Langmuir</i> , 0, , .	3.5	0
14016	Unraveling the Interaction of a Neurological Drug Rivastigmine with Human Insulin Protein: A Biophysical Method in Combination with Molecular Docking and Molecular Dynamics Simulation. , 2023, 2, .		0
14017	Smartphone-based polydiacetylene colorimetric sensor for point-of-care diagnosis of bacterial infections. <i>Smart Materials in Medicine</i> , 2024, 5, 140-152.	6.7	0
14018	Molecular Mechanisms behind Conformational Transitions of the Influenza Virus Hemagglutinin Membrane Anchor. <i>Journal of Physical Chemistry B</i> , 2023, 127, 9450-9460.	2.6	0
14019	EphrinA5 regulates cell motility by modulating Snhg15/DNA triplex-dependent targeting of DNMT1 to the Ncam1 promoter. <i>Epigenetics and Chromatin</i> , 2023, 16, .	3.9	0
14020	Protein compactness and interaction valency define the architecture of a biomolecular condensate across scales. <i>ELife</i> , 0, 12, .	6.0	1
14021	Structural basis for the activity regulation of Salt Overly Sensitive 1 in Arabidopsis salt tolerance. <i>Nature Plants</i> , 2023, 9, 1915-1923.	9.3	4

#	ARTICLE	IF	CITATIONS
14022	Cryo-EM structure of human PAPP-A2 and mechanism of substrate recognition. Communications Chemistry, 2023, 6, .	4.5	0
14023	Injectable tissue prosthesis for instantaneous closed-loop rehabilitation. Nature, 2023, 623, 58-65.	27.8	6
14024	The complex impact of cancer-related missense mutations on the stability and on the biophysical and biochemical properties of MAPK1 and MAPK3 somatic variants. Human Genomics, 2023, 17, .	2.9	0
14025	Energy coupling and stoichiometry of Zn <sup>2+</sup> /H <sup>+</sup> antiport by the prokaryotic cation diffusion facilitator YiiP. ELife, 0, 12, .	6.0	3
14026	Mechanical properties of boron nitride nanotube reinforced PEEK composite: a molecular dynamics study. Nanocomposites, 2023, 9, 148-158.	4.2	0
14027	Investigation of the structure, stability, and relative solubility of psilocybin in water and pure organic solvents: A molecular simulation study. Journal of Molecular Liquids, 2023, 392, 123479.	4.9	0
14028	Hydrophobic gating in bundle-crossing ion channels: a case study of TRPV4. Communications Biology, 2023, 6, .	4.4	2
14029	Defining neutralization and allostery by antibodies against COVID-19 variants. Nature Communications, 2023, 14, .	12.8	1
14030	RNAs undergo phase transitions with lower critical solution temperatures. Nature Chemistry, 2023, 15, 1693-1704.	13.6	6
14031	The molecular mechanism of the effects of the anti-neuropathic ligands on the modulation of the Sigma-2 receptor: An in-silico study. International Journal of Biological Macromolecules, 2024, 254, 127925.	7.5	0
14032	Conformational dynamics of I $\pm$ -synuclein and study of its intramolecular forces in the presence of selected compounds. Scientific Reports, 2023, 13, .	3.3	0
14033	Enthalpy of dissociation of the mixed methane + propane sll hydrate along the three-phase equilibrium line. Molecular Physics, 0, , .	1.7	0
14034	Energetic and structural insights behind calcium induced conformational transition in calmodulin. Proteins: Structure, Function and Bioinformatics, 2024, 92, 384-394.	2.6	0
14035	Exploration of phytochemical compounds against Marburg virus using QSAR, molecular dynamics, and free energy landscape. Molecular Diversity, 0, , .	3.9	2
14036	Targeting tachykinin peptides involved in viral infections through in silico approach: Screening the unforeseen potency of serratiopeptidase. Journal of Molecular Liquids, 2023, 392, 123504.	4.9	0
14037	Cell-free biosynthesis combined with deep learning accelerates de novo-development of antimicrobial peptides. Nature Communications, 2023, 14, .	12.8	8
14038	Dual function of OmpM as outer membrane tether and nutrient uptake channel in diderm Firmicutes. Nature Communications, 2023, 14, .	12.8	0
14039	Anomalous lateral diffusion of lipids during the fluid/gel phase transition of a lipid membrane. Physical Chemistry Chemical Physics, 2023, 25, 31431-31443.	2.8	1

#	ARTICLE	IF	CITATIONS
14040	Novel insights into the effects of asphaltenes on oil phase properties: Crude oil, oil-water interface, and graphene oxide synergistic demulsification. <i>Journal of Molecular Liquids</i> , 2023, 391, 123405.	4.9	0
14041	Simulated pressure changes in LaCl suggest a link between hydration and functional conformational changes. <i>Biophysical Chemistry</i> , 2024, 304, 107126.	2.8	0
14042	Enhancing aromatics extraction by double salt ionic liquids: Rational screening&mdash;validation and mechanistic insights. <i>AIChE Journal</i> , 2024, 70, .	3.6	0
14043	Effects of ion type and concentration on the structure and aggregation of the amyloid peptide <sc>A</sc>I <sup>216</sup> 22. <i>Proteins: Structure, Function and Bioinformatics</i> , 0, , .	2.6	2
14044	Nucleation and Growth of Amyloid Fibrils. <i>Journal of Physical Chemistry B</i> , 2023, 127, 9759-9770.	2.6	4
14045	Effect of Temperature on Flow-Induced Crystallization of Isotactic Polypropylene: A Molecular-Dynamics Study. <i>Macromolecules</i> , 2023, 56, 8417-8427.	4.8	0
14046	Patterns in interactions of variably acetylated xylans with hydrophobic cellulose surfaces. <i>Cellulose</i> , 2023, 30, 11323-11340.	4.9	0
14047	Evaluating the gas storage capacity of 1,3-dioxolane&mdash;hydrogen binary hydrates via molecular simulations. <i>Journal of Molecular Liquids</i> , 2024, 393, 123542.	4.9	0
14048	Single-layer MoS <sub>2</sub> solid-state nanopores for coarse-grained sequencing of proteins. <i>Frontiers in Nanotechnology</i> , 0, 5, .	4.8	0
14049	Decoding dissociation of sequence-specific protein&mdash;DNA complexes with non-equilibrium simulations. <i>Nucleic Acids Research</i> , 2023, 51, 12150-12160.	14.5	0
14050	The stability and dynamics of the A <sup>240</sup> /A <sup>242</sup> interlaced mixed fibrils. <i>Journal of Biomolecular Structure and Dynamics</i> , 0, , 1-14.	3.5	0
14051	ATP-Bound State of the Uncoupling Protein 1 (UCP1) from Molecular Simulations. <i>Journal of Physical Chemistry B</i> , 2023, 127, 9685-9696.	2.6	0
14052	Molecular mechanisms underlying nanowire formation in pristine phthalocyanine. <i>Physical Chemistry Chemical Physics</i> , 2023, 25, 30259-30268.	2.8	0
14053	Molecular dynamics study of the mechanical properties of drug loaded model systems: A comparison of a polymersome with a bilayer. <i>Journal of Chemical Physics</i> , 2023, 159, .	3.0	0
14055	Identifying potential compounds from <i>Bacopa monnieri</i> (brahmi) against coxsackievirus A16 RdRp targeting HFM disease (tomato flu). <i>Medicine in Novel Technology and Devices</i> , 2023, 20, 100270.	1.6	0
14056	Unraveling the complexity of Exendin-4 folding through two distinct pathways. <i>Journal of Mathematical Chemistry</i> , 0, , .	1.5	0
14057	Hyaluronan-arginine enhanced and dynamic interaction emerges from distinctive molecular signature due to electrostatics and side-chain specificity. <i>Carbohydrate Polymers</i> , 2024, 325, 121568.	10.2	0
14058	Zika virus prM protein contains cholesterol binding motifs required for virus entry and assembly. <i>Nature Communications</i> , 2023, 14, .	12.8	1

#	ARTICLE	IF	CITATIONS
14059	Unsupervised deep learning for molecular dynamics simulations: a novel analysis of proteinâ€“ligand interactions in SARS-CoV-2 M <sup>pro</sup> . RSC Advances, 2023, 13, 34249-34261.	3.6	0
14060	Understanding the Role of Activation Loop Mutants in Drug Efficacy for FLT3-ITD. Cancers, 2023, 15, 5426.	3.7	0
14061	In-depth theoretical study on the structures of betaine-1,2-propanediol based deep eutectic solvents. Journal of Molecular Liquids, 2023, 392, 123453.	4.9	0
14062	Electrostatic interactions of enzymes in non-aqueous conditions: insights from molecular dynamics simulations. Journal of Biomolecular Structure and Dynamics, 0, , 1-14.	3.5	0
14063	In silico study of the impact of oxidation on pyruvate transmission across the hVDAC1 protein channel. Archives of Biochemistry and Biophysics, 2024, 751, 109835.	3.0	0
14064	Theoretical models of staurosporine and analogs uncover detailed structural information in biological solution. Journal of Molecular Graphics and Modelling, 2024, 126, 108653.	2.4	0
14065	<sc><i>PTMâ€“Psi</i></sc>: A python package to facilitate the computational investigation of <sc><i>p</i></sc>ostâ€“<sc><i>t</i></sc>ranslational <sc><i>m</i></sc>odification on <sc><i>p</i></sc>rotein <sc><i>s</i></sc>tructures and their <sc><i>i</i></sc>mpacts on dynamics and functions. Protein Science, 2023, 32, .	7.6	0
14066	Alkyl Derivatives of Perylene Photosensitizing Antivirals: Towards Understanding the Influence of Lipophilicity. International Journal of Molecular Sciences, 2023, 24, 16483.	4.1	0
14067	Dynamical correlations in simple disorder and complex disorder liquids. Journal of Molecular Liquids, 2024, 393, 123421.	4.9	1
14068	Rate-enhancing PETase mutations determined through DFT/MM molecular dynamics simulations. New Journal of Chemistry, 2023, 48, 45-54.	2.8	1
14069	CLIP-Seq analysis enables the design of protective ribosomal RNA bait oligonucleotides against <i>C9ORF72</i> ALS/FTD poly-GR pathophysiology. Science Advances, 2023, 9, .	10.3	1
14070	Machine Learning Subtle Conformational Change due to Phosphorylation in Intrinsically Disordered Proteins. Journal of Physical Chemistry B, 2023, 127, 9433-9449.	2.6	2
14071	Nanoscale creep mechanism of clay through MD modeling with hexagonal particles. International Journal for Numerical and Analytical Methods in Geomechanics, 2024, 48, 538-565.	3.3	0
14072	Revealing the interaction between peptide drugs and permeation enhancers in the presence of intestinal bile salts. Nanoscale, 2023, 15, 19180-19195.	5.6	1
14073	Physical Chemistry of Chloroquine Permeation through the Cell Membrane with Atomistic Detail. Journal of Chemical Information and Modeling, 2023, 63, 7124-7132.	5.4	1
14074	Accurate calculation of affinity changes to the close state of influenza A M2 transmembrane domain in response to subtle structural changes of adamantyl amines using free energy perturbation methods in different lipid bilayers. Biochimica Et Biophysica Acta - Biomembranes, 2024, 1866, 184258.	2.6	0
14075	Activation and substrate specificity of the human P4-ATPase ATP8B1. Nature Communications, 2023, 14, .	12.8	0
14076	Engineering the fracture resistance of 2H-transition metal dichalcogenides using vacancies: An in-silico investigation based on HRTEM images. Materials Today, 2023, 70, 17-32.	14.2	0

#	ARTICLE	IF	CITATIONS
14077	Structural and Functional Insights into the Stealth Protein CpsY of <i>Mycobacterium tuberculosis</i> . <i>Biomolecules</i> , 2023, 13, 1611.	4.0	0
14078	Pathway analysis of host responses to dengue virus serotype 2 infection and inhibition of viral envelope protein by naringenin from <i>Ganoderma lucidum</i> . <i>Journal of Biosciences</i> , 2023, 48, .	1.1	0
14079	The GET insertase exhibits conformational plasticity and induces membrane thinning. <i>Nature Communications</i> , 2023, 14, .	12.8	1
14080	Inter-BRCT linker is probably the most intolerant region of the BRCA1 BRCT domain. <i>Journal of Biomolecular Structure and Dynamics</i> , 0, , 1-13.	3.5	0
14081	Understanding why constant energy or constant temperature may affect nucleation behavior in MD simulations: A study of gas hydrate nucleation. <i>Journal of Chemical Physics</i> , 2023, 159, .	3.0	0
14082	CGCompiler: Automated Coarse-Grained Molecule Parametrization via Noise-Resistant Mixed-Variable Optimization. <i>Journal of Chemical Theory and Computation</i> , 2023, 19, 8384-8400.	5.3	2
14083	Multi-targeting of virulence factors of <i>P. aeruginosa</i> by $\beta$ -lactam antibiotics to combat antimicrobial resistance. <i>Journal of Biomolecular Structure and Dynamics</i> , 0, , 1-19.	3.5	1
14084	Theoretical study of protein adsorption on graphene/h-BN heterostructures. <i>Physical Chemistry Chemical Physics</i> , 2023, 25, 31206-31221.	2.8	0
14085	Surface-Enhanced Raman Scattering-Based Surface Chemotaxonomy: Combining Bacteria Extracellular Matrices and Machine Learning for Rapid and Universal Species Identification. <i>ACS Nano</i> , 2023, 17, 23132-23143.	14.6	0
14086	In Silico Evaluation of Oligomeric Representations for Molecularly Imprinted Polymer Modeling Using a Biological Template. <i>Journal of Chemical Information and Modeling</i> , 2023, 63, 6740-6755.	5.4	0
14087	Structural insights into the activation mechanism of phosphoinositide 3-kinase alpha. <i>Computational Biology and Chemistry</i> , 2024, 108, 107994.	2.3	0
14088	Hypoxia increases persulfide and polysulfide formation by AMP kinase dependent cystathionine gamma lyase phosphorylation. <i>Redox Biology</i> , 2023, 68, 102949.	9.0	2
14089	Molecular Simulations of Ionic Liquids at Charged Graphite Interfaces. <i>Journal of Physical Chemistry C</i> , 2023, 127, 22917-22933.	3.1	0
14090	Inferring free-energy barriers and kinetic rates from molecular dynamics via underdamped Langevin models. <i>Journal of Chemical Physics</i> , 2023, 159, .	3.0	0
14091	Mode and mechanism of water droplet breakup in oil under high-voltage and high-frequency pulsed electric fields. <i>Journal of Molecular Liquids</i> , 2023, 392, 123500.	4.9	0
14092	HDAC inhibition by <i>Nigella sativa</i> L. sprouts extract in hepatocellular carcinoma: an approach to study anti-cancer potential. <i>Journal of Biomolecular Structure and Dynamics</i> , 0, , 1-19.	3.5	0
14093	Elevator-like movements of prestin mediate outer hair cell electromotility. <i>Nature Communications</i> , 2023, 14, .	12.8	3
14094	Mechanisms of Fibroblast Growth Factor 21 Adsorption on Macroion Layers: Molecular Dynamics Modeling and Kinetic Measurements. <i>Biomolecules</i> , 2023, 13, 1709.	4.0	0

#	ARTICLE	IF	CITATIONS
14095	Size matters: asphaltenes with enlarged aromatic cores promote heat transfer in organic phase-change materials. <i>Physical Chemistry Chemical Physics</i> , 2023, 25, 32196-32207.	2.8	0
14096	Toward Metal Extraction from Regolith: Theoretical Investigation of the Solvation Structure and Dynamics of Metal Ions in Ionic Liquids. <i>Journal of Physical Chemistry B</i> , 2023, 127, 9985-9996.	2.6	0
14097	Exploring the conformational dynamics and thermodynamics of <i>EGFR</i> S768I and G719X + S768I mutations in non-small cell lung cancer: An <i>in silico</i> approaches. <i>Open Life Sciences</i> , 2023, 18, .	1.4	0
14098	Molecular Dynamics Simulation Studies on the Micromorphology and Proton Transport of Nafion/Ti3C2Tx Composite Membrane. <i>Chinese Journal of Polymer Science (English Edition)</i> , 2024, 42, 373-387.	3.8	0
14099	Interaction between a water-soluble anionic porphyrin and human serum albumin unexpectedly stimulates the aggregation of the photosensitizer at the surface of the albumin. <i>International Journal of Biological Macromolecules</i> , 2024, 255, 128210.	7.5	2
14100	How does aggregation of doxorubicin molecules affect its solvation and membrane penetration?. <i>New Journal of Chemistry</i> , 2023, 47, 22063-22077.	2.8	0
14101	Structural insights into the co-aggregation of A $\beta$ 2 and tau amyloid core peptides: Revealing potential pathological heterooligomers by simulations. <i>International Journal of Biological Macromolecules</i> , 2024, 254, 127841.	7.5	1
14102	Redox-Based Defect Detection in Packed DNA: Insights from Hybrid Quantum Mechanical/Molecular Mechanics Molecular Dynamics Simulations. <i>Journal of Chemical Theory and Computation</i> , 2023, 19, 8434-8445.	5.3	0
14103	Designing a polyvalent vaccine targeting multiple strains of varicella zoster virus using integrated bioinformatics approaches. <i>Frontiers in Microbiology</i> , 0, 14, .	3.5	0
14104	Exploring preferred binding domains of <scp>IgG1 mAbs</scp> to multimodal adsorbents using a combined biophysics and simulation approach. <i>Biotechnology Progress</i> , 0, , .	2.6	0
14105	Molecularâ€Level Insight into Impact of Additives on Film Formation and Molecular Packing in Y6â€based Organic Solar Cells. <i>Small</i> , 0, , .	10.0	0
14106	Graphene quantum dots blocking the channel egresses of cytochrome P450 enzyme (CYP3A4) reveals potential toxicity. <i>Scientific Reports</i> , 2023, 13, .	3.3	0
14107	Optimizing biodegradable plastics: Molecular dynamics insights into starch plasticization with glycerol and oleic acid. <i>Journal of Molecular Graphics and Modelling</i> , 2024, 126, 108674.	2.4	0
14108	Atomic insights into the inhibition of R3 domain of tau protein by epigallocatechin gallate, quercetin and gallic acid. <i>Biophysical Chemistry</i> , 2024, 305, 107142.	2.8	0
14109	Collagen Structured Hydration. <i>Biomolecules</i> , 2023, 13, 1744.	4.0	0
14110	Hydrophobic Interaction-Induced Topology-Independent Destabilization of G-Quadruplex. <i>Biochemistry</i> , 2023, 62, 3430-3439.	2.5	2
14111	Targetâ€ligand binding affinity from single point enthalpy calculation and elemental composition. <i>Physical Chemistry Chemical Physics</i> , 2023, 25, 31714-31725.	2.8	0
14112	Conformational plasticity and allosteric communication networks explain Shelterin protein TPP1 binding to human telomerase. <i>Communications Chemistry</i> , 2023, 6, .	4.5	0



#	ARTICLE	IF	CITATIONS
14113	Flow regime transition of multicomponent oil in shale nanopores. <i>Fuel</i> , 2024, 359, 130431.	6.4	1
14114	Microscopic insights into poly- and mono-crystalline methane hydrate dissociation in Na-montmorillonite pores at static and dynamic fluid conditions. <i>Energy</i> , 2024, 288, 129755.	8.8	0
14115	Cognitive impairment in long-living adults: a genome-wide association study, polygenic risk score model and molecular modeling of the APOE protein. <i>Frontiers in Aging Neuroscience</i> , 0, 15, .	3.4	1
14116	Effect of Terahertz Waves on the Structure of the A $\beta$ 242 Monomer, Dimer, and Protofibril: Insights from Molecular Dynamics Simulations. <i>ACS Chemical Neuroscience</i> , 2023, 14, 4128-4138.	3.5	0
14117	Deciphering the Role of Anions of Ionic Liquids in Modulating the Structure and Stability of ct-DNA in Aqueous Solutions. <i>Langmuir</i> , 2023, 39, 17318-17332.	3.5	0
14118	Solvent effects on extractant conformational energetics in liquid-liquid extraction: a simulation study of molecular solvents and ionic liquids. <i>Physical Chemistry Chemical Physics</i> , 0, , .	2.8	0
14119	Comparative Analysis of Protein Surface Hydrophobicity Maps Determined by Sparse Sampling INDUS and Spatial Aggregation Propensity. <i>Journal of Physical Chemistry B</i> , 2023, 127, 10304-10314.	2.6	0
14120	Shear-Enhanced Ion Rejection during Seawater Freezing. <i>Journal of Physical Chemistry B</i> , 2023, 127, 10404-10410.	2.6	0
14121	Molecular annotation of G protein variants in a neurological disorder. <i>Cell Reports</i> , 2023, 42, 113462.	6.4	0
14122	Membrane potential accelerates sugar uptake by stabilizing the outward facing conformation of the Na/glucose symporter vSGLT. <i>Nature Communications</i> , 2023, 14, .	12.8	0
14123	An atypical GABARAP binding module drives the pro-autophagic potential of the AML-associated NPM1c variant. <i>Cell Reports</i> , 2023, 42, 113484.	6.4	0
14124	An extended Tudor domain within Vreteno interconnects Gtsf1L and Ago3 for piRNA biogenesis in <i>Bombyx mori</i> . <i>EMBO Journal</i> , 2023, 42, .	7.8	2
14125	Competition between superconductivity and molecularization in the quantum nuclear behavior of lanthanum hydride. <i>Physical Review B</i> , 2023, 108, .	3.2	1
14126	Structure-based virtual screening, ADMET analysis, and molecular dynamics simulation of Moroccan natural compounds as candidates for the SARS-CoV-2 inhibitors. <i>Natural Product Research</i> , 0, , 1-8.	1.8	2
14127	Molecular Dynamics Simulation on the Charge Transport Properties in a Salt-in-Ionic Liquid Electrolyte. <i>Journal of Physical Chemistry B</i> , 2023, 127, 10434-10446.	2.6	0
14128	Development of a scalable single process for producing SARS-CoV-2 RBD monomer and dimer vaccine antigens. <i>Frontiers in Bioengineering and Biotechnology</i> , 0, 11, .	4.1	0
14129	Pterostilbene-Isothiocyanate Inhibits Proliferation of Human MG-63 Osteosarcoma Cells via Abrogating $\beta$ -Catenin/TCF-4 Interaction—A Mechanistic Insight. <i>ACS Omega</i> , 2023, 8, 43474-43489.	3.5	0
14130	Machine learning molecular dynamics reveals the structural origin of the first sharp diffraction peak in high-density silica glasses. <i>Scientific Reports</i> , 2023, 13, .	3.3	1

#	ARTICLE	IF	CITATIONS
14131	A computational simulation appraisal of banana lectin as a potential anti-SARS-CoV-2 candidate by targeting the receptor-binding domain. Journal of Genetic Engineering and Biotechnology, 2023, 21, 148.	3.3	1
14132	Design and Multiple Performance Evaluation of Green Sustainable Process for Azeotropes Separation via Extractive Distillation. ACS Sustainable Chemistry and Engineering, 2023, 11, 16849-16881.	6.7	3
14133	Five similar anthocyanidin molecules display distinct disruptive effects and mechanisms of action on A $\beta$ 1-42 protofibril: A molecular dynamic simulation study. International Journal of Biological Macromolecules, 2024, 256, 128467.	7.5	1
14134	Structural basis for human Cav1.2 inhibition by multiple drugs and the neurotoxin calciseptine. Cell, 2023, 186, 5363-5374.e16.	28.9	2
14135	Viscosity reduction mechanism of surface-functionalized Fe <sub>3</sub> O <sub>4</sub> nanoparticles in different types of heavy oil. Fuel, 2024, 360, 130535.	6.4	0
14136	Salt Effects on Caffeine across Concentration Regimes. Journal of Physical Chemistry B, 2023, 127, 10253-10265.	2.6	0
14137	Multiscale Molecular Dynamics Simulations of Ice-Binding Proteins. Methods in Molecular Biology, 2024, , 185-202.	0.9	0
14138	Osmotic Force Balance Evaluation of Aqueous Electrolyte Osmotic Pressures and Chemical Potentials. Journal of Chemical Theory and Computation, 2023, 19, 8826-8838.	5.3	1
14139	Improved Protein Model in SPICA Force Field. Journal of Chemical Theory and Computation, 2023, 19, 8967-8977.	5.3	3
14140	Assessing the Binding Mode of a Splicing Modulator Stimulating Pre-mRNA Binding to the Plastic U2AF2 Splicing Factor. Journal of Chemical Information and Modeling, 2023, 63, 7508-7517.	5.4	1
14141	Solution critical temperature through Excess-entropy-Diffusivity lens. Journal of Molecular Liquids, 2024, 394, 123785.	4.9	0
14142	Stuttering associated with a pathogenic variant in the chaperone protein cyclophilin 40. Brain, 2023, 146, 5086-5097.	7.6	1
14143	Conductivity and Transference Numbers in Lithium Salt-Doped Block Copolymeric Ionic Liquid Electrolytes. Macromolecules, 2023, 56, 9750-9765.	4.8	0
14144	Periplasmic chitooligosaccharide-binding protein requires a three-domain organization for substrate translocation. Scientific Reports, 2023, 13, .	3.3	0
14145	Inhibition of SARS-CoV-2 NSP15 by Uridine-5'-Monophosphate Analogues Using QSAR Modelling, Molecular Dynamics Simulations, and Free Energy Landscape. Saudi Pharmaceutical Journal, 2024, 32, 101914.	2.7	0
14146	Investigating the Vapor-Phase Adsorption of Aroma Molecules on the Water-Vapor Interface using Molecular Dynamics Simulations. Langmuir, 2023, 39, 17889-17902.	3.5	1
14147	Further extension of the Madrid-2019 force field: Parametrization of nitrate (NO <sub>3</sub> <sup>-</sup> ) and ammonium (NH <sub>4</sub> <sup>+</sup> ) ions. Journal of Chemical Physics, 2023, 159, .	3.0	1
14148	Tld1 is a regulator of triglyceride lipolysis that demarcates a lipid droplet subpopulation. Journal of Cell Biology, 2024, 223, .	5.2	2

#	ARTICLE	IF	CITATIONS
14150	HPTLC based quantification of $\beta$ -sitosterol from the leaves of <i>Nyctanthes arbor-tristis</i> and <i>in-silico</i> prediction of potential drug targeted towards cancer therapy. Journal of Biomolecular Structure and Dynamics, 0, , 1-8.	3.5	1
14151	Designing and Computational Analysis of Chimeric Avian Influenza Antigen: A Yeast-Displayed Universal and Cross-Protective Vaccine Candidate. , 2023, 1, 1-15.		0
14152	Unveiling a medium-range structural commonality of amorphous alloys. Journal of Non-Crystalline Solids, 2024, 624, 122696.	3.1	0
14153	Physics infused machine learning force fields for 2D materials monolayers. , 0, 3, .		0
14157	Molecular insights into the synergistic mechanisms of hybrid CO <sub>2</sub> -surfactant thermal systems at heavy oil-water interfaces. Energy, 2024, 286, 129476.	8.8	3
14158	Evaluation of Supervised Machine Learning Algorithms and Computational Structural Validation of Single Nucleotide Polymorphisms Related to Acute Liver Injury with Paracetamol. Current Drug Metabolism, 2023, 24, .	1.2	0
14159	Martensitic Phase Transition in TiNi Thin Plates with Different Surface Crystallographic Orientations. , 2023, , .		0
14160	Controlling Supramolecular Fiber Formation of Nucleopeptide by Guanosine Triphosphate. Biomacromolecules, 2023, 24, 5678-5686.	5.4	0
14161	Deciphering specificity and cross-reactivity in tachykinin NK1 and NK2 receptors. Journal of Biological Chemistry, 2023, 299, 105438.	3.4	0
14163	Lipid and cholesterol modulate the dynamics of SARS-CoV-2 viral ion channel ORF3a and its pathogenic variants. International Journal of Biological Macromolecules, 2024, 254, 127986.	7.5	0
14164	Combined Computationalâ€Biochemical Approach Offers an Accelerated Path to Membrane Protein Solubilization. Journal of Chemical Information and Modeling, 2023, 63, 7159-7170.	5.4	0
14165	Effects of surfactants on droplet deformation and breakup in water-in-oil emulsions under DC electric field: A molecular dynamics study. Fuel, 2024, 358, 130328.	6.4	1
14167	Wetting and spreading of AgCuTi on Fe substrate at high temperatures: A molecular dynamics study. Journal of Materials Research and Technology, 2023, 27, 5783-5790.	5.8	0
14168	Drug repurposing for targeting fibronectin in treatment of endometriosis and cancers. Journal of Biomolecular Structure and Dynamics, 0, , 1-17.	3.5	0
14169	Structure-Based Optimization of Carbendazim-Derived Tubulin Polymerization Inhibitors through Alchemical Free Energy Calculations. Journal of Chemical Information and Modeling, 2023, 63, 7228-7238.	5.4	0
14170	Construction of quercetin-fucoidan nanoparticles and their application in cancer chemo-immunotherapy treatment. International Journal of Biological Macromolecules, 2024, 256, 128057.	7.5	0
14171	Analysis of stabilization mechanisms in $\beta$ -lactoglobulin-based amorphous solid dispersions by experimental and computational approaches. European Journal of Pharmaceutical Sciences, 2024, 192, 106639.	4.0	1
14172	Mechanism of substrate binding and transport in BASS transporters. ELife, 0, 12, .	6.0	0

#	ARTICLE	IF	CITATIONS
14173	<i>K</i> -Means Clustering Coarse-Graining (KMC-CG): A Next Generation Methodology for Determining Optimal Coarse-Grained Mappings of Large Biomolecules. Journal of Chemical Theory and Computation, 2023, 19, 8987-8997.	5.3	0
14175	Computational and in vitro targeting of HUVECs by ARA-Linker-TGF $\beta$ 1L3 through VEGFR2. Molecular Simulation, 2024, 50, 137-147.	2.0	0
14177	Design of a new potent Alzheimer's disease inhibitor based on QSAR, molecular docking and molecular dynamics investigations. Chemical Physics Impact, 2023, 7, 100361.	3.5	4
14178	Lightweight Extendable Stacking Framework for Structure Classification in Atomistic Simulations. Journal of Chemical Theory and Computation, 2023, 19, 8332-8339.	5.3	0
14179	Integrated workflow for the identification of new GABA <sub>A</sub> positive allosteric modulators based on the <i>in silico</i> screening with further <i>in vitro</i> validation. Case study using Enamine's stock chemical space. Molecular Informatics, 2024, 43, .	2.5	0
14180	Molecular mechanism of calcitriol enhances membrane water permeability. Biochimica Et Biophysica Acta - Molecular and Cell Biology of Lipids, 2024, 1869, 159430.	2.4	0
14181	Micro-Solvation of Propofol in Propylene Glycol-Water Binary Mixtures: Molecular Dynamics Simulation Studies. Journal of Physical Chemistry B, 0, , .	2.6	0
14183	Conformational transitions of the HIV-1 Gag polyprotein upon multimerization and gRNA binding. Biophysical Journal, 2023, , .	0.5	1
14184	The Challenges of Using COSMO-RS To Describe Polymer Solution Behavior. Industrial & Engineering Chemistry Research, 2023, 62, 20936-20944.	3.7	1
14187	In vitro and in silico evaluation of the antimicrobial and antioxidant activities of spiropyrazoline oxindole congeners. Arabian Journal of Chemistry, 2024, 17, 105465.	4.9	1
14188	Density and Viscosity of (Ethyl Acetate + Diethyl Succinate) Mixtures: Experimental Measurements and Molecular Dynamics Simulations. Journal of Chemical & Engineering Data, 0, , .	1.9	0
14189	Cyclic Peptides as Aggregation Inhibitors for Sickle Cell Disease. Journal of Medicinal Chemistry, 0, , .	6.4	0
14190	Molecular mechanism of regulation of RhoA GTPase by phosphorylation of RhoGDI. Biophysical Journal, 2023, , .	0.5	0
14192	<i>In silico</i> exploration and <i>in vitro</i> validation of the filarial thioredoxin reductase inhibitory activity of Scytonemin and its derivatives. Journal of Biomolecular Structure and Dynamics, 0, , 1-13.	3.5	0
14193	The non-thermal influences of ultrasound on cell membrane: A molecular dynamics study. Journal of Molecular Structure, 2024, 1299, 137140.	3.6	0
14194	Structure-guided design of a trivalent nanobody cluster targeting SARS-CoV-2 spike protein. International Journal of Biological Macromolecules, 2024, 256, 128191.	7.5	1
14196	Molecular dynamics simulations reveal methylation in Me-GDGTs as a microbial low-temperature adaptation. Chemical Geology, 2024, 644, 121844.	3.3	0
14198	Modeling the release of vinpocetine from microcapsules based on sodium alginate and chitosan by molecular dynamics. , 2023, 22, 68-75.	0.3	0

#	ARTICLE	IF	CITATIONS
14199	Thermal Sensitivity of the Enzymatic Activity of Î²-Glucosidase: Simulations Lend Mechanistic Insights into Experimental Observations. <i>Biochemistry</i> , 2023, 62, 3440-3452.	2.5	0
14202	Investigating ionic liquid hydration effects at high temperatures: Insights from classic molecular dynamics simulations. <i>Journal of Molecular Liquids</i> , 2024, 393, 123662.	4.9	0
14203	The dynamics of <i>Escherichia coli</i> FtsZ dimer. <i>Journal of Biomolecular Structure and Dynamics</i> , 0, , 1-14.	3.5	0
14204	Influence of ZrF4 additive on the local structures and thermophysical properties of molten NaF-BeF2. <i>Journal of Molecular Liquids</i> , 2024, 393, 123681.	4.9	0
14205	Seawater-based methane storage via mixed CH4/1,3-dioxane hydrates: Insights from experimental and molecular dynamic simulations. <i>Chemical Engineering Journal</i> , 2024, 479, 147721.	12.7	0
14206	Total revalorization of high impact polystyrene (HIPS): enhancing styrene recovery and upcycling of the rubber phase. <i>Green Chemistry</i> , 0, , .	9.0	0
14207	Spidroins under the Influence of Alcohol: Effect of Ethanol on Secondary Structure and Molecular Level Solvation of Silk-Like Proteins. <i>Biomacromolecules</i> , 2023, 24, 5638-5653.	5.4	0
14208	Martini 3 Force Field Parameters for Protein Lipidation Post-Translational Modifications. <i>Journal of Chemical Theory and Computation</i> , 2023, 19, 8901-8918.	5.3	0
14209	Functional Groups Accessibility and the Origin of Photoluminescence in N/Oâ€containing Bottomâ€ Carbon Nanodots. <i>ChemNanoMat</i> , 2024, 10, .	2.8	0
14210	Linear and Ring Polypeptides Complexed with Oppositely Charged Surfactants. The Cohesion of the Complexes as Revealed in Atomistic Simulations. <i>Soft Matter</i> , 0, , .	2.7	0
14211	Chilling alcohol on the computer: isothermal compressibility and the formation of hydrogen-bond clusters in liquid propan-1-ol. <i>European Physical Journal E</i> , 2023, 46, .	1.6	0
14212	DypB peroxidase for aflatoxin removal: New insights into the toxin degradation process. <i>Chemosphere</i> , 2024, 349, 140826.	8.2	0
14213	Unlocking the mysterious polytypic features within vaterite CaCO3. <i>Nature Communications</i> , 2023, 14, .	12.8	0
14214	Computer simulation of carbonization and graphitization of coal. <i>Nanotechnology</i> , 2024, 35, 095703.	2.6	1
14215	Structureâ€Interaction Relationship of Polymyxins with Lung Surfactant. <i>Journal of Medicinal Chemistry</i> , 0, , .	6.4	0
14216	Synergistic Effect of Hyperactive Antifreeze Protein on Inhibition of Gas-Hydrate Growth by Hydrophobic and Hydrophilic Groups. <i>Journal of Physical Chemistry B</i> , 0, , .	2.6	0
14217	Synthesis and Characterization of Ionic Li+@C70 Endohedral Fullerene. <i>Chemistry - A European Journal</i> , 0, , .	3.3	0
14218	Combined Classical and Flooding Molecular Dynamics Simulations of The Mip-Rapamycin and FKBP12-Rapamycin Complexes. <i>Jurnal Kimia Sains Dan Aplikasi</i> , 2023, 26, 300-309.	0.4	0

#	ARTICLE	IF	CITATIONS
14221	Prediction of Toluene/Water Partition Coefficients of SAMPL9 compounds: Comparison of the molecular dynamics force fields GAFF/RESP and GAFF/IPolQ-Mod+LJ-fit. Physical Chemistry Chemical Physics, 0, , .	2.8	0
14222	Synthesis and evaluation of hybrid sulfonamide–chalcones with potential antileishmanial activity. Archiv Der Pharmazie, 2024, 357, .	4.1	0
14223	Self-Defensive Antimicrobial Shape Memory Polyurethanes with Honey-Based Compounds. ACS Applied Materials & Interfaces, 0, , .	8.0	0
14225	Accelerating and Automating the Free Energy Perturbation Absolute Binding Free Energy Calculation with the RED-E Function. Journal of Chemical Information and Modeling, 2023, 63, 7755-7767.	5.4	1
14226	Acetylation of Nanocellulose: Miscibility and Reinforcement Mechanisms in Polymer Nanocomposites. ACS Nano, 0, , .	14.6	0
14227	Titin domains with reduced core hydrophobicity cause dilated cardiomyopathy. Cell Reports, 2023, 42, 113490.	6.4	0
14229	Oxidation-induced superelasticity in metallic glass nanotubes. Nature Materials, 0, , .	27.5	0
14231	Computationally Designed Molecules Modulate ALS-Related Amyloidogenic TDP-43 <sup>307–319</sup> Aggregation. ACS Chemical Neuroscience, 2023, 14, 4395-4408.	3.5	1
14232	Diffusion and Coalescence of Phosphorene Monovacancies Studied Using High-Dimensional Neural Network Potentials. Journal of Physical Chemistry C, 0, , .	3.1	0
14233	An Uncertainty-Guided Deep Learning Method Facilitates Rapid Screening of CYP3A4 Inhibitors. Journal of Chemical Information and Modeling, 0, , .	5.4	0
14234	Theoretical Investigation of Lead Perovskite PbXO <sub>3</sub> (X = Ti, Zr, and Hf) for Potential Thermoelectric Applications: Hybrid-DFT Approach. Energy & Fuels, 0, , .	5.1	0
14235	An OrthoBoXY-method for various alternative box geometries. Physical Chemistry Chemical Physics, 0, , .	2.8	1
14236	Mechanisms of DNA-Mediated Allostery. Physical Review Letters, 2023, 131, .	7.8	0
14237	Modelling and Molecular Dynamics Predict the Structure and Interactions of the Glycine Receptor Intracellular Domain. Biomolecules, 2023, 13, 1757.	4.0	0
14239	Exploring the role of cyclodextrins as a cholesterol scavenger: a molecular dynamics investigation of conformational changes and thermodynamics. Scientific Reports, 2023, 13, .	3.3	1
14240	Phospholipids are imported into mitochondria by VDAC, a dimeric beta barrel scramblase. Nature Communications, 2023, 14, .	12.8	1
14241	Analysis of bioactive compounds of <i>Olea europaea</i> as potential inhibitors of SARS-CoV-2 main protease: a pharmacokinetics, molecular docking and molecular dynamics simulation studies. Journal of Biomolecular Structure and Dynamics, 0, , 1-12.	3.5	0
14242	Evolution towards simplicity in bacterial small heat shock protein system. ELife, 0, 12, .	6.0	0



#	ARTICLE	IF	CITATIONS
14243	Membrane platform protein PulF of the <i>Klebsiella</i> type II secretion system forms a trimeric ion channel essential for endopilus assembly and protein secretion. MBio, 0, , .	4.1	0
14245	Biological evaluation, molecular modeling and dynamic simulation of IDQ bulk and IDQNPs: Organo nano-bio interface in the medical field. Journal of Molecular Structure, 2024, 1301, 137288.	3.6	1
14246	Development of machine learning interatomic potential for zinc. Computational Materials Science, 2024, 233, 112723.	3.0	0
14247	De novo drug designing coupled with brute force screening and structure guided lead optimization gives highly specific inhibitor of METTL3: a potential cure for Acute Myeloid Leukaemia. Journal of Biomolecular Structure and Dynamics, 0, , 1-14.	3.5	0
14249	Specific protonation of acidic residues confers K <sup>+</sup> selectivity to the gastric proton pump. Journal of Biological Chemistry, 2023, , 105542.	3.4	0
14250	Unveiling the structural organisation of carvacrol through X-ray scattering and molecular Dynamics: A comparative study with liquid thymol. Journal of Molecular Liquids, 2024, 394, 123778.	4.9	0
14251	Quantifying the Nearly Random Microheterogeneity of Aqueous <i>tert</i> -Butyl Alcohol Solutions Using Vibrational Spectroscopy. Journal of Physical Chemistry Letters, 0, , 11376-11383.	4.6	0
14252	Trapping a non-cognate nucleotide upon initial binding for replication fidelity control in SARS-CoV-2 RNA dependent RNA polymerase. Physical Chemistry Chemical Physics, 2024, 26, 1792-1808.	2.8	0
14253	AAP-MSMD: Amino Acid Preference Mapping on Protein-Protein Interaction Surfaces Using Mixed-Solvent Molecular Dynamics. Journal of Chemical Information and Modeling, 0, , .	5.4	0
14254	Selection of Aptamers for Use as Molecular Probes in AFM Detection of Proteins. Biomolecules, 2023, 13, 1776.	4.0	0
14255	Scrutinizing the protein hydration shell from molecular dynamics simulations against consensus small-angle scattering data. Communications Chemistry, 2023, 6, .	4.5	1
14256	New Insights into the LANCL2-ABA Binding Mode towards the Evaluation of New LANCL Agonists. Pharmaceutics, 2023, 15, 2754.	4.5	1
14257	Synthesis, structure elucidation, SC-XRD/DFT, molecular modelling simulations and DNA binding studies of 3,5-diphenyl-4,5-dihydro-1 <i>H</i> -pyrazole chalcones. Journal of Biomolecular Structure and Dynamics, 0, , 1-16.	3.5	0
14258	Structure and Elasticity of Mitochondrial Membranes: A Molecular Dynamics Simulation Study. Journal of Physical Chemistry B, 2023, 127, 10778-10791.	2.6	1
14259	Molecular insights into the differential membrane targeting of maximin 1 in prokaryotic and eukaryotic cells. Journal of Biomolecular Structure and Dynamics, 0, , 1-14.	3.5	0
14260	Revealing the Formation Dynamics of Janus Polymer Particles: Insights from Experiments and Molecular Dynamics. Journal of Chemical Information and Modeling, 2023, 63, 7453-7463.	5.4	0
14261	Villin headpiece unfolding upon binding to boridene mediated by the "anchoring-perturbation" mechanism. IScience, 2024, 27, 108577.	4.1	0
14262	Nonuniversal impact of cholesterol on membranes mobility, curvature sensing and elasticity. Nature Communications, 2023, 14, .	12.8	0

#	ARTICLE	IF	CITATIONS
14263	Peptide Power: Mechanistic Insights into the Effect of Mitochondria-Targeted Tetrapeptides on Membrane Electrostatics from Molecular Simulations. <i>Molecular Pharmaceutics</i> , 2023, 20, 6114-6129.	4.6	1
14264	Dissociation line and driving force for nucleation of the nitrogen hydrate from computer simulation. <i>Journal of Chemical Physics</i> , 2023, 159, .	3.0	0
14265	Amino acid ionic liquids as efficient catalysts for CO <sub>2</sub> capture: A combined static and dynamic approach. <i>Results in Surfaces and Interfaces</i> , 2024, 14, 100175.	2.4	0
14266	Investigation of the interfacial phenomena in the presence of nonionic surfactants and a silica nanoparticle at the n-decane-water interface: Insights from molecular dynamics simulation. <i>Journal of Molecular Liquids</i> , 2024, 394, 123789.	4.9	0
14267	Protein stability in a natural deep eutectic solvent: Preferential hydration or solvent slaving?. <i>Journal of Chemical Physics</i> , 2023, 159, .	3.0	1
14268	Monovalent metal ion binding promotes the first transesterification reaction in the spliceosome. <i>Nature Communications</i> , 2023, 14, .	12.8	0
14269	Variations of the Mycobacterium abscessus F-ATP synthase subunit a-c interface alter binding and potency of the anti-TB drug bedaquiline. <i>Biochemical and Biophysical Research Communications</i> , 2024, 690, 149249.	2.1	1
14270	Deep learning structural insights into heterotrimeric alternatively spliced P2X <sub>7</sub> receptors. <i>Purinergic Signalling</i> , 0, , .	2.2	0
14271	Molecular basis and cellular functions of vinculin-actin directional catch bonding. <i>Nature Communications</i> , 2023, 14, .	12.8	2
14272	Probing Reactivity with External Forces: The Case of Nitroacetamides in Water. <i>Molecules</i> , 2024, 29, 9.	3.8	0
14273	Adsorption of zwitterionic oligomer-grafted silica nanoparticles on rock surface in enhanced oil recovery studied by molecular dynamics simulations. <i>Colloids and Surfaces A: Physicochemical and Engineering Aspects</i> , 2024, 684, 133013.	4.7	0
14274	Serine-129 phosphorylation of Î±-synuclein is an activity-dependent trigger for physiologic protein-protein interactions and synaptic function. <i>Neuron</i> , 2023, 111, 4006-4023.e10.	8.1	4
14275	Immunoinformatics-aided rational design of a multi-epitope vaccine targeting feline infectious peritonitis virus. <i>Frontiers in Veterinary Science</i> , 0, 10, .	2.2	1
14276	RNA G-quadruplex folding is a multi-pathway process driven by conformational entropy. <i>Nucleic Acids Research</i> , 2024, 52, 87-100.	14.5	1
14278	Insights on the conformation and appropriate drug-target sites on retinal IMPDH1 using the 604-aa isoform lacking the C-terminal extension. <i>Research in Pharmaceutical Sciences</i> , 2023, 18, 638-647.	1.8	0
14279	The ternary phase diagram of nitrogen doped lutetium hydrides can not explain its claimed high T <sub>c</sub> superconductivity. <i>New Journal of Physics</i> , 2023, 25, 123008.	2.9	1
14280	Structural insights into ACE2 interactions and immune activation of SARS-CoV-2 and its variants: an <i>in-silico</i> study. <i>Journal of Biomolecular Structure and Dynamics</i> , 0, , 1-14.	3.5	0
14281	Influence of Anion Species on Liquid-Liquid Phase Separation in [EMIm] <sup>+</sup> [X] <sup>-</sup> /Benzene Mixtures. <i>Journal of Physical Chemistry B</i> , 2023, 127, 10583-10591.	2.6	0

#	ARTICLE	IF	CITATIONS
14282	Underpinning beneficial maize response to application of minimally processed homogenates of red and brown seaweeds. <i>Frontiers in Plant Science</i> , 0, 14, .	3.6	0
14283	Molecular dynamics simulations on the interactions between nucleic acids and a phospholipid bilayer. <i>Chinese Physics B</i> , 0, , .	1.4	0
14284	SlyB encapsulates outer membrane proteins in stress-induced lipid nanodomains. <i>Nature</i> , 2024, 626, 617-625.	27.8	1
14285	Molecular insights into anti-Protozoal action of natural compounds against <i>Cryptosporidium parvum</i> : a molecular simulation study. <i>Journal of Biomolecular Structure and Dynamics</i> , 0, , 1-17.	3.5	0
14286	Integrated Quantum-Classical Protocol for the Realistic Description of Solvated Multinuclear Mixed-Valence Transition-Metal Complexes and Their Solvatochromic Properties. <i>Journal of Chemical Theory and Computation</i> , 2024, 20, 1306-1323.	5.3	0
14287	Decoding the therapeutic landscape of alpha-linolenic acid: a network pharmacology and bioinformatics investigation against cancer-related epigenetic modifiers. <i>Journal of Biomolecular Structure and Dynamics</i> , 0, , 1-26.	3.5	1
14293	Deciphering Lipid Arrangement in Phosphatidylserine/Phosphatidylcholine Mixed Membranes: Simulations and Experiments. <i>Langmuir</i> , 0, , .	3.5	0
14294	Using Metadynamics to Reveal Extractant Conformational Free Energy Landscapes. <i>Journal of Physical Chemistry B</i> , 0, , .	2.6	0
14295	Data-driven prediction of $\beta$ 2 integrin activation pathways using nonlinear manifold learning and deep generative modeling. <i>Biophysical Journal</i> , 2023, , .	0.5	0
14296	Molecular Insight into the Effect of Polymer Topology on Wettability of Block Copolymers: The Case of Amphiphilic Polyurethanes. <i>Langmuir</i> , 0, , .	3.5	0
14297	Modeling Substrate Entry into the P-Glycoprotein Efflux Pump at the Blood–Brain Barrier. <i>Journal of Medicinal Chemistry</i> , 0, , .	6.4	0
14298	Construing the Interactions of Coumarin Derivatives with the Main Protease of Stomach Pepsin Using Spectroscopic and Computational Analyses: Insights into the Binding Thermodynamics, Antifibrillation Studies, and Enzymatic Assay. <i>ACS Food Science &amp; Technology</i> , 0, , .	2.7	0
14299	Strong and selective interactions of palmatine with G-rich sequences in TRF2 promoter; experimental and computational studies. <i>Journal of Biomolecular Structure and Dynamics</i> , 0, , 1-15.	3.5	0
14302	The innate interfacial elastic strain field of a transformable B2 precipitate embedded in an amorphous matrix. <i>Npj Computational Materials</i> , 2023, 9, .	8.7	0
14303	Large mechanical properties enhancement in ceramics through vacancy-mediated unit cell disturbance. <i>Nature Communications</i> , 2023, 14, .	12.8	0
14304	Shocker’s Molecular Dynamics Protocol and Tool for Accelerating and Analyzing the Effects of Osmotic Shocks. <i>Journal of Chemical Theory and Computation</i> , 2024, 20, 212-223.	5.3	0
14305	<i>In silico</i> identification and characterization of small molecule binding to the CD1d immunoreceptor. <i>Journal of Biomolecular Structure and Dynamics</i> , 0, , 1-19.	3.5	0
14306	Designing a Multiepitope Vaccine against Eastern Equine Encephalitis Virus: Immunoinformatics and Computational Approaches. <i>ACS Omega</i> , 0, , .	3.5	1

#	ARTICLE	IF	CITATIONS
14307	Four-dimensional imaging for cryo-electron microscopy experiments using molecular simulations and manifold learning. Journal of Computational Chemistry, 0, , .	3.3	0
14308	Molecular dynamics simulations show how antibodies may rescue HIV-1 mutants incapable of infecting host cells. Journal of Biomolecular Structure and Dynamics, 0, , 1-11.	3.5	0
14309	Biophysical basis of filamentous phage tactoid-mediated antibiotic tolerance in P. aeruginosa. Nature Communications, 2023, 14, .	12.8	1
14310	Unraveling viral drug targets: a deep learning-based approach for the identification of potential binding sites. Briefings in Bioinformatics, 2023, 25, .	6.5	0
14311	Palmitoylation of the Glucagon-like Peptide-1 Receptor Modulates Cholesterol Interactions at the Receptor-Lipid Microenvironment. Journal of Physical Chemistry B, 0, , .	2.6	1
14312	Preventing amyloid- $\beta$ oligomerization and aggregation with berberine: Investigating the mechanism of action through computational methods. International Journal of Biological Macromolecules, 2024, 258, 128900.	7.5	0
14314	Elucidating the microscopic origin of observed anti-correlation between the protein-protein and protein-water interaction energies. Chemical Physics Impact, 2024, 8, 100421.	3.5	0
14315	Computational Prediction of Coiled-Coil Protein Gelation Dynamics and Structure. Biomacromolecules, 0, , .	5.4	0
14316	Structural Insights into the Activation of Human Aryl Hydrocarbon Receptor by the Environmental Contaminant Benzo[a]pyrene and Structurally Related Compounds. Journal of Molecular Biology, 2024, 436, 168411.	4.2	1
14317	BthTX-I, a phospholipase A2-like toxin, is inhibited by the plant cinnamic acid derivative: Chlorogenic acid. Biochimica Et Biophysica Acta - Proteins and Proteomics, 2023, , 140988.	2.3	0
14318	Size Matters: A Computational Study of Hydrogen Absorption in Ionic Liquids. Journal of Chemical Information and Modeling, 0, , .	5.4	0
14321	Molecular Dynamics Simulation of an Iron(III) Binding Site on the Fc Domain of IgG1 Relevant for Visible Light-Induced Protein Fragmentation. Molecular Pharmaceutics, 2024, 21, 501-512.	4.6	0
14322	Generalized polarization and time-resolved fluorescence provide evidence for different populations of Laurdan in lipid vesicles. Journal of Photochemistry and Photobiology B: Biology, 2024, 250, 112833.	3.8	0
14323	Atomistic ensemble of active SHP2 phosphatase. Communications Biology, 2023, 6, .	4.4	0
14324	Comprehensive in silico discovery of c-Src tyrosine kinase inhibitors in cancer treatment: A unified approach combining pharmacophore modeling, 3D QSAR, DFT, and molecular dynamics simulation. Journal of King Saud University - Science, 2024, 36, 103076.	3.5	1
14325	Structural mechanism of TRPV5 inhibition by econazole. Structure, 2024, 32, 148-156.e5.	3.3	0
14326	The effects of side chain engineering on the morphology and charge transport of the A <sub>1</sub> type of non-fullerene acceptor: a multiscale study. Physical Chemistry Chemical Physics, 2024, 26, 2666-2677.	2.8	0
14327	Twofold Machine-Learning and Molecular Dynamics: A Computational Framework. Computers, 2024, 13, 2.	3.3	0

#	ARTICLE	IF	CITATIONS
14328	Surface Display and Engineering of Laccase CotA for Increased Growth of <i>Pseudomonas putida</i> on Lignin. <i>ChemCatChem</i> , 2024, 16, .	3.7	0
14329	Excited States of $\alpha$ -Guanidine-III Riboswitch Contribute to Guanidinium Binding through Both Conformational and Induced-Fit Mechanisms. <i>Journal of Chemical Theory and Computation</i> , 0, , .	5.3	0
14331	Molecular mechanisms in the destabilization of the two types of R3-R4 tau fibrils associated with chronic traumatic encephalopathy. <i>Physical Chemistry Chemical Physics</i> , 0, , .	2.8	0
14332	Unraveling the Molecular Mechanisms of Alcohol-Mediated Skin Permeation Enhancement: Insights from Molecular Dynamics Simulations. <i>Langmuir</i> , 0, , .	3.5	0
14333	Mechanical forces control the valency of the malaria adhesin VAR2CSA by exposing cryptic glycan binding sites. <i>PLoS Computational Biology</i> , 2023, 19, e1011726.	3.2	0
14334	Quantitative Ensemble Interpretation of Membrane Paramagnetic Relaxation Enhancement (mPRE) for Studying Membrane-Associated Intrinsically Disordered Proteins. <i>Journal of the American Chemical Society</i> , 2024, 146, 791-800.	13.7	0
14335	Effect of Water-Soluble Polymers on the Dynamics of Carbon Dioxide Sorption by Lime-Based Sorbents. <i>Catalysis in Industry</i> , 2023, 15, 325-332.	0.7	0
14337	Identification and stability analysis of potential ADP-ribose modification sites on vascular endothelial growth factor (VEGF) through molecular dynamics simulation. <i>Journal of Biomolecular Structure and Dynamics</i> , 0, , 1-9.	3.5	0
14338	Atomistic Insights into Hydrogen-Bonded Supramolecular Capsule Self-Assembly Dynamics. <i>Journal of Physical Chemistry C</i> , 0, , .	3.1	0
14339	Separation of Protein Corona from Nanoparticles at the Intracellular Acidic Condition: Effect of Protonation on Nanoparticle-Protein and Protein-Protein Interactions. <i>Physical Chemistry Chemical Physics</i> , 0, , .	2.8	0
14340	Investigating the bispecific lead compounds against methicillin-resistant <i>Staphylococcus aureus</i> SarA and CrtM using machine learning and molecular dynamics approach. <i>Journal of Biomolecular Structure and Dynamics</i> , 0, , 1-18.	3.5	0
14341	Exclusive Ion Recognition Using Host-Guest Sandwich Complexes. <i>Physical Chemistry Chemical Physics</i> , 0, , .	2.8	0
14342	Fluctuation Relations to Calculate Protein Redox Potentials from Molecular Dynamics Simulations. <i>Journal of Chemical Theory and Computation</i> , 0, , .	5.3	1
14343	Molecular docking and MD simulations reveal protease inhibitors block the catalytic residues in Prp8 intein of <i>Aspergillus fumigatus</i> : a potential target for antimycotics. <i>Journal of Biomolecular Structure and Dynamics</i> , 0, , 1-16.	3.5	0
14344	Liquid-Vapor Interface of Aqueous Ethylene Glycol Solutions: A Molecular Dynamics Study. <i>Langmuir</i> , 0, , .	3.5	0
14345	The role of hydrogen bonding in solubilizing camptothecin in hydrophilic and hydrophobic ionic liquids. <i>Green Chemical Engineering</i> , 2023, , .	6.3	0
14346	Enhanced Coarse-Grained Molecular Dynamics Simulation with a Smoothed Hybrid Potential Using a Neural Network Model. <i>Journal of Chemical Theory and Computation</i> , 0, , .	5.3	0
14347	Inhibition of the C1s Protease and the Classical Complement Pathway by 6-(4-Phenylpiperazin-1-yl)Pyridine-3-Carboximidamide and Chemical Analogs. <i>Journal of Immunology</i> , 0, , .	0.8	0

#	ARTICLE	IF	CITATIONS
14348	Network pharmacology, molecular docking and molecular dynamics simulation of chalcone scaffold-based compounds targeting breast cancer receptors. Journal of Biomolecular Structure and Dynamics, 0, , 1-16.	3.5	0
14349	Bioinspired mineral-in-shell nanoarchitectonics: Functional empowerment of mineral precursors for guiding intradental mineralization. Nano Research, 2024, 17, 4338-4349.	10.4	0
14350	Unveiling Arformoterol as a potent LSD1 inhibitor for breast cancer treatment: A comprehensive study integrating 3D-QSAR pharmacophore modeling, molecular docking, molecular dynamics simulations and in vitro assays. International Journal of Biological Macromolecules, 2024, 258, 129048.	7.5	0
14351	Adaptive lambda schemes for efficient relative binding free energy calculation. Journal of Computational Chemistry, 2024, 45, 855-862.	3.3	0
14352	Combination of a pH-responsive peptide amphiphile and a conventional antibiotic in treating Gram-negative bacteria. Journal of Colloid and Interface Science, 2024, 659, 397-412.	9.4	1
14353	Temperature-Transferable Coarse-Grained Models for Volumetric Properties of Poly(lactic Acid). Journal of Physical Chemistry B, 0, , .	2.6	0
14354	Aromatic vs alicyclic: Hydrophobicity of the ionic liquid on protein stability and fibril formation. Journal of Molecular Liquids, 2023, , 123920.	4.9	0
14355	Discovery of Potential Prolyl-tRNA Synthetase Allosteric Inhibitor Through Virtual Screening and In Vitro Assay against Plasmodium falciparum. Jordan Journal of Pharmaceutical Sciences, 2023, 16, 880-900.	1.1	0
14356	pSPICA Force Field Extended for Proteins and Peptides. Journal of Chemical Information and Modeling, 0, , .	5.4	0
14357	Comparative Analysis of Inhibitor Binding to Peroxiredoxins from Candidatus Liberibacter asiaticus and Its Host Citrus sinensis. Applied Biochemistry and Biotechnology, 0, , .	2.9	0
14358	Atomistic Simulations of Polydisperse Lignin Melts Using Simple Polydisperse Residue Input Generator. Biomacromolecules, 2024, 25, 767-777.	5.4	0
14359	Investigation of hydrogen-propane hydrate formation mechanism and optimal pressure range via hydrate-based hydrogen storage. Fuel, 2024, 361, 130791.	6.4	0
14360	Theoretical insights into the HO—induced oxidation of chlorpyrifos pesticide: Mechanism, kinetics, ecotoxicity, and cholinesterase inhibition of degradants. Chemosphere, 2023, , 141085.	8.2	0
14361	Neighbor List Artifacts in Molecular Dynamics Simulations. Journal of Chemical Theory and Computation, 2023, 19, 8919-8929.	5.3	1
14362	On the Na <sup>+</sup> transport and electrochemical stability window in NaTFSI:NMA deep eutectic solvent. Journal of Molecular Liquids, 2024, 395, 123930.	4.9	0
14363	The juxtamembrane linker of synaptotagmin 1 regulates Ca <sup>2+</sup> binding via liquid-liquid phase separation. Nature Communications, 2024, 15, .	12.8	1
14364	Protein-lipid interactions and protein anchoring modulate the modes of association of the globular domain of the Prion protein and Doppel protein to model membrane patches. Frontiers in Bioinformatics, 0, 3, .	2.1	0
14365	Flagellar motor protein-targeted search for the druggable site of <i>Helicobacter pylori</i> . Physical Chemistry Chemical Physics, 2024, 26, 2111-2126.	2.8	0



#	ARTICLE	IF	CITATIONS
14366	Tautomeric contributions to the absorption spectrum of [2,2â€²-bipyridyl]-3,3â€²-diol in water unveiled by molecular dynamics with accurate quantum mechanically derived force-fields. Journal of Molecular Liquids, 2024, 396, 123898.	4.9	0
14367	Probing binding and occlusion of substrate in the human creatine transporterâ€”by computation and mutagenesis. Protein Science, 2024, 33, .	7.6	0
14368	Discovery of dual rho-associated protein kinase 1 (ROCK1)/apoptosis signalâ€”regulating kinase 1 (ASK1) inhibitors as a novel approach for non-alcoholic steatohepatitis (NASH) treatment. BMC Chemistry, 2024, 18, .	3.8	0
14369	Phase-Dependent Adsorption of Myelin Basic Protein to Phosphatidylcholine Lipid Bilayers. Membranes, 2024, 14, 15.	3.0	0
14370	Mechanism of water transport through the lipid membrane with trichogin GA IV. Molecular dynamics study. Journal of Molecular Liquids, 2024, 396, 123948.	4.9	0
14371	Molecular Modeling of the Fluorination Effect on the Penetration of Nanoparticles across Lipid Bilayers. Langmuir, 2024, 40, 1295-1304.	3.5	0
14372	Transport and inhibition mechanism for VMAT2-mediated synaptic vesicle loading of monoamines. Cell Research, 2024, 34, 47-57.	12.0	3
14373	Kinetics of Oriented Attachment of Mica Crystals. Inorganic Chemistry, 2024, 63, 1367-1377.	4.0	0
14374	Structural basis for partial agonism in 5-HT3A receptors. Nature Structural and Molecular Biology, 2024, 31, 598-609.	8.2	0
14375	Investigating the effects of four medicinal plants against dengue virus through QSAR modeling and molecular dynamics studies. Journal of Biomolecular Structure and Dynamics, 0, , 1-18.	3.5	0
14376	Relationship between Protein-Induced Membrane Curvature and Membrane Thermal Undulation. Journal of Physical Chemistry B, 2024, 128, 515-525.	2.6	0
14377	Structural insights into the activation and inhibition of CXC chemokine receptor 3. Nature Structural and Molecular Biology, 2024, 31, 610-620.	8.2	1
14378	Investigating the role of dispersion corrections and anharmonic effects on the phase transition in SrZrS3: A systematic analysis from AIMD free energy calculations. Journal of Chemical Physics, 2024, 160, .	3.0	0
14379	Molecular dynamics simulations of the oil spill-treating phase-selective organogelator N-acetyl-L-isoleucine-N'-n-octyl amide. Journal of Molecular Liquids, 2024, 397, 123960.	4.9	0
14380	Computational insights into overcoming resistance mechanisms in targeted therapies for advanced breast cancer: focus on EGFR and HER2 co-inhibition. Journal of Biomolecular Structure and Dynamics, 0, , 1-12.	3.5	0
14381	Molecular study on the growth mechanism of CO2-H2 binary hydrate promoted by electric field. Fuel, 2024, 363, 130924.	6.4	0
14382	Molecular mechanism of decoupling between the fluorescence anisotropy thermograms of diphenylhexatriene and the thermotropic phase transitions of biomimetic ion pair amphiphile bilayers. Journal of Molecular Liquids, 2024, 395, 123959.	4.9	0
14383	Machine learned force-fields for an Ab-initio quality description of metal-organic frameworks. Npj Computational Materials, 2024, 10, .	8.7	1

#	ARTICLE	IF	CITATIONS
14384	Aggregation, structure and water permeability of membrane-embedded helical A $\beta$ oligomers. <i>Physical Chemistry Chemical Physics</i> , 2024, 26, 5128-5140.	2.8	0
14385	Molecular insights on the formation of inclusion complexes between Natural and Synthetic cyclodextrins and 7-O-methyl-aromadendrin. <i>Journal of Molecular Structure</i> , 2024, 1303, 137480.	3.6	0
14386	Atomistic simulations of RNA duplex thermal denaturation: Sequence- and forcefield-dependence. <i>Biophysical Chemistry</i> , 2024, 307, 107167.	2.8	0
14387	Computational insight into the effect of alkyl chain length in tetraalkylammonium-based deep eutectic solvents. <i>Journal of Molecular Graphics and Modelling</i> , 2024, 128, 108717.	2.4	0
14388	Exploring Ring Conformation in Uronate Monosaccharides: Insights from <i>Ab Initio</i> Calculations and Classical Molecular Dynamics Simulations. <i>Journal of Physical Chemistry B</i> , 2024, 128, 472-491.	2.6	0
14389	Ligand coupling mechanism of the human serotonin transporter differentiates substrates from inhibitors. <i>Nature Communications</i> , 2024, 15, .	12.8	0
14390	Madrid-2019 force field: An extension to divalent cations Sr <sup>2+</sup> and Ba <sup>2+</sup> . <i>Journal of Chemical Physics</i> , 2024, 160, .	3.0	0
14391	Decoding the secrets: how conformational and structural regulators inhibit the human 20S proteasome. <i>Frontiers in Chemistry</i> , 0, 11, .	3.6	0
14392	Solute interaction-driven and solvent interaction-driven liquid-liquid phase separation induced by molecular size difference. <i>Journal of Chemical Physics</i> , 2024, 160, .	3.0	0
14393	Molecular Dynamics Simulation of the Adsorption and Diffusion of C <sub>8</sub> Aromatic Isomers in MIL-47(V). <i>Langmuir</i> , 2024, 40, 2385-2395.	3.5	0
14394	<i>Ferulago bernardii</i> as a New Source of $\alpha$ -Pinene Binds to ctDNA: <i>In Silico</i> and <i>In Vitro</i> Studies. <i>Chemistry and Biodiversity</i> , 2023, 20, .	2.1	0
14395	Interaction of C-terminal Truncated Beta-amyloid Peptides with Human Serum Albumin. <i>Current Proteomics</i> , 2023, 20, 145-157.	0.3	1
14396	Molecular dynamics simulations and FTIR spectroscopy investigations on the hydration, transport, and dielectric properties of the NaF(aq) system at various concentrations. <i>Chemical Physics Impact</i> , 2024, 8, 100400.	3.5	0
14397	In silico studies of anti-oxidative and hot temperament-based phytochemicals as natural inhibitors of SARS-CoV-2 Mpro. <i>PLoS ONE</i> , 2023, 18, e0295014.	2.5	0
14398	Rapid Experimental Screening of High-Entropy Diborides for Superior Oxidation Resistance. <i>Advanced Functional Materials</i> , 0, , .	14.9	1
14400	Calculation of Melting Temperature Using Nonequilibrium Thermodynamic Integration Methods. <i>Advanced Theory and Simulations</i> , 2024, 7, .	2.8	0
14401	Guidelines for Free-Energy Calculations Involving Charge Changes. <i>Journal of Chemical Theory and Computation</i> , 2024, 20, 914-925.	5.3	0
14402	Digestion of lipid micelles leads to increased membrane permeability. <i>Nanoscale</i> , 2024, 16, 2642-2653.	5.6	0

#	ARTICLE	IF	CITATIONS
14403	Optimizing Phosphopeptide Structures That Target 14-3-3 $\mu$ in Cutaneous Squamous Cell Carcinoma. ACS Omega, 2024, 9, 2719-2729.	3.5	0
14404	Probing the role of protein conformational changes in the mechanism of prenylated-FMN-dependent phenazine-1-carboxylic acid decarboxylase. Journal of Biological Chemistry, 2024, 300, 105621.	3.4	0
14405	Solubility of Gases and Free Volume Evolution in R-BAPB Polyimide: Molecular Dynamics Simulations and Analytical Theory Insights into Cooling Velocity Effect. Macromolecules, 2024, 57, 586-596.	4.8	0
14406	Revolutionizing aqueous Zn-ion batteries: Precision control of H <sub>2</sub> O activity and Zn deposition through ammonium oxalate additive. Chemical Engineering Journal, 2024, 481, 148544.	12.7	0
14408	On the dual behaviour of water in octanol-rich aqueous <i>n</i>-octanol mixtures: an X-ray scattering and computer simulation study. Physical Chemistry Chemical Physics, 2024, 26, 4099-4110.	2.8	0
14409	Searching for Structure: Characterizing the Protein Conformational Landscape with Clustering-Based Algorithms. Journal of Chemical Information and Modeling, 2024, 64, 470-482.	5.4	0
14410	Structure, flexibility and hydration properties of lignin dimers studied with Molecular Dynamics simulations. Holzforschung, 2024, 78, 98-108.	1.9	0
14411	Hydration of biologically relevant tetramethylammonium cation by neutron scattering and molecular dynamics. Physical Chemistry Chemical Physics, 2024, 26, 3208-3218.	2.8	0
14414	Curvature sensing lipid dynamics in a mitochondrial inner membrane model. Communications Biology, 2024, 7, .	4.4	0
14416	Effects of Temperature on Novel Molecular Perovskite Energetic Material (C <sub>6</sub> H <sub>14</sub> N <sub>2</sub> )[NH <sub>4</sub> (ClO <sub>4</sub> ) <sub>3</sub> ]: A Molecular Dynamics Simulation. ACS Omega, 0, , .	3.5	0
14417	Molecular dynamics simulations support a preference of cyclotide kalata B1 for phosphatidylethanolamine phospholipids. Biochimica Et Biophysica Acta - Biomembranes, 2024, 1866, 184268.	2.6	0
14418	Identification of coumarin derivatives targeting acetylcholinesterase for Alzheimer's disease by field-based 3D-QSAR, pharmacophore model-based virtual screening, molecular docking, MM/GBSA, ADME and MD Simulation study. Current Research in Structural Biology, 2024, 7, 100124.	2.2	0
14419	Graph-Neural-Network-Based Unsupervised Learning of the Temporal Similarity of Structural Features Observed in Molecular Dynamics Simulations. Journal of Chemical Theory and Computation, 2024, 20, 819-831.	5.3	0
14420	Identification of approved drugs with ALDH1A1 inhibitory potential aimed at enhancing chemotherapy sensitivity in cancer cells: an in-silico drug repurposing approach. Journal of Biomolecular Structure and Dynamics, 0, , 1-15.	3.5	0
14422	Mechanisms of ion transport in lithium salt-doped zwitterionic polymer-supported ionic liquid electrolytes. Journal of Chemical Physics, 2024, 160, .	3.0	0
14424	Modulation of Al <sup>2+</sup> 16â€“22 aggregation by glucose. Physical Chemistry Chemical Physics, 2024, 26, 5038-5044.	2.8	0
14425	Structural characterization of the antimicrobial peptides myxinidin and WMR in bacterial membrane mimetic micelles and bicelles. Biochimica Et Biophysica Acta - Biomembranes, 2024, 1866, 184272.	2.6	0
14426	Novel coreâ€“shell and recyclable gas hydrate promoter for efficient solidified natural gas storage. Energy Conversion and Management, 2024, 301, 118059.	9.2	1

#	ARTICLE	IF	CITATIONS
14427	Molecular dynamics simulations of HIV-1 matrix-membrane interactions at different stages of viral maturation. <i>Biophysical Journal</i> , 2024, 123, 389-406.	0.5	1
14428	Structural and functional premise of transport protein transthyretin in the sight of silver and zinc oxide nanoparticles through atomistic simulations. <i>Inorganica Chimica Acta</i> , 2024, 563, 121923.	2.4	0
14429	Comprehensive Molecular Dynamics Study of Oxygen Diffusion in Carbon Mesopores: Insights for Designing Fuel-Cell Catalyst Supports. <i>Langmuir</i> , 2024, 40, 1674-1687.	3.5	0
14430	Role of conformational entropy in low melting point of ionic liquids: a molecular dynamics simulation study. <i>Bulletin of the Chemical Society of Japan</i> , 2024, 97, .	3.2	1
14431	Classification of MLH1 Missense VUS Using Protein Structure-Based Deep Learning-Ramachandran Plot-Molecular Dynamics Simulations Method. <i>International Journal of Molecular Sciences</i> , 2024, 25, 850.	4.1	0
14432	A computational examination of the therapeutic advantages of fourth-generation ALK inhibitors TPX-0131 and repotrectinib over third-generation lorlatinib for NSCLC with ALK F1174C/L/V mutations. <i>Frontiers in Molecular Biosciences</i> , 0, 10, .	3.5	0
14433	Impact of the Unstirred Water Layer on the Permeation of Small-Molecule Drugs. <i>Journal of Chemical Information and Modeling</i> , 2024, 64, 933-943.	5.4	0
14435	Inhibition of polymorphic MexXYâ€œOprM efflux system in <i>Pseudomonas aeruginosa</i> clinical isolates by Berberine derivatives. <i>ChemMedChem</i> , 2024, 19, .	3.2	0
14436	Insights into the conformational, secondary structural, dynamical and hydration pattern changes of glucose mediated glycosylated HSA: a molecular dynamics approach. <i>Journal of Biomolecular Structure and Dynamics</i> , 0, , 1-13.	3.5	0
14437	Single-phase local-high-concentration solid polymer electrolytes for lithium-metal batteries. <i>Nature Energy</i> , 2024, 9, 386-400.	39.5	0
14439	Influence of Peptoid Sequence on the Mechanisms and Kinetics of 2D Assembly. <i>ACS Nano</i> , 2024, 18, 3497-3508.	14.6	0
14440	The anisotropy of deformation twinning in bcc materials: Mechanical loading, temperature effect, and twinâ€œtwin interaction. <i>Acta Materialia</i> , 2024, 266, 119681.	7.9	0
14442	Atomic diffusion in liquid gallium and gallium-nickel alloys probed by quasielastic neutron scattering and molecular dynamic simulations. <i>Journal of Physics Condensed Matter</i> , 2024, 36, 175403.	1.8	0
14444	Timeâ€œtemperature correlations of amorphous thermoplastics at large strains based on molecular dynamics simulations. <i>Mechanics of Materials</i> , 2024, 190, 104926.	3.2	0
14449	Gallic acid forms V-amylose complex structure with starch through hydrophobic interaction. <i>International Journal of Biological Macromolecules</i> , 2024, 260, 129408.	7.5	0
14450	Structure-based virtual screening and molecular dynamics studies to explore potential natural inhibitors against 3C protease of foot-and-mouth disease virus. <i>Frontiers in Veterinary Science</i> , 0, 10, .	2.2	1
14451	Exploration of a mutant enzyme protein with active site fluctuations at 330Â°K via machine learning and molecular dynamics simulations. <i>AIP Advances</i> , 2024, 14, .	1.3	0
14452	Interaction between Permeation Enhancers and Lipid Bilayers. <i>Journal of Physical Chemistry B</i> , 2024, 128, 1668-1679.	2.6	0

#	ARTICLE	IF	CITATIONS
14453	Elucidating the structure of donor–acceptor conjugated polymer aggregates in liquid solution. <i>Soft Matter</i> , 2024, 20, 1824-1833.	2.7	0
14454	Significance of the Disulfide Bridge in the Structure and Stability of Metalloprotein Azurin. <i>Journal of Physical Chemistry B</i> , 2024, 128, 973-984.	2.6	0
14455	A hybrid molecular dynamics/machine learning framework to calculate the viscosity and thermal conductivity of Ar, Kr, Xe, O, and $\text{H}_2\text{O}$ .		0
14456	Fine Tuning Water States in Hydrogels for High Voltage Aqueous Batteries. <i>ACS Nano</i> , 2024, 18, 3101-3114.	14.6	1
14457	An atomistic study of effects of temperature and Ni element on the phase transition and wear behavior of NiTi shape memory alloy. <i>Tribology International</i> , 2024, 192, 109309.	5.9	0
14458	Acceleration of Molecular Simulations by Parametric Time-Lagged tSNE Metadynamics. <i>Journal of Physical Chemistry B</i> , 2024, 128, 903-913.	2.6	0
14459	Application of temperature-dependent and steered molecular dynamics simulation to screen anti-dengue compounds against Marburg virus. <i>Journal of Biomolecular Structure and Dynamics</i> , 0, , 1-20.	3.5	0
14460	Comparison of two peroxidases with high potential for biotechnology applications – HRP vs. APEX2. <i>Computational and Structural Biotechnology Journal</i> , 2024, 23, 742-751.	4.1	0
14461	Elucidating the Membrane Binding Process of a Disordered Protein: Dynamic Interplay of Anionic Lipids and the Polybasic Region. <i>ACS Physical Chemistry Au</i> , 2024, 4, 167-179.	4.0	0
14462	High UV damage and low repair, but not cytosine deamination, stimulate mutation hotspots at ETS binding sites in melanoma. <i>Proceedings of the National Academy of Sciences of the United States of America</i> , 2024, 121, .	7.1	0
14463	Hfe Permease and <i>Haemophilus influenzae</i> Manganese Homeostasis. <i>ACS Infectious Diseases</i> , 2024, 10, 436-452.	3.8	0
14464	Computing Accurate True Self-Diffusion Coefficients and Shear Viscosities Using the OrthoBoXY Approach. <i>Journal of Physical Chemistry B</i> , 2024, 128, 1040-1052.	2.6	0
14465	The counteracting influence of 2-hydroxypropyl substitution and the presence of a guest molecule on the shape and size of the $\beta$ -cyclodextrin cavity. <i>Physical Chemistry Chemical Physics</i> , 2024, 26, 11531-11544.	2.8	0
14466	Enticing a Proton using Single Ammonia Molecule as Bait. <i>Journal of Physical Chemistry B</i> , 2024, 128, 1022-1028.	2.6	0
14467	Computational exploration of microsomal cytochrome P450 3A1 enzyme modulation by phytochemicals of <i>Cichorium intybus</i> L.: Insights into drug metabolism. <i>Biopharmaceutics and Drug Disposition</i> , 2024, 45, 15-29.	1.9	0
14468	Unravelling carbohydrate binding module 21 (CBM21) dynamics of interaction with amylose. <i>Carbohydrate Polymers</i> , 2024, 330, 121792.	10.2	0
14469	Experimental Measurements and Molecular Simulations on the Liquid Density and Viscosity of Pentaerythritol Tetraacetate. <i>International Journal of Thermophysics</i> , 2024, 45, .	2.1	0
14470	Disulfide bridge-dependent dimerization triggers FGF2 membrane translocation into the extracellular space. <i>ELife</i> , 0, 12, .	6.0	0

#	ARTICLE	IF	CITATIONS
14471	Computer Aided Structure-Based Drug Design of Novel SARS-CoV-2 Main Protease Inhibitors: Molecular Docking and Molecular Dynamics Study. <i>Computation</i> , 2024, 12, 18.	2.0	0
14472	Inosine-Induced Base Pairing Diversity during Reverse Transcription. <i>ACS Chemical Biology</i> , 2024, 19, 348-356.	3.4	0
14473	Structural and Dynamic-Based Characterization of the Recognition Patterns of E7 and TRP-2 Epitopes by MHC Class I Receptors through Computational Approaches. <i>International Journal of Molecular Sciences</i> , 2024, 25, 1384.	4.1	0
14474	Tandem repeats of highly bioluminescent <sc>NanoLuc</sc> are refolded noncanonically by the <sc>Hsp70</sc> machinery. <i>Protein Science</i> , 2024, 33, .	7.6	0
14475	Tracing the substrate translocation mechanism in P-glycoprotein. <i>ELife</i> , 0, 12, .	6.0	0
14476	Martini on the Rocks: Can a Coarse-Grained Force Field Model Crystals?. <i>Journal of Physical Chemistry Letters</i> , 2024, 15, 1079-1088.	4.6	0
14477	Inhibiting the oligomerization of mycobacterial DNA-directed RNA polymerase (RNAP) using natural compound via in-silico techniques. <i>Medicine in Novel Technology and Devices</i> , 2024, 21, 100286.	1.6	0
14478	Rational design for novel heterocyclic based Donepezil analogs for Alzheimerâ€™s disease: an in silico approach. <i>Journal of Biomolecular Structure and Dynamics</i> , 0, , 1-12.	3.5	0
14479	Structural and thermodynamic characterization of allosteric transitions in human serum albumin with metadynamics simulations. <i>Physical Chemistry Chemical Physics</i> , 2024, 26, 6436-6447.	2.8	0
14480	Understanding the Positive Role of Ionic Liquids in CO<sub>2</sub> Capture by Poly(ethylenimine). <i>Journal of Physical Chemistry B</i> , 2024, 128, 1079-1090.	2.6	0
14481	Is the Local Ion Density Sufficient to Drive NaCl Nucleation from the Melt and Aqueous Solution?. <i>Journal of Physical Chemistry B</i> , 2024, 128, 1012-1021.	2.6	1
14482	Variational autoencoder for design of synthetic viral vector serotypes. <i>Nature Machine Intelligence</i> , 2024, 6, 147-160.	16.0	0
14483	Adsorption in Action: Molecular Dynamics as a Tool to Study Adsorption at the Surface of Fine Plastic Particles in Aquatic Environments. <i>ACS Omega</i> , 2024, 9, 5142-5156.	3.5	0
14484	Redox-driven confinement of quinone with imidazole in sub-nanometer sized porous carbon space mitigating chemical degradation for aqueous energy storage. <i>Journal of Materials Chemistry A</i> , 2024, 12, 5778-5792.	10.3	0
14485	Recalibrating the Experimentally Derived Structure of the Metastable Surface Oxide on Copper via Machine Learning-Accelerated <i>In Silico</i> Global Optimization. <i>ACS Nano</i> , 2024, 18, 4559-4569.	14.6	0
14486	Identification of amentoflavone as a potent SARS-CoV-2 M<sup>pro</sup> inhibitor: a combination of computational studies and inÂ vitro biological evaluation. <i>Journal of Biomolecular Structure and Dynamics</i> , 0, , 1-19.	3.5	0
14487	Molecular simulation of ultrasonic assisted diamond grit scratching 4H-SiC single-crystal. <i>Tribology International</i> , 2024, 192, 109330.	5.9	0
14489	Molecular Insights into the Influence of Major Marine Ions on Carbon Dioxide Hydrate Growth. <i>Crystal Growth and Design</i> , 2024, 24, 1380-1388.	3.0	0



#	ARTICLE	IF	CITATIONS
14490	Hydration induced mechanical degradation in the Y-doped BaZrO <sub>3</sub> solid oxide. Computational Materials Science, 2024, 235, 112824.	3.0	0
14491	Threading Subunits for Polymers to Predict the Equilibrium Ensemble of Solid Polymer Electrolytes. Journal of Physical Chemistry Letters, 2024, 15, 1227-1233.	4.6	0
14492	Structural insights into the semiquinone form of human Cytochrome P450 reductase by DEER distance measurements between a native flavin and a spin labelled nonâ€œcanonical amino acid. Chemistry - A European Journal, 2024, 30, .	3.3	0
14494	Ca <sup>2+</sup> pre-intercalated bilayered vanadium oxide for high-performance aqueous Mg-ion batteries. Energy Storage Materials, 2024, 66, 103212.	18.0	0
14497	Divergence among Local Structure, Dynamics, and Nucleation Outcome in Heterogeneous Nucleation of Close-Packed Crystals. Journal of Physical Chemistry Letters, 2024, 15, 1279-1287.	4.6	0
14498	Protocol-dependent frictional granular jamming simulations: cyclical, compression, and expansion. , 0, 3, .		0
14499	Structures of complete extracellular receptor assemblies mediated by IL-12 and IL-23. Nature Structural and Molecular Biology, 2024, 31, 591-597.	8.2	0
14501	The Inhibition Effect of Epigallocatechin-3-Gallate on the Co-Aggregation of Amyloid-Î² and Human Islet Amyloid Polypeptide Revealed by Replica Exchange Molecular Dynamics Simulations. International Journal of Molecular Sciences, 2024, 25, 1636.	4.1	0
14502	Predicting the Geometry of Coreâ€œShell Structures: How a Shape Changes with Constant Added Thickness. Journal of Physical Chemistry B, 2024, 128, 1317-1324.	2.6	0
14503	Molecular docking, molecular dynamics, MM/PBSA approaches and bioactivity studies of nepetanudoside B isolated from endemic <i>Nepeta aristata</i>. Journal of Biomolecular Structure and Dynamics, 0, , 1-14.	3.5	1
14504	Campesterol and dithymoquinone as a potent inhibitors of SARS cov-2 main proteasesâ€œpromising drug candidates for targeting its novel variants. Journal of Biomolecular Structure and Dynamics, 0, , 1-15.	3.5	0
14505	Computer aided aptamer selection for fabrication of electrochemical sensor to detect Aflatoxin B<sub>1</sub>. Journal of Biomolecular Structure and Dynamics, 0, , 1-14.	3.5	0
14506	Elucidating the reversible and irreversible self-assembly mechanisms of low-complexity aromatic-rich kinked peptides and steric zipper peptides. Nanoscale, 2024, 16, 4025-4038.	5.6	0
14507	Multiscale Molecular Dynamics Simulations of an Active Self-Assembling Material. Journal of Physical Chemistry B, 2024, 128, 1266-1274.	2.6	0
14508	Discovery of lipid binding sites in a ligand-gated ion channel by integrating simulations and cryo-EM. ELife, 0, 12, .	6.0	0
14509	Observing growth and interfacial dynamics of nanocrystalline ice in thin amorphous ice films. Nature Communications, 2024, 15, .	12.8	0
14511	Zn<sup>2+</sup> Binding Increases Parallel Structure in the AÎ²(16â€œ22) Oligomer by Disrupting Salt Bridge in Antiparallel Structure. Journal of Physical Chemistry B, 2024, 128, 1385-1393.	2.6	0
14512	Beyond the electrical double layer model: ion-dependent effects in nanoscale solvent organization. Physical Chemistry Chemical Physics, 2024, 26, 6726-6735.	2.8	0

#	ARTICLE	IF	CITATIONS
14513	Improved Protein Dynamics and Hydration in the Martini3 Coarse-Grain Model. Journal of Chemical Information and Modeling, 2024, 64, 837-850.	5.4	0
14514	PopShift: A Thermodynamically Sound Approach to Estimate Binding Free Energies by Accounting for Ligand-Induced Population Shifts from a Ligand-Free Markov State Model. Journal of Chemical Theory and Computation, 2024, 20, 1036-1050.	5.3	0
14515	Solubility of CO <sub>2</sub> in salty water: adsorption, interfacial tension and salting out effect. Molecular Physics, 0, , .	1.7	0
14516	Computational Approaches to Evaluate the Acetylcholinesterase Binding Interaction with Taxifolin for the Management of Alzheimer's Disease. Molecules, 2024, 29, 674.	3.8	0
14517	Computationally guided synthesis of carbon coated mesoporous silica materials. Carbon, 2024, 221, 118891.	10.3	0
14518	Acylation of MLKL Impacts Its Function in Necroptosis. ACS Chemical Biology, 2024, 19, 407-418.	3.4	0
14519	Unravelling the molecular interactions behind the formation of PEG/PPG aqueous two-phase systems. Physical Chemistry Chemical Physics, 2024, 26, 7308-7317.	2.8	0
14520	Sensing membrane voltage by reorientation of dipolar transmembrane peptides. Biophysical Journal, 2024, 123, 584-597.	0.5	0
14521	Flip-flop dynamics in smectic liquid-crystal organic semiconductors revealed by molecular dynamics simulations. Chemical Communications, 2024, 60, 2192-2195.	4.1	0
14522	Growth kinetics of amyloid-like fibrils: An integrated atomistic simulation and continuum theory approach. , 2024, 3, .		1
14523	Uncovering the Crystalline Packing Advantages of Asymmetric Y6 Series Acceptors for Efficient Additive-insensitive and Intrinsically Stable Organic Solar Cells. Advanced Energy Materials, 2024, 14, .	19.5	0
14524	Identification of Residues Potentially Involved in Optical Shifts in the Water-Soluble Chlorophyll <i>a</i> -Binding Protein through Molecular Dynamics Simulations. Journal of Physical Chemistry B, 2024, 128, 1371-1384.	2.6	0
14525	Effects of Bacillus in Pectobacterium quorum quenching: A survey of two different acyl-homoserine lactonases. Folia Microbiologica, 0, , .	2.3	0
14526	Force field benchmark of asphalt materials: Density, viscosity, glass transition temperature, diffusion coefficient, cohesive energy density and molecular structures. Journal of Molecular Liquids, 2024, 398, 124166.	4.9	0
14527	Viscosity of Pectin-[BMIM][PF6] electrolytes and the interplay of ion-ion interactions. Journal of Molecular Liquids, 2024, 397, 124159.	4.9	0
14529	Allosteric regulation in SARS-CoV-2 spike protein. Physical Chemistry Chemical Physics, 2024, 26, 6582-6589.	2.8	0
14530	Exploring the Function of (+)-Naltrexone Precursors: Their Activity as TLR4 Antagonists and Potential in Treating Morphine Addiction. Journal of Medicinal Chemistry, 2024, 67, 3127-3143.	6.4	0
14531	A molecular arm: the molecular bending-unbending mechanism of integrin. Biomechanics and Modeling in Mechanobiology, 0, , .	2.8	0

#	ARTICLE	IF	CITATIONS
14532	Decoding the dynamics of BCL9 triazole stapled peptide. Biophysical Chemistry, 2024, 307, 107197.	2.8	0
14533	Temperature-induced suppression of structural disproportionation in paramagnetic quantum materials. Journal of Applied Physics, 2024, 135, .	2.5	1
14534	Unveiling the molecular interaction of hepatitis B virus inhibitor, entecavir with human serum albumin through computational, microscopic and spectroscopic approaches. Journal of Biomolecular Structure and Dynamics, 0, , 1-14.	3.5	0
14535	Molecular and quantum mechanical insights of conformational dynamics of Maltosyl-Î²-Cyclodextrin/Formononetin supramolecular complexes. Journal of Molecular Liquids, 2024, 397, 124196.	4.9	1
14536	Substituent effects on the coordination of benzo-21-crown-7 and dibenzo-21-crown-7 with cesium: Insights from computational chemistry and nuclear magnetic resonance spectroscopy. Journal of Molecular Liquids, 2024, 397, 124169.	4.9	0
14537	The accuracy limit of chemical shift predictions for species in aqueous solution. Physical Chemistry Chemical Physics, 2024, 26, 6386-6395.	2.8	0
14538	The elementary reactions for incorporation into crystals. Proceedings of the National Academy of Sciences of the United States of America, 2024, 121, .	7.1	0
14539	Formalizing Coarse-Grained Representations of Anisotropic Interactions at Multimeric Protein Interfaces Using Virtual Sites. Journal of Physical Chemistry B, 2024, 128, 1394-1406.	2.6	0
14540	Molecular Modeling of the Adsorption of an Egg Yolk Protein on a Water–Oil Interface. Langmuir, 0, , .	3.5	1
14541	Stability of Cytoplasmic Membrane of <i>Escherichia coli</i> Bacteria in Aqueous and Ethanolic Environment. Langmuir, 2024, 40, 2893-2906.	3.5	0
14542	Proline–Tyrosine Ring Interactions in Black Widow Dragline Silk Revealed by Solid-State Nuclear Magnetic Resonance and Molecular Dynamics Simulations. Biomacromolecules, 2024, 25, 1916-1922.	5.4	0
14543	Mechanism of RGD-conjugated nanodevice binding to its target protein integrin Î± <sub>V</sub> Î² <sub>3</sub> by atomistic molecular dynamics and machine learning. Nanoscale, 2024, 16, 4063-4081.	5.6	0
14544	Phase transitions of fluorotelomer alcohols at the water   alkane interface studied <i>via</i> molecular dynamics simulation. Soft Matter, 2024, 20, 2243-2257.	2.7	1
14546	Structural studies of catalytic peptides using molecular dynamics simulations. Methods in Enzymology, 2024, , .	1.0	0
14547	<i>In silico</i> and structural investigation of sulfonamides targeting VraSR two component system in methicillin-resistant <i>Staphylococcus aureus</i> . Journal of Biomolecular Structure and Dynamics, 0, , 1-21.	3.5	0
14548	Chlorination-improved adsorption capacity of microplastics for antibiotics: A combined experimental and molecular mechanism investigation. Journal of Hazardous Materials, 2024, 467, 133734.	12.4	0
14551	Non–Sacrificial Additive Enables a Non–Passivating Cathode Interface for 4.6 V Li   LiCoO <sub>2</sub> Batteries. Advanced Energy Materials, 2024, 14, .	19.5	0
14552	Molecular insights into the absorption of SO <sub>2</sub> with amine alkyl organosilicon and its optimal absorption temperature. Separation and Purification Technology, 2024, 340, 126660.	7.9	0

#	ARTICLE	IF	CITATIONS
14553	Insights into the effects of 1,3-dioxolane on the growth of sl CO <sub>2</sub> hydrate: A molecular dynamics simulation study. <i>Fuel</i> , 2024, 364, 131143.	6.4	0
14554	Three-step docking by WIPI2, ATG16L1, and ATG3 delivers LC3 to the phagophore. <i>Science Advances</i> , 2024, 10, .	10.3	0
14555	Fluorinated benzoxazinones designed via <scp>MIAâ€‘QSAR</scp>, docking and molecular dynamics as protoporphyrinogen <scp>IX</scp> oxidase inhibitors. <i>Journal of the Science of Food and Agriculture</i> , 0, , .	3.5	0
14556	Molecular Dynamics Study of Protein Aggregation at Moving Interfaces. <i>Molecular Pharmaceutics</i> , 2024, 21, 1214-1221.	4.6	0
14557	On the diffusion of carbamazepine, acetaminophen and atenolol in water: An experimental and theoretical approach. <i>Fluid Phase Equilibria</i> , 2024, 580, 114056.	2.5	0
14558	Investigation on potential allergenic peptides and critical amino acids of the digestive products of glycated Î±-lactalbumin via allergenicity evaluation and molecular dynamic simulation. <i>LWT - Food Science and Technology</i> , 2024, 195, 115800.	5.2	0
14559	Nanoparticles insert a three dimensional cavity structure of proteins for function inhibition: The Case of CeO <sub>2</sub> and SARS-CoV-2. <i>Nano Today</i> , 2024, 55, 102183.	11.9	1
14560	Atomistic Insight into the Lipid Nanodomains of Synaptic Vesicles. <i>Journal of Physical Chemistry B</i> , 2024, 128, 2707-2716.	2.6	0
14561	Synthesis of lipid-linked precursors of the bacterial cell wall is governed by a feedback control mechanism in <i>Pseudomonas aeruginosa</i> . <i>Nature Microbiology</i> , 2024, 9, 763-775.	13.3	0
14562	Molecular Dynamics Simulation of Nanometer-Sized Carbon Nitride Polyaniline (C<sub>3</sub>N) Binding to Small Intestinal Epithelial Cell Membranes. <i>ACS Applied Nano Materials</i> , 2024, 7, 3817-3825.	5.0	0
14563	<i>In silico</i> investigations and molecular insights for designing tRNA-encoded peptides as potential therapeutics for targeting over-expressed receptors in breast cancer. <i>Journal of Biomolecular Structure and Dynamics</i> , 0, , 1-17.	3.5	0
14564	Mutual Adjacency of Components Molecules in Aqueous TBA and TMAO Solutions. <i>Journal of Structural Chemistry</i> , 2024, 65, 149-159.	1.0	0
14566	Molecular dynamics studies on the thermodynamic and structural properties of hydrogen bonds in a novel mixture of dual amino acid ionic liquid â€‘ H <sub>2</sub> O. <i>Journal of Molecular Liquids</i> , 2024, 398, 124235.	4.9	0
14567	Interferon-Î³ as a Potential Inhibitor of SARS-CoV-2 ORF6 Accessory Protein. <i>International Journal of Molecular Sciences</i> , 2024, 25, 2155.	4.1	0
14568	Discovery of A Novel Series of Quinazolineâ€‘Thiazole Hybrids as Potential Antiproliferative and Anti-Angiogenic Agents. <i>Biomolecules</i> , 2024, 14, 218.	4.0	0
14569	Simulation data for engineering graphene quantum dot epoxy nanocomposites using molecular dynamics. <i>Data in Brief</i> , 2024, 53, 110169.	1.0	0
14570	Unraveling the Microscopic Mechanism of Molecular Ion Interaction with Monoclonal Antibodies: Impact on Protein Aggregation. <i>Molecular Pharmaceutics</i> , 2024, 21, 1285-1299.	4.6	0
14571	Discovery of anticancer compound possessing potential to bind Î³-secretase catalytic subunit and inhibit notch promoter activity. <i>Journal of Biomolecular Structure and Dynamics</i> , 0, , 1-16.	3.5	0

#	ARTICLE	IF	CITATIONS
14572	Molecular dynamics simulation as a promising approach for computational study of liquid crystal-based aptasensors. Journal of Biomolecular Structure and Dynamics, 0, , 1-13.	3.5	0
14573	Kinetic description of water transport during spontaneous emulsification induced by Span 80. Nanoscale, 2024, 16, 4056-4062.	5.6	0
14574	A close look at the hydration layer and at the premelting layer of K-feldspar. Molecular Physics, 0, , .	1.7	0
14575	Shielding&Anchoring Double Protection Tactics of Imidazo[1,2&b]pyridazine Additive for Ultrastable Zinc Anode. Advanced Functional Materials, 0, , .	14.9	0
14576	Estimating the phase diagrams of deep eutectic solvents within an extensive chemical space. Communications Chemistry, 2024, 7, .	4.5	0
14577	Efficient delivery of carotenoids to adipocytes with albumin. Physical Chemistry Chemical Physics, 2024, 26, 7865-7876.	2.8	2
14578	Probing the dynamic landscape of peptides in molecular assemblies by synergized NMR experiments and MD simulations. Communications Chemistry, 2024, 7, .	4.5	0
14579	Myomerger Induces Membrane Hemifusion and Regulates Fusion Pore Expansion. Biochemistry, 2024, 63, 815-826.	2.5	0
14580	Alternative splicing generates a novel ferroportin isoform with a shorter C&terminal and an intact iron&and hepcidin&binding property. IUBMB Life, 0, , .	3.4	0
14581	Molecular basis of VEGFR1 autoinhibition at the plasma membrane. Nature Communications, 2024, 15, .	12.8	0
14582	Achievements and Prospects of Molecular Dynamics Simulations in Thermofluid Sciences. Energies, 2024, 17, 888.	3.1	0
14583	Unraveling the Significance of Mg<sup>2+</sup> Dependency and Nucleotide Binding Specificity of H-RAS. Journal of Physical Chemistry B, 2024, 128, 1618-1626.	2.6	0
14584	Characterizing Aptamer Interaction with the Oncolytic Virus VV-GMCSF-Lact. Molecules, 2024, 29, 848.	3.8	0
14585	Molecular Insights into the Inhibition and Disaggregation Effects of EGCG on AÎ²40 and AÎ²42 Cofibrillation. Journal of Physical Chemistry B, 2024, 128, 1843-1853.	2.6	0
14586	Peptide translocation across asymmetric phospholipid membranes. Biophysical Journal, 2024, 123, 693-702.	0.5	0
14587	Determinants for 1-alkyl-3-methylimidazolium chloride-induced modulation of thermodynamic stability and CO-association dynamics of horse ferrocycytochrome c. Journal of Molecular Liquids, 2024, 398, 124227.	4.9	0
14588	Effects of anthocyanidins on the conformational transition of AÎ²(1-42) peptide: Insights from molecular docking and molecular dynamics simulations. Journal of Molecular Graphics and Modelling, 2024, 129, 108732.	2.4	0
14590	Hierarchical Assembly of Single-Stranded RNA. Journal of Chemical Theory and Computation, 2024, 20, 2246-2260.	5.3	1

#	ARTICLE	IF	CITATIONS
14591	Nanobody engineering for SARS-CoV-2 neutralization and detection. Microbiology Spectrum, 2024, 12, .	3.0	0
14592	Cyclodextrins: Establishing building blocks for AI-driven drug design by determining affinity constants in silico. Computational and Structural Biotechnology Journal, 2024, 23, 1117-1128.	4.1	0
14593	UNRAVELLING THE INTERACTION BETWEEN GARCINISIDONE-A AND HER2 PROTEIN IN BREAST CANCER: A COMPUTATIONAL STUDY. International Journal of Applied Pharmaceutics, 0, , 99-104.	0.3	0
14596	CHEK2 germline variants identified in familial nonmedullary thyroid cancer lead to impaired protein structure and function. Journal of Biological Chemistry, 2024, 300, 105767.	3.4	0
14597	Molecular Dynamics Simulations of Polyelectrolyte Complexes. Biomacromolecules, 2024, 25, 1468-1480.	5.4	0
14598	Preparation, physicochemical characterization, and computational studies of aldehyde aroma compounds/cyclodextrin inclusion complexes. Industrial Crops and Products, 2024, 211, 118245.	5.2	0
14599	Solidâ€“Liquidâ€“Solution Phases in Poly(diallyldimethylammonium)/Poly(acrylic acid) Polyelectrolyte Complexes at Varying Temperatures. Macromolecules, 2024, 57, 2363-2375.	4.8	0
14600	Unveiling the mechanism of thermal catalytic oxidation of HCHO from the kiln exhaust gas using Sc-decorated Cr<sub>2</sub>CO<sub>2</sub>-MXenes. Journal of Materials Chemistry A, 2024, 12, 6671-6680.	10.3	0
14602	Inhibitory effects of nobiletin-mediated interfacial instability of bile salt emulsified oil droplets on lipid digestion. Food Chemistry, 2024, 444, 138751.	8.2	0
14604	Closing the Gap between Experiment and Simulationâ”€A Holistic Study on the Complexation of Small Interfering RNAs with Polyethylenimine. Molecular Pharmaceutics, 2024, 21, 2163-2175.	4.6	0
14605	Submicron-thick single anion-conducting polymer electrolytes. , 0, , .		0
14606	Insertases scramble lipids: Molecular simulations of MTCH2. Structure, 2024, 32, 505-510.e4.	3.3	0
14607	Tracing the Antibacterial Performance of Bis-Imidazolium-based Ionic Liquid Derivatives. ACS Applied Bio Materials, 2024, 7, 1558-1568.	4.6	0
14608	Multivalent Ion-Mediated Polyelectrolyte Association and Structure. Macromolecules, 2024, 57, 1941-1949.	4.8	0
14609	Homologous mutations in human Î², embryonic, and perinatal muscle myosins have divergent effects on molecular power generation. Proceedings of the National Academy of Sciences of the United States of America, 2024, 121, .	7.1	0
14610	Structural mechanisms of Î±7 nicotinic receptor allosteric modulation and activation. Cell, 2024, 187, 1160-1176.e21.	28.9	0
14611	Complex phase diagram and supercritical matter. Physical Review E, 2024, 109, .	2.1	0
14612	The Role of ZO-2 in Modulating JAM-A and Î³-Actin Junctional Recruitment, Apical Membrane and Tight Junction Tension, and Cell Response to Substrate Stiffness and Topography. International Journal of Molecular Sciences, 2024, 25, 2453.	4.1	0



#	ARTICLE	IF	CITATIONS
14613	From dietary lignans to cancer therapy: Integrative systems analysis of enterolactone's molecular targets and signaling pathways in combatting cancer stem cells in triple-negative breast cancer. Food Bioscience, 2024, 58, 103732.	4.4	0
14614	Pectin Nanoporous Structures Prepared via Salt-Induced Phase Separation and Ambient Azeotropic Evaporation Processes. Biomacromolecules, 2024, 25, 1709-1723.	5.4	0
14615	Investigation of thermal stress effects during annealing of hafnia-made thin film using molecular dynamics simulations. Microelectronic Engineering, 2024, 288, 112158.	2.4	0
14616	Design of target specific peptide inhibitors using generative deep learning and molecular dynamics simulations. Nature Communications, 2024, 15, .	12.8	0
14617	Binding mechanism of full-length AÎ²40 peptide to a mixed lipid bilayer. Frontiers in Chemistry, 0, 12, .	3.6	0
14618	The Signature of Fluctuations of the Hydrogen Bond Network Formed by Water Molecules in the Interfacial Layer of Anionic Lipids. Biophysica, 2024, 4, 92-106.	1.4	0
14619	Antimycobacterial Drugs as a Novel Strategy to Inhibit Pseudomonas aeruginosa Virulence Factors and Combat Antibiotic Resistance: A Molecular Simulation Study. Microbiology Research, 2024, 15, 290-313.	1.9	0
14620	Beneficial Effects of Sideritis clandestina Extracts and Sideridiol against Amyloid Î² Toxicity. Antioxidants, 2024, 13, 261.	5.1	0
14621	Effects of 1-butyl-3-methyl-imidazolium acetate on the solution behavior of melittin: A molecular dynamics study. Journal of Ionic Liquids, 2024, 4, 100081.	2.7	0
14622	Proteinâ€™lipid acyl chain interactions: Depth-dependent changes of segmental mobility of phospholipid in contact with bacteriorhodopsin. Biophysical Chemistry, 2024, 308, 107204.	2.8	0
14623	The Jarzynski binding free energy can effectively rank ligand-protein affinities in inadequate samplings. Chemical Physics Letters, 2024, 840, 141145.	2.6	0
14624	Mechanism and cellular function of direct membrane binding by the ESCRT and ERES-associated Ca <sup>2+</sup> -sensor ALG-2. Proceedings of the National Academy of Sciences of the United States of America, 2024, 121, .	7.1	0
14625	<i>In silico</i> assessment of a natural small molecule as an inhibitor of programmed death ligand 1 for cancer immunotherapy: a computational approach. Journal of Biomolecular Structure and Dynamics, 0, , 1-21.	3.5	0
14626	Impact of DNA on interactions between core proteins of Hepatitis B virus-like particles comprising different C-terminals. International Journal of Biological Macromolecules, 2024, 263, 130365.	7.5	0
14627	Barnacle cement protein as an efficient bioinspired corrosion inhibitor. Communications Materials, 2024, 5, .	6.9	0
14628	Increasing the polarity of Î²-lapachone does not affect its binding capacity with bovine plasma protein. International Journal of Biological Macromolecules, 2024, 263, 130279.	7.5	0
14629	Additive Molar Volumes in Amorphous Ca/Sr Carbonate Solid Solutions. Journal of Physical Chemistry C, 2024, 128, 4070-4078.	3.1	0
14630	Myelin Basic Protein Attenuates Furin-Mediated Bri2 Cleavage and Postpones Its Membrane Trafficking. International Journal of Molecular Sciences, 2024, 25, 2608.	4.1	0

#	ARTICLE	IF	CITATIONS
14631	Ion-Induced PIP2 Clustering with Martini3: Modification of Phosphate-Ion Interactions and Comparison with CHARMM36. Journal of Physical Chemistry B, 2024, 128, 2134-2143.	2.6	0
14632	Melting and Bubble Formation in a Double-Stranded DNA: Microscopic Aspects of Early Base-Pair Opening Events and the Role of Water. Journal of Physical Chemistry B, 2024, 128, 2076-2086.	2.6	0
14633	Ferroelectric Phase Transition in Barium Titanate Revisited with Ab Initio Molecular Dynamics. Materials, 2024, 17, 1023.	2.9	0
14634	Machine Learning Deciphered Molecular Mechanistics with Accurate Kinetic and Thermodynamic Prediction. Journal of Chemical Theory and Computation, 0, , .	5.3	0
14635	Structural and energetic analysis of NS5 protein inhibition by small molecules in Japanese encephalitis virus using machine learning and steered molecular dynamics approach. Journal of Biomolecular Structure and Dynamics, 0, , 1-18.	3.5	0
14636	Study of the evolution of nano-bubbles/droplets generated in water by CO2-Hydrate dissociation via molecular-dynamics simulation. AIP Conference Proceedings, 2024, , .	0.4	0
14637	Molecular guidelines for promising antimicrobial agents. Scientific Reports, 2024, 14, .	3.3	0
14638	Strain-induced two-dimensional relaxor ferroelectrics in Se-doped PbTe. Physical Review B, 2024, 109, .	3.2	0
14639	Sequence Sensitivity in Membrane Remodeling by Polyampholyte Condensates. Journal of Physical Chemistry B, 2024, 128, 2087-2099.	2.6	0
14640	Serine protease inhibitor 3 (Serp13) from <i>Penaeus vannamei</i> selectively interacts with <i>Vibrio parahaemolyticus</i> PirA <sup>vp</sup> . Journal of Fish Diseases, 0, , .	1.9	0
14641	A multi-scale numerical approach to study monoclonal antibodies in solution. APL Bioengineering, 2024, 8, .	6.2	0
14642	Molecular Dynamics Investigation of Lipid-Specific Interactions with a Fusion Peptide. Biomolecules, 2024, 14, 285.	4.0	0
14644	A release of local subunit conformational heterogeneity underlies gating in a muscle nicotinic acetylcholine receptor. Nature Communications, 2024, 15, .	12.8	0
14645	Solvent-Dependent Emissions Properties of a Model Aurone Enable Use in Biological Applications. Journal of Fluorescence, 0, , .	2.5	0
14646	Mechanism of Membrane Curvature Induced by SNX1: Insights from Molecular Dynamics Simulations. Journal of Physical Chemistry B, 2024, 128, 2144-2153.	2.6	0
14648	SNAP25 disease mutations change the energy landscape for synaptic exocytosis due to aberrant SNARE interactions. ELife, 0, 12, .	6.0	0
14649	Cellulose-Carboxymethyl Hydrogels: Computational Exploration of Their Nanostructure and Mechanical Properties. Biomacromolecules, 2024, 25, 1989-2006.	5.4	0
14650	Understanding Self-Assembly and Molecular Packing in Methylcellulose Aqueous Solutions Using Multiscale Modeling and Simulations. Biomacromolecules, 2024, 25, 1682-1695.	5.4	0

#	ARTICLE	IF	CITATIONS
14651	Understanding a point mutation signature D54K in the caspase activation recruitment domain of NOD1 capitulating concerted immunity via atomistic simulation. Journal of Biomolecular Structure and Dynamics, 0, , 1-17.	3.5	0
14652	Synthesis, insertion, and characterization of SARS-CoV-2 membrane protein within lipid bilayers. Science Advances, 2024, 10, .	10.3	0
14653	Visualizing Ultrasound Sources Using Signal Time Reversal in the Particle Dynamics Model. Acoustical Physics, 2023, 69, 884-896.	1.0	0
14654	Close-Up Look at Electronic Spectroscopic Signatures of Common Pharmaceuticals in Solution. Journal of Physical Chemistry B, 2024, 128, 2432-2446.	2.6	0
14655	Ionic Pairing and Selective Solvation of Butylmethylimidazolium Chloride Ion Pairs in DMSOâ€“Water Mixtures: A Comprehensive Examination via Molecular Dynamics Simulations and Potentials of Mean Force Analysis. Journal of Physical Chemistry B, 2024, 128, 2168-2180.	2.6	0
14656	Submillisecond Atomistic Molecular Dynamics Simulations Reveal Hydrogen Bond-Driven Diffusion of a Guest Peptide in Proteinâ€“RNA Condensate. Journal of Physical Chemistry B, 2024, 128, 2347-2359.	2.6	0
14657	Novel thiazolidin-4-one benzenesulfonamide hybrids as PPARÎ³ agonists: Design, synthesis and in vivo anti-diabetic evaluation. European Journal of Medicinal Chemistry, 2024, 269, 116279.	5.5	0
14658	Understanding the basis of thermostability for enzyme â€œNanolucâ€“towards designing industry-competent engineered variants. Journal of Biomolecular Structure and Dynamics, 0, , 1-14.	3.5	0
14659	The Deinococcus protease PprI senses DNA damage by directly interacting with single-stranded DNA. Nature Communications, 2024, 15, .	12.8	0
14661	Rapid simulation of glycoprotein structures by grafting and steric exclusion of glycan conformer libraries. Cell, 2024, 187, 1296-1311.e26.	28.9	0
14663	Dissecting the chiral recognition of TLR4/MD2 with Neoseptin-3 enantiomers by molecular dynamics simulations. Physical Chemistry Chemical Physics, 2024, 26, 9309-9316.	2.8	0
14664	Liquidâ€“Vapor Coexistence and Spontaneous Evaporation at Atmospheric Pressure of Common Rigid Three-Point Water Models in Molecular Simulations. Journal of Physical Chemistry B, 2024, 128, 2457-2468.	2.6	0
14665	The genomic landscape of <i>CYP2D6</i> variation in the Indian population. Pharmacogenomics, 2024, 25, 147-160.	1.3	0
14666	Main role of fractal-like nature of conformational space in subdiffusion in proteins. Physical Review E, 2024, 109, .	2.1	0
14667	Exploring Free Energies of Specific Protein Conformations Using the Martini Force Field. Journal of Chemical Theory and Computation, 2024, 20, 2273-2283.	5.3	0
14668	Sequence-dependent material properties of biomolecular condensates and their relation to dilute phase conformations. Nature Communications, 2024, 15, .	12.8	0
14669	Connection between partial pressure, volatility, and the Soret effect elucidated using simulations of nonideal supercritical fluid mixtures. Journal of Chemical Physics, 2024, 160, .	3.0	0
14670	Polycaprolactone/polyacrylic acid/graphene oxide composite nanofibers as a highly efficient sorbent to remove lead toxic metal from drinking water and apple juice. Scientific Reports, 2024, 14, .	3.3	0

#	ARTICLE	IF	CITATIONS
14671	Decoding Molecular Mechanism Underlying Human Olfactory Receptor OR8D1 Activation by Sotolone Enantiomers. Journal of Agricultural and Food Chemistry, 2024, 72, 5403-5415.	5.2	0
14672	Analysis of Poly(ethylene terephthalate) degradation kinetics of evolved IsPETase variants using a surface crowding model. Journal of Biological Chemistry, 2024, 300, 105783.	3.4	0
14673	Synthesis, in silico studies, and inÂvitro biological evaluation of newly-designed 5-amino-1 <i>H</i>-tetrazole-linked 5-fluorouracil analog as a potential antigastric-cancer agent. Journal of Biomolecular Structure and Dynamics, 0, , 1-19.	3.5	0
14674	Molecular cloning, biophysical and <i>in silico</i> studies of Human papillomavirus 33ÂE2 DNA binding domain. Journal of Biomolecular Structure and Dynamics, 0, , 1-20.	3.5	0
14675	The dynamic competition mechanism between the topologically close-packed and BCC structures during crystallization of undercooled zirconium. Chemical Physics, 2024, 581, 112238.	1.9	0
14676	Phosphopeptide binding to the N-SH2 domain of tyrosine phosphatase SHP2 correlates with the unzipping of its central I <sup>2</sup> -sheet. Computational and Structural Biotechnology Journal, 2024, 23, 1169-1180.	4.1	0
14677	Unraveling the underlying structural & transport mechanism of lithium-ion within Lithium bis(trifluoromethanesulfonyl)imide subjected to organic & inorganic matrix based Eutectogel. Journal of Power Sources, 2024, 600, 234270.	7.8	0
14678	Role of Protonation States in the Stability of Molecular Dynamics Simulations of High-Resolution Membrane Protein Structures. Journal of Physical Chemistry B, 2024, 128, 2304-2316.	2.6	0
14680	Mutational analysis in Corynebacterium stationis MFS transporters for improving nucleotide bioproduction. Applied Microbiology and Biotechnology, 2024, 108, .	3.6	0
14681	Thermodynamic and molecular mechanisms of ionic liquids for acetylene dehydration. AIChE Journal, 0, , .	3.6	0
14682	Unraveling the molecular dynamics of sugammadex-rocuronium complexation: A blueprint for cyclodextrin drug design. Carbohydrate Polymers, 2024, 334, 122018.	10.2	0
14683	Understanding the uniaxial-deformation behavior of stable and unstable CO2 hydrates under squeezing and stretching conditions. Materials Today Chemistry, 2024, 37, 101975.	3.5	0
14684	Identification of bioactive compounds of Zanthoxylum armatum as potential inhibitor of pyruvate kinase M2 (PKM2): Computational and virtual screening approaches. Heliyon, 2024, 10, e27361.	3.2	0
14685	Predicting Spin-Dependent Phonon Band Structures of HKUST-1 Using Density Functional Theory and Machine-Learned Interatomic Potentials. International Journal of Molecular Sciences, 2024, 25, 3023.	4.1	0
14686	Effect of Impurities on the Formation of End-Group Clusters in Natural Rubber: Phenylalanine Dipeptide as an Impurity Protein. Macromolecules, 2024, 57, 2588-2608.	4.8	0
14687	Interface Water Assists in Dimethyl Sulfoxide Crossing and Poration in Model Bilayer. Langmuir, 2024, 40, 5764-5775.	3.5	0
14688	<i>Switching Go</i>...<i>-Martini</i> for Investigating Protein Conformational Transitions and Associated Proteinâ€Lipid Interactions. Journal of Chemical Theory and Computation, 2024, 20, 2618-2629.	5.3	0
14689	Searching for low thermal conductivity materials for thermal barrier coatings: A theoretical approach. Physical Review Materials, 2024, 8, .	2.4	0

#	ARTICLE	IF	CITATIONS
14690	Unraveling Partial Coalescence Between Droplet and Oilâ€‘Water Interface in Water-in-Oil Emulsions under a Direct-Current Electric Field via Molecular Dynamics Simulation. <i>Langmuir</i> , 2024, 40, 5992-6003.	3.5	0
14691	Oleic Acid Could Act as a Channel Blocker in the Inhibition of nAChR: Insights from Molecular Dynamics Simulations. <i>Journal of Physical Chemistry B</i> , 2024, 128, 2398-2411.	2.6	0
14692	Tuning Supramolecular Chirality in Iodinated Amphiphilic Peptides Through Tripeptide Linker Editing. <i>Biomacromolecules</i> , 2024, 25, 2277-2285.	5.4	0
14693	Effect of Organic Solvents on the Activity, Stability and Secondary Structure of asclepain cl, Using FTIR and Molecular Dynamics Simulations. <i>Protein Journal</i> , 0, , .	1.6	0
14694	Repurposing of SARS-CoV-2 compounds against Marburg Virus using MD simulation, mm/GBSA, PCA analysis, and free energy landscape. <i>Journal of Biomolecular Structure and Dynamics</i> , 0, , 1-20.	3.5	0
14695	Molecular docking, ADME-Tox, DFT and molecular dynamics simulation of butyroyl glucopyranoside derivatives against DNA gyrase inhibitors as antimicrobial agents. <i>Journal of Molecular Structure</i> , 2024, 1307, 137930.	3.6	0
14696	Microstructure of dendrimers functionalized with folic acid as studied by molecular dynamics simulations. <i>Journal of Molecular Liquids</i> , 2024, 399, 124396.	4.9	0
14697	Building Water Models Compatible with Charge Scaling Molecular Dynamics. <i>Journal of Physical Chemistry Letters</i> , 2024, 15, 2922-2928.	4.6	0
14698	Cytotoxic monastrol derivatives as adjective inhibitors of drug-resistant Eg5: a molecular dynamics perspective. <i>Journal of Biomolecular Structure and Dynamics</i> , 0, , 1-14.	3.5	0
14699	Identification of novel AKT1 inhibitors from <i>Sapria himalayana</i> bioactive compounds using structure-based virtual screening and molecular dynamics simulations. <i>BMC Complementary Medicine and Therapies</i> , 2024, 24, .	2.7	0
14700	Molecular dynamics study of the thermodynamic properties of triglyceride/methanol mixtures in the presence of cosolvent. <i>Journal of Molecular Liquids</i> , 2024, 399, 124431.	4.9	0
14701	Molecular basis of JAK2 activation in erythropoietin receptor and pathogenic JAK2 signaling. <i>Science Advances</i> , 2024, 10, .	10.3	0
14702	Investigating the Aryl Hydrocarbon Receptor Agonist/Antagonist Conformational Switch Using Well-Tempered Metadynamics Simulations. <i>Journal of Chemical Information and Modeling</i> , 2024, 64, 2021-2034.	5.4	0
14703	Molecular Crowding Alters the Interactions of Polymyxin Lipopeptides within the Periplasm of <i>E. coli</i> : Insights from Molecular Dynamics. <i>Journal of Physical Chemistry B</i> , 2024, 128, 2717-2733.	2.6	0
14704	Computational highâ€‘pressure chemistry: Ab initio simulations of atoms, molecules, and extended materials in the gigapascal regime. <i>Wiley Interdisciplinary Reviews: Computational Molecular Science</i> , 2024, 14, .	14.6	0
14705	Free-energy landscape and spinodals for the liquidâ€‘liquid transition of the TIP4P/2005 and TIP4P/Ice models of water. <i>Journal of Chemical Physics</i> , 2024, 160, .	3.0	0
14706	Effect of solid solution and vacancies on the mechanical properties of Cu(Al)/Al <sub>2</sub> Cu/(Cu)Al layered gradient heterostructures. <i>Physica B: Condensed Matter</i> , 2024, 680, 415845.	2.7	0
14707	Chemically Specific Systematic Coarse-Grained Polymer Model with Both Consistently Structural and Dynamical Properties. <i>Jacs Au</i> , 2024, 4, 1018-1030.	7.9	0

#	ARTICLE	IF	CITATIONS
14708	Resolving coupled pH titrations using alchemical free energy calculations. Journal of Computational Chemistry, 2024, 45, 1444-1455.	3.3	0
14709	Time-resolved cryo-EM of G-protein activation by a GPCR. Nature, 0, , .	27.8	0
14710	Cooperative Membrane Binding of HIV-1 Matrix Proteins. Journal of Physical Chemistry B, 2024, 128, 2595-2606.	2.6	0
14711	Temperature dependence of the dynamics and interfacial width in nanoconfined polymers via atomistic simulations. Journal of Chemical Physics, 2024, 160, .	3.0	0
14712	Bending of a lipid membrane edge by annexin A5 trimers. Biophysical Journal, 2024, 123, 1006-1014.	0.5	0
14713	Mechanistic insights into interactions between ionizable lipid nanodroplets and biomembranes. Journal of Biomolecular Structure and Dynamics, 0, , 1-11.	3.5	0
14714	VirtuousPocketome: a computational tool for screening proteinâ€“ligand complexes to identify similar binding sites. Scientific Reports, 2024, 14, .	3.3	0
14715	MemPrep, a new technology for isolating organellar membranes provides fingerprints of lipid bilayer stress. EMBO Journal, 2024, 43, 1653-1685.	7.8	0
14716	Molecular Insights into the Differential Effects of Acetylation on the Aggregation of Tau Microtubule-Binding Repeats. Journal of Chemical Information and Modeling, 2024, 64, 3386-3399.	5.4	0
14717	Differences in the Membrane-Binding Properties of Flaviviral Nonstructural 1 (NS1) Protein: Comparative Simulations of Zika and Dengue Virus NS1 Proteins in Explicit Bilayers. ACS Bio & Med Chem Au, 0, , .	3.7	0
14718	Assessment of water purification by IRMOF-1 based on rGO as a new nanoengineered adsorbent: Insights from adsorption mechanism. Journal of Molecular Liquids, 2024, 400, 124485.	4.9	0
14719	The mutual and dynamic role of TSPO and ligands in their binding process: An example with PK-11195. Biochimie, 2024, , .	2.6	0
14720	Mechanistic Insight into the Mechanical Unfolding of the Integral Membrane Diacylglycerol Kinase. JACS, 2024, 4, 1422-1435.	7.9	0
14721	The Absorption Mechanisms of CO <sub>2</sub> , H <sub>2</sub> S and CH <sub>4</sub> Molecules in [EMIM][SCN] and [EMIM][DCA] Ionic Liquids: A Computational Insight. Fluid Phase Equilibria, 2024, 581, 114080.	2.5	0
14722	In silico and in vivo study of anti-inflammatory activity of Morinda longissima (Rubiaceae) extract and phytochemicals for treatment of inflammation-mediated diseases. Journal of Ethnopharmacology, 2024, 328, 118051.	4.1	0
14725	Unlocking bacterial defense: Exploring the potent inhibition of NorA efflux pump by coumarin derivatives in Staphylococcus aureus. Microbial Pathogenesis, 2024, 190, 106608.	2.9	0
14726	Assessing the mechanism of fastâ€“cycling cancerâ€“associated mutations of <scp>Rac1</scp> small <scp>Rho GTPase</scp>. Protein Science, 2024, 33, .	7.6	0
14727	Molecular Insights into the Impact of Mutations on the Binding Affinity of Targeted Covalent Inhibitors of BTK. Journal of Physical Chemistry B, 2024, 128, 2874-2884.	2.6	0



#	ARTICLE	IF	CITATIONS
14728	Identification of Antiviral Phytocompounds as Potential Anti-Dengue Agents against DENV NS2B/NS3 Protease: An Integrated Molecular Modelling and Dynamics Approach. <i>ChemistrySelect</i> , 2024, 9, .	1.5	0
14729	RAPP-containing arrest peptides induce translational stalling by short circuiting the ribosomal peptidyltransferase activity. <i>Nature Communications</i> , 2024, 15, .	12.8	0
14731	Identification of Î²-cyclodial-derived mono-carbonyl curcumin analogs as potential interleukin-6 inhibitor to treat wound healing through QSAR, molecular docking, MD simulation, MM-GBSA calculation. <i>Journal of Biomolecular Structure and Dynamics</i> , 0, , 1-12.	3.5	0
14732	Computational Studies of Cannabis Derivatives as Potential Inhibitors of SARS-CoV-2 Mpro. <i>Chemistry Africa</i> , 0, , .	2.4	0
14733	Regulating and understanding the compatibility of sulfide composite solid-state electrolyte in nickel-rich lithium metal batteries. <i>Journal of Power Sources</i> , 2024, 602, 234366.	7.8	0
14734	Investigation of Rare Earth Element Binding to a Surface-Bound Affinity Peptide Derived from EF-Hand Loop I of Lanmodulin. <i>ACS Applied Materials &amp; Interfaces</i> , 2024, 16, 16912-16926.	8.0	0
14736	Molecular mechanism for the interaction of natural products with ionic liquids: Insights from MD and DFT study. <i>Journal of Molecular Liquids</i> , 2024, 399, 124440.	4.9	0
14737	Molecular Basis for the Involvement of Mammalian Serum Albumin in the AGE/RAGE Axis: A Comprehensive Computational Study. <i>International Journal of Molecular Sciences</i> , 2024, 25, 3204.	4.1	0
14738	Selective Removal of Chlorophyll and Isolation of Lutein from Plant Extracts Using Magnetic Solid Phase Extraction with Iron Oxide Nanoparticles. <i>International Journal of Molecular Sciences</i> , 2024, 25, 3152.	4.1	0
14739	A binding site for phosphoinositides described by multiscale simulations explains their modulation of voltage-gated sodium channels. <i>ELife</i> , 0, 12, .	6.0	0
14740	NMR Study of Water-Soluble Carotenoid Crocin: Formation of Mixed Micelles, Interaction with Lipid Membrane and Antioxidant Activity. <i>International Journal of Molecular Sciences</i> , 2024, 25, 3194.	4.1	0
14741	Unraveling motion in proteins by combining NMR relaxometry and molecular dynamics simulations: A case study on ubiquitin. <i>Journal of Chemical Physics</i> , 2024, 160, .	3.0	0
14742	Acceleration of Solvation Free Energy Calculation via Thermodynamic Integration Coupled with Gaussian Process Regression and Improved Gelman-Rubin Convergence Diagnostics. <i>Journal of Chemical Theory and Computation</i> , 2024, 20, 2570-2581.	5.3	0
14743	In-silico design novel phenylsulfonyl furoxan and phenstatin derivatives as multi-target anti-cancer inhibitors based on 2D-QSAR, molecular docking, dynamics and ADMET approaches. <i>Molecular Simulation</i> , 2024, 50, 470-492.	2.0	0
14744	Efficient and accurate binding free energy calculation of AÎ²<sub>9â€“40</sub> protofilament propagation. <i>Proteins: Structure, Function and Bioinformatics</i> , 0, , .	2.6	0
14745	Structures and Dynamics of Î²-Rich Oligomers of ATTR (105â€“115) Assembly. <i>ACS Chemical Neuroscience</i> , 2024, 15, 1356-1365.	3.5	0
14746	Integrated preservation of water activity as key to intensified chemoenzymatic synthesis of bio-based styrene derivatives. <i>Communications Chemistry</i> , 2024, 7, .	4.5	0
14747	Anti-agglotiation of gas hydrate. , 2024, , 479-522.		0

#	ARTICLE	IF	CITATIONS
14748	General concepts of geologic carbon sequestration, gas hydrate, and molecular simulation. , 2024, , 1-66.		0
14749	Understanding and fine tuning the propensity of ATP-driven liquidâ€“liquid phase separation with oligolysine. Physical Chemistry Chemical Physics, 2024, 26, 10568-10578.	2.8	0
14750	Adsorption Isotherm and Mechanism of Ca <sup>2+</sup> Binding to Polyelectrolyte. Langmuir, 2024, 40, 6212-6219.	3.5	0
14751	De novo antioxidant peptide design via machine learning and DFT studies. Scientific Reports, 2024, 14, .	3.3	0
14752	Effect of <scp>hexylâ€“branched</scp> backbone size on the size distribution and coalescence of free volume around an amphiphilic molecule. Polymer Engineering and Science, 0, , .	3.1	0
14753	Effect of citral partitioning on structural and mechanical properties of lipid membranes. European Physical Journal: Special Topics, 0, , .	2.6	0
14754	Molecular dynamics of the human RhD and RhAG blood group proteins. Frontiers in Chemistry, 0, 12, .	3.6	0
14755	In Silico Investigation of Parkin-Activating Mutations Using Simulations and Network Modeling. Biomolecules, 2024, 14, 365.	4.0	0
14756	Cryo-electron Microscopy and Molecular Modeling Methods to Characterize the Dynamics of Tau Bound to Microtubules. Methods in Molecular Biology, 2024, , 77-90.	0.9	0
14757	A closer examination of the nature of atomic motion in the interfacial region of crystals upon approaching melting. Journal of Chemical Physics, 2024, 160, .	3.0	0
14758	Modulation of Phospholipase A <sub>2</sub> Membrane Activity by Anti-inflammatory Drugs. Langmuir, 2024, 40, 7038-7048.	3.5	0
14759	4-(Azolyl)-Benzamidines as a Novel Chemotype for ASIC1a Inhibitors. International Journal of Molecular Sciences, 2024, 25, 3584.	4.1	0
14760	Exploring Product Release from Yeast Cytosine Deaminase with Metadynamics. Journal of Physical Chemistry B, 2024, 128, 3102-3112.	2.6	0
14761	Electric field induced the changes in structure and function of human transforming growth factor beta receptor type I: from molecular dynamics to docking. Journal of Biomolecular Structure and Dynamics, 0, , 1-12.	3.5	0
14762	Theoretical study on symmetric and asymmetric stacking in the self-assembly of bola-amphiphilic peptides into membranes with mixtures of EF4E and KF4K. Journal of Molecular Liquids, 2024, 400, 124535.	4.9	0
14763	Membrane Catalyzed Formation of Nucleotide Clusters and Their Role in the Origins of Life: Insights from Molecular Simulations and Lattice Modeling. Journal of Physical Chemistry B, 2024, 128, 3121-3132.	2.6	0
14764	Inherent limitations of the hydrogen-bonding UPy motif as self-healing functionality for polymer electrolytes. , 0, , .		0
14765	3,4-Ethylenedioxythiophene Hydrogels: Relating Structure and Charge Transport in Supramolecular Gels. Chemistry of Materials, 2024, 36, 3092-3106.	6.7	0

#	ARTICLE	IF	CITATIONS
14766	Deciphering the Molecular Mechanisms of Reactive Metabolite Formation in the Mechanism-Based Inactivation of Cytochrome p450 1B1 by 8-Methoxypsoralen and Assessing the Driving Effect of phe268. Molecules, 2024, 29, 1433.	3.8	0
14767	pH Dependence of HSF1 trimerization is shaped by intramolecular interactions. Biochemical and Biophysical Research Communications, 2024, 709, 149824.	2.1	0
14768	Investigation of the behavior of water and oil droplets on nanostructured surfaces: a molecular dynamics simulation study. Journal of Mechanical Science and Technology, 2024, 38, 1249-1257.	1.5	0
14769	Studying the ssDNA loaded adeno-associated virus aggregation using coarse-grained molecular dynamics simulations. International Journal of Pharmaceutics, 2024, 655, 123985.	5.2	0
14770	Dynamic effects on the nonlinear optical properties of donor acceptor stenhouse adducts: insights from combined MD + QM simulations. Physical Chemistry Chemical Physics, 0, , .	2.8	0
14771	Mn <sup>2+</sup> -induced structural flexibility enhances the entire catalytic cycle and the cleavage of mismatches in prokaryotic argonaute proteins. Chemical Science, 2024, 15, 5612-5626.	7.4	0
14772	Structural insights into the octamerization of glycerol dehydrogenase. PLoS ONE, 2024, 19, e0300541.	2.5	0
14773	In Vitro and In Silico Explorations of the Protein Conformational Changes of Corynebacterium glutamicum MshA, a Model Retaining GT-B Glycosyltransferase. Biochemistry, 2024, 63, 939-951.	2.5	0
14774	Delineating the impact of N21D mutation on the conformational preferences and structural transitions in human islet amyloid polypeptide. Journal of Molecular Liquids, 2024, 401, 124528.	4.9	0
14776	Structure and assembly of a bacterial gasdermin pore. Nature, 2024, 628, 657-663.	27.8	0
14777	Hydroxychloroquine interaction with phosphoinositide 3-kinase modulates prostate cancer growth in bone microenvironment: In vitro and molecular dynamics based approach. International Journal of Biological Macromolecules, 2024, 266, 130912.	7.5	0